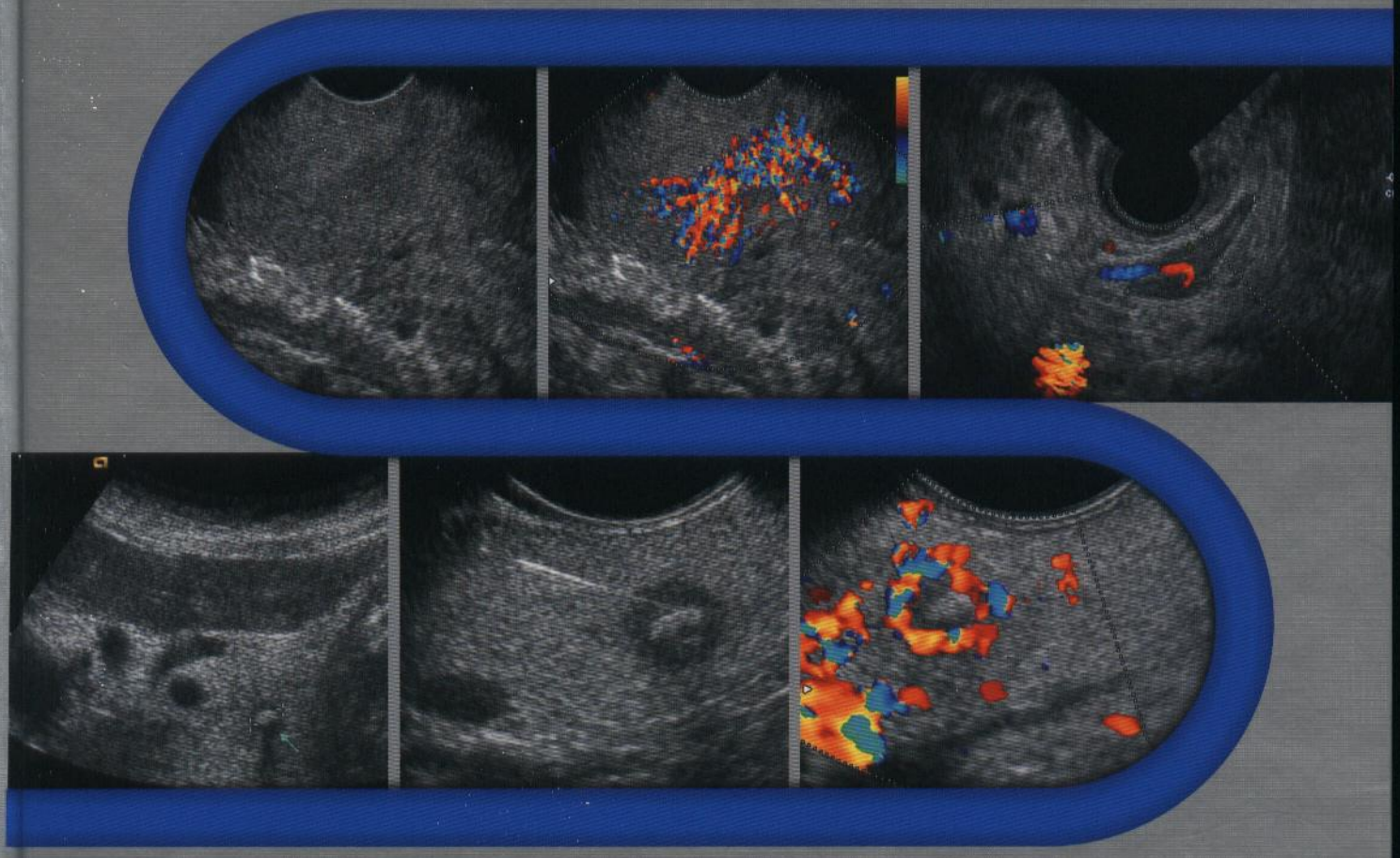
Endoscopic Ultrasound

An Introductory Manual and Atlas

Editor
Christoph Frank Dietrich



Thieme

Endoscopic Ultrasound

An Introductory Manual and Atlas

Christoph Frank Dietrich, MD
Professor
Department of Internal Medicine 2
Caritas Hospital Bad Mergentheim
Germany

With contributions by
H Allgayer, PG Arcidiacono, HD Becker, T Beyer, B Braden, E Burmester, S Carrara, R Eberhardt, S Faiss, W Fischbach, H Frey, A Fritscher-Ravens, M Giovannini, C Greis, FJ Herth, M Hocke, S Hollerbach, J Janssen, C Jenssen, PH Kann, M Krasnik, T Leineweber, M Mayr, J Mertens, H Neye, J Niehaus, D Nuernberg, C Ortiz-Moyano, M Sailer, H Seifert, HW Sudholt, T Topalidis, P Vilmann

Foreword by Wolfgang F Caspary

906 illustrations
94 tables

Thieme
Stuttgart · New York

1 Basics of Radial Endoscopic Ultrasound

M. Hocke

Introduction

Endoscopic ultrasound today demands the highest level of expertise from physicians working in endoscopy. The method requires a unique combination of familiarity with endoscopic practices and experience in ultrasound. When it is properly carried out and critically assessed, it makes extensive diagnostic and therapeutic applications possible.

However, newcomers to this field often find themselves facing a mountain of problems, despite having a thorough knowledge of endoscopy and sonography. The consequent frustration can result in this valuable method being abandoned. The following chapter therefore aims to simplify the examination technique and make it more accessible, so that it can be carried out successfully after a little practice.

Ten Golden Rules

Firstly, we can introduce the "10 golden rules of endoscopic ultrasound" that every practitioner should have at his or her disposal in order to regain perspective when difficulties arise during the examination (in both radial and longitudinal ultrasound). These rules were compiled by an endoscopic ultrasound specialist, Dr. U. Will, and have been collated, experienced, and tested in practice by the author of this chapter.

1. If you can't see anything, withdraw.
2. Always turn the instrument clockwise.
3. No air, always use suction.
4. Use your knowledge of anatomy for orientation.
5. Stay at the back of the stomach.
6. Only make small movements.
7. Do nothing!
8. Use water.
9. Remember the power of endoscopic ultrasound.
10. When in doubt, trust those with more experience.

Notes on the "Golden Rules"

1. During an endoscopic ultrasound examination, you will frequently find yourself with an image in which nothing is recognizable. In this situation, you should gradually bring the scope back until a recognizable marker appears. From this point you can proceed anew with the examination.

2. Slight clockwise twisting of the instrument may be necessary to keep the papilla of Vater in the same position, especially in the descending duodenum. This can also help avoid slippage of the scope from the duodenum into the stomach (a similar phenomenon can be observed in endoscopic retrograde cholangiopancreatography).

3. Air is the enemy of endoscopic ultrasound—applying continuous suction during the entire examination should be standard.

4. Problems can occur when you first orient yourself visually using specific structures and then start trying to construct an ultrasound image. The air needed for good visibility will prevent the ultrasound from working, and there will be a large discrepancy between the visual appearance of the structure and the ultrasound image. It is always preferable to locate a structure on a purely endoscopic ultrasound image, using anatomical markers for orientation.

5. Positioning the instrument at the back wall of the stomach can often help when perspective has been lost, as the important markers are easy to recognize from this location.

6. The biggest mistake made by beginners is to move the scope too far in one go. Large movements lead to the markers being overlooked and therefore to a loss of orientation during the examination.

7. Not moving the instrument does not mean keeping it in one place. The peristaltic movements alone result in a gradual change of view through the different levels, without any action on the part of the operator. This is an excellent, unhurried way of mentally ordering the structures as you see them.

8. In hollow, air-filled organs such as the gastric body and fundus regions, filling with water can produce unexpectedly effective images.

9. When this technique is carried out correctly, the practitioner will begin to see the extensive range of possible applications.

10. Experience colors vision; two examiners looking at the same image may interpret what they see very differently.

Patient Preparation

The patient should be made aware in advance of the risks and effectiveness of the procedure. Endoscopic ultrasound is not suitable as a screening method and should only be used to answer specific questions.

The risk of complications with diagnostic endoscopic ultrasound, at 0.05%, and the 30-day mortality, at 0.003%, are very low, but they are not completely negligible. The main risk is the danger of perforation by the 3–4 cm stiff tip of the instrument used in both radial and longitudinal equipment.

Light sedation (with midazolam or propofol) is recommended for the examination, which should be carried out with the patient lying on the left side. The patient should not consume any food for 8 hours before the procedure.

Examination Procedures

In principle, the procedure used in the examination depends on the question being posed. For the newcomer, the easiest phenomena to examine and diagnose are protuberances in the gastrointestinal tract and surface tumors. The instrument is positioned directly in front of the relevant area, and after a preparatory stream of water has been applied (with an air-free balloon filled with water to a diameter of 5–10 mm), the examination can take place under continuous suction. However, although this process is easy to carry out in the duodenum, antrum, and esophagus, the presence of air and the many folds present in the gastric body and fundus regions make it more difficult there. Often, filling the stomach with 200–300 mL water can result in an adequate image in these areas. The most difficult areas to examine are the angular notch and the fundus region. Occasionally, turning the patient onto his or her back after the water has been introduced can help here.

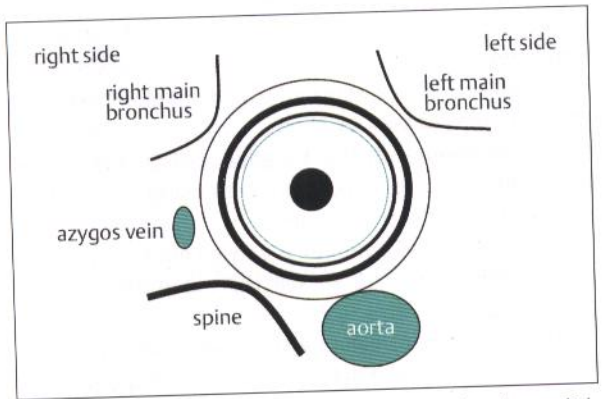


Fig. 1.1 Orientation during examination with the radial method. In general, the view resembles that in computed tomography—i. e., the anatomy is viewed from underneath.

Small protuberances in the gastrointestinal tract are often difficult to capture with the balloon method alone. The examiner should make certain that mucosal masses are "smoothed out" with the balloon and therefore remain hidden from the image. These should preferably be examined using the miniprobe method, which makes it possible to locate lesions more precisely.

The most difficult endoscopic ultrasound procedure is examining extraintestinal organs and structures. Success here depends on excellent knowledge of ultrasound anatomy, so that pathological structures can be detected by recognizing markers.

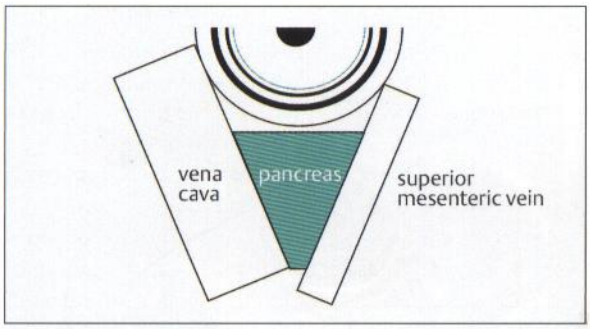
As a rule, the operator should make sure that the radial endoscopic ultrasound instruments are standardized for a computed-tomographic (CT) view—i. e., viewing the patient from underneath. This can best be seen in the mediastinum. It is essential to remember that when the descending aorta and spine are at the bottom edge of the picture, the image will appear mirrored: the right main bronchus appears on the left side of the image, the left on the right (Fig. 1.1).

To maintain orientation during the imaging process, it is necessary to identify a series of standard ultrasound cross-sections in the gastrointestinal tract. This should be carried out during every examination. The following sections aim to describe each cross-section and the best technique for locating it.

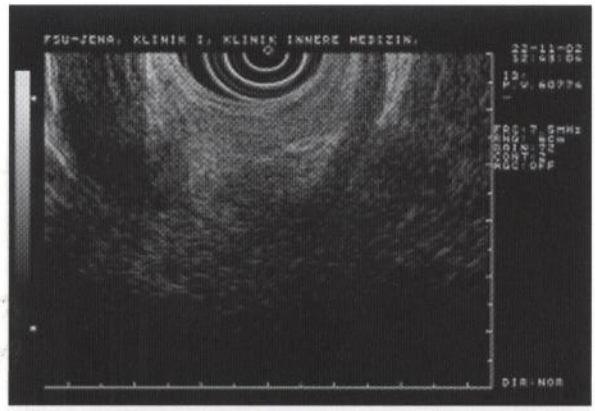
Cross-Section of the Descending Duodenum

To produce images of extraintestinal structures, begin by positioning the scope in the descending duodenum by sight in the same way as in the endoscopic retrograde cholangiopancreatography (ERCP) method, and then straighten it slowly. The water-filled balloon should normally be used to improve the contact. Continuous suction can be controlled with the left hand, which can also angle the tip of the scope as far upward as possible to optimize the contact with the intestine. Sideways movements are not made using the small wheel, but by turning the instrument itself with the right hand—optimally turning the whole instrument at the shaft.

As the scope is withdrawn slowly from this relatively blind position, two anatomical markers will become visible: the vena cava and aorta can be seen as a wide echo-free band on the left side of the screen, and the superior mesenteric vein and artery as a narrow band with a weak echo on the right side. These two markers produce a forward-pointing triangle, which surrounds parts of the body of the pancreas and, more importantly, the uncinate pancreas. This position is optimally suited for examination and diagnosis. The aorta on the left of the image and the superior mesenteric artery on the right, in addition to the confluence of the superior mesenteric artery and the aorta toward the bottom of the image, form a V shape. As this is the first recognizable

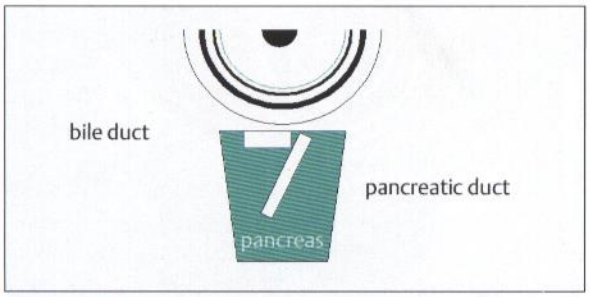


a

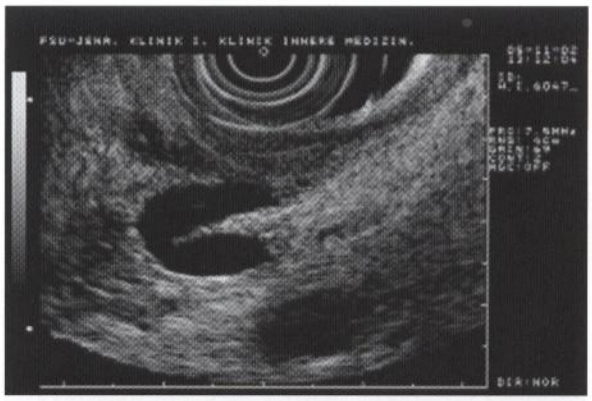


b

Fig. 1.**2a, b** Standard cross-section of the descending duodenum. Anatomical markers: superior mesenteric artery and vein, aorta, vena cava.



a



b

Fig. 1.**3a, b** Standard cross-section of the papilla of Vater. Anatomical markers: pancreatic duct, bile duct.

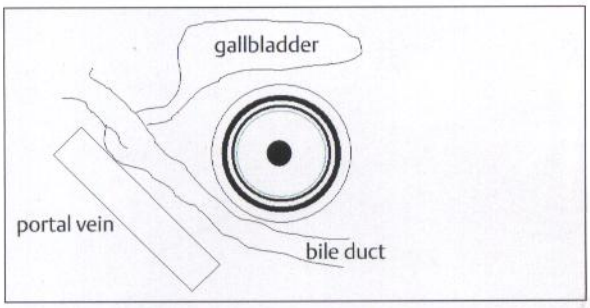
image to appear while the scope is being withdrawn from the descending duodenum, a view of the pancreas opens up—the "golden V"—when this position has been reached (Fig. 1.**2**).

Cross-Section of the Papilla of Vater

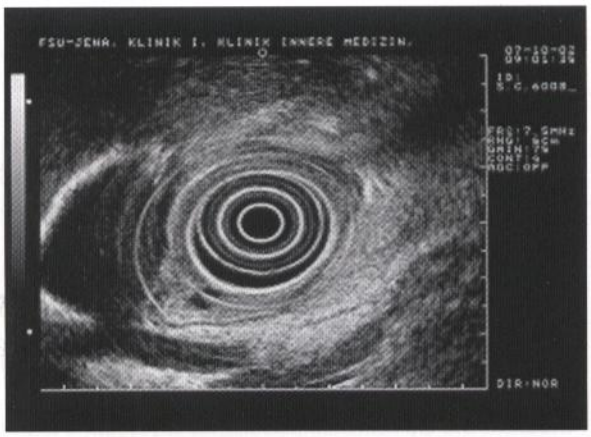
From this section in the descending duodenum, the instrument should be withdrawn while the shaft is turned slightly to the right. The first marker to become visible is the pancreatic duct in the head of the pancreas. This appears as a narrow, echo-free structure in the middle of the easily visible pancreatic tissue stretching from the bottom left to the top right of the view. When this has been located, keep it in the middle of the image and follow it upward to the right by turning the instrument further clockwise and by withdrawing the instrument to the papilla of Vater. The correct position has been reached when a second tubular structure starts to appear on the left, at the junction of the pancreatic duct and the duodenum. This represents the bile duct. When both markers have been correctly identified, imaging and examination of the papilla of Vater can be carried out, using slow forward and backward movements (Fig. 1.**3**).

Cross-Section of the Duodenal Bulb

After the examination of the papilla of Vater, stop turning the instrument to the right, hold the bile duct in the center of the image, and then turn the instrument at the shaft slightly to the left. This movement allows the tip of the scope slowly to relocate itself into the duodenal bulb (as in ERCP). The instrument repositions itself in such a way that the bile duct lets itself be untwisted lengthways, and eventually an image is produced that should be recognizable from percutaneous ultrasound. In this position, the bile duct can be viewed up to the hepatic duct bifurcation near the ultrasound head, and the accompanying portal vein can be seen on the side furthest from the head of the scope. The extrahepatic bile ducts can be examined optimally from this position. Near the middle of the bile duct, the bifurcation of the cystic duct can be seen. This often encircles the bile duct and leads to the gallbladder, which is on the left in the image (Fig. 1.**4**).

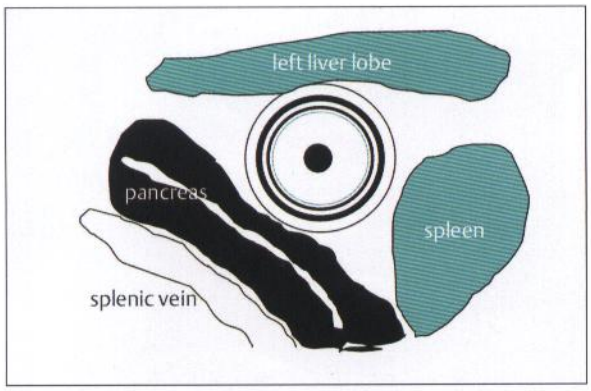


a

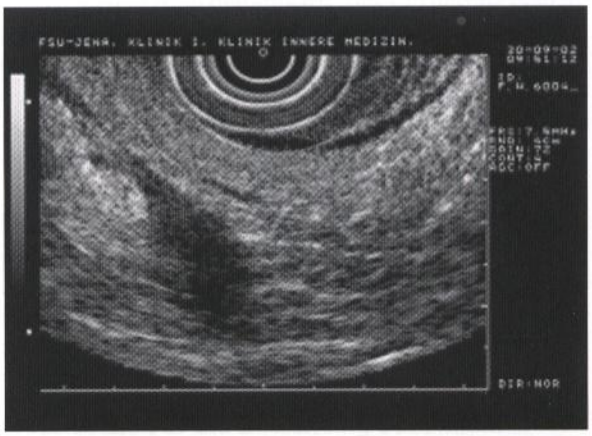


b

Fig. 1.4a, b Standard cross-section of the duodenal bulb. Anatomical markers: bile duct, gallbladder, portal vein.



a



b

Fig. 1.5a, b Standard cross-section of the stomach. Anatomical markers: pancreas, splenic vein.

Cross-Section of the Stomach

After examination of the porta hepatis, withdrawing the scope further often leads to invagination of the bulb into the stomach. Emptying the balloon slightly and filling it again usually results in the instrument, due to the pull exerted, becoming located in an optimal position to examine the body of the pancreas. Without moving the instrument, this should become visible on the bottom left and can be recognized by the dorsally positioned splenic vein. This section is easy to interpret, as it is similar to percutaneous ultrasound diagnosis. An important clue for orientation is the left liver lobe, which appears at the top of the picture. Loosening the large wheel and straightening the tip of the scope by means of clockwise and anticlockwise twisting at the shaft makes it possible to see the entire body and tail of the pancreas, as well as a large part of the pancreatic head. The spleen rounds off the image on the right side (Fig. 1.5).

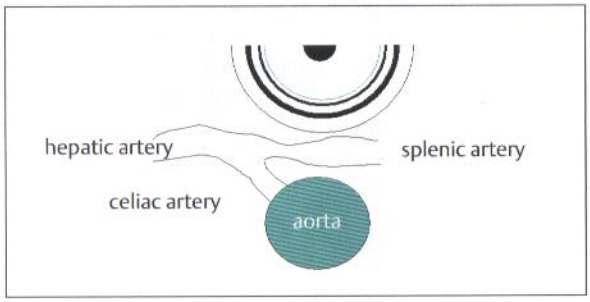
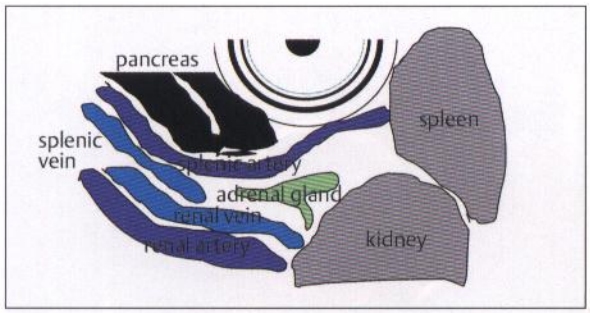


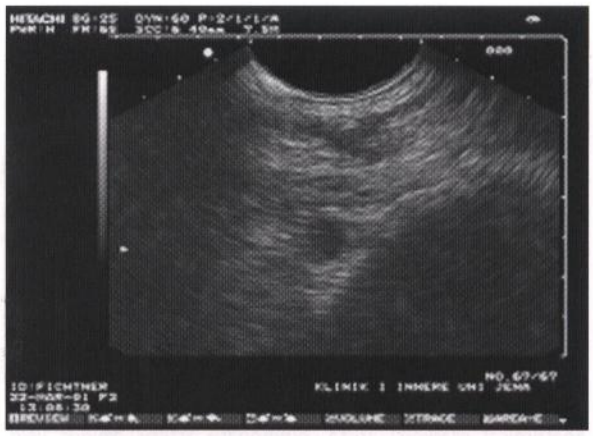
Fig. 1.6 Standard cross-section of the para-aortic region. Anatomical marker: aorta.

Cross-Section of the Para-Aortic Region

Withdrawing further leaves the upper pancreas behind, and the abdominal aorta soon comes into view as an easily found marker at the bottom of the image. Experience shows that the junctions of the large abdominal vessels can only be recognized in part; in good conditions, however, the confluence of the celiac artery can be seen, with the splenic artery coursing to the left and the hepatic artery coursing to the right of the image (Fig. 1.6).

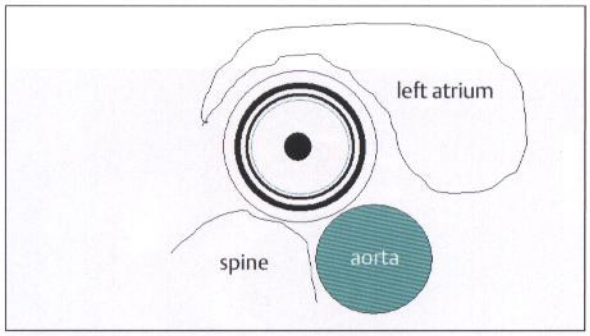


a

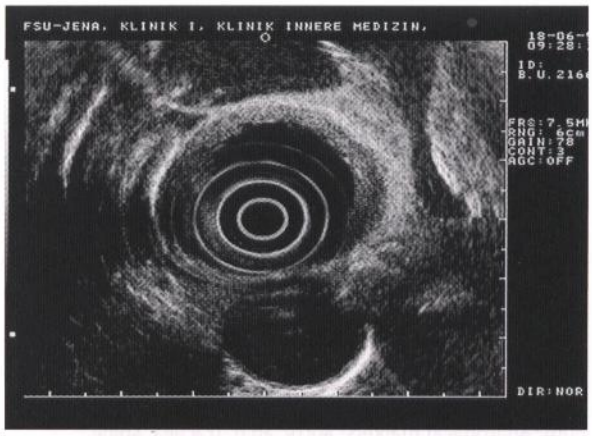


b

Fig. 1.**7a, b** Standard cross-section of the adrenal gland. Anatomical markers: pancreatic tail, left kidney, left renal vessels and spleen.



a



b

Fig. 1.**8a, b** Standard cross-section of the lower mediastinum. Anatomical markers: left atrium, aorta, spine.

Cross-Section of the Adrenal Glands

From this position at the confluence of the large abdominal vessels, the scope should now be pushed back again somewhat, while twisting the shaft slightly clockwise. This movement makes it possible to return via the fundus region to the tail of the pancreas, first passing the spleen and then the kidney, both on the right side of the image. The left adrenal gland can be found on the upper side of the kidney, framed by the splenic artery and splenic vein, as well as the left renal vein. Holding this pelican-shaped structure in the center of the image will quickly result in it coming closer to the wall of the stomach, which is the position from which it can be examined most effectively (Fig. 1.**7**).

Cross-Section of the Lower Mediastinum

All of the structures surrounding the upper gastrointestinal tract have now been examined. An examination of the mediastinum should now form the conclusion of the procedure. With the exception of the diagnosis of changes on the surface of the gastrointestinal tract, this is the easiest task, thanks to the anatomical markers.

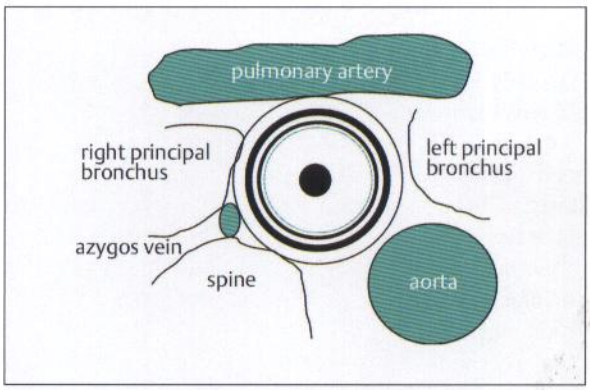
It has proved advantageous always to assume that the organs of the mediastinum have the same locations, so the examination should be carried out with the spine and descending aorta at the lower edge of the image as standard. After the scope has been withdrawn, the left atrium should be visible as a marker at the top edge of the image (Fig. 1.**8**).

Cross-Section of the Central Mediastinum

As the instrument is withdrawn further, a large tubular structure should be seen crossing the top of the picture; this is the pulmonary artery. The sharp air reflexes of the left main bronchus on the right side of the picture and the right main bronchus on the left side can also be identified. On the left of the picture, next to the spine, there is another tubular structure—the azygos vein (Fig. 1.**9**).

Cross-Section of the Upper Mediastinum

As the scope is withdrawn further, the two principal bronchi converge into the trachea at the top of the picture, and the confluence of the ascending aorta and

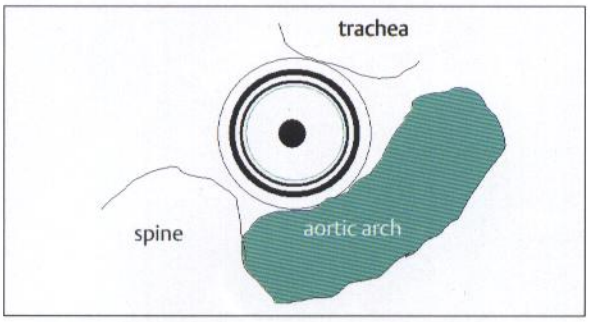


a



b

Fig. 1.**9a, b** Standard cross-section of the central mediastinum. Anatomical markers: aorta, pulmonary artery, azygos vein, main bronchus.



a



b

Fig. 1.**10a, b** Standard cross-section of the upper mediastinum. Anatomical markers: aortic arch, trachea, spine.

the descending aorta in the aortic arch can be seen on the bottom right, with the cervical and brachial vessels leading off it. Experience has shown that the examination of these structures using the radial method and the filled balloon should be discontinued here, as it leads to increased discomfort for the patient (Fig. 1.**10**).

These sections, as explained above, are designed to help the examiner maintain perspective in the difficult radial anatomy of the upper gastrointestinal tract and to help him or her return to a recognizable structure when orientation is occasionally lost.

■ Rating Levels of Skill in the Endoscopic Ultrasound Method

It is extremely important to judge one's own ability in endoscopic ultrasonography critically, in order to recognize opportunities for diagnostic improvement using this powerful method. Each practitioner can match his or her own achievements against the stages of learning and assess his or her results accordingly. Four stages of learning are generally recognized.

1. Justified lack of confidence. This can be recognized by complete reliance on the instructor. An independent diagnosis at this stage is almost impossible. Problems often occur even in bringing the instrument into the descending duodenum. Finding the papilla section marker is unsuccessful 75% of the time. In comparison with percutaneous ultrasonography, the results of endoscopic ultrasonography are often poorer. These problems are common when fewer than 50 examinations have been carried out.

2. Unjustified confidence. After a few successes, the practitioner is inclined to overrate his or her own ability. It is in the interests of the method and the patients to recognize this phase quickly and to keep it as short as possible. Clear signs of this stage are attempts to diagnose the malignancy of masses beyond the range of this image-based method. Other signs are, for example, not recognizing cholangiolithiasis, which is then diagnosed with ERCP, or failing to notice surface lesions 5–10 mm in size in the gastrointestinal tract. A lack of

perspective is common in this phase; the practitioner fixes firmly on the structures he or she recognizes and loses an overview of the surroundings. This stage is often found in those who have carried out up to 100 independent examinations.

3. Unjustified lack of confidence. Several misdiagnoses can cause practitioners to lose faith in themselves and the method. Many give up on the method at this point, although their own experience is much more advanced than they realize. This phase can be recognized by a tendency only to describe what is being seen and to avoid making a working or hypothetical diagnosis. The practitioner is heavily reliant on other image-based diagnostic methods (such as computed tomography and percutaneous ultrasonography) and bases his or her results on these, even when these do not quite match the findings on endoscopic ultrasound. This stage is usually found in those who have carried out approximately 150 independent examinations.

4. Justified confidence. After these first stages have been passed, the enormous potential of this method starts to become apparent. The practitioner is able to make confident diagnoses and, when necessary, to prescribe interventional therapy (e.g., correct diagnosis of an infected pancreatic pseudocyst followed by endoscopic ultrasound cyst drainage). The practitioner who regularly checks his or her results and critically assesses them will find that the possibilities of the method are almost unlimited.

2 Longitudinal EUS Anatomy

J. Janssen

Introduction

Endoscopic ultrasonography (EUS) started in the 1980s with mechanical radial scanners, which provide a circumferential overview of the gastrointestinal wall and surrounding structures. This specific imaging method was quickly accepted, and reports about difficult anatomic orientation were rare—probably due to the resemblance of the images to those provided by computed tomography (CT). Some 10 years later, longitudinal electronic scanners were developed, allowing biopsies to be taken and EUS interventions to be carried out with real-time guidance. Despite the high resolution and good image quality provided, these systems had, and are still having, difficulty in becoming accepted as routine diagnostic instruments as well. The main obstacle is the impression that anatomic orientation is more difficult, resulting in a longer learning curve.

The image produced with linear EUS is similar to that in conventional ultrasound images. The lack of a circumferential view has to be compensated for by 360° rotation with the echoendoscope. Skilled ultrasonographers and endoscopists, including those with experience in endoscopic retrograde cholangiopancreatography (ERCP), are therefore likely to succeed more easily with linear EUS.

Since the very beginnings of longitudinal EUS, several groups have been concerned with the issues involved in education and training in EUS [1–4]. Workshops and meetings provide an opportunity to learn the examination technique, as well as useful tricks, from experts. However, hands-on training requires a familiar setting and cannot be offered in workshops.

When various EUS centers are compared, it is surprising to see how many different approaches to linear EUS there are, each represented by successful experts. The technique presented in this chapter thus describes only one of several ways of performing linear EUS.

The Philosophy of the Examination

The underlying idea is to develop EUS anatomy along landmarks and guiding structures. The need for endoscopic control is negligible; the exact position of the tip of the echoendoscope is of no interest.

EUS Landmarks

The *long axis* in the chest and abdomen is represented by the *thoracic and abdominal aorta*, which can be imaged from the esophagus and stomach. The *pancreas* is the *transverse axis* in the abdomen. The third guiding structure (which is of lesser importance) is the *inferior vena cava* (IVC), which can be imaged from the descending part of the duodenum.

The Examination Sequence

As the aorta is used as the main longitudinal anatomic axis, it seems reasonable to pick up this structure as early as possible whilst introducing the scope. As the aorta is followed, further anatomic structures become visible, as described in detail later. Thus, the examination starts orally and subsequently extends to the aboral areas. Usually, the region of interest is imaged repeatedly, with the instrument being moved forward and backward while the scope is rotated, as appropriate. Until the pylorus has to be passed, there is normally no need for endoscopic guidance, except to examine small mural lesions. Air insufflation is therefore not necessary, and close contact between the probe and the gastrointestinal wall is established more easily.

Caution: whenever the echoendoscope cannot be moved easily, endoscopic guidance is mandatory to avoid injuring or even perforating the gastrointestinal wall.

Deep introduction of the echoendoscope into the duodenum is not required for several EUS indications, such as the staging of esophageal cancer. Intubation of the duodenum is necessary in order to visualize the anatomic area around the pancreatic head or common bile duct, or both.

Special Linear EUS Anatomy

EUS Anatomy Displayed from the Esophagus

After the echoendoscope has been introduced, the first anatomic structure seen is the aortic arch, at about 22 cm from the incisors. The branching of the left subclavian artery can be detected immediately, or after

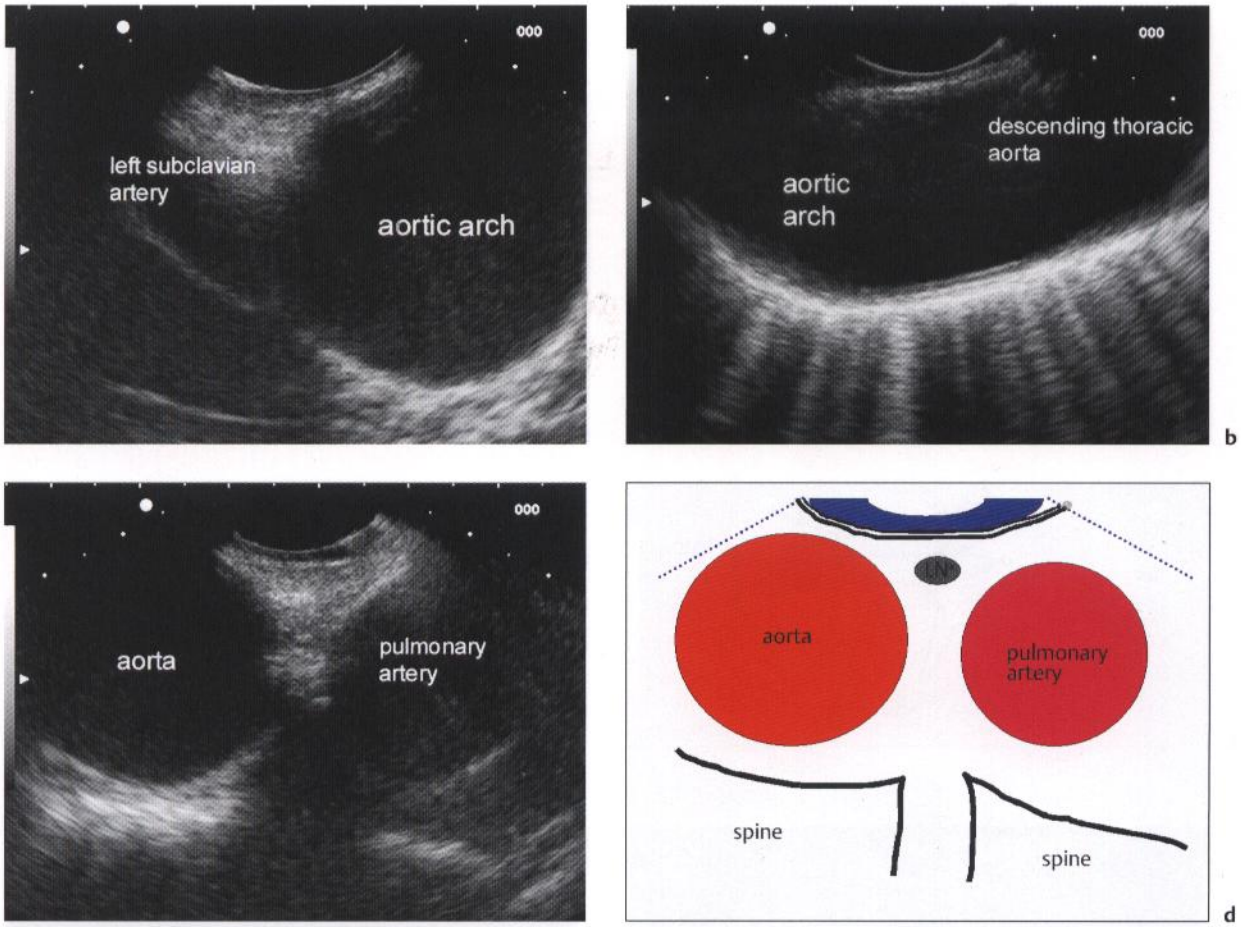


Fig. 2.**1a** The aortic arch and left subclavian artery are seen at 22 cm from the incisors. **b** When the scope is turned counterclockwise, the arch can be followed into the descending thoracic aorta. **c** When the instrument is rotated clockwise and slightly pushed, the aortopulmonary window becomes visible. **d** The anatomic outline of the aortopulmonary window. LN: level 5 lymph node (American Thoracic Society map).

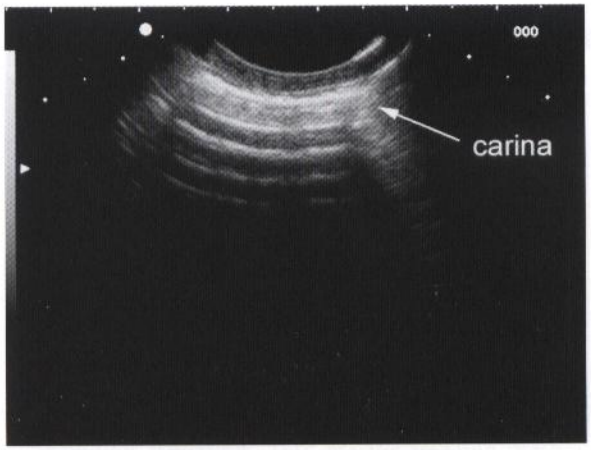
turning the scope slightly to the left (Fig. 2.**1a**). Continuing the rotation in a counterclockwise direction along the aortic arch leads to the descending thoracic aorta (Fig. 2.**1b**), which can easily be followed caudally by pushing the scope and adjusting the wheels to adapt the probe to the longitudinal axis of the aorta.

The aortopulmonary window, covering level 5 lymph nodes according to the American Thoracic Society (ATS) map, can also be depicted starting at the aortic arch, with the instrument now being rotated clockwise and moved slightly forward (Fig. 2.**1c**).

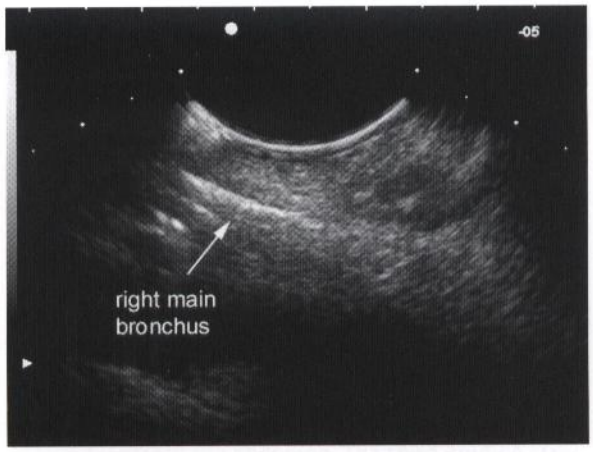
The trachea is found about 18–25 cm from the incisors by rotating the probe to the front (about 180° when starting from the descending aorta). It is sonographically characterized by a bright line with dorsal reverberating artifacts, which are caused by the intratracheal air (Fig. 2.**2a**). As the scope is moved forward, the line will end at the carina of the trachea. The infracarinal area is the region of the posterior level 7 lymph nodes according to the ATS map, which can hardly be entered with mediastinoscopy. For visualization of the right main bronchus, the instrument has to be rotated clockwise (Fig. 2.**2b**). For the left main bronchus the imaging procedure is reversed.

Tip: If one scans *to the front* (e. g., trachea/bronchi), the scope has to be rotated *equivocally* (e. g., to the right) to display a structure lateral to the starting point (e. g., on the right side). If the probe is directed *dorsally*—e. g., toward the aorta—the instrument has to be rotated *unequivocally* to visualize structures on one or the other side of the aorta.

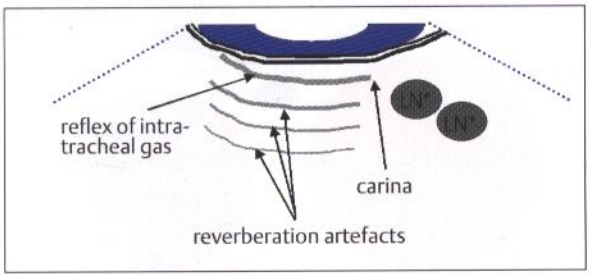
As the instrument is pushed forward, the left atrium of the heart is seen as a dominant cardiac structure close to the esophagus (Fig. 2.**3a**). Modifying the direction of the scanner in accordance with the individual situation is helpful for inspecting more distant parts of the heart (aortic and mitral valve, left ventricle) and the associated large vessels (ascending thoracic aorta, pulmonary trunk, pulmonary veins) (Fig. 2.**3a–c**).



a

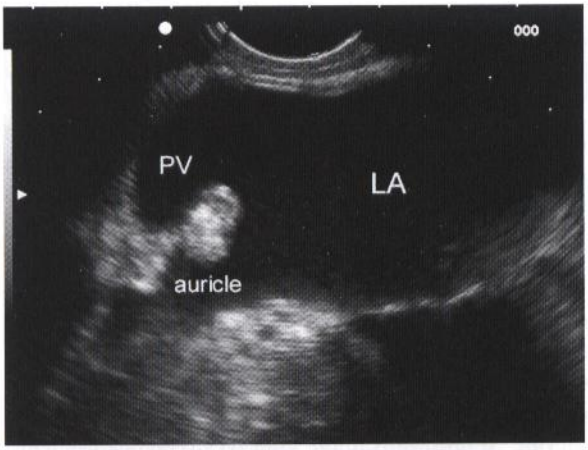


b

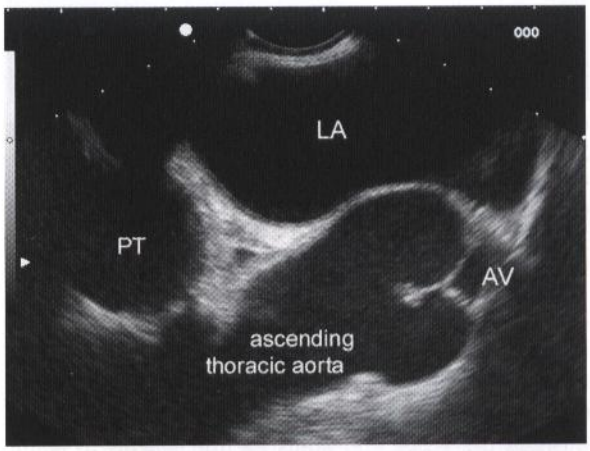


c

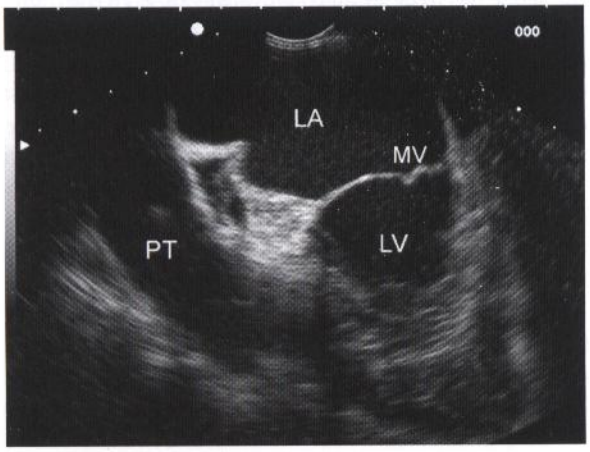
Fig. 2.2a Gas filling in the trachea produces a bright line with dorsal reverberation artifacts. **b** Clockwise rotation and some angulation of the probe are necessary for visualization of the right main bronchus. **c** Scheme of the trachea and infracarinal lymph-node area. LN: posterior level 7 lymph node (American Thoracic Society map).



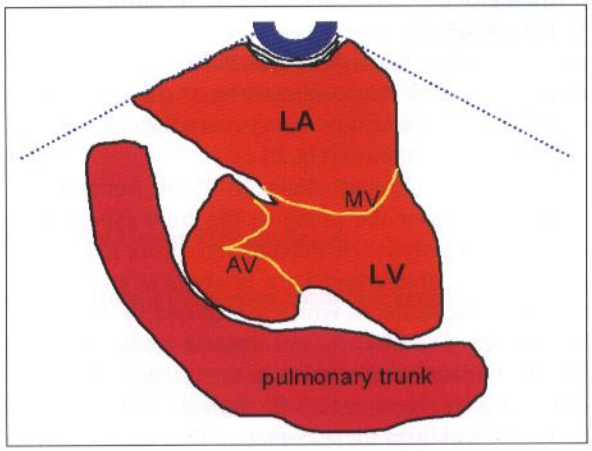
a



b



c



d

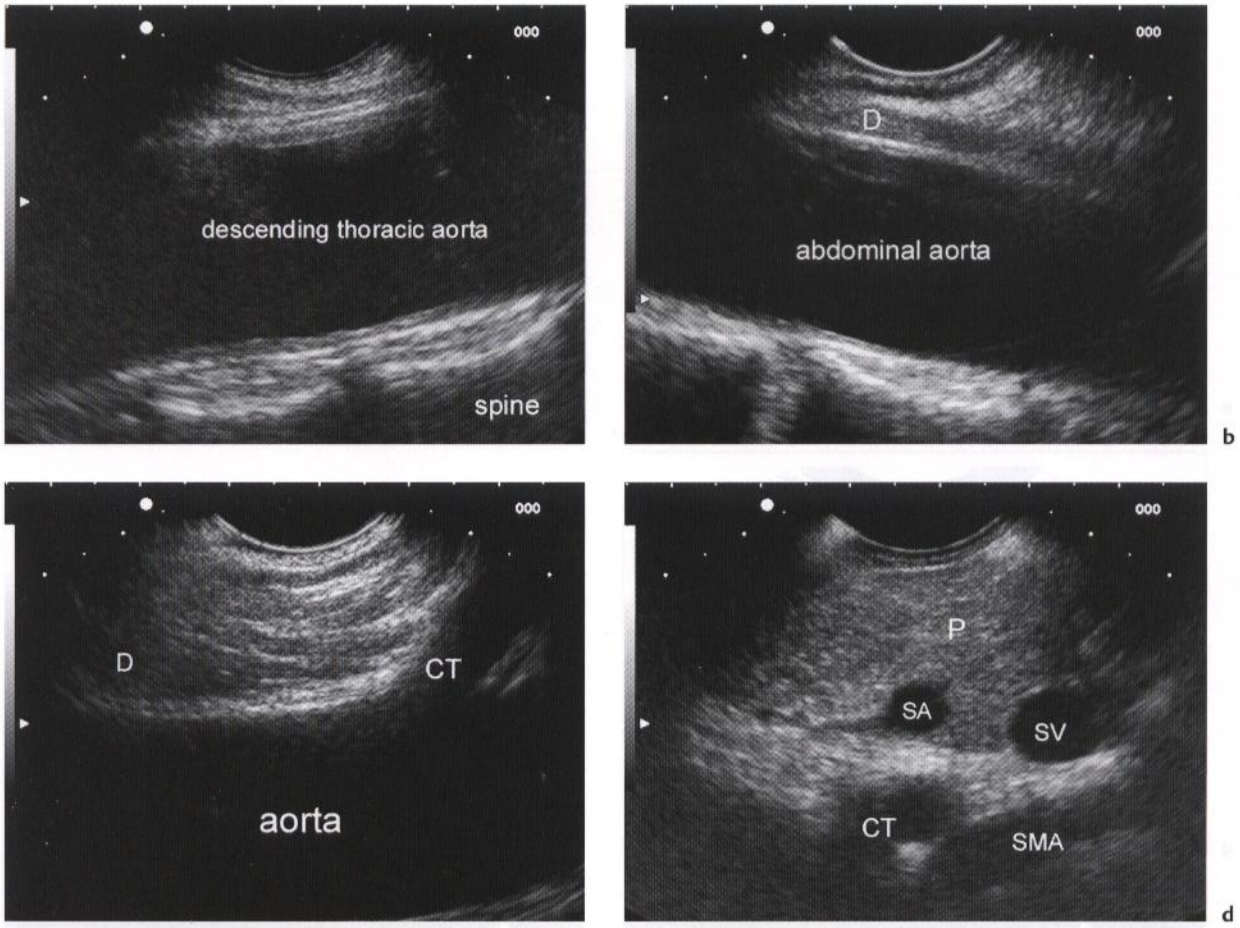


Fig. 2.**4a** The echoendoscope is pushed forward along the descending thoracic aorta into the abdomen. **b** The entrance is marked by the hypoechoic left crus of the diaphragm (D). **c, d** This is followed by the cranial aortic branches, the celiac trunk (CT), and the superior mesenteric artery (SMA in **d**). P: pancreatic body; SA: splenic artery, SV: splenic vein.

Fig. 2.**4e–g** ▷

EUS Anatomy Imaged from the Stomach

As the descending thoracic aorta is followed (Fig. 2.**4a**), the left crus of the diaphragm is seen as a hypoechoic structure ventral to the aorta (Fig. 2.**4b**). This marks the transition into the abdomen. As the stomach is entered, it is important to deflect the probe to maintain close contact with the dorsal gastric wall. In this way, the descending aorta can be followed continuously from the thorax into the abdomen. Intra-abdominally, the cranial abdominal aortic branches, celiac trunk, and superior mesenteric artery (SMA) can usually be seen (Fig. 2.**4c**, **d**).

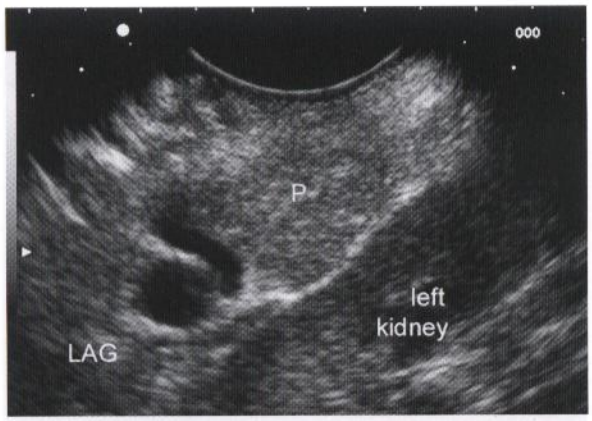
◁ Fig. 2.**3a–d** EUS anatomy of the heart. The left atrium (LA) is the dominant structure close to the esophagus. Small movements of the probe make it possible to visualize the mitral valve (MV), left ventricle (LV), aortic valve (AV), ascending thoracic aorta, and pulmonary trunk (PT). **d** Scheme of the most prominent cardiac structures. PV: pulmonary vein.

The SMA is the decisive landmark for finding the pancreatic body, which is always located ventral to the SMA (Fig. 2.**4d**).

The pancreas is scanned longitudinally in a craniocaudal direction. With clockwise rotation and slight retraction of the scope toward the spleen, the pancreatic body and the tail are imaged. In most cases, the left adrenal gland is simultaneously visualized at the left side of the aorta (Figs. 2.**4e**, 2.**5a**). The adrenal crura can be elaborated by slight movements of the scope tip (Fig. 2.**5b**). Advancing the probe caudally will reveal the left kidney (Fig. 2.**4e**].

After one has returned to the SMA and continued the counterclockwise rotation, the right part of the pancreatic body and the cranial parts of the pancreatic head, including the portal venous confluence and the common bile duct outside the pancreas, are examined (Fig. 2.**6**).

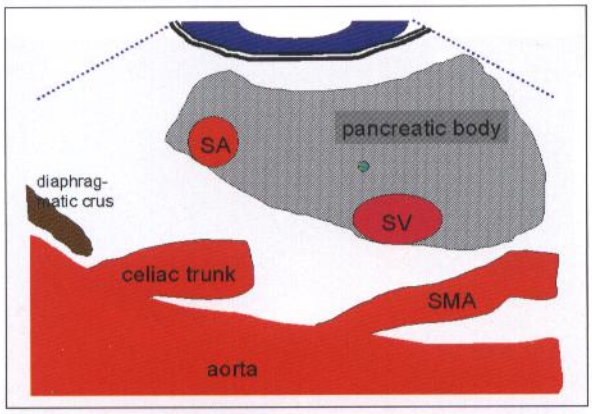
This procedure ensures a fast and complete examination of the pancreas, except for the caudal parts of the pancreatic head. It is important to carry out the rotations



e

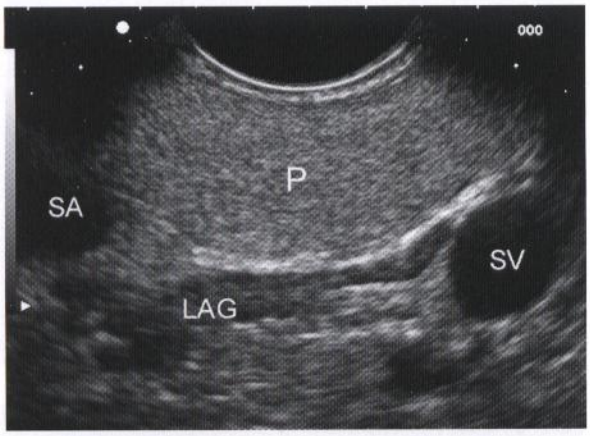


f

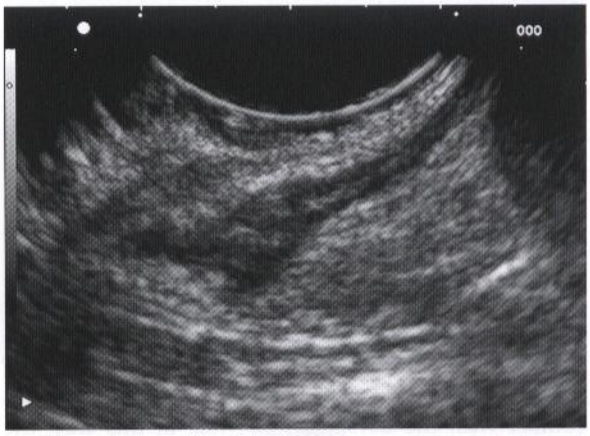


g

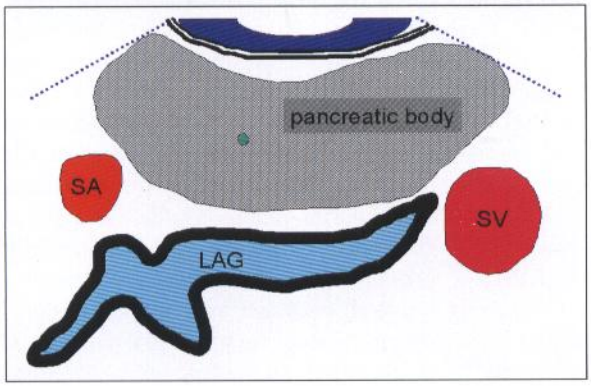
Fig. 2.**4e** Clockwise rotation and slight retraction of the probe allow visualization of the pancreatic body (P), left adrenal gland (LAG) and left kidney, and finally the splenic hilum (**f**). **g** Scheme of the anatomic structures that can usually be located from the abdominal aorta. SA: splenic artery; SV: splenic vein; SMA: superior mesenteric artery.



a

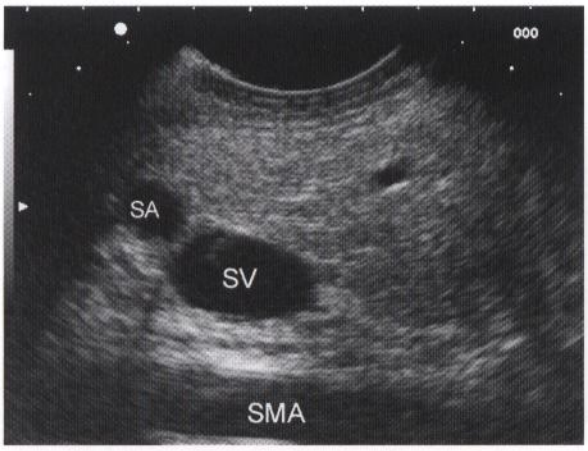


b

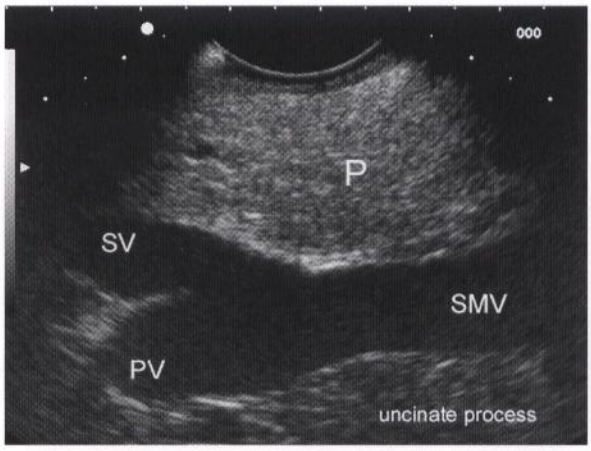


c

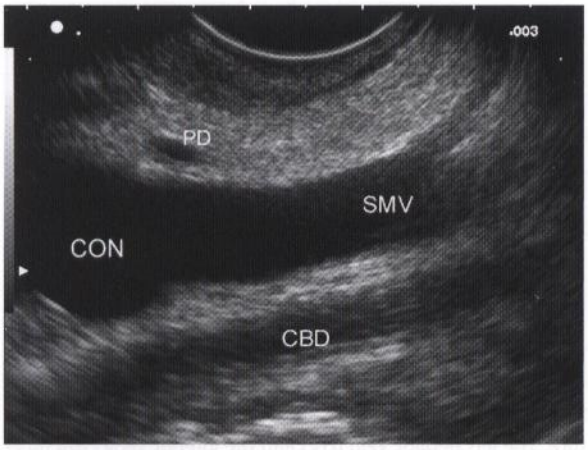
Fig. 2.**5a** The left adrenal gland (LAG) is located at the left side of the aorta and is imaged by slight clockwise rotation of the instrument, starting at the aorta along the pancreatic body (P). SA: splenic artery; SV: splenic vein. **b** The substructure of the adrenal gland—i. e., the hypoechoic cortex and the hyperechoic medulla—can be differentiated well. **c** Outline of the anatomic relationship between the pancreatic body and the left adrenal gland. LAG: left adrenal gland; SA: splenic artery; SV: splenic vein.



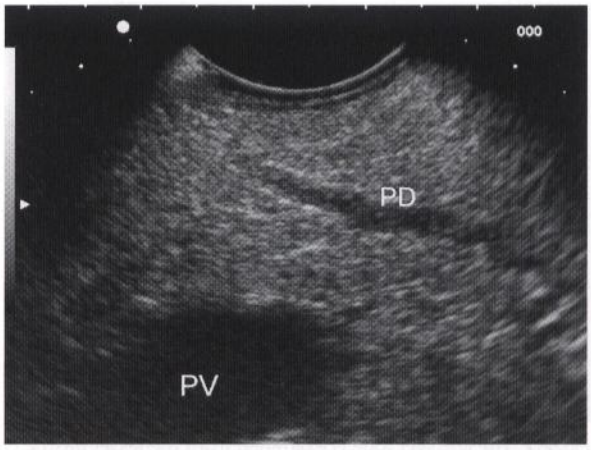
a



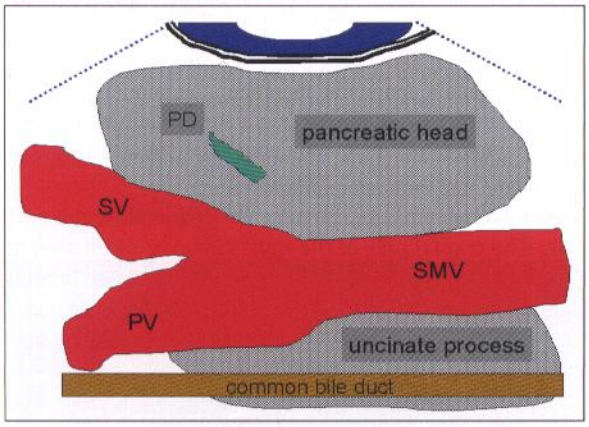
b



c



d



e

Fig. 2.**6a–c** Starting at the longitudinal image of the superior mesenteric artery (SMA), counterclockwise rotation of the probe results in imaging of the portal venous confluence (CON in **c**) and the cranial pancreatic head (P in **b**). Dorsally, the common bile duct (CBD) is seen. PD: pancreatic duct; PV: portal vein; SA: splenic artery; SMV: superior mesenteric vein; SV: splenic vein. **d** Angulation of the probe allows visualization of the pancreatic duct (PD), which crosses the confluence ventrally. PV: portal vein. **e** A schematic summary of the details within and around the pancreatic head, displayed from the stomach. PD: pancreatic duct; PV: portal vein; SV: splenic vein; SMV: superior mesenteric vein.

slowly and to ensure that the complete craniocaudal extent of the organ is imaged. There is no need to produce the classic cross-sectional images of the pancreas familiar from transcutaneous ultrasonography and radial EUS.

It is always possible to scan through the left liver lobe from the oral lesser curvature of the stomach (Fig. 2.**7**). When the probe is rotated and angulated as appropriate, the left hepatic vein running into the IVC (Fig. 2.**7a**), the left hepatic duct (Fig. 2.**7b**), and the left branch of the portal vein including the hepatoumbilical ligament (Fig. 2.**7c**) can be visualized.

EUS Anatomy Imaged from the Duodenum

For exploration of the entire pancreatic head, the papilla of Vater, and the distal common bile duct, it is necessary for the scope to pass into the descending duodenum under endoscopic guidance (Figs. 2.**8**, 2.**9**). The instrument is straightened in the way familiar from ERCP. We

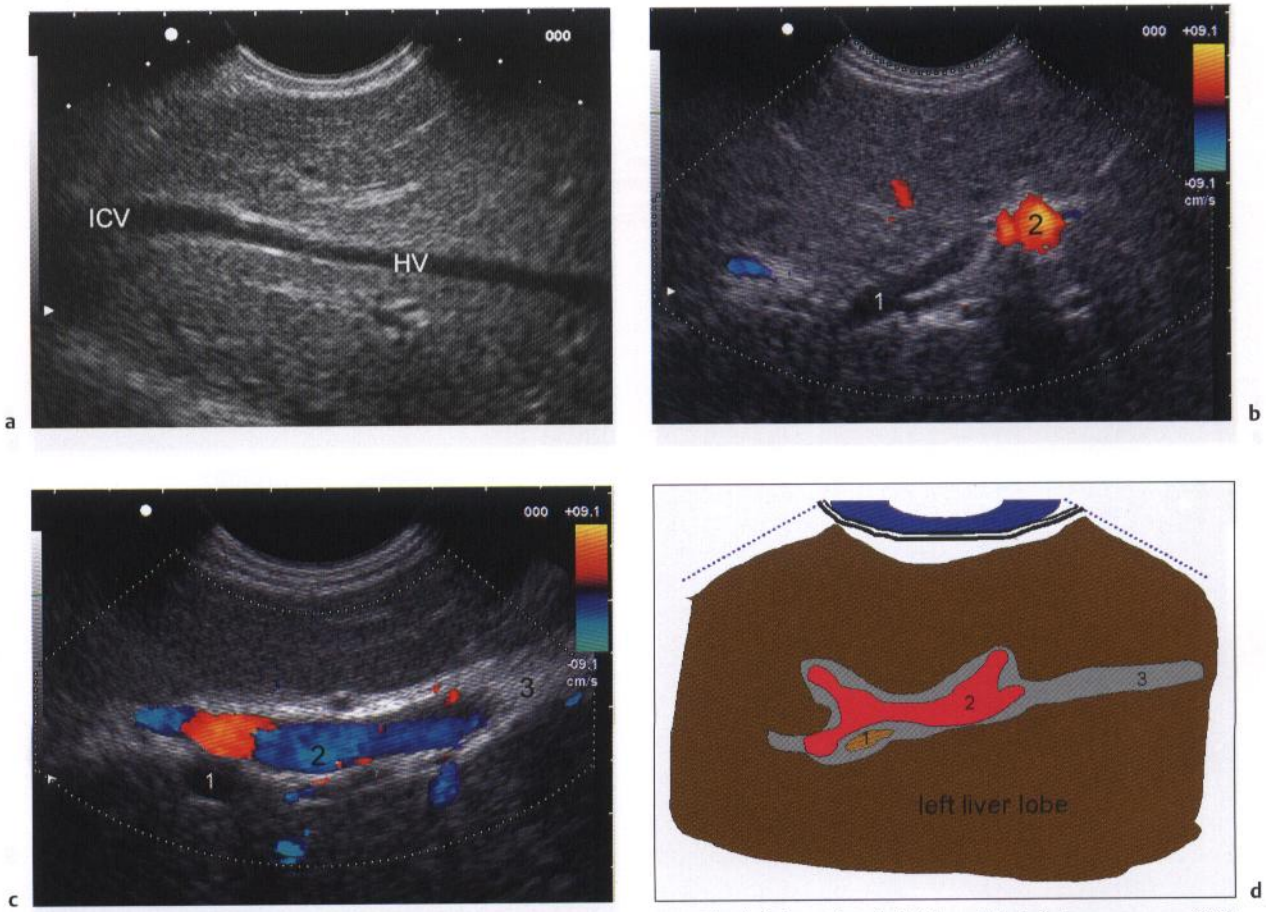


Fig. 2.7 The left liver lobe is examined from the lesser gastric curvature. The left hepatic vein (HV) and the inferior vena cava (ICV) (**a**), the left hepatic duct (1), the left branch of the portal vein (2), and the hepatoumbilical ligament (3) can be inspected (**b–d**).

prefer to place the patient in the prone position if the focus of the examination is on the periampullary region or the distal common bile duct. The probe is adherent to the duodenal wall at the minor side. If the insertion depth of the instrument is correct, the caudal pancreatic head and the uncinate process can be seen. The scope is slowly retracted step by step. At each step, rotation of the instrument is necessary to scan through the entire pancreatic head, thus compensating for the absence of a radial view with the linear probe. The superior mesenteric vessels can be imaged behind the pancreatic head in a precise horizontal section. The vein is seen closer to the probe and the artery more distant (Fig. 2.**8b**).

The papilla of Vater is identified as a small hypoechoic structure (Fig. 2.**8c**), which can often be differentiated from pancreatic tissue during the procedure described above, except in very hypoechoic (young) organs. If it is difficult to find the papilla, it is advisable to couple to it under endoscopic guidance.

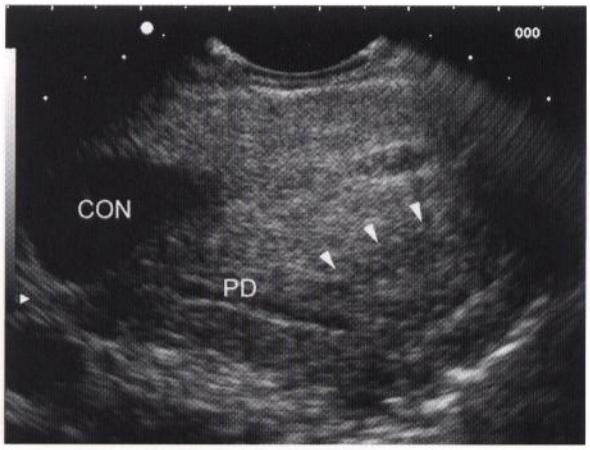
The common bile duct and the pancreatic duct each run into the papilla of Vater. The two ducts can be followed by thorough retraction of the scope, with the wheels being adjusted and the instrument rotated under guidance from the ultrasound image (Fig. 2.**9**). It may be difficult to detect small ducts within a hypoechoic pancreas. EUS imaging conditions improve whenever the ducts are dilated.

The IVC is found by turning the echoendoscope dorsally. The cranial pole of the right kidney is often seen in this position as well. The right adrenal is located behind the IVC and can be imaged by pulling the scope back and following the IVC cranially toward the superior duodenal flexure (Fig. 2.**10**).

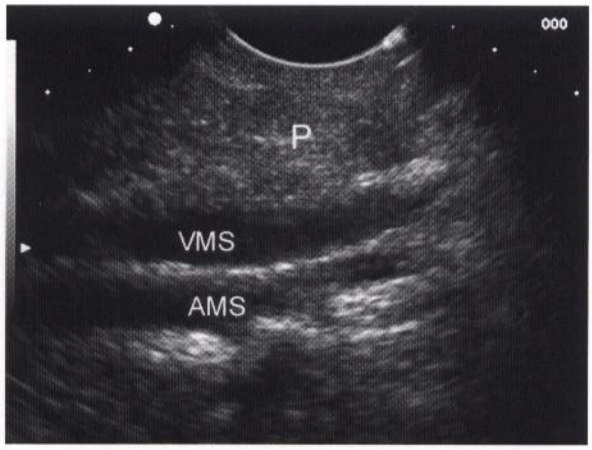
As one moves back into the duodenal bulb, the probe can be directed cranially to allow inspection of the structures of the liver hilum. Color Doppler imaging facilitates correct identification of the vessels (Fig 2.**11a**). Further retraction of the instrument is needed to visualize the gallbladder (Fig. 2.**11b**).

■ Examination of the Gastrointestinal Wall

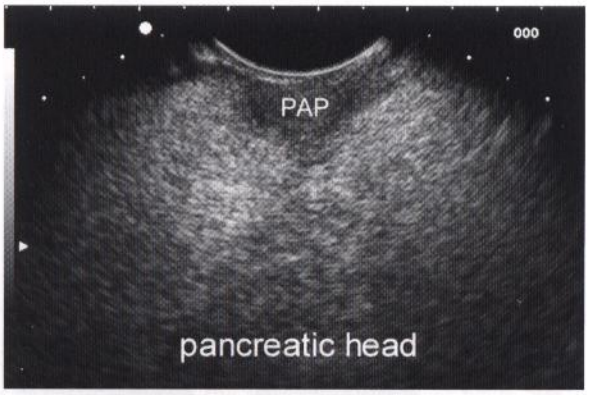
Lesions in the gastrointestinal wall are examined endosonographically as a specially targeted issue after endoscopy. It is therefore hardly ever necessary to scan the



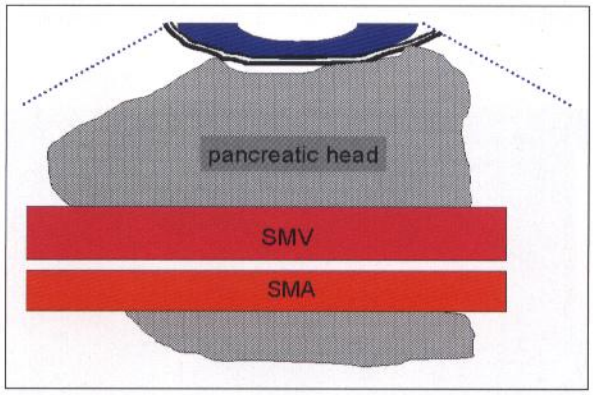
a



b

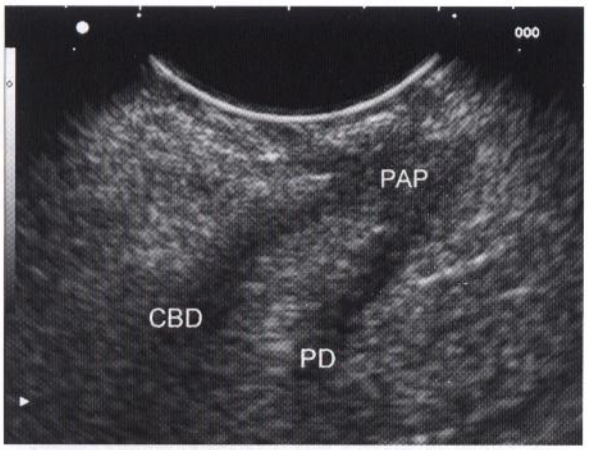


c

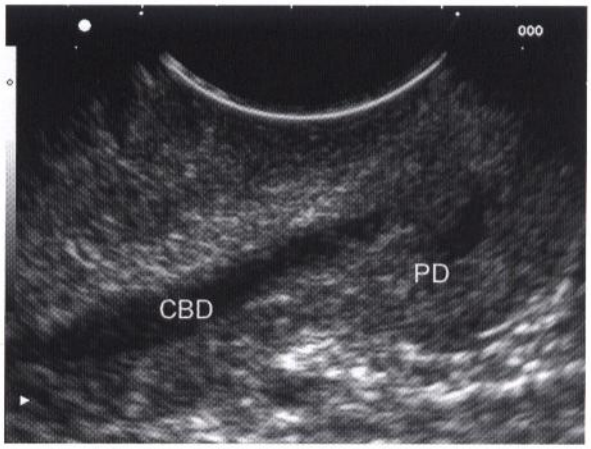


d

Fig. 2.**8** The pancreatic head imaged in the endoscopic retrograde cholangiopancreatography (ERCP) position after straightening of the instrument. **a** The ventral pancreas (arrowheads) is hypoechoic, contrasting with the more hyperechoic dorsal pancreas. CON: portal venous confluence; PD: pancreatic duct. **b** With precise horizontal scanning, the superior mesenteric vessels are visualized behind the pancreatic head. AMS: superior mesenteric artery: P: pancreatic head; VMS: superior mesenteric vein. **c** The papilla of Vater (PAP) is a small hypoechoic structure, which can usually be differentiated from the pancreatic tissue. **d** Scheme of the pancreatic head and superior mesenteric vessels, imaged from the descending duodenum. SMV: superior mesenteric vein; SMA: superior mesenteric artery.



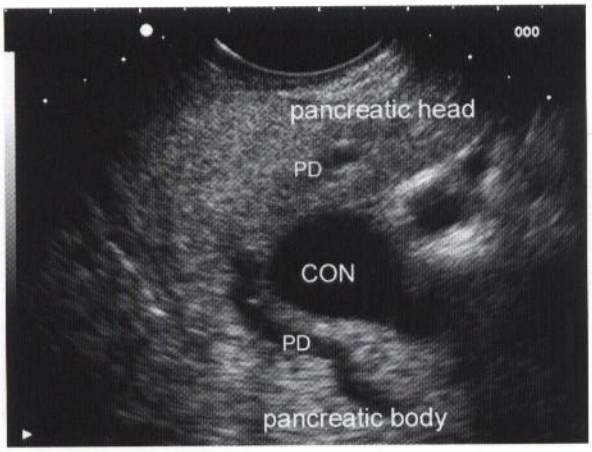
a



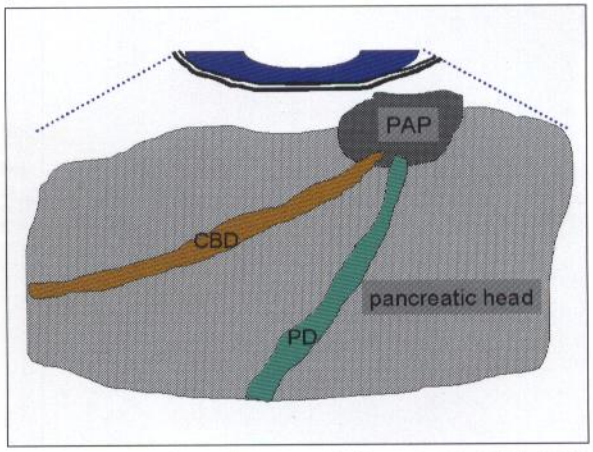
b

Fig. 2.**9a** The common bile duct (CBD) and pancreatic duct (PD) are imaged by small movements after visualization of the papilla of Vater (PAP). **b** The two ducts can be followed separately by retracting the echoendoscope and adjusting the orientation of the tip. CBD: common bile duct; PD: pancreatic duct.

Fig. 2.**9c, d** ▷

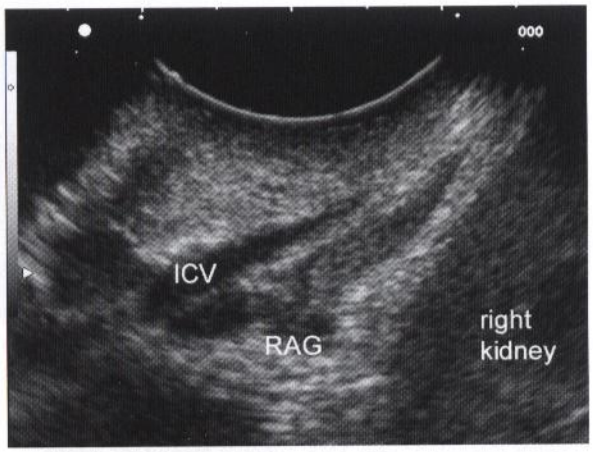


c

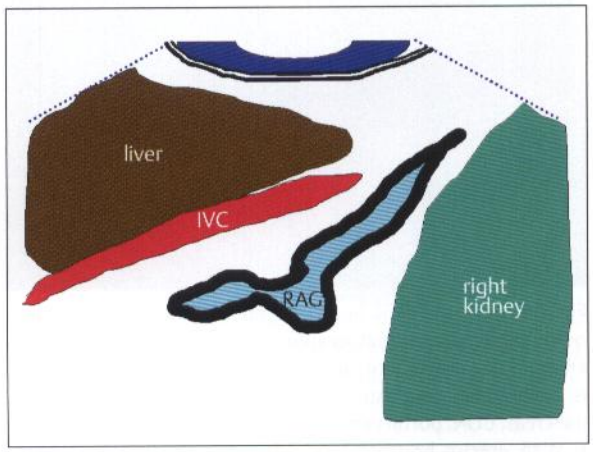


d

Fig. 2.**9c** The image of the pancreatic duct here is complementary to the image from the stomach shown in Fig. 2.**6d**. CON: confluence; PD: pancreatic duct. **d** The typical periampullary anatomy. CBD: ; PAP: papilla of Vater; PD: pancreatic duct.



a



b

Fig. 2.**10a** The right adrenal gland (RAG) is best found by retracting the probe along the inferior vena cava (IVC). **b** The position of the right adrenal gland at the top of the right kidney and behind the inferior caval vein. IVC: inferior vena cava; RAG: right adrenal gland.

complete wall of the upper gastrointestinal tract in a screening fashion.

Large lesions are found with EUS alone, whereas small ones can be identified under endoscopic guidance more quickly. To investigate the mural layers without compression, it is advisable to fill the lumen with water. Nevertheless, an experienced endosonographer is able to adapt the linear probe to the wall with as little pressure as necessary, thus imaging five or even seven layers of the normal or infiltrated gastrointestinal wall (Fig. 2.**12**). As the near scanning field of the modern probes has improved significantly, water filling of a mounted balloon is not necessary.

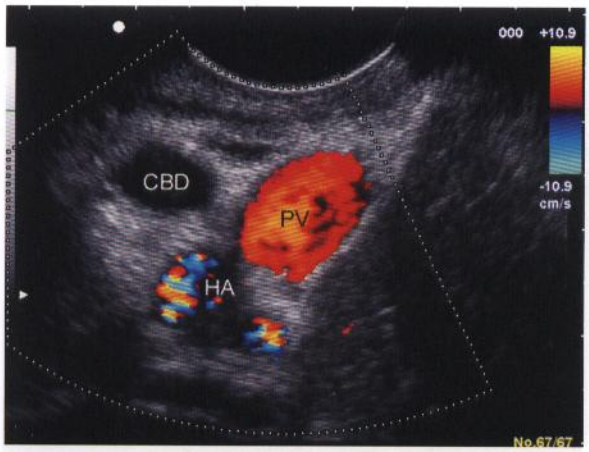
It is important to scan the gastrointestinal wall vertically in order to image the true thickness of the wall. Oblique scanning leads to overestimation of the thickness and may suggest an infiltrating process.

Conclusion

In our experience, the approach to linear EUS anatomy described here helps beginners find their way through the anatomic forest of EUS. Concentrating on the ultrasound image instead of the endoscopic image makes it easier to adapt the course of the examination to the individual anatomy and pathological findings. Sooner or later, each examiner is able to find his or her own way of performing EUS, modifying and unifying the examination strategies suggested by different experts.

References

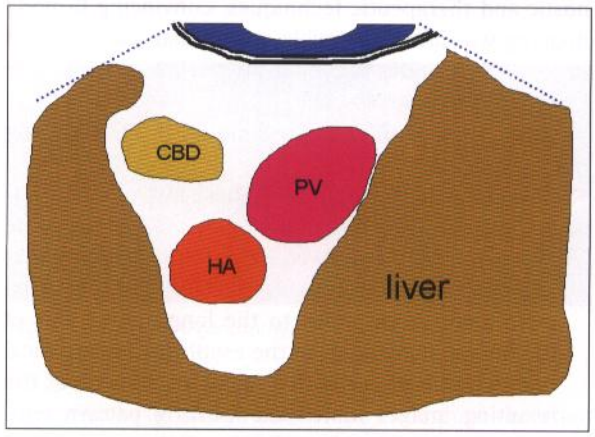
1. Janssen J, Greiner L. Examination technique and general principles. In: Rösch T, Will U, Chang KJ, editors. Longitudinal endosonography: atlas and manual for use in the upper gastrointestinal tract. Berlin: Springer, 2001:11–9.



a

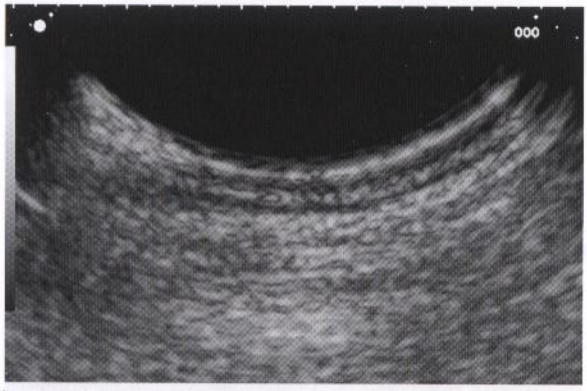


b

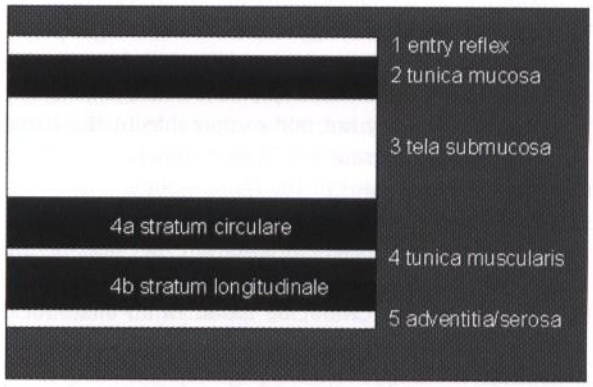


c

Fig. 2.**11a** Turning the probe cranially allows inspection of the vessels of the liver hilum. Color Doppler helps identify the vessels. CBD: common bile duct; HA: hepatic artery; PV: portal vein. **b** After retraction, the gallbladder (GB) is seen. **c** Schematic illustration of the anatomy of the liver hilum. **CBD: common bile duct; HA: hepatic artery; PV: portal vein.**



a



b

Fig. 2.**12a** Imaging of the gastric wall layers with conventional linear EUS (10 MHz) without water filling or a balloon. **b** The endosonographic wall layers correlate with the histological ones.

2. Burmester E, Leineweber T, Hacker, Tiede U, Hütteroth TH, Höhne KH. EUS meets VOXEL-MAN: three-dimensional anatomic animation of linear-array endoscopic ultrasound images. Endoscopy 2004;36:726–30.
3. Bhutani MS, Hoffmann BJ, Hawes RH. A swine model for teaching endoscopic ultrasound (EUS) imaging and intervention under EUS guidance. Endoscopy 1998;30:605–9.
4. Sorbi D, Vazquez-Sequeiros E, Wiersema MJ. A simple phantom for learning EUS-guided FNA. Gastrointest Endosc 2003;57:580–3.

3 EUS meets VOXEL-MAN: a Computer-Based Training System for Longitudinal EUS

T. Leineweber, E. Burmester

Introduction

The indications for endoscopic ultrasound (EUS) have changed fundamentally in recent years. Starting with the interpretation of B-mode images, the range of indications has expanded to include more invasive diagnostic and therapeutic techniques. Convincing B-mode imaging was always possible with radial scanners, but invasive techniques can only be carried out with the longitudinal echoendoscope.

There are two different techniques in EUS imaging (Fig. 3.**1**):

- *Radial scanning* (radial EUS). These instruments generate a 270°/360° radial picture at a 90° angle to the axis of the endoscope (Fig. 3.**1**, right side). This results in a cross-sectional imaging modality as long as the instrument corresponds to the longitudinal axis of the human body—e. g., in the esophagus. Anatomical orientation is easier with a radial instrument, as the resulting images match the viewing pattern with other cross-sectional modalities such as computed tomography (Fig. 3.**2**).
- *Longitudinal scanning* (longitudinal EUS). These instruments generate longitudinal sector images parallel to the axis of the endoscope (Fig. 3.**1**). Interpreting the anatomical sections depicted is a challenge, as the resulting pictures are not comparable to the usual computed tomography (CT) or magnetic resonance imaging (MRI) scans of the human body. The examiner therefore needs to have excellent skills in order to achieve the correct orientation. Because of the flexible tip of the endoscope, multiple sections are available, which cannot be found in an anatomical atlas. For these reasons, longitudinal EUS is the most difficult technique to learn (Fig. 3.**3**).

For a considerable period, the main indication for endoscopic ultrasound was imaging of the wall of the gastrointestinal tract. High-frequency scanners allowed high-resolution imaging of the wall layers, with improved staging of tumors of the wall. The new longitudinal echoendoscopes provide a new spectrum of diagnostic invasive indications (such as EUS-guided fine-needle

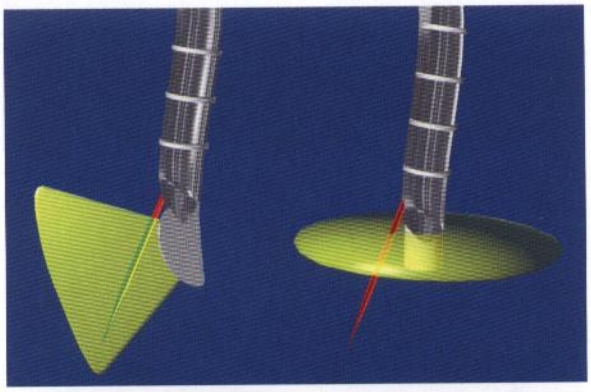


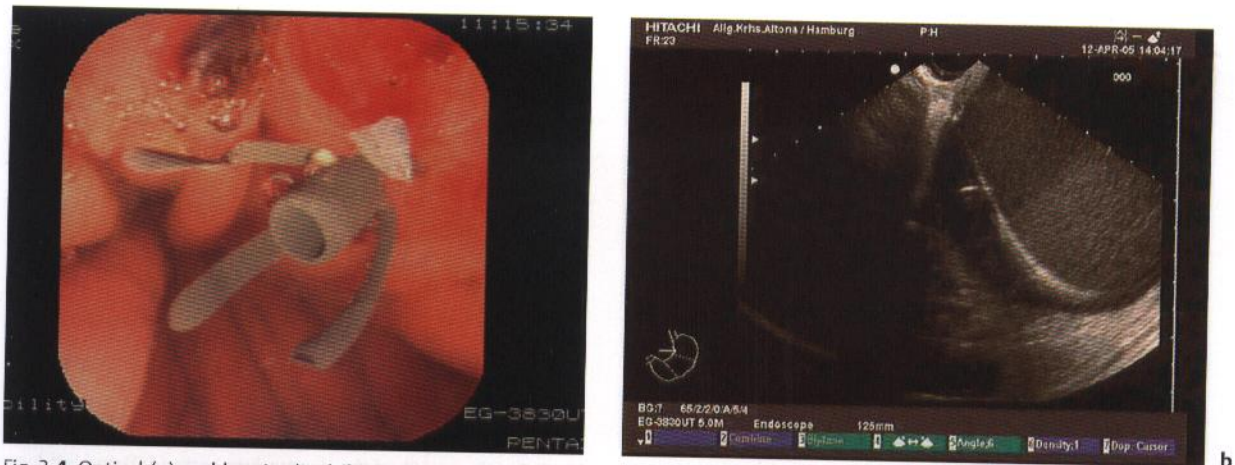
Fig. 3.**1** The two types of endoscopic ultrasound (EUS). *Left:* longitudinal EUS; *right:* radial EUS.



Fig. 3.**2** Radial EUS image of the body of the pancreas.



Fig. 3.**3** Longitudinal EUS image of the head of the pancreas, with a migrated gallstone in the dilated pancreatic duct.



a b

Fig. 3.4 Optical (**a**) and longitudinal (**b**) EUS images of pancreatic pseudocyst drainage.

aspiration, EUS-FNA) and therapeutic invasive indications such as EUS-guided drainage of pancreatic pseudocysts (Fig. 3.**4**).

Controlling each step with endoscopic ultrasound is the crucial item in these invasive procedures. For this reason, longitudinal echoendoscopes provide needle control. The scanner head has the same orientation as the axis of the endoscope, and the needle moves within the ultrasound field (Fig. 3.**1**).

Excellent anatomical knowledge is important in order to minimize the risk of injuring sensitive structures during invasive procedures and to enable one to recognize the relationship between vessels and organs.

The *EUS meets VOXEL-MAN* digital versatile disk (DVD) was created in order to simulate the movements of an endosonographic transducer in the human body, so as to make it easier to learn longitudinal EUS and minimize the risk for patients.

■ EUS meets VOXEL-MAN

EUS meets VOXEL-MAN is a personal computer–based training system that consists of three main parts [1–6]:

- Anatomical simulation of longitudinal EUS
- Atlas of longitudinal "VOXEL-MAN" anatomy and ultrasound anatomy
- Video sequences of real-time examinations with integrated "VOXEL-MAN" simulation

The anatomical simulation shows the cross-sectional anatomy using the VOXEL-MAN model [1,2]. This three-dimensional anatomical model is based on the U.S. National Library of Medicine's Visual Human Project data.

At six reference positions in the esophagus, stomach, and duodenum, anatomical scenes were calculated using a QuickTime video-recording format. Using the computer mouse within the scenes, the user can simulate two basic movements of the endoscope—rotation and angulation. Thus, the scanner head can be rotated for 360° on the endoscope's axis and 20° in the longitudinal axis. Using these six reference positions, all of the crucial anatomical landmarks in longitudinal endoscopic ultrasonography can be depicted. Most of these landmarks are vessels the user has to identify exactly, as the scanner is not visible during the examination.



Fig. 3.5 VOXEL-MAN anatomy.

The integrated knowledge base shows all the anatomical structures in the model and allows the user to look for anatomical structures in the region of interest in three languages (German, English, and Latin).

Each anatomical image (Fig. 3.**5**) shows:

- A three-dimensional overview, with the position of the scanner head in the human body and its relationship to the most important anatomical landmarks (left side).
- The corresponding anatomical cross-section, with a mask overlay depicting only the representation of real endoscopic ultrasound (right side).

The atlas shows striking parallelism between the VOXEL-MAN anatomy and real endoscopic ultrasound images (Fig. 3.**6**). The video sequences demonstrate real-time longitudinal anatomy and the steps in an examination, in order to "translate" the VOXEL-MAN anatomy into the real-time examination. *EUS meets VOXEL-MAN* thus represents an interactive longitudinal simulation of



Fig. 3.**6** Parallelism between VOXEL-MAN and ultrasound anatomy: the pancreaticoduodenal artery (PDA) and pancreatic head (P).

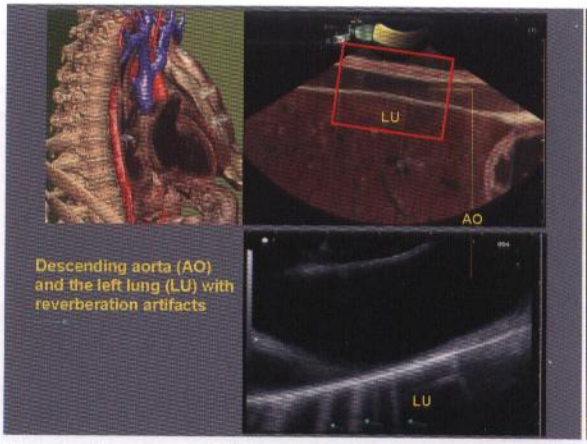


Fig. 3.**7** Atlas image of the descending aorta (AO) and left lung (LU), with reverberation artifacts (arrows)

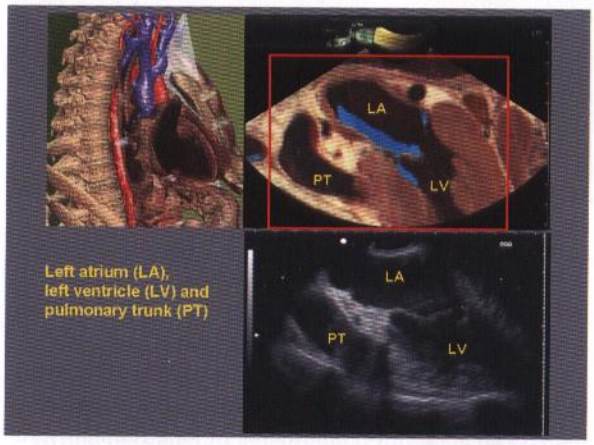


Fig. 3.**8** Atlas image of the left atrium (LA) of the heart, left ventricle (LV), and pulmonary trunk (PT).

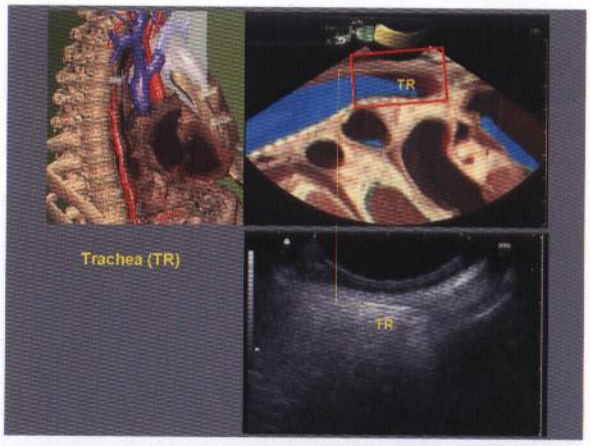


Fig. 3.**9** Atlas image of the trachea (TR).

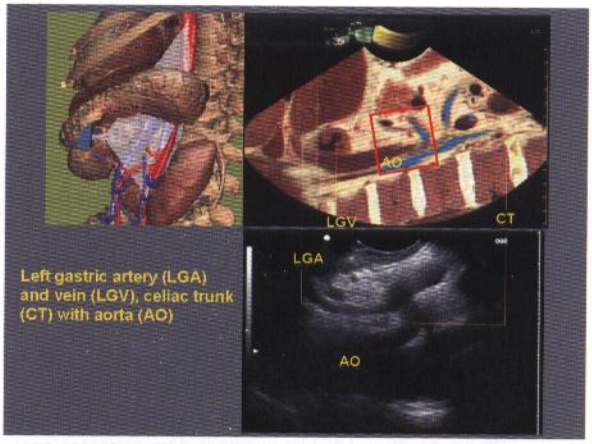


Fig. 3.**10** Atlas image of the left gastric artery (LGA) and vein (LGV), with the celiac trunk (CT) and aorta (AO).

endoscopic ultrasound using a detailed computer-based three-dimensional anatomical model [3–6].

Systematic Approach to an EUS Examination

Familiarity with the reference positions and the anatomical landmarks corresponding to them is crucial for an EUS examination. During the examination, reference positions must not be followed systematically (in a craniocaudal or caudocranial direction).

These are the reference positions and their corresponding anatomical landmarks:

- Reference position 1: upper esophagus, descending aorta (Fig. 3.**7**), aortic arch, azygos vein.
- Reference position 2: middle esophagus, heart (Fig. 3.**8**), right pulmonary artery, trachea (Fig. 3.**9**), bronchus, and aortopulmonary window.
- Reference position 3: gastric fundus, abdominal aorta (part IV) with exiting celiac trunk (Fig. 3.**10**), splenic

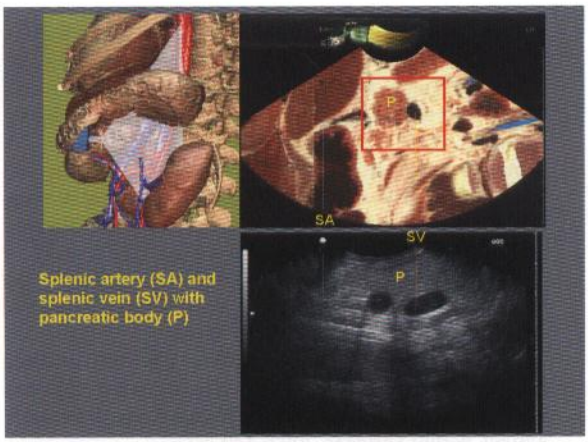


Fig. 3.**11** Atlas image of the splenic artery (SA) and vein (SV), with the pancreatic body (P).

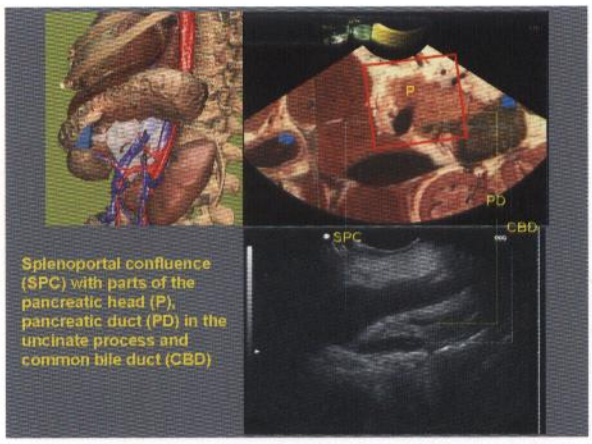


Fig. 3.**12** Atlas image of the splenoportal confluence (SPC), with parts of the pancreatic head (P), the pancreatic duct (PD) in the uncinate process, and common bile duct (CBD).

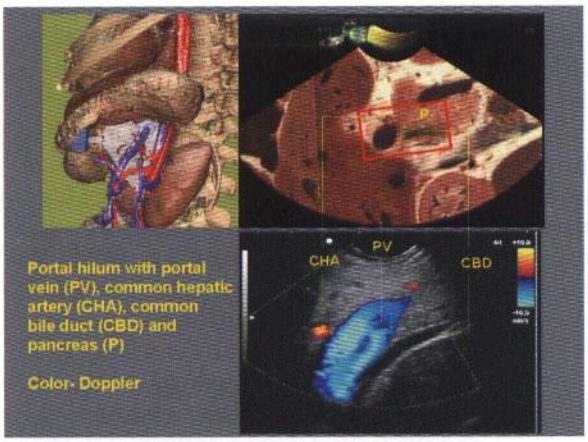


Fig. 3.**13** Atlas image of the portal hilum with the portal vein (PV), common hepatic artery (CHA), common bile duct (CBD), and pancreas (P). The vessels are shown with color Doppler imaging.

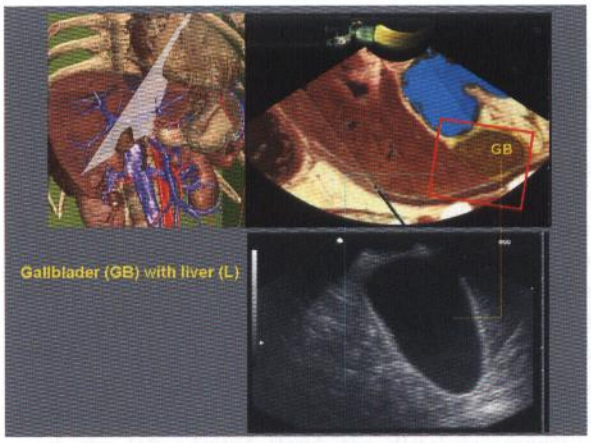


Fig. 3.**14** Atlas image of the gallbladder (GB) with the liver.

artery and splenic vein with pancreatic body and tail (Fig. 3.**11**), splenoportal confluence (Fig. 3.**12**), left lobe of the liver.

- Reference position 4: duodenal bulb, portal hilum (Fig. 3.**13**), gallbladder (Fig. 3.**14**), common bile duct.
- Reference position 5: papilla region, mesenteric vessels, head of the pancreas with pancreatic duct (Fig. 3.**15**), common bile duct, cystic duct.
- Reference position 6: deep parts of the duodenum, abdominal aorta (part V), and inferior vena cava (Fig. 3.**16**).

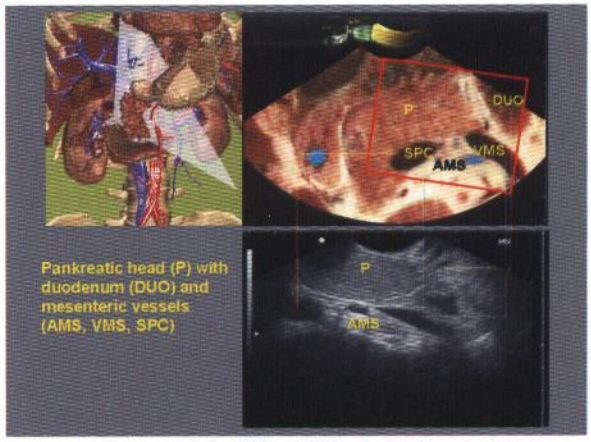


Fig. 3.**15** Atlas image of the pancreatic head (P) with the duodenum (DUO) and mesenteric vessels. AMS: superior mesenteric artery; VMS: superior mesenteric vein; SPC: splenoportal confluence.

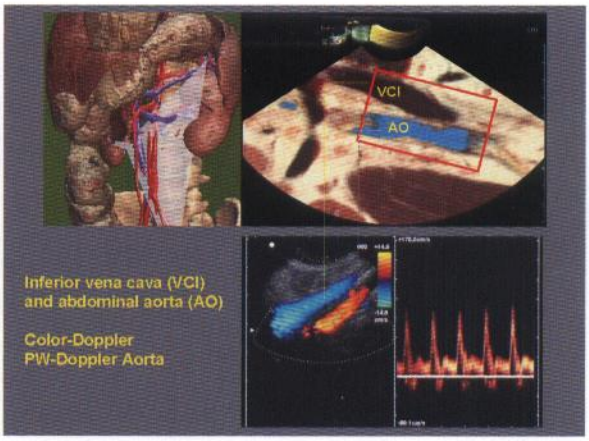


Fig. 3.**16** Atlas image of the inferior vena cava (VCI) and abdominal aorta (AO), with color Doppler and pulsed-wave Doppler imaging of the aorta.

References

1. Höhne KH, Pflesser B, Pommert A, Priesmeyer K, Riemer M, Schiemann T, et al. VOXEL-MAN 3D navigator: inner organs. Regional, systemic and radiological anatomy. Heidelberg: Springer, 2000 (3 CD-ROMs, ISBN 3-540-14759-4).
2. Pommert A, Höhne KH, Pflesser B, Richter E, Riemer M, Schiemann T, et al. Creating a high-resolution spatial/symbolic model of the inner organs based on the Visible Human. Med Image Anal 2001;5:221–8.
3. Hacker S, Tiede U, Burmester E, Leineweber T, Höhne KH. Ein virtuelles Trainingssystem für endoskopische Longitudinal-Ultraschalluntersuchungen. In: Meiler M, Saupe D, Kruggel F, editors. Bildverarbeitung für die Medizin 2002. Algorithmen – Systeme – Anwendungen. Proceedings des Workshop vom 10.–12. März 2002 in Leipzig. Informatik Aktuell. Berlin: Springer, 2002: 149–52.
4. Hacker S, Tiede U, Burmester E, Leineweber T, Höhne KH. A virtual training system for linear-type endoscopic ultrasonography. In: Lemke HU, Vannier MW, Inamura K, Farman AG, Doi K, Reiber JHC, editors. CARS 2002: computer-assisted radiology and surgery. Proceedings of the 16th International Congress and Exhibition, Paris, June 26–29, 2002. Heidelberg: Springer, 2002: 1–5.
5. Burmester E, Hollerbach S. [Report on the "Endoscopic Ultrasound" working session of the German Society for Digestive and Metabolic Diseases in Bonn, 11.9.2002; in German.] Z Gastroenterol 2003;41:362–7.
6. Burmester E, Leineweber T, Hacker S, Tiede U, Hütteroth TH, Höhne KH. EUS meets Voxel-Man: three-dimensional anatomic animation of linear-array endoscopic ultrasound images. Endoscopy 2004;36:726–30.

4 Miniprobes

H. Seifert, C.F. Dietrich

Introduction

During the last 10 years, endoscopic ultrasound (EUS) has gained wide acceptance as the method of choice for the local staging of gastrointestinal tumors. It allows visualization of the intestinal wall and of surrounding structures with a resolution unequaled by other imaging modalities. However, EUS continued for a long time to be a specialty requiring expensive equipment, echoendoscopes dedicated to the technique, and special training of examiners. With the advent of flexible high-frequency miniprobes that can be introduced through the working channel of any endoscope, EUS became available as an additional and very powerful diagnostic tool during routine endoscopic procedures. While conventional transabdominal ultrasonography (TUS) using the most sophisticated techniques provides excellent images of almost every anatomical region in the abdomen, miniprobes can be directed to very small structures of interest that can only be targeted under direct endoscopic guidance. It is thought that structures missed on TUS can be identified with miniprobes and vice versa, making the two methods ideal and complementary partners in modern gastrointestinal imaging.

After a discussion of a few technical considerations and practical remarks, useful applications of EUS miniprobes (see Table 4.1) and future perspectives for the technique are discussed below, on the basis of the available published evidence and the authors' experience. Examples are given in various other chapters.

Technical Considerations and Practical Remarks

Miniprobes for routine diagnostic use are usually high-frequency mechanical scanners with a diameter of 1.7–3.4 mm that can be introduced through the working channel of any flexible endoscope. Frequently asked questions regarding the clinical application of miniprobes include the following.

Which frequency should be used? The available miniprobes cover a frequency range of 12–30 MHz, with higher frequencies corresponding to lesser penetration depth. There have been no systematic studies comparing miniprobes of different frequencies for a single application. In the authors' experience, 20-MHz probes are most useful for all applications. With lower frequencies, visualization of the extramural anatomy and staging of advanced tumors may be easier. However, for the extramural anatomy, conventional EUS with radial or longitudinal scanners provides similar frequencies (7.5–12 MHz) and superior image quality, and for advanced tumors, EUS local staging seems of limited relevance. With higher frequencies (30 MHz), fine resolution of the intestinal wall would be excellent, but with the drawback of losing sight of almost any external structure. As long as there is at best very limited evidence correlating ultrasound morphology with histology, 20 MHz appears to provide the ideal compromise between excellent local resolution and visualization of the relevant surrounding anatomy. At this frequency, with a penetration depth of about 2 cm, a considerable part of the abdominal anatomy can be seen. This perigastric and periduodenal (and sometimes also pericolonic) volume of 2 cm comprises the periesophageal area and part of the mediastinal lymph nodes, the aorta, pericardial and pleural fluid, infradiaphragmatic and perigastric lymph nodes, the splenic hilum, celiac trunk, splenic artery and vein, the pancreas and pancreatic duct, the left adrenal gland, the distal common bile duct (CBD), and sometimes liver hilum, part of the gallbladder, and free abdominal fluid. In addition, the intestinal wall with adherent lesions is seen with superior resolution. This is true of both intraluminal and intraductal applications; for lesions in the pancreatic or the bile duct, a periductal cylinder of 1–2 cm correctly represents the region of interest.

Diameter, rigidity and shape: are they important? Theoretically, a minimal diameter would be most desirable. It would allow easy introduction even through narrow working channels and atraumatic cannulation of the papilla of Vater for pancreatic or biliary intraductal ultrasonography (IDUS). Rigidity of the tip should be minimal in order to allow steering with the Albarran lever without breaking the transducer. The tip should be rounded and smooth, as otherwise it could be trapped by mucosal folds, leading to injury to the mucosa and damage to the probe. Alternatively, probes with a guide wire port at their tip are very useful for wire-guided IDUS, but are also restricted to this technique. In the authors' experience, very slim probes (< 2 mm) are easy to handle, but at the cost of inferior image quality. For

Table 4.1 Applications of miniprobes in the gastrointestinal tract

Application	Targets	Examples
Examination of structures within or adjacent to the intestinal wall	• Mucosal neoplasias • Submucosal tumors • Myogenic tumors, GIST • Paraesophageal or paragastric lymph nodes • Vascular formations (varices) • All organs within 2 cm from the intestine	• Cancer staging (EEC, EGC, endoscopic mucosal resection) • Differentiation of unknown structures (e.g., cystic vs. solid) • Focal pancreatic lesions
IDUS	Bile duct and pancreatic duct with surrounding tissue	Small pancreatic and biliary tumors, stones, staging of CCC
EDUS	Distal bile duct and pancreatic duct	Small CBD stones Small periampullary tumors

CBD, common bile duct; CCC, cholangiocarcinoma; EDUS, extraductal ultrasound; EEC, early esophageal cancer; EGC, early gastric cancer; IDUS, intraductal ultrasound; GIST, gastrointestinal stromal tumor.

most universal use, a 2.5-mm probe with a flexible, blunted tip appears at present to be the best compromise.

How is sonographic coupling to the wall accomplished? Is a balloon required? Although balloons are available, sonographic coupling to the intestinal wall is better obtained by direct contact between the probe and the mucosal surface or, for small superficial lesions, by injecting some saline or tap water. The use of large-channel endoscopes that allow instillation as well as aspiration of water while the miniprobe is inserted can therefore be recommended. Using a balloon sheath increases the diameter of the probe from 2.5 or 2.0 mm to 3.6 mm, thereby preventing effective suction even with a large-channel endoscope (3.7 mm). For endobronchial ultrasonography (EBUS), balloons are necessary to obtain adequate coupling [1,2].

What about durability and price? The durability of different miniprobes has improved considerably in recent years. However, they can still easily be damaged by one mistake—trapping them with the duodenoscope's elevator. Most often, they lose functionality due to small breaks in the plastic sheath close to the tip, leading to air bubbles disturbing the image. In some miniprobes, the plastic sheath can be exchanged—a very cost-effective repair. We believe that miniprobes should be available at a reasonable price, as part of the advanced endoscopic armamentarium. If they were capable of replacing conventional EUS for many of its applications, then even now they would represent a cost-effective alternative. The lack of adequately defined reimbursement for EUS in some countries should not lead to the disappearance of a powerful diagnostic tool such as this.

Before physicians embark on miniprobe EUS, it is recommended that they compare the latest developments from different companies with regard to image quality, possible applications, and price. If handled properly, a miniprobe should last for at least 80–100 applications (including IDUS) (Table 4.1).

■ Miniprobe Applications in the Gastrointestinal Tract

Examination of Structures Within and Adjacent to the Intestinal Wall

Miniprobe EUS has been reported to be valuable for the staging of colorectal neoplasms (T staging accuracy 90%), cholangiocellular carcinoma (T staging accuracy 89%, N staging 60%), lymphoma, and esophageal and pancreatic tumors [3–9]. The literature is summarized in Table 4.2 [4,7,10–15].

In stenosing esophageal tumors, EUS staging with miniprobes appears to be recommendable, as passage is always possible without prior bougienage or balloon dilation of the stenosis. As long as any form of therapy other than endoscopic palliation is intended, this type of traumatic approach to a tumor contradicts the principles of oncology. In addition, in advanced esophageal tumors, the value of EUS staging appears to be questionable. Most stenosing tumors of the esophagus can be expected to be T3 N1 [16]—all the more so when the tumor boundaries are beyond the reach of the miniprobe (i.e., 20 mm).

In "submucosal" tumors, myogenic lesions are easily differentiated from submucosal or intramucosal ones. Vascular lesions such as gastric angiodysplasia or eroded vessels after ulcer bleeding are clearly visualized, and there may be substantial therapeutic implications.

In comparison with conventional endosonography using 7.5-MHz large-diameter instruments, miniprobe ultrasonography allows safe passage through high-grade malignant esophageal strictures; higher accuracy rates for T staging; and similar rates for N staging [7].

After endoscopic mucosal resection (EMR) became an important therapeutic option for early esophageal and gastric cancer, miniprobe EUS staging was found to be the most valuable method of preinterventional local staging [11]. In 46 patients with gastric cancers, the miniprobe EUS findings were compared with histopathological findings after treatment. The total accuracy of

Table 4.2 Miniprobe ultrasound in the evaluation of various diseases

Method	Disease	Accuracy (%)	Sensitivity (%)	Specificity (%)	PPV	NPV	Reference
IDUS	Biliary obstruction	89.1	91.1	80	n.a.	n.a.	[4]
EUS	Biliary obstruction	75.6	75.7	75	n.a.	n.a.	[4]
UMP	Gastric cancer	71.7	n.a.	n.a.	n.a.	n.a.	[4]
EUS	Esophageal carcinoma	62	n.a.	n.a.	n.a.	n.a.	[7]
MPS	Esophageal carcinoma	86.8	n.a.	n.a.	n.a.	n.a.	[7]
MPS	Gastric cancer with lymph-node involvement	80	73	89	n.a.	n.a.	[10]
MPS	Esophageal cancer	90	n.a.	n.a.	n.a.	n.a.	[10]
MPS	Esophageal cancer with lymph-node involvement	78	75	80	n.a.	n.a.	[10]
MPS	Gastric cancer	82	n.a.	n.a.	n.a.	n.a.	[10]
MPS	Gastric cancer all tumors	61	n.a.	n.a.	n.a.	n.a.	[11]
MPS	Gastric cancer T1	72	n.a.	n.a.	n.a.	n.a.	[11]
MPS	Gastric cancer T2–4	40	n.a.	n.a.	n.a.	n.a.	[11]
MPS	Gastric cancer nodal staging, overall	69	n.a.	n.a.	n.a.	n.a.	[11]
MPS	Gastric cancer N0	86	n.a.	n.a.	n.a.	n.a.	[11]
MPS	Gastric cancer N1	25	n.a.	n.a.	n.a.	n.a.	[11]
MPS	Gastric cancer N2	14	n.a.	n.a.	n.a.	n.a.	[11]
IDUS	Papillary adenocarcinoma	90	89	90	n.a.	n.a.	[12]
IDUS	Bile duct cancer	76	89	50	n.a.	n.a.	[13]
IDUS	Pancreatic carcinoma		75	67	n.a.	n.a.	[14]
ERCP	Pancreatic carcinoma		37	67	n.a.	n.a.	[14]
CT	Pancreatic carcinoma		37	33	n.a.	n.a.	[14]
EUS	Pancreatic carcinoma	n.a.	50	67	n.a.	n.a.	[14]
IDUS	Biliary tract tumor	n.a.	89	89	n.a.	n.a.	[14]
ERCP	Biliary tract tumor	n.a.	78	88	n.a.	n.a.	[14]
CT	Biliary tract tumor	n.a.	33	60	n.a.	n.a.	[14]
EUS	Biliary tract tumor	n.a.	33	75	n.a.	n.a.	[14]
EUS	Pancreatic cancer	n.a.	92.9	58.3	n.a.	n.a.	[15]
CT	Pancreatic cancer	n.a.	64.3	66.7	n.a.	n.a.	[15]
ERP	Pancreatic cancer	n.a.	85.7	66.7	n.a.	n.a.	[15]
IDUS	Pancreatic cancer	n.a.	100	91.7	n.a.	n.a.	[15]

CT, computed tomography; ERCP, endoscopic retrograde cholangiopancreatography; ERP, endoscopic retrograde pancreatography; EUS, endoscopic ultrasonography; IDUS, intraductal ultrasonography; MPS, miniprobe sonography; n.a.: data not available; NPV, negative predictive value; PPV, positive predictive value; UMP, ultrasound miniprobe.

miniprobe EUS relative to the depth of tumor invasion was 71.7% (33 of 46 patients). The accuracy for T1m tumor diagnosis was 75.7% (22 of 29 patients). For T1sm lesions, it was 76.9% (10 of 13 patients), but the accuracy for T2 tumor diagnosis was low due to ultrasound attenuation. When the analysis was carried out on the basis of the size of tumor, the accuracy was 50.0% (nine of 18 patients) for all tumors larger than 20 mm in diameter and 85.7% (24 of 28 patients) for all tumors smaller than 20 mm [17].

Gastric mucosa-associated lymphoid tissue (MALT) lesions have been accurately visualized with miniprobe EUS [6]. During the follow-up period after therapy, in patients with normal miniprobe ultrasonography findings (n = 15), the histological examination confirmed complete remission in all patients. Hypoechoic thickening of the mucosa or submucosa, or both, was seen in nine patients. Endoscopic biopsies in four of these nine patients revealed recurrent lymphoma [6].

In 63 patients with tumors of the colon or rectum, miniprobe ultrasonography revealed carcinoma in five of 30 broad-based polyps, although adenomas were diagnosed on endoscopy. Correct assessment of lymph-node involvement was obtained in 47 of 55 patients. On the basis of the miniprobe ultrasonography findings, management was modified in seven of the 63 patients [3].

Despite the excellent resolution of small anatomical structures provided, miniprobe EUS is not a substitute for histological analysis. In ulcerated or polypoid lesions,

malignancy must be confirmed or excluded by biopsy; this applies in particular to the follow-up situation after radiotherapy or chemotherapy.

Extraductal Ultrasonography

Extraductal ultrasound (EDUS), as opposed to intraductal ultrasound (IDUS; see Chapter 5) is defined as endoscopic ultrasound with miniprobes visualizing the distal CBD from the duodenal, extraductal position. EDUS is a noninvasive application of miniprobes, without the need to cannulate the ostium and without altering the organ of interest. The distal CBD and in many instances also the distal pancreatic duct can be visualized in an unaltered state. EDUS allows excellent visualization of the distal common bile duct and detects small stones with a sensitivity of 94% and a specificity of 99%.

■ Future Developments

Linear miniprobes with electronic scanners (no mechanical parts). Three-dimensional display and the ability to review endoluminal ultrasound data interactively may improve the staging of gastrointestinal tumors [18]. In a small series of patients with cholangiocellular carcinoma, three-dimensional intraductal ultrasonography allowed accurate assessment of tumor invasion of the right hepatic artery in 88% of cases, the portal vein in 100%, and pancreatic parenchyma in 100% [12]. These preliminary data are encouraging for further evaluation of this technique. Spatial three-dimensional reconstructions of high-resolution IDUS images combined with cholangioscopic images and histopathology or cytopathology findings obtained via percutaneous transhepatic access may become a powerful diagnostic technique for planning differential therapy of cholangiocarcinoma.

■ Conclusions

The preliminary results show that miniprobe ultrasonography can in many cases enhance the examination of structures within and adjacent to the intestinal wall. This technique is easily carried out during routine endoscopy, and is therefore helpful in everyday routine conditions due to the view beyond the gastrointestinal wall that it provides.

References

1. Hurter T, Hanrath P. Endobronchial sonography: feasibility and preliminary results. Thorax 1992;47:565–7.
2. Herth F, Becker HD, Manegold C, Drings P. Endobronchial ultrasound (EBUS) assessment of a new diagnostic tool in bronchoscopy for staging of lung cancer. Onkologie 2001; 24:151–4.
3. Hunerbein M, Totkas S, Ghadimi BM, Schlag PM. Preoperative evaluation of colorectal neoplasms by colonoscopic miniprobe ultrasonography. Ann Surg 2000;232:46–50.
4. Menzel J, Poremba C, Dietl KH, Domschke W. Preoperative diagnosis of bile duct strictures: comparison of intraductal ultrasonography with conventional endosonography. Scand J Gastroenterol 2000;35:77–82.
5. Tamada K, Nagai H, Yasuda Y, Tomiyama T, Ohashi A, Wada S, et al. Transpapillary intraductal US prior to biliary drainage in the assessment of longitudinal spread of extrahepatic bile duct carcinoma. Gastrointest Endosc 2001;53:300–7.
6. Lugering N, Menzel J, Kucharzik T, Koch P, Herbst H, Tiemann M, et al. Impact of miniprobes compared to conventional endosonography in the staging of low-grade gastric malt lymphoma. Endoscopy 2001;33:832–7.
7. Menzel J, Hoepffner N, Nottberg H, Schulz C, Senninger N, Domschke W. Preoperative staging of esophageal carcinoma: miniprobe sonography versus conventional endoscopic ultrasound in a prospective histopathologically verified study. Endoscopy 1999;31:291–7.
8. Ariyama J, Suyama M, Satoh K, Wakabayashi K. Endoscopic ultrasound and intraductal ultrasound in the diagnosis of small pancreatic tumors. Abdom Imaging 1998;23:380–6.
9. Seifert H, Wehrmann T, Hilgers R, Gouder S, Braden B, Dietrich CF. Catheter probe extraductal EUS reliably detects distal common bile duct abnormalities. Gastrointest Endosc 2004;60:61–7.
10. Hunerbein M, Ghadimi BM, Haensch W, Schlag PM. Transendoscopic ultrasound of esophageal and gastric cancer using miniaturized ultrasound catheter probes. Gastrointest Endosc 1998;48:371–5.
11. Akahoshi K, Chijiiwa Y, Sasaki I, Hamada S, Iwakiri Y, Nawata H, et al. Preoperative TN staging of gastric cancer using a 15 MHz ultrasound miniprobe. Br J Radiol 1997;70:703–7.
12. Tamada K, Kanai N, Tomiyama T, Ohashi A, Wada S, Satoh Y, et al. Prediction of the histologic type of bile duct cancer by using intraductal ultrasonography. Abdom Imaging 1999; 24:484–90.
13. Tamada K, Kanai N, Ueno N, Ichiyama M, Tomiyama T, Wada S, et al. Limitations of intraductal ultrasonography in differentiating between bile duct cancer in stage T1 and stage T2: in-vitro and in-vivo studies. Endoscopy 1997;29:721–5.
14. Menzel J, Domschke W, Konturek JW, Gillessen A, Foerster E. [Intraductal ultrasound in the pancreaticobiliary duct system; in German.] Dtsch Med Wochenschr 1997;122:41–9.
15. Furukawa T, Tsukamoto Y, Naitoh Y, Hirooka Y, Hayakawa T. Differential diagnosis between benign and malignant localized stenosis of the main pancreatic duct by intraductal ultrasound of the pancreas. Am J Gastroenterol 1994;89: 2038–41.
16. Vickers J, Alderson D. Influence of luminal obstruction on oesophageal cancer staging using endoscopic ultrasonography. Br J Surg 1998;85:999–1001.
17. Okamura S, Tsutsui A, Muguruma N, Ichikawa S, Sogabe M, Okita Y, et al. The utility and limitations of an ultrasonic miniprobe in the staging of gastric cancer. J Med Invest 1999;46:49–53.
18. Hunerbein M, Ghadimi BM, Gretschel S, Schlag PM. Three-dimensional endoluminal ultrasound: a new method for the evaluation of gastrointestinal tumors. Abdom Imaging 1999;24:445–8.

5 Intraductal Ultrasound

B. Braden, H. Seifert, C.F. Dietrich

Following initial reports on the intravascular use of high-frequency filiform miniprobes, biliary and pancreatic intraductal ultrasonography (IDUS) led to impressive imaging of these ducts and to valuable diagnostic information complementary to endoscopic retrograde cholangiopancreatography (ERCP), especially in patients with intraductal papillary tumors—further enhancing the potential of endoscopic ultrasonography [1–3]. Although there are some features that are typical of malignant lesions, there are no criteria sufficiently reliable to allow differentiation between benign and malignant biliary or pancreatic lesions.

Miniprobes with outer diameters of only 2–3 mm can be inserted through the instrument channel of standard endoscopes and provide high-frequency ultrasound images. The flexibility and small diameter of miniprobes allow intraductal ultrasonography (IDUS) in the biliary tract and pancreatic duct, as well as in the endobronchial system.

High-frequency endoscopic ultrasound (EUS) probes are not well suited for screening examinations. The high resolution of miniprobes is useful for further differentiating and characterization of pathological structures that have been identified with other imaging methods (e.g., endoscopy or transabdominal ultrasound) or to answer specific clinical questions (e.g., suspected choledocholithiasis).

Due to wear on the instruments, miniprobes have a short lifespan when used intraductally, and this is still a drawback with this endosonographic technique. No cost–benefit analyses have so far been published.

■ Technical Developments

In comparison with conventional endosonography, miniprobes work at substantially higher frequencies (12–30 MHz). This results in a high resolution (0.07–0.18 mm) that allows precise differentiation of the discrete wall layers in the esophagus, stomach, and bowel. Electronic miniprobes have a ring at the top that incorporates 64 transducer elements, which produce a 360° image. Electronic miniprobes are highly flexible, but have the disadvantage of restricted lateral resolution. In contrast, mechanical systems produce a 360° image with significantly better resolution, with a rotating transducer at the top of the probe.

New miniprobe developments, with controlled automated retraction over a defined distance, allow three-dimensional reconstruction after complex image processing.

Continuing research on probe design, which may improve the durability of the instruments and extend the depth of penetration, may encourage more widespread use of this novel technology.

■ Intraductal Ultrasound of the Hepatobiliary System

Small-caliber miniprobes can be inserted into the bile duct during ERCP. Prior papillotomy makes insertion easier, but may not be essential. Wire-guided miniprobes allow cannulation of the bile duct in nearly 100% of cases without previous sphincterotomy [4]. Miniprobes can also be placed in specific intrahepatic bile ducts over a selectively placed guide wire. The position of the probe can be controlled radiographically during endoscopic retrograde cholangiography (ERC).

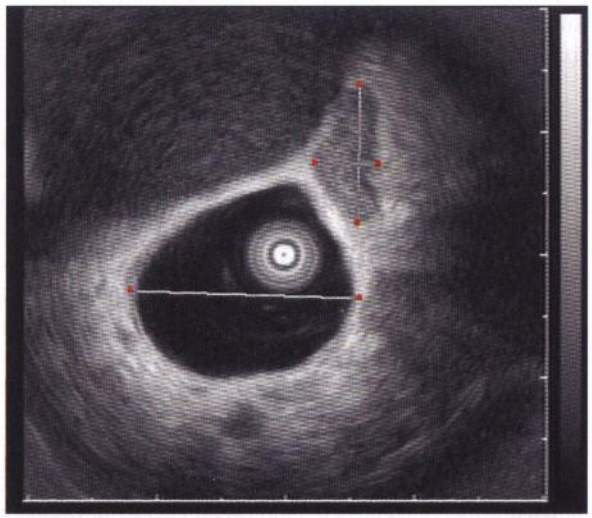
IDUS prolongs the examination time only marginally (about 5–10 min). It has been reported that it does not increase the complication rate with ERCP (one case of mild pancreatitis in 400 patients) [5].

Biliary IDUS provides a high-resolution display of structures in the hepatoduodenal ligament (portal vein, hepatic artery, and lymph nodes) (Fig. 5.**1**) [6]. Close to the papilla of Vater, IDUS depicts the surrounding pancreatic parenchyma with a penetration depth of 2 cm. In the intrahepatic position, the miniprobe shows parallel branches of the portal vein and the surrounding liver parenchyma.

IDUS distinguishes three layers of the normal wall of the bile duct. The fine inner and more echogenic layer corresponds to the transition echo. The next layer, less echogenic, matches the mucosa and muscularis propria (fibromuscular layer). The outer more echogenic layer corresponds to the fatty tissue of the subserosa, the serosa, and the transition echo to neighboring organs [7].



a



b



c

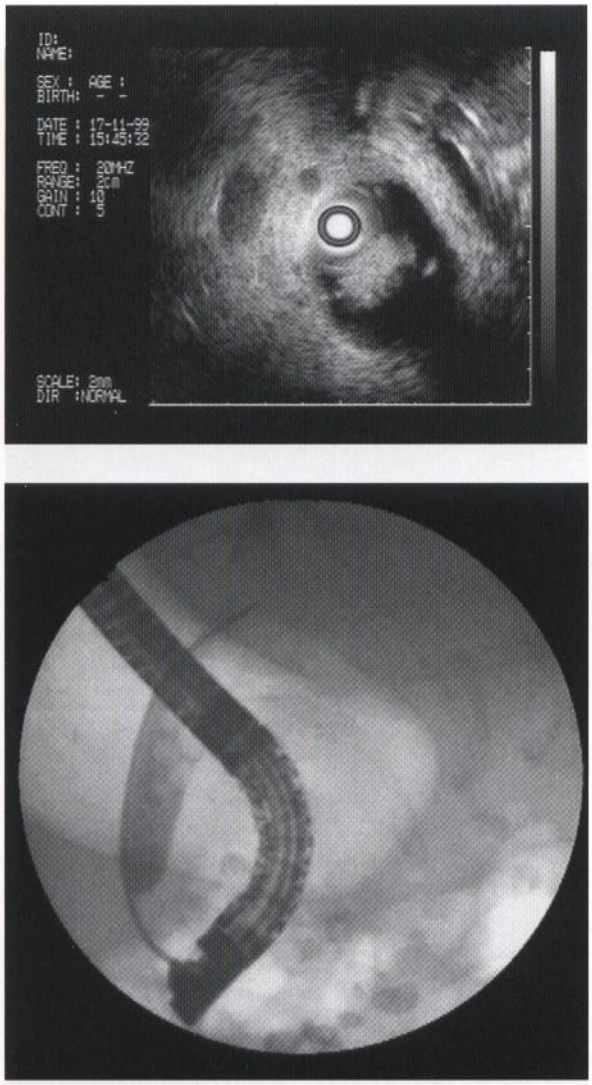
Fig. 5.1 Anatomy of the bile duct. **a** Intraductal (common bile duct) imaging of the pancreatic duct close to the papilla. **b** A lymph node in the hepatoduodenal ligament close to the cystic duct [6]. **c** The origin of the cystic duct. PV: portal vein; A: hepatic artery; CY: cystic duct.

Choledocholithiasis

With both transabdominal ultrasonography and computed tomography, it can sometimes be difficult to detect gallstones in the bile duct. Interpreting magnetic resonance imaging (MRI) of the bile duct is still a sophisticated exercise. ERCP is therefore still the gold standard in the diagnosis and treatment of choledocholithiasis. However, even on ERCP, small stones may be overlooked, and it is difficult to distinguish between aerobilia and small stones. Conventional endosonography from a duodenal position has a high sensitivity of 95% for detecting choledocholithiasis, similar to that of ERCP [8].

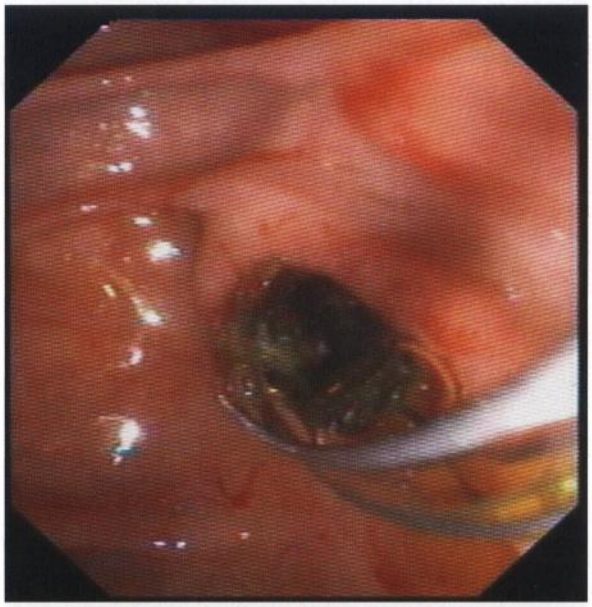
The best results reported for detecting choledocholithiasis were obtained with IDUS of the bile duct [9,10]. In a prospective study by Palazzo, 97% of bile duct stones were detected with the miniprobe, 81% during ERCP, 61% with intravenous cholangiography, and 45% by transabdominal ultrasonography [11]. Particular advantages of IDUS are that it makes it easier to distinguish between air, sludge, and stones and that it provides high resolution even of small stones (< 5 mm in diameter). IDUS of the bile duct can therefore be a valuable tool for diagnosing choledocholithiasis. If (wire-guided) IDUS of the bile duct is negative, sphincterotomy can be avoided. In contrast to invasive IDUS, we prefer extraductal ultrasound (EDUS; see also Chapter 20 on EUS of the hepatobiliary system) in most cases [12] (see below).

Review of the literature. IDUS is useful for detecting small residual bile duct stones during endoscopic balloon sphincteroplasty when stones are fragmented by mechanical lithotripsy, or when there is evidence of a dilated bile duct (> 10 mm) [13]. In 62 patients suspected to have bile duct stones, the accuracy of ERC combined with IDUS for diagnosing bile duct stone and/or sludge was higher than that of ERC alone (97% vs. 87%; $P < 0.05$). With dilated bile ducts, the diagnostic accuracy of ERC combined with IDUS was also higher than that of ERC alone (95.5% vs. 72.7%; $P < 0.05$). Additional diagnostic information provided by IDUS included identification of cystic duct stones in five patients, characterization of bile duct strictures in two patients, and choledochal varices in one patient [14]. In 65 patients in



a

b



c

Fig. 5.2 Choledocholithiasis. **a** Intraductal ultrasonography, showing choledocholithiasis and the accompanying acoustic shadow. **b** The corresponding endoscopic retrograde cholangiogram. **c** The corresponding endoscopic image.

whom there was a strong suspicion of choledocholithiasis, the IDUS probe was inserted by means of the duodenoscope into the bile duct without a sphincterotomy. All stones identified by IDUS or retrograde cholangiography were removed after endoscopic sphincterotomy. The final diagnosis was choledocholithiasis in 59 patients. The bile duct diameter ranged from 0.6 to 2.3 cm, and the stone size from 2 mm to 2 cm. IDUS successfully identified all stones in these patients [15]. Examples are shown in Figs 5.**2** and 5.**3**; by contrast, adenoma of the papilla with intraductal growth is illustrated in Fig. 5.**4**.

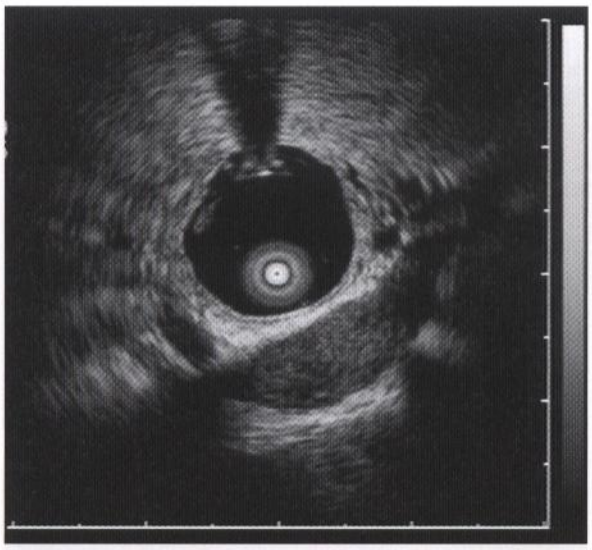
Bile Duct Strictures

IDUS can help distinguish between benign and malignant bile strictures. The criteria for malignancy are less echogenic lesions extending beyond the borders of the organ, irregular ductal surfaces, interruption of the typical ultrasound wall layering, and a heterogeneous echo pattern.

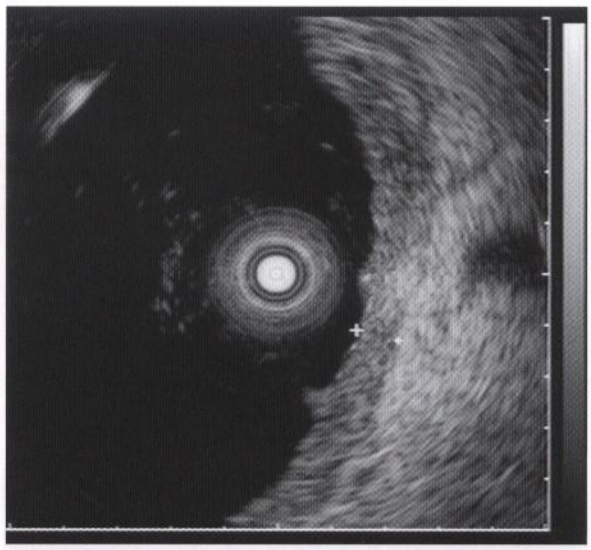
High-grade stenoses may require dilation of the bile duct using balloon catheters before the miniprobe can pass.

In comparison with conventional endoscopic ultrasound, IDUS has proved to be superior for predicting the benign or malignant status of biliary structures and the resectability of biliary tumors [16]. When ERCP was supplemented with IDUS, the accuracy of correct differentiation between malignant and benign strictures increased significantly to 88% and was superior to that of magnetic resonance cholangiopancreatography (MRCP) [17].

It may be possible to distinguish scarred strictures after cholecystectomy and in patients with Mirizzi syndrome from tumor stenosis of invasive cancers (although this is a controversial issue.



a



b

Fig. 5.3a Choledocholithiasis with cholangitis. **b** Wall thickening is seen between the markers (scale: 2 mm).

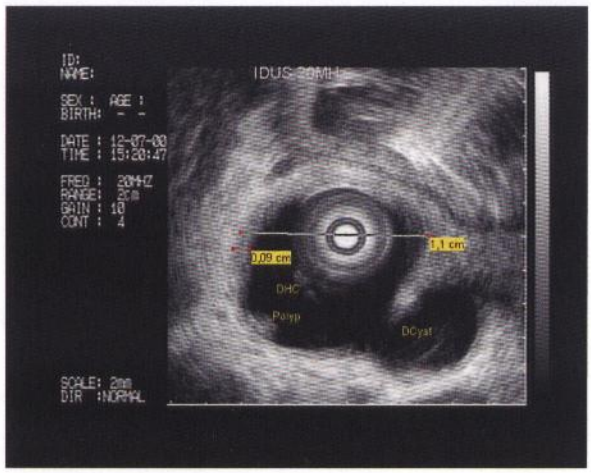


Fig. 5.4 Adenoma of the papilla with intraductal growth. Intraductal ultrasound is particularly helpful for detecting intraductal growth (polyps) and therefore indicates when surgery is required. DHC: common hepatic duct. DCyst: ductal cyst.

If polypoid structures are detected adhering to the biliary wall, a histological examination should be carried out. The likelihood of malignancy increases with the size of the polypoid lesion (> 8 mm).

Primary sclerosing cholangitis is characterized by multifocal concentric strictures. Whether IDUS may be helpful in early screening for cholangiocellular carcinoma in these patients is still unclear. However, the diagnostic dilemma in ultrasonography is that it is difficult to distinguish between inflammatory conditions and tumor infiltration [18] (Fig. 5.5).

Cholangiocellular Carcinoma

Cholangiocellular carcinoma expands along the ductal structures. IDUS is able to determine the longitudinal extension of bile duct tumors, which is crucial for the prediction of resectability. Tumor invasion of the surrounding organs and blood vessels can be detected with IDUS, as well as infiltration of the pancreatic parenchyma, the portal vein, or the hepatic artery.

The limited depth of penetration restricts the diagnostic power of IDUS in determining the expansion of the tumor and the infiltration of lymph nodes beyond the hepatoduodenal ligament. IDUS is not capable of assessing the M and N stages. A thickening of the biliary wall can be caused by inflammation or tumor infiltration. Endosonography cannot provide any certainty in differentiating between inflammation and neoplastic infiltration, and is therefore inaccurate for predicting the T stage. Normally, inflammation causes symmetric wall thickening, while neoplastic wall alterations have an asymmetrical appearance (Fig. 5.6). Papillary adenomatosis is regarded as benign in most cases, but malignant transformation is possible (Fig. 5.7).

Review of the literature. It is not possible to distinguish between strictures or inflammatory or neoplastic lesions [19]. IDUS cannot reliably distinguish between bile duct cancer in stage T1 and that in stage T2 [20]. EUS is useful in assessing portal vein invasion by cholangiocarcinomas at the middle and distal common bile duct (with an accuracy of 91%), but is less accurate (57%) in assessing invasion at the proximal bile duct [21–23]. While IDUS proved useful for assessing the extent of bile duct cancer invasion into the right hepatic artery, it did not demonstrate the hepatic artery proper or the left hepatic artery sufficiently for diagnosing vascular involvement [21–23].

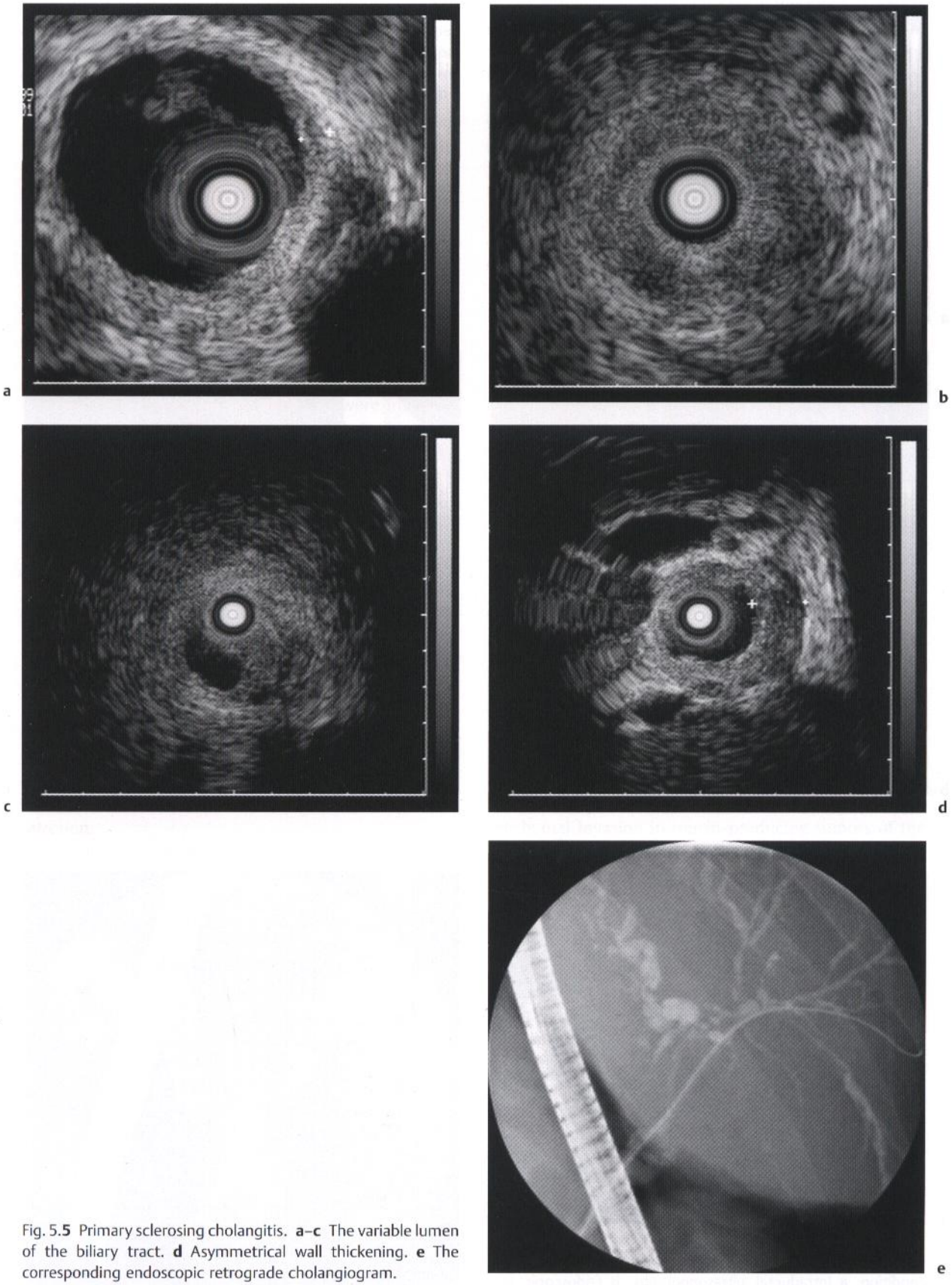
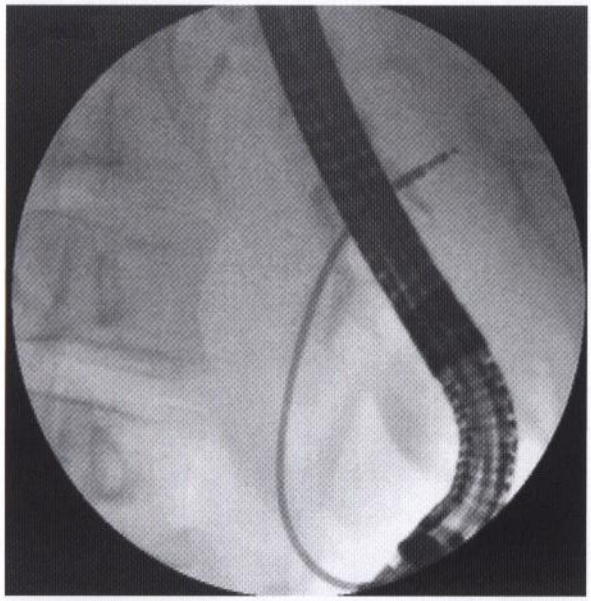


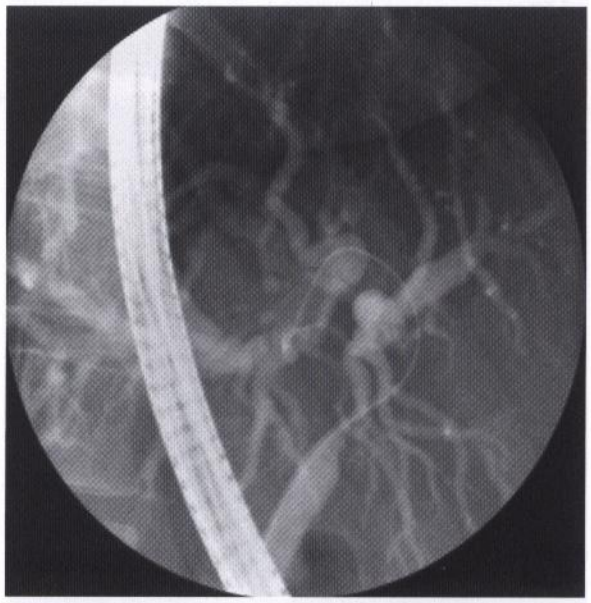
Fig. 5.5 Primary sclerosing cholangitis. **a–c** The variable lumen of the biliary tract. **d** Asymmetrical wall thickening. **e** The corresponding endoscopic retrograde cholangiogram.



a

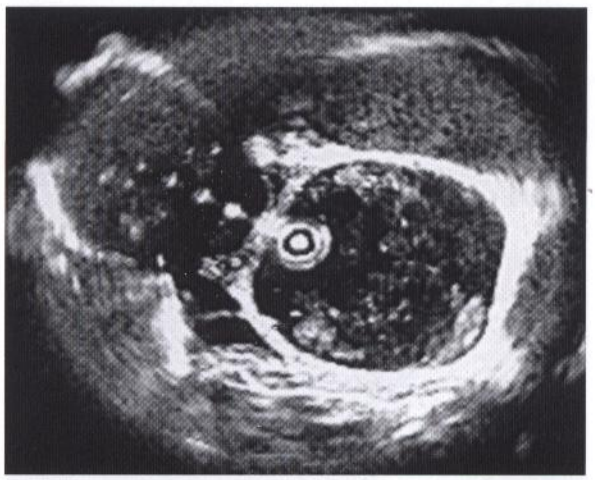


b



c

Fig. 5.6a Cholangiocellular carcinoma. The lesion is characterized by destructive growth and invasion, but neoplastic changes are difficult to distinguish from inflammatory reactions. **b** The position of the miniprobe in the corresponding endoscopic retrograde cholangiogram. **c** ERCP.



a



b

Fig. 5.7 Biliary tract papillomatosis. This is a benign and rare condition. **a** Intraductal ultrasonography. **b** Endoscopic retrograde cholangiography.

In 18 patients with extrahepatic bile duct cancer, the accuracy of IDUS, EUS, and angiography in assessing pancreatic parenchymal invasion was 100%, 78%, and 61%, respectively. However, IDUS was not capable of assessing pancreatic capsular invasion [24].

In 62 patients with presumed malignant strictures of the bile duct, IDUS was carried out using an ultrasonic probe (diameter 2.0 mm, frequency 20 MHz). Following IDUS, a bile duct biopsy was performed. The IDUS images of the tumor were classified as polypoid lesions, localized wall thickening, intraductal sessile tumors, sessile tumor outside of the bile duct, or absence of apparent lesions. The IDUS findings were compared with the histological findings and clinical course. Multiple regression analysis showed that the presence of a sessile tumor (intraductal or outside of the bile duct; $P < 0.05$), tumor size greater than 10 mm ($P < 0.001$), and an interrupted wall structure ($P < 0.05$) were independent variables predictive of malignancy. It was concluded that IDUS criteria can predict malignancy when biopsy fails [25]. Probably, with the techniques currently available, optimal planning of hepatobiliary surgery for cholangiocellular carcinoma requires a combination of ERC or percutaneous cholangiography and cholangioscopy, IDUS, TUS, and possibly MRCP and angiography. Assessment of the surgical margins with IDUS alone was found to be inaccurate in some cases [26].

■ IDUS of the Pancreatic Ducts

Conducting IDUS of the pancreatic duct involves a risk of inducing acute pancreatitis. Although the risk is considered to be fairly low (< 1%) [27,28], it may depend on the examiner's level of experience as well as on patient selection.

Although miniprobes can often be inserted into the pancreatic duct without prior sphincterotomy, the contorted course of the duct may make further intubation difficult. The investigation often has to be stopped at the genu.

Using a 20-MHz miniprobe, the boundary of the pancreatic duct appears as a hyperechoic layer. Higher-frequency miniprobes (30 MHz) depict three layers—two hyperechoic layers and an intermediate hypoechoic layer.

IDUS can be helpful for differentiating between benign and malignant strictures of the pancreatic duct. IDUS can depict the signs of chronic pancreatitis (calcifications, fibrosis, pancreatic lithiasis, small cysts). According to studies by Furukawa et al. [28], IDUS can distinguish between strictures of the pancreatic duct caused by focal pancreatitis and tumor stenosis with an accuracy of 90%. In addition, IDUS can assess tumor infiltration into the splenic, mesenteric, and portal veins.

IDUS may also be useful in the differential diagnosis of cystic pancreatic tumors (serous cystadenoma, mucinous cystadenoma, mucinous cystadenocarcinoma, intraductal papillary mucinous cystic tumor). Early identification of these lesions is important, as the management and outcome differ from those for ductal pancreatic adenocarcinoma.

Neuroendocrine tumors of the pancreas (gastrinoma, insulinoma, glucagonoma, VIPoma, somatostatinoma) are rare neoplasms that may arise sporadically or in association with a hereditary endocrine neoplasia syndrome. They require precise imaging and localization for the planning of resection.

Even intraoperatively, up to 20% of insulinomas and up to 50% of gastrinomas are difficult to find. Results of initial studies indicate that IDUS may be able to improve the localization of neuroendocrine tumors in the pancreas in comparison with conventional methods (such as EUS and octreotide receptor scintigraphy) [29]. Even tiny lesions can be detected using the high resolution provided by miniprobes [30]. In a few cases, the additional information provided by the IDUS results may allow organ-preserving enucleation instead of pancreatic resection.

Review of the literature. In the diagnosis of 239 patients with pancreatic disease (including 48 cancers, 90 mucin-producing tumors, seven islet-cell tumors, two metastatic pancreatic tumors, seven serous cystadenomas, one pancreatic teratoma, three solid cystic tumors, 49 cases of chronic pancreatitis, 25 cases of focal pancreatitis, and seven cases of pancreatolithiasis), IDUS was able to image the entire cross-section of the portal vein and other large veins. IDUS was useful in detecting carcinoma in situ and small tumors, in assessing the intraductal spread of the tumor and its pancreatic parenchymal invasion in mucin-producing tumors of the main duct, and in assessing the indications for surgery by revealing mural nodules in mucin-producing tumors of the ductal branches. IDUS was also useful in evaluating the feasibility of partial resection of the tumor in mucin-producing tumors of the ductal branches and pancreatic islet-cell tumors, in accurately locating multiple lesions in pancreatic islet-cell cancer, and in differentiating between benign and malignant cases of localized stenosis of the main pancreatic duct related to pancreatic stenting. With IDUS, it was possible to identify the site of pancreatic stones in order to assess the need for endoscopic treatment. Acute pancreatitis as a complication occurred in one of the 239 patients who underwent IDUS (0.4%) [28]. Very small neuroendocrine pancreatic tumors were diagnosed by pancreatic IDUS [29] (Table 5.**1**).

Table 5.1 Indications for intraductal ultrasonography (IDUS)

Biliary tract
• Suspected choledocholithiasis (?)
• Differentiating between benign and malignant biliary strictures (?)
• Local tumor staging (?)
Pancreas
• Differentiating between benign and malignant pancreatic strictures (?)
• Local tumor staging (?)
• Characterization of cystic tumors (?)
• Localization of neuroendocrine tumors not detectable on EUS (?)

IDUS in Patients with Tumors of the Papilla and with Sphincter of Oddi Dysfunction

In contrast to pancreatic carcinoma, tumors of the papilla of Vater can usually be resected and therefore have a better prognosis. Adenomas in the papilla of Vater are premalignant conditions. The choice of the resection method depends on the presence of intraductal growth. Intraductal extension of the tumor requires pylorus-preserving pancreatoduodenectomy (the Whipple operation), while extraductal adenoma can be resected endoscopically. IDUS allows visualization of the papilla of Vater, including the sphincter of Oddi. IDUS depicts papillary tumors and detects neoplastic intraductal growth or infiltration of the surrounding structures. In contrast to other imaging methods such as computed tomography (CT) and EUS, IDUS has a high level of sensitivity. However, IDUS may overlook lymph-node infiltration by papillary carcinoma, due to its limited depth of penetration.

In 21 patients with suspected biliary sphincter of Oddi dysfunction, IDUS of the papilla was technically feasible and safe, but could not be used as a substitute for sphincter of Oddi manometry [31].

Conclusion

Intraductal endosonography is particularly valuable for diagnosing stenoses of unknown origin in the common bile duct. It must be borne in mind that IDUS (like other ultrasound methods, as well as CT and MRI) is not able to differentiate reliably between benign and malignant lesions. In most cases, extraductal EUS techniques are sufficient.

References

1. Furukawa T, Naitoh Y, Tsukamoto Y, Mitake M, Yamada M, Ishihara A, et al. New technique using intraductal ultrasonography for the diagnosis of diseases of the pancreatobiliary system. J Ultrasound Med 1992;11:607–12.
2. Furukawa T, Tsukamoto Y, Naitoh Y, Hirooka Y, Katoh T. Evaluation of intraductal ultrasonography in the diagnosis of pancreatic cancer. Endoscopy 1993;25:577–81.
3. Furukawa T, Tsukamoto Y, Naitoh Y, Mitake M, Hirooka Y, Hayakawa T. Differential diagnosis of pancreatic diseases with an intraductal ultrasound system. Gastrointest Endosc 1994;40:213–9.
4. Tamada K, Nagai H, Yasuda Y, Tomiyama T, Ohashi A, Wada S, et al. Transpapillary intraductal US prior to biliary drainage in the assessment of longitudinal spread of extrahepatic bile duct carcinoma. Gastrointest Endosc 2001;53:300–7.
5. Levy MJ, Vazquez-Sequeiros E, Wiersema MJ. Evaluation of the pancreaticobiliary ductal systems by intraductal US.- Gastrointest Endosc 2002;55:397–408.
6. Dietrich CF, Lee JH, Herrmann G, Tueber G, Roth WK, Zeuzem S. Enlargement of perihepatic lymph nodes in relation to liver histology and viremia in patients with chronic hepatitis C. Hepatology 1997;26:467–72.
7. Noda Y, Fujita N, Kobayashi G, Kimura K, Yago A, Yuki T, et al. [Comparison of echograms by a microscanner and histological findings of the common bile duct: in vitro study; in Japanese.] Nippon Shokakibyo Gakkai Zasshi 1997;94:172–9.
8. Palazzo L, Girollet PP, Salmeron M, Silvain C, Roseau G, Canard JM, et al. Value of endoscopic ultrasonography in the diagnosis of common bile duct stones: comparison with surgical exploration and ERCP. Gastrointest Endosc 1995;42:225–31.
9. Linghu EQ, Cheng LF, Wang XD, Wang ZQ, Yang YS, Li W, et al. Intraductal ultrasonography and endoscopic retrograde cholangiography in diagnosis of extrahepatic bile duct stones: a comparative study. Hepatobiliary Pancreat Dis Int 2004;3:129–32.
10. Moon JH, Cho YD, Cha SW, Cheon YK, Ahn HC, Kim YS, et al. The detection of bile duct stones in suspected biliary pancreatitis: comparison of MRCP, ERCP, and intraductal US. Am J Gastroenterol 2005;100:1051–7.
11. Palazzo L. Which test for common bile duct stones? Endoscopic and intraductal ultrasonography. Endoscopy 1997;29:655–65.
12. Seifert H, Wehrmann T, Hilgers R, Gouder S, Braden B, Dietrich CF. Catheter probe extraductal EUS reliably detects distal common bile duct abnormalities. Gastrointest Endosc 2004;60:61–7.
13. Ohashi A, Ueno N, Tamada K, Tomiyama T, Wada S, Miyata T, et al. Assessment of residual bile duct stones with use of intraductal US during endoscopic balloon sphincteroplasty: comparison with balloon cholangiography. Gastrointest Endosc 1999;49:328–33.
14. Das A, Isenberg G, Wong RC, Sivak MV Jr, Chak A. Wire-guided intraductal US: an adjunct to ERCP in the management of bile duct stones. Gastrointest Endosc 2001;54:31–36.
15. Tseng LJ, Jao YT, Mo LR, Lin RC. Over-the-wire US catheter probe as an adjunct to ERCP in the detection of choledocholithiasis. Gastrointest Endosc 2001;54:720–3.
16. Menzel J, Poremba C, Dietl KH, Domschke W. Preoperative diagnosis of bile duct strictures: comparison of intraductal

ultrasonography with conventional endosonography. Scand J Gastroenterol 2000;35:77–82.
17. Domagk D, Wessling J, Reimer P, Hertel L, Poremba C, Senninger N, et al. Endoscopic retrograde cholangiopancreatography, intraductal ultrasonography, and magnetic resonance cholangiopancreatography in bile duct strictures: a prospective comparison of imaging diagnostics with histopathological correlation. Am J Gastroenterol 2004;99: 1684–9.
18. Hirche TO, Russler J, Braden B, Schuessler G, Zeuzem S, Wehrmann T, et al. Sonographic detection of perihepatic lymphadenopathy is an indicator for primary sclerosing cholangitis in patients with inflammatory bowel disease. Int J Colorectal Dis 2004;19:586–94.
19. Tamada K, Kanai N, Tomiyama T, Ohashi A, Wada S, Satoh Y, et al. Prediction of the histologic type of bile duct cancer by using intraductal ultrasonography. Abdom Imaging 1999; 24:484–90.
20. Ueno N, Nishizono T, Tamada K, Ichiyama M, Wada S, Tomiyama T, et al. Diagnosing extrahepatic bile duct stones using intraductal ultrasonography: a case series. Endoscopy 1997;29:356–60.
21. Tamada K, Ido K, Ueno N, Ichiyama M, Tomiyama T, Nishizono T, et al. Assessment of hepatic artery invasion by bile duct cancer using intraductal ultrasonography. Endoscopy 1995;27:579–83.
22. Tamada K, Ido K, Ueno N, Ichiyama M, Tomiyama T, Nishizono T, et al. Assessment of portal vein invasion by bile duct cancer using intraductal ultrasonography. Endoscopy 1995;27:573–8.
23. Tamada K, Ido K, Ueno N, Kimura K, Ichiyama M, Tomiyama T. Preoperative staging of extrahepatic bile duct cancer with intraductal ultrasonography. Am J Gastroenterol 1995;90: 239–46.
24. Tamada K, Ueno N, Ichiyama M, Tomiyama T, Nishizono T, Wada S, et al. Assessment of pancreatic parenchymal invasion by bile duct cancer using intraductal ultrasonography. Endoscopy 1996;28:492–6.
25. Tamada K, Tomiyama T, Wada S, Ohashi A, Satoh Y, Ido K, et al. Endoscopic transpapillary bile duct biopsy with the combination of intraductal ultrasonography in the diagnosis of biliary strictures. Gut 2002;50:326–31.
26. Dietrich CF, Seifert H, Schreiber-Dietrich D, Caspary WF, Wehrmann T. Benigne Papillomatose der Gallenwege: Eine sonographische Blickdiagnose? [abstract]. Ultraschall Med 1998;19:88.
27. Menzel J, Domschke W. Intraductal ultrasonography (IDUS) of the pancreato-biliary duct system: personal experience and review of literature. Eur J Ultrasound 1999;10:105–15.
28. Furukawa T, Oohashi K, Yamao K, Naitoh Y, Hirooka Y, Taki T, et al. Intraductal ultrasonography of the pancreas: development and clinical potential. Endoscopy 1997;29:561–9.
29. Menzel J, Domschke W. Intraductal ultrasonography may localize islet cell tumours negative on endoscopic ultrasound. Scand J Gastroenterol 1998;33:109–12.
30. Yamao K, Okubo K, Sawaka A, Hara K, Nakamura T, Suzuki T, et al. Endoluminal ultrasonography in the diagnosis of pancreatic diseases. Abdom Imaging 2003;28:545–55.
31. Wehrmann T, Stergiou N, Riphaus A, Lembcke B. Correlation between sphincter of Oddi manometry and intraductal ultrasound morphology in patients with suspected sphincter of Oddi dysfunction. Endoscopy 2001;33:773–7.

6 Radial EUS, Linear EUS, or Ultrasound Miniprobe: Which Is the Most Suitable Device?

J. Janssen, C.F. Dietrich

The Development of EUS: a Short Historical Survey

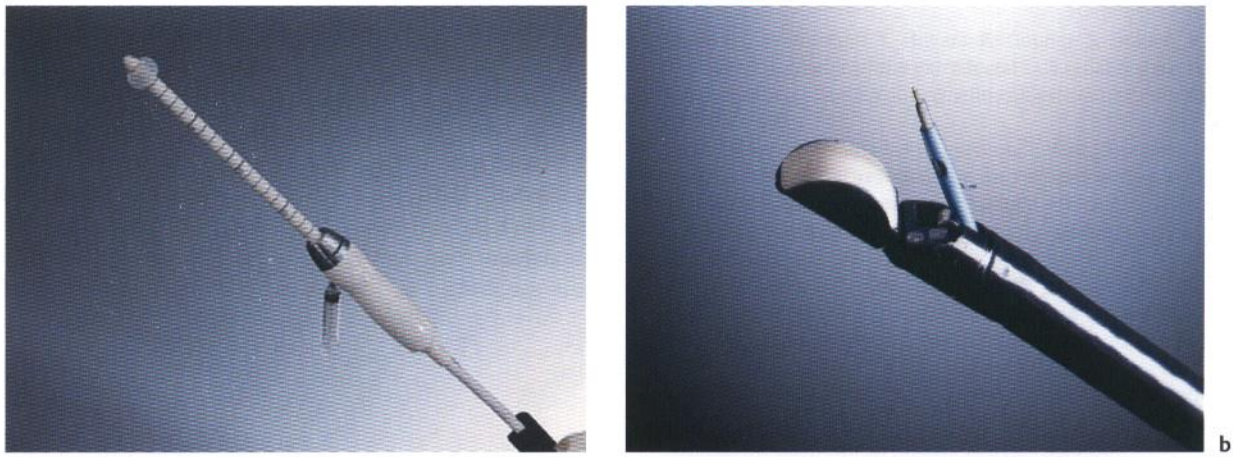
Shortly after ultrasound first became available as a diagnostic imaging method in medicine [1], its use was expanded by Wild et al., who presented an intracavitary rectal application in 1957 [2]. The principle of using a blind, rigid probe has been maintained and further improved for vaginal and rectal ultrasonography (Fig. 6.**1a**).

Endoscopic ultrasonography (EUS) with flexible instruments has developed quickly since the early 1980s [3] and is now accepted as indispensable tool in gastroenterology and associated fields. Apart from other indications, EUS is essential for the pretherapeutic local staging of gastrointestinal tumors. It is the method of choice for determining the origin and type of submucosal lesions. The use of longitudinal systems makes it possible to carry out fine-needle biopsy of lesions close to the gastrointestinal tract and local interventions guided by real-time EUS.

The development of flexible echoendoscopes started with mechanical radial scanners (5 MHz, 360°), which were mounted on top of a conventional endoscope [3]. Soon after this, prototype echoendoscopes based on the radial mechanical technique were manufactured by the Olympus Corporation [4]. Subsequent models worked with a frequency range of 5–12 MHz and dominated clinical applications for some 10 years. Most of the relevant studies on diagnostic EUS were conducted using this type of instrument.

At the beginning of the 1990s, a novel longitudinally scanning echoendoscope was presented and produced in series (Hitachi/Pentax FG-32UA) [5]. This instrument had an electronic scanner at frequencies of 5–10 MHz and allowed vessels to be examined using pulsed Doppler and color Doppler (Fig. 6.**1b**). In comparison with the mechanical devices, electronic scanners provided significantly better spatial resolution and higher imaging quality, especially in the near field. The fundamental advantage of the linear scanner is that it allows real-time controlled EUS-guided biopsy and interventions. Needles can be introduced through a working channel, and their tip is moved forward into the tissue within the scanning plane [6]. The combination of these interventional instruments with color flow Doppler imaging reduces the risk of bleeding during puncture and transmural insertion of drains. Nowadays, modern radial scanners also work electronically, incorporating Doppler facilities and providing better spatial resolution.

The ultrasound miniprobe was also developed at the same time as longitudinal scanners. The miniprobe is characterized by its small caliber and high ultrasound frequency (7.5–30 MHz), which provides high resolution, but at the expense of penetration depth. These probes were initially used in intracoronary ultrasonography [7–9], and the applications were later extended to



a b

Fig. 6.**1** The modern rigid rectal probe (**a**) and flexible longitudinal echoendoscope (**b**) for diagnostic and interventional endoscopic ultrasonography.

the gastrointestinal field [10]. The miniprobe is inserted into the working channel of a standard endoscope; endoscopy and EUS can thus be combined in a single examination. The small caliber of the instrument makes it possible to explore narrow tumor stenoses and allows intraductal biliary or pancreatic ultrasonography. Miniprobes usually work mechanically and produce a radial 360° image. The main disadvantage of these devices is their small penetration depth (2–3 cm) at frequencies of 20–30 MHz. Their use is therefore limited when the focus of the examination is on the surroundings of the gastrointestinal wall—e.g., for the exploration of lymph nodes and the pancreas (reviewed in [11]).

The main obstacles to the widespread use of EUS are its limited (although still expanding) range of indications and the high initial costs and operating costs. It depends on the structure of local departments whether the purchase of one or more types of EUS instrument is economically justifiable. If only one system is to be bought, the choice of the correct type of EUS unit is also an issue.

In centers with low annual numbers of examinations, it is economically mandatory for the basic ultrasound unit to be usable for transabdominal, vascular, and cardiac ultrasonography as well. All EUS equipment manufacturers now offer variable-use systems. The initial costs for a standard echoendoscope are about $60 000–80 000. Experience shows that the lifetime of an instrument used at a frequency of 500 examinations per year is about 3 years. Purchasing a second echoendoscope is profitable above a frequency of three or four examinations per day. The lifetime of a miniprobe is highly dependent on the experience and the care of the examiner and on the uses to which the instrument is put (e.g., esophageal applications versus intraductal ultrasonography). Reports on the average number of examinations carried out with one probe vary from 10 to 90. The price of a miniprobe is about $2000–3000.

During the last 10 years, the quality of all of the EUS systems available on the market has significantly improved. However, there are specific differences between the systems. The following sections provide general comparisons between linear and radial standard EUS systems and ultrasound miniprobes, without concentrating on specific instruments that are currently available.

■ Miniprobe Versus Conventional EUS

The indisputable advantage of miniprobe ultrasonography is that it makes it possible to carry out endoscopy and EUS during a single session. An ideal indication for this method is the evaluation of submucosal tumors or unclear external impressions [11]. The only precondition for this is that the basic ultrasound unit should be immediately available, rather than being used for routine examinations by another physician in a different room.

High-frequency miniprobe ultrasonography is limited by its low penetration depth. Systematic exploration of the pancreas and lymph-node areas or other structures more distant from the gastrointestinal wall is therefore not generally possible, although it has been done successfully in several cases. The second disadvantage is that it is not possible to carry out real-time controlled fine-needle aspiration biopsy (FNAB) with the miniprobe.

The outer diameter of standard echoendoscopes is approximately 12.5–14.5 mm. In contrast to the miniprobe, these instruments are not able to pass high-grade tumor stenoses and do not allow intraductal ultrasound (IDUS) examinations. However, the unresectability of a stenosing esophageal cancer can often be confirmed with conventional EUS just by scanning the oral end of the tumor; bougienage is therefore not necessary in these cases. If passage is mandatory in order to determine the exact stage of the tumor, bougienage can precede EUS. The perforation risk is low with this procedure [12,13].

Miniprobes are often preferred in the staging of early gastrointestinal cancer before endoscopic treatment. Studies have reported good results with high-frequency miniprobes in this setting (see Chapter 4), but there have as yet been no studies prospectively comparing the miniprobe with modern electronic conventional EUS systems. These new-generation instruments, working at 10–12 MHz, provide excellent spatial resolution including the near field, which in our opinion is comparable with the quality of miniprobe imaging (Fig. 6.**2**). Irrespective of the EUS system used, problems resulting from concomitant inflammation, causing overstaging, or due to the location of the tumor (e.g., in the cardia) have not been solved. It therefore seems unnecessary to debate whether one system or another is preferable, since the ultimate assessment of the tumor stage, and of whether oncological surgery is needed due to deep submucosal infiltration, is made by the pathologist after endoscopic resection.

In conclusion, the only *specific* indications that cannot be investigated with conventional EUS in comparison with miniprobe ultrasonography are those involving IDUS. Nevertheless, advocates of the miniprobe appreciate the high resolution it provides and its rapid availability in connection with endoscopy.

■ Conventional Radial EUS Versus Conventional Longitudinal EUS

Most data on the accuracy of EUS in the staging of gastrointestinal tumors are derived from studies conducted with radial scanners in the 1980s. The number of

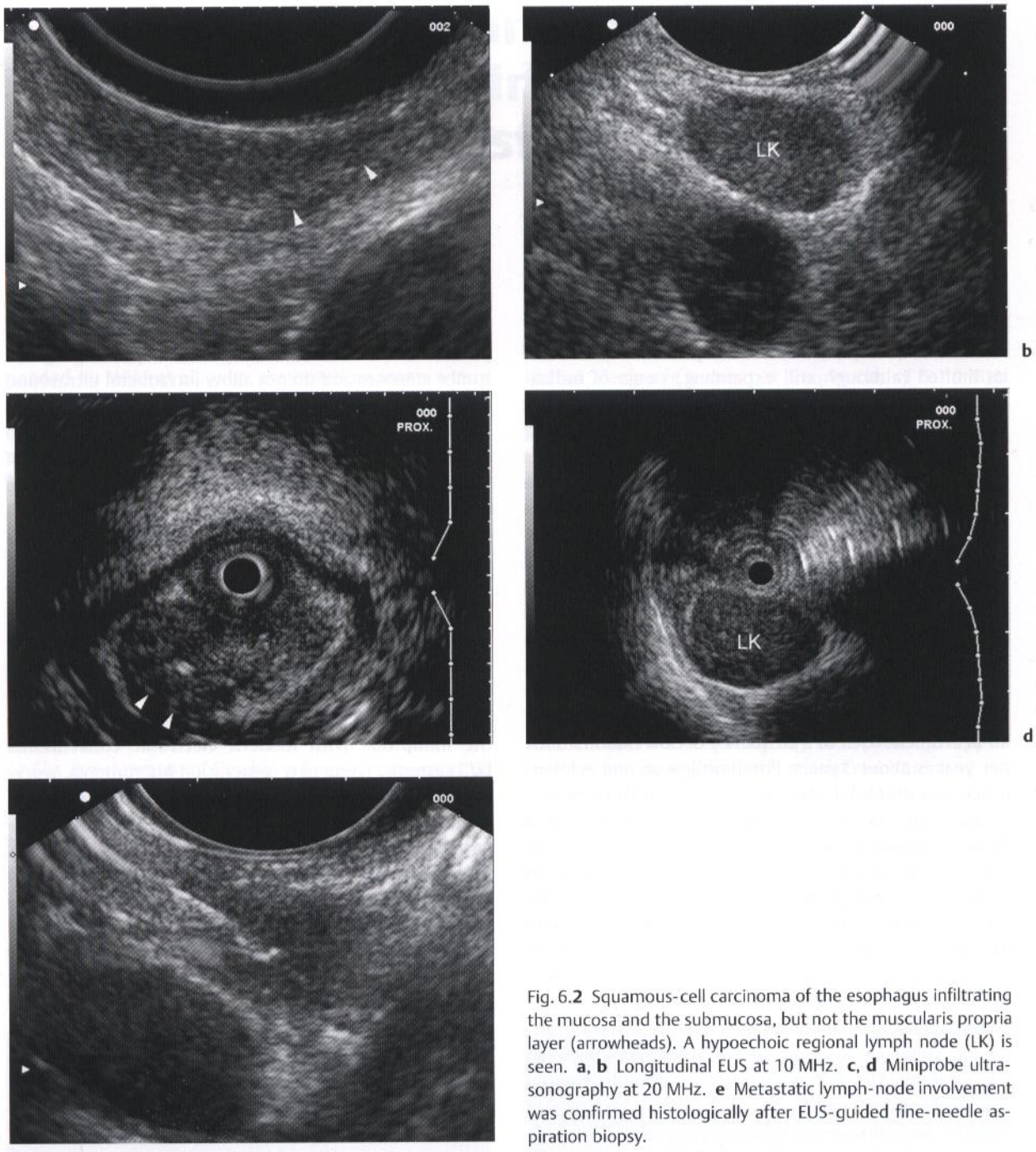
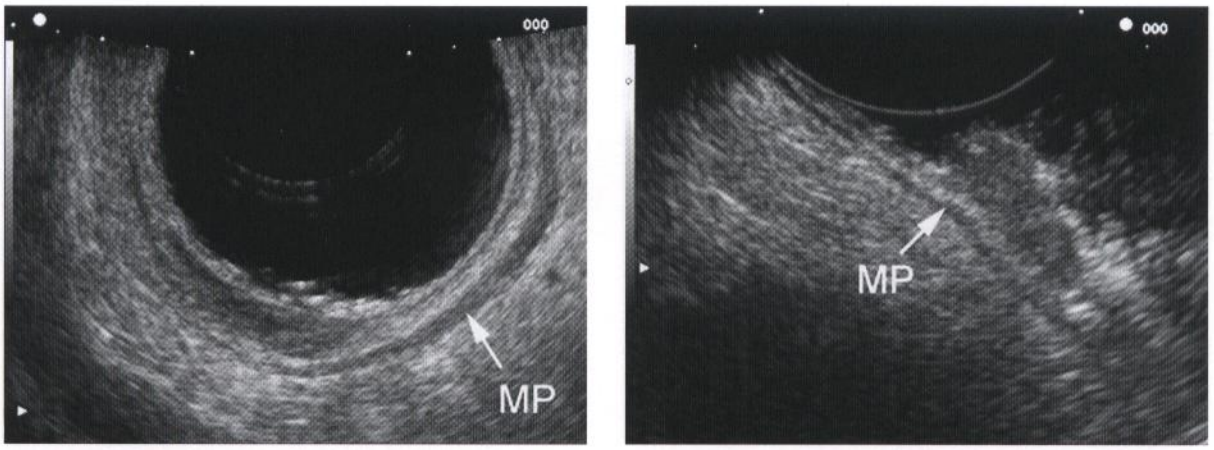


Fig. 6.2 Squamous-cell carcinoma of the esophagus infiltrating the mucosa and the submucosa, but not the muscularis propria layer (arrowheads). A hypoechoic regional lymph node (LK) is seen. **a**, **b** Longitudinal EUS at 10 MHz. **c**, **d** Miniprobe ultrasonography at 20 MHz. **e** Metastatic lymph-node involvement was confirmed histologically after EUS-guided fine-needle aspiration biopsy.

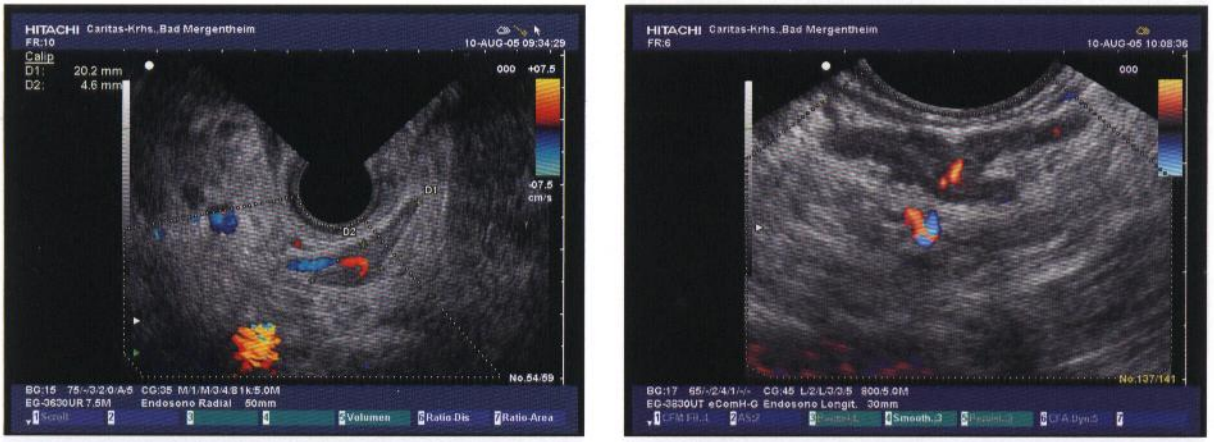
studies dealing with the diagnostic capabilities of linear EUS is still small. The quality of radial and linear EUS is probably comparable in the staging of pancreatic cancer [14], the evaluation of suspected pancreatic disease [15], and the detection of bile duct stones [16,17]. Although longitudinal EUS is widely used for the staging of gastrointestinal wall tumors, there has only been one prospective study demonstrating that linear and radial EUS are equivalent in the staging of esophageal cancer [18]. In contrast to the 1980s, only early-stage esophageal and rectal carcinomas are primarily operated on nowadays. If EUS reveals a locally advanced tumor stage, patients primarily undergo neoadjuvant therapy. The conditions for conducting studies comparing EUS results and the pathological tumor stage have therefore significantly changed. Nevertheless, the few data currently available suggest that linear EUS is not poorer than radial EUS in the assessment of gastrointestinal wall tumors.

The decisive difference between radial and longitudinal EUS is that the linear technique allows biopsies to



a b

Fig. 6.**3** A malignant rectal polyp in the mucosa, with no infiltration into the submucosa. The same result is convincingly demonstrated with both rigid radial EUS (**a**) and flexible longitudinal EUS (**b**). MP: muscularis propria.



a b

Fig. 6.**4** A normal adrenal gland (between the markers), displayed with radial scanning (**a**) and longitudinal scanning (**b**). The adrenal hilum and adrenal vessels are delineated with both methods. Miniprobe ultrasound via the longitudinal probe was of no value (not shown).

be taken and interventions to be carried out with real-time EUS guidance. Many studies have shown that EUS-guided FNAB of lymph nodes, pancreatic lesions, the left adrenal gland, and other structures close to the gastrointestinal tract is safe and highly accurate [19–21]. The frequency of punctures is about 20–30% of all EUS examinations in centers offering this method. The complication risk is low. The short distances between the tip of the instrument and the targeted lesion minimize the risk of tract metastases. Lymph nodes as small as 3–5 mm can be reliably punctured and the question of whether there is metastatic nodal disease in pancreatic carcinoma can be explored before surgery. Lymph nodes and tumors in the dorsal mediastinum can be evaluated histologically. As the more invasive method, mediastinoscopy can be replaced in a significant proportion of patients.

EUS was initially carried out in large university medical centers, from which initial experience was reported and the development of the radial EUS examination technique was promoted and spread. Examiners who have learnt EUS in these centers and left to work in peripheral hospitals are most familiar with the radial technique. Consequently, longitudinal scanners are still not used for diagnostic EUS in many centers, mainly because of the different orientation and examination technique, which is thought to be more difficult. Longitudinal EUS is often carried out for biopsy in addition to previous diagnostic radial EUS.

Our experience shows that the learning curve for linear EUS can be shortened through structured training and by taking a systematic approach toward EUS anatomy [22]. We therefore believe that the conventional linear probe is an all-round instrument that has no significant disadvantages in comparison with the radial system (Fig. 6.**3**).

Figures 6.**4**–6.**8** present comparisons of EUS systems in different organ systems. In all of the patients, longitudinal and radial scanning were of similar value,



a



b



c

Fig. 6.5 A pancreatic metastasis in a patient with adrenal gland carcinoma, displayed with the radial (**a**) and longitudinal (**b**) techniques. **c** Elastography is also possible with both techniques; the longitudinal technique is illustrated here, indicating inhomogeneous elasticity.



a



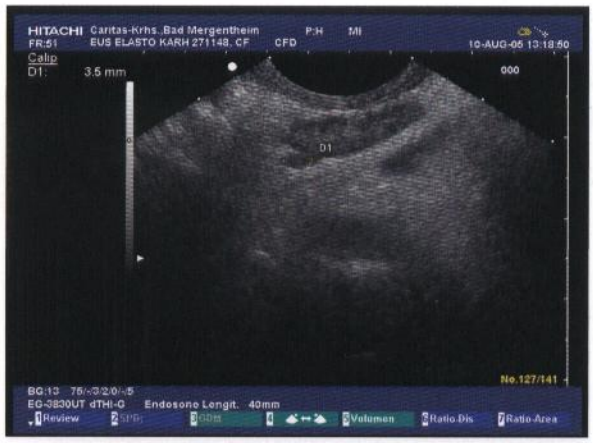
b

Fig. 6.6 Subcarinal lymph nodes. Normal subcarinal lymph nodes can be displayed with the radial (**a**) and longitudinal (**b**) techniques.

Fig. 6.6c, d ▷



c



d

Fig. 6.**6** Pathological lymph-node infiltration (about 4 mm) can also be displayed with both methods (**c**, **d**), whereas tumor puncture is only possible with the longitudinal scanner. Miniprobe ultrasound via the longitudinal probe was of no value (not shown). PA: pulmonary artery; T: tumor.



a



b



c



d

Fig. 6.**7** Large fold gastritis associated with *Helicobacter pylori* infection, displayed using longitudinal scanning (**a**), radial techniques (**b**), and miniprobe technology via the longitudinal echoendoscope (**c–e**). RFG: Riesenfaltengastritis (= large mucosal fold gastritis), see also page 42 Fig. 6.**7e**

Fig. 6.**7e** ▷



Fig. 6.7e see also Fig. 6.7a–d



a



b



c



d

Fig. 6.8 Rectal carcinoma with T1 sm3 infiltration, displayed with radial scanning (**a**, **b**) and miniprobe (**c**, **d**). Longitudinal scanning was of less value. MU: muscularis propria.

whereas the miniprobe was advantageous in the gastrointestinal wall.

■ Which Is the EUS Technique of the Future?

As EUS-guided FNAB is indispensable for all EUS examiners, one can conclusively recommend linear probes as all-round instruments for users who only want to purchase a single system. This is particularly so since lon-

gitudinal EUS is equivalent or even better than radial EUS for plain diagnostic imaging. Special indications that require miniprobes (e.g., stenoses, IDUS) are relatively rare and can be dealt with after bougienage or with extraductal ultrasonography using the standard linear probe. However, miniprobes are a useful addition to the EUS equipment if affordable and if the specific indications are encountered in the department. Only large EUS centers will be able to justify the purchase of all three of the EUS systems described.

References

1. Howry DH, Bliss WR. Ultrasonic visualization of soft tissue structures of the body. J Lab Clin Med 1952;40:579–92.
2. Wild JJ, Reid JM. In: Kelly E, Editor. Ultrasound in Biology and Medicine. American Institute of Biological Sciences 1957;1:30–45.
3. Strohm WD, Phillip J, Hagenmuller F, Classen M. Ultrasonic tomography by means of an ultrasonic fiberendoscope. Endoscopy 1980;12:241–4.
4. Lux G, Heyder N, Lutz H, Demling L. Endoscopic ultrasonography: technique, orientation and diagnostic possibilities. Endoscopy 1982;14:220–5.
5. Vilmann P, Khattar S, Hancke S. Endoscopic ultrasound examination of the upper gastrointestinal tract using a curved-array transducer: a preliminary report. Surg Endosc 1991;5:79–82.
6. Vilmann P, Hancke S, Henriksen FW, Jacobsen GK. Endosonographically-guided fine needle aspiration biopsy of malignant lesions in the upper gastrointestinal tract. Endoscopy 1993;25:523–7.
7. Meyer CR, Chiang EH, Fechner KP, Fitting DW, Williams DM, Buda AJ. Feasibility of high-resolution, intravascular ultrasonic imaging catheters. Radiology 1988;168:113–6.
8. Gussenhoven WJ, Essed CE, Frietman P, Mastik F, Lancee C, Slager C, et al. Intravascular echographic assessment of vessel wall characteristics: a correlation with histology. Int J Card Imaging 1989;4:105–16.
9. Yock PG, Linker DT, Angelsen BA. Two-dimensional intravascular ultrasound: technical development and initial clinical experience. J Am Soc Echocardiogr 1989;2:296–304.
10. Engstrom CF, Wiechel KL. Endoluminal ultrasound of the bile ducts. Surg Endosc 1990;4:187–90.
11. Menzel J, Domschke W, Brambs HJ, Frank N, Hatfield A, Nattermann C, et al. [Mini-probe ultrasound of the upper gastrointestinal tract: 1995 state of the art and perspectives. Workshop on Mini-Probe Ultrasound in Gastroenterology, Münster, 28 October 1995; in German.]. Ultraschall Med 1996;17:143–8.
12. Pfau PR, Ginsberg GG, Lew RJ, Faigel DO, Smith DB, Kochman ML. Esophageal dilation for endosonographic evaluation of malignant esophageal strictures is safe and effective. Am J Gastroenterol 2000;95:2813–5.
13. Wallace MB, Hawes RH, Sahai AV, Van Velse A, Hoffman BJ. Dilation of malignant esophageal stenosis to allow EUS guided fine- needle aspiration: safety and effect on patient management. Gastrointest Endosc 2000;51:309–13.
14. Gress F, Savides T, Cummings O, Sherman S, Lehman G, Zaidi S, et al. Radial scanning and linear array endosonography for staging pancreatic cancer: a prospective randomized comparison. Gastrointest Endosc 1997;45:138–42.
15. Kochman ML, Elta GH, Bude R, Nostrant TT, Scheiman JM. Utility of a linear array ultrasound endoscope in the evaluation of suspected pancreatic disease. J Gastrointest Surg 1998;2:217–22.
16. Kohut M, Nowakowska-Dulawa E, Marek T, Kaczor R, Nowak A. Accuracy of linear endoscopic ultrasonography in the evaluation of patients with suspected common bile duct stones. Endoscopy 2002;34:299–303.
17. Lachter J, Rubin A, Shiller M, Lavy A, Yasin K, Suissa A, et al. Linear EUS for bile duct stones. Gastrointest Endosc 2000;51:51–4.
18. Siemsen M, Svendsen LB, Knigge U, Vilmann P, Jensen F, Rasch L, et al. A prospective randomized comparison of curved array and radial echoendoscopy in patients with esophageal cancer. Gastrointest Endosc 2003;58:671–6.
19. Janssen J, Johanns W, Luis W, Greiner L. [Clinical value of endoscopic ultrasound-guided transesophageal fine needle puncture of mediastinal lesions; in German]. Dtsch Med Wochenschr 1998;123:1402–9.
20. Dietrich CF, Wehrmann T, Hoffmann C, Herrmann G, Caspary WF, Seifert H. Detection of the adrenal glands by endoscopic or transabdominal ultrasound. Endoscopy 1997;29:859–64.
21. Fritscher-Ravens A, Sriram PV, Bobrowski C, Pforte A, Topalidis T, Krause C, et al. Mediastinal lymphadenopathy in patients with or without previous malignancy: EUS-FNA-based differential cytodiagnosis in 153 patients. Am J Gastroenterol 2000;95:2278–84.
22. Janssen J, Greiner L. Examination technique and general principles. In: Rösch T, Will U, Chang KJ. Longitudinal endosonography: atlas and manual for use in the upper gastrointestinal tract. Berlin: Springer, 2001:11–9.

7 Ultrasound Contrast Agents and Contrast-Enhanced Ultrasonography

C. Greis, C.F. Dietrich

Introduction

Imaging the internal organs is crucially important for identifying diseases and for treatment and follow-up. Diagnostic imaging has made tremendous technological progress in recent years, making possible ever more advanced and more detailed examinations of anatomy and physiology. In addition to techniques such as multislice computed tomography (CT), whole-body magnetic resonance imaging (MRI) and positron-emission tomography (PET), which require large and expensive machines, there is still a substantial need for easily available, patient-friendly, and inexpensive methods such as ultrasonography. However, the technique needs to fully meet the standards of modern diagnostic imaging in all respects.

These requirements have become substantially more demanding over the years. Following the introduction of contrast agents, the original simple imaging of anatomical structures was extended to the imaging of the blood supply (vessels and perfusion) and, most recently, the imaging of molecular structures (molecular imaging) with the aid of tissue-specific contrast agents. All such investigations can in principle be carried out with sonography as well. This chapter provides an overview of the contrast agents currently available, with their most important properties, and of contrast-specific sonographic techniques that allow selective imaging of contrast agent signals.

The basis of all sonographic examinations is B-mode sonography, which uses differences in echogenicity in tissue to produce detailed high-resolution images of anatomical structures. In addition, Doppler sonography allows imaging of the blood flow in vessels and the derivation of spectra for the quantitative determination of blood flow over time. However, Doppler sonography has serious limitations: it only functions at fairly high flow rates (greater than the wall motion), for flow in a defined direction toward or away from the transducer, and for adequate flow volumes. Imaging of capillary flow (small volumes, very slow speeds), particularly in tumors with complex vascular architecture, is not possible using this technique. For this purpose, contrast agents that allow the imaging of blood on the basis of specific parts of the contrast-agent signal are required.

Ultrasound contrast agents were originally developed in order to improve the contrast of weak (noisy) echo signals, but a combination with contrast-specific scanner techniques made a completely new application available: B-mode imaging of very small quantities of contrast agent (equivalent to blood volumes) in tissue (parenchyma). This requires sensitive detection (right down to the individual microbubbles) and selective detection (to distinguish between tissue signals and noise) of the contrast agent, making it possible to image the blood supply in tissue.

This type of contrast-specific sonography firstly allows the imaging of vascularity and vessel geometry in organs (capillary volume); and secondly can image and quantify the passage of a contrast agent bolus through the vascular system in real time (capillary flow). Capillary volume and capillary flow are the determinants of parenchymal perfusion.

Historical Background

The principle of ultrasound contrast agents has been known for more than 30 years, since Gramiak and Shah observed strong ultrasound echo signals in blood following the injection of indocyanine green [1]. The signals were formed as a result of air bubbles that were co-administered during the rapid bolus injection. Since that time, the intentional creation of air or gas bubbles of this type has been used to produce echogenic solutions that make the hypoechoic blood visible using ultrasound.

Home-made ultrasound contrast agents of this type were prepared, for example, through vigorous shaking of physiological saline or viscous infusion solutions or by sonicating radiographic contrast agents. As their lack of stability inhibited pulmonary passage, they were mainly used for shunt diagnosis [2,3] or to image myocardial perfusion after intracoronary administration [4,5].

Since 1991, standardized ultrasound contrast agents have been available for right-heart diagnosis (Echovist) and, since 1995, ultrasound contrast agents that are stable on passage through the lungs (Levovist) have been commercially available. Since 2001, second-generation contrast agents containing gases with low solubility in water have been on the market (SonoVue), and have substantially increased the stability and duration of the contrast.

■ Classification of Ultrasound Contrast Agents

Blood Pool Contrast Agents

The original objective in developing standardized ultrasound contrast agents was to obtain products that pass through the lungs, making contrast imaging of the entire vascular system possible after intravenous injection (blood-pool agents). Most products available or in development today fall into this category. Ideally, blood-pool contrast agents should be transported freely in the bloodstream without leaving the vascular bed or accumulating in specific tissues (Table 7.**1**).

Some of these contrast agents do not move perfectly freely with the bloodstream, but have some tissue-specific affinity. This means that they accumulate in specific tissues—e.g., the reticuloendothelial cells in the liver and spleen—at the end of the vascular phase. This effect has been described for Levovist [6,7] and NC100100 [8,9] and can be used diagnostically to identify functional liver tissue in the late, liver-specific, phase (i.e., after the end of the vascular phase). Care needs to be taken to ensure that the late-phase examination is not recorded too soon, to avoid overlap with the portal venous phase.

Tissue-Specific Contrast Agents

These are contrast agents that have a high affinity to specific tissues or molecular structures and which therefore accumulate specifically in these tissues. In principle, this includes the above blood-pool contrast agents with liver-specific late phases. In the narrower sense, however, it is taken to mean contrast agents with a shell containing structures with high molecular affinities (e.g., antibody fragments).

Currently, no tissue-specific contrast agents are available for use in humans, but several substances are in preclinical development [10–14]. Contrast agents of this type make it possible to detect intravascular thrombi, plaques, or inflammation, for example.

Table 7.**1** Blood-pool ultrasound contrast agents: overview of products

Name	Manufacturer	Shell	Gas	Approved
Echovist*	Schering	Galactose	Air	1991
Albunex	Molecular Biosystems	Albumin	Air	1993
Levovist	Schering	Galactose	Air	1995
Optison	GE/Amersham	Albumin	Perfluoropropane	1998
SonoVue	Bracco	Phospholipids	Sulfur hexafluoride	2001
Definity	Bristol-Myers Squibb	Phospholipids	Perfluoropropane	2001 (USA)

* Does not pass through the lungs.

Drug-Delivery Systems

The shells of ultrasound contrast agents can be used not only for the transport of gases or air, but can also transport drugs in the body. The release of these drugs then takes place locally, either through nonspecific rupture of the shell after specific binding to the target tissue (target-specific microbubbles) or by selective local rupture of the freely circulating microbubbles in the target area (e.g., by exposure to ultrasound). Systems of this type can be used for the transport of conventional drugs or even of DNA or RNA fragments (e.g., antisense molecules) [15,16]. After initial in-vitro and in-vivo experiments with stains and marker DNA, studies are now underway with functional DNA and have already resulted in measurable clinical effects in animal studies. It is helpful that ultrasound can be used not just to release the active substance, but also allows penetration into the tissue (sonoporation). Products of this type are already in preclinical testing.

Intracavitary Contrast Agents

These were generally developed as blood-pool contrast agents; however, the administration route is not intravenous, but rather by catheter or needle into a body cavity. Established indications are contrast hysterosalpingosonography to assess the patency of the tubes when investigating fertility [17], and voiding urosonography to investigate vesicoureterorenal reflux, particularly in children [18].

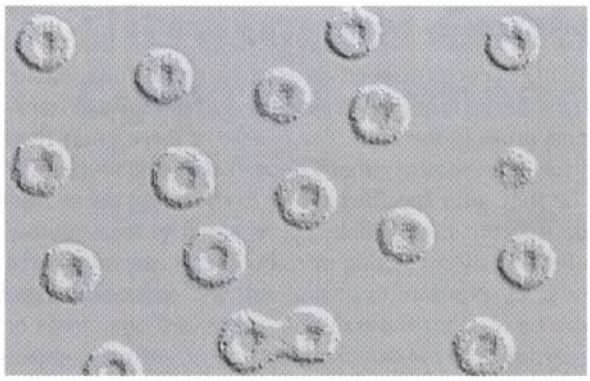
Oral Contrast Agents

These are actually negative contrast agents, as they do not produce echogenicity, but eliminate the interfering echogenicity in the gastrointestinal tract caused by the presence of air. At present, the sole product approved for this purpose has only been approved in the USA (SonoRx). The drinkable liquid contains cellulose fibers that adsorb the air that causes interference, thus allowing overlap-free examination of organs behind the gastrointestinal tract [19].

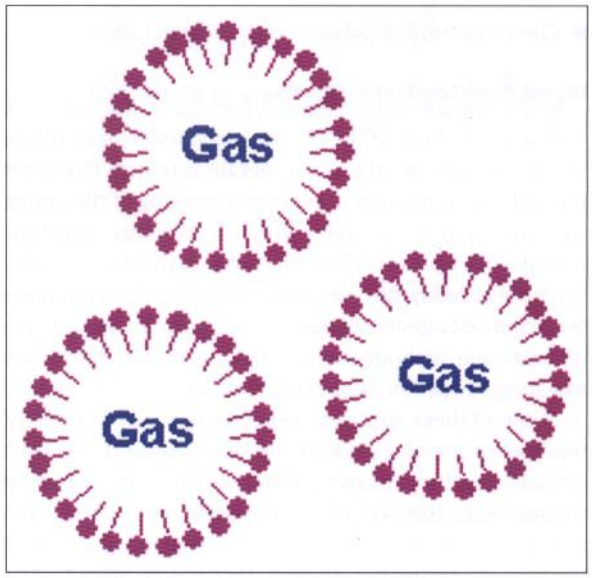
■ Mode of Action of Ultrasound Contrast Agents

Structure

The basic principle of ultrasound contrast agents is the creation of many small interfaces with high echogenicity. This is ideally achieved using gaseous microbubbles. To increase the stability of microbubbles in the blood and achieve a standardized size, the bubbles are surrounded by a shell. There are products with hard shells (e.g., galactose microparticles, denatured albumin) and



a



b

Fig. 7.1 Composition of an ultrasound contrast agent microbubble. Microscopic image (**a**) and schematic configuration (**b**) of SonoVue microbubbles. A flexible outer shell of phospholipids surrounds the enclosed SF6 gas. The phospholipids form a monolayer, with the lipid side facing inward (toward the gas) and the hydrophilic side pointing outward (toward the blood).

products with flexible shell membranes (e.g., phospholipid shells). In terms of the gas, a distinction is made between products containing air (first-generation products) and those with low-solubility gases (second-generation products) (Fig. 7.**1**). The latter produce longer-lasting contrast, as the gas they contain only dissolves slowly in the surrounding blood.

The microbubbles usually have a diameter of 2–10 µm, which is about the size of the red blood cells. Unlike common CT and MRI contrast agents, therefore, they do not pass into the interstitial fluid, but remain confined to the vascular system (blood-pool contrast agents). This substantially simplifies the assessment of tissue perfusion, as the contrast agent distribution can be considered equivalent to the distribution of the blood. Luckily, the resonance frequency of microbubbles of this size is in the region of the sound frequencies used for diagnostic imaging, which makes it possible to generate a harmonic response.

Echogenic Properties

When sound waves strike the microbubbles, they are reflected from the surface. More precisely, the process is known as backscattering. The backscattered sound waves have the same wavelength as the emitted sound waves. This backscattering behavior is referred to as the linear behavior of the microbubbles. The microbubbles in ultrasound contrast agents are very effective backscatterers. They increase the signal intensity by more than 30 dB [20], which corresponds to a factor of 1000 in the received sound intensity.

However, as the sound pressure increases, nonlinear behavior of the microbubbles becomes increasingly prominent. The bubbles first start to oscillate, sending out harmonic oscillations [21,22], and then, as the sound pressure increases further, the microbubbles become unstable, start to split up, and finally break down. In the process, they send out a brief high-energy signal (stimulated acoustic emission, SAE) [23,24] (Fig. 7.**2**).

In principle, all ultrasound contrast agents show this behavior, but the absolute level of sound energy at which the harmonic response and the rupture of the microbubbles sets in varies from one contrast agent to another. Microbubbles with flexible shells start to oscillate at low sound energies and show pronounced harmonic behavior. Hard-shelled contrast agents, on the other hand, give a very good SAE signal on rupture.

During oscillation, the microbubbles produce a nonlinear echo signal [25]. This is because the compression of the microbubbles against the pressure of the inner gas content is less than the expansion. This leads to asymmetrical fluctuation of the bubble diameter, which is no longer linearly dependent on the sound pressure (Fig. 7.**3**).

Dosage and Administration

Ultrasound contrast agents are usually administered by intravenous bolus injection. To achieve the fastest and most complete possible wash-in of the contrast agent bolus, flushing with 5–10 mL of physiological saline is recommended [26]. The injection should ideally be given in a large-volume arm vein, with the syringe connected to the indwelling cannula directly or via the straight part of a T connector. If there are compelling reasons for interposing an infusion tube, it must be as short as possible and the inner lumen should be not too

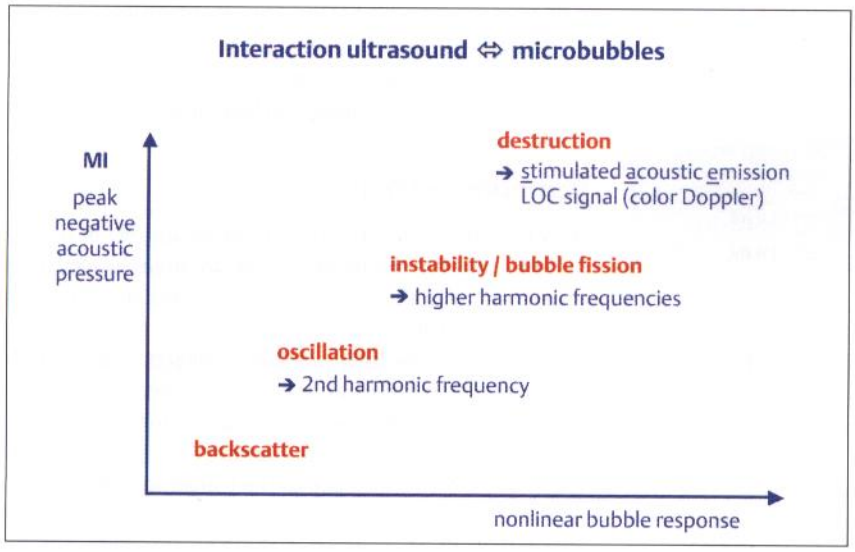


Fig. 7.**2** Behavior of microbubbles as a function of insonation pressure. The behavior of microbubbles in the acoustic field depends primarily on the insonation pressure. If the acoustic pressure is very low, passive backscattering of the input signal occurs. At somewhat higher acoustic pressures, the microbubbles start to oscillate at their resonance frequency. If the acoustic pressure is too high, the microbubbles break down. LOC: loss of correlation; MI: mechanical index.

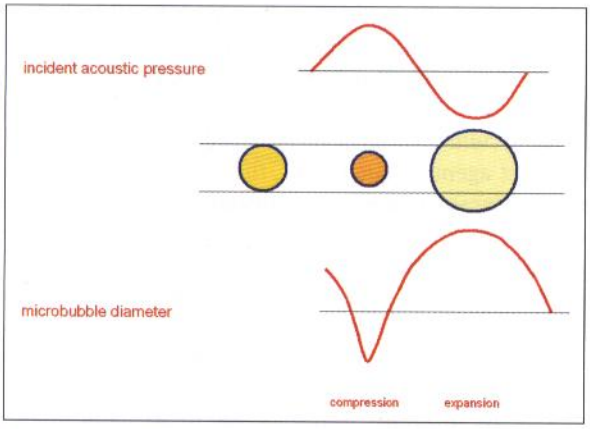


Fig. 7.**3** Oscillation of microbubbles in a sound field. Compression of the microbubbles during the high-pressure phase (against the internal gas pressure) is less than expansion in the low-pressure phase. The fluctuation in the diameter of the microbubbles is therefore asymmetrical and is not a linear function of pressure fluctuation—a nonlinear response.

tight. Particularly for measuring perfusion profiles (e.g., to characterize lesions), the injection has to be given rapidly in order to obtain sharp temporal separation.

After the bolus injection, there is a rapid increase in the microbubble concentration, followed by a slow wash-out over several minutes. Attention has to be given to three threshold values (Fig. 7.**4**):

- *System saturation.* This threshold is frequently reached right at the start of contrast wash-in and gives rise to saturation artifacts and (in color Doppler) blooming effects.
- *Attenuation threshold.* Above this threshold, there is a strong echo signal close to the transducer because of the high microbubble concentration; distal to this there is shadowing, like that seen behind hyperechoic tissue structures.
- *Detection threshold.* Below this threshold, the microbubble concentration is too low and the microbubbles can no longer be detected.

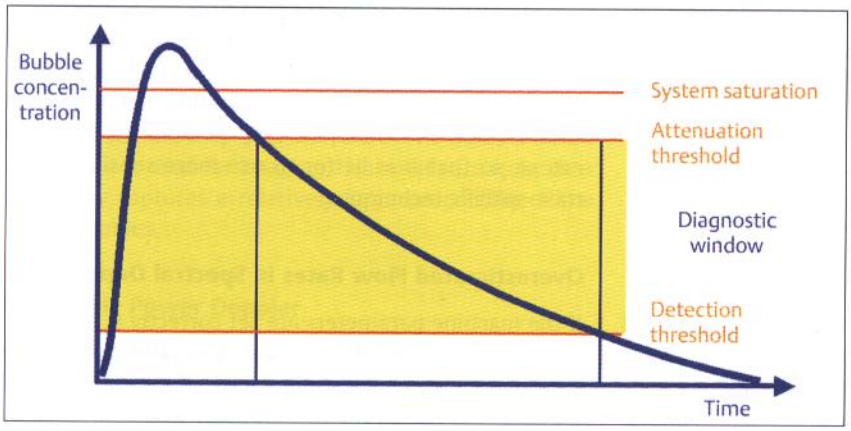


Fig. 7.**4** Course of the microbubble concentration in blood after bolus administration. After bolus injection, there is a rapid increase in the contrast-agent concentration up to a maximum (peak intensity), followed by a somewhat slower wash-out phase. If the attenuation threshold or even system saturation is reached at the maximum, artifacts such as shadowing or blooming can occur.

Table 7.2 Recommended doses of different ultrasound contrast agents

Product	Concentration	Dose
Levovist	200 mg/mL	10–16 mL
	300 mg/mL	5–10 mL
	400 mg/mL	5–8 mL
Optison		0.5–3.0 mL
SonoVue		2.0–2.4 mL

The diagnostic window within which the bubble concentration is optimal for imaging is located between the detection threshold and the attenuation threshold. The absolute level of these thresholds depends on the machine used, the contrast software installed, and the machine settings. Most machines now have presets suitable for contrast agents, allowing rapid selection of the most important parameters for optimal contrast imaging.

The signal strength (gray value or power Doppler intensity) is an approximately linear function of the bubble concentration, allowing quantitative assessment of the perfusion. However, this only applies at contrast agent concentrations that are not too high (below the attenuation threshold).

The optimal dose of contrast agent depends, among other things, on the technique used (B-mode, Doppler, harmonic mode, etc.), the settings and sensitivity of the ultrasound machine, the target organ, and the contrast enhancement required. With the newer second-generation contrast agents, doses of 1–5 mL are usually adequate. The quantity of gas they contain is very low (e.g., only 8 µL/mL in the case of SonoVue), which illustrates the high sensitivity of contrast agent imaging. The dosages shown Table 7.2 are recommended as standard values.

If longer contrast times with uniform contrast enhancement are required, a continuous infusion of microbubbles can be given [26,27]. The infusion rate has to be adjusted so as to give uniform contrast without saturation artifacts. For longer infusion times, it should be noted that the microbubbles float toward the top of the carrier liquid over time and become concentrated in the surface of the liquid in the syringe. Regular, or preferably continuous, mixing of the solution is recommended (e.g., with special infusion pumps).

■ Artifacts Caused by Contrast Agents

Saturation Artifacts

The high amplitude of the backscattered signal can lead to saturation of the receiver electronics at high microbubble concentrations. In color Doppler, this takes the form of smearing of the color signal (color blooming), which also occurs at high color amplification or transmitter power [28]. This effect often occurs shortly after wash-in of the contrast agent and disappears as the microbubble concentration declines again.

Destruction Artifacts

At very high sound pressures, large quantities of microbubbles become unstable and finally break down. This gives rise to high energy signals (stimulated acoustic emission). If these signals mix with normal backscattered signals, they lead to an artificial echo image (bubble noise) [28]. However, when such signals are generated deliberately, they can be used for imaging.

The destruction of microbubbles in regions of high sound pressure (e.g., close to the transducer in the focal plane) can also lead to attenuation phenomena that simulate lack of contrast enhancement. This can be avoided by reducing the sound energy and/or lowering the focal plane.

During sonography of regions with low blood-flow velocities (capillary beds) that section of the image only fills up again very slowly after destruction of the microbubbles. This can lead to bleaching of the contrast effect in tissue, which could be misinterpreted as an absence of contrast agent. In such cases, the perfusion can still be imaged by sonography at a reduced imaging rate (intermittent imaging) [29,30]. Individual images (frames) are recorded and displayed as still images until the next frame is captured. The length of the delay is normally 1–10 s (i.e., 1 frame is recorded every 1–10 s), depending on the strength of the blood flow. Recording of the frames can also be synchronized with the cardiac pulse (triggered imaging). However, in newer procedures, bubble rupture is usually avoided by reducing the transmission power (i.e., using a low mechanical index procedure).

Shadow Artifacts

If the microbubble concentration is too high, very strong echo signals are produced close to the transducer, leading to shadowing or attenuation of deeper-lying structures [31]. The effect corresponds to the attenuation phenomenon behind very echogenic structures. Increasing the signal intensity by administering higher doses of contrast agent is therefore only possible to a limited extent, so that it is better to use more sensitive, contrast-specific techniques.

Overestimated Flow Rates in Spectral Doppler

If the machine parameters are set correctly (i.e., amplification, wall filter, etc.), correct flow rates can also be measured with contrast-enhanced ultrasonography. If the signal is too strong, the Doppler gain may have to

be reduced. There may be differences in the measured values in comparison with ultrasonography without contrast enhancement, if the maximum flow rate (i.e., the upper limit of the Doppler spectral curve) is not detected because the signal strength is too low [28,32]. This is often the case for pathological flow in small volumes (e.g., flow in a stenosis, reflux jet, or shunt flow). In this situation, contrast enhancement contributes to more reliable measurement.

■ Contrast-Specific Imaging Procedures

Contrast-specific imaging procedures make use of the nonlinear behavior of the contrast-agent microbubbles for selective imaging of the ultrasound contrast agent, and thus of the blood volume.

There are numerous technical approaches to separating the (nonlinear) contrast-agent echo from the (linear) tissue echo and the artifact echoes (noise, speckle, clutter, motion artifacts in Doppler, etc.). The objective of each of these procedures is to optimize the contrast–tissue ratio and the contrast–noise ratio.

Frequency Filter Procedures

In frequency filter procedures (harmonic imaging), the nonlinear signals in the region of the second harmonic frequency (i.e., twice the transmitted frequency) are separated out by means of a filter. Thus, only a part of the frequency spectrum that consists exclusively of nonlinear signals is used for imaging. The filter removes those parts of the signal at the fundamental frequency f0 and only those signals in the region of the second harmonic frequency are used for imaging (Fig. 7.**5**).

The advantage of this procedure that it reduces the tissue signal (although, because of the formation of harmonics during the propagation of the sound wave, the echoes are not completely suppressed) and provides a clear reduction in noise artifacts (e.g., clutter). The contrast signal is thus more intense in comparison with the tissue (signal–tissue ratio) and noise (signal–clutter ratio), but not completely selective. The disadvantage of harmonic imaging is the need to use narrow-band transducers with lower resolution (to avoid overlapping of the two frequency bands) and the high sound energy required (as the most intense part of the backscattered signal is not used for imaging). Harmonic imaging thus generally ruptures a relatively large proportion of the microbubbles.

Harmonic Power Doppler

Color Doppler uses an autocorrelation procedure to calculate the Doppler signal—i.e., it compares two echoes recorded a short time apart and interprets changes as

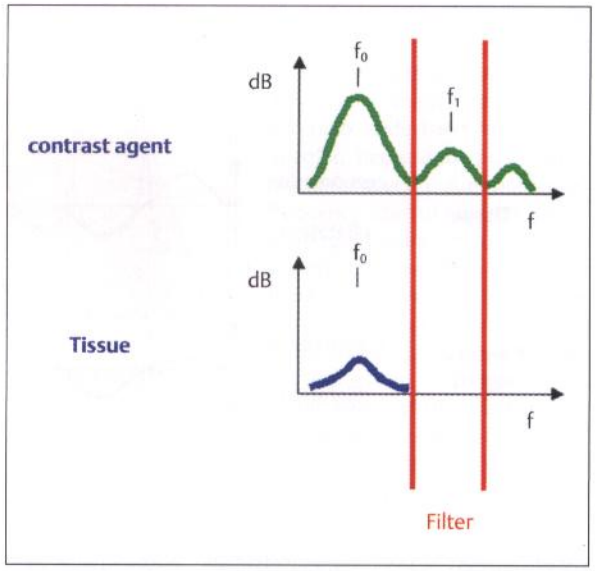


Fig. 7.**5** The principle of harmonic imaging. In harmonic imaging, contrast-specific parts of the signal are separated from tissue signals using a frequency filter. However, this also suppresses nonlinear signals in the range of the fundamental frequency.

movement. As mentioned above, harmonic imaging uses high sound energies, rupturing a relatively large number of microbubbles. Color Doppler interprets the disappearance of the microbubbles (erroneously) as very rapid movement and displays the corresponding color-coded signal on the monitor. It thus gives rise to a microbubble-dependent "Doppler" signal of high intensity (and random direction). In regions of very low blood flow (such as capillary regions)—i.e., where there is no velocity-based Doppler signal—harmonic power Doppler can be used to image the distribution of microbubbles (perfusion imaging). In this case, high intensity (bright signal) means a large number of microbubbles, and thus a high blood volume.

The advantage of this procedure is real-time subtraction of the background signal (tissue) and a color-coded image corresponding to the microbubble concentration (if the machine settings are correct). The disadvantage is high sensitivity to motion artifacts.

Pulse Summation Procedures

Pulse summation procedures (pulse inversion, phase inversion, or wide-band harmonic imaging) use a completely different technique to separate nonlinear and linear signals (Fig. 7.**6**). Several consecutive sound waves from a single scan line are evaluated together. In the simplest case, a positive wave and a negative wave (with inverted phase) are subtracted from one another, resulting in cancellation of the signal. Linear signals are thus not displayed. On the other hand, nonlinear signals (formed due to the different reactions of microbubbles

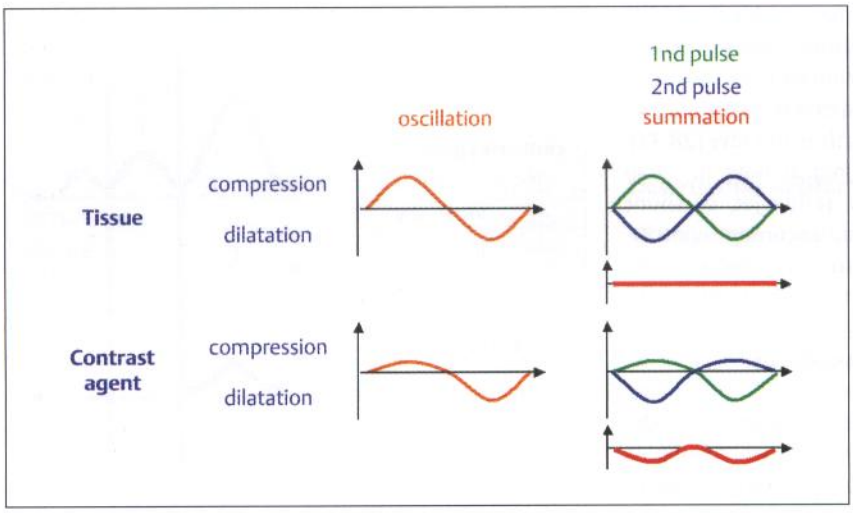


Fig. 7.**6** The principle of the pulse summation procedure (pulse/phase inversion). In the pulse summation procedure, the contrast-specific parts of the signal are separated from the tissue signal by co-evaluation of several successive pulse sequences. This produces very good suppression of the tissue signal and high sensitivity for contrast-agent signals.

Table 7.**3** Imaging procedures specific for contrast agents

Manufacturer	Machine platform	Name of the procedure*
Aloka	ProSound SSD-5500	Extended Pure Harmonic Detection (E-PHD)
Esaote	EsaTune	Contrast Tuned Imaging (CnTI)
	Technos MPX	Contrast Tuned Imaging (CnTI)
GE	Logic 7	Coded Phase Inversion (cPI)
	Logic 9	Coded Phase Inversion (cPI)
Hitachi	EUB 6500	Dynamic Contrast Harmonic Imaging (dCHI-W)
	EUB 8500	Dynamic Contrast Harmonic Imaging (dCHI-W)
Philips	ATL HDI 5000	Pulse Inversion Harmonic Contrast Imaging (PI)
		Power Pulse Inversion Harmonic Contrast Imaging (PPI)
		Agent Detection Imaging (ADI)
		Microvascular Imaging (MVI)
	Sonus 5500	Power Modulation (PM)
	Sonus 7500	Power Modulation (PM)
Siemens	Acuson Sequoia	Coherent Contrast Imaging (CCI) Cadence Contrast Pulse Sequencing (CPS)
	Elegra	Ensemble Contrast Imaging (ECI)
	Antares	Cadence Contrast Agent Imaging (CCAI)
		Cadence Contrast Pulse Sequencing (CPS)
Toshiba	Aplio	Contrast Tissue Discrimination (CTD)

* Manufacturer's trade name.

to positive and negative waves) do not cancel out during this calculation and are displayed [33,34].

Instead of simple pulse inversion, other mathematical techniques (e. g., doubling and subsequent halving of the amplitude, digital coding, etc.) can be used.

All of the main equipment manufacturers now offer one or more contrast-specific imaging procedures. However, all of the procedures are based on one of the two principles, or a combination of the two. A sequential summation image is sometimes also used, allowing reconstruction of the course of the microvessels from the paths of the microbubbles passing through. The manufacturers are constantly improving and further developing the techniques.

In general, all of the procedures either use high sound energy (high mechanical index procedures), with destruction of the microbubbles forming the basis of the signal specific to the contrast agent, or very low sound energy (low mechanical index procedures), in which the persistent oscillation of the microbubbles forms the basis of the contrast-specific signal. The choice of the optimal procedure depends on contrast agent used. Microbubbles with thick, rigid shells are more suitable for high mechanical index (MI) procedures, while those with thin, flexible shells are better for low-MI procedures. Table 7.**3** provides an overview of the contrast-specific procedures currently available.

The significant advantage of pulse summation procedures is that (in contrast to harmonic imaging) wide-band transducers with better spatial resolution can again be used (Fig. 7.**7**). However, because several (short) pulses have to be transmitted per scan line, the frame rate is lower than for normal B-mode images.

As a result of the use of the entire frequency spectrum, the signal strength as a whole is higher than in classical harmonic imaging. In addition to the better spatial resolution, wide-band harmonic imaging produ-

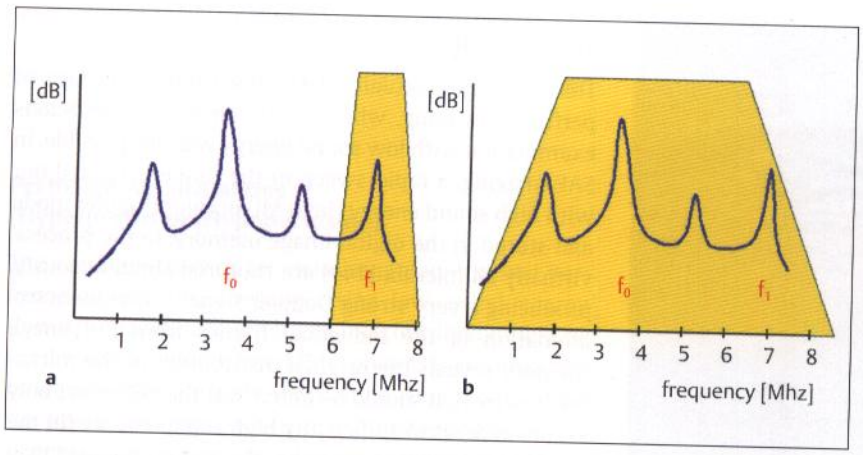


Fig. 7.7 Use of the full bandwidth in the pulse summation procedure (wide-band harmonic imaging). **a** Harmonic imaging (narrow-band). **b** Wide-band harmonic imaging. Because the pulse summation procedure does not use a frequency filter to separate contrast-agent signals from tissue signals, it is possible to use wide-band transducers with better spatial resolution, as in normal B-mode sonography. This is the origin of the term "wide-band harmonic imaging" (**b**), which is sometimes used in contrast to normal harmonic imaging with narrow-band transducers (**a**).

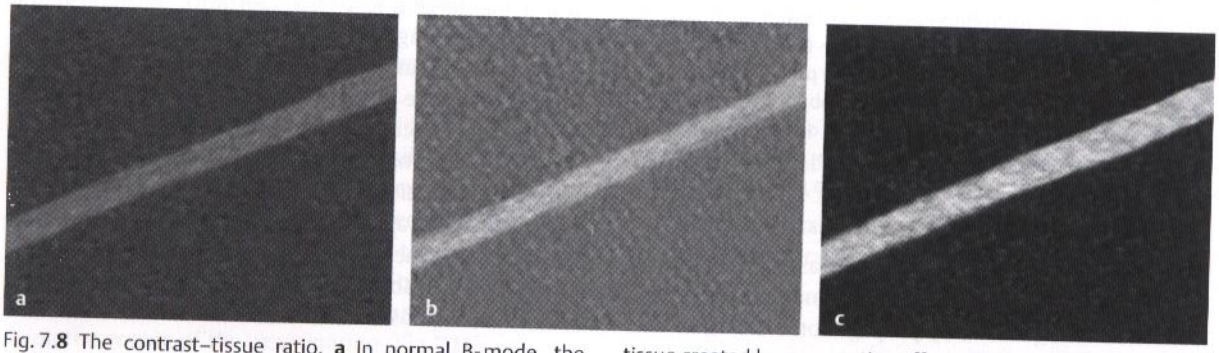


Fig. 7.8 The contrast–tissue ratio. **a** In normal B-mode, the contrast signal from the blood is considerably enhanced, about to the level of the tissue signal. However, this sometimes gives rise to an anti-contrast effect—i. e., the blood and tissue signals reach a similar gray value that can no longer be differentiated. Advantages of B-mode: high spatial resolution and high frame rate; disadvantages: relatively weak contrast signal and no separation from the tissue signal. **b** Harmonic imaging makes the contrast-agent signals relatively stronger and substantially suppresses the tissue signals. However, nonlinear signals from the tissue created by propagation effects (known as tissue harmonics) do appear in the image. Advantages of harmonic imaging (the frequency filter mode): strong contrast signal and high frame rate; disadvantages: reduced spatial resolution and only partial separation from the tissue signal. **c** Pulse summation procedures provide optimal imaging of the contrast-agent signal, with almost complete suppression of tissue signals. Advantages of the pulse summation mode: strong contrast signal, full spatial resolution, and complete separation from the tissue signals; disadvantage: slightly reduced frame rate.

ces a further improved contrast–tissue ratio (with virtually complete suppression of the tissue signal) [34] (Fig. 7.8).

Investigations at Very Low Insonation Power (Low-MI Imaging)

Because pulse summation procedures use the entire frequency spectrum for imaging, the energy backscattered from the microbubbles can be used substantially more effectively. It is therefore possible to use significantly lower transmitter powers than for harmonic imaging, which results in less destruction of the microbubbles. Particularly with newer products with flexible shells (e. g., SonoVue, Definity), it is possible to use minimal sound pressure (mechanical index < 0.1), at which microbubbles oscillate for a long time, emitting strong harmonic signals, without being destroyed. This makes it possible to image parenchymal blood flow with continuous transmission (real-time perfusion imaging) [35].

The transmitter power is nowadays normally shown on the machine monitor as the mechanical index (MI). The MI is calculated from the maximum negative sound pressure divided by the square root of the sound frequency. It should be noted that the actual local sound pressure in the sound field varies greatly because of the beam geometry and the increasing attenuation in deeper layers. In addition, the methods of calculation used by different machine manufacturers are not the same. The absolute MI values can therefore only be taken as indicative, and are not directly comparable from machine to machine.

As a general rule, the harmonic response of the microbubbles does increase with an increasing mechanical

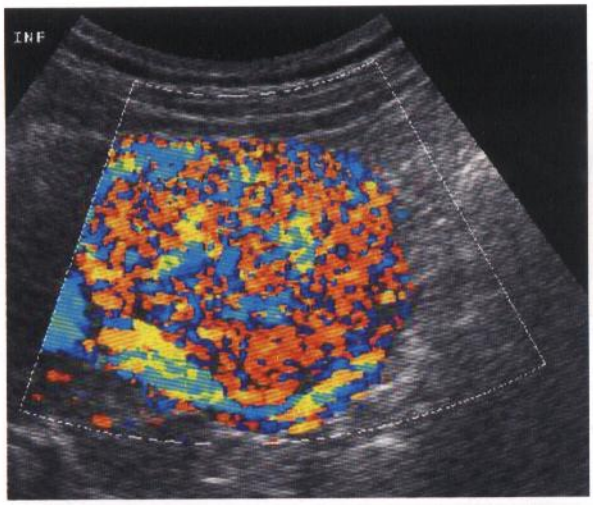


Fig. 7.**9** Stimulated acoustic emission (SAE) imaging. In SAE, virtually all of the microbubbles are destroyed at the same time. This produces a very intense wide-band signal, which can be used as a brief flash for virtually all procedures. In color Doppler, the disappearance of the microbubbles is misinterpreted as rapid movement and therefore displayed as a (chaotic) velocity signal. However, longer-term imaging of the kinetics of the contrast agent is not possible with this method.

index (creating a more intense contrast signal), but (to an even greater extent) so do the harmonic components from the tissue (caused by propagation effects), so that the overall contrast–tissue ratio deteriorates. In addition, destruction of the microbubbles increases. Appropriate adjustment of the insonation power (MI) is therefore essential for good contrast imaging.

Flash Echo Imaging

In general, the objective of this contrast-specific imaging procedure is continuous imaging of the blood supply in tissue, as far as possible without destroying microbubbles. Despite this, in certain situations it may be desirable to briefly destroy all microbubbles in the insonation field during continuous imaging, using a pulse of high sound energy (a flash or burst) [36].

The brief destruction of the microbubbles during a continuous examination in low-MI mode allows imaging of the refilling of the capillary bed (replenishment) and thus the assessment of the dynamics of perfusion [37]. The blood flow in capillaries is so slow that replenishment with new microbubbles takes several seconds. The time until full contrast intensity is reached again (the slope of the replenishment curve) is a measure of the blood flow, whereas the intensity is a measure of the blood volume. Multiplying the two values together provides a parameter for assessing parenchymal perfusion (see the section on quantitative evaluation below).

SAE Imaging

This technique actually dates from the early days of perfusion imaging, when interference-free continuous examination with low sound energy was not possible. In SAE imaging, a rapid sweep of the tissue is carried out with high sound energy (high MI) in color Doppler mode and stored in the digital image memory. In the process, virtually all microbubbles are ruptured simultaneously, producing a very strong Doppler signal. Subsequent examination of the individual frames from the image memory reveals the original distribution of the microbubbles [6,7]. It should be noted that the SAE effect only occurs in areas of sufficiently high sound energy (in the near field); in deeper regions, the sound pressure may be too low to break the microbubbles. Although this is the most sensitive procedure for detecting microbubbles, it has largely lost its importance because of the technical advantages of real-time imaging (Fig. 7.**9**).

SAE imaging can be carried out with any normal color Doppler machine and is technically very simple, as standardized machine settings can be used and image acquisition only has to be carried out once, a few minutes after injection of the contrast agent. This means that the contrast agent can be administered in daylight, before starting the ultrasound examination. However, it is only ever possible to record an instantaneous image, and ultrasound loses its real-time character.

■ Qualitative Evaluation

Vascular Geometry

Contrast-enhanced B-mode sonography can image veins and arteries at a high spatial resolution without blooming and independent of direction. Panorama sweeps and three-dimensional reconstructions are possible [38] (Fig. 7.**10**). The imaging of afferent and efferent vessels and the capillary circulation makes it possible to image vascular abnormalities. Vascular geometry can make an important contribution to the characterization of focal lesions.

The possibility of destruction of microbubbles must be borne in mind when examining blood vessels with contrast-enhanced ultrasonography. In large-volume vessels or vessels with high flow rates, bubbles destroyed in the image plane are rapidly replenished, so that real-time imaging can be carried out with relatively high sound energy. However, in small vessels with low flow rates (e.g., capillary beds), replenishment with fresh contrast agent is very slow, so either a reduced image rate (intermittent imaging) or very low sound energy (low-MI imaging) have to be used for examinations. These effects can be used to produce images with different weighting. Depending on the issue being in-

vestigated, it is possible to image just the afferent vessels with high flow rates (flow-based imaging) or the entire vasculature including capillaries (volume-based imaging).

Perfusion Abnormalities (Hyperperfusion/Hypoperfusion)

The optimal approach for examining parenchymal perfusion is real-time imaging, using low sound energy (low-MI imaging). Intermittent imaging should only be used when a suitable low-MI technique is not available or when extremely high sensitivity is required to detect the tiniest perfusion signals (e.g., to image perfusion in hypovascular metastases). This has to be borne in mind, of course, when interpreting the results, and the description of the vascularity must always be carried out in comparison with the surrounding normal tissue. A more sensitive technique would never change a hypovascular lesion into a hypervascular lesion, even if it did reveal the presence of contrast agent.

Using low sound energy (low-MI imaging), continuous examination of a region is possible, allowing the assessment of a certain region for or repeatedly at different time points. This allows unlimited examination of the organ (e.g., the liver) throughout the period of contrast enhancement, making it possible to detect and simultaneously characterize lesions, and greatly simplifying the course of the examination (Fig. 7.**11**).

The continuous examination allows easy assessment of contrast-agent dynamics in tissue. Contrast ultrasonography has the advantage that the examination can be performed continuously from the start of the injection, so that all phases of perfusion can be observed (even the very early, rapid, processes). This should always be used. Only with very slow, late processes (e.g., in hemangiomas), the examination can be interrupted after about 1 min for periods of about 30 s, to give both the patient and the examiner a rest. When the various flow phases are being examined in liver tissue, it is easy to recognize abnormal uptake of contrast agent in focal lesions and use it diagnostically. The results are comparable with phase images in computed tomography.

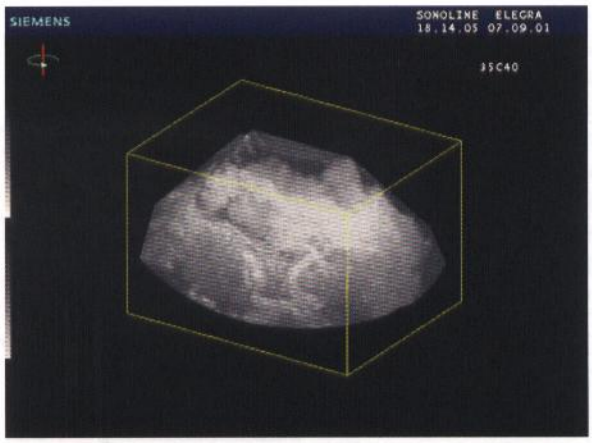


Fig. 7.**10** Three-dimensional representation of the vascular geometry of a lesion. The vascular geometry of the afferent and efferent vessels and of the capillary network of a lesion in the spleen, infiltrated (mainly in the peripheral regions) by a T cell lymphoma.

■ Quantitative Evaluation

Bolus Kinetics

The wash-in and wash-out kinetics of the contrast agent after a bolus injection can also be measured quantitatively. To do this, a region of interest (ROI) is generally specified and the total pixel intensity in this region is recorded as a function of time. The measurement can be carried out off-line from the video signal, or preferably

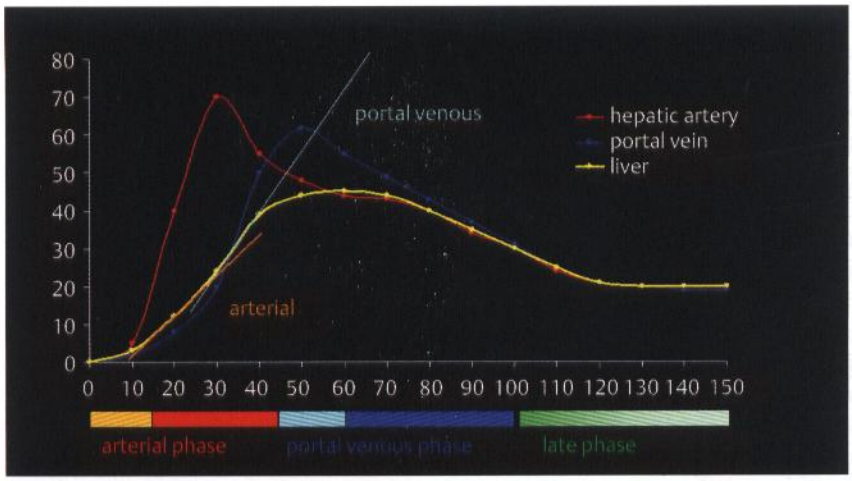


Fig. 7.**11** Contrast phases in the liver. Because of the dual blood supply to the liver through the hepatic artery and portal vein, two separate sets of wash-in kinetics can be observed at different times. Initially, there is contrast enhancement due to wash-in from the hepatic artery (the arterial phase) and then, approximately 30–40 s later, contrast enhancement due to wash-in from the portal vein is seen. Because the normal liver parenchyma is mainly supplied by the portal vein, the contrast enhancement in liver tissue is substantially stronger in the portal venous phase.

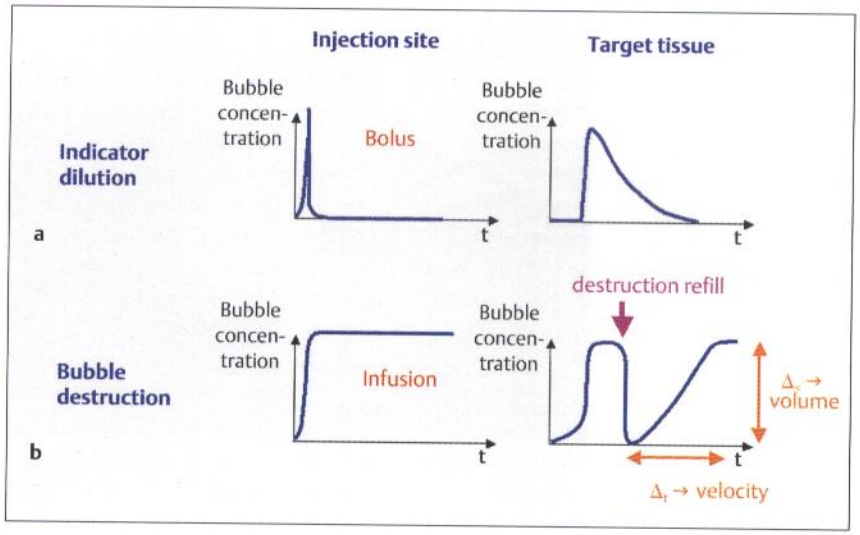


Fig. 7.**12** Bolus and replenishment kinetics. **a** In classical bolus kinetics, the change in contrast in the target tissue is recorded after a fast bolus injection. However, cardiopulmonary passage after an intravenous injection always results in the bolus diffusing apart and being diluted, which adversely affects the temporal resolution. **b** In replenishment kinetics, the increase in the signal occurs as a result of replenishment directly from the afferent vessels after local destruction of the microbubbles in the sound field directly, so that a very high level of temporal resolution is achieved.

from the digital data set in the memory. Care must be taken to ensure that no distortion of the measured values occurs during post-processing in the ultrasound equipment (particularly when using the video signal).

The recording of bolus kinetics follows the principle of indicator dilution theory. For a homogeneous distribution of microbubbles in blood, the height of the washout curve is a measure of the blood volume and the washout time is a measure of the blood flow. However, exact application of this principle requires an exact bolus time point, which is not strictly obtained following an intravenous injection. However, the small injection volume of modern contrast agents is an advantage in this respect.

The major advantage of ultrasound contrast agents and their microbubbles is that they represent a genuine intravascular marker which, unlike other contrast agents (e.g., in CT, MRI, or with nuclear tracers) do not pass into the interstitial space or the intracellular fluid.

Transit Time Analysis

In transit time analysis, a simultaneous continuous measurement is carried out in the afferent and efferent vessels of an organ. The exact time of onset of contrast wash-in is recorded. The transit time—i.e., the time required for blood to flow through an organ—can be determined from the time difference between inflow and outflow. The transit time can be regarded as a measure of the general perfusion of an organ. It is increased in generalized hypoperfusion and shortened in the presence of arteriovenous shunts. Transit time analysis can therefore be used to look for occult hepatic lesions (with arteriovenous shunts).

Replenishment Kinetics

A fundamental problem with using bolus kinetics is the prolonged wash-in time following intravenous injection, which is due to venous pooling and the bolus drifting apart during passage through the heart and lungs. This limits the diagnostic value of the method for rapid wash-in profiles, despite the intravascular character of the microbubbles. The ability to use a single flash to rupture virtually all microbubbles in a capillary bed within fractions of a second opens up fresh scope for this principle.

Instead of wash-in and wash-out of a bolus injection, the replenishment after rupture of the microbubbles can be investigated starting from a constant contrast level. This technique is also known as the negative bolus technique. The initial level of contrast agent can be kept constant—for example, through continuous infusion.

In replenishment kinetics, the intensity is a measure of the blood volume in tissue, and the time taken to return to the previous intensity (or the slope of the refill curve) is a measure of the flow rate. Multiplication of these two parameters provides a measure of perfusion in the tissue. To determine the absolute perfusion (mL/min/g), this value would have to be standardized by weighting it for the tissue in the measured area (Fig. 7.**12**).

Depletion Kinetics

If the destruction of the microbubbles is arranged so that only some of the bubbles in the sound field are destroyed during the recording of one image frame (by adjusting the insonation energy and image rate), fractional signal attenuation is achieved over several frames. The number of frames required until all the microbubbles are destroyed (i.e., until the signal is completely

quenched) depends on the amount of contrast agent present (i.e., the blood volume) and the amount of replenishment between two frames (i.e., the blood flow). The quenching time thus reflects the local perfusion and can be used to investigate relative differences in perfusion. The advantage of this method is the short measurement time (only about 1 s) for the complete kinetics. It is thus possible to measure several sets of kinetics (e.g., in several focal planes) after a simple bolus injection (at the inflow maximum).

Parametric Imaging

Parametric imaging is based on the measurement of wash-out or replenishment curves of this type and the calculation of characteristic, curve-specific parameters (e.g., time to peak, slope of the peak, half-life, area under the curve, etc.). However, the calculation is not carried out for a large region of interest, but separately for each individual pixel. The corresponding curve parameters can be color-coded for each pixel. Thus, for example, flow rate images or volume images can show regions of high flow or volume in brighter colors. Parametric images of this type make it possible to document the complete contrast-agent dynamics on a single image.

■ Clinical Indications for Contrast-Enhanced Ultrasonography

Doppler Signal Enhancement (Vascular Flow)

Originally, ultrasound contrast agents were developed both to image body cavities to improve the delineation of contours (e.g., identification of the endocardium in echocardiography) and especially to enhance the Doppler signal—so they are still often known as signal enhancers, even though their uses now extend far beyond that. Enhancement of the Doppler signal is always necessary if the signal without contrast agent is too weak, or rather if the signal–noise ratio is too poor (otherwise it would be simpler to increase the amplifier setting on the machine). The crucial point is that the contrast agent (the signal enhancer) selectively enhances the useful signal, but not the noise. However, the better the ultrasound machine used, the less need there is for this type of Doppler signal enhancement. Modern high-end color Doppler machines can usually provide an adequate Doppler signal without contrast enhancement.

However, when the signal–noise ratio is inadequate for an unambiguous diagnosis in individual cases, injection of a signal enhancer is the method of choice. This may occur in regions with very low flow volumes, for example (e.g., residual volume in a severe stenosis) or very slow flow (e.g., aneurysms). When there is vascular occlusion, the signal enhancer increases the diagnostic accuracy, because the absence of a flow signal could also be caused by too low a signal strength (below the noise filter) or an unfavorable vessel angle (e.g., in a bend in the vessel).

Signal enhancers are very important in organs that are difficult to examine with ultrasonography, such as the brain, however. Cerebral ultrasonography is only possible through an acoustic window in the skull (transcranial ultrasound), and the sound cone is substantially attenuated. In this case, signal enhancers usually allow a diagnostic examination with a high diagnostic value.

Diagnosis of Ischemia

In contrast to the large vessels, both the signal strength and the flow rate of blood in the capillary beds are too low to produce a detectable Doppler signal. In this case, an ultrasound contrast agent is necessary to allow any imaging of the blood volume at all. The contrast agent does not just function as an image enhancer, but also as a marker, the passage of which through the organ can be observed as a function of time. This allows dynamic assessment of the blood supply (perfusion).

With the aid of additional quantitative techniques, as described above, it is possible to identify and assess regional or global hypoperfusion. For example, it is possible to detect stenosis in the afferent artery as relative ischemia in the upstream parenchyma. This allows hemodynamic quantification of stenoses (e.g., in the renal artery, coronary arteries, etc). If necessary, functional examinations can be carried out as well—e.g., after administration of a vasoactive substance.

Diagnosis of Traumatic Lesions

Blunt traumatic injuries can lead to structural defects in organs that are difficult or impossible to detect with noncontrast ultrasonography, particularly if the capsule is still intact and there is little or no free fluid. After administration of the contrast agent, it is generally possible to recognize all disturbances of the microvascular system clearly. Tissue ruptures appear as a black line in contrasted parenchyma and hematomas as extensive unperfused areas.

Detection of Focal Lesions

Focal lesions are detected either by identifying hyperperfusion or hypoperfusion in comparison with the surrounding tissue, or through changes in the wash-in kinetics of the contrast agent. The classification as hyperperfused or hypoperfused is thus made in comparison with the surrounding normal tissue and is always related to a particular time point. An early arterial hyperperfused lesion may appear hypoperfused during the portal venous phase.

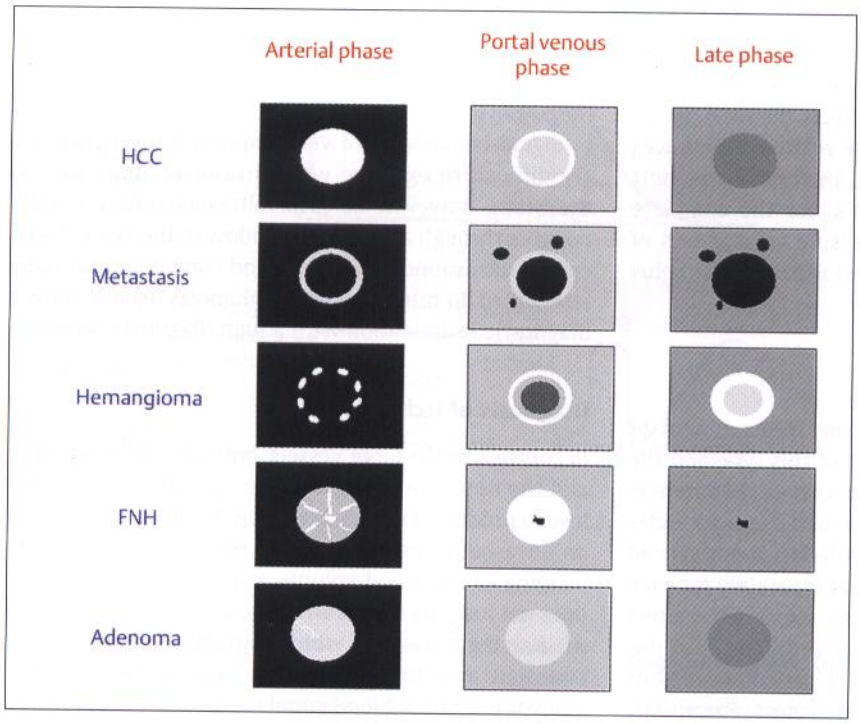


Fig. 7.**13** Characteristic contrast patterns in hepatic lesions. Focal hepatic lesions show characteristic remodeling of the vascular supply, which may include arterialization. The increased arterial supply is usually followed by a reduction in the portal venous supply. This results in temporal and geometric changes in the wash-in profile of the lesion, which can be used for characterization. FNH: focal nodular hyperplasia; HCC: hepatocellular carcinoma.

Hyperperfused lesions can generally be seen during the arterial phase as regions of high contrast enhancement (white spots). On high-intensity sonography (bubble destruction), the high flow rates mean that they show intense contrast at short delay times. On the other hand, hypoperfused lesions can be detected in the portal venous phase as black spots against the clearly contrasted normal liver tissue.

Focal lesions of nonhepatic tissue (e.g., metastases from extrahepatic tumors) can be detected by the absence of accumulation of liver-specific contrast agents (e.g., Levovist). Lesions of this type appear as accumulation defects in the late-phase images.

Characterization of Focal Lesions

In the first place, contrast-enhanced ultrasonography can be used to assess whether a lesion is strongly perfused or not. Modern ultrasound equipment has excellent contrast resolution and can identify even slightly altered regions of the liver (e.g., regional fatty changes) as suspect regions. Such findings are often obtained incidentally in routine examinations and show no symptoms. If no increased arterial perfusion can be seen in such regions, a benign process can usually be assumed.

Because of the double blood supply via the portal vein and the hepatic artery, focal lesions in the liver often do not display general hyperperfusion or hypoperfusion, but a complex temporal and spatial pattern of hyperenhancement and hypoenhancement, depending on the phase of flow. Some lesions have a characteristic vascular pattern (e.g., wheel spokes) or perfusion pattern (e.g., halo contrast, iris diaphragm phenomenon), which makes it possible to characterize the lesion [39]. However, not all lesions show the typical aspects of the particular lesion type, due to hemorrhagic or deteriorating changes. Nevertheless, if a characteristic perfusion pattern is observed and if it corresponds to the patient's clinical picture, a definitive diagnosis can usually be made (Fig. 7.**13**).

Monitoring of Interventions and Treatment Follow-Up

Contrast-enhanced ultrasonography is an excellent method for monitoring and follow-up of percutaneous ablation therapy (alcohol injection, radiofrequency therapy, laser ablation, etc.). Vital and nonvital tissue is very easy to distinguish on the basis of the vascularization. Because monitoring can be carried out during the intervention itself, any necessary further treatment can be initiated immediately, in the same session. Because of the gas artifacts formed during thermoablation, a pause is required between the end of treatment and checking the results. In general, however, an initial assessment of the position and size of the necrotic area is possible 5–10 min after the end of treatment.

With hyperperfused lesions (e.g., hepatocellular carcinomas), care has to be taken to ensure complete ablation of the hyperperfused tissue. However, hyperemic regions around the ablated area as a result of the treatment must not be misinterpreted as hyperperfused tis-

sue. With hypoperfused lesions (e.g., metastases) only indirect assessment of the necrotic area is possible. The contrast defect in the portal venous phase must be larger than the original lesion (about 0.5–1.0 cm as a safety distance).

It is also possible to monitor the outcome of radiotherapy or chemotherapy. Regression of the vascularization allows earlier assessment of the onset of treatment success than is possible simply by assessing the reduction in size. However, this approach still needs to be examined in clinical studies.

■ Safety Aspects

There are four major risks associated with ultrasound contrast agents: the toxicological risk, the embolic risk, the anaphylactic risk, and the generation of biological effects due to ultrasound-induced cavitation.

Ultrasound contrast agents are made up of air or an inert gas and a shell of nontoxic material. They do not contain any components with toxic potential, and are only administered in very small quantities. No toxic effects are known, nor has clinical use revealed any toxic side effects of clinical significance either. In most cases, the injection is tolerated extremely well.

The embolic risk is also negligible, as commercial ultrasound contrast agents consist of microbubbles with a standardized size distribution and pass freely through the capillaries. No signs of induced ischemia have been observed in functional clinical studies of the heart and brain. Even highly sensitive electroencephalography was only found to show mild alerting reactions (caused by the audible pulse sounds of the transducer) with contrast agents and ultrasonography, and no pathological signs [40,41]. An assessment by the European Committee for Medical Ultrasound Safety (ECMUS) concluded that the toxic and embolic potential of ultrasound contrast agents is of no clinical significance [42].

In general, the injection of macromolecular substances and colloidal/particulate solutions involves a certain risk of anaphylactic reactions (triggered by corresponding antibodies) or anaphylactoid reactions (triggered by interaction with mediators, such as histamine) [43]. Macromolecular substances are contained in ultrasound contrast agents as components of the shell (e.g., albumin), and/or as excipients to adjust the osmotic value (e.g., macrogol). In isolated cases, pseudoallergic reactions have been observed after administration of an ultrasound contrast agent. Such pseudoallergic reactions may be comparatively harmless (sensation of warmth, flushing) or even very dramatic (dyspnea, bradycardia, hypotension, anxiety). In such cases, the patient must be treated symptomatically [44,45] (e.g., H1/H2-blockers, glucocorticosteroids, epinephrine if necessary). In patients with severely impaired cardiac function (e.g., coronary heart disease, acute or chronic heart failure) the fall in blood pressure as a result of pseudoallergic reactions can lead to complications, with transient myocardial ischemia. Although pseudoallergic reactions of this type are very rare, the examiner should be prepared for them and appropriate emergency equipment should be available.

One potential risk of ultrasound contrast agents is ultrasound-induced cavitation [46]. In the low-pressure phase of the sound wave, the fluid in the blood can be pulled away from the microbubbles, so that a free gas bubble is formed. In the subsequent high-pressure phase, this gas bubble collapses, releasing a large amount of energy in a small area, which leads to a large rise in temperature. This can lead to the formation of free radicals, electromagnetic radiation (sonoluminescence), and lysis of neighboring cells [42].

The induction of biological effects of this type has been demonstrated many times in in-vitro experiments [47–53], but in conditions that do not correspond to the situation in vivo—using very high contrast agent concentrations (> 0.2%), very long transmitter pulse times (> 2 μs), very high sound energies (MI > 1.9), and/or nonphysiological hematocrit values. No significant biological effects have yet been observed with clinically relevant values for these parameters [52,54].

Numerous experiments have been carried out to detect such biological effects in vivo as well. In most cases, no cavitation was observed, even after the injection of saline containing air bubbles. No endothelial damage was observed [42]. However, transient pores in the endothelium, which close again after a short time (< 1 s), may form. During this time, substances and/or blood components can pass into the tissue. In unfavorable conditions, this could lead to petechial hemorrhage. The extent of this endothelial perforation is directly proportional to the microbubble concentration (i.e., the contrast-agent dose) and the insonation energy used. The use of low doses of contrast (with a gas volume of only a few microliters) and low sound energies (low-MI imaging) substantially reduces this risk. Therapeutically, this effect—known as sonoporation—can be used for targeted drug delivery. The optimal insonation energies, frequencies, pulse sequences, and microbubble concentrations for this are currently being investigated in a number of preclinical studies.

Free radicals are only formed in the blood, and not (as in radiography) in tissue. In the blood, they only survive for a few milliseconds and are captured by blood components. In one experiment in mice, low-grade hemolysis was observed, but it was only < 4% and had virtually no clinical significance [55].

At clinically relevant sound pressures (0.6–1.6 MPa), microbubbles are ruptured relatively slowly (in the order of 1 ms), and cavitation effects only occur after multiple pulses of high intensity [56]. There is a clear

sound-energy threshold for the occurrence of such biological effects. This has led to the introduction of parameters and upper limits for the energy emitted by ultrasound equipment. The best known is the mechanical index (MI) [57], which is shown on the monitor of most machines.

The safety of contrast-enhanced ultrasonography was demonstrated in numerous clinical studies during approval procedures for the contrast agents. No significant changes in the blood or laboratory values have been found after contrast-enhanced examinations. A critical evaluation of the available results by the European Committee for Medical Ultrasound Safety (ECMUS) showed that, although it appears possible for microbubbles or non-degassed saline to increase the probability of ultrasound-induced cavitation, the clinical significance of this effect is small [42]. It was, however, recommended that treatment with high-energy therapeutic ultrasound or lithotripsy should not be carried out within 1 day of the administration of an ultrasound contrast agent.

References

1. Gramiak R, Shah PM. Echocardiography of the aortic root. Invest Radiol 1968;3:356–66.
2. Nemec JJ, Marwick TH, Lorig RJ, Davison MB, Chimowitz MI, Litowitz H, et al. Comparison of transcranial Doppler ultrasound and transesophageal contrast echocardiography in the detection of interatrial right-to-left shunts. Am J Cardiol 1991;68:1498–502.
3. Kasper W, Geibel A, Tiede N, Just H. Patent foramen ovale in patients with haemodynamically significant pulmonary embolism. Lancet 1992;340:561–4.
4. Feinstein SB, Lang RM, Dick C, Neumann A, Al Sadir J, Chua KG, et al. Contrast echocardiography during coronary arteriography in humans: perfusion and anatomic studies. J Am Coll Cardiol 1988;11:59–65.
5. Sabia PJ, Powers ER, Jayaweera AR, Ragosta M, Kaul S. Functional significance of collateral blood flow in patients with recent acute myocardial infarction: a study using myocardial contrast echocardiography. Circulation 1992;85: 2080–9.
6. Blomley MJ, Albrecht T, Cosgrove DO, Patel N, Jayaram V, Butler BJ, et al. Improved imaging of liver metastases with stimulated acoustic emission in the late phase of enhancement with the US contrast agent SH U 508A: early experience. Radiology 1999;210:409–16.
7. Albrecht T, Blomley MJ, Heckemann RA, Cosgrove DO, Jayaram V, Butler BJ, et al. [Stimulated acoustic emissions with the ultrasound contrast medium Levovist: a clinically useful contrast effect with liver-specific properties; in German.]. Röfo Fortschr Geb Rontgenstr Neuen Bildgeb Verfahr 2000;172:61–7.
8. Needlemann L, Blomley M, Albrecht T, Hoffmann CW, Olstad MA, Leen EL. Liver parenchyma contrast-enhanced ultrasound: preliminary results of a multi-center study for liver lesion detection [abstract]. Radiology 2000; 217 (Suppl):305.
9. Leen EL, Albrecht T, Harvey CJ, Goldberg BB, Olstad MA, Cosgrove DO. Multicenter study of Sonazoid-enhanced pulse inversion harmonic imaging in the characterisation of focal hepatic lesions: preliminary results [abstract]. Radiology 2000;217(Suppl):458.
10. Lanza GM, Wallace KD, Scott MJ, Cacheris WP, Abendschein DR, Christy DH, et al. A novel site-targeted ultrasonic contrast agent with broad biomedical application. Circulation 1996;94:3334–40 [published erratum in Circulation 1997;95:2458].
11. Klibanov AL, Hughes MS, Marsh JN, Hall CS, Miller JG, Wible JH, et al. Targeting of ultrasound contrast material: an in vitro feasibility study. Acta Radiol Suppl 1997;412:113–20.
12. Lanza GM, Wallace KD, Fischer SE, Christy DH, Scott MJ, Trousil RL, et al. High-frequency ultrasonic detection of thrombi with a targeted contrast system. Ultrasound Med Biol 1997;23:863–70.
13. Lanza GM, Trousil RL, Wallace KD, Rose JH, Hall CS, Scott MJ, et al. In vitro characterization of a novel, tissue-targeted ultrasonic contrast system with acoustic microscopy. J Acoust Soc Am 1998;104:3665–72.
14. Unger EC, McCreery TP, Sweitzer RH, Shen D, Wu G. In vitro studies of a new thrombus-specific ultrasound contrast agent. Am J Cardiol 1998;81:58G–61G.
15. Price RJ, Skyba DM, Kaul S, Skalak TC. Delivery of colloidal particles and red blood cells to tissue through microvessel ruptures created by targeted microbubble destruction with ultrasound. Circulation 1998;98:1264–7.
16. Shohet RV, Chen S, Zhou YT, Wang Z, Meidell RS, Unger RH, et al. Echocardiographic destruction of albumin microbubbles directs gene delivery to the myocardium. Circulation 2000;101:2554–6.
17. Hamilton JA, Larson AJ, Lower AM, Hasnain S, Grudzinskas JG. Routine use of saline hysterosonography in 500 consecutive, unselected, infertile women. Hum Reprod 1998;13: 2463–73.
18. Darge K, Troeger J, Duetting T, Zieger B, Rohrschneider W, Moehring K, et al. Reflux in young patients: comparison of voiding US of the bladder and retrovesical space with echo enhancement versus voiding cystourethrography for diagnosis. Radiology 1999;210:201–7.
19. Lev-Toaff AS, Langer JE, Rubin DL, Zelch JV, Chong WK, Barone AE, et al. Safety and efficacy of a new oral contrast agent for sonography: a phase II trial. AJR Am J Roentgenol 1999;173:431–6.
20. Kaps M, Schaffer P, Beller KD, Seidel G, Bliesath H, Wurst W. Phase I: transcranial echo contrast studies in healthy volunteers. Stroke 1995;26:2048–52.
21. Schrope BA, Newhouse VL. Second harmonic ultrasonic blood perfusion measurement. Ultrasound Med Biol 1993; 19:567–79.
22. Burns PN. Harmonic imaging with ultrasound contrast agents. Clin Radiol 1996;51(Suppl 1):50–5.
23. Burns PN, Fritzsch T, Weitschies W, Uhlendorf V, Hope-Simson D, Powers JE. Pseudo-Doppler shifts from stationary tissue due to stimulated emission of ultrasound from a new microsphere contrast agent [abstract]. Radiology 1995; 197:402.
24. Blomley MJ, Albrecht T, Cosgrove D, Jayaram V, Patel N, Butler BJ, et al. Stimulated acoustic emission imaging ("sono-scintigraphy") with the ultrasound contrast agent Levovist: a reproducible Doppler ultrasound effect with potential clinical utility. Acad Radiol 1998;5(Suppl 1): S236–9.
25. De Jong N, Frinking PJ, Bouakaz A, Goorden M, Schourmans T, Jingping X, et al. Optical imaging of contrast agent micro-

bubbles in an ultrasound field with a 100-MHz camera. Ultrasound Med Biol 2000;26:487–92.
26. Becher H, Burns PN. Contrast agents for ultrasound. In: Becher H, Burns PN, editors. Handbook of contrast echocardiography. Berlin: Springer, 2000: 5–16.
27. Correas JM, Burns PN, Lai X, Qi X. Infusion versus bolus of an ultrasound contrast agent: in vivo dose-response measurements of BR1. Invest Radiol 2000;35:72–9.
28. Forsberg F, Liu JB, Burns PN, Merton DA, Goldberg BB. Artifacts in ultrasonic contrast agent studies. J Ultrasound Med 1994;13:357–65.
29. Porter TR, Xie F. Transient myocardial contrast after initial exposure to diagnostic ultrasound pressures with minute doses of intravenously injected microbubbles: demonstration and potential mechanisms. Circulation 1995;92: 2391–5.
30. Wei K, Skyba DM, Firschke C, Jayaweera AR, Lindner JR, Kaul S. Interactions between microbubbles and ultrasound: in vitro and in vivo observations. J Am Coll Cardiol 1997; 29:1081–8.
31. Bos LJ, Piek JJ, Spaan JA. Effects of shadowing on the time-intensity curves in contrast echocardiography: a phantom study. Ultrasound Med Biol 1996;22:217–27.
32. Strauss AD, Beller KD. Arterial parameters under echo contrast enhancement. Eur J Ultrasound 1997;5:31–8.
33. Bauer A, Hauff P, Lazenby J, von Behren P, Zomack M, Reinhardt M, et al. Wideband harmonic imaging: a novel contrast ultrasound imaging technique. Eur Radiol 1999;9(Suppl 3):S364–7.
34. Burns PN, Wilson SR, Simpson DH. Pulse inversion imaging of liver blood flow: improved method for characterizing focal masses with microbubble contrast. Invest Radiol 2000;35:58–71.
35. Wilson SR, Burns PN, Muradali D, Wilson JA, Lai X. Harmonic hepatic US with microbubble contrast agent: initial experience showing improved characterization of hemangioma, hepatocellular carcinoma, and metastasis. Radiology 2000;215:153–61.
36. Kamiyama N, Moriyasu F, Mine Y, Goto Y. Analysis of flash echo from contrast agent for designing optimal ultrasound diagnostic systems. Ultrasound Med Biol 1999;25:411–20.
37. Wei K, Jayaweera AR, Firoozan S, Linka A, Skyba DM, Kaul S. Quantification of myocardial blood flow with ultrasound-induced destruction of microbubbles administered as a constant venous infusion. Circulation 1998;97:473–83.
38. Dietrich CF. [3D real-time contrast enhanced ultrasonography: a new technique; in German.] Röfo Fortschr Geb Rontgenstr Neuen Bildgeb Verfahr 2002;174:160–3.
39. Schuessler G, Ignee A, Hirche T, Dietrich CF. [Improved detection and characterization of liver tumors with echo-enhanced ultrasound; in German.] Z Gastroenterol 2003;41:1167–76.
40. Seidel G, Kaps M, Verleger R, Meyrer R, Greis C. Einfluss eines Spherosomenhaltigen Echokontrastmittels (BY963) auf die EEG-Aktivität während der transkraniellen Duplexsonographie [abstract]. Akt Neurol 1996;23(Suppl):S49.
41. Seidel G, Kaps M, Verleger R, Greis C. Improvement of color-coded duplex sonography in patients with insufficient acoustic bone window using the new echo contrast agent BY963: a safety study [abstract]. Cerebrovasc Dis 1996;6 (Suppl 3): 37.
42. Rott HD. Safety of ultrasonic contrast agents. European Committee for Medical Ultrasound Safety. Eur J Ultrasound 1999;9:195–7.
43. Ring J, Brockow K, Behrendt H. History and classification of anaphylaxis. Novartis Found Symp 2004;257:6–16.
44. Walther A, Bottiger BW. [Out-of-hospital treatment of anaphylactoid reactions; in German]. Internist (Berl) 2004;45: 296–304.
45. Thomsen HS, Morcos SK. Management of acute adverse reactions to contrast media. Eur Radiol 2004;14:476–81.
46. Mornstein V. Cavitation-induced risks associated with contrast agents used in ultrasonography. Eur J Ultrasound 1997;5:101–11.
47. Miller DL, Thomas RM, Williams AR. Mechanisms for hemolysis by ultrasonic cavitation in the rotating exposure system. Ultrasound Med Biol 1991;17:171–8.
48. Williams AR, Kubowicz G, Cramer E. The effects of the microbubble suspension SHU 454 (Echovist) on ultrasound-induced cell lysis in a rotating tube exposure system. Echocardiography 1991;8:423–33.
49. Holland CK, Roy RA, Apfel RE, Crum LA. In vitro detection of cavitation induced by a diagnostic ultrasound system. IEEE Trans 1992;29:95–101.
50. Miller DL, Thomas RM. Ultrasound contrast agents nucleate inertial cavitation in vitro. Ultrasound Med Biol 1995;21: 1059–65.
51. Miller DL, Thomas RM. Contrast-agent gas bodies enhance hemolysis induced by lithotripter shock waves and high-intensity focused ultrasound in whole blood. Ultrasound Med Biol 1996;22:1089–95.
52. Miller DL, Gies RA, Chrisler WB. Ultrasonically induced hemolysis at high cell and gas body concentrations in a thin-disc exposure chamber. Ultrasound Med Biol 1997; 23:625–33.
53. Everbach EC, Makin IR, Francis CW, Meltzer RS. Effect of acoustic cavitation on platelets in the presence of an echo-contrast agent. Ultrasound Med Biol 1998;24:129–36.
54. Uhlendorf V, Hoffmann C. Nonlinear acoustical response of coated microbubbles in diagnostic ultrasound. Proc IEEE Ultrasonics Symp 1994;3:1559–62.
55. Dalecki D, Raeman CH, Child SZ, Cox C, Francis CW, Meltzer RS, et al. Hemolysis in vivo from exposure to pulsed ultrasound. Ultrasound Med Biol 1997;23:307–13.
56. Shi WT, Forsberg F, Tornes A, Ostensen J, Goldberg BB. Destruction of contrast microbubbles and the association with inertial cavitation. Ultrasound Med Biol 2000;26: 1009–19.
57. Meltzer RS. Food and Drug Administration ultrasound device regulation: the output display standard, the "mechanical index," and ultrasound safety [editorial]. J Am Soc Echocardiogr 1996;9:216–20.

8 Three-Dimensional Linear Endoscopic Ultrasound

A. Fritscher-Ravens, H. Neye

Introduction

Endoscopic ultrasound (EUS) for gastrointestinal or pancreatic lesions can provide results comparable with those of other imaging techniques such as helical computed tomography (CT) and magnetic resonance tomography (MRI) [1,2]. In contrast to CT and MRI, the image slices acquired during transabdominal ultrasound or EUS can be selected freely and are set up by the examiner's hands selecting the base layer through voluntary movements. This freedom of movement has the disadvantage that it can potentially produce blurred anatomy and distorted images. It can make it difficult to obtain reliable volume measurements. The addition of three-dimensional (3D) reconstruction to EUS may help overcome some of these shortcomings.

Three-dimensional reconstruction of the two-dimensional ultrasound images has been reported for transabdominal ultrasonography and mechanical radial endoscopic ultrasonography, particularly in the staging of rectal tumors [3–6]. Although no significant advantages were observed with radial 3D as an addition to EUS for rectal tumor staging, the stereoscopic visualization appeared to allow a better understanding of the spread of the lesion [4,5].

Three-dimensional reconstruction in radial EUS can be achieved relatively easily in comparison with linear probes, as the two-dimensional scans that are to be converted into the 3D images are obtained with the inbuilt transducer placed in a fixed position, and the images acquired can therefore be clearly related to each other.

Technical advances have allowed the development of 3D imaging systems using transabdominal ultrasound, by placing a reference point within the ultrasound field using sensors attached to the ultrasound probe. This allows the coordinates of the changes in angulation to be tracked. Hardly any research has so far been conducted on the possibility of 3D image acquisition with linear-array endoscopic ultrasound. The difficulty involved—that any angulation or torque of the transducer will produce a variety of scans from different planes and positions, which are neither parallel to nor at a fixed angle to each other—has yet to be overcome and appears to be more challenging than with transabdominal transducers or radial EUS.

This chapter attempts to present some of the problems with linear endoscopic ultrasound and 3D acquisition and to help the reader understand why this technique has not been given the full attention for further development that is required. It will also describe the two different methods developed and tested in studies in experimental animals. One of these new techniques has also been used in patients, to investigate whether 3D imaging may be able to provide information additional to that already available with two-dimensional EUS imaging.

One of the two 3D systems used was custom-made, while the other was a modified commercially available 3D acquisition system built for transabdominal ultrasound. It was converted for linear EUS and used in a small pilot study in patients. The production of technical equipment for routine use of 3D linear EUS is currently still awaited.

Background

The development of ultrasound imaging started with the amplitude mode (A-mode). The intensity of the reflected sound waves was demonstrated by the amplitude of the sound waves along a single x-axis. The transition from A-mode to B-mode, in which a y-axis was added to the existing x-axis and when gray-scale imaging was used to display the processed signals, led to dramatic improvements in the clarity and interpretability of the ultrasound images, and this greatly facilitated the success of ultrasonography as an imaging technique.

In US, but also in endoscopic ultrasound, the examiner can freely create the x-axis and y-axis anywhere in the human body manually when manoeuvring the ultrasound transducer. This is a great advantage in comparison with CT and MRI, as the other imaging techniques are limited to the fixed sagittal, transverse, and coronary planes. However, the disadvantages include distortion of the lesions imaged, blurred anatomy, and incorrect volume measurements.

Although examiners became used to dealing with these disadvantages, this led to a desire for three-dimensional viewing of the targets in order to overcome some of the difficulties [7,8]. The notion of being able to view any lesion in three-dimensional space—a cube with x, y and z axes—is very attractive (Fig. 8.**1**). Any mass

could be viewed from different angles and its volume could be measured correctly, providing more information about the target and in particular about possible malignancy (Fig. 8.**4**).

During the last 10 years, 3D acquisition systems for transabdominal ultrasonography have been developed, with a standard technique for routine use. This has been shown to be particularly valuable for examining the unborn child [7–9]. Some technical problems had to be overcome, which are similar to the those involved in the development of a 3D acquisition system for linear endoscopic ultrasound.

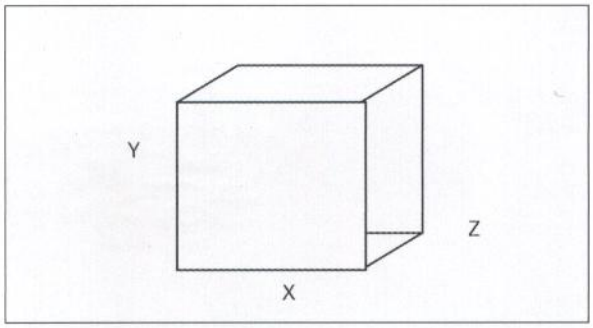


Fig. 8.**1** A cube with x, y and z axes, within which any scanned lesion can be converted into a three-dimensional shape.

■ Technical Considerations

A prerequisite for any three-dimensional reconstruction of an ultrasound image is solving the problem of obtaining a sequence of two-dimensional images in a defined, geometrical relationship, so that the subsequent transformation into a three-dimensional cube is in the correct relationship to the original. Three-dimensional reconstruction has become routine with other imaging techniques such as magnetic resonance imaging and computed tomography. This is relatively easy to achieve with these techniques, as the two-dimensional images obtained are in a precisely defined and structured relationship to each other. This is not the case with ultrasound. The constant movement and flexible guidance of the ultrasound transducer, as well as the uneven surface of the human body, make a coordinated sequence of images for spatial reconstruction difficult to obtain.

There are several possible options that can be used to achieve the correct transformation of a variety of two-dimensional ultrasound images into a three-dimensional space. Described below, the methods need to define the coordinates of each of the numerous pixels of any image in order to allow the image to be transformed.

■ Transformation Methods

Parallel Guidance of the Transducer

The simplest solution for generating a coordinated sequence of images is to mount a conventional transducer into or onto a device in which it can be moved back and forth in a parallel fashion to capture a certain number of images at a defined distance from each other. This can be achieved by moving a crystal array in a parallel fashion within a transducer. These transducers are not small, and large spaces need to be covered in order to obtain images of a whole organ. For instance, if a kidney 11 cm in size has to be imaged, the entire 11 cm have to be covered with an up-and-down movement of the transducer in order to acquire the image.

Rotation

Rotating the image plane can also provide three-dimensional images. If convex-array transducers are used, contact between the transducer and the skin can be limited to a very small area to examine a large volume of the abdomen. This eliminates some of the negative aspects of the parallel movement approach. There are two ways of acquiring images—rotation around a vertical axis and horizontal rotation.

Vertical rotation. The transducer needs to be rotated along its vertical axis, which is the axis that is in line with the ultrasound waves. However, all two-dimensional images of the one image plane along the vertical axis overlap. The distance of the single imaging planes from each other increases with the distance to the vertical axis. This may result in higher interpolarization and thus incorrect reconstruction of the three-dimensional images.

Horizontal rotation. The rotational axis is inside the ultrasound probe, orthogonal to the direction of the sound wave. This avoids the overlapping of image planes that occurs with the rotational axis. The crystal array is flexible and can be moved with the support of a motor above the target lesion being examined. This technique makes it possible to record two-dimensional image planes that are situated at a constant and clearly defined angle to each other.

Freehand Ultrasound

The examiner can steer the transducer in any direction imaginable over or toward the target to be examined. The ultrasound transducer produces a two-dimensional image of the scanned area at all times. As the transducer is moved, variable image planes are received that lie in a variety of positions relative to each other and are not positioned constantly parallel to each other or at some other clearly defined angle as with three-dimensional CT image reconstruction.

Each of the image planes is recorded and stored in the ultrasound system's computer. To reconstruct a 3D im-



Fig. 8.2 The heavy 10-cm transmitter has been placed next to the abdominal wall of the patient on her bed. The 3-cm lightweight sensor has been attached to the shaft of the echoendoscope.

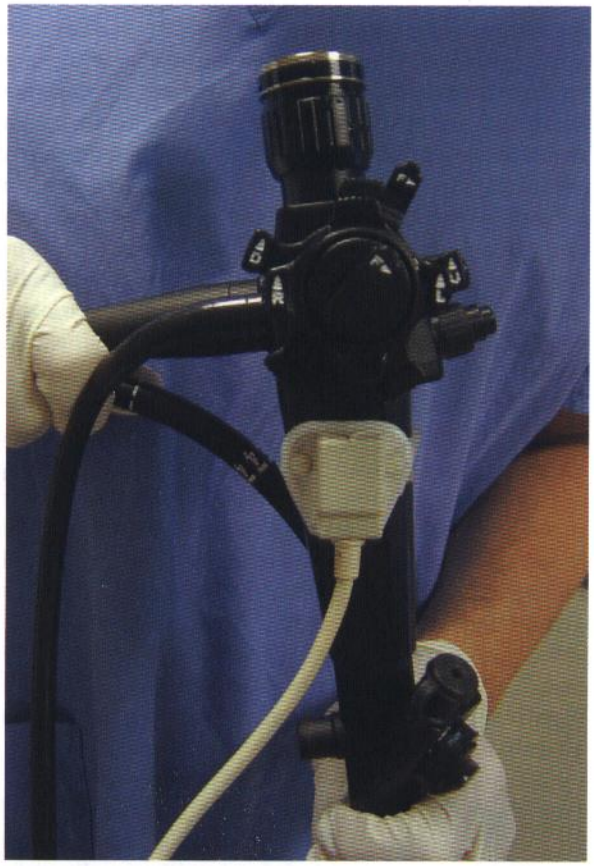


Fig. 8.3 The 3-cm lightweight sensor, attached to the shaft of the echoendoscope. It transmits any movements made within the electromagnetic field created by the heavy cube device.

age, all of the image planes have to be transferred into a regular pattern. Several hundred of the image planes that are related to each other have to be put into their correct location within the cube. For this purpose, the location and orientation of the transducer needs to be known at the time of the recording. This can be achieved with movable arms in which every change in angulation and rotation is measured electronically; infrared devices or electromagnetic sensors can also be used. With the help of any of these tools, the position can be measured with a precision of about 1 mm.

Current Methods for Linear 3D Endoscopic Ultrasound

Sumiyama et al. have developed a prototype 3D linear EUS system equipped with an electromagnetic sensor, allowing positional measurement with six degrees of freedom [10,11]. The sensor has to be attached to the control section of the echoendoscope outside the patient [10]. The rotational data from the scope are extracted using specially developed algorithms to minimize the severe deformation of the 3D images [10] produced by discrepancies in motion between the ultrasound probe at the tip of the scope and the control section with the positioning sensor outside the patient. The miniature positioning sensor, attached to the tip of the scope, required the use of an overtube for intubation in the first prototype tests, but not in subsequent studies [11]. It was thought that the overtube would facilitate smooth rotation of the scope to acquire satisfactory 3D images without distortion. Further investigations revealed that the anatomical structures of the esophagus and diaphragm also allowed smooth rotation [10], making the overtube redundant. This device has been tested in experimental animal settings, but patient data are at present still awaited.

Our own group converted an electromagnetic positioning/tracking system commercially available for transabdominal ultrasonography (Echotec, Hitachi Ultrasound, Tokyo, Japan) for use in linear endoscopic ultrasound. An electromagnetic 2-kg block-shaped transmitter, 10 cm^3 in size, served as one part of the positioning system (the more voluminous part). Before the examination, this was positioned next to the patient's abdominal wall (Fig. 8.**2**) and connected to a computer to create an image. This heavy, block-shaped transmitter generates a spherical magnetic field with an effective range of about 70 cm, which serves for reference purposes. Within this spatial field, the position and movements of a second device, a 3-cm lightweight sensor, can be determined at any time. The sensor can be fitted onto the shaft of a conventional echoendoscope without limiting the examiner's freedom of movement (Fig. 8.**3**). The sensor records the movements made by the tip of the echoendoscope that contains the ultrasound transducer. The examiner therefore has to transmit all of his or her movements carefully from the distal tip to the proximal shaft of the echoendoscope. The 3D volume is scanned by a vertical shift of the entire echoendoscope. As with the system used by Sumiyama

et al. [10,11], this sensor was able to differentiate between six different degrees of freedom: shifts in the X, Y, and Z directions and rotation around the X, Y, and Z axes. The combination of the sensor and transmitter ensures that two-dimensional (2D) images can be spatially related to specific positions for conversion into a complete 3D volume image (Figs 8.**4**, 8.**5**). After 2D image acquisition, the system calculates the spatial relationships of the individual pixels.

Incorrect manual shifting and movements that are too rapid produce artifacts during generation of the 3D images, resulting in black holes within the reconstructed 3D image.

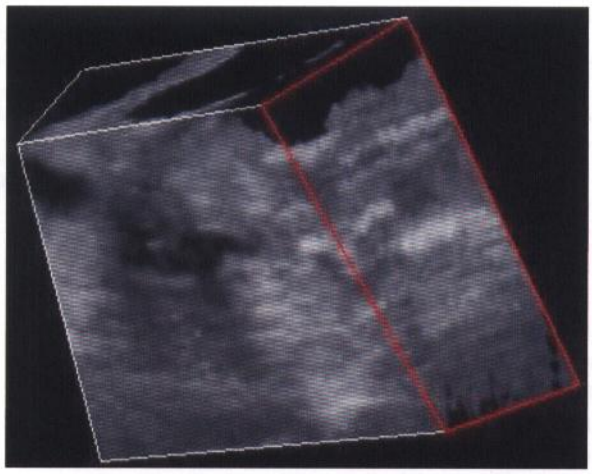


Fig. 8.**4** Two-dimensional EUS images are spatially related to specific positions and then converted into a complete three-dimensional volume image—in this case, the pancreatic head with a tumor across the pancreatic duct and portal vein.

■ 3D EUS Examination in Patients

We conducted a pilot study to evaluate vascular involvement in pancreatic cancer [12]. The examiner was blinded to the results of previous imaging studies, but was informed about the possible presence of a pancreatic mass lesion and its suspected location within the pancreas. All of the patients were referred for pancreatic surgery and underwent routine EUS and EUS-guided fine-needle aspiration (FNA) first, before additional 3D evaluation was carried out. Immediately after the scans had been taken, the reconstructed 3D volumetric image was converted into a form that could be displayed on a two-dimensional flat screen monitor, using perspective distortions and the edges of a cube to increase three-dimensional perception. Multiplanar reconstruction out of the volume data set, rotation and translation on three axes, photorealistic visualization or transparency, brightness, contrast, and color modes, as well as a zoom mode, were possible.

Twenty-two patients with lesions in the head of the pancreas were staged with EUS-FNA for tissue diagnosis and had 3D evaluation as an add-on procedure, with the image generation taking approximately 10 more minutes. The 3D images offered additional clinically valuable information, although the images produced were sometimes blurred and of poor quality. Distinct but subtle changes in vessel behavior were detectable in the 3D images, since views from below the vessels were very valuable. These advantages of 3D application made it possible to suggest vessel compression rather than invasion in three of 10 patients in whom vascular invasion was detected on 2D imaging. Three-dimensional image interpretation gave a false-negative result for vascular invasion in only one patient. Conventional EUS image interpretation gave four false-positive patients for vascular invasion. This improvement in the ability to distinguish between vascular invasion and compression appears to be one advantage of 3D EUS.

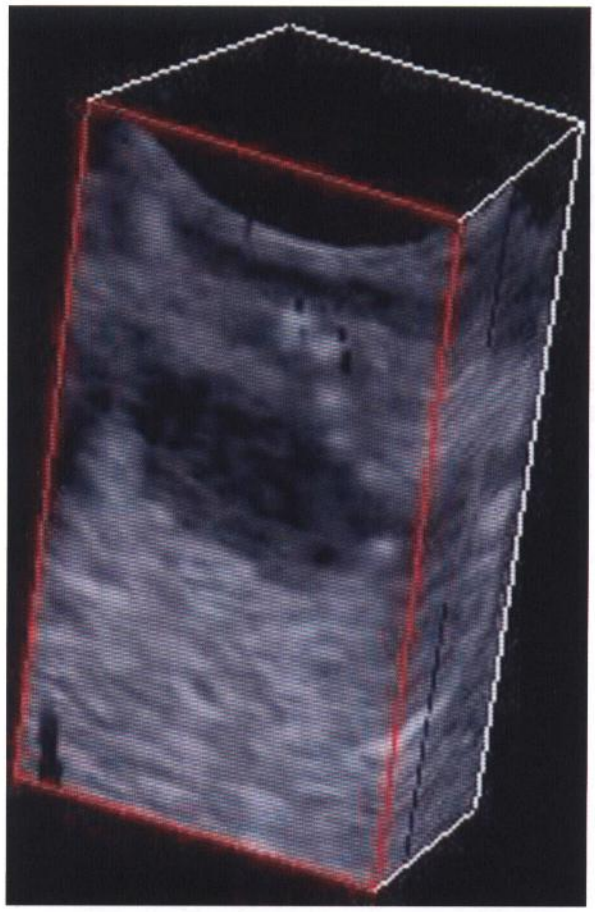


Fig. 8.**5** A three-dimensional image of stones, with acoustic shadowing within the pancreatic duct. The image shows the normal-sized and stone-free common bile duct at the top of the image; the stone-filled pancreatic duct beneath it; and the portal vein, represented by the large hypoechoic mass beneath the two ducts.

Conclusion

Linear 3D endoscopic ultrasonography appears to be a good option to help overcome some of the minor disadvantages of 2D echoendoscopy. However, technical improvements and the development of a specific 3D acquisition system for linear EUS are prerequisites which examiners need to be equipped with before any further clinical studies can be carried out. The development of an ultrathin sensor to directly obtain positional data for the ultrasound probe via the accessory channel might make it possible to resolve some of the current problems. More bench tests and objective evaluation of the accuracy and reproducibility of such systems might help exclude system problems and produce a 3D system that can be used for routine examinations.

References

1. Dewitt J, Ciaccia D, Leblanc J, et al. Prospective comparison of endoscopic ultrasound and dual phase helical computer tomography for the preoperative evaluation of known or suspected pancreatic malignancy: final results [abstract]. Gastrointest Endosc 2003;57:AB 99.
2. Howard T, Chin AC, Stein EW, Kopecky KK, Wiebke EA. Value of helical computed tomography, angiography, and endoscopic ultrasound in determining resectability of periampullary carcinoma. Am J Surg 1997;174:237–41.
3. Kim JC, Cho YK, Kim, SY, Park SK, Lee MG. Comparative study of three-dimensional and conventional endorectal ultrasonography used in rectal cancer staging. Surg Endosc 2002;16:1280–5.
4. Hünerbein M, Schlag M. Three-dimensional endosonography for staging of rectal tumor. Ann Surg 1997;225:432–8.
5. Hünerbein M, Pegios W, Rau B, Vogl TJ, Felix R, Schlag M. Prospective comparison of endorectal ultrasound, three-dimensional endorectal ultrasound, and endorectal MRI in the preoperative evaluation of rectal tumors: preliminary results. Surg Endosc 2000;14:1005–9.
6. Szilvas A, Szekely G, Tarjan Z, Fornet B. Three-dimensional ultrasonography, virtual coloscopy and endorectal magnetic resonance imaging in the diagnosis of complicated inflammatory bowel disease. Endoscopy 2002;34:94–9.
7. King DL, King DL Jr, Shao MY. Three-dimensional spatial registration and interactive display of position and orientation of real-time ultrasound images. J Ultrasound Med 1990;9:525–32.
8. Merz E. Use of 3D ultrasound technique in prenatal diagnosis. Ultraschall Med 1995;16:154–61.
9. Mueller GM, Weiner CP, Yankowitz J. Three-dimensional ultrasound in the evaluation of fetal head and spine anomalies. Obstet Gynecol 1996;88:372–8.
10. Sumiyama K, Suzuki N, Kakutani H, et al. A novel 3-dimensional EUS technique for real-time visualization of the volume data reconstruction process. Gastrointest Endosc 2002;55:723–8.
11. Sumiyama K, Suzuki N, Tajiri H. A linear-array freehand 3-D endoscopic ultrasound. Ultrasound Med Biol 2003;29:1001–6.
12. Fritscher-Ravens A, Knoefel WT, Krause C, Swain CP, Brandt L, Patel K. Three-dimensional linear endoscopic ultrasound: feasibility of a novel technique applied for the detection of vessel involvement of pancreatic masses. Am J Gastroenterol 2005;100:1296–1302.

9 Sonoelastography: a New Ultrasound Modality for Assessing Tissue Elasticity

H. Frey, C.F. Dietrich

Introduction

It is well known that inflammatory conditions and tumors lead to an alteration of the normal tissue structure, causing hardening of the tissue and a change in its elasticity. The elasticity modulus is a measure of the stress that is applied to tissue structures relative to the strain or deformation produced. Figure 9.**1** shows a graph of the elasticity coefficient for different breast tissues [1].

Assessing and visualizing tissue elasticity provides the clinician with potentially important information that can be used in the diagnosis of tumors and inflammatory conditions. Various ultrasound techniques have been developed and experimentally evaluated in recent years for visualizing the elastic properties of tissue.

Figure 9.**2** demonstrates the different effect of compression on hard and soft tissue. Soft tissues are compressed more than hard tissue structures under the same pressure. This deformation can be detected from the ultrasound data and can be displayed. The sonoelastography modality described here uses standard ultrasound probes, and there is no requirement for additional equipment such as pressure or vibration measurement systems. The procedure is similar to that in conventional color Doppler examination. Measurements of tissue elasticity are acquired in real time and presented as a color overlay on the conventional B-mode image.

Technical Characteristics

Conventional ultrasound images (B-mode images) are constructed from ultrasound signals that are reflected back from tissue boundaries within the body. The ultrasound signal is also attenuated by tissues to an extent that depends on the tissue density. The returning signals are reconstructed and displayed. Because tumors often have a similar echogenicity to that of the adjacent tissue, it can be very difficult or even impossible to delineate a tumor with conventional B-mode imaging. However, malignancies are often associated with a change in tissue hardness. Sonoelastography is an ultrasound technique that is capable of displaying tissue hardness in order to provide the clinician with important additional diagnostic information. The technique is especially useful in lesions that are not easily palpated—providing tissue differentiation by quantifying the tissue elasticity.

A technique known as the extended combined autocorrelation method provides the mathematical basis for the sonoelastography method described below. The returning radiofrequency echo patterns are compared over time. If the transducer has not moved during a given time and no pressure is applied to the scanned tissues, the received echo patterns will be the same, provided there is no respiratory or cardiac motion. If gentle pressure is applied to the tissues, the radiofrequency echo patterns will change. If the distance be-

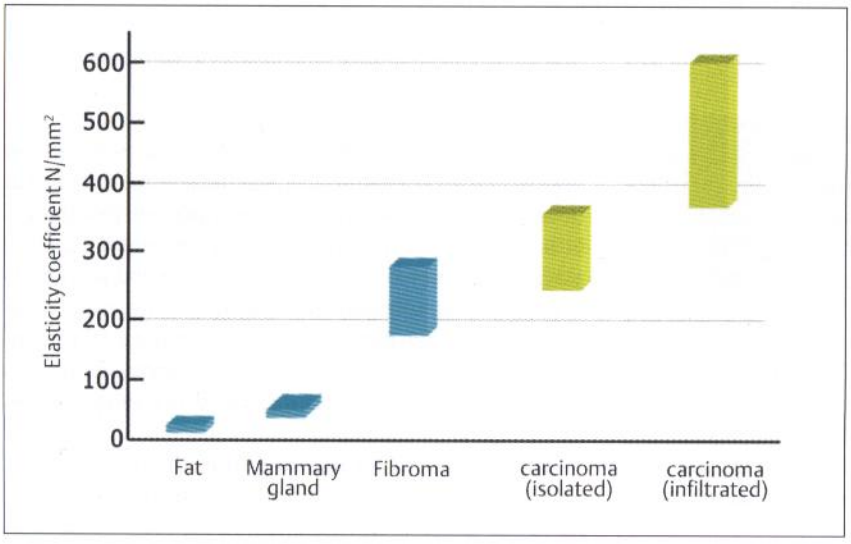


Fig. 9.**1** Coefficients of elasticity in various tissues in the breast (adapted from [1]).

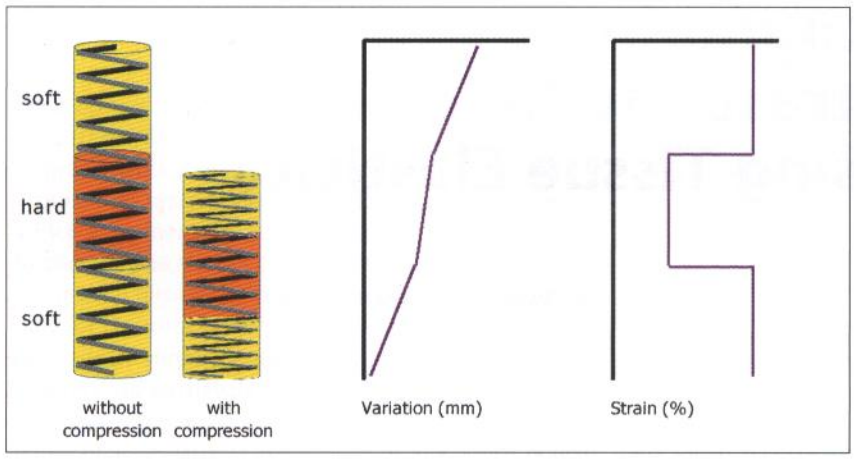


Fig. 9.2 The elasticity characteristics of various tissues under compression, based on a spring-coil model. When the same pressure is applied, a soft (more elastic) spring coil is compressed more than a hard spring.

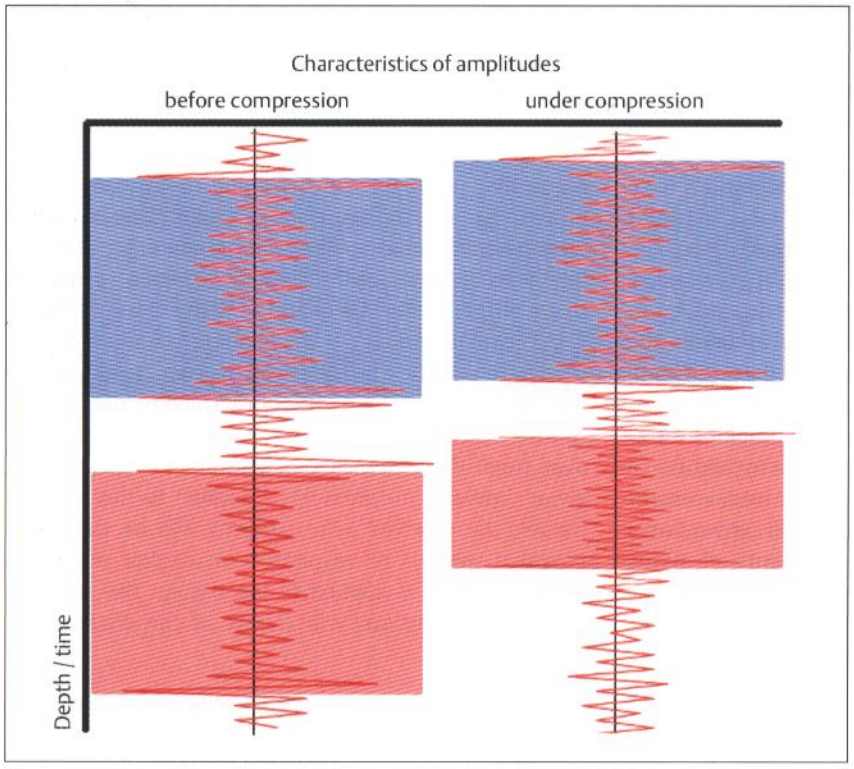


Fig. 9.3 Radiofrequency signals for an ultrasound vector without compression (left) and with compression (right). Compression in hard tissue areas is shown as blue and compression in soft tissue areas is red.

tween two reflectors remains the same, it is a "harder" tissue area. If this distance decreases, then it represents elastically deformable tissue (Fig. 9.3). The echo patterns in the adjacent tissue areas are also analyzed in order to detect possible lateral displacement of the compressed tissue area.

For example, a round echogenic tissue structure moves vertically under compression, and if it is a hard, nondeformable structure without lateral displacement, it remains as a circular image with the same diameter. However, if the same structure is displaced laterally with compression, it is detected as a circular structure but with a smaller diameter.

With the extended combined autocorrelation method, it is possible to acquire measurements in real time and display them simultaneously on the Hitachi EUB-8500 platform. Using this technology, large displacements can be analyzed very quickly and accurately in comparison with conventional autocorrelation methods. An accurate mathematical explanation of the sonoelastography mode based on the extended combined autocorrelation method is described presented by Yamakawa and Shiina [2].

The strain field is calculated from the displacement, allowing conclusions to be drawn regarding the elasticity of the tissue area examined. Areas characterized as

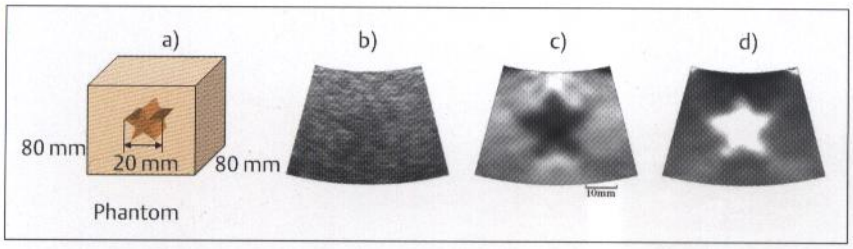


Fig. 9.**4a** A tissue elasticity phantom, with an inclusion mimicking a star-shaped tumor. **b** The B-mode image of the stellate inclusion. The structure is very difficult to visualize. By contrast, the stellate inclusion is easily seen in the deformation image (**c**) and elasticity image (**d**).

soft tissue appear as areas of high strain, whereas hard tissue structures appear as areas with lower elasticity.

As sonoelastography developed, it became apparent that the procedure had to be integrated into a routine examination procedure using standard linear or curved transducers, as well as specialist transducers for endovaginal, endorectal, laparoscopic, and endoscopic applications. The method was also developed without any need for additional equipment (for example, to induce pressure or vibration in the tissues), providing a user-friendly system for routine clinical use.

The calculation of the tissue elasticity distribution is carried out by means of a three-dimensional tissue phantom together with a 3D finite element method (3D-FEM). The finite element method (FEM) is a type of mathematical analysis that is used in engineering science to develop complex statistical components for calculating stress deformation and also complex flow fields and flow processing. Using this technique, complex geometrical structures are divided into small components (finite elements). The deformation of a structure such as a cube is well known, and the power that is introduced at the edge of the cube can be calculated. The calculation can be done first for each cube and then for the structure as a whole.

In the sonoelastography mode described below, the finite element method is used inversely. The structure being examined is divided into 30 000 equal cubes. Before compression, it is assumed that the tissue elasticity (measured using the modulus of elasticity or Young's modulus, E) is constant throughout. After compression, the resulting displacement is measured for each finite element (cube), and the deformation of the edges of the cube can be calculated and the strain evaluated. The FEM confirms the tissue elasticity of each individual cube. The iterative process depends on different variables (e.g., the power, velocity, duration, and surface distribution of the induced compression). This iterative process is repeated until predefined thresholds are reached. The exact mathematical process involved in calculating tissue elasticity is described by Nitta et al. [3] and Yamakawa and Shiina [4].

■ Research Results

The performance of real-time sonoelastography using the extended combined autocorrelation method and the 3D finite element method have been investigated using phantoms and in-vivo experiments. Figure 9.**4a** shows a phantom containing a gelatin cube that has been used to mimic a tumor. The stellate tumor contains a concentration of 30% gelatin, whilst the surrounding tissue has a concentration of 10%. The materials are made of polyethylene dust. Figure 9.**4b** shows the phantom in B-mode imaging. It is not possible to visualize the simulated tumor clearly, as its echogenicity is similar to that of the surrounding gelatin. Figures 9.**4c** and **d** show the same structure in sonoelastography mode, with the stellate structure clearly visible in the deformation image and elasticity image.

To provide better visualization of tumors and to characterize them, the elastogram is displayed in color and provided as a transparent overlay on the conventional B-mode image. Hard tissue structures are displayed in blue, and soft structures are encoded in red (Fig. 9.**5**). Sonoelastography is a real-time method. Using the Hitachi EUB-8500 system, the frame rate varies from 10 to 35 images per second, depending on the size of the area analyzed (the region of interest).

In addition, quantification of the color display can be provided using a number of algorithms. At present, this is still carried out "offline," using digital video scans. Real-time quantification that accurately determines the elasticity values is currently being developed and

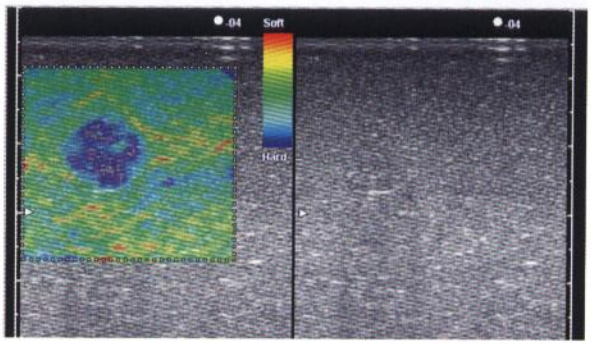


Fig. 9.**5** A tissue elasticity image (left), with hard tissue areas shown in blue and soft tissue areas in red/green. The right side of the monitor image shows the corresponding B-mode display.

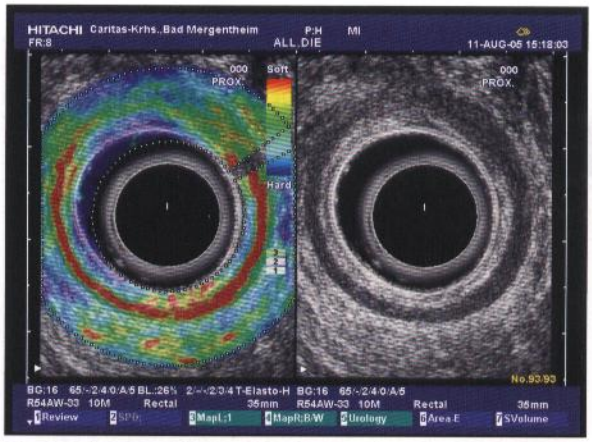


Fig. 9.6 The normal internal and external anal sphincter, showing excellent differentiation with sonoelastography. The internal anal sphincter is shown in red and the external anal sphincter in green.

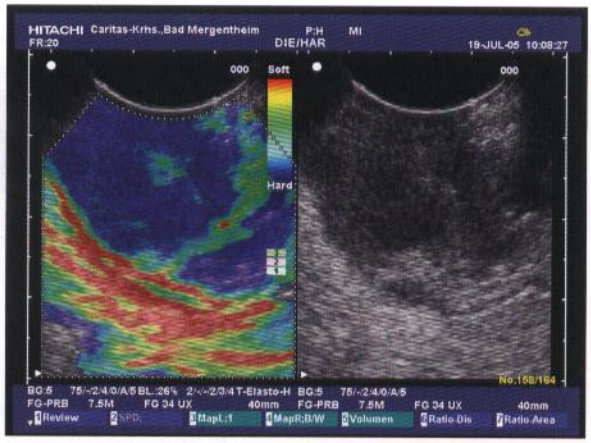
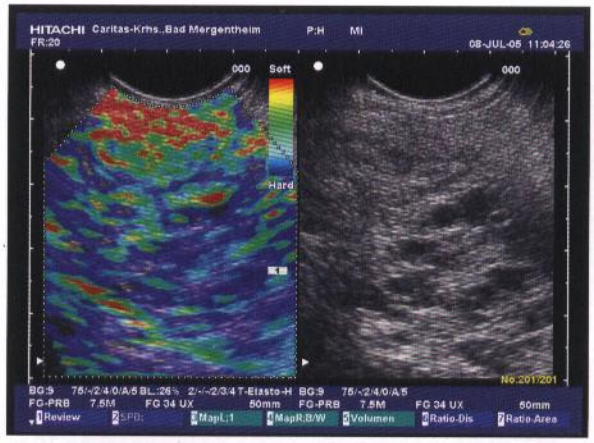
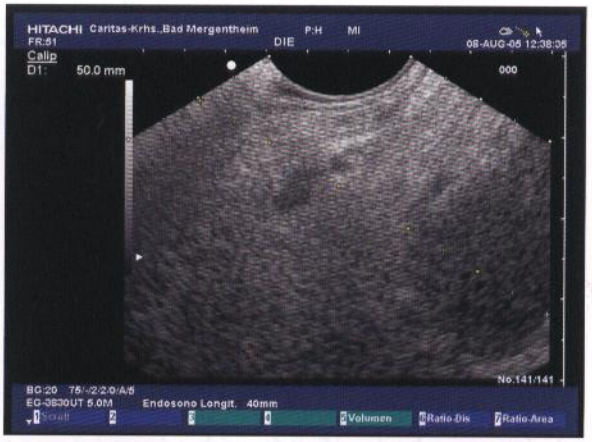


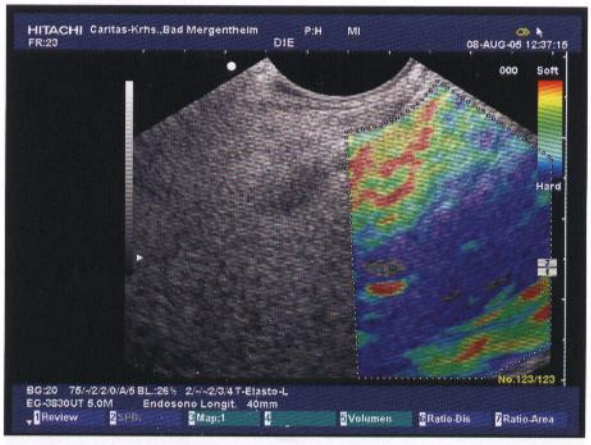
Fig. 9.7 Colorectal carcinoma. The hard carcinoma tissue is displayed in blue, in contrast to the surrounding tissue.



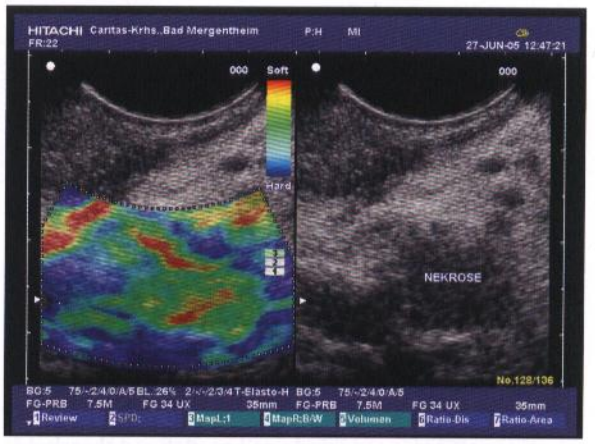
a



b

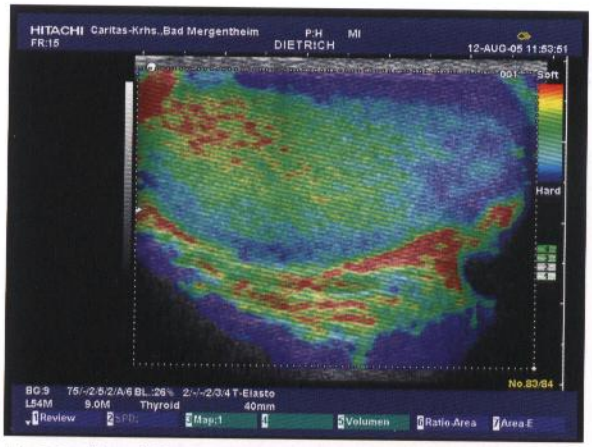


c

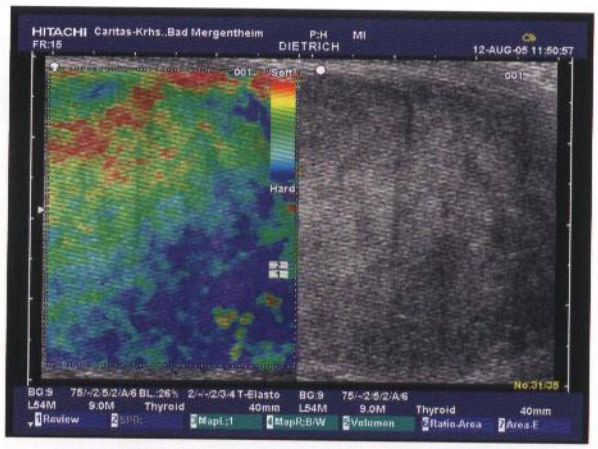


d

Fig. 9.8a A large (serous) microcystic adenoma. The more distally located cystic parts are shown in blue (hard), whereas the more proximally located solid components are shown in red (soft). **b**, **c** In patients with carcinoma, the solid component is harder than the surrounding tissue. **d** Pancreatic necroses are soft.



a



b

Fig. 9.**9a, b** A diffuse infiltrating teratoma of the testis.

will soon be incorporated into the system. Elastography is a widely discussed topic in the current literature [5–18].

■ Sonoelastography in the Clinical Setting

Conventional ultrasound endoscopes are used for sonoelastography of the anorectum, pancreas, and the mediastinal lymph nodes. Electronic longitudinal ultrasound endoscopes, or fiberoptic or electronic radial endoscopes can all be used. The advantage of using endoscopic ultrasound with elastography is that aspiration can be carried out immediately in any suspicious area. The gentle curvature on the surface of the longitudinal endoscope is particularly well adapted for applying uniform pressure on tissues.

To perform sonoelastography, the ultrasound endoscope is positioned in the same way as for a conventional endosonography examination. The area to be evaluated is defined by a region of interest (ROI) in exactly the same way as in a color Doppler examination. For sonoelastography, little additional compression is required, as the pressure from the pulsation of the surrounding vessels is normally sufficient. A sensitive system setting is required. The ROI has to be sufficiently large, with the area of the lesion being no more than 50% of the size of the ROI, to allow the sonoelastography image to display the elasticity of the lesion relative to the surrounding tissues. Research aiming to allow accurate definition of elasticity is currently in progress. If the ROI is too small, the relative elasticity differences within the lesion are displayed and the hardness of the lesion relative to the normal surrounding tissue is not seen.

Figures 9.**6**–9.**8** present clinical examples of the endorectal wall and sphincters, as well as the pancreas. Other examples appear in various chapters of the present book. For example, elastography is helpful and produces reproducible findings for detecting circumscribed lymph-node infiltration in patients with malignant lymph-node involvement.

It should be borne in mind that elastography is mainly helpful in superficially located organs in which pressure can be accurately applied, as shown in Fig. 9.**9**, demonstrating a diffuse infiltrating teratoma of the testis.

References

1. Krouskop TA, Wheeler TM, Kallel F, Garra BS, Hall T. Elastic moduli of breast and prostate tissues under compression. Ultrason Imaging 1998;20:260–74.
2. Yamakawa M, Shiina T. Strain estimation using the extended combined autocorrelation method. Jpn J Appl Phys 2001;40:3872–6.
3. Nitta N, Yamakawa M, Shiina T, Ueno E, Doyley MM, Bamber JC. Tissue elasticity imaging based on combined autocorrelation method and 3-D tissue model. In: Schneider SC, Levy M, McAvoy BR, editors. Proceedings of the IEEE Ultrasonics Symposium 1998. Piscataway, NJ: Institute of Electrical and Electronics Engineers, 1998: 1447–50.
4. Yamakawa M, Shiina T. Tissue elasticity reconstruction based on 3-dimensional finite-element model. Jpn J Appl Phys 1999;38:3393–8.
5. Frey H. [Real-time elastography: a new ultrasound procedure for the reconstruction of tissue elasticity; in German.] Radiologe 2003;43:850–5.
6. Ophir J, Cespedes I, Ponnekanti H, Yazdi Y, Li X. Elastography: a quantitative method for imaging the elasticity of biological tissues. Ultrason Imaging 1991;13:111–34.
7. Shiina T, Doyley MM, Bamber JC. Strain imaging using combined RF and envelope autocorrelation processing. In: Levy M, Schneider SC, McAvoy BR, editors. Proceedings of the IEEE Ultrasonics Symposium 1996. Piscataway, NJ: Institute of Electrical and Electronics Engineers, 1997: 1331–6.
8. Lorenz A, Ermert H, Sommerfeld HJ, Garcia-Schurmann M, Senge T, Philippou S. [Ultrasound elastography of the prostate: a new technique for tumor detection; in German.] Ultraschall Med 2000;21:8–15.
9. Cespedes I, Ophir J. Reduction of image noise in elastography. Ultrason Imaging 1993;15:89–102.

10. Bonnefous O, Pesque P. Time domain formulation of pulse-Doppler ultrasound and blood velocity estimation by cross correlation. Ultrason Imaging 1986;8:73–85.
11. Konofagou E, Ophir J. A new elastographic method for estimation and imaging of lateral displacements, lateral strains, corrected axial strains and Poisson's ratios in tissues. Ultrasound Med Biol 1998;24:1183–99.
12. Gao L, Parker KJ, Alam SK, Lernel RM. Sonoelasticity imaging: theory and experimental verification. J Acoust Soc Am 1995;97:3875–86.
13. Srinivasan S, Kallel F, Ophir J. The effects of digitization on the elastographic signal-to-noise ratio. Ultrasound Med Biol 2002;28:1521–34.
14. Srinivasan S, Kallel F, Souchon R, Ophir J. Analysis of an adaptive strain estimation technique in elastography. Ultrason Imaging 2002;24:109–18.
15. Maurice RL, Bertrand M. Speckle-motion artifact under tissue shearing. IEEE Trans Ultrason Ferroelectr Freq Control 1999;46:584–94.
16. Lubinski MA, Emelianov SY, O'Donnell M. Speckle tracking methods for ultrasonic elasticity imaging using short-time correlation. IEEE Trans Ultrason Ferroelectr Freq Control 1999;46:82–96.
17. Kallel F, Ophir J. A least-squares strain estimator for elastography. Ultrason Imaging 1997;19:195–208.
18. Ermert H, Lorenz A, Pesavento A. Elasticity imaging: new imaging modalities. Proceedings of the First European Medical and Biological Engineering Conference (EMBEC), Vienna, 4–7 November 1999. Med Biol Eng Computing 1999;37(Suppl 2 Pt II):954–5.

10 EUS-Guided Biopsy: Equipment and Technique

H.W. Sudholt, P. Vilmann

Introduction

The development of endoscopic ultrasound scanning (EUS) began in the early 1980s with mechanical, radial-scanning transducers [1–3]. Despite excellent imaging resolution, the method did not gain widespread popularity until the development of EUS-guided fine-needle aspiration (EUS-FNA) biopsy [4–8]. For many years, efforts to characterize specific lesions and differentiate between them using EUS imaging alone postponed the necessary development of tissue sampling guided by endosonography. EUS-FNA is now carried out routinely at many endoscopic centers, and the procedure is clearly having a major impact on the therapeutic management of patients by providing definitive tissue diagnosis of lesions outlined by endosonography. EUS-FNA is obviously by no means limited to the field of gastroenterology, since the gastrointestinal tract traverses through anatomical regions related to other medical specialties such as pulmonology, thoracic surgery, internal medicine, oncology, urology, gynecology, and endocrinology [9–11]. There is also considerable evidence that EUS-FNA in experienced hands can replace many other far more invasive and risky diagnostic procedures, such as mediastinoscopy, diagnostic laparoscopy, and even laparotomy or thoracotomy [12–14].

One of the main strengths of EUS-FNA in comparison with radiographic imaging methods with percutaneous biopsy is the close proximity of the transducer to the regions of interest. This means that even minute lesions, down to a size of 5 mm, can be imaged and consequently biopsied. However, the technique is not easy to master, and considerable energy and effort need to be invested before an examiner's technique reaches an acceptable success rate comparable to that reported in the literature, at about 90–95%, with an overall sensitivity and specificity of 90% and 100%, respectively. The aim of the present chapter is to describe the technique of EUS-guided biopsy in detail, based on a literature review and our extensive experience with this method.



Fig. 10.1 Pentax EG-3830UT.

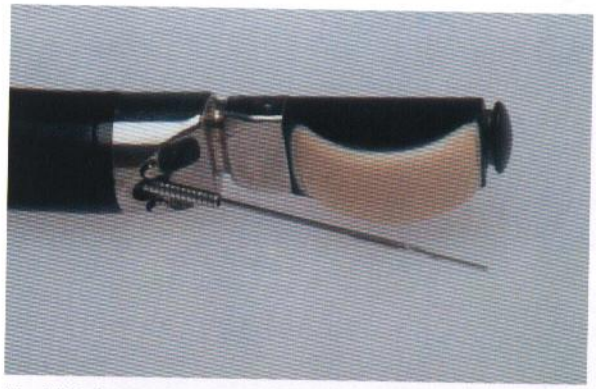


Fig. 10.2 Pentax FG-34UX.

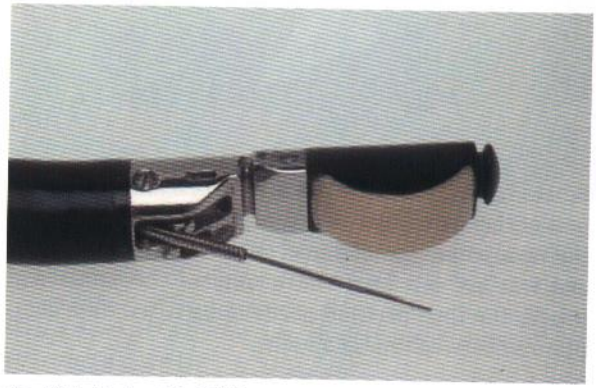


Fig. 10.3 Pentax FG-36UX.

Endoscopes

Table 10.1 and Figs. 10.1–10.5 show the endoscopes that are currently commercially available for EUS-guided diagnostic fine-needle biopsy. Some of these devices have

Table 10.1 Endoscopes currently commercially available for endoscopic ultrasound-guided diagnostic fine-needle aspiration biopsy

Manufacturer	Series	Model	Description	Working channel (mm)	Albarran
Pentax		FG-34UX	Fiberoptic ultrasound endoscope, diameter 12.1 mm, working length 1250 mm, viewing angle 105°	2.0	–
		FG-36UX	Fiberoptic ultrasound endoscope, diameter 12.1 mm, working length 1250 mm, viewing angle 105°	2.4	+
		FG-38UX	Fiberoptic ultrasound endoscope, diameter 12.8 mm, working length 1250 mm, viewing angle 60°	3.2 *	–
		EG-36U	Video ultrasound endoscope, diameter 12.1 mm, working length 1250 mm, viewing angle 130°	2.4	+
		EG-3830UT	Video ultrasound endoscope, diameter 12.8 mm, working length 1250 mm, viewing angle 120°	3.8 *	+
Olympus	EUS EXERA	GF-UCT160-OL5	Ultrasonic video biopsy endoscope for FNA	2.8	+
	EUS EXERA	GF-UC160P-OL5	Ultrasonic video biopsy endoscope for treatment and FNA	3.7	+
Olympus/Aloka	EUS	GF-UCT140-AL5	Ultrasonic video biopsy endoscope for FNA	2.8	+
	EUS	GF-UC140P-AL5	Ultrasonic video biopsy endoscope for treatment and FNA	3.7	+
Olympus/Philips	EUS	GF-UC160P-AT8	Ultrasonic video biopsy endoscope for FNA	2.8	+
	EUS	GF-UCT160-AT8	Ultrasonic video biopsy endoscope for treatment and FNA	3.7	+
Toshiba/Fujinon	EUS	PEF-708FA	Ultrasonic video biopsy endoscope for FNA	2.8	–

* Treatment and biopsy. FNA: fine-needle aspiration.

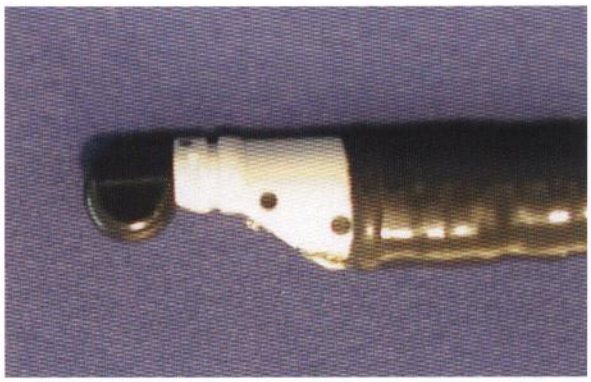


Fig. 10.4 Olympus GF-UC140P-AL5.



Fig. 10.5 Fujinon PEF-708FA.

an Albarran lever (elevator) to facilitate needle positioning. Several aspects need to be taken into consideration when one is choosing a biopsy instrument, including the Albarran, the stiffness/flexibility and length of the distal part of the endoscope, the diameter of the distal end of the endoscope, the diameter of the working channel, and last but not least the quality of the ultrasound image. The final decision needs to be based on a compromise between these options.

Biopsy Needles

In the early 1990s, special biopsy equipment was developed by one of the authors (P.V.) and Søren Hancke in collaboration with the German accessory company GIP-Medizintechnik (now Medi-Globe Ltd.), leading to the final breakthrough for the EUS-guided biopsy method [15]. A wide range of different needle systems are now available (Table 10.2). All of the other biopsy equipment for EUS-FNA that is currently available on the market is based on the same construction principles, so that the EUS-FNA procedure can be explained on the basis of the original design of the Hancke–Vilmann needle system.

Table 10.**2** Biopsy needles

Manufacturer	Model	Needle (G)	Specific features	Adjustable sheath length
Medi-Globe	Hancke–Vilmann	19–22	Reusable aspiration instrument with metal spiral sheath	–
Medi-Globe	SonoTip II	19–22	Disposable kit, Teflon-coated metal spiral sheath	+
Olympus	NA-10J-1	22	Reusable aspiration device, with metal spiral sheath	–
Olympus	NA-11J-KB Power Shot	22	Reusable, power shot function with metal spiral sheath	+
Olympus	NA-00H-8022 EZ Shot)	22	Disposable kit, hard plastic sheath	–
Wilson-Cook	EUSN-1, 19, 25	19–25	Disposable kit, with different needle-sheath materials	+
Wilson-Cook	ECHO-1-22	22	Disposable standard needle with plastic lock	+
Wilson-Cook	ECHO-2-22	22	Same needle as above, but with metal spiral lock	+
Wilson-Cook	ECHO-19	19	Disposable needle	+
Wilson-Cook	ECHO-25	25	Disposable, very thin with high flexibility	+
Wilson Cook	EUSN-19-QC Quick-Core	19U2<	Tru-Cut histology needle, with power-shot mechanism	+

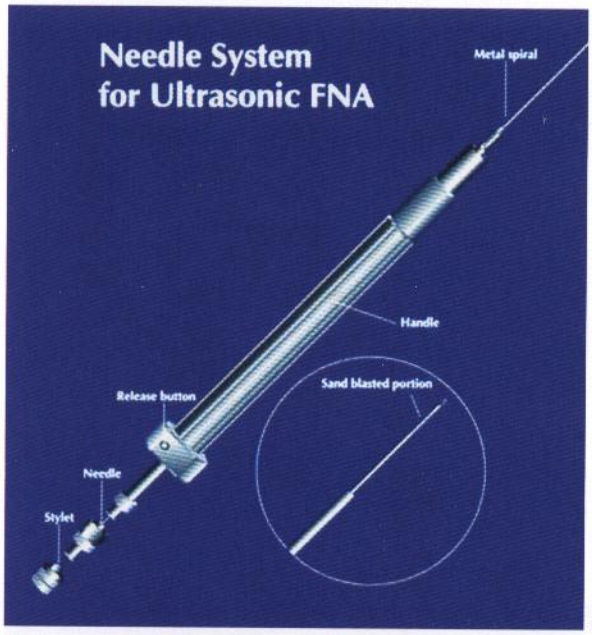
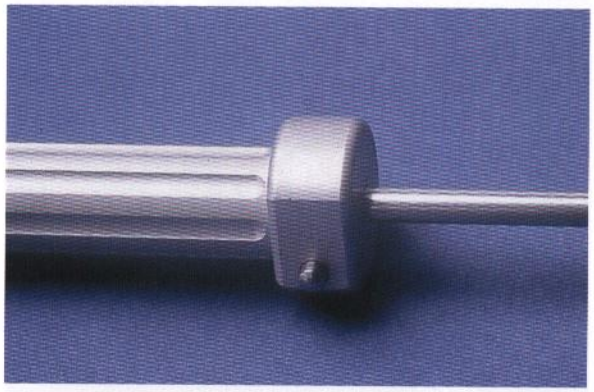


Fig. 10.**6** The Hancke–Vilmann multiple-use needle system (Medi-Globe).



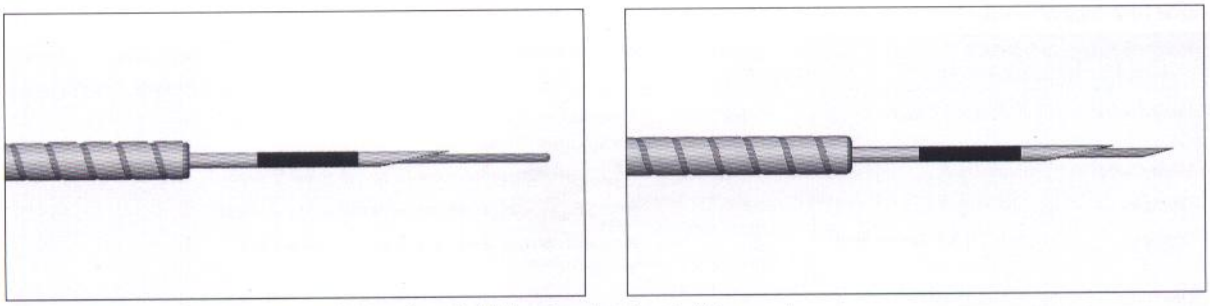
a



b

Fig. 10.**7a** When the needle is completely retracted inside the sheath, the position can be fixed with a button to avoid accidental forward movement of the needle tip. **b** The stylet is unprotected when the needle piston is unlocked. This may cause damage to the working channel during introduction of the needle assembly.

The core of the biopsy instrument is a stiff steel needle 170 cm long. The needle is manipulated using a handle piston inside the biopsy handle (or outside it with the Olympus and Wilson-Cook systems) (Fig. 10.**6**). The handle piston with the needle transmits any movements made by the examiner directly to the needle tip without compressing the needle, so that it can even be used to penetrate hard tumors. The handle piston can be locked and unlocked by means of a button (or screw) to avoid advancement of the needle during introduction and withdrawal of the biopsy assembly (Fig. 10.**7**).



a b

Fig. 10.**8** Stylets can either be round (**a**) or beveled (**b**) at the distal end of the needle.



Fig. 10.**9** The SonoTip I single-use system (Medi-Globe; no longer available, replaced by SonoTip II).

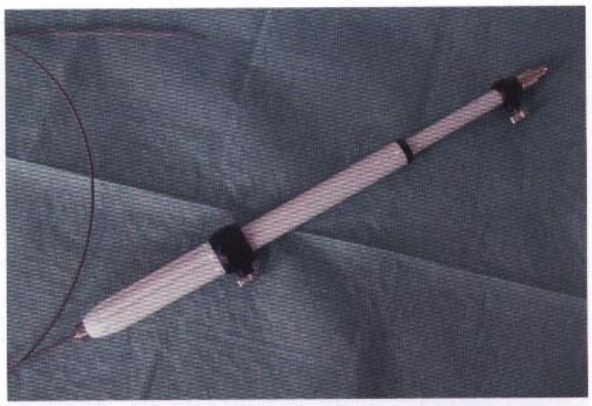


Fig. 10.**10** The SonoTip II single-use system (Medi-Globe).

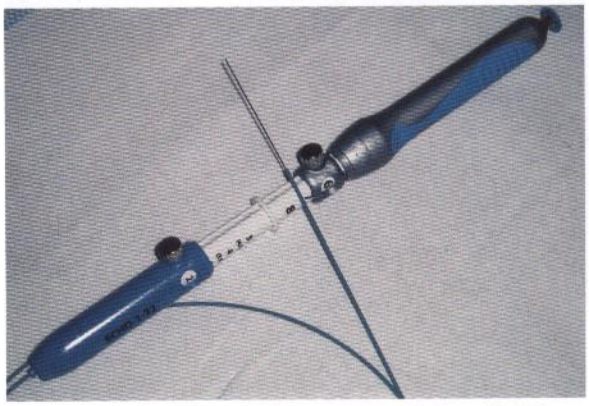


Fig. 10.**11** The Echo-Tip single-use system (Wilson-Cook).

The needle is supported by a stable metal spiral sheath, which is firmly connected to the aluminum handle. The handle can be firmly connected to the endoscope using a Luer lock. When the handle is screwed onto the endoscope's Luer connection, the metal spiral extends 4–5 mm out of the distal outlet of the working channel, so that the needle cannot damage the endoscope's instrument channel as it is being introduced.

Inside the needle, there is a stylet with the important feature (in the original version) of having a rounded tip, to avoid perforating the spiral and damaging the endoscope's working channel, requiring very expensive repairs. Nowadays the needle is also available with an optional beveled stylet (Fig. 10.**8**).

The instruments described above represent the conventional biopsy equipment developed by Vilmann and Hancke. In these instruments, the steel needle is disposable, while the other components can be reused a number of times. Due to the variety of customer requirements, Medi-Globe, Olympus, and Wilson-Cook have developed single-use plastic kits that can be disposed of completely (Figs. 10.**9**–10.**12**). These innovations also

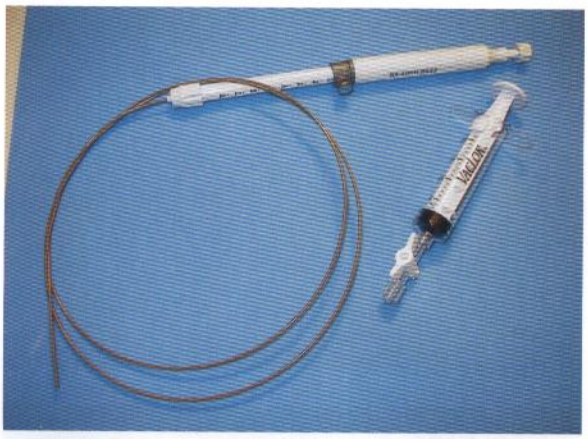


Fig. 10.**12** The EZ shot single-use system (Olympus).

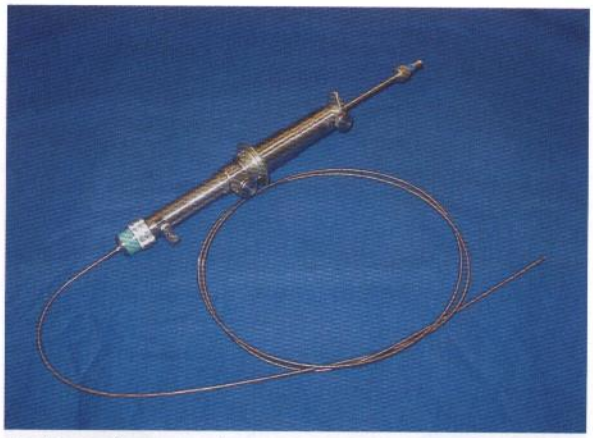


Fig. 10.**13** The Power Shot reusable spring-loaded needle system (Olympus).

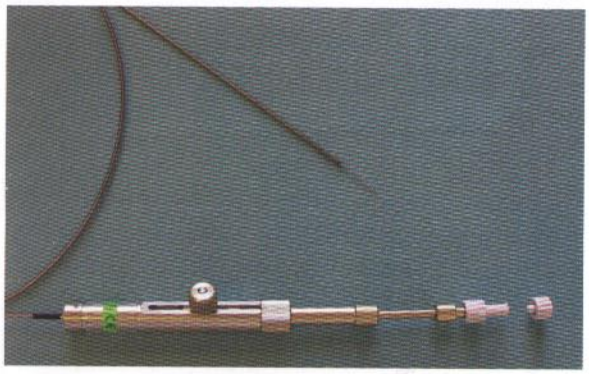


Fig. 10.**14** The conventional multiple-use needle system (Olympus NA-10J-1).

make it possible to adjust the length of the needle sheaths to match the variable lengths of the endoscope working channels. However, many examiners still use the conventional biopsy equipment, which with its purely metal components provides a high degree of stability and guide precision, as this can be advantageous for biopsies of hard tumors. In addition to the aspiration needle equipment, the disposable kits also contain a syringe with a three-way stopcock that makes handling easier. An automatic spring-loaded biopsy system (Olympus PowerShot; Fig. 10.**13**) is also available; this has a metal spring that can forcefully shoot the needle out up to 3 cm (the depth is adjustable).

There are a wide range of different sheath designs, either consisting of metal rings with or without Teflon coating, or sheaths made entirely of Teflon or other plastic types (Figs. 10.**14**, 10.**15**). Different sizes of sheath diameter are available; the larger sheath diameter sizes (Medi-Globe Ltd.) are preferable for biopsies using large-channel endoscopes. The sheath diameters available from Medi-Globe are either 1.8 mm or 2.7 mm.

A different needle material has also recently become available, with nitinol being used instead of stainless steel. This new needle system should also be able to incorporate a shape-memory function (Fig. 10.**16**). This is a recent development, and experience with the system is at present limited. To increase the visibility of the

	Sheath		Stylet	Needle
Order no.	French size	Design	Tip	Gauge
ECHO-1-22	5.2 - 4.5		Beveled	22
ECHO-3-22	5.2		2 mm ball tip	22
ECHO-19	5.2 - 4.0		2 mm ball tip	19
ECHO-25	5.2 - 4.5		2 mm ball tip	25
ECHO-20-CPN*	6.0		N/A	20

U.S. Patent Number: 5,081,997.

Celiac plexus neurolysis - available summer 2003. Not for sale in the USA. Cone-tip needle with side holes for injection of neurolysing agents.

Fig. 10.**15** Different needle types and sheath designs (Wilson-Cook).

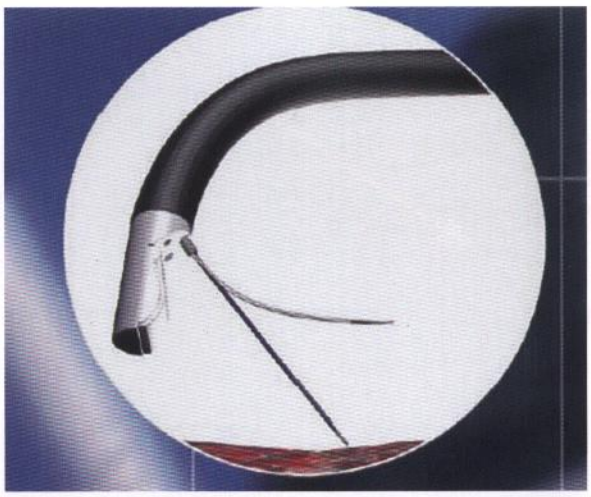
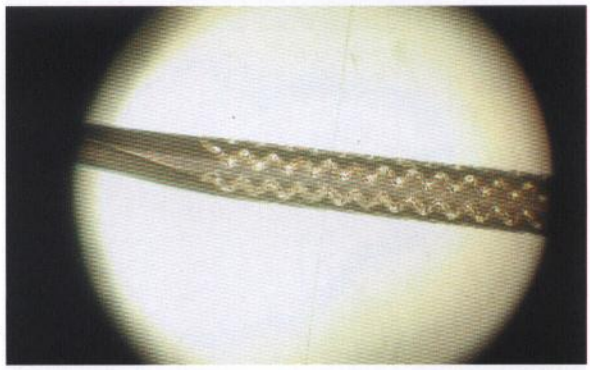


Fig. 10.**16** The new Medi-Globe single-use aspiration nitinol needle. The needle, featuring a memory effect, prevents bending of the cannula.



a



b

Fig. 10.**17a, b** Different laser-treated needle tips for enhanced ultrasonic needle visualization. ▷



a

Fig. 10.**18** The Quick-Core spring-loaded histological Tru-Cut needle (Wilson-Cook). **a** Round-type stylet. **b** Beveled-type stylet.



b

needle during EUS-FNA, the various manufacturers each have specific designs for the distal few centimeters of the needle tip, with different laser-produced marks in the metal (Fig. 10.**17**).

In the authors' experience, there are no major differences between the various designs with regard to needle monitoring and visualization, but there are variations in the way they appear on the ultrasound image.

Only one histological Tru-Cut needle with a spring-loaded shot mechanism is currently available (the Quick-Core needle from Wilson-Cook) (Fig. 10.**18**).

■ Examination Room

Due to the lengths of the instrument and other required equipment, the examination room should be sufficiently large. The stiff 170-cm needle has a high level of residual stress, so that carelessness in small rooms can result in injury to the medical staff. Priority should be given to ensuring that there is sufficient space to place the endoscope, with a working surface nearby for the smear preparation.

The biopsy instrument should be used with sterile gloves as far as possible, to avoid iatrogenic infections with hospital germs.

■ Preparation of the Patient

EUS-FNA can be carried out safely as an outpatient procedure in most cases. Laboratory tests are only necessary in selected patients—e.g., those receiving anticoagulation treatment or with known or potential bleeding disorders. As with all endoscopic procedures, the patient should fast for at least 2–4 hours. It is recommended that the examination should be carried out with the patient sedated as usual for endoscopy, with midazolam (3–6 mg) and fentanyl (50–100 µg). Low-dose midazolam (2–3 mg) in combination very low-dose propofol (3–5 mg) as required is used mainly in Germany. However, in most other European countries, the administration of propofol is only permitted for anesthesiologists.

■ Biopsy Procedure (Tables 10.3–10.5)

Before an EUS-guided biopsy procedure is started, several issues need to be taken into consideration. Firstly, the indication needs to be correct and patient safety should be considered. It is advisable for inexperienced examiners not to start with the most difficult types of biopsy. Contrary to what might be expected, the stomach wall is the most difficult area to biopsy, since the wall tends to move considerably along with the needle, and several of the indications in this location are submucosal tumors, which are difficult to diagnose with fine-needle aspiration—e.g., gastrointestinal stromal tumors and leiomyomas. Table 10.**3** lists the levels of difficulty of the various procedures in increasing order, based on our own experience. Our advice is that examiners should start with a biopsy of a large mediastinal tumor that is suspicious for lung cancer; in most cases, these lesions are very easy to target and the diagnosis is easy to obtain.

Cooperation by the patient is an important prerequisite for a complication-free biopsy procedure. Sudden movements have to be avoided in order to prevent injuries. Of course, the biopsy must not be carried out

Table 10.**3** Levels of difficulty of endoscopic ultrasound-guided fine-needle aspiration biopsy, in increasing order

1	Large mediastinal tumors
2	Mediastinal lymph nodes
3	Liver lesions
4	Adrenals
5	Perigastric lymph nodes
6	Pancreatic body and tail tumors
7	Peripancreatic lymph nodes
8	Pancreatic head tumors
9	Stomach wall (submucosal tumors)

Table 10.**4** Biopsy recommendations

- Establish firm transducer contact with the gastrointestinal wall
- Straighten the endoscope
- Use a four-hand procedure in difficult cases
- Take multiple biopsies
- Remove the stylet inside the lesion
- Ensure full monitoring of the needle
- Release the Albarran when inside the lesion

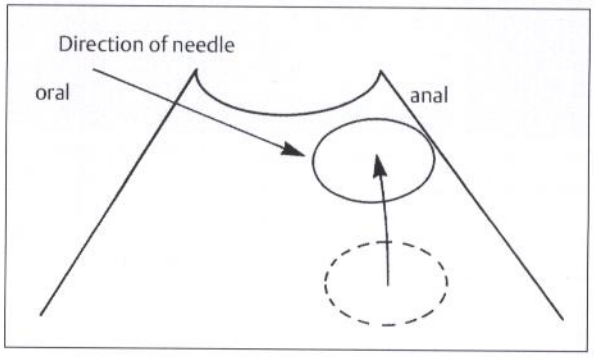


Fig. 10.**19** Positioning the lesion at the top margin of the image.

when there is a vessel between the transducer and the tumor, or when the lesion cannot be properly positioned.

Firstly, the transducer has to be brought into a stable position in front of the lesion to be biopsied. As the prick angle is quite small, it is advantageous to position the lesion at the top margin of the image using the control device before introducing the needle (Fig. 10.**19**). The metal spiral (together with the retracted needle) is then introduced into the biopsy channel, and care must be taken to ensure that the needle piston is securely locked. Introducing the metal spiral with a needle that is sticking out by 1–2 mm at the distal end can severely damage the endoscope.

Table 10.**5** The biopsy procedure: tips and tricks

Preparation	
Before introducing the needle, check the biopsy equipment with this checklist	• Make sure the needle and stylet are firmly screwed and connected • Make sure the needle is not extending distally from the metal spiral • Make sure the needle piston is locked firmly in the handle
After introducing the needle into the instrument channel	• Is the handle firmly screwed and connected with the Luer lock on the endoscope's channel inlet? (Keep checking firm seating of this during the biopsy procedure)
Before advancing the needle	• Is the metal spiral sheath visible in the endoscopic image?
Before the basic biopsy procedure	• Check the precise positioning of the transducer in front of the biopsy target, which should be in the needle's potential pointing direction • Exclude significant interposed vessels using color Doppler ultrasound or by assessing the tumor vascularization
Biopsy procedure	• Advance the needle (after releasing the lock button) together with the stylet up to the inner surface of the gastrointestinal tract. The needle and insertion direction are now visible in the ultrasound image • If using a *round* stylet, retract it about 5 mm into the needle. A *beveled* stylet can be advanced together with the needle • The needle is advanced into the lesion, with careful ultrasound monitoring; the stylet is reintroduced to exclude obstructing tissue plugs inside the needle tip and then completely removed and kept sterile • Low pressure is created using a 10-mL syringe, and while the low pressure is maintained the needle is moved about 5–10 times forward and back in the lesion • The low pressure is slowly released while the needle is still *inside the lesion* • If insufficient acoustic coupling is experienced in the duodenum initially during the biopsy procedure, fill the balloon shortly after needle contact with the duodenal wall • If mounting of the biopsy instrument is difficult due to bending of the endoscope in the duodenum, withdraw the endoscope to the stomach and reenter after mounting the needle • Release the elevator after EUS-guided tumor penetration, to reduce the resistance against the needle • The entire needle assembly can only be removed from the endoscope after complete retraction of the needle into the sheath (note the lock position). If the needle is not retracted completely, it may damage the entire instrument channel • The specimen is either expelled onto glass slides with air, using a syringe, or distributed evenly by reintroducing the stylet



Fig. 10.**20** A needle system firmly attached to the endoscope's biopsy inlet. A syringe with suction is mounted during the aspiration biopsy.

The spiral is fully inserted and the handle with the Luer lock is firmly screwed onto the biopsy channel (Fig. 10.**20**).

Two methods can be used to ensure that the sheath protects the entire length of the endoscope's working channel. Using the endoscope's lens, it can be observed that the sheath is extending from the distal end to a secure distance of 3–5 mm; alternatively, the position of the sheath can be checked by ultrasound. The latter technique is safe and advisable in experienced hands, but the first method should be used by those who are less experienced. However, ultrasound checking has the drawback that the transducer has to be lifted away from the mucosa and the ultrasound view of the lesion. A new firm contact then has to be made and the optimal transducer position has to be regained before the biopsy can be performed.

The needle should only be moved forward when the handle is firmly screwed onto the biopsy channel and the sheath is visible at the distal end (Figs. 10.**7**, 10.**20**).

This is to avoid damage to the working channel due to unintended disconnection of the Luer lock connection during the biopsy.

Checking the ultrasound image, the examiner has to try to keep a very firm and stable contact between the transducer and the inner surface of the gastrointestinal tract. The endoscope should be straightened, especially when puncturing the pancreatic head, as in the endoscopic retrograde cholangiopancreatography (ERCP) position, as these tumors are often very hard to biopsy and the resistance to needle movements should be as low as possible.

Once the position has been carefully adjusted, the needle with the attached stylet should be advanced until the biopsy direction can be estimated and the target of the biopsy can be reached easily.

An Albarran is undoubtedly advantageous when very deep lesions have to be reached. However, it needs to be taken into account that the needle with the stylet is very stiff and that activation of the Albarran causes considerable strain on the sheath, biopsy needle, and stylet. Moreover, the flexion makes it more difficult to move the needle forward and backward during the biopsy procedure; when hard tumors are being penetrated, it even increases the resistance, which is already quite high. In most cases, it is possible to adjust the direction of the biopsy needle insertion very precisely using the endoscope's conventional handle control buttons (Fig. 10.**21**).

The needle, still with the stylet, is then advanced up to the inner surface (mucosa) of the gastrointestinal tract. The next step depends on the type of stylet being used—either round or sharp (beveled). The round type leads to significantly less damage to the instrument channel and is preferable for those with less experience. When a biopsy is being carried out with a beveled stylet, the needle can be advanced into a lesion immediately after it has been moved into position. If a round stylet is being used, it has to be retracted by a few millimeters (as it normally extends beyond the needle tip by 1–2 mm) before the actual penetration through the gut wall is carried out. After the stylet has been retracted, the needle tip is exposed and can freely penetrate the tissue. Further retraction of the stylet should not be done, in order to avoid obstructive tissue plugs from superficial layers inside the biopsy needle. It is often unavoidable that a few cells from the gut wall (gastric mucosa, duodenal mucosa, esophageal mucosa) appear in the cytological material. Consequently, it is very important to provide the cytologist with precise information about the method and route of the biopsy.

With the stylet retracted but still inside the needle, the biopsy needle is now moved forward into the lesion under full ultrasound guidance (Fig. 10.**22**). It should be emphasized that complete monitoring of the needle tip is important whenever possible. There are a few cases in

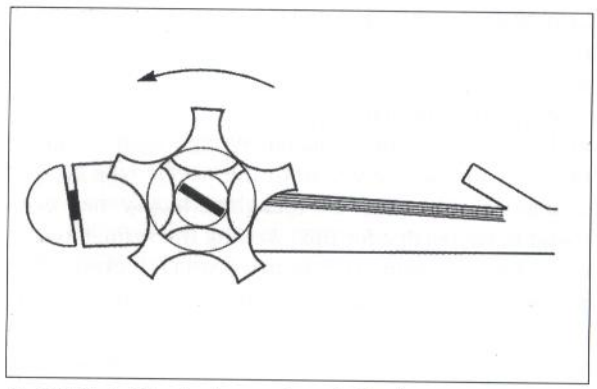


Fig. 10.**21** Anticlockwise turning of the large control wheel, with deflection of the distal tip, lifts the lesion closer to the transducer.



Fig. 10.**22** Endoscopic ultrasound-guided biopsy of an insulinoma in the tail of the pancreas. The needle should be clearly visible during the entire biopsy procedure.

which a punch technique is the only way to penetrate a hard lesion. However, this technique should not be used as standard. After penetration into the middle of a lesion, the stylet is removed completely. One of the present authors (P.V.) always reintroduces the stylet into the needle before complete removal, in order to expel possible tissue plugs from superficial layers that are obstructing the needle lumen. This should of course only be done in cases in which there is no tumor interposed between the transducer and the target lesion, to avoid tumor seeding.

When hard tumors are being punctured, bending of the needle is sometimes observed; this may create problems with monitoring the needle tip and may potentially cause injury to the surrounding structures, particularly the vessels. If severe bending of the needle is experienced, a new needle should be chosen for a repeat biopsy. There is also a tendency during needle advancement for the transducer to be pushed away from the mucosa, so that the ultrasound image is lost. This occurs particularly during pancreatic biopsies. Loss of the ultrasound image and thus of ultrasound needle monitoring

in these cases can be avoided to some extent by inflating the balloon immediately after initial mucosal contact with the needle.

When the optimal needle position is reached in the middle of the lesion, a 10-mL syringe with a locking device is firmly screwed onto the needle (the type of syringe usually used for Menghini biopsy has been found to be reliable for this). Pulling the syringe piston creates low pressure. The syringe piston is locked in this position for permanent suction. The needle is now moved to and fro 5–10 times inside the lesion with full ultrasound guidance. If considerable resistance is experienced when using the Albarran during the biopsy, one should try to neutralize the Albarran as soon as the needle tip is in the middle of the lesion. With the needle tip still in the lesion, suction is slowly released, and the needle is retracted (cautiously, as there is a danger of injury and contamination) inside the needle sheath and locked in a secure position. The complete needle assembly is now removed by disconnection from the inlet of the endoscope.

Consideration also needs to be given to the endoscope used when the type of needle is being selected. Biopsy can be carried out safely with large-channel endoscopes. However, ultrasound control during the needle during biopsy is more difficult with standard needle systems, as there is a size difference between the needle sheath and the working channel. There is a tendency to lose sight of the needle on the ultrasound image when the needle sheath is floppy and unsupported by the endoscope working channel. This can be reduced using the Albarran, which holds the sheath in a firm position. However, needles with an extended sheath size that fits the endoscope's working channel better are preferable.

If several lesions are present during an EUS examination, it has to be decided how many of the lesions, which lesions, and in which order they should be biopsied. Careful consideration is mandatory here, taking the TNM staging of each disease into account. It is obvious that a lesion that is suspected to be a distant metastasis should be biopsied before the local lymph nodes, with the primary lesion following last, in successive order, if the same needle is to be used. If this is not done, it is possible for false-positive up-staging of the disease to occur. If a new, more distant lesion is detected after an initial biopsy, a completely new needle should be chosen.

■ Preparing the Smear

In normal conditions after fine-needle aspiration biopsy, it is recommended that the biopsy material should immediately be expelled with air from the syringe onto the prepared specimen slides. Another method that can be recommended in EUS-FNA is to reintroduce the stylet into the needle and move it slowly forward. This creates high pressure in the needle and the material can be expelled carefully and in a controlled way droplet by droplet onto the specimen slides. The decisive advantage of this method is that numerous specimens of the same quality can be prepared, whereas with the air expulsion method, there is a risk of the material being expelled in an uncontrolled way. Stylet expulsion is particularly advantageous, as immunohistochemical stains are often necessary and are becoming more and more important. With this method, it is easy to identify cylinders that can be processed during histological analysis. However, the diagnostic benefit of histological specimens should not be overrated, as cytology also allows excellent immunohistochemical examination.

The smearing technique should be discussed with the cytopathologist. Personally, we smear the material with a second specimen slide that is placed smoothly on top of the first one and retracted, with a second specimen being obtained. Others recommend that, in addition to smearing of the material, a microhistological cylinder should be prepared, fixed with formalin, and processed into a cell block for histological evaluation.

The subsequent procedure, particularly fixation, should also be discussed with the cytologist. No general advice can be given here; basically, the specimen can be air-dried and fixed later, but some cytopathologists recommend immediate fixing and coloring of the smear. There is some evidence in the literature that it is preferable to have an attending cytopathologist in the examination room for immediate evaluation of the specimen. When a ready-to-use staining liquid is applied, it is possible to assess and evaluate the adequacy of the specimen even after only a few minutes. However, in the authors' experience, this is not absolutely necessary if ultrasound monitoring of the needle during the biopsy is optimal and if the macroscopic appearance of the material shows that it contains minute tissue fragments.

■ Limitations and Complications

The increasingly widespread use of ultrasound-guided fine-needle biopsy certainly owes something to the fact that it is regarded as a low-complication method. A multicenter study by Wiersema et al. [16] showed that the complication rate was about 2%, with the majority being minor complications. Complications often consist only biopsy-point bleeding that is clinically insignificant. Heavier bleeding is rare; it may occur rarely due to shearing of the mucosa by the needle and due to injury to adjacent vessels when restless and nervous patients are being examined.

The infection rate is also remarkably low, so that antibiotic prophylaxis is not usually necessary. Biopsy of pancreatic pseudocysts is an exception to this, in

which it has been shown that antibiotic prophylaxis is preferable, as there is a relatively high risk of infection [17]. Pancreatitis has been reported as a complication, particularly when pancreatic biopsies are carried out in patients with benign pancreatic diseases [15].

Tumor-cell seeding has always been a matter of debate and concern; however, there are as yet no "hard facts" providing evidence that this is a potential risk. Penetrating through malignant tissue to reach a suspicious lesion is in any case not recommended. An example of this might be a patient with gastric or esophageal cancer, with a suspicious lymph node adjacent to the primary tumor.

Despite the rapid technological advances being made with other imaging methods, endoscopic ultrasonography has strengthened its position as a diagnostic method, particularly since the development of the fine-needle biopsy technique. It is therefore all the more important to take advantage of the diagnostic advantages and low complication rate of EUS by standardizing the procedure and providing training programs, so that it becomes even more widely used in gastrointestinal practice.

References

1. Fukuda M, Nakano Y, Saito K, Hirarta K, Terada S, Urushizaki I. Endoscopic ultrasonography in the diagnosis of pancreatic carcinoma: the use of a liquid-filled stomach method. Scand J Gastroenterol Suppl 1984;94:65–76.
2. DiMagno EP, Buxton JL, Regan PT, Hattery RR, Wilson DA, Suarez JR, et al. Ultrasonic endoscope. Lancet 1980;i: 629–31.
3. Strohm WD, Phillip J, Hagenmüller F, Classen M. Ultrasonic tomography by means of an ultrasonic fiberendosope. Endoscopy 1980;12:241–4.
4. Vilmann P, Jacobsen GK, Henriksen FW, Hancke S. Endoscopic ultrasonography with guided fine needle aspiration biopsy in pancreatic disease: a new diagnostic procedure. Gastrointest Endosc 1992;38:172–3.
5. Vilmann P, Hancke S, Henriksen FW, Jacobsen GK. Endosonographically-guided fine needle aspiration biopsy of malignant lesions in the upper gastrointestinal tract. Endoscopy 1993;25:523–7.
6. Vilmann P, Hancke S, Henricksen FW, Jacobsen GK. Endoscopic ultrasonography-guided fine-needle aspiration biopsy of lesions in the upper gastrointestinal tract. Gastrointest Endosc 1995;41:230–5.
7. Vilmann P. Endoscopic ultrasonography with curved array transducer in diagnosis of cancer in and adjacent to the upper gastrointestinal tract: scanning and guided fine needle aspiration biopsy [dissertation]. Copenhagen: Munksgaard, 1998.
8. Giovannini M, Seitz JF, Monges G, Perrier H, Rabbia I. Fine-needle aspiration cytology guided by endoscopic ultrasonography: results in 141 patients. Endoscopy 1995;27: 171–7.
9. Vilmann P. Endoscopic ultrasonography-guided fine-needle aspiration biopsy of lymph nodes. Gastrointest Endosc 1996;43(2 Pt 2):S24–9.
10. Pedersen BH, Vilmann P, Folke K, Jacobsen GK, Krasnik M, Milman N, et al. Endoscopic ultrasonography and real-time guided fine-needle aspiration biopsy of solid lesions of the mediastinum suspected of malignancy. Chest 1996;110: 539–44.
11. Pedersen BH, Vilmann P, Milman N, Folke K, Hancke S. Endoscopic ultrasonography with guided fine needle aspiration biopsy of a mediastinal mass lesion. Acta Radiol 1995; 36:326–8.
12. Larsen SS, Krasnik M, Vilmann P, Jacobsen GK, Petersen JH, Fauerskov P, et al. Endoscopic ultrasound guided biopsy of mediastinal lesions has a major impact on patient management. Thorax 2002;57:98–103.
13. Larsen SS, Vilmann P, Krasnik M, Dirksen A, Clementsen P, Maltbaek N, et al. Endoscopic ultrasound guided biopsy performed routinely in lung cancer staging spares futile thoracotomies: preliminary results from a randomised clinical trial. Lung Cancer 2005;49:377–85.
14. Larsen SS, Vilmann P, Krasnik M, Dirksen A, Clementsen P, Skov BG, et al. Endoscopic ultrasound guided biopsy versus mediastinoscopy for analysis of paratracheal and subcarinal lymph nodes in lung cancer staging. Lung Cancer 2005;48: 85–92.
15. Vilmann P, Hancke S. A new biopsy handle instrument for endoscopic ultrasound-guided fine-needle aspiration biopsy. Gastrointest Endosc 1996;43:238–42.
16. Wiersema MJ, Vilmann P, Giovannini M, Chang KJ, Wiersema LM. Endosonography-guided fine-needle aspiration biopsy: diagnostic accuracy and complication assessment. Gastroenterology 1997;112:1087–95.
17. Chang KJ, Katz KD, Durbin TE, Erickson RA, Butler JA, Lin F, et al. Endoscopic ultrasound-guided fine-needle aspiration. Gastrointest Endosc 1994;40:694–9.

11 Tips and Tricks for Fine-Needle Puncture

T. Beyer, T. Topalidis

Introduction

There is a very wide range of morphological equivalents for a pathological structure that is visualized on ultrasonography. Options include inflammatory conditions, benign or malignant tumors, and metastases. Cytological or histological confirmation of the diagnosis is often required in order to distinguish between the different possibilities. The hints and tips presented here are intended for cytological aspiration biopsy—better known as fine-needle aspiration biopsy (FNAB).

The advantages of the current microinvasive technique include:

- A high level of patient acceptance
- The high diagnostic yield
- A low risk of complications
- Low cost

These considerations have led to this valuable method being accepted throughout the world.

Definition of Fine-Needle Puncture

Various different terms are used for the fine-needle puncture technique (needle diameter < 1 mm) in everyday clinical practice:

- Fine-needle aspiration (FNA)
- Fine-needle aspiration biopsy (FNAB)
- Fine-needle aspiration cytology (FNAC)
- Fine-needle biopsy (FNB)
- Fine-needle cytology (FNC)

A variety of fine-needle systems are now commercially available, which can be used with endoscopic ultrasound (EUS) equipment for imaging-guided biopsy procedures. The main advantage of EUS-guided fine-needle puncture appears to be the ability to control the needle tip in real time during the puncture process. However, the results depend not only on the puncture process, but also on the processing of the resulting specimen and the quality of the cytologist.

Unfortunately, there is as yet no standard procedure for specimen processing. There is no consensus on whether it is necessary to use a fixation process for the specimens, or if so, whether fixation should be carried out before or after smearing onto the microscopic slide. Nor is it clear which fixation method is best. However, we would like to discuss and clarify the following questions here:

- What fixation methods are available?
- How should the specimens be stained?
- Is it possible to create a standard for cytological diagnosis?

Cytological Examination

Nine steps are involved in a normal cytological examination process, according to Lopes Cardozo [1]:

- Indication for fine-needle aspiration
- Choice of the best way of obtaining the specimen
- Process of taking the specimen
- Preparation of the specimen
- Fixation process
- Staining process
- Preliminary analysis of the material
- Formulating a diagnosis on the basis of clinical information
- Matching the diagnosis to the patient's disease

All of these diagnostic steps are equally important in order to obtain an optimal result. Normally, steps 1–5 and 9 are carried out by the clinical practitioner, whereas steps 6–8 are carried out by the cytologist. In our opinion, steps 2, 3 and 9 are the most difficult and require perfect teamwork between the clinical practitioner and the cytologist in order to ensure the best possible result.

It is important to mention two different ways of obtaining a cytological diagnosis at this point. On the one hand, there are central cytology laboratories with no direct connection to the clinical practitioner (as in the case of one of the present authors, T.T); on the other hand, cytologically trained clinical practitioners (as in the case of the other author, T.B.) may have a direct link to a clinical department (such as pulmonology). The goal in both cases is to match the cytological specimens to the correct diagnosis. The cytologically trained clinical practitioner carries out a simultaneous preliminary analysis during the puncture process, which is advantageous as it reduces the number of specimen collections. This results in better patient comfort and increases the sensitivity of the method. On the other hand, the cytol-

ogy specialist naturally has a wider knowledge of different diseases and can use immunocytology to obtain a clearer diagnosis.

■ Collection

It is important to obtain an optimal view of the lesion in question after an EUS examination of the patient. The most important consideration is to find the shortest possible route to the target, avoiding the surrounding blood vessels. One advantageous way of doing this is to use an assistant to control the needle movement into the lesion (in real-time puncture) while the examiner controls the echoendoscope to maintain optimal positioning. After the needle has entered the target, the stylet has to be removed. A syringe with a volume of 10 cm^3 should then be placed attached at the end of the needle and used to produce suction (pressure below atmospheric level). While continuous suction through the syringe is being maintained, the needle should be passed through the lesion movement forward and backward in a fan-like. After three to five needle passes, the suction should be released and the needle removed (Fig. 11.**1**).

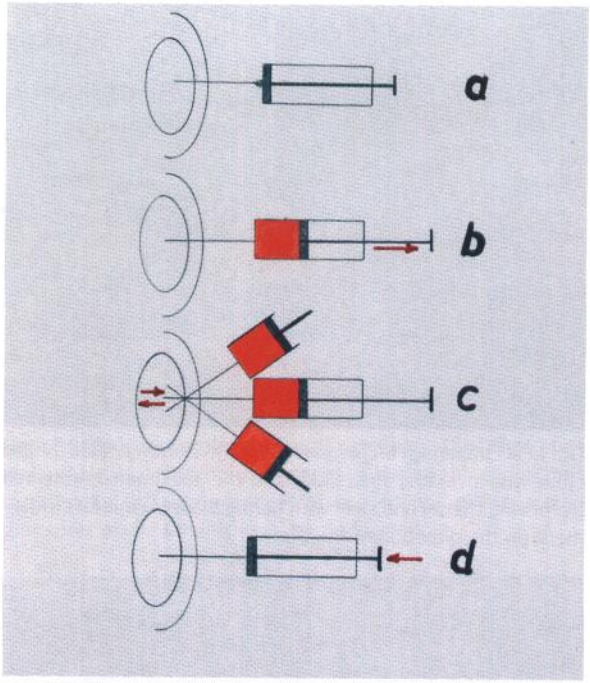


Fig. 11.**1** The fine-needle aspiration procedure. **a** Introducing the needle into the lesion. **b** Creating suction using a syringe. **c** The fan-like pattern of needle passes (three to five passes). **d** Releasing the suction and removing the needle.

■ Specimen Handling

After the puncture process has been carried out, the fine-needle aspiration system should immediately be removed from the echoendoscope, and a new 10 cm^3 syringe filled with 10 mL air should be placed at the end of the needle system. The collected specimen has to be spread onto slides by carefully emptying the air-filled syringe through the needle. During this process, the tip of the needle has to be held directly on the slide to ensure that only small portions of the specimen are released. Alternatively, the stylet can be carefully reintroduced into the needle and the resulting pressure can be used to eject the specimen (Figs. 11.**2**, 11.**3**).

Immediately after this, the specimen should be smeared gently but quickly using another slide. The smaller the specimen drops, the thinner the specimen layer on the slide (Figs. 11.**4**, 11.**5**). Too much pressure during the spreading process should be avoided, as it increases cell artifacts.

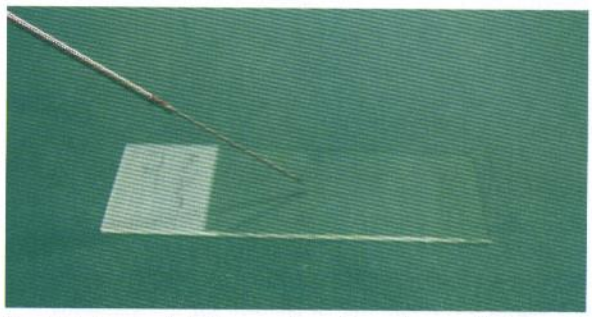


Fig. 11.**2** Removal of the specimen from the needle (step 1). The Hancke–Vilmann fine-needle aspiration system is being used here.

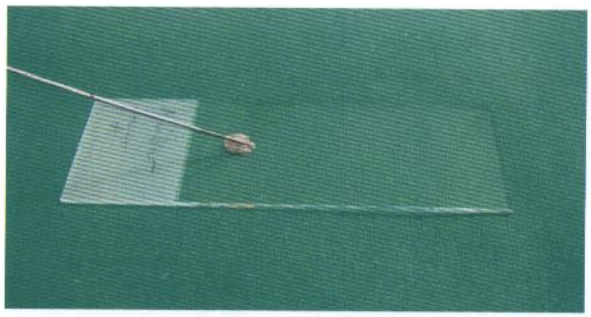


Fig. 11.**3** Removal of the specimen from the needle (step 2). Releasing drop-like portions onto the slide. It is important to prevent the resulting specimen from drying out by preparing no more than two or three slides and then immediately smearing them using another slide.

■ Fixation

The fixation process is very important for the microscopic image, and fixation should be carried out immediately after the smearing of the specimen. The method of fixation used depends on the type and size of the specimen, as well as on the staining method chosen

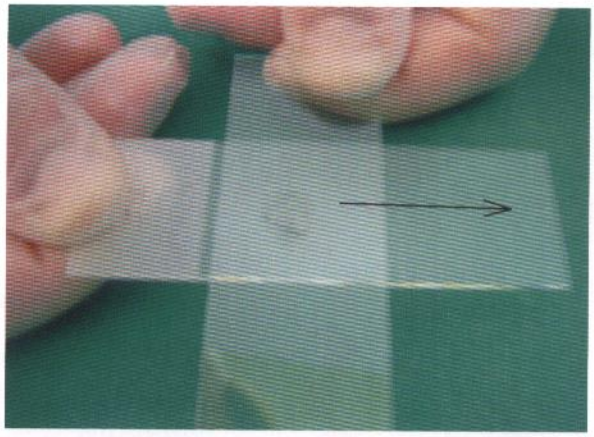


Fig. 11.4 Smearing technique (step 1). Another slide is laid cross-wise over the first slide, and the specimen is smeared by moving the second slide with gentle pressure but fast movement (in the direction of the arrow).

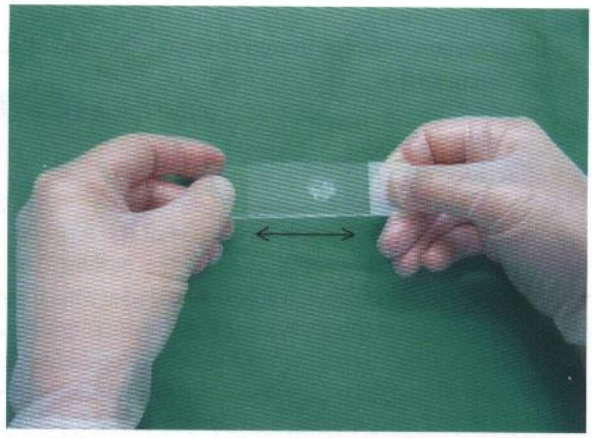


Fig. 11.5 Smearing technique (step 2). Another slide should be laid directly over the first slide. The two slides are moved against each other quickly, but with gentle pressure.

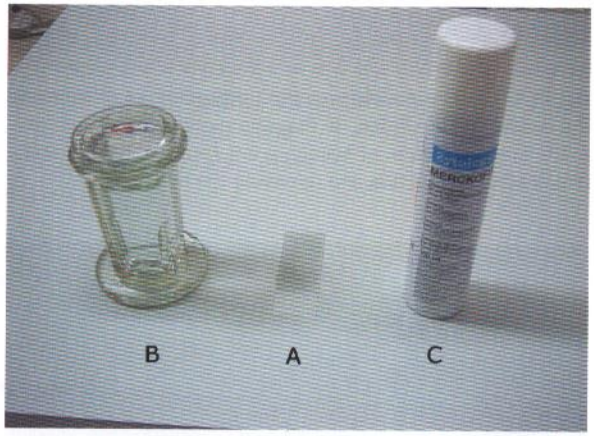


Fig. 11.6 Three types of fixation. **a** Air-drying fixation. **b** Chemical liquid fixation (alcohol or Delaunay solution), with immersion of the loaded slides in a 95% alcohol solution for a period of 30 min. **c** Chemical spray fixation.

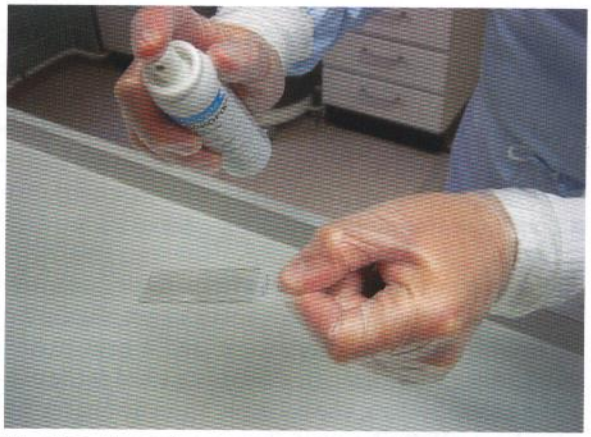


Fig. 11.7 Chemical spray fixation. This is best for subsequent staining using Papanicolaou solution or hematoxylin–eosin (HE) solution. Agreement from the cytologist is required before this is used. The loaded slide should be sprayed several times from a distance of 20–30 cm immediately after smearing. After spraying, the slides should be left in a horizontal position for 20 min.

afterward. There are two different fixation methods (Figs. 11.6–11.8):

- Air-drying fixation
- Chemical fixation

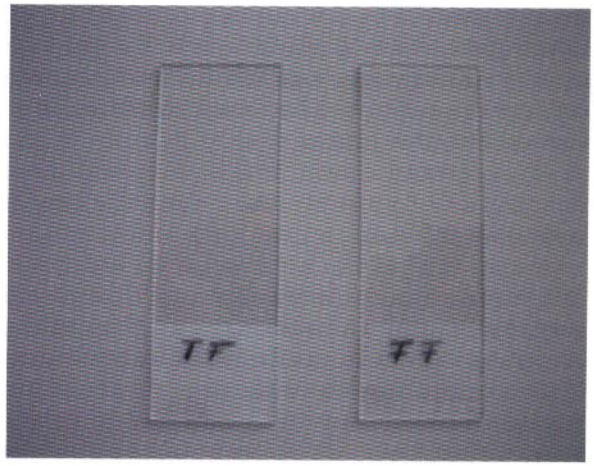


Fig. 11.8 Air-drying fixation or chemical fixation? Air-drying fixation is quick and therefore allows staining to be carried out at the bedside (with May–Grünwald–Giemsa staining or Pappenheim staining). It is also suitable for immunocytochemical examinations. Chemical fixation is necessary for Papanicolaou or hematoxylin–eosin staining and needs to be agreed on with the cytologist beforehand.

Air-drying fixation allows later staining using May–Grünwald–Giemsa solution (MGG), as well as immunocytochemical staining methods, and in the authors' opinion appears to be preferable to chemical fixation methods. Chemical fixation substances (alcohol, Delaunay solution, chemical spray fixation) allows later staining using Papanicolaou solution or hematoxylin-eosin solution. In this case, the fixation process has to be started immediately (< 5 s) after smearing. The specimen on the slide must still be moist during the fixation process, to avoid severe cell artifacts that could prevent proper examination by the cytologist. There should be a label on every slide stating the type of fixation used and the name of the patient, in order to avoid mistakes and to ensure the optimal choice of staining method.

■ Staining

The air-drying method has proved to be the best way of allowing a quick "bedside" staining process such as Hemacolor (Merck Inc., Darmstadt, Germany) (Figs. 11.**9**–11.**11**).

■ Request Form, Clinical Data, Questions of Interest

It is essential for the cytologist to have important clinical facts from the patient's history in order to find the correct answer to the question being posed. Unfortunately, only little information is often provided on the request form. It should be noted that data protection between the clinical physician and the cytologist is usually very strictly adhered to.

The following information is the minimum necessary to provide the best cytological results:

- Type of specimen
- Origin of specimen
- Important facts in the patient's history, for example:
  - Any previous carcinoma; if so, then an indication of the histological type and grading should be given
  - Known diagnosis
  - Important pathological data from the patient's laboratory results
- Question posed
- Needle track

On the other hand, the cytologist has to provide answers to the following questions:

- Is the material representative?
- What was the origin of the material?
- Is it an inflammatory process or a neoplasia?
- Is the neoplasia benign or malignant?
- In case of metastasis, what is the origin of the cancer?



Fig. 11.**9** Bedside cytology (clinical cytology). This allows fast preliminary evaluation of the specimen during the endoscopic investigation. If a sampling error occurs, up to two repeat punctures of the lesion should be performed.

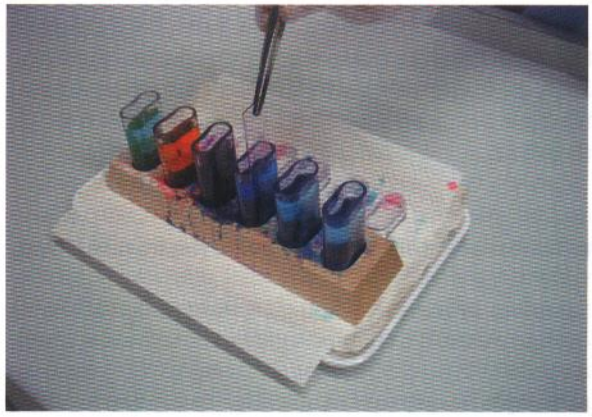


Fig. 11.**10** A fast staining kit (Hemacolor; Merck no. 11661). Solution 1: the fixation solution (5 × 1 s). Solution 2: the staining substance red (3 × 1 s). Solution 3: the blue staining substance (6 × 1 s). Solution 4: buffer solution (2 × 1 s). Solution 5: buffer solution (2 × 1 s). Solution 6: buffer solution (2 × 1 s). The advantages of the staining kit are that it is a simple and fast method, one can check one's own results, and it is a time-saving technique.

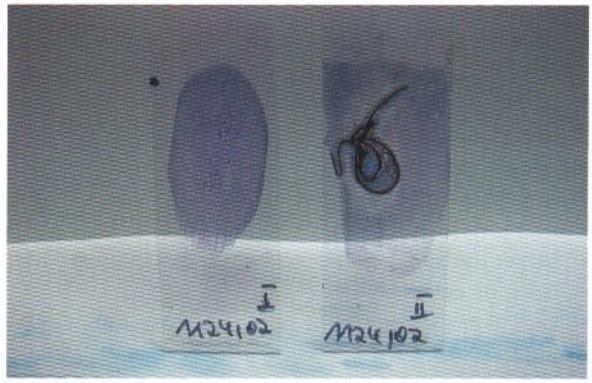


Fig. 11.**11** Which is the ideal smear? I: An ideal smear—rich in cells (macroscopic small dark blue pixels, homogeneously dispersed). II: An unusable smear, with large amounts of coagulated material and lumps.

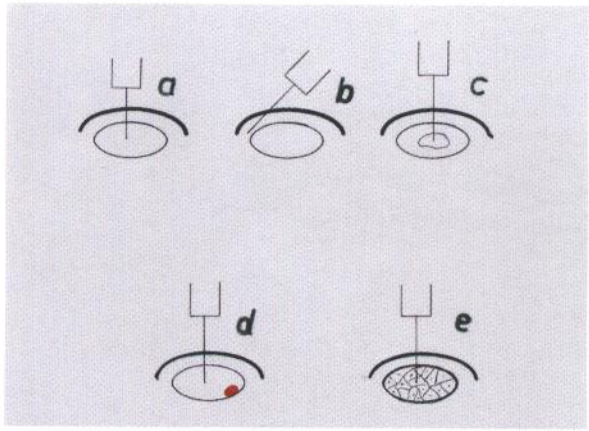


Fig. 11.12 Sampling errors. **a** The best scenario: correct needle positioning and optimal fine-needle aspiration. **b** Missing the target. **c** Cystic, hemorrhagic, or necrotic material. **d** Missing the cancer in a benign lesion. **e** Low cell content in the lesion, or sclerotic lesion.

Not all material contains the right cells for cytological analysis. In our own experience, the incidence of usable cells being present in all loaded slides is 89% [2] (Fig. 11.12).

Causes of Errors in Fine-Needle Aspiration Biopsy

Sampling process: missing the target; not obtaining enough material from the target; material not representative.

Sample handling: smearing, fixing and staining process; cytologist's level of experience.

Capabilities and Limitations of Cytology

Capabilities. The primary aim in cytology is to distinguish between malignant and benign specimens. False-positive results are mainly due to mistakes by the cytologist, and may include:

- Granulomatous inflammations
- Cell artifacts caused by previous radiation or chemotherapy
- Benign tumors

False-negative results are often due to mistakes by the clinical physician, and may include:

- Target too small for a specimen to be obtained
- Necrotic material
- Lack of proficiency in the fine-needle aspiration technique

Limitations.

- Information about the infiltration of the lesion: invasion of the lymphatic system; invasion of different layers and/or vessels.
- Exclusion of malignancy using a single fine-needle aspiration with an inadequate specimen.
- Differentiation and classification of anaplastic or immature tumors and non-Hodgkin's or Hodgkin's lymphomas is nearly impossible using normal cell-staining methods. In these cases, immunocytochemical staining methods are required.

Standardized Documentation of Findings

The cytological documentation should contain:

- A description of the patient's history relevant to the specimen
- A description of the quality of the material (e.g., six air-dried, unstained slides with material)
- A description of the cells present
- A diagnosis, including the expected grade of malignancy:
  - Material not representative
  - Representative material with no signs of malignancy (negative)
  - Malignant cells not clearly ruled out (doubtful)
  - Malignant cells probable (suspicion)
  - Malignant cells visible (positive)

It should be noted that neither method (histology or cytology) is infallible. In all cases, the cytological diagnosis should be evaluated in conjunction with the patient's symptoms.

References

1. Lopes Cardozo P., In: Früherkennung des Krebses, Hrsg. A. Linke. Schattauer, Stuttgart 1962.
2. Beyer T., Klinischer Stellenwert der endosonographisch gesteuerten transmuralen Feinnadelbiopsie für den Pneumologen. Dissertation, Medizinische Fakultät der Universität Leipzig. 2003.

12 Complications of Endoscopic Ultrasound: Risk Assessment and Prevention

C. Jenssen, M. Mayr, D. Nürnberg

Endoscopic ultrasound (EUS) and EUS-guided interventions, including fine-needle aspiration biopsy (EUS-FNA) and Tru-Cut biopsy, have become an accepted part of the diagnosis, staging, and treatment of gastrointestinal diseases, as well as in benign and malignant pulmonary disorders. In Germany, EUS systems are now used not only in university medical centers but also in the majority of gastroenterology units. Despite more than 20 years' experience and a growing number of examinations and interventions, there are few published prospective data on the safety, risks, and complications of the procedures. Most reports on complications of EUS have been sporadic observations from single centers, or have been based on reviews or retrospective studies [1].

■ EUS-Specific Factors Contributing to the Risk of Complications

Endoscopic ultrasound systems differ from traditional forward-viewing and oblique-viewing endoscopes in the rigidity and stiffness of the tip of the scope, which carries the ultrasound transducer, and in that they have a somewhat larger diameter. In addition, most echoendoscopes have a longer nonflexible segment just proximal to the transducer. The examination time in EUS is in most cases significantly longer than standard esophagogastroduodenoscopy. With the exception of one electronic radial scanning echoendoscope (Pentax/Hitachi), all echoendoscopes currently available are oblique-viewing instruments. Intubation and advancement of the echoendoscopes, especially in the esophagus, are therefore semi-blind maneuvers.

EUS-FNA and EUS-guided Tru-Cut biopsy (TCB) differ from forceps biopsies in that all of the layers of the nonsterile gastrointestinal tract and sterile extraintestinal anatomical structures are penetrated in order to obtain access to the target organ or structure. The target lesions are often neighboring vascular structures and may have pathological vascularization themselves. This is why it is not possible to apply data from studies on the safety of upper gastrointestinal endoscopy to endoscopic ultrasound.

■ Complications of Diagnostic EUS

Perforation (Table 12.1)

In a survey of the members of the American Endosonography Club published in 2001, 86 members reported 16 cervical esophageal perforations among 43 852 upper gastrointestinal EUS procedures with radial echoendoscopes (0.03%) [2]. Almost all of the patients in whom perforations occurred were elderly; seven of the 16 patients (44%) had a history of difficult intubation in previous endoscopic investigations. Large cervical osteophytes were identified in three cases.

In nine of the 16 patients with cervical esophageal perforation (56%), the procedure was being carried out by an investigator with less than 1 year of experience in endoscopic ultrasonography. Two patients required surgery. In 13 of the 15 surviving patients (81%), the complication was managed successfully with conservative treatment. One patient died [2].

Another early multicenter survey from Europe [3] reported 13 esophageal perforations in 37 915 radial EUS examinations (0.03%), accounting for 68% of all complications. The majority of these patients (77%) had undergone pre-EUS dilation of esophageal strictures

Table 12.1 Possible risk factors for gastrointestinal perforation in endoscopic ultrasound investigations

Risk factor	References
Lack of operator experience	Das et al. 2001 [2], Jenssen 2004 [4], Lachter 2005 [7]
Esophagus	
Cancer of the esophagus and EGJ	Das et al. 2001 [2], Mortensen et al. 2005 [8], Rösch et al. 1993 [3]
Dilation of esophageal stricture before EUS	Das et al. 2001 [2], Mortensen et al. 2005 [8], Rösch et al. 1993 [3]
Advanced age of patient	Das et al. 2001 [2]
Difficult previous endoscope introduction	Das et al. 2001 [2]
Large cervical osteophytes	Das et al. 2001 [2]
Duodenum	
Diverticula	Jenssen 2004 [4], Lachter 2005 [7]
Electronic curvilinear echoendoscopes with long, rigid tip	Lachter 2005 [7]

EGJ: esophagogastric junction; EUS: endoscopic ultrasonography.

Table 12.2 Complications of diagnostic endoscopic ultrasonography (EUS), EUS-guided fine-needle aspiration (FNA), and EUS-guided fine-needle interventions (FNI) in 18 centers in Germany (2004) [4]. The experience of the EUS centers participating in the survey varied from 55 EUS procedures (in 1 year) to 8800 EUS procedures (over 12 years). EUS-FNA and EUS-FNI were performed in only 12 of the 18 centers, with experience varying substantially: EUS-FNA: minimum 14 (1 year), maximum 1600 (8 years); EUS-FNI: minimum three (1 year), maximum 400 (8 years). Complications were reported by 11 of the 18 centers, all of which had experience in more than 400 EUS procedures. The mortality rate for all EUS procedures was 0.008%; the mortality rate for all EUS-guided interventions was 0.38%

Complications	Diagnostic EUS (n = 32 001)	EUS-FNA (n = 4616)	EUS-FNI (n = 788)	All EUS procedures (n = 37 405)
Major complications				22 (0.06%)
Conservative management [1]	0	4	1	5
Interventional management	0	1	1	2
Surgery [2]	6	2	7	15
Minor complications				7 (0.02%)
Minor bleeding (no treatment)	0	7	0	7
All complications	6 (0.02%) [3]	14 (0.30%) [4]	9 (1.14%) [5, 6]	29 (0.08%) [6]

[1] Acute pancreatitis (n = 3); bleeding requiring transfusion (n = 2).
[2] Perforation (n = 11); pancreatic cyst infection (n = 1); pancreatic cyst infection and acute pancreatitis (n = 1); mediastinal cyst infection (n = 1); large mediastinal hematoma and hematothorax (n = 1).
[3] Esophageal perforation (n = 3); duodenal perforation (n = 3); all perforations were managed surgically.
[4] Bleeding requiring transfusion (n = 1); bleeding requiring surgical treatment and transfusion (n = 1); bleeding requiring no treatment (n = 7); cyst infection and acute pancreatitis requiring surgical treatment (n = 1); pancreatic cyst infection requiring antibiotic treatment (n = 1); acute pancreatitis requiring conservative treatment (n = 2); mediastinal abscess requiring endoscopic treatment (n = 1).
[5] Perforation of pseudocyst wall requiring surgery (n = 3); bleeding requiring blood transfusion (n = 1); bile peritonitis requiring surgery (n = 1); pseudocyst infection requiring surgical treatment (n = 2); pseudocyst infection requiring endoscopic treatment (n = 1); immediate stent dislocation into a pseudocyst requiring delayed surgery (n = 1).
[6] Three deaths after EUS-guided treatment for pancreatic pseudocysts and peripancreatic necrosis (bleeding, peritonitis).

to allow complete staging of esophageal cancer, including the celiac lymph-node station [3].

In 2004, we carried out a survey in German centers performing endoscopic ultrasonography [4]. Fourteen of the 18 centers that responded to the questionnaire reported keeping a prospective registry of complications. Esophageal perforation occurred in only three of 32 001 reported diagnostic EUS procedures (0.009%). None of the perforations was related to previous dilation of esophageal strictures. Stenosing esophageal cancer was present in only one case. Duodenal perforations occurred in three additional cases (0.009%). One duodenal perforation was related to a duodenal diverticulum. All of the perforations were managed surgically, and all the patients survived [4] (Table 12.2). In a large series of 233 endoscopic ultrasound-guided fine-needle aspiration biopsies in patients with presumed pancreatic cancer, Raut and colleagues reported on two cases of duodenal perforation requiring surgical intervention (0.86%). There was no luminal narrowing of the duodenum in either case [5]. One case report has been published describing an iatrogenic duodenal perforation during endoscopic ultrasonography, which was managed successfully by endoscopic closure with Hemoclips, followed by conservative treatment [6].

A national survey in Israel investigated the mortality associated with diagnostic EUS [7]. Ten of 12 reported cases of death related to EUS (seven in Israel and four from outside the country) resulted from duodenal tears, leading to retroperitoneal perforations. A further case occurred as a consequence of esophageal perforation. At least five cases of duodenal perforation involved patients with duodenal diverticula [7]. The only published prospective single-center evaluation of complications in diagnostic endoscopic ultrasonography is from a department of surgical gastroenterology in Denmark, including 3324 consecutive patients who underwent upper gastrointestinal endoscopic ultrasonography between 1991 and 2002 [8]. Esophageal perforation occurred in five of 10 cases with complications (0.15% of all investigations; 0.94% of all patients with esophageal cancer). Balloon dilation had been carried out before the EUS examination in two cases. All five patients with esophageal perforation made a full recovery with conservative treatment (n = 4) or surgical treatment (n = 1) [8].

Aspiration

Endosonographic visualization of the gastrointestinal wall and of adjacent structures depends on appropriate acoustic coupling of the transducer to the gastrointestinal wall, either using a water-filled balloon at the tip of the echoendoscope or of the high-frequency ultrasound miniprobe or by filling the gastrointestinal lumen with water. Since water-filling of the upper gastrointestinal tract is frequently used, the low frequency of reported cases of aspiration is somewhat surprising. There have only been three reported cases of aspiration of water followed by aspiration pneumonia in endosonographic examinations [7,9].

In the Danish prospective study, tracheal suction was needed in 15 of 293 patients (5.1%), and one patient aspirated during the procedure (0.3%). The "water-in-stomach" method was only used in nine patients (3.1%) [8].

Bacteremia

Few data are available concerning the frequency of bacteremia after diagnostic EUS without fine-needle aspiration biopsy. Janssen et al. [10] investigated 100 consecutive patients undergoing diagnostic EUS with a curvilinear echoendoscope by obtaining two pairs of blood cultures immediately before and 5 min after EUS. Significant bacteremia (*Streptococcus viridans* and *Propionibacterium* species; *S. mitis*) occurred in only two patients (20%; two of nine patients with esophageal carcinoma) after an EUS investigation for staging of esophageal carcinoma [10]. Levy et al. [11] noted transient bacteremia in one of 52 patients who underwent diagnostic EUS with a radial-scanning echoendoscope (1.9%). None of these three patients with bacteremia after diagnostic EUS in the two studies developed symptoms of infection [10,11].

■ Complications with EUS-FNA and EUS-Guided Interventions

Patients who undergo EUS-FNA or EUS-guided interventions are more likely to experience complications or to report symptoms following EUS in comparison with patients undergoing diagnostic EUS [4,12] (Table 12.**2**). The major complications reported with EUS-FNA are infections in cystic lesions, bleeding, and acute pancreatitis [1,13].

Bacteremia and Infectious Complications

Bacteremia after EUS-FNA in the upper gastrointestinal tract appears to be a rare event. Its frequency has been investigated in three prospective studies including 202 patients [10,11,14]. In one study with 100 patients, all blood cultures obtained 30 min and 60 min after the procedure were negative, except in six patients in whom the culture was positive for coagulase-negative *Staphylococcus*, which the investigators regarded as a contaminant [14]. Among the 102 patients in the studies by Janssen et al. and Levy et al. mentioned above, five patients had bacteremia after EUS-FNA (*Streptococcus viridans* in three cases; *Streptococcus* group F; Gram-negative bacillus). No signs or symptoms of infection developed in any of the patients [10,11]. Other large series reporting EUS-FNA in solid pancreatic masses have noted febrile episodes at a rate of 0.4–1.0% [15,16]. One case was reported of pyrexia and abdominal pain after EUS-FNA of a large pancreatic head mass, followed by extensive acute portal vein thrombosis [17].

In addition to one case of fever that resolved on antibiotics after mediastinal lymph-node EUS-FNA in 82 patients, there has only been one report of a serious infectious complication of EUS-FNA of the mediastinal lymph nodes. After EUS-guided aspiration biopsy of a mediastinal lymph-node metastasis from hepatocellular carcinoma, a mediastinal abscess developed. The iatrogenic abscess was treated successfully by EUS-guided drainage and subsequent endoscopic closure of the resulting esophagomediastinal fistula [18]. There has only been one report of infection after EUS-FNA of a subepithelial tumor [19].

EUS-FNA of rectal, colonic, perirectal and pericolic mass lesions appears to be a safe procedure. There has only been one report mentioning one infectious complication in 24 cases of transrectal and transcolonic EUS-FNA of pelvic masses [20]. In a prospective risk assessment of bacteremia in 27 patients undergoing EUS-FNA of rectal and perirectal lesions, the only two cases of positive blood cultures were considered to be contaminants (coagulase-negative *Staphylococcus, Moraxella*). None of the patients developed true-positive blood cultures or suffered immediate or delayed infectious complications [21]. In two other investigations of the role of EUS-FNA in submucosal tumors and extrinsic masses of the colon and rectum, there were also no complications in 22 and 48 patients, respectively, who underwent transrectal or transcolonic EUS-FNA [22,23].

EUS-FNA of cystic lesions in the retroperitoneal space or pancreas, and particularly in the mediastinum, appears to carry a significant risk of infectious complications. In a large multicenter study of EUS-FNA, two of 18 patients with EUS-FNA of a cystic pancreatic lesion without any preprocedural antibiotic prophylaxis developed cyst infection [24]. In spite of substantially growing numbers of EUS-FNA procedures for cystic lesions in the pancreas, there have only been two reports of infection after EUS-FNA of cystic pancreatic lesions despite prophylactic antibiotics [25,26].

EUS-FNA of bronchogenic and other mediastinal cysts may cause cyst infection, mediastinitis, and severe sepsis. There have been reports of three cases of mediastinitis following EUS-FNA or EUS-TCP of mediastinal mass lesions, which (on the basis of computed tomography of the thorax in one case and the EUS appearance in the other two) had been suspected to be lymph-node metastases, but proved to be bronchogenic cysts. Since metastatic lymph nodes were suspected in all three cases, antibiotics had not been administered [27–29]. In another case of transesophageal diagnostic aspiration of a foregut duplication cyst, subclinical cyst infection developed despite preprocedural antibiotic prophylaxis [30].

EUS-guided celiac plexus block (EUS-CPB) may lead to retroperitoneal abscess, which has only been reported in three cases in a large single-center series [31]. However, in one multicenter risk assessment in 41 patients undergoing EUS-CPB, no infectious complications were observed after the procedure; 46.3% the patients were receiving proton-pump inhibitors (PPIs), and no antibiotic prophylaxis was administered in 58.5% of the procedures [32].

Bile Peritonitis and Cholangitis

Bile peritonitis is a severe complication which may develop due to inadvertent penetration or perforation of the common bile duct when EUS-FNA of a pancreatic mass is being carried out in patients with biliary obstruction [33] or after failure of an attempt at EUS-guided transduodenal cholangiography or bile-duct drainage [4,34].

An attempt at EUS-guided gallbladder bile aspiration resulted in bile peritonitis in two of the first three patients who were enrolled in a study to identify patients with microlithiasis as a cause of idiopathic pancreatitis. These complications prompted the investigators to discontinue the study [35].

In an international survey of the indications, yield, and safety of EUS-FNA of liver lesions, one case of death due to septic cholangitis associated with EUS-FNA of a liver metastasis was reported. The background was an occluded biliary stent, with biliary obstruction secondary to pancreatic cancer [36].

As a consequence of mechanical irritation caused by the tip of the scope or by a water-filled balloon, endoscopic ultrasonography of the pancreas may cause proximal or distal biliary stent migration, possibly followed by cholangitis [37].

Acute Pancreatitis

Four large studies of EUS-FNA of pancreatic mass lesions have reported iatrogenic acute pancreatitis following EUS-FNA, with rates ranging from 0.4% to 2.0% [9,12,26,38]. A pooled analysis of 4909 EUS-FNAs of solid pancreatic masses from 19 EUS centers in the United States identified 14 cases of iatrogenic postprocedural acute pancreatitis (0.29%) [39]. The frequency of acute pancreatitis in individual centers ranged from 0% to 2.35%. Only two centers (413 cases of pancreatic EUS-FNA, two cases of acute pancreatitis) assessed complications of EUS-FNA in a prospective manner. Some of the centers with retrospective complication assessment did not report any cases of iatrogenic acute pancreatitis, suggesting that cases of acute pancreatitis may have been underreported for the retrospective cohort. Interestingly, the survey found that half of the patients who had acute pancreatitis after EUS-FNA had benign disease, suggesting that these patients may carry a higher risk. Another possible risk factor for iatrogenic acute pancreatitis after EUS-FNA appears to be a history of acute recurrent pancreatitis [39]. This observation is in good accordance with experience with percutaneous pancreatic FNA. In the German survey, all four patients with reported acute pancreatitis after EUS-FNA of pancreatic mass lesions turned out to have benign disease (acute recurrent pancreatitis, one case; chronic pancreatitis with inflammatory mass, two cases; solitary serous pancreatic cyst, one case; Table 12.**2**) [4]. In a large retrospective series of EUS-FNA in patients with pancreatic cystic lesions, acute pancreatitis occurred in six of 603 cases (1%) [25]. Two studies investigated the value of EUS-FNA and EUS-TCP in the diagnosis of chronic pancreatitis. Mild acute pancreatitis developed in two of 27 patients (7.4%) after EUS-FNA [40] and in one of 16 patients (6%) as a consequence of EUS-TCB [41].

EUS-guided pancreatogastrostomy is a complex procedure that is only indicated for the treatment of severe pain in selected patients with pancreatic ductal dilation inaccessible to transpapillary endoscopic therapy. In a small series in a center with extensive experience in interventional pancreatic procedures, two of 28 patients (7.1%) developed an acute episode of pancreatitis after transgastric EUS-guided drainage of the dilated pancreatic duct [42].

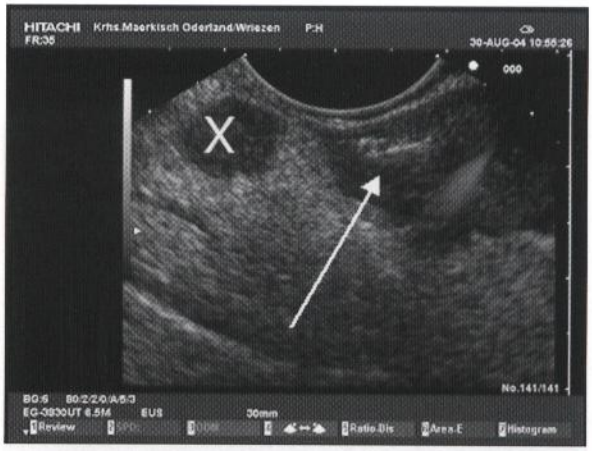
Hemorrhage

Self-limiting mild intraluminal bleeding due to EUS-FNA has been reported to occur in as many as 4% of cases [16]. In a prospective study evaluating the risk of extraluminal hemorrhage caused by EUS-FNA, only three cases of mild extraluminal hemorrhage were observed among 227 patients (1.3%) [43]. Extraluminal bleeding after EUS-FNA can be visualized with endoscopic ultrasound very well. The bleeding appears as an expanding hypoechoic region adjacent to the sampled lesion (Figs. 12.**1**–12.**3**) [43].

In the survey of 18 German EUS centers mentioned above (4616 EUS-FNAs; Table 12.**2**), mild and self-limiting bleeding after EUS-FNA occurred in seven patients. One patient was treated with low-molecular-weight heparin (LWMH) immediately after the procedure and developed a large mediastinal hematoma and hematothorax. Seven units of packed red cells had to be transfused, and thoracoscopy was performed. Another patient needed transfusion of four units of packed red cells after EUS-FNA of pancreatic head carcinoma with portal hypertension (bleeding in 0.19% of all EUS-FNAs) [4]. Patients with highly vascularized lesions—for example, neuroendocrine tumors and some metastases, as well as patients with cystic lesions—may be at greater risk (Figs. 12.**1**, 12.**4**). In a retrospective study of EUS-FNA of pancreatic cystic lesions in 50 patients, Varadarajulu and

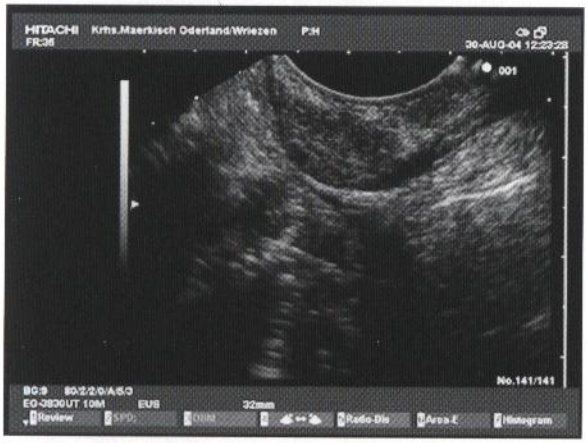


a



b

Fig. 12.**1** Mild extraluminal hemorrhage (arrow) after endoscopic ultrasound-guided fine-needle aspiration (EUS-FNA) of a small neuroendocrine pancreatic tumor (X). **a** Before EUS-FNA. **b** Approximately 5 min after a second needle pass. The patient did not develop any symptoms.

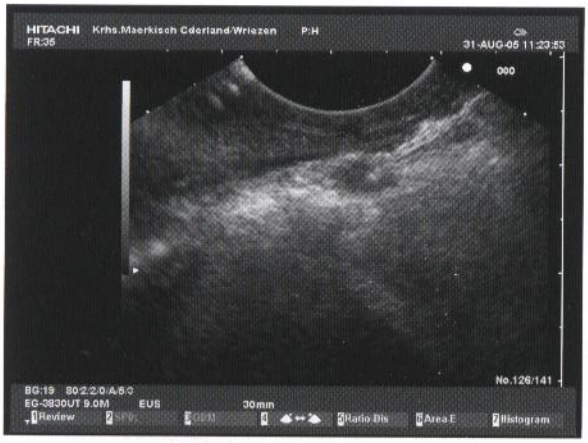


a

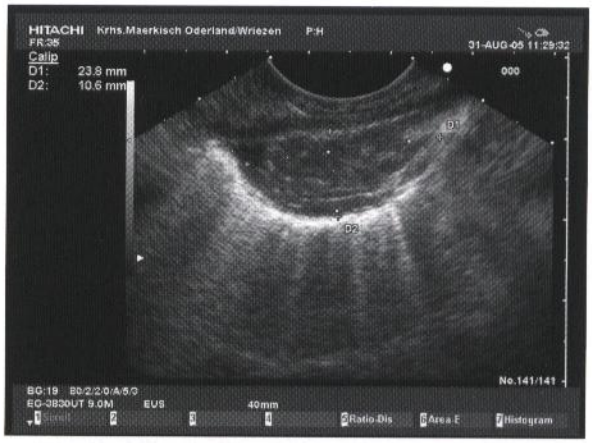


b

Fig. 12.**2** A minute hematoma in the gastric wall after endoscopic ultrasound-guided fine-needle aspiration (EUS-FNA) of a small subepithelial tumor in a patient with cancer of the large intestine. **a** Appearance before EUS-FNA. **b** A small echogenic intramural hematoma after three needle passes. The EUS-FNA was nondiagnostic; pathological examination following surgical wedge resection revealed a pancreatic rest.



a



b

Fig. 12.**3** Extraesophageal bleeding after endoscopic ultrasound-guided fine-needle aspiration (EUS-FNA) of a small mediastinal lymph node after neoadjuvant chemotherapy in a patient with non–small-cell lung cancer. **a** EUS-FNA. **b** The hematoma appeared immediately after the first needle pass.



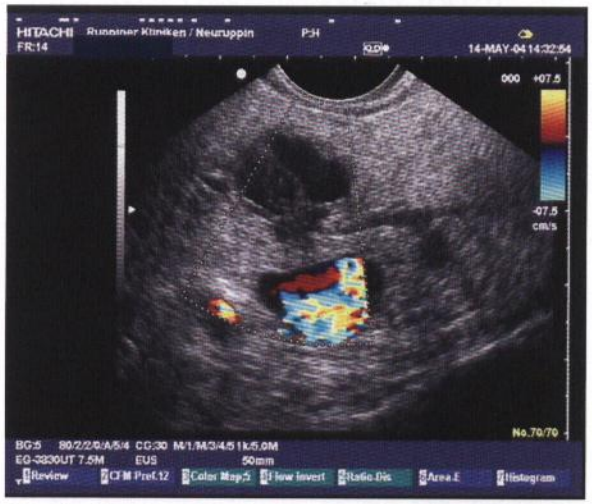
a



b



c



d

Fig. 12.4 Intraluminal cyst hemorrhage after diagnostic endoscopic ultrasound-guided fine-needle aspiration (EUS-FNA) of a septated pancreatic cystic lesion. **a**, **b** The cystic lesion before EUS-FNA; the color Doppler does not show any vessels in the cyst wall. **c** A hyperechogenic area within the cyst after EUS-FNA. The bleeding stopped spontaneously. At the time of puncture, the bleeding was immediately recognized with color-coded duplex ultrasound and originated from a small septation inside the cyst. **d** The appearance of the cyst 14 days after EUS-FNA. The patient did not develop any symptoms.

Eloubedi identified three cases of acute intracystic hemorrhage (6%) [44]. Two patients experienced abdominal pain transiently, and none of the three patients required blood transfusions. Intracystic bleeding was readily recognized during the investigation as an expanding hyperechoic area around the site of needle puncture within the targeted cyst (Fig. 12.**4**). It was not possible to identify any risk factors contributing to the bleeding events. None of the patients with acute intracystic hemorrhage had taken nonsteroidal anti-inflammatory drugs (NSAIDs), including aspirin, during the week before the procedure [44].

A prospective analysis compared the risk of bleeding after EUS-FNA or EUS-TCB in patients taking NSAIDs, aspirin, or prophylactic LWMH to those who were not treated. Only one of 28 patients (3.6%) taking potentially risky drugs developed extraluminal bleeding, in comparison with five of the 196 patients (2.6%) without such medication. There appears to be no additional risk of bleeding related to EUS-FNA in patients taking aspirin, NSAIDs, or prophylactic LMWH [45].

There have been two reports of fatal extraluminal bleeding after EUS-FNA of solid pancreatic lesions. One patient developed uncontrolled bleeding from a pseudoaneurysm and died. The FNA was carried out using a radial-scanning echoendoscope [46]. The other patient developed massive gastrointestinal bleeding 6 h after EUS-FNA of a pancreatic cancer. Autopsy revealed disseminated cancer, but no bleeding from the EUS puncture areas [8].

Therapeutic EUS-guided interventions may carry an elevated risk of bleeding complications, despite the use of color-coded duplex sonography [4] (Fig. 12.**5**).

Tumor Cell Seeding

Needle-tract seeding is a rare complication after percutaneous fine-needle biopsy of intra-abdominal tumors. Based on large retrospective series, its frequency is estimated to be as low as 0.003–0.009% of cases [47–52]. However, one prospective comparative study reported the incidence of needle-tract implantation of hepatocellular carcinoma and pancreatic carcinoma after ultrasound-guided percutaneous puncture to be about 1.5% [53].

The actual frequency of EUS-FNA related needle-tract seeding is unknown, but three recent case reports have raised concern that the substantial increase in the numbers of EUS-FNA procedures being carried out in the diagnosis of pancreatic masses may lead to further cases of this harmful complication. In one case, a large gastric wall implantation metastasis with retroperitoneal invasion (50 × 30 mm) was diagnosed 16 months after potentially curative resection of a small (8 mm) T1N0M0 carcinoma of the pancreatic tail. The tumor had previously been sampled using transgastric EUS-FNA (with five needle passes) [54]. In the second case, transgastric EUS-FNA (one needle pass) of a melanoma metastasis to a perigastric lymph node was complicated by a large (30 mm) gastric implantation metastasis along the needle tract. It was detected and resected 6 months later in the course of surgical resection of the lymph-node metastasis after neoadjuvant chemotherapy had been administered [55].

The potential risk of peritoneal carcinomatosis due to transgastric EUS-FNA of pancreatic malignancies was highlighted by a reported case of peritoneal dissemination of an intraductal papillary mucinous tumor (IPMT) of the pancreas following EUS-FNA of the tumor [56]. Nevertheless, the risk of peritoneal carcinomatosis appears to be significantly lower with EUS-FNA in comparison with percutaneous FNA under computed-tomographic or ultrasound guidance [57].

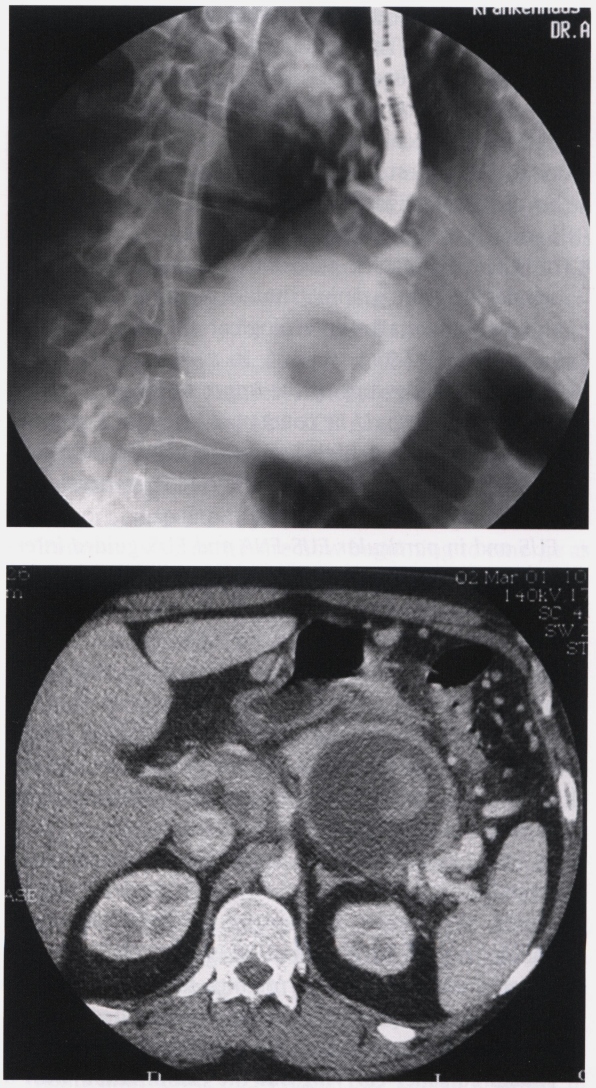


Fig. 12.**5** Intraluminal bleeding after endoscopic ultrasound-guided pseudocystogastrostomy. **a** The fluoroscopic image. **b** The computed tomogram after termination of the procedure.

■ Prevention of EUS-Related Complications

Strategies aimed at minimizing the potential risk of EUS, EUS-FNA, and EUS-guided interventions include:

- Adequate education and training of examiners.
- Deep familiarity with the results of previous investigations and of possible therapeutic implications.
- Appropriate consideration of the patient's clinical condition and of the indications and contraindications of the investigation or procedure.
- Careful consideration of a meaningful clinical strategy for investigating and treating each individual patient.
- Optimization of the prerequisites and conditions for the planned investigation or procedure.

Suggested Ways of Preventing Complications

- *Participation in supervised training programs in EUS, EUS-FNA, and EUS-guided interventions.* EUS, EUS-FNA, and EUS-guided interventions are complex, technically demanding procedures in which the findings are difficult to interpret and which require advanced skills in diagnostic and therapeutic endoscopy, outstanding experience in diagnostic ultrasonography, and a fundamental understanding of the

anatomy of the gastrointestinal tract and surrounding structures. The guidelines for credentialing and granting privileges for endoscopic ultrasound published by the American Society for Gastrointestinal Endoscopy recommend a minimum of 150 supervised EUS investigations, including 75 pancreatobiliary EUS investigations and 50 EUS-FNA procedures, to establish comprehensive competence in all aspects of EUS [58]. Specific guidelines for training in endoscopic ultrasonography should be implemented in the national gastroenterological societies' training programs [59,60].

- *Diagnostic endoscopy of the upper or lower gastrointestinal tract should be conducted before EUS* and the echoendoscope or high-frequency ultrasound miniprobe most suitable for the intended investigation or procedure should be selected.
- *EUS and in particular EUS-FNA and EUS-guided interventions should only be carried out in cooperative and adequately sedated patients.* The oxygen saturation, heart rate, and (whenever possible and necessary) blood pressure and electrocardiography should be monitored.
- *Water filling in the upper gastrointestinal tract should be restricted to the minimum amount needed* and the endoscopy unit and team should be prepared for carrying out nasopharyngeal suction.
- In EUS examinations of the pancreas, biliary duct, ampulla, and duodenum in patients with biliary stents, *the correct position of the stent should be checked before the examination is completed.*
- *When there is luminal narrowing—for instance, in patients with esophageal carcinoma—care needs to be taken when maneuvering the echoendoscope and one should consider carrying out the examination with a transendoscopic high-frequency ultrasound miniprobe. Dilation and passage of the stricture should only be carried out in selected cases.* A malignant esophageal stricture restricts passage of the echoendoscope in approximately one-third of investigations for esophageal cancer staging and may limit complete evaluation of the tumor depth and lymph nodes at the celiac axis [61]. On the other hand, EUS is currently the most accurate modality available for locoregional staging of esophageal carcinoma. In comparison with the limited diagnostic accuracy of computed tomography, EUS in combination with FNA is highly accurate for detecting and assessing lymph-node metastases at the celiac axis. EUS in combination with EUS-FNA of suspicious celiac lymph nodes is essential for effective decision-making and may therefore potentially reduce the costs as well as the complications of managing patients with esophageal cancer, by preventing unnecessary thoracotomies [62,63]. In addition, EUS staging leads to appropriate administration of neoadjuvant therapy in patients with locally advanced disease and is associated with a recurrence-free survival advantage and an overall survival advantage in these patients [64]. This is why it is justified to carry out dilation before passage of a curvilinear echoendoscope through a malignant esophageal stricture in selected patients, in order to gain access to the celiac axis region to look for and aspirate celiac lymph nodes. Prospective studies of the role of dilation in patients with obstructing esophageal cancer undergoing EUS examinations by experienced endosonographers have not found any association between perforation and dilation [65]. However, in the case of high-grade strictures in one study, a substantial rate (24%) of esophageal perforation as a result of either wire-guided dilation, or as a direct consequence of the endosonographic staging procedure, was reported. On the other hand, 19 of 21 patients with a high-grade malignant stenosis were found to have stage III or IV disease on histopathological examination of the surgical specimen [61]. This is why we do not recommend dilation and complete endosonographic staging in patients with very tight malignant strictures. Dilation or bougienage should be limited to the minimal diameter needed for passage of the echoendoscope. Sequential dilation to a maximum of 16 mm has been reported in four studies with 160 patients, with no perforations [65–68]. One large multicenter study demonstrated the safety of through-the-scope balloon dilation before complete EUS staging of esophageal cancer. A perforation occurred in one of 71 cases [69]. Negotiating the echoendoscope through the tumor with the tip of the video scope closely following the path of the guide wire used for dilation under fluoroscopic guidance may help prevent perforation after dilation [70]. Dilation should be limited to patients in whom detection of celiac lymph-node metastases would change the course of treatment. Patients who are not suitable for surgery or neoadjuvant treatment schedules due to significant co-morbidity or liver metastases (identified on ultrasonography or computed tomography) should be excluded from dilation. Using a tapered-tip, wire-guided, nonoptical radial echoendoscope [71,72] or through-the-scope high-frequency ultrasound miniprobes [73–77] allows complete staging of obstructing esophageal cancer in most cases, but does not allow cytological or histological confirmation of suspected celiac lymph-node metastases.
- EUS-FNA should not be performed:
  - In patients without adequate sedation.
  - In patients receiving anticoagulation treatment or with coagulopathy.
  - Without sufficient optical needle control.
  - In patients with untreated bile duct obstruction (liver, pancreatic head, ampulla).

  - In patients in whom the results of EUS-FNA are unlikely to have any clinical impact [13].
- *Whenever possible, use color-coded duplex sonography (CCDS) or the color-power angio (CPA) mode before puncture* to avoid vessels and highly vascularized structures in the needle trajectory.
- *Before EUS-FNA of a large, solid-appearing mediastinal mass lesion, all appropriate methods should be used to exclude cystic lesions:*
  - Computed tomography (CT) or magnetic resonance imaging (MRI) before EUS-FNA.
  - CCDS or CPA to confirm that the structure really is solid, characterized by the detection of blood flow inside the lesion.
  - If there is any uncertainty regarding the solid character of the lesion, ultrasound contrast enhancement should be used to confirm the flow signals.
- *EUS-FNA of pancreatic masses should be restricted to those patients in whom definitive cytological diagnosis of the lesion is likely to alter the management significantly.* Knowing when to carry out EUS-FNA is as important as being able to perform the procedure itself [13]. In general, there is no indication for EUS-FNA of a pancreatic mass lesion that is typical of adenocarcinoma in patients who have no criteria of unresectability [13,78]. We would suggest the following indications for EUS-FNA of pancreatic masses:
  - *Unresectable mass:* documentation of malignancy and histological type before palliative (or neoadjuvant) chemotherapy or radiation therapy.
  - *Solid pancreatic mass lesions atypical for adenocarcinoma* (for example, suspected metastases, lymphoma, cystadenoma, or neuroendocrine tumor): cytological or histological diagnosis in most cases will alter the course of therapy (avoiding surgical interventions, limited resections, chemotherapy, radiotherapy). More recent EUS techniques (CCDS, CPA, ultrasound contrast enhancement, ultrasound elastography) may help select resectable pancreatic masses that are atypical of pancreatic adenocarcinoma and should therefore be sampled.
  - If the patient is reluctant to undergo major pancreatic surgery without a definitive histological diagnosis, EUS-FNA appears to be the safest and most efficacious method of tissue acquisition [13]. In such cases, transgastric EUS-FNA of pancreatic mass lesions should be avoided in order to minimize the risk of implantation metastasis or intraperitoneal cancer dissemination.
- *Tru-Cut needles should be used with caution and only in selected cases* [1,79]. *One should not use 19-gauge aspiration needles for diagnostic purposes.* There are several advantages and disadvantages of using EUS-guided Tru-Cut biopsy (EUS-TCB) to obtain a tissue diagnosis. Small series appear to indicate that EUS-TCB in the hands of very experienced investigators is not associated with an increased risk of complications [79]. However, none of the studies conducted to date has addressed the issue of safety sufficiently and in comparison with EUS-FNA. On the other hand, there are several technical difficulties with this technique—for example, inadequate tissue acquisition when the echoendoscope is in a duodenal position [28] or in suspected nonfocal chronic pancreatitis [41]. In one study, the overall accuracy of EUS-TCB specimens was greater than that of EUS-FNA specimens, particularly for subepithelial mass lesions and lymphomas (88% vs. 29%; $P < 0.05$). The same study also suggested that fewer needle passes may be required when using EUS-TCB needles in comparison with EUS-FNA needles, especially for tissue acquisition from pancreatic neoplasms [80]. Subepithelial tumors, suspected lymphoma, and suspected autoimmune pancreatitis are now beginning to emerge as special indications for EUS-TCB, as it provides an opportunity for histological versus cytological examination and because it has greater diagnostic efficacy and accuracy in comparison with EUS-FNA. In solid or cystic pancreatic masses, particularly in the pancreatic neck, body, and tail, there may be some advantages of EUS-TCB over EUS-FNA [79]. A prospective comparison of a 19-gauge versus a 22-gauge needle for performing EUS-FNA of solid pancreatic masses did not show any diagnostic superiority for the larger needle. On the other hand, complications and technical difficulties only occurred with the 19-gauge needle [81]; 19-gauge needles are only necessary in EUS-guided therapeutic interventions, as they allow the introduction of 0.35-inch guide wires.
- *Antibiotic prophylaxis should be administered in patients undergoing EUS-FNA or EUS-guided drainage of cystic lesions (pancreas, peripancreatic, mediastinal). Antibiotic prophylaxis should also be considered in patients undergoing transrectal and transcolonic EUS-FNA* [1]. Antibiotic prophylaxis appears to reduce the incidence of clinically relevant infectious complications of EUS-FNA performed to sample cystic lesions of the pancreas. There are no data comparing EUS-FNA of cystic lesions with or without antibiotic prophylaxis in a prospective manner. However, in contrast to the high rate of cyst infections in older studies in which antibiotic prophylaxis was not provided, one large previous series (including 603 patients) using antibiotic prophylaxis reported only one infectious complication [25]. Some experts also recommend periprocedural antibiotic prophylaxis for EUS-FNA of the perirectal space [82] and for EUS-guided celiac plexus block in patients taking PPIs [83]. However, there are no valid data supporting routine use of antibiotics for these indications [21,32].
- *Complications should be assessed in a prospective manner and all complications that occur should be ana-*

lyzed. Prospective risk assessment is an essential prerequisite for the analysis and prevention of complications. Careful prospective studies show higher complication rates than retrospective studies. The American Society for Gastrointestinal Endoscopy recommends that specific quality indicators (in particular indications, sedation, immediate and delayed complications, procedure success) should be tracked routinely in all patients undergoing EUS [84].

■ Summary: Morbidity and Mortality of EUS and EUS-FNA

Diagnostic EUS without EUS-FNA is a safe procedure. The complication rates are comparable to those in diagnostic endoscopy of the upper gastrointestinal tract [1]. The most common complications are perforations of the esophagus and of the duodenum. Perforation may be made more likely by the specific mechanical and optical properties of echoendoscopes. To minimize the risk of perforation, examiners should be aware of the specific features of the echoendoscope used, as well as of the specific anatomical situation in the patient (e.g., esophageal stenosis, duodenal diverticula). Esophageal dilation before EUS staging of esophageal carcinoma should be avoided in very tight stenoses and in all cases in which the results of complete locoregional staging will probably not alter the course of management for the patient.

Most complications of EUS are associated with EUS-FNA. The overall complication rate of EUS-FNA appears to be between 0.3% and 6.3%. The mortality is close to zero [4,8,9,13,24,36,46,85]. The major complications are bleeding, acute pancreatitis, and infectious complications [1,13,85]. Cystic lesions are associated with an increased risk of infectious and bleeding complications in comparison with solid lesions [24,44]. Infection of pancreatic cystic lesions appears to have been substantially eliminated by prophylactic antibiotic use. The risk of bleeding is not increased in patients who are taking aspirin, NSAIDs, or prophylactic LWMH. EUS-FNA of benign pancreatic lesions appears to be associated with a higher risk than EUS-FNA of pancreatic malignancies. Tumor cell seeding and peritoneal dissemination are very rarely reported serious events.

Complications occurring with EUS, EUS-FNA, and EUS-FNI should be assessed in a prospective manner in all endoscopy units.

Adequate education and training in EUS and EUS-FNA is the essential prerequisite for minimizing the risk and enhancing the efficacy of endosonographic examinations and interventions. Restricting EUS-FNA only to patients in whom the cytological or histological results can be expected to change the course of management is the best way of preventing the complications of EUS-FNA.

References

1. Adler DG, Jacobson BC, Davila RE, Hirota WK, Leighton JA, Qureshi WA, et al. ASGE guideline: complications of EUS. Gastrointest Endosc 2005;61:8–12.
2. Das A, Sivak MV Jr, Chak A. Cervical esophageal perforation during EUS: a national survey. Gastrointest Endosc 2001;53:599–602.
3. Rösch T, Dittler HJ, Fockens P, Yasuda K, Lightdale C. Major complications of endoscopic ultrasonography: results of a survey of 42 105 cases [abstract]. Gastrointest Endosc 1993;39:344.
4. Jenssen C. Complications of endoscopic ultrasound in 18 German centers: report of a survey [unpublished data, 2004].
5. Raut CP, Grau AM, Staerkel GA, Kaw M, Tamm EP, Wolff RA, et al. Diagnostic accuracy of endoscopic ultrasound-guided fine-needle aspiration in patients with presumed pancreatic cancer. J Gastrointest Surg 2003;7:118–26.
6. Sebastian S, Byrne AT, Torreggiani WC, Buckley M. Endoscopic closure of iatrogenic duodenal perforation during endoscopic ultrasound. Endoscopy 2004;36:245.
7. Lachter J. Mortality from EUS [abstract]. Gastrointest Endosc 2005;61: AB 118.
8. Mortensen MB, Fristrup C, Holm FS, Pless T, Durup J, Ainsworth AP, et al. Prospective evaluation of patient tolerability, satisfaction with patient information, and complications in endoscopic ultrasonography. Endoscopy 2005;37: 146–53.
9. O'Toole D, Palazzo L, Arotcarena R, Dancour A, Aubert A, Hammel P, et al. Assessment of complications of EUS-guided fine-needle aspiration. Gastrointest Endosc 2001;53:470–4.
10. Janssen J, Konig K, Knop-Hammad V, Johanns W, Greiner L. Frequency of bacteremia after linear EUS of the upper GI tract with and without FNA. Gastrointest Endosc 2004;59: 339–44.
11. Levy MJ, Norton ID, Wiersema MJ, Schwartz DA, Clain JE, Vazquez-Sequeiros E, et al. Prospective risk assessment of bacteremia and other infectious complications in patients undergoing EUS-guided FNA. Gastrointest Endosc 2003; 57:672–8.
12. Eloubeidi MA, Chen VK, Pratibhu PP, Geels W, Wilcox CM. A prospective evaluation of immediate, acute, and 30-day complication assessment after endoscopic ultrasonography (EUS): a large single endosonographer's experience [abstract]. Gastrointest Endosc 2003; 57: AB 106.
13. Erickson RA. EUS-guided FNA. Gastrointest Endosc 2004; 60:267–79.
14. Barawi M, Gottlieb K, Cunha B, Portis M, Gress F. A prospective evaluation of the incidence of bacteremia associated with EUS-guided fine-needle aspiration. Gastrointest Endosc 2001;53:189–92.
15. Chang KJ, Nguyen P, Erickson RA, Durbin TE, Katz KD. The clinical utility of endoscopic ultrasound-guided fine-needle aspiration in the diagnosis and staging of pancreatic carcinoma. Gastrointest Endosc 1997;45:387–93.
16. Voss M, Hammel P, Molas G, Palazzo L, Dancour A, O'Toole D, et al. Value of endoscopic ultrasound guided fine needle aspiration biopsy in the diagnosis of solid pancreatic masses. Gut 2000;46:244–9.
17. Matsumoto K, Yamao K, Ohashi K, Watanabe Y, Sawaki A, Nakamura T, et al. Acute portal vein thrombosis after EUS-guided FNA of pancreatic cancer: case report. Gastrointest Endosc 2003;57:269–71.

18. Will U, Meyer F, Bosseckert H. Successful endoscopic management of iatrogenic mediastinal infection and subsequent esophagomediastinal fistula, following endosonographically guided fine-needle aspiration biopsy. Endoscopy 2005;37:88–90.
19. Grandval P, Picon M, Coste P, Giovannini M, Thomas P, Lafon J. [Infection of submucosal tumor after endosonography-guided needle biopsy; in French.] Gastroenterol Clin Biol 1999;23:566–8.
20. Faias S, Kaplan R, Hawes RH, Romagnuolo J, Paquin SC, Chong AK, et al. Role of endoscopic ultrasound with guided fine needle aspiration (EUS-FNA) in the diagnosis of pelvic masses [abstract]. Gastrointest Endosc 2005;61:AB 276.
21. Levy MJ, Kumar KS, Norton ID, Yusuf TE, Clain JE, Harewood GC, et al. Prospective risk assessment of bacteremia in patients undergoing endoscopic ultrasound guided fine needle aspiration (EUS FNA) of rectal and perirectal lesions [abstract]. Gastrointest Endosc 2004;59:AB 108.
22. Sailer M, Bussen D, Fein M, Freys S, Debus SE, Thiede A, et al. Endoscopic ultrasound-guided transrectal biopsies of pelvic tumors. J Gastrointest Surg 2002;6:342–6.
23. Sasaki Y, Niwa Y, Hirooka Y, Ohmiya N, Itoh A, Ando N, et al. The use of endoscopic ultrasound-guided fine-needle aspiration for investigation of submucosal and extrinsic masses of the colon and rectum. Endoscopy 2005;37:154–60.
24. Wiersema MJ, Vilmann P, Giovannini M, Chang KJ, Wiersema LM. Endosonography-guided fine-needle aspiration biopsy: diagnostic accuracy and complication assessment. Gastroenterology 1997;112:1087–95.
25. Lee LS, Saltzman JR, Bounds BC, Poneros JM, Brugge WR, Thompson CC. EUS-guided fine needle aspiration of pancreatic cysts: a retrospective analysis of complications and their predictors. Clin Gastroenterol Hepatol 2005;3:231–6.
26. Williams DB, Sahai AV, Aabakken L, Penman ID, van Velse A, Webb J, et al. Endoscopic ultrasound guided fine needle aspiration biopsy: a large single centre experience. Gut 1999;44:720–6.
27. Annema JT, Veselic M, Versteegh MI, Rabe KF. Mediastinitis caused by EUS-FNA of a bronchogenic cyst. Endoscopy 2003;35:791–3.
28. Varadarajulu S, Fraig M, Schmulewitz N, Roberts S, Wildi S, Hawes RH, et al. Comparison of EUS-guided 19-gauge Trucut needle biopsy with EUS-guided fine-needle aspiration. Endoscopy 2004;36:397–401.
29. Wildi SM, Hoda RS, Fickling W, Schmulewitz N, Varadarajulu S, Roberts SS, et al. Diagnosis of benign cysts of the mediastinum: the role and risks of EUS and FNA. Gastrointest Endosc 2003;58:362–8.
30. Ryan AG, Zamvar V, Roberts SA. Iatrogenic candidal infection of a mediastinal foregut cyst following endoscopic ultrasound–guided fine-needle aspiration. Endoscopy 2002;34:838–9.
31. Mahajan RJ, Nowell W, Theerathorn P, Lipscomb A, Hart R, Adams L. Empyema after endoscopic ultrasound guided celiac plexus pain block (EUS-CPB) in chronic pancreatitis (CP): experience at an academic center [abstract]. Gastrointest Endosc 2002;55:AB 101.
32. George J, Grobmann CR, Jowell PS, Michael H, Pollack B, Gress F. Risk assessment of infectious complications in patients undergoing endoscopic ultrasound (EUS) guided celiac plexus block (CPB): a multicenter experience [abstract]. Gastrointest Endosc 2005;61:AB 279.
33. Chen HY, Lee CH, Hsieh CH. Bile peritonitis after EUS-guided fine-needle aspiration. Gastrointest Endosc 2002;56:594–6.
34. Kahaleh M, Shami VM, Wang P, Tokar J, Adams RB, Yeaton P. Interventional endoscopic ultrasound cholangiography (IEUC): mid-term follow-up of 18 cases [abstract]. Gastrointest Endosc 2005;61:AB 285.
35. Jacobson BC, Waxman I, Parmar K, Kauffman JM, Clarke GA, Van Dam J. Endoscopic ultrasound-guided gallbladder bile aspiration in idiopathic pancreatitis carries a significant risk of bile peritonitis. Pancreatology 2002;2:26–9.
36. tenBerge J, Hoffman BJ, Hawes RH, Van Enckevort C, Giovannini M, Erickson RA, et al. EUS-guided fine needle aspiration of the liver: indications, yield, and safety based on an international survey of 167 cases. Gastrointest Endosc 2002;55:859–62.
37. Gaylord KM, Nawras A. Incidence of biliary stent migration as a direct complication of performing endoscopic ultrasound. Gastrointest Endosc 2005;61:AB 279.
38. Gress F, Michael H, Gelrud D, Patel P, Gottlieb K, Singh F, et al. EUS-guided fine-needle aspiration of the pancreas: evaluation of pancreatitis as a complication. Gastrointest Endosc 2002;56:864–7.
39. Eloubeidi MA, Gress FG, Savides TJ, Wiersema MJ, Kochman ML, Ahmad NA, et al. Acute pancreatitis after EUS-guided FNA of solid pancreatic masses: a pooled analysis from EUS centers in the United States. Gastrointest Endosc 2004; 60:385–9.
40. Hollerbach S, Klamann A, Topalidis T, Schmiegel WH. Endoscopic ultrasonography (EUS) and fine-needle aspiration (FNA) cytology for diagnosis of chronic pancreatitis. Endoscopy 2001;33:824–31.
41. DeWitt J, McGreevy K, LeBlanc J, McHenry L, Cummings O, Sherman S. EUS-guided Trucut biopsy of suspected nonfocal chronic pancreatitis. Gastrointest Endosc 2005;62:76–84.
42. Tessier G, Hittelet A, Bories E, Le Moine O, Giovannini M, Devière J. EUS-guided pancreatogastrostomy for the treatment of pain in patients with pancreatic ductal dilatation inaccessible for transpapillary therapy. Gastrointest Endosc 2005;61:AB 303.
43. Affi A, Vazquez-Sequeiros E, Norton ID, Clain JE, Wiersema MJ. Acute extraluminal hemorrhage associated with EUS-guided fine needle aspiration: frequency and clinical significance. Gastrointest Endosc 2001;53:221–5.
44. Varadarajulu S, Eloubeidi MA. Frequency and significance of acute intracystic hemorrhage during EUS-FNA of cystic lesions of the pancreas. Gastrointest Endosc 2004;60:631–5.
45. Meenan J, Doig L, Vu C. The safety of endosonography-guided FNA and/ or trucut biopsy in patients on aspirin, NSAIDs or prophylactic low molecular weight heparin. Gastrointest Endosc 2005;61:AB 293.
46. Gress FG, Hawes RH, Savides TJ, Ikenberry SO, Lehman GA. Endoscopic ultrasound-guided fine-needle aspiration biopsy using linear array and radial scanning endosonography. Gastrointest Endosc 1997;45:243–50.
47. Buscarini L, Fornari F, Bolondi L, Colombo P, Livraghi T, Magnolfi F, et al. Ultrasound-guided fine-needle biopsy of focal liver lesions: techniques, diagnostic accuracy and complications. A retrospective study on 2091 biopsies. J Hepatol 1990;11:344–8.
48. Fornari F, Civardi G, Cavanna L, Di Stasi M, Rossi S, Sbolli G, et al. Complications of ultrasonically guided fine-needle abdominal biopsy: results of a multicenter Italian study and review of the literature. The Cooperative Italian Study Group. Scand J Gastroenterol 1989;24:949–55.
49. Smith EH. The hazards of fine-needle aspiration biopsy. Ultrasound Med Biol 1984;10:629–34.

50. Smith EH. Complications of percutaneous abdominal fine-needle biopsy: review. Radiology 1991;178:253–8.
51. Weiss H, Duntsch U. [Complications of fine needle puncture: DEGUM survey II; in German.] Ultraschall Med 1996;17:118–30.
52. Weiss H, Duntsch U, Weiss A. [Risks of fine needle puncture: results of a survey in West Germany (German Society of Ultrasound in Medicine survey); in German.] Ultraschall Med 1988;9:121–7.
53. Kosugi C, Furuse J, Ishii H, Maru Y, Yoshino M, Kinoshita T, et al. Needle tract implantation of hepatocellular carcinoma and pancreatic carcinoma after ultrasound-guided percutaneous puncture: clinical and pathologic characteristics and the treatment of needle tract implantation. World J Surg 2004;28:29–32.
54. Paquin SC, Gariepy G, Lepanto L, Bourdages R, Raymond G, Sahai AV. A first report of tumor seeding because of EUS-guided FNA of a pancreatic adenocarcinoma. Gastrointest Endosc 2005;61:610–1.
55. Shah JN, Fraker D, Guerry D, Feldman M, Kochman ML. Melanoma seeding of an EUS-guided fine needle track. Gastrointest Endosc 2004;59:923–4.
56. Hirooka Y, Goto H, Itoh A, Hashimoto S, Niwa K, Ishikawa H, et al. Case of intraductal papillary mucinous tumor in which endosonography-guided fine-needle aspiration biopsy caused dissemination. J Gastroenterol Hepatol 2003;18:1323–4.
57. Micames C, Jowell PS, White R, Paulson E, Nelson R, Morse M, et al. Lower frequency of peritoneal carcinomatosis in patients with pancreatic cancer diagnosed by EUS-guided FNA vs. percutaneous FNA. Gastrointest Endosc 2003;58:690–5.
58. Eisen GM, Dominitz JA, Faigel DO, Goldstein JA, Petersen BT, Raddawi HM, et al. Guidelines for credentialing and granting privileges for endoscopic ultrasound. Gastrointest Endosc 2001;54:811–4.
59. Krakamp B, Janssen J, Menzel J, Schafer A, Runzi M, Arbeitsgemeinschaft für endoskopischen Ultraschall in Nordrhein-Westfalen (AGEUS). [Requirements and recommendations for performing endosonographies; in German.] Z Gastroenterol 2004;42:157–66.
60. Van Dam J, Brady PG, Freeman M, Gress F, Gross GW, Hassall E, et al. Guidelines for training in endoscopic ultrasound. Gastrointest Endosc 1999;49:829–33.
61. Van Dam J, Rice TW, Catalano MF, Kirby T, Sivak MV Jr. High-grade malignant stricture is predictive of esophageal tumor stage: risks of endosonographic evaluation. Cancer 1993;71:2910–7.
62. Chang KJ, Soetikno RM, Bastas D, Tu C, Nguyen PT. Impact of endoscopic ultrasound combined with fine-needle aspiration biopsy in the management of esophageal cancer. Endoscopy 2003;35:962–6.
63. Lightdale CJ, Kulkarni KG. Role of endoscopic ultrasonography in the staging and follow-up of esophageal cancer. J Clin Oncol 2005;23:4483–9.
64. Harewood GC, Kumar KS. Assessment of clinical impact of endoscopic ultrasound on esophageal cancer. J Gastroenterol Hepatol 2004;19:433–9.
65. Parmar KS, Zwischenberger JB, Reeves AL, Waxman I. Clinical impact of endoscopic ultrasound-guided fine needle aspiration of celiac axis lymph nodes (M1a disease) in esophageal cancer. Ann Thorac Surg 2002;73:916–20.
66. Kallimanis GE, Gupta PK, al-Kawas FH, Tio LT, Benjamin SB, Bertagnolli ME, et al. Endoscopic ultrasound for staging esophageal cancer, with or without dilation, is clinically important and safe. Gastrointest Endosc 1995;41:540–6.
67. Pfau PR, Ginsberg GG, Lew RJ, Faigel DO, Smith DB, Kochman ML. Esophageal dilation for endosonographic evaluation of malignant esophageal strictures is safe and effective. Am J Gastroenterol 2000;95:2813–5.
68. Wallace MB, Hawes RH, Sahai AV, Van Velse A, Hoffman BJ. Dilation of malignant esophageal stenosis to allow EUS guided fine-needle aspiration: safety and effect on patient management. Gastrointest Endosc 2000;51:309–13.
69. Jacobson BC, Shami VM, Larghi A, Chi KD, Kahaleh M, Dye C, et al. TTS-balloon dilatation for EUS staging of esophageal cancer: a multi-center safety study [abstract]. Gastrointest Endosc 2005;61:AB 115.
70. Chandrashekar MV, Richardson DL, Preston S, Karat D, Griffin SM. Perforation of a nonobstructing gastro-oesophageal carcinoma by oblique-viewing endoscopic ultrasound videoscope: a need for a safe technique. Endoscopy 2002;34:934
71. Bowrey DJ, Clark GW, Roberts SA, Maughan TS, Hawthorne AB, Williams GT, et al. Endosonographic staging of 100 consecutive patients with esophageal carcinoma: introduction of the 8-mm esophagoprobe. Dis Esophagus 1999;12:258–63.
72. Mallery S, Van Dam J. Increased rate of complete EUS staging of patients with esophageal cancer using the nonoptical, wire-guided echoendoscope. Gastrointest Endosc 1999;50:53–7.
73. Hunerbein M, Ghadimi BM, Haensch W, Schlag PM. Transendoscopic ultrasound of esophageal and gastric cancer using miniaturized ultrasound catheter probes. Gastrointest Endosc 1998;48:371–5.
74. Menzel J, Domschke W. Gastrointestinal miniprobe sonography: the current status. Am J Gastroenterol 2000;95:605–16.
75. Menzel J, Hoepffner N, Nottberg H, Schulz C, Senninger N, Domschke W. Preoperative staging of esophageal carcinoma: miniprobe sonography versus conventional endoscopic ultrasound in a prospective histopathologically verified study. Endoscopy 1999;31:291–7.
76. Sahai AV. Balloon-assisted esophageal intubation to prevent cervical perforation during EUS. Gastrointest Endosc 2002;55:140–1.
77. Schembre D, Chak A, Stevens P, Isenberg G, Sivak MV Jr, Lightdale CJ. Prospective evaluation of balloon-sheathed catheter US system. Gastrointest Endosc 2001;53:758–63.
78. Rösch T. [Puncture of every mass lesion in the pancreas? Point of view of gastroenterology; in German.] Dtsch Med Wochenschr 2004;129:1827.
79. Levy MJ, Wiersema MJ. EUS-guided Trucut biopsy. Gastrointest Endosc 2005;62:417–26.
80. Levy MJ, Jondal ML, Clain J, Wiersema MJ. Preliminary experience with an EUS-guided trucut biopsy needle compared with EUS-guided FNA. Gastrointest Endosc 2003;57:101–6.
81. Levy MJ, Clain JE, Keeney GL, Norton ID, Vazquez-Sequeiros E, Wiersema MJ. Prospective comparison of a 19 versus 22 gauge needle for performing endosonography guided fine needle aspiration of solid pancreatic neoplasms [abstract]. Gastrointest Endosc 2005;61:AB 289.
82. Schwartz DA, Harewood GC, Wiersema MJ. EUS for rectal disease. Gastrointest Endosc 2002;56:100–9.
83. Gress F, Schmitt C, Sherman S, Ciaccia D, Ikenberry S, Lehman G. Endoscopic ultrasound-guided celiac plexus block

for managing abdominal pain associated with chronic pancreatitis: a prospective single center experience. Am J Gastroenterol 2001;96:409–16.

84. Johanson JF, Cooper G, Eisen GM, Freeman M, Goldstein JL, Jensen DM, et al. Quality assessment of endoscopic ultrasound. Gastrointest Endosc 2002;55:798–801.

85. Eloubeidi MA, Chen VK, Eltoum IA, Jhala D, Chieng DC, Jhala N, et al. Endoscopic ultrasound-guided fine needle aspiration biopsy of patients with suspected pancreatic cancer: diagnostic accuracy and acute and 30-day complications. Am J Gastroenterol 2003;98:2663–8.

13 Esophagus, Stomach, Duodenum

C.F. Dietrich, S. Faiss

Introduction

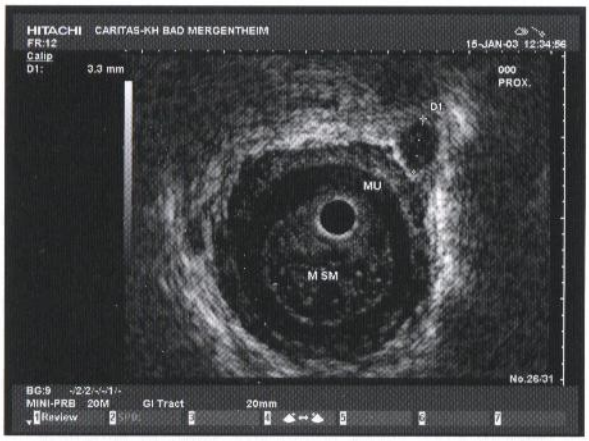
Endoscopic ultrasonography (EUS) is an extremely valuable tool for the local staging of various types of gastrointestinal tumor. Initial enthusiastic reports on the technique's diagnostic value were later qualified, but EUS-guided fine-needle aspiration (EUS-FNA) has extended the method's range of applications.

Wall layers in the esophagus, stomach, and duodenum. The accuracy of EUS measurement of the thickness of the gastrointestinal wall depends on physiological peristalsis; a contracted segment can resemble a thickened intestinal wall. Published studies provide some reference values for the "normal" thickness of the gastrointestinal wall, but these tend to have a wide range due to the use of different examination techniques (e.g., more or less application pressure) and technical parameters (such as the frequency used and the accuracy of measurement), and in addition there is considerable interobserver variability. As in conventional transabdominal ultrasonography of the bowel, EUS can delineate five layers in the wall of the esophagus, stomach, and duodenum (Table 13.**1**). In the esophagus, the muscularis propria can be divided into a hypoechoic inner layer (ring) and a hypoechoic outer layer (longitudinal). A hyperechoic connective-tissue layer can be detected between these two layers of muscle (Fig. 13.**1**, Table 13.**1**). Further differentiation of the mucosa is possible in some cases, but is of less clinical significance.

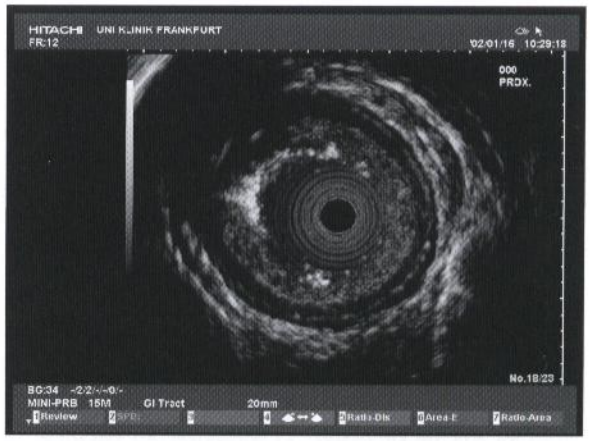
Table 13.**1** Endoscopic ultrasound (EUS) layers in the normal esophageal, gastric, and duodenal wall

EUS morphology of the gastrointestinal wall	Interpretation
Hyperechoic inner layer	Physical entrance echo (transition between the lumen and the mucosa)
Hypoechoic inner layer	Mucosa
Hyperechoic middle layer	Submucosa
Hypoechoic outer layer	Muscularis propria
Hyperechoic outer layer	Physical emission echo (serosa, adventitia/surroundings)

Although acoustic changes in the impedance cannot in principle be equated with the histological structure of the intestinal wall, the endosonographic image of the layers can provide orientation. Edema, cellular infiltration, cicatricial changes, and neoplastic masses can produce an endosonographic image of a thickened intestinal wall. Hypoechoic parts of the intestinal wall predominate when there are active inflammatory processes. However, echogenicity alone is not a sufficient marker of inflammatory activity. In addition, echogenicity may be biased by the frequency of the transducer used. Mucosal edema with normal or slightly reduced



a



b

Fig. 13.**1** The layers of the esophageal wall. **a** Normal esophageal layers, showing the mucosa (M) and submucosa (SM), as well as the muscularis propria (MU). A small normal perigastric lymph node is also visible. **b** The inner (ring) muscular and outer (longitudinal) muscular layer are visible.

peristalsis can lead to accentuated intestinal layers. By contrast, the typical layers of the intestinal wall can be disrupted by invasive processes (such as neoplasms and lymphomas) (Figs. 13.**2**, 13.**3**).

■ Esophagus

Orientation

Thorough anatomical knowledge of the abdominal and thoracic region, familiarity with different imaging qualities (e.g., radial or linear EUS and the effects of the angle of the acoustic level relative to the tip of the EUS probe), a feeling for the position of the probe tip, and a strong three-dimensional spatial sense are necessary for correct anatomical classification of findings in the intestinal wall. In addition to having good endoscopic skills and familiarity with ultrasound, examiners have to go through an extensive learning process to be able to grasp the different and variable acoustic levels in EUS. Basically, the gastrointestinal tract and the adjacent organs can be examined at the horizontal, sagittal, frontal, and subsequently at mixed and variable levels. With the radial EUS scanners currently available, the acoustic level that is mapped is pivotable in a user-defined way. This means that different views from cranial and caudal, as well as from any other optional position, can be obtained without moving the probe tip.

Older EUS devices (e.g., the Olympus UM-3 generation) only had two settings. However, these systems already had remarkable spatial resolution. In addition to anatomical knowledge and a basic understanding of the special imaging view provided by EUS devices, observing specific conventions during the course of an examination is useful for maintaining continuous anatomical orientation. In the ideal case, the EUS device can be passed through the gastrointestinal tract with only ultrasound and manual guidance, without endoscopic viewing. Rotating the stem of the EUS device produces comparable rotation of the EUS image, so that optional imaging positions can be achieved. In EUS, the esophagus is usually examined with the spine at the 6-o'clock position and the patient's left side at the 3-o'clock position. This approach facilitates comparison with other imaging modalities (such as computed tomography). However, other different approaches are also used.

Optimizing the Examination

Filling the organ with water and/or using a water-filled balloon at the tip of the EUS device can help provide a better view. Starting in the distal part of the esophagus, water filling can be carried out to improve the imaging quality. Filling the balloon slightly after inserting the scope can help prevent mucosal damage by smoothing the potentially traumatic tip of the device. Water filling of the lumen is contraindicated in the proximal part of the esophagus, due to the risk of aspiration.



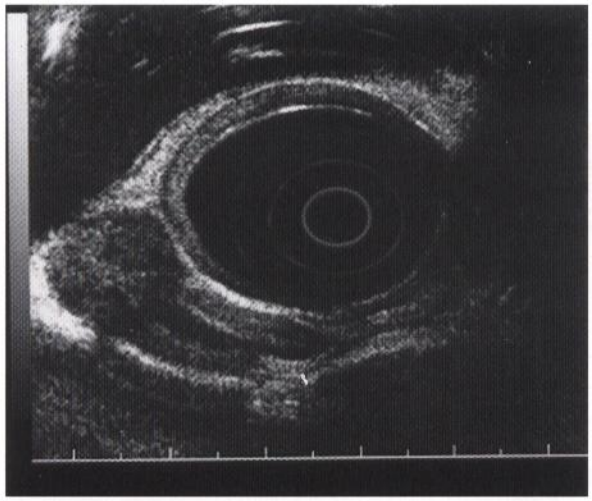
Fig. 13.**2** Disrupted layers of the esophageal wall in a patient with an initial mucosal tear. This type of initial mucosal tear, as well as a conventional biopsy, can lead to intramural bleeding or edema, with considerable changes in the layers that prevent adequate endosonographic assessment.



Fig. 13.**3** Disrupted layers of the esophageal wall after radiotherapy. Due to a variety of changes, and particularly as a result of fusion of the anatomical layers, re-staging with EUS after radiotherapy is not possible.

Indications

EUS is indicated for the staging malignant tumors in patients with no distant metastases, and for clarifying unclear findings. Endosonographic assessment of the esophageal wall is the method of choice and provides unrivaled resolution.



a



b

Fig. 13.4 A leiomyoma is visible in the outer muscular layer on radial endoscopic ultrasound (**a**) and miniprobe ultrasonography (**b**).



Fig. 13.5 Endoscopic ultrasound (EUS) demonstration of a lipoma, achieved by assigning the submucosa as the underlying anatomical layer. The echogenicity depends on the size of the fat droplets and the EUS frequency used. Lipomas can be hypoechoic but are more often hyperechoic or mixed.

Benign Diseases

The value of EUS in histologically confirmed benign diseases of the esophagus is unclear. There have been no prospective studies on the clinical impact of EUS in benign esophageal diseases. Depending on the presence of Barrett's epithelium, differences in the thickness of the esophageal wall can be measured endosonographically, but as these lie in a range of less than 1 mm they have not become clinically relevant. However, EUS is helpful for clarifying submucosal lesions and assessing impressions on the esophageal wall. EUS can distinguish between stromal tumors, which are often encountered —e.g., leiomyoma (Fig. 13.**4**), fibroma, lipoma (Fig. 13.**5**), hemangioma, myxoma—and rare epithelial tumors (such as cysts and papillomas). The symptoms of the various lesions are not characteristic; the principal symptom is dysphagia. Before endoscopic resection of such tumors, vessels need to be excluded as the cause of mucosal or submucosal swelling in order to avoid fatal complications.

The success of treatment for esophageal varices is assessed endoscopically. Conventional EUS can provide adequate assessment of intraluminal and extramural varices that are not endoscopically visible, but the management implications of this are not clear (Fig. 13.**6**).

Malignant Tumors of the Esophagus

Malignant intratumoral and extramural tumor growth can normally be evaluated very well with EUS. However, tumor-related esophageal stenoses that prevent passage of the endoscope are problematic, since in these cases the transverse acoustic level leads to overestimation of the extent of the tumor.

Many studies have shown that small T1 esophageal carcinomas cannot be definitely assigned to the mucosa or submucosa using conventional EUS. However, the distinction is essential for assessing whether endoscopic mucosal resection of these small tumors is possible. It has yet to be seen whether the problem of assessing the depth of tumor infiltration can be solved with high-frequency EUS miniprobes. Whether a T1 carcinoma has only infiltrated the mucosa or has already penetrated into to the submucosa has substantial prognostic relevance. In patients with submucosal tumor invasion, the rate of lymph-node metastases is much higher in comparison with those who only have mucosal invasion. T1 tumors with submucosal invasion are not therefore not suitable for primary endoscopic therapy. Clear differentiation between T2 and T3 esophageal carcinomas is also challenging in relation to the prognosis and surgical strategy. Peritumoral edema or inflammatory infiltration, or both, can give tumors a hypoechoic margin that is difficult to distinguish from the tumor itself. The malignant status of circumscribed esophageal lesions

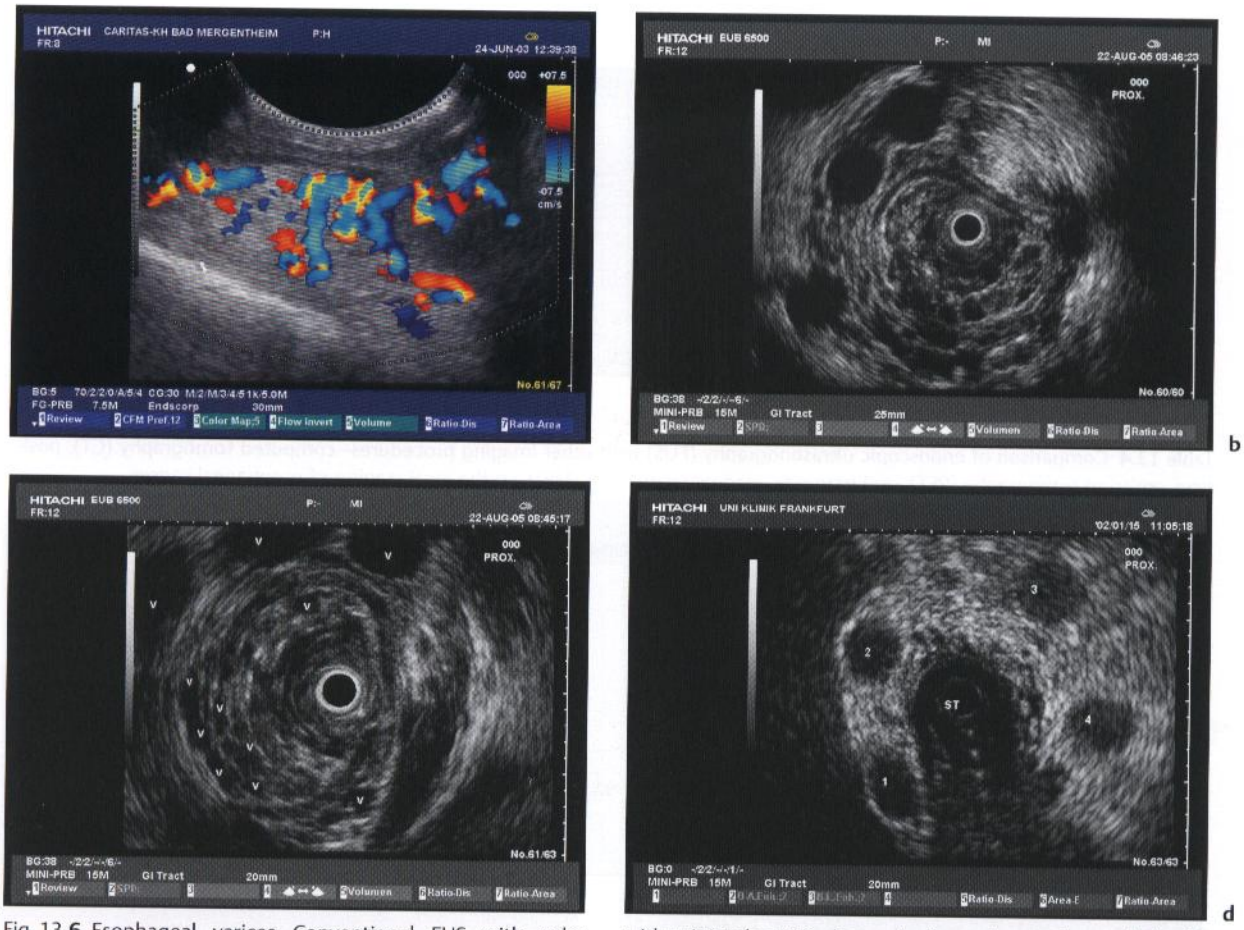


Fig. 13.**6** Esophageal varices. Conventional EUS with color Doppler is helpful for identifying submucosal or extramural esophageal varices (**a**). Esophageal varices can also be detected with miniprobe EUS, demonstrating extramural vessels (**a**, **b**), intramucosal varices (**c**) and thrombosed vessels after treatment of fundus varices (**d**). ST: stomach.

can only be assessed with histological examination of representative biopsies (as the gold standard). Attempts have been made to develop EUS criteria for malignancy, but the initial cancer diagnosis in the gastrointestinal tract is always established using a histological examination of endoscopic biopsies.

Operability is the deciding criterion in the assessment of malignant esophageal tumors. The reported accuracy of EUS for assessing the extent of tumors (T staging) is 80–90%, slightly higher than that in the stomach. The current value of EUS is described below on the basis of the published data; more critical reports have appeared recently. EUS examination of the esophagus is an established diagnostic method that still provides the only way of distinguishing between the different layers of the esophageal wall. Several publications have shown that EUS is superior not only to computed tomography (CT) but also to more recent imaging techniques such as positron-emission tomography (PET) (Tables 13.**2**–13.**4**) [1–7].

Table 13.**2** The accuracy of T staging with endoscopic ultrasonography (EUS) in comparison with computed tomography (CT) in patients with esophageal carcinomas or carcinomas of the gastroesophageal junction

First author, ref.	Patients (n)	Method	T total	T1	T2	T3	T4
Botet [1]	50	EUS	92%	n.a.	n.a.	n.a.	n.a.
	42	CT	42%	n.a.	n.a.	n.a.	n.a.
Ziegler [2]	37	EUS	89%	n.a.	n.a.	n.a.	n.a.
		CT	51%	n.a.	n.a.	n.a.	n.a.
Kienle [3]	117	EUS	69%	63%	52%	77%	50%
	36	CT	33%	100%	26%	36%	–
Weaver [4]	52	EUS	83%	88% *		85%	40%
		CT	77%	70% *		80%	50%

N.a.: not available. * T1 and T2 together.

Table 13.3 Accuracy (N-stage) of EUS compared with CT in patients with esophageal carcinomas or carcinomas of the gastro-esophageal junction

First author, ref.	Patients (n)	Method	N total	N0	N1	N2
Botet [1]	50	EUS	88%	n.a.	n.a.	n.a.
	42	CT	74%	n.a.	n.a.	n.a.
Ziegler [2]	37	EUS	69%	n.a.	n.a.	n.a.
		CT	51%	n.a.	n.a.	n.a.
Kienle [3]	117	EUS	79%	71%	85% *	
	36	CT	67%	47%	84% *	
Weaver [4]	52	EUS	81%	68%	83% *	
		CT	81%	84%	74% *	

N.a.: not available. * N1 and N2 together.

Table 13.4 Comparison of endoscopic ultrasonography (EUS) with other imaging procedures—computed tomography (CT), positron-emission tomography (PET), and magnetic resonance imaging (MR))—in the local staging of esophageal cancer

First author, ref.	Patients (n)	Method	T stage			N stage		
			Sensitivity	Specificity	Accuracy	Sensitivity	Specificity	Accuracy
Rasanen [5]	42	EUS	n.a.	n.a.	63%	89%	54%	75%
		CT	n.a.	n.a.	n.a.	47%	92%	66%
		PET	n.a.	n.a.	n.a.	37%	100%	63%
Flamen [6]	43	EUS	42%	94%	71%	63%	88%	85%
		CT	41%	83%	64%	22%	96%	78%
		PET	74%	90%	82%	39%	97%	83%
Berger [7]	Review	EUS	58–91%	82–99%	n.a.	77–89%	75–85%	n.a.
		CT	25%	94%	n.a.	11–77%	71–95%	n.a.
		PET	n.a.	n.a.	n.a.	28–39%	95–100%	n.a.

Table 13.5 Endoscopic ultrasound T staging of esophageal carcinomas

First author, ref.	Patients (n)	Sensitivity	Specificity	Accuracy
Rösch [8]	Review	n.a.	n.a.	85%
Weaver [4]	52	72%	85%	83%

N.a.: not available.

Table 13.6 Accuracy of endoscopic ultrasound for T staging of esophageal carcinomas

First author, ref.	Patients (n)	T (total)	T1	T2	T3	T4
Nattermann [9]	44	80%	75%	71%	91%	67%
Rösch [8]	Review	n.a.	84%	73%	89%	89%
Souquet [10]	82	77	n.a.	n.a.	n.a.	n.a.
Salminen [11]	32	66%	14%	40%	90%	–
Saunders [12]	Review	n.a.	75–82%	64–85%	89–94%	88–100%
Menzel [13]	30	57%	33%	57%	75%	50%
	53	87% *	43% *	88% *	96% *	100% *
Vazquez-Sequeiros [14]	37	84%	50%	100%	88%	0%
Weaver [4]	52	83%	88% **		85%	40%

N.a.: not available. * Data from miniprobes (15/20 MHz). ** T1 and T2 together

T Stage

The sensitivity of EUS for T staging in esophageal carcinoma is 85–95% (Table 13.**5**) [4,8]. However, there is some variation in the accuracy depending on the specific T stage (Table 13.**6**) [4,8–14]. In addition, as EUS is not capable of differentiating between tumor infiltration and concomitant inflammatory reactions, overstaging on EUS continues to be a problem (Figs. 13.**7**–13.**12**).

N Stage

Studies have shown that EUS has a sensitivity of 70–80% for N staging in esophageal carcinoma (Table 13.7) [4,8,9,11,15,16].

Table 13.7 Endoscopic ultrasound N staging of esophageal carcinomas

First author, ref.	Patients (n)	Sensitivity	Specificity	Accuracy
Rösch [8]	Review	n.a.	n.a.	75–80%
Rice [15]	22	70%	70%	59%
Dittler [16]	167	75%	70%	73%
Nattermann [9]	44	91%	64%	84%
Weaver [4]	52	91%	68%	81%

N.a.: not available.

Fine-Needle Aspiration

EUS-guided fine-needle aspiration (FNA) can improve the results in the staging of esophageal carcinomas

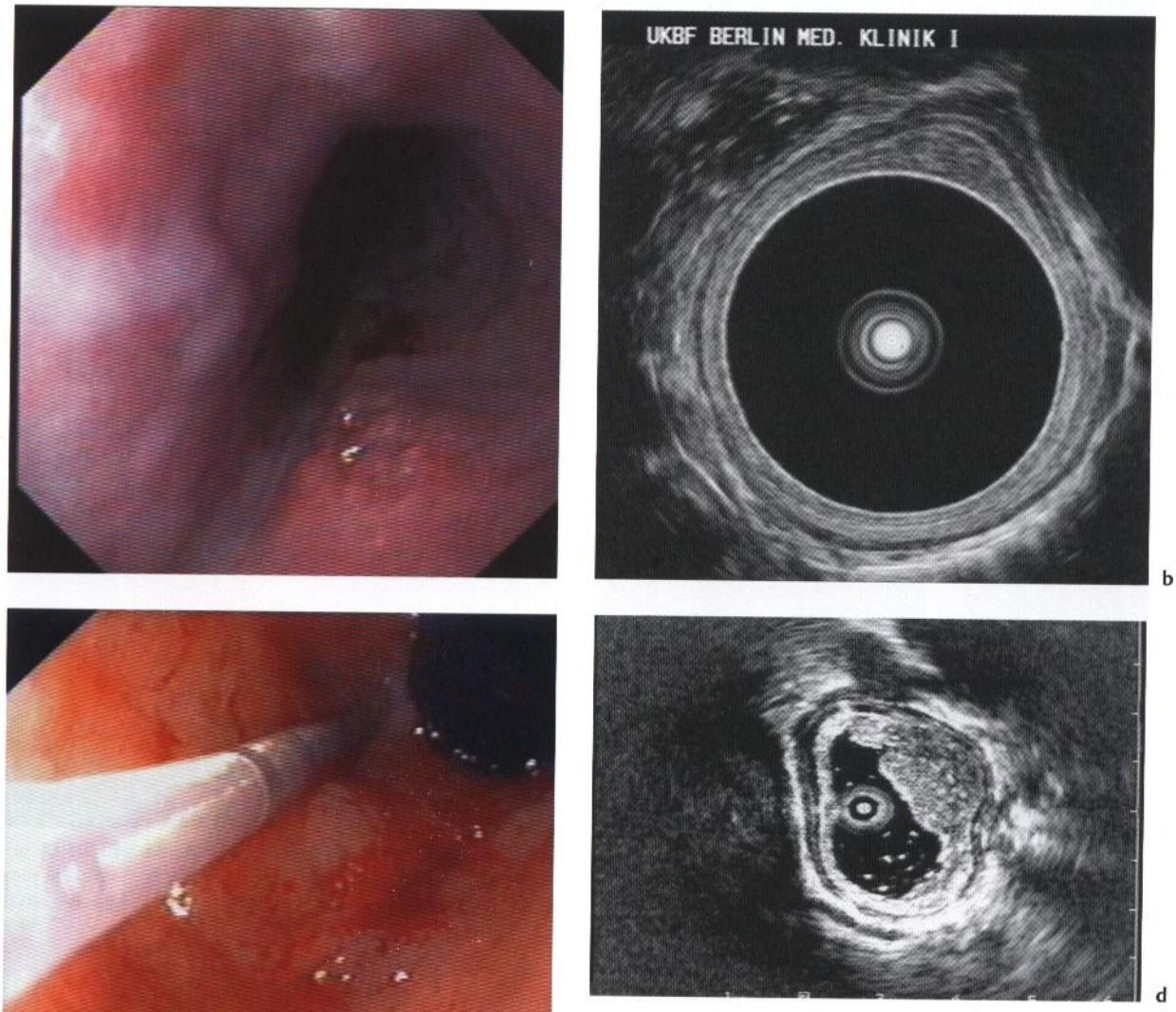


Fig. 13.7 T1 esophageal cancer, with mucosal and submucosal invasion. **a–c** Ideally, the EUS miniprobe should be used under endoscopic vision without pressure. **d** The EUS miniprobe provides unrivaled optical resolution.

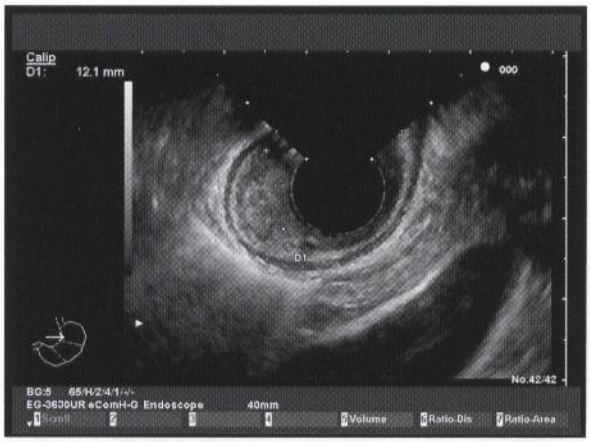
Fig. 13.7e–i ▷



e



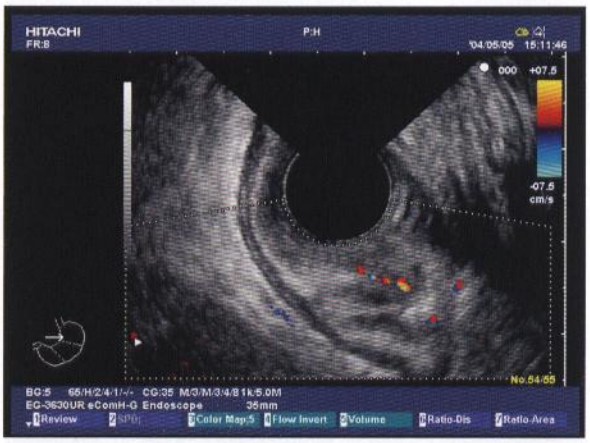
f



g



h



i

Fig. 13.**7e–i** Other forms of T1m (**e**) and T1sm tumors (**f**, **g**). The morphology depends on the inflammatory reaction. **h**, **i** Hyperplastic polyps may not be identifiable macroscopically (**h**); color Doppler imaging, demonstrating a normal vascular architecture, is helpful here (**i**).

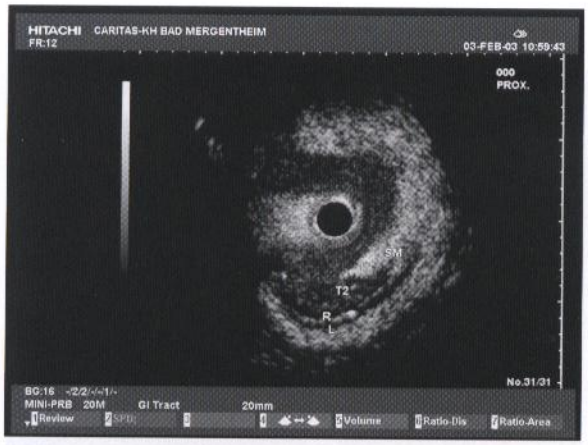
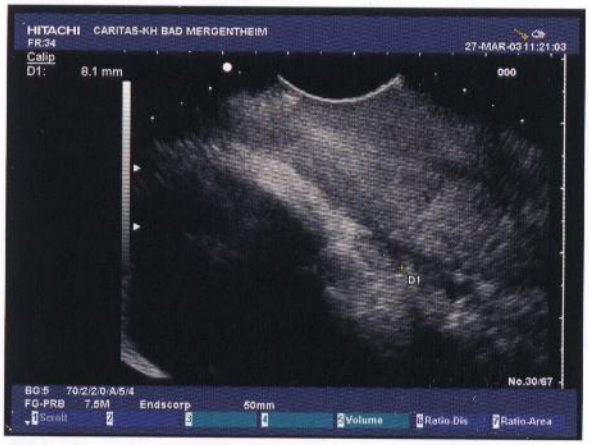


Fig. 13.**8** EUS miniprobe findings in T2 esophageal cancer, with invasion of the submucosal (SM) and muscular layer. In this case, the different depth of invasion is very well demonstrated. R: internal (ring) muscular layer. L: external (longitudinal) muscular layer. Due to the limited acoustic penetration with EUS miniprobes, adequate staging of periesophageal lymph nodes is not possible.



Fig. 13.**9** T2N1 esophageal carcinoma. Due to the limited acoustic penetration of EUS miniprobes, adequate staging of periesophageal lymph nodes is not possible. Conventional EUS is recommended for periesophageal lymph-node staging (as in the 4-mm periesophageal lymph node marked here). Conventional EUS also allows EUS-guided fine-needle aspiration of the lymph nodes, particularly for assessment of celiac lymph-node metastases.



a



b

Fig. 13.**10** T3 esophageal carcinoma (between the marks). Tumor invasion into the periesophageal connective tissue can be detected reliably with conventional EUS (**a**), as well as with the EUS miniprobe (**b**). Inflammatory reactions and atypical vessels affecting the T3 stage need to be taken into consideration.

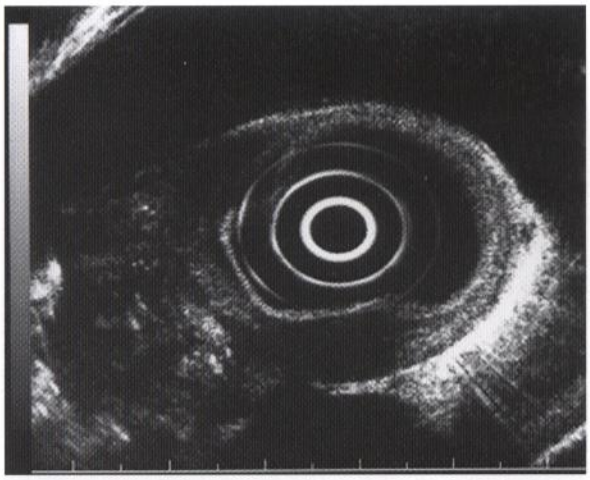
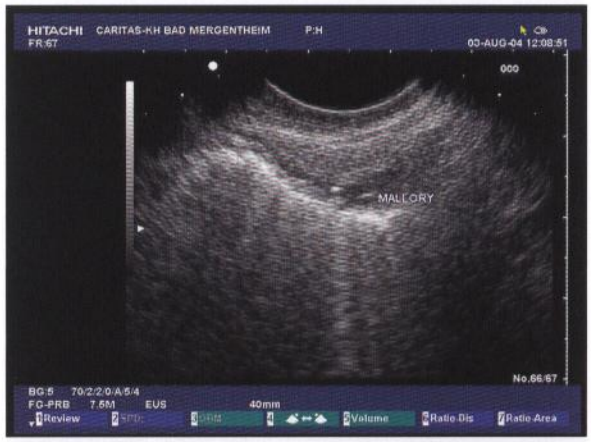


Fig. 13.**11** T4 esophageal carcinoma. The T4 stage of esophageal carcinoma is defined as infiltration of the mediastinal vessels (such as the aorta, in this case) or infiltration of the heart.



a



b

Fig. 13.**12** EUS staging after dilation. **a** Due to intramural bleeding and edema, EUS staging after dilation of malignant esophageal stenoses is not reliable and leads to overstaging, as seen in this case in a patient with a T2 carcinoma. **b** In a patient with a Mallory–Weiss lesion, air echoes are seen deep in the esophageal wall, showing that EUS staging is only of value in patients with histologically confirmed malignancies. ▷

Table 13.**8** Endoscopic ultrasound-guided fine-needle aspiration of lymph nodes in the staging of esophageal carcinomas

First author, ref.	Patients (n)	Sensitivity	Specificity	Accuracy
Vazquez-Sequeiros [18]	31	93%	100%	93%
Eloubeidi [19]	51	98%	100%	98%
Parmar [20]	20	100%	100%	100%
Murata [21]	Review	81–97%	83–100%	83–97%
Vazquez-Sequeiros [18]	124	83%	93%	87%

[17], as has been shown by several reports comparing the method with CT and with conventional EUS without FNA (Tables 13.**8**, 13.**9**) [18–22].

The accuracy of re-staging with EUS after chemoradiotherapy for esophageal and gastric tumors is currently a matter of controversy. After chemoradiotherapy, inflammatory and cicatricial processes cannot be distinguished from malignant infiltration, and routine EUS after radiotherapy is not at present accepted. However, local tumor recurrence in the anastomotic region after adequate previous surgery is an exception to this. As in primary tumor staging, local tumor recurrences also have to be confirmed histologically. Due to the underlying inflammatory and cicatricial changes, EUS of suspected local tumor recurrences has a relatively high level of sensitivity, but with low specificity.

Periesophageal structures can usually be assessed and even small lymph nodes can be detected. However, it has been shown that the morphology of lymph nodes that can be detected with EUS (their size, shape, acoustic pattern, and margins) is not sensitive enough to identify definite malignant infiltration. This is because, on the one hand, there may only be microscopic malignant infiltration of the lymph nodes, while on the other, peritumoral lymph nodes with inflammatory changes may meet the criteria for malignancy. These criteria are the number (more than

Table 13.9 Diagnostic value of endoscopic ultrasound-guided fine-needle aspiration (EUS-FNA) in the N staging of esophageal carcinomas, in comparison with endoscopic ultrasonography (EUS) and computed tomography (CT)

First author, ref.	Patients	Method	Sensitivity	Specificity	Accuracy
Parmar [20]	20/40	EUS+FNA	100%	100%	100%
	40	EUS	100%	50%	90%
	40	CT	30%	67%	35%
Murata [21]	Review	EUS-FNA	81–97%	83–100%	83–97%
		EUS	49–99%	33–99%	71–96%
Vazquez-Sequeiros [18]	124	EUS-FNA	83%	93%	87%
		EUS	71%	79%	74%
		CT	29%	89%	51%
Chang [22]	18	EUS-FNA	n.a.	n.a.	89%
		EUS	n.a.	n.a.	83%
		CT	n.a.	n.a.	56%

N.a.: not available.

three) and size (> 5 mm) of the lymph nodes; a round shape with a hypoechoic acoustic pattern; and precise delimitation from the surroundings.

EUS of the esophagus is useful for assessing the prognosis (for T staging, N staging, and providing the patient with information), for decision-making on whether curative or palliative surgery should be carried out, and for assessing the effectiveness of preoperative (neoadjuvant) treatment (e.g., chemoradiotherapy).

The relationship between an esophageal cancer and the tracheal bifurcation can be clearly demonstrated. This relationship is important and has treatment implications. Depending on the surgical approach, even non-metastatic T3 tumors distal to the bifurcation can be resected. Depending on whether there are any distal metastases, preoperative neoadjuvant chemoradiotherapy is recommended for proximal T3 lesions and all T4 malignancies. In patients with distal metastases and tumor-related dysphagia, palliative stenting of the esophagus is beneficial. In severe stenoses of this type, which cannot be passed with conventional EUS devices, the thickness of the esophageal wall is usually more than 2 cm and in nearly all cases the tumors are in stages T3 or T4. It is not yet clear whether traversing these stenoses with thinner EUS devices (known as blind probes) or miniprobes is of any practical value. Typically, the examination is limited by the reduced depth of penetration of the high-frequency miniprobes.

■ Stomach

Orientation

In terms of its position, shape, and size, the stomach has a variable and rather longitudinal (rather than horizontal) alignment and lies on the left side and to the left of the spine. After it enters the stomach, the EUS device is rotated nearly 90° to the right. The lesser curvature of the stomach is in the 12-o'clock position and the anterior wall is in the 3-o'clock position.

As in passage from the cardia to the fundus, the position of the EUS device is changed completely when the angular notch is passed and the prepyloric antrum is entered (Fig. 13.**13**). An additional change is made in the position of the device after it has passed through the duodenal bulb, with the instrument being rotated to the left into its original position, as in the esophagus. Orientation in the deep duodenum, correlating with the body axis, thus resembles that in the esophagus, with the spine (the dorsal reference structure) in the 6-o'clock position, the kidney (the right lateral reference structure) in the 9-o'clock position, and the pancreatic head in the 3-o'clock position.

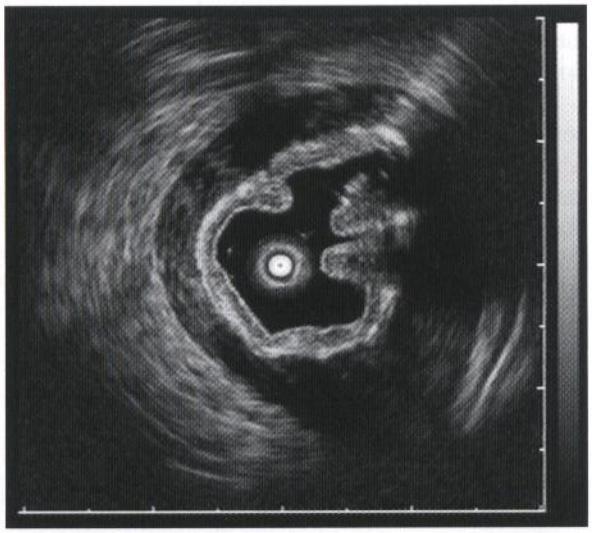
Optimizing the Examination

A 0.9% isotonic saline solution (300–500 mL) can be introduced into the stomach. However, some endoscopists prefer to work without filling the stomach with liquid. Simeticone (activated dimethicone) can be administered a few minutes before the examination to prevent intragastric foam. It is a matter of controversy whether the patient's position should be changed for assessment of the gastric fundus. For better assessment of the periduodenal structures (especially the pancreatic head), it is helpful to inflate the balloon at the echoendoscope's tip with water when it is in the duodenal bulb.

In most cases, additional external water-filling is not possible in the duodenum, but the internal duodenal fluid is sufficient. Because of their anatomical location and their air content, some areas of the duodenum and stomach (such as the cardia, fundus, parts of the anterior wall and antrum, the distal part of the duodenal bulb) are more difficult to evaluate. Repeated water-filling and suction of air bubbles, as well as changing the patient's position, is



a



b



c

necessary for adequate examinations. For evaluation of the cardia, fundus, and lesser curvature of the stomach, it is necessary to position the patient with the head downward or on the right side, while avoiding aspiration.

Because of the variability of the stomach and duodenum, orthograde angling of the acoustic level is necessary in order to avoid misinterpreting artificial swelling in the duodenal or gastric wall. The effects of compression by the EUS device can lead to limited visualization of discrete mucosal lesions and should therefore also be avoided. For adequate evaluation of structures in the intestinal wall, it is essential to keep a fair distance from the target. A high-frequency EUS miniprobe inserted through the endoscope's working channel and used without relevant compression is helpful for assessing smaller lesions.

Indications

The indications and examination criteria for evaluating the cardia and stomach are in principle similar to those for esophageal examinations. Due to the variable position of the stomach and consequently of the EUS device, the sensitivity and specificity of the method for diagnosing and staging gastric lesions are lower than in the esophagus.

Benign Gastric Lesions

Gastric polyps can be assigned to the superficial mucosa layer reliably with EUS (Figs. 13.**14**, 13.**15**).

Definitive diagnosis and classification of a gastric polyp is only possible after complete removal and histological work-up of the polyp. Before endoscopic removal, transmural growth of larger polyps can be excluded with EUS.

Conventional EUS is only of marginal relevance for diagnosing gastric ulcers, as the diagnosis has to be confirmed histologically. In penetrating ulcers, malignant tumor growth may be simulated on EUS. Although a correlation has been demonstrated between the depth of penetration and the time to ulcer healing, the value of EUS for evaluating ulcer healing is a matter of contro-

Fig. 13.**13** The different layers of the gastric wall. The configuration of the gastric wall layers varies in different locations and when different ultrasound devices are used. **a** Wall layers in the gastric corpus. **b**, **c** Wall layers in the antrum, with an accentuated muscular layer (**b**) and using a different technique (**c**); ee: physical entrance echo; mu: mucosa; sm: submucosa; mp: muscularis propria.

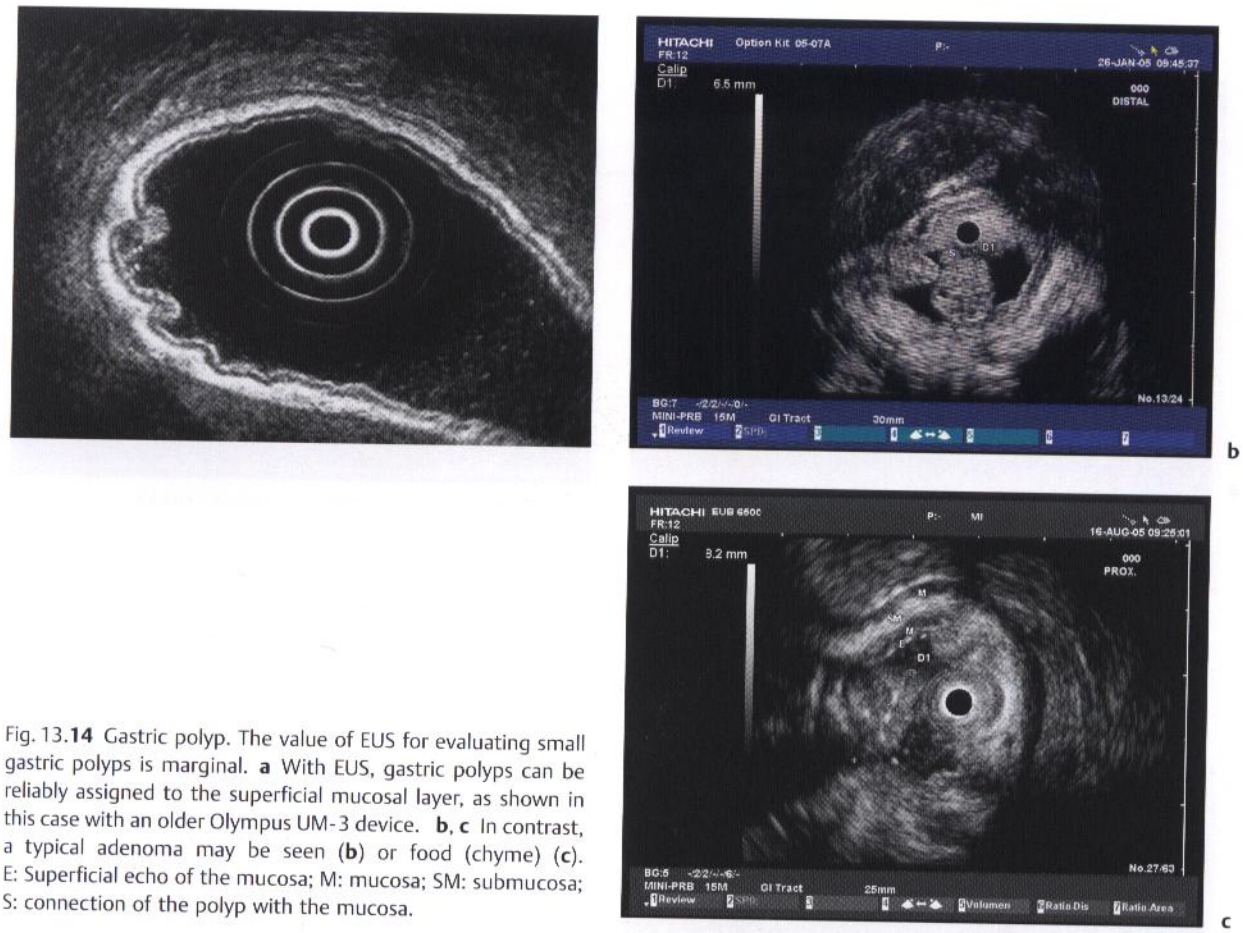


Fig. 13.**14** Gastric polyp. The value of EUS for evaluating small gastric polyps is marginal. **a** With EUS, gastric polyps can be reliably assigned to the superficial mucosal layer, as shown in this case with an older Olympus UM-3 device. **b**, **c** In contrast, a typical adenoma may be seen (**b**) or food (chyme) (**c**). E: Superficial echo of the mucosa; M: mucosa; SM: submucosa; S: connection of the polyp with the mucosa.

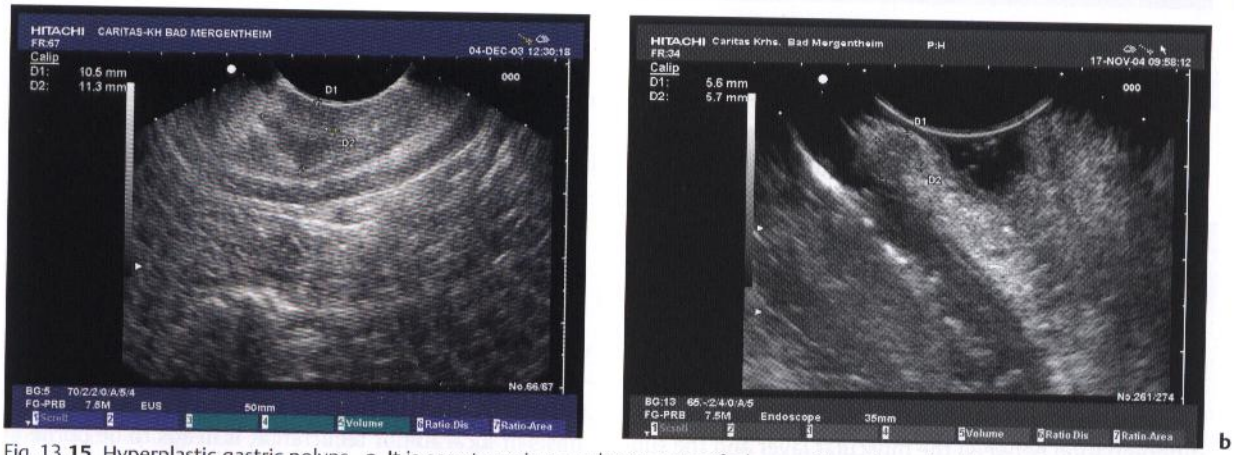


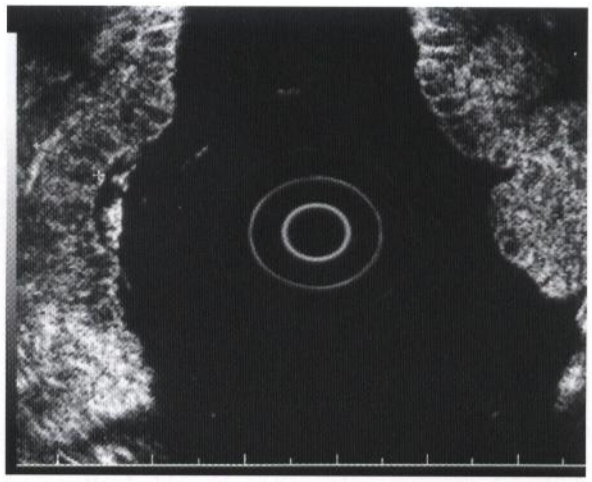
Fig. 13.**15** Hyperplastic gastric polyps. **a** It is easy to assign a polyp to a specific layer with endoscopic ultrasound (in this case, the mucosa). **b** In this example, the hyperplastic polyp is only displayed at the tip of the fold.

versy and the method ultimately has no practical relevance. The diagnostic impact of conventional EUS in other inflammatory diseases, such as Crohn's disease, is also limited.

In the evaluation of large folds in the stomach, suggestive findings can be detected by conventional EUS, but histological confirmation of the diagnosis remains obligatory. Foveolar hyperplasia of the stomach and Ménétrier's disease, with swelling of only the two inner layers, have to be distinguished from other entities (such as diffuse gastric cancer, linitis plastica, and gastric lymphoma). Intramural vessels in patients with portal hypertension can be excluded with EUS. The value of EUS in relation to large gastric folds is that it allows intramural vessels to be excluded before endoscopic resection of a gastric fold (Fig. 13.**16**).



a



b



c

Fig. 13.**16** Large-fold gastritis. **a**, **b** Ménétrier's disease, with thickening of the mucosa and submucosa. **c** Portal hypertension (PHTN).

Gastric Cancer

The TNM classification is used for the staging of gastric cancer (Tables 13.**10**, 13.**11**) [23]; a histological classification is also used (Table 13.**12**) [24]. The T1 stage has infiltration into the mucosa and submucosa, but without invasion into the muscularis propria. In superficial T1 tumors with mucosal tumor growth, EUS can show inconspicuous gastric layers. A histologically confirmed gastric cancer without changes on EUS is therefore classified as stage T1. Stage T2 is defined as infiltration into the muscular layer (T2a) or into the subserosa (T2b), but differentiation between the muscular layer and the subserosa is not possible with ultrasound in patients who do not have ascites. Definitive differentiation between T2 and T3 tumors is therefore not possible. Stage T3 involves tumor infiltration through the serosa into the visceral peritoneum, without infiltration of neighboring organs. Stage T4 is defined by tumor invasion into neighboring organs (e.g., the colon, liver, and pancreas).

Gastric cancers are normally hypoechoic, but hyperechoic tumors also sometimes occur.

The N stage is divided into stage N0 without metastatic lymph nodes, stage N1 with metastatic perigastric lymph nodes less than 3 cm from the tumor, and stage N2 with metastatic lymph nodes more than 3 cm from the tumor or lymph nodes along the left gastric artery, hepatic artery, splenic artery, and all the other mesenteric branches. Due to limited penetration depth, more distant lymph-node metastases cannot be diagnosed with EUS. EUS is superior to CT and transabdominal ultrasonography in the staging of gastric cancer. The possibility of gastric wall metastases (e.g., from melanoma or ovarian carcinoma) should be considered.

After gastrectomy, EUS is helpful for detecting malignant infiltration of regional lymph nodes. In the diagnosis of local tumor recurrence, it needs to be borne in mind that inflammatory processes and connective tissue can lead to false-positive results. The problems with EUS in the stomach are the same here as in the esophagus.

In patients in whom surgical resection is contraindicated and in whom local endoscopic tumor removal is possible, EUS staging is extremely valuable. EUS miniprobes are helpful in these cases in particular. Differentiation between the mucosal and submucosal T1 stages is possible, which is of considerable importance for curative endoscopic tumor therapy. The importance of perigastric lymph-node metastases in patients with

Table 13.**10** The TNM classification of malignant tumors [23]

Stage	Description
TX	Primary tumor not assessed
T0	No primary tumor
Tis	Carcinoma in situ: intraepithelial tumor without invasion into the lamina propria mucosae
T1	Tumor with invasion into the lamina propria mucosae or submucosa
T2	Tumor with invasion into the muscularis propria or subserosa
T3	Tumor with penetration of the visceral serosa and without infiltration into neighboring organs *
T4	Tumor with infiltration into neighboring organs *
NX	Regional lymph nodes not assessed
N0	No regional lymph-node metastases
N1**	Regional lymph-node metastases, 1–6 lymph nodes
N2**	Regional lymph-node metastases, 7–15 lymph nodes
N3**	Regional lymph-node metastases, > 15 lymph nodes
MX	Distant metastases not assessed
M0	No distant metastases
M1	Distant metastases

* Neighboring organs: spleen, transverse colon, liver, diaphragm, pancreas, abdominal wall, adrenal gland, kidney, small bowel and retroperitoneal region.

** Local lymph nodes are the perigastric lymph nodes along the greater and lesser curvature of the stomach; the lymph nodes along the branches of the celiac trunk (left gastric artery, hepatic artery, splenic artery) and along the hepatoduodenal ligament (compartment I lymph nodes less than 3 cm from the primary tumor). Compartment II: lymph-node metastases more than 3 cm from the primary tumor along the branches of the celiac trunk; compartment III: lymph nodes in the region of the root of the mesentery and retropancreatic lymph nodes are considered to be distant metastases.

Table 13.**11** International Union against Cancer (UICC) classification of malignant tumors [23]

Stage			
0	Tis	N0	M0
Ia	T1	N0	M0
Ib	T1	N1	M0
	T2	N0	M0
II	T1	N2	M0
	T2	N1	M0
	T3	N0	M0
IIIa	T2	N2	M0
	T3	N1	M0
	T4	N0	M0
IIIb	T3	N2	M0
IV	T1–3	N3	M0
	T4	N1–3	M0
	Any T	Any N	M1

Tis: intraepithelial carcinoma without invasion of the lamina propria mucosae.

Table 13.**12** The Lauren histological classification of gastric cancer [24]

1	Not applicable (no adenocarcinoma, no signet-ring cell cancer or undifferentiated carcinoma)
2	Intestinal type (polypoid growth, well demarcated, good prognosis)
	Well differentiated
	Moderately differentiated
	Poorly differentiated
3	Diffuse type (infiltrative growth, poorly demarcated)
4	Mixed type

T1 carcinomas was mentioned above. This is of great importance for planning endoscopic treatment and assessing the patient's prognosis. Conventional EUS is also important in view of the increasing numbers of laparoscopic operations being carried out.

Review of the Literature

Due to its high resolution, EUS is superior to other imaging modalities (especially CT) in the staging of malignant gastric tumors (Tables 13.**13**–13.**16**) [17,25–29]. This is especially true for T1 and T2 stage gastric cancer. With the increasing use of endoscopic mucosal resection in the treatment of early gastric cancer, endosonographic examination of the stomach is becoming increasingly important. In these cases, high-frequency miniprobes with 15, 20, or even 30 MHz provide excellent resolution of the gastric wall, which helps in differentiating T1 carcinomas into several subtypes. This is helpful for identifying patients with early gastric cancer who are eligible for therapeutic endoscopic mucosal resection. Typical findings are shown in Figs. 13.**17**–13.**26**.

Table 13.**13** Accuracy of endoscopic ultrasonography in the T staging of gastric cancer

First author, ref.	Patients (n)	T total	T1	T2	T3	T4
Wang [17]	119	70%	68%	67%	81%	53%
Willis [25]	116	78%	80%	61%	94%	82%
	Review	83%	72%	89%	79%	82%
Xi [26]	32	80%	100% *	71%	88%	73%

* Using 7.5, 12, and 20 MHz.

Table 13.**14** Accuracy of endoscopic ultrasonography in the N staging of gastric cancer

First author, ref.	Patients (n)	N total	N0	N1	N2
Wang [17]	119	65%	73%	69%	52%
Willis [25]	116	77%	84%	75%	65%
	Review	70%	87%	67%	61%
Xi [26]	32	69%	70%	67% pos. LN	n.a.

N.a.: not available; LN: lymph nodes.

Table 13.**15** Accuracy of endoscopic ultrasonography (EUS) in the T staging of gastric cancer, in comparison with helical computed tomography (CT)

First author, ref.	Patients (n)	Method	T total	T1	T2	T3	T4
Kuntz [27]	82	EUS	n.a.	100%	81%	61%	100%
	Review	EUS	60–90%	n.a.	n.a.	n.a.	n.a.
	94	CT	58%		57% *	34%	75%
Habermann [28]	51	EUS	86%	–	90%	79%	100%
		CT	76%	–	83%	63%	100%
Polkowski [29]	88	EUS	63%	36%	55%	80%	33%
		CT	44%	18%	22%	56%	38%

N.a.: not available. * T1 and T2 together.

Table 13.**16** Accuracy of endoscopic ultrasonography (EUS) in the N staging of gastric cancer, in comparison with helical computed tomography (CT)

First author, ref.	Patients (n)	Method	N total	N0	N1	N2
Kuntz [27]	82	EUS	n.a.	82%	89% *	
	94	HCT	n.a.	48%	83% *	
Habermann [28]	51	EUS	90%	100%	83%	84%
		HCT	70%	84%	42%	74%
Polkowski [29]	88	EUS	47%	64%	36%	43%
		HCT	52%	50%	54%	51%

N.a.: not available. * T1 and T2 together.

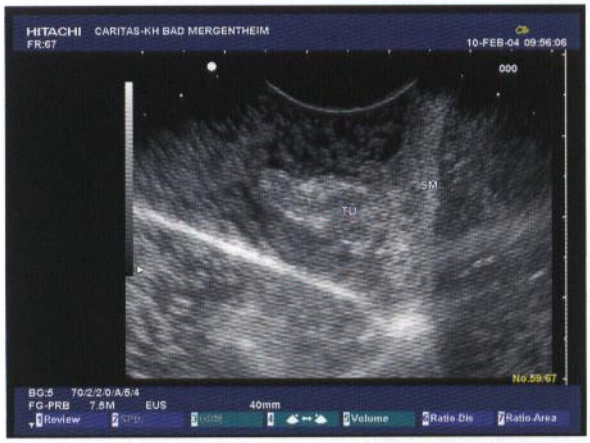


Fig. 13.**17** Exophytic T1 gastric cancer. The tumor (TU) is well distinguished from the deeper muscular layer. Local endoscopic tumor therapy is technically possible. SM: submucosa.

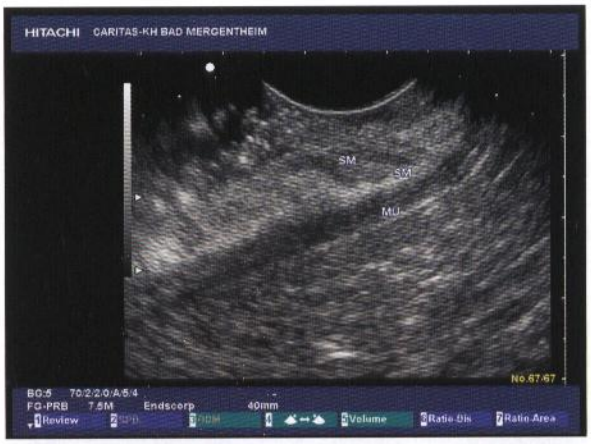


Fig. 13.**18** Excavated T1 gastric cancer. The excavated form of gastric cancer seen here is associated with a poor prognosis and is difficult to classify in comparison with exophytic tumors, in which the underlying layers can be assessed precisely. Submucosal (SM) infiltration is seen in this case. MU: muscularis propria.



Fig. 13.**19** T1 gastric cancer, imaged with an endoscopic ultrasound (EUS) miniprobe. The detailed resolution of superficial lesions is better with high-resolution miniprobes than with conventional EUS.

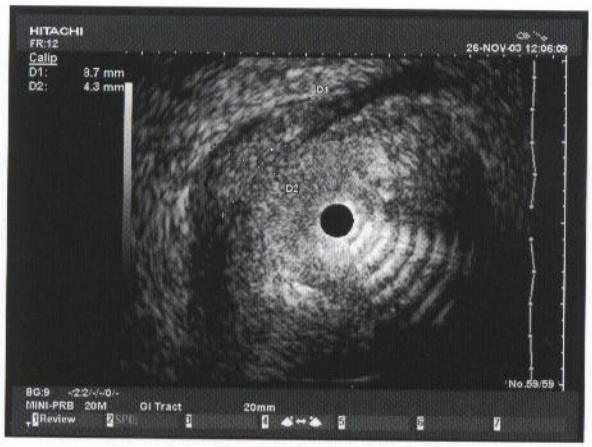
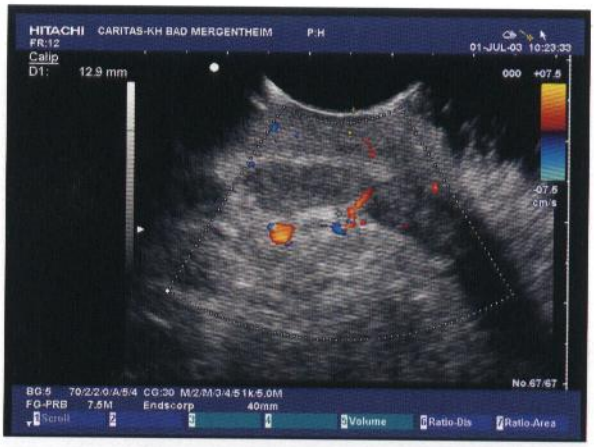


Fig. 13.**20** T2 gastric cancer. Hyperechoic infiltration of the muscular layer is well visualized. There is no penetration through the gastric wall.



a



b



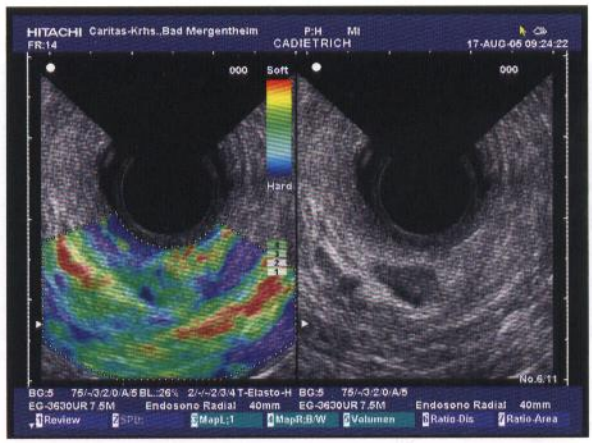
c



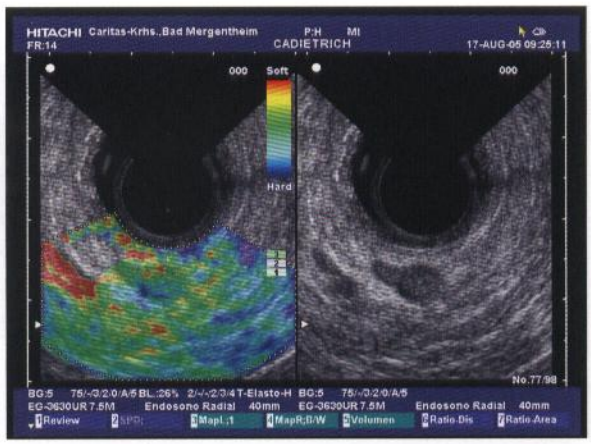
d

Fig. 13.**21** T3 gastric cancer. **a** It can be difficult to differentiate between T2 and T3 gastric carcinomas with endoscopic ultrasound alone, due to inflammatory reactions around the tumor. **b, c** Color and power Doppler imaging can be helpful for detecting vessels and assessing tumor invasion. **d** Another example, with lymph-node infiltration. Typically, there is no shift between the stomach and the surrounding tissue.

Fig. 13.**21e, f** ▷



e



f

Fig. 13.**21e, f** Elastography is helpful and provides reproducible results in detecting circumscribed lymph-node infiltration.



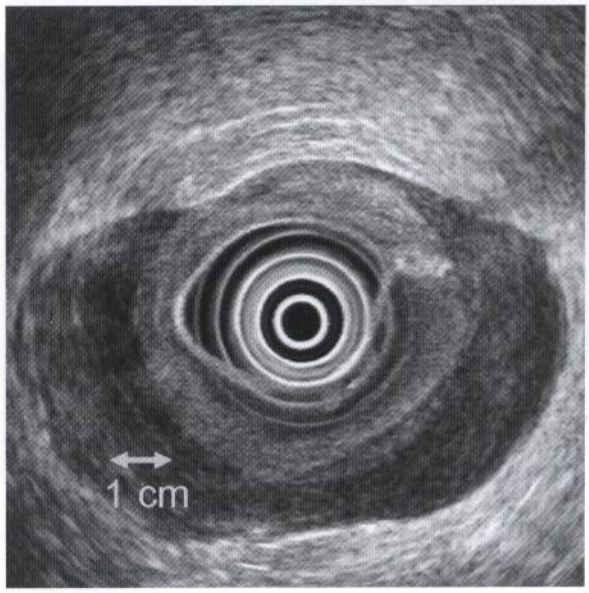
a



b



c



d

Fig. 13.**22** T4N1 gastric cancer. **a** Tumor invasion into the pancreas (T4). **b** Lymph-node metastases. **c** A small liver metastasis with segmental biliary congestion. **d** Linitis plastica.



Fig. 13.**23** Endoscopic ultrasound findings in peritoneal carcinosis, with infiltration of the serosa and muscularis propria by a tumor originating in the pancreas.

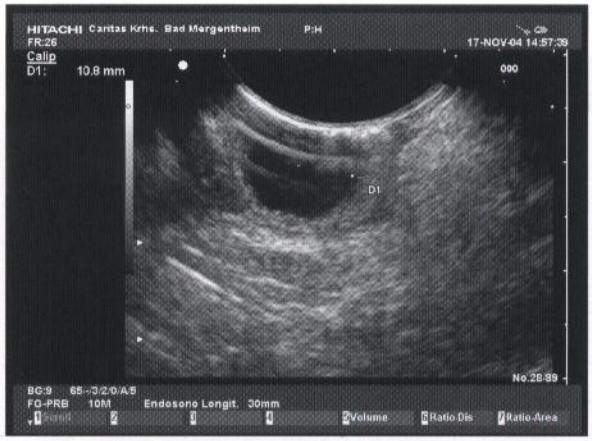


Fig. 13.**24** An intramucosal metastasis from a small-cell lung carcinoma is seen between the markers.

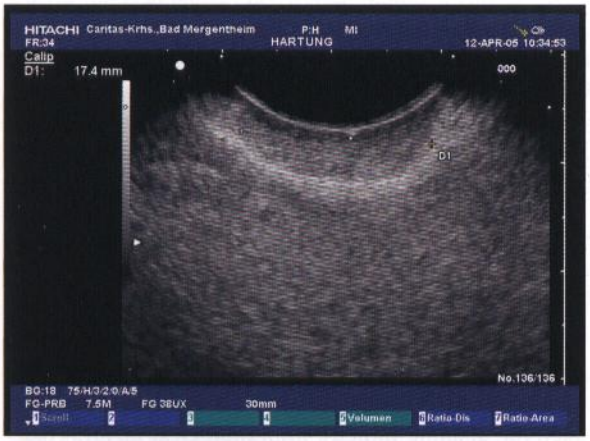
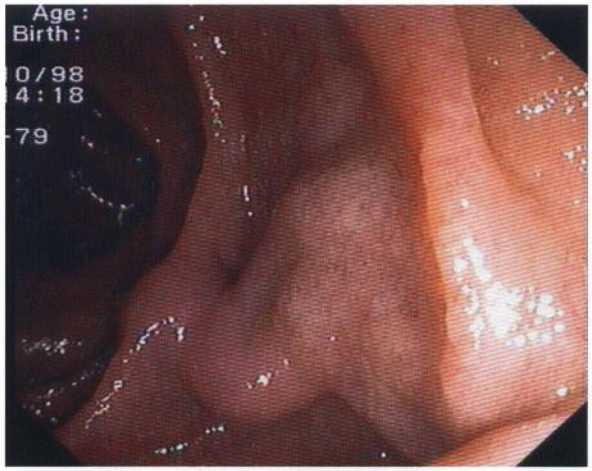


Fig. 13.**25** A neuroendocrine tumor (between the markers), mimicking gastric carcinoma infiltrating the submucosa.



a



b



c

Fig. 13.**26** Osler's disease. **a**, **b** Vascular abnormalities in Osler's disease can produce an impression like that of submucosal tumors. **c** They can be very well detected with EUS.

Table 13.**17** Predisposing factors for the development of malignancies in the small intestine

- Familial adenomatous polyposis
- Genetically determined tumor diseases (e.g., hereditary nonpolyposis colorectal cancer, HNPCC) and multiple primary malignant neoplasia, MPMN)
- Cowden syndrome
- Peutz–Jeghers syndrome
- Chronic inflammatory bowel diseases—e.g., Crohn's disease (predisposing factors: high inflammatory activity, involvement of the small bowel or isolated parts of the small bowel)
- Celiac disease (treatment-resistant)
- Hereditary or acquired immunodeficiency

Table 13.**18** Benign tumors of the small intestine

Lesion	Characteristics
Adenoma	A frequent epithelial tumor in the small bowel, with the frequency increasing from proximal to distal. Risk of malignancy: 30–50%; specific feature: familiar polyposis syndromes
Leiomyoma	A frequent mesenchymal and symptomatic tumor in the small bowel (especially the jejunum). Leading symptom: occult bleeding and obstruction. Caution: gastrointestinal stromal tumor (GIST)
Lipoma	Predilection in the ileum; mostly asymptomatic
Hamartoma	E.g., Peutz–Jeghers syndrome, defined genetic defect (*LKB1/STK11* gene on chromosome 19p); mucocutaneous, melanoid pigments. Increased risk of malignancies (small bowel, colorectal cancer, pancreas, breast, and testicle). Increased epithelial components are not found in hamartomas
Other	Inflammatory pseudotumors (e.g., Crohn's disease, postradiation enteritis)

Table 13.**19** Malignant tumors of the small intestine

Entity	Characteristics
Carcinoma	Frequent malignant tumor of the small bowel (> 50%). Predilection: duodenum and jejunum more than ileum; association with Crohn's disease and celiac disease; influence of genetic disorders (K-*ras*, erbB2, p53, etc.)
Sarcoma	Sarcomas develop from mesenchymal tissue (e.g., leiomyosarcoma from smooth muscle in the intestinal wall) and metastasize relatively early (e.g., to the liver). Treatment of choice: curative or palliative surgery, as the benefit of chemotherapy or radiotherapy has not yet been established
Kaposi's sarcoma	A frequent tumor in acquired immune deficiency syndrome (AIDS); mostly asymptomatic and diagnosed endoscopically as an incidental finding. Due to recurrent tumor manifestations, surgical resection is not promising
Other	Depending on the different tissue types, a large number of rare malignant tumors of the small intestine can be observed

■ Small Bowel

Due to the difficulty of diagnosing diseases in the small intestine, the value of EUS in evaluating these diseases is unclear. Correct staging and differential diagnosis of small-bowel diseases require adequate histological work-up, which is often only possible after surgical resection. The same principles apply as in EUS of the esophagus and stomach. In experienced hands, analogous decisions can therefore be obtained easily. Some specific characteristics of neoplastic diseases in the small intestine are discussed below.

Despite the large surface area of the intestine and faster proliferation of the epithelial cells in comparison with the colon, benign tumors (30–50%) and malignant tumors (50–70%) in the small bowel are rare (< 5% of all gastrointestinal tumors, 0.1% of all malignant tumors; incidence one in 10^5). The incidence of colon cancer is more than 50 times higher. The available data on the frequency of tumors in the different parts of the small intestine are inconsistent. Distal (benign) tumors (in the ileum) are more frequent than proximally located tumors (in the duodenum and jejunum). However, the frequency of malignant intestinal tumors decreases from proximal to distal (duodenum 50%, jejunum 30%, ileum 20%). Adenocarcinomas, carcinoids, lymphomas, and sarcomas are the most frequently diagnosed malignant tumors in the small bowel. The frequency increases in older patients. Many possible etiological reasons for the relatively low incidence of these tumors have been discussed; in addition to the fast transit time and the low viscosity of the diluted intestinal fluid (low rate of bacteria, alkaline milieu), immunological factors (macrophages, T and B cells, IgA secretion) in the mucosa play an important role. Many (rare) diseases predispose to malignancies in the small intestine (Tables 13.**17**–13.**20**).

Over 50% of tumors in the small intestine are asymptomatic. The most frequently observed findings are chronic (occult) bleeding, abdominal pain, and obstruction (ileus or subileus). Although 90% of the patients have uncharacteristic symptoms at the time of diagnosis, small-intestinal tumors are normally diagnosed at an advanced stage of the disease (with intestinal bleeding, ileus, stenoses, invagination, perforation). Signs of invasive tumor disease should be noted (e.g., jaundice when there is biliary involvement).

Tumors of the small bowel are difficult to detect when endoscopically inaccessible parts of the small intestine are affected. Enteroclysis (Sellink) is the method with the best results. Only 50–60 cm of the proximal jejunum can be reached with push enteroscopy, so that the benefits of this method depend on the tumor location. High-resolution transabdominal ultrasonography and helical CT can be very useful in specific cases, but definitive diagnosis can usually only be obtained by laparotomy. As in all other tumors, the prognosis with

Table 13.**20** Classification of benign and malignant tumors of the small intestine according to the primary tissue. For gastrointestinal stromal tumors (GISTs), see Chapter 14).

Tumor genesis	Benign	Malignant
Epithelial	Adenoma	Adenocarcinoma
Mesenchymal	Fibroma	Fibrosarcoma
Smooth muscle	Leiomyoma	Leiomyosarcoma
Fatty tissue	Lipoma	Liposarcoma
Blood vessels	Hemangioma	Hemangiosarcoma, Kaposi's sarcoma
Lymphatic vessels	Lymphangioma	Lymphangiosarcoma
Lymphatic tissue	Pseudolymphoma	Lymphoma
Nerval tissue	Neurofibroma	Neurofibrosarcoma
Glia	Neurilemmoma	Neurofibrosarcoma
Enterochromaffin cells		Carcinoid, gastrinoma, insulinoma
Pluripotent stem cell	Hamartoma	Malignant mixed tumors (teratoma, adenocarcinoid, adenosquamous carcinoma)

these lesions depends on the tumor stage, histology, grading, and available treatment modalities. The 5-year survival rates are lower in patients with adenocarcinomas and sarcomas in comparison with those with carcinoids and lymphomas.

References

1. Botet JF, Lightdale CJ, Zauber AG, Gerdes H, Winawer SJ, Urmacher C, et al. Preoperative staging of gastric cancer: comparison of endoscopic US and dynamic CT. Radiology 1991;181:426–32.
2. Ziegler K, Sanft C, Zeitz M, Friedrich M, Stein H, Haring R, et al. Evaluation of endosonography in TN staging of oesophageal cancer. Gut 1991;32:16–20.
3. Kienle P, Buhl K, Kuntz C, Dux M, Hartmann C, Axel B, et al. Prospective comparison of endoscopy, endosonography and computed tomography for staging of tumours of the oesophagus and gastric cardia. Digestion 2002;66:230–6.
4. Weaver SR, Blackshaw GR, Lewis WG, Edwards P, Roberts SA, Thomas GV, et al. Comparison of special interest computed tomography, endosonography and histopathological stage of oesophageal cancer. Clin Radiol 2004;59:499–504.
5. Rasanen JV, Sihvo EI, Knuuti MJ, Minn HR, Luostarinen ME, Laippala P, et al. Prospective analysis of accuracy of positron emission tomography, computed tomography, and endoscopic ultrasonography in staging of adenocarcinoma of the esophagus and the esophagogastric junction. Ann Surg Oncol 2003;10:954–60.
6. Flamen P, Lerut A, Van Cutsem E, De Wever W, Peeters M, Stroobants S, et al. Utility of positron emission tomography for the staging of patients with potentially operable esophageal carcinoma. J Clin Oncol 2000;18:3202–10.
7. Berger AC, Scott WJ. Noninvasive staging of esophageal carcinoma. J Surg Res 2004;117:127–33.
8. Rösch T. Endosonographic staging of esophageal cancer: a review of literature results. Gastrointest Endosc Clin N Am 1995;5:537–47.
9. Nattermann C, Dancygier H. [Endoscopic ultrasound in preoperative TN staging of esophageal cancer: a comparative study between endosonography and computerized tomography; in German.] Ultraschall Med 1993;14:100–5.
10. Souquet JC, Napoleon B, Pujol B, Keriven O, Ponchon T, Descos F, et al. Endoscopic ultrasonography in the preoperative staging of esophageal cancer. Endoscopy 1994;26:764–6.
11. Salminen JT, Farkkila MA, Ramo OJ, Toikkanen V, Simpanen J, Nuutinen H, et al. Endoscopic ultrasonography in the preoperative staging of adenocarcinoma of the distal oesophagus and oesophagogastric junction. Scand J Gastroenterol 1999;34:1178–82.
12. Saunders HS, Wolfman NT, Ott DJ. Esophageal cancer: radiologic staging. Radiol Clin North Am 1997;35:281–94.
13. Menzel J, Hoepffner N, Nottberg H, Schulz C, Senninger N, Domschke W. Preoperative staging of esophageal carcinoma: miniprobe sonography versus conventional endoscopic ultrasound in a prospective histopathologically verified study. Endoscopy 1999;31:291–7.
14. Vazquez-Sequeiros E, Wiersema MJ, Clain JE, Norton ID, Levy MJ, Romero Y, et al. Impact of lymph node staging on therapy of esophageal carcinoma. Gastroenterology 2003;125:1626–35.
15. Rice TW, Boyce GA, Sivak MV. Esophageal ultrasound and the preoperative staging of carcinoma of the esophagus. J Thorac Cardiovasc Surg 1991;101:536–43.
16. Dittler HJ, Siewert JR. Role of endoscopic ultrasonography in esophageal carcinoma. Endoscopy 1993;25:156–61.
17. Wang JY, Hsieh JS, Huang YS, Huang CJ, Hou MF, Huang TJ. Endoscopic ultrasonography for preoperative locoregional staging and assessment of resectability in gastric cancer. Clin Imaging 1998;22:355–9.
18. Vazquez-Sequeiros E, Norton ID, Clain JE, Wang KK, Affi A, Allen M, et al. Impact of EUS-guided fine-needle aspiration on lymph node staging in patients with esophageal carcinoma. Gastrointest Endosc 2001;53:751–7.
19. Eloubeidi MA, Wallace MB, Reed CE, Hadzijahic N, Lewin DN, Van Velse A, et al. The utility of EUS and EUS-guided fine needle aspiration in detecting celiac lymph node metastasis in patients with esophageal cancer: a single-center experience. Gastrointest Endosc 2001;54:714–9.
20. Parmar KS, Zwischenberger JB, Reeves AL, Waxman I. Clinical impact of endoscopic ultrasound-guided fine needle aspiration of celiac axis lymph nodes (M1a disease) in esophageal cancer. Ann Thorac Surg 2002;73:916–20.

21. Murata Y, Ohta M, Hayashi K, Ide H, Takasaki K. Preoperative evaluation of lymph node metastasis in esophageal cancer. Ann Thorac Cardiovasc Surg 2003;9:88–92.
22. Chang KJ, Soetikno RM, Bastas D, Tu C, Nguyen PT. Impact of endoscopic ultrasound combined with fine-needle aspiration biopsy in the management of esophageal cancer. Endoscopy 2003;35:962–6.
23. Sobin LH, Wittekind C, editors. TNM classification of malignant tumours, 6th ed. New York : Wiley-Liss, 2002 (UICC, International Union against Cancer).
24. Lauren P. The two histological main types of gastric carcinoma: diffuse and so-called intestinal-type carcinoma: an attempt at a histo-clinical classification. Acta Pathol Microbiol Scand 1965;64:31–49.
25. Willis S, Truong S, Gribnitz S, Fass J, Schumpelick V. Endoscopic ultrasonography in the preoperative staging of gastric cancer: accuracy and impact on surgical therapy. Surg Endosc 2000;14:951–4.
26. Xi WD, Zhao C, Ren GS. Endoscopic ultrasonography in preoperative staging of gastric cancer: determination of tumor invasion depth, nodal involvement and surgical resectability. World J Gastroenterol 2003;9:254–7.
27. Kuntz C, Herfarth C. Imaging diagnosis for staging of gastric cancer. Semin Surg Oncol 1999;17:96–102.
28. Habermann CR, Weiss F, Riecken R, Honarpisheh H, Bohnacker S, Staedtler C, et al. Preoperative staging of gastric adenocarcinoma: comparison of helical CT and endoscopic US. Radiology 2004;230:465–71.
29. Polkowski M, Palucki J, Wronska E, Szawlowski A, Nasierowska-Guttmejer A, Butruk E. Endosonography versus helical computed tomography for locoregional staging of gastric cancer. Endoscopy 2004;36:617–23.

14 Endoscopic Ultrasound in Subepithelial Tumors of the Gastrointestinal Tract

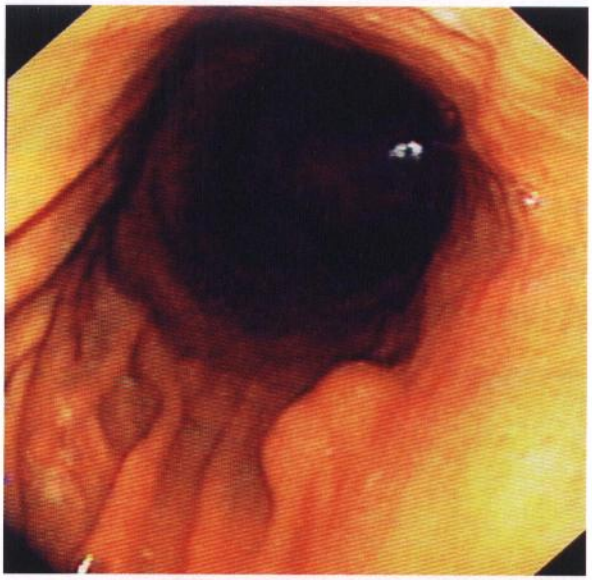
C. Jenssen, C.F. Dietrich

One of the classical indications for endoscopic ultrasonography (EUS) is the investigation of possible subepithelial tumors and the differential diagnosis, classification, and follow-up of these lesions [1–5]. There are no reliable data on the incidence of subepithelial tumors and other submucosal lesions of the gastrointestinal tract, since in the majority of cases they remain asymptomatic and undiagnosed throughout life. Postmortem studies have found mesenchymal esophageal tumors (leiomyomas) in 5% of cases, and mesenchymal gastric tumors in half of all patients who died over the age of 50 years [5]. Such tumors are diagnosed much less frequently in living patients, although with the increasing use of endoscopy they are now being discovered more often. Usually, they represent an incidental finding and may be entirely unrelated to the clinical question that prompted the endoscopic examination in the first place [6]. The endoscopic findings may vary from subtle protrusions to tiny polyps or large, protruding mass lesions (Figs. 14.**1**, 14.**2**).

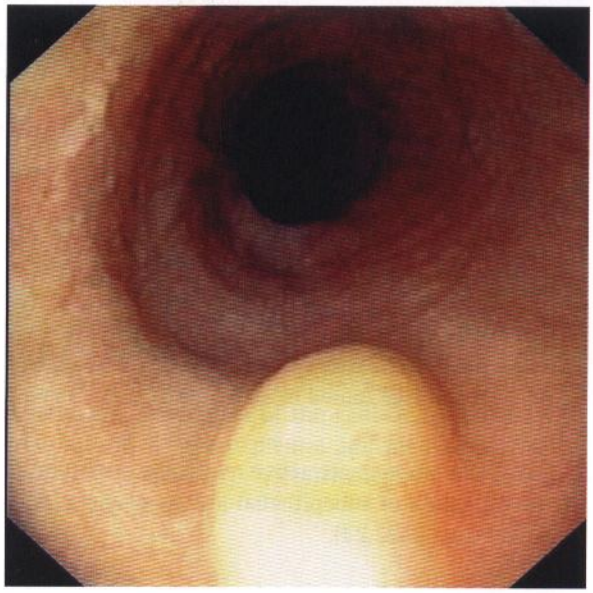
The distribution of subepithelial tumors in the upper gastrointestinal tract is not uniform. The stomach is the organ most frequently involved (in about 60% of cases); approximately 30% of subepithelial tumors are found in the esophagus, and only about 10% in the duodenum [7,8,9].

We carried out 125 endosonographic examinations for subepithelial lesions over a period of 50 months. In 84% of the examinations, the presenting symptoms appeared to be unrelated to the subepithelial lesion. Subepithelial tumors only cause gastrointestinal hemorrhage (Fig. 14.**3**), dysphagia, or symptoms of intestinal obstruction in rare cases [8,10,11].

As with radiographic methods, endoscopy is not capable of differentiating reliably between subepithelial tumors, intramural varices, and wall impressions caused by extraluminal lesions [1,3,12–17]. In addition, it is not possible to diagnose the lesion type, the depth and extent of an intramural lesion, or whether neighboring organs are involved [13,15,18]. Endoscopic biopsy is usually unhelpful, as it only provides samples of the mucosa covering a subepithelial lesion, not tissue from the lesion itself. More invasive methods of tissue sampling, such as "buttonhole" or jumbo biopsies, have a low diagnostic yield and carry a high risk (Fig. 14.**4**) [19–21].



a



b

Fig. 14.**1a** Endoscopic view of a small gastric subepithelial tumor (a gastrointestinal stromal tumor) on the back wall of the gastric body. **b** Endoscopic view of a small esophageal subepithelial tumor (a granular-cell tumor).

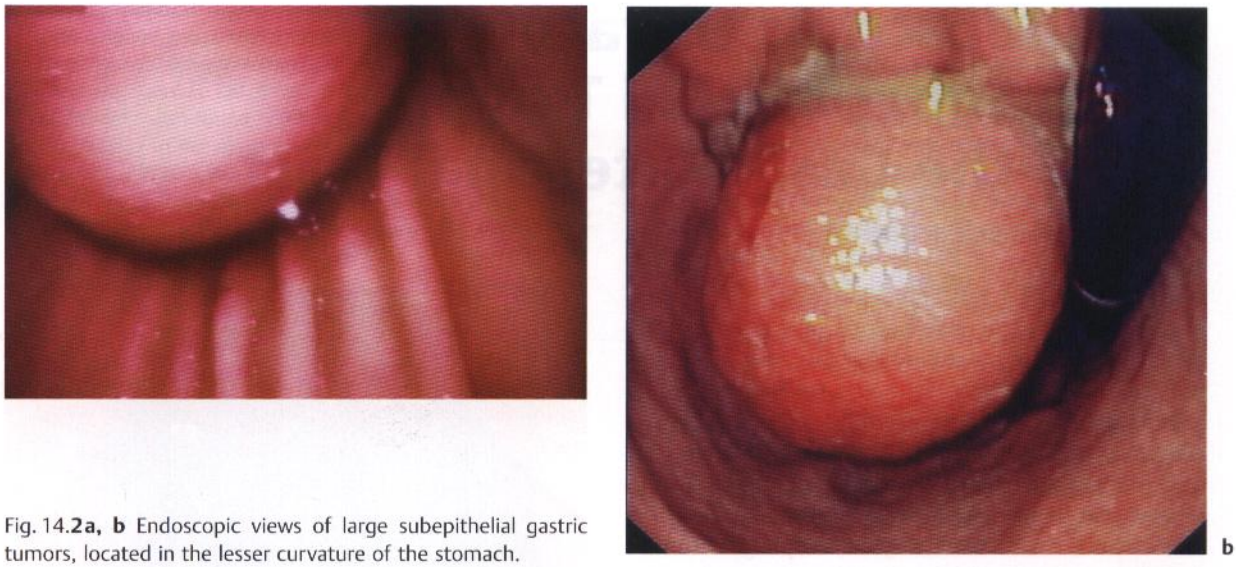


Fig. 14.2a, b Endoscopic views of large subepithelial gastric tumors, located in the lesser curvature of the stomach.

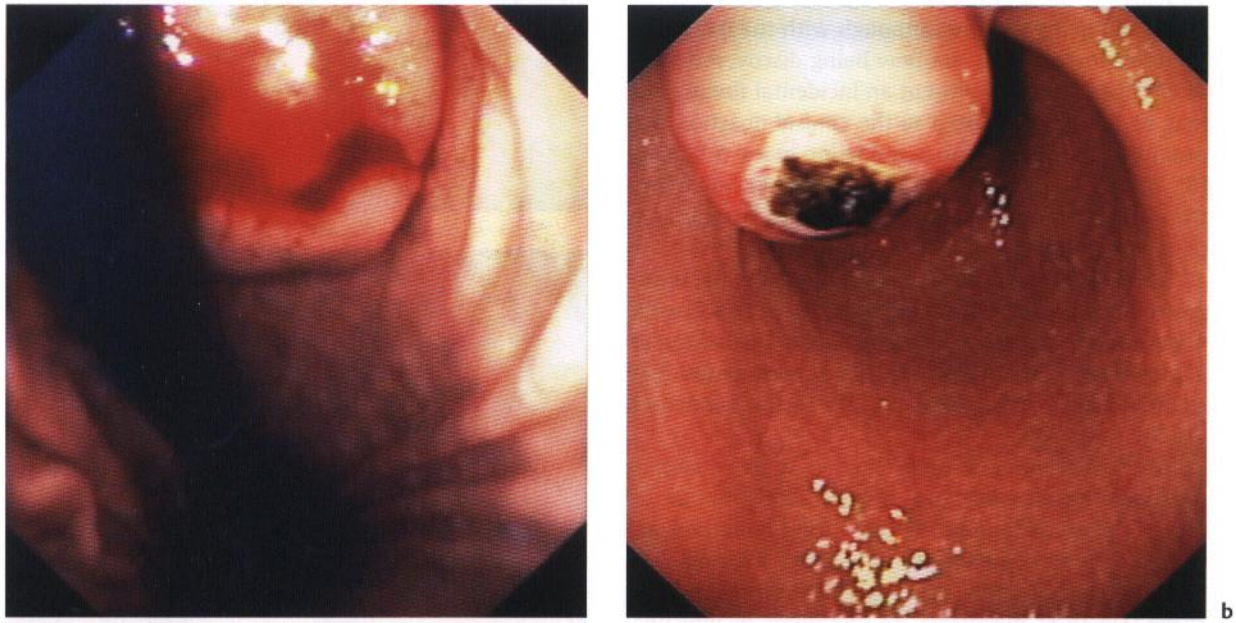
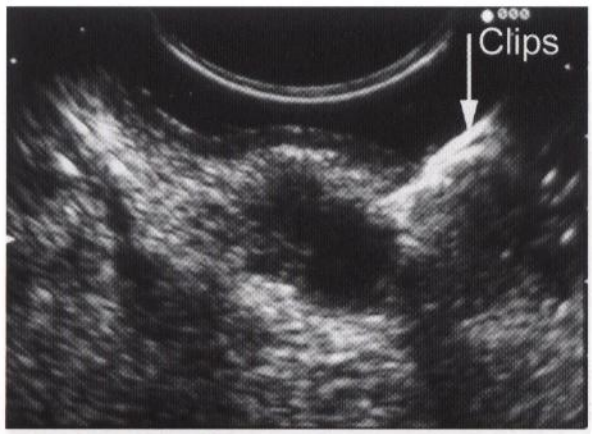


Fig. 14.3 Hemorrhage caused by subepithelial gastric tumors. **a** Overt bleeding (retrograde view). **b** Ulceration with adherent clot.

EUS is therefore an attractive noninvasive method in the investigation of subepithelial lesions of the gastrointestinal tract [8,22,23].

Subepithelial Tumors versus Extramural Impressions (Lesions Mimicking Subepithelial Tumors)

Endoscopic ultrasound is a highly reliable method for differentiating between subepithelial lesions and wall impressions caused by extramural lesions [3,18,24–29]. Observer agreement in the diagnosis of extramural lesions causing wall protrusion is excellent [30]. In comparison with other methods such as barium contrast, endoscopy with biopsy, and computed tomography (CT), EUS shows considerable superiority in the diagnosis of such lesions, and should therefore be regarded as the investigation of first choice [12,14–16,31]. There have been numerous studies reporting that among lesions endoscopically suspected to be subepithelial tumors, the proportion of extramural lesions causing wall impressions is in the range of 14–42% [15,24,25,32–34]. In our own patients, we found extramural impression effects in 23% (29 of 125) of the endosonographic examinations conducted for suspected subepithelial tumors. Extramural wall protrusions of this type are usu-



a



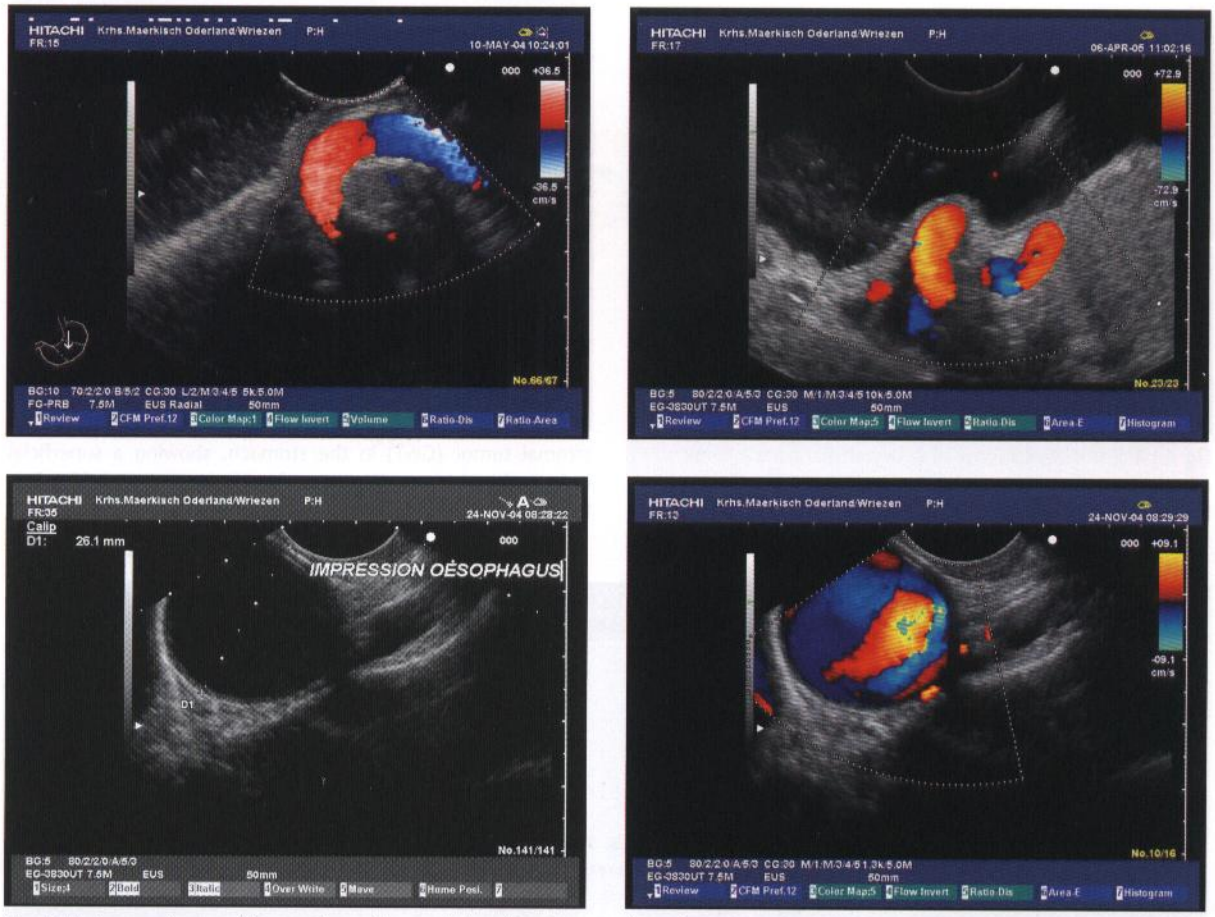
b

Fig. 14.**4** Buttonhole biopsy of subepithelial gastric tumors. **a** EUS view of a subepithelial neuroendocrine tumor with a hemoclip after hemorrhage **b** EUS view of a gastrointestinal stromal tumor (GIST) in the stomach, showing a superficial defect after biopsy. Clinically, there was recurrent bleeding from the biopsy site.

Table 14.**1** Causes of wall protrusion/impression

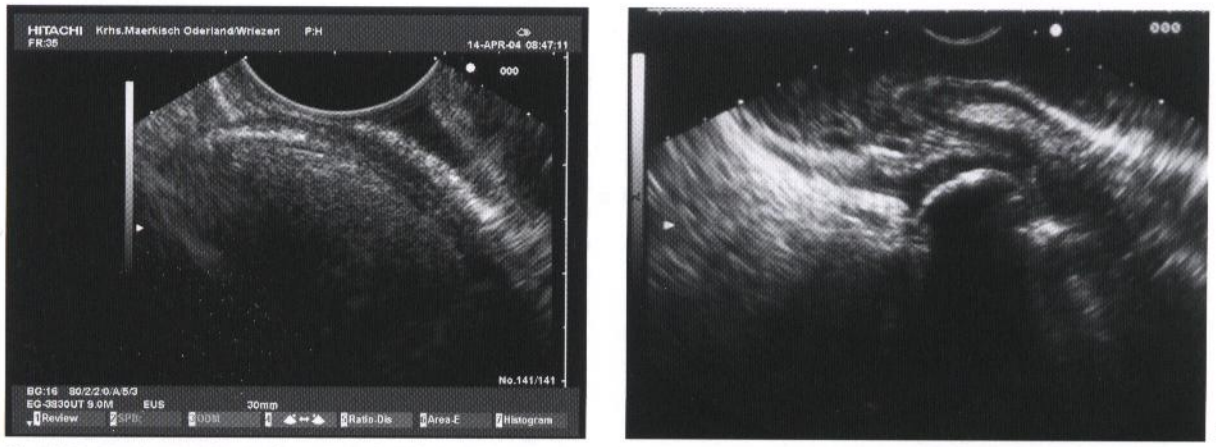
	Chen et al. 2001 [24] n = 238 (1993–2001)	**Our own patients 2002 n = 125 (2000–2002)**
Patients with subepithelial tumors	183 (76.9%)	96 (76.8%)
Patients with wall impressions caused by extramural structures	55 (23.1%)	29 (23.2%)
Transient impression	6 (10.9%)	8 (27.6%)
Neighboring organs	32 (58.2%) (10 × spleen, 6 × splenic vessels, 9 × gallbladder, 3 × liver, 3 × pancreas, 1 × intestine)	9 (31%) (6 × splenic vessels, 3 × spleen, 2 × intestine, 1 × pancreas, 1 × liver, 1 × uterus)
Benign lesions	12 (21.8%) (7 hepatic cysts, 2 hepatic hemangiomas, 1 splenic cyst, 1 pancreatic cyst)	3 (10.3%) (2 pancreatic cysts, 1 concealed gallbladder perforation)
Malignant lesions	5 (9.1%) (3 hepatic tumors, 1 pancreatic tumor, 1 splenic tumor)	3 (10.3%) (1 pancreatic tumor, 1 splenic tumor, 1 hepatic tumor)

ally caused by neighboring structures such as the spleen, splenic blood vessels, gallbladder, pancreas, liver, ovaries, uterus, or occasionally the intestine. More rarely, benign pathological changes in neighboring organs can cause wall impressions mimicking subepithelial tumors. In the upper gastrointestinal tract, such lesions may be cysts in the liver, pancreas, or spleen, mediastinal cysts, inflammatory lesions of the gallbladder or pancreas, benign tumors of the liver and spleen, adrenal gland adenomas, arteriovenous malformations, or arterial aneurysms. Only very rarely are external wall impressions caused by malignant tumors of the neighboring organs (e.g., carcinoma of the gallbladder, colon, pancreas, uterus or ovary, pleural and mediastinal malignancies, lymphoma) [5,14,17,24,25,35] (Table 14.**1**, Figs. 14.**5**–14.**8**).



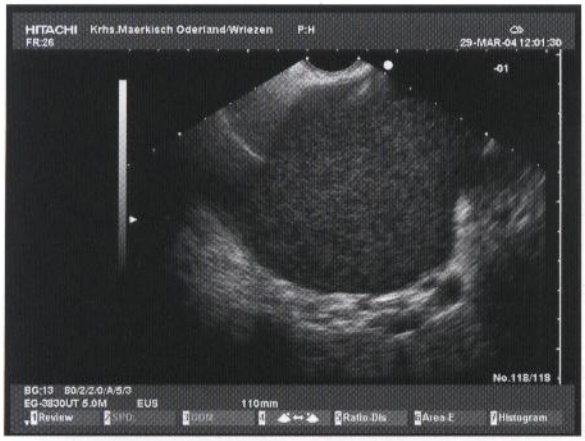
a b c d

Fig. 14.5 Impressions on the gastric wall caused by adjacent vessels. **a, b** Impressions on the gastric fundus made by elongated splenic arteries. **c, d** An impression on the upper esophagus made by the aortic arch (**c**, gray-scale image; **d,** color-coded view).

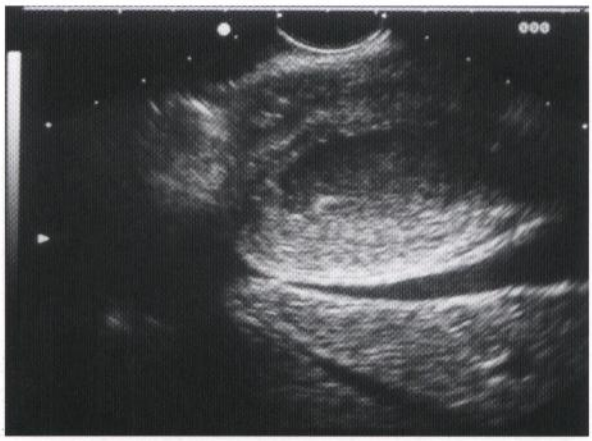


a b

Fig. 14.6a An impression on the stomach wall caused by a sludge-filled gallbladder with wall thickening (chronic cholecystitis). **b** A concealed gallbladder perforation.



a



b

Fig. 14.**7** Impressions on the stomach wall caused by fluid mass lesions. **a** A pseudocyst in the tail of the pancreas. **b** A liver abscess in a patient with chronic pancreatitis.



a



b

Fig. 14.**8** Impressions on the stomach wall (fundus) made by a tumor of the spleen (**a**) and a large carcinoma in the pancreatic tail (**b**).

Pitfalls

- High-frequency ultrasound miniprobes have a limited depth of penetration. They make it possible to exclude subepithelial tumors, but they are often insufficient to allow detailed imaging and diagnosis of extramural structures which cause external wall impressions.
- When using a curvilinear echoendoscope, it is possible to mistake a hypertrophied pyloric sphincter for a subepithelial tumor in the fourth hypoechoic layer, especially if the hypertrophy is asymmetrical (Figs. 14.**9**, 14.**10**).
- Gastrointestinal stromal tumors (GISTs), especially in the stomach, may be connected to the fourth hypoechoic layer (tunica muscularis) only by a thin stalk, with the remainder of the tumor being located extraluminally. Such tumors, especially epithelioid GISTs (leiomyoblastomas), are easily mistaken for a malignant lymph node, because their morphology and echogenicity may be very similar [36,37]. If a

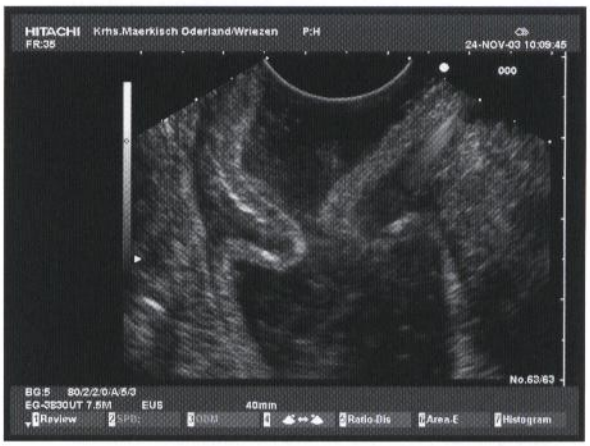
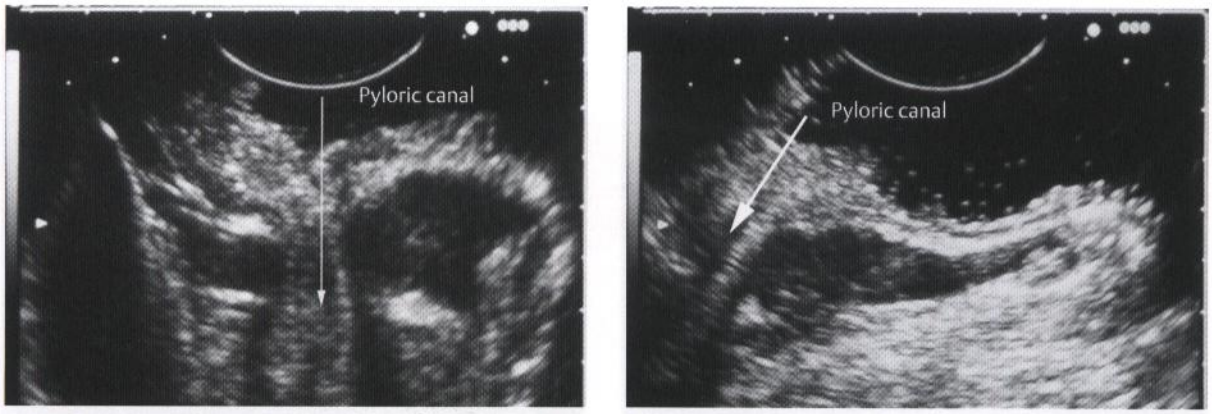


Fig. 14.**9** Symmetrical hypertrophy of the pyloric sphincter.



a b

Fig. 14.**10** Asymmetric hypertrophy of the pyloric sphincter (**a**, transverse view; **b**, longitudinal view).

fine-needle biopsy of such a tumor is performed and the examiner assumes that he or she is obtaining material from a suspicious lymph node, there is a danger that a GIST may be wrongly diagnosed as a metastasis from an epithelial malignancy [36].

Endosonographic Description and Classification of Subepithelial Lesions

All of the echoendoscopes currently available (mechanical and electronic radial echoendoscopes, electronic curvilinear-array echoendoscopes), as well as high-frequency miniprobes, provide detailed views of the wall structure of gastrointestinal organs and make it possible to determine which layer of the wall subepithelial lesions originate from [4,29,38–40]. In addition, it is generally possible to measure the size of a lesion in two imaging planes. Two previous studies have demonstrated that EUS measures the subepithelial tumor size accurately in comparison with surgically resected specimens, with the exception of large lesions that extend beyond the sonographic penetration depth [16,41].

Practical Hints

- Particularly important for follow-up studies: results obtained with radial scanning echoendoscopes (width and thickness) cannot be directly compared with measurements obtained with longitudinal scanning echoendoscopes (thickness and longitudinal diameter).
- High-frequency miniprobes are particularly useful in subepithelial lesions with a diameter of less than 20 mm, especially if an endoscopic therapeutic intervention is planned for the same session [38, 39, 42–45].
- In the investigation of subepithelial tumors, EUS not only provides B-mode views of the lesion. In addition, it is also possible to study the perfusion of a lesion using color-coded duplex sonography [46] (Fig. 14.**11**) and to perform endoscopic ultrasound-guided fine-needle aspiration (EUS-FNA) (Fig. 14.**12**) [7, 9, 37, 44, 47–61] as well as EUS-guided Tru-Cut biopsies (EUS-TCB) [60,62]. In addition, EUS-guided injection can be used to separate submucosal tumors from the muscular layer before endoscopic resection [63]. In selected cases, EUS has been used to assist in the obliteration of subepithelial vascular malformations [64] and for EUS-guided ethanol injection for treatment of a GIST [65].
- If the body of the stomach, the rectum, or the duodenum are being examined, we recommend filling the lumen of these organs in order to obtain adequate acoustic coupling. When the esophagus or gastric antrum are being examined, it may sometimes be helpful to use water-filled balloons. In selected cases, filling the lumen with simeticone (dimethicone) solution may help define the border of a lesion more clearly.
- Good technique is essential to be able to measure the longitudinal extent of a tumor, to determine which mural layer it arises from, and to study its internal structure. Especially if a curvilinear-array echoendoscope is being used, one should remember to advance and retract slowly to ensure optimal flexion of the tip of the endoscope, and to make certain that the endoscope attaches to the central longitudinal axis of the tumor.

The endosonographic classification of subepithelial tumors is based on their outline, echogenicity, echohomogeneity, and internal echo pattern, as well as their demarcation from or infiltration of adjacent layers. Their echogenicity is compared to the muscularis propria (low echogenicity), the submucosal layer (high echogenicity), and to the lumen of the organ being examined, which should be filled with water or with water-filled balloons and therefore be anechoic [33,66]. Some authors differentiate echogenicity in greater detail by also using the

Table 14.**2** Endoscopic ultrasound description of subepithelial lesions

Endoscopic findings

- Localization
- Changes in the mucosa in the area of the protrusion (e.g., erythema, lymphangiectasia, erosions, ulceration, blood clots, active bleeding, color)
  - Sessile vs. pedunculated
  - Additional findings: central nidus, consistency, mobility, pillow sign, tenting

Endosonographic findings

- Diameter measured in two orthogonal planes
- Layer of origin (possible/not possible to determine; 2nd hypoechoic layer–3rd hyperechoic layer–4th hypoechoic layer; extramural)
- Margin (smooth/irregular)
- Can the lesion be distinguished from neighboring structures? (Yes/no; cannot be separated from ...; clearly infiltrates ...)
- Are the covering layers intact? (No mucosal defect; localized mucosal defect, mucosal and submucosal defect = ulceration; ulceration extending into the tumor)
- Solid; cystic; mixed solid and cystic
- Echogenicity (anechoic, hypoechoic, hyperechoic/mixed echogenicity)
- Texture (homogeneous, inhomogeneous—diffusely inhomogeneous vs. inhomogeneous with defined internal structures)
- Defined internal structures: echogenic strains; echogenic spots (without echo extinction); calcification (echogenic reflexes with echo extinction); tubular structures; cystic structures: solitary/some/multiple

Other findings

- If possible: show presence of blood vessels on color-coded duplex sonography (CCDS); estimate perfusion with color power angio (CPA) mode: no/some/multiple perfusion signals
- Suspicious-looking local or regional lymph nodes (morphology, location, number)
- Any hepatic lesions (in the parts of the liver that are visible): morphology, location, number
- Free fluid in the peritoneal cavity; pleural effusion



a



b

Fig. 14.**11** Color-coded duplex sonography of subepithelial tumors. **a** An extramurally located benign gastrointestinal stromal tumor (GIST) of the stomach. **b** A submucosal granulomatous tumor in the rectum.

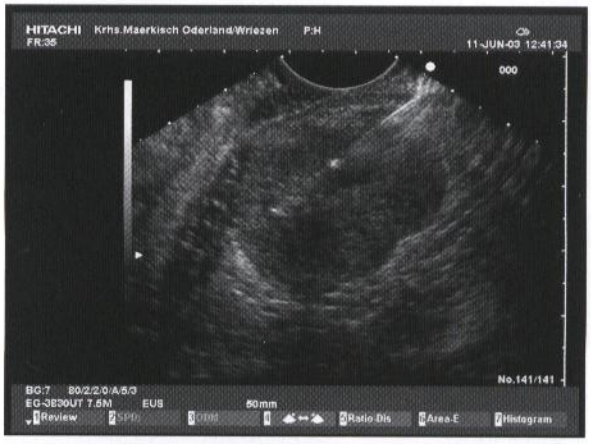


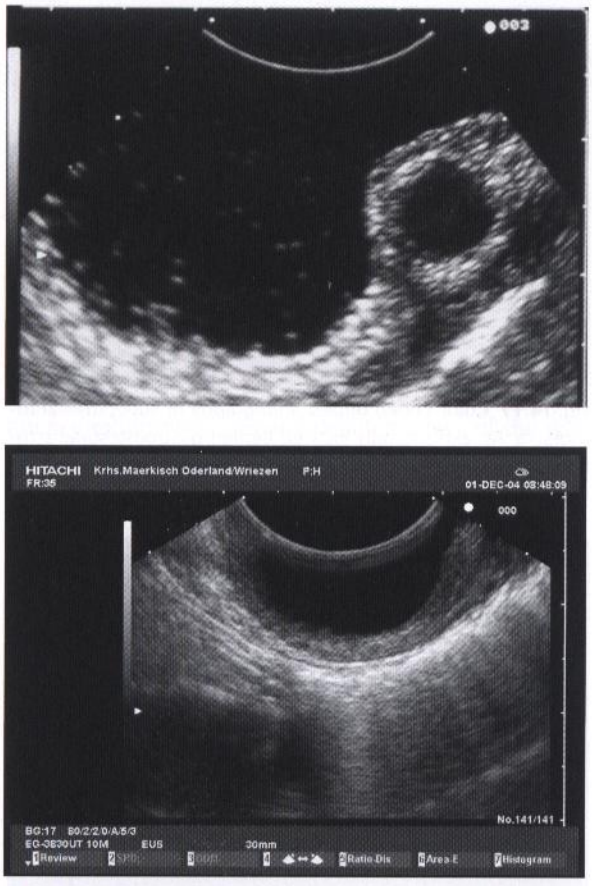
Fig. 14.**12** EUS-guided fine-needle aspiration (EUS-FNA) of a subepithelial tumor in the gastric body.

parenchyma of the spleen for comparison [67]. Further criteria that can be used to classify subepithelial tumors are the extent of compressibility using the tip of the echoendoscope, the presence of ulceration, the presence of sonomorphologically abnormal or enlarged lymph-nodes, and the presence of a connection between the intramural lesion and extramural structures [6,18,22, 33,34] (Table 14.**2**).

Using electronic echoendoscopes with color-coded Doppler and color power angio functions makes it possible to assess the perfusion of subepithelial structures, which may sometimes simplify and accelerate the diagnostic process [46]. As a modification of the classification used by Hizawa et al. [33], we suggest classifying

Table 14.3 Classification of subepithelial lesions

Vascular
Varices
Vascular malformations and hemangiomas
Cystic
• Simple cysts (solitary or multiple)
• Polycystic/septated cyst
• Mixed solid cystic lesions
Solid
• Hyperechoic (homogeneous, heterogeneous, inhomogeneous)
• Hypoechoic (homogeneous, heterogeneous, inhomogeneous)
• Mixed echogenicity (heterogeneous)



a

b

Fig. 14.13 The difficulty of differentiating between small anechoic lesions and subepithelial tumors with low echogenicity. Is it a cyst or a solid, hypoechoic tumor in the gastric wall (**a**) or esophageal wall (**b**)?

subepithelial lesions according to the categories shown in Table 14.**3**.

The criteria discussed in Tables 14.**2** and 14.**3** should enable the examiner to determine the type of lesion and to judge whether or not the lesion may be malignant. In addition, the criteria should be helpful in deciding which further investigations and therapeutic options may be indicated. Numerous examiners have attempted to correlate the histopathological characteristics of subepithelial lesions with specific sonomorphological findings (Table 14.**4**).

Pitfalls

- The degree of "echogenicity" is a very subjective criterion when studying stromal tumors of the gastrointestinal tract. A study comparing the findings of five experienced endosonographers found very poor interobserver reproducibility, with a kappa value of 0.12 [68].
- In small lesions close to the transducer (e.g., in the esophagus), it is very difficult to differentiate between anechoicity and low echogenicity. This can lead to diagnostic errors (e.g., cyst versus leiomyoma) [69] (Fig. 14.**13**).
- The echogenicity of subepithelial tumors depends on their cellular density—the higher this is, the lower the echogenicity—and also on the number and size of internal structures such as cysts or blood vessels. Numerous small cystic changes or small blood vessels evoke numerous interface reflections and can cause a paradoxically high echogenicity [67,70,71].
- Although no comparative studies have been published, the echogenicity of a lesion and its homogeneity appear to depend on the scanning frequency used, as well as on the various physical parameters and settings of the ultrasound system.

The diagnosis of vascular subepithelial lesions can usually also be made if color-coded Doppler sonography (CCDS) is not available [72]. If the diagnosis has not already been made by conventional endoscopy, varices can easily be recognized by following their course, by their compressibility, and by demonstration of extramural collateral vessels. However, the diagnosis can be made more quickly using CCDS, and additional information can be obtained—for example, a portosplenic thrombosis may be recognized (Figs. 14.**14**–14.**16**).

Intramural cavernous hemangiomas are very rare [73,74], but they can be diagnosed much more easily using CCDS (Fig. 14.**17**).

Table 14.**4** Endoscopic ultrasound criteria in subepithelial lesions

Echogenicity	Type of lesion	Wall layers	Tumor characteristics
Anechoic	Cysts (various types)	3 (submucosa) extramural	Dorsal enhancement
	Varices	3 (submucosa) extramural	Vascular structure can be followed, perfusion imaging, perforating veins
	Lymphangioma	3 (submucosa)	Frequently polypoid and polycystic, no perfusion, compressible
	Cavernous hemangioma	3 (submucosa)	Polycystic appearance, perfusion visible
Hypoechoic	Gastrointestinal mesenchymal tumor (GIST, leiomyoma, schwannoma)	4 (muscularis propria) or 2 muscularis (mucosae)	Leiomyomas: usually in the esophagus and in the second hypoechoic layer of the lower gastrointestinal tract; GISTs: usually in the stomach
	Granular-cell tumor (Abrikosov's tumor)	3 (submucosa) and 4 (muscularis propria)	Usually homogeneous with smooth margin, usually < 20 mm, frequently in the esophagus
	Neuroendocrine tumors (carcinoids)	3 (submucosa), possibly no margin to layers 2 and 4	"Pepper-and-salt" appearance of inner texture, round, smooth margins, visible perfusion, usually in the rectum and duodenum
	Inflammatory fibroid polyps	2 muscularis (mucosae) and 3 (submucosa)	Usually with poorly defined margins, homogeneously low echogenicity, usually in the stomach
	Metastases	Do not respect layers	
	Submucosal cancer	Layers poorly defined or lost	Mixed homogeneity, possibly lymphadenopathy
	Lymphoma	Layers 2-4, separation lost	Multinodular, homogeneously low echogenicity, lymphadenopathy possible
	Rarely: amyloid, focal inflammation, endometriosis		
Hyperechoic	Lipoma, fibrolipoma	3 (submucosa)	Homogeneous echogenicity (possibly some slight irregularities)
Mixed echogenicity	Heterotopic pancreas	3 (submucosa)	Internal structure showing ducts or microcysts; central "umbilicus-like" indentation, usually in the gastric antrum
	Malignant mesenchymal tumors (GIST, leiomyosarcoma)	Usually 4 (muscularis propria) as origin, but often does not respect layers	Characteristic findings: containing cysts or hyperechoic structures, irregular margin, size > 40 mm, exophytic growth
	Fibrovascular polyp	3 (submucosa)	Polypoid
	Spontaneous esophageal hematoma	3 (submucosa)	Overall low echogenicity with discrete hyperechoic foci
	Wall abscess	3 (submucosa)	Possibly gaseous inclusions

GIST: gastrointestinal stromal tumor.



a b

Fig. 14.**14a, b** Vascular subepithelial lesions: giant varices in the cardia.

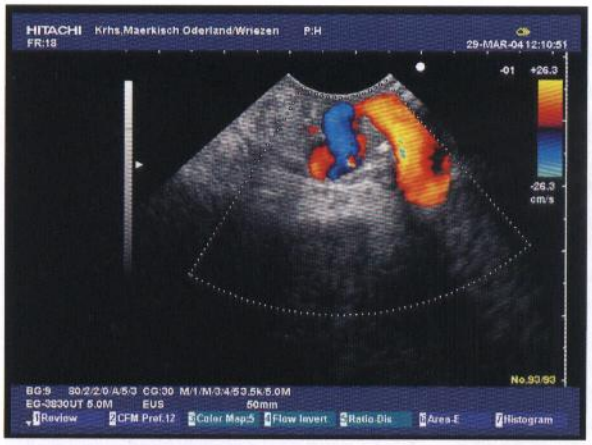
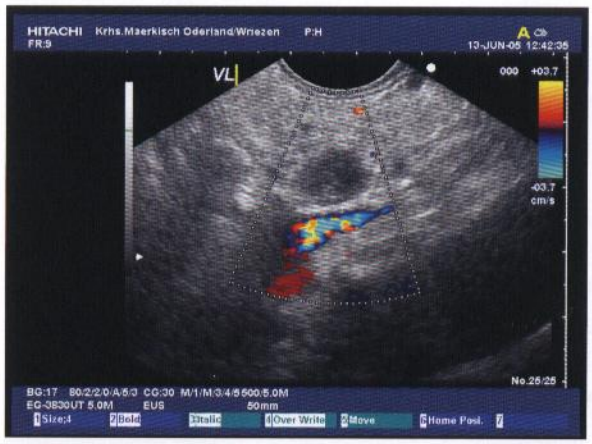


Fig. 14.**15** Vascular subepithelial lesions: varices in the gastric fundus.

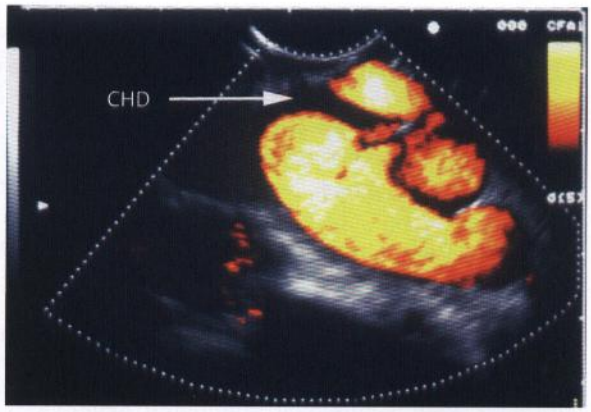
Cystic and Solid Cystic Subepithelial Lesions

Anechoic nonvascular subepithelial lesions account for a large variety of underlying diagnoses. They may represent different types of cysts [48], mucosal heterotopias located in the submucosal layer, Brunner's gland hamartomas, cystic lymphangiomas (lymphatic cysts), or more rarely pancreatic heterotopias, mesenchymal tumors with cystic degeneration, gastritis cystica profunda or colitis cystica profunda, tuberculomas, mural abscesses or empyema [75–78], or mucoceles [79].

This multitude of differential diagnoses makes it difficult to reach a confident diagnosis. To simplify the diagnostic process, the examiner should differentiate between simple cystic lesions, polycystic/septated lesions, and solid cystic subepithelial lesions [33,80] (Table 14.**5**).



a



b

Fig. 14.**16** Recent splenic vein thrombosis (**a**) and portal vein cavernoma (**b**). CHD: common hepatic duct.



a



b

Fig. 14.**17a, b** Cavernous hemangioma of the rectum.

Simple submucosal cysts have been found endosonographically in the esophagus, in the stomach, in the duodenum, and near the cecal pole [79]. Simple submucosal cysts are round anechoic lesions with a smooth margin that can only be slightly compressed with the tip of the echoendoscope and which show dorsal enhancement. Occasionally, sedimented debris can be seen in the lumen of the cyst. Duplication cysts can usually be recognized through a duplicated wall, although this is not always visible. In appropriate cases, EUS-FNA can be helpful for the further diagnostic and therapeutic management [5,29,48,82–87].

Cystic and cavernous lymphangiomas are the most frequently encountered polycystic subepithelial lesions. They are usually found in the small and large intestine, more rarely in the stomach, and very rarely in the esophagus. They are benign lesions that consist of cavities or dilated lymphatic vessels situated in the submucosal or mucosal layers. Their inner wall is covered by an epithelial layer, and they are subdivided by irregular septal structures that consist of smooth muscle or connective tissue. Depending on their size and location, they may occasionally cause symptoms. Endoscopically, they usually appear as soft, broad-based polypoid structures, which are covered with normal or erythematous mucosa. They are easily compressible with forceps. In the duodenum and small intestine, it is often possible to find mucosal lymphangiectasia, evident from multiple dot-shaped whitish mucosal elevations. Somewhat more rarely, cystic lymphangiomas may have a pedicle [88]. Endosonographically, lymphangiomas are usually found in the third hyperechoic layer, although sessile lesions in particular may extend to the second hypoechoic layer. The endosonographic picture may vary depending on the size and number of the dilated lymphatic vessels and depending on the extent to which bundles of smooth muscle and connective tissue subdivide the lesion. If the lymphangioma consists of moderately dilated tortuous lymphatic vessels, or if it contains small cysts, EUS will usually show multiple hypoechoic or anechoic structures, possibly with hyperechoic subdivisions. Such lymphangiomas may also appear as simple or septated round or oval anechoic lesions in the third hyperechoic layer (Fig.14.**18**). However, if the lymphatic vessels are very small (diameter < 1 mm), the lymphangioma will appear as a slightly inhomogeneous submucosal tumor with medium echogenicity [70,80,88–92].

Heterotopia of the gastric mucosa. A very similar appearance with the same endosonographic localization in layers 2 and 3 can be found for the different types of subepithelial *heterotopia of the gastric mucosa*, as well as *hyperplasia of Brunner's glands* and *gastric and duodenal hamartomas* [33,93–96]. The range of endosonographic findings extends from simple submucosal cysts, which may also be multiple, through polycystic lesions with hyperechoic septa, to inhomogeneous hyperechoic submucosal tumors with small cystic areas. A special scenario is gastritis cystica profunda, which appears as a polycystic lesion and can often be found near the anastomosis after gastric surgery [97–99] (Figs. 14.**19**, 14.**20**).

Endoscopically, these lesions appear as broad-based or stalked polyps. Subepithelial heterotopia of the gastric mucosa is frequently (19–100%) associated with gastric cancer, particularly if multiple lesions are present. Occasionally, the carcinoma may arise from the subepithelial heterotopia [96–98,80,100–102].

Heterotopic pancreatic tissue. A further differential diagnosis of cystic subepithelial lesions is heterotopic pancreatic tissue, which is usually located in the stomach, or more rarely in the duodenum or close to the papilla. Occasionally, pancreatic heterotopia may appear as a simple or septated anechoic lesion with smooth

Table 14.**5** Endoscopic ultrasound of cystic subepithelial lesions

Simple cystic	• Duplication cysts
	• Bronchogenic cysts
	• Heterotopic gastric mucosa
	Rare:
	• Brunner's gland hamartoma
	• Mucocele
	• Intramural pancreatic pseudocyst
	• Abscess of the stomach wall (low echogenicity)
	• Pancreatic heterotopia
Multicystic	• Lymphangioma
	• Heterotopic gastric mucosa and gastritis cystica profunda
	• Brunner's gland hamartoma
Solid cystic	• Pancreatic heterotopia
	• Lymphangioma
	Rare:
	• Tuberculoma
	• GIST with cystic degeneration

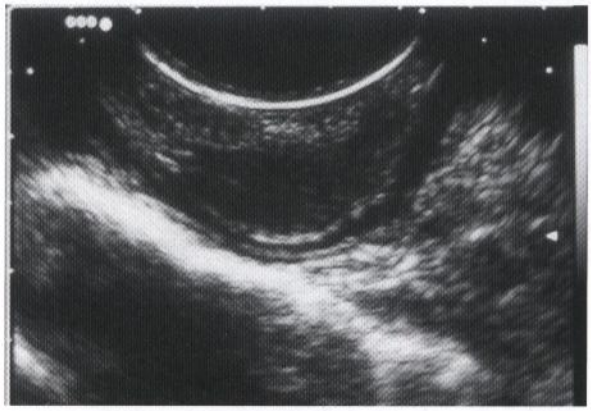
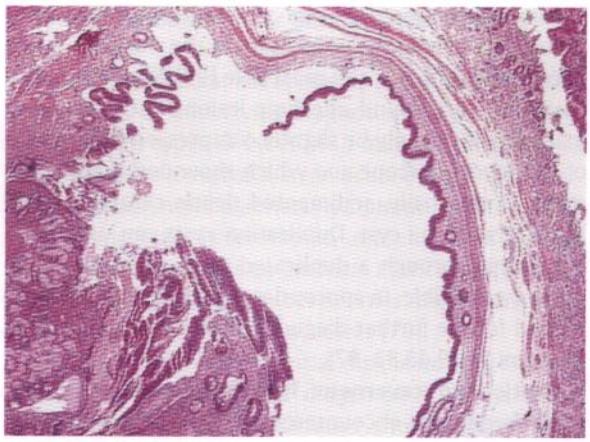


Fig. 14.**18** Submucosal lymphangioma in the esophagus.



a



b

Fig. 14.**19** Submucosal cystic heterotopia in the gastric mucosa, situated in the gastric antrum. **a** Radial 15-MHz ultrasound miniprobe. **b** Histological confirmation after endoscopic resection (histological image courtesy of S. Wagner and S. Bartho, Königswusterhausen, Germany).

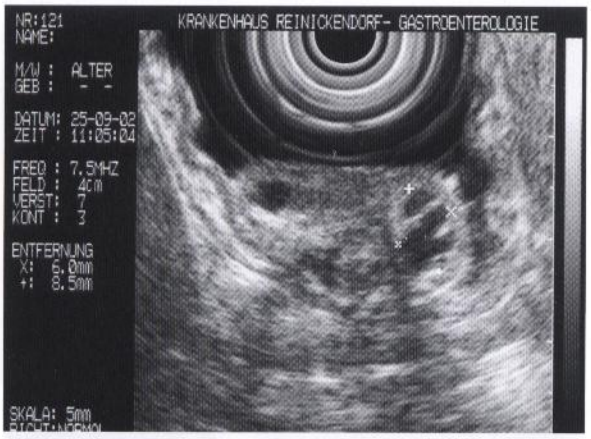


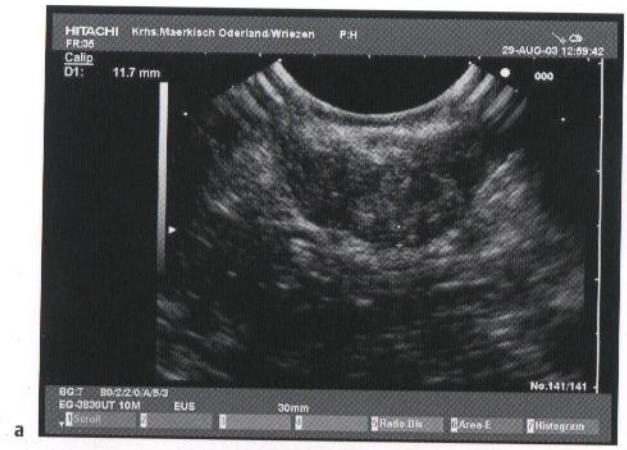
Fig. 14.**20** Gastritis cystica profunda close to the anastomosis after a Billroth II gastrectomy (with a mechanical radial echoendoscope; courtesy of M. Mayr, Berlin).

margins, which is located in the third echogenic layer [86]. However, it usually appears as a heterogeneous hypoechoic subepithelial lesion with poorly defined margins, which may contain cystic spaces, duct-like structures, finely scattered hyperechoic spots, and occasionally calcifications [33,80,103–107]. The irregular margins are caused by lobulated acinar tissue, and the mixed echogenicity is due to ducts, cysts, lobulated tissue, areas of fat, and bundles of muscle fibers [106]. A characteristic feature of submucosal pancreatic heterotopia is a thickening of the fourth layer adjacent to the mass. In a series of 10 pancreatic heterotopias located in the stomach that were studied both endosonographically and histologically, five were only located in the third echogenic layer (submucosa) and could be easily differentiated from the fourth layer (separate type). In the remaining five cases, the lesion extended into the third echogenic and fourth hypoechoic layer (fusion type) [106]. Although the endosonographic findings are so variable, they correlate well with the histological findings [106], and when the endoscopic findings (usually situated in the antrum, central umbilication) are also taken into account, pancreatic heterotopia may be diagnosed endosonographically with a reasonable degree of certainty (Fig. 14.**21**). In a study of six patients, an endosonographically suspected diagnosis of pancreatic heterotopia was confirmed histologically in all cases after endoscopic resection [69].

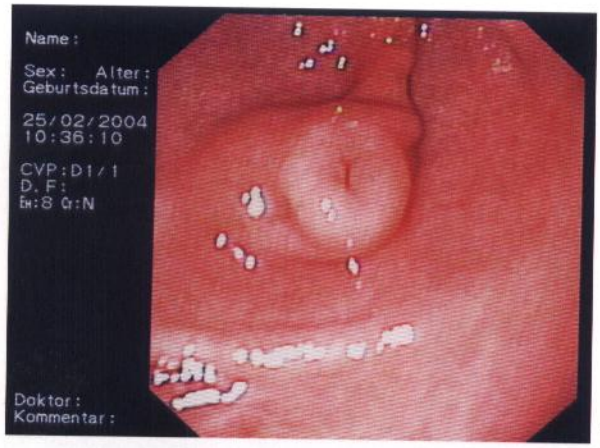
■ Solid Subepithelial Lesions

Lipomas are the most common echogenic subepithelial lesions. They usually appear as flat or sessile polypoid lesions, although they may have a stalk. They are classically located in the right colon, but can also appear in the stomach and duodenum. Frequently, an endosonographic examination is not required if the endoscopic findings are unequivocal (slightly yellow shimmering through the mucosa, pillow sign) [6,18]. Endosonographically, lipomas appear as intensely hyperechoic, entirely homogeneous well-demarcated lesions located in the third echogenic layer (submucosa). Some inhomogeneities can sometimes be seen, particularly if the tumor is large [6, 14, 16, 18, 28, 29 ,33, 40, 90, 108] (Fig. 14.**22**).

Interobserver agreement for diagnosing a lipoma is good [30]. The differential diagnosis includes fibromas and, in the esophagus, fibrovascular polyps (fibrolipomas). The latter consist of a mixture of mesenchymal tissues and also contain fatty tissue. Only the lipomatous areas appear homogeneously echogenic, whereas the fibrous and muscular parts of these polyps show less echogenicity [109].



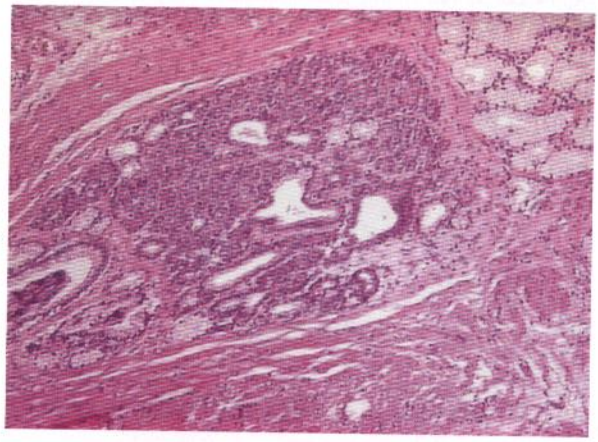
a



b

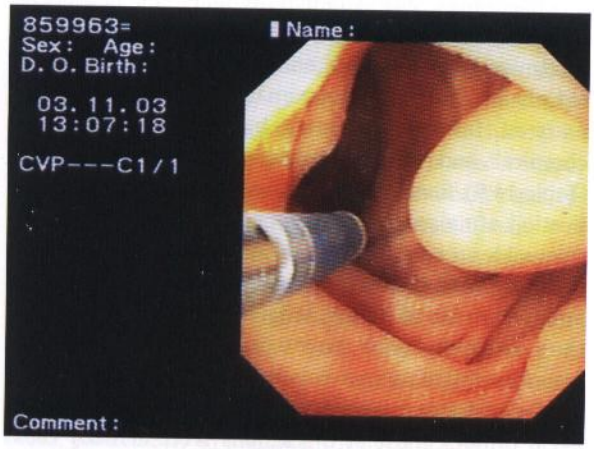


c

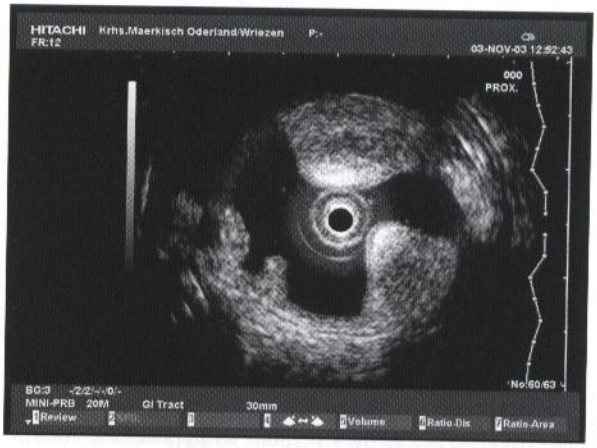


d

Fig. 14.**21** Heterotopic pancreatic tissue in the stomach. **a** The typical EUS features of the fusion type—i. e., with the muscular layer also affected, as confirmed histologically after surgical resection. **b–d** The separate type—i. e., with only the submucosa affected. **b** The endoscopic image, with central umbilication. **c** The EUS appearance. **d** Histological confirmation after endoscopic resection (histological image courtesy of S. Bartho and S. Wagner, Königswusterhausen, Germany).



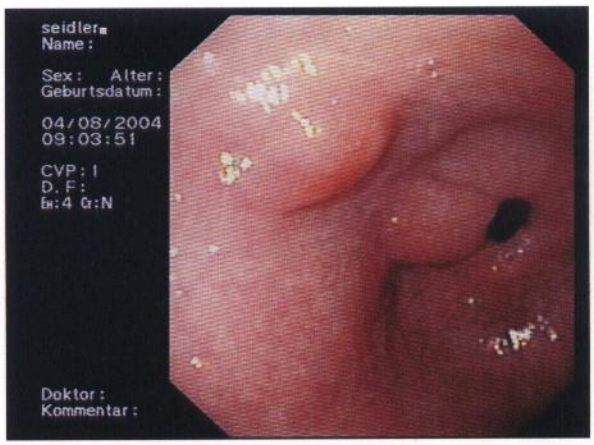
a



b

Fig. 14.**22** Submucosal lipomas in the upper gastrointestinal tract, viewed endoscopically. **a** The duodenal lumen filled with water, with the radial 15-MHz ultrasound miniprobe being introduced through the endoscope. **b** The corresponding EUS view obtained with the 15-MHz ultrasound miniprobe.

Fig. 14.**22c, d** ▷

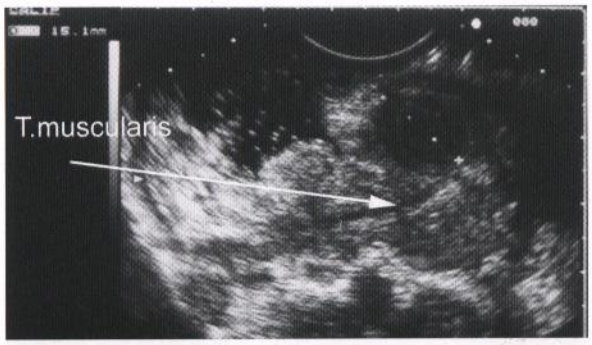


c



d

Fig. 14.**22c, d** Flat submucosal lipomas in the antrum, visualized endoscopically and with the 15-MHz ultrasound miniprobe).



a



b

Fig. 14.**23a, b** Submucosal abscesses following acute episodes of chronic pancreatitis.

In exceptional cases, inflammatory fibroid polyps (IFPs) may appear hyperechoic if numerous small blood vessels cause multiple interface reflections [67,110].

Hypoechoic subepithelial tumors are a very heterogeneous group. They pose a number of problems for the examiner. In our own patients, examined over a period of 50 months, 62 of 88 (70.5%) nonvascular subepithelial lesions showed low echogenicity. The range of diagnoses includes benign tumors such as leiomyomas, granular-cell tumors, neurinomas, pancreatic heterotopias, and inflammatory fibroid polyps (IFPs), but also includes benign and malignant gastrointestinal stromal tumors (GISTs), neuroendocrine tumors, leiomyosarcomas, and submucosal metastases. Very rarely, amyloidosis [111], endometriosis [59,90,112], cavernous hemangiomas [73,74], and inflammatory tumors and abscesses [76–78] (Fig. 14.**23**) may present as hypoechoic subepithelial lesions.

Gastrointestinal stromal tumors (GISTs). In the early large endosonographic series [12, 14, 16, 28, 29, 31, 40], hypoechoic mesenchymal tumors arising from one of the two muscular layers and histologically showing either a spindle-cell or an epithelioid structure were either classified as myogenic tumors (leiomyomas, leiomyoblastomas, and leiomyosarcomas) or neurogenic tumors (schwannoma, neurofibroma). GISTs were only recognized as a separate entity fairly recently and can mainly be found in the stomach. They can be differentiated from leiomyomas by their immunohistochemical and genetic characteristics [10,11,113–116] (Table 14.**6**). Because of the recent change in the classification of mesenchymal tumors of the gastrointestinal tract, older reports need to be viewed in the light of this information. A recent pathological study that examined archived tissue of subepithelial mesenchymal tumors of the gastrointestinal tract previously classified as smooth-muscle tumors (leiomyomas and leiomyosarcomas) demonstrated that, with the exception of esophageal tumors, most of the lesions were actually GISTs [81].

The clinical presentation of GIST varies widely and includes incidentally found small benign tumors, tumors of uncertain prognosis, and highly malignant tumors with predominantly hepatic and peritoneal metastases.

Conversely, lymph-node metastases are exceedingly rare [6,116–118].

GISTs are now defined as mesenchymal spindle-cell, epithelioid, or rarely pleomorphic tumors of the gastrointestinal tract which—in contrast to myogenic or neurogenic tumors—express Kit protein (stem cell factor receptor protein, CD117) [10, 11, 113–117, 119–121] (Table 14.**6**). Histogenetically, these tumors probably originate from a CD34-positive subset of gastrointestinal pacemaker cells (interstitial cells of Cajal) or a pluripotent precursor cell. Mutations of the c-*kit* gene, which produces the Kit protein, lead to ligand-independent activation of Kit tyrosine kinase, which can frequently be found in malignant GISTs, as can certain chromosomal abnormalities [116,119]. The relative risk of malignancy of a GIST primarily depends on the number of mitoses per 50 high-power fields (HPF) and on its size. Only tumors smaller than 5 cm and with a low mitotic count (< 5/50 HPF) are regarded as benign [10, 113, 115–117, 121, 122] (Table 14.**7**).

Leiomyomas —i.e., benign gastrointestinal mesenchymal tumors with muscular differentiation—can be found in the second hypoechoic layer (the lamina muscularis mucosae) as well as in the fourth hypoechoic layer (the tunica muscularis). Endosonographically, they appear as homogeneously hypoechoic, sometimes almost anechoic tumors with smooth margins. Occasionally, leiomyomas may contain calcifications. Depending on their size and age, both leiomyomas and benign GISTs may develop regressive changes that appear as anechoic or hyperechoic regions, and they may develop an irregular shape, which may make it difficult or impossible to differentiate them from malignant mesenchymal tumors (Fig. 14.**24**).

Gastrointestinal stromal tumors (GISTs) and the more rarely occurring neurogenic mesenchymal gastrointestinal tumors do not differ endosonographically from myogenic mesenchymal gastrointestinal tumors. It is therefore not possible to differentiate between these three tumor types purely by relying on endosonographic criteria [6–8,18,26]. Only one small study including 24 gastrointestinal mesenchymal tumors reported endosonographic differences between GISTs and other gastrointestinal mesenchymal tumors. A marginal halo was found in 12 of 19 GISTs and in both of the schwannomas, but not in any of the three leiomyomas. The echogenicity of GISTs was low, but higher than that of the normal muscularis propria layer, whereas the echogenicity of leiomyomas and schwannomas was usually low. Lobulation of the tumor surface was documented only in GISTs, particularly in malignant lesions [123].

Table 14.**6** Phenotypic characterization of gastrointestinal mesenchymal tumors

Myogenic tumors (leiomyomas, leiomyoblastomas and leiomyosarcomas)
• Histologic subtypes: 30% epithelioid, 70% spindle-cellular. The malignant type (leiomyosarcoma) is very rare.
• Can mainly be found in the esophagus and the lamina muscularis mucosae of the lower gastrointestinal tract.
Actin +, desmin +, NSE –, PGP –, S100 –, CD117 (KIT) –, CD34 (+), vimentin –
Neurogenic tumors (schwannoma, neurofibroma, ganglioneuroma)
• Usually occur in the stomach, very rarely in the esophagus and intestine.
• Nearly always benign.
Actin –, desmin –, NSE +, PGP +, S100 +, CD117 (KIT) –, CD34 (+), vimentin +
Undifferentiated or poorly differentiated = gastrointestinal stromal tumor (GIST)
Synonyms: interstitial Cajal-cell tumor (ICC tumor); gastrointestinal pacemaker cell tumor (GIPACT)
Subgroup: gastrointestinal autonomic nerve tumor (GANT)
May show incomplete neurogenic, myogenic or mixed neurogenic–myogenic differentiation.
Occurrence: 60–70% in the stomach, 20–25% in the small intestine, 5% colorectal, < 5% in the esophagus
Actin (+), desmin (+), NSE –, PGP –, S100 (+), CD117 (KIT) +, CD34 +, vimentin +

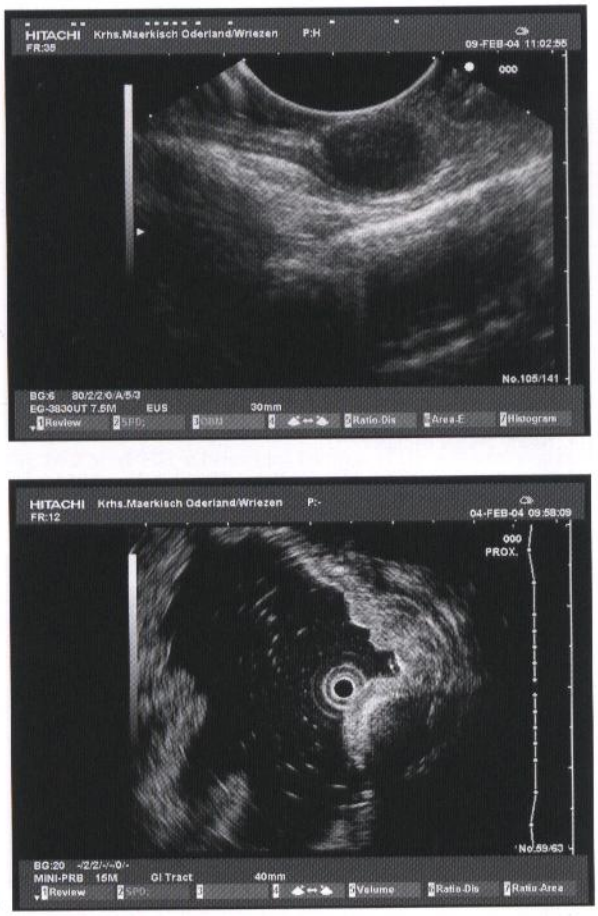
NSE: neuron-specific enolase, PGP: protein gene product.

Table 14.**7** Prognostic criteria in gastrointestinal stromal tumors [10,122]

Risk of malignant behavior	Tumor size (cm)	Number of mitoses per high-power field
Very low risk	< 2	< 5/50
Low risk	2–5	< 5/50
Intermediate risk	< 5	6–10/50
	5–10	< 5/50
High risk	> 5	> 5/50
	> 10	Any mitotic rate
	Any size	> 10/50

Pitfalls

- The endosonographic diagnosis of subepithelial tumors is influenced by subjective judgment and the examiner's experience. Observer agreement among 10 experienced sonographers was excellent for recognizing cystic lesions (kappa 0.80) and external impression (kappa 0.94), and it was good for recognizing lipomas (kappa 0.65). However, agreement was significantly reduced for diagnosing leiomyomas (kappa 0.53) and vascular structures (kappa 0.54). Observer agreement was poor for diagnosing other subepithelial tumors (metastases, carcinoid, pancreatic heterotopia; kappa 0.34) [30].



a

b

Fig. 14.**24** Submucosal leiomyomas of the esophagus **a** Originating from the lamina muscularis mucosae, with smooth margins and homogeneously hypoechoic. **b** Gastric leiomyoma, with extensive calcification and dorsal extinction. The layer of origin is therefore uncertain (15-MHz ultrasound miniprobe).

- Flow velocities in cavernous hemangiomas may be so low that the correct diagnosis may be missed [74].
- An atypical ultrastructure may lead to misclassification. Occasionally, lipomas may show a slightly inhomogeneous texture and GISTs may show medium echogenicity or cystic regions [33,80]. Pancreatic heterotopia may appear as a septated cyst [86] or may contain calcifications [107] and inflammatory fibroid polyps, and gastrointestinal lymphangiomas may appear hyperechoic [67,70,71,110].

Practical Hints

- There is such a wide variety of hypoechoic subepithelial tumors that the examiner should refrain from trying to make a definite diagnosis of the tumor type. Instead, he or she should give a detailed description of the findings and offer a list of differential diagnoses.
- To date, the value of contrast-enhanced CCDS in diagnosing subepithelial lesions has not been sufficiently studied [46]. However, in our experience it does help differentiate between very hypoechoic solid lesions and anechoic cystic lesions. It also increases diagnostic certainty for cavernous hemangiomas.
- It is possible to increase the diagnostic yield by taking into account pathological and anatomical data such as the predilection sites for specific tumors, and endosonographic findings such as the layer of origin or the tumor outline [124] (Table 14.**8**).

Hypoechoic Subepithelial Tumors of the Esophagus

Leiomyomas. In the esophagus, benign leiomyomas are both the most common subepithelial tumor and the most common mesenchymal tumor. Leiomyomas are typically located in the middle or lower third of the esophagus. Esophageal leiomyomas can originate from the second hypoechoic layer (muscularis mucosae) [125] as well as from the fourth hypoechoic layer (muscularis propria) [69,126]. If a hypoechoic tumor is found in this location, the endosonographic diagnosis of a leiomyoma is reasonably reliable, particularly because GISTs are only rarely seen in the esophagus [7,8,126,127]. However, very small leiomyomas may be mistaken for intramural cysts, as they may appear almost anechoic (Figs. 14.**13**, 14.**24a**). A Japanese study compared the endosonographic diagnosis of 26 endoscopically resected esophageal tumors (among which there were 19 leiomyomas) with the histological diagnosis. Two leiomyomas (diameter 8 mm and 20 mm) had been classified as cysts endosonographically, whereas a cyst of 9 mm diameter had been classified as a leiomyoma. For three leiomyomas, the endosonographic classification was uncertain, and one was thought to be a granular-cell tumor [69]. Esophageal leiomyomas only rarely exceed a size of 30 mm, they only very rarely have a stalk, and sometimes a diffuse growth of multiple leiomyomas (esophageal leiomyomatosis) is observed [126,128,129].

Granular-cell tumors are the second most common hypoechoic subepithelial tumor in the esophagus (also known as myoblastic myoma or Abrikosov's tumor). The histogenetic origins of this rare tumor are possibly Schwann cells. Only 5–9% of granular-cell tumors arise in the gastrointestinal tract, and they are then usually located in the esophagus. Immunohistochemically, the tumor is positive for S100 protein and normally also for neuron-specific enolase. These tumors are usually benign, and like leiomyomas and leiomyoblastomas they are usually found in the lower and middle third of the esophagus. Multiple tumors may occur. Endoscopically, granular-cell tumors have a yellowish hue, but in contrast to lipomas their consistency is rather firm. En-

Table 14.**8** Diagnosing the type of hypoechoic subepithelial lesions relative to their location

Esophagus	Leiomyoma	Predominantly lower third, layers 2 and 4, homogeneous, smooth margins
	Abrikosov's tumor	Usually layers 3 and 4, homogeneous with smooth margins, nearly always < 20 mm
	Very rarely: GIST, leiomyosarcoma, IFP	
Stomach	GIST	Usually layers 2 and 4, more rarely "extramural," variable size and inhomogeneity
	Rare: leiomyoma, schwannoma, neuroendocrine tumor (carcinoid), IFP, metastases, submucosal cancer, lymphoma, pancreatic heterotopia	
	Very rare: leiomyosarcoma, focal inflammation	
Duodenum	Neuroendocrine tumor (carcinoid)	Small, slightly inhomogeneous, usually layers 2 and 3
	Rare: GIST, Abrikosov's tumor	
	Very rare: IFP, metastases, lymphoma, amyloid	
Colon	Leiomyoma	Small, homogeneous with smooth margins, usually layer 2
	Rare: GIST, leiomyosarcoma, IFP, Abrikosov's tumor, endometriosis	
	Very rare: metastases, lymphoma	
Rectum	Neuroendocrine tumor (carcinoid)	Small, slightly inhomogeneous, usually layers 2 and 3
	Leiomyoma	Small, homogeneous with smooth margins, usually layer 2
	Rare: GIST, leiomyosarcoma, local subepithelial cancer recurrences, Abrikosov's tumor, endometriosis	

GIST: gastrointestinal stromal tumor; IFP: inflammatory fibroid polyp.

dosonographically, they appear as homogeneously hypoechoic lesions with a smooth margin, which rarely exceed a size of 20 mm. They can usually be found in the second hypoechoic layer (lamina muscularis mucosae) or the third echogenic layer (tunica submucosa) [130] (Figs. 14.**1b**,14.**25**, 14.**38e–g**).

However, high-frequency miniprobes may visualize a more heterogeneous echo texture and unclear margins, reflecting the mixture of laterally scattering tumor cells, fibrosis, and muscularis mucosae in granular-cell tumors, and may therefore be useful for differentiating esophageal granular-cell tumors from leiomyomas [131]. Malignant granular-cell tumors are rare. They show infiltrative growth, are frequently larger than 40 mm, and tend to cause lymphatic metastases. These characteristics are easily recognized by endosonography [130].

Inflammatory fibroid polyps (IFPs). Very rarely, the differential diagnosis for hypoechoic subepithelial tumors of the esophagus may include IFPs, which—as in the stomach—are located in the second and third layers and have poorly defined margins [132,133]. Other rare differential diagnoses include GISTs and leiomyosarcomas [134]. Only 5% of GISTs occur in the esophagus, which is thus the least common location in which these are found. There have been no published reports of endosonographically diagnosed esophageal GISTs. Leiomyosarcomas of the esophagus occur even more rarely than GISTs [127] (Fig. 14.**26**).

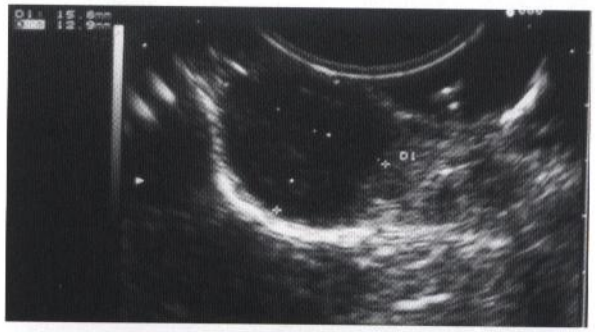


Fig. 14.**25** A granular-cell tumor in the esophagus. The tumor is displacing the surrounding tissues, but there is no infiltrative growth.

Hypoechoic Subepithelial Tumors of the Stomach

Gastrointestinal stromal tumors (GISTs). In contrast to the esophagus, GISTs are the most common hypoechoic subepithelial tumors in the stomach. Approximately two-thirds of GISTs are found in the stomach. Gastric leiomyomas are very rare and are almost invariably found in the cardia [115,116,135]. It can therefore be assumed that papers published in the 1980s and 1990s that described the endosonographic characteristics of "leiomyomas," "leiomyoblastomas," and "leiomyosarcomas" of the stomach were probably referring to GISTs in the majority of cases [12, 14, 16, 28, 29, 31, 40, 68, 136, 137]. The size of the lesions varies from a few milli-

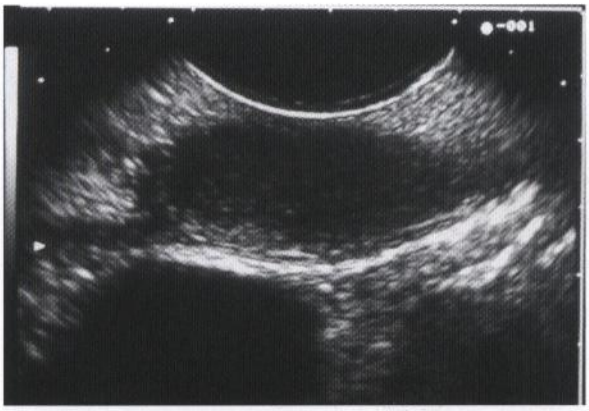


Fig. 14.**26** A leiomyosarcoma in the esophagus. The esophageal lumen has been filled with simeticone (dimethicone) solution to improve visualization of the tumor.



Fig. 14.**27** A large extramural gastrointestinal stromal tumor (GIST) in the stomach, showing necrotic areas and obvious hyperperfusion.

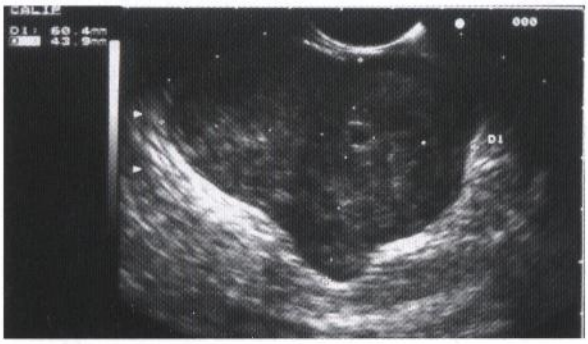


Fig. 14.**28** Gastric schwannoma. The diagnosis was confirmed histologically by fine-needle biopsy. The tumor was found in an 80-year-old woman and did not change over a period of several years.

meters to a few centimeters. While smaller tumors are often incidental findings, larger tumors may be symptomatic—e.g., they may cause gastrointestinal hemorrhage (Fig. 14.**3**).

GISTs can occur in all mural layers, although they are usually found in the second or fourth hypoechoic layers. Occasionally GISTs that are mainly located extramurally have been observed. They are connected to the fourth hypoechoic layer only by a thin hypoechoic strand, which may easily be missed [36] (Figs. 14.**10a**, 14.**27**).

Schwannomas of the stomach are extremely rare. They cannot be differentiated from GISTs endosonographically (Fig. 14.**28**).

Inflammatory fibroid polyps (IFPs). are another rare differential diagnosis in hypoechoic subepithelial tumors of the stomach. They are situated in the submucosal layer and consist of acapsular loose perivascular connective tissue, which contains an eosinophilic inflammatory infiltrate [67,71,110]. To differentiate them from GISTs, it is important to bear in mind that IFPs are also positive for CD34, but do not express CD117 [81, 115, 116, 135].

Neuroendocrine tumors (carcinoids) of the stomach. The characteristics of these lesions are poorly defined margins, localization in the submucosal layer, and an inhomogeneous hypoechoic ("pepper-and-salt") appearance [33,108] (Fig. 14.**4a**).

Gastric metastases from malignant tumors, which in some 50% of cases may appear as subepithelial tumors endoscopically, and malignant lymphomas or gastric adenocarcinoma with purely submucosal polypoid growth, are also very rare [9;138–141] (Fig. 14.**29**).

Hypoechoic Subepithelial Tumors of the Duodenum

No large reviews have been published on the prevalence and endosonographic characteristics of subepithelial tumors of the duodenum. One series described 114 subepithelial tumors of the gastrointestinal tract, all of which were examined with EUS, with the diagnosis subsequently being confirmed histologically. In this study, 27 tumors were seen in the duodenum, 15 of which originated from the Brunner glands and had a partially cystic appearance [139]. In four endosonographic studies of hypoechoic subepithelial tumors of the duodenum, a histological diagnosis was obtained for a total of 50 tumors. The authors found nine neuroendocrine tumors (carcinoid), one granular-cell tumor, one leiomyoblastoma, one leiomyoma, one schwannoma, one inflammatory vascular polyp, and two lymphomas [45,69,136,142]. A case study described inflammatory fibroid polyps in the duodenum. Their endosonographic appearance was consistent with the known criteria for gastric IFPs [143]. The great majority of the rare mesenchymal tumors of the duodenum are gastrointestinal



a



b

Fig. 14.**29** Malignant subepithelial tumors. **a** A subepithelial hypoechoic T-cell lymphoma in the stomach. **b** A subepithelial metastasis from an ovarian carcinoma, mimicking a gastrointestinal stromal tumor.



Fig. 14.**30** A hypoechoic subepithelial duodenal tumor just below the papilla of Vater, coexisting with chronic calcifying pancreatitis. Histological examination after surgical resection showed that the lesion was a benign gastrointestinal stromal tumor (GIST), along with chronic pancreatitis.



Fig. 14.**31** Endometriosis of the rectum, located in the submucosal layer, cannot be differentiated from the tunica muscularis.

stromal tumors (GISTs) (Fig. 14.**30**); leiomyomas and leiomyosarcomas are very rare [144].

Hypoechoic Subepithelial Tumors of the Colon and Rectum

Lipomas and lymphangiomas are the most common subepithelial tumors of the colon and rectum. However, in a study of 45 patients in whom a subepithelial tumor was suspected on endoscopy or radiography, there were 22 hypoechoic tumors that were diagnosed as six different tumor types—six leiomyomas and three leiomyosarcomas (possibly GISTs), seven cases of endometriosis, two malignant lymphomas, three postoperative cancer recurrences, and one mucocele of the appendix [90].

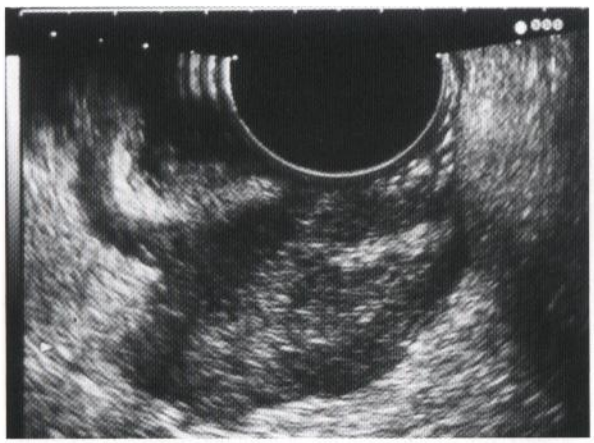
Gastrointestinal stromal tumors or leiomyomas/leiomyosarcomas were endosonographically located in the fourth hypoechoic layer. It was sometimes difficult or impossible to differentiate them from endometriosis of the colon, which may on occasion have a spindle-shaped appearance [90].

Endometriosis. In the rectum, endometriosis may appear as an extramural lesion, or—if it arises from a pelvic endometric nodulus—it may appear as a hypoechoic lesion that infiltrates the fourth hypoechoic layer or rarely the third echogenic layer [112] (Fig. 14.**31**).

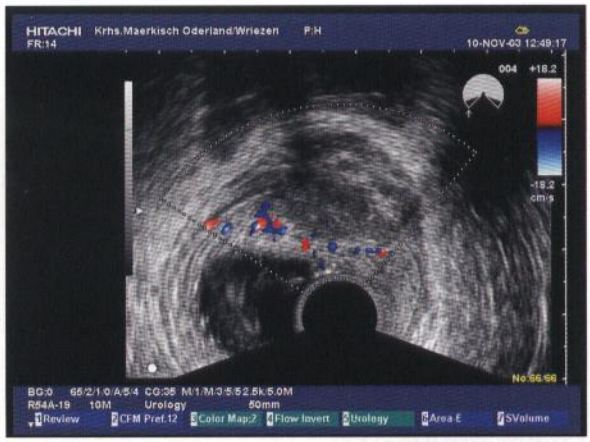
Rectal cancer recurrences (Fig. 14.**32a**), submucosally growing rectal cancers (Fig. 14.**32b**, **c**), and lymphomas show irregular margins.

Leiomyosarcomas (or malignant GISTs) were larger than 40 mm, had a round or lobulated appearance, and in comparison to benign leiomyomas/GISTs showed more inhomogeneities with echogenic foci [90].

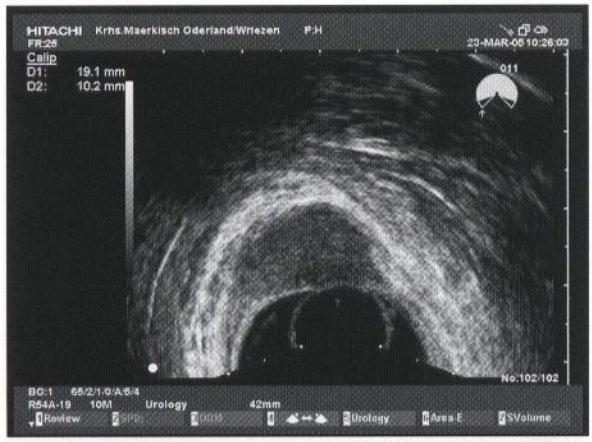
Neuroendocrine tumors (carcinoids) are the predominant tumor type in the rectum. Endosonographically, they uniformly appear as well-demarcated, round hypoechoic tumors located in the submucosal layer, with the internal structure resembling a "pepper-and-



a



b



c

Fig. 14.**32** Rectal cancer with subepithelial growth. **a** Recurrent subepithelial rectal cancer, following a previous surgical resection. **b** Rectal cancer of the signet-ring cell type, with subepithelial growth and infiltration beyond the deep muscle layer. **c** Primary cancer of the anorectal transitional zone, with a subepithelial growth pattern and infiltration of the deep muscle layer.

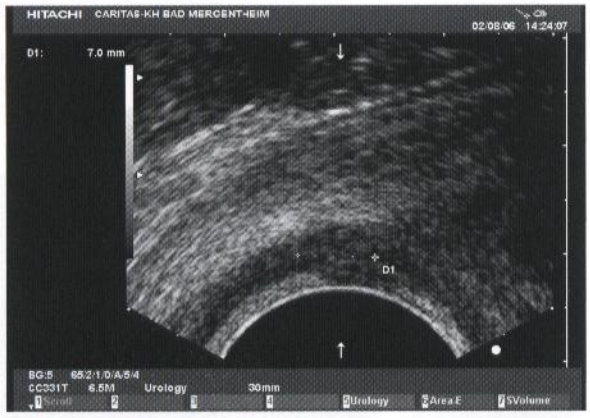


Fig. 14.**33** A neuroendocrine tumor in the rectum (7 mm), infiltrating the fourth ultrasound layer. Endoscopic resection is therefore not possible.

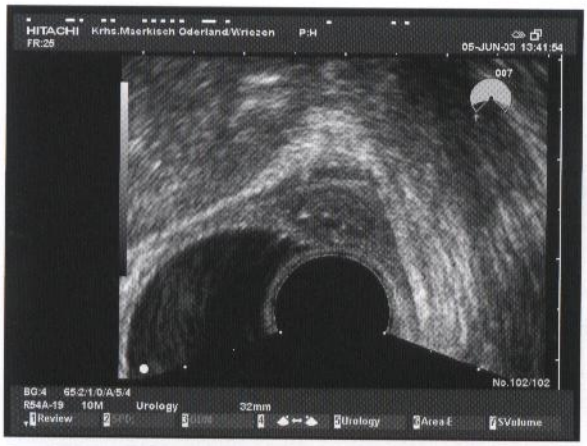
salt" pattern. EUS is very helpful for treatment planning [45,145,146] (Fig. 14.**33**).

Granular-cell tumors are very rare in the lower gastrointestinal tract. Their endosonographic appearance shows the same characteristics as in the esophagus [147].

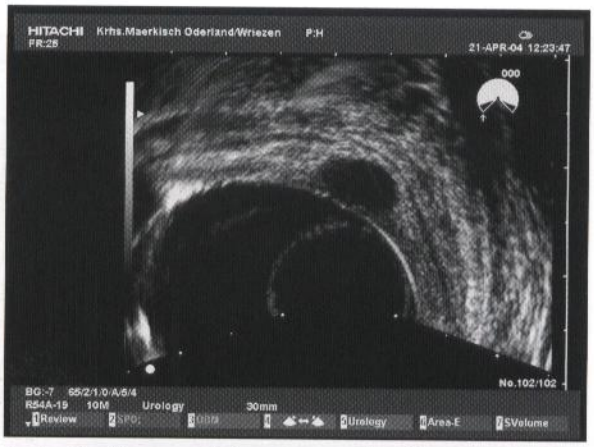
Amyloidosis is a rare diagnosis. Only one case of solitary amyloidosis localized in the transverse colon has been described, presenting as a homogeneously hypoechoic smooth oval lesion located in the third echogenic layer [111].

Schwannomas of the colon and rectum are very rare and, independent of their size, they are always benign [148]. Leiomyosarcomas of the colon and rectum occur much more rarely than GISTs and usually appear as large polypoid tumors. As elsewhere, differentiation of the different phenotypes of mesenchymal tumors in the lower gastrointestinal tract is only possible with immunohistochemical methods [115,125,148,149].

There have been no endosonographic follow-up studies of hypoechoic mesenchymal tumors of the colon and rectum, and endosonographic markers of malignancy have not been described. The following details are therefore based on pathological and anatomical studies: small hypoechoic mesenchymal tumors located in the lamina muscularis mucosae are almost invariably benign leiomyomas [125] (Fig. 14.**34a**). In contrast to the stomach, GISTs in the colon can only be regarded as benign if they measure less than 10 mm and have a low number of mitoses (< 5/50 HPF) [148]. In the rectum, GISTs measuring less than 20 mm with a low mitotic count are nearly always benign [149] (Fig. 14.**34b**).



a



b

Fig. 14.**34** Small subepithelial tumors of the rectum. **a** A leiomyoma of the muscularis mucosae, with small calcifications. **b** A small hypoechoic gastrointestinal stromal tumor (GIST), located in the muscularis mucosae. The diagnosis was confirmed histologically after endoscopic resection.

■ Assessment of the Biological Behavior of Hypoechoic Subepithelial Tumors

The pathological and anatomical assessment of the behavior of mesenchymal tumors of the gastrointestinal tract is more difficult and less reliable than the pathological and anatomical assessment of the biological behavior of epithelial neoplasms. Differences between published studies are largely due to relatively small numbers of patients, different follow-up periods, various definitions of the term "high power field" (HPF), and other reasons. To a large extent, tumor behavior can be judged by the number of mitotic changes per 50 HPF and the size of the tumor. In the upper gastrointestinal tract, only tumors measuring less than 50 mm and with a low number of mitoses (< 5/50 HPF for GISTs and < 2/50 HPF for leiomyomas) are deemed to be benign (very low risk, low risk) (Table 14.**7**). Despite this, there have been a number of cases in which the pathological and anatomical picture of gastrointestinal mesenchymal tumors supported a benign lesion, but in which the clinical course was malignant—specifically with the development of intraperitoneal dissemination and hepatic metastases. The biological behavior of mesenchymal neoplasms also appears to depend on their location. In addition, the number of mitoses and the degree of cell differentiation may vary within a mesenchymal tumor [113,115,116,121]. When these pathologic and anatomical difficulties are taken into account, it is easy to see that using only EUS criteria to assess the biological behavior of hypoechoic tumors originating from the muscular layers of the gastrointestinal tract is problematic [26,120]. Despite these limitations, it has been possible in some series, in which the findings were verified histologically, to define criteria with some predictive value for assessing the biological behavior of mesenchymal subepithelial tumors [26,34,47,68,123,150–153] (Table 14.**9**; for overview and discussion, see Polkowski et al. 2005 [7] and Polkowski and Butruk 2005 [8]).

In a study of 56 submucosal gastrointestinal mesenchymal tumors in which the endosonographic findings were controlled by histological assessments, hypoechoic subepithelial tumors with a diameter of less than 30 mm, a regular outline, and a homogeneous texture (Fig. 14.**35**) were always benign. However, 63% of the benign gastrointestinal mesenchymal tumors did not meet all three of these criteria for benign behavior [153].

In the eight larger endosonographic studies with histological controls, the following criteria were markers of malignancy: irregular outline, presence of echogenic or cystic internal structures, inhomogeneous echo pattern, diameter exceeding 30–40 mm, and the presence of enlarged local lymph nodes [26,33,34,68,139,150–153] (Fig. 14.**36**).

An ex-vivo analysis of five GISTs shortly after surgical resection found that hyperechoic foci or stranding around the periphery of the tumor on EUS were due to fibrotic changes; circumscribed echogenic areas represented areas of hyalinized necrosis, and cystic parts were found to be fluid-filled nonepithelialized cavities [43]. In our own patients, we have found that older hemorrhages appeared as very hypoechoic or anechoic tumor areas on EUS (Fig. 14.**36c**). More than 90% of malignant subepithelial mesenchymal tumors of the upper gastrointestinal tract show at least one of the criteria of malignancy mentioned above. However, these may also occur in a high percentage of benign tumors [154]. In the published series, the presence of two EUS criteria of malignancy (e. g., irregular outline and cystic internal structures, or an inhomogeneous echo pattern and size > 40 mm) was highly specific for malignant gastrointestinal mesenchymal tumors, but was not sufficiently sensitive to be able to diagnose malignant tumors reliably by endoscopic ultrasound [26,33,34,139,150,153,154].

Table 14.9 Endoscopic ultrasound assessment of the biological behavior of hypoechoic subepithelial tumors

Source	Benign	Characteristic	Malignant	Evaluation
Chak et al. 1997 [68] (n = 35)	≤ 40 mm	Size	> 40 mm	Evaluation by 5 experts; 2/3 main criteria met: sensitivity 80–90% no main criterion for malignancy met: specificity 89–100%
	Regular	Extraluminal contour	Irregular	
		Echogenic foci > 3 mm	+	
		Internal cystic structures > 4 mm	+	
Palazzo et al. 2000 [153] (n = 56) (22 malignant or borderline)	≤ 30 mm	Size	> 30 mm	All 3 main criteria for benign met: sensitivity 37%, specificity 100% 1/3 main criteria for malignancy met: sensitivity 91%, specificity 88%; 2/3 main criteria for malignancy met: sensitivity 23%, specificity 100%
	Regular	Extraluminal contour	Irregular	
		Internal cystic structures > 4 mm	+	
		Suspicious-appearing lymph nodes	+	
		Exophytic growth	+	
	Homogeneous	Internal echo pattern	Inhomogeneous	
Will et al. 2001 [34] (n = 41) (17 malignant)	≤ 40 mm	Size	> 40 mm	Both main criteria for malignancy met: sensitivity 71%, specificity 81%
	Homogeneous	Internal echo pattern	Inhomogeneous	
		Cystic/tubular internal structures	+	
Nickl et al. 2002 [151] (n = 102) (9 malignant, 21 borderline)	None	Ulceration	+	Tumors located in the stomach are more frequently malignant. Surgery of tumors with ulceration, > 30 mm, with irregular outline that were not round or oval and showed enlarged lymphnodes: 100% of malignant tumors and > 95% of borderline tumors diagnosed. No correlation between malignancy and presence of hyperechoic/hypoechoic foci
	< 30 mm	Size	≥ 30 mm	
	Regular, round or oval	Contour	irregular	



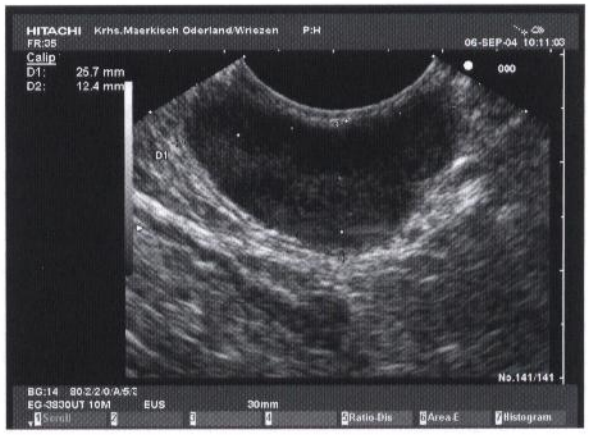
a



b



c



d

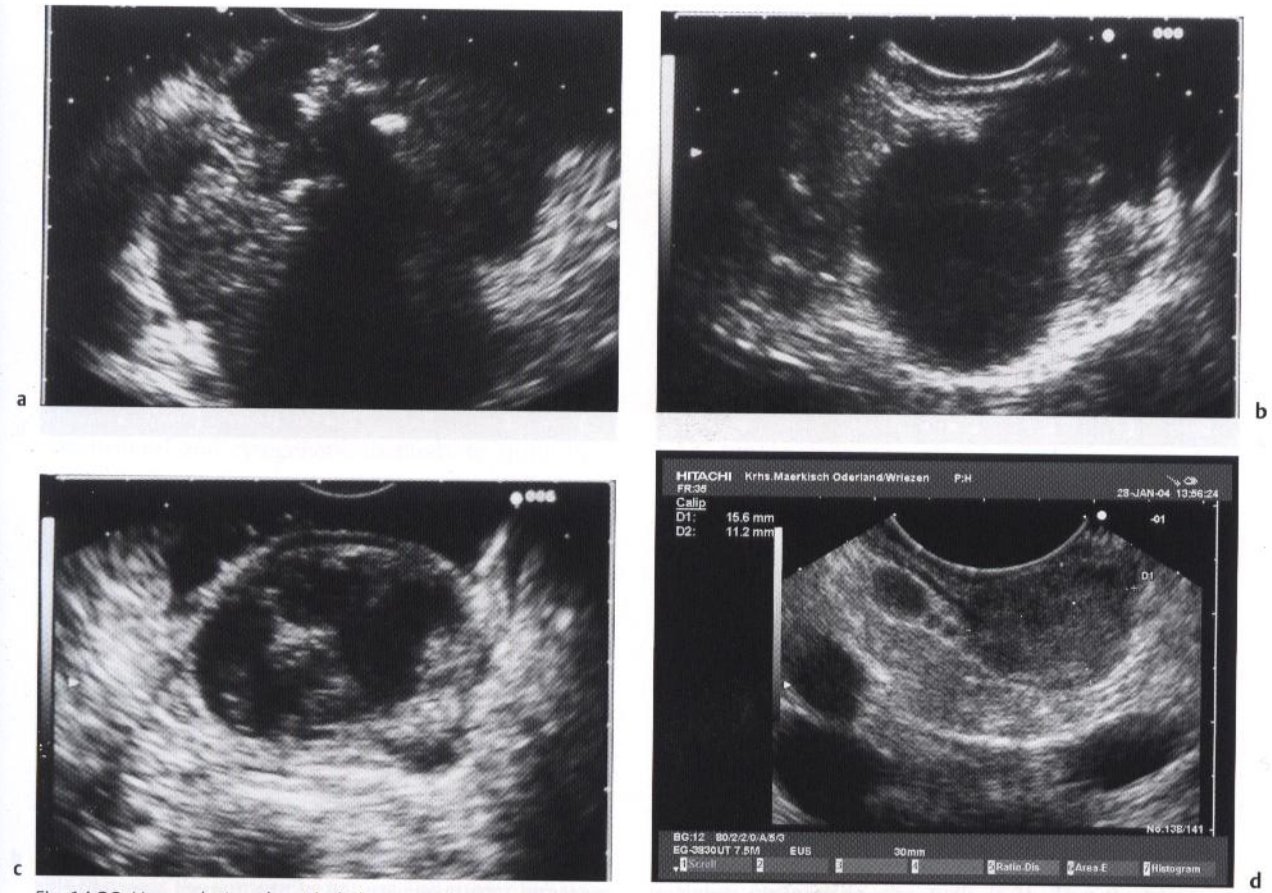


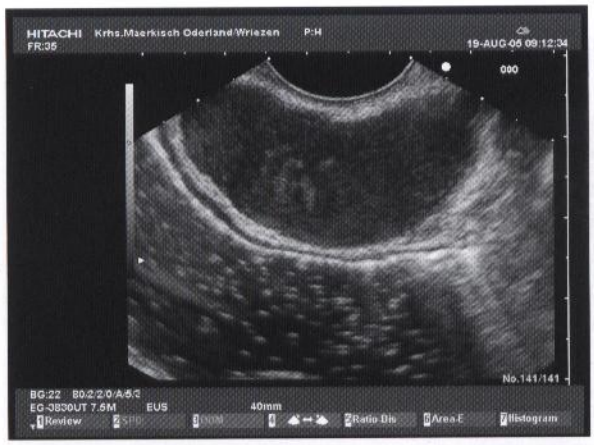
Fig. 14.**36** Hypoechoic subepithelial tumors that are malignant according to EUS criteria. **a** Duodenum: ulceration, size > 60 mm, with an inhomogeneous texture. **b** Stomach: the endoscopic appearance and endoscopic biopsy suggested an anaplastic gastric carcinoma. The EUS findings led to a review and correction of the histological diagnosis to malignant gastrointestinal stromal tumor (GIST), which was confirmed after surgical resection. **c** Obvious inhomogeneities, with infiltrative growth. The histological diagnosis was borderline GIST. **d** Some minor inhomogeneities, with definitely enlarged lymph nodes. Histological examination of the surgical specimen showed that it was a benign GIST.

When biological tumor behavior is being assessed, it is important to remember that the prevalence of malignant mesenchymal tumors depends on their location. Small mesenchymal tumors of the colon and rectum that arise from the lamina muscularis mucosae (the second hypoechoic layer) are almost exclusively leiomyomas and not GISTs [125]. Similarly, and independently of the layer of origin, benign leiomyomas are the predominant mesenchymal tumor in the esophagus. They occur much more frequently than GISTs or leiomyosarcomas, which are extremely rare [127]. A large multicenter study by Nickl et al. showed that a gastric location was a positive predictor of malignancy [151].

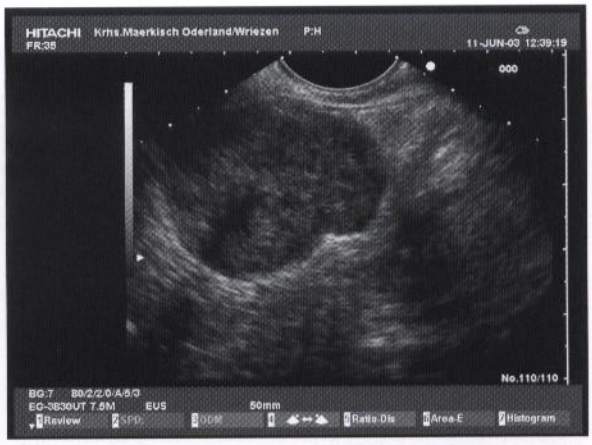
◁ Fig. 14.**35** Hypoechoic subepithelial tumors that are benign according to EUS criteria. **a** An incidental finding in the gastric body. No external compression was visible on endoscopy. **b** A minor external impression from a small homogeneously hypoechoic tumor with smooth margins, arising from the tunica muscularis of the stomach. **c** A small hypoechoic tumor in the gastric body, again arising from the tunica muscularis. **d** A pseudopedunculated hypoechoic tumor in the upper stomach, with smooth margins, arising from the tunica muscularis of the cardia.

Pitfalls

- The criteria for judging biological tumor behavior discussed above are very examiner-dependent. In the only published study to date, agreement between experienced observers in assessing biological behavior according to endosonographic criteria varied from unsatisfactory (cystic or echogenic internal structures) to moderate (heterogeneity, irregular outline) [30].
- Depending on size and age, benign leiomyomas and GISTs may develop an irregular outline and regressive changes, which appear as an inhomogeneous echo pattern or as anechoic or hypoechoic areas. These changes may make it difficult or impossible to distinguish these tumors from malignant mesenchymal tumors (Fig. 14.**37**).



a



b



c



d

Fig. 14.**37a–d** Examples in which assessment of the biological behavior of hypoechoic subepithelial tumors using endoscopic ultrasound led to equivocal results: size 40 mm, with mild or moderate inhomogeneity. All of the tumors were resected surgically and found to be benign. The more obvious inhomogeneities in **c** and **d** were due to hemorrhage.

- In our own series and in the series published by Ando et al. [47], one malignant GIST tumor was found that according to the criteria presented by Palazzo et al. [153] would have been regarded as definitely benign: the tumor had a smooth margin, was homogeneously hypoechoic, and was smaller than 30 mm. However, the histological examination revealed definite malignant changes.
- The criteria for judging the biological behavior of mesenchymal tumors are almost exclusively based on tumors of the upper gastrointestinal tract. It is not known whether these can be generalized to the lower gastrointestinal tract. GISTs in the colon show biologically malignant behavior when are larger than 10–20 mm [148]. In the series reported by Kameyama et al. [90], it was not possible to distinguish "leiomyomas" from "leiomyosarcomas" of the colon reliably using endoscopic ultrasound.

In summary, we consider that the endosonographic criteria are not sufficiently reliable in the assessment of the biological behavior of hypoechoic subepithelial tumors for EUS to be used as the only investigation for therapeutic decision-making.

■ EUS-Guided Fine-Needle Aspiration

Endoscopic ultrasound-guide fine-needle aspiration (EUS-FNA) is helpful for obtaining cytological material from lymph nodes and pancreatic tumors. Obtaining adequate specimens from subepithelial tumors with EUS-FNA is technically demanding, and in studies from the 1990s the sensitivity, specificity, and accuracy of cytological evaluation of intramural lesions was unacceptably low [155,156]. There are only a few cytological characteristics suggesting malignancy, such as dominant single cells or very rarely pleomorphic or hyperchromatic nuclei. However, the cytological assessment of fine-needle aspirates is not sufficient for assessing the behavior of GISTs, in particular because the cytological appearance of epithelioid GIST may mimic that of an adenocarcinoma or neuroendocrine tumor [36,157,158].

More recently, several studies have been published suggesting that the yield of EUS-FNA in the diagnosis of solid subepithelial tumors can be improved by optimizing needles and aspiration techniques and using immunocytochemical and immunocytogenetic analysis. Using cytological smears, immunocytochemical methods

make it reliably possible to determine the subtype of gastrointestinal mesenchymal tumors, and it is now also possible to carry out mutational analysis of the *KIT* gene [51,54,58,158–161]. In hypoechoic subepithelial tumors, cytological and immunocytochemical criteria make it possible differentiate between GISTs and—for example—neuroendocrine tumors [162], gastric glomus tumors [50], peripheral nerve sheath tumors [58], and Abrikosov's tumors [163]. Since myogenic, neurogenic, and undifferentiated gastrointestinal mesenchymal tumors behave differently, and because the number of mutations of the *KIT* gene and the degree of malignancy of GISTs are closely correlated [116], it may in the future be easier to predict tumor behavior by using immunocytochemical and cytogenetic methods to study fine-needle aspirates. Growing experience with EUS-FNA of subepithelial tumors has increased the rate at which adequate specimens are collected, and the method is now approaching the diagnostic yield of EUS-FNA of pancreatic mass lesions and lymph nodes [7, 9, 47, 55–57, 59, 61]. EUS-FNA with a modified sampling technique makes it possible to obtain core tissue specimens from subepithelial tumors, which can then be examined histologically and immunohistochemically, providing a wider range of diagnostic options than cytological smears or cell blocks. Ando et al. used a 22-G aspiration needle to obtain core specimens from 23 gastrointestinal mesenchymal tumors with EUS guidance. They were able to assess the tumor phenotype and tumor behavior correctly by staining for CD117, CD34, muscle actin, and S100 protein and by determining the number of mitoses and the Ki-67 labeling index [47]. Similar results have been reported by other Japanese groups [55,57,61,163]. The usefulness and safety of Tru-Cut needles (EUS-TCB) and guillotine needles for obtaining tissue from subepithelial tumors under endosonographic guidance has also been tested successfully [37,60,62,164,165]. The diagnostic yield of core biopsy with various types of needle appears to be better than with traditional cytological biopsy [7,165], and is sufficient for the diagnosis of gastrointestinal mesenchymal tumors and the assessment of their malignant potential before therapeutic decisions [55,57,61,159].

■ EUS-Guided Treatment of Subepithelial Lesions

With endoscopic ultrasound, it is possible to determine the layer of origin of subepithelial lesions reliably, both with radial high-frequency miniprobes [38, 39, 42, 45, 69, 166, 167] and with conventional echoendoscopes. This may also be useful for therapeutic interventions: some endoscopic resection techniques that were originally developed for removing epithelial lesions—particularly the techniques of endoscopic mucosal resection and endoscopic submucosal resection [52]—can also be used with different technical variations to resect small subepithelial tumors arising from the second hypoechoic or third echogenic layer. With the exception of stalked tumors, most authors would regard a size of > 20 mm (30 mm maximum) and a lack of separation from the fourth hypoechoic layer as a contraindication to endoscopic resection [45,69,70,80,136,166,168,169]. Various methods of resection have been described [169]: conventional snare resection of pedunculated subepithelial tumors, snare resection after prior submucosal injection with saline [45,69,136,170,171], snare resection using a ligation device [172], endoscopic enucleation using a snare or an insulated-tip knife [173,174], and partial snare resection ("unroofing") of cystic tumors [80]. In our department, we have successfully used the method of endoscopic submucosal tumor resection with a transparent cap [170] (first described by Inoue et al. [175] to resect flat mucosal neoplasms) or snare resection using a ligation device to resect several submucosal pancreatic heterotopias in the stomach and several other small tumors arising from the second hypoechoic or third echogenic layer of the esophagus and stomach (Fig. 14.**38**).

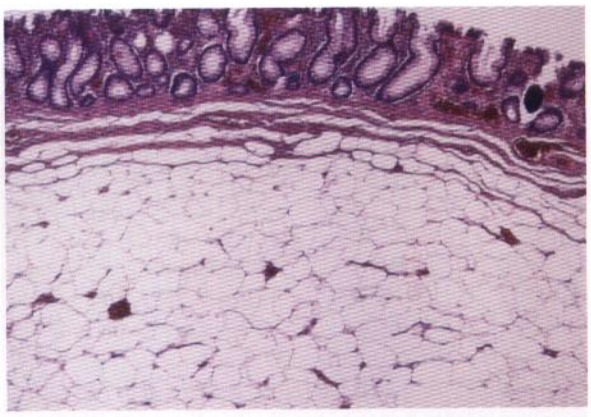
When endosonographic guidance is used for injection of normal saline to separate the tumor from surrounding tissues, endoscopy has even been used successfully to resect subepithelial tumors arising from the fourth hypoechoic layer (the tunica muscularis propria) without perforating the wall [63]. The decision on whether to resect a subepithelial tumor depends on several considerations—in particular, the patient's symptoms, the endosonographic and endoscopic features of the tumor, its potential to cause complications, the patient's comorbidities, and local expertise and the availability of the various resection techniques. The endoscopic resection of subepithelial tumors sometimes appears to be the most effective strategy for obtaining an unequivocal histopathological tissue diagnosis in comparison with EUS-FNA or jumbo biopsy [20,52,172].

Pitfalls and Practical Hints

- Submucosal injection of normal saline may cause the mucosal surface to level off near the submucosal tumor if it is not done sufficiently close to the tunica muscularis and directly beneath the tumor. This may result in the resection being unsuccessful. If the subepithelial tumor extends to the fourth hypoechoic layer, the injection should therefore in selected cases either be carried out with EUS guidance [63], or, if done endoscopically, the length of the needle and the depth of the injection have to be adapted to the depth of the lesion. It may be useful to create a depot of physiological saline between the tunica muscularis and the tumor to minimize the trauma caused by coagulation and consequently the risk of perforation.



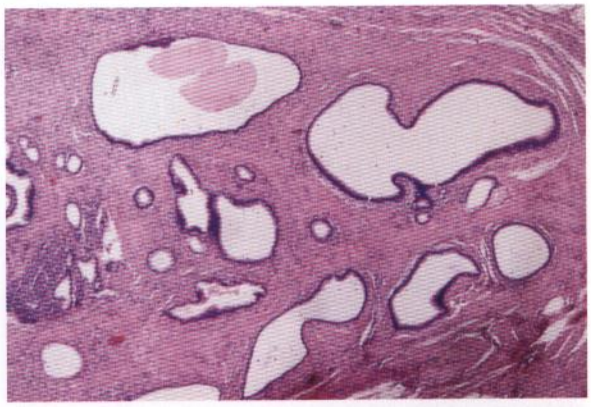
a



b



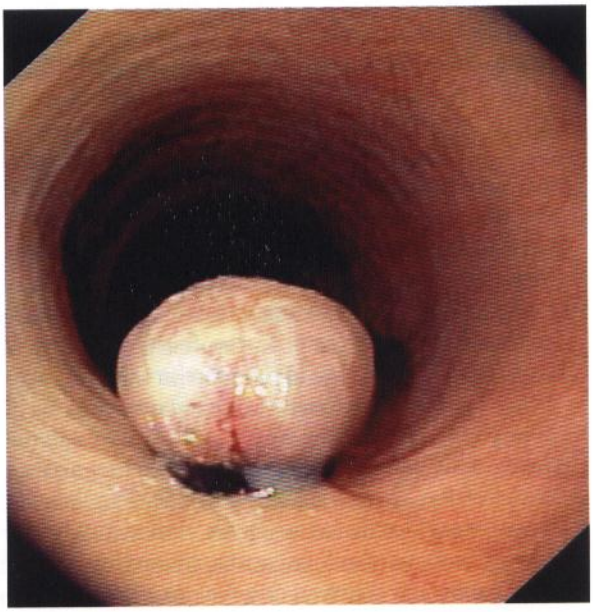
c



d



f



e

Fig. 14.**38** Endoscopic submucosal resection of small submucosal tumors. **a** A resected lipoma. **b** The corresponding histological specimen. **c** Resected gastric pancreatic heterotopia. **d** The corresponding histological specimen. **e** An esophageal granular-cell tumor after rubber-band ligation before endoscopic snare resection. **f** Endosonographic image (15-MHz ultrasound miniprobe) before rubber-band ligation.

Fig. 14.**38g** ▷

- The endoscopic resection of tumors arising from the tunica muscularis propria or infiltrating this layer carries a considerable risk of perforation [174]. In addition, radical resection of these tumors may be technically impossible.

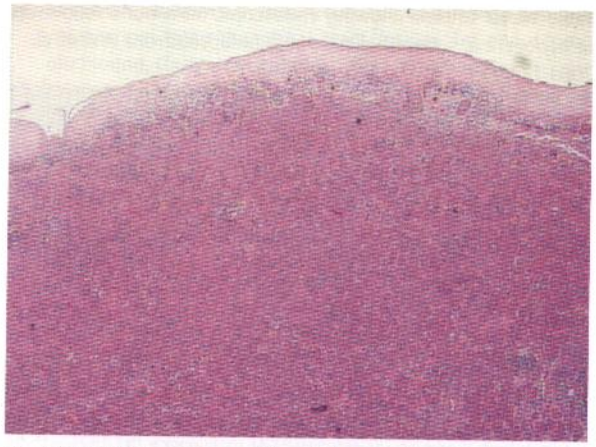
Diagnostic and Therapeutic Strategy for Subepithelial Lesions in the Gastrointestinal Tract

Endoscopic ultrasound should be used to exclude the presence of extramural impressions and varices, both of which may mimic subepithelial tumors. Subepithelial lesions should then be analyzed in accordance with a standardized protocol (Table 14.**2**) and, if possible, a diagnosis should be made.

If tumors are symptomatic (hemorrhage, pain, stenosis, endocrine activity), endoscopic or surgical treatment is always indicated. Endoscopic ultrasound may be useful here for assessing whether a tumor can be resected endoscopically, and it may be able to guide the submucosal injection of physiological saline to assist in endoscopic resection. EUS may also provide the surgeon with additional preoperative information on the topography of the tumor, its depth of infiltration, and possibly the presence of enlarged lymph-nodes. It is usually possible to resect a tumor endoscopically if its size does not exceed 20 mm (or 30 mm if in a suitable location) and if it is easily detachable from the fourth hypoechoic layer, perhaps after submucosal injection of physiological saline. Larger pedunculated subepithelial tumors may also be resected by endoscopy. In such cases, our experience shows that it is useful to assess the stalk with CCDS to estimate the risk of hemorrhage and to initiate measures to reduce this risk (e.g., Endoloop). In some selected cases, special endoscopic techniques (en-bloc resection using insulated-tip knives) also make it possible to resect larger nonpedunculated subepithelial tumors [174].

In the presence of asymptomatic subepithelial tumors, the task of endoscopic ultrasonography is to differentiate between:

- Definitely benign lesions that do not require any treatment or follow-up.
- Probably benign lesions, which should either be treated with endoscopic methods or followed up at regular intervals.
- Possibly malignant lesions, which either require further investigation with fine-needle aspiration or Tru-Cut biopsy, or which require endoscopic or surgical resection.
- Definitely malignant lesions (e.g., infiltrative growth), or probably malignant lesions, which require complete surgical resection.



g

Fig. 14.**38g** The corresponding histological specimen. We are grateful to H. Martin, Berlin (**b**, **d**) and S. Bartho and S. Wagner, Königswusterhausen, Germany (**g**), for providing the histological images.

In this scenario, EUS may reduce the use of cost-intensive, potentially dangerous, and often unhelpful further diagnostic procedures [176]. Endoscopic mucosal and submucosal resection techniques nowadays have to be regarded as well-established procedures with a low complication rate. Given that both the patient and physician may feel rather alarmed by the diagnostic uncertainties in hypoechoic subepithelial tumors of the gastrointestinal tract, we consider that the threshold for initiating endoscopic treatment should be low.

The only definitely benign subepithelial lesions that require neither treatment nor follow-up are typical lipomas. We can support the recommendation that submucosal cysts should be excluded from treatment or follow-up [34] only in the case of typical solitary monocystic lesions. The group of multiple cystic, polycystic, and solid cystic subepithelial tumors is large and heterogeneous. It includes various forms of cystic subepithelial heterotopia in the gastric mucosa, which may be associated with gastric cancer [97,100], some cases of pancreatic heterotopia, which very rarely may be associated with adenocarcinoma [106,177] or may develop complications [103,178,179], and GISTs with cystic degeneration [33]. In such lesions, endoscopic resection or partial resection should be the aim whenever possible [80]. Endosonographic follow-up is an alternative option.

Endosonographic follow-up also appears to be an acceptable alternative to endoscopic resection in a subgroup of hypoechoic subepithelial tumors. The risk of a surveillance strategy instead of endoscopic or surgical resection is low in small (< 30 mm) hypoechoic subepithelial tumors with well-defined margins if they are homogeneous and if the layer of origin can be easily visualized without any signs of infiltration. During the follow-up, the tumor should not show any increase in size or any change in echotexture [34]. In some smaller studies, the number of hypoechoic subepithelial tumors

Table 14.**10** Criteria allowing endoscopic ultrasound follow-up of hypoechoic subepithelial tumors (adapted from Will et al. 2001 [34])

- The patient is asymptomatic (specifically: no hemorrhage, no intestinal obstruction)
- Tumor size ≤ 30 mm (or ≤ 20 mm in the colon and rectum)
- Smooth outline
- Homogeneous texture without cystic internal structures; layer of origin clearly discernible; no evidence of infiltrative growth
- No enlarged local lymph nodes
- During follow-up: no significant increase in size (e.g., > 10 mm or 50%) [51], no change in texture, patient remains asymptomatic.
- If fine-needle aspiration performed: no definite or equivocal cytological or histological criteria of malignancy [51,182]

Table 14.**11** Criteria for surgical or endoscopic resection of subepithelial tumors (adapted from Will et al. 2001 [34])

- Tumor is causing symptoms (specifically hemorrhage or intestinal obstruction)
- Tumor size > 30 mm
- Irregular outline
- Inhomogeneous echotexture (particularly cystic cavities)
- Layer of origin not clearly delineated, signs of infiltration
- Enlarged local lymph nodes
- Cytological or histological studies suggesting possible malignancy

in which a significant increase in size was observed during the follow-up period was very low [180,181]. As there are only sparse data on the natural course of hypoechoic subepithelial tumors [7], a surveillance strategy should be discussed with each patient on an individual basis (Table 14.**10**) [34,51,182].

In addition to this group of hypoechoic subepithelial tumors, we would recommend endosonographic follow-up for cystic and solid cystic lesions (probable lymphangiomas, hemangiomas, pancreatic heterotopia, cystic hamartomas) that are not referred for histological investigation or endoscopic resection.

We recommend a follow-up examination 6 months after the initial diagnosis, then again 6 months later, and finally 2 years after the diagnosis. Further follow-up does not appear to be indicated [183]. In the large intestine and in the rectum, the cut-off for follow-up rather than intervention should be reduced to a tumor size of 20 mm, because of the different biological behavior of gastrointestinal stromal tumors in the lower gastrointestinal tract [149]. On the other hand, the risk of a follow-up strategy is considerably lower in esophageal hypoechoic subepithelial tumors in comparison with tumors of gastral localization [7,159]. One considerable problem with this follow-up program may be low attendance rates for surveillance examinations. In one prospective multicenter trial, a follow-up strategy for patients with hypoechoic subepithelial tumors without EUS features predictive of malignancy proved to be unsuccessful because of low patient compliance and lack of cost-effectiveness [151,152,183]. An interesting alternative for endosonographic follow-up of subepithelial gastric tumors might be abdominal ultrasound surveillance. Three studies have shown that the great majority of subepithelial tumors of the stomach that have previously been diagnosed endoscopically or with EUS can be detected and measured using abdominal ultrasonography of the water-filled stomach [184–186].

If all subepithelial tumors that do not meet the above criteria were surgically removed because of suspected malignancy, the prevalence of tumors that were found to be benign after resection would be very high (e.g., 65% in Will et al. [34]). In the patients we saw over an investigation period of 50 months, approximately one-third of hypoechoic subepithelial tumors met one of the EUS criteria for malignancy, and a further third met at least two of these criteria (Fig. 14.**37**). We would therefore suggest that, in patients with asymptomatic tumors with one marker of possible malignancy (e.g., size between 30 and 50 mm, inhomogeneous texture), the decision between follow-up or surgical removal should also be based on the results of cytological and histological examinations. This is particularly worth considering if the risk of surgery is high or if the patient does not wish to undergo surgery. In such a scenario, it is important to try to obtain a core specimen (with EUS-FNA or EUS Tru-Cut biopsy), as cytological biopsy is of no value for assessing the malignant potential of GISTs. Modern methods of investigation, such as immunohistochemistry and immunocytochemistry for determining the phenotype (CD117) and proliferative activity (Ki-67, MIB-1), and perhaps in the future also cytogenetic methods of analyzing mutations in the *KIT* gene, need to be included in histocytological processing of the tissue samples obtained.

All asymptomatic subepithelial tumors that meet any of the following criteria definitely require surgical (or endoscopic) intervention: at least two of the endosonographic criteria for malignancy; development of symptoms during follow-up; significant increase in size (+ 10 mm or > 50%); changes in the EUS appearance during the follow-up; cytological, histological, immunohistochemical, immunocytochemical, or cytogenetic criteria of a malignant or potentially malignant neoplasm [34] (Table 14.**11**).

In subepithelial tumors of the stomach that arise from the second or third layer, measure up to 20 mm, and cannot be confidently diagnosed as simple lipomas or cysts, the threshold for proceeding to endoscopic resection should be low. In such cases, EUS-FNA is unhelpful in deciding whether or not to operate [54]. Among hypoechoic subepithelial tumors that were resected because they fulfilled at least two of the endo-

sonographic criteria for malignancy, up to 20% of the lesions were benign in published studies with highly selected patients [34,68]. In our own patient population, the proportion was 64%.

We do not agree with Will et al. [34] that all subepithelial tumors that are positive for CD117 and CD34 should be resected, regardless of whether they meet any other criteria for malignancy [34], since 70–80% of gastrointestinal stromal tumors that are positive for these immunohistochemical markers turn out to have a low or very low risk of malignant behavior [115,116,135].

When presented with a specimen of a spindle-cell or epithelioid gastrointestinal mesenchymal tumor, the pathologist should not only perform the standard macroscopic and histological investigations. In addition, he or she should use immunohistochemical methods to determine the phenotype and should also assess the presence of markers of proliferation—e.g., MIB-1/Ki-67 or proliferating cell nuclear antigen (PCNA). It is not yet known whether postoperative adjuvant chemotherapy with the tyrosine kinase inhibitor imatinib (Glivec, Gleevec) is indicated, although this drug is highly effective in metastasizing or inoperable malignant gastrointestinal stromal tumors [117].

References

1. Gordon SJ, Rifkin MD, Goldberg BB. Endosonographic evaluation of mural abnormalities of the upper gastrointestinal tract. Gastrointest Endosc 1986;32:193–8.
2. Lambert R, Caletti G, Cho E, et al. International workshop on the clinical impact of endoscopic ultrasound in gastroenterology. Endoscopy 2000;32:549–84.
3. Rifkin MD, Gordon SJ. Sonoendoscopic evaluation of extraesophageal and extragastric abnormalities: a review. Scand J Gastroenterol Suppl 1986;123:68–73.
4. Strohm WD, Classen M. Benign lesions of the upper GI tract by means of endoscopic ultrasonography. Scand J Gastroenterol Suppl 1986;123:41–6.
5. Van Stolk RU. Subepithelial lesions. In: Van Dam J, Sivak MV, editors. Gastrointestinal endosonography. Philadelphia: Saunders, 1999: 153–65.
6. Hwang JH, Kimmey MB. The incidental upper gastrointestinal subepithelial mass. Gastroenterology 2004;126:301–7.
7. Polkowski M. Endoscopic ultrasound and endoscopic ultrasound-guided fine-needle biopsy for the diagnosis of malignant submucosal tumors. Endoscopy 2005;37:635–45.
8. Polkowski M, Butruk E. Submucosal lesions. Gastrointest Endosc Clin N Am 2005;15:33–54, viii.
9. Mallery S, Lai R, Bardales R, Stelow E, Debol S, Stanley M. EUS-guided needle aspiration (EUS-FNA) in subepithelial GI-tract masses (SIGIM): results in 105 lesions [abstract]. Gastrointest Endosc 2004;59: AB 234.
10. Davila RE, Faigel DO. GI stromal tumors. Gastrointest Endosc 2003;58:80–8.
11. Saund MS, Demetri GD, Ashley SW. Gastrointestinal stromal tumors (GISTs). Curr Opin Gastroenterol 2004;20:89–94.
12. Boyce GA, Sivak MV Jr, Rösch T, et al. Evaluation of submucosal upper gastrointestinal tract lesions by endoscopic ultrasound. Gastrointest Endosc 1991;37:449–54.
13. Faivre J, Bory R, Moulinier B. Benign tumors of oesophagus: value of endoscopy. Endoscopy 1978;10:264–8.
14. Rösch T, Classen, M. Gastroenterologic endosonography: textbook and atlas. Stuttgart: Thieme, 1992.
15. Rösch T, Kapfer B, Will U, et al. Endoscopy is not sufficient for a reliable diagnosis of upper GI submucosal tumors (SMT) [abstract]. Gastrointest Endosc 1999;49: AB 212.
16. Rösch T, Lorenz R, Dancygier H, et al. Endosonographic diagnosis of submucosal upper gastrointestinal tract tumors. Scand J Gastroenterol 1992;27:1–8.
17. Rösch T, Lorenz R, von Wichert A, et al. Gastric fundus impression caused by splenic vessels: detection by endoscopic ultrasound. Endoscopy 1991;23(2):85–7.
18. Hwang JH, Saunders MD, Rulyak SJ, et al. A prospective study comparing endoscopy and EUS in the evaluation of GI subepithelial masses. Gastrointest Endosc 2005;62: 202–8.
19. Cantor MJ, Davila ER, Faigel DO. Yield of tissue sampling for submucosal lesions evaluated by EUS: a comparison between forceps biopsies and endoscopic submucosal-mucosal resection [abstract]. Gastrointest Endosc 2004;59:AB 234.
20. Hunt GC, Smith PP, Faigel DO. Yield of tissue sampling for submucosal lesions evaluated by EUS. Gastrointest Endosc 2003;57:68–72.
21. Rösch T, Kapfer B, Will U, et al. Endoscopic ultrasound (EUS) reduces the risk of large particle biopsy in upper GI submucosal lesions: a prospective study in 150 patients [abstract]. Gastrointest Endosc 1999;49:AB 212.
22. Eckardt AJ, Wassef W. Diagnosis of subepithelial tumors in the GI tract: endoscopy, EUS, and histology: bronze, silver, and gold standard? Gastrointest Endosc 2005;62:209–12.
23. Zhang QL, Nian WD. Endoscopic ultrasonography diagnosis in submucosal tumor of stomach. Endoscopy 1998;30(Suppl 1):A69–A71.
24. Chen TK, Wu CH, Lee CL, et al. Endoscopic ultrasonography to study the causes of extragastric compression mimicking gastric submucosal tumor. J Formos Med Assoc 2001;100: 758–61.
25. Motoo Y, Okai T, Ohta H, et al. Endoscopic ultrasonography in the diagnosis of extraluminal compressions mimicking gastric submucosal tumors. Endoscopy 1994;26:239–42.
26. Rösch T, Kapfer B, Will U, et al. Accuracy of endoscopic ultrasonography in upper gastrointestinal submucosal lesions: a prospective multicenter study. Scand J Gastroenterol 2002;37:856–62.
27. Tio TL, Tytgat GN, Hartog Jager FC. Endoscopic ultrasonography for the evaluation of smooth muscle tumors in the upper gastrointestinal tract: an experience with 42 cases. Gastrointest Endosc 1990;36:342–50.
28. Yasuda K, Nakajima M, Kawai K. Endoscopic ultrasonography in the diagnosis of submucosal tumor of the upper digestive tract. Scand J Gastroenterol Suppl 1986;123: 59–67.
29. Yasuda K, Nakajima M, Yoshida S, et al. The diagnosis of submucosal tumors of the stomach by endoscopic ultrasonography. Gastrointest Endosc 1989;35:10–5.
30. Gress F, Schmitt C, Savides T, et al. Interobserver agreement for EUS in the evaluation and diagnosis of submucosal masses. Gastrointest Endosc 2001;53:71–6.

31. Rösch T. Endoscopic ultrasonography in upper gastrointestinal submucosal tumors: a literature review. Gastrointest Endosc Clin N Am 1995;5:609–14.
32. De Angelis C, Carucci P, Curri F, Peyre S, Arena V, Maglione V, et al. Role of endoscopic ultrasonography in therapeutic decision making and in following-up gastrointestinal submucosal tumors and extraluminal compressions [abstract]. Gastrointest Endosc 2000;51[4 Part 2]:AB 223.
33. Hizawa K, Kawasaki M, Kouzuki T, et al. Endosonographic classifications of gastrointestinal submucosal tumors. Dig Endosc 2000;12:120–5.
34. Will U, Reinholz G, Bosseckert H. Wertigkeit der Endosonographie submuköser Tumore des oberen GIT [abstract]. Ultraschall Med 2001;22(Suppl):S118.
35. Shudo R, Yazaki Y, Sakurai S, et al. Adrenal adenoma mimicking a submucosal tumor of the stomach. Dig Endosc 2001;13:99–103.
36. Fritscher-Ravens A, Sriram PV, Schroder S, et al. Stromal tumor as a pitfall in EUS-guided fine-needle aspiration cytology. Gastrointest Endosc 2000;51:746–9.
37. Fujisaki J, Chibai M. Endoscopic ultrasonography guided needle biopsy for submucosal tumors. Dig Endosc 2001;13(Suppl 1):S57–S58.
38. Buscarini E, Stasi MD, Rossi S, et al. Endosonographic diagnosis of submucosal upper gastrointestinal tract lesions and large fold gastropathies by catheter ultrasound probe. Gastrointest Endosc 1999;49:184–91.
39. Xu GQ, Li YW, Han YM, et al. Miniature ultrasonic probes for diagnosis and treatment of digestive tract diseases. World J Gastroenterol 2004;10:1948–53.
40. Yasuda K, Cho E, Nakajima M, et al. Diagnosis of submucosal lesions of the upper gastrointestinal tract by endoscopic ultrasonography. Gastrointest Endosc 1990;36(2 Suppl): S17–S20.
41. Murata Y, Yoshida M, Akimoto S, et al. Evaluation of endoscopic ultrasonography for the diagnosis of submucosal tumors of the esophagus. Surg Endosc 1988;2:51–8.
42. Koch J, Halvorsen RA, Jr, Levenson SD, et al. Prospective comparison of catheter-based endoscopic sonography versus standard endoscopic sonography: evaluation of gastrointestinal-wall abnormalities and staging of gastrointestinal malignancies. J Clin Ultrasound 2001;29:117–24.
43. Krinsky ML, Savides TJ, Behling CA. Ex-vivo correlation of endosonographic features with pathologic findings in gastric stromal tumors [abstract]. Gastrointest Endosc 2001;53:AB 170.
44. Tombazzi CE, Tio TL, Mayoral W, et al. FNA and mucosectomy in submucosal GI-lesions in adjunct to EUS/ CUS [abstract]. Gastrointest Endosc 2000;51:AB 287.
45. Waxman I, Saitoh Y, Raju GS, et al. High-frequency probe EUS-assisted endoscopic mucosal resection: a therapeutic strategy for submucosal tumors of the GI tract. Gastrointest Endosc 2002;55:44–9.
46. Niwa Y, Kobayashi S. Color Doppler-enhanced endoscopic ultrasonographic diagnosis of upper gastrointestinal submucosal lesions. Gastrointest Endosc 1998;47:95–6.
47. Ando N, Goto H, Niwa Y, et al. The diagnosis of GI stromal tumors with EUS-guided fine needle aspiration with immunohistochemical analysis. Gastrointest Endosc 2002;55: 37–43.
48. Eloubeidi MA, Cohn M, Cerfolio RJ, et al. Endoscopic ultrasound-guided fine-needle aspiration in the diagnosis of foregut duplication cysts: the value of demonstrating detached ciliary tufts in cyst fluid. Cancer 2004;102:253–8.
49. Gu M, Ghafari S, Nguyen PT, et al. Cytologic diagnosis of gastrointestinal stromal tumors of the stomach by endoscopic ultrasound-guided fine-needle aspiration biopsy: cytomorphologic and immunohistochemical study of 12 cases. Diagn Cytopathol 2001;25:343–50.
50. Gu M, Nguyen PT, Cao S, et al. Diagnosis of gastric glomus tumor by endoscopic ultrasound-guided fine needle aspiration biopsy: a case report with cytologic, histologic and immunohistochemical studies. Acta Cytol 2002;46:560–6.
51. Kinoshita K, Isozaki K, Tsutsui S, et al. Endoscopic ultrasonography-guided fine needle aspiration biopsy in follow-up patients with gastrointestinal stromal tumours. Eur J Gastroenterol Hepatol 2003;15:1189–93.
52. Kwok H, Nguyen PT, Lee JG, Christie CJ, Chang KJ. Fine needle aspiration (FNA) vs. endoscopic mucosal resection (EMR): optimizing tissue acquisition during endoscopic ultrasound (EUS) evaluation of submucosal lesions [abstract]. Gastrointest Endosc 2004;59:AB 237.
53. Matsui M, Goto H, Niwa Y, et al. Preliminary results of fine needle aspiration biopsy histology in upper gastrointestinal submucosal tumors. Endoscopy 1998;30:750–5.
54. Niwa Y, Goto H, Hirooka Y, Kojima K, Ando K, Hayakawa T, et al. Diagnosis of gastric submucosal tumors by endoscopic ultrasound (EUS); only image vs. EUS-guided fine needle biopsy [abstract]. Gastrointest Endosc 2000;51(4 Part 2):AB 300.
55. Okubo K, Yamao K, Nakamura T, et al. Endoscopic ultrasound-guided fine-needle aspiration biopsy for the diagnosis of gastrointestinal stromal tumors in the stomach. J Gastroenterol 2004;39:747–53.
56. Sasaki Y, Niwa Y, Hirooka Y, et al. The use of endoscopic ultrasound-guided fine-needle aspiration for investigation of submucosal and extrinsic masses of the colon and rectum. Endoscopy 2005;37:154–60.
57. Sawaki A, Okubo K, Mizuno N, Ashida R, Nakamura T, Tajika M, et al. Preoperative diagnosis of GISTs using endoscopic ultrasonography guided fine needle aspiration biopsy (EUS-FNAB) [abstract]. Gastrointest Endosc 2004;59:AB 237.
58. Stelow EB, Lai R, Bardales RH, et al. Endoscopic ultrasound-guided fine-needle aspiration cytology of peripheral nerve-sheath tumors. Diagn Cytopathol 2004;30:172–7.
59. Vander Noot MR III, Eloubeidi MA, Chen VK, et al. Diagnosis of gastrointestinal tract lesions by endoscopic ultrasound-guided fine-needle aspiration biopsy. Cancer 2004;102: 157–63.
60. Yadav D, Levy MJ, Schwartz D, et al. EUS-guided trucut biopsy for diagnosis of an esophageal stromal tumor: case report. Gastrointest Endosc 2003;58:457–60.
61. Yamao K, Ohashi K, Nakamura T, Suzuki T, Koshikawa S. Endoscopic ultrasound guided fine needle aspiration for the diagnosis of the gastrointestinal submucosal tumors [abstract]. Gastrointest Endosc 2000;51(4 Part 2):AB 163.
62. Ribeiro A, Vernon S, Quintela P. EUS-guided trucut biopsy with immunohistochemical analysis of a gastric stromal tumor. Gastrointest Endosc 2004;60:645–8.
63. Sun S, Wang M, Sun S. Use of endoscopic ultrasound-guided injection in endoscopic resection of solid submucosal tumors. Endoscopy 2002;34:82–5.
64. Pedersen FM, Vilmann P, Bytzer P. Gastric arteriovenous malformation: Doppler EUS-guided diagnosis and therapy. Gastrointest Endosc 2002;55:597–9.
65. Gunter E, Lingenfelser T, Eitelbach F, et al. EUS-guided ethanol injection for treatment of a GI stromal tumor. Gastrointest Endosc 2003;57:113–5.

66. Okanobu H, Hata J, Haruma K, et al. A classification system of echogenicity for gastrointestinal neoplasms. Digestion 2005;72:8–12.
67. Matsushita M, Hajiro K, Okazaki K, et al. Gastric inflammatory fibroid polyps: endoscopic ultrasonographic analysis in comparison with the histology. Gastrointest Endosc 1997; 46:53–7.
68. Chak A, Canto MI, Rösch T, et al. Endosonographic differentiation of benign and malignant stromal cell tumors. Gastrointest Endosc 1997;45:468–73.
69. Kojima T, Takahashi H, Parra-Blanco A, et al. Diagnosis of submucosal tumor of the upper GI tract by endoscopic resection. Gastrointest Endosc 1999;50:516–22.
70. Hizawa K, Aoyagi K, Kurahara K, et al. Gastrointestinal lymphangioma: endosonographic demonstration and endoscopic removal. Gastrointest Endosc 1996;43:620–4.
71. Matsushita M, Takakuwa H, Nishio A. Characteristic endosonographic features of gastric inflammatory fibroid polyps. Endoscopy 2001;33:729–30.
72. Kono K, Sekikawa T, Iino H, et al. A case of arteriovenous malformation in the submucosal layer of the stomach. J Gastroenterol 1994;29:340–3.
73. Arafa UA, Fujiwara Y, Shiba M, et al. Endoscopic resection of a cavernous haemangioma of the stomach. Dig Liver Dis 2002;34:808–11.
74. Tominaga K, Arakawa T, Ando K, et al. Oesophageal cavernous haemangioma diagnosed histologically, not by endoscopic procedures. J Gastroenterol Hepatol 2000;15:215–9.
75. Choong NW, Levy MJ, Rajan E, et al. Intramural gastric abscess: case history and review. Gastrointest Endosc 2003;58:627–9.
76. Messmann H, Hollerbach S, Gross V, et al. [Multiple gastric wall abscesses: a rare differential endosonographic diagnosis of submucous stomach tumors; in German.] Z Gastroenterol 1995;33:170–2.
77. Soon MS, Yen HH, Soon A, et al. Endoscopic ultrasonographic appearance of gastric emphysema. World J Gastroenterol 2005;11:1719–21.
78. Will U, Masri R, Bosseckert H, et al. Gastric wall abscess, a rare endosonographic differential diagnosis of intramural tumors: successful endoscopic treatment. Endoscopy 1998; 30:432–5.
79. Mizuma N, Kabemura T, Akahoshi K, et al. Endosonographic features of mucocele of the appendix: report of a case. Gastrointest Endosc 1997;46:549–52.
80. Hizawa K,Matsumoto T, Kouzuki T, et al. Cystic submucosal tumors in the gastrointestinal tract: endosonographic findings and endoscopic removal. Endoscopy 2000;32:712–4.
81. Miettinen M, Sobin LH, Sarlomo-Rikala M. Immunohistochemical spectrum of GISTs at different sites and their differential diagnosis with a reference to CD117 (KIT). Mod Pathol 2000;13:1134–42.
82. Faigel DO, Burke A, Ginsberg GG, et al. The role of endoscopic ultrasound in the evaluation and management of foregut duplications. Gastrointest Endosc 1997;45:99–103.
83. Geller A, Wang KK, DiMagno EP. Diagnosis of foregut duplication cysts by endoscopic ultrasonography. Gastroenterology 1995;109:838–42.
84. Guibaud L, Fouque P, Genin G, et al. Case report: CT and ultrasound of gastric and duodenal duplications. J Comput Assist Tomogr 1996;20:382–5.
85. Pontes JM, Cadime A, Pereira E, Catre A. Value of endoscopic ultrasound in the diagnosis and treatment of unusual gastrointestinal cystic lesions [abstract]. Gastrointest Endosc 2000; 51(4 Part 2):AB 286.
86. Riyaz A, Cohen H. Ectopic pancreas presenting as a submucosal gastric antral tumor that was cystic on EUS. Gastrointest Endosc 2001;53:675–7.
87. Van Dam J, Rice TW, Sivak MV Jr. Endoscopic ultrasonography and endoscopically guided needle aspiration for the diagnosis of upper gastrointestinal tract foregut cysts. Am J Gastroenterol 1992;87:762–5.
88. Kim KM, Choi KY, Lee A, et al. Lymphangioma of large intestine: report of ten cases with endoscopic and pathologic correlation. Gastrointest Endosc 2000;52:255–9.
89. Ishikawa N, Fuchigami T, Kikuchi Y, et al. EUS for gastric lymphangioma. Gastrointest Endosc 2000;52:798–800.
90. Kameyama H, Niwa Y, Arisawa T, et al. Endoscopic ultrasonography in the diagnosis of submucosal lesions of the large intestine. Gastrointest Endosc 1997;46:406–11.
91. Kim HS, Lee SY, Lee YD, et al. Gastric lymphangioma. J Korean Med Sci 2001;16:229–32.
92. Kochman ML, Wiersema MJ, Hawes RH, et al. Preoperative diagnosis of cystic lymphangioma of the colon by endoscopic ultrasound. Gastrointest Endosc 1997;45:204–6.
93. Changchien CS, Hsu CC, Hu TH. Endosonographic appearances of Brunner's gland hamartomas. J Clin Ultrasound 2001;29:243–6.
94. Kaufman DJ, Al Kharrat H, Weiss S, et al. EUS-guided endoscopic removal of a large Brunner's gland hamartoma. Gastrointest Endosc 2003;58:313–4.
95. Matsushita M, Hajiro K, Takakuwa H, et al. Characteristic EUS appearance of Brunner's gland hamartoma. Gastrointest Endosc 1999;49:670–2.
96. Soon MS, Lin OS, Yeh KT. Gastric mucosal heterotopia in the gastric submucosa: an evaluation by EUS. Gastrointest Endosc 1999;49(4 Pt 1):534–7.
97. Chung HK, Kim EJ, Kim DJ, Kim HS, Park SH, Lee MS, et al. Clinical significance of gastritis cystica polyposa and role of endoscopic ultrasonography [abstract]. Gastrointest Endosc 2000;51(4 Part 2]:AB 163.
98. Okada M, Iizuka Y, Oh K, et al. Gastritis cystica profunda presenting as giant gastric mucosal folds: the role of endoscopic ultrasonography and mucosectomy in the diagnostic work-up. Gastrointest Endosc 1994;40:640–4.
99. Shudo R, Horita K, Takahashi K, et al. A case of gastritis cystica polyposa showing a characteristic endoscopic ultrasonogram. Digest Endosc 2000;12:68–72.
100. Hizawa K, Suekane H, Kawasaki M, et al. Diffuse cystic malformation and neoplasia-associated cystic formation in the stomach: endosonographic features and diagnosis of tumor depth. J Clin Gastroenterol 1997;25:634–9.
101. Niizawa M, Ishida H, Morikawa P, et al. Diffuse heterotopic submucosal cystic malformation of the stomach: ultrasonographic diagnosis. Gastrointest Radiol 1992;17:9–12.
102. Ohtsuka H, Ikeda M, Morozumi A, et al. Diagnosis of multiple submucosal cysts of the stomach by endoscopic ultrasonography. Dig Endosc 2001;13:207–11.
103. Fekete F, Noun R, Sauvanet A, et al. Pseudotumor developing in heterotopic pancreas. World J Surg 1996;20:295–8.
104. Hase S, Nakazawa S, Yoshino J, et al. [A study on gastric and small intestinal aberrant pancreas by endoscopic ultrasonography: with special reference to comparison with histological appearance]. Nippon Shokakibyo Gakkai Zasshi 1989;86:1684–91.
105. Jovanovic I, Knezevic S, Micev M, et al. EUS mini probes in diagnosis of cystic dystrophy of duodenal wall in heterotopic pancreas: a case report. World J Gastroenterol 2004;10:2609–12.

106. Matsushita M, Hajiro K, Okazaki K, et al. Gastric aberrant pancreas: EUS analysis in comparison with the histology. Gastrointest Endosc 1999;49(4 Pt 1):493–7.
107. Oka R, Okai T, Kitakata H, et al. Heterotopic pancreas with calcification: a lesion mimicking leiomyosarcoma of the stomach. Gastrointest Endosc 2002;56:939–42.
108. Chak A. EUS in submucosal tumors. Gastrointest Endosc 2002;56(4 Suppl):S43–S48.
109. Schuhmacher C, Becker K, Dittler HJ, et al. Fibrovascular esophageal polyp as a diagnostic challenge. Dis Esophagus 2000;13:324–7.
110. Matsushita M, Okazaki K. Atypical EUS features of gastric inflammatory fibroid polyps. Gastrointest Endosc 2005; 61:637–8.
111. Watanabe T, Kato K, Sugitani M, et al. A case of solitary amyloidosis localized within the transverse colon presenting as a submucosal tumor. Gastrointest Endosc 1999; 49:644–7.
112. Roseau G, Dumontier I, Palazzo L, et al. Rectosigmoid endometriosis: endoscopic ultrasound features and clinical implications. Endoscopy 2000;32:525–30.
113. Franquemont DW. Differentiation and risk assessment of gastrointestinal stromal tumors. Am J Clin Pathol 1995; 103:41–7.
114. Graadt van Roggen JF, van Velthuysen ML, Hogendoorn PC. The histopathological differential diagnosis of gastrointestinal stromal tumours. J Clin Pathol 2001;54:96–102.
115. Miettinen M, Lasota J. Gastrointestinal stromal tumors: definition, clinical, histological, immunohistochemical, and molecular genetic features and differential diagnosis. Virchows Arch 2001;438:1–12.
116. Miettinen M, Lasota J. Gastrointestinal stromal tumors (GISTs): definition, occurrence, pathology, differential diagnosis and molecular genetics. Pol J Pathol 2003;54:3–24.
117. Blay JY, Bonvalot S, Casali P, et al. Consensus meeting for the management of gastrointestinal stromal tumors. Report of the GIST Consensus Conference of 20–21 March 2004, under the auspices of ESMO. Ann Oncol 2005; 16:566–78.
118. Nowain A, Bhakta H, Pais S, et al. Gastrointestinal stromal tumors: clinical profile, pathogenesis, treatment strategies and prognosis. J Gastroenterol Hepatol 2005;20:818–24.
119. Debiec-Rychter M, Lasota J, Sarlomo-Rikala M, et al. Chromosomal aberrations in malignant gastrointestinal stromal tumors: correlation with c-KIT gene mutation. Cancer Genet Cytogenet 2001;128:24–30.
120. Nickl NJ. Gastrointestinal stromal tumors: new progress, new questions. Curr Opin Gastroenterol 2004;20:482–7.
121. Strickland L, Letson GD, Muro-Cacho CA. Gastrointestinal stromal tumors. Cancer Control 2001;8:252–61.
122. Fletcher CD, Berman JJ, Corless C, et al. Diagnosis of gastrointestinal stromal tumors: a consensus approach. Hum Pathol 2002;33:459–65.
123. Okai T, Minamoto T, Ohtsubo K, et al. Endosonographic evaluation of *c-kit*-positive gastrointestinal stromal tumor. Abdom Imaging 2003;28:301–7.
124. Wiech T, Walch A, Werner M. Histopathological classification of nonneoplastic and neoplastic gastrointestinal submucosal lesions. Endoscopy 2005;37:630–4.
125. Miettinen M, Sarlomo-Rikala M, Sobin LH. Mesenchymal tumors of muscularis mucosae of colon and rectum are benign leiomyomas that should be separated from gastrointestinal stromal tumors: a clinicopathologic and immunohistochemical study of eighty-eight cases. Mod Pathol 2001;14:950–6.
126. Xu GQ, Zhang BL, Li YM, et al. Diagnostic value of endoscopic ultrasonography for gastrointestinal leiomyoma. World J Gastroenterol 2003;9:2088–91.
127. Miettinen M, Sarlomo-Rikala M, Sobin LH, et al. Esophageal stromal tumors: a clinicopathologic, immunohistochemical, and molecular genetic study of 17 cases and comparison with esophageal leiomyomas and leiomyosarcomas. Am J Surg Pathol 2000;24:211–22.
128. Calabrese C, Fabbri A, Fusaroli P, et al. Diffuse esophageal leiomyomatosis: case report and review. Gastrointest Endosc 2002;55:590–3.
129. Kuo MJ, Yeh HZ, Chen GH, et al. Diffuse esophageal leiomyomatosis with a pedunculated polyp. J Gastroenterol 2004;39:1205–9.
130. Palazzo L, Landi B, Cellier C, et al. Endosonographic features of esophageal granular cell tumors. Endoscopy 1997; 29:850–3.
131. Yazumi S, Takahashi R, Kajiyama T, et al. Comparison of histological analysis and endosonographic features in esophageal granular cell tumors. Dig Endosc 2003;15: 284–8.
132. Costa PM, Marques A, Tavora, et al. Inflammatory fibroid polyp of the esophagus. Dis Esophagus 2000;13:75–9.
133. Devereaux BM, Leblanc JK, Kesler K, et al. Giant fibrovascular polyp of the esophagus. Endoscopy 2003;35:970–2.
134. Aimoto T, Sasajima K, Kyono S, et al. Leiomyosarcoma of the esophagus: report of a case and preoperative evaluation by CT scan, endoscopic ultrasonography and angiography. Gastroenterol Jpn 1992;27:773–9.
135. Miettinen M, Sobin LH, Lasota J. Gastrointestinal stromal tumors of the stomach: a clinicopathologic, immunohistochemical, and molecular genetic study of 1765 cases with long-term follow-up. Am J Surg Pathol 2005;29: 52–68.
136. Kawamoto K, Yamada Y, Furukawa N, et al. Endoscopic submucosal tumorectomy for gastrointestinal submucosal tumors restricted to the submucosa: a new form of endoscopic minimal surgery. Gastrointest Endosc 1997;46: 311–7.
137. Nakazawa S, Yoshino J, Nakamura T, et al. Endoscopic ultrasonography of gastric myogenic tumor: a comparative study between histology and ultrasonography. J Ultrasound Med 1989;8:353–9.
138. Arantes V, Logrono R, Faruqi S, et al. Endoscopic sonographically guided fine-needle aspiration yield in submucosal tumors of the gastrointestinal tract. J Ultrasound Med 2004;23:1141–50.
139. Kawamoto K, Yamada Y, Utsunomiya T, et al. Gastrointestinal submucosal tumors: evaluation with endoscopic US. Radiology 1997;205:733–40.
140. Oda I, Kondo H, Yamao T, et al. Metastatic tumors to the stomach: analysis of 54 patients diagnosed at endoscopy and 347 autopsy cases. Endoscopy 2001;33:507–10.
141. Takahashi T, Otani Y, Yoshida M, et al. Gastric cancer mimicking a submucosal tumor diagnosed by laparoscopic excision biopsy. J Laparoendosc Adv Surg Tech A 2005; 15:51–6.
142. Inai M, Sakai M, Kajiyama T, et al. Endosonographic characterization of duodenal elevated lesions. Gastrointest Endosc 1996;44:714–9.
143. Soon MS, Lin OS. Inflammatory fibroid polyp of the duodenum. Surg Endosc 2000;14:86.

144. Miettinen M, Kopczynski J, Makhlouf HR, et al. Gastrointestinal stromal tumors, intramural leiomyomas, and leiomyosarcomas in the duodenum: a clinicopathologic, immunohistochemical, and molecular genetic study of 167 cases. Am J Surg Pathol 2003;27:625–41.
145. Fujishima H, Misawa T, Maruoka A, et al. Rectal carcinoid tumor: endoscopic ultrasonographic detection and endoscopic removal. Eur J Radiol 1993;16:198–200.
146. Matsumoto T, Iida M, Suekane H, et al. Endoscopic ultrasonography in rectal carcinoid tumors: contribution to selection of therapy. Gastrointest Endosc 1991;37:539–42.
147. Nakachi A, Miyazato H, Oshiro T, et al. Granular cell tumor of the rectum: a case report and review of the literature. J Gastroenterol 2000;35:631–4.
148. Miettinen M, Sarlomo-Rikala M, Sobin LH, et al. Gastrointestinal stromal tumors and leiomyosarcomas in the colon: a clinicopathologic, immunohistochemical, and molecular genetic study of 44 cases. Am J Surg Pathol 2000;24:1339–52.
149. Miettinen M, Furlong M, Sarlomo-Rikala M, et al. Gastrointestinal stromal tumors, intramural leiomyomas, and leiomyosarcomas in the rectum and anus: a clinicopathologic, immunohistochemical, and molecular genetic study of 144 cases. Am J Surg Pathol 2001;25:1121–33.
150. Brand B, Oesterhelweg L, Binmoeller KF, et al. Impact of endoscopic ultrasound for evaluation of submucosal lesions in gastrointestinal tract. Dig Liver Dis 2002;34: 290–7.
151. Nickl N, Gress F, McClave S, Fockens P, Chak A, Savides T, et al. Hypoechoic intramural tumor study: final report [abstract]. Gastrointest Endosc 2002;55:AB 98.
152. Nickl NJ, Behling C, McClave S, Chak A, Odegaard S, Rösch T, et al. Specific EUS features can identify hypoechoic masses which are not benign stromal cell tumors [abstract]. Gastrointest Endosc 1999;49[4 Part 2]:AB 211.
153. Palazzo L, Landi B, Cellier C, et al. Endosonographic features predictive of benign and malignant gastrointestinal stromal cell tumours. Gut 2000;46:88–92.
154. Hur BW, Chun HJ, Kang CD, Lee JW, Jeen YT, Song CW, et al. Reassessment of usefulness of EUS in differentiation of benign and malignant gastric stromal tumors which were diagnosed according to pathologic guidelines of Ackerman's surgical pathology [abstract]. Gastrointest Endosc 2000;51(4 Part 2):AB 215.
155. Wiersema MJ, Vilmann P, Giovannini M, et al. Endosonography-guided fine-needle aspiration biopsy: diagnostic accuracy and complication assessment. Gastroenterology 1997;112:1087–95.
156. Williams DB, Sahai AV, Aabakken L, et al. Endoscopic ultrasound guided fine needle aspiration biopsy: a large single centre experience. Gut 1999;44:720–6.
157. Dong Q, McKee G, Pitman M, et al. Epithelioid variant of gastrointestinal stromal tumor: Diagnosis by fine-needle aspiration. Diagn Cytopathol 2003;29:55–60.
158. Li SQ, O'Leary TJ, Buchner SB, et al. Fine needle aspiration of gastrointestinal stromal tumors. Acta Cytol 2001;45: 9–17.
159. Hunt GC, Rader AE, Faigel DO. A comparison of EUS features between CD-117 positive GI stromal tumors and CD-117 negative GI spindle cell tumors. Gastrointest Endosc 2003;57:469–74.
160. Rader AE, Avery A, Wait CL, et al. Fine-needle aspiration biopsy diagnosis of gastrointestinal stromal tumors using morphology, immunocytochemistry, and mutational analysis of *c-kit*. Cancer 2001;93:269–75.
161. Wieczorek TJ, Faquin WC, Rubin BP, et al. Cytologic diagnosis of gastrointestinal stromal tumor with emphasis on the differential diagnosis with leiomyosarcoma. Cancer 2001;93:276–87.
162. Acs G, McGrath CM, Gupta PK. Duodenal carcinoid tumor: report of a case diagnosed by endoscopic ultrasound-guided fine-needle aspiration biopsy with immunocytochemical correlation. Diagn Cytopathol 2000;23:183–6.
163. Liu K, Madden JF, Olatidoye BA, et al. Features of benign granular cell tumor on fine needle aspiration. Acta Cytol 1999;43:552–7.
164. Caletti GC, Brocchi E, Ferrari A, et al. Guillotine needle biopsy as a supplement to endosonography in the diagnosis of gastric submucosal tumors. Endoscopy 1991;23: 251–4.
165. Levy MJ, Jondal ML, Clain J, et al. Preliminary experience with an EUS-guided trucut biopsy needle compared with EUS-guided FNA. Gastrointest Endosc 2003;57:101–6.
166. Nesje LB, Laerum OD, Svanes K, et al. Subepithelial masses of the gastrointestinal tract evaluated by endoscopic ultrasonography. Eur J Ultrasound 2002;15:45–54.
167. Wallace MB, Hoffman BJ, Sahai AS, et al. Imaging of esophageal tumors with a water-filled condom and a catheter US probe. Gastrointest Endosc 2000;51:597–600.
168. Chang KJ, Yoshinaka R, Nguyen P. Endoscopic ultrasound-assisted band ligation: a new technique for resection of submucosal tumors. Gastrointest Endosc 1996;44:720–2.
169. Shim CS, Jung IS. Endoscopic removal of submucosal tumors: preprocedure diagnosis, technical options, and results. Endoscopy 2005;37:646–54.
170. Kajiyama T, Hajiro K, Sakai M, et al. Endoscopic resection of gastrointestinal submucosal lesions: a comparison between strip biopsy and aspiration lumpectomy. Gastrointest Endosc 1996;44:404–10.
171. Yasuda I, Tomita E, Nagura K, et al. Endoscopic removal of granular cell tumors. Gastrointest Endosc 1995;41:163–7.
172. Wehrmann T, Martchenko K, Nakamura M, et al. Endoscopic resection of submucosal esophageal tumors: a prospective case series. Endoscopy 2004;36:802–7.
173. Park YS, Park SW, Kim TI, et al. Endoscopic enucleation of upper-GI submucosal tumors by using an insulated-tip electrosurgical knife. Gastrointest Endosc 2004;59: 409–15.
174. Rösch T, Sarbia M, Schumacher B, et al. Attempted endoscopic en bloc resection of mucosal and submucosal tumors using insulated-tip knives: a pilot series. Endoscopy 2004;36:788–801.
175. Inoue H, Takeshita K, Hori H, et al. Endoscopic mucosal resection with a cap-fitted panendoscope for esophagus, stomach, and colon mucosal lesions. Gastrointest Endosc 1993;39:58–62.
176. Sahai AV, Siess M, Kapfer B, et al. Endoscopic ultrasonography for upper gastrointestinal submucosal lesions: a cost minimization analysis with an international perspective. Am J Gastroenterol 2003;98:1989–95.
177. Matsuki M, Gouda Y, Ando T, et al. Adenocarcinoma arising from aberrant pancreas in the stomach. J Gastroenterol 2005;40:652–6.
178. Green PH, Barratt PJ, Percy JP, et al. Acute pancreatitis occurring in gastric aberrant pancreatic tissue. Am J Dig Dis 1977;22:734–40.

179. Matsushita M, Hajiro K, Takakuwa H. Acute pancreatitis occurring in gastric aberrant pancreas accompanied by paralytic ileus. Am J Gastroenterol 1997;92:2121–2.
180. Meining A, Rösch T, Taffanek M, Kapfer B, Lorenz R, Allescher HD, et al. Endosonographic follow-up of upper GI submucosal tumors: does it change management? [abstract]. Gastrointest Endosc 2000;51(4 Part 2):AB 162.
181. Melzer E, Fidder H. The natural course of upper gastrointestinal submucosal tumors: an endoscopic ultrasound survey. Isr Med Assoc J 2000;2:430–2.
182. Sato T, Peiper M, Fritscher-Ravens A, et al. Strategy of treatment of submucosal gastric tumors. Eur J Med Res 2005;10:292–5.
183. Nickl NJ, Wackerbarth S, Gresse F, Fockens P, McClave S, Chak A, et al. Management of hypoechoic intramural tumors: a decision tree analysis of EUS-directed vs. surgical management [abstract]. Gastrointest Endosc 2000;51(4 Part 2):AB 176.
184. Futagami K, Hata J, Haruma K, et al. Extracorporeal ultrasound is an effective diagnostic alternative to endoscopic ultrasound for gastric submucosal tumours. Scand J Gastroenterol 2001;36:1222–6.
185. Polkowski M, Palucki J, Butruk E. Transabdominal ultrasound for visualizing gastric submucosal tumors diagnosed by endosonography: can surveillance be simplified? Endoscopy 2002;34:979–83.
186. Tsai TL, Changchien CS, Hu TH, et al. Demonstration of gastric submucosal lesions by high-resolution transabdominal sonography. J Clin Ultrasound 2000;28:125–32.

15 Endosonographic Diagnosis and Treatment Planning in Gastrointestinal Lymphoma

W. Fischbach

Introduction

The gastrointestinal tract is by far the most frequent site of manifestation for extranodal non-Hodgkin's lymphomas (NHLs). Primary gastrointestinal lymphomas are today regarded as an independent entity, and there are differences between gastric lymphomas and intestinal lymphomas with regard to etiology, histomorphology, and clinical course. The World Health Organization (WHO) classification, dating from 2002 (Table 15.1), deliberately avoids classification into low-grade and high-grade NHL [1]. However, a distinction of this type would still be useful from the clinical point of view. In its present form, the classification does take account of the fact that there is no conclusive evidence for the existence of a sequential development of high-grade lymphomas from low-grade ones.

More than 70% of primary gastrointestinal NHLs present as gastric lymphomas. In terms of numbers, marginal-zone B-cell lymphomas of the mucosa-associated lymphoid tissue (MALT) type are predominant. The majority of intestinal lymphomas, which represent up to 20–30% of cases, are high-grade B-cell and T-cell lymphomas. Colonic lymphomas are a rarity, at 2%. Multiple-organ involvement in the gastrointestinal tract is seen in some 6% of cases [2]. The etiopathogenetic significance of *Helicobacter pylori* infection for the development of gastric lymphoma is well established, with convincing data from epidemiological, morphological, and molecular-biological studies, as well as animal experiments [3]. These insights have led to the use of eradication therapy as the treatment of first choice in patients with stage I low-grade lymphoma and as part of the initial staging procedure. Mucosal immune-regulatory changes resulting from untreated gluten-sensitive celiac disease or chronic infections, as well as congenital or acquired immune-deficiency syndromes, are recognized risk factors for intestinal lymphomas.

Table 15.1 World Health Organization classification of gastrointestinal non-Hodgkin's lymphomas [1]

B-cell lymphomas
Marginal-zone B-cell lymphoma of the MALT type
Follicular lymphoma (grades I–III)
Mantle-cell lymphoma (lymphomatous polyposis)
Diffuse large B-cell lymphoma with/without MALT-type components
Burkitt's lymphoma
Immune deficiency–associated lymphoma
T-cell lymphomas
Enteropathy-associated T-cell lymphoma (EATCL)
Peripheral T-cell-lymphoma (non-EATCL)

MALT: mucosa-associated lymphoid tissue.

Clinical Presentation

The clinical picture of gastrointestinal lymphomas in nonspecific. It is characterized by abdominal discomfort, pain, vomiting, diarrhea, weight loss, and manifest or occult bleeding. However, gastric lymphomas are also quite often an incidental finding at endoscopy. In general, it can be stated that complications such as obstruction, perforation, or bleeding are observed more frequently in intestinal lymphomas than in gastric lymphomas—which may in part be due to the fact that diagnosing them is more difficult and consequently takes place later.

Diagnosis and Staging

The diagnostic procedure focuses on two aspects:

- Precise histological classification and typing of the lesion (low-grade, secondary high-grade, high-grade)
- The accuracy of clinical staging

These are the two decisive prognostic factors and determinants of treatment [4,5]. Careful endoscopic and biopsy diagnosis and accurate staging are the essential prerequisite for adequate treatment.

Gastric lymphomas are accessible to endoscopic viewing. Esophagogastroduodenoscopy is therefore of the utmost importance for the diagnosis. In view of the nonspecific appearance of gastric lymphomas [6] and potential sources of error in diagnostic work-up with endoscopy and biopsy (with discrepancies between the endoscopy and biopsy diagnosis and the definitive classification based on the surgical specimen in up to 26% of cases [7]), biopsy methods involving what is known as gastric mapping are required. This means:

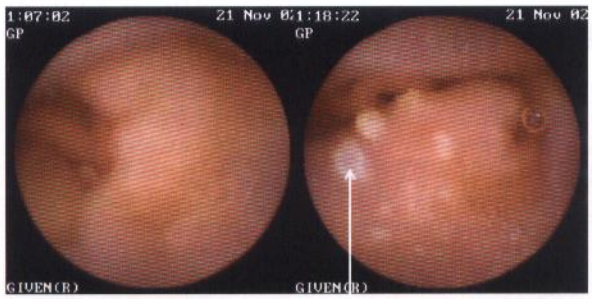


Fig. 15.1 Capsule endoscopy, demonstrating normal mucosa and a follicular lymphoma (arrow).

- Taking 8–10 biopsies from suspicious areas
- Four-quadrant biopsies from normal-appearing mucosa in the antrum and gastric body
- Two biopsies from the fundus
- Rapid urease testing in the antrum and gastric body.

This procedure ensures adequate histological, immunohistochemical, and molecular-biological diagnosis. As in the diagnosis of dysplasia, a second expert opinion from one of the reference centers in the lymphoma network should be always obtained. There are two consequences for everyday routine work. Firstly, the gastric mapping procedure usually requires a second endoscopy examination, since a biopsy technique of this type is not usually carried out during the initial investigation. Secondly, *H. pylori* eradication therapy should be postponed until the findings from the reference histology are available, since previous antibacterial treatment often makes a definitive diagnosis of lymphoma more difficult, or even impossible.

The particular difficulty with intestinal lymphomas lies in the limited endoscopic and biopsy access that is possible. This often means that exploratory laparoscopy or laparotomy is needed to establish the diagnosis, with a biopsy encompassing the whole wall—assuming that complications such as bleeding or perforation do not make emergency surgery necessary in any case.

It is to be hoped that new methods such as double-balloon enteroscopy and capsule endoscopy (Fig. 15.**1**) will in the future allow improved noninvasive methods of diagnosing intestinal NHLs. In addition, capsule endoscopy makes it possible to identify the intestinal manifestation expected in some 6% of cases of gastric lymphoma when there is multiple-organ gastrointestinal involvement [2]. We are currently testing this in a prospective study in which all patients with newly diagnosed gastric lymphomas undergo capsule endoscopy during the staging process.

If a diagnosis of gastrointestinal lymphoma is established, various examinations follow to allow assessment of the spread of the lymphoma ("staging"):

- Endoscopic ultrasonography (EUS)
- Ileocolonoscopy
- Radiographic small-bowel double-contrast imaging or Sellink magnetic resonance imaging
- Cervical and abdominal ultrasonography
- Computed tomography of the chest and abdomen
- Cytological and histological assessment of a bone-marrow puncture

For staging, the Ann Arbor classification is still used, with Musshoff's modification and taking the Radaszkiewicz subclassification of stage I into account (Table 15.**2**). It would be desirable for the Paris staging system to become established [8], as it is more modern, is based on the TNM classification, and better reflects the specific characteristics of gastrointestinal lymphomas [8].

■ Relevance of EUS

The prognostic relevance of the subclassification of stages I and II into stage I1, I2, and II1 (Table 15.**2**) has been confirmed [5]. Avoiding surgical resection by determining the histopathological stage can be only achieved with EUS, as it is the only imaging procedure that makes it possible to differentiate the gastric wall

Table 15.**2** Staging of primary gastrointestinal lymphomas

Ann Arbor system	Lugano system	TNM classification	Spread of lymphoma
E* I 1	I 1	T1 N0 M0	Mucosa, submucosa
E I 2	I 2	T2 N0 M0	Muscularis propria, subserosa
E I 2	I 2	T3 N0 M0	Serosal penetration
E I 2	II E**	T4 N0 M0	Infiltration of adjacent organs or tissues
E II 1	II 1 E	T1–4 N1 M0	Infiltration of regional lymph nodes (compartments I+II)
E II 2	II 1 E	T1–4 N2 M0	Infiltration of lymph nodes beyond the regional stations (compartment III), including retroperitoneal, mesenterial and para-aortic lymph nodes
III	–	T1–4 N3 M0	Infiltration of infradiaphragmatic and supradiaphragmatic lymph nodes
IV	IV	T1–4 N0–3 M1	Dissemination of the lymphoma

* E: primary extranodal location. ** E: infiltration of adjacent organs in continuity.

layers and that visualizes perigastric lymph nodes. EUS is therefore an essential part of the staging procedure for gastric lymphomas. What does it show? How good is it?

The endosonographic appearance of gastric lymphomas varies depending on their shape. They may present as focal nodular infiltration of the mucosa (Fig. 15.**2**) or as diffuse, circumscribed mucosal thickening (Fig. 15.**3a**). In the latter case, the normal structure of the gastric wall in the antrum (Fig. 15.**3b**) can be clearly distinguished from the lymphoma in the gastric body. A mixed appearance, with thickened mucosa and focal loss of the normal gastric wall layers, can sometimes be seen (Fig. 15.**4**). Tumor growth through all of the wall layers (Fig. 15.**5**) is characteristic of stage I2 or T3 (Table 15.**2**); infiltration of adjacent organs or tissues (Fig. 15.**6**) represents stage I2 or T4; and involvement of perigastric lymph nodes (Fig. 15.**7**) represents stage II1 or T1–4N1.

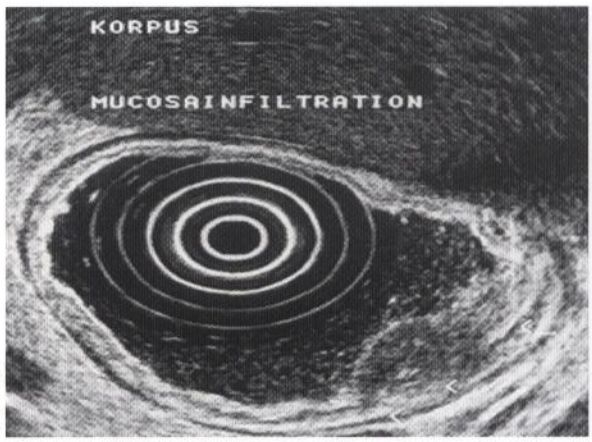
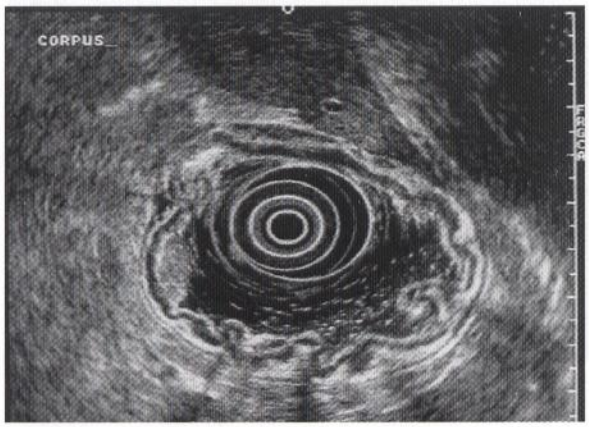


Fig. 15.**2** Focal nodular infiltration of the gastric mucosa by a marginal-zone B-cell lymphoma of the MALT type (stage I1 or T1)



a



b

Fig. 15.**3a** Circumscribed mucosal thickening of the gastric body by a marginal-zone B-cell lymphoma of MALT type (stage I1 or T1). **b** Normal gastric wall findings in the antrum.



Fig. 15.**4** Thickened mucosa (right) and focal loss of the normal gastric wall layers (left) due to a marginal-zone B-cell lymphoma of MALT type (stage I2 or T2).

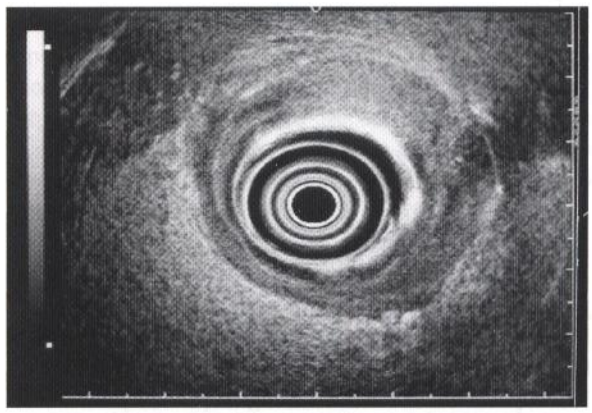
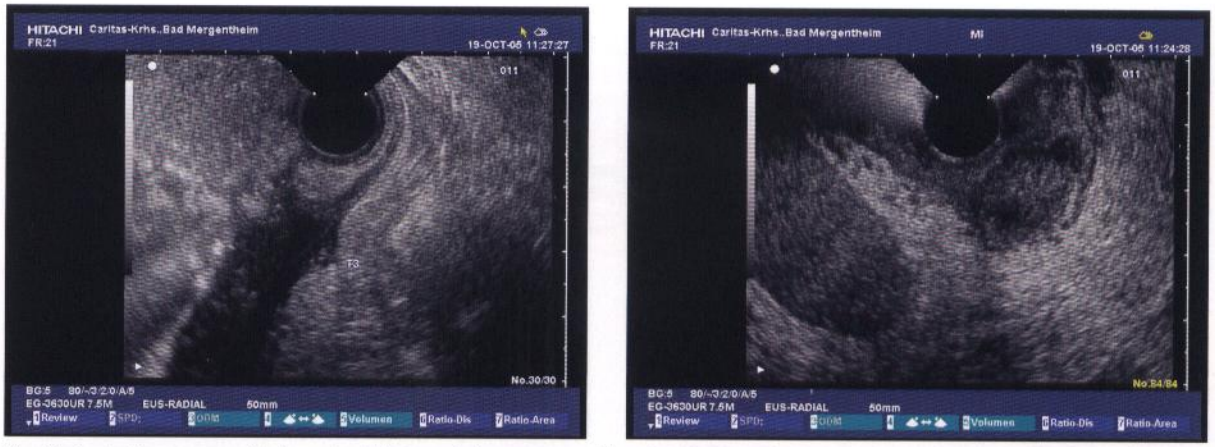


Fig. 15.**5** Circular growth through all layers of the gastric wall by a marginal-zone B-cell lymphoma of MALT type (T3 here). Note the relationship of the tumor to the muscularis layer.



a b

Fig. 15.**6a, b** Tumor growth through all layers of the gastric wall and continuous infiltration of adjacent tissues by a diffuse large B-cell lymphoma (final diagnosis stage T4).



a b

Fig. 15.**7a, b** Involvement of three perigastric lymph nodes by a diffuse large B-cell lymphoma.

EUS has been regarded as the best method for local staging of gastric carcinoma for quite some time [9]. However, the endosonographic data on gastric lymphoma are in fact scarce and are mainly derived from a few prospective studies including only small numbers of patients [10,11]. In the first German–Austrian multicenter study on gastrointestinal lymphoma, all patients with gastric lymphoma in stages I and II (except those undergoing exclusive *H. pylori* eradication therapy) were referred for surgical resection [7]. This made it possible to compare the diagnostic accuracy of preoperative EUS with the gold standard of the histopathological staging in a large series [12]. At first sight, the results are disappointing. EUS correctly classified the lymphoma in 37 of 70 patients (53%). The sensitivity of EUS in assessing the depth of lymphoma infiltration (59%) and lymph-node status (71%) were unsatisfactory. The explanation for these findings is probably the multicenter nature of the study, which included 34 centers at a time (in the mid-1990s) when experience with EUS was still generally limited. Increasing experience, technical improvements such as the use of mini-echoendoscopes, and EUS-guided biopsies of perigastric lymph nodes have since improved the accuracy of EUS. Definitive data are still lacking, however, and will probably remain so in view of the current trend toward nonsurgical treatment methods for gastric lymphomas. For the same reason, studies in which EUS was used to evaluate the longitudinal lymphoma infiltration and to determine the margins for partial resection of the stomach can now be regarded as historical.

Since conservative treatment strategies are now preferred, assessing the response to radiotherapy and chemotherapy is a new challenge for EUS in the future. Sackmann and co-workers have shown that the regression of lymphoma after successful eradication of *H. pylori* can be reliably predicted by EUS [13], and this finding has been confirmed by a Japanese group [14]. It remains to be seen whether the use of miniprobes will be capable of providing more precise information on the depth of lymphoma infiltration in comparison with conventional EUS. EUS is of course not indicated in intestinal lymphomas.

■ Treatment Planning

In patients with stage I MALT lymphoma, *H. pylori* eradication is the initial treatment of choice. It leads to complete remission of the lymphoma in some 80% of cases [3]. There was some doubt for a considerable period as to whether this does in fact represent long-term treatment success. However, long-term follow-up reports have now been published that impressively demonstrate that this is indeed the case and suggest that *H. pylori* eradication provides a genuine chance of a cure in the majority of these patients [15].

Most recently, it has also emerged that patients with minimal residual disease after successful eradication therapy—i. e., normalization of the endoscopic findings but persistent residual lymphoma on histology—also have a favorable prognosis [16]. In these patients, a "watch-and-wait" strategy, with regular endoscopic and biopsy check-ups (every 3 months in the first 2 years, then 6-monthly, and then annually after 5 years) is a well-justified approach, particularly since all of the other treatment options still remain open.

Patients with *H. pylori*–negative recurrence of stage I gastric MALT lymphoma, with an initially negative *H. pylori* status (including serological findings), and all patients in stage II are referred for radiotherapy. This is probably as effective as surgical resection [17], as the preliminary results of a prospective randomized study in Germany have suggested, while preserving the organ and thus offering a better quality of life. Radiotherapy is now usually carried out using the method of extended-field irradiation at a dosage of 30 Gy, with local saturation of the tumor region at 10 Gy. In patients in stage II, an abdominal bath is preferred in some centers, although this is associated with a much higher level of toxicity.

In the rare cases (maximum 10%) of MALT lymphomas in advanced stages III and IV, treatment measures are in principle questionable, in view of the lack of a curative approach, the often mild clinical symptoms, and the slowness of tumor progression. If an active approach is decided on, common chemotherapeutic agents such as chlorambucil or combination protocols such as cyclophosphamide, hydroxydaunorubicin (doxorubicin, adriamycin), Oncovin (vincristine), and prednisone *(CHOP), and recently also fludarabine, may be considered. There is no standard treatment in this situation. Chemotherapy* is the undisputed treatment of choice for high-grade lymphomas in all stages. CHOP-21 or CHOP-14, with or without growth factors, can still be regarded as the standard here. Following chemotherapy, involved-field radiotherapy at a dosage of 36–40 Gy has so far been generally recommended, although chemotherapy alone can certainly claim to be curative.

Surgical resection of gastric lymphomas is reserved for complications such as bleeding or perforation, or may provide an alternative to radiotherapy if the patient requests it.

Table 15.**3** Stage-adapted treatment strategies in low-grade gastric lymphomas (MALT) and high-grade gastric lymphomas (diffuse large B-cell with or without MALT components) gastric lymphomas (grade of evidence)

Stage	Low-grade (MALT lymphoma)	High-grade (diffuse large B-cell lymphoma with/without MALT components)
I1 (T2N0M0)	*H. pylori* eradication (IIa)	Chemotherapy ± radiation (IIa)
I2 (T2N0M0)	*H. pylori* eradication (III)	Chemotherapy ± radiation (IIa)
I1–2 (T1–2N0M0)*	Radiation (surgery) (IIa)	
I1–2 (T1–2N0M0 MRD)	Watch and wait (IV)	
II1–2 (T1–4N1–2M0)	Radiation (surgery) (IIa)	Chemotherapy ± radiation (IIa)
III (T1–4N3M0)	Chemotherapy (IIa)	Chemotherapy ± radiation (IIa)
IV (T1–4N0–3M1)	Chemotherapy (IIa)	Chemotherapy ± radiation (IIa)

MRD: minimal residual disease.
Surgery only in cases of complications or at the patient's request.
* *H. pylori*–negative, no response to eradication therapy, recurrences.

The current treatment recommendations for gastric lymphoma are summarized in Table 15.**3**. Clearly defined treatment recommendations such as those outlined for gastric lymphomas are not yet available for intestinal lymphomas.

References

1. Jaffe ES, Harris NL, Stein H, Vardiman JW, eds. Pathology and genetics of tumours of haematopoetic and lymphoid tissues. Lyons: IARC Press, 2002. (World Health Organization classification of tumours, 3.)
2. Koch P, del Valle F, Berdel WE, Willich NA, Reers B, Hiddemann W, et al. Primary gastrointestinal non-Hodgkin's lymphoma, 1: anatomic and histologic distribution, clinical features, and survival data of 371 patients registered in the German Multicenter Study GIT NHL 01/92. J Clin Oncol 2001;19:3861–73.
3. Fischbach W. [Gastrointestinal lymphoma: etiology, pathogenesis and therapy; in German.] Internist (Berl) 2000; 41:831–40.
4. Cogliatti SB, Schmid U, Schumacher U, Eckert F, Hansmann ML, Hedderich J, et al. Primary B-cell gastric lymphoma: a clinicopathological study of 145 patients. Gastroenterology 1991;101:1159–70.
5. Radaszkiewicz T, Dragosics B, Bauer P. Gastrointestinal malignant lymphomas of the mucosa-associated lymphoid tissue: factors relevant to prognosis. Gastroenterology 1992; 102:1628–38.

6. Kolve M, Fischbach W, Greiner A, Wilms K. Differences in endoscopic and clinicopathological features of primary and secondary gastric non-Hodgkin's lymphoma. Gastrointestinal Lymphoma Study Group. Gastrointest Endosc 1999; 49:307–15.
7. Fischbach W, Dragosics B, Kolve-Goebeler ME, Ohmann C, Greiner A, Yang Q, et al. Primary gastric B-cell lymphoma: results of a prospective multicenter study. The German-Austrian Gastrointestinal Lymphoma Study Group. Gastroenterology 2000;119:1191–202.
8. Ruskone-Fourmestraux A, Dragosics B, Morgner A, Wotherspoon A, De Jong D. Paris staging system for primary gastrointestinal lymphomas. Gut 2003;52:912–3.
9. Caletti G, Fusaroli P, Bocus P. Endoscopic ultrasonography. Digestion 1998;59:509–29.
10. Palazzo L, Roseau G, Ruskone-Fourmestraux A, Rougier P, Chaussade S, Rambaud JC, et al. Endoscopic ultrasonography in the local staging of primary gastric lymphoma. Endoscopy 1993;25:502–8.
11. Schüder G, Hildebrandt U, Kreissler-Haag D, Seitz G, Feifel G. Role of endosonography in the surgical management of non-Hodgkin's lymphoma of the stomach. Endoscopy 1993;25:509–12.
12. Fischbach W, Goebeler-Kolve ME, Greiner A. Diagnostic accuracy of EUS in the local staging of primary gastric lymphoma: results of a prospective, multicenter study comparing EUS with histopathologic stage. Gastrointest Endosc 2002;56:696–700.
13. Sackmann M, Morgner A, Rudolph B, Neubauer A, Thiede C, Schulz H, et al. Regression of gastric MALT lymphoma after eradication of *Helicobacter pylori* is predicted by endosonographic staging. MALT Lymphoma Study Group. Gastroenterology 1997;113:1087–90.
14. Nakamura S, Matsumoto T, Suekane H, Takeshita M, Hizawa K, Kawasaki M, et al. Predictive value of endoscopic ultrasonography for regression of gastric low grade and high grade MALT lymphomas after eradication of *Helicobacter pylori*. Gut 2001;48:454–60.
15. Fischbach W, Goebeler-Kolve ME, Dragosics B, Greiner A, Stolte M. Long term outcome of patients with gastric marginal zone B cell lymphoma of mucosa-associated lymphoid tissue (MALT) following exclusive *Helicobacter pylori* eradication therapy: experience from a large prospective series. Gut 2004;53:34–7.
16. Fischbach W, Goebeler-Kolve M, Starostik P, Greiner A, Muller-Hermelink HK. Minimal residual low-grade gastric MALT-type lymphoma after eradication of *Helicobacter pylori*. Lancet 2002;360:547–8.
17. Koch P, del Valle F, Berdel WE, Willich NA, Reers B, Hiddemann W, et al. Primary gastrointestinal non-Hodgkin's lymphoma, 2: combined surgical and conservative or conservative management only in localized gastric lymphoma—results of the prospective German Multicenter Study GIT NHL 01/92. J Clin Oncol 2001;19:3874–83

16 Endoscopic Ultrasound in Chronic Pancreatitis

C. Jenssen, C.F. Dietrich

■ Difficulties in Diagnosing Chronic Pancreatitis

Establishing a definite diagnosis of chronic pancreatitis is a challenging task. The definition of the diagnosis itself is already problematic—for example, it is often not possible to differentiate clearly between recurrent attacks of acute pancreatitis and the early stages of chronic pancreatitis. The history and presenting symptoms may be nonspecific, which may result in up to 4 of 10 patients being initially misdiagnosed as "nonspecific dyspepsia" [1]. The correct diagnosis of chronic pancreatitis is, on average, only made 60 months after the original presentation [2]. Simple pancreatic function tests (e.g., fecal pancreatic elastase) and widely available noninvasive imaging methods such as abdominal ultrasonography and computed tomography (CT) are not sufficiently sensitive to diagnose the early stages of chronic pancreatitis. Percutaneous biopsy of the pancreas can be used to confirm a suspected diagnosis of chronic pancreatitis. However, it is a very invasive method, and since the extent of disease may vary widely within different areas of the pancreas, it may not necessarily be diagnostic. Its routine use is not recommended. Up to now, a combination of endoscopic retrograde cholangiopancreatography (ERCP) and the secretin-pancreozymin test have been regarded as the reference standard for diagnosing chronic pancreatitis [3]. However, ERCP does carry a considerable procedural risk, is unpleasant for the patient, and it is very expensive [4–6]. Magnetic resonance cholangiopancreatography (MRCP) is so far not being used routinely, but it appears to be a promising method for the future [7].

In chronic pancreatitis, functional deficits, morphological changes, and the degree of pain are not always closely correlated. The extent of changes in the pancreatic duct system and the extent of impairment of the exocrine function correlate closely in only about three-quarters to four-fifths of patients [2,8]. There are patients with severely damaged pancreatic ducts who have normal exocrine and endocrine pancreatic function, and some of these patients may be completely asymptomatic for years. In contrast, clinically significant impairment of pancreatic function does not have to be associated with severe ductal changes. Some 5–10% of patients with chronic pancreatitis are initially pain-free and only develop symptoms later on due to endocrine and exocrine dysfunction [2,4,8].

It is difficult to judge the significance of mild or early changes in the pancreatic duct system and the pancreatic parenchyma, particularly because the normal appearance of the pancreas already varies widely with age. It may also be impossible to differentiate early chronic pancreatitis from scarring after acute pancreatitis, and from asymptomatic fibrosis of the pancreas [3–5,9].

In up to 30% of cases of chronic pancreatitis or recurrent acute pancreatitis, it is not possible to determine the etiology of the disease, despite a detailed history and extensive investigations [8,10]. Even if a diagnosis of chronic pancreatitis is established, it may still be difficult to determine the exact nature of focal cystic or solid changes within the pancreas [11].

The following imaging methods are available for diagnosing chronic pancreatitis and its complications:

- Radiographic methods: plain radiography, computed tomography (CT).
- Magnetic resonance imaging (MRI), magnetic resonance cholangiopancreatography (MRCP).
- Endoscopic methods: endoscopic retrograde cholangiopancreatography (ERCP), endoscopic ultrasonography (EUS).
- Abdominal ultrasonography (US), possibly with color-coded duplex sonography (CCDS). Chronic pancreatitis can be diagnosed with abdominal ultrasound in accordance with the criteria used in the Cambridge classification. This classification uses a combination of diagnostic criteria, each of which in itself is nonspecific (Table 16.**1**) [2,5,12,13].

In contrast to ERCP, which only allows investigation of the ductal system, ultrasound allows visualization of both the ductal system and of the pancreatic parenchyma. In addition, it is noninvasive, the patient is not exposed to roentgen rays, and, at least in theory, ultrasound should also be able to detect any complications of chronic pancreatitis, particularly if it is used with CCDS [13–19]. However, in comparison with the reference standard of ERCP and the secretin–pancreozymin test, the sensitivity of abdominal ultrasound is relatively low (60–70%), to a large extent probably due to the retroperitoneal location of the pancreas [5,16,20]. The sensitivity of abdominal ultrasound is particularly low for diagnosing the early stages of chronic pancreatitis.

Table 16.1 The Cambridge classification of chronic pancreatitis for endoscopic retrograde cholangiopancreatography (ERCP) and abdominal ultrasonography/computed tomography (CT) [12,13]. (Adapted from Glasbrenner et al. [5] and Lankisch [2])

Stage	ERCP	Abdominal ultrasonography, CT
Normal (0)	No pathological changes; good quality study of the entire pancreatic duct system must be obtained	No pathological changes (main pancreatic duct < 2 mm, homogeneous parenchymal structure, normal size and shape)
Uncertain (1)	Normal main pancreatic duct, pathological changes in less than three side branches	One pathological change: • Main pancreatic duct 2–4 mm • Pancreas enlarged (up to twice normal size)
Mild (2)	Normal main pancreatic duct, pathological changes in more than three side branches	Two or more pathological changes: • Cysts < 10 mm • Irregular main pancreatic duct • Focal acute pancreatitis • Heterogeneous parenchymal structure • Hyperechoic pancreatic duct wall • Contour irregularities (pancreatic head or body)
Moderate (3)	As "mild", plus abnormal main pancreatic duct	All of the criteria mentioned above
Severe (4)	As "moderate", plus one or more of the following changes: • Cysts > 10 mm • Pancreas more than twice the normal size • Intraductal filling defects • Pancreatic duct calculi/calcifications • Duct obstruction (stricture) • Severe dilation or irregularities of the main pancreatic duct • Involvement of adjacent organs (ultrasound, CT)	

■ Endosonography of the Pancreas

In virtually all patients with normal upper gastrointestinal anatomy, EUS makes it possible to visualize the entire pancreas, the neighboring blood vessels, and the common bile duct from various scanning positions in the stomach and duodenum. This is not possible with abdominal ultrasound, and the local resolution provided by the endosonographic images is unsurpassed by any other imaging method. Despite there being some technical differences, this applies to both radial and curvilinear endosonography [9,21–24]. The large majority of published data were obtained with mechanical radial scanning echoendoscopes with a transducer frequency of 7.5 MHz. In addition, electronic curvilinear, and more recently electronic radial, scanning echoendoscopes also allow visualization of the large vessels adjacent to the pancreas with CCDS, and, by using ultrasound contrast enhancement, they may show perfusion as well as pathological changes within the parenchyma of the pancreas [25–31].

Because of the anatomical position of the stomach, the endosonographic appearance of the pancreas when viewed with a curvilinear-array transducer resembles its appearance when viewed with abdominal ultrasound. In addition, it is possible to view different planes of the pancreatic head by positioning the transducer in the duodenum [22,24,32] (Fig. 16.**1**).

In contrast to ERCP, with endosonography it is not only possible to view changes in the pancreatic duct, but changes in the parenchyma can also be taken into account for diagnostic considerations. The procedural risk of EUS is, however, much lower than that of ERCP. Limitations may arise, as with ERCP, in patients with pyloric stenoses or after surgery, particularly after complete resection of the stomach.

The normal endosonographic appearance of the pancreas is characterized by specific criteria for size, contour, parenchyma, and ducts (Table 16.**2**) [9, 22, 24, 33, 34]. However, since the imaging planes are less standardized than in CT, for example, the diameter of the pancreatic head has limited diagnostic significance.

To be able to diagnose pathological changes in the pancreas, it is also important to be aware of normal anatomical variants. For example, the width of the pancreatic duct and the echogenicity of the parenchyma increase with age [9,35]. Hyperechogenicity in the pancreatic parenchyma has been observed in about 25% of EUS investigations and was found to be related to age, to a higher body mass index, and to the absence of chronic pancreatitis [34]. In addition, the ventral part (the embryological "ventral anlage") of the pancreas sonographically appears as a variably well demarcated hypoechoic structure situated in the dorsal and inferior part of the pancreatic head, and may be detected in about 75% of patients undergoing EUS for nonpancreatic indications [22,36]. Detection of the ventral anlage on EUS is less likely in patients with diabetes mellitus, with the sonographic features of chronic pancreatitis, with a mass lesion in the pancreatic head, or with pancreas divisum [36–38] (Fig. 16.**2**).

With some experience, it is also possible to diagnose anatomical variants of the pancreatic duct. Pancreas divisum is present if the course of the pancreatic duct

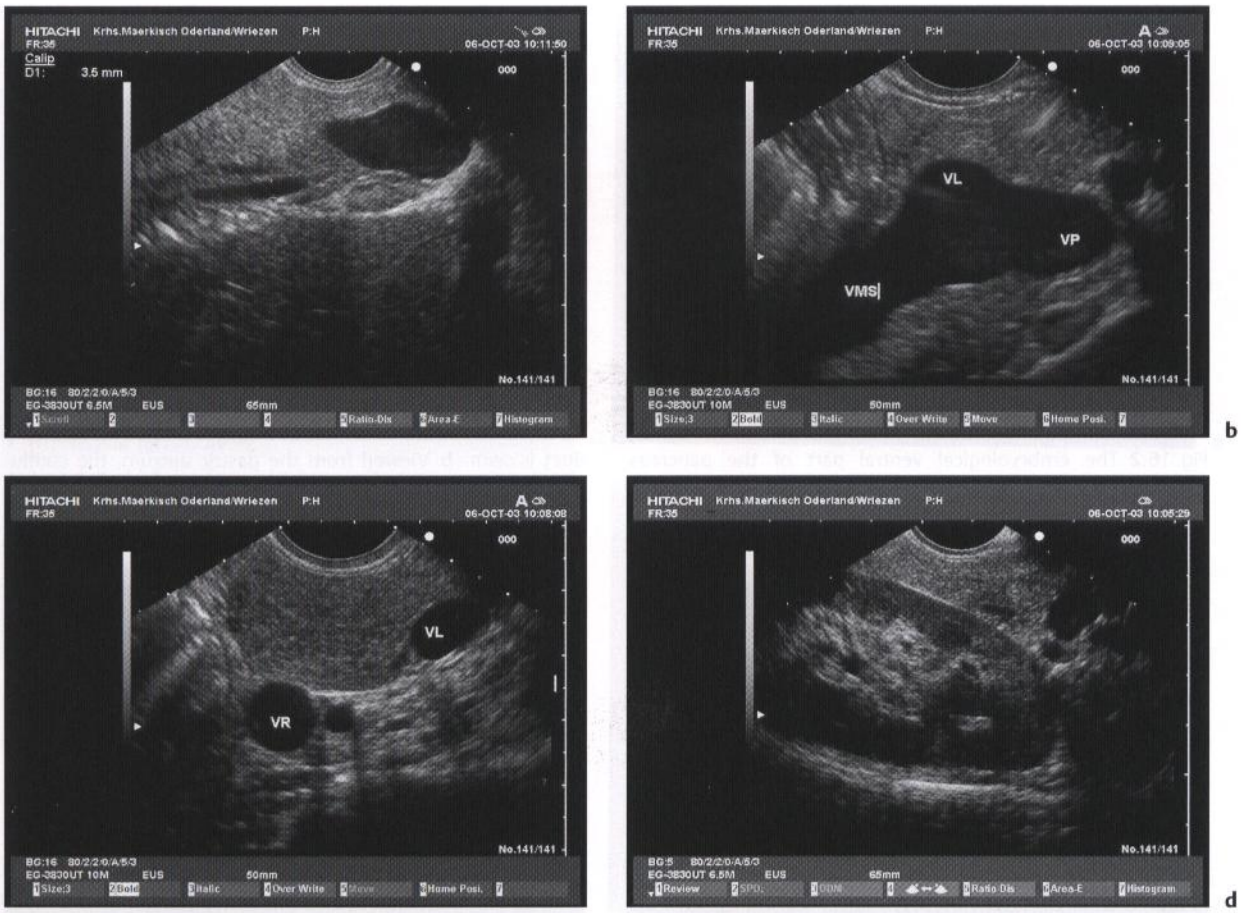
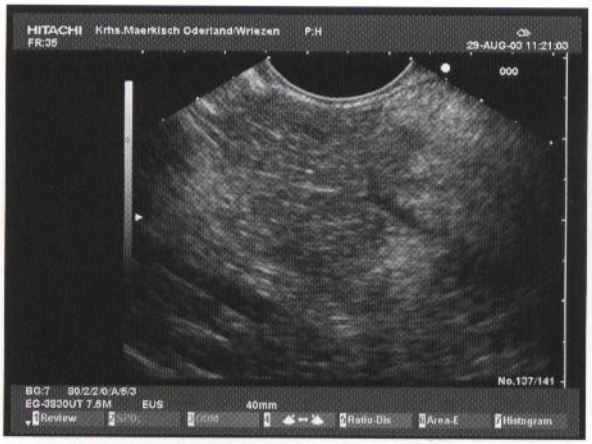


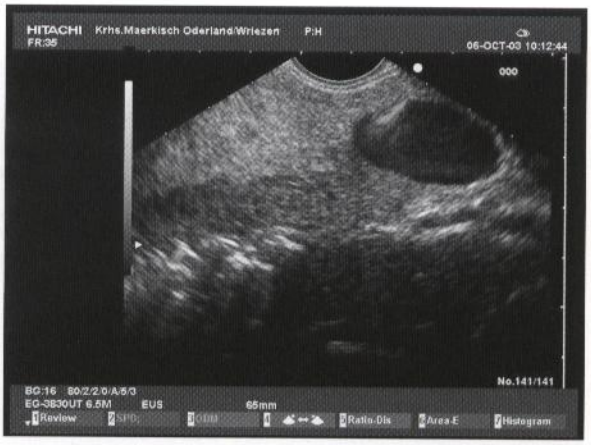
Fig. 16.1 The pancreas, viewed with a curvilinear-array echoendoscope. **a** Seen from the gastric antrum, the confluence of the portal vein is a helpful anatomical landmark. The distal common bile duct and the main pancreatic duct are easily recognizable. **b** The confluence of the portal vein and pancreatic neck. VP: portal vein; VMS: superior mesenteric vein; VL: splenic vein. **c** View of the distal pancreatic body, seen from the gastric body. The splenic vein and splenic artery are anatomical landmarks. VR: left renal vein; VL: splenic vein. **d** View of the pancreatic tail, adjacent to the left kidney, seen from the upper gastric body.

Table 16.2 Endoscopic ultrasonography of the pancreas: normal findings [9,22,24,33]

Characteristic	Normal appearance
Size	Measurements as for abdominal ultrasonography and CT: • Pancreatic head: 25–30 mm • Pancreatic body: up to 20 mm • Pancreatic tail: 20–30 mm
Contour	Smooth, fine, slightly hyperechoic outline of the pancreatic capsule. *Variant:* if the parenchyma is hyperechoic ("lipomatosis"), it is difficult to differentiate the pancreatic tissue from the peripancreatic fatty tissue
Parenchyma	Medium echogenicity, regular lobulation by fine, hyperechoic internal echo reflexes ("pepper-and-salt appearance") *Variants:* With increasing echogenicity of the parenchyma, the physiological heterogeneity of the parenchyma is lost and replaced by a more homogeneous appearance [34]. The ventral part (embryological ventral anlage) of the pancreas can be differentiated as a variably well demarcated structure with lower echogenicity and variably regular lobulation
Pancreatic duct	Anechoic smooth linear structure, sometimes slightly hyperechoic contour, width < 2 mm (in the pancreatic body)

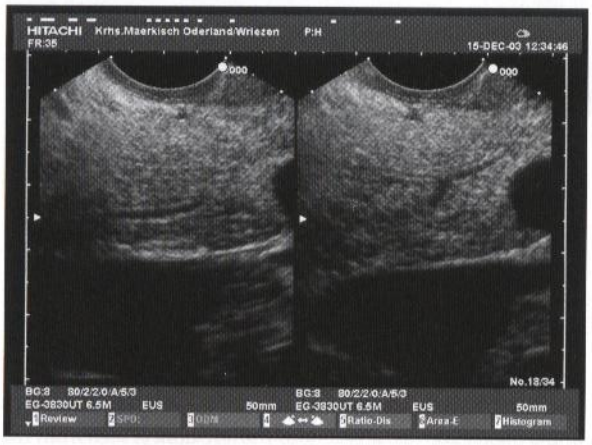


a



b

Fig. 16.2 The embryological ventral part of the pancreas, viewed with a curvilinear-array echoendoscope. **a** Viewed from the descending part of the duodenum, the pancreatic duct is seen. **b** Viewed from the gastric antrum, the confluence of the portal vein can be used for orientation.



a



b



c

Fig. 16.3 Exclusion of pancreas divisum. **a, b** Continuous visualization of the pancreatic duct from the ventral to the dorsal part of the pancreas. **c** Pancreas divisum in a patient with recurrent acute pancreatitis: there is a separate orifice of the dorsal pancreatic duct at the minor papilla in pancreas divisum. Pancreas divisum can be confirmed and treated with endoscopic retrograde cholangiopancreatography.

cannot be followed from its origin at the ampulla of Vater through the ventral part to the dorsal part of the pancreas, or if the pancreatic duct cannot be visualized within the ventral part of the pancreas. Architectural distortion due to chronic pancreatitis may favor false-positive diagnoses of pancreas divisum [39–41]. It may also sometimes be possible to visualize the separate orifices of the common bile duct at the major papilla and of the dorsal pancreatic duct at the minor papilla (Fig. 16.**3c**). Conversely, it is possible to exclude pancreas divisum reliably using endoscopic ultrasound if it is possible to follow the pancreatic duct continuously

Table 16.**3** Endoscopic ultrasound criteria for chronic pancreatitis according to Lees [18], Lees et al. [19], and Wiersema et al. [42]

Ductal criteria
• Increased echogenicity of the pancreatic duct wall
• Irregular contour of the main pancreatic duct
• Dilated side branches (within the body or tail)
• Ductal calculi
• Dilation of the main pancreatic duct (> 3 mm head; > 2 mm body; > 1 mm tail)
• Stricture with dilation of the main pancreatic duct*
• Interruption of the duct with formation of cysts*
Parenchymal criteria
• Hyperechoic foci (1–2 mm)
• Accentuated lobular pattern (2–5 hypoechoic areas surrounded by hyperechoic septa)
• Focal hypoechoic areas
• Parenchymal cysts (> 2 mm)
• Irregular echogenic strains*
• Enlargement of the pancreas*

* Only given as a criterion by Lees [18] and Lees et al. [19].



Fig. 16.**4a, b** Parenchymal criteria: inhomogeneities, echogenic foci, and echogenic strains.

from the ventral to the dorsal pancreas, or between the papilla of Vater and the pancreatic neck [9,40,41] (Figs. 16.**2a**, 16.**3a, b**).

■ Endosonographic Criteria for Chronic Pancreatitis

The endosonographic criteria for chronic pancreatitis follow the ultrasound criteria which were developed by Jones et al. [13] and were included in the Cambridge Classification (Table 16.**1**). The original 13 criteria developed in 1986 by Lees et al. [18,19], were revised and modified by Wiersema et al. in 1993 [42]. In 30 patients in whom chronic pancreatitis had been confirmed by ERCP and/or an (intraductal) secretin test, calcifications and calculi in the pancreatic duct were found to have a positive predictive value of 100% for diagnosing chronic pancreatitis. From this study, the authors developed nine criteria (five ductal and four parenchymal), which now form the basis of most published studies on EUS in chronic pancreatitis [38] (Table 16.**3**, Figs. 16.**4**–16.**10**) [18,19,42].

In their study of the different stages of chronic pancreatitis, Catalano et al. [43] modified the criteria developed by Wiersema et al. [42] slightly and added "inhomogeneous echo-pattern" and a "lobular outer gland margin," so that their classification included 11 criteria (the Milwaukee classification, with five ductal and six parenchymal criteria; Table 16.**4**) [43].

The endosonographic diagnosis of chronic pancreatitis previously established by ERCP (class 2–4 in the Cambridge classification) requires at least three of the nine endosonographic criteria in the modified Wiersema classification [44]. Higher negative and positive predictive values for EUS are obtained if the threshold for "normal" is set at a maximum of two pathological criteria, and if at least five of nine pathological criteria have to be fulfilled to establish a diagnosis of "abnormal" [9,44]. However, other authors have suggested that a diagnosis of chronic pancreatitis can already be made if, in the presence of an appropriate clinical history, only one pathological criterion is present [43,45].

One of the problems with using a threshold number of criteria for the EUS diagnosis of chronic pancreatitis [9,44] is that some of the criteria are related to each other—for example, ductal dilation and parenchymal atrophy (Fig. 16.**10**); echogenic strains and honeycomb pattern (Figs. 16.**4**, 16.**5**); hypoechoic parenchyma and

Table 16.4 Endoscopic ultrasound criteria for chronic pancreatitis according to Catalano et al. [43] (the Milwaukee criteria)

Ductal criteria
• Dilation of the main pancreatic duct (> 3 mm)
• Tortuous pancreatic duct
• Intraductal echogenic foci
• Echogenic duct wall
• Ectatic side branches
Parenchymal criteria
• Inhomogeneous echo pattern
• Foci of reduced echogenicity (1–3 mm)
• Foci of increased echogenicity
• Prominent interlobular septa
• Lobular outer gland margin
• Large echo-free cavities (> 5 mm)



a



b

Fig. 16.**5a, b** Parenchymal criteria: accentuated lobularity (honeycomb pattern); the pancreatic capsule shows increased echogenicity and is slightly irregular.



a



b

Fig. 16.**6** Ductal criteria. The pancreatic duct is slightly dilated; the duct wall shows increased echogenicity and is slightly irregular. In addition, some parenchymal criteria are visible—an increased lobular pattern (**a**) and an indistinct border between the ventral and the dorsal part of the pancreas (**b**).

increased echogenicity in the duct wall (Figs. 16.**6b**, 16.**7b**). However, in cases of extreme ductal ectasia and parenchymal atrophy, it is possible that some parenchymal criteria, such as echogenic foci and strains, may not be visualized (Fig. 16.**10**). In such cases, the required threshold number of criteria may not be met, although the picture would clearly be that of advanced chronic pancreatitis. In other cases, a marked honeycomb pattern in the absence of ductal ectasia may make it difficult to recognize subtle ductal changes.

All studies are in agreement that "calcification" and "calculi" provide the highest diagnostic power [9, 42–44,

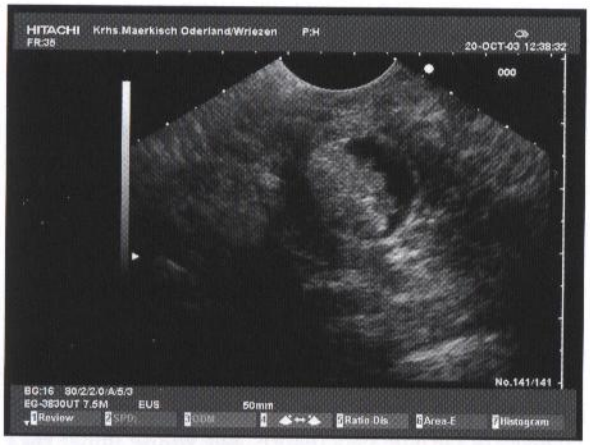


a



b

Fig. 16.**7** Typical endosonographic appearance of chronic pancreatitis. **a** A moderately dilated pancreatic duct; the duct is irregular within the pancreatic neck. **b** Marked dilation of the pancreatic duct in the tail, with dilation and irregular contour of one of the side branches. The parenchyma is inhomogeneous, and the capsule appears irregular and shows increased echogenicity.



a



b

Fig. 16.**8** Chronic pancreatitis with a small pseudocyst, which is partially filled with detritus. **a** Very inhomogeneous parenchyma. **b** Color power angio (CPA) mode. There is hyperperfusion around the margin of the pseudocyst.

46]. Further predictors of a diagnosis of chronic pancreatitis are the number of endosonographic parenchymal criteria met and a clinical history of alcohol abuse [44]. So far, there have been no studies of the validity of the above criteria in larger groups of patients, and the criteria have only recently been correlated with clinical data such as age, sex, history of alcohol abuse, smoking, and clinical symptoms [35,47–49].

Observer agreement between experienced examiners in making a diagnosis of chronic pancreatitis is moderate, both for radial systems [50,51] and for curvilinear EUS systems [50]. It is similar to the level of agreement in classifying hemorrhagic gastric ulcers using the Forrest classification. Only one study determined the agreement between radial and curvilinear systems and found it to be moderate [50]. To achieve sufficient competence in interpreting endosonographic findings in suspected chronic pancreatitis, in comparison with the consensus of a panel of experts, it has been suggested that it is necessary to undergo a supervised training program consisting of 15–40 examinations of patients with chronic pancreatitis [52].

■ Comparison of Methods: Is EUS More Sensitive than ERCP for Diagnosing Chronic Pancreatitis?

On the basis of the criteria discussed in the previous section, the sensitivity of EUS for diagnosing chronic pancreatitis is at least as good as that of ERCP, which is commonly regarded as the reference standard, and it appears to be superior to that of other imaging methods (US, CT, MRI/MRCP) (Table 16.**5**) [7,42,45,53,54]. However, more detailed comparison is difficult for several reasons. Firstly, many of the endosonographic studies investigated highly selected patients, who were fre-

Table 16.5 The accuracy of endoscopic ultrasonography (EUS) in the diagnosis of chronic pancreatitis, in comparison with endoscopic retrograde cholangiopancreatography (ERCP) in patients examined due to suspected pancreatic pathology. The reference standard was either a combination of ERCP, pancreatic function tests, and clinical criteria [42,53,54], or changes in the ERCP findings over time [45]

First author, year (ref.)	Sensitivity of EUS	Sensitivity of ERCP	Specificity of EUS	Patients (n)
Wiersema 1993 [42]	80%	50% [1]	86%	30
Giovannini 1994 [54]	93%	76%	56%	17
Buscail 1995 [53] [2]	88%	74%	100%	81
Kahl 2002 [45]	100%	80.7%	-- [3]	130

1. Sensitivity only for "early chronic pancreatitis" (sensitivity of EUS for "early chronic pancreatitis": 86%).
2. Sensitivity: computed tomography (CT) 75%; abdominal ultrasound 58%; specificity: ERCP 100%, CT 95%, abdominal ultrasound 75%.
3. This study did not include any patients in whom chronic pancreatitis was not suspected clinically. It was therefore not possible to determine the specificity of EUS.

quently suffering from severe chronic pancreatitis. Secondly, the diagnostic reference standard used differs between studies, with diagnostic methods used including ERCP [44,45,55–57], indirect pancreatic function tests [55], a combination of ERCP and the secretin test [43], or a combination of different tests together with clinical criteria [42,53]. However, it is well known that only a small proportion of patients with slightly abnormal findings on ERCP (Cambridge categories 1 and 2) meet any of the clinical criteria for chronic pancreatitis [4]. Only one study, so far only published as an abstract, related endosonographic findings to the histology of resected pancreatic tissue [58]. Another study related the endosonographic diagnosis to cytological findings obtained with endoscopic ultrasound-guided fine-needle aspiration (EUS-FNA) [55].

Several studies have shown that, in patients who meet the ERCP criteria for chronic pancreatitis (Cambridge classes 2–4), a mean of 4.4 [44] or a median of six (range three to seven) out of nine [45] EUS criteria for chronic pancreatitis were present in the endosonographic examination.

Some studies have shown that, in patients with clinically suspected chronic pancreatitis, endosonography was able to identify changes consistent with this diagnosis, even though ERCP did not show any changes in the pancreatic duct [42–45,56,57]. For example, in a study of 43 patients with clinically suspected chronic pancreatitis, Nattermann et al. [56,57] found endosonographic criteria for chronic pancreatitis in 27 patients who had no changes in the pancreatic duct on ERCP. The combined results of the studies by Catalano et al. [43], Sahai et al. [44], and Wiersema et al. [42] show that 25% of patients with clinically suspected chronic pancreatitis and normal ERCP had abnormal findings on EUS. Similarly, 40% of patients with clinically suspected chronic pancreatitis and normal pancreatic function tests were found to have abnormalities on EUS [4]. In the study by Sahai et al., the 30 patients in whom ERCP did not support the clinically suspected diagnosis of chronic pancreatitis had a mean of 3.2 criteria of chronic pancreatitis on endosonography [44]. The most commonly observed endosonographic findings in patients with clinically suspected chronic pancreatitis but normal ductography (ERCP) were parenchymal inhomogeneities (accentuation of lobularity, honeycomb pattern), increased echogenicity of the pancreatic duct, and changes in the contour of the pancreas. However, since the above studies used a cross-sectional design with no follow-up, the significance of abnormal endosonographic findings in patients with suspected chronic pancreatitis but normal ERCP findings and/or pancreatic function tests remains controversial. There is still uncertainty regarding whether EUS can be used reliably to diagnose early chronic pancreatitis [4, 9, 38, 59–62]. This is partly due to the fact that some of the ultrasound and endosonographic criteria for chronic pancreatitis may also be present in asymptomatic individuals with no clinical symptoms of pancreatic disease, either with or without a history of alcohol abuse [35,47–49,63]. However, the significance of abnormal findings on EUS in the presence of a normal ERCP may be different in symptomatic patients who have a history of alcohol abuse. In a region with a high prevalence of chronic pancreatitis, Kahl et al. studied a group of 38 patients with a history of chronic alcohol abuse and recurring upper abdominal pain who had at least one (median two) of the endosonographic (parenchymal) changes of chronic pancreatitis, but whose initial ERCP showed no ductal changes. After a median follow-up of 18 months, 22 of the patients (68.8%) developed changes typical of chronic pancreatitis on ERCP. The authors concluded that EUS may be more sensitive than ERCP for diagnosing early chronic pancreatitis, but that the endosonographic findings have to be interpreted against the background of the clinical history [45].

Another study reported that in a cohort of 127 patients with dyspepsia but no clinical markers of pancreatic disease, approximately half met at least four of the pathological endosonographic criteria for chronic pancreatitis [1]. On the other hand, there are conflicting results with direct pancreatic function testing and endoscopic ultrasonography in the investigation of patients with suspected minimal changes in chronic pancreatitis [64]. When one bears in mind the conflicting results of the studies referred to above, it is difficult to interpret the significance of these findings as long as no follow-up data for this population are available. It is possible that in diagnostically uncertain cases (endosonographic parenchymal criteria met, but normal ERCP; suspicion of autoimmune pancreatitis), cytological or histological ex-

amination using EUS-FNA [55,65] or EUS Tru-Cut biopsy (EUS-TCB) [66] may be helpful. However, since pancreatic EUS-FNA carries a considerable risk, especially in patients with a history of pancreatitis [67,68], while EUS-TCB has a limited diagnostic yield [69] and definite cytological or histological diagnosis of chronic pancreatitis may only have a limited influence on the clinical management, the diagnostic value of EUS-guided FNA and TCB remains to be determined.

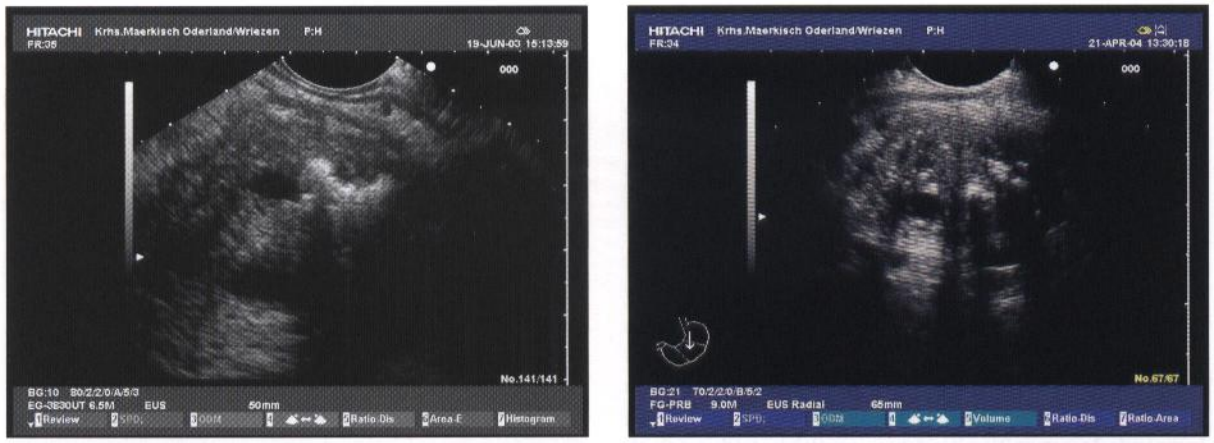
In Summary: The currently available studies suggest that EUS is at least as sensitive as ERCP in the diagnosis of chronic pancreatitis, and that it should replace the latter if making this diagnosis is the only indication for an examination. However, the normal appearance of the pancreas may be very variable, particularly in elderly patients. In addition, it may be difficult or impossible to differentiate between residual changes of acute pancreatitis, alcohol-induced toxic fibrosis of the pancreas, and chronic pancreatitis. As is also true for ERCP and pancreatic function tests, the specificity of endoscopic ultrasound is highly dependent on the patient group studied, or, in individual cases, on the clinical setting. If the clinical findings and patient's history are not taken into account, there is a risk of overdiagnosing chronic pancreatitis when using endosonography [4,70,71].

If EUS is performed only shortly after an episode of acute pancreatitis—i. e., within 4 weeks of it—it is not possible to confirm or exclude a diagnosis of chronic pancreatitis reliably [70]. Any modification of the cut-off number of endosonographic criteria required to establish a reliable diagnosis should take into account the patient's age and average regular alcohol intake [49].

A diagnosis of chronic pancreatitis can be made with a high degree of certainty if five or more of the nine endosonographic criteria are met. In patients younger than 60 without significant regular alcohol consumption, the detection of only three or more endosonographic criteria is highly predictive of chronic pancreatitis [49]. In such cases, further investigation is not required, and ERCP is only indicated for therapeutic interventions. Conversely, advanced chronic pancreatitis can be excluded if EUS only shows up to two pathological findings. ERCP, pancreatic function tests, or other complex investigations for diagnosing chronic pancreatitis will probably be unhelpful and are not required. If the clinical presentation strongly suggests the presence of chronic pancreatitis (typical abdominal pain, chronic alcohol abuse), it appears that the presence of a small number of endosonographic parenchymal criteria is specific for diagnosing early chronic pancreatitis, which cannot be diagnosed by ERCP or pancreatic function tests. Since the difference between acute recurrent pancreatitis and chronic pancreatitis is the progression of morphological and functional changes over time in chronic pancreatitis, the diagnosis may be more easily made by repeated endosonographic follow-up examinations than by more invasive tests. In the future, studies are required that will correlate the endosonographic findings of chronic pancreatitis with histological findings, and that will determine their individual diagnostic significance. In addition, long-term follow-up studies including symptomatic and asymptomatic patients with abnormal findings on EUS, but with normal ERCP and pancreatic function tests, are needed.

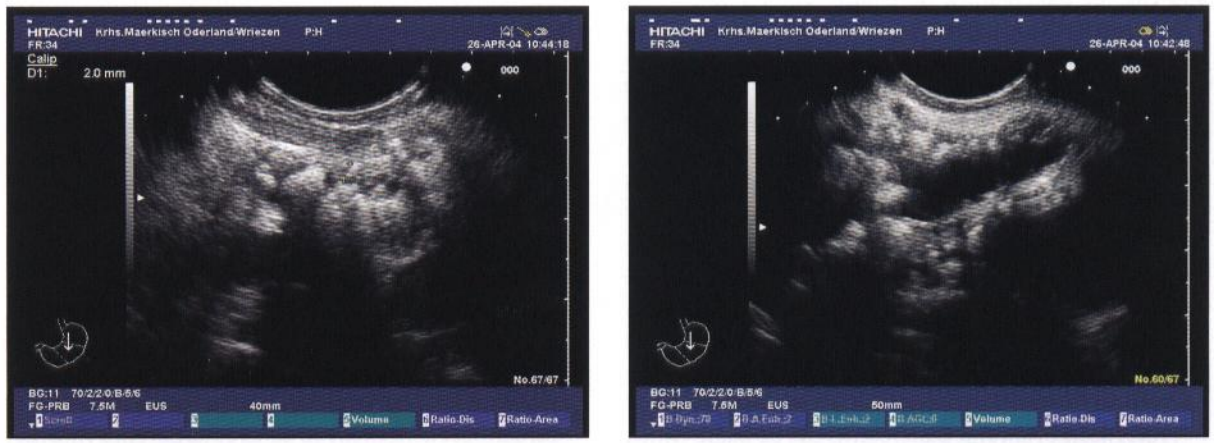
Pitfalls

- *Anatomic variants.* A ventral anlage is recognized in up to three-quarters of endosonographic examinations. In comparison with the dorsal pancreas, the ventral pancreas tends to show lower echogenicity and a more inhomogeneous structure. It is possible to misinterpret this hypoechoic ventral pancreas for a tumor or for focal chronic pancreatitis [9,36,38]. In our experience, this is a common mistake in less experienced examiners.
- It may be difficult to differentiate the pancreas from visceral fatty tissue in patients with marked abdominal obesity (large amounts of visceral fat) who also have marked fatty changes of the pancreas [9,34].
- Age-related changes in the pancreatic echotexture can be extremely variable. The pancreatic duct may become slightly ectatic, the echogenicity of the parenchyma and of the contours of the capsule and the ducts may increase, and the pancreas may develop an increasingly lobular structure. These changes cannot be differentiated from the changes in early chronic pancreatitis with certainty [9,35,38,49] (Fig. 16.**11**).
- Structural changes in the pancreatic parenchyma that would be consistent with an endosonographic diagnosis of chronic pancreatitis may be present in asymptomatic patients with a history of alcohol abuse, in heavy smokers, and in patients with nonspecific dyspepsia. In such cases, a diagnosis of chronic pancreatitis merely based on the EUS criteria may not necessarily be correct [1,38,47,48,71].
- Hyperechogenic foci and a hyperechogenic pancreatic duct wall are relatively nonspecific endosonographic findings, which may also be present in patients with no clinical markers of pancreatic disease. The duct wall is frequently hyperechoic in heavy smokers, and hyperechogenic foci are more common in men [63, 71]. These changes, as well as an increased lobular parenchymal pattern, may also be found in patients with chronic alcohol abuse who have a diffusely fibrosed pancreas but no chronic pancreatitis [47, 48, 71] (Fig. 16.**11a**).
- Large calcifications and pancreatic calculi cause dorsal echo extinction and make it impossible to assess the pancreatic tissue situated dorsal to the calcification (Figs. 16.**9**, 16.**10a**).



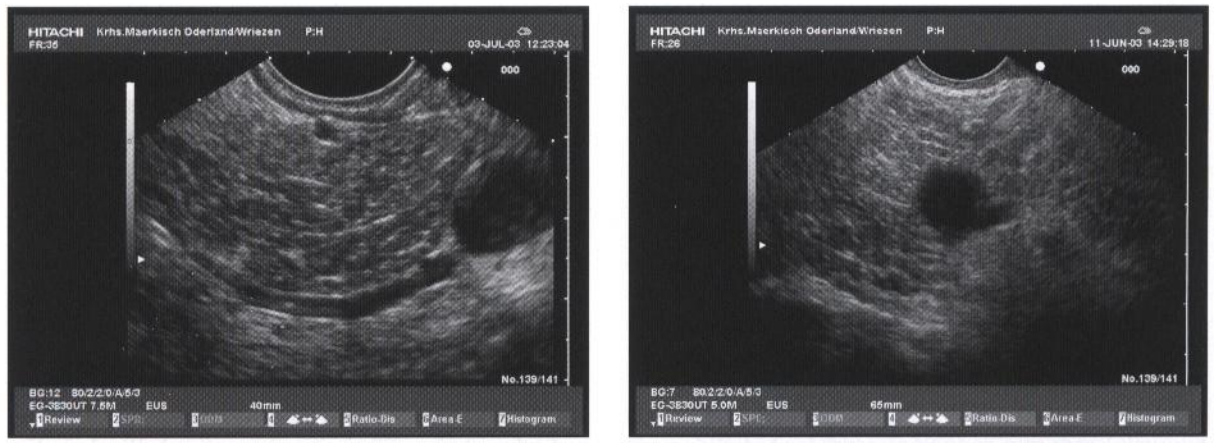
a b

Fig. 16.**9** Hyperechoic reflexes with shadowing can be differentiated into pancreatic stones (**a**) or parenchymal calcifications (**b**).



a b

Fig. 16.**10** Advanced chronic pancreatitis with calcifications, marked parenchymal atrophy, pancreatic stones (**a**), and marked dilation of the distal pancreatic duct (**b**).



a b

Fig. 16.**11** Minimal changes in the echo texture of the pancreatic parenchyma. **a** In a young patient with significant regular alcohol abuse. **b** In an elderly woman with no clinical criteria for chronic pancreatitis.

Table 16.**6** Suggested staging system for chronic pancreatitis, based on the Cambridge classification (see Table 16.**1**)

Cambridge category	Criteria
Category 0 (no chronic pancreatitis)	None
Category 1 *	1–2 criteria, but no dilation or irregularity of the pancreatic duct and no calcification/pancreatic duct calculi
Category 2 (mild chronic pancreatitis)	At least three criteria, such as hypoechogenic areas, hyperechogenic foci, hyperechogenic strains, marked lobulation of the pancreatic parenchyma, hyperechogenic duct wall. No dilation or irregularity of the pancreatic duct and no calcification/pancreatic duct stones
Category 3 (moderate chronic pancreatitis)	At least five criteria, including obvious irregularities in the pancreatic duct (dilation, obvious variability of the diameter, dilated side branches). No calcification/pancreatic duct calculi and no pseudocysts > 10 mm
Category 4 (severe chronic pancreatitis)	At least seven criteria; presence of calcifications/pancreatic duct calculi and/or of pseudocysts > 10 mm

* In the presence of a typical patient history or symptoms, classification as "early chronic pancreatitis" or "minimal-change chronic pancreatitis" is possible.

■ Endosonographic Staging of Chronic Pancreatitis

EUS staging of chronic pancreatitis should follow the Cambridge classification [12]. There are no internationally consistent EUS staging systems. Nattermann and Dancygier carried out a qualitative correlation of the ERCP grades in the Cambridge classification with endosonographic findings, indirectly weighting the findings into minor and major criteria [56]. The endosonographic staging developed by Hollerbach et al. follows a similar principle [55]. In contrast, Catalano et al. [43] classified the presence of one or two of 11 endosonographic criteria as mild chronic pancreatitis (Cambridge category 2), the presence of three to five of 11 criteria as moderate chronic pancreatitis (Cambridge category 3), and the presence of more than five of 11 criteria as severe chronic pancreatitis (Cambridge category 4). We would suggest a staging system as outlined in Table 16.**6**. This is based on the Cambridge classification and takes into account the qualitative weighting of criteria developed by Nattermann et al. [56,57], Dancygier [59], and Hollerbach et al. [55]. It also takes account of the findings by Sahai et al., who quantitatively correlated EUS findings with severity graded according to ERCP [9,44].

■ Diagnosis of Complications of Chronic Pancreatitis

It is usually possible to diagnose the common sequelae of chronic pancreatitis or of acute recurrent pancreatitis, such as pancreatic pseudocysts, stenosis of the common bile duct, and portal or splenic vein thrombosis, using abdominal ultrasound or CT. Endosonography is therefore only rarely required [14,16]. CCDS is more sensitive than CT for diagnosing vascular complications [15]. However, if only abdominal ultrasound is used, it may still be difficult to demonstrate small pseudocysts or splenic vein thrombosis near the pancreatic tail, or, independent of the location, partial or locally restricted portal vein thrombosis. In patients in whom abdominal ultrasound is not diagnostic, endosonography with CCDS is often useful for showing thromboses and occlusions of the portal and splenic veins, as well as portosystemic shunts [72–74]. Ultrasound contrast enhancement can be used to improve the reliability of EUS in diagnosing portal and splenic vein thromboses [25–27]. In our experience, endoscopic ultrasound with systems capable of CCDS and color power angio (CPA)—electronic curvilinear and radial-array—can now be regarded as the most sensitive method of diagnosing vascular complications, chronic pancreatitis, or acute recurrent pancreatitis (Figs. 16.**12**–16.**17**).

A detailed assessment of pancreatic pseudocysts and of post-pancreatitis abscesses is important, as it may have therapeutic implications (Figs. 16.**18**, 16.**19**).

Tubular stenoses of the common bile duct and their underlying pathology can be reliably demonstrated with endoscopic ultrasound (Fig. 16.**20**).

■ Etiological Information

EUS can provide etiological information only in patients with obstructive chronic pancreatitis (Fig. 16.**21**) or with idiopathic acute (recurrent) pancreatitis [10,70,75–80]. In a relatively large study, one-third of all patients with idiopathic acute (recurrent) pancreatitis who were examined with EUS and with ERCP and sphincter of Oddi manometry showed changes consistent with at least moderately severe chronic pancreatitis. An underlying tumor was found in 10% of the patients, and gallstones were present in a similar proportion [10]. Very similar results were found in an endosonographic study of 370 patients with primary and idiopathic acute recurrent pancreatitis [70]. More than four EUS criteria of chronic pancreatitis were found in 19.9% of patients with primary idiopathic acute pancreatitis and in 40.8% of pa-

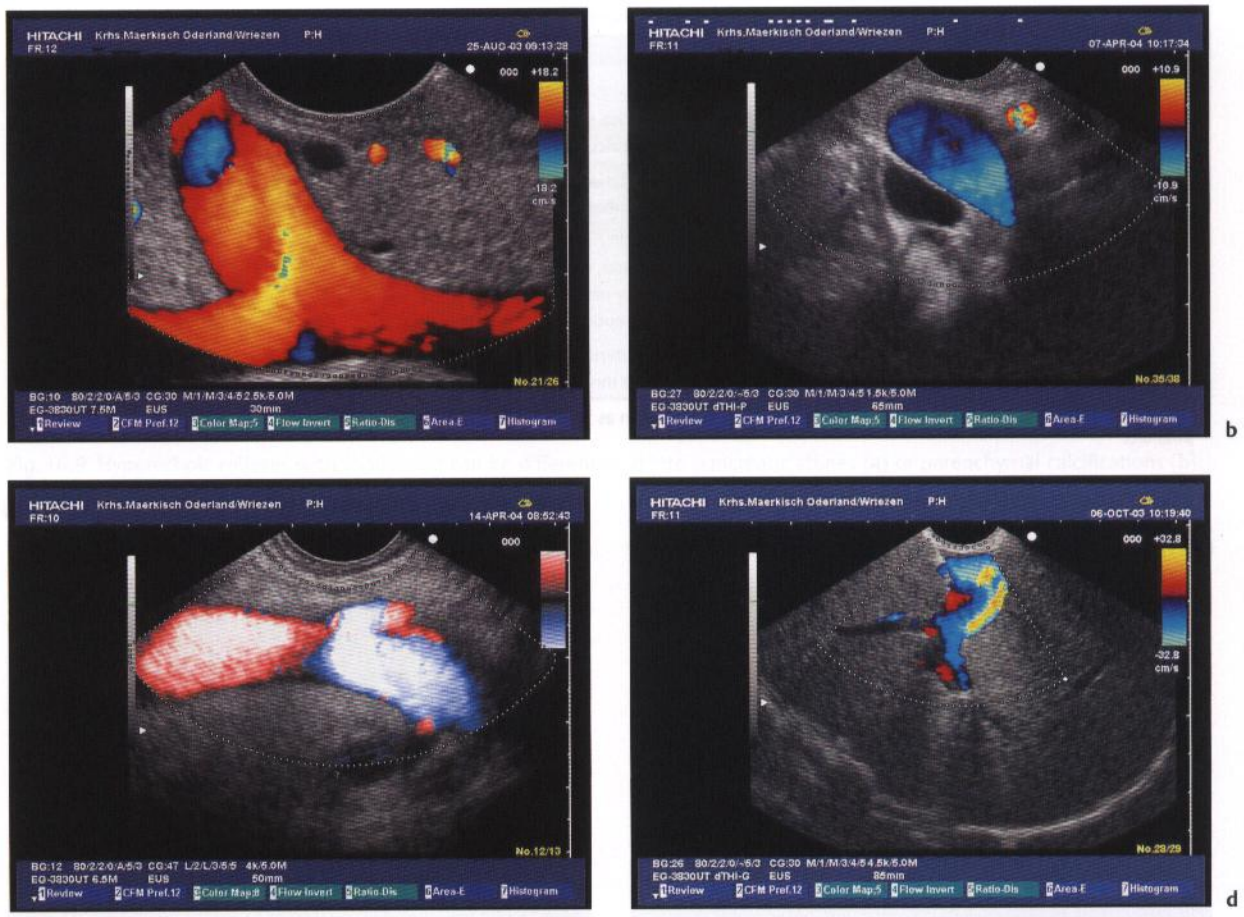


Fig. 16.**12** Endosonographic imaging of the portosplenic vessels. **a** The confluence of the portal vein. **b** The portal vein in the portal region of the liver. **c** The splenic vein within the pancreatic body. **d** The splenic vessels in the hilar region of the spleen.

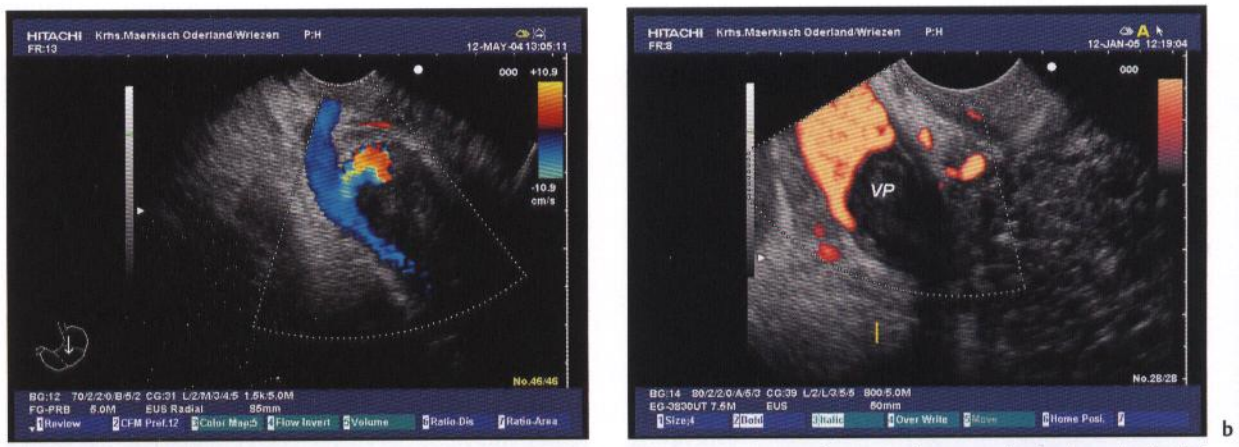


Fig. 16.**13** Thrombosis of the portal vessels as a complication of chronic pancreatitis. **a**, **b** Incomplete portal vein thrombosis with periduodenal collaterals. VP: portal vein.

Fig. 16.**13c–f** ▷

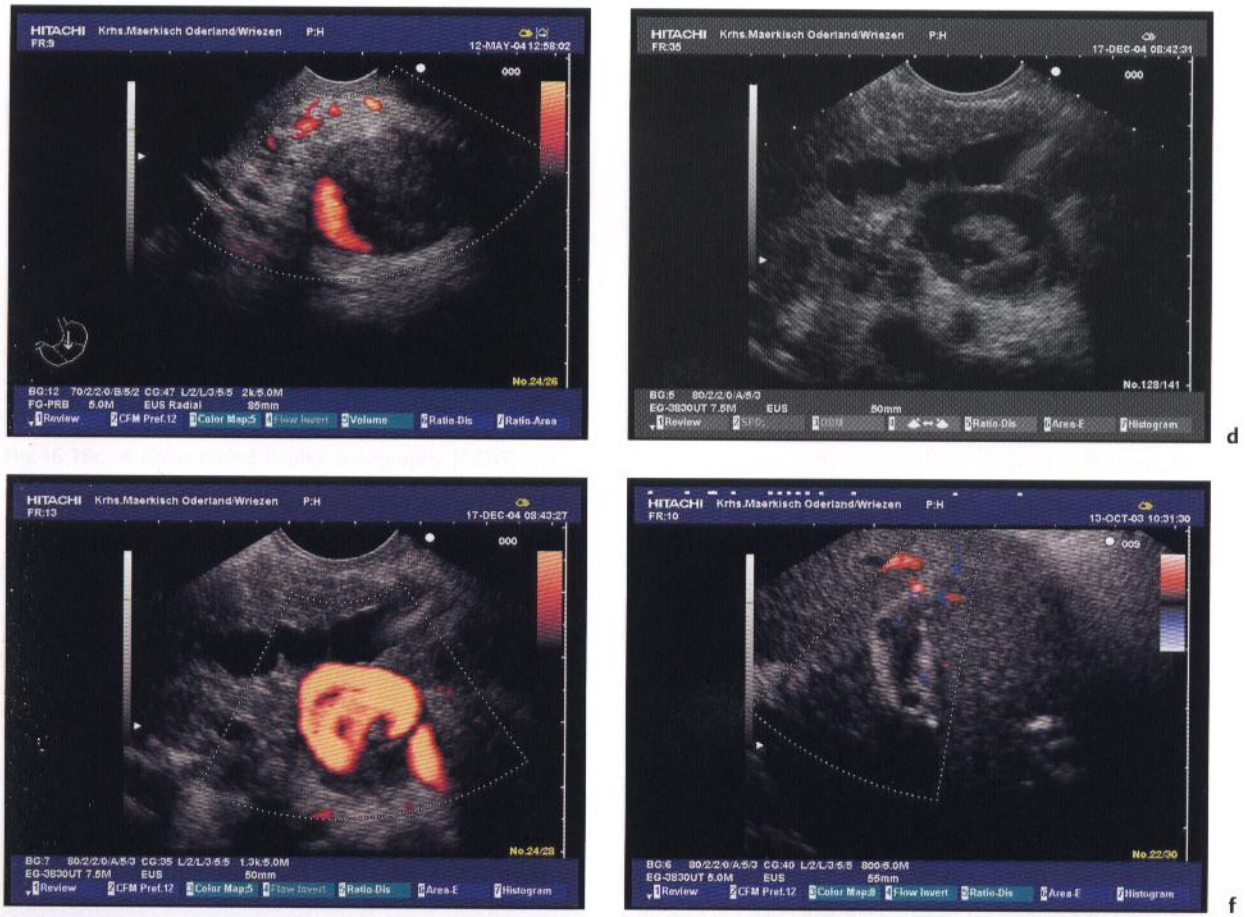


Fig. 16.**13c** Dilated confluence of the portal vessels, with a large thrombus surrounded by some remaining blood flow. **d, e** The confluence of the portal vessels with incomplete thrombosis; the dilation and irregular contour of the main pancreatic duct should be noted. **f** Extension of a portal vein thrombus into an intrahepatic branch of the portal vein.

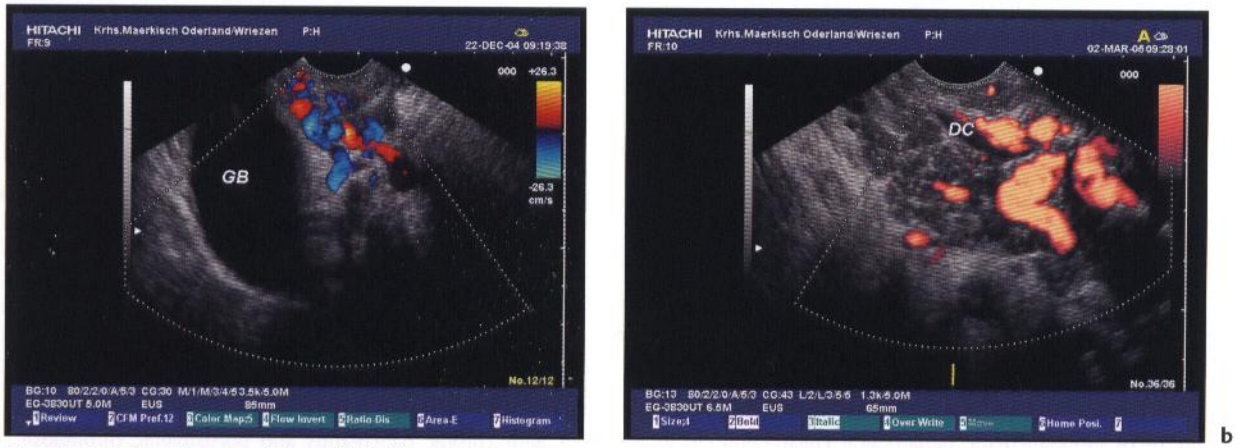


Fig. 16.**14** Collaterals around the gallbladder (**a**) and around the common bile duct (**b**) in patients with chronic pancreatitis and thrombosis of the portal veins. DC: bile duct; GB: gallbladder.

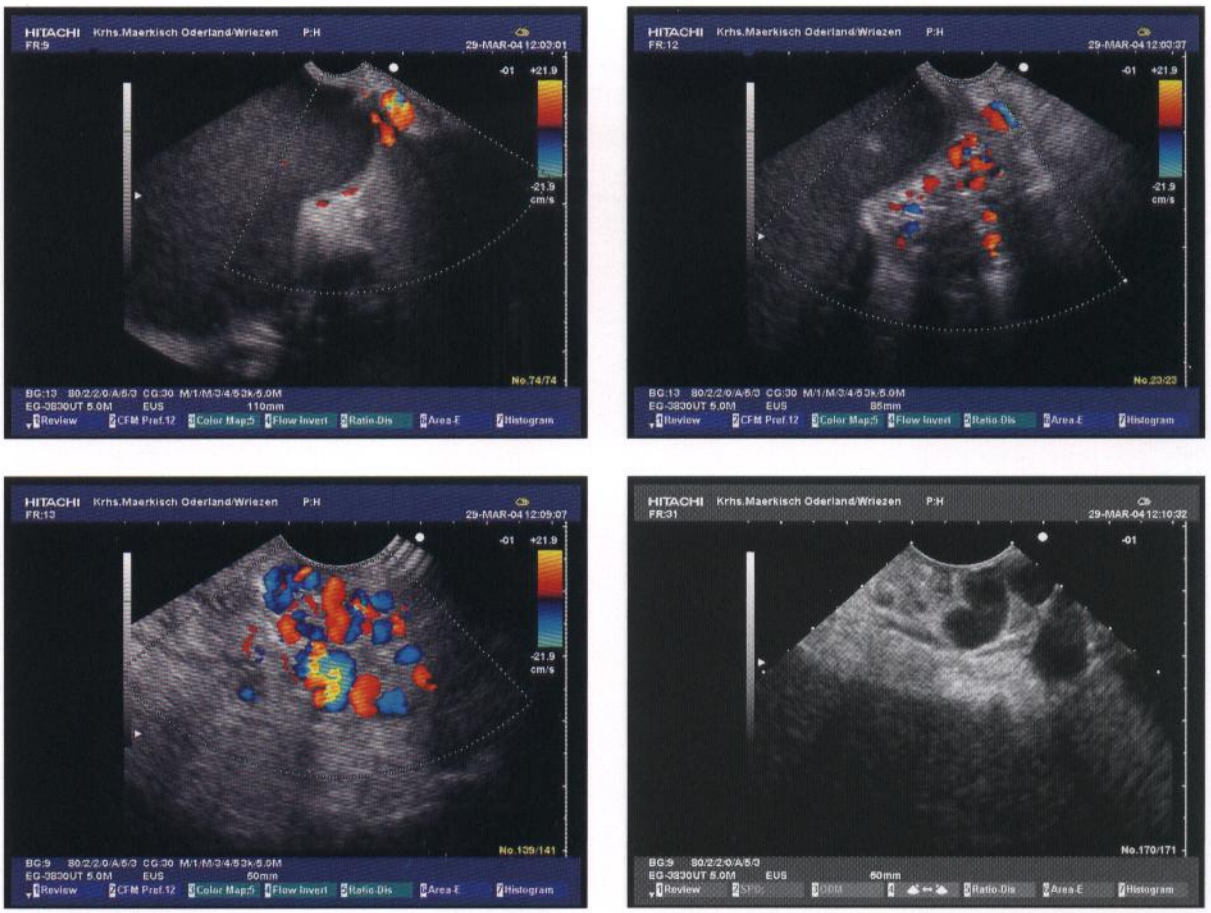


Fig. 16.**15a** A space-occupying pseudocyst in the pancreatic tail. **b–d** The lesion led to hilar splenic vein thrombosis, with hepatopetal and hepatofugal collaterals, cavernous transformation of the splenic vein (**b, c**), and gastric fundic varices (**d**).

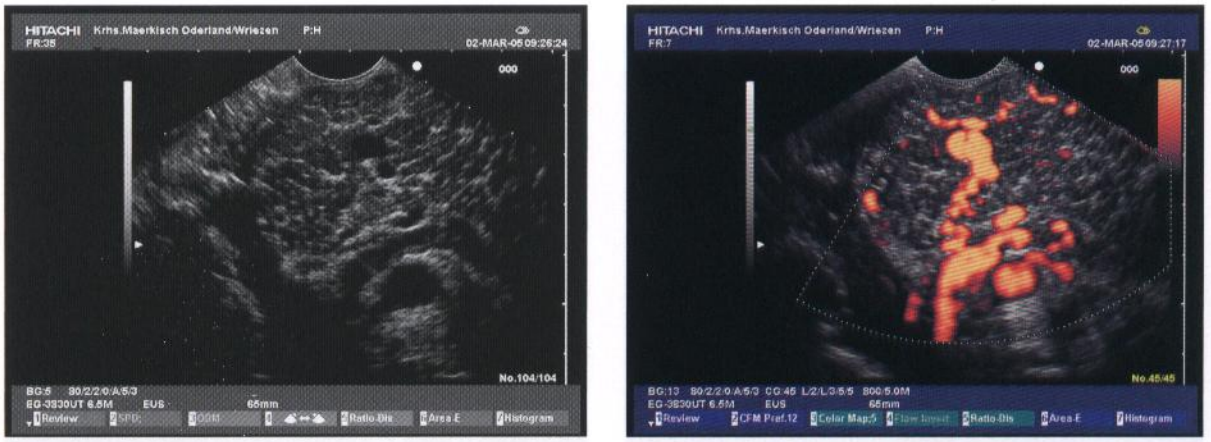
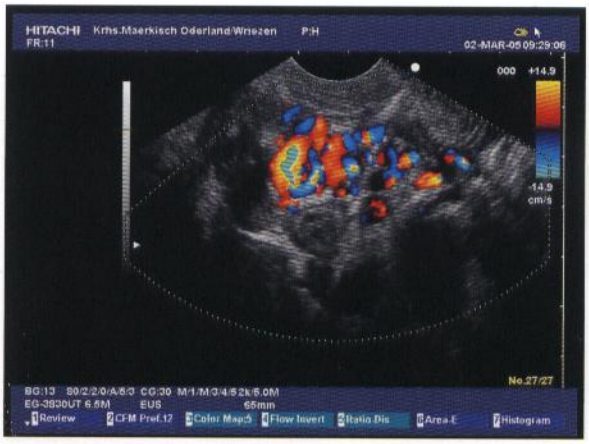


Fig. 16.**16** Intrapancreatic hepatopetal collateralization in a patient with chronic pancreatitis and portosplenic thrombosis. **a** Distinct structural inhomogeneity in the pancreatic tail (echogenic spots, accentuated lobulation, suspicion of dilated side branches). **b** Color power angio (CPA) mode reveals intrapancreatic collaterals, presumed to be dilated side branches.

Fig. 16.**16c, d** ▷



c

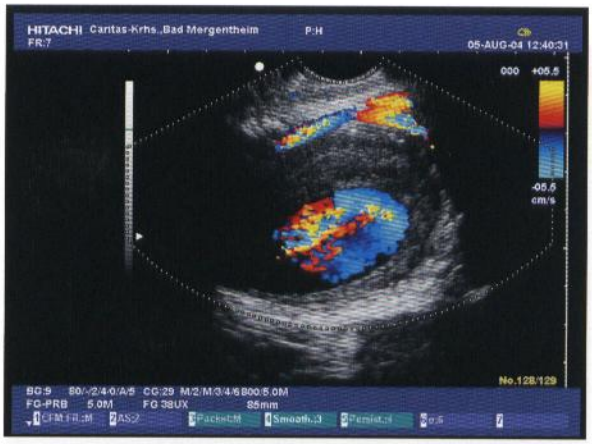


d

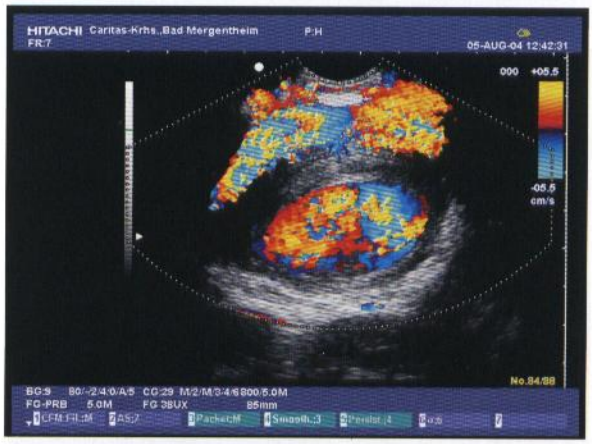
Fig. 16.**16c, d** Color-coded duplex sonography (CCDS) also demonstrates peripancreatic collateral vessels (**c**) and the causative thrombosis of the splenic vein (**d**).



a



b



c

Fig. 16.**17** A false aneurysm in chronic pancreatitis, with hemorrhage into a pseudocyst. **a** Without color-coded duplex sonography (CCDS). **b** With CCDS. **c** After contrast enhancement by intravenous administration of the ultrasound contrast agent SonoVue.

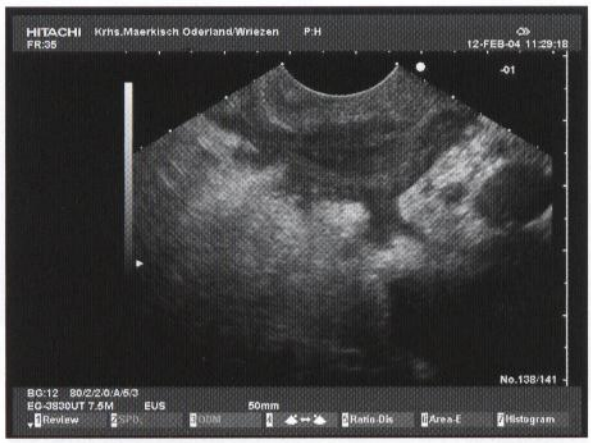


a



b

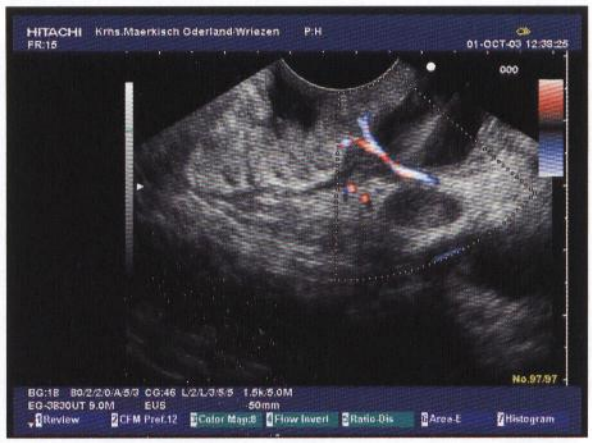
Fig. 16.**18** Large pancreatic pseudocysts. **a** A pseudocyst containing finely dispersed hyperechoic reflexes. **b** A pseudocyst filled with some hyperechoic debris.



a



b



c

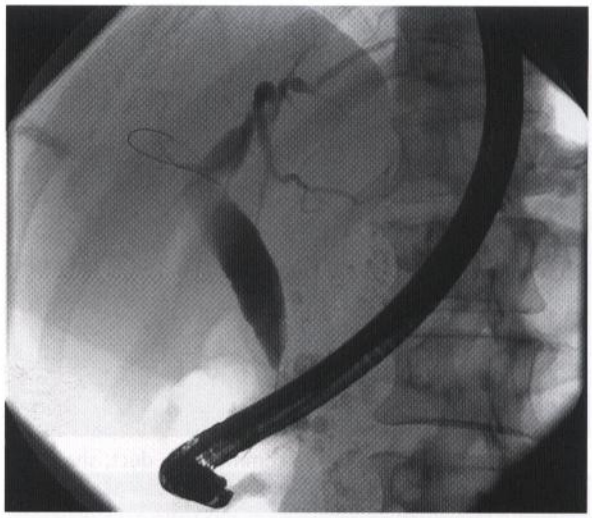


d

Fig. 16.**19** A small mural pseudocyst in a patient with rim pancreatitis and recurrent pyloric stenosis. **a** Hypoechoic material in the duodenopancreatic rim, with duodenal wall thickening. **b** Periduodenal pseudocyst. **c, d** Mural Pseudocyst with perifocal vessels and an enlarged peripancreatic lymph node.

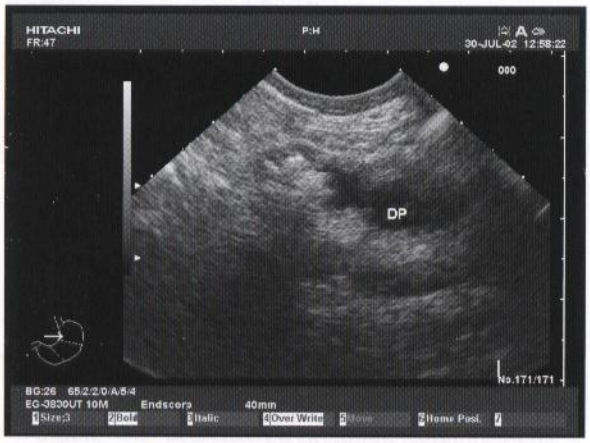


a



b

Fig. 16.**20a** Endosonographic view of a tubular stenosis of the distal common bile duct in a patient with chronic calcifying pancreatitis. **b** The corresponding endoscopic retrograde cholangiopancreatography (ERCP) view.



a



b

Fig. 16.**21a, b** Obstructive chronic pancreatitis caused by pancreatic duct stones. DP: pancreatic duct.

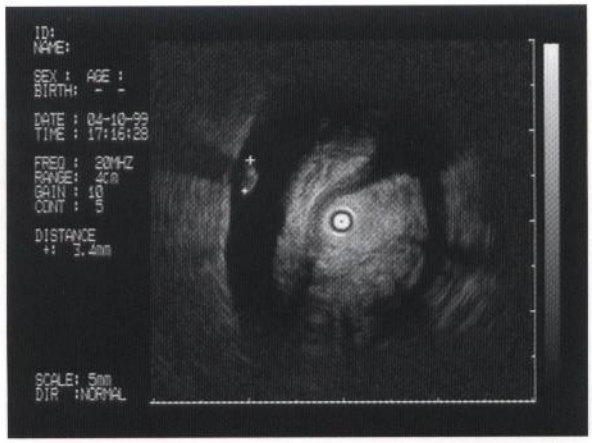
tients with idiopathic acute recurrent pancreatitis. Other possible causes of idiopathic acute pancreatitis that were detected by EUS in this large group of patients included biliary sludge or stones (gallbladder or bile ducts, 13.5%); solid and cystic pancreatic neoplasms (3.5%), and pancreas divisum (7.3%) [70]. Extraductal ultrasound (EDUS) using high-frequency miniprobes can be used to demonstrate pancreatic duct obstruction and its underlying causes, such as tumors of the papilla, ductal adenocarcinomas, intraductal papillary mucinous tumors (IPMTs), or obstructive calcifications and calculi [81,82] (Fig. 16.**22**).

EUS has been shown to have a high level of sensitivity for diagnosing calculi in the common bile duct, which are frequently responsible for causing acute recurrent pancreatitis, when mechanical radial scanners are used [83–85], when EDUS with high-frequency miniprobes is used [81,82], and recently also with electronic curvilinear scanners [86–88] (Fig. 16.**23**). In addition, endosonography can also demonstrate microcalculi in the gallbladder, which may sometimes not be visible on abdominal ultrasound [77,89] (Fig. 16.**24**).

EUS can be helpful in deciding whether or not invasive therapeutic interventions should be undertaken, and it may help avoid more risky and complex investigations such as ERCP and sphincter of Oddi manometry [10,76,86,90]. However, dynamic endosonography of the pancreas with secretin stimulation is not sufficiently sensitive to replace sphincter of Oddi manometry. Nevertheless, an obstructive cause of pancreatitis can be diagnosed reliably by observing that the diameter of the main pancreatic duct increases by at least 1 mm when stimulated with secretin. Similarly, occlusion of a pancreatic duct stent can be diagnosed using the same method [91]. An interesting observation was made in the only study published on this subject so far; Catalano et al. found that when using dynamic endosonography with secretin stimulation, they were able to identify

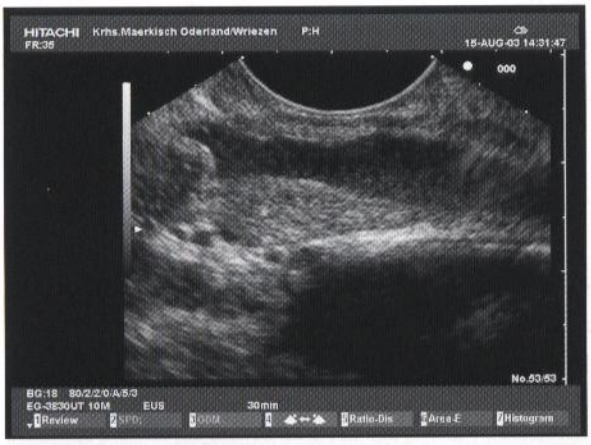


a

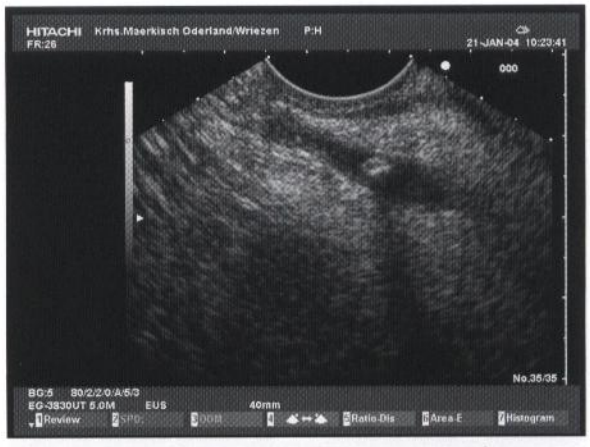


b

Fig. 16.**22** A small stone in the common bile duct, shown by extraductal endosonography (EDUS) with an endoscopic high-frequency miniprobe. Small stones of this type in undilated bile ducts may be missed on endoscopic retrograde cholangiopancreatography.

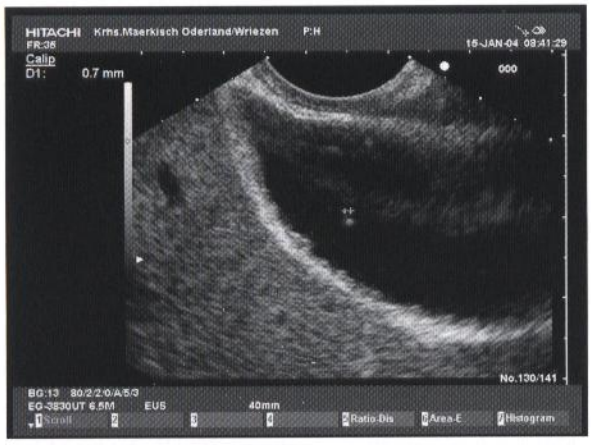


a

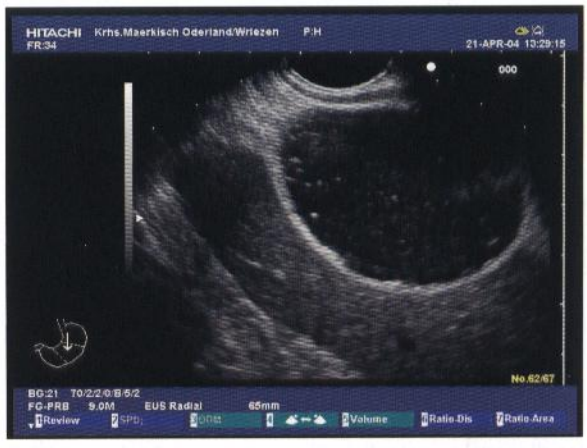


b

Fig. 16.**23a, b** Small common bile duct stones can be reliably visualized using endoscopic ultrasound.



a



b

Fig. 16.**24a, b** Microcalculi in the gallbladder as a possible cause for pancreatitis—visualized by endoscopic ultrasound, but not visible on abdominal ultrasound.

patients with chronic pancreatitis and pancreas divisum who subsequently benefited from endoscopic stent placement [91].

Practical Hints

- It is important to define the diagnostic aim of an EUS examination in chronic pancreatitis, bearing in mind the patient's individual clinical background.
- An endosonographic diagnosis of chronic pancreatitis should usually not be made only shortly (up to approximately 4 weeks) after an acute attack of pancreatitis [70]. Diagnostic aims in such a situation might be exclusion of chronic pancreatitis; identification of the underlying etiology of the acute attack; diagnosis of complications [60].
- Isolated changes in the ventral part of the pancreas [37] should not be used to make a diagnosis of chronic pancreatitis if the remainder of the pancreas appears normal [9].
- A diagnosis of chronic pancreatitis must be made on the basis of the established EUS criteria, taking the patient's clinical background and history into account.
- A complete endosonographic examination in acute recurrent pancreatitis or (suspected) chronic pancreatitis not only entails evaluation of the entire pancreas, but also assessment of the extrahepatic bile ducts and the portal vessels, if possible using CCDS and/or CPA.
- A full diagnostic evaluation should include a statement regarding whether the suspected diagnosis of chronic pancreatitis can be confirmed, the degree of diagnostic certainty, and the staging of severity in accordance with the Cambridge classification. In addition, the presence of possible complications of chronic pancreatitis should be determined, underlying etiological factors should be sought, and if appropriate, suggestions for therapeutic interventions should be offered.

Differential Diagnosis, Diagnostic Problems, and Pitfalls

Areas in which diagnostic difficulties may arise are in differentiating between neoplastic lesions and focal or segmental inflammatory masses, in the diagnostic interpretation of cystic lesions, and in the etiological diagnosis of ductal dilations.

Pancreatic Cancer versus Focal Inflammatory Masses

The life expectancy of patients with chronic pancreatitis is reduced [92]. They have an up to 19-fold increased risk of developing pancreatic cancer, which is most likely due to smoking being a common risk factor

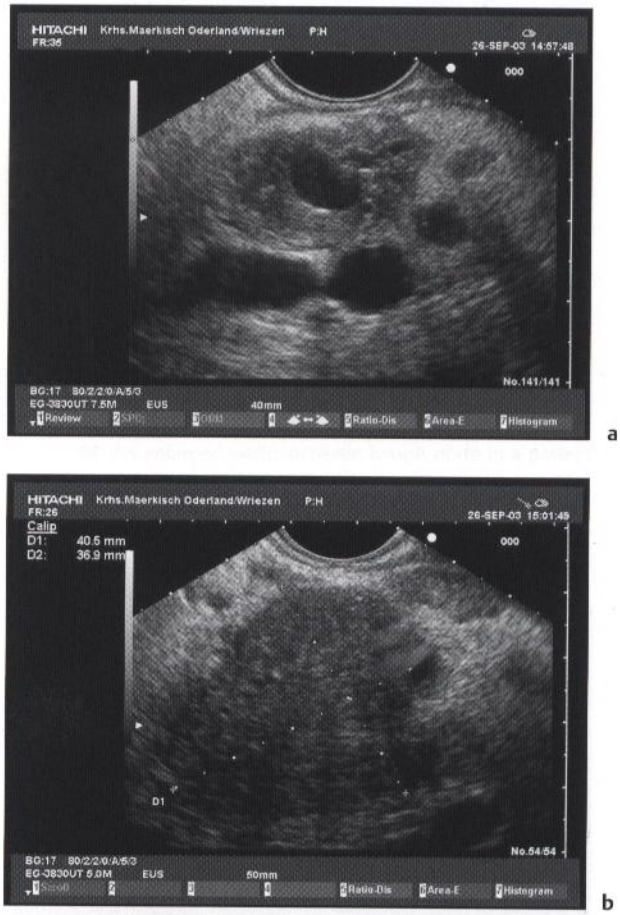
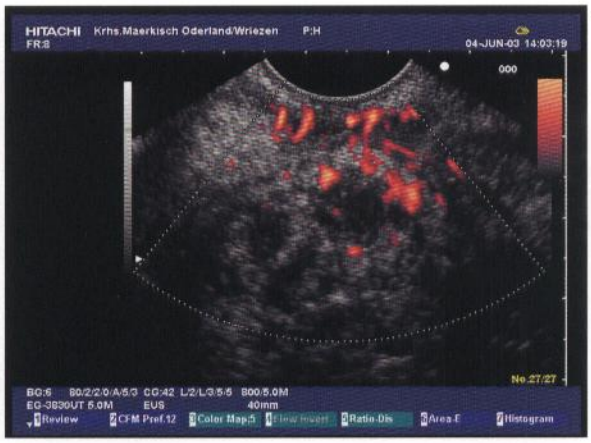


Fig. 16.**25a** Changes consistent with chronic pancreatitis located in the pancreatic tail. **b** The underlying cause is a large cancer in the pancreatic head.

[93–95]. However, a proximal pancreatic tumor may well be the underlying reason for developing obstructive chronic pancreatitis. In a study of 103 patients with proven pancreatic cancer but no history of chronic pancreatitis, half of the patients had at least one of the endosonographic criteria for chronic pancreatitis—mostly dilation and a hyperechogenic wall in the main pancreatic duct. When at least four of the endosonographic criteria were found, 17% of the patients were diagnosed as having chronic pancreatitis in addition to their pancreatic cancer [96]. (Fig. 16.**25**)

Focal inflammatory masses may mimic changes typical of a pancreatic cancer on CT or abdominal ultrasound, and even on ERCP. Two large surgical studies found benign inflammatory lesions in 6–9% of patients who underwent surgery for lesions that even retrospectively appeared highly suspicious for pancreatic cancer [97,98]. A substantial proportion of these tumor-like forms of pancreatitis appear to belong to the only recently recognized clinical entity of autoimmune pancreatitis or lymphoplasmacytic sclerosing pancreatitis [97–101]. In a series of 442 patients who underwent pancreaticoduo-



◁ Fig. 16.**26** Hypoechoic mass lesions in chronic pancreatitis may have numerous underlying diagnoses, and it is not possible to differentiate reliably between necrosis and carcinoma.

Fig. 16.**27a–d** Contrast-enhanced endosonography in patients with chronic pancreatitis and hypoechoic lesions in the pancreatic head. **a, b** After injection of only 0.6 mL of SonoVue, there is obvious enhancement of the pancreatic head, which is enlarged due to chronic inflammation. However, the hypoechoic lesion is spared, suggesting the presence of a small adenocarcinoma. **c, d** In the second patient, there is enhancement of the entire hypoechoic lesion after injection of 2,5 mL SonoVue, suggesting an inflammatory pseudotumor.
▽



a



b



c



d

denectomy [97], 47 patients (10.6%) with histopathologically benign disease were identified, 40 of whom had undergone surgery due to a clinical suspicion of pancreatic malignancy. Fourteen patients turned out to have chronic pancreatitis (29.8%), and 11 patients (23.4%) were classified as having lymphoplasmacytic sclerosing pancreatitis [97]. The characteristic EUS findings for autoimmune pancreatitis include a diffusely enlarged, hypoechoic pancreas that lacks the features of regular chronic pancreatitis (lobularity, heterogeneous foci) or a solitary hypoechoic mass in the pancreatic head. A hyperechoic, narrowed pancreatic duct and concentric wall thickening in the distal common bile duct, causing bile duct stenosis, are additional features frequently found in autoimmune pancreatitis. Pancreatic pseudocysts and peripancreatic fluid collections do not appear to be common findings in autoimmune pancreatitis [65,102,103].

Endosonography has been found to be a highly sensitive method of diagnosing solid pancreatic lesions in patients with or without chronic pancreatitis. However, differentiation between malignant and inflammatory lesions remains difficult [65, 104–111] (Figs. 16.**26**, 16.**27**).

This is particularly true because markedly enlarged peripancreatic lymph nodes may also be present in chronic pancreatitis as well as in autoimmune pancreatitis [65], and autoimmune pancreatitis may involve large vessels [65] (Fig. 16.**28**).

Nattermann et al. studied 12 different endosonographic criteria in 69 inflammatory lesions and 61 malignant tumors. They were unable to identify any characteristics that reliably allowed differentiation between the two types of lesion [109]. For example, the lesions showed irregular or indistinct margins with similar frequency (86% versus 84%). Rösch et al. found similar results [111]. Endosonographic changes that were more common in focal inflammatory lesions, though neither very sensitive nor specific, included coarsely speckled hyperechoic foci (23% versus 7%) [109]. However, endosonographic criteria for the infiltration of duodenum or stomach, and for the infiltration of neighboring vessels, were much less commonly found in focal inflammatory lesions: 7% versus 30% and 9% versus 39%, respectively [109]. In a small group of patients with both pancreatic cancer and chronic pancreatitis, the authors observed that, in contrast to inflammatory masses, in all patients with cancerous masses the calcifications were limited to the periphery of the hypoechoic tumors [106] (Figs. 16.**25b**, 16.**29a**).

It is possible to increase the diagnostic yield of endosonography markedly using echo-enhanced CCDS [25–29,112–114]. As in recent findings in echo-enhanced ultrasonography [14,115–119], adenocarcinomas of the pancreas appear almost exclusively hypoperfused endosonographically and may only occasionally show a hyperperfused rim [28, 29, 112, 113] (Fig. 16.**28a**, **b**). Conversely, inflammatory lesions (but also neuroendocrine tumors, serous cystadenomas, mucinous tumors, and metastases from renal-cell carcinomas) show obvious enhancement of the perfusion signal, certainly after application of echo-contrast enhancers [28, 29, 31, 102, 112, 113] (Figs. 16.**28a**, **b**, 16.**30**). In autoimmune pancreatitis, echo enhancement also results in mild to marked enhancement of the pancreatic parenchyma and the thickened wall of the distal common bile duct; the grade of lesion vascularity correlates with the pathological grade of inflammation and correlates inversely with the grade of fibrosis associated with autoimmune pancreatitis [102, 120]. Perfusion signals inside the mass lesion are only rarely observed in adenocarcinomas, regardless of whether abdominal ultrasound or endosonography is used [112, 115]. One problem is that focal necrosis as a consequence of acute attack of chronic pancreatitis is also characterized by the absence of perfusion signals inside the lesion contrasting with pronounced vascular signals in the surrounding inflamed parenchyma (Fig. 16.**29**).



Fig. 16.**28** An enlarged peripancreatic lymph node in a patient with chronic pancreatitis.

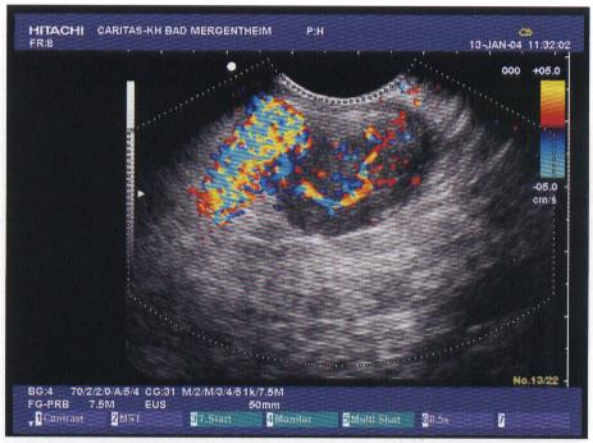


a



b

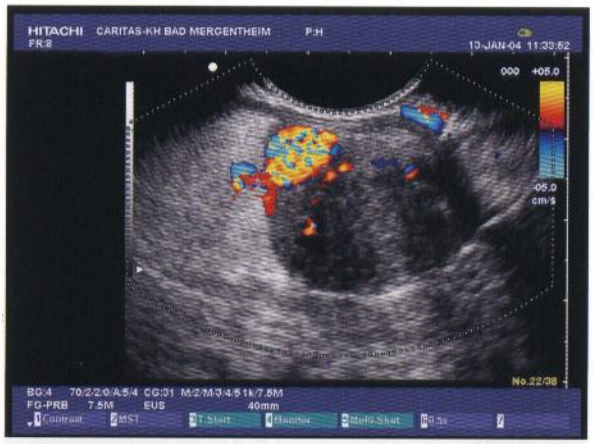
Fig. 16.**29a, b** Endoscopic ultrasound-guided fine-needle aspiration (EUS-FNA) in a patient with acute recurrent pancreatitis and a solid cystic mass lesion in the pancreatic tail. Turbid fluid was aspirated. The cytological and histological findings were typical of necrotic changes.



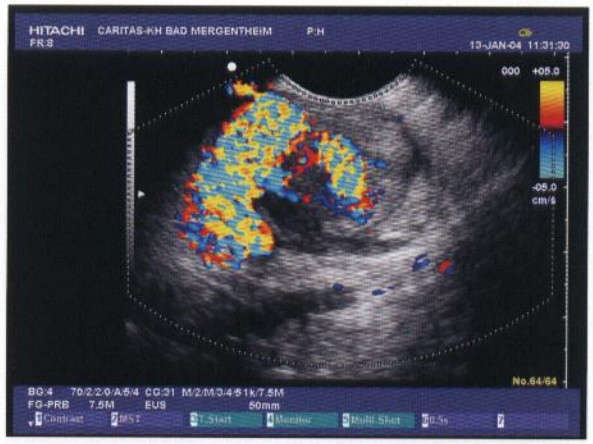
a



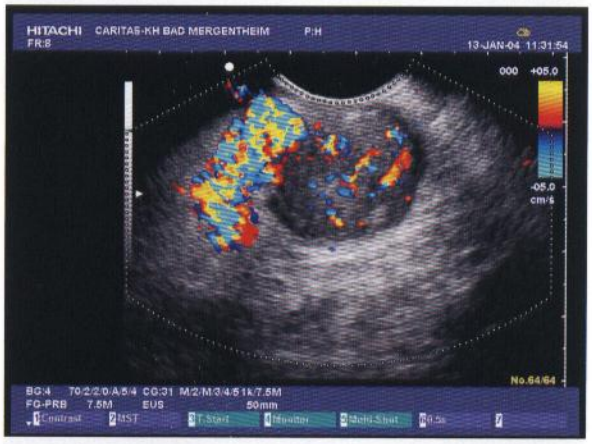
b



c



d



e

Fig. 16.**30** A hypoechoic mass in the pancreatic tail, suspected to be adenocarcinoma. **a** Color-coded duplex endoscopic ultrasound clearly delineates the splenic artery next to the mass lesion, but demonstrates no perfusion inside the lesion. **b–e** Following intravenous injection of the contrast-enhancing agent SonoVue, several vascular signals are identified inside the lesion. After surgical resection, the histological examination excluded adenocarcinoma (the ultimate diagnosis was chronic pancreatitis).

An increased level of CA19-9 (> 500 U/L) in the serum of patients with chronic pancreatitis and with a focal pancreatic lesion is highly specific for a diagnosis of adenocarcinoma of the pancreas [121].

EUS-FNA generally has very high sensitivity (> 95%) for diagnosing adenocarcinoma of the pancreas [122–124]. However, it is unable to resolve the differential-diagnostic dilemma of hypoechoic mass lesions in patients with chronic pancreatitis. In such patients, the diagnostic sensitivity of EUS-FNA, even in highly specialized centers, has been reported to be between only 44% and 80% [104,108,125–128] (Fig. 16.**29**). Analysis of the K-*ras* point mutation in specimens obtained with EUS-FNA may enhance the diagnostic accuracy in indeterminate cases. In one previous investigation, the K-*ras* point mutation was found in 74% of pancreatic cancers and 0% of focal pancreatitis lesions [127].

We would recommend that patients with chronic pancreatitis and a focal hypoechoic, hypoperfused lesion should be referred for surgery without delay if the clinical and imaging findings strongly suggest the presence of a resectable adenocarcinoma. Patients with chronic pancreatitis in whom CCDS shows a well-perfused lesion and in whom the CA19-9 level is low should undergo EUS-FNA. If this shows findings typical of chronic pancreatitis or autoimmune pancreatitis, we suggest that as an alternative to surgery the patient might want to undergo further follow-up examinations, at least in the short term. So far, there have been no systematic studies on whether the combined use of (echo-enhanced) color-coded duplex endosonography and EUS-FNA increases the reliability of the diagnostic findings. In our own experience, we have found that contrast-enhanced color-coded duplex endosonography helps define the margins of the suspicious tumor, facilitating targeting of the lesion, and thus increases the diagnostic yield in patients with chronic pancreatitis and suspected adenocarcinoma (Figs. 16.**28**, 16.**30**).

Pseudocyst versus Simple Cyst versus Cystic Neoplasia versus Pseudoaneurysm

If CCDS is used, it is relatively easy to differentiate between cystic lesions and pseudoaneurysms, both with abdominal sonography and with endosonography (Fig. 16.**17**). With mechanical radial echoendoscopes, this differentiation is more difficult. It is then based on demonstrating or excluding the presence of blood vessels communicating with the lesion, and this is not always reliably possible.

It is much more difficult—although from the point of view of prognostic assessment and treatment extremely important—to differentiate between pseudocysts (80–90% of cystic pancreatic lesions), simple nonneoplastic cysts, and benign or malignant cystic neoplasms (serous or mucinous cystadenoma; mucinous cystadenocarcinoma; intraductal papillary mucinous tumors: approximately 10% of cystic lesions within the pancreas) (see Figs. 16.**31**, 16.**33**, 16.**36**).

Lesions that occur only very rarely include cystic islet-cell tumors, cystic lymphangiomas, solid pseudopapillary tumors, cystic teratomas, and paragangliomas or ganglioneuromas [129–136]. The incidence of pancreatic cystic lesions is much higher than previously reported. The widespread use of modern high-quality cross-sectional imaging and ultrasound has dramatically increased the number of patients in whom asymptomatic pancreatic cysts are discovered incidentally [17, 132, 137].

A Japanese group have presented an endosonographic classification of cystic pancreatic lesions, consisting of six morphological subtypes: thick wall type; protruding tumor type; thick septal type; microcystic

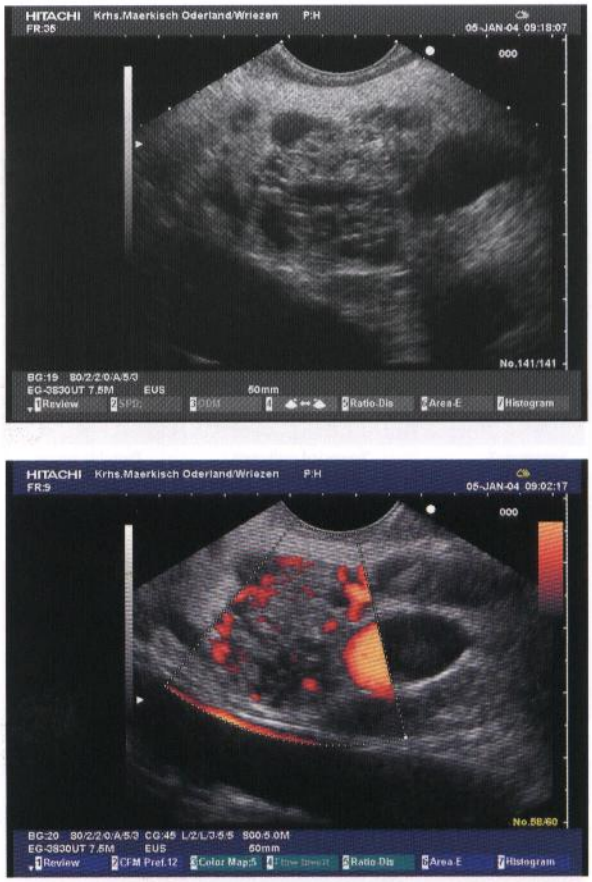


Fig. 16.**31** Cystic mass lesions in the pancreas. **a, b** Serous microcystic adenoma.

type; thin septal type; and simple type. Retrospectively, they were able to achieve reliable differentiation between neoplastic and nonneoplastic cystic pancreatic lesions using this classification [138]. A similarly reliable method of differentiation (with a sensitivity of 92%), which is only based on morphological criteria, has been presented by a group at the Mayo Clinic. They found that a wall thickness of 3 mm or greater, macroseptation (all cyst compartments > 10 mm), the presence of mass or intratumoral growth, and cystic dilation of the main pancreatic duct were criteria for malignancy [135]. Similarly, Gress et al. [139] suggested that solid cystic or complex cystic mass lesions were typically malignant. Intraductal mucinous adenocarcinomas may sometimes also have hyperechogenic foci inside the solid part [139]. On the other hand, considerable interobserver disagreement has been reported among eight experienced endosonographers with regard to the diagnosis of neoplastic versus nonneoplastic cystic lesions, the specific type, and the specific EUS features of cystic pancreatic lesions [140].

Small incidental simple pancreatic cysts that have initially been classified as benign do not undergo malignant change or cause morbidity or mortality, even if

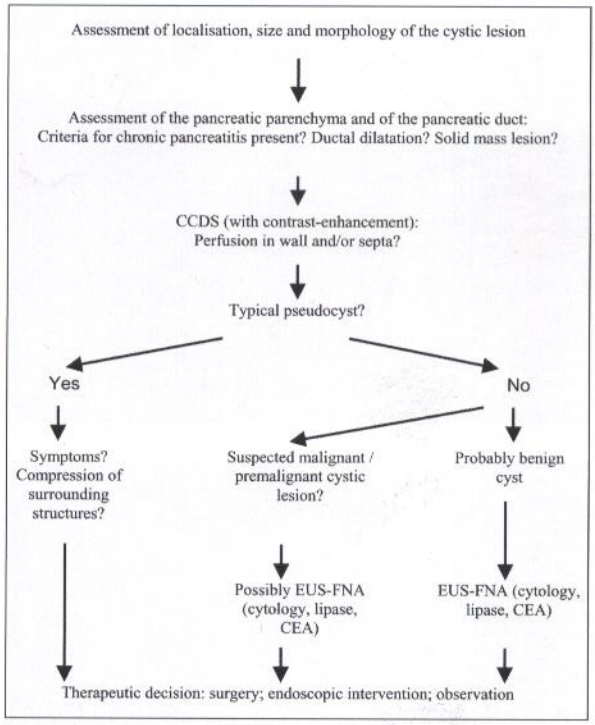


Fig. 16.**32** Flow chart for the differential diagnosis of cystic lesions of the pancreas [11,129,130,136,137,151]. CCDS: color-coded duplex sonography; CEA: carcinoembryonic antigen; EUS-FNA: endoscopic ultrasound-guided fine-needle aspiration.

followed up for a long period [141,142]. There have been several prospective studies of cystic pancreatic lesions before surgical removal. In contrast to earlier studies, they found that several criteria—e.g., wall thickness, presence of septa, presence of solid parts, and lymphadenopathy—were not sufficiently reliable to differentiate between benign and malignant lesions if the patient's clinical history and the morphology of the pancreatic parenchyma were not known [143–145]. The sensitivity of diagnosing malignant and/or premalignant mucinous cysts can be increased by using a combination of endosonographic morphology, cytology of the fluid within the cyst, and the level of carcinoembryonic antigen (CEA) [133, 134, 136, 137, 145–150] (Fig. 16.**32**), (Table 16.**7**). Measuring the CEA level in the fluid within the cyst has been found to be superior to measuring other tumor markers. However, there is considerable overlapping of CEA levels between the various types of pancreatic cystic lesion. The CEA cut-off levels reported in different studies vary substantially. CA19-9 may be nonspecifically raised in inflammatory processes [129,130,145,149]. The presence of high levels of pancreatic enzymes is typical of pseudocysts, but may also occur in cystic neoplasms that communicate with the pancreatic ducts [129,130,136]. In selected cases, injecting secretin during EUS may be useful for differentiating small cystic lesions of the pancreas; this causes enlargement of pseudocysts that communicate with the pan-

Table 16.**7** Morphological, cytological, and biochemical criteria for different cystic lesions of the pancreas [129–131,134,135,137–139,145,146,148,150,152].

Entity	Morphological characteristics	Cytology of the cyst contents	Biochemistry
Serous cystadenoma	Microcystic, rarely macrocystic; thin septa, blood vessels within the septa	Thin, translucent fluid; small, cuboid epithelia containing glycogen	Lipase usually low; CEA low (< 5 ng/mL)
Mucinous cystadenoma (adenocarcinoma)	Macrocystic, thick septa, thick wall, potentially intramural tumor	Viscous fluid; fluid stains positive for mucin; mucinous columnar epithelial cells with variable atypia	CEA high (> 192 ng/mL [1], 400 ng/mL [2], 800 ng/mL [3])
Intraductal papillary mucinous tumor (IPMT)	Dilation of the duct without stricture, solid mural noduli, probably non-anechoic content, variable morphology	Viscous fluid; fluid stains positive for mucin; mucinous columnar epithelial cells with variable atypia	No data
Pseudocyst	Simple cyst or cyst with thin septa, sometimes echogenic debris; changes in the pancreatic parenchyma	Thin, muddy-brown fluid; negative fluid staining for mucin; histiocytes, macrophages, neutrophils, but no epithelial cells	Lipase +++; CEA low (usually < 5 ng/mL)
Simple cyst	Simple cyst or cyst with thin septa	Epithelial cells; no atypical cells	Lipase variable; CEA low
Cystic neuroendocrine tumor	Solid tumor with a large unilocular cyst	Thin, sometimes bloody fluid; monomorphic endocrine tumor cells, staining positive for chromogranin A and synaptophysin	No data
Solid pseudopapillary tumor	Tumor with cystic and solid components (variably)	Bloody fluid, sometimes with necrotic debris; monomorphic cells with round nuclei and eosinophilic, foamy cytoplasm; positive staining for vimentin and alpha-1-antitrypsin	No data

CEA: carcinoembryonic antigen.
1. Brugge et al. 2004 [145].
2. Frossard et al. 2003 [146].
3. Van der Waaij et al. 2005 [150].

creatic duct, but cystic neoplasms do not change in size [153].

In addition to biochemical and cytological investigations of the cystic fluid and other cost-intensive tests, we consider that morphological assessment of the entire pancreas and consideration of the clinical background (e.g., whether the patient has previously had episodes of acute pancreatitis or has a history of alcohol abuse) need to be taken into account and may well be more important [11,129,130,147–149] (Fig. 16.**32**).

However, it is important to remember that mucinous cystadenomas may present with acute recurrent pancreatitis. Doing without further investigation of a cystic pancreatic lesion is only acceptable if the clinical context, the (endo-)sonographic morphology of the pancreas and of the cystic lesion, and the findings of any other imaging examinations are taken into account, and if the lesion appears typical of a pseudocyst. If the diagnosis of a pseudocyst is uncertain, or if a cystic neoplasm is suspected, it depends on the degree of diagnostic uncertainty whether, before proceeding to surgery, the clinician may wish to undertake EUS-FNA of the contents of the cyst for cytological and biochemical studies [122, 129, 130, 136, 137, 146, 148, 150, 151] (Table 16.**7**; Fig. 16.**33**).

In the case of EUS-FNA of cystic pancreatic lesions, antibiotic prophylaxis is mandatory [134]. The age of the patients is also an independent risk factor for malignancy and should be considered when making therapeutical decisions. However, the decision on whether to carry out surgical resection of a pancreatic cystic lesion has to weigh up the risk of surgery against the risk of malignancy [137].

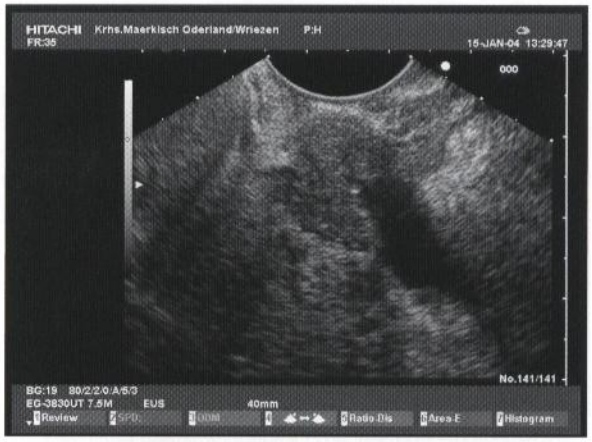
Dilation of the Main Pancreatic Duct

Dilation of the main pancreatic duct and its branches is one of the classical endosonographic characteristics of chronic pancreatitis and usually occurs together with an irregular, hyperechogenic duct contour [9, 42–44, 56, 57, 60]. In elderly people, mild dilation of the pancreatic ducts without any changes in the duct contour is frequent and can be regarded as normal [9,35] (Fig. 16.**11b**). If the duct is clearly dilated, it is always necessary to look for an underlying tumor at the papilla or in the pancreatic head. Endoscopic ultrasound is the most suitable diagnostic method here [81] (Fig. 16.**34**).

In a large series of patients with pancreatic cancer who were studied prospectively for the presence of characteristics of chronic pancreatitis, a dilated pancreatic duct was present in just over half of the patients [96] (Fig. 16.**25**). If the common bile duct and the pancreatic duct are both dilated from the level of the papilla, the differential diagnosis also includes benign stenosis of the papilla, adenomyomatosis, or obstruction by a stone [81] (Figs. 16.**21**, 16.**35**).



Fig. 16.**33** Aspiration of a macrocystic adenoma of the pancreas.



a



b

Fig. 16.**34a, b** Obvious dilation of the pancreatic duct in the presence of tumors of the papilla. CON: portal confluence; P: pancreatic duct.

A further important differential diagnosis is an intraductal papillary mucinous tumor (IPMT). IPMTs are characterized by small polypoid structures within the wall of the pancreatic duct, combined with duct dilation, cystic lesions, and solid lesions [129–131] (Fig. 16.**36**). In such



a

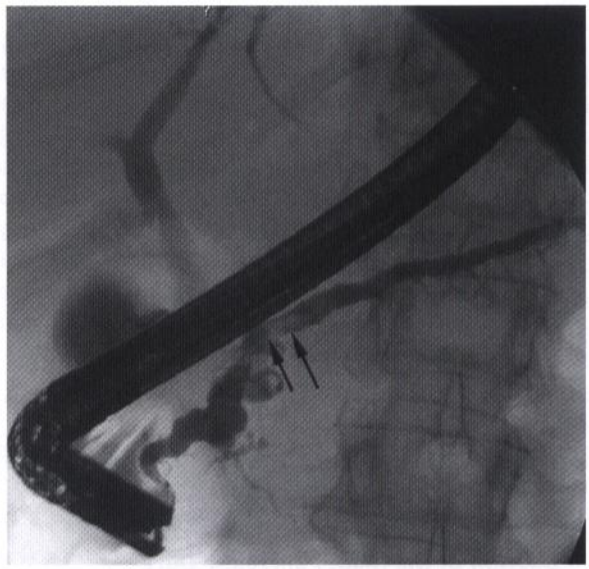


b

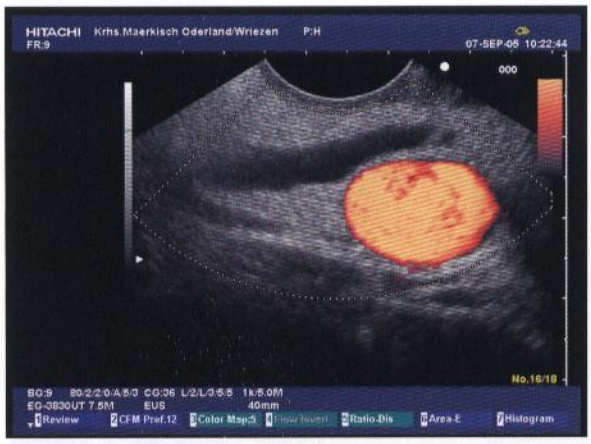
Fig. 16.**35a, b** Benign stenosis of the papilla.



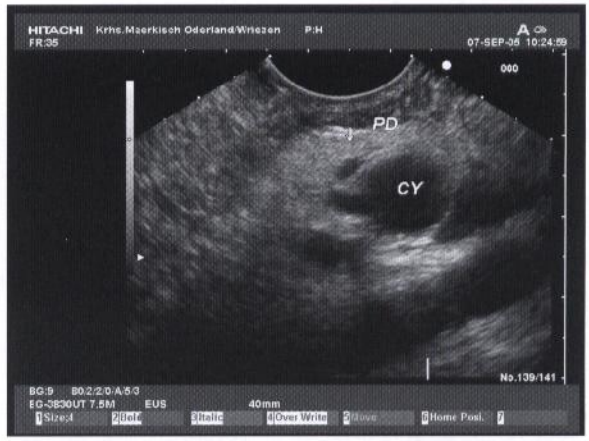
a



b



c



d

Fig. 16.**36** Intraductal papillary mucinous tumors (IPMT) of the pancreas. **a** EUS view of an IPMT of the main duct type. **b** ERCP view of an IPMT of the main duct type. There is obvious dilation of the pancreatic ducts, a bizarre pattern in the absence of any stenosis (endoscopic appearance of a fish-mouth papilla), and indistinct intraductal filling defects (arrows). **c, d** An IPMT of the branch duct type. **c** There is marked dilation of the smoothly outlined main pancreatic duct (color-coded: portal confluence). **d** A small cystic (CY) lesion in the pancreatic body, communicating with a dilated side branch of the main pancreatic duct (PD).

Table 16.**8** Endoscopic ultrasound (EUS)-guided therapeutic interventions in chronic pancreatitis

EUS- guided intervention	Success rate/efficacy	First author, year (ref.)
EUS-assisted and EUS-guided pancreatic pseudocyst drainage (pseudocystogastrostomy, pseudocystoduodenostomy)	– Case reports and case series with high technical and clinical success rates – Safe also in cases of portal hypertension and intervening vessels [155]	Giovannini 1998 [156], Inui 2001 [157], Seifert 2000, 2001 [158,159], Sriram 2005 [155], Vilmann 1998 [160], Wiersema 1996, 2001 [161,162]
EUS-guided transmural necrosectomy and drainage of (peri)pancreatic necrosis and abscess	Case series (30 patients), high technical and clinical success rates	Fuchs 2000 [163], Seewald 2005 [164], Seifert 2000 [159]
EUS-guided celiac ganglion block/neurolysis	– Improvement of pain in 50/90 patients (55%), persistent benefit beyond 12 weeks in 26% [165] – Less efficacy in comparison with pain control in patients with pancreatic cancer [167] – More effective than CT- guided block [166]	Gress 1999, 2001 [165,166], Wiersema 1998 [167]
EUS-assisted main pancreatic duct drainage using the rendezvous-technique: antegrade transgastric or transduodenal pancreatography, transmural and subsequently transductal guide-wire placement, retrograde transpapillary stent drainage by ERCP	Three reports including six patients (technical and clinical success in three patients)	Bataille 2002 [168], Mallery 2003 [169], Will 2005 [170]
EUS-guided main pancreatic duct drainage (antegrade pancreaticoduodenostomy and pancreaticogastrostomy)	– Technical success in 25/28 patients (89%) [171] – Clinical benefit (pain relief and fistula closure) in 75% (cumulative data from [171,174])	Arvanitakis 2005 [171], François 2002 [172], Kahaleh 2003 [173], Tessier 2005 [174]

cases, endosonography-guided aspiration of the pancreatic duct with antibiotic protection (e.g., ciprofloxacin for 5 days, starting with the intervention), with biochemical and cytological investigation of the aspirate, has been found to be a safe method with a high diagnostic yield [144,154]. If solid lesions of the pancreas are also present, these should be aspirated as well [129].

The Contribution of EUS to the Treatment of Chronic Pancreatitis

Endoscopic ultrasonography has added several options and advantages to the armamentarium of therapeutic endoscopy for chronic pancreatitis. There is an expanding role of EUS in the planning and guidance of drainage procedures of pancreatic pseudocysts. Several other EUS-guided interventions in chronic pancreatitis have also recently been developed (Table 16.**8**) [155–174].

The decision on whether to carry out EUS-guided or endoscopic drainage of a pancreatic pseudocyst depends on a number of different issues. Clinical and endosonographic findings, as well as potentially the findings of other investigations, influence which interventional method and specific methodology will be used (Table 16.**9**). For example, the interventional methods may differ depending on whether a pseudocyst, a complicated pseudocyst, or necrotic tissue is present [60,134,158,159,164,175,176] (Fig. 16.**37**).

Table 16.**9** Diagnostic issues to be considered before endoscopic ultrasound (EUS)-guided or endoscopic drainage of a pancreatic pseudocyst

- Is the lesion a typical pancreatic pseudocyst, or could the differential diagnosis include a cystic neoplasm, a pseudoaneurysm, or other benign cystic lesions?
- Are the symptoms the patient is presenting with most likely due to the pseudocyst? (Size and location, anatomical relation to other structures, possible compression of neighboring structures)
- Are there any diagnostic hints that the pseudocyst may be communicating with the pancreatic duct?
- What is the location of the pseudocyst in relation to the wall of the stomach and the duodenum?
- Is the pseudocyst (or post-pancreatic abscess) located in a parenchymal organ (spleen, liver)?
- How thick is the wall of the pseudocyst? Are there blood vessels within the wall of the pseudocyst or within any septa (if present)?
- Are there blood vessels or normal pancreatic parenchyma located between the pseudocyst and the gastrointestinal wall that might be injured during an aspiration?
- Is left-sided portal hypertension present, for example with gastric varices?
- Does the pseudocyst contain solid structures (sequesters) or sediment?
- Are there clinical or endosonographic markers for a potential infection of the pseudocyst (abscess)?
- Is additional exudate or free fluid present?

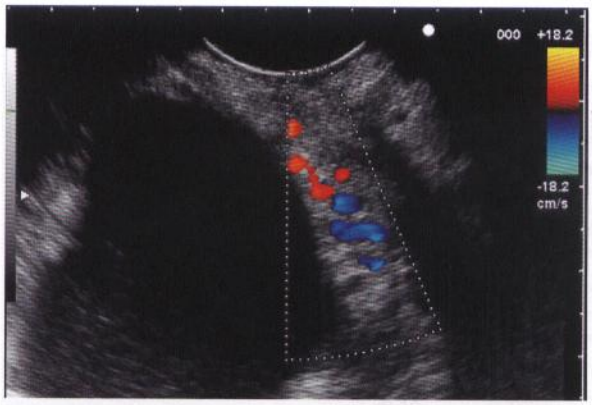
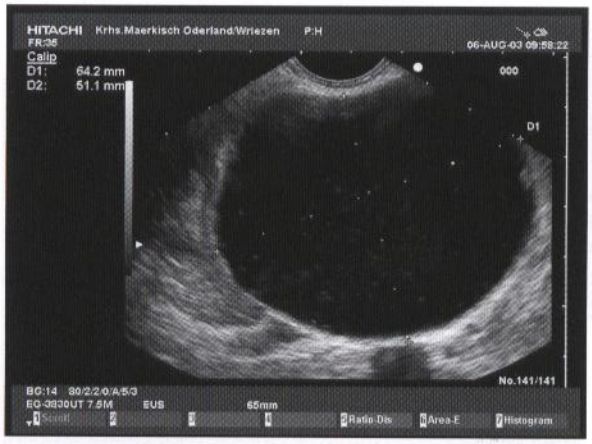


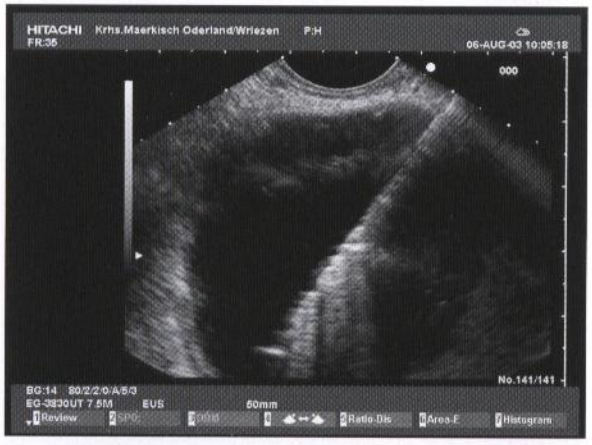
Fig. 16.**37** Collateral vessels located between the wall of the pseudocyst and the stomach wall.



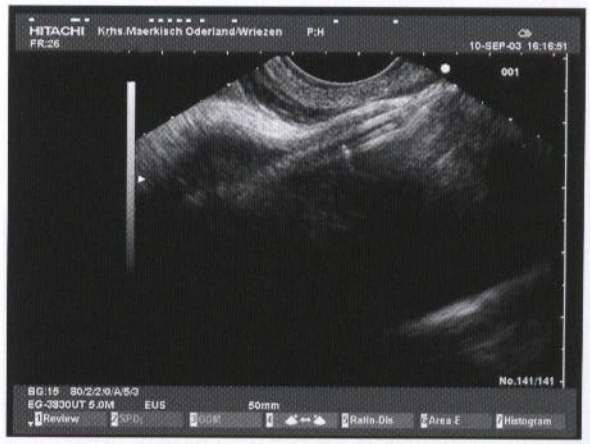
a



b



c



d

Fig. 16.**38** Endoscopic ultrasound-guided drainage of a pseudocyst. **a** There is close contact between the wall of the pseudocyst and the gastric wall. **b** Incision with the electrosurgical needle. **c, d** Insertion of a 10-Fr endoprosthesis via a guide wire.

In a prospective study of 32 patients who were scheduled to undergo endoscopic drainage of a pancreatic pseudocyst, the endosonographic findings changed the therapeutic plan in more than one-third of the cases [176]. In our experience, one question that remains difficult to answer with endoscopic ultrasound is whether a pseudocyst is communicating with the pancreatic duct. We would therefore recommend that before endosonographic or endoscopic drainage of a pseudocyst, ERCP should be performed, providing the option of transpapillary drainage (Fig. 16.**38**).

Endoscopic ultrasound may also be helpful in planning other therapeutic interventions for chronic pancreatitis, particularly if ERCP is negative or shows an interruption of contrast within the duct during endoscopic retrograde pancreatography. In such cases, it is

often possible to identify the reason for the interruption of the contrast medium by using endosonography [177]. It may be possible to differentiate between stones in the pancreatic duct and parenchymal calcifications, or to diagnose pancreas divisum. Endosonography can therefore make a useful contribution to the selection and planning of extracorporeal shock-wave lithotripsy (ESWL), surgical procedures, aggressive endoscopic interventions, or endosonography-guided drainage procedures in the common bile duct or main pancreatic duct [60,151]. In this context, the findings reported by Catalano et al. [91] are of interest; using dynamic secretin-stimulated endosonography in patients with pancreas divisum and a history of chronic pancreatitis, it was possible to identify patients capable of benefiting from endoscopic stent placement.

In selected patients with negative endoscopic retrograde pancreatography findings, it may be possible to use endosonography to puncture the pancreatic duct and inject contrast medium, thereby making pancreatography possible [178,179]. This technique allows subsequent EUS-guided transmural or EUS-assisted transpapillary drainage of the obstructed pancreatic duct in symptomatic patients in whom endoscopic retrograde access to the obstructed main pancreatic duct is not possible (Table 16.**8**) [168–174].

Pitfalls

- Marked dilation of the pancreatic duct may be caused not only by chronic pancreatitis, but also by an intraductal mucinous tumor or by an obstructing proximal tumor of the pancreas or papilla (Figs. 16.**34**–16.**36**). Conversely, an obstructing proximal tumor of the pancreas may cause chronic pancreatitis.
- Enlarged lymph nodes may be present in chronic pancreatitis, autoimmune pancreatitis, or acute recurrent pancreatitis. However, they may also represent lymph-node metastases from a pancreatic carcinoma [106]. (Fig. 16.**27**)
- Extension into neighboring structures is not always a sign of pancreatic cancer. It may also be present in chronic pancreatitis with focal inflammatory changes and in autoimmune pancreatitis [65,107,109].
- In the presence of chronic pancreatitis, the diagnostic accuracy of EUS-FNA for focal hypoechoic mass lesions or cystic pancreatic lesions is too low to refrain from surgical intervention in patients with a suspicious lesion who are otherwise surgically fit [104,108,122,125–130,136,137,146,150,151].

Practical Hints

- If the main pancreatic duct is dilated, its whole course, including the papilla, has to be inspected in detail. The examiner should particularly look for tumors at the papilla and near the ampulla, treatable benign obstructions of the pancreatic duct, associated cystic or solid mass lesions, and small polypoid tumors indicating the presence of IPMT (Figs. 16.**34**–16.**36**).
- If electronic curvilinear or radial echoendoscopes are used, CCDS—possibly with contrast enhancement—should always be used to look for thrombotic complications of chronic pancreatitis or acute recurrent pancreatitis (Figs. 16.**12**–16.**16**; 16.**17**), to differentiate between cystic lesions and pseudoaneurysms and/or cavernomas of the portal vein (Fig. 16.**17**), and possibly to improve the etiological diagnosis of solid or cystic mass lesions (Figs. 16.**26**, 16.**27**).
- In addition, CCDS should be used before endoscopic/endosonographic drainage of pseudocysts to identify interposed gastric or duodenal varices and extragastric collaterals (Figs. 16.**15**, 16.**19**, 16.**37**). Exerting too much pressure with the transducer should be avoided.
- In the presence of chronic pancreatitis, the limitations of EUS-FNA in the differential diagnosis of solid and cystic mass lesions should be borne in mind.
- Particular indications for EUS-FNA are as follows:
  - To increase the probability of excluding malignant/premalignant changes in a lesion which, according to EUS and CCDS, is highly likely to be benign (for example, serous cystadenoma, focal inflammatory lesions, hemorrhagic pseudocyst).
  - Patients with a high clinical and endosonographic suspicion of an unresectable adenocarcinoma and/or pancreatic metastases in the presence of chronic pancreatitis (before palliative therapy).
  - Suspicion of borderline lesions (neuroendocrine tumors, mucinous cystadenoma, lymphoma) before surgical intervention.
  - Dilation of the pancreatic duct of unknown etiology (to diagnose IPMT).
- As patients with a long history of chronic pancreatitis have an increased risk of developing pancreatic cancer, new solid mass lesions should always be looked for in such cases. No validated recommendations are available at present for endosonographic follow-up in patients with moderate or severe chronic pancreatitis. Since the life expectancy in patients with chronic pancreatitis is reduced [92], and since the surgical results in the treatment of pancreatic cancer are poor, it seems unlikely that regular endosonographic follow-up in patients with chronic pancreatitis would have a positive influence on the prognosis. However, in patients with additional risk factors (positive family history, hereditary pancreatitis, smoking), one might want to consider regular follow-up from the age of 50 years [180].

Conclusions

Particularly because of its lower complication rate in comparison with ERCP, EUS is playing an increasingly important role in the diagnosis and management of chronic pancreatitis—without, however, being able to solve all the diagnostic difficulties. Some authors have already declared that endosonography is the new reference standard for imaging in chronic pancreatitis [5, 151]. This view is based on the method's high local imaging resolution, combined with its ability to allow assessment of both the pancreatic parenchyma and the structure of the pancreatic ducts. An international panel of experts has stated that EUS is a suitable method for the diagnosis of early chronic pancreatitis, for the etiological diagnosis of pancreatic duct stenosis, and for management planning in patients with pancreatic pseudocysts [122]. In addition, endoscopic ultrasound also plays an important role in the diagnosis of idiopathic acute pancreatitis and autoimmune pancreatitis.

A study conducted in a Danish community hospital reported that over a 3-year period, suspected benign pancreaticobiliary disease was the most rapidly increasing indication for EUS. It was also the most common indication, ranking even higher than the staging of gastrointestinal and pancreatic tumors. Eighty-six percent of ERCPs scheduled for the investigation of suspected benign pancreaticobiliary disease were no longer considered to be required after EUS had been carried out [181].

With the exception of calcification, extreme caution should be exercised when interpreting isolated parenchymal abnormalities on EUS as an early sign of chronic pancreatitis. The clinical background and the results of further diagnostic tests—for example, EUS-FNA or pancreatic function tests—should always be taken into account.

Some weaknesses of EUS include differentiation between chronic pancreatitis and normal age-related changes; differentiation between residues of acute pancreatitis and diffuse alcohol-toxic fibrosis; and the diagnostic interpretation of hypoechoic pancreatic mass lesions, as well as cystic pancreatic lesions, in patients with chronic pancreatitis. In all of these diagnostic dilemmas, other imaging methods such as helical CT, MRI, MRCP, and positron-emission tomography (PET) are also unable to provide sufficient diagnostic accuracy. The decision on whether to investigate suspicious-looking solid or cystic lesions further using early surgical exploration, complex and invasive methods such as EUS-FNA, contrast-enhanced CCDS, or functional endosonography with secretin stimulation, has to be based on each patient's individual clinical background.

If endoscopic ultrasound is to be widely used and if it is to be regarded as the reference standard for morphological imaging in the diagnosis of chronic pancreatitis, it will be necessary to develop a catalogue of internationally recognized diagnostic criteria and a staging system compatible with the Cambridge classification. In addition, future examiners should be trained in centers with a considerable degree of expertise and experience in the diagnosis and management of chronic pancreatitis. In experienced hands, EUS has a considerable part to play in planning the management of pseudocysts, peripancreatic necrotic tissue, pancreatic duct obstruction, stenosis of the common bile duct, pancreatic lithiasis, and dysfunction of the sphincter of Oddi. In addition to providing a large amount of diagnostic information, EUS may also be used for carrying out therapeutic interventions.

References

1. Sahai AV, Mishra G, Penman ID, et al. EUS to detect evidence of pancreatic disease in patients with persistent or nonspecific dyspepsia. Gastrointest Endosc 2000;52:153–9.
2. Lankisch PG. Sicherheit bei der Diagnostik der chronischen Pankreatitis. Was ist wirklich erforderlich? Dtsch Med Wochenschr 2001;126:96–101.
3. Lankisch PG, Seidensticker F, Otto J, et al. Secretin-pancreozymin test (SPT) and endoscopic retrograde cholangiopancreatography (ERCP): both are necessary for diagnosing or excluding chronic pancreatitis. Pancreas 1996;12:149–52.
4. Forsmark CE. The diagnosis of chronic pancreatitis. Gastrointest Endosc 2000;52:293–8.
5. Glasbrenner B, Kahl S, Malfertheiner P. Modern diagnostics of chronic pancreatitis. Eur J Gastroenterol Hepatol 2002; 14:935–41.
6. Hawes RH. Comparison of diagnostic modalities: EUS, ERCP, and fluid analysis. Gastrointest Endosc 1999;49: S74–S76.
7. Pungpapong S, Wallace MB, Woodward TA, Raimondo M. Accuracy of endoscopic ultrasonography and magnetic resonance cholangiopancreatography for the diagnosis of chronic pancreatitis [abstract]. Gastrointest Endosc 2005; 61:AB 298.
8. Lankisch PG, Assmus C, Maisonneuve P, et al. Epidemiology of pancreatic diseases in Luneburg County: a study in a defined German population. Pancreatology 2002;2:469–77.
9. Sahai AV. EUS and chronic pancreatitis. Gastrointest Endosc 2002;56(4 Suppl):S76–S81.
10. Coyle WJ, Pineau BC, Tarnasky PR, et al. Evaluation of unexplained acute and acute recurrent pancreatitis using endoscopic retrograde cholangiopancreatography, sphincter of Oddi manometry and endoscopic ultrasound. Endoscopy 2002;34:617–23.
11. Hernandez LV, Bhutani MS. Endoscopic ultrasound and pancreatic cysts: a sticky situation! Am J Gastroenterol 2001; 96:3229–30.
12. Axon AT, Classen M, Cotton PB, et al. Pancreatography in chronic pancreatitis: international definitions. Gut 1984; 25:1107–12.
13. Jones SN, Lees WR, Frost RA. Diagnosis and grading of chronic pancreatitis by morphological criteria derived by ultrasound and pancreatography. Clin Radiol 1988;39:43–8.
14. Dietrich CF, Becker D. Signalverstärkte Farbdopplersonographie des Abdomens. Constance, Germany: Schnetztor, 2002.

15. Dorffel T, Wruck T, Ruckert RI, et al. Vascular complications in acute pancreatitis assessed by color duplex ultrasonography. Pancreas 2000;21:126–33.
16. Erk JU, Bunk A, Schentke KU. Die transabdominelle Sonographie in der Diagnostik der chronischen Pankreatitis. Verdauungskr 1997;1:118–123.
17. Ikeda M, Sato T, Morozumi A, et al. Morphologic changes in the pancreas detected by screening ultrasonography in a mass survey, with special reference to main duct dilatation, cyst formation, and calcification. Pancreas 1994;9:508–12.
18. Lees WR. Endoscopic ultrasonography of chronic pancreatitis and pancreatic pseudocysts. Scand J Gastroenterol Suppl 1986;123:123–9.
19. Lees WR, Vallon AG, Denyer ME, et al. Prospective study of ultrasonography in chronic pancreatic disease. Br Med J 1979;i:162–4.
20. Hollerbach S, Ruser J, Ochs A, et al. [Current status of abdominal pancreatic ultrasound: a retrospective analysis of 585 pancreatic ultrasound examinations; in German.] Med Klin (Munich) 1994;89:7–13.
21. Bhutani MS. Endoscopic ultrasound in pancreatic diseases: indications, limitations, and the future. Gastroenterol Clin North Am 1999;28:747–70, xi.
22. Hawes RH, Zaidi S. Endoscopic ultrasonography of the pancreas. Gastrointest Endosc Clin N Am 1995;5:61–80.
23. Niwa K, Hirooka Y, Niwa Y, et al. Comparison of image quality between electronic and mechanical radial scanning echoendoscopes in pancreatic diseases. J Gastroenterol Hepatol 2004;19:454–9.
24. Vilmann P, Hancke S. Endoscopic ultrasound scanning of the upper gastrointestinal tract using a curved linear array transducer: "the linear anatomy." Gastrointest Endosc Clin N Am 1995;5:507–21.
25. Bhutani MS. Contrast agents for endoscopic ultrasound. Gastrointest Endosc 1998;47:324.
26. Bhutani MS, Barde CJ. Contrast-enhanced gastrointestinal trans-abdominal and endoscopic ultrasonography: an idea whose time has come. Am J Gastroenterol 1997;92: 1976–80.
27. Bhutani MS, Hoffman BJ, Van Velse A, et al. Contrast-enhanced endoscopic ultrasonography with galactose microparticles: SHU508 A (Levovist). Endoscopy 1997;29:635–9.
28. Hirooka Y, Goto H, Ito A, et al. Contrast-enhanced endoscopic ultrasonography in pancreatic diseases: a preliminary study. Am J Gastroenterol 1998;93:632–5.
29. Hirooka Y, Itoh A, Goto H. Contrast-enhanced endoscopic ultrasonography in the diagnosis of pancreato-biliary diseases. Dig Endosc 2004;16(Suppl 2):S245–S248.
30. Kasono K, Hyodo T, Suminaga Y, et al. Contrast-enhanced endoscopic ultrasonography improves the preoperative localization of insulinomas. Endocr J 2002;49:517–22.
31. Ueno N, Ozawa Y. Pancreatic cancer evaluated by contrast-enhanced color Doppler endoscopic ultrasonography. Dig Endosc 2002;14:184–7.
32. Chang KJ, Erickson RA. A primer on linear array endosonographic anatomy. Gastrointest Endosc 1996;43(2 Pt 2): S43–S47.
33. Will U, Zinsser E, Bosseckert H. Die Endosonographie in der Diagnostik der chronischen Pankreatitis. Verdauungskr 1997;15:137–142.
34. Lucido ML, Lai R, Guda NM, Mallery S. Hyperechoic pancreas (HEP) on EUS and associated patient factors [abstract]. Gastrointest Endosc 2005;61:AB 290.
35. Rajan E, Clain JE, Levy MJ, et al. Age-related changes in the pancreas identified by EUS: a prospective evaluation. Gastrointest Endosc 2005;61:401–6.
36. Savides TJ, Gress FG, Zaidi SA, et al. Detection of embryologic ventral pancreatic parenchyma with endoscopic ultrasound. Gastrointest Endosc 1996;43:14–9.
37. Lucido ML, Lai R, Guda NM, Mallery S. Factors associated with detection of the ventral anlage (VA) on EUS [abstract]. Gastrointest Endosc 2005;61:AB 290.
38. Wiersema MJ, Wiersema LM. Endosonography of the pancreas: normal variation versus changes of early chronic pancreatitis. Gastrointest Endosc Clin N Am 1995;5:487–96.
39. Bhutani MS, Hoffman BJ, Hawes RH. Diagnosis of pancreas divisum by endoscopic ultrasonography. Endoscopy 1999; 31:167–9.
40. Lai R, Freeman ML, Cass OW, et al. Accurate diagnosis of pancreas divisum by linear-array endoscopic ultrasonography. Endoscopy 2004;36:705–9.
41. Tessier G, Sahai A. A prospective validation of multiple EUS criteria to diagnose or to exclude pancreas divisum: EUS can accurately exclude pancreas divisum, but ERCP is still required for a definitive diagnosis [abstract]. Gastrointest Endosc 2005;61:AB 302.
42. Wiersema MJ, Hawes RH, Lehman GA, et al. Prospective evaluation of endoscopic ultrasonography and endoscopic retrograde cholangiopancreatography in patients with chronic abdominal pain of suspected pancreatic origin. Endoscopy 1993;25:555–64.
43. Catalano MF, Lahoti S, Geenen JE, et al. Prospective evaluation of endoscopic ultrasonography, endoscopic retrograde pancreatography, and secretin test in the diagnosis of chronic pancreatitis. Gastrointest Endosc 1998;48:11–7.
44. Sahai AV, Zimmerman M, Aabakken L, et al. Prospective assessment of the ability of endoscopic ultrasound to diagnose, exclude, or establish the severity of chronic pancreatitis found by endoscopic retrograde cholangiopancreatography. Gastrointest Endosc 1998;48:18–25.
45. Kahl S, Glasbrenner B, Leodolter A, et al. EUS in the diagnosis of early chronic pancreatitis: a prospective follow-up study. Gastrointest Endosc 2002;55:507–11.
46. Catalano MF, Geenen JE. Diagnosis of chronic pancreatitis by endoscopic ultrasonography. Endoscopy 1998;30(Suppl 1): A111–A115.
47. Bhutani MS. Endoscopic ultrasonography: changes of chronic pancreatitis in asymptomatic and symptomatic alcoholic patients. J Ultrasound Med 1999;18:455–62.
48. Hastier P, Buckley MJ, François E, et al. A prospective study of pancreatic disease in patients with alcoholic cirrhosis: comparative diagnostic value of ERCP and EUS and long-term significance of isolated parenchymal abnormalities. Gastrointest Endosc 1999;49:705–9.
49. Vazquez-Sequeiros E, Boixeda D, Moreira V, Plaza AG. New endoscopic ultrasound (EUS) criteria for diagnosis of chronic pancreatitis (CP) [abstract]. Gastrointest Endosc 2004;59:AB 223.
50. Lai R, Wiersema MJ, Sahai AV, et al. Blinded comparison of linear and radial endoscopic ultrasound (EUS) for the evaluation of chronic pancreatitis [abstract]. Gastrointest Endosc 2001;53:AB 170.
51. Wallace MB, Hawes RH, Durkalski V, et al. The reliability of EUS for the diagnosis of chronic pancreatitis: interobserver agreement among experienced endosonographers. Gastrointest Endosc 2001;53:294–9.

52. Wallace MB, Affi A, Eloubeidi MA, et al. How much experience is required to correctly interpret EUS features of chronic pancreatitis? A multicenter prospective trial of third tier EUS trainees compared to a consensus of experts [abstract]. Gastrointest Endosc 2000;51:AB 176.
53. Buscail L, Escourrou J, Moreau J, et al. Endoscopic ultrasonography in chronic pancreatitis: a comparative prospective study with conventional ultrasonography, computed tomography, and ERCP. Pancreas 1995;10:251–7.
54. Giovannini M, Seitz JF. Endoscopic ultrasonography with a linear-type echoendoscope in the evaluation of 94 patients with pancreatobiliary disease. Endoscopy 1994;26:579–85.
55. Hollerbach S, Klamann A, Topalidis T, et al. Endoscopic ultrasonography (EUS) and fine-needle aspiration (FNA) cytology for diagnosis of chronic pancreatitis. Endoscopy 2001;33:824–31.
56. Nattermann C, Goldschmidt AJ, Dancygier H. [Endosonography in chronic pancreatitis: a comparative study of endoscopic retrograde pancreatography and endoscopic sonography; in German.] Ultraschall Med 1992;13:263–70.
57. Nattermann C, Goldschmidt AJ, Dancygier H. Endosonography in chronic pancreatitis: a comparison between endoscopic retrograde pancreatography and endoscopic ultrasonography. Endoscopy 1993;25:565–70.
58. Zimmerman MJ, Mishra G, Lewin D, et al: Comparison of EUS findings with histopathology in chronic pancreatitis [abstract]. Gastrointest. Endosc. 1997;45:AB 185.
59. Dancygier H. Endoscopic ultrasonography in chronic pancreatitis. Gastrointest Endosc Clin N Am 1995;5:795–804.
60. Wallace MB, Hawes RH. Endoscopic ultrasound in the evaluation and treatment of chronic pancreatitis. Pancreas 2001;23:26–35.
61. Wiersema MJ. Diagnosing chronic pancreatitis: shades of gray. Gastrointest Endosc 1998;48:102–6.
62. Zuccaro G Jr, Sivak MV Jr. Endoscopic ultrasonography in the diagnosis of chronic pancreatitis. Endoscopy 1992;24(Suppl 1):347–9.
63. Jafri SF, Muthusamy R, Hernandez M, Chang KJ, Ngyen P. Prospective prevalence of endoscopic ultrasound (EUS) criteria for chronic pancreatitis (CP) in patients undergoing routine upper EUS [abstract]. Gastrointest Endosc 2001;53: AB 168.
64. Chowdhury R, Bhutani MS, Mishra G, et al. Comparative analysis of direct pancreatic function testing versus morphological assessment by endoscopic ultrasonography for the evaluation of chronic unexplained abdominal pain of presumed pancreatic origin. Pancreas 2005;31:63–8.
65. Farrell JJ, Garber J, Sahani D, et al. EUS findings in patients with autoimmune pancreatitis. Gastrointest Endosc 2004; 60:927–36.
66. Dewitt J, McGreevy K, LeBlanc J, et al. EUS-guided Trucut biopsy of suspected nonfocal chronic pancreatitis. Gastrointest Endosc 2005;62:76–84.
67. Eloubeidi MA, Gress FG, Savides TJ, et al. Acute pancreatitis after EUS-guided FNA of solid pancreatic masses: a pooled analysis from EUS centers in the United States. Gastrointest Endosc 2004;60:385–9.
68. Gress F, Michael H, Gelrud D, et al. EUS-guided fine-needle aspiration of the pancreas: evaluation of pancreatitis as a complication. Gastrointest Endosc 2002;56:864–7.
69. Levy MJ, Reddy RP, Wiersema MJ, et al. EUS-guided trucut biopsy in establishing autoimmune pancreatitis as the cause of obstructive jaundice. Gastrointest Endosc 2005; 61:467–72.
70. Yusoff IF, Raymond G, Sahai AV. A prospective comparison of the yield of EUS in primary vs. recurrent idiopathic acute pancreatitis. Gastrointest Endosc 2004;60:673–8.
71. Yusoff IF, Sahai AV. A prospective, quantitative assessment of the effect of ethanol and other variables on the endosonographic appearance of the pancreas. Clin Gastroenterol Hepatol 2004;2:405–9.
72. Lai L, Brugge WR. Endoscopic ultrasound is a sensitive and specific test to diagnose portal venous system thrombosis (PVST). Am J Gastroenterol 2004;99:40–4.
73. Lewis JD, Faigel DO, Morris JB, et al. Splenic vein thrombosis secondary to focal pancreatitis diagnosed by endoscopic ultrasonography. J Clin Gastroenterol 1998;26:54–6.
74. Wiersema MJ, Chak A, Kopecky KK, et al. Duplex Doppler endosonography in the diagnosis of splenic vein, portal vein, and portosystemic shunt thrombosis. Gastrointest Endosc 1995;42:19–26.
75. Chen RY, Hawes RH. Idiopathic acute pancreatitis: is EUS worth doing? Am J Gastroenterol 2002;97:1244–6.
76. Frossard JL, Sosa-Valencia L, Amouyal G, et al. Usefulness of endoscopic ultrasonography in patients with "idiopathic" acute pancreatitis. Am J Med 2000;109:196–200.
77. Liu CL, Lo CM, Chan JK, et al. EUS for detection of occult cholelithiasis in patients with idiopathic pancreatitis. Gastrointest Endosc 2000;51:28–32.
78. Norton SA, Alderson D. Endoscopic ultrasonography in the evaluation of idiopathic acute pancreatitis. Br J Surg 2000;87:1650–5.
79. Tandon M, Topazian M. Endoscopic ultrasound in idiopathic acute pancreatitis. Am J Gastroenterol 2001;96:705–9.
80. Vazquez-Sequeiros E, Boixeda-Miquel D, Moreira-Vincente V, Garcia-Plaza A. Prospective assessment of the role of endoscopic ultrasound in the diagnosis of idiopathic acute relapsing pancreatitis [abstract]. Gastrointest Endosc 2005; 61:AB 304.
81. Dietrich CF, Gouder S, Hocke M, Schuessler G, Ignee A. [Endoscopic ultrasound in the differential diagnosis of choledocholithiasis; in German.] Endosk Heute 2004; 17:160–6.
82. Seifert H, Wehrmann T, Hilgers R, et al. Catheter probe extraductal EUS reliably detects distal common bile duct abnormalities. Gastrointest Endosc 2004;60:61–7.
83. Canto MI, Chak A, Stellato T, et al. Endoscopic ultrasonography versus cholangiography for the diagnosis of choledocholithiasis. Gastrointest Endosc 1998;47:439–48.
84. Palazzo L, O'Toole D. EUS in common bile duct stones. Gastrointest Endosc 2002;56(4 Suppl):S49–S57.
85. Prat F, Amouyal G, Amouyal P, et al. Prospective controlled study of endoscopic ultrasonography and endoscopic retrograde cholangiography in patients with suspected common bile duct lithiasis. Lancet 1996;347:75–9.
86. Kohut M, Nowak A, Nowakowska-Dulawa E, et al. Endosonography with linear array instead of endoscopic retrograde cholangiography as the diagnostic tool in patients with moderate suspicion of common bile duct stones. World J Gastroenterol 2003;9:612–4.
87. Kohut M, Nowakowska-Dulawa E, Marek T, et al. Accuracy of linear endoscopic ultrasonography in the evaluation of patients with suspected common bile duct stones. Endoscopy 2002;34:299–303.
88. Lachter J, Rubin A, Shiller M, et al. Linear EUS for bile duct stones. Gastrointest Endosc 2000;51:51–4.

89. Thorboll J, Vilmann P, Jacobsen B, et al. Endoscopic ultrasonography in detection of cholelithiasis in patients with biliary pain and negative transabdominal ultrasonography. Scand J Gastroenterol 2004;39:267–9.
90. Levy P, Boruchowicz A, Hastier P, et al. Diagnostic criteria in predicting a biliary origin of acute pancreatitis in the era of endoscopic ultrasound: multicentre prospective evaluation of 213 patients. Pancreatology 2005;5:450–6.
91. Catalano MF, Lahoti S, Alcocer E, et al. Dynamic imaging of the pancreas using real-time endoscopic ultrasonography with secretin stimulation. Gastrointest Endosc 1998;48: 580–7.
92. Lowenfels AB, Maisonneuve P, Cavallini G, et al. Prognosis of chronic pancreatitis: an international multicenter study. International Pancreatitis Study Group. Am J Gastroenterol 1994;89:1467–71.
93. Lowenfels AB, Maisonneuve P, Cavallini G, et al. Pancreatitis and the risk of pancreatic cancer. International Pancreatitis Study Group. N Engl J Med 1993;328:1433–7.
94. Lowenfels AB, Maisonneuve P, Lankisch PG. Chronic pancreatitis and other risk factors for pancreatic cancer. Gastroenterol Clin North Am 1999;28:673–85, x.
95. Talamini G, Falconi M, Bassi C, et al. Incidence of cancer in the course of chronic pancreatitis. Am J Gastroenterol 1999;94:1253–60.
96. Parasher G, Alasadi R, Chang KJ, Ngyen PT. Endoscopic ultrasound (EUS) changes of chronic pancreatitis (CP) are common among patients with pancreatic cancer [abstract]. Gastrointest Endosc 2002;55:AB 250.
97. Abraham SC, Wilentz RE, Yeo CJ, et al. Pancreaticoduodenectomy (Whipple resections) in patients without malignancy: are they all "chronic pancreatitis"? Am J Surg Pathol 2003;27:110–20.
98. Van Gulik TM, Reeders JW, Bosma A, et al. Incidence and clinical findings of benign, inflammatory disease in patients resected for presumed pancreatic head cancer. Gastrointest Endosc 1997;46:417–23.
99. Notohara K, Burgart LJ, Yadav D, et al. Idiopathic chronic pancreatitis with periductal lymphoplasmacytic infiltration: clinicopathologic features of 35 cases. Am J Surg Pathol 2003;27:1119–27.
100. Weber SM, Cubukcu-Dimopulo O, Palesty JA, et al. Lymphoplasmacytic sclerosing pancreatitis: inflammatory mimic of pancreatic carcinoma. J Gastrointest Surg 2003;7:129–37.
101. Yadav D, Notahara K, Smyrk TC, et al. Idiopathic tumefactive chronic pancreatitis: clinical profile, histology, and natural history after resection. Clin Gastroenterol Hepatol 2003;1:129–35.
102. Hyodo N, Hyodo T. Ultrasonographic evaluation in patients with autoimmune-related pancreatitis. J Gastroenterol 2003;38:1155–61.
103. Sahani DV, Kalva SP, Farrell J, et al. Autoimmune pancreatitis: imaging features. Radiology 2004;233:345–52.
104. Baron PL, Aabakken LE, Cole DJ, et al. Differentiation of benign from malignant pancreatic masses by endoscopic ultrasound. Ann Surg Oncol 1997;4:639–43.
105. Barthet M, Hastier P, Buckley MJ, et al. Eosinophilic pancreatitis mimicking pancreatic neoplasia: EUS and ERCP findings–is nonsurgical diagnosis possible? Pancreas 1998;17:419–22.
106. Barthet M, Portal I, Boujaoude J, et al. Endoscopic ultrasonographic diagnosis of pancreatic cancer complicating chronic pancreatitis. Endoscopy 1996;28:487–91.
107. Brand B, Pfaff T, Binmoeller KF, et al. Endoscopic ultrasound for differential diagnosis of focal pancreatic lesions, confirmed by surgery. Scand J Gastroenterol 2000;35: 1221–8.
108. Canto MIF, Kantsevoy SV, Smith CL, McClelland L, Kalloo AN. Tumor versus pseudotumor? A prospective study of factors associated with missed cancers and nondiagnostic EUS-FNA in patients with pancreatobiliary lesions [abstract]. Gastrointest Endosc 2000;51:AB 170.
109. Nattermann C, Goldschmidt AJ, Dancygier H. [Endosonography in the assessment of pancreatic tumors: a comparison of the endosonographic findings of carcinomas and segmental inflammatory changes; in German]. Dtsch Med Wochenschr 1995;120:1571–6.
110. Okai T, Fujii T, Ida M, et al. EUS and ERCP features of nonalcoholic duct-destructive, mass-forming pancreatitis before and after treatment with prednisolone. Abdom Imaging 2002;27:74–6.
111. Rösch T, Lorenz R, Braig C, et al. Endoscopic ultrasound in pancreatic tumor diagnosis. Gastrointest Endosc 1991;37: 347–52.
112. Becker D, Strobel D, Bernatik T, et al. Echo-enhanced color- and power-Doppler EUS for the discrimination between focal pancreatitis and pancreatic carcinoma. Gastrointest Endosc 2001;53:784–9.
113. Kato T, Tsukamoto Y, Naitoh Y, et al. Ultrasonographic and endoscopic ultrasonographic angiography in pancreatic mass lesions. Acta Radiol 1995;36:381–7.
114. Kitano M, Kudo M, Maekawa K, et al. Contrast-enhanced harmonic EUS: a method to visualize microcirculation in digestive organs [abstract]. Gastrointest Endosc 2005;61: AB 288.
115. Ozawa Y, Numata K, Tanaka K, et al. Contrast-enhanced sonography of small pancreatic mass lesions. J Ultrasound Med 2002;21:983–91.
116. Rickes S, Malfertheiner P. Echo-enhanced sonography: an increasingly used procedure for the differentiation of pancreatic tumors. Dig Dis 2004;22:32–8.
117. Rickes S, Unkrodt K, Neye H, et al. [Differential diagnosis of frequent pancreatic tumors with echo-enhanced power-Doppler sonography: presentation of case reports; in German.] Z Gastroenterol 2002;40:235–40.
118. Rickes S, Unkrodt K, Neye H, et al. Differentiation of pancreatic tumours by conventional ultrasound, unenhanced and echo-enhanced power Doppler sonography. Scand J Gastroenterol 2002;37:1313–20.
119. Rickes S, Unkrodt K, Ocran K, et al. [Evaluation of Doppler ultrasonography criteria for the differential diagnosis of pancreatic tumors; in German.] Ultraschall Med 2000; 21:253–8.
120. Numata K, Ozawa Y, Kobayashi N, et al. Contrast-enhanced sonography of autoimmune pancreatitis: comparison with pathologic findings. J Ultrasound Med 2004;23:199–206.
121. Alasadi R, Berdy A, Parasher G, et al. The diagnostic value of CA 19-9 in patients with suspected pancreatic cancer and chronic pancreatitis on endoscopic ultrasound (EUS) [abstract]. Gastrointest Endosc 2002;55:AB 245.
122. Lambert R, Caletti G, Cho E, et al. International workshop on the clinical impact of endoscopic ultrasound in gastroenterology. Endoscopy 2000;32:549–84.
123. Wiersema MJ, Vilmann P, Giovannini M, et al. Endosonography-guided fine-needle aspiration biopsy: diagnostic accuracy and complication assessment. Gastroenterology 1997;112:1087–95.

124. Williams DB, Sahai AV, Aabakken L, et al. Endoscopic ultrasound guided fine needle aspiration biopsy: a large single centre experience. Gut 1999;44:720–6.
125. Catalano MF, Fazel A, Quadri A, Geenen JE. Factors that influence accuracy of tissue sampling in pancreatic mass lesions: an EUS-FNA study. Gastrointest Endosc 2002;55: AB 246.
126. Fritscher-Ravens A, Brand L, Knofel WT, et al. Comparison of endoscopic ultrasound-guided fine needle aspiration for focal pancreatic lesions in patients with normal parenchyma and chronic pancreatitis. Am J Gastroenterol 2002;97:2768–75.
127. Takahashi K, Yamao K, Okubo K, et al. Differential diagnosis of pancreatic cancer and focal pancreatitis by using EUS-guided FNA. Gastrointest Endosc 2005;61:76–9.
128. Varadarajulu S, Tamhane A, Eloubeidi MA. Yield of EUS-FNA of pancreatic masses in the presence or absence of chronic pancreatitis [abstract]. Gastrointest Endosc 2005;61:AB 304.
129. Brugge WR. The role of EUS in the diagnosis of cystic lesions of the pancreas. Gastrointest Endosc 2000;52(6 Suppl):S18–S22.
130. Brugge WR. Role of endoscopic ultrasound in the diagnosis of cystic lesions of the pancreas. Pancreatology 2001;1: 637–40.
131. Brugge WR. Evaluation of pancreatic cystic lesions with EUS. Gastrointest Endosc 2004;59:698–707.
132. Brugge WR, Lauwers GY, Sahani D, et al. Cystic neoplasms of the pancreas. N Engl J Med 2004;351:1218–26.
133. Hernandez LV, Mishra G, Forsmark C, et al. Role of endoscopic ultrasound (EUS) and EUS-guided fine needle aspiration in the diagnosis and treatment of cystic lesions of the pancreas. Pancreas 2002;25:222–8.
134. Jacobson BC, Baron TH, Adler DG, et al. ASGE guideline: The role of endoscopy in the diagnosis and the management of cystic lesions and inflammatory fluid collections of the pancreas. Gastrointest Endosc 2005;61:363–70.
135. Sedlack R, Affi A, Vazquez-Sequeiros E, et al. Utility of EUS in the evaluation of cystic pancreatic lesions. Gastrointest Endosc 2002;56:543–7.
136. Van Dam J. EUS in cystic lesions of the pancreas. Gastrointest Endosc 2002;56(4 Suppl):S91–S93.
137. Brugge WR. Should all pancreatic cystic lesions be resected? Cyst-fluid analysis in the differential diagnosis of pancreatic cystic lesions: a meta-analysis. Gastrointest Endosc 2005;62:390–1.
138. Koito K, Namieno T, Nagakawa T, et al. Solitary cystic tumor of the pancreas: EUS–pathologic correlation. Gastrointest Endosc 1997;45:268–76.
139. Gress F, Gottlieb K, Cummings O, Sherman S, Lehman G. Endoscopic ultrasound characteristics of mucinous cystic neoplasms of the pancreas. Am J Gastroenterol 2000;95: 961–5.
140. Ahmad NA, Kochman ML, Brensinger C, et al. Interobserver agreement among endosonographers for the diagnosis of neoplastic versus nonneoplastic pancreatic cystic lesions. Gastrointest Endosc 2003;58:59–64.
141. Handrich SJ, Hough DM, Fletcher JG, et al. The natural history of the incidentally discovered small simple pancreatic cyst: long-term follow-up and clinical implications. AJR Am J Roentgenol 2005;184:20–3.
142. Ikeda M, Sato T, Ochiai M, et al. Ultrasonographic follow-up study of small pancreatic cysts of unknown etiology. Bildgebung 1993;60:209–14.
143. Ahmad NA, Kochman ML, Lewis JD, et al. Can EUS alone differentiate between malignant and benign cystic lesions of the pancreas? Am J Gastroenterol 2001;96:3295–300.
144. Brandwein SL, Farrell JJ, Centeno BA, et al. Detection and tumor staging of malignancy in cystic, intraductal, and solid tumors of the pancreas by EUS. Gastrointest Endosc 2001;53:722–7.
145. Brugge WR, Lewandrowski K, Lee-Lewandrowski E, et al. Diagnosis of pancreatic cystic neoplasms: a report of the cooperative pancreatic cyst study. Gastroenterology 2004;126:1330–6.
146. Frossard JL, Amouyal P, Amouyal G, et al. Performance of endosonography-guided fine needle aspiration and biopsy in the diagnosis of pancreatic cystic lesions. Am J Gastroenterol 2003;98:1516–24.
147. Levy MJ, Clain JE. Evaluation and management of cystic pancreatic tumors: emphasis on the role of EUS FNA. Clin Gastroenterol Hepatol 2004;2:639–53.
148. O'Toole D, Palazzo L, Hammel P, et al. Macrocystic pancreatic cystadenoma: the role of EUS and cyst fluid analysis in distinguishing mucinous and serous lesions. Gastrointest Endosc 2004;59:823–9.
149. Sand JA, Hyoty MK, Mattila J, et al. Clinical assessment compared with cyst fluid analysis in the differential diagnosis of cystic lesions in the pancreas. Surgery 1996; 119:275–80.
150. Van der Waaij LA, van Dullemen HM, Porte RJ. Cyst fluid analysis in the differential diagnosis of pancreatic cystic lesions: a pooled analysis. Gastrointest Endosc 2005;62: 383–9.
151. Snady H. Endoscopic ultrasonography in benign pancreatic disease. Surg Clin North Am 2001;81:329–44.
152. Song MH, Lee SK, Kim MH, et al. EUS in the evaluation of pancreatic cystic lesions. Gastrointest Endosc 2003;57: 891–6.
153. Ikeda M, Sato T, Ochiai M, et al. Morphological changes of small pancreatic cysts in response to secretin stimulation: observation by endoscopic ultrasonography. Dig Dis Sci 1993;38:648–52.
154. Lai R, Stanley MW, Bardales R, et al. Endoscopic ultrasound-guided pancreatic duct aspiration: diagnostic yield and safety. Endoscopy 2002;34:715–20.
155. Sriram PV, Kaffes AJ, Rao GV, et al. Endoscopic ultrasound-guided drainage of pancreatic pseudocysts complicated by portal hypertension or by intervening vessels. Endoscopy 2005;37:231–5.
156. Giovannini M, Bernardini D, Seitz JF. Cystogastrotomy entirely performed under endosonography guidance for pancreatic pseudocyst: results in six patients. Gastrointest Endosc 1998;48:200–3.
157. Inui K, Yoshino J, Okushima K, et al. EUS-guided one-step drainage of pancreatic pseudocysts: experience in 3 patients. Gastrointest Endosc 2001;54:87–9.
158. Seifert H, Dietrich C, Schmitt T, et al. Endoscopic ultrasound-guided one-step transmural drainage of cystic abdominal lesions with a large-channel echo endoscope. Endoscopy 2000;32:255–9.
159. Seifert H, Wehrmann T, Schmitt T, et al. Retroperitoneal endoscopic debridement for infected peripancreatic necrosis. Lancet 2000;356:653–5.
160. Vilmann P, Hancke S, Pless T, et al. One-step endosonography-guided drainage of a pancreatic pseudocyst: a new technique of stent delivery through the echo endoscope. Endoscopy 1998;30:730–3.

161. Wiersema MJ. Endosonography-guided cystoduodenostomy with a therapeutic ultrasound endoscope. Gastrointest Endosc 1996;44:614–7.
162. Wiersema MJ, Baron TH, Chari ST. Endosonography-guided pseudocyst drainage with a new large-channel linear scanning echoendoscope. Gastrointest Endosc 2001;53: 811–3.
163. Fuchs M, Reimann FM, Gaebel C, et al. Treatment of infected pancreatic pseudocysts by endoscopic ultrasonography-guided cystogastrostomy. Endoscopy 2000;32: 654–7.
164. Seewald S, Groth S, Omar S, et al. Aggressive endoscopic therapy for pancreatic necrosis and pancreatic abscess: a new safe and effective treatment algorithm (videos). Gastrointest Endosc 2005;62:92–100.
165. Gress F, Schmitt C, Sherman S, et al. Endoscopic ultrasound-guided celiac plexus block for managing abdominal pain associated with chronic pancreatitis: a prospective single center experience. Am J Gastroenterol 2001;96: 409–16.
166. Gress F, Schmitt C, Sherman S, et al. A prospective randomized comparison of endoscopic ultrasound- and computed tomography-guided celiac plexus block for managing chronic pancreatitis pain. Am J Gastroenterol 1999;94: 900–5.
167. Wiersema MJ, Harada N, Wiersema LM. Endosonography guided celiac plexus neurolysis efficacy in chronic pancreatitis and malignant disease. Acta Endosc 1998;28: 67–79.
168. Bataille L, Deprez P. A new application for therapeutic EUS: main pancreatic duct drainage with a "pancreatic rendezvous technique." Gastrointest Endosc 2002;55:740–3.
169. Mallery S, Matlock J, Freeman ML. EUS-guided rendezvous drainage of obstructed biliary and pancreatic ducts: report of 6 cases. Gastrointest Endosc 2004;59:100–7.
170. Will U, Meyer F, Manger T, Wanzar I. Endoscopic ultrasound-assisted rendezvous maneuver to achieve pancreatic duct drainage in obstructive chronic pancreatitis. Endoscopy 2005;37:171–3.
171. Arvanitakis M, Delhaye M, Matos C, et al. EUS-guided pancreaticoduodenostomy: a new technique for main pancreatic duct drainage in acute and chronic pancreatitis [abstract]. Gastrointest Endosc 2005;61:AB 222.
172. François E, Kahaleh M, Giovannini M, et al. EUS-guided pancreaticogastrostomy. Gastrointest Endosc 2002;56: 128–33.
173. Kahaleh M, Yoshida C, Yeaton P. EUS antegrade pancreatography with gastropancreatic duct stent placement: review of two cases. Gastrointest Endosc 2003;58:919–23.
174. Tessier G, Hittelet A, Bories E, Le Moine O, Giovannini M, Devière J. EUS-guided pancreatogastrostomy for the treatment of pain in patients with pancreatic ductal dilatation inaccessible for transpapillary endoscopic therapy [abstract]. Gastrointest Endosc 2005;61:AB 303.
175. Fockens P. EUS in drainage of pancreatic pseudocysts. Gastrointest Endosc 2002;56(4 Suppl):S93–S97.
176. Fockens P, Johnson TG, van Dullemen HM, et al. Endosonographic imaging of pancreatic pseudocysts before endoscopic transmural drainage. Gastrointest Endosc 1997;46: 412–6.
177. Fazel A, Moezardalan K, Kalaghchi B, Forsmark C. The isolated pancreatic duct (PD) stricture with negative brush cytology: EUS for the detection of underlying malignancy. Gastrointest Endosc 2005;61:AB 277.
178. Gress F, Ikenberry S, Sherman S, et al. Endoscopic ultrasound-directed pancreatography. Gastrointest Endosc 1996;44:736–9.
179. Wiersema MJ, Sandusky D, Carr R, et al. Endosonography-guided cholangiopancreatography. Gastrointest Endosc 1996;43:102–6.
180. Canto MI, Goggins M, Yeo CJ, et al. Screening for pancreatic neoplasia in high-risk individuals: an EUS-based approach. Clin Gastroenterol Hepatol 2004;2:606–21.
181. Ainsworth AP, Mortensen MB, Durup J, et al. Clinical impact of endoscopic ultrasonography at a county hospital. Endoscopy 2002;34:447–50.

17 Pancreatic Adenocarcinoma: the Role of Endoscopic Ultrasonography

P.G. Arcidiacono, S. Carrara

Introduction

Pancreatic cancer is the fourth leading cause of cancer death in Western countries. It is unusual in persons under the age of 45, while after the age of 50 its frequency increases linearly. The increase in the incidence ranges from two per 100 000 per year in patients aged 40–44 to 67 per 100 000 per year in patients older than 75 [1]. At the age of 70, the mortality due to pancreatic cancer is approximately 60 deaths per 100 000 persons per year. Some 74 000 new cases of pancreatic cancers were diagnosed in 2000 in Europe [2].

Pancreatic cancers can arise from both the exocrine and endocrine cells. Among pancreatic tumors, about 95% develop from the exocrine portion of the pancreas, including the ductal epithelium, acinar cells, connective tissue, and lymphatic tissue. Approximately 75% of pancreatic carcinomas occur in the head or neck of the pancreas, 15–20% occur in the body of the pancreas, and 5–10% occur in the tail. Typically, pancreatic cancer first metastasizes to regional lymph nodes and then to the liver and less commonly to the lungs. It can also directly invade surrounding visceral organs such as the duodenum, stomach, and colon. It spreads rapidly, is seldom detected at an early stage, and is extremely difficult to treat. Symptoms such as jaundice, abdominal pain, and weight loss may not appear until the disease is quite advanced. By that time, the cancer is likely to have spread to other tissues and surgical removal is no longer possible. This is why it has been termed the "silent killer." The annual mortality rate approximates the annual incidence rate, reflecting the short survival time associated with pancreatic cancer [3].

Overall, fewer than 5% of patients are still alive 5 years after the diagnosis. The EUROCARE study analyzed the survival in 49 074 patients with pancreatic cancer at 1, 3, and 5 years after diagnosis, and the figures were 15.9%, 5.4%, and 4.1%, respectively [4]. The data were similar in men and women. The median survival time for all patients with advanced cancer is about 4–6 months.

For many years, little was known about the pancreas; it was one of the most difficult organs to study, due to its deep location in the abdomen, often inaccessible to traditional ultrasonography and too distant to biopsy. The complexity of pancreatic disease and the richness of the organ's anatomical relationships also made the approach to this gland a challenge even for the best surgeons. Researchers are now beginning to understand the genetic basis and the pathogenesis of the disease, and imaging technologies are developing new and sophisticated techniques for diagnosing and staging pancreatic cancer.

Ultrasonography, computed tomography (CT), and endoscopic retrograde cholangiopancreatography (ERCP) have been the conventional imaging modalities in the management of pancreatic cancer. Endoscopic ultrasonography (EUS) developed in the 1980s after high-frequency ultrasound transducers were combined with endoscopes in order to overcome the physical limitations of transabdominal ultrasonography (which is obstructed by fat, air, and bone).

Initially, EUS was used to confirm and stage solid masses for which a suspicion of malignancy had been raised with other imaging techniques or in the clinical examination. As the technology improved and dedicated accessories were developed, and as endosonographers' experience with the method grew, applications for EUS continued to expand. Nowadays it is also used to diagnose and follow up benign or borderline diseases, and it is often required for evaluation of focal enlargement of the gland, in the absence of a definite mass with other imaging methods. It has been demonstrated that a CT finding of fullness or enlargement of the pancreas may be a sign of malignancy and that EUS may be able to identify a mass [5,6]. In this case, fine-needle aspiration (FNA) biopsy is carried out under endosonographic guidance.

The probe, which can be positioned in the esophagus, stomach, and duodenum, provides ultrasound images of the gastrointestinal wall, distinguishing the different parietal layers and producing transmural images of the surrounding structures. Two types of echoendoscope were initially developed—the radial-scanning instrument, with scans perpendicular to the scope's axis, providing radial 360° images similar to those of CT; and the convex linear-array instrument, in which the scanning plane is parallel to the scope's longitudinal axis. The radial echoendoscope was first developed by the Olympus Corporation, while Pentax and Hitachi developed the convex linear-array probe, with an oblique forward optical view. No differences between the two types of instrument have been found with regard to the accuracy of pancreatic cancer staging [7].

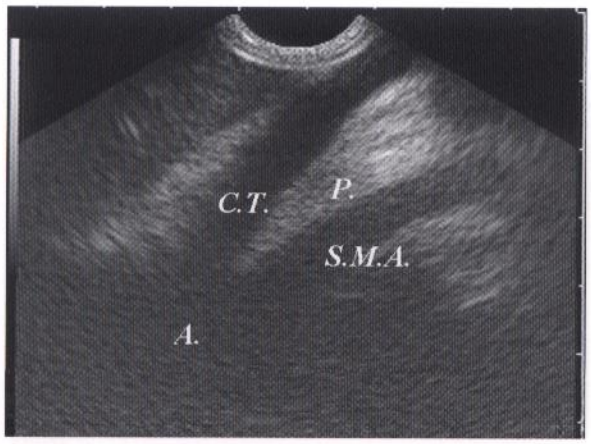


Fig. 17.**1** The origin of the celiac trunk (CT) and superior mesenteric artery (SMA) from the aorta (A); imaging from the proximal stomach. P: pancreas.

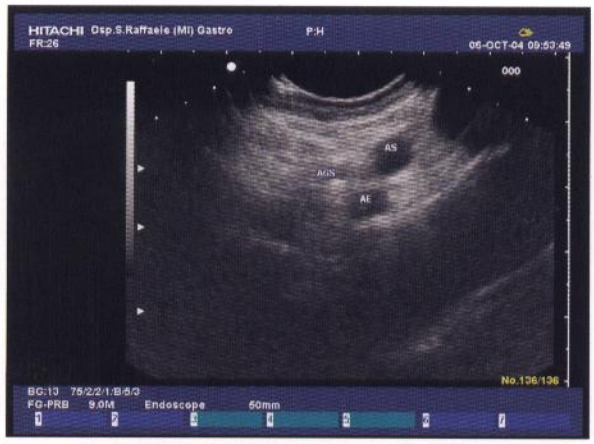


Fig. 17.**2** The celiac trunk division with its branches, the left gastric artery (AGS), splenic artery (AS) and hepatic artery (AE).



a



b

Fig. 17.**3a** The hepatic hilum from the stomach. CBD: common bile duct; AE: hepatic artery; VP: portal vein. **a** Color flow image. **b** Without color flow.

The linear-array echoendoscope is described in this chapter, as it is the instrument used for interventional procedures. It has a biopsy channel, the size of which varies from model to model. The probe is sheathed with a latex balloon that can be filled with water to allow acoustic coupling. The tip of the instrument is equipped with an elevator to angle the accessories exiting from the biopsy channel. The transducer operates at different frequencies, from 5 to 10 MHz. The frequency is inversely proportional to the penetration depth of ultrasound; at 5 MHz, ultrasound penetrates approximately 8 cm, while at 10 MHz the penetration field of ultrasound is about 4 cm.

The patient is positioned in the left lateral decubitus position, as for any standard upper endoscopy procedure. Informed consent is obtained. Conscious sedation can be administered with midazolam and meperidine. The ideal condition is deep sedation with assistance from an anesthetist. The patient is monitored during and after the procedure.

■ Principles of the Technique

Examination of the pancreas starts from the proximal stomach. The most important landmark here is the descending aorta, with the emergence of the celiac trunk and, 1 or 2 centimeters below it, the superior mesenteric artery (Fig. 17.**1**).

The celiac trunk divides into three branches—the left gastric artery, the splenic artery, and the hepatic artery (Fig. 17.**2**). Just past the cardia, the tip of the echoendoscope is placed against the lesser curvature. From this point, a scan of the hepatic hilum (Fig. 17.**3**) with the portal vein as far as the splenomesenteric confluence (Fig. 17.**4**) is obtained by rotating the wrist clockwise on the instrument. The splenic vein and the splenic artery are important landmarks for imaging the body of the pancreas, where the main pancreatic duct is seen as two parallel hyperechoic lines; its lumen is usually virtual, but it may vary from 1 to 3 mm (Figs. 17.**5**, 17.**6**).



Fig. 17.4 The splenic vein (VS) and superior mesenteric vein (VMS) entering the confluence. CBD: common bile duct; CORPO: pancreatic body; TESTA: pancreatic head; VPORTA: portal vein; AS: splenic artery.



Fig. 17.5 View of the pancreatic body (CORPO) from the stomach. The splenic vessels are important landmarks for visualizing the body and the tail of the pancreas. The splenic artery is proximal to the splenic vein. RENESX: left kidney; AS: splenic artery; VS: splenic vein.

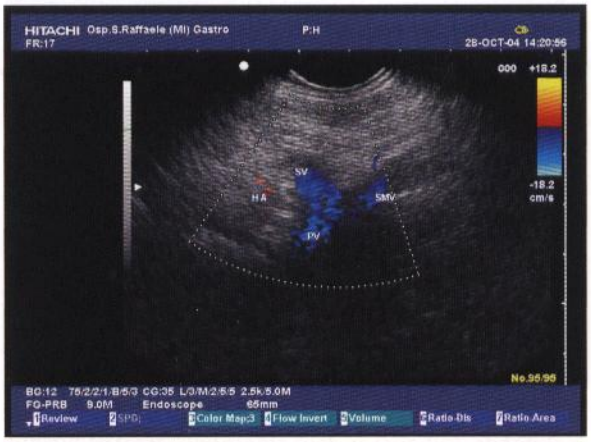


Fig. 17.6 The pancreatic body, with the splenic vein (SV) and the superior mesenteric vein (SMV) forming the portal vein (PV). HA: hepatic artery.



Fig. 17.7 A color flow image of the abdominal vessels from the posterior wall of the stomach. The pancreatic body is seen with the superior mesenteric artery (AMS) emerging from the aorta and the superior mesenteric vein (VMS), and the left renal vein (VRSX) crossing the aorta below the SMA.

The splenic artery has a cephalic location, and its course is more serpiginous than that of the vein. The splenic vein is larger and oval in shape, while the artery is round. As the splenic vessels are followed along the posterior wall of the stomach to the splenic hilum, and as the tip is rotated more to the right, the tail of the pancreas is visualized as far as the spleen and, below, the left kidney. For the tail to be seen, the instrument has to be withdrawn slightly, as the tail courses upward and leftward. The pancreatic neck is imaged from the stomach as the tip is advanced further into the antrum. The main landmark, the superior mesenteric artery, imaged longitudinally, courses posterior to the pancreas, parallel to the splenomesenteric confluence. From this position, the probe displays the pancreatic neck and visualizes one of the most important crossroads for the staging of vascular involvement in patients with pancreatic cancer: the portal vein, the splenomesenteric confluence, with the splenic vein and the superior mesenteric vein, and the superior mesenteric artery (Figs. 17.**4**, 17.**7**).

If there is portal vein obstruction, collaterals may be seen along the gastric and duodenal walls; color Doppler is helpful for recognizing these vessels. The transducer is then advanced to the descending duodenum, past the ampulla of Vater, and the instrument is straightened into the short position. Air in the duodenal lumen is suctioned, and the latex balloon on the probe is inflated with water; the duodenal lumen may also be filled with water to improve acoustic coupling. From this position, a full scan of the pancreatic head and uncinate process is



Fig. 17.**8** The uncinate process seen from the duodenum. The portal confluence (PC) is seen with its vessels—the superior mesenteric vein (SMV) and splenic vein (SV). PH: pancreatic head.



Fig. 17.**9** The pancreatic head (TESTA) from the duodenum, with the mesenteric vessels, the superior mesenteric vein (VMS) and the superior mesenteric artery (AMS).

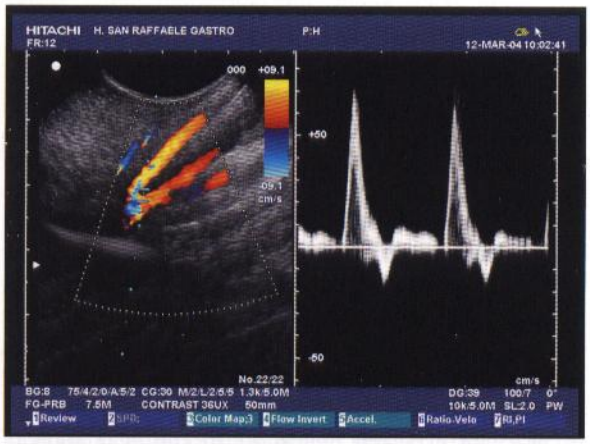


Fig. 17.**10** A color and fast Fourier transform (FFT) Doppler image of the mesenteric vessels seen from the duodenum.



Fig. 17.**11** The uncinate process with the veins and, more deeply, the superior mesenteric artery (AMS), which is located below the portal confluence (PC). PH: pancreatic head; VMS: superior mesenteric vein; VS: splenic vein.

obtained (Fig. 17.**8**)—from the mesenteric vessels (vein and artery), with the echoendoscope rotated to the right, to the aorta, with rotation to the left (Figs. 17.**9**–17.**11**).

The probe is maneuvered and withdrawn with fine movements. The superior mesenteric vein is followed as far as the confluence. Here, the neck of the pancreas is also visualized from the duodenum, and this image complements the previous scan obtained from the stomach. Two different areas of the pancreatic head can be identified, due to their different embryogenesis—the dorsal and the ventral pancreas. Their echogenicity differs; the ventral part may appear more hypoechoic, mimicking a pseudotumor, although its structure is homogeneous, while the dorsal part is more hyperechoic, as it is richer in interacinar fat tissue. The ampulla of Vater is seen as a hypoechoic, well-delineated structure (Fig. 17.**12**) from which the two ducts—the common bile duct (upper) and the main pancreatic duct (lower)—can be traced and followed into the pancreatic head (Fig. 17.**13**). While the ampulla is being imaged, one must ensure that the probe is not pressed too hard against the duodenal wall, to avoid compression artifacts. The common bile duct can be followed as far as the hepatic hilum, with the tip being withdrawn and lifted. As the tip is withdrawn from the major ampulla, the minor ampulla and Santorini's duct (the accessory pancreatic duct) are imaged (Fig. 17.**14**).

The normal pancreatic parenchyma has a characteristic homogeneous "salt-and-pepper" echo texture. Its echo structure is similar to that of the liver in young people. In older people and in the obese, it is more hyperechoic.

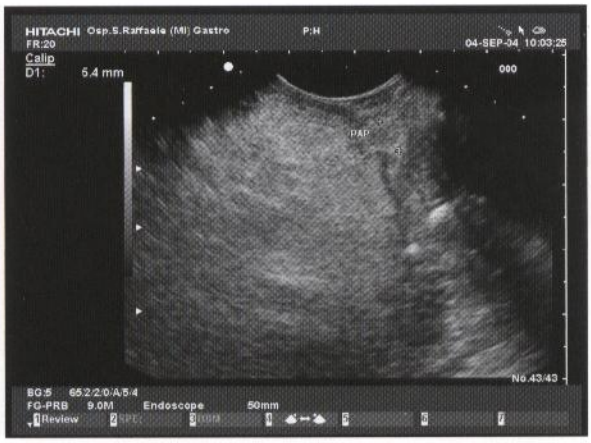


Fig. 17.**12** Scanning of the normal papilla of Vater (PAP) from the duodenum.



Fig. 17.**13** View of the common bile duct (CBD) and distal pancreatic duct (Wirsung's duct, W) in the pancreatic head from the descending duodenum. The two ducts are shown in a longitudinal section that passes into the papilla, the smooth, hypoechoic area on the right of the image.

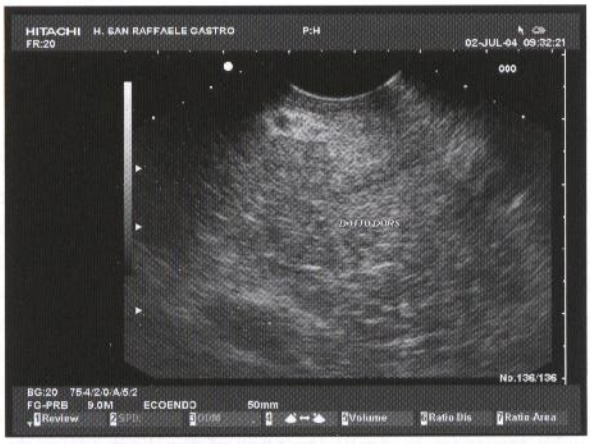


Fig. 17.**14** A view of Santorini's duct (SD, the accessory pancreatic duct) from the descending duodenum. Once the papilla of Vater has been visualized, the transducer is withdrawn further, with fine movements; the minor papilla comes into view, and Santorini's duct can be followed into the pancreatic head.

Staging

The prognosis in cancer depends on how advanced the tumor is at the time of diagnosis. Accurate staging is essential to allow the best treatment decisions to be made, particularly in selecting patients for surgery and patients for chemotherapy or palliative procedures. Pancreatic adenocarcinoma is classified using the tumor, node, and metastasis (TNM) staging system, which was modified in 2002 by the American Joint Committee on Cancer [8]. This classification assigns tumors that are invading the portal venous system (previously staged as T4) to stage T3. Although surgery is technically feasible, invasion of the portal vein, superior mesenteric vessels, and celiac trunk usually precludes surgical resection [9] (Tables 17.**1**, 17.**2**).

Older and more recent imaging modalities are available to help in the diagnosis of pancreatic carcinoma: transabdominal ultrasonography (TUS), computed tomography (CT), endoscopic ultrasonography (EUS), magnetic resonance imaging (MRI), endoscopic retrograde cholangiopancreatography (ERCP), and positron-emission tomography (PET). EUS is one of the most sensitive techniques for detecting pancreatic masses, with a high accuracy rate that ranges from 78% to 94% for T staging and from 64% to 82% for N staging [10–12].

Many studies have examined the role of EUS in the detection of suspected pancreatic masses not defined by cross-sectional imaging techniques, and it has been found that EUS has better sensitivity for lesions less than 3 cm in size, with the best advantage for lesions less than 2 cm in size [13]. In a recent review, Hunt and Faigel pooled data from four studies, comparing the accuracy of EUS and helical CT in the evaluation of pancreatic cancer [14]. They noted that EUS detected more tumors (97% versus 73%), that it was more accurate for determining tumor resectability (91% versus 73%), and that it was more sensitive for detecting vascular involvement (91% versus 64%). However, newer and more sophisticated multiphasic helical CT scans have shown better accuracy for detecting small cancers (< 2 cm), with a sensitivity of 97% and a specificity of 100% [15].

DeWitt et al. [16] compared endoscopic ultrasonography with multidetector CT for detecting and staging pancreatic cancer and concluded that EUS was superior for tumor detection (98% versus 86%; $P = 0.01$), but equivalent to multidetector CT for nodal staging and assessment of resectability (88% versus 92%). Detection of lesions 25 mm or smaller in size did not significantly differ between EUS and multidetector CT (89% versus 53%; $P = 0.077$). In patients who underwent surgery, the overall accuracy of EUS staging was superior to that of CT (67% versus 41%; $P = 0.007$).

T stage. The T stage reflects the tumor characteristics and invasion of adjacent structures. The tumor is

usually imaged as a focal, hypoechoic mass. Lesions of huge dimensions are inhomogeneous due to fibrosis and necrotic tissue, and they may have anechoic foci and poorly defined margins. Small cancers (< 2 cm) are more homogeneous, with smooth borders. There is a clear demarcation between the hypoechogenicity of the tumor and the surrounding healthy pancreatic tissue or fat tissue. Tumors with a homogeneous echo texture similar to that of the surrounding pancreas, with only a mild hypoechoic pattern, are often well-differentiated, less aggressive cancers (Fig. 17.**15**).

Usually, there are no calcifications in a tumor arising from a "healthy" pancreas, while cancers originating from chronic pancreatitis may be surrounded by calcifications. The endosonographer has to recognize an area with less calcification in the context of chronic pancreatitis, as this is suspicious for malignancy and a biopsy has to be directed toward the area. If there is diffuse enlargement of the gland, lymphoma has to be included in the differential diagnosis; lymphomas are often huge and multifocal, with an ultrasound pattern similar to that of acute pancreatitis. In describing the T stage, the endosonographer has to note the size of the tumor and its relationship with the surrounding organs, particularly with the duodenum, the stomach, and the common bile duct. The parietal layers of the duodenum have to be observed in order to exclude invasion if there is a tumor of the pancreatic head. In this case, the normal layered architecture of the duodenal wall is lost and replaced with hypoechoic tissue. Dilation of the main pancreatic duct is a sign that may suggest the presence of an obstructing mass downstream. The dilated duct is different from that observed in chronic pancreatitis, as in this case the dilation is uniform and regular. Tumors in the head of the pancreas are usually diagnosed earlier than those in the body or tail, because of the close relationship with the common bile duct and the subsequent obstructive jaundice (Fig. 17.**16**).

The differential diagnosis of a pancreatic solid mass has to include inflammatory masses such as chronic and autoimmune pancreatitis, and other kinds of tumor. Clinical, laboratory, and imaging tests have to be evaluated in order to reach the final diagnosis, and FNA has to be carried out if there is a strong suspicion of cancer. Some centers have suggested that biopsies should not be carried out in lesions that will undergo surgery. The surgeons argue that a negative cytological result may be a sampling error that will not preclude surgery. On the other hand, passage of the needle into a tumor may contaminate the peritoneum with tumor cells. The risk of carcinomatous seeding secondary to EUS-guided FNA is very low; the needle path is short, and in addition, the tract passed by the needle is resected at the time of surgery [17]. In addition, EUS-FNA through the duodenum does not breach the peritoneal cavity, and this should prevent peritoneal seeding. Another aspect in

Table 17.**1** TNM staging

Tumor (T)	
TX	Primary tumor cannot be assessed
T0	No evidence of primary tumor
Tis	Carcinoma in situ
T1	Tumor limited to the pancreas, 2 cm or smaller in largest diameter
T2	Tumor limited to the pancreas, larger than 2 cm in larger diameter
T3	Tumor extension beyond the pancreas (i.e., duodenum, bile duct, portal or superior mesenteric vein) but not involving the celiac axis or superior mesenteric artery
T4	Tumor involving the celiac axis or superior mesenteric arteries
Regional lymph nodes (N)	
NX	Regional lymph nodes cannot be assessed
N0	No regional lymph node metastasis
N1	Regional lymph node metastasis
Distant metastasis (M)	
MX	Distant metastasis cannot be assessed
M0	No distant metastasis
M1	Distant metastasis

Table 17.**2** The results of the TNM staging system can be grouped into these stages

Stage 0	Tis, N0, M0
Stage IA	T1, N0, M0
Stage IB	T2, N0, M0
Stage IIA	T3, N0, M0
Stage IIB	T1–3, N1, M0
Stage III	T4, any N, M0
Stage IV	Any T, any N, M1

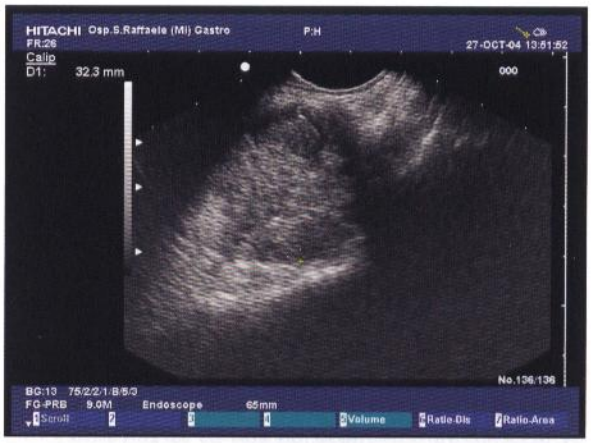


Fig. 17.**15** A lesion 3 cm in size in the head of the pancreas. The larger the lesion, the more inhomogeneous the echo texture.

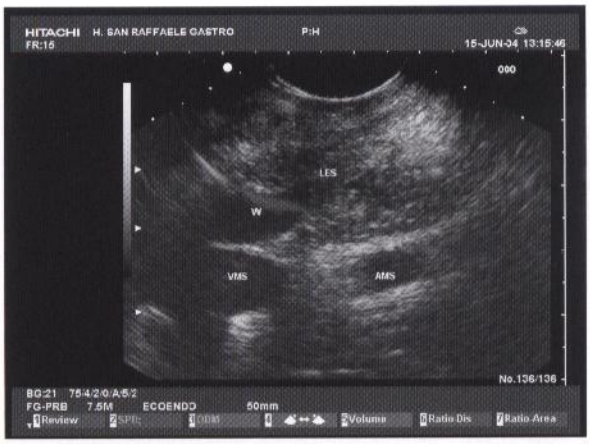


Fig. 17.**16** A pancreatic head lesion (LES) occluding the main pancreatic duct (Wirsung's duct, W), which is dilated. AMS: superior mesenteric artery; VMS: superior mesenteric vein.



Fig. 17.**17** A pancreatic lesion (LES) occluding the superior mesenteric vein (VMS). A cuff of hypoechoic tissue is visible around the superior mesenteric artery (AMS). VP: portal vein.

favor of EUS-FNA is the need to obtain cytological identification of a tumor mass before initiating neoadjuvant therapy.

Despite the good resolution of EUS, pancreatic cancer may be missed with the method in certain conditions: chronic pancreatitis with a severely inhomogeneous echo texture; diffuse infiltration by the tumor; a prominent ventral/dorsal split; and in patients who have had a recent episode of acute pancreatitis (< 4 weeks), where edema can conceal a focal lesion. These factors have been reported in a recent study by Bhutani and colleagues [18]. The accuracy of T staging is also affected by peritumoral inflammation and by large tumors that cause ultrasound attenuation. Various studies have shown that EUS is more accurate in cancers less than 3 cm in size [19].

Intravenous contrast media have been used to help differentiate between benign inflammatory pseudotumoral masses and pancreatic cancer. The initial studies were carried out with transabdominal ultrasound, with good results being reported. Contrast enhancement showed marked hyperperfusion in cases of neuroendocrine tumors or inflammatory lesions, whereas pancreatic carcinoma typically showed a hypoperfused pattern [20,21]. Contrast agents are now also being used for EUS examinations [22]. The contrast agents consist of stabilized microbubbles that range in size from 2 to 8 µm (the size of an erythrocyte) and have outer shells to prevent coagulation and aggregation. They can therefore be injected intravenously with no risk of thrombosis, and they cross the pulmonary capillaries in that same way that blood cells do. The presence of contrast in the bloodstream increases the ultrasound signal intensity and consequently the sensitivity of the equipment for detecting small vessels with slow flow. The contrast is injected as an intravenous bolus, and enhancement persists for approximately 3–5 min. This new technique is safe, involving no risk of pancreatitis or thrombosis, and does not expose the patient to ionizing radiation. It is useful in differentiating between an inflammatory pancreatic mass and a ductal carcinoma, and it can be used to guide biopsies in an area of suspicion.

The second step, after the identification and description of the primary lesion, is the evaluation of the vascular structures surrounding the pancreas. This is one of the most important criteria for the resectability of pancreatic cancer (Fig. 17.**17**). Since its very beginnings, EUS has been regarded as the most accurate preoperative method for evaluating tumor resectability. The criteria for assessing vascular invasion have been examined by Brugge et al. [23] and Snady et al. [24], with an accuracy of 55–94% being reported. When assessing vascular involvement, the endosonographer has to note:

- Any loss of interface between the tumor and the vessel wall
- The presence of tumor in the vessel lumen (seen as echoic material)
- Collateral vessels
- Irregularity in the vessel wall

If there is an intact hyperechoic interface between the tumor and the vessel, one can be sure that the tumor does not involve the vessel, while complete encasement of the vessel by the tumor is a sign of involvement. Initial studies demonstrated the high sensitivity and specificity of EUS for assessing vascular invasion; however, most of these studies suffered from bias, in that EUS was compared with surgical palpation in unresectable cancers. This surgical method is extremely subjective and susceptible to interobserver variability [10–12]. More recent studies have found that EUS is not so accurate for predicting resectability. In a blinded reevaluation of videotapes, Rösch et al. found that the ultrasound features of vascular invasion did not show sensitivity and specificity values greater than 80% [25]. Recent reports have

focused on reassessing the accuracy of EUS for predicting vascular involvement. The only gold standard for comparison with EUS assessment of invasion is the surgical specimen, with histological analysis. Aslanian and colleagues compared EUS with vascular resection and histological evidence of vascular invasion in 30 resected pancreatic cancers [26]. They found that EUS had poor predictive accuracy for the diagnosis of vascular invasion. The sensitivity, specificity, positive predictive value, and negative predictive value were 63%, 64%, 43%, and 80%, respectively, for vascular adherence; and 50%, 58%, 28%, and 82%, respectively, for vascular invasion. The loss of a hyperechoic interface between the tumor and the vessel, previously regarded as a major criterion for vascular invasion, was found to be a poor predictor of vascular involvement. Peritumoral inflammatory tissue may be one of the causes of endosonographic overdiagnosis of vascular invasion. What appears to be vascular adherence may be only fibrosis and edema, seen as a smooth hypoechoic area. On the other hand, CT sometimes underdiagnoses vascular involvement. The two methods are therefore complementary; EUS provides an opportunity for biopsies to be taken and CT provides broad imaging of the abdomen, making it possible to diagnose distant metastases. The authors conclude that if the sonographic features of vascular invasion are absent, EUS usually excludes involvement of the portal confluence, but when sonographic signs of vascular involvement are present, they may not be reliable for diagnosis. Dilated and collateral veins may sometimes be seen in patients with invasion or thrombosis of the portal vein system.

The assessment of vascular invasion may be more difficult in the arteries, particularly with the superior mesenteric artery, which is deeper and more distant from the probe; in this case, the accuracy of EUS is lower than that for detecting portal or splenic veins [23–25]. This difficulty is thought to be due to the fact that arteries are smaller than veins and have a more tortuous course, which is difficult to follow along its entire path. Arteries often show signs of encasement rather than clear invasion with tumoral growth in their lumen, perhaps because the vessel walls are thicker than those in venous structures (Fig. 17.**18**).

N stage. The accuracy of EUS for N staging lies in the range of 64–82% [12]. Although EUS is highly sensitive for detecting regional lymph nodes, it has difficulties in distinguishing between malignant and inflammatory adenopathy. Catalano et al. [27] suggested some predictive features of malignancy: lymph nodes are considered malignant when they have a round shape and are homogeneous and hypoechoic, with sharp margins, and if they have a diameter of 10 mm or more. Loss of the hyperechoic center is a sign of malignancy. A lymph node with an elongated shape that is heterogeneous and hyperechoic is usually reactive, but it may sometimes

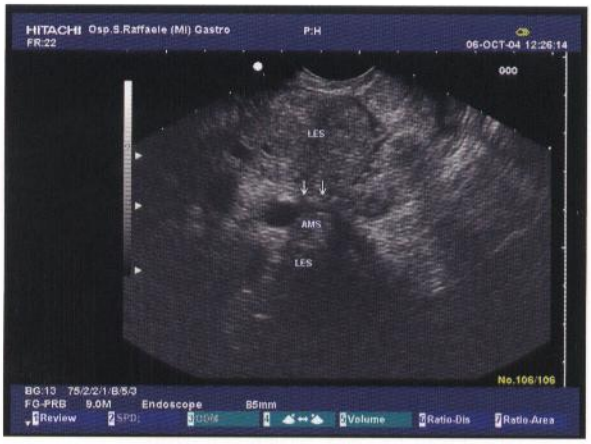


Fig. 17.**18** A huge pancreatic lesion (LES), with infiltration (arrows) into the superior mesenteric artery (AMS).

have micrometastases that are not detectable with ultrasound; in this case, the endosonographic features of malignancy are not sufficient to allow prediction of the real nature of the enlarged node, and EUS-FNA is needed in order to resolve the issue (Fig. 17.**19**).

The main node stations to image are the perigastric, periduodenal, and celiac nodes, and the hepatic hilum. Mediastinal adenopathy, detected in about 5% of patients with pancreaticobiliary cancer, has a prognostic value and precludes surgical resection in patients with pancreatic cancer [28]. The endosonographer should therefore routinely explore the mediastinal stations.

M stage. As far as M staging is concerned, EUS is not capable of identifying distant metastases, but is useful for detecting ascites and metastases in the left hepatic lobe.

EUS-guided fine needle aspiration biopsy (EUS-FNA)

EUS provides high-resolution images of lesions and is an accurate tool for diagnosing pancreatic masses, but it has one primary limitation: its low specificity (about 75%) [29] and inability to differentiate between malignant and inflammatory pancreatic masses. The specificity of EUS can be significantly increased by using EUS-guided FNA. Since the initial studies of the technique, EUS-FNA has been found to have a high specificity (100%) and accuracy rate (95%) [30]. It has been shown to have a relatively low complication rate, with a major complication rate of 1% [31] and a low risk of tumor seeding. EUS-FNA through the duodenum has the advantage of not passing through the peritoneal cavity, which should prevent peritoneal seeding; moreover, in resectable tumors, the area through which the needle has passed is removed.

The necessity of obtaining a cytological or histological sample in order to diagnose pancreatic cancer before surgery remains controversial. Varadarajulu and Elou-



a

b

Fig. 17.**19a** A peripancreatic lymph node (LINF) with a malignant appearance. **b** EUS-guided fine-needle aspiration of the node.

Table 17.**3** Indications for endoscopic ultrasound-guided fine-needle aspiration (EUS-FNA) [32]

- To document a diagnosis of malignancy in a patient with an unresectable mass as a prerequisite for adjuvant chemotherapy or radiotherapy
- To exclude other tumor types such as lymphoma, small-cell metastasis, or neuroendocrine cancer that may require a different management strategy
- To determine a diagnosis in patients who are reluctant to undergo major surgery without a definitive diagnosis
- To document the absence of malignancy when the pretest probability of malignancy is low

beidi listed the indications for EUS-FNA in a recent review of the use of EUS in pancreatic cancer (Table 17.**3**) [32].

Tissue diagnosis is almost always required in unresectable cancers before chemotherapy, radiotherapy (palliative or neoadjuvant), or nonsurgical palliative treatment for obstructive jaundice are started. The histological nature of a pancreatic tumor can also change the management approach; for example, a pancreatic lymphoma requires medical treatment rather than surgery.

■ EUS-FNA Technique

Lesions located in the pancreatic head and uncinate process are biopsied from the duodenum, while those located in the body and tail are biopsied from the stomach. Color Doppler is used to display the lesion and surrounding structures, in order to avoid vascular structures along the needle path.

Once the target lesion has been visualized, with the transducer in a steady position, the tip is pushed against the gastrointestinal wall, and the up–down and left–right wheels are locked. Keeping a steady position is often easier from the duodenum, for pancreatic head cancer, than from the stomach, for cancers of the pancreatic body and tail. A biopsy from the stomach may require more energy and a firm hit, as the gastric folds present resistance to needle passage. The needle is can be easily introduced if the procedure is carried out in a straight position. If the tip is flexed too much or the echoendoscope is looped, advancement of the needle is difficult and it may be dangerous for the instrument. Excessive pushing of the needle may cause a hole in the endoscope's working channel. If resistance is encountered, the instrument should be withdrawn and straightened until needle passage becomes easier, without resistance. Most pancreatic solid tumors are as hard as stone, due to the desmoplastic reaction typical of these cancers, and strong needle penetration is needed.

The needle used for EUS-FNA is equipped with a stylet covered by a protective spiral sheath. The stylet prevents the needle from clogging due to tissue or blood as it is advanced into the target lesion. During the FNA procedure, the catheter is inserted into the biopsy channel. Before the puncture, the stylet is withdrawn a few millimeters to expose the sharp tip of the needle. The tip is then advanced with real-time endoscopic ultrasound guidance until the needle tip is seen within the lesion. The needle appears as a hyperechoic line; artifacts due to reflections produced by the metal are easily recognized. If the needle is not fully visualized, fine adjustments of the transducer position usually restore the correct image. Once the lesion has been penetrated, the stylet is advanced to the original position to clean the needle of cells or clots that have entered during passage through the gastrointestinal wall. The stylet is then removed, suction is applied through a 10-mL syringe, and the needle is moved to and fro 5–10 times inside the lesion. The suction is then released, the needle is retracted into the catheter, and the entire catheter is removed from the echoendoscope. The aspirate is then placed on glass slides for smears using Papanicolau and Wright–Giemsa stains. The presence of a cytology technician or cytopathologist in the endoscopy room during the procedure is important for assessing the adequacy of the specimen after each pass. This helps the endosonographer decide whether further passes are needed.

The number of passes needed to provide an adequate sample is still a matter of controversy. An average of three or four passes appears to provide definitive cytologic diagnosis [33,34]. In a technological review of EUS-FNA, Erickson explained in a very clear way the advantages, disadvantages, and complications of the procedure [35]. There appear to be no clinical or EUS features predictive of the number of passes needed. The major determinant of FNA pass numbers appears to be the tumor differentiation; some cases in which 10 or more passes were needed have been reported in well-differentiated cancers [36] (Figs. 17.**20**, 17.**21**).

Ductal and parenchymal changes have been observed in patients with pancreatic or biliary stents, due to edema and fibrosis, resulting in abnormalities in the echogenicity and texture of the tissue surrounding the stent (Fig. 17.**22**). As a foreign body, the plastic or metal stent creates a fibrotic reaction around the duct, altering the diagnostic value of endosonography and making FNA more difficult. Air in the biliary ducts may cause interference and reverberations, and the stent may cause shadowing that conceals the surrounding tissues. This is known to create artifacts and fibrosis that make it more difficult to carry out FNA, as the needle has to touch hard tissue and it is sometimes necessary for it to pass through the stent. Despite the method's high level of accuracy, its low negative predictive value (NPV) limits the usefulness of EUS-FNA in these cases. Even in the presence of a negative cytological result, malignancy cannot be ruled out, particularly if clinical and laboratory tests are strongly suspicious for cancer. Agarwal et al. reported a NPV of 22% with EUS-FNA in patients with obstructive jaundice and biliary strictures. In seven of the eight patients with false-negative results, a plastic stent had been previously placed in the bile duct [37]. In addition, indeterminate biliary strictures may also be benign, without a clearly defined mass. In these cases, the edema caused by stent placement may resemble a focal lesion. Despite of these difficulties, we consider that EUS-FNA is an important tool for reaching a cytological diagnosis, even in patients with biliary or pancreatic stents; the availability of a cytology technician is very important in these cases.

EUS-FNA is not only useful as a prognostic indicator, but also has a substantial effect on cost savings. It can avoid major surgery in unresectable patients and it helps in the management of patients (establishing the need for palliative treatment, chemotherapy, or minimally invasive procedures). In a study of the clinical value of EUS-FNA, Chang et al. showed that it led to cost savings of approximately $3300 per patient, due to the avoidance of surgery [30].

In conclusion, EUS and CT are complementary methods in the diagnosis and staging of pancreatic cancer. Technological developments have provided EUS with new accessories to improve the diagnosis, such as con-

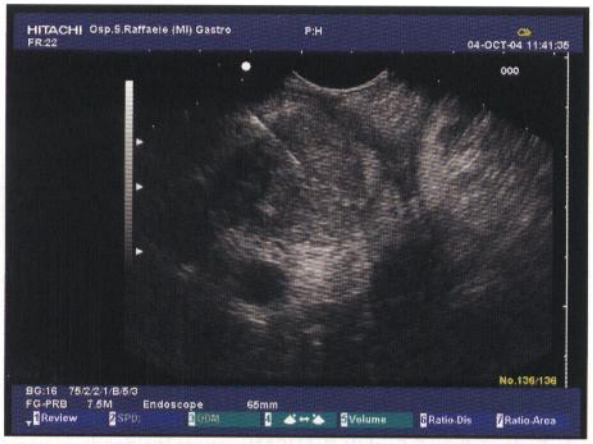


Fig. 17.**20** EUS-guided fine-needle aspiration biopsy of a mass in the head of the pancreas. The lesion is hypoechoic, with defined margins. The needle is visible as a hyperechoic line.



Fig. 17.**21** EUS-guided fine-needle aspiration of a tumor in the head of the pancreas.



Fig. 17.**22** A malignant lesion in the pancreatic head, with a stent placed in the bile duct. The stent appears as two parallel hyperechoic lines. The lesion does not have defined margins and may be difficult to distinguish from the edema caused by the stent.

trast enhancement and most importantly the option of carrying out guided fine-needle aspiration biopsies. EUS is now emerging not only as a purely imaging technique, but also as a method of guiding the delivery of new treatments for pancreatic cancer, and it can be helpful in the palliative treatment of pancreatic cancer. New therapeutic applications of EUS, such as injection therapy with genetic or immunological agents and radiofrequency therapy, have yet to be fully assessed in large multicenter trials in order to define their real clinical value.

References

1. Ferlay J, Bray F, Sankila R. EUCAN: cancer incidence, mortality, and prevalence in the European Union. International Agency for Research on Cancer, ENCR, European Network of Cancer Registries, Europe Against Cancer Programme. Lyons: IARC Press, 1999. (IARC cancerBase, no. 4.)
2. Ferlay J, Bray F, Pisani P, Parkin DM. GLOBOCAN 2000: cancer incidence, mortality, and prevalence worldwide. WHO International Agency for Research on Cancer. Lyons: IARC Press, 2001. (IARC cancerBase, no. 5.)
3. Coleman MP, Babb P, Daniecki P. Cancer survival trends in England and Wales, 1971–1995: deprivation and NHS region. London: Stationery Office, 1999. (Studies in medical and population subjects, no. 61.)
4. Roazzi P, Capocaccia R, Santaquilani M, Carrani E. Electronic availability of EUROCARE-3 data: a tool for further analysis. Ann Oncol 2003;14(Suppl 5):v150–5.
5. Horwhat JD, Gerke H, Baillie J. Focal or diffuse "fullness" of the pancreas on CT is usually benign, but yield of malignancy, albeit small, justifies EUS +/– FNA [abstract]. Gastrointest Endosc 2004;59:AB 230.
6. Ho S, Bonasera R, Pollack B. The utility of endoscopic ultrasound (EUS) in evaluating CT findings of fullness or enlargement of the pancreas: a large single center experience. Am J Gastroenterol 2003;98:S295.
7. Gress F, Savides T, Cummings O, Sherman S, Lehman G, Zaidi S, et al. Radial scanning and linear array endosonography for staging pancreatic cancer: a prospective randomized comparison. Gastrointest Endosc 1997;45:138–42.
8. Greene FL. Exocrine pancreas. In: American Joint Committee on Cancer, editors. AJCC cancer staging manual, 6th ed. New York: Springer, 2002: 157–64.
9. Rösch T, Classen M. Endosonographic staging of pancreatic cancer. In: Van Dam J, Sivak MV Jr, editors. Gastrointestinal endosonography. Philadelphia: Saunders, 1999:245–250.
10. Gress F, Hawes RH, Savides TJ, Ikenberry SO, Cummings O, Kopecky KK, et al. Role of EUS in preoperative staging of pancreatic cancer: a large single-center experience. Gastrointest Endosc 1999;50:786–91.
11. Palazzo L, Roseau G, Gayet B, Vilgrain V, Belghiti J, Fekete F, et al. Endoscopic ultrasonography in the diagnosis and staging of pancreatic adenocarcinoma. Endoscopy 1993; 25:143–50.
12. Yasuda K, Mukai H, Nakajima M, Kawai K. Staging of pancreatic carcinoma by endoscopic ultrasonography. Endoscopy 1993;25:151–5.
13. Rösch T, Braig C, Gain T, Feuerbach S, Siewert JR, Schusdziarra V, et al. Staging of pancreatic and ampullary carcinoma by endoscopic ultrasonography: comparison with conventional sonography, computed tomography and angiography. Gastroenterology 1992;102:188–99.
14. Hunt GC, Faigel DO. Assessment of EUS for diagnosing, staging, and determining respectability of pancreatic cancer: a review. Gastrointest Endosc 2002;55:232–37.
15. Bronstein YL, Loyer EM, Kaur H, Choi H, David C, DuBrow RA, et al. Detection of small pancreatic tumors with multiphasic helical CT. AJR Am J Roentgenol 2004;182:619–23.
16. DeWitt J, Devereaux B, Chriswell M, McGreevy K, Howard T, Imperiale TF, et al. Comparison of endoscopic ultrasonography and multidetector computer tomography for detecting and staging pancreatic cancer. Ann Intern Med 2004;141:753–63.
17. Micames C, Jowell PS, White R, Paulson E, Nelson R, Morse M, et al. Lower frequency of peritoneal carcinomatosis in patients with pancreatic cancer diagnosed by EUS-guided FNA vs percutaneous FNA. Gastrointest Endosc 2003;58: 690–5.
18. Bhutani MS, Gress FG, Giovannini M, Erickson RA, Catalano MF, Chak A, et al. The No Endosonographic Detection of Tumor (NEST) study: a case series of pancreatic cancers missed on endoscopic ultrasonography. Endoscopy 2004; 36:385–89.
19. Nakaizumi A, Uehara H, Iishi H, Tatsuta M, Kitamura T, Kuroda C, et al. Endoscopic ultrasonography in diagnosis and staging of pancreatic cancer. Dig Dis Sci 1995;40: 696–700.
20. Rickes S, Malfertheiner P. Echo-enhanced sonography: an increasingly used procedure for the differentiation of pancreatic tumors. Dig Dis 2004;22:32–8.
21. D'Onofrio M, Mansueto G, Falconi M, Procacci C. Neuroendocrine pancreatic tumor: value of contrast enhanced ultrasonography. Abdom Imaging 2004;29:246–58.
22. Becker D, Strobel D, Bernatik T, Hahn EG. Echo-enhanced color- and power-Doppler EUS for the discrimination between focal pancreatitis and pancreatic parenchyma. Gastrointest Endosc 2001;53:784–89.
23. Brugge WR, Lee MJ, Kelsey PB, Schapiro RH, Warshaw AL. The use of EUS to diagnose malignant portal venous system invasion by pancreatic cancer. Gastrointest. Endosc 1996; 43:561–7.
24. Snady H, Bruckner H, Siegel J, Cooperman A, Neff R, Kiefer L. Endoscopic ultrasonographic criteria of vascular invasion by potentially resectable pancreatic tumors. Gastrointest Endosc 1994;40:326–33.
25. Rösch T, Dittler HJ, Strobel K, Meining A, Schusdziarra V, Lorenz R, et al. Endoscopic ultrasound criteria for vascular invasion in the staging of cancer of the head of the pancreas: a blind reevaluation of videotapes. Gastrointest Endosc 2000;52:469–77.
26. Aslanian H, Salem R, Lee J, Andersen D, Robert M, Topazian M. EUS diagnosis of vascular invasion in pancreatic cancer: surgical and histologic correlates. Am J Gastroenterol 2005;100:1381–5.
27. Catalano MF, Sivak MV Jr, Rice T, Gragg LA, Van Dam J. Endosonographic features predictive of lymph node metastasis. Gastrointest Endosc 1994;40:442–6.
28. Agarwal B, Gogia S, Eloubeidi MA, Correa AM, Ho L, Collins BT. Malignant mediastinal lymphadenopathy detected by staging EUS in patients with pancreatobiliary cancer. Gastrointest Endosc 2005;61:849–53.
29. Rösch T, Lorenz R, Braig C, Feuerbach S, Siewert JR, Schusdziarra V, et al. Endoscopic ultrasound in pancreatic tumor diagnosis. Gastrointest Endosc 1991;37:347–52.

30. Chang KJ, Nguyen P, Erickson RA, Durbin TE, Katz KD. The clinical utility of endoscopic ultrasound-guided fine-needle aspiration in the diagnosis and staging of pancreatic carcinoma. Gastrointest Endosc 1997;45:387–93.
31. Chang K, Wiersema M, Giovannini M. Multicenter collaborative study on endoscopic ultrasound (EUS) guided fine needle aspiration (FNA) of the pancreas [abstract]. Gastrointest Endosc 1996;43:A507.
32. Varadarajulu S, Eloubeidi MA. Frequency and significance of acute intracystic hemorrhage during EUS-FNA of cystic lesions of the pancreas. Gatsrointest Endosc 2004;60:631–5.
33. Erickson RA, Sayage-Rabie L, Beisner RS. Factors impacting endoscopic ultrasound-guided fine needle aspiration passes for pancreatic malignancies. Gastrointest Endosc 2000;51: 184–90.
34. Wiersema MJ, Vilmann P, Giovannini M, Chang KJ, Wiersema LM. Endosonography-guided fine-needle aspiration biopsy: diagnostic accuracy and complication assessment. Gastroenterology 1997;112:1087–95.
35. Erickson RA. EUS-guided FNA. Gastrointest Endosc 2004; 60:267–79.
36. Lin F, Staerkel G. Cytologic criteria for well differentiated adenocarcinoma of the pancreas in fine-needle aspiration biopsy specimens. Cancer 2003;99:44–50.
37. Agarwal B, Abu-Hamda E, Molke KL, Correa AM, Ho L. Endoscopic ultrasound-guided fine needle aspiration and multidetector spiral CT in the diagnosis of pancreatic cancer. Am J Gastroenterol 2004;99:844–50.

18 Benign and Malignant (Cystic) Tumors of the Pancreas

C.F. Dietrich, C. Jenssen

Introduction

Various types of benign and malignant cystic tumor can occur in the pancreas. Cystic lesions in the pancreas can be divided pathologically into retention cysts, pseudocysts, and cystic neoplasms. Distinguishing between the various types of lesion has important prognostic and therapeutic implications. Cystic lesions of the pancreas are associated with systemic disease—e. g., cystic fibrosis and von Hippel–Lindau disease. In the latter, the reported incidence is approximately 10–20%. In a recent study, 77% of 158 consecutive patients had lesions in the pancreas, including cysts, serous cystadenomas, and neuroendocrine tumors. Most patients had no symptoms related to peptide hormone secretion. As a result, many of these lesions are diagnosed incidentally in surveillance examinations—e. g., for renal tumors. Anatomic or intensive biochemical studies reveal pancreatic tumors in up to 80% of patients with multiple endocrine neoplasia type 1. The World Health Organization (WHO) classification of pancreatic tumors is summarized in Table 18.**1**.

Table 18.**1** The World Health Organization (WHO) classification of pancreatic tumors

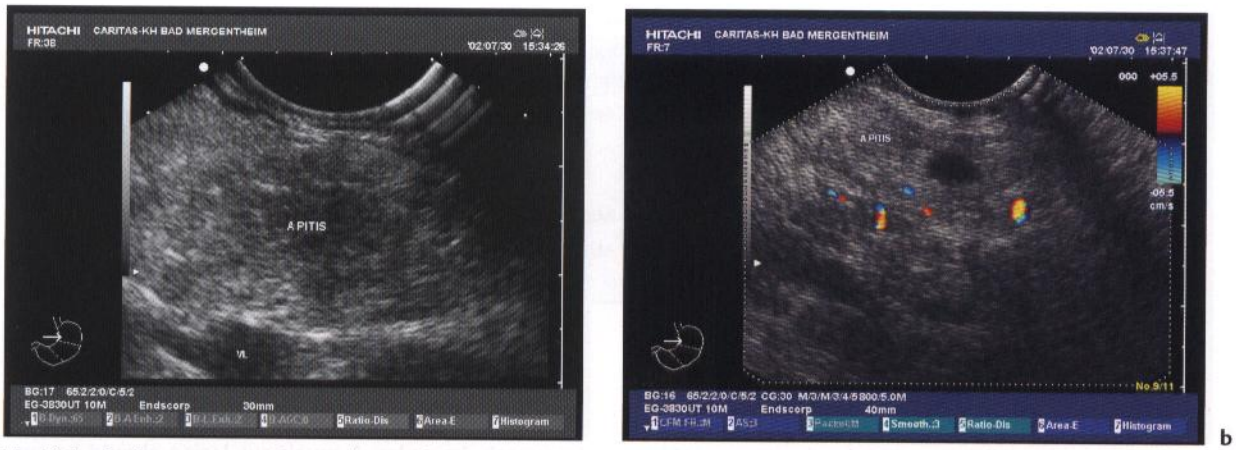
Benign
Serous cystadenoma
Mucinous cystadenoma
Intraductal papillary mucinous adenoma
Mature teratoma
Borderline
Mucinous cystic tumor with moderate dysplasia
Intraductal mucinous papillary tumor with moderate dysplasia
Solid pseudopapillary tumor
Malignant
Highly ductal dysplasia, carcinoma in situ
Ductal adenocarcinoma
Serous cystadenocarcinoma
Mucinous cystadenocarcinoma
Intraductal papillary mucinous carcinoma
Acinar-cell carcinoma
Solid pseudopapillary carcinoma
Pancreatic blastoma
Osteoclasts similar to giant-cell tumor
Mixed carcinoma

Simple cysts. Simple (true or retention) cysts of the pancreas are often small, fluid-containing spaces lined with normal duct and centroacinar cells. They are usually incidental findings with no clinical significance and can be left untreated. They are found in about of 25% of patients with cystic fibrosis [1].

Pseudocysts. Pancreatic pseudocysts develop as a result of pancreatic inflammation and necrosis. Most pseudocysts communicate with the pancreatic ductal system and contain high concentrations of enzymes. The walls of pseudocysts are formed by adjacent structures and consist of fibrous and granulation tissue and are therefore not lined with normal duct and centroacinar cells. The lack of an epithelial lining thus distinguishes pseudocysts from true cystic lesions of the pancreas. A pseudocyst should be suspected in patients with a recent history of pancreatitis and an elevated serum amylase concentration, when the lesion contains enzyme-rich watery fluid and communicates with the pancreatic duct as assessed by endoscopic retrograde cholangiopancreatography (ERCP). The diagnostic implications of pancreatic pseudocysts are described in the respective sections below.

When a diagnosis of pseudocyst is made, the management is mostly determined by the symptoms. Asymptomatic pseudocysts that are not increasing in size can be monitored, even if they are large. Symptoms should be treated either with resection (for lesions in the body or tail of the pancreas) or drainage (for lesions anywhere in the pancreas). Drainage can be carried out with endoscopic ultrasound (EUS) guidance, either into the stomach or (less favorably) into the duodenum or via the percutaneous route [2–10]. Pseudocysts can also be drained surgically by anastomosing the stomach, duodenum, or jejunum to the cyst wall. The therapeutic implications mainly depend on the locally available expertise and clinicians' preferences, since none of the methods has been shown to be superior to the others. EUS management is discussed in Chapter 19.

EUS in acute pancreatitis (Fig. 18.**1**) is carried out routinely to demonstrate the biliary etiology, but has rarely been used to assess the degree of necrosis.



a b

Fig. 18.**1a, b** Acute pancreatitis. Exudates and necrosis can be delineated with high-resolution EUS, using color Doppler imaging.

■ Cystic Neoplasms

At least four different types of cystic neoplasms in the pancreas have been described.

- Mucinous cystadenoma/cystadenocarcinoma
- Intraductal papillary mucinous neoplasm (mucinous duct ectasia)
- Serous cystadenoma
- Papillary cystic neoplasm (also known as pseudopapillary neoplasm or solid pseudopapillary tumor)

Epidemiology. Mucinous cystadenoma is the most common type of cystic neoplasm and serous cystadenoma is the second most common cystic tumor in the pancreas. Papillary cystic neoplasm (or tumor, also known as solid pseudopapillary neoplasm or tumor) is the least common type of pancreatic cystic neoplasm [11,12]. Cystic lesions of the pancreas, even when found incidentally, may have a malignant potential and require diagnostic evaluation regardless of their size.

Diagnosis. The EUS findings by themselves are not accurate enough to diagnose the type of cystic lesion of the pancreas definitively, or to determine its malignant potential in all cases. Endoscopic ultrasound-guided fine-needle aspiration (EUS-FNA) with assessment of tumor markers may increase the accuracy [13].

Cytology. Cytological analysis of the cyst fluid obtained using EUS-FNA lacks sensitivity, but has a high level of specificity for malignancies and mucinous cystic neoplasms. Measurement of cyst fluid amylase, lipase, and various tumor markers such as carcinoembryonic antigen (CEA) and CA19-9 is clinically useful. One study examined 341 patients who underwent EUS-FNA of pancreatic cystic lesions. Cyst fluid was analyzed for CEA, CA72-4, CA125, CA19-9, and CA15-3. A histological diagnosis was obtained in 112 patients who underwent surgical resection (68 with mucinous lesions, seven with serous, 27 with inflammatory, five with endocrine, and five with other types of cystic lesion). Using a cut-off value of 192 ng/mL, CEA levels were the most accurate method of differentiating between mucinous and non-mucinous cystic lesions (sensitivity 73%, specificity 84%). There was no combination of tests that provided greater accuracy than CEA alone [14]. In addition, biopsies may not be diagnostic, since such samples frequently do not contain cells that are representative of the entire cyst lining. The relatively low sensitivity and specificity levels raise questions about the reliability of these methods for assessing the need for surgery in individual patients.

Histology. Cytological examination of the cystic fluid may allow diagnosis if either glycogen-rich cells (suggesting serous cystadenoma) or mucin-containing cells (suggesting mucinous lesions) are present. However, false-negative cytology is not unusual, and mucus-secreting cells can be found in the normal pancreatic duct lining. In patients with suspected serous cystadenoma, a core biopsy for histology is required if the lesion appears solid, in order to avoid surgery.

Safety. FNA of cystic lesions is generally safe. Prophylactic antibiotics should be administered to patients undergoing EUS-FNA, ERCP, or endoscopic drainage procedures for (inflammatory) cystic lesions of the pancreas.

Differential diagnosis (Table 18.**2**) It is sometimes difficult to distinguish between pseudocysts and serous and mucinous tumors, since the latter may contain enzyme-rich fluid, communicate with the ductal system, and may be seen in patients with symptoms of recent pancreatitis.

Endoscopic ultrasound may make it possible to distinguish between serous and mucinous neoplasms by revealing a mass composed of either many tiny cysts (microcystic), showing a solid-appearing hypervascular tumor, or showing several large cysts (macrocystic). Serous cystadenomas typically have a central scar and central vessel, similar to focal nodular hyperplasia in the liver. This finding can often also be seen with trans-

Table 18.2 Differential diagnosis of cystic lesions of the pancreas

Type	Age (years)	Location in pancreas	Malignant potential	Communication with the duct
Simple retention cyst		Mainly head	None	Rarely
Pseudocyst			None	Frequently
Serous cystadenoma			Very low	Rarely
Mucinous cystadenoma	40–50	Mainly body and tail	High	Occasionally
IPMN	60-70	Mainly head	Moderate–high	Typically
Solid pseudopapillary neoplasm	20-40		Moderate	Rarely

IPMN: intraductal papillary mucinous neoplasm.

abdominal ultrasonography. However, even with these findings, it is not possible to exclude the presence of a malignancy, especially a neuroendocrine tumor [15].

Therapy. The EUS findings by themselves are not sufficiently accurate to diagnose the type of cystic lesion of the pancreas definitively or to determine its malignant potential in all cases, and surgery is therefore mandatory, depending on the patient's age and comorbidity. In patients with histologically confirmed serous cystadenomas, which are only accessible via the transabdominal route or using EUS-guided Tru-Cut biopsy [16], careful follow-up may be possible.

The management of patients with uncertain cystic lesions is difficult. In a study including 398 patients with cystadenomas from 73 institutions, 372 of whom underwent surgery, accurate preoperative diagnosis of the tumor type was achieved in only 20% of those who were ultimately diagnosed with serous cystadenomas, 30% of those with mucinous cystadenomas, and 29% of those with mucinous cystadenocarcinomas [17]. Many experts and pancreatic surgeons therefore recommend resection for even moderately suspicious lesions in the body and tail of the pancreas, and for highly suspicious lesions in the head of the gland.

There are currently no established endoscopic treatments for cystic neoplasms of the pancreas. EUS and ERCP should be always considered before surgical or percutaneous drainage of pancreatic pseudocysts, in order to optimize patient selection. In one preliminary study, EUS-guided ethanol lavage of unilocular and septate cystic lesions of the pancreas was used in 25 patients with small cystic pancreatic lesions, 68% of whom with fluid characteristic of mucinous neoplasms. Complete resolution of the cysts was observed on follow-up imaging in eight of the patients (35%). Five patients with persistent cysts underwent resection, and histological evidence of epithelial ablation was seen [18].

Mucinous Cystadenoma and Cystadenocarcinoma

Mucinous cystadenomas consist of one or more macrocystic spaces lined with mucus-secreting cells and are typically located in the body or tail of the pancreas. It is often difficult to make the diagnosis on the basis of biopsy or aspiration samples, as the cellular lining is frequently irregular. A mucinous lesion should be suspected when one or more macrocytic spaces containing mucin are found. Most of these mucinous tumors are malignant at time of diagnosis, and benign forms have a high potential for malignant transformation (Figs. 18.**2**, 18.**3**). During ERCP, tissue sampling with brushing, and/or biopsy, and/or pancreatic fluid collection, should be carried out whenever possible.

When the diagnosis of a mucinous cystadenoma is made, the lesion should be resected, due to the high potential for malignant change, but also depending on the patient's age and comorbidity. Distal pancreatectomy should be carried out for lesions in the tail or body of the pancreas, and pancreaticoduodenectomy should be carried out for lesions in the pancreatic head.

Another type of mucinous tumor of the pancreas is intraductal papillary mucinous neoplasm (IPMN) or mucinous duct ectasia. The relationship between IPMNs (in which an increasing incidence is being observed) and mucinous cystadenoma/cystadenocarcinomas is not yet clear [15].

Intraductal Papillary Mucinous Neoplasm (Mucinous Duct Ectasia)

IPMNs were first described in 1982 in patients suspected of having pancreatic carcinoma who had a favorable outcome. A variety of confusing synonyms have been used—e.g., mucinous ductal ectasia, mucin-producing carcinoma, intraductal mucin-producing tumor, intraductal papillary hyperplasia, intraductal papillary tumor, intraductal papillary neoplasm, etc. Intraductal papillary mucinous neoplasms show dilated ductal segments lined with mucus-secreting cells and may be located within the head of the pancreas or diffusely throughout the organ. IPMNs have been subclassified into a main duct type (MDT-IPMN, 75%) and a branch duct type (BDT-IPMN, often in the uncinate process) based on the anatomical involvement of the pancreatic duct. In comparison with mucinous cystadenomas, they have a lower but still relatively high malignant potential. The BDT-IPMN subtype is associated with less aggressive

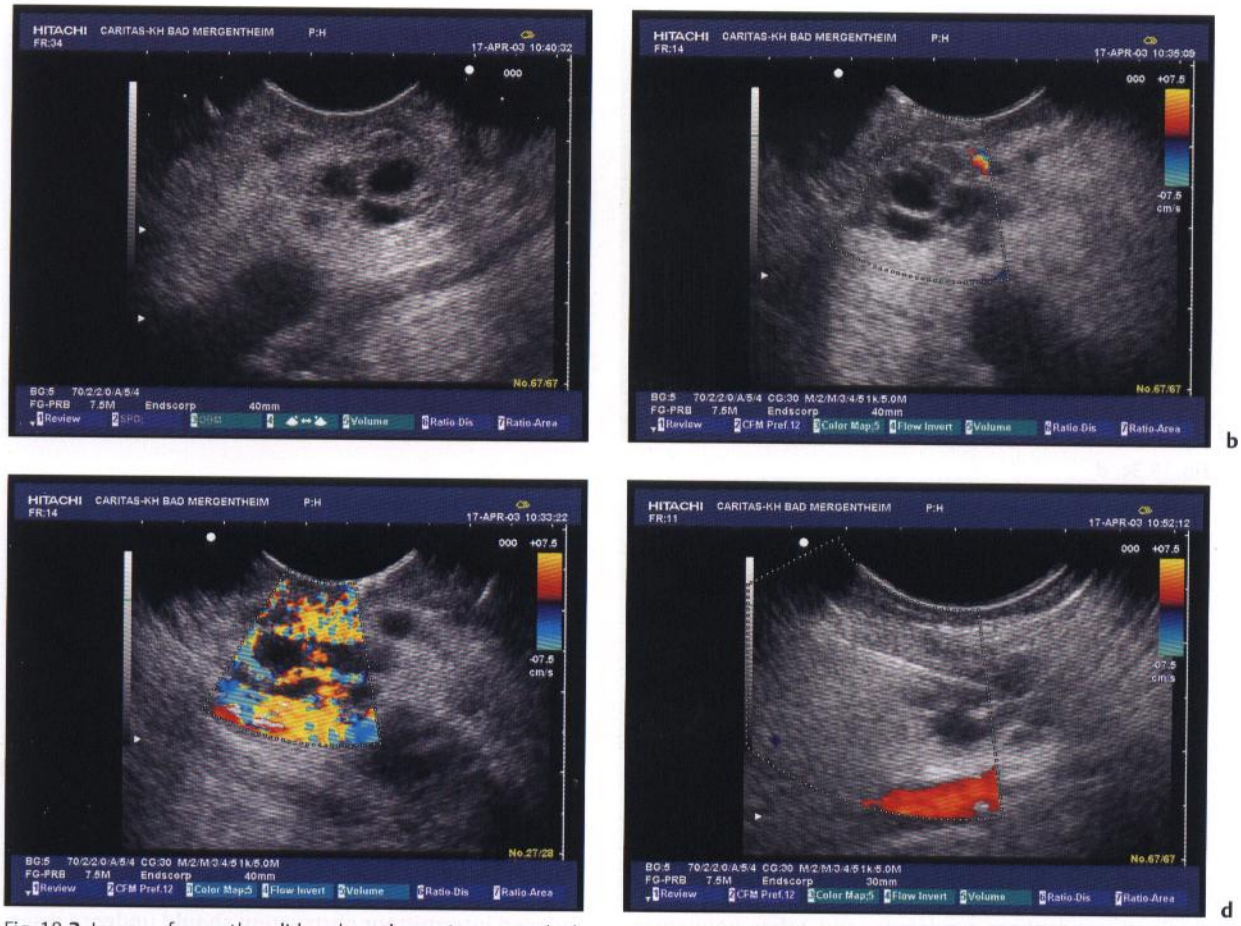


Fig. 18.**2** Image of a partly solid and partly cystic mass, which was identified as a pseudocyst with an external transabdominal examination. **a** B-mode. **b** Color duplex ultrasonography. **c** Vascularization of the tumor areas is identified after application of the echo contrast agent SonoVue. **d** The tumor areas were aspirated in the same procedure. The cytological and histological diagnosis confirmed that the lesion was a mucinous cystadenoma, with no signs of malignancy.

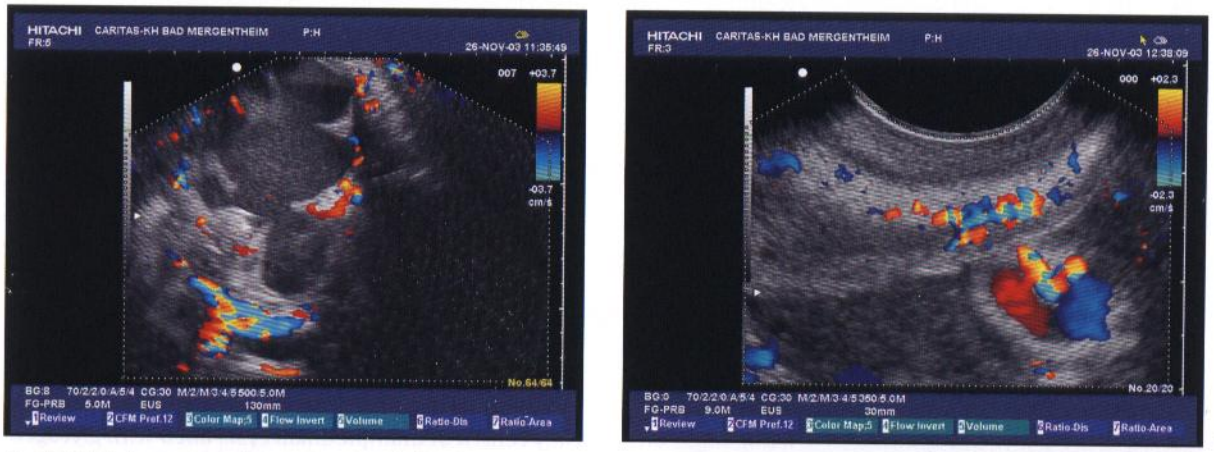
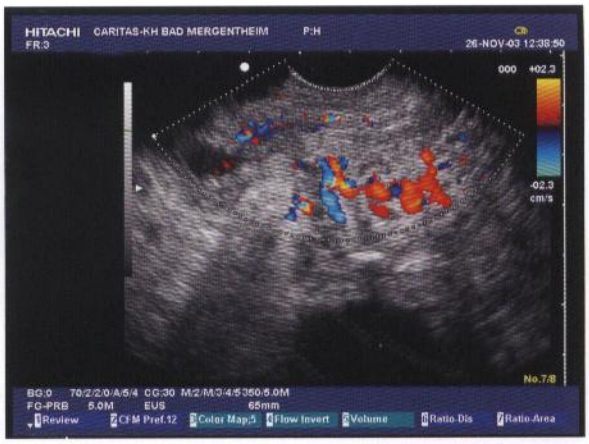


Fig. 18.**3** Mucinous cystadenocarcinoma of the pancreas with mucus-containing cysts (**a**) and vascularized septa (**b**) and collaterals due to portal vein thrombosis (**c**, **d**).

Fig. 18.**3c, d** ▷



c



d

Fig. 18.**3c, d**

histological features in comparison with the MDT-IPMN subtype. The majority of patients with IPMNs do not have invasive cancer at time of diagnosis, and the rate of progression appears to be extremely slow (approximately 15–20 years) [19,20].

Epidemiology. IPMNs have most commonly been described in men over the age of 60, some of whom have symptoms suggestive of chronic obstructive pancreatitis or acute recurrent pancreatitis due to intermittent obstruction of the pancreatic duct with mucus plugs. The etiology of IPMN is unclear. It has been described in association with familial adenomatous polyposis, Peutz–Jeghers syndrome, and other nonpancreatic tumors.

Diagnosis. There are three classic signs of IPMN: a segmental or diffusely dilated main pancreatic duct > 10 mm in diameter without involvement of the common bile duct; a patulous ampullary orifice ("fish-mouth"), frequently with mucus secretion (specific but not sensitive); and mural nodules > 10 mm (MDT-IPMN) or multiple small cysts (5–20 mm) (BDT-IPMN). Dilation of the pancreatic duct to over 10 mm and cysts larger than 20 mm are suggestive of malignancy. Intraductal ultrasonography can be helpful for assessing the tumor extent in MDT-IPMNs, but is rarely performed. EUS-FNA of the dilated pancreatic duct, including mural nodules and especially of solid components of the tumor, may be helpful in the diagnosis (Figs. 18.**4**, 18.**5**). Histopathological analysis tends to underestimate the tumor grade [21].

Tumor markers are elevated in less than 25% of patients and are not helpful indicators of malignant transformation. Pancreatic secretions can be tested for molecular markers such as K-*ras*, P53, and telomerase activity, but the results have so far been inconsistent.

Differential diagnosis. The differential diagnosis of IPMN includes chronic obstructive pancreatitis, mucinous cystic tumors of the pancreas, and rarely pancreatic ductal adenocarcinoma.

Therapy. When an IPMN is diagnosed, the lesion should be resected, due to the high potential for malignant change, but also depending on the patient's age and comorbidity and the type of lesion involved. BDT-IPMNs less than 2.5 cm in diameter with a thin wall, without papillary wall protrusions, without thick septum-like structures, and without dilation of the main pancreatic duct progress very slowly. In view of the risks of pancreatic surgery, close monitoring—for example, with periodical EUS examinations—may be justified in patients with these lesions [19,22].

Patients with recurrent pancreatitis caused by IPMN-induced intermittent obstruction should undergo resection of the mucous-secreting abnormal portion of the pancreas. Distal pancreatectomy, pancreaticoduodenectomy, or even total pancreatectomy, depending on the location and extent of the lesion, may be necessary. In our experience, patients with recurrent pancreatitis who are not suitable for surgery may benefit from endoscopic therapy.

Serous Cystadenoma

Microcystic pancreatic adenomas were formerly considered a rarity. Nowadays, with technological advances in the equipment, localized changes in the pancreas are much more frequently observed. In contrast to mucous cystadenomas and IPMNs, serous cystadenomas have a very low potential for malignant transformation. Tumors are distributed throughout the pancreas without predilection (Fig. 18.**6**). Histologically, the lesions typically consist of multiple small cysts lined with glycogen-rich cells, with a regular vascular architecture.

It has been found useful to remove larger cylinders of tissue, as the specimens obtained with EUS-FNA are only sufficient for determining malignancy, but not for classifying the tumor type. In patients with suspected serous cystadenomas, core biopsies for histology are therefore required if the lesion appears solid, in order to avoid



a



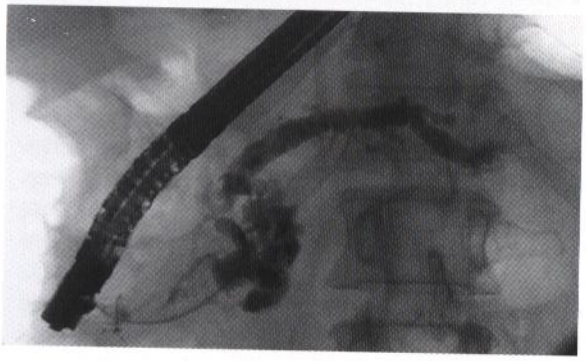
b



c



d



e



f

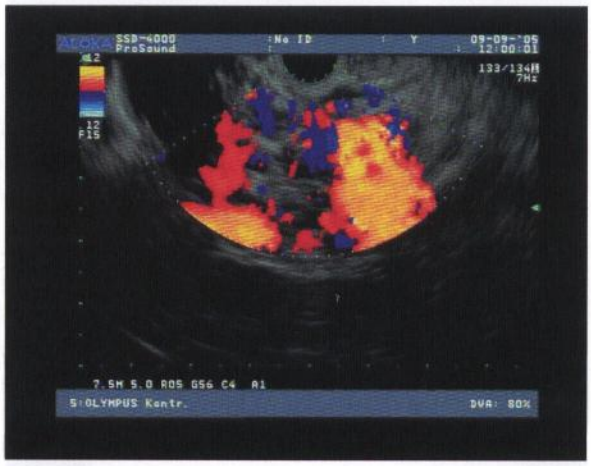
Fig. 18.4 Intraductal papillary mucinous neoplasms (IPMNs) of the pancreas (main duct type). **a** Tortuous dilation of the main pancreatic duct in the pancreatic neck. **b** Cystic spaces with not completely anechoic luminal contents in the pancreatic body. **c** The orifice of the main pancreatic duct is wide open. **d** There is also dilation of the accessory pancreatic duct, viewed from the minor papilla. **e, f** The corresponding endoscopic retrograde cholangiopancreatography (ERCP) images show tortuous dilation and cystic cavities in the pancreatic head and neck, as well as dilation of the main pancreatic duct in the body and tail of the pancreas: opacification from the major (**e**) and from the minor (**f**) papilla.



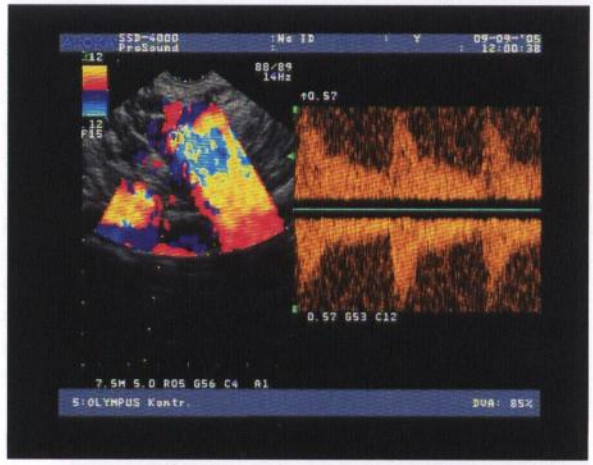
a



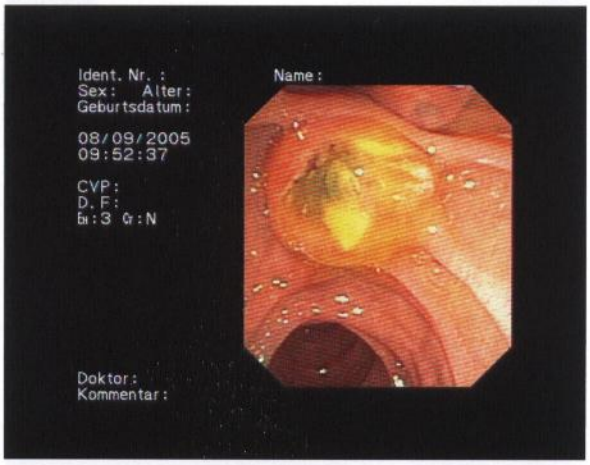
b



c



d



e

Fig. 18.5 Intraductal papillary mucinous neoplasms (IPMNs) of the pancreas (courtesy of M. Hocke). **a, b** B-mode. **c** Color Doppler imaging. **d** Spectral analysis. **e** Endoscopic image.

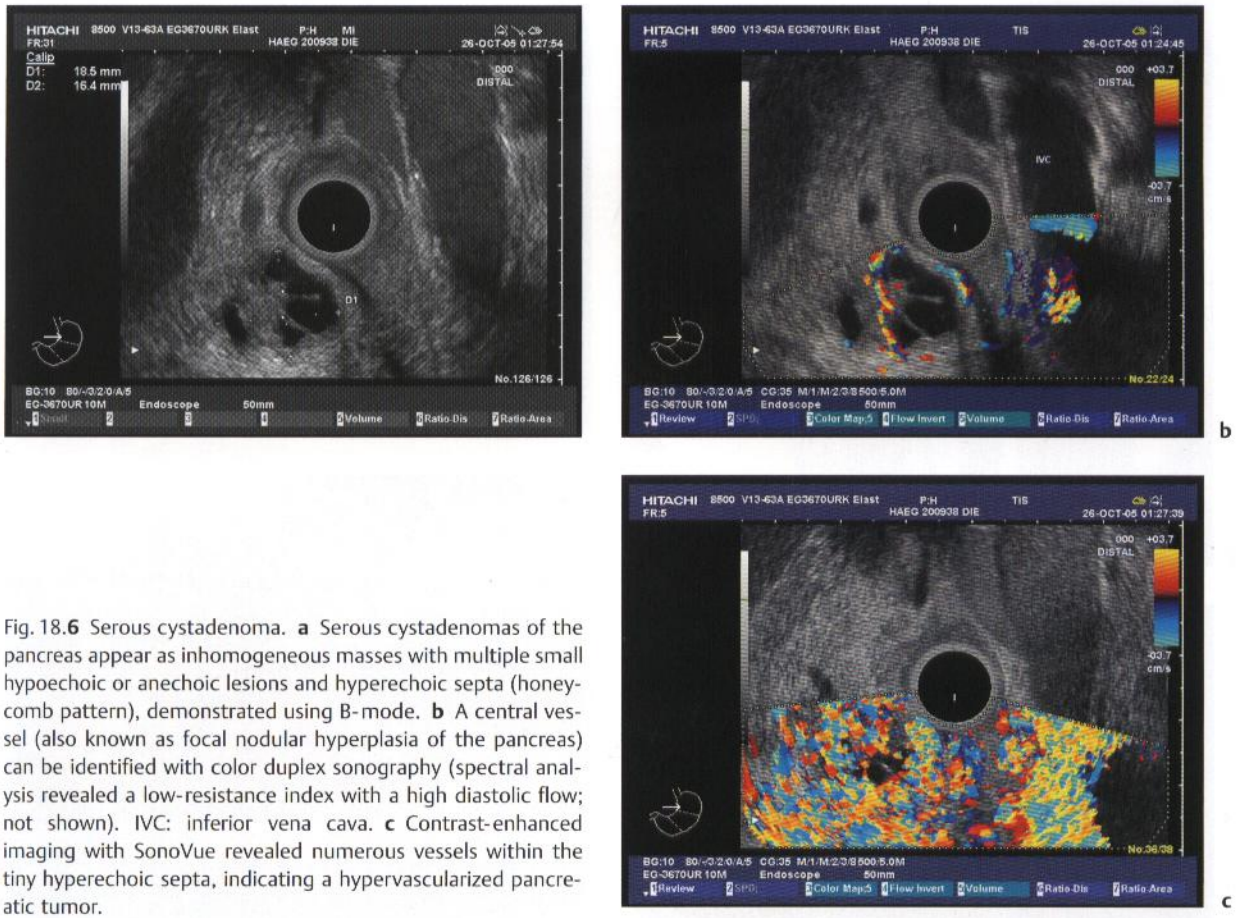


Fig. 18.**6** Serous cystadenoma. **a** Serous cystadenomas of the pancreas appear as inhomogeneous masses with multiple small hypoechoic or anechoic lesions and hyperechoic septa (honeycomb pattern), demonstrated using B-mode. **b** A central vessel (also known as focal nodular hyperplasia of the pancreas) can be identified with color duplex sonography (spectral analysis revealed a low-resistance index with a high diastolic flow; not shown). IVC: inferior vena cava. **c** Contrast-enhanced imaging with SonoVue revealed numerous vessels within the tiny hyperechoic septa, indicating a hypervascularized pancreatic tumor.

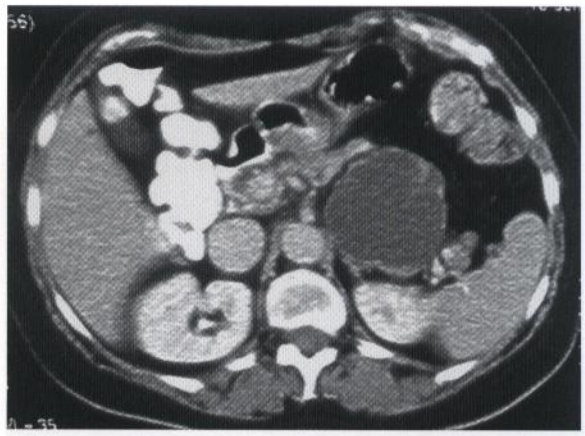
surgery. The results of a recent pilot study suggested that EUS-TCB is capable of collecting sufficient tissue in cases of serous cystadenoma [16]. In a patient with a definitive diagnosis of a serous cystadenoma, the management is determined by age, comorbidity, symptoms, progression, and lesion location. Symptomatic or enlarging serous cystadenomas in healthy young patients should be resected. Lesions in the body or tail of the pancreas require distal pancreatectomy, while those in the head of the gland are enucleated or resected with pancreaticoduodenectomy. Small, asymptomatic, and nonenlarging serous cystadenomas can be monitored, as the risk of malignant change is very low. The optimal interval for repeating imaging examinations in such patients is not known, but should be not longer than 12 months.

Papillary Cystic Neoplasm (Solid Pseudopapillary Neoplasm)

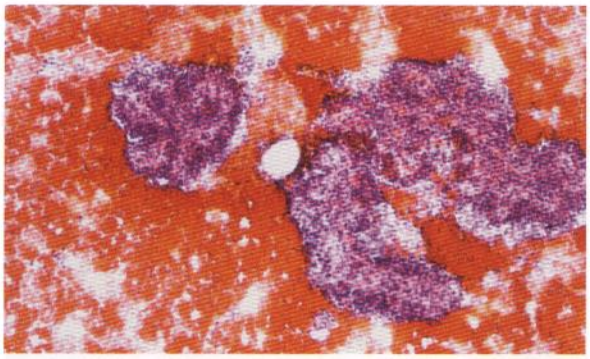
Papillary cystic neoplasms (also known as pseudopapillary neoplasms or solid pseudopapillary tumors) usually occur in young women, have a low malignant potential, and are most commonly found in the tail or body of the pancreas. EUS shows a mixed solid and cystic encapsulated tumor with distinct margins (Fig. 18.**7**). There are sometimes a few calcifications. The tumors are often very large. EUS-FNA shows very distinctive cytopathological features, which make it possible to distinguish this type from other pancreatic neoplasms. Cytopathological slides show branching papillae with myxoid and fibrovascular stroma. The tumor cells are monomorphic, with round nuclei and an eosinophilic, foamy cytoplasm. The cystic components contain bloody fluid, sometimes with necrotic debris. Immunoreactivity for vimentin, alpha-1-antitrypsin, neuron-specific enolase, and progesterone receptor is typical of this rare type of pancreatic tumor [23,24]. Patients with solid pseudopapillary tumors of the pancreas have a very good prognosis if the tumor is resected completely. However, recurrences and even metastases may occur in a small number of cases. Histological prediction of the malignant potential is not yet possible. The most important differential diagnosis to consider is neuroendocrine tumor of the pancreas [25]. The type of resection depends on the location of the tumor.



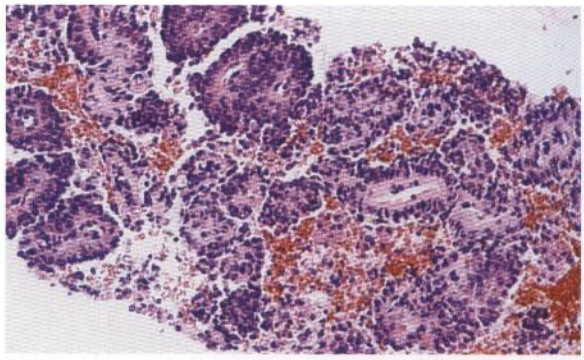
a



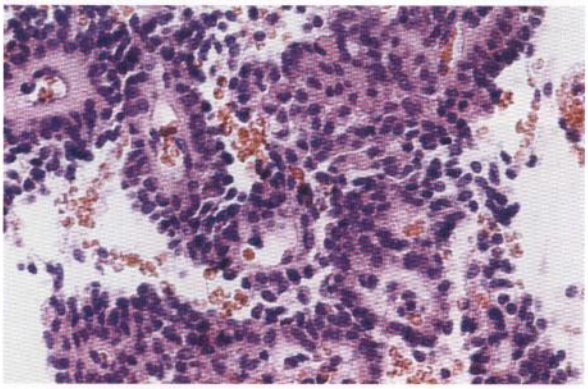
b



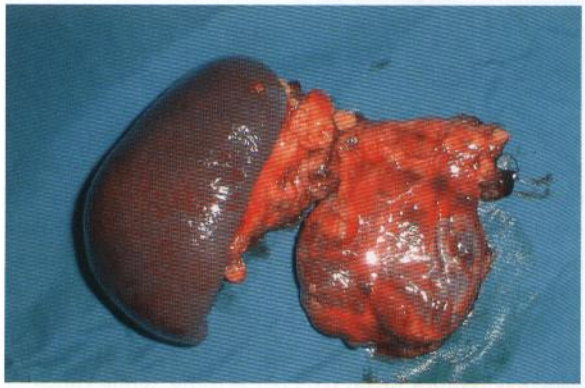
c



d



e



f

Fig. 18.**7a–f** Solid pseudopapillary neoplasm of the pancreas: cystic tumor of the pancreatic tail in a 45-year-old asymptomatic woman. The tumor is predominantly cystic with some solid parts (**a** EUS; **b** CT). EUS–FNA shows the characteristic branching papillae with myxoid and fibrovascular stroma. Tumor cells are isomorphic. The prominent nuclei are rounded, slightly hyperchromatic, and show no mitotic activity. Tumor cells stained positive for vimentin, NSE, and progesterone receptor. Staining for CA 19-9, CEA, MFN 116, synaptophysin, and chromogranin A was negative. The proliferative activity (Ki-67 labeling index: 1%) was low (**c** cell smears, hematoxilin and eosin, x 100; **d, e** core biopsy, hematoxilin and eosin, x 200 and x 400, courtesy of Dr. B. Fiedler, Berlin, Germany). **f** Resection of the pancreatic tail, the tumor, and the spleen was carried out (courtesy of Dr. G. Reiche, Strausberg, Germany).

Teratoma of the Pancreas

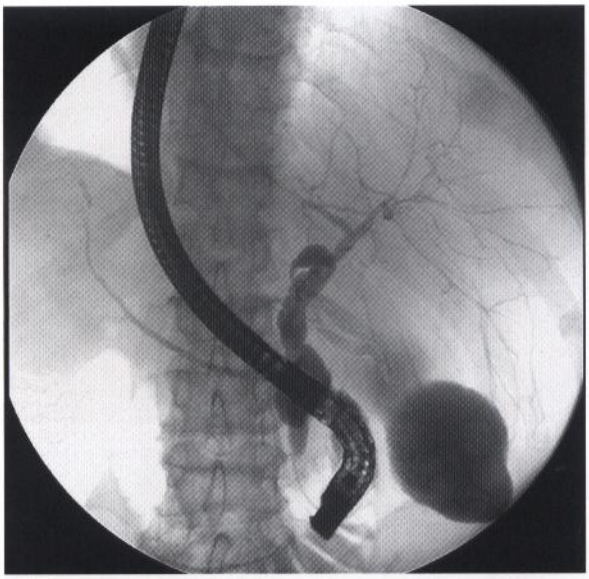
Teratoma of the pancreas is mentioned in the WHO classification and represents a very rare entity (Fig. 18.**8**).

Rare Cystic Neoplasms and Miscellaneous Pancreatic Lesions Mimicking Cystic Neoplasms

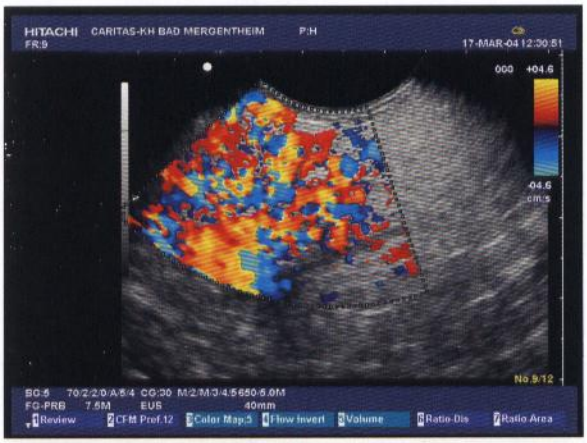
A large variety of cystic pancreatic lesions should be considered in the differential diagnosis—e.g., lymphoepithelial cysts, cystic neuroendocrine tumors, the cystic form of acinar-cell carcinoma (Fig. 18.**9**), mucin-produc-



a



b



c



d



e

Fig. 18.**8** Mature pancreatic teratoma. **a** B-mode sonography shows a weakly echogenic mass with central calcification (8 × 6 mm in size). **b** Endoscopic retrograde cholangiopancreatography shows blockage of the distally positioned part of the pancreatic duct, raising a suspicion of pancreatic carcinoma. **c, d** Contrast-enhanced endoscopic ultrasonography proved useful for characterization, as the vessels are visible and only the central part is not seen. **e** The diagnosis was only reached histologically; EUS-guided aspiration was not completely unambiguous.

Fig. 18.**8f–l** ▷



f



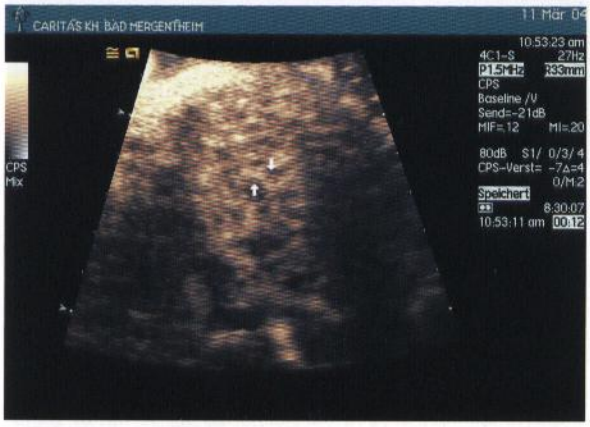
g



h



i



j



k



l

Fig. 18.**8f, g** The transabdominal findings were compared side by side. With the ductal blockage, these were primarily interpreted as signs of pancreatitis. **h–l** After contrast enhancement, the color power method showed concentration in the tumor tissue, ruling out a single calcified structure and allowing a diagnosis of neoplasia.

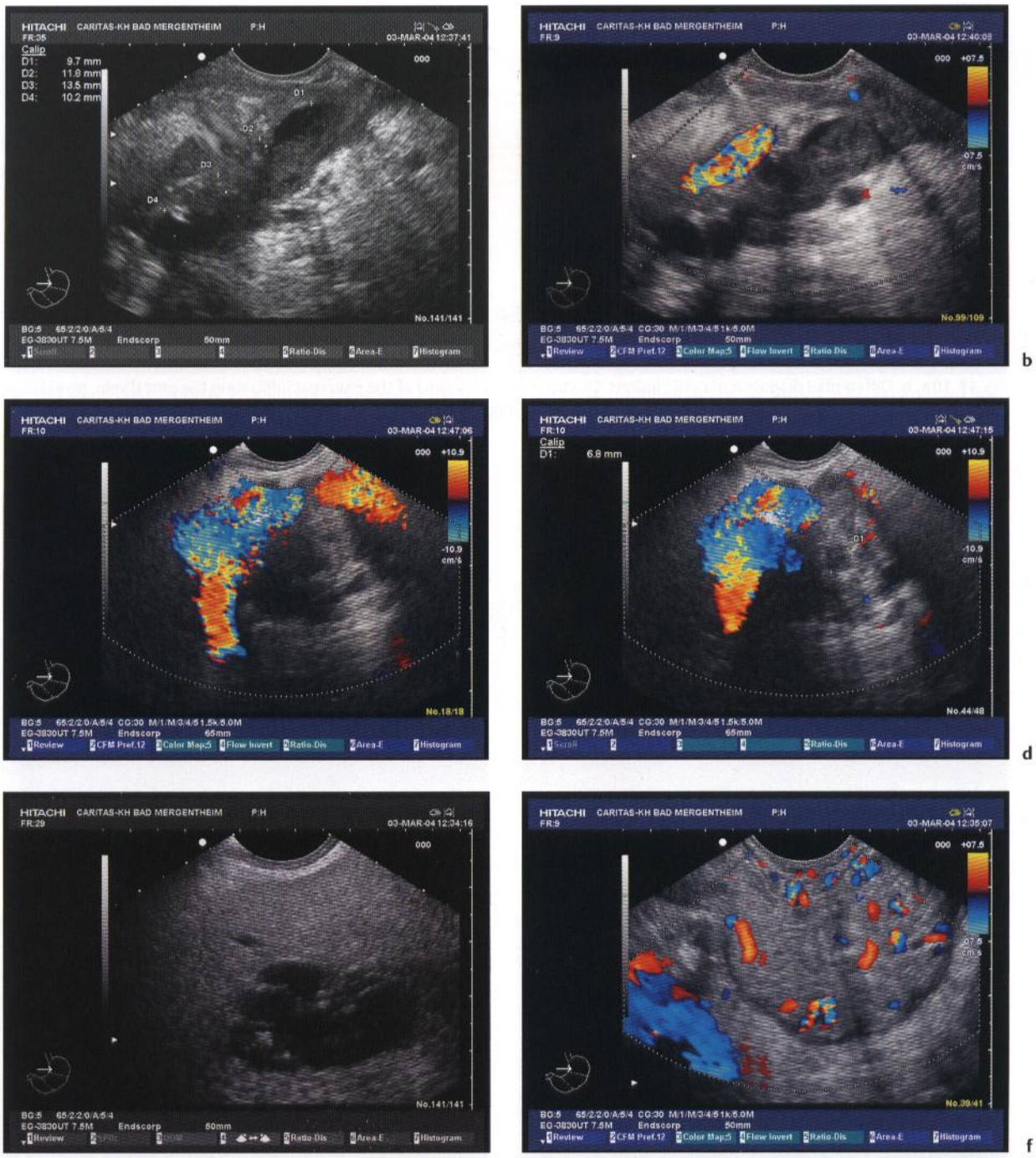


Fig. 18.**9** Acinar-cell carcinoma. **a** Conventional B-mode image of a portal vein thrombosis, with varying stages of development between the markers. **b** On color duplex ultrasonography, there are no signs of flow in the portal vein, although the splenic artery is visible. **c, d** Contrast enhancement with SonoVue shows that the tumor areas are barely supplied with blood, which can be taken as an indication of malignancy. **e, f** In the same examination, it was possible to identify metastases in the liver (**e**), as well as extended circulation surrounding the gastric fundus region (varices, **f**). The diagnosis of the rare condition of acinar-cell carcinoma was confirmed histologically.

ing ductal adenocarcinomas (Figs. 18.**10**, 18.**11**) [26], primary pancreatic lymphomas (Fig. 18.**12**), which are much more rare than the involvement in systemic disease, and cystic metastatic disease. Interobserver variability has been reported to be high for many aspects of the EUS assessment [27] (Fig. 18.**13**).



a b

Fig. 18.**10a, b** Differential diagnosis of cystic lesions. Ductal adenocarcinoma of the pancreas infiltrating the portal vein, revealed by color Doppler imaging demonstrating turbulence, may rarely create the impression of a pseudocystic lesion [26].



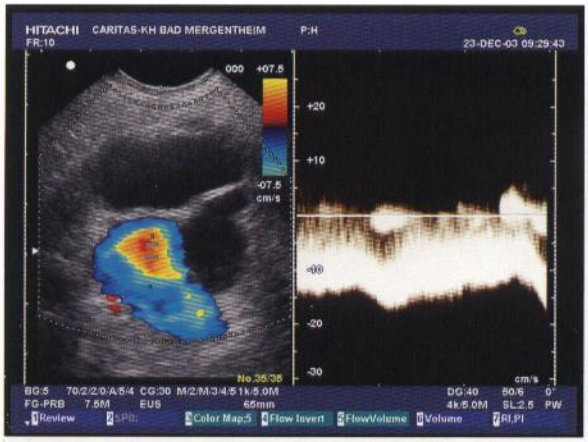
a b



c d

Fig. 18.**11a, b** Small retropapillary ductal adenocarcinomas may present as small cystic lesions, confused by the enlarged common hepatic bile duct and main pancreatic duct. **(b, c)** Color Doppler imaging is helpful in identifying the ducts and vessels. PAP: papilla.

Fig. 18.**11e–f** ▷



e



f

Fig. 18.**11d, e** Color Doppler imaging can also identify the tumor. **f** The final diagnosis can be confirmed using EUS-guided fine-needle aspiration. AL: splenic artery; MA: stomach.



Fig. 18.**12** An isolated non-Hodgkin's lymphoma (NHL) in the pancreas. Non-Hodgkin's lymphoma of the pancreas is a rare lesions, but it may be seen particularly in patients with acquired immune deficiency syndrome (AIDS) and may present in the form of cystic-type lesions. Color Doppler imaging is helpful in differentiating the infiltration from the vessel.



a



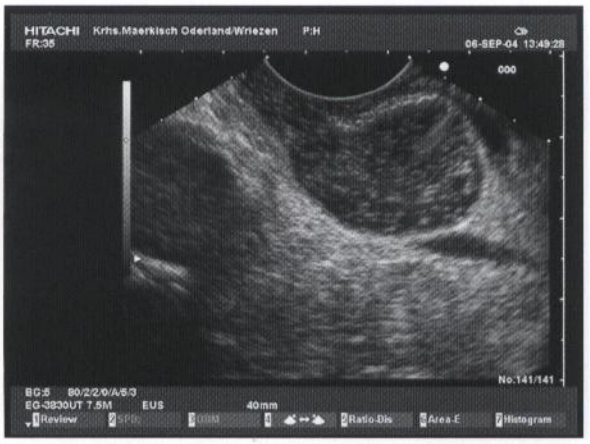
b

Fig. 18.**13** A possible pitfall in the diagnosis of cystic pancreatic tumors. **a** EUS shows a large, well-delineated, heterogeneous mass in the pancreatic head with a honeycomb pattern, resembling a microcystic serous adenoma. **b** Color-coded duplex imaging does not show any vascular signals inside the lesion, but after air insufflation into the duodenum, a few hyperechoic mobile reflexes (arrowheads) were seen inside the lesion, representing a very large duodenal diverticulum displacing the pancreatic head (hypoechoic ventral anlage (VA) and common bile duct (CBD) on the right side of the image).

Fig. 18.**13c–d** ▷



c



d

Fig. 18.13c, d For comparison, these images show a typical example of a duodenal diverticulum. At the beginning of the examination, after air insufflation, there are hyperechoic peripancreatic and periduodenal reflexes (**c**); water filling allows the diagnosis of a periduodenal diverticulum (**d**).

■ Neuroendocrine Tumors (Table 18.3)

Definition and epidemiology. Neuroendocrine pancreatic tumors are considered to be rare tumors of the pancreas or peripancreatic region (stomach or duodenal wall). More than 50% of these tumors (up to 85%) secrete biologically active hormones or demonstrate biochemical abnormalities, resulting in specific clinical syndromes. Although the tumors have a similar histological appearance, they can be distinguished by the use of immunostaining for the hormone being secreted.

Pancreatic endocrine tumors are named after the predominant hormone that they secrete. Insulinomas are reported to be the most common type of tumor, accounting for 60% of pancreatic endocrine tumors. Gastrinomas are the second most common type, occurring in about 20% of cases. Glucagonomas, somatostatinomas, and tumors secreting vasoactive intestinal peptide (VIPomas) are much rarer. The 15–40% of tumors that are nonfunctional do not become apparent clinically until they are large enough to impinge on adjacent structures and cause symptoms due to mass effects. We have diagnosed the latter form much more commonly than has recently been reported, and in our own series they are the most frequently encountered entity.

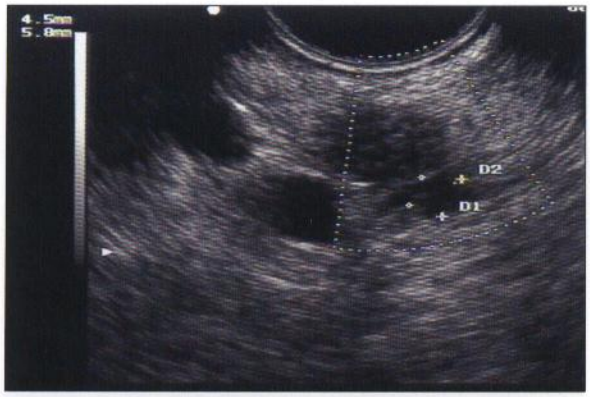
Biological behavior. The clinical behavior of pancreatic endocrine tumors can be benign or malignant, and it is difficult to assess the malignant potential on the basis of the histological appearance. Since benign and malignant pancreatic endocrine tumors are not distinguishable histologically, the absence or presence of metastases (either nodal or distant) has been used to make this distinction. However, this criterion alone is not an ideal indicator of the prognosis, since some benign tumors recur.

Table 18.3 Neuroendocrine tumors of the pancreas

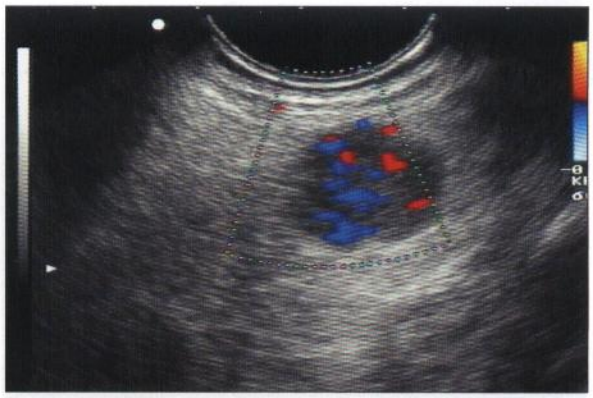
Benign	Benign and borderline	Borderline	Malignant
Hormone-secreting, easily differentiated	Hormone-secreting, easily differentiated	Hormone-secreting, easily differentiated	Hormone-secreting or nonsecreting, difficult to differentiate
Insulinomas < 2 cm	Insulinomas 2–4 cm	Insulinomas > 3 cm	Intermediate or small-cell carcinomas
Other < 1 cm	Other 1–2 cm	Other > 2 cm	
Nonsecreting, easily differentiated	Nonsecreting, easily differentiated	Nonsecreting, easily differentiated	
< 2 cm	2–3 cm	> 3 cm	
No invasion of blood vessels	No invasion of blood vessels	Possible invasion of blood vessels	
Up to 2 mitoses/HPF and up to 2% Ki-67-positive cells	More than 2 mitoses or more than 2% Ki-67 positive cells		

HPF, high-power field.

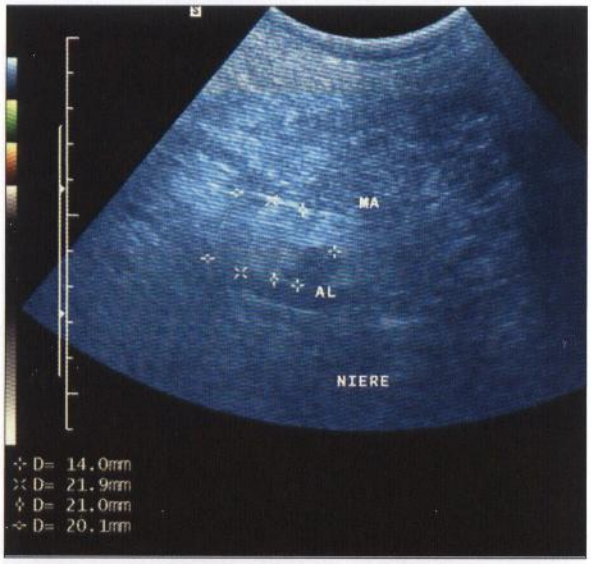
Symptoms. Pancreatic endocrine tumors—most often insulinomas or gastrinomas—become clinically apparent in approximately half of the patients with this disorder. However, subclinical involvement is more common.



a

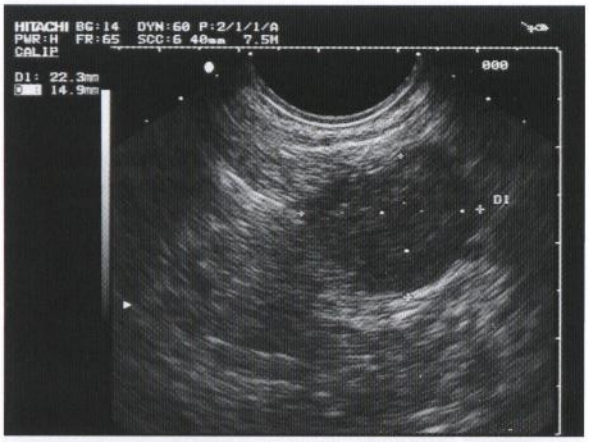


b



c

Fig. 18.**14** Neuroendocrine tumor: insulinoma. A small cyst is delineated next to a small lesion in the pancreatic tail. **a** B-mode. **b** Color Doppler imaging. **c** Transabdominal imaging. AL: splenic artery; MA: stomach.



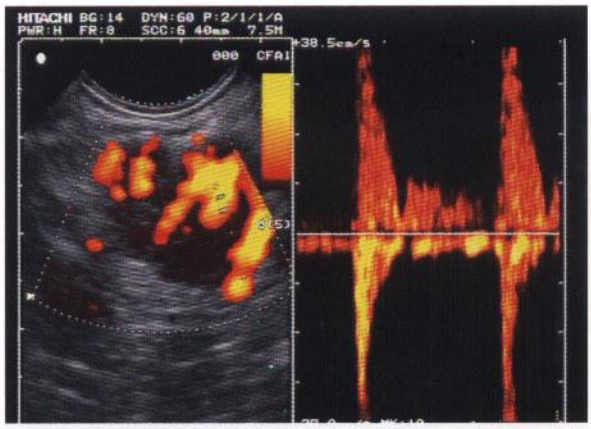
a



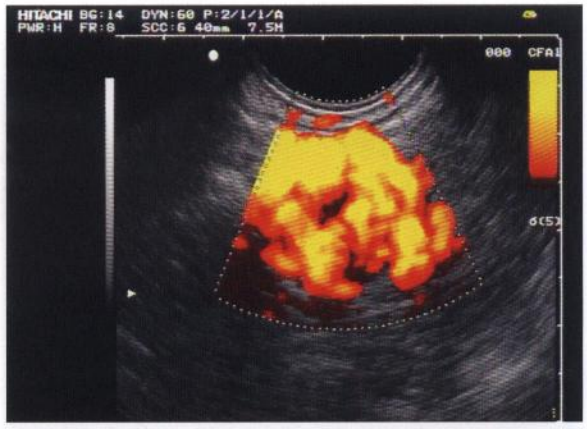
b

Fig. 18.**15** Insulinoma. **a** B-mode. **b** Color Doppler imaging.

Fig. 18.**15c–d** ▷

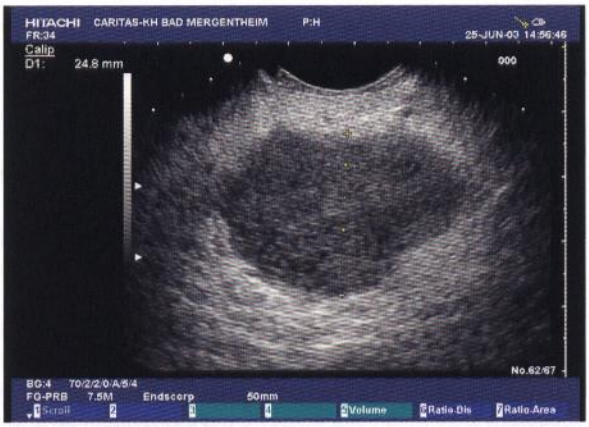


c



d

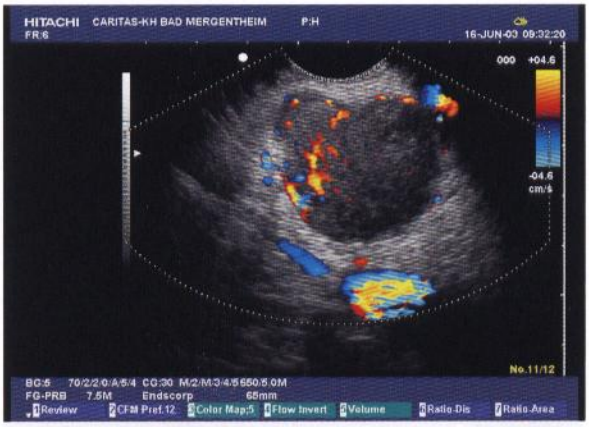
Fig. 18.**15c** Fast Fourier transform (FFT) analysis. **d** Contrast-enhanced ultrasonography.



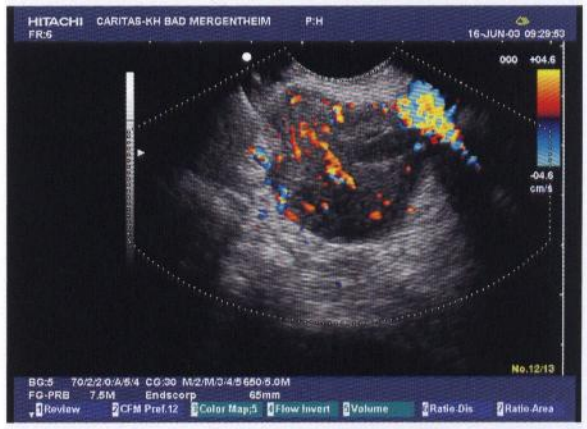
a



b



c



d



e

Fig. 18.**16** Semimalignant neuroendocrine tumor of the pancreas. **a** A 36-year-old patient presented with a clearly defined localized pancreatic mass. **b** Minor cystic changes; color duplex sonography shows no blood supply—typical of neuroendocrine tumors. **c, d** After contrast enhancement with SonoVue, vascularization becomes clearly visible on the edges of the tumor. **e** EUS-guided aspiration and removal of potentially malignant cells. Histological assessment of the surgical specimen confirmed a neuroendocrine tumor with malignant transformation.

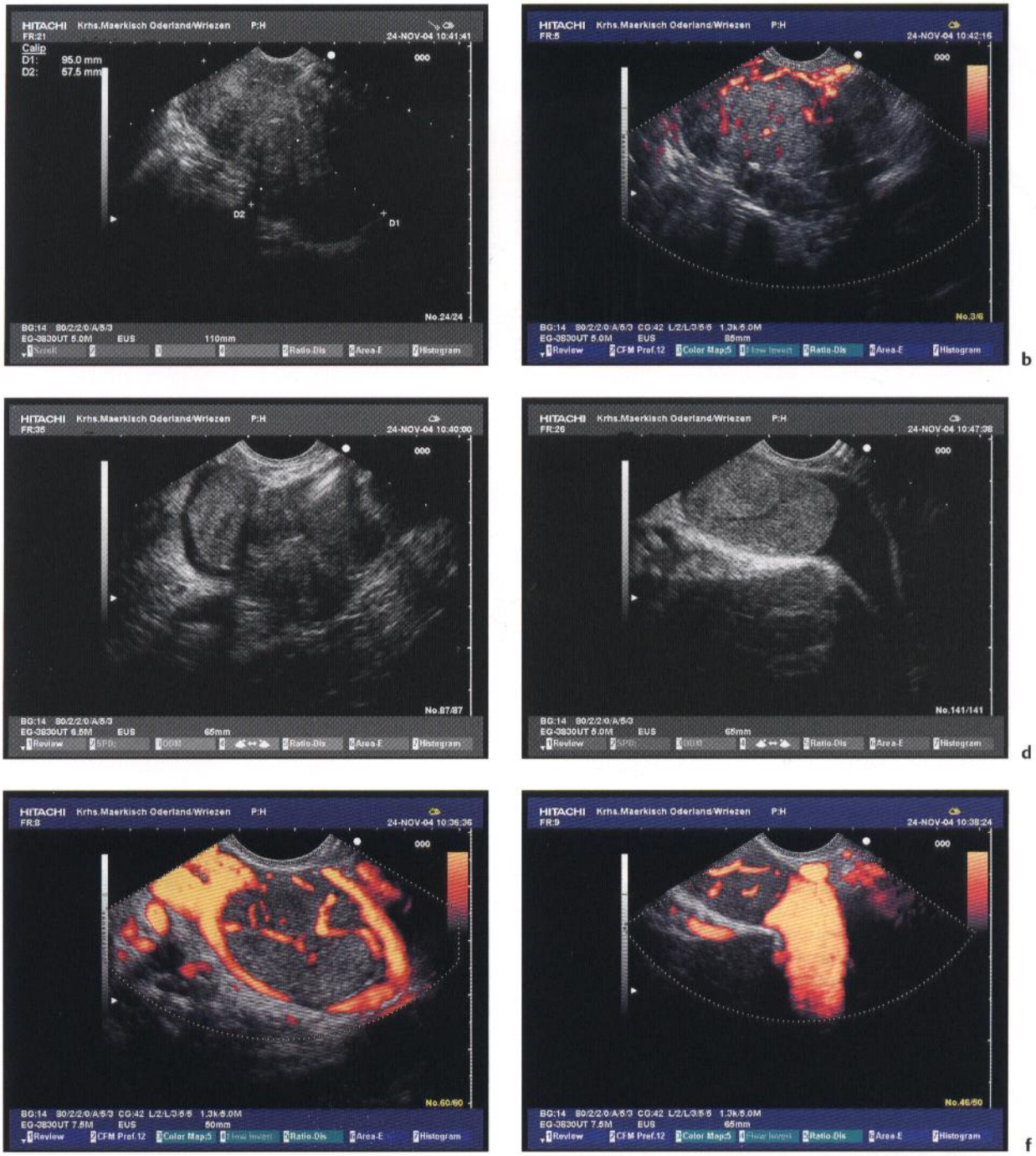
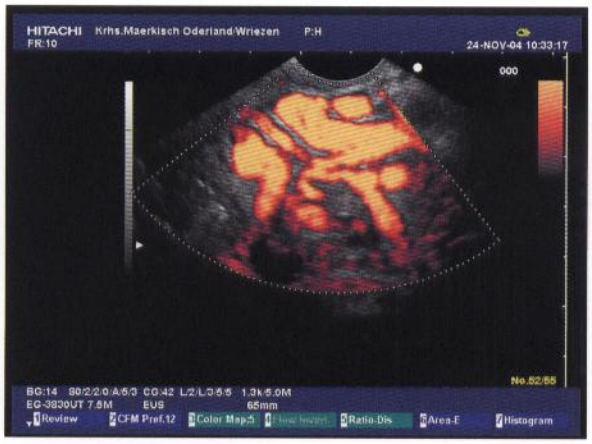
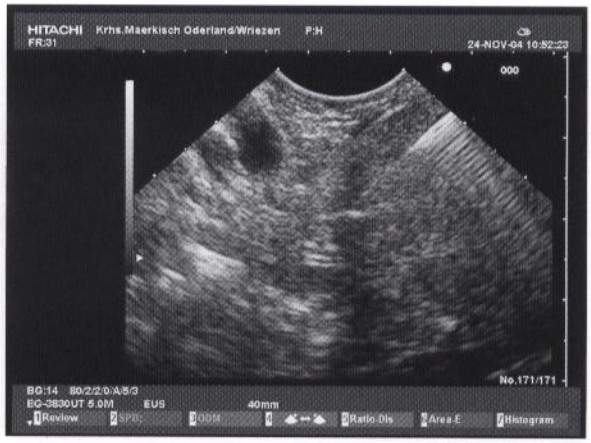


Fig. 18.**17** Large nonfunctioning pancreatic neuroendocrine tumor in an asymptomatic 68-year-old woman. The tumor was identified on transabdominal ultrasonography. **a** Endoscopic ultrasound showed a very large, inhomogeneous and hypoechoic tumor in the pancreatic body and tail, infiltrating and totally occluding the splenic vein. **b** Color-coded duplex imaging shows vascular signals inside the tumor. **c, d** The tumor is infiltrating the portal vein, forming a tumor thrombus (**c**) that extends into the porta hepatis (**d**). **e, f** Color-coded duplex imaging shows vascular signals within the tumor thrombus, so that it can be distinguished from an appositional fibrin thrombus.

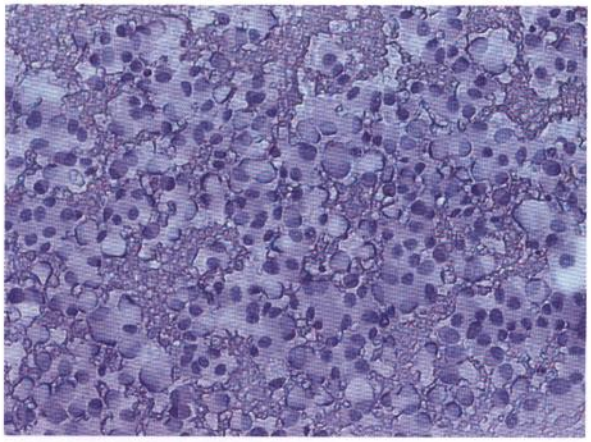
Fig. 18.**17g–k** ▷



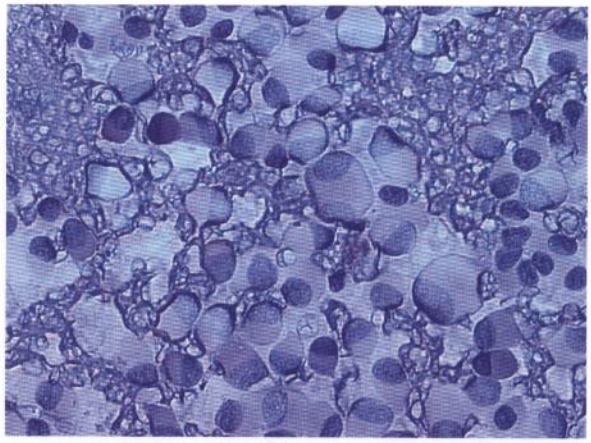
g



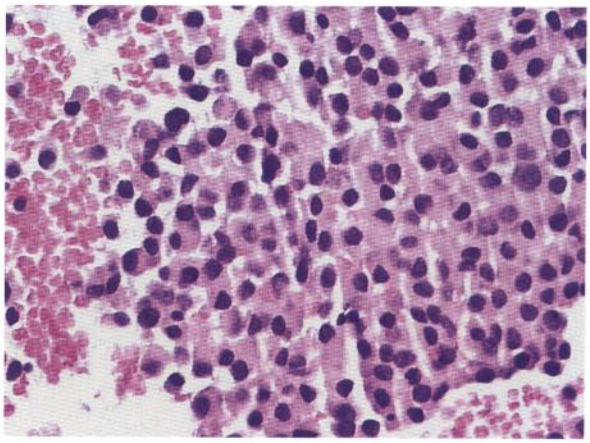
h



i



j



k

Fig. 18.**17g, h** Despite considerable numbers of peripancreatic portoportal collaterals (**g**), transgastric EUS-guided fine-needle aspiration was carried out using a 22-gauge aspiration needle, without any complications (**h**). **i, j** The bloody cytological smears showed numerous ovoid large cells, with bright cytoplasm. The variably large nuclei are located eccentrically, some of them containing nucleoli. A few of the tumor cells contain giant or double nuclei (Papanicolaou, x 200, x 400. **k** Histological examination of some small cylinders was possible and showed tumor cells with enlarged hyperchromatic nuclei and perinuclear brightening of the cytoplasm (hematoxylineosin, x 200; courtesy of Dr. Wagner, Königswusterhausen, Germany). Immunohistochemical staining was positive for chromogranine A and synaptophysine.

Diagnosis. Once a diagnosis is made, the primary tumor has to be localized and the presence of metastases has to be assessed. EUS is also used to evaluate the response to chemotherapy. Pancreatic endocrine tumors are often small and hard to detect with radiographic techniques. Since these tumors are rare, it is difficult to compare the accuracy of the various imaging tests.

Endoscopic ultrasound provides the highest resolution of the pancreas and can distinguish structures as small as < 2–3 mm. EUS has also proved to be a useful tool for identifying tumors in the duodenal wall and peripancreatic lymph nodes. EUS-guided fine-needle aspiration biopsy may help identify the type of tumor, but may not be sufficiently accurate to exclude the diagnosis in all cases. In one early report in patients who had negative ultrasound and computed tomography (CT) scans, EUS detected endocrine tumors in the pancreas with a high level of sensitivity (82%) and specificity (95%) [28]. The excellent results of this initial study were confirmed in several other studies including

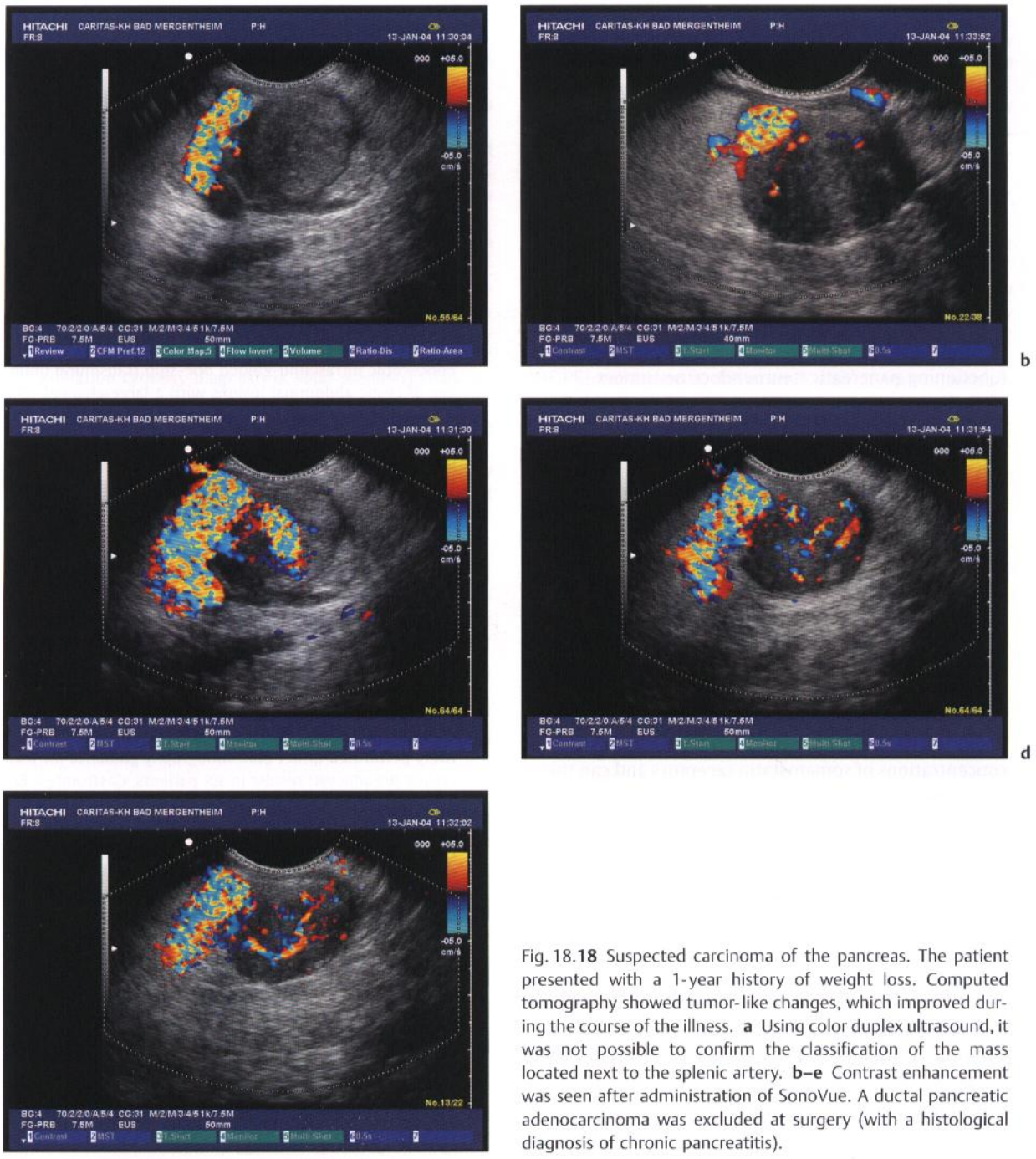


Fig. 18.**18** Suspected carcinoma of the pancreas. The patient presented with a 1-year history of weight loss. Computed tomography showed tumor-like changes, which improved during the course of the illness. **a** Using color duplex ultrasound, it was not possible to confirm the classification of the mass located next to the splenic artery. **b–e** Contrast enhancement was seen after administration of SonoVue. A ductal pancreatic adenocarcinoma was excluded at surgery (with a histological diagnosis of chronic pancreatitis).

some 300 patients. In comparison with abdominal ultrasound, CT, magnetic resonance imaging, angiography, and somatostatin-receptor scintigraphy, endoscopic ultrasound is clearly superior for localizing endocrine pancreatic tumors preoperatively. The sensitivity of EUS in detecting pancreatic gastrinomas and insulinomas has been reported to be in the range of 79–100%. EUS can therefore be regarded as method of choice for localizing pancreatic neuroendocrine tumors.

EUS-FNA may be of value in particular for differentiating between nonfunctioning pancreatic neuroendocrine tumors and other pancreatic neoplasms, in order to avoid extended pancreatic surgery. EUS-FNA is also effective and accurate in establishing the diagnosis of functioning pancreatic neuroendocrine tumors [29,30].

Preliminary experience with intraductal techniques has suggested that these may be helpful in a few cases. However, experience is limited, and the technique is not widely available.

Typically, neuroendocrine tumors are hypoechoic, well-circumscribed, and hypervascularized in comparison with the surrounding tissue (Figs. 18.**14**–18.**18**). Some tumors may resemble peripancreatic lymph nodes, as they may be connected to the pancreas by a small vascular stalk. Cystic degeneration can typically be observed mainly in larger tumors and in up to 50% of liver metastases (data not yet published).

Other imaging techniques. *Somatostatin-receptor scintigraphy.* Neuroendocrine tumors may have high concentrations of somatostatin receptors and can therefore sometimes be imaged with a radiolabeled form of the somatostatin analogue. Somatostatin-receptor scintigraphy has proved particularly effective for visualizing gastrinomas and glucagonomas, as well as nonfunctioning pancreatic tumors. As somatostatin-receptor scintigraphy fails to identify most insulinomas, it should not be used as a primary imaging test.

Intraoperative localization. Intraoperative ultrasonography (IOUS) has been used in combination with palpation of the pancreas with promising results, with a sensitivity for tumor detection of up to 83–100%. IOUS is not so far capable of replacing preoperative imaging.

Prognosis. The prognostic impact of hormone secretion is unclear. Although several studies have suggested that the survival in patients with nonfunctional tumors is poorer than in those with functional lesions, others have found no differences in the survival.

Therapy. Curative surgical resection can be attempted if there is no metastatic disease. If metastatic disease is present, its extent has to be determined so that optimal treatment can be instituted (e.g., cytoreductive surgery or chemotherapy).

References

1. Dietrich CF, Chichakli M, Hirche TO, Bargon J, Leitzmann P, Wagner TO, et al. Sonographic findings of the hepatobiliary-pancreatic system in adult patients with cystic fibrosis. J Ultrasound Med 2002;21:409–16.
2. Seifert H. [Endoscopic treatment of chronic pancreatitis; in German.] Schweiz Rundsch Med Prax 2005;94:911–23.
3. Seifert H, Faust D, Schmitt T, Dietrich C, Caspary W, Wehrmann T. Transmural drainage of cystic peripancreatic lesions with a new large-channel echo endoscope. Endoscopy 2001;33:1022–6.
4. Seifert H, Wehrmann T, Schmitt T, Zeuzem S, Caspary WF. Retroperitoneal endoscopic debridement for infected peripancreatic necrosis. Lancet 2000;356:653–5.
5. Seifert H, Dietrich C, Schmitt T, Caspary W, Wehrmann T. Endoscopic ultrasound-guided one-step transmural drainage of cystic abdominal lesions with a large-channel echo endoscope. Endoscopy 2000;32:255–9.
6. Jenssen C, Dietrich CF. [Endoscopic ultrasound in chronic pancreatitis; in German.] Z Gastroenterol 2005;43:737–49.
7. Francois E, Kahaleh M, Giovannini M, Matos C, Devière J. EUS-guided pancreaticogastrostomy. Gastrointest Endosc 2002;56:128–33.
8. Giovannini M, Moutardier V, Pesenti C, Bories E, Lelong B, Delpero JR. Endoscopic ultrasound-guided bilioduodenal anastomosis: a new technique for biliary drainage. Endoscopy 2001;33:898–900.
9. Giovannini M, Pesenti C, Rolland AL, Moutardier V, Delpero JR. Endoscopic ultrasound-guided drainage of pancreatic pseudocysts or pancreatic abscesses using a therapeutic echo endoscope. Endoscopy 2001;33:473–7.
10. Giovannini M, Bernardini D, Seitz JF. Cystogastrotomy entirely performed under endosonography guidance for pancreatic pseudocyst: results in six patients. Gastrointest Endosc 1998;48:200–3.
11. Compagno J, Oertel JE. Mucinous cystic neoplasms of the pancreas with overt and latent malignancy (cystadenocarcinoma and cystadenoma): a clinicopathologic study of 41 cases. Am J Clin Pathol 1978;69:573–80.
12. Compagno J, Oertel JE. Microcystic adenomas of the pancreas (glycogen-rich cystadenomas): a clinicopathologic study of 34 cases. Am J Clin Pathol 1978; 69:289–98.
13. Frossard JL, Amouyal P, Amouyal G, Palazzo L, Amaris J, Soldan M, et al. Performance of endosonography-guided fine needle aspiration and biopsy in the diagnosis of pancreatic cystic lesions. Am J Gastroenterol 2003;98:1516–24.
14. Brugge WR, Lewandrowski K, Lee-Lewandrowski E, Centeno BA, Szydlo T, Regan S, et al. Diagnosis of pancreatic cystic neoplasms: a report of the Cooperative Pancreatic Cyst Study. Gastroenterology 2004;126:1330–6.
15. Brugge WR. Evaluation of pancreatic cystic lesions with EUS. Gastrointest Endosc 2004;59:698–707.
16. Levy MJ, Smyrk TC, Reddy RP, Clain JE, Harewood GC, Kendrick ML, et al. Endoscopic ultrasound-guided trucut biopsy of the cyst wall for diagnosing cystic pancreatic tumors. Clin Gastroenterol Hepatol 2005;3:974–9.
17. Le Borgne J, De Calan L, Partensky C. Cystadenomas and cystadenocarcinomas of the pancreas: a multi-institutional retrospective study of 398 cases. French Surgical Association. Ann Surg 1999;230:152–61.
18. Gan SI, Thompson CC, Lauwers GY, Bounds BC, Brugge WR. Ethanol lavage of pancreatic cystic lesions: initial pilot study. Gastrointest Endosc 2005;61:746–52.

19. Farrell JJ, Brugge WR. Intraductal papillary mucinous tumor of the pancreas. Gastrointest Endosc 2002;55:701–14.
20. Furukawa T, Kloppel G, Volkan Adsay N, Albores-Saavedra J, Fukushima N, Horii A, et al. Classification of types of intraductal papillary-mucinous neoplasm of the pancreas: a consensus study. Virchows Arch 2005;447:794–9.
21. Maire F, Couvelard A, Hammel P, Ponsot P, Palazzo L, Aubert A, et al. Intraductal papillary mucinous tumors of the pancreas: the preoperative value of cytologic and histopathologic diagnosis. Gastrointest Endosc 2003;58:701–6.
22. Kobayashi G, Fujita N, Noda Y, Ito K, Horaguchi J, Takasawa O, et al. Mode of progression of intraductal papillary-mucinous tumor of the pancreas: analysis of patients with follow-up by EUS. J Gastroenterol 2005;40:744–51.
23. Bardales RH, Centeno B, Mallery JS, Lai R, Pochapin M, Guiter G, et al. Endoscopic ultrasound-guided fine-needle aspiration cytology diagnosis of solid-pseudopapillary tumor of the pancreas: a rare neoplasm of elusive origin but characteristic cytomorphologic features. Am J Clin Pathol 2004;121:654–62.
24. Master SS, Savides TJ. Diagnosis of solid-pseudopapillary neoplasm of the pancreas by EUS-guided FNA. Gastrointest Endosc 2003;57:965–8.
25. Kosmahl M, Peters K, Anlauf M, Sipos B, Pauser U, Luttges J, et al. [Solid pseudopapillary neoplasms: enigmatic entity with female preponderance; in German.] Pathologe 2005;26:41–5.
26. Bunk A, Pistorius S, Konopke R, Ockert D, Kuhlisch E, Saeger HD. [The value of colour duplex sonography in the assessment of surgical resectability of pancreatic tumors; in German.] Ultraschall Med 2001;22:265–73.
27. Meining A, Dittler HJ, Wolf A, Lorenz R, Schusdziarra V, Siewert JR, et al. You get what you expect? A critical appraisal of imaging methodology in endosonographic cancer staging. Gut 2002;50:599–603.
28. Rösch T, Lightdale CJ, Botet JF, Boyce GA, Sivak MV Jr, Yasuda K, et al. Localization of pancreatic endocrine tumors by endoscopic ultrasonography. N Engl J Med 1992;326:1721–6.
29. Fritscher-Ravens A, Sriram PV, Krause C, Atay Z, Jaeckle S, Thonke F, et al. Detection of pancreatic metastases by EUS-guided fine-needle aspiration. Gastrointest Endosc 2001;53:65–70.
30. Fritscher-Ravens A. Endoscopic ultrasound and neuroendocrine tumors of the pancreas. JOP 2004;5:273–81.

19 Pancreatic Interventions

H. Seifert, C.F. Dietrich

Introduction

Due to its retroperitoneal position, the pancreas is difficult to reach using all of the conventional surgical techniques, including open or laparoscopic surgery. From the endosonographic point of view, however, it is only a few millimeters from the transducer—a distance corresponding to the thickness of the duodenal or gastric wall. The development of endoscopic ultrasound (EUS) therefore led to the development of EUS-guided interventions in the pancreas. These interventions almost always relate to peripancreatic fluid collections, usually resulting from acute or chronic pancreatitis.

In the early 1980s, for patients with chronic pancreatitis, the alternatives to letting the process run its spontaneous course, on the one hand, and carrying out pancreatectomy with unsatisfactory results on the other, included surgical drainage procedures with dilation of the pancreatic duct in cases of obstruction. At about the same time, alternative techniques were developed, with the objective of making the resection less radical and the drainage less invasive: resection of the head of the pancreas, preserving the duodenum, and endoscopic decompression using pancreatic papillotomy, extraction of stones, and stent placement. At the same time, as part of the new endoscopic treatments for chronic pancreatitis, the first endoscopic transpapillary and transmural drainage procedures were carried out in pancreatic pseudocysts. These endoscopic techniques have been found to be technically successful, with low complication rates, and not just in individual cases. It has also been established that successful puncture and drainage can at least reduce the often considerable symptoms. This form of treatment has developed substantially, particularly with the aid of endosonography.

Table 19.1 Normal methods of clinical description of peripancreatic fluid collections

Criteria	Terms used
Medical history, age	Acute/chronic, mature/immature
Underlying illness	Post-pancreatitis, idiopathic, neoplastic
Symptoms	Symptomatic/asymptomatic
Size	Microcystic, large (> 6 cm), small (≤ 6 cm)
Shape	Monocystic/polycystic, causing bulging/no bulging, septate/nonseptate
Image of contents	Anechoic/hypoechoic/echogenic
Content as aspirate	Serous, liquid, mucinous, putrid, hemorrhagic ("chocolate cyst"), solid, infected/sterile, amylase present/absent
Boundaries	With/without wall, sharply/poorly delineated, arched–round, complex/branched
Connections	With/without fistula to: pancreatic duct, stomach, ascites, retroperitoneum, pleura, mediastinum, other cysts
Position	Intrapancreatic/extrapancreatic, head–body–tail
Malignancy	Benign/malignant

Cystic Pancreatic Lesions: Definition and Classification

Pathological cavities in the region of the pancreas can be classified using a wide variety of characteristics. In clinical practice, lesions can be described from various points of view (Table 19.**1**) [1–4], although the characteristics of one category (e. g., size) do not necessarily allow conclusions to be drawn about another category (such as the prognosis).

This situation has led to some uncertainty regarding the classification and definition of cystic lesions of this type. The most important questions in clinical practice are answered by simple sonomorphological characterization of the lesions with regard to shape, size, position, and echo pattern. This applies in particular when the technique also provides information about the topographical and pathological anatomy of the vessels and of the pancreatic and bile ducts, and when information about the development of the cysts can be obtained over a period of a few weeks. Information of similar value to that provided by ultrasound can also be obtained with magnetic resonance imaging (MRI) and computed tomography (CT).

A second classification in terms of the etiology and pathogenesis on the basis of the sonomorphology and medical history, but sometimes not until endoscopic retrograde cholangiopancreatography (ERCP) or histological assessment have been carried out (Table 19.**2**).

Awareness of these differential-diagnostic alternatives is important during the endoscopic drainage of cystic lesions. In particular, malignant tumors, which may not always be cystic adenocarcinomas, must not be overlooked. Even acute or chronic pancreatitis can

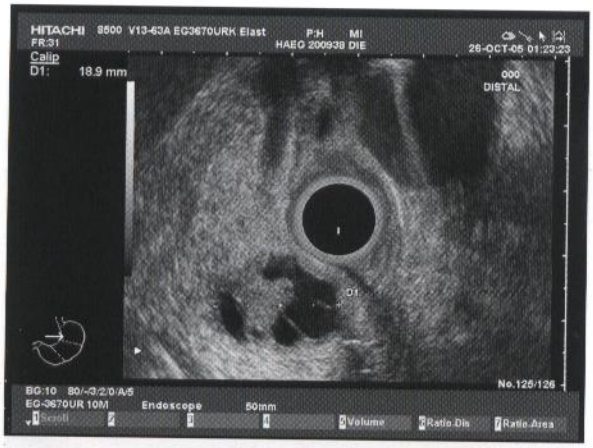


Fig. 19.**1** Polycystic serous pancreatic adenoma. Endosonography, radial scanner (3670 UR). The tumor as a whole has a roundish border. It displays larger cysts, but also honeycombed, microcystic areas. The surrounding pancreatic parenchyma is normal.

Table 19.**2** Classification of cystic peripancreatic lesions in relation to etiology and pathogenesis

Diagnosis	Comments
Result of pancreatitis	Pseudocysts and other lesions (see the Atlanta classification, Table 19.**3**)
Duodenal wall cysts	Intramural. Genesis unclear; caused by ectopic pancreas or inflammation of the head of the pancreas?
Idiopathic pancreatic cysts	Rare, sporadic, or in polycystic disease
Cystic pancreatic tumors	Microcystic or macrocystic, serous or mucinous. Malignancy in principle unclear
Genuine pancreatic cysts	Rare, probably mostly cystadenoma
Pancreas duplication cysts	Rare, benign [1]
Lymphocele	Benign, rare, in parenchyma; the surroundings are normal, the edges smooth and very delicate, no wall [2]
Hydatid disease	Rare [3,4]
Wall abscess	Rare, EUS demonstrates the position in the wall of the stomach

EUS: endoscopic ultrasonography.



Fig. 19.**2** Mucus-producing pancreatic tumor. **a** The tumor was revealed by a fishmouth papilla. The viscous mucus forced the pancreatic ostium wide open. **b** The mucus filled the pancreatic duct system, which had a cystically dilated appearance on EUS (longitudinal scanner, 7.5 MHz, Pentax FG38-UX, Pentax, Hamburg, Germany). **c** The corresponding endoscopic retrograde cholangiogram.

cause or possibly be the consequence of a pancreatic carcinoma.

Malignant pancreatic tumors, the prevalence of which among cystic pancreatic processes is estimated to be at about 5–10%, are the most important differential diagnosis. Detailed descriptions of the classification and diagnosis of cystic pancreatic tumors have recently been published [5–7].

In cases of cystic pancreatic processes, serous or mucinous neoplasia should always be considered; they cannot always be recognized using the typical microcystic or polycystic shape or by mucous filling of the duct (Figs. 19.**1**–19.**4**) [8].

The most accurate method of imaging various cystic lesions is endosonography. By far the majority of peripancreatic fluid collections are the result of episodes of pancreatitis. Following less convincing attempts to classify pseudocysts systematically, the classification shown in Table 19.**3** [9] was finally proposed for fluid collections caused by pancreatitis, as part of the Atlanta classification of acute pancreatitis. The Atlanta classification includes the common *postacute fluid collections,* which are not sharply delimited and often resolve spontaneously, and are filled with clear (anechoic) fluid; *pseudocysts* surrounded by a fibrous wall; and *necroses*—three findings that can also be differentiated very easily on a clinical basis. In practice, however, such pure findings

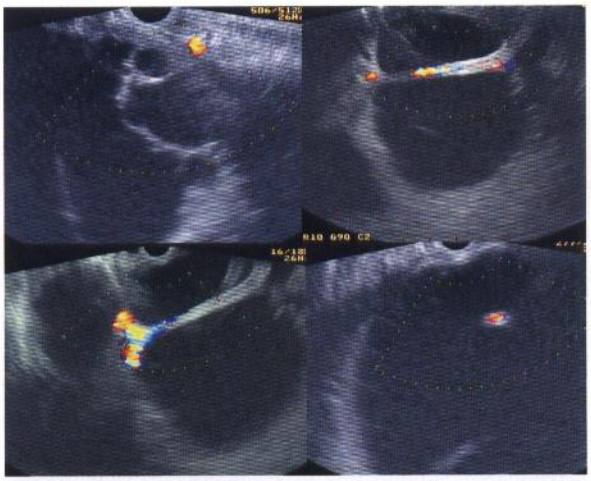


Fig. 19.**3a–d** A huge cystic retroperitoneal finding dorsal to the stomach, with anechoic contents, delicate septa, and unusually with arteries flowing through the lumen. There was no definite pancreatitis in the medical history, and no changes in the pancreatic parenchyma as found in chronic pancreatitis. Transmural drainage was not carried out due to the suspect finding, and open surgery was carried out instead. Histological analysis showed that the lesion was a benign pseudocyst.

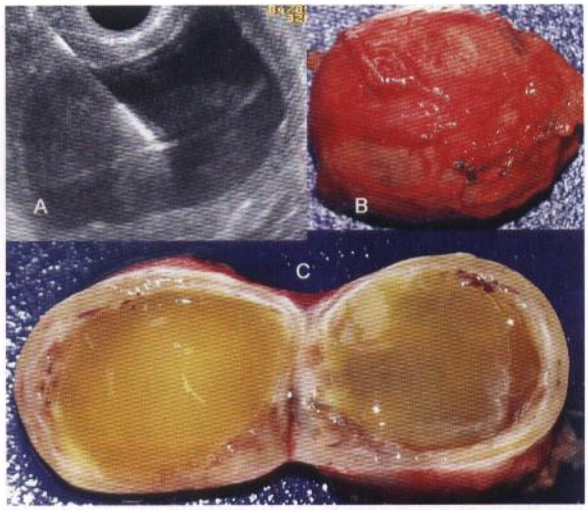


Fig. 19.**4a** A cystic lesion in the body of the pancreas with a strong wall, thickened dorsally, and anechoic contents, in a 46-year-old patient with no signs of acute or chronic pancreatitis in the medical history or abdominal ultrasound findings. The symptoms included a slight pulling sensation during vigorous movement. **b, c** Surgically, a previously unreported type of pancreatic ganglioneuroma was enucleated [8]. EUS-guided fine-needle aspiration revealed highly viscous mucus. The course was uncomplicated. This example shows how difficult it can be to distinguish between cystic lesions following pancreatitis and neoplastic lesions.

Table 19.**3** Clinical classification of peripancreatic fluid collections in accordance with the 1992 Atlanta classification [9]

Description	Definition	Clinical manifestation	Pathology	Comments
Acute fluid collections	Fluid collections in or on the pancreas, occurring early in the course of acute pancreatitis and lacking a wall	Occurs in 30–50%; spontaneous regression in approx. 50%. Most easily detected by sonography	Sometimes contaminated with bacteria, composition variable, fluid	Can develop into pseudocysts or abscesses. Cause cannot be predicted
Pancreatic necrosis	Diffuse or focal tissue necrosis, typically together with peripancreatic fatty tissue necrosis	Detection by sonography, dynamic computed tomography or MRI	The necroses can involve fatty tissue and all parts of the pancreas. Sometimes with hemorrhage.	Can become infected, and is then life-threatening (fine-needle biopsy, bacteriography of the aspirate)
Infected necrosis			Contains pus and necrotic tissue	Life-threatening, indication for surgical treatment
Acute pseudocyst	Fluid collection present more than 4 weeks after acute pancreatitis, with a wall of fibrous or granulation tissue	Clinical symptoms depend on position and size; most easily detected by sonography with CT	Usually contains pancreatic juice with high enzyme concentration; is (initially) sterile, sometimes contaminated with bacteria	Often has fistula connecting to pancreatic duct. Danger of infection
Chronic pseudocyst	Fluid collection with a wall of fibrous or granulation tissue in chronic pancreatitis, without previous episodes of acute pancreatitis	Clinical symptoms depend on position and size, most easily detected by sonography or CT	Usually contains pancreatic juice with high enzyme concentrations, is (initially) sterile, sometimes contaminated with bacteria	Often has fistula connecting to pancreatic duct. Danger of infection
Pancreatic or peripancreatic abscess	Circumscribed peripancreatic putrid abscess that occurs as a result of acute pancreatitis or pancreatic trauma	Symptoms variable, as for pseudocyst; in addition, occasionally clinical picture of sepsis	Contains pus, no or very little necrosis, synonymous with infected pseudocyst, but also with liquefied and infected circumscribed necrosis	Less threatening than infected necrosis, easier to treat

CT: computed tomography; MRI: magnetic resonance imaging.

are the exception, and transitional states are the norm. If it is difficult even to draw a clear line between acute pancreatitis and acute episodes of chronic pancreatitis, it is certainly difficult and unreliable to attempt a clear clinical classification of their "cystic" complications, with superimposition of older and more recent findings, liquid and solid, echogenic and hypoechoic, sterile, contaminated and infected (putrid) cysts with more or less well-defined walls (and anatomic delimitation). Despite these limitations, the Atlanta classification is currently the best and only clinically useful classification of pancreatogenic cysts, precisely because it bows to practice and attempts to use different categories to do justice to the characteristics of quite different types of cyst.

The classification proposed by Nealon and Walser in 2002 [10] is based solely on the anatomy of the pancreatic duct:

- Type I: normal duct with no communication with the pseudocyst
- Type II: normal duct, communication with the pseudocyst
- Type III: otherwise normal duct with stricture, no communication with the pseudocyst
- Type IV: otherwise normal duct with stricture, communication with the pseudocyst
- Type VI: otherwise normal duct with complete cut-off
- Type VII: chronic pancreatitis, no duct–pseudocyst communication
- Type VIII: chronic pancreatitis, duct–pseudocyst communication

This classification addresses the important and previously unclear issue of the influence of communications between the pancreatic duct and the fluid collection on the treatment strategy and its chances of success. Using their own retrospective data, the authors show that percutaneous drainage has little chance of success when a communication is present.

The present authors have not found that it is beneficial to make the treatment procedure dependent on the existence of this type of communication, particularly since the existence of a fistula of this type is often difficult to establish and even more difficult to rule out. This fact is also reflected in the large differences between the values for the prevalence of such fistulas reported by different authors. The values vary between 6%, cited by Neoptolemos [11], 20% by Barthet et al. [12], and up to 60% by Nealon et al. [13]. Large pseudocysts or necrotic cavities, inflammatory swelling of the head of the pancreas or of the duodenal wall, or scarring and calcification in chronic pancreatitis can change the normal anatomy to such an extent that endoscopic retrograde pancreatography (ERP) is impossible or very difficult. Even if the pancreatic duct can be examined, fistulas often cannot be clearly identified due to compression caused by the cystic lesions and calcification. In addition, a high level of injection pressure is often required, and—especially for very large pseudocysts—large quantities of contrast agent are needed in order to clearly identify the communication between the pancreatic duct and pseudocyst, necrotic cavity, or even stomach, mediastinum, abdominal cavity, or bile duct. We avoid this sort of procedure, which involves a substantial risk of introducing bacterial contamination (almost always) or manifest septic complications. In addition, the anatomy can often be imaged without any problems following decompression of the pseudocyst or necrotic cavity. Magnetic resonance cholangiopancreatography (MRCP) is not capable of detecting narrow fistulas in complex anatomy either, so it is not an alternative to ERCP. On the other hand, if the latter is easy to do and shows a clear communication between the duct and the pseudocyst, transpapillary drainage is often successful on its own. It has not been demonstrated whether, in such cases, it is better to fit the pancreatic duct with a stent to bridge the fistula (our preference, which we like to combine with transmural drainage) or to drain the cyst directly through the fistula.

None of the classifications of cystic lesions mentioned are suitable for stratifying patients according to the severity of the condition. In clinical practice, an overview of aspects covered by the individual classifications, the serum C-reactive protein (CRP) level, and symptoms during the course of the illness provide a tried-and-tested basis for the treatment strategy.

■ Epidemiology

Pseudocysts are typical complications of chronic pancreatitis. They are found in up to 60% of surgical specimens from patients with chronic pancreatitis, and, according to Stolte [14], are found more often in preparations with segmental (48%) than with nonsegmental (23%) chronic pancreatitis. In large clinically recorded populations with chronic pancreatitis, pseudocysts have been described in 23% of patients (56 of 245) [15]. These data relate to a symptomatic and consequently treated population (usually treated surgically). The actual prevalence of pancreatic pseudocysts and other cystic lesions in chronic pancreatitis, including uncomplicated courses, is presumably substantially lower.

Values cited for the incidence of peripancreatic fluid accumulations in acute pancreatitis lie between 14% [16] and (when detected with CT) over 50% [17].

Pancreatic necroses develop in approximately 5% (17 of 348) [18] to 20% (38 of 194) [19] of patients with acute pancreatitis. Up to 70% of them have primary infection. In recent publications, the mortality rate due to infected necroses has been reported to be 10–35%.

In 100 patients included in a study in Glasgow [20], the mortality rate due to pseudocysts of biliary origin, at 22%, was distinctly higher than for pseudocysts of alcoholic origin, at 5%. The overall figure was 12%; only patients with postacute pseudocysts who had undergone surgery were included. In most cases, the cause of death was sepsis or hemorrhage. All patients with chronic pseudocysts survived. A mortality rate of 5–15% has generally been reported for cystic lesions following pancreatitis. However, it is scarcely possible to give a figure for the spontaneous course, as the patients detected epidemiologically have usually been treated and thus represent a selection.

With very few exceptions, the data shown here apply to "publication-relevant" groups of patients in fairly large centers—i.e., only to the more severe courses of the clinical pictures concerned. The incidence and prevalence of problems and complications may therefore have been overestimated. However, selection of this sort also applies in general to patients, including those undergoing interventional treatment.

■ Etiopathogenesis

Peripancreatic or intrapancreatic fluid collections can have various origins and are probably often the result of several pathological mechanisms working together.

Severe acute pancreatitis gives rise to peripancreatic fatty tissue necroses, occasionally with large fields of necrosis surrounding the pancreas like a coat and spreading along the fibrous tissue septa to the intrapancreatic fatty tissue, on the one hand, and to the more distant extrapancreatic fatty tissue (mesentery, omental bursa, retroperitoneum) on the other. Pseudocysts containing hemorrhagic and necrotic material develop from the larger necrosis fields within 7–30 days of the acute necrosis. With time, they separate themselves more clearly from their surroundings through the formation of granulation tissue. They not infrequently communicate with the pancreatic duct. Confluent intrapancreatic fatty tissue necroses are usually replaced by sclerotic tissue. This fibrotic process can involve the interlobular pancreatic ducts and encourage the development of chronic pancreatitis. Intrapancreatic pseudocysts can also persist due to communication with the ductal system and lead to local complications due to compression of the environment. In dogs, it has been shown that a pseudocyst takes about 6 weeks to develop a "mature" fibrous wall.

Post-traumatic pancreatic pseudocysts are not common; in large populations, they represent a maximum of 5%. In children, they mainly occur after pancreatic rupture due to car accidents or due to trauma from bicycle handlebars. If the pancreatic duct remains continuous, spontaneous regression is possible.

Despite important recent evidence concerning the genetic and autoimmune pathogenesis of acute and chronic pancreatitis, the concept of more or less mechanical development is still the most important idea guiding the therapeutic procedure and the patient's well-being. Stolte's discussion of this subject from 1984 [14], based on thorough morphometric investigations, remains valid: whatever the nature of the etiology or course of the pancreatitis, "in the end, there is always an area of scar tissue. So the various subdivisions of chronic pancreatitis, with their histological types and duct patterns only appear to be snapshots of a continuous, progressive process ... There is a vicious circle of self-perpetuation in chronic pancreatitis." The fact that a persistent fistula, traumatic rupture of the duct, and pancreas divisum are established causes or contributing factors in the formation of pseudocysts supports the view that the impaired flow is at least partly mechanical in origin.

■ Therapeutic Approaches

Any therapeutic intervention has to be weighed up in comparison with alternative treatments. Surgical or endoscopic interventions are only justified if their risk is lower than that of the spontaneous course or of noninvasive approaches. Different therapeutic strategies, including open surgery, have to be discussed with the patient to provide a basis for informed consent to any therapy. These alternatives are therefore considered here.

Objectives of Treatment

As in the treatment of chronic pancreatitis in general, a treatment strategy for pancreatogenic cystic lesions can serve very different purposes. As emergency treatment in acute complications such as rupture or hemorrhage, the objective is to avert the immediate danger, which is almost always achieved by surgery and does not require any discussion. In the case of infected pseudocysts or necroses, the prevention of life-threatening septic complications is without question an absolute indication for surgery. The situation is similar for compression stenoses of the bile duct, duodenum, or stomach, which require surgery.

However, the most common reason for surgical treatment of pseudocysts is severe pain, followed by nausea and vomiting (as a consequence of the above-mentioned compression of the gastric and intestinal lumen), loss of weight, and jaundice. However, in the surgical literature, clear reference to the indications or the objectives of the intervention is not always made, with the common cause being severe pain in chronic pancreatitis.

In asymptomatic or oligosymptomatic patients with large or persistent cysts, the prevention of likely complications of the spontaneous course (see below) always influences the therapeutic objectives, although there are no reliable data regarding the incidence of these. The complications can also be considered to include loss of the endocrine or exocrine function of the pancreas. In this case, maintaining the function of the organ (or preventing its loss in the "natural" course of the disease) would be the therapeutic objective. In the context of organ conservation, the treatment of cystic lesions—which is justified even for isolated lesions for improvement of symptoms—should be understood as only part of the decompressive and drainage treatment of the chronic pancreatitis. In this way, surgery has achieved encouraging results [21–23]. Endoscopic interventions are generally based on the hypothesis that reconstructing the normal anatomy, usually by drainage of congested regions, and restoring the normal flow of pancreatic juice can lead to an improvement in the symptoms and sometimes of the entire clinical course. In a multicenter retrospective analysis of more than 1000 patients with chronic pancreatitis, the symptoms improved in the long term in 65% of patients and in the short term in 85% [24].

Spontaneous Course

The expected spontaneous course of a pancreatic pseudocyst depends on the time of observation. If a cystic lesion develops during the acute phase of pancreatitis, it is very probably peripancreatic edema with a good chance of spontaneous regression. Clinically, acute fluid collections of this type can correspond to a pseudocyst.

Spontaneous regression rates of 7% [8], 12% [25], 28% [26], and 60% [27,28] have been reported, sometimes depending on the size of the cyst. According to some authors, spontaneous regression of pseudocysts is unlikely after more than 6 weeks. On the other hand, Vitas and Sarr, who retrospectively analyzed patients with pancreatic pseudocysts who were treated at the Mayo Clinic in the years 1980–85, came to a different conclusion [29]. Of 114 patients, 46 were given primary treatment by surgery. Only six (9%) of the remaining 68 patients, who were treated conservatively, had serious complications during a mean observation period of 46 months; 19 of them ultimately underwent elective surgery. Overall, the pseudocyst regressed spontaneously in 57% of the patients treated conservatively, in 38% of them more than 6 months after the diagnosis. Among these, seven patients had cysts more than 10 cm in diameter which regressed without complications. The authors conclude that, contrary to the earlier view, even older and very large pseudocysts can regress spontaneously; that a "wait-and-see" approach is therefore justified in most patients.

Relevant complications of the spontaneous course include hemorrhage, rupture, and infection. The incidence of these is difficult to specify, as it is normal to try to avoid such complications using surgical treatment. No reports on the spontaneous course in large populations of patients over prolonged observation periods are available.

Hemorrhagic complications—which can manifest as hemosuccus pancreaticus, and also as fulminant hemorrhage into a pseudocyst or as a consequence of cyst rupture—mostly arise from the splenic artery. The artery is affected by local reactions resulting from pancreatitis and can develop pseudoaneurysms as a typical complication in about 3% of patients. Rupture of the pseudoaneurysm then leads to arterial bleeding. Major arteries originating from the celiac trunk, and not infrequently the splenic artery or hepatic artery, often pass directly by the walls of cystic lesions. They can be clearly seen there using ultrasonography even without Doppler imaging, whereas smaller vessels can only be seen with EUS. The splenic vein lies in the immediate vicinity in most cases of pancreatitis and pseudocysts. If it is affected by the inflammatory process, the typical complication is splenic vein thrombosis. This is apparent from the almost pathognomonic endoscopic picture of isolated gastric varices (without esophageal varices), sometimes together with duodenal varices. Bleeding varices can develop as life-threatening sequelae. The literature contains a large number of case studies on this topic, but there is no reliable information on the incidence of such vascular and hemorrhagic complications.

The same applies to spontaneous rupture of pseudocysts. Sankaran and Walt [30] observed spontaneous rupture in 19 of 131 pseudocysts (15%), with hemorrhage in four cases. Because of the high rate of spontaneous complications (33%), the authors advocate surgical drainage. Such a high rate of spontaneous complications has not been confirmed in the few other papers on the spontaneous course. Nevertheless, Seiler et al. [31], on the basis of 154 patients with complicated chronic pancreatitis, describe the formation of pseudocysts as the most important prognostic risk factor, correlating highly significantly not only with pain but also with a higher incidence of vascular complications and a significantly higher risk of mortality (7.1%) than for patients without pseudocysts (1.8%).

There have been isolated reports of fistulas to the stomach, and of the spread of pseudocysts into the mediastinum with rupture or fistula into the esophagus, pseudoachalasia, or cardiac compression.

There is no reliable information on the incidence of spontaneous infection of initially sterile pseudocysts. Kolars et al. [32] found bacterial infection in 17 of 51 (33%) pseudocysts, although this was in a group of hospitalized patients who later underwent surgery—i.e., certainly not a representative population.

Imrie et al. [20] reported a mortality rate of 22% for patients with pancreatic pseudocysts of biliary origin (27% of the group), significantly higher than the mortality rate of 5% for pseudocysts of alcohol-induced origin (59% of the patients). In 1979, Bradley et al. [33] recommended that pseudocysts should not be kept under observation for long, as 41% of 54 patients with pancreatic cysts developed complications after an observation period of 2–4 months, with a mortality rate of 14%—higher than with surgical intervention.

Conservative Treatment

Patients with symptomatic cystic lesions have generally already undergone weeks or months of conservative treatment by various hospitals and doctors, require high doses of analgesics, and have undergone prolonged hospital stays and periods of fasting, often with parenteral feeding. They are referred because of the failure of these treatments. For most of the patients encountered here, conservative treatment is no longer a genuine alternative; instead, they specifically represent "the failures of the waiting game" [34].

Although treatment with somatostatin analogues has been repeatedly suggested for chronic pancreatitis, the usefulness of these agents has at best been demonstrated in combination with surgical treatment. They are of doubtful efficacy in conservative treatment regimens, at least in relation to pain.

Parenteral nutrition is at best of limited use in the treatment of symptomatic pseudocysts. In addition, it is not a low-risk therapy; potentially severe complications should be taken into consideration.

Interventional Treatment

Surgical Procedures

The objective of surgical treatment has been defined for decades. It consists of avoiding the various complications by removing necrotic and infected material and through drainage and lavage of existing cavities. The first successful treatment of a pancreatic pseudocyst by excision was carried out in 1882 by Bozeman [35]. The first external drainage by marsupialization was described the following year by Gussenbauer [36], a method that was still being practiced in recent times. Resection is now avoided. The objectives are to relieve cystic cavities and to carry out gentle (manual) removal of easily mobilized necrotic tissue. Cystic processes are opened and either drained externally or into the stomach (the first pseudocystogastrostomy was carried out in 1921 by Jedlica [37]), the duodenum (the first pseudocystoduodenostomy was carried out in 1928 by Hahn [38]), or the jejunum (the first pseudocystojejunostomy was carried out in 1931 by Jurasz [39]). In the last two cases, surgical anastomoses are established between the pseudocysts and the intestinal lumen and, in the case of the jejunum, Roux-en-Y anastomoses as well. The prerequisite for this type of cystointestostomy is that the cyst must have a wall that can be sutured. For this reason alone, the surgical literature often recommends waiting 5–6 weeks after the acute attack or the development of the cystic lesion before surgery, to provide sufficient time for a fibrous wall to form.

In the case of surgery, as for any other form of treatment, the question arises of whether different cystic lesions require specific therapeutic strategies. The procedure may depend on the clinical picture, the presence of infection, the pathogenesis, the morphology, etc. Infected and uninfected lesions should in principle be treated differently, with classical pseudocysts on the one hand and infected necroses on the other representing two very different clinical extremes in peripancreatic fluid collections. The most important aspects of these from a surgical viewpoint are therefore described in brief below.

The best surgical technique is a matter of dispute and may perhaps be a question both of the anatomical circumstances in the individual case and the surgeon's experience. Longitudinal opening and anastomosis of the pancreatic duct (Partington–Rochelle pancreaticojejunostomy) is favored by many, but—like endoscopic techniques—only secures drainage without reliably removing the chronic inflammatory foci frequently present in the head of the pancreas. In addition, the main problem of a pancreatogenic distal bile duct stenosis remains untreated. Whether resection of the head of the pancreas conserving the duodenum or a modified Whipple procedure with pancreaticoduodenectomy (whether or not conserving the pylorus) should be preferred in this case is still a matter of debate even among specialists. Jimenez et al. were unable to identify any advantage of pylorus-conserving pancreaticoduodenectomy over the classical Whipple procedure [40].

In a randomized study, Izbicki et al. found that a combination of a drainage operation and local resection of the pancreatic head was slightly better than pylorus-conserving resection of the pancreatic head [22], and a recent randomized study showed that the duodenum-conserving technique was clearly better than the classical Kausch–Whipple procedure in terms of pain, quality of life, and the patient's nutritional status [41]. As a rule of thumb, it may be stated that classical procedures for the treatment of the complications of chronic pancreatitis should solve all anatomical problems as rigorously as possible, so that further regular endoscopic treatment efforts after surgery can be expected to be unnecessary. A severely inflamed and often stenotic duodenum, a fibrotic bile duct that is stenotic over a long distance, and a long-standing "pseudotumor" in the head of the pancreas should be removed, and drainage secured. The

outcome is considered to depend on the size of the inflamed head of the pancreas. In rare cases, a splenectomy may also be indicated. However, left subphrenic abscesses penetrating the spleen can also be successfully treated endoscopically [42]. Nealon and Walser found that, in the presence of ductal changes and pseudocysts, surgical drainage of the pancreatic duct without drainage of the cyst itself was adequate [43].

In a prospective and randomized study comparing endoscopic and surgical treatment, 35% of the surgically treated and 15% of the endoscopically treated patients were pain-free after 5 years, and approximately half showed improvement in each case. Thus, if the less invasive endoscopic technique does not lead to success as the primary therapy, surgery is a good alternative [44]. Left resection of the pancreas has led to unsatisfactory results and should at best be considered in exceptional cases.

Data on intraportal autologous islet transplantation after pancreatectomy provide hope that more than half of those affected may be able to remain independent of insulin treatment.

Pseudocysts. Once CT and sonography in particular allowed precise morphological description of cystic lesions in the course of their development, the question of the correct time for surgical intervention became more urgent. Warshaw found that the waiting period for spontaneous regression of pseudocysts after acute pancreatitis or an acute episode of chronic pancreatitis should be 6 weeks [34]; in chronic pancreatitis without an acute episode, one should wait for persistence for more than 4–6 weeks, but thick walls and cicatricial ductal changes are unlikely. The author regarded a connection between the cyst and the pancreatic duct as a precondition for spontaneous regression. The specified minimum age of 4–6 weeks was calculated from the time of diagnosis, so it can only be regarded as reliable if the cyst was observed at the time it developed—i. e., in the course of acute pancreatitis. This "maturation period," which is still often considered to be necessary even today, originated in a number of papers by surgeons and does not appear to be essential from the endoscopic point of view.

Because of the good chances of regression, surgery does not appear to be justified in patients with asymptomatic retroperitoneal pancreatic pseudocysts. Treatment is usually regarded as indicated in the case of symptomatic, infected, or very large pseudocysts.

Multiple pancreatic pseudocysts, which are reported in about 10% of the affected patients, place particular demands on surgical drainage. In a recently published study [45], pseudocysts were the most common indication for surgery in 231 patients with chronic pancreatitis.

Necroses. Up to 20% of patients with acute pancreatitis develop pancreatic necrosis. A secondary infection can be expected in more than 50% of these cases; this is regarded as an indication for an open drainage operation and is associated with a mortality rate of 10–15%. There is wide agreement on the indication for surgical treatment of infected necroses. The mortality rate is given as 10–35%.

Conservative treatment of sterile necroses is increasingly being advocated. According to this view, careful necrosectomy should be reserved for patients with extensive necroses, a clinical picture of sepsis, and multiple-organ failure. Every resection in acute pancreatitis becomes excessive treatment if vital tissue capable of recovery is removed as well. Bradley considers that surgical debridement of sterile necroses is not indicated, as it does not improve the course of the disease and leads to secondary infection in 25% of cases. For infected necroses, he believes that surgery is the treatment of choice, although the optimal drainage technique needs to be discussed, "despite occasional anecdotal reports of successful management by transcutaneous or endoscopic means" [46]. Other centers recommend removal of sterile necroses as well [47] and report a mortality rate of less than 10% after surgical debridement [48]. The debridement has to be as complete as possible, as residual infected necrotic material adversely affects the prognosis.

Percutaneous Drainage

Percutaneous drainage of uncomplicated pancreatic pseudocysts is a low-risk procedure when appropriate sonographic techniques are used, and it can produce good results, at least in the short term. It can be controlled by CT or sonography [49, 50].

Adams and Anderson [51] reported retrospectively on 52 CT-controlled punctures of pancreatic pseudocysts. The mortality rate was 0%, but the rate of infection in the puncture channel was 48%. The advantage of this method in comparison with surgery is the lower mortality rate (0 vs. 7%), the lack of surgical trauma, and the fact that surgical treatment remains an option.

Some authors consider that percutaneous drainage is promising in normal ductal anatomy but is not indicated in chronically altered ductal anatomy with fistulas or strictures.

Van Sonnenberg et al. reported success rates of more than 90% after percutaneous puncture and drainage, despite 51% (of 101) pseudocysts having a primary infection [50]. The authors emphasized that large-caliber catheters and patience (average duration of drainage 33 days, maximum 119 days) are decisive for success; the mortality rate in patients with infected cysts was 8% [52].

Percutaneous debridement of pancreatic necroses with special catheters has also been reported; this requires very long examination and exposure times.

Endoscopic Transmural Drainage

The endoscopic treatment of intrapancreatic or peripancreatic fluid collections can be carried out using transpapillary drainage or transmural puncture and drainage. The transmural procedure should always be carried out under endosonographic guidance, as hemorrhagic complications can be avoided and complex anatomical situations can be mastered in this manner. This is a view that cannot be based on comparative research studies; due to the immediate practical evidence, experienced investigators with access to EUS would regard such studies as unacceptable.

The first transmural cyst puncture, reported in 1975 by Rogers et al. [53], was only successful in the short term, as a relapse occurred. After only one further case report on the endoscopic transgastric method had been published, the technique of internal gastrocystic drainage, established percutaneously with ultrasound guidance and gastroscopic control, was developed by Hancke, Henriksen, and others. This technique produced promising results. Recently, there have been occasional reports of good results with combined percutaneous– endoscopic transgastric cyst drainage with ultrasound guidance.

However, the more rigorous procedure using gastroscopy was direct endoscopic puncture, favorable results with which in somewhat larger numbers of patients were then published [54]. Sahel et al. reported on 19 patients who underwent endoscopic cystoduodenostomy [55]. Eleven of the patients had communications between the cyst and the ductal system, which had no discernible effect on the clinical outcome. The complications that occurred were two cases of hemorrhage, one of which was fatal, and two perforations in patients without visible compression of the intestinal wall by the pseudocyst. Cremer et al. reported good success rates over 7 years, with only one hemorrhage as a complication, in 22 patients who underwent cystogastrostomy via a nasocystic catheter [56]. They mention the presence of an impression on the enteric wall by the cyst as a prerequisite for this procedure. In suitable cases, they regarded surgical treatment as the option of second choice after endoscopy. This report was followed by publications on the successful treatment of pancreatic pseudocysts, and also of abscesses by transpapillary drainage. Various instruments have been developed for endoscopic cyst drainage.

In 1999, Terblanche's group published their technical success rate, complication rate, and relapse rate for endoscopic drainage of pancreatic pseudocysts [57]. Among 66 pancreatic pseudocysts, 34 (52%) were suitable for endoscopic treatment, namely when they caused bulging of the stomach or duodenal wall. Endoscopic drainage was successful in 24 cases (71%), and the success rate with a follow-up period of 46 months was 62%, with a relapse rate of 7%. The factors held responsible for failure were a thick cyst wall, unfavorable position, and association with necrotizing pancreatitis.

Endoscopic transmural puncture was initially restricted to lesions with clear bulging of the gastric or duodenal wall caused by the cyst, as reliable hits could not otherwise be achieved and substantial complications such as puncture of the gallbladder, and hemorrhage in particular, were to be feared. In addition, the proportion of cystic lesions accessible to endoscopic treatment in these conditions was distinctly limited. Even large pseudocysts or abscesses do not necessarily cause bulging in adjacent sections of the intestine. Infected necroses are not normally clearly visible with endoscopy. Although conventional sonography provides more or less reliable preliminary information about the topography of the possible puncture site in this situation, no exact statements can be made about the vascular situation, and the combined endoscopic–sonographic procedure proved to be very complex and difficult. The unavoidable insufflation of air through the endoscope led to loss of the transgastric sonographic image. With the development of endosonography, the almost ideal method became available. The anatomical situation in the pancreas and surrounding structures, and their positions relative to the intestinal wall, could now be imaged precisely from the stomach and duodenum. Longitudinal scanners also provided reliable identification of larger vessels close to the point of puncture so that they could be avoided.

Baron et al. recently reported a long-term success rate for endoscopic treatment of chronic pseudocysts (according to the Atlanta classification) of 92%, and for acute pseudocysts and necroses of 70–75%. The rate of complications for pseudocysts was barely 20%, for necroses almost twice as high [58].

Even extensive, solid, and infected retroperitoneal necroses can be successfully treated endoscopically using the transmural procedure and direct debridement [59, 60].

Preliminary anatomical remarks. For endoscopic therapy, the entire expanse of a cyst has to be accessible from the stomach or duodenum, whether via a transpapillary route through the pancreatic duct or by transmural puncture. What this means in concrete terms, and the method to be used to establish the prerequisites for endoscopic treatment, are matters of controversy. The question of which pathoanatomical conditions favor the endoscopic procedure and which argue for surgical treatment is also open. For this reason, some preliminary remarks concerning the anatomy of pancreatogenic fluid collections are given here. This will certainly not include anything new to abdominal surgeons, but may include some aspects that are not so familiar to internal-medicine specialists. It is essential to be aware of the mesenteric relationships and retroperitoneal connections when carrying out endoscopic surgery.

The retroperitoneal position of the pancreas determines the spread, as well as the limits, of pancreatogenic cystic lesions. The pancreas extends retroperitoneally between the duodenum and the splenic hilum. Anteriorly, it is only separated from the stomach by the omental bursa, so that it is directly next to it. The omental bursa is normally only a gap between two peritoneal membranes and cannot be seen directly with imaging methods. However, if it is filled with fluid and prevented by adhesions from draining into the free abdominal cavity through the omental foramen, it appears as a cystic structure between the pancreas and stomach. Intact or even necrotic peripancreatic or pancreatic tissue can thus be found dorsal to this "pseudocyst," or in its lumen. Fluid collections in the omental bursa may be adjacent to the stomach or duodenum. Their greatest extent generally follows the transverse pancreas, and they can normally be drained completely from a single point. Usually, the best opportunity for puncture is from the body of the stomach.

During endoscopic puncture, particular attention has to be paid to the splenic artery and the dorsal pancreatic artery, which usually emerges from it close to the celiac trunk. In typical anatomy, the latter has two branches—one to the arteries of the head of the pancreas to the right and the other (in this connection the important one) to the left, often strong and passing into the parenchyma (or necrosis) in the direction of the splenic hilum. Along with the pancreatic branches of the splenic artery, there are arteries supplying the stomach in the region of the puncture.

On transduodenal puncture, attention has to be paid to the artery in the duodenal concavity, which is fed by the hepatic artery and the superior mesenteric artery. The superior pancreaticoduodenal artery (from the gastroduodenal artery) and the inferior pancreaticoduodenal artery (from the superior mesenteric artery) communicate at the back of the head of the pancreas at about the level of the major duodenal papilla.

Veins can also lead to hemorrhage following transmural puncture; the veins concerned are almost always collateral veins in splenic vein thrombosis or portal hypertension, in the context of cirrhosis of the liver. Splenic vein thrombosis is a common and typical complication of inflammatory or compressive processes in the pancreatic capsule. Endoscopically, and especially endosonographically, there is a typical pattern of gastric varices, especially in the fundus, without esophageal varices (hepatopetal flow, if cirrhosis of the liver is absent), with major veins in the splenic hilum and dorsal of the stomach wall. Not infrequently, the vessels are precisely in the area of the optimal transmural puncture point.

Indications. Interventional treatment is always indicated in patients with pseudocysts or peripancreatic necroses with septic complications. However, the situation is usually much less clear in clinical practice. Cystic bodies containing putrid matter are often oligosymptomatic or asymptomatic. Large pseudocysts, and especially extensive necrosis, can persist for weeks or even months, during antibiotic treatment sometimes with CRP declining or remaining in the moderately increased pathological range and stable. If the symptoms do not require surgical intervention, only involving persistent nausea, a more or less troublesome lack of appetite, and a feeling of pressure of varying severity, it is not easy to decide on whether to carry out endoscopic or surgical intervention. In some patients with extensive necroses, we have successfully waited until the lesions had finally consolidated. A procedure of this type requires patience (2–3 months) and involves a risk of septic complications. If the intervention is delayed until septic complications absolutely require it, the success of treatment appears impressive, but the risks increase. There are no reliable data on the best time for an intervention. It may be that, because of its minimal tissue trauma, endoscopic EUS-guided retroperitoneal decompression or debridement is justified earlier than the surgical procedure. There are no comparative prospective data on this issue.

Urgent indications for interventional therapy in pseudocysts or retroperitoneal necroses include:

- Obstruction of the stomach or duodenum
- Pain
- Vomiting
- Hemorrhage
- Septic complications (fever, increase in CRP)

Uncertain indications include:

- Feeling of fullness
- Loss of appetite
- Weight loss
- Persistence or increase in size
- Influence on vessels, close to vessels
- Bacterial contamination (positive aspirate without symptoms)

When there are no urgent indications for surgery—which include a request for treatment by the patient after receiving detailed information—we always monitor the course for 2–6 weeks. If there is no improvement during this period, we tend to operate even for the "uncertain indications." If CRP is normal and there is no sign of bacterial infection, prophylactic antibiotic treatment is not generally indicated, as recently shown by the German ASAP Study Group [61].

Practical procedure for endoscopic treatment of cystic peripancreatic lesions. Although liquid cyst contents can be drained through conventional plastic stents, solid necroses require a more aggressive procedure. The retroperitoneal space is punctured directly from the stomach or duodenum with a suitable EUS endoscope [8,42,62–64]. A transmural window is created using through-the-scope balloon dilation with an

8-mm balloon (Max-Force, Microvasive Inc. Boston, Massachusetts, USA), followed by an 18-mm or 20-mm balloon. Direct endoscopic debridement of the necrotic material is carried out through this window, and is initially repeated every 2–3 days. In some cases, the necrotic cavity is not restricted to the omental bursa, but has wide-ranging retroperitoneal branches, which have to be conscientiously drained.

The most important *principles of the endoscopic strategy* are:

- Firstly, reconstruction of the normal flow of pancreatic juice, transpapillary drainage of the *entire* pancreatic duct (no "uncoupled" areas should be allowed). Special catheters and wires are often required to do this. The duct has to be cleaned (with extraction of stones) and defects have to reconstructed along its entire length (with plastic stents).
- Secondly, transmural decompression, drainage, and lavage of cystic lesions. The window has to be large enough: if necessary, endoscopic debridement of necroses should be carried out. No infected necroses should be left behind. EUS is essential; large vessels are associated with a high risk in larger interventions. No undrained lacunae should be left behind; if necessary, percutaneous puncture of perforating abscesses in the pelvis should be carried out.

If these two principles are successfully observed, even extensive fluid collections (ascites, pleural effusions, large abscesses) disappear rapidly and fistulas dry up (Fig. 19.**5**). Endoscopic sealing of fistulas with tissue glue is rarely necessary.

Endoscopic treatment requires patience and experience, and should best be carried out by a combined gastroenterology and abdominal surgery team.

There are strong arguments for the view that mobile patients should be able to eat immediately after surgery, and thus against the use of nasocystic drains (which are very irritating and easily dislodged).

Preinterventional diagnosis. ***Patient information and consent.*** The patient should be briefed on the day before the procedure regarding alternative techniques (see above) and their risks, and in particular the risks of endoscopic transmural fenestration—hemorrhage, incorrect puncture (gallbladder), infections, and septic complications, surgery, low mortality rate. In addition, the typical risks of endoscopy (aspiration, dental damage, pancreatitis) and sedation should be mentioned.

Laboratory tests. Coagulation, cholestasis, raised CRP (procalcitonin is probably not better than CRP as a marker of bacterial infection), kidney function, cancer (hyperparathyroidism as a possible cause of pancreatitis of "unclear origin").

Doppler sonography. Recent imaging findings for the abdominal organs, their relative positions, vascularity, exclusion of anatomical details likely to lead to complications (pseudoaneurysms, varices, kidney and liver cysts, large gallbladder, extended branched systems, possible tumors) as close as possible to the time of surgery.

CT with contrast agents or MRI. Anatomical overview of the abdomen (considerable overlap with the ultrasound examination) and mediastinum, objectively evaluable images (which the radiographer interprets and the surgeon accepts, and which can later confirm the correct diagnosis) (Fig. 19.**6**).

EUS (potentially in preparation for puncture). Information briefing about possible interventions (green light for surgery even before the first intervention). Precise imaging (Fig. 19.**7**) [60] of the relative positions of the target structure and its surroundings, the best puncture position (vascularity), the pancreatic parenchyma (possible tumors, chronic pancreatitis, calcification), multiple cystic lesions, communications, imaging of pancreatic duct (occlusions by strictures or intraductal stones, possible prestenotic dilation, maintained or interrupted continuity, possible blockage in the necrosis).

ERCP (often carried out in the same session as EUS). An information briefing should be provided regarding possible interventions. ERCP should *not* be carried out if the papilla is difficult to access, if very large compressive processes are causing displacement and affect the anatomy, when surgical treatment is likely anyway in conditions that are still sterile (contamination of the ducts almost always occurs when contrast agents are used). An initial ERP is helpful for the intervention. If technically feasible, reconstruction of the pancreatic duct in the presence of occlusions, diagnosis of a pancreas divisum, bile duct stenosis, or detection of a ductal injury can indicate the appropriate form of treatment. In some cases, even endoscopic treatment of abscesses or infected necroses using an exclusively transpapillary technique is successful.

Reconstruction of the pancreatic duct, ensuring transpapillary flow and as far as possible maintaining continuity into the tail must *always* be attempted. If dominant stenoses persist, then prestenotic congestion and resulting recurrence of the cyst is inevitable.

The Transmural Operation

Position. The standard position is on the left side (with the least risk of aspiration).

Sedation. The authors have found that sedation with propofol is optimal.

Preliminary endoscopy. Before the transmural puncture, one should "sound out the terrain" using a large-diameter endoscope (normally a gastroscope). If necessary, the stomach should be emptied and one should identify or exclude abnormalities (stenoses, scars, ulcers, anatomical variants). Alternatively, a mod-

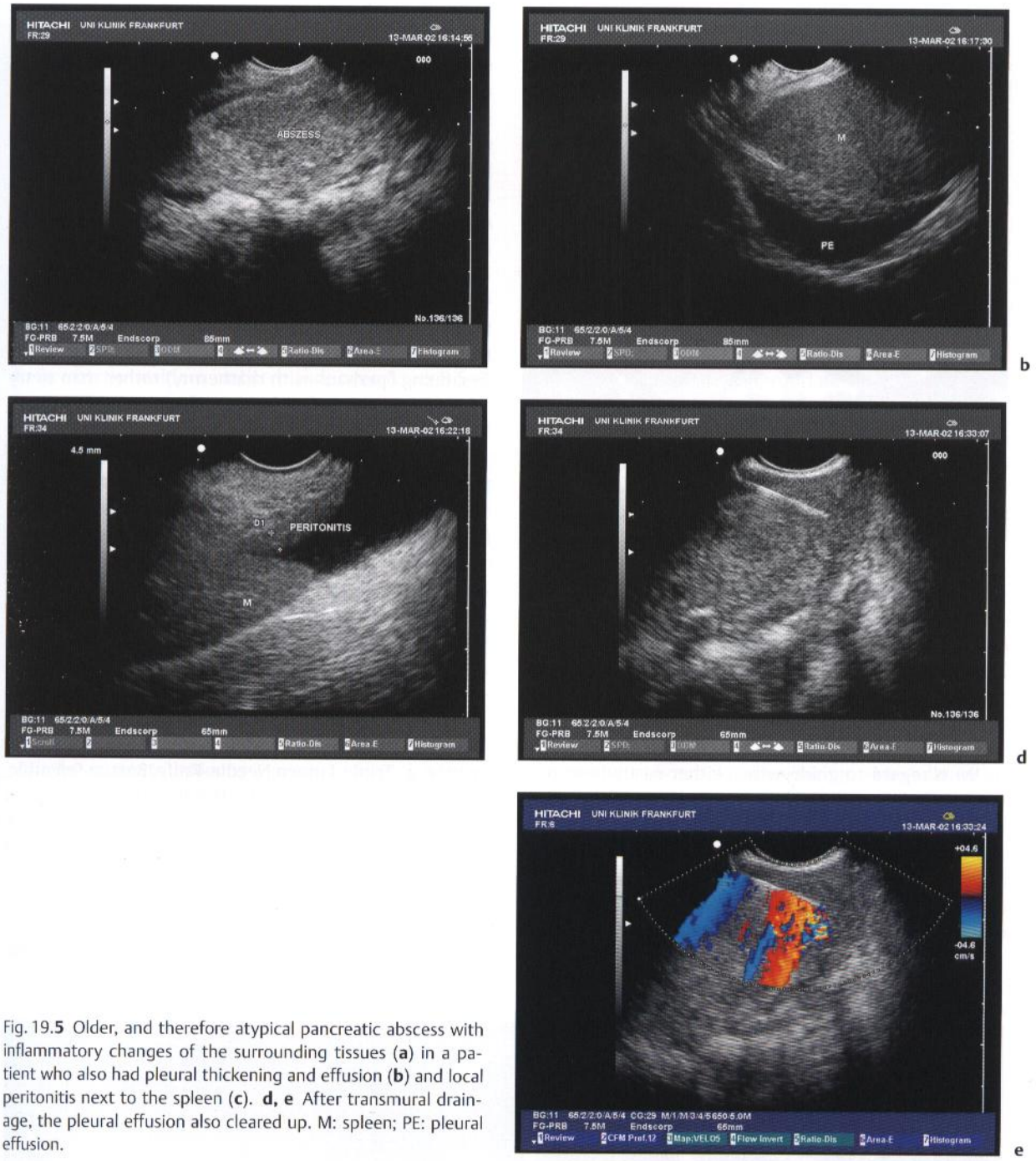


Fig. 19.**5** Older, and therefore atypical pancreatic abscess with inflammatory changes of the surrounding tissues (**a**) in a patient who also had pleural thickening and effusion (**b**) and local peritonitis next to the spleen (**c**). **d, e** After transmural drainage, the pleural effusion also cleared up. M: spleen; PE: pleural effusion.

ern endoscope with a video chip and extra-large 6-mm working channel should be used.

EUS-guided transmural drainage, debridement of necroses. In principle, two different puncture techniques are available:

- Sharp puncture with a needle and without diathermy.
- Passage into the cavity with diathermy current.

Without diathermy. Stiff, large-diameter needles should be used (Echo-19, Wilson-Cook, Winston-Salem, North Carolina, USA). Large-diameter stiff needles are usually easy visualized endosonographically. They maintain their direction relatively reliably, and even fix the transducer to the puncture point. They almost always allow diagnostic aspiration of material for bacteriology and pathology (with the exception of solid necroses). In particular, the risk of hemorrhage is low, as the procedure only leads to puncture on the axis of the defined

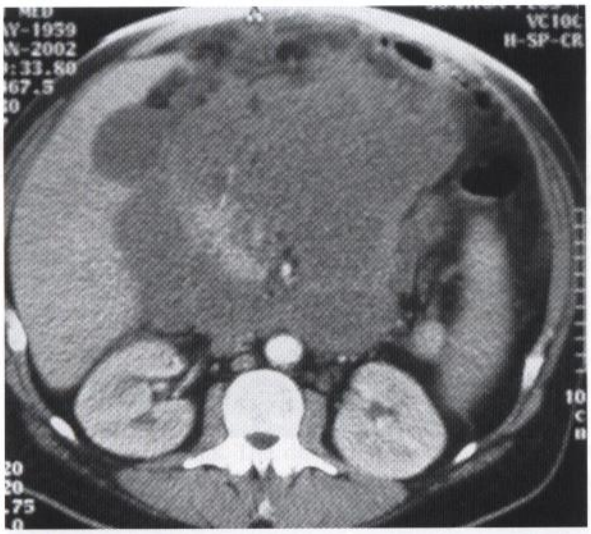


Fig. 19.6 The computed tomogram shows an extensive retroperitoneal necrosis. After transmural fenestration, about 1500 mL of pus and solid necroses was drained, followed by notable clinical improvement.

channel, rather than a cut to the side of it. Large-diameter needles can be used with a guide wire passing through the needle. Alternatively, a 1-mm needle with a fitted Teflon dilator or pusher–stent combination has proved successful for puncture and drainage in one step [42]. Unfortunately, only prototypes of such combinations are so far available.

With regard to guide wires, either easily bent pure steel wires have to be used, or the fundamental principle of never passing coated wires through sharp needles has to be breached. When advancing the needle or retracting the wire, the coating may be peeled off, or the tip of the wire could even be cut off. Thus, if one is using bend-resistant wires with hydrophilic and atraumatic radiopaque ends, which are otherwise very suitable, after stable placement of the wire in the punctured cavity (if possible with several turns), the needle must always be drawn back and removed. The guide wire can then be used either (when using echoendoscopes with narrow working channels) to replace the echoendoscope with a therapeutic gastroscope or duodenoscope (depending on availability and the anatomical situation), or drainage can be carried out directly. The use of puncture needles for complex interventions always involves the risk of damaging the working channel of the endoscope (with extremely expensive repairs). This usually happens when drawing back and then advancing the needle again, so that the fundamental rule is: if the situation is unclear, it is better to start in an orderly way from the beginning (perhaps with diathermy) rather than to try to "rescue" an attempt that has already been started.

The procedure without diathermy reaches its limits when the very tough wall of the retroperitoneal cavity is in the way of the needle. If forced puncture is attempted, the endosonographic image goes out of control, the tip of the needle departs from the plane of the image, and the transducer becomes uncoupled from the wall. With modern endoscopes, which produce an excellent endoscopic images, the operation can then sometimes be completed under endoscopic guidance. In such cases, diathermy-assisted methods have advantages.

With diathermy current. This technique uses needle-knife papillotomes with a cutting wire (rather than a blade) and an extra lumen for aspiration and the guide wire (e. g., Triple-Lumen Needle-Knife, Boston Scientific, Natick, Massachusetts, USA). The puncture point has to be selected particularly carefully in this technique, since unlike stiff needles, the needle-knife is not capable of fixing the transducer in position. With the position stable, the needle is advanced into the mucous membrane and then advanced along the axis with diathermy current (e. g., Endo-Cut). The puncture channel is burnt free.



Fig. 19.7 Even at the first endoscopic examination, the miniprobe showed the most important features in this case. **a** At the bottom of the image, there is a normal stomach wall with typical stratification, behind that, there is pancreatic tissue, at the top only the mucosal layer, and behind that no pseudocyst but an abscess in the gastric wall. **b** This image shows a preserved anterior gastric wall on the right, while on the left gastric wall is no longer present and there is only an amorphous boundary layer (complete necrosis of the posterior gastric wall); behind that, there is hypoechoic tissue with gas bubbles. **c** The longitudinal scanner shows extensive infected necroses in the same patient. Successful treatment was carried out by transmural debridement, with resection of large necrotic masses and the ischemic–necrotic spleen [60].

Caution: if the position is unstable, sideways cutting into the stomach wall (with major arteries) or tissue outside the EUS plane is possible. The diathermy effect can be visualized very well with endosonography. It clearly shows the position of the needle-knife (which is otherwise often difficult to see) and produces impressive effects at this point on reaching the cyst lumen. At that point, the guide wire and/or catheter has to be advanced further into the punctured lumen (*caution:* only the thin cutting wire should be in the lumen; the guide wire should be outside, between the layers).

As an alternative to the needle-knife, specially developed puncture sets can be used. The Giovannini Needle Wire (Wilson-Cook) has a special guide wire with a diathermy tip inside a catheter and, over it, an 8.5-Fr stent, which is placed in one step. The Cystotome (Wilson-Cook) combines a needle-knife with a ring-shaped 10-Fr electrocauterizer.

Irrespective of the technique used, the following principles and prerequisites apply:

- Experienced endoscopist (better: two physicians) and two experienced endoscopy assistants
- Potent suction (massive releases of pus or bleeding is possible after puncture), Hemoclips to stop bleeding, epinephrine, collection containers for aspirate for diagnosis (particularly bacteriology, also amylase, CEA, cytology, possibly hematocrit). Photodocumentation should be carried out if available
- Puncture equipment
- Catheter, stents, balloons
- Prograde endoscope
- Possibly nasocystic catheter or percutaneous endoscopic gastrostomy (PEG; a matter of preference)
- Preoperative antibiotic prophylaxis with sulbactam and ampicillin (Unacid), ciprofloxacin

The operation.

- The best position for puncture has to be established.
  - There should be intimate contact between the cavity to be punctured and the intestinal wall. The optimal puncture point is typically transgastric, just below the cardia, at approximately 41–45 cm from the incisors (tail, body, spleen abscesses, infradiaphragmatic spread, to splenic hilum) or about at the level of the angular notch of the stomach, 45–50 cm from the incisors (pancreatic head region, extension to the porta hepatis, bile duct, retrocecal) through the posterior gastric wall to the omental bursa, or the descending duodenum back toward the pancreatic head region, slightly above the major duodenal papilla.
  - The arteries should be avoided, especially when using diathermy (Fig. 19.**8**). Are there any vessels interposed along the puncture route? Is there a perfused solid "necrotic area"? Are there any vessels in the cyst wall, especially dorsal? Are gastric wall arteries or varices present? (Searching should be carried out with *minimal* pressure from the transducer and compression.) Retracting the instrument from the wall is possible, with optical inspection of the puncture site (Fig. 19.**9**).
  - The minimum possible bending of the instrument should be carried out (often difficult).
- Puncture of the cyst with a 19-G aspiration biopsy needle.
- Aspiration of cyst fluid in a stable position:
  - Bacteriology (blood culture bottles)
  - Laboratory tests (amylase, lipase, leucocyte count, CEA)
  - Cytology
- Introduction of an appropriate (e.g., 0.018-inch) guide wire with a flexible tip (which should be advanced as far as possible, until two or three loops form in the cyst, to ensure that the wire is in a stable position)
- Withdrawal of the puncture needle and bougienage of the access route with a 7-Fr or 8.5-Fr dilator.

Options after successful puncture, with the wire or catheter in place:

- Insertion of a plastic transmural stent (such as a double-pigtail stent or a U-shaped, suspended stent), which is often sufficient for uncomplicated pseudocysts. It is sometimes sensible to use several stents.
- A nasocystic irrigation catheter allows regular irrigation and radiographic monitoring, especially of infected cysts. However, these are easily dislocated and are very troublesome for the patient. Combination with a transmural stent is useful.
- Balloon dilation of the transmural window with an 8-mm balloon through the endoscope (up to 20 mm) (Fig. 19.**10**). This step is essential for infected necroses with solid contents. Dilation to the desired diameter can be carried out in steps over several days, or immediately at the first step (as the present authors prefer). With large windows, no additional plastic drain is required.
- Insertion of the endoscope through the 15–20-mm window into the retroperitoneal cyst and endoscopic debridement of demarcated necroses. Any endoscope can be used; large-channel therapeutic gastroscopes have proved successful, as have side-viewing instruments in special cases or thin 6-mm gastroscopes for the irrigation of narrow recesses.

After the operation. There are even fewer standards for the procedure after successful drainage than for the puncture technique itself. The procedure is determined to a large extent by the peculiarities of the individual case, but also by the technical facilities available and, not least, the investigator's experience. For this reason, no treatment instructions can be given here, and

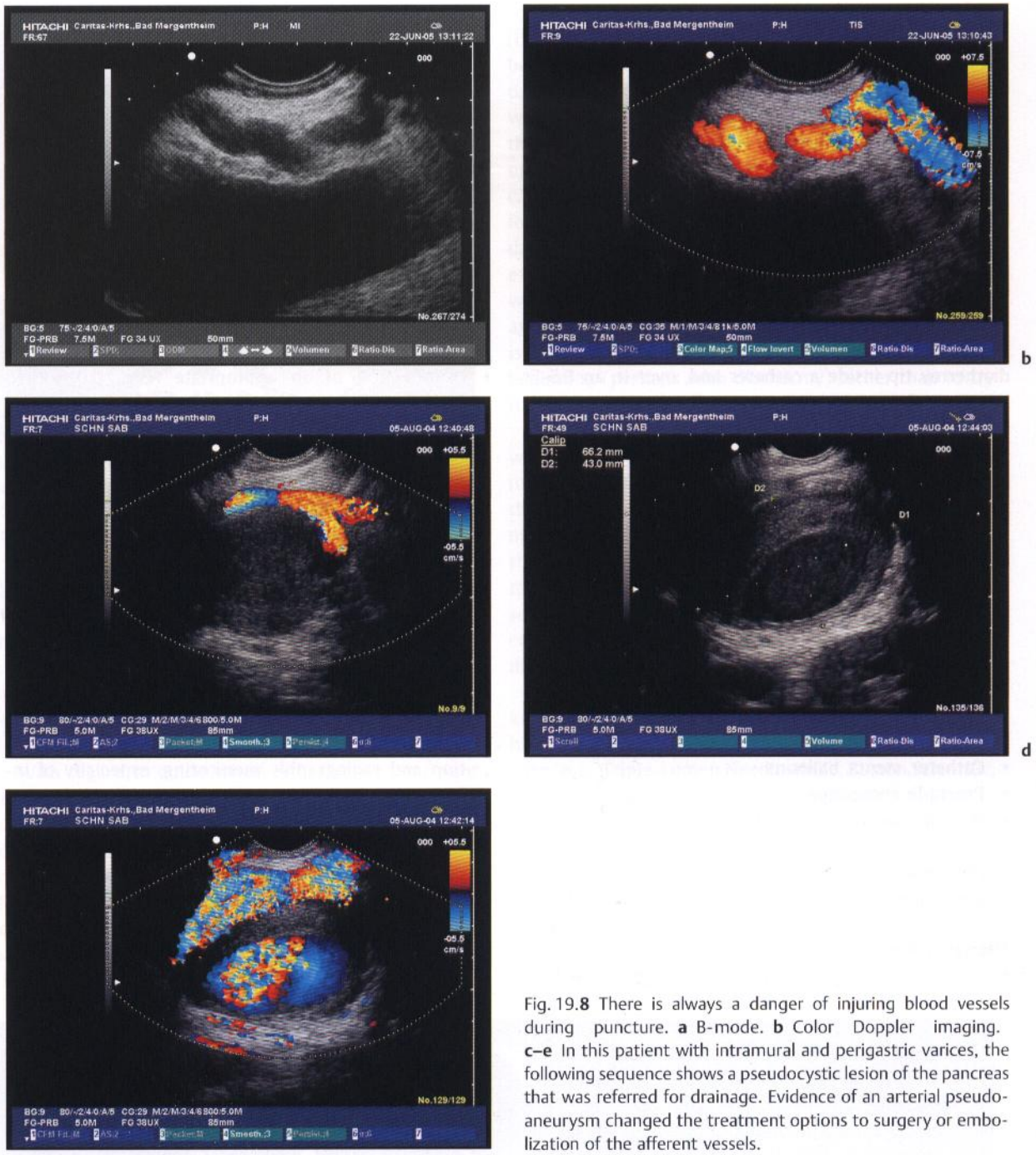


Fig. 19.**8** There is always a danger of injuring blood vessels during puncture. **a** B-mode. **b** Color Doppler imaging. **c–e** In this patient with intramural and perigastric varices, the following sequence shows a pseudocystic lesion of the pancreas that was referred for drainage. Evidence of an arterial pseudoaneurysm changed the treatment options to surgery or embolization of the afferent vessels.

only the most important comments on the endoscopic treatment of cystic retroperitoneal lesions can be offered.

- Initially, after major interventions (debridement of infected necroses, retroperitoneal endoscopy), there is often a *transient increase in CRP*. Clinically, patients improve immediately after decompression of large cysts or abscesses, and even after debridement clinical improvement usually starts at the latest on day 2.
- Infected cavities have to be cleaned up as soon as possible. In the case of abscesses, this means systematic irrigation; in the case of infected necroses, repeated debridement with careful (often very difficult) visits to the retroperitoneal recesses, which typically lie in the region to the left of the splenic hilum and retrocecally on the right (Fig. 19.**11**). At present, inadequate instruments still have to be used (baskets, balloons, irrigation catheters with

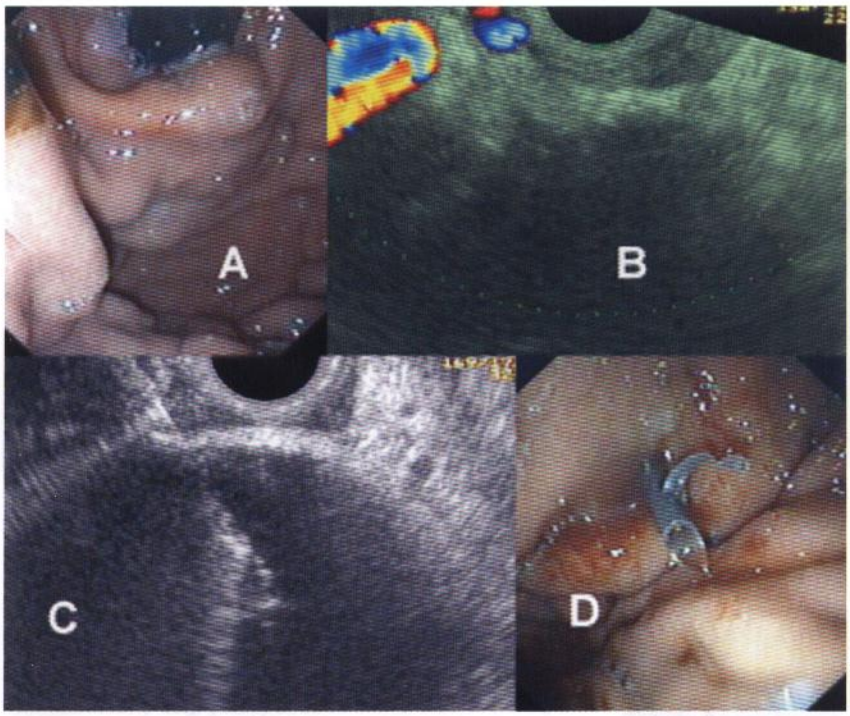


Fig. 19.**9a** Pronounced fundic varices in splenic vein thrombosis. **b, c** The Doppler image helps the varices to be avoided during EUS-guided puncture (**c**) and drainage of the large pseudocyst. **d** Placement of a plastic stent, with no hemorrhage.

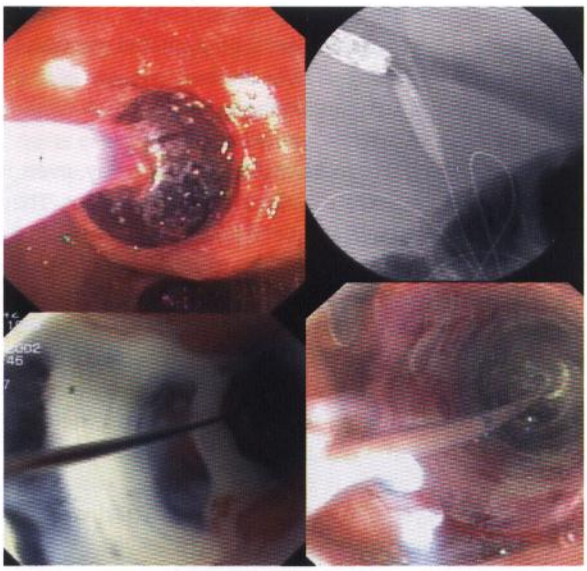


Fig. 19.**10a–d** Various aspects of transmural balloon dilation. Balloon filling, either pneumatic or with a diluted contrast agent, makes the air easier to draw out. Direct endoscopic guidance means that radiographic support is not necessarily required.

atraumatic wires). *It is essential to avoid damage to blood vessels.* Puncture of large veins involves a risk of *fatal air embolisms,* and *arterial hemorrhages* have to be treated surgically. Vessels with patent lumens (often thrombosed in necrotic zones) can be identified with EUS miniprobes (Fig. 19.**12**).

- Initially, it is better for irrigation to be too frequent rather than not frequent enough. It should be carried out with nasocystic or transmural access (PEG with a long section in the cavity), preferably several times daily, endoscopically every 2–3 days. There are no data regarding the best irrigation solution. We have used taurine in necrotic cavities, but this did not have any particularly impressive effects. For endoscopic irrigation, we otherwise use saline containing gentamicin (80 mg/500 mL) and, if necessary, a little contrast agent. Most of the solution is reaspirated. Instilling large volumes of physiological saline via nasogastric irrigation tubes leads to nausea and symptoms due to the volume, so that it has limitations.
- The *transmural window* in the stomach is usually unproblematic; it closes spontaneously so quickly that it is often difficult to locate after a few days and needs to be dilated again. The wall of the duodenum is thinner and closes somewhat more slowly. The window should be kept open until the lumen of the cavity only has a minimal image (and only on EUS or with direct contrast). If the wall of the cavity is clean and greasy coatings have been replaced by granulation tissue, retroperitoneal endoscopic procedures are no longer required. The window can be kept open for irrigation and drainage with a 10-Fr stent.
- The right time to consider that the treatment is complete and to remove all transmural place-holders is often difficult, and always has to be decided on a case-by-case basis. Sometimes the decision takes



Fig. 19.**11a–c** From the retroperitoneal cavity (**b**; stomach with air and contrast, with the endoscope in the transmural window), it is possible to reach extensive recesses that need to be irrigated and cleaned. **a** Retrocecal **c** With spontaneous connection and drainage into a sigmoid anastomosis..

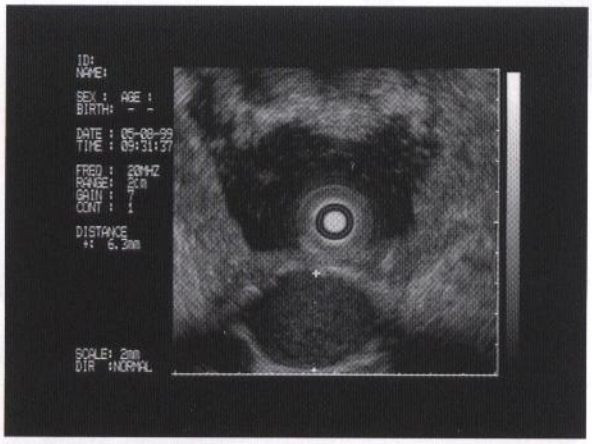


Fig. 19.**12** The miniprobe inside the retroperitoneal necrotic cavity (through a therapeutic gastroscope). A large artery (the splenic artery) is seen immediately next to the cavity.

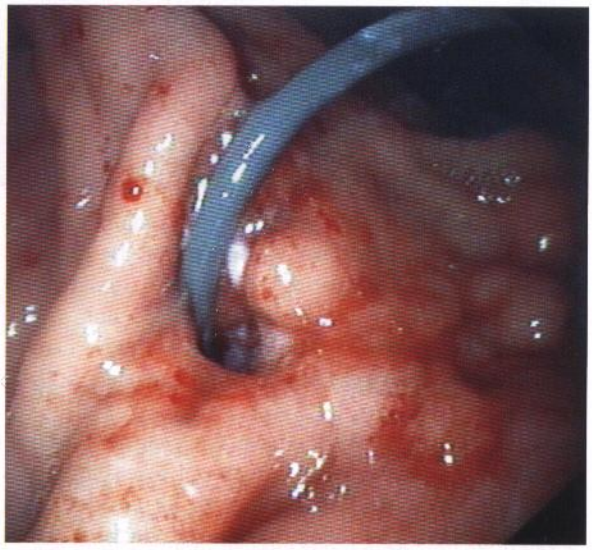


Fig. 19.**13** The transmural window in the stomach, with a suspended U stent (10-Fr Teflon, bent with hot air) in place to keep it open.

place automatically, if the cavity becomes granulated and the last place-holder detaches itself (this is not possible with the classic double-pigtail stents; we use U-shaped Teflon stents approximately 6 cm long) (Fig. 19.**13**). Treatment of uncomplicated pseudocysts is usually complete after 4 weeks.

- If the window closes earlier than expected, we wait to see what will happen even in the presence of a residual cyst. If it becomes larger and leads to symptoms and a relapse, we puncture it again.
- Patients can resume eating on the first day, even if they have large transmural windows of 2 cm. They should be rapidly mobilized and treated as outpatients as soon as possible. When pulmonary complications occur, or intensive treatment or co-morbidities make the patient bedridden and immobilized, we have observed very slow and difficult courses.
- Perioperative antibiotic prophylaxis is always administered—the duration of this can be left to the clinician's judgment. We have often found *Candida* infection in large necrotic cavities, and generally do not treat this systematically. The infection disappears with the appearance of granulation tissue.
- Perhaps the most important point is that treatment must always be carried out as part of an overall plan to restore normal pancreatic flow. The endoscopy team need to have mastered all the methods of surgical endoscopy in the pancreas. Transpapillary therapy can be carried out before or after transmural puncture, but to be successful, there has to be free transpapillary flow, as otherwise pseudocysts and

fistulas will persist. It is always necessary to weigh up whether the intended drainage effect could also be achieved, or could exclusively be achieved, with the transpapillary route alone.

- Minor injuries to the bile duct with escape of bile into the retroperitoneal cavity can be treated with transpapillary stents.
- Constructive cooperation with an experienced abdominal surgeon is always required. Pancreatic surgery is a typical field for an abdominal surgery center. Collaboration should be ensured even from the planning stage.
- If an unfavorable course starts to develop, usually because of extensive fatty tissue necroses that cannot all be reached by endoscopy (Fig. 19.**14**), with septic complications, an increase in CRP after initial improvement, and failure to improve despite technically successful drainage, one should move to an early open surgical procedure rather than defending the endoscopic approach.



Fig. 19.**14** Autopsy specimen. There is suppurating fatty tissue necrosis in the entire left kidney position. Extensive findings such as these cannot be successfully treated endoscopically.

■ Summary and Prospects

EUS with modern, Doppler-enabled, large-channel longitudinal scanners has opened up new dimensions in surgical endoscopy that have not yet been exhausted by a long way. In the field of abdominal surgery, and laparoscopic surgery in particular, there are exciting prospects especially for interventions in the retroperitoneal cavity, particularly in the pancreas and its surroundings. EUS-supported interventions, along with other endoscopic procedures, have the most important role in the treatment of the complications of acute and chronic pancreatitis. EUS is superior to all other imaging procedures in the diagnosis of the numerous possible pathoanatomical changes (Fig. 19.**15**) (Table 19.**4**).

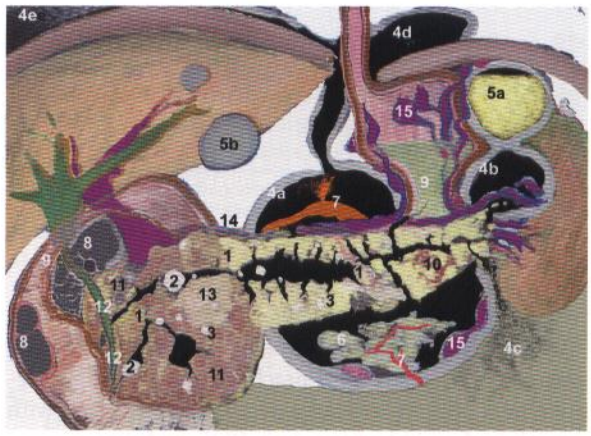


Fig. 19.**15** Morphological complications of acute and chronic pancreatitis and differential diagnoses are best assessed by endosonography (see Table 19.**4**).

Table 19.**4** Complications of pancreatitis (key to Fig. 19.**15**)

No.	Complication	Symptoms	Diagnosis	Treatment of choice
1	Stricture	Pain	ERP, EUS, US, MRCP	Stent, drainage surgery
2	Stone in duct	Pain	US, EUS, ERP, MRCP	EPT, extraction, lithotripsy, ESWL, surgery
3	Stone (calcification) in parenchyma	Pain	US, EUS, radiography	ESWL, surgery
4	Fistula to:			Always secure transpapillary flow. Endoscopic drainage transpapillary and/or transmural. Possibly percutaneous puncture. Any extrapancreatic juice can lead to tissue necroses
4a	Bursa (pseudocyst)	Size-dependent sensation of fullness, loss of appetite, pressure	US, EUS, ERP	
4b	Pseudocyst in splenic hilum	Sensation of pressure	US, EUS, ERP	
4c	Ascites	Sensation of fullness, weight gain	US, EUS, ERP	
4d	Mediastinum	None	US, EUS, ERP	
4e	Pleural effusion (usually on the left)	Dyspnea	US, radiography, EUS, ERP	

Continued ▷

Table 19.4 Complications of pancreatitis (key to Fig. 19.15) (Continued)

No.	Complication	Symptoms	Diagnosis	Treatment of choice
5	Abscess	Fever, malaise	US, EUS, ERP, CT	Endoscopic drainage transpapillary and/or transmural
5a	Infradiaphragmatic/ intrasplenic	Often with few symptoms	US, EUS, ERP, CT	
5b	Intrahepatic		US, EUS, ERP, CT	
6	Necrosis	Variable (in infection fever, loss of appetite)	US, EUS, CT	In infection, transmural debridement or surgery
7	Arteries in the necrosis (pseudoaneurysm)	Only on hemorrhage	US, EUS + Doppler	Angiography, embolization
8	Duodenal wall cysts	Usually none	Endoscopy, EUS	None, possibly incision or puncture
9	Compression of pylorus/ duodenum with retention	Nausea, loss of appetite, pain	US, EGD	Cyst drainage, pancreatic head resection
10	Focal inflammations	Pain	? EUS	Duct decompression? Elimination of the noxa?
11	Inflammatory pseudotumor of the head of the pancreas	Pain, nausea	US, EUS, CT, MRI	Pancreatic head resection
12	Bile duct stenosis by compression and fibrosis	Jaundice, pruritus, fever	US, EUS, ERC	Cyst drainage, duct stent (short term), pancreatic head resection, choledochojejunostomy
13	Pancreatic carcinoma	Nonspecific	(EUS + FNAC??)	Resection
14	Occlusion of the splenic vein by compression/ thrombosis	None	US/EUS + Doppler, MRI	Cyst drainage
15	Fundic varices, collateral circulation	None, hemorrhage	EGD	Histoacryl obliteration in hemorrhage, splenectomy

CT: computed tomography; EGD: esophagogastroduodenoscopy; EPT: endoscopic papillotomy; ERP: endoscopic retrograde pancreatography; ESWL: extracorporeal shock-wave lithotripsy; EUS: endoscopic ultrasonography; FNAC: fine-needle aspiration cytology; MRCP: magnetic resonance cholangiopancreatography; MRI: magnetic resonance imaging; US: ultrasonography.

Endoscopic transmural drainage of pseudocysts is a long-established standard practice, and endoscopic debridement of even very large necroses—in one case with resection of an ischemic spleen [60]—and direct transmural puncture of a pancreatic duct not accessible by the transpapillary route [65,66] illustrate the possibilities that are available here. Suitable specialized instruments now need to be developed for these methods, and prospective treatment protocols are even more urgently required. If possible, the techniques should be used in centers with appropriate endoscopic and open surgical expertise and collaboration. Appropriate staffing and technical resources are required for such centers, and in particular, appropriate recognition of these complex procedures within the framework of therapeutic procedures in hospitals is needed.

References

1. Black PR, Welch KJ, Eraklis AJ. Juxtapancreatic intestinal duplications with pancreatic ductal communication: a cause of pancreatitis and recurrent abdominal pain in childhood. J Pediatr Surg 1986;21:257–61.
2. Kazumori H, Sizuku T, Ueki T, Uchida Y, Yamamoto S. Lymphoepithelial cyst of the pancreas. J Gastroenterol 1997; 32:700–3.
3. Papadimitriou J. Pancreatic abscess due to infected hydatid disease. Surgery 1987;102:880–2.
4. Regan JK, Brown RD, Marrero JA, Malik P, Rosenberg F, Venu RP. Chronic pancreatitis resulting from primary hydatid disease of the pancreas: a case report and review of the literature. Gastrointest Endosc 1999;49:791–3.
5. Brugge WR, Lauwers GY, Sahani D, Fernandez-del Castillo C, Warshaw AL. Cystic neoplasms of the pancreas. N Engl J Med 2004;351:1218–26.
6. Kosmahl M, Pauser U, Peters K, Sipos B, Luttges J, Kremer B, et al. Cystic neoplasms of the pancreas and tumor-like lesions with cystic features: a review of 418 cases and a classification proposal. Virchows Arch 2004;445:168–78.
7. Levy MJ, Clain JE. Evaluation and management of cystic pancreatic tumors: emphasis on the role of EUS FNA. Clin Gastroenterol Hepatol 2004;2:639–53.
8. Seifert H, Faust D, Schmitt T, Dietrich C, Caspary W, Wehrmann T. Transmural drainage of cystic peripancreatic lesions with a new large-channel echo endoscope. Endoscopy 2001;33:1022–6.
9. Bradley EL 3rd. A clinically based classification system for acute pancreatitis. Summary of the International Symposium on Acute Pancreatitis, Atlanta, Ga, September 11 through 13, 1992. Arch Surg 1993;128:586–90.
10. Nealon WH, Walser E. Main pancreatic ductal anatomy can direct choice of modality for treating pancreatic pseudocysts (surgery versus percutaneous drainage). Ann Surg 2002;235:751–8.

11. Neoptolemos JP. Endoscopic sphincterotomy in acute gallstone pancreatitis. Br J Surg 1993;80:547–9.
12. Barthet M, Bugallo M, Moreira LS, Bastid C, Sastre B, Sahel J. Management of cysts and pseudocysts complicating chronic pancreatitis: a retrospective study of 143 patients. Gastroenterol Clin Biol 1993;17:270–6.
13. Nealon WH, Townsend CM Jr, Thompson JC. Preoperative endoscopic retrograde cholangiopancreatography (ERCP) in patients with pancreatic pseudocyst associated with resolving acute and chronic pancreatitis. Ann Surg 1989;209: 532–8.
14. Stolte M. Chronische Pankreatitis. Erlangen, Germany: Perimed, 1984.
15. Ammann RW, Akovbiantz A, Largiader F, Schueler G. Course and outcome of chronic pancreatitis: longitudinal study of a mixed medical-surgical series of 245 patients. Gastroenterology 1984;86(5 Pt 1):820–8.
16. Lankisch PG, Burchard-Reckert S, Petersen M, Lehnick D, Schirren CA, Kohler H, et al. Morbidity and mortality in 602 patients with acute pancreatitis seen between the years 1980–1994. Z Gastroenterol 1996;34(6):371–7.
17. Siegelman SS, Copeland BE, Saba GP, Cameron JL, Sanders RC, Zerhouni EA. CT of fluid collections associated with pancreatitis. AJR Am J Roentgenol 1980;134:1121–32.
18. Allardyce DB. Incidence of necrotizing pancreatitis and factors related to mortality. Am J Surg 1987;154:295–9.
19. Bradley EL, Allen K. A prospective longitudinal study of observation versus surgical intervention in the management of necrotizing pancreatitis. Am J Surg 1991;161:19–24.
20. Imrie CW, Buist LJ, Shearer MG. Importance of cause in the outcome of pancreatic pseudocysts. Am J Surg 1988;156(3 Pt 1):159–62.
21. Beger HG, Schlosser W, Siech M, Poch B. The surgical management of chronic pancreatitis: duodenum-preserving pancreatectomy. Adv Surg 1999;32:87–104.
22. Izbicki JR, Bloechle C, Broering DC, Knoefel WT, Kuechler T, Broelsch CE. Extended drainage versus resection in surgery for chronic pancreatitis: a prospective randomized trial comparing the longitudinal pancreaticojejunostomy combined with local pancreatic head excision with the pylorus-preserving pancreatoduodenectomy. Ann Surg 1998;228: 771–9.
23. Nealon WH, Thompson JC. Progressive loss of pancreatic function in chronic pancreatitis is delayed by main pancreatic duct decompression: a longitudinal prospective analysis of the modified Puestow procedure. Ann Surg 1993; 217:458–66.
24. Rösch T, Daniel S, Scholz M, Huibregtse K, Smits M, Schneider T, et al. Endoscopic treatment of chronic pancreatitis: a multicenter study of 1000 patients with long-term follow-up. Endoscopy 2002;34:765–71.
25. Andersson R, Janzon M, Sundberg I, Bengmark S. Management of pancreatic pseudocysts. Br J Surg 1989;76:550–2.
26. Aranha GV, Prinz RA, Esguerra AC, Greenlee HB. The nature and course of cystic pancreatic lesions diagnosed by ultrasound. Arch Surg 1983;118:486–8.
27. Czaja AJ, Fisher M, Marin GA. Spontaneous resolution of pancreatic masses (pseudocysts?): development and disappearance after acute alcoholic pancreatitis. Arch Intern Med 1975;135:558–62.
28. Yeo CJ, Bastidas JA, Lynch-Nyhan A, Fishman EK, Zinner MJ, Cameron JL. The natural history of pancreatic pseudocysts documented by computed tomography. Surg Gynecol Obstet 1990;170:411–7.
29. Vitas GJ, Sarr MG. Selected management of pancreatic pseudocysts: operative versus expectant management. Surgery 1992;111:123–30.
30. Sankaran S, Walt AJ. The natural and unnatural history of pancreatic pseudocysts. Br J Surg 1975;62:37–44.
31. Seiler CA, Boss MA, Czerniak A, Gertsch P, Berne TV, Blumgart L. Complications of chronic pancreatitis. Dig Surg 1997;14:540–5.
32. Kolars JC, Allen MO, Ansel H, Silvis SE, Vennes JA. Pancreatic pseudocysts: clinical and endoscopic experience. Am J Gastroenterol 1989;84:259–64.
33. Bradley EL, Clements JL, Jr., Gonzalez AC. The natural history of pancreatic pseudocysts: a unified concept of management. Am J Surg 1979;137:135–41.
34. Warshaw A. Pain in chronic pancreatitis: patients, patience, and the impatient surgeon [editorial]. Gastroenterology 1984;86(5 Pt 1):987–9.
35. Bozeman N. Removal of a cyst of the pancreas weighing twenty and one-half pounds. Med Rec 1882;21:46–7.
36. Gussenbauer C. Zur operativen Behandlung der Pankreas-Cysten. Arch Klin Chir 1883;29:355–64.
37. Jedlica R. Eine neue Operationsmethode der Pankreascysten (Pancreatogastrostomie). Zentralbl Chir 1923;50:132.
38. Hahn O. Beitrag zur Behandlung der Pankreasfisteln. Klin Chir 1928;143(73):73.
39. Jurasz A. Zur Frage der operativen Behandlung der Pankreascysten. Arch Klin Chir 1931;164:272–9.
40. Jimenez RE, Fernandez-Del Castillo C, Rattner DW, Warshaw AL. Pylorus-preserving pancreaticoduodenectomy in the treatment of chronic pancreatitis. World J Surg 2003;27: 1211–6.
41. Witzigmann H, Max D, Uhlmann D, Geissler F, Schwarz R, Ludwig S, et al. Outcome after duodenum-preserving pancreatic head resection is improved compared with classic Whipple procedure in the treatment of chronic pancreatitis. Surgery 2003;134:53–62.
42. Seifert H, Dietrich C, Schmitt T, Caspary W, Wehrmann T. Endoscopic ultrasound-guided one-step transmural drainage of cystic abdominal lesions with a large-channel echo endoscope. Endoscopy 2000;32:255–9.
43. Nealon WH, Walser E. Duct drainage alone is sufficient in the operative management of pancreatic pseudocyst in patients with chronic pancreatitis. Ann Surg 2003;237: 614–20.
44. Dite P, Ruzicka M, Zboril V, Novotny I. A prospective, randomized trial comparing endoscopic and surgical therapy for chronic pancreatitis. Endoscopy 2003;35:553–8.
45. Malka D, Hammel P, Sauvanet A, Rufat P, O'Toole D, Bardet P, et al. Risk factors for diabetes mellitus in chronic pancreatitis. Gastroenterology 2000;119:1324–32.
46. Bradley EL 3rd. Operative vs non-operative management in sterile necrotizing pancreatitis. HPB Surg 1997;10:188–91.
47. Rattner DW, Legermate DA, Lee MJ, Mueller PR, Warshaw AL. Early surgical debridement of symptomatic pancreatic necrosis is beneficial irrespective of infection. Am J Surg 1992;163:105–9.
48. Fernandez-del Castillo C, Rattner DW, Makary MA, Mostafavi A, McGrath D, Warshaw AL. Debridement and closed packing for the treatment of necrotizing pancreatitis. Ann Surg 1998;228:676–84.
49. Hancke S, Pedersen JF. Percutaneous puncture of pancreatic cysts guided by ultrasound. Surg Gynecol Obstet 1976;142: 551–2.

50. Van Sonnenberg E, Wittich GR, Casola G, Brannigan TC, Karnel F, Stabile BE, et al. Percutaneous drainage of infected and noninfected pancreatic pseudocysts: experience in 101 cases. Radiology 1989;170(3 Pt 1):757–61.
51. Adams DB, Anderson MC. Percutaneous catheter drainage compared with internal drainage in the management of pancreatic pseudocyst. Ann Surg 1992;215:571–6.
52. Van Sonnenberg E, Wittich GR, Chon KS, HB DA, Casola G, Easter D, et al. Percutaneous radiologic drainage of pancreatic abscesses. AJR Am J Roentgenol 1997;168:979–84.
53. Rogers BH, Cicurel NJ, Seed RW. Transgastric needle aspiration of pancreatic pseudocyst through an endoscope. Gastrointest Endosc 1975;21:133–4.
54. Kozarek RA, Brayko CM, Harlan J, Sanowski RA, Cintora I, Kovac A. Endoscopic drainage of pancreatic pseudocysts. Gastrointest Endosc 1985;31:322–7.
55. Sahel J, Bastid C, Pellat B, Schurgers P, Sarles H. Endoscopic cystoduodenostomy of cysts of chronic calcifying pancreatitis: a report of 20 cases. Pancreas 1987;2:447–53.
56. Cremer M, Devière J, Engelholm L. Endoscopic management of cysts and pseudocysts in chronic pancreatitis: long-term follow-up after 7 years of experience. Gastrointestinal Endoscopy 1989;35:1–9.
57. Beckingham IJ, Krige JE, Bornman PC, Terblanche J. Long term outcome of endoscopic drainage of pancreatic pseudocysts. Am J Gastroenterol 1999;94:71–4.
58. Baron TH, Harewood GC, Morgan DE, Yates MR. Outcome differences after endoscopic drainage of pancreatic necrosis, acute pancreatic pseudocysts, and chronic pancreatic pseudocysts. Gastrointest Endosc 2002;56:7–17.
59. Seewald S, Groth S, Omar S, Imazu H, Seitz U, de Weerth A, et al. Aggressive endoscopic therapy for pancreatic necrosis and pancreatic abscess: a new safe and effective treatment algorithm (videos). Gastrointest Endosc 2005;62:92–100.
60. Seifert H, Wehrmann T, Schmitt T, Zeuzem S, Caspary WF. Retroperitoneal endoscopic debridement for infected peripancreatic necrosis. Lancet 2000;356:653–5.
61. Isenmann R, Runzi M, Kron M, Kahl S, Kraus D, Jung N, et al. Prophylactic antibiotic treatment in patients with predicted severe acute pancreatitis: a placebo-controlled, double-blind trial. Gastroenterology 2004;126:997–1004.
62. Giovannini M, Bernardini D, Seitz JF. Cystogastrotomy entirely performed under endosonography guidance for pancreatic pseudocyst: results in six patients. Gastrointest Endosc 1998;48:200–3.
63. Giovannini M, Pesenti C, Rolland AL, Moutardier V, Delpero JR. Endoscopic ultrasound-guided drainage of pancreatic pseudocysts or pancreatic abscesses using a therapeutic echo endoscope. Endoscopy 2001;33:473–7.
64. Vilmann P, Hancke S, Pless T, Schell-Hincke JD, Henriksen FW. One-step endosonography-guided drainage of a pancreatic pseudocyst: a new technique of stent delivery through the echo endoscope. Endoscopy 1998;30:730–3.
65. Burmester E, Niehaus J, Leineweber T, Huetteroth T. EUS-cholangio-drainage of the bile duct: report of 4 cases. Gastrointest Endosc 2003;57:246–51.
66. Mallery S, Matlock J, Freeman ML. EUS-guided rendezvous drainage of obstructed biliary and pancreatic ducts: report of 6 cases. Gastrointest Endosc 2004;59:100–7.

20 Endosonography of the Hepatobiliary System

C.F. Dietrich, M. Hocke, H. Seifert

Definitions

The term "cholelithiasis" refers to the presence of gallstones in the extrahepatic biliary tract. Depending on the location of the concrement, a further distinction is made between cholecystolithiasis and choledocholithiasis. A combination of the two conditions can be expected in 15% of the patients.

Reliability of Examination Methods for Detecting Gallstones

The reported accuracy of examination methods is measured using four indices: sensitivity, specificity, and positive and negative predictive values (Table 20.**1**). Cholecystolithiasis can be detected by transabdominal ultrasound with a high level of sensitivity (Fig. 20.**1**, Table 20.**2**) [1–7], but choledocholithiasis is more difficult do diagnose transabdominally (Table 20.**3**) [8–16]. Tables 20.**4**–20.**9** [8,9,11–13,16,17–44] present a review of the literature for the different methods used.

Choledocholithiasis can be detected with conventional endoscopic ultrasonography (EUS), which is routinely used as a diagnostic procedure, especially in France. However, many clinical centers do not use EUS for routine diagnosis, as it does not allow therapeutic interventions and involves a need to switch ultrasound machines. Endoscopic retrograde cholangiopancreatography (ERCP) is currently regarded as the diagnostic gold standard, with a reported success rate of 90–96%. However, the value of diagnostic ERCP may have been considerably overestimated, as the rate of correctly diagnosed choledocholithiasis appears to be much lower—particularly since small gallstones (< 3 mm in diameter) with normal or even dilated bile ducts are easily overlooked even in ERCP.

A combination of ERCP with endoscopic sphincterotomy (EST) is the treatment of choice in patients with choledocholithiasis, but this is an invasive technique that is associated with a significant risk of complications for the patient. With regard to the potential complications of the procedure, a distinction needs to be made between early and late complications. Typical early complications include pancreatitis, cholangitis, cholecystitis, bleeding, and perforation. In addition, EST leads to permanent dysfunction of the sphincter of

Table 20.**1** Definition of terms used in assessing the accuracy of diagnostic tests

Term	Definition
Sensitivity (%)	True positives/(true-positives + false-negatives)
Specificity (%)	True-negatives/(true-negatives + false-positives)
Positive predictive value (PPV) (%)	True-positives/total positives
Negative predictive value NPV (%)	True-negatives/total negatives
Accuracy (%)	True-positives + true-negatives)/ total number
Youden index (%)	Sensitivity + specificity – 1

Table 20.**2** Reported detection rates for cholecystolithiasis using transabdominal ultrasonography

Ref.	Sensitivity(%)	Specificity(%)
[1]	98	94–98
[2]	70	100
[3]	97	92
[4]	91	99
[5]	98	–
[6]	91	100
[7]	87	93

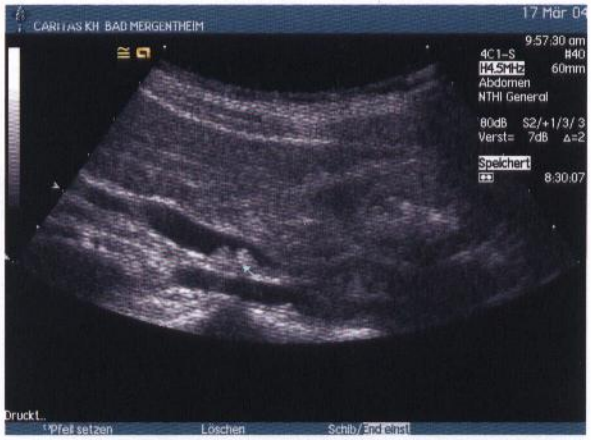


Fig. 20.**1** Transabdominal imaging of choledocholithiasis. The lack of acoustic shadowing is a typical phenomenon in primary choledocholithiasis.

Table 20.3 Detection of choledocholithiasis using transabdominal ultrasonography: review of the literature

Ref.	Patients (n)	Sensitivity (%)	Specificity (%)	NPV (%)	PPV (%)	Gold standard
[8]	62	25	100	56	100	ERCP with or without EST or IOC
[9]	52	80	94	–	–	ERCP/EST or surgical exploration
[10]	–	38	100	–	–	No results
[11]	35	47	90	–	–	ERCP/EST
[12]	142	63	95	–	–	ERCP with or without EST or surgical exploration
[13]	36	50	100	74	100	ERCP/EST
[14]	50	100	97	92	100	ERCP/PTC
[15]	132	68	–	–	–	ERCP/EST
[16]	29	38	100	–	–	ERCP

ERCP: endoscopic retrograde cholangiopancreatography; EST: endoscopic sphincterotomy; IOC: intraoperative cholangiography; NPV: negative predictive value; PPV: positive predictive value; PTC: percutaneous transhepatic cholangiography.

Table 20.4 Detection of choledocholithiasis with computed tomography: review of the literature

Ref.	Patients (n)	Sensitivity (%)	Specificity (%)	Gold standard
[12]	155	71	97	ERCP and EST
[17]	220	23–37	–	ERCP
[18]	82	86	98	ERCP
[19] *	101	96	–	Direct cholangiography
[19]	101	60	–	Direct cholangiography
[20]	40	80	100	ERCP
[21]	80	89	98	CT cholangiography
[22]	51	88	97	ERCP
[23]	52	85	88	ERCP
[11]	35	47	95	ERCP with or without EST

Helical CT cholangiography. CT: computed tomography; ERCP: endoscopic retrograde cholangiopancreatography; EST: endoscopic sphincterotomy.

Table 20.5 Detection of choledocholithiasis using endoscopic ultrasonography: review of the literature

Ref.	Patients (n)	Sensitivity (%)	Specificity (%)	NPV (%)	PPV (%)	Gold standard
[8]	62	97	100	97	100	ERCP with or without EST
[9]	52	100	100	–	–	ERCP and EST or surgical exploration
[24]	50	100	97	100	92	Surgical exploration
[25]	32	100	95	100	91	ERCP and EST
[26]	20	75	100	–	–	Surgical exploration
[27]	50	97	77	–	–	ERCP with or without EST
[28]	240	85	93	96	75	Surgical exploration
[29]	422	95	96	96	95	Surgical exploration
[23]	52	91	100	–	–	ERCP with or without EST
[30]	119	93	97	88	98	ERCP and EST
[11]	35	100	100	–	–	ERCP and EST
[12]	155	96	100	–	–	ERCP with or without EST or surgical exploration
[31]	100	97	98	–	–	ERCP and EST
[13]	36	91	100	95	100	ERCP and EST
[32]	50	88	96	–	–	ERCP and EST

ERCP: endoscopic retrograde cholangiopancreatography; EST: endoscopic sphincterotomy; NPV: negative predictive value; PPV: positive predictive value.

Table 20.**6** Detection of choledocholithiasis using magnetic resonance cholangiopancreatography (MRCP): review of the literature

Ref.	Patients (n)	Sensitivity (%)	Specificity (%)	NPV (%)	PPV (%)	Gold standard
[25]	43	100	73	100	63	ERCP and EST
[33]	146	98	89	99	84	ERCP or surgical exploration
[34]	28	40	96	88	66	ERCP
[35]	74	100	97	–	–	ERCP
[36]	35	100	50	100	87	ERCP and EST
[37]	50	95	96	–	–	ERCP, IOC, or surgical exploration
[38]	133	84	96	93	91	ERCP
[16]	29	91	98	–	–	ERCP

ERCP: endoscopic retrograde cholangiopancreatography; EST: endoscopic sphincterotomy; IOC: intraoperative cholangiography; NPV: negative predictive value; PPV: positive predictive value.

Table 20.**7** Detection of choledocholithiasis using intraductal ultrasonography (IDUS)

Ref.	Patients (n)	Accuracy (%)	Sensitivity (%)	Specificity (%)	NPV (%)	PPV (%)	Gold standard
[39]	31	97	–	–	–	–	EST [3] or surgical exploration
[40]	81	95	–	–	–	–	EST [3]
[41]	65	97	100	67	–	–	EST [3]
[42]	62	97 [1]/87 [2]	–	–	–	–	EST [3]

EST: endoscopic sphincterotomy; NPV: negative predictive value; PPV: positive predictive value.
1. ERCP with IDUS.
2. ERCP without IDUS.
3. Endoscopic sphincterotomy.

Table 20.**8** Comparison of the diagnostic accuracy of endoscopic ultrasonography and other imaging techniques in relation to the detection of choledocholithiasis

Ref.	Patients (n)	EUS (%)	US (%)	CT (%)	ERCP (%)	MRCP (%)
[9]	52	100	80	83	–	–
[25]	43	97	–	–	–	82
[34]	30	89	–	–	–	61
[23]	52	94	–	86	–	–
[13]	36	97	83	–	89	–
[41]	65	97	–	–	94	–
[31]	100	98	–	–	96	–

CT: computed tomography; ERCP: endoscopic retrograde cholangiopancreatography; EUS: endoscopic ultrasonography; MRCP: magnetic resonance cholangiopancreatography; US: ultrasonography.

Table 20.**9** Detection of choledocholithiasis using endoscopic retrograde cholangiopancreatography (ERCP). Endoscopic sphincterotomy (EST) was used as the gold standard

Ref.	Patients (n)	Sensitivity (%)	Specificity (%)	NPV (%)	PPV (%)
[30]	119	89	100	83	100
[43]	–	84–89	97–100	88	100
[11]	35	100	–	–	–
[41]	65	100	67	–	–
[17]	220	67–81	–	–	–
[31]	100	97	–	–	–
[44] *	72	90	98	–	–
[13]	36	92	–	–	–

NPV: negative predictive value; PPV: positive predictive value. * The gold standard used was intraoperative cholangiography.

Table 20.**10** Incidence of complications in endoscopic retrograde cholangiopancreatography (ERCP) and endoscopic sphincterotomy (EST)

Ref.	Procedures (n)	Total complication rate (%)	Pancreatitis (%)	Cholangitis (%)	Bacterial complications (%)
[45]	2444	5	2	1	–
[46]	590	2–9	2–4	1	–
[47]	118	5	3	–	3
[48]	2769	4	1	1	–
[49]	51	16	4	–	–
[50	32	30	12	3	–
[51]	50	4	2	–	–
[52]	80	6	–	–	–
[53]	238	7	3	1	–
[54]	2347	10	5	–	–
[55]	180	12	8	1	–

All of the studies included diagnostic and therapeutic ERCP procedures.

Table 20.**11** Incidence of complications in endoscopic retrograde cholangiopancreatography (ERCP) and endoscopic sphincterotomy (EST)

Ref.	Procedures (n)	Bleeding (%)	Perforation (%)	Death (%)	Other (%)
[45]	2444	1	1	0	1
[46]	590	0 –3	1–2	0 - 1	–
[47]	118	–	–	–	–
[48]	2769	1	1	0	1
[49]	51	4	8	–	–
[50]	32	9	6	–	–
[51]	50	2	–	–	–
[52]	80	–	–	–	–
[53]	238	2	1	–	–
[54]	2347	2	–	0,5	–
[55]	180	–	1	–	–

All of the studies included diagnostic and therapeutic ERCP procedures.

Table 20.**12** Diagnosis of choledocholithiasis by endosonography

Ref.	Patients (n)	Sensitivity (%)	Specificity (%)	NPV (%)	PPV (%)	Gold standard
[8]	62	97	100	97	100	ERCP with or without EST
[9]	52	100	100	–	–	ERCP and EST or surgical exploration
[24]	50	100	97	100	92	Surgical exploration
[25]	32	100	95	100	91	ERCP and EST
[27]	50	97	77	–	–	ERCP with or without EST
[28]	240	85	93	96	75	Surgical exploration
[29]	422	95	96	96	95	Surgical exploration
[23]	52	91	100	–	–	ERCP with or without EST
[30]	119	93	97	88	98	ERCP and EST
[11]	35	100	100	–	–	ERCP and EST
[12]	155	96	100	–	–	ERCP with or without EST or surgical exploration
[31]	100	97	98	–	–	ERCP and EST
[13]	36	91	100	95	100	ERCP and EST
[32]	50	88	96	–	–	ERCP and EST

ERCP: endoscopic retrograde cholangiopancreatography; EST: endoscopic sphincterotomy; NPV: negative predictive value; PPV: positive predictive value.

Oddi. Late complications include recurrent gallstones (3–20%) and papillary stenosis (2–6%). The total rate of complications is reported to be in the range of 2–30%. A review of the literature on the incidence of various complications in ERCP and EST is presented in Tables 20.**10** and 20.**11** [45–55].

In addition to the significant risk of complications, there are many differential diagnoses of choledocholithiasis that require neither ERCP for diagnosis nor EST for therapy. When this is borne in mind, initial use of a reliable and less invasive method of diagnosis, associated with a lower rate of complications, would be advantageous in order to confirm choledocholithiasis and establish an adequate indication for EST. Conventional endosonography meets these requirements and facilitates reliable diagnosis of choledocholithiasis before more invasive procedures are carried out. Table 20.**12** presents a review of the literature [8, 9, 11–13, 23–25, 27–32].

EUS provides excellent visualization of the proximal and distal common bile duct (Fig. 20.**2**), and of the ampulla and left intrahepatic bile ducts, with a very high sensitivity for even very small stones. In 96% of the patients, the entire length of the common bile duct



a



b

Fig. 20.**2a** A normal duodenal papilla (between the markers) in routine conditions. **b** In a few patients, the orifice of the common hepatic bile duct and pancreatic duct can be imaged separately. The common bile duct orifice (1) and the pancreatic duct orifice (2) are indicated here.

can be visualized, but imaging of the bile ducts of the right lobe of the liver and the hepatic hilum is more difficult. The results of endosonography have been shown to be independent of the size of the concrement or the diameter of the bile duct, and gallstones smaller than 2 mm have been detected even in dilated bile ducts. Another major advantage of endosonography is the very low rates of morbidity and mortality associated with the procedure, and there have been no reports of severe complications. In summary, conventional EUS is a safe, reliable, and minimally invasive method of detecting choledocholithiasis.

The relevance of endosonography for diagnosing cholecystolithiasis before cholecystectomy has yet to be examined and can only be determined in large prospective studies including sufficient numbers of patients with and without cholecystolithiasis. Unexpected diagnostic results, such as benign papillary stenosis and anatomic variations in the bile duct system, need to be taken into account in advance.



Fig. 20.**3** Imaging of choledocholithiasis using extraductal ultrasound (EDUS). Ideally, minuscule concrements only a few millimeters in size (microlithiasis) can be identified even in bile ducts of normal width. Concrements of this type may not be invisible on endoscopic retrograde cholangiopancreatography.

■ Miniprobe EUS and Extraductal Ultrasound

EUS miniprobes introduced through the working channel of a regular endoscope can be used in the same way as ordinary endoscopy accessories such as biopsy forceps. With a penetration depth of about 2 cm, they allow visualization of considerable areas of important anatomy around the upper gastrointestinal tract. Catheter probes may be able to cover most of the indications for conventional diagnostic EUS; this would certainly apply to pathological structures in the intestinal wall. Interventional procedures may be reserved for longitudinal scanners with stiff shafts and wide working channels.

The distal common bile duct (CBD), running from the major duodenal papilla up to the liver just behind the duodenal wall, is certainly within the reach of diagnostic miniprobe EUS. Extraductal ultrasonography (EDUS) of the distal CBD for the detection of choledocholithiasis, with the miniprobe in a duodenal position, was investigated in a prospective study including 119 patients with suspected choledocholithiasis [30]. The probe was introduced through a duodenoscope and first placed on the duodenal papilla to image the sphincter, and then moved slightly more cranially to scan the distal CBD and pancreatic duct. A diagnosis of choledocholithiasis was made when hyperechoic structures not adherent to the ductal wall were detected, with or without acoustic shadowing (Fig. 20.**3**). ERCP with EST and pull-through of a Dormia basket were used as the gold standard. The EDUS diagnosis of choledocholithiasis was confirmed in 33 of 34 patients (97%). As expected, EDUS

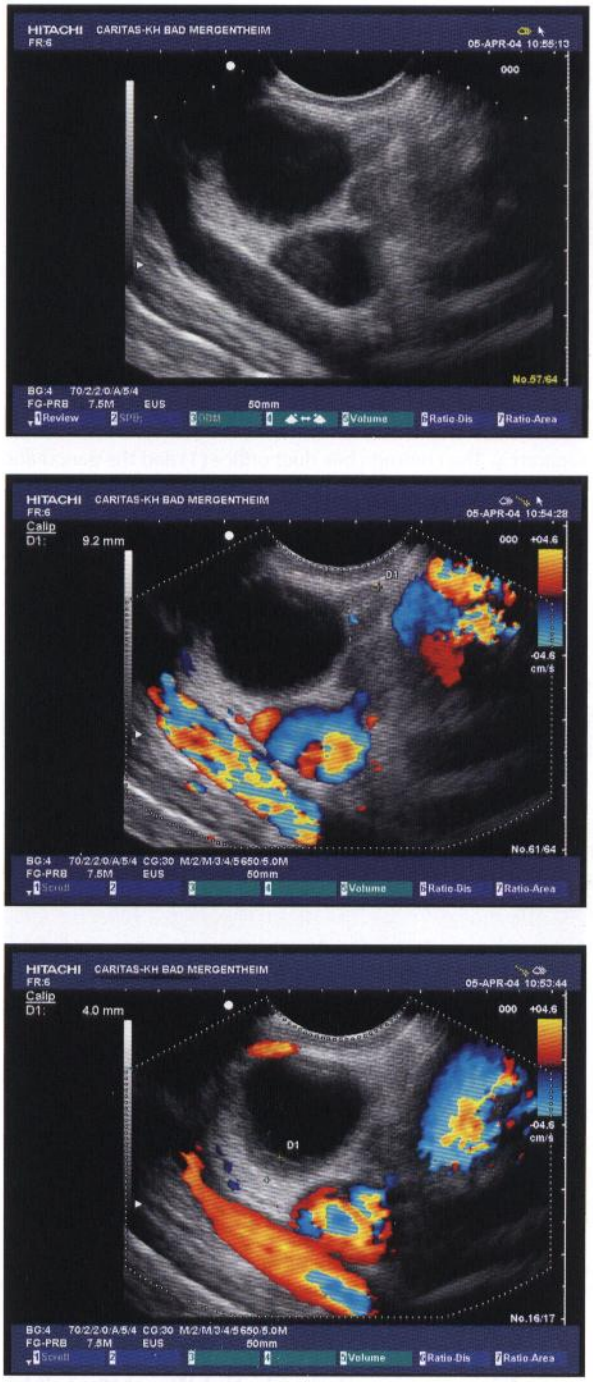


Fig. 20.**4a** Conventional endosonographic imaging of an adenoma in the papilla of Vater. **b** The use of color duplex ultrasonography has been shown to facilitate correct detection of ductal structures. Blood vessels are detected within the adenoma here (between the markers). **c** It is important to remember that adenomas can develop multilocularly, especially in the extrahepatic bile ducts (between the markers here).

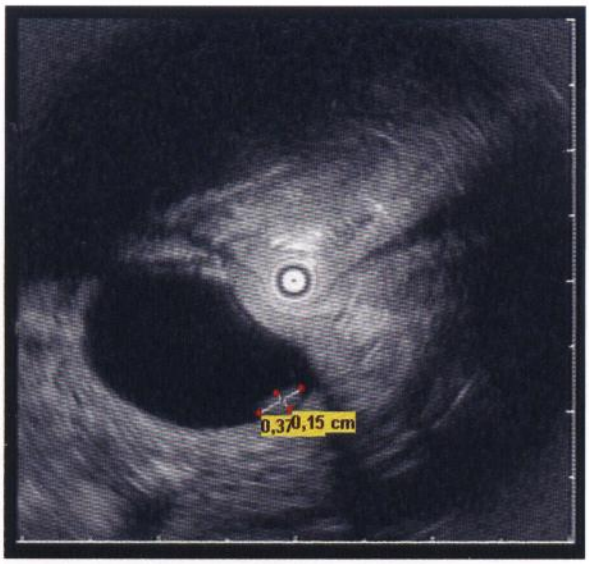
failed to detect peripheral lesions. The study shows that EDUS can reliably detect pathological lesions in the distal common bile duct, particularly small concrements, and can therefore avoid the need for sphincterotomy, with the associated complications.

Additional diagnostic applications of EDUS for the duodenal papilla were evaluated in another prospective study including 150 patients with similar diagnostic issues and methods. It was shown that in addition to choledocholithiasis, chronic pancreatitis, adenomas of the papilla, adenomas of the bile duct, and primary sclerosing cholangitis (PSC) were capable of being detected reliably using this method [57]. In summary, EUS or EDUS is indicated before cholecystectomy, especially in patients who are at intermediate risk, and these techniques appear to be superior to other diagnostic methods. In addition, EUS is definitely indicated for staging of carcinoma of the ampulla of Vater. EUS is less important in the staging of cholangiocellular carcinoma than it is for pathologic processes in the papilla. Intraductal ultrasonography (IDUS) has diagnostic value particularly in stenoses of unknown origin in the common bile duct.

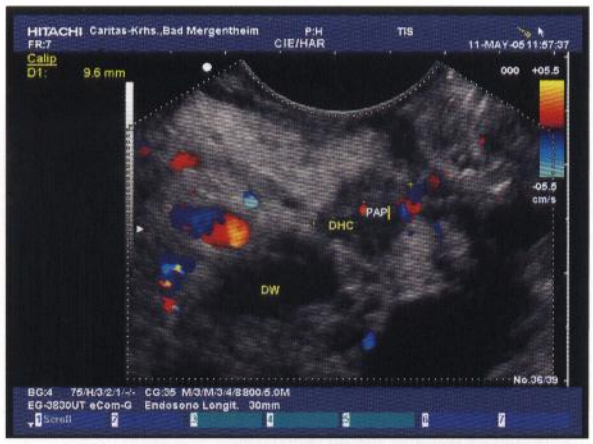
When evaluating tumors of the bile ducts, it needs to be borne in mind that tumors in the immediate vicinity of the papilla are much easier to diagnose and classify than intrahepatic tumors. Klatskin tumors that are located more proximally can often not be classified adequately with endosonography. In the case of bile duct carcinoma, lymph-node metastases are not associated with the T stage in the TNM classification, and the accuracy of diagnosis of lymph-node infiltration is reported to be 50–60%. Adequate comparisons between conventional endosonography and intraductal ultrasound have not yet been reported, although several case reports are available. What is known as the "common channel" can be visualized well with endosonography.

■ Adenoma and Carcinoma of the Papilla of Vater

In the same way as carcinomas of the pancreas, tumors of the papilla of Vater are classified using the TNM staging system. T1 tumors are confined to the papilla, without infiltration of the duodenal wall. T2 is characterized by invasion of the duodenal wall no deeper than the duodenal muscularis propria. T3 means that invasion of the pancreas is less than 2 cm; T4 includes tumors invading the pancreas by more than 2 cm or invading neighboring vessels or organs. The N classification categorizes the presence (N1) or absence (N0) of pathological lymph nodes. More sophisticated and differentiated staging systems have not proved helpful. It is not possible to distinguish between a T1 papillary carcinoma and an adenoma using endosonography (Figs. 20.**4**, 20.**5**); histological assessment is required for this crucial differ-

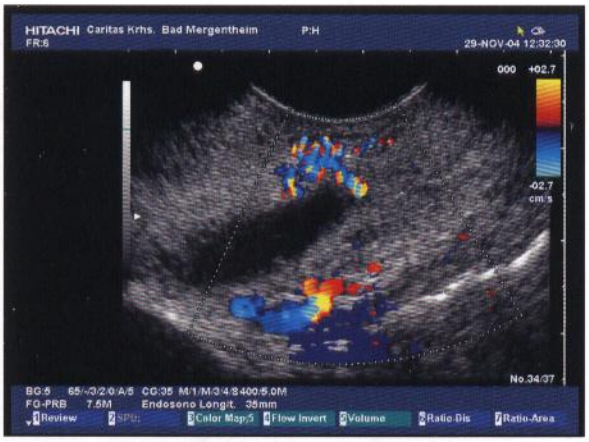


a



b

Fig. 20.**5a, b** Adenoma of the papilla, visualized with EUS. **c** In contrast to miniprobe ultrasonography, the conventional technique allows imaging of blood vessels with color duplex ultrasonography. The beginning of the common hepatic duct (DHC) and pancreatic duct (DW) are also shown. PAP: papilla.



a



b

Fig. 20.**6** Rare pathological conditions in the papilla. **a** The papilla of Vater with inflammation (papillitis). **b** Color Doppler imaging showing aerobilia after endoscopic retrograde cholangiopancreatography.

entiation. Multiloculated tumors have to be taken into account. It is also difficult with EUS to distinguish between inflammatory alterations after the expulsion of gallstones or after endoscopic sphincterotomy and malignant processes. The differential diagnosis of papillitis or adenomyomatosis of the bile duct with EDUS is equally difficult.

■ EUS of the Papillary Region, Adenomyomatosis

The papilla of Vater is a smooth muscle containing an outlet system for the common bile duct and the main pancreatic duct, which frequently (but not always) join to form a single orifice. Specifically, the papilla consists of the circular muscle of the common bile duct and an additional circular muscle that encloses the two ducts. The normal size of the major duodenal papilla is 10 × 5 mm. It can be visualized endosonographically (Figs. 20.**2**, 20.**6**).

There can be many causes of dilation of the common bile duct as a sign of biliary obstruction. In addition to cholangiolithiasis, benign and malignant neoplasms such as adenomas, neuroendocrine tumors, or adenocarcinomas of the papilla are possible causes. A less well known, but in our experience not uncommon, condition is what is known as stenotic papillitis or adenomyomatosis of the papilla (Fig. 20.**7**). The prevalence of this condition is frequently underestimated and was approximately 50% in older autopsy studies. In a more recent study, Elek and colleagues [56] describe an inflammatory alteration of the papilla as the reason for biliary obstruction in 36% of their patients. Adenomatous hyperplasia and adenomyomatosis were observed in 5% and 7% of

Table 20.**13** The Milwaukee classification of sphincter of Oddi dysfunction

Stage	Biliary pain	Elevated liver function tests	Bile duct dilation > 12 mm
I	+	+	+
II	+	–	+
III	+	–	–

Table 20.**14** Criteria for adenomyomatosis

- Concentric thickening of the papillary region
- Mixed echogenic, predominantly echodense alterations in the papilla
- Smooth borders of the tumor
- Preserved layers of the duodenal wall
- Convex growth of the tumor
- As the most important criterion, a funnel-shaped narrowing and filiform discharge of the common bile duct into the papilla. Typical findings are illustrated in Fig. 20.**7**

Table 20.**15** Criteria for noninvasive neoplasm of the papilla (e.g., adenoma, neuroendocrine tumor)

- Intraluminal growth
- Preserved duodenal wall layers
- Homogeneous structure
- Narrowing of the common bile duct due to compression
- Proximal ductal dilation
- Size frequently > 1 cm

Table 20.**16** Criteria for a malignant tumor of the papilla of Vater

- Irregular borders
- Heterogeneous, predominantly poorly echogenic structure
- Disruption of duodenal wall layering
- Invasion of the duodenal wall, pancreas, ducts, and blood vessels
- Suspicious lymph nodes

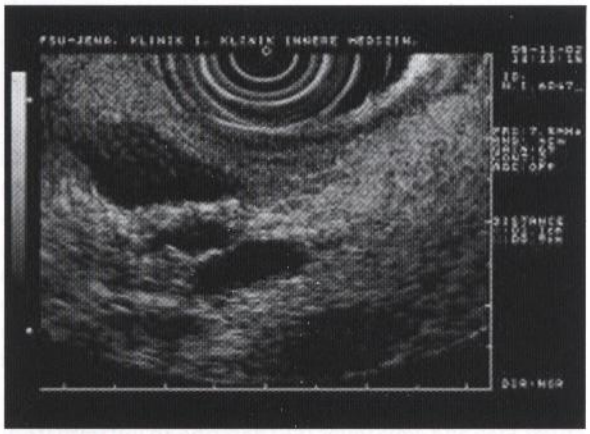


Fig. 20.**7** Adenomyomatosis of the papilla, with funnel-shaped narrowing of the common bile duct.

examinations, respectively. The clinical symptoms of these conditions are reflected in the Milwaukee classification of sphincter of Oddi dysfunction (Table 20.**13**).

Clinical experience shows that adenomyomatosis is more often seen in elderly women with a history of cholecystectomy, but may also be seen in any patient with increasing age. Pathomorphology shows an increase in the musculature of the sphincter apparatus, with or without a simultaneous inflammatory reaction. Since muscular hypertrophy in biopsies is not necessarily regarded as abnormal by pathologists, close collaboration between the endoscopist and pathologist is required.

At present, the only reliable imaging method for identifying adenomyomatosis of the papilla of Vater is endosonography. Only endosonography allows visualization of the papillary region with sufficient magnification for alterations in the sphincter apparatus to be diagnosed. According to Will et al. [58], pathological findings were observed in the papillary region in 311 of 4832 endosonographic examinations. Of these, 183 were further confirmed by biopsy or surgery, showing that EUS has a sensitivity of 92.3% and a specificity of 75.3% for detecting papillary carcinoma, with an accuracy of 82%. The criteria used in the study are listed in Table 20.**14**. Criteria for a noninvasive neoplasia of the papilla (e.g., adenomas, neuroendocrine tumors) are listed in Table 20.**15**.

It should be emphasized that it is not possible to distinguish between extensive adenomyomatosis and adenoma of the papilla of Vater using endosonographic criteria alone. Further histological examination and verification are required in these cases. An example of a neuroendocrine tumor is shown in Fig. 20.**8**. Criteria for the differential diagnosis of a malignant tumor of the papilla of Vater are listed in Table 20.**16**; a typical example is shown in Fig. 20.**9**.

The detailed diagnosis of papillary lesions is therefore an important area of application for endosonography before further diagnostic or therapeutic procedures such as sphincterotomy, papillectomy, or surgical intervention are carried out.

■ Cholangiocellular Carcinomas

Carcinomas of the bile duct are classified using the TNM system. T1 is defined as tumor growth within the ductal wall while the outer border is still smooth. T2 tumors invade the periductal connective tissue, resulting in an irregular border. T3 is characterized by invasion of neighboring organs or vessels. As in carcinoma of the pancreas, invasion into the portal vein is the decisive prognostic marker. The N classification designates the presence (N1) or absence (N0) of pathological lymph nodes.

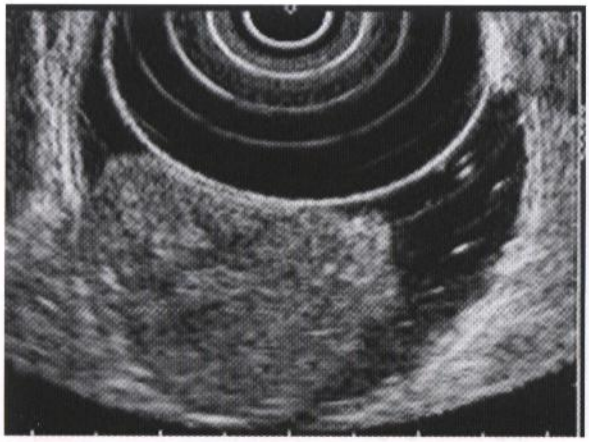


Fig. 20.**8** A neuroendocrine tumor of the papilla of Vater, with a homogeneous structure and preserved duodenal wall layers.

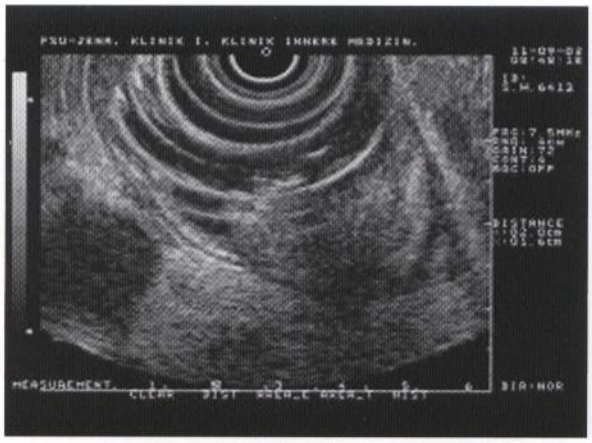


Fig. 20.**9** Carcinoma of the papilla of Vater with invasive growth. The duodenal wall layering is disrupted, and the lesion is poorly echogenic, with an irregular base).

■ Carcinomas of the Gallbladder

Carcinomas of the gallbladder are also classified using the TNM system. T1 shows invasion no deeper than the muscularis propria, with a smooth border. T2 shows invasion of the gallbladder serosa, but the tumor is still contained in the gallbladder and does not invade the liver. In T3, there is invasion of the liver no deeper than 2 cm and in T4, the tumor is invading the liver by more than 2 cm or penetrating into adjacent organs. The N classification categorizes the presence (N1) or absence (N0) of pathological lymph nodes. As with other tumors of the upper gastrointestinal tract, definitive distinction between inflammatory and neoplastic alterations or changes in the connective tissue is not possible with EUS. In some cases, an endosonographic diagnosis of adenomyomatosis, cholesterol polyps, and other forms of gallbladder pathology (e.g., cholecystolithiasis) can be made, although there is no indication for endosonography in these differential diagnoses. The relevance of endosonography for the diagnosis of invasive tumor growth in primary sclerosing cholangitis is unknown. As with the findings in examinations of the esophagus, stomach, and duodenum, inflammatory alterations can lead to narrowing of the bile duct, which can mimic an invasive tumor in the ductal wall.



a



b

Fig. 20.**10** Choledocholithiasis. **a** Longitudinal scanning. **b** Radial scanning.

Fig. 20.**10c** ▷

■ Conclusions

EUS (or EDUS) is indicated before cholecystectomy, particularly in patients with an intermediate risk of choledocholithiasis. EUS appears to be superior to other diagnostic methods, particularly in patients with microlithiasis. It has been shown that longitudinal scanning, radial EUS, or miniprobe ultrasonography are of similar value in the detection of choledocholithiasis; Figs. 20.**10**–20.**12** show comparisons of these different methods. Periductal changes in elasticity are illustrated in Fig. 20.**13**. In addition, EUS is definitely indicated for staging of carci-



Fig. 20.**10c** Miniprobe imaging. It can be seen that longitudinal scanning, radial EUS, and miniprobe ultrasonography provide similarly good imaging results.



a



b



c



d

Fig. 20.**11** The retropapillary region in a patient with choledocholithiasis. **a** Longitudinal scanning. **b** Radial scanning. **c** Miniprobe imaging. PAP: papilla. **d** The miniprobe (MS) is also shown with the longitudinal echoendoscope.

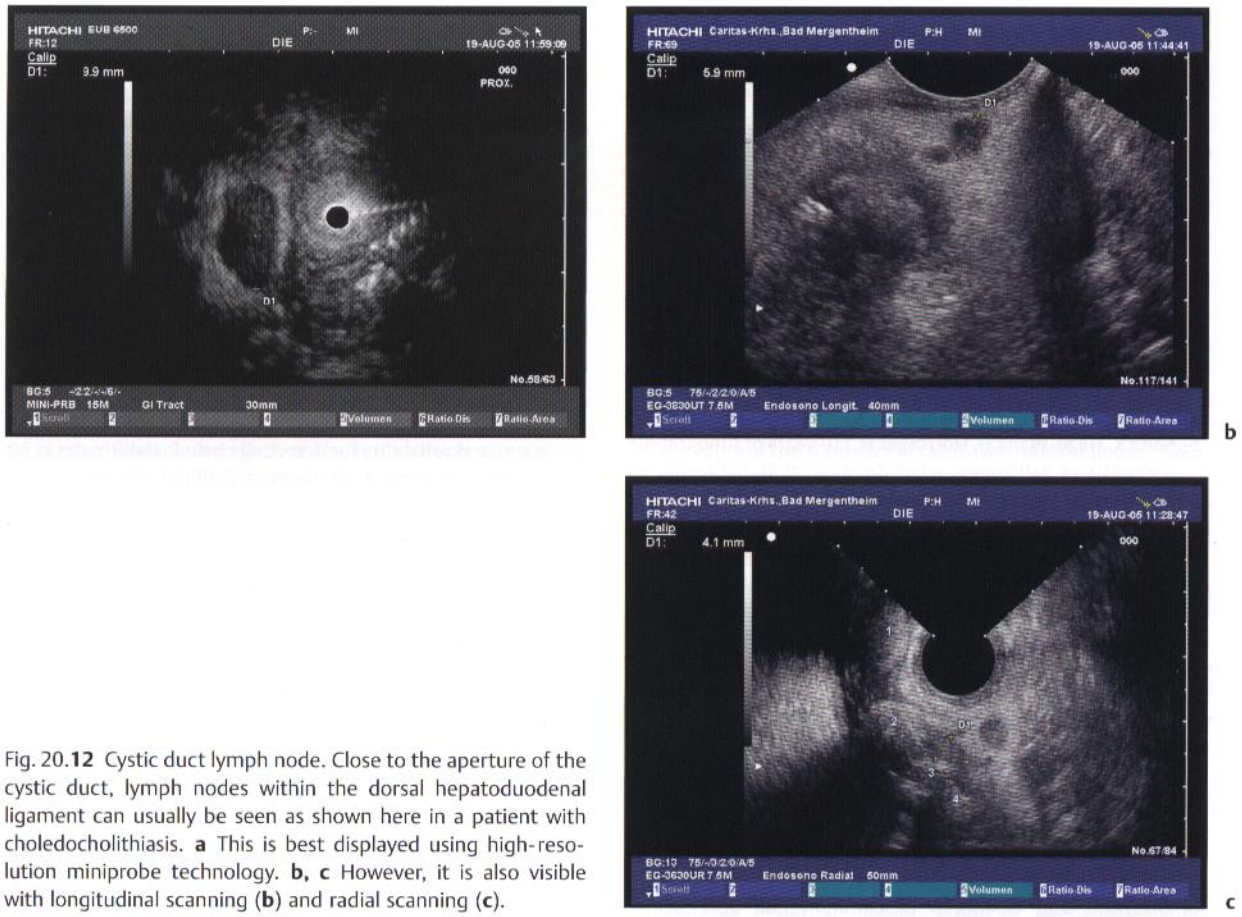


Fig. 20.**12** Cystic duct lymph node. Close to the aperture of the cystic duct, lymph nodes within the dorsal hepatoduodenal ligament can usually be seen as shown here in a patient with choledocholithiasis. **a** This is best displayed using high-resolution miniprobe technology. **b, c** However, it is also visible with longitudinal scanning (**b**) and radial scanning (**c**).

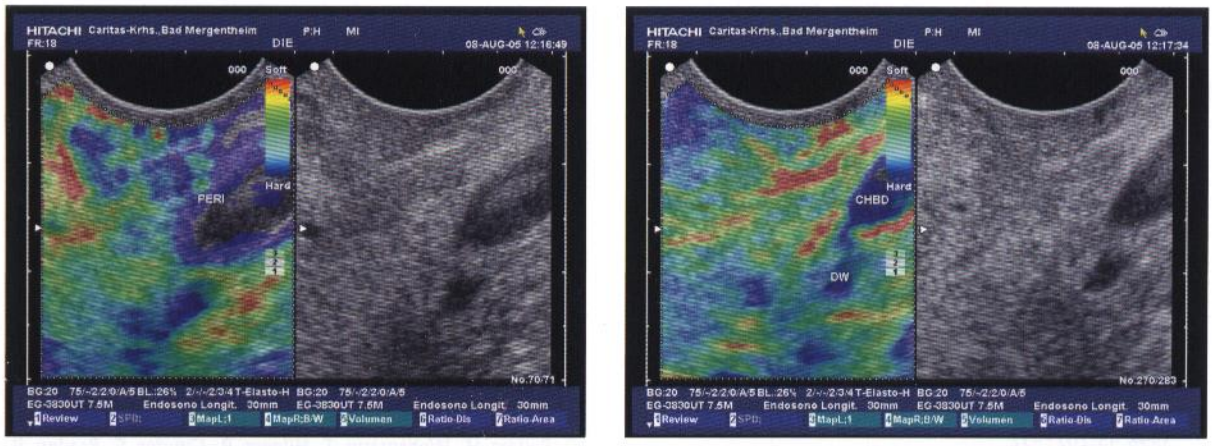


Fig. 20.**13** Pericholangitis. **a** Periductal fibrosis (PERI) in a patient with chronic cholangitis, reproducibly demonstrated with elastography (blue indicates harder elasticity here). **b** CHBD: common hepatic bile duct. DW: duct of Wirsung (pancreatic duct).

noma of the ampulla of Vater. EUS is less important for the staging of cholangiocellular carcinoma than for pathological processes in the papilla.

References

1. Cooperberg PL, Burhenne HJ. Real-time ultrasonography: diagnostic technique of choice in calculous gallbladder disease. N Engl J Med 1980;302:1277–9.
2. Di Nardo R, Urbano D, Drudi FM, Chianta GL, Tortora A, De Simone P, et al. [Ultrasonography in the preoperative assessment of candidates for laparoscopic cholecystectomy: examination technique and results; in Italian.] Radiol Med (Torino) 1996;92:605–9.
3. Fang R, Pilcher JA, Putnam AT, Smith T, Smith DL. Accuracy of surgeon-performed gallbladder ultrasound. Am J Surg 1999;178:475–9.
4. Krook PM, Allen FH, Bush WH Jr, Malmer G, MacLean MD. Comparison of real-time cholecystosonography and oral cholecystography. Radiology 1980;135:145–8.
5. Seitz K, Hege-Blank U, Holzinger H. [10 years of sonographic diagnosis of gallstones: what do surgical statistics tell us about its reliability? In German.] Ultraschall Med 1987;8: 121–5.
6. Silidker MS, Cronan JJ, Scola FH, Moore MM, Schepps B, Thompson W, et al. Ultrasound evaluation of cholelithiasis in the morbidly obese. Gastrointest Radiol 1988;13:345–6.
7. Goodman AJ, Neoptolemos JP, Carr-Locke DL, Finlay DB, Fossard DP. Detection of gallstones after acute pancreatitis. Gut 1985;26:125–32.
8. Amouyal P, Amouyal G, Levy P, Tuzet S, Palazzo L, Vilgrain V, et al. Diagnosis of choledocholithiasis by endoscopic ultrasonography. Gastroenterology 1994;106:1062–7.
9. Amouyal P, Palazzo L, Amouyal G, Ponsot P, Mompoint D, Vilgrain V, et al. Endosonography: promising method for diagnosis of extrahepatic cholestasis. Lancet 1989;ii: 1195–8.
10. Diagnosis and treatment of common bile duct stones (CBDS). Results of a consensus development conference. Scientific Committee of the European Association for Endoscopic Surgery (E.A.E.S.). Surg Endosc 1998;12(6):856–64.
11. Sugiyama M, Atomi Y. Acute biliary pancreatitis: the roles of endoscopic ultrasonography and endoscopic retrograde cholangiopancreatography. Surgery 1998;124:14–21.
12. Sugiyama M, Atomi Y. Endoscopic ultrasonography for diagnosing choledocholithiasis: a prospective comparative study with ultrasonography and computed tomography. Gastrointest Endosc 1997;45:143–6.
13. Chak A, Hawes RH, Cooper GS, Hoffman B, Catalano MF, Wong RC, et al. Prospective assessment of the utility of EUS in the evaluation of gallstone pancreatitis. Gastrointest Endosc 1999;49:599–604.
14. Kumar M, Prashad R, Kumar A, Sharma R, Acharya SK, Chattopadhyay TK. Relative merits of ultrasonography, computed tomography and cholangiography in patients of surgical obstructive jaundice. Hepatogastroenterology 1998;45:2027–32.
15. Shim CS, Joo JH, Park CW, Kim YS, Lee JS, Lee MS, et al. Effectiveness of endoscopic ultrasonography in the diagnosis of choledocholithiasis prior to laparoscopic cholecystectomy. Endoscopy 1995;27:428–32.
16. Varghese JC, Liddell RP, Farrell MA, Murray FE, Osborne H, Lee MJ. The diagnostic accuracy of magnetic resonance cholangiopancreatography and ultrasound compared with direct cholangiography in the detection of choledocholithiasis. Clin Radiol 1999;54:604–14.
17. Pasanen P, Partanen K, Pikkarainen P, Alhava E, Pirinen A, Janatuinen E. Ultrasonography, CT, and ERCP in the diagnosis of choledochal stones. Acta Radiol 1992;33:53–6.
18. Pickuth D, Spielmann RP. Detection of choledocholithiasis: comparison of unenhanced spiral CT, US, and ERCP. Hepatogastroenterology 2000;47:1514–7.
19. Cabada Giadas T, Sarria Octavio de Toledo L, Martinez-Berganza Asensio MT, Cozcolluela Cabrejas R, Alberdi Ibanez I, et al. Helical CT cholangiography in the evaluation of the biliary tract: application to the diagnosis of choledocholithiasis. Abdom Imaging 2002;27:61–70.
20. Jimenez Cuenca I, del Olmo Martinez L, Perez Homs M. Helical CT without contrast in choledocholithiasis diagnosis. Eur Radiol 2001;11:197–201.
21. Takahashi M, Saida Y, Itai Y, Gunji N, Orii K, Watanabe Y. Reevaluation of spiral CT cholangiography: basic considerations and reliability for detecting choledocholithiasis in 80 patients. J Comput Assist Tomogr 2000;24:859–65.
22. Neitlich JD, Topazian M, Smith RC, Gupta A, Burrell MI, Rosenfield AT. Detection of choledocholithiasis: comparison of unenhanced helical CT and endoscopic retrograde cholangiopancreatography. Radiology 1997;203:753–7.
23. Polkowski M, Palucki J, Regula J, Tilszer A, Butruk E. Helical computed tomographic cholangiography versus endosonography for suspected bile duct stones: a prospective blinded study in non-jaundiced patients. Gut 1999;45: 744–9.
24. Aubertin JM, Levoir D, Bouillot JL, Becheur H, Bloch F, Aouad K, et al. Endoscopic ultrasonography immediately prior to laparoscopic cholecystectomy: a prospective evaluation. Endoscopy 1996;28:667–73.
25. De Ledinghen V, Lecesne R, Raymond JM, Gense V, Amouretti M, Drouillard J, et al. Diagnosis of choledocholithiasis: EUS or magnetic resonance cholangiography? A prospective controlled study. Gastrointest Endosc 1999;49:26–31.
26. Edmundowicz SA, Aliperti G, Middleton WD. Preliminary experience using endoscopic ultrasonography in the diagnosis of choledocholithiasis. Endoscopy 1992;24:774–8.
27. Lachter J, Rubin A, Shiller M, Lavy A, Yasin K, Suissa A, et al. Linear EUS for bile duct stones. Gastrointest Endosc 2000;51:51–4.
28. Montariol T, Msika S, Charlier A, Rey C, Bataille N, Hay JM, et al. Diagnosis of asymptomatic common bile duct stones: preoperative endoscopic ultrasonography versus intraoperative cholangiography: a multicenter, prospective controlled study. French Associations for Surgical Research. Surgery 1998;124(1):6–13.
29. Palazzo L, Girollet PP, Salmeron M, Silvain C, Roseau G, Canard JM, et al. Value of endoscopic ultrasonography in the diagnosis of common bile duct stones: comparison with surgical exploration and ERCP. Gastrointest Endosc 1995; 42:225–31.
30. Seifert H, Wehrmann T, Hilgers R, Gouder S, Braden B, Dietrich CF. Catheder probe extraductal EUS reliably detects distal common bile duct abnormalities. Gastrointest Endosc 2004;60:61–67.
31. Liu CL, Lo CM, Chan JK, Poon RT, Lam CM, Fan ST, et al. Detection of choledocholithiasis by EUS in acute pancreatitis: a prospective evaluation in 100 consecutive patients. Gastrointest Endosc 2001;54:325–30.
32. Norton SA, Alderson D. Prospective comparison of endoscopic ultrasonography and endoscopic retrograde cholangiopancreatography in the detection of bile duct stones. Br J Surg 1997;84:1366–9.

33. Taylor AC, Little AF, Hennessy OF, Banting SW, Smith PJ, Desmond PV. Prospective assessment of magnetic resonance cholangiopancreatography for noninvasive imaging of the biliary tree. Gastrointest Endosc 2002;55:17–22.
34. Scheiman JM, Carlos RC, Barnett JL, Elta GH, Nostrant TT, Chey WD, et al. Can endoscopic ultrasound or magnetic resonance cholangiopancreatography replace ERCP in patients with suspected biliary disease? A prospective trial and cost analysis. Am J Gastroenterol 2001;96:2900–4.
35. Lomas DJ, Bearcroft PW, Gimson AE. MR cholangiopancreatography: prospective comparison of a breath-hold 2D projection technique with diagnostic ERCP. Eur Radiol 1999; 9:1411–7.
36. Linares Torres P, Vivas Alegre S, Espinel Diez J, Rueda Castanon R, Munoz Nunez F, Dominguez Carbajo A, et al. [Current status of endoscopic retrograde cholangiopancreatography: what is the effect of the introduction of magnetic resonance cholangiography? In Spanish.] Gastroenterol Hepatol 2001;24:483–8.
37. Hussein FM, Alsumait B, Aman S, Sinan T, Alkandari K, da Hniya MH, et al. Diagnosis of choledocholithiasis and bile duct stenosis by magnetic resonance cholangiogram. Australas Radiol 2002;46:41–6.
38. Griffin N, Wastle ML, Dunn WK, Ryder SD, Beckingham IJ. Magnetic resonance cholangiopancreatography versus endoscopic retrograde cholangiopancreatography in the diagnosis of choledocholithiasis. Eur J Gastroenterol Hepatol 2003;15:809–13.
39. Ueno N, Nishizono T, Tamada K, Ichiyama M, Wada S, Tomiyama T, et al. Diagnosing extrahepatic bile duct stones using intraductal ultrasonography: a case series. Endoscopy 1997;29:356–60.
40. Ohashi A, Ueno N, Tamada K, Tomiyama T, Wada S, Miyata T, et al. Assessment of residual bile duct stones with use of intraductal US during endoscopic balloon sphincteroplasty: comparison with balloon cholangiography. Gastrointest Endosc 1999;49(3 Pt 1):328–33.
41. Tseng LJ, Jao YT, Mo LR, Lin RC. Over-the-wire US catheter probe as an adjunct to ERCP in the detection of choledocholithiasis. Gastrointest Endosc 2001;54:720–3.
42. Das A, Isenberg G, Wong RC, Sivak MV Jr, Chak A. Wire-guided intraductal US: an adjunct to ERCP in the management of bile duct stones. Gastrointest Endosc 2001;54: 31–6.
43. Berthou JC, Drouard F, Charbonneau P, Moussalier K. Evaluation of laparoscopic management of common bile duct stones in 220 patients. Surg Endosc 1998;12:16–22.
44. Frey CF, Burbige EJ, Meinke WB, Pullos TG, Wong HN, Hickman DM, et al. Endoscopic retrograde cholangiopancreatography. Am J Surg 1982;144:109–14.
45. Masci E, Toti G, Mariani A, Curioni S, Lomazzi A, Dinelli M, et al. Complications of diagnostic and therapeutic ERCP: a prospective multicenter study. Am J Gastroenterol 2001; 96:417–23.
46. Halme L, Doepel M, von Numers H, Edgren J, Ahonen J. Complications of diagnostic and therapeutic ERCP. Ann Chir Gynaecol 1999;88:127–31.
47. Brandes JW, Scheffer B, Lorenz-Meyer H, Korst HA, Littmann KP. ERCP: complications and prophylaxis a controlled study. Endoscopy 1981;13:27–30.
48. Loperfido S, Angelini G, Benedetti G, Chilovi F, Costan F, De Berardinis F, et al. Major early complications from diagnostic and therapeutic ERCP: a prospective multicenter study. Gastrointest Endosc 1998;48:1–10.
49. Thatcher BS, Sivak MV Jr, Tedesco FJ, Vennes JA, Hutton SW, Achkar EA. Endoscopic sphincterotomy for suspected dysfunction of the sphincter of Oddi. Gastrointest Endosc 1987; 33:91–5.
50. Neoptolemos JP, Bailey IS, Carr-Locke DL. Sphincter of Oddi dysfunction: results of treatment by endoscopic sphincterotomy. Br J Surg 1988;75:454–9.
51. Roberts-Thomson IC, Toouli J. Is endoscopic sphincterotomy for disabling biliary-type pain after cholecystectomy effective? Gastrointest Endosc 1985;31:370–73.
52. Geenen JE, Hogan WJ, Dodds WJ, Toouli J, Venu RP. The efficacy of endoscopic sphincterotomy after cholecystectomy in patients with sphincter-of-Oddi dysfunction. N Engl J Med 1989;320:82–7.
53. Wojtun S, Gil M, Gil J. Recognition of ERC-induced pancreatitis in patients with choledocholithiasis by an analysis of laboratory findings. Hepatogastroenterology 2000;47: 550–3.
54. Freeman ML, Nelson DB, Sherman S, Haber GB, Herman ME, Dorsher PJ, et al. Complications of endoscopic biliary sphincterotomy. N Engl J Med 1996;335:909–18.
55. Sharma SK, Larson KA, Adler Z, Goldfarb MA. Role of endoscopic retrograde cholangiopancreatography in the management of suspected choledocholithiasis. Surg Endosc 2003;17:868–71.
56. Elek G, Gyori S, Toth B, Pap A. Histological evaluation of preoperative biopsies from ampulla Vateri. Pathol Oncol Res 2003;9:32–41.
57. Seifert H, Wehrmann T, Hilgers R, Gouder S, Braden B, Dietrich CF. Catheter probe extraductal EUS reliably detects distal common bile duct abnormalities. Gastrointest Endosc 2004;60:61–67 and unpublished data.
58. Dietrich CF, Seifert H, Gouder S, Hocke M. Endosonographie des hepatobiliären Systems. Endoskopischer Ultraschall, eine Einführung. Schnetztor Verlag Konstanz 2005, pp. 254–271.

21 Endoscopic Ultrasound Imaging of the Adrenals

C.F. Dietrich, P.H. Kann

Introduction

Endosonographic imaging of the adrenal glands, and the systematic use of the method in diagnostic procedures for adrenal diseases, have been reported for almost 10 years. Endosonographic imaging of the left adrenal gland was first described by Chang et al. [1]. In a small group of 31 patients, the normal left adrenal gland was delineated using endoscopic ultrasonography (EUS) in 97% of cases; detection of the right adrenal gland was only reported in one patient, with a J-shaped stomach. Imaging of the right adrenal gland was therefore initially found to be more problematic.

In the meantime, a great deal of experience has been gained in carrying out endosonographic imaging of the adrenal glands and in assessing the value of this diagnostic technique [2–18]. Both the imaging quality and precise identification of healthy—i.e., morphologically normal—tissue in the adrenals have markedly improved. In particular, modifying the imaging technique for the right adrenal gland made a substantial contribution to progress in this area. It is now possible to distinguish between the medulla and cortex in both adrenals, very small tumors can be identified, and in particular, atrophic adrenals can be demonstrated as a manifestation of autoimmune Addison's disease.

Examination Technique

Due to the complementary role of transabdominal and endoscopic ultrasound for examining the adrenal glands, both methods are described here.

Transabdominal Examination Technique

Cadaver studies. The transabdominal and endoscopic examination technique has recently been validated in corpses. To establish the correct identification and echo pattern of the adrenal glands, the sonographic appearance was documented.

Right adrenal gland. The right adrenal gland is examined in a slightly left lateral position, with the patient's right hand raised above the head to widen the intercostal space. The right adrenal gland is located using the upper pole of the kidney, the inferior vena cava, the crus of the diaphragm, and the margin of the liver as guiding structures. The inferior vena cava, as the medial border, can be always delineated, as well the crus of the diaphragm. For correct identification, the typical echo pattern (bright, dark, bright, dark, and bright echo lines), defined by the pathological anatomical study, has to be visualized. The thickness was measured as 5 ± 1 mm (range 4–8 mm). The thickness of the adrenal wings, measured in their middle representative symmetrical portion in healthy control individuals, was comparable to the EUS findings. Both were slightly larger than the documented diameters in the cadavers. This may have been due to pressure from the directly applied transducer on the adrenal gland, or differences in blood filling.

Left adrenal gland. The left adrenal gland can be examined with the patient in a supine or slightly (right) oblique position, with the left hand raised above the head to widen the intercostal space. Typically, it is seen between the upper pole of the left kidney, pancreatic tail, spleen, crus of the diaphragm, and aorta. In some cases, better visualization is achieved by applying the transducer ventrally, documenting the celiac trunk, splenic and left renal vessels, pancreas, aorta, and left kidney.

Identification of normal adrenal glands, and particularly the right adrenal gland, is possible with transabdominal ultrasonography in most healthy individuals. Reported differences in the detection rate of the adrenal glands may also be due to differences in the equipment used. However, EUS is capable of detecting almost all left and most right adrenal glands, if required.

Endoscopic Ultrasound Examination Technique

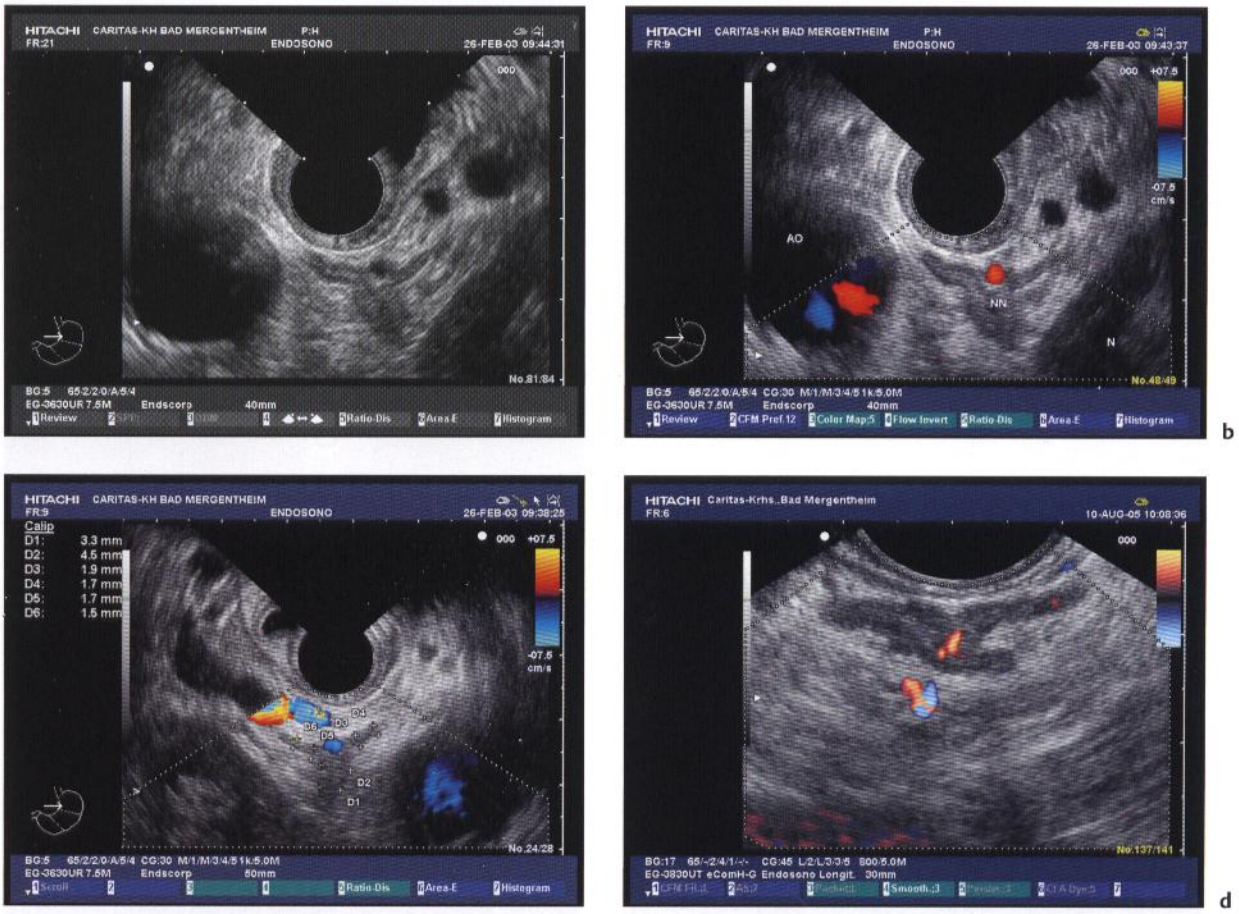
Endosonographic imaging of the adrenals is carried out more easily with a longitudinal echoendoscope, but is also possible with radial transducers. Using these instruments, the adrenal glands can be visualized best by sector scanning; switching the frequency from 7.5 to 5.0 MHz is sometimes useful, as it improves the imaging of the right adrenal gland, which is frequently further away from the transducer than the left adrenal gland, within a range of < 30 mm. In addition, the device also provides the option of carrying out EUS-guided fine-needle aspiration biopsy of adrenal masses in patients who may benefit from cytological and histological assessment.

Sedation. The echoendoscope is inserted with the patient lying on the left side. Since imaging of the adrenals often involves detection or exclusion of very small morphological changes, sufficient sedation is mandatory. The authors use different approaches to sedation. One author (C.F.D.) always uses propofol sedation without local anesthesia; the other (P.H.K.) prefers the following approach: after administering local anesthesia of the pharynx with a spray, and an intravenous injection of atropine (0.25 mg), premedication is carried out with pentazocine (30 mg) and diazepam (10–20 mg).

Left adrenal gland. Landmarks for correct identification of the left adrenal are the cranial pole of the left kidney, the distal pancreatic tail, and the splenic vessels. Typically, after entering the stomach the transducer is kept toward the left posterior gastric wall and shows a variable section of the abdominal aorta at 45 cm; a little more caudally, the upper pole of the left kidney is seen. The transducer should be angulated slightly medially and retracted. The adrenal gland is seen on the way between the upper pole of the left kidney and the aorta, just below the splenic vein. The fact that it typically overlaps the aorta ventromedially by about 0.5 cm is very helpful in finding the correct position. In some cases, the left adrenal gland can also be seen with the transducer in the ascending part of the duodenum. For correct identification, the typical sonographic echo pattern (bright, dark, bright, dark, and bright echo lines) has to be documented. The mean EUS examination time for the left adrenal gland has been reported to be 2 ± 1 min, starting on entry into the stomach, demonstrating that the procedure is not time-consuming (Fig. 21.**1**).

Due to its vicinity to the posterior gastric wall, miniprobe ultrasonography of the left adrenal gland is also possible (Fig. 21.**2**).

Right adrenal gland. Imaging of the right adrenal gland is easiest to carry out when the transducer is placed in the antrum, just in front of the pylorus, after which the patient should lie on the right side. The transducer is now flexed fully toward the right, so that the tip of the echoendoscope is behind the angular notch. With the transducer in this position, the echoendoscope is carefully retracted until the landmarks (the cranial pole of the right kidney, inferior cava vein, caudal parts



a b c d

Fig. 21.**1a** A normal left adrenal gland imaged using conventional B-mode. **b, c** Color Doppler imaging, showing the hilum with the afferent artery (**b**) and efferent vein (**c**). NN: adrenal; AO: aorta; N; kidney. **d** Longitudinal scanning.

Fig. 21.**1e** ▷



e

Fig. 21.**1e** Radial scanning. The adrenal hilum and adrenal vessels can be delineated with both methods. Miniprobe ultrasound with longitudinal scanning is of no value (not shown).

of the liver, and the portal vein) can be identified. After this, the right adrenal gland can be imaged behind the inferior cava vein. As in the transabdominal examination, this technique makes it possible to distinguish between the echoes generated by the adrenal medulla and those generated by the cortex (Fig. 21.**3**).

Adrenal gland morphology. It is possible to visualize abnormalities in the structure of the adrenal glands, although the relevance of these has not yet been fully assessed. For example, in patients with genetic disorders such as multiple endocrine neoplasia types 2a and 2b and von Hippel–Lindau disease, it is now possible to identify clear hyperplasia of the adrenal medulla. Further studies are needed in order to clarify whether this is a preliminary stage in the development of manifest pheochromocytoma, in the same way that there is a progression from C cell hyperplasia to medullary thyroid carcinoma.

■ Indications for EUS of the Adrenal Glands

On this basis of the information currently available, the following can be regarded as valid indications for endosonography of the adrenal glands:

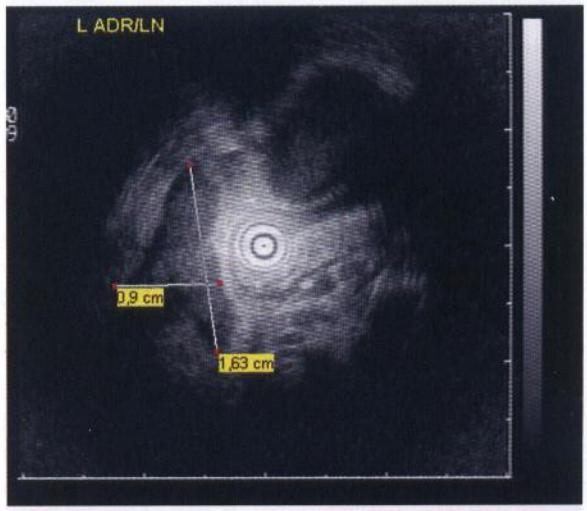
- Detection of small adrenal tumors
- Characterization of adrenal tumors
- Assessing criteria of malignancy in adrenal tumors
- Early detection of recurrences of malignant adrenal tumors
- Preoperative identification of morphologically healthy parts of the adrenals
- Detection of extra-adrenal/ectopic tumors (pheochromocytomas)
- Differentiation between different entities in adrenal insufficiency
- EUS-guided fine-needle aspiration biopsy



a



b

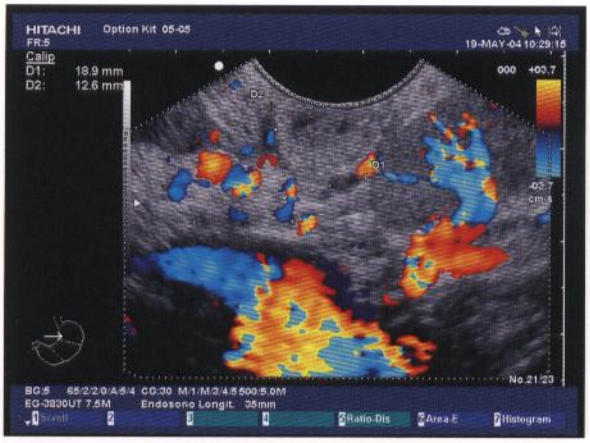


c

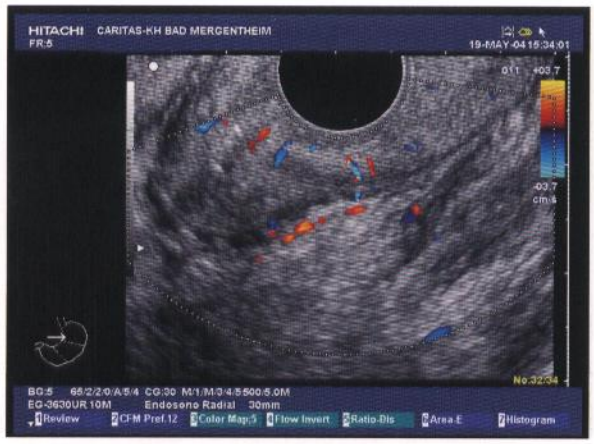
Fig. 21.**2a–c** Imaging of a normal left adrenal gland using miniprobe technology next to the pancreas.

■ Pathological Findings

Detection of small adrenal tumors. Endosonography of the adrenal glands makes it possible to detect morphological abnormalities such as nodular formations in the adrenals, down to a diameter of about 3 mm



a



b

Fig. 21.**3a** The right adrenal gland, between the markers. **b** Color Doppler imaging demonstrates the hilum as well.

(Fig. 21.**4**). In addition, nodular hyperplasia occurring in multiple endocrine neoplasia type 1 can be identified. There is some evidence that endosonography of the adrenal glands may be superior to magnetic resonance imaging and/or computed tomography (CT) in relation to small adrenal tumors, with postoperative histological assessment being used as the gold standard.

Incidentalomas. Incidentally found adrenal tumors without hormone production are known as incidentalomas. These can be found in up to 5% of transabdominal examinations, as well as CT and EUS examinations, in unselected populations. Surgery is recommended in patients with tumors 4–6 cm in size and/or tumor growth. Fine-needle aspiration cytology is helpful in the diagnosis of lymphoma and metastases (Fig. 21.**5**).

In the case of enlarged adrenals, it is also possible to identify lipid-containing tumors such as myelolipoma, due to their high echogenicity. Adrenal cysts are rare and have the typical features known from conventional sonography in other organs (Fig. 21.**6**).

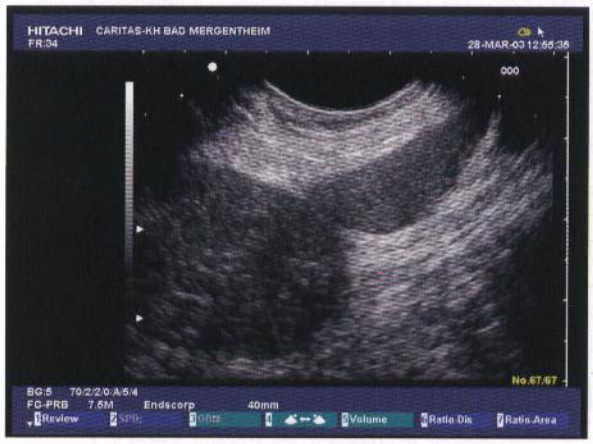
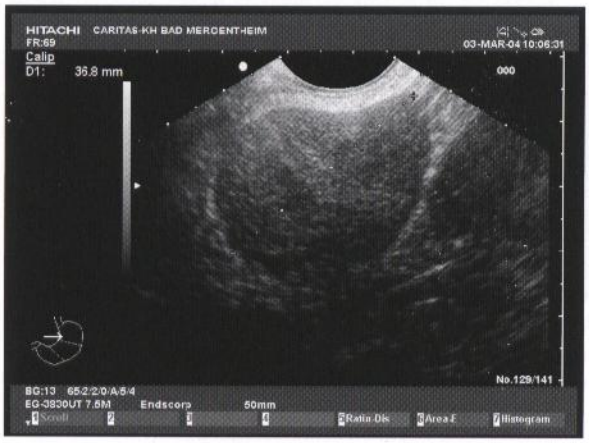
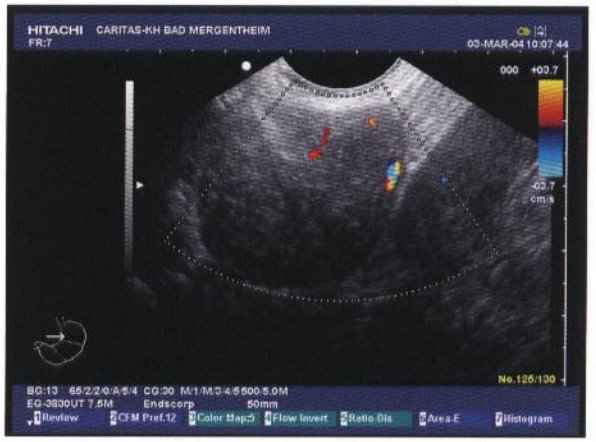


Fig. 21.**4** Diffuse enlargement of the left adrenal gland, often observed as a nonspecific finding in elderly patients.



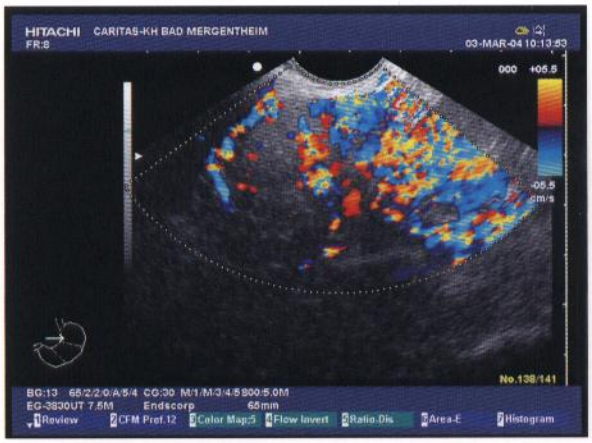
a



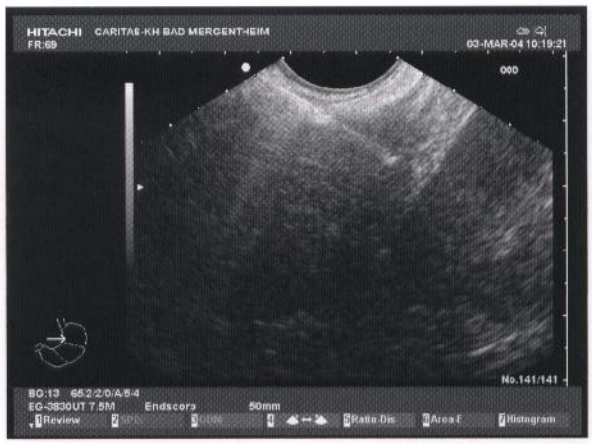
b

Fig. 21.**5** Incidentaloma. **a** B-mode. **b** Color duplex scanning.

Fig. 21.**5c, d** ▷



c



d

Fig. 21.5c Contrast-enhanced ultrasound using SonoVue. **d** Puncture.

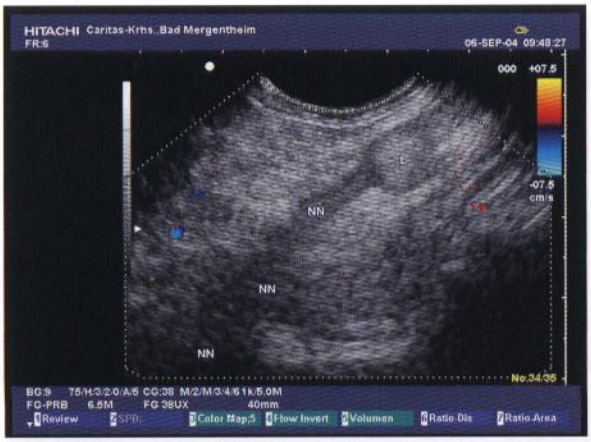


Fig. 21.6 A small hyperechoic tumor in the left adrenal gland (NN): a typical lipid-containing myelolipoma (M).

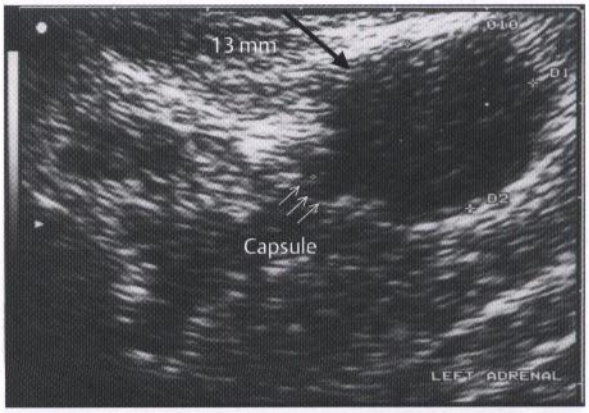


Fig. 21.7 A solitary adenoma (arrow) in the left adrenal gland (lateral limb) in Conn's syndrome (primary aldosteronism).

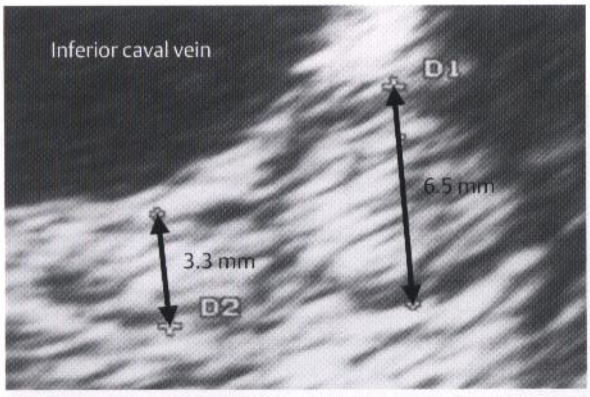
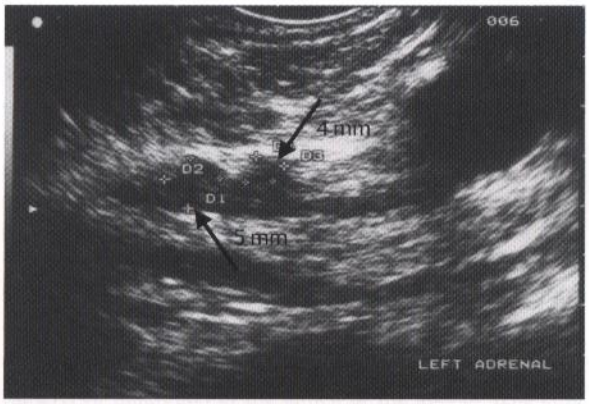


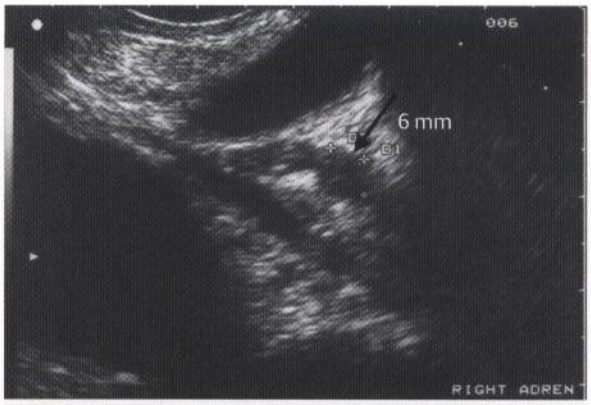
Fig. 21.8 Nodular transformation (assessed histologically as nodular hyperplasia) in the body of the right adrenal gland in a patient with rapidly progressive virilization.



Fig. 21.9 A solitary adenoma (arrow) in the right adrenal gland (lateral limb) in a patient with Cushing's syndrome independent of adrenocorticotropic hormone (ACTH).



a



b

Fig. 21.**10a, b** Hyperplasia of the adrenal glands (arrows; morphologically nodular) in idiopathic hyperaldosteronism.



Fig. 21.**11** Hyperplasia of the adrenal medulla in a patient with multiple endocrine neoplasia (MEN) type 2a.

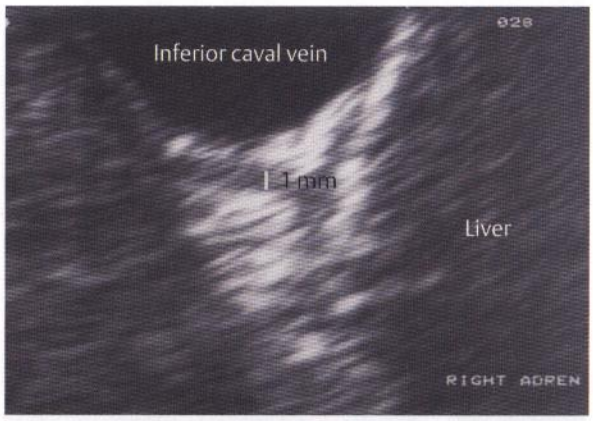


Fig. 21.**12** Marked atrophy of the adrenal glands (the right adrenal is shown here) in a patient with autoimmune Addison's disease.

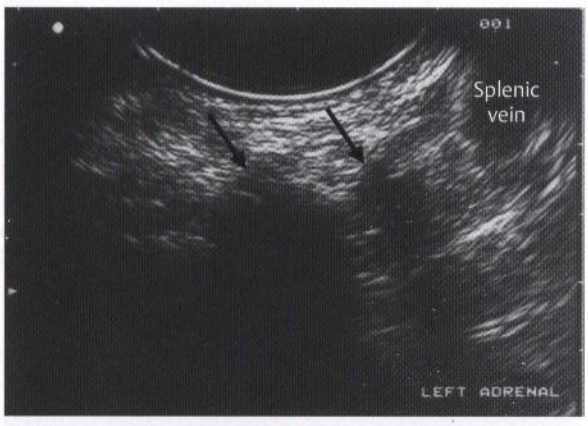


Fig. 21.**13** Calcification of the left adrenal gland in adrenal tuberculosis and primary adrenal insufficiency.

Characterization of adrenal tumors. Micronodular hyperplasia of the adrenal glands can be identified by EUS as a rare morphological substrate of Cushing's syndrome independent of adrenocorticotropic hormone (ACTH). It is easily distinguished from unilateral, solitary adenoma of one adrenal gland.

In the differential diagnosis of primary hyperaldosteronism, endosonography allows the identification of unilateral adenoma. Important criteria for this appear to be a round or oval shape of the tumor and detection of the border of the normal adrenal tissue. Bilateral adrenal hyperplasia can also be imaged and differentiation between a diffuse type or nodular morphology is possible. The precise differential diagnosis is very important clinically, since in the first case surgery is indicated, while in the second case medical treatment is mandatory.

Figures 21.**7**–21.**11**) show examples of various hormone-producing tumors and hyperplasia. Figures 21.**12** and 21.**13**) show examples of atrophy in patients with insufficiency.

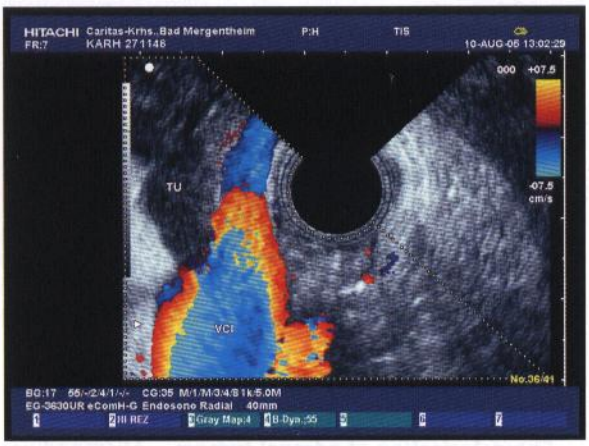
Assessment criteria for malignancy in adrenal tumors. Preoperative detection of criteria for malignancy is very important during the planning of the surgical strategy for adrenal masses. Endocrinologists and endocrine surgeons may consider endoscopic resection to be the wrong approach in such cases.

Adrenocortical carcinomas are generally heterogeneous and have a complex echo pattern, but malignant and benign pheochromocytomas can also have the same characteristics. Heterogeneity of an adrenal tumor is therefore not a clear criterion for malignancy (Fig. 21.**14**). The value of endosonography is that it can demonstrate or exclude infiltration of neighboring organs as a valid criterion for malignancy. In addition, the detection of effusion is suggestive of malignancy. Detection of local or regional lymph-node metastases and vascular invasion is a clear criterion for malignancy.

Early detection of recurrences of malignant adrenal tumors. In the postoperative care of adrenocortical carcinomas and pheochromocytomas, endosonography allows detection of small recurrences in the tumor area and in neighboring regions earlier than with other techniques.

Preoperative identification of morphologically normal parts of the adrenals. Bilateral adrenal masses are detected in some cases, particularly in diseases with genetic causes such as multiple endocrine neoplasia types 2a and 2b and von Hippel–Lindau disease. The patients affected are often young. It is very important to know preoperatively whether there are morphologically completely normal parts of an adrenal gland that can be left in situ, in order to avoid the need for lifelong substitution treatment with adrenal steroid hormones in these patients.

Detection of extra-adrenal/ectopic masses (pheochromocytomas). The typical symptoms and hormonal findings of a pheochromocytoma are the principal reason for morphological diagnostic procedures being carried out in the adrenals. However, some of these tumors are ectopic, either para-adrenal or in other regions of the body. In these circumstances, endosonography allows detection of ectopic tumors (Fig. 21.**15**).



a



b



c



d

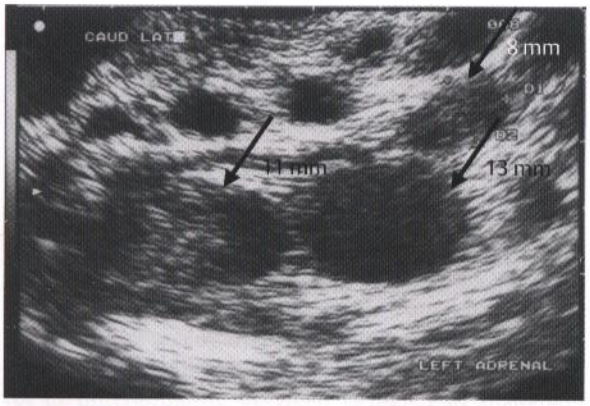
Fig. 21.**14** A right adrenal gland tumor (TU) infiltrating the inferior vena cava (VCI). While visualization was comparable with the radial (**a**) and longitudinal (**b**) systems, tumor puncture is only possible with the longitudinal scanner. **c** Miniprobe ultrasound (MINI) was not helpful in delineating tumor infiltration. The miniprobe position is shown here with the longitudinal scanner. **d** The corresponding miniprobe image, showing the inferior vena cava (VCI).

Fig. 21.**14e** ▷

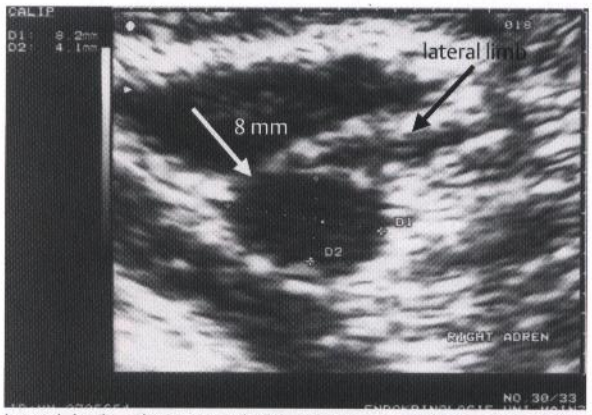


e

Fig. 21.**14e** Infiltration of the lumen of the inferior vena cava (VCI) was only visualized using the longitudinal probe.



a



b

Fig. 21.**15** Pheochromocytomas in both adrenal glands (three on the left, **a**; one on the right, **b**) in a patient with multiple endocrine neoplasia type 2a, with clear identification of morphologically normal parts of the right adrenal gland in the lateral limb. This part of the organ was left in situ during surgery, allowing the patient to avoid lifelong substitution treatment with steroid hormones.

Differentiation of different causes of adrenal insufficiency. Different diseases causing adrenocortical insufficiency have typical morphologies, which can be detected using endosonography. Autoimmune Addison's disease is associated with marked atrophy of the adrenal glands. Calcifications in the organs are suggestive of adrenal insufficiency following adrenal tuberculosis. Adrenal metastases are typically large and hypoechoic, and clear identification and histopathological differentiation can be achieved with EUS-guided fine-needle aspiration biopsy.

EUS-guided fine-needle aspiration biopsy. Endosonography allows guided fine-needle aspiration biopsies of the adrenal glands. In most cases, this makes a definitive diagnosis possible. The following points apply to the indication for fine-needle aspiration biopsy of the adrenal glands:

- Biopsy of an adrenal mass makes it possible to differentiate between adrenal tissue and nonadrenal tissue—i. e., in particular, detection of metastases and/or lymphomas.
- Differentiation between adrenocortical adenoma and adrenocortical carcinoma is not possible with fine-needle aspiration biopsy. This is therefore not an indication for biopsy.
- Due to complications reported in the literature resulting from mechanical manipulations of pheochromocytomas, fine-needle aspiration biopsy of adrenal masses should not be carried out unless pheochromocytoma has been excluded.

■ Conclusion and Summary

Endosonographic imaging of the adrenal glands has developed from an experimental procedure into an established diagnostic method. Endosonography conducted by an experienced investigator in patients who have received sufficient premedication is a harmless procedure for the patient. The complication rate is comparable to that with conventional gastroscopy, there is no radiation exposure, the diagnostic value and clinical

impact are high, and the procedure is inexpensive. The technique is therefore an advantageous one in the diagnosis and differentiation of adrenal diseases.

References

1. Chang KJ, Erickson RA, Nguyen P: Endoscopic ultrasound (EUS) and EUS-guided fine-needle aspiration of the left adrenal gland. Gastrointest Endosc 1997;44:568–72.
2. Chhieng DC, Jhala D, Jhala N, Eltoum I, Chen VK, Vickers S, et al. Endoscopic ultrasound-guided fine-needle aspiration biopsy: a study of 103 cases. Cancer 2002;96:232–9.
3. Dietrich CF, Wehrmann T, Hoffmann C, Herrmann G, Caspary WF, Seifert H. Detection of the adrenal glands by endoscopic or transabdominal ultrasound. Endoscopy 1997;29: 859–64.
4. Heinz-Peer G, Honigschnabl S, Schneider B, Niederle B, Kaserer K, Lechner G. Characterization of adrenal masses using MR imaging with histopathologic correlation. AJR Am J Roentgenol 1999;173:15–22.
5. Kann P, Bittinger F, Hengstermann C, Engelbach M, Beyer J. Endosonographische Darstellung der Nebennieren: Eine neue Methode. Ultraschall Med 1998;19:4–9.
6. Kann P, Hengstermann C, Heussel CP, Bittinger F, Engelbach M, Beyer J. Endosonography of the adrenal glands: normal size—pathological findings. Exp Clin Endocrinol Diabetes 1998;106:123–9.
7. Kann P, Heintz A, Bittinger F, Herber S, Kunt T, Beyer J. Endosonographie bei kleinen Nebennierenraumforderungen: Morphologischer Nachweis der mikro- und makronodulären Nebennierenrindenhyperplasie in vivo als Ursache einer autonomen Sekretion von Steroidhormonen. Tumordiagn Ther 1999;20:135–43.
8. Kann P, Heintz A, Bittinger F, Kessler S, Forst T, Weis A, et al. Bildgebende Diagnostik der Nebennieren: neue Aspekte durch die Einführung der Endosonographie. Minimal Inv Chir 2000;9:58–61.
9. Kann PH, Wirkus B, Behr T, Klose KH, Meyer S. Endosonographic imaging of benign and malignant pheochromocytomas. J Clin Endocrinol Metab 2004;89:1694–7.
10. Kann PH. Endosonographic imaging of the adrenals. Endoscopy 2005;37:244–53.
11. Korobkin M, Brodeur FJ, Francis IR, Quint LE, Dunnick NR, Londy F. CT time-attenuation washout curves of adrenal adenomas and nonadenomas. AJR Am J Roentgenol 1998; 170:747–52.
12. Langer P, Bartsch DK, Fendrich V, Kann PH, Rothmund M, Zielke A. Minimalinvasive operative Therapie des organischen Hyperinsulinismus. Dtsch Med Wochenschr 2005;13 0:514–8.
13. Meyer S, Bittinger F, Keth A, von Mach MA, Kann P. Endosonographically controlled transluminal fine needle aspiration biopsy: diagnostic quality by cytologic and histopathologic classification. Dtsch Med Wochenschr 2003;128: 1585–91.
14. Müller MF, Meyerberger C, Bertschinger P, Schaer R, Marincek B. Pancreatic tumors: evaluation with endoscopic US, CT, and MR imaging. Radiology 1994;190:745–51.
15. Reincke M, Allolio B. Das Nebenniereninzidentalom. Dt Aerztebl 1995;92:A764–70.
16. Sample WF. A new technique for the evaluation of the adrenal gland with gray scale ultrasonography. Radiology 1977;124:463–9.
17. Trojan J, Schwarz W, Sarrazin CM, Thalhammer A, Vogl T, Dietrich CF. Role of ultrasonography in the detection of small adrenal masses. Ultraschall Med 2002;81:96–100.
18. Vilmann P. Endoscopic ultrasound-guided fine-needle biopsy in Europe. Endoscopy 1998;30(Suppl 1):A161–2.

22 Contrast-Enhanced EUS in the Pancreas

M. Hocke, C.F. Dietrich

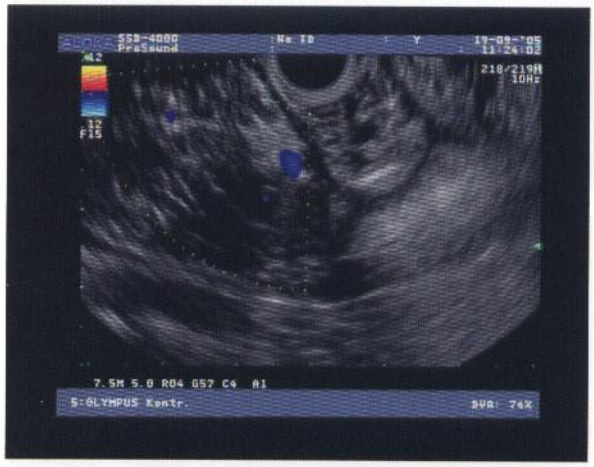
■ Detection

The potential of contrast-enhanced endoscopic ultrasound (EUS) to detect pancreatic lesions that are not identified with conventional endoscopic ultrasound is limited. This situation is also unlikely to change, since it is difficult to improve the local resolution of endoscopic ultrasound, and with correct positioning of the scope and mastery of the examination technique, even structures only a few millimeters in size can be clearly recognized.

■ Characterization of Malignancy

The primary aim in using contrast enhancement in endoscopic ultrasound, therefore, is to improve the assessment of malignancy in pathological changes by optimizing the imaging of vessel distribution. Endoscopic ultrasound with amplified echo signals has been found helpful in differentiating between benign and malignant pancreatic tumors, although a definitive conclusion cannot be reached in every case. Initial attempts to diagnose malignant areas in cases of chronic pancreatitis have been very promising. Above and beyond this, however, it has become apparent that with improved equipment and classification of the pancreatic vascular structures, the quality of malignancy assessment in pancreatic tumors can be greatly improved. The examination of patients with undiagnosed pancreatic masses has shown that pancreatic adenocarcinomas have a few arteries with an irregular configuration and that focal pancreatitis demonstrates both veins and arteries with a regular tree-like distribution (Figs. 22.**1**, 22.**2**).

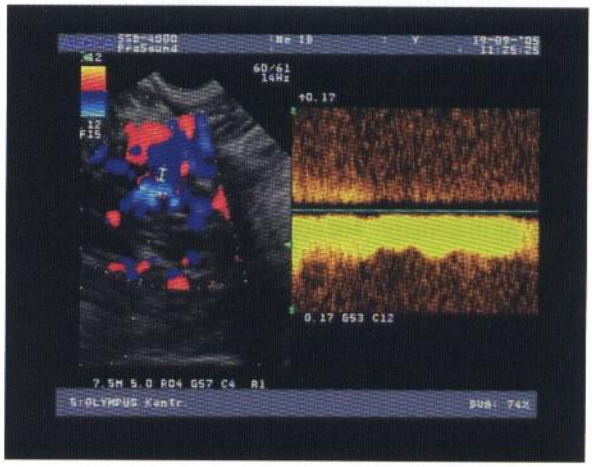
Endoscopic ultrasound is also useful for clarifying less common localized pancreatic growths. It is particularly valuable in cases of hypervascularization of microcystic pancreatic adenomas or neuroendocrine tumors, as well as macrocystic ones, although these are less well de-



a



b



c

Fig. 22.**1** Chronic pancreatitis. **a** No evidence of vascularization on power Doppler imaging before contrast administration. **b** Evidence of long, regular blood vessels, homogeneously distributed, after contrast administration. **c** Evidence of arterial and venous signals on Doppler imaging.

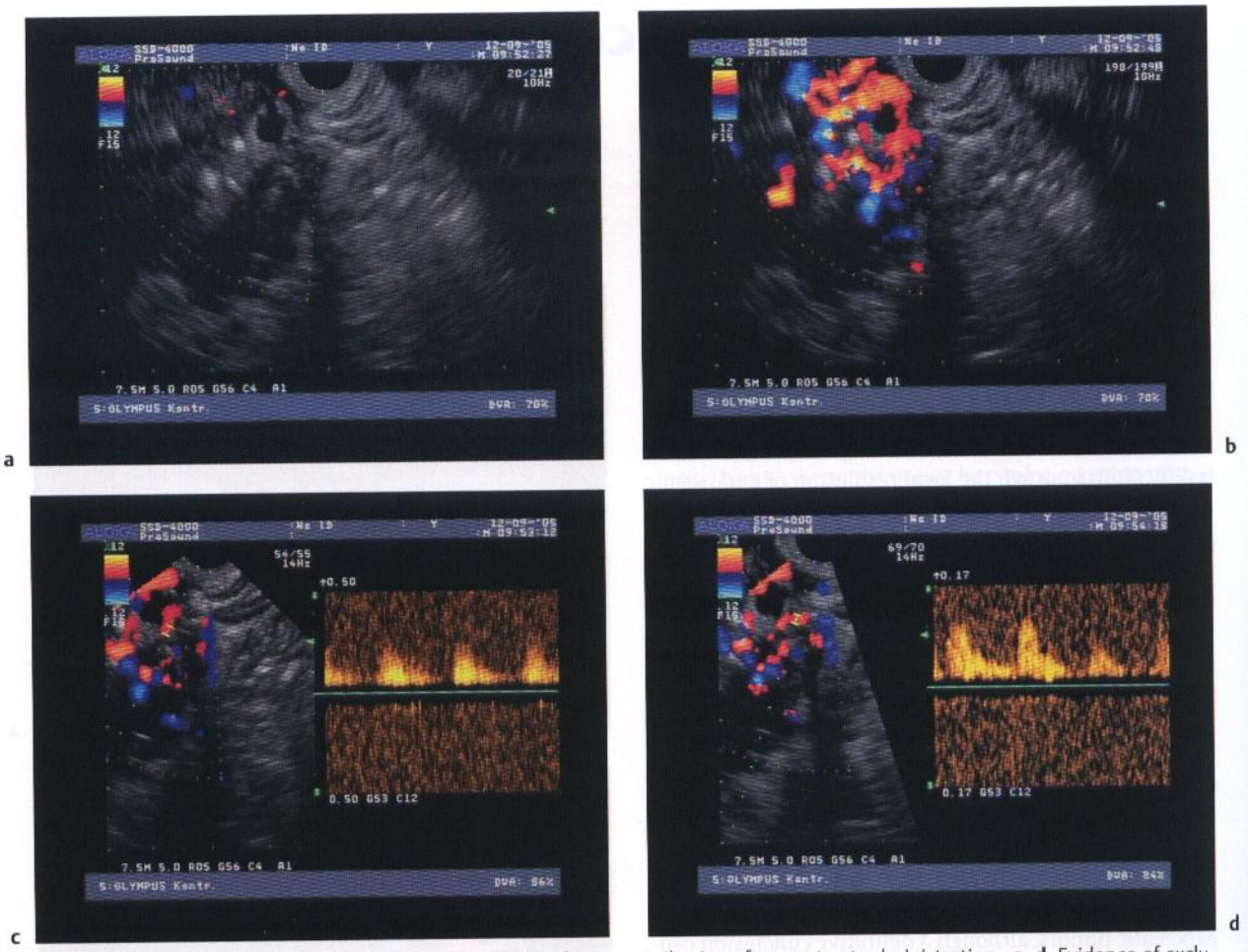


Fig. 22.2 Pancreatic carcinoma. **a** No evidence of vessels on power Doppler imaging before contrast administration. **b** Evidence of short, irregular vessels with an inhomogeneous distribution after contrast administration. **c, d** Evidence of exclusively arterial signals on Doppler imaging.

lineated (Figs. 22.3, 22.4). The lesions can be diagnosed relatively reliably using color duplex endoscopic ultrasound and contrast-enhanced sonography. It is essential to make a differentiated diagnosis when there are mixed pancreatic tumors with different degrees of malignancy and in cases of hypervascularized pancreatic metastases, which are relatively often diagnosed using modern imaging, but which play a lesser role in determining the prognosis. In cases of hypervascularized pancreatic metastases, it is also important to take into consideration the possibility that they are metastases from renal adenocarcinoma, melanoma, small-cell bronchial carcinoma, or mammary carcinoma.

With the help of EUS-guided fine-needle aspiration, endoscopic ultrasound represents an important tool in the diagnosis of pancreatic tumors. Preliminary data indicate that it is already possible today to do without histological specimens and rely on cytological specimens. This hypothesis is currently being tested—for example, at Topalidis's cytology laboratory in Hanover, Germany (who kindly provided the images for Fig. 22.4).

Review of the Literature [1]

Contrast-enhanced transabdominal ultrasound techniques were recently introduced. Administration of liver-specific microbubbles using Levovist makes it possible to detect metastases smaller than 1 cm and improved the ability to differentiate between benign and malignant lesions [2–4]. Due to the complexity of the (intermittent) examination technique, with a high mechanical index and bubble destruction, the method was found to be difficult to use routinely. More recent advances using SonoVue combined with low mechanical index techniques improved the transabdominal use of contrast-enhanced techniques, allowing real-time imaging with or without three-dimensional reconstruction [5].

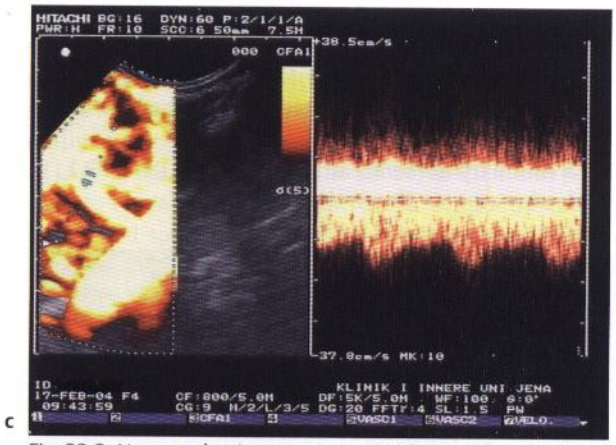
Several studies have been carried out to assess the potential role of contrast-enhanced endoscopic ultrasonography. Initial data on the practicality of using first-generation contrast enhancers were published by Bhutani et al. [6], who were able to demonstrate better



a

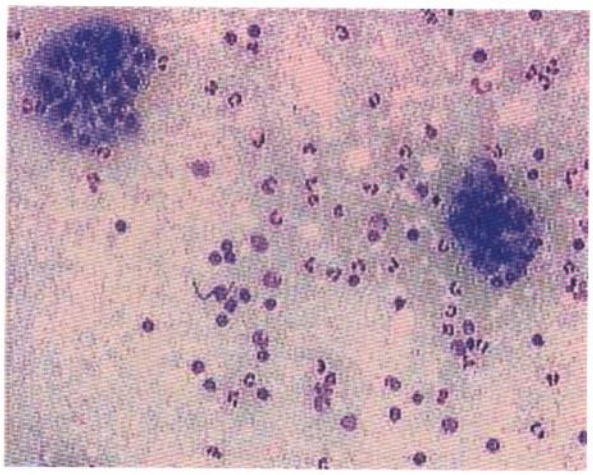


b

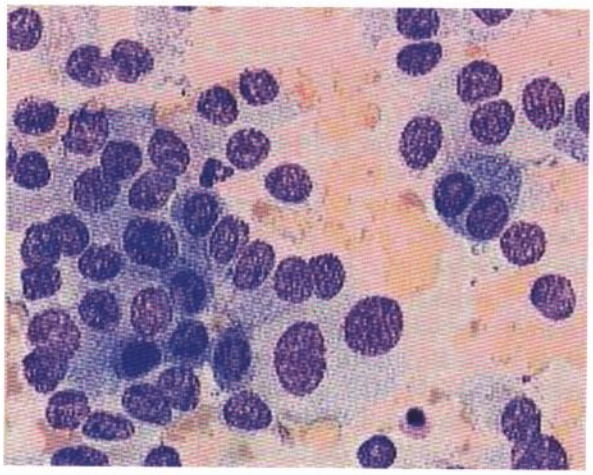


c

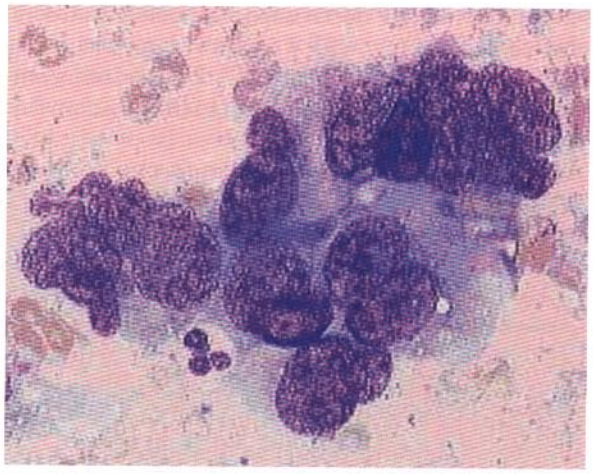
Fig. 22.3 Neuroendocrine tumor. **a** Evidence of vessels on power Doppler imaging, even before contrast administration. **b** Evidence of a long, regular vessel structure after contrast administration. **c** Evidence of both arterial and venous signals on Doppler imaging.



a



b



c

Fig. 22.4 Cytological images (courtesy of T. Topalidis, Hanover). **a** Chronic pancreatitis. **b** Undifferentiated pancreatic carcinoma. **c** Neuroendocrine carcinoma.

imaging of vessels in swine after administration of Levovist. It should be noted that only one study has been conducted to date using second-generation contrast agents, and there no research has been published yet on contrast-specific software.

Recognizing malignant neoplasia in chronic pancreatitis has always been difficult. The gold standard is still surgery. Although the introduction of EUS-guided fine-needle aspiration has made this easier, an improved noninvasive method of detecting malignant tissue would be preferable. In a recently published study, contrast-enhanced EUS was used to distinguish between benign and malignant pancreatic lesions. Using conventional EUS criteria, the sensitivity was 73% and the specificity 83% for pancreatic cancer. Using contrast-enhanced EUS, detection of 51 of 56 patients with malignant pancreatic lesions increased the sensitivity to 91%. In 28 of 30 patients with chronic inflammatory pancreatic disease, the diagnosis was correctly recognized, giving a specificity value of 93.3% [7].

As in studies using contrast-enhanced transabdominal ultrasound [8–11], ductal adenocarcinoma of the pancreas was found to be hypoenhancing in an EUS study by Hirooka et al. [12] using Albunex. The authors found that Albunex improved the endoscopic ultrasound diagnosis in examinations of the gallbladder and pancreas. They were able to show enhancement in the various layers of tissue and absence of it in pancreatic carcinoma. However, it should be noted that all of the investigations were based on contrast differences that could be detected using a mechanical radial scanner.

Optison was also used in a small study by Becker et al. [13] to differentiate ductal adenocarcinoma from focal chronic pancreatitis, with a sensitivity of 94% and a specificity of 100%. Interestingly, neuroendocrine tumors were not distinguishable from inflammation. This is the only report in the current literature describing the use of second-generation ultrasound contrast enhancers with electronic scanners.

In a case report, insulinoma was found to be distinguishable from the main pancreatic duct, with a separation of 3 mm, so that enucleation instead of pancreatectomy was considered preoperatively [14].

Bile duct carcinoma at the hepatic bifurcation was differentiated from primary and secondary sclerosing cholangitis by analyzing the enhancement pattern of the wall of the bile ducts; hypoenhancement was found to be a typical sign of malignancy [15]. In five patients with autoimmune pancreatitis, strong enhancement of the thickened wall of the common bile duct after injection of Levovist was able to rule out pancreaticobiliary malignancy [16]. The accuracy of predicting the T staging of malignancies of the gallbladder using contrast-enhanced endoscopic ultrasound with Albunex was better than with conventional EUS, improving from 79% to 93% [17].

Contrast-enhanced endoscopic ultrasound was also used in patients with gastric and esophageal cancer, and improved the accuracy of T staging from 77% to 90%. Most malignant lesions showed no enhancement [17].

The detection of perforating veins in patients with esophageal varices due to portal hypertension as a predictive sign of recurrence was improved by the use of Levovist-enhanced Doppler techniques. Using unenhanced endoscopic ultrasonography, 31% of patients with recurrent esophageal varices, and none of the patients without recurrences, were shown to have perforating veins. Using contrast-enhanced EUS, 76% of patients with recurrences were found to have perforating veins. Again, none of the patients who had no recurrences showed this sign.

A summary of the literature is given in Table 22.1 [1].

Table 22.1 Findings in contrast-enhanced endoscopic ultrasound techniques, as reported in the literature [1]

Criteria evaluated	Lesions	Patients (n)	Method	Conclusion	Reference
To detect perforating veins as a criterion for recurrence of esophageal varices	Esophageal varices	29	CE-EUS, Levovist, color/power Doppler	Detection of perforating veins in patients with vs. without recurrence of varices in EUS: 31% vs. 0%; in CE-EUS: 76% vs. 0%	[19]
To describe esophageal varices	Esophageal varices	62	CE-EUS, Levovist, color/power Doppler	Levovist improves the diagnostic quality of EUS, providing improved images	[20]
Concentric wall thickening of the common bile duct	Common bile duct	5	CE-EUS, EUS, IDUS, Levovist	Strong enhancement after Levovist rules out pancreaticobiliary malignancy in autoimmune-related pancreatitis	[16]
Enhancement of bile duct wall	Primary (2) and secondary sclerosing cholangitis (1), bile duct carcinoma of the hepatic bifurcation (4)	7	CE-IDUS, Levovist, quantitative assessment	The wall of the bile duct is not enhanced in bile duct carcinoma but in sclerosing cholangitis	[15]
Hypoperfusion as a criterion for malignancy	Solid pancreatic masses	23	CE-EUS, Optison, color/power Doppler	Sensitivity 94%, specificity 100% for malignancy	[13]

Table 22.1 Findings in contrast-enhanced endoscopic ultrasound techniques, as reported in the literature [1] (Continued)

Criteria evaluated	Lesions	Patients (n)	Method	Conclusion	Reference
Negative enhancement as a criterion for malignancy	Esophageal (4), gastric carcinoma (30), gastric myogenic tumors (5), gastric ulcers (3)	42	CE-EUS, Albunex, high MI B-mode	In gastric cancer, improved accuracy of T staging from 77% to 90%; sharper delineation of tumors	[18]
To evaluate pancreas saving operability	Insulinoma of the pancreas, detected by CT	Case study	CE-EUS Levovist®	Enhancement, distance to pancreatic duct was 3 mm so enucleation was possible	[13]
enhancement in ductal adenocarcinoma and pseudocysts	Ductal adenocarcinoma (11), mucin producing tumors (10), pseudocysts (5), islet-cell tumors (4), chronic pancreatitis (4), serous cystadenoma (3)	37	CE-EUS, Albunex®	Combined evaluation of fundamental and contrast enhanced images of EUS useful for diagnosis of pancreatic diseases	[11]
To differentiate different lesions of the gall bladder	Adenocarcinoma of the gall bladder (12), adenosquamous carcinoma (2), cholesterol polyp (6), cholecystitis (10), adenomyomatosis (8)	38	CE-EUS, Albunex®	No enhancement in adenosquamous carcinomas and cholesterol polyps; accuracy for detection of tumor invasion using CE-EUS improved from 79 to 93%	[16]

CE: contrast enhanced; CT: computed tomography; EUS: endoscopic ultrasonography; IDUS: intraductal ultrasonography; MI: mechanical index.

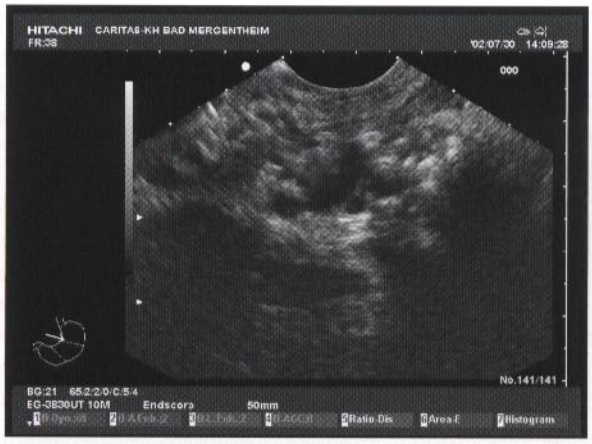
■ Wide-Band Harmonic Imaging

Although EUS has become an established procedure during the last 20 years, real-time contrast applications using a low mechanical index (MI) have been limited to the transabdominal approach. Recent advances in technology have allowed the development of new endoscopic systems, making it possible to use low MI contrast-enhanced imaging techniques (wide-band harmonic imaging using endoscopic ultrasonography is currently at a preliminary stage).

During the arterial phase of about 10–20 s, it is possible to characterize the celiac trunk, common hepatic artery, and splenic artery as arterial target vessels. It is also possible to demonstrate the portal vein and its branches, as well as collaterals, in patients with portal vein thrombosis. In contrast to angiographic imaging, parenchymal enhancement was only possible in patients who did not have underlying liver disease. The enhancement was strongest and homogeneous in a band of approximately 2–4 cm around the level of the focal zone. No significant bubble destruction was visualized. This method is limited by a depth of penetration of just over 50 mm, due to higher harmonic frequency ranges used. As with all new methods, a learning curve needs to be taken into account, since steady and targeted transducer manipulation is a prerequisite for optimal image documentation [1] (Fig. 22.**5**).

■ Lymph Nodes

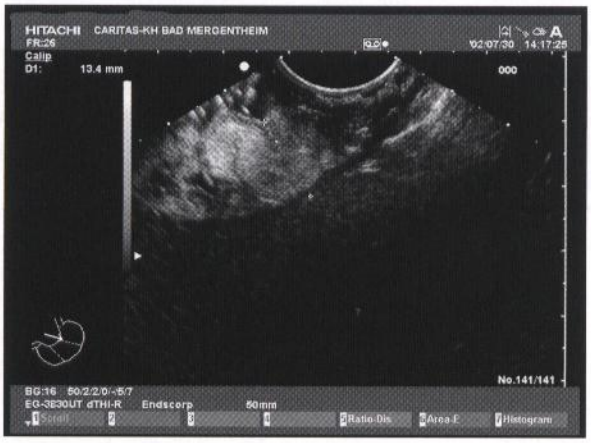
Contrast-enhanced endoscopic ultrasound is particularly important for assessing malignancy in mediastinal or abdominal lymph nodes (Figs. 22.**6**–22.**8**). It has been shown in case reports that malignant infiltration of regional lymph nodes can be better imaged and aspirated with guidance from endoscopic ultrasound. Analysis of the vascular structure has proved to be useful here, as lymph nodes are normally fed by arteries through their sinus and drained correspondingly by veins. These changes can also be corroborated by the histopathology. When the vessel invasion extends beyond the capsule, it should be assumed that the infiltration of the lymph node is malignant, although this criterion has not yet been sufficiently evaluated in the current literature. The criteria for size, shape, and echo pattern analysis that have been described are ambiguous in many cases. Unfortunately, research to date has not yet demonstrated any clear superiority for contrast-enhanced analysis of the vascular distribution in determining whether the enlargement of lymph nodes is benign or malignant. An as yet unpublished study on this issue analyzed the vascularization tendencies in various lymph nodes before and after contrast administration and verified the results by carrying out fine-needle aspiration immediately after the examination. A total of 63 patients were included in the study. Using normal endoscopic ultrasound diagnosis, 24 of 29 cases of benign lymph-node enlargement were correctly identified (specificity 82.7%); after contrast administration, this increased to 27 of the 29 cases (a specificity of 93.1%). Twenty-seven



a



b



c

Fig. 22.**5a–c** Wide-band harmonic imaging. The first images using contrast-enhanced low mechanical index wide-band harmonic imaging equipment produced very promising results. The circulation surrounding a portal vein thrombosis is visible in a contrasted image.



a



b

Fig. 22.**6** Ventral and dorsal imaging of the perihepatic lymph-node group in the hepatoduodenal ligament in a patient with suspected lymphoma. **a** B-mode sonography showed lymph nodes enlarged to 43 mm in the direct vicinity of the common hepatic artery and portal vein. **b** No relevant vessels were identified on color duplex sonography.

Fig. 22.**6c–f** ▷

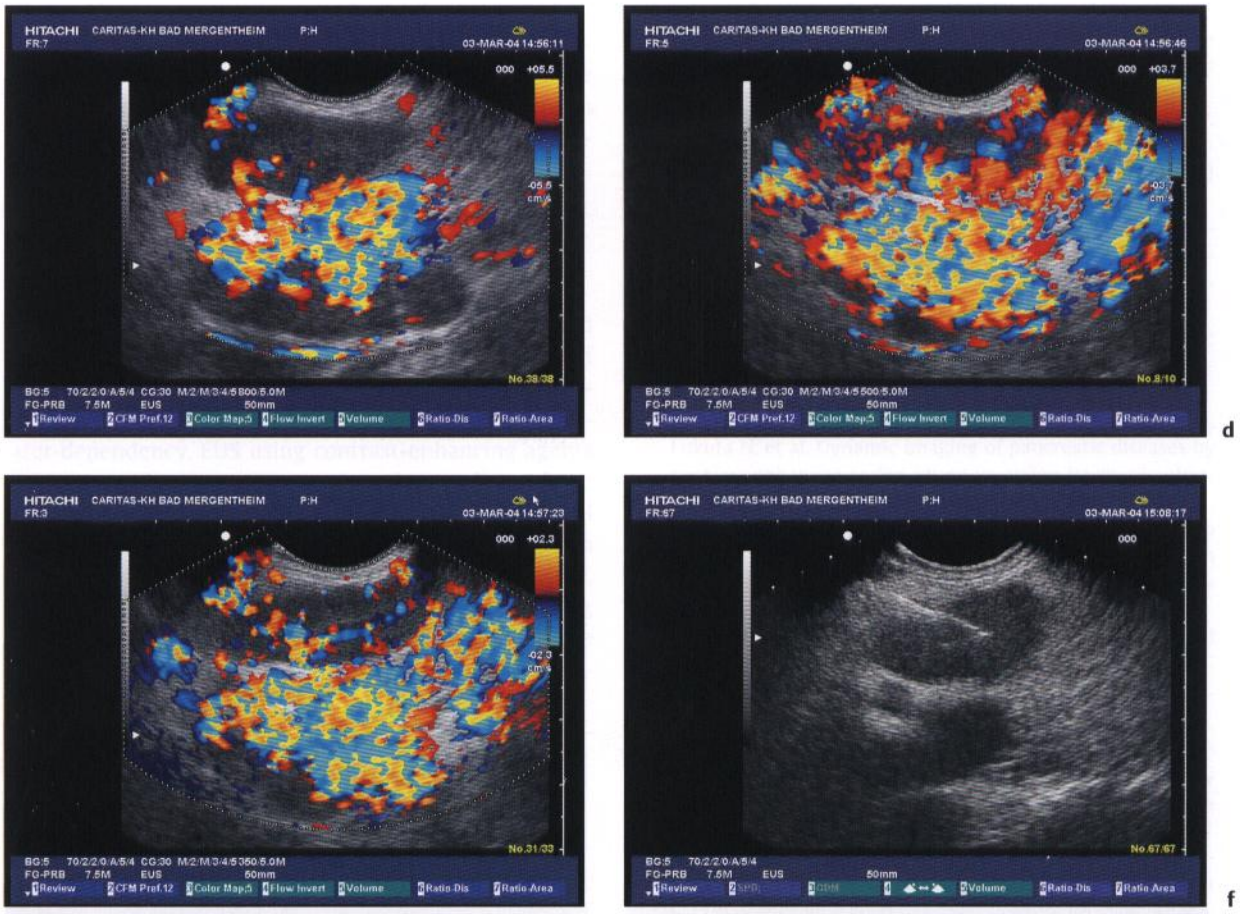


Fig. 22.**6c–e** After administration of the contrast agent SonoVue, the lymph-node sinus is clearly recognizable both ventrally and dorsally in the hepatoduodenal ligament, with no damaged vascular structure or localized infiltration. **f** Endoscopic ultrasound-guided fine-needle aspiration demonstrated granulomatous inflammation qualified by a hepatic manifestation of sarcoidosis.

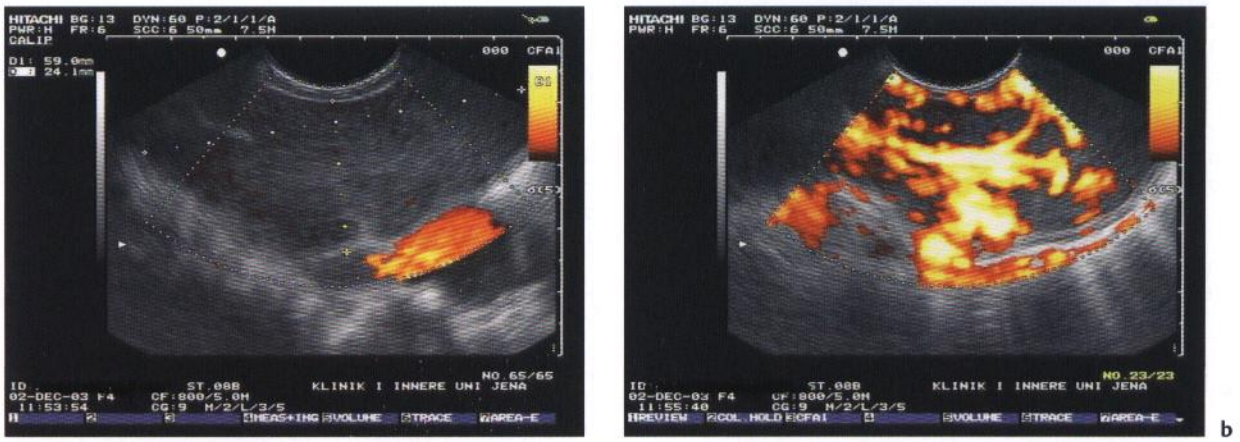
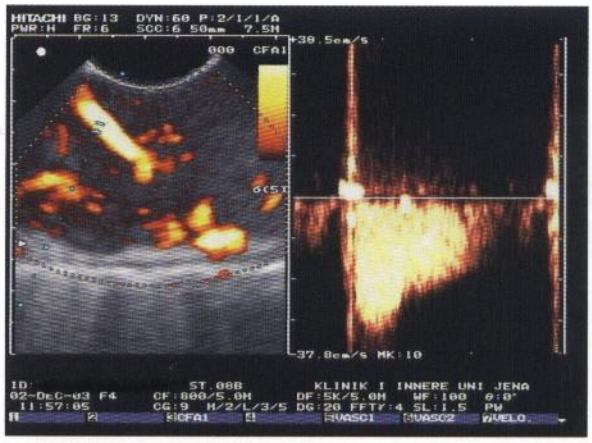


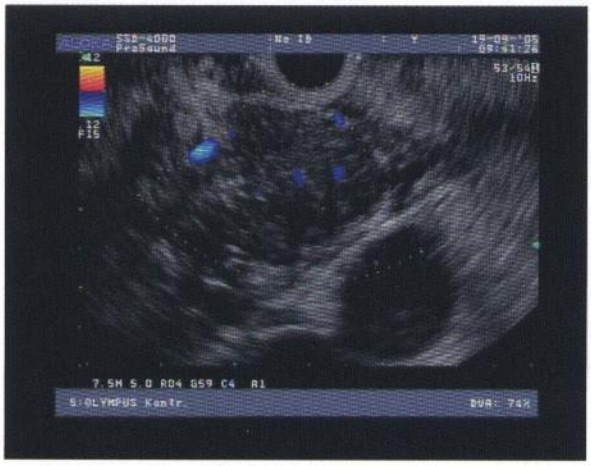
Fig. 22.**7a–c** Another example of sarcoidosis before and after contrast administration. Note the preserved lymph node architecture.

Fig. 22.**7c** ▷



c

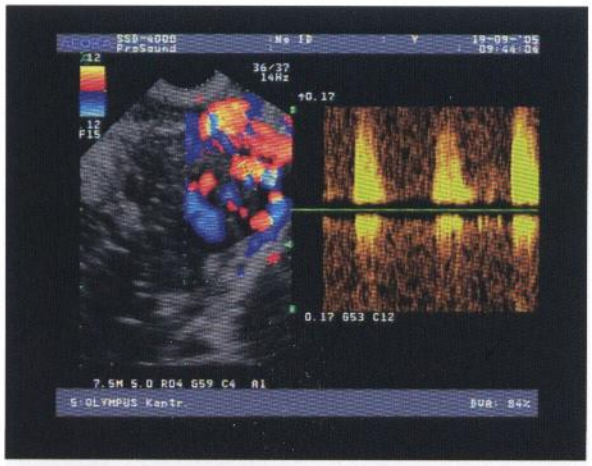
Fig. 22.**7c** Another example of sarcoidosis before and after contrast administration. Note the preserved lymph node architecture.



a



b



c

Fig. 22.**8** A malignant lymph node before and after contrast administration. The vascular distribution is not regular, and only arterial vessels are seen.

of 34 malignant lymph nodes were correctly diagnosed with normal endoscopic ultrasound (sensitivity 73.5%). However, when the criteria for vascularization assessment after the introduction of contrast enhancer were taken into account, the results deteriorated to 22 of 34 cases (sensitivity 64.7%). The majority of false-positive findings with contrast-enhanced endosonography were malignant lymphomas (n = 6). Using this technique, no difference was observed in the vascular lymph-node pattern between benign lymph nodes and lymph-node enlargements caused by malignant lymphomas, and this was the problem that mainly led to the poor results.

These data suggest contrast-enhanced assessment of lymph nodes is not capable of improving visual differentiation between malignant and benign lymph-node enlargements. However, further trials would be useful in order to define the criteria for differentiation more precisely.

Prospects

Ultrasonography is currently the most commonly used imaging modality in many countries. The advantages of endoscopic ultrasonography (e.g., lack of radiation exposure and relatively low cost) are limited by its operator-dependency. EUS using contrast-enhancing agents might be able to improve our understanding of the morphological imaging methods by allowing additional analysis of functional criteria such as perfusion, with better characterization of tumors, lymph-node staging, and organ infiltration, for example. Improved imaging documentation of this type would improve confidence in the sonographic method. Other possible new applications might be lymph-node biopsies guided by contrast-enhanced imaging, with demarcation of the infiltrated site even in small lymph nodes.

References

1. Dietrich CF, Ignee A, Frey H. Contrast-enhanced endoscopic ultrasound with low mechanical index: a new technique. Z Gastroenterol 2005;43:1219–23.
2. Harvey CJ, Blomley MJ, Eckersley RJ, Heckemann RA, Butler-Barnes J, Cosgrove DO. Pulse-inversion mode imaging of liver specific microbubbles: improved detection of subcentimetre metastases. Lancet 2000;355:807–8.
3. Blomley M, Albrecht T, Cosgrove D, Jayaram V, Patel N, Butler-Barnes J, et al. Stimulated acoustic emission imaging ("sono-scintigraphy") with the ultrasound contrast agent Levovist: a reproducible Doppler ultrasound effect with potential clinical utility. Acad Radiol 1998;5(Suppl 1): S236–9.
4. Dietrich CF, Ignee A, Trojan J, Fellbaum C, Schuessler G. Improved characterisation of histologically proven liver tumours by contrast enhanced ultrasonography during the portal venous and specific late phase of SHU 508A. Gut 2004;53:401–5.
5. Dietrich CF. [3D real time contrast enhanced ultrasonography: a new technique; in German.] Röfo Fortschr Geb Rontgenstr Neuen Bildgeb Verfahr 2002;74:160–3.
6. Bhutani MS, Hoffman BJ, van Velse A, Hawes RH. Contrast-enhanced endoscopic ultrasonography with galactose microparticles: SHU 508A (Levovist). Endoscopy 1997;29: 635–9.
7. Hocke M, Schulze E, Gottschalk P, Topalidis T, Dietrich CF. Contrast-enhanced endoscopic ultrasound in discrimination between focal pancreatitis and pancreatic cancer. World J Gastroenterol 2006;12:246–50.
8. Rickes S, Unkrodt K, Ocran K, Neye H, Lochs H, Wermke W. [Evaluation of Doppler ultrasonography criteria for the differential diagnosis of pancreatic tumors]. Ultraschall Med 2000;21:253–8.
9. Rickes S, Unkrodt K, Neye H, Ocran KW, Wermke W. Differentiation of pancreatic tumours by conventional ultrasound, unenhanced and echo-enhanced power Doppler sonography. Scand J Gastroenterol 2002;37:1313–20.
10. Ding H, Kudo M, Onda H, Nomura H, Haji S. Sonographic diagnosis of pancreatic islet cell tumor: value of intermittent harmonic imaging. J Clin Ultrasound 2001;29:411–6.
11. Kitano M, Kudo M, Maekawa K, Suetomi Y, Sakamoto H, Fukuta N, et al. Dynamic imaging of pancreatic diseases by contrast enhanced coded phase inversion harmonic ultrasonography. Gut 2004;53:854–9.
12. Hirooka Y, Goto H, Ito A, Hayakawa S, Watanabe Y, Ishiguro Y, et al. Contrast-enhanced endoscopic ultrasonography in pancreatic diseases: a preliminary study. Am J Gastroenterol 1998;93:632–5.
13. Becker D, Strobel D, Bernatik T, Hahn EG. Echo-enhanced color- and power-Doppler EUS for the discrimination between focal pancreatitis and pancreatic carcinoma. Gastrointest Endosc 2001;53:784–9.
14. Kasono K, Hyodo T, Suminaga Y, Sugiura Y, Namai K, Ikoma A, et al. Contrast-enhanced endoscopic ultrasonography improves the preoperative localization of insulinomas. Endocr J 2002;49:517–22.
15. Hyodo T, Hyodo N, Yamanaka T, Imawari M. Contrast-enhanced intraductal ultrasonography for thickened bile duct wall. J Gastroenterol 2001;36:557–9.
16. Hyodo N, Hyodo T. Ultrasonographic evaluation in patients with autoimmune-related pancreatitis. J Gastroenterol 2003;38:1155–61.
17. Hirooka Y, Naitoh Y, Goto H, Ito A, Hayakawa S, Watanabe Y, et al. Contrast-enhanced endoscopic ultrasonography in gallbladder diseases. Gastrointest Endosc 1998;48:406–10.
18. Nomura N, Goto H, Niwa Y, Arisawa T, Hirooka Y, Hayakawa T. Usefulness of contrast-enhanced EUS in the diagnosis of upper GI tract diseases. Gastrointest Endosc 1999;50: 555–60.
19. Sato T, Yamazaki K, Toyota, J et al. Perforating veins in recurrent esophageal varices evaluated by endoscopic color Doppler ultrasonography with a galactose-based contrast agent. J Gastroenterol 2004;39:422–428.
20. Sato T, Yamazaki K, Toyota J et al. Evaluation of hemodynamics in esophageal varices. Value of endoscopic color Doppler ultrasonography with a galactose-based contrast agent. Hepatol Res 2003;25:55–61.

23 Incidental Findings in the Surrounding Organs (Miscellaneous)

C.F. Dietrich

■ Common Incidental Findings

The term "incidental findings" refers to unexpected findings in the surrounding organs that are not within the typical indications for routine endoscopic ultrasonography (EUS). They are much more common than expected. This chapter discusses incidental findings reported in the author's own publications on transabdominal ultrasonography. I would be most grateful if readers were willing to contribute further case reports on incidental findings for future editions of this book.



Fig. 23.**1** Lung embolism with infarction, discovered incidentally in a patient being examined to exclude a pancreatic mass.

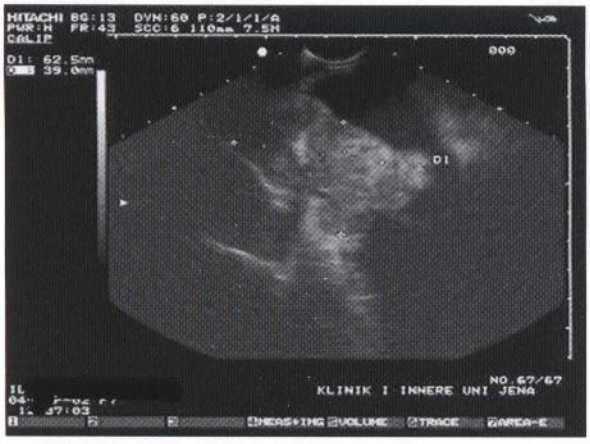


Fig. 23.**2** Angiomyosarcoma of the left atrium, diagnosed by endoscopic ultrasound-guided fine-needle aspiration. (Courtesy of M. Hocke).

Thyroid. The thyroid can be routinely imaged with EUS. Thoracic goiter can be found in many patients with EUS, but parathyroid tumors may be diagnosed in only a few selected patients.

Lung parenchyma. Pleural effusion and lung infarction can be seen using endoscopic ultrasound if the defects are close to the esophagus, or next to the spleen or left liver lobe [1,2]. Changes in the lung parenchyma should be noted even if a systematic examination of the parenchyma does not appear worthwhile (Fig. 23.**1**).

Heart. In individual cases, the potential of EUS can extend much further; we have been able to assess cardiac masses using fine-needle aspiration in two patients, without complications (Fig. 23.**2**). In one of these cases, a paracardiac lipoma with an impression on the left atrium was diagnosed, and in the other an extremely malignant angiomyosarcoma of the left atrium was confirmed, allowing appropriate therapy to be started.

Liver (left liver lobe). The left liver lobe can always be examined (at least in part), whereas only parts of the right liver lobe can be visualized.

Focal hepatic lesions. Typical focal liver lesions seen with endoscopic ultrasound are small subcapsularly located cholangiofibromas and hemangiomas (Figs. 23.**3**, 23.**4**). Liver tumors have the same B-mode and color Doppler imaging characteristics as in transabdominal imaging [3,4] (Figs. 23.**5**–23.**7**).

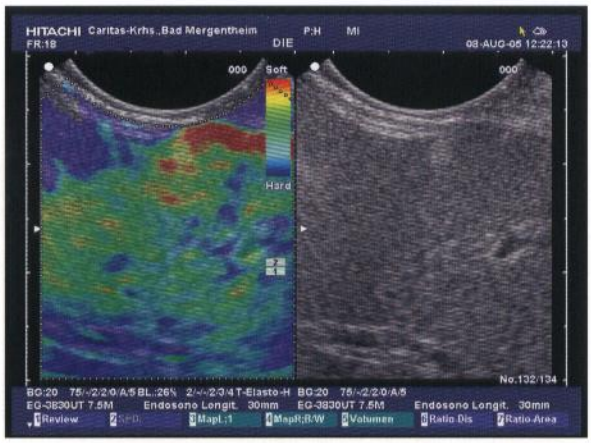
Diffuse liver disease. Diffuse liver disease—e.g., fatty liver with areas of different fatty infiltration around the liver veins, as well as next to the round ligament—can often be displayed in patients who have lost weight due to malignancies, as well as in those receiving corticosteroid treatment and patients with diabetes and many other diseases [5,6] (Fig. 23.**8**).

Perihepatic lymphadenopathy is a typical sign of inflammatory parenchymal liver disease and can be seen in chronic virus hepatitis, primary biliary cirrhosis, primary sclerosing cholangitis, as well as in malignant liver disease. It is important to be aware of this in the differential diagnosis [7–10]. Normal perihepatic lymph nodes < 20 mm in size can be demonstrated in up to 75% of healthy individuals (Fig. 23.**9**).

Gallbladder. The gallbladder can be examined from the duodenal bulb in most cases. Carcinomas of the gallbladder are discussed in Chapter 20. In some cases, an endosonographic diagnosis of adenomyomatosis,



a



b

Fig. 23.**3a** Cholangiofibromas (between the markers) are typically found in a subcapsular location and are less than 10 mm in diameter. **b** On elastography, they show similar elasticity to that of the surrounding liver tissue.



Fig. 23.**4** Hemangioma. Typical hemangiomas (in this case confirmed histologically, due to a suspected pancreatic malignancy) are found to have afferent vessels on power Doppler sonography.



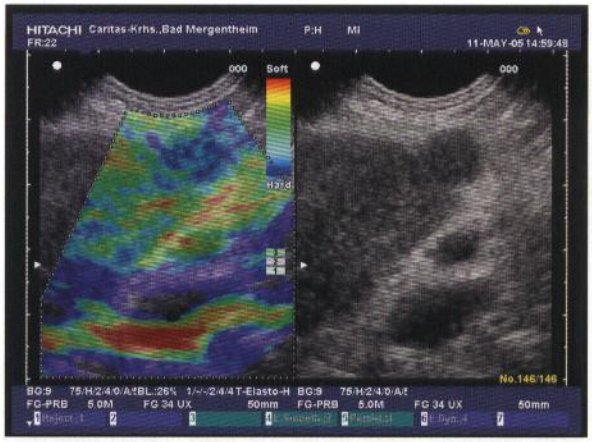
a



b

Fig. 23.**5** Liver metastases. **a** Small liver metastases may only be visible with EUS, particularly in patients with pancreatic cancer patients who are being examined for staging purposes. **b** Lesions in a subdiaphragmatic location are particularly difficult to identify with computed tomography and magnetic resonance imaging.

Fig. 23.**5c, d** ▷



c

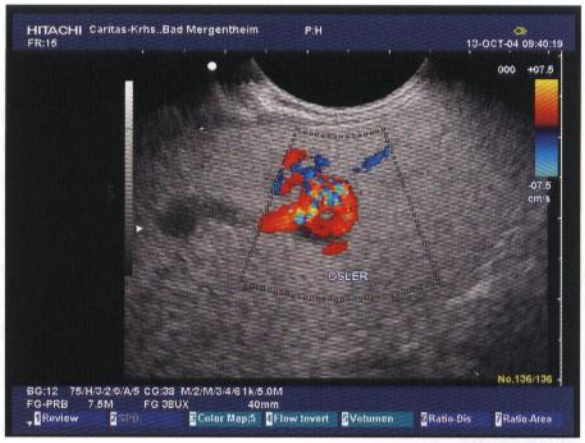


d

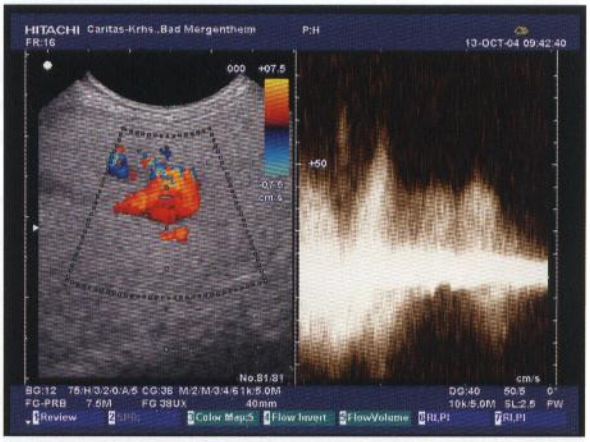
Fig. 23.**5c** The differences in elasticity displayed with elastography in a small exophytic metastasis should be noted. **d** Diffuse malignant infiltration can be demarcated using elastography.



a



b

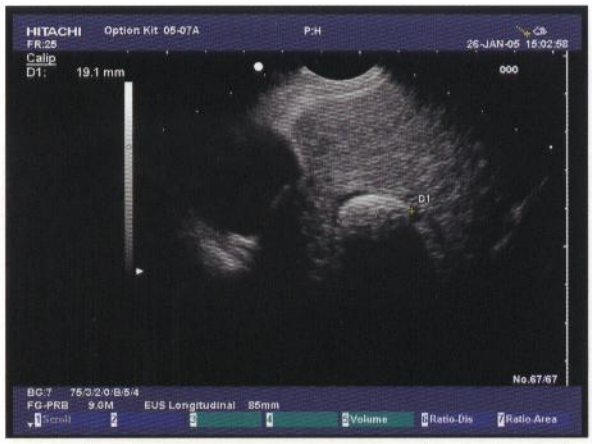


c

Fig. 23.**6a** Osler's disease should be suspected in patients with atypical cysts; color Doppler imaging (**b**) and continuous duplex scanning (**c**) are helpful in the diagnosis.



a



b

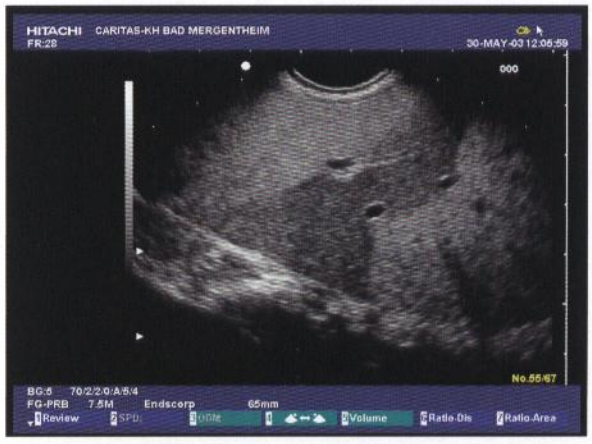
Fig. 23.**7** Caroli's disease. The differential diagnosis of cystic lesions with debridement (**a**) and calcifications (**b**) includes Caroli's disease.



a



b



c

Fig. 23.**8a** Fatty liver with areas of different fatty infiltration can mimic liver tumors. **b, c** Typically, the hepatic architecture is not destroyed.



a b

Fig. 23.**9** Normal perihepatic lymph nodes < 20 mm in size can be demonstrated in up to 75% of healthy individuals. The regular architecture of the lymph-node sinus next to the common hepatic artery (AHC) should be noted. **a** B-mode. **b** Color Doppler imaging.



a b

Fig. 23.**10a** Cholecystolithiasis is easily demonstrated using EUS, particularly in patients with microlithiasis (see also Chapter 20). **b** More confusing images result in patients with aerobilia.

cholesterol polyps, microgallbladder [11], and other forms of gallbladder pathology (e.g., cholecystolithiasis) can be made, although there is no indication for endosonography in these differential diagnoses (Figs. 23.**10**, 23.**11**). As in other tumors of the upper gastrointestinal tract, a definite endosonographic distinction between inflammatory and neoplastic alterations or changes in connective tissue is not possible.

Kidney, urogenital system. The upper pole of the left kidney can be visualized in almost all patients (see Chapter 21). Landmarks for correct identification of the cranial pole of the left kidney are the aorta, the pancreatic tail, the splenic vessels, and the left adrenal gland. Typically, after entering the stomach, the transducer should be kept toward the left posterior gastric wall, showing a variable section of the abdominal aorta at 45 cm; slightly more caudally, the upper pole of the left kidney is seen. In some cases, the kidney and ureter can also be seen by positioning the transducer in the ascending part of the duodenum—a route that is used in only a few patients (Figs. 23.**12**–23.**14**).

Retroperitoneum. Incidental findings of enlarged retroperitoneal lymph nodes may be found in particular in patients with asymptomatic lymphoma, tuberculosis, and many other diseases (Fig. 23.**15**).

Spleen. The spleen can be visualized by identifying the aorta, pancreatic tail, splenic vessels, cranial pole of the left kidney, and left adrenal gland (Figs. 23.**16**, 23.**17**). Typically, after entering the stomach, the transducer should be kept toward the left posterior gastric wall, showing a variable section of the abdominal aorta at 45 cm; slightly more caudally, the upper pole of the left kidney is seen. In this partly inverted position, the endoscope has to be pushed forward into the gastric fundus.

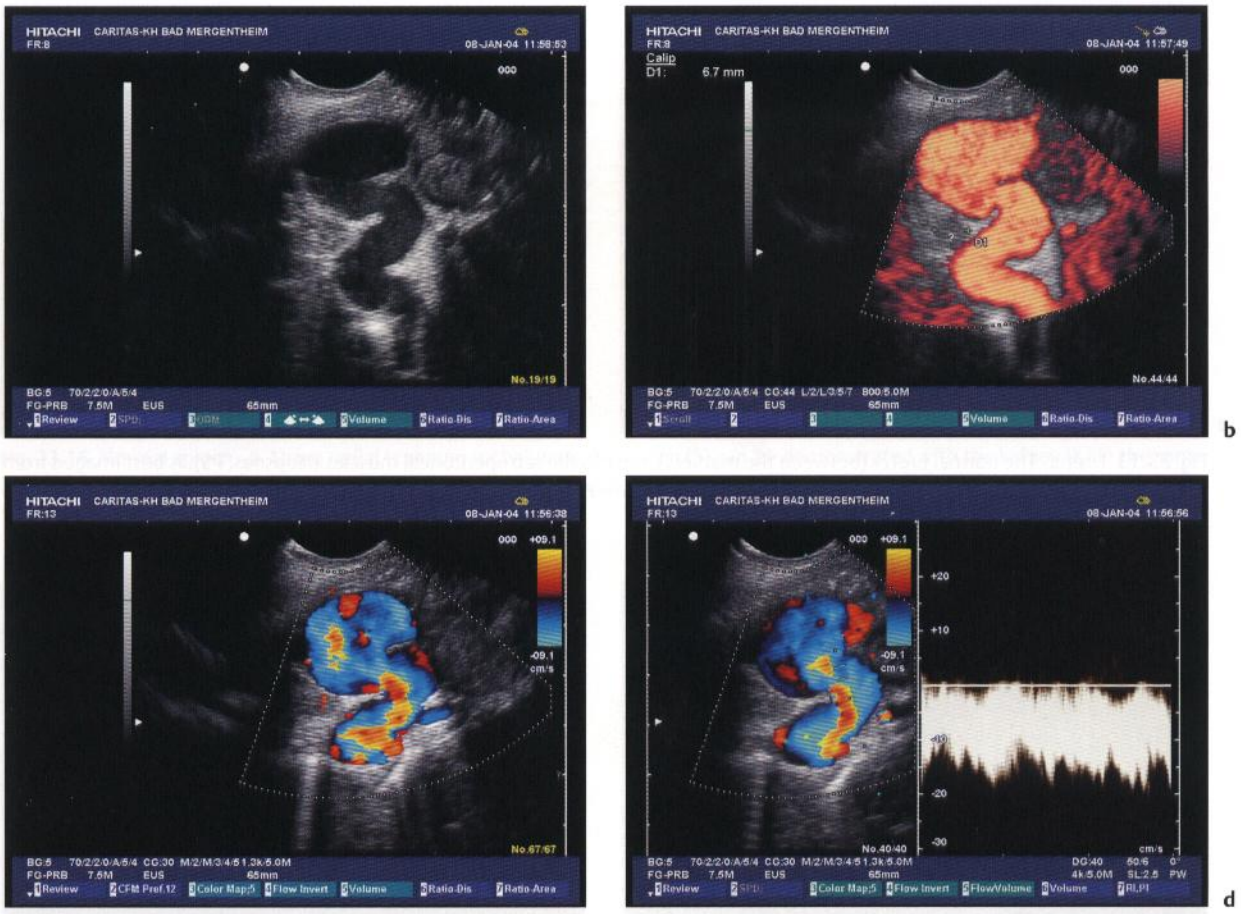
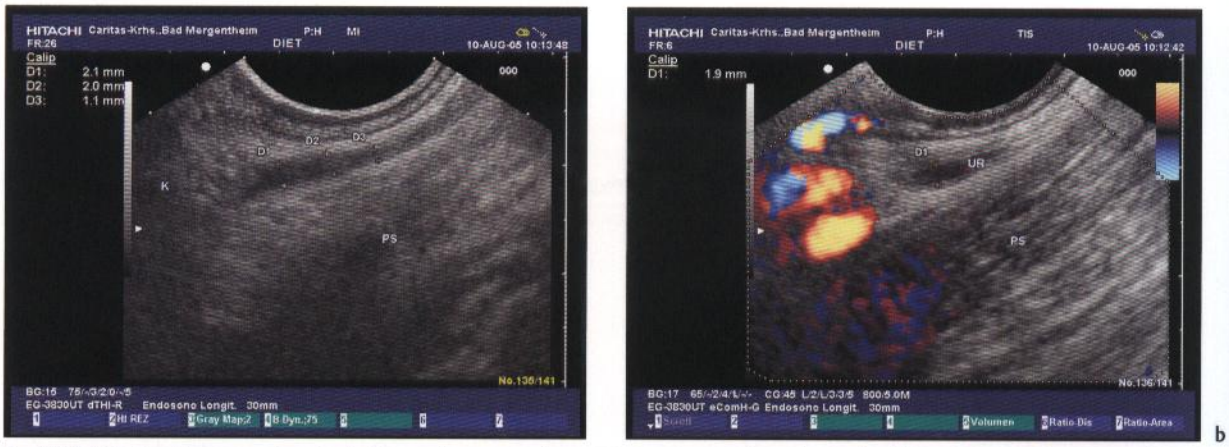


Fig. 23.**11** Perihepatic varices. **a** Large varices and Cruveilhier–Baumgarten syndrome produce confusing images when B-mode imaging is used **b–d** Power Doppler (**b**), color Doppler (**c**), and coded duplex scanning (**d**) are helpful for defining the underlying vessels.

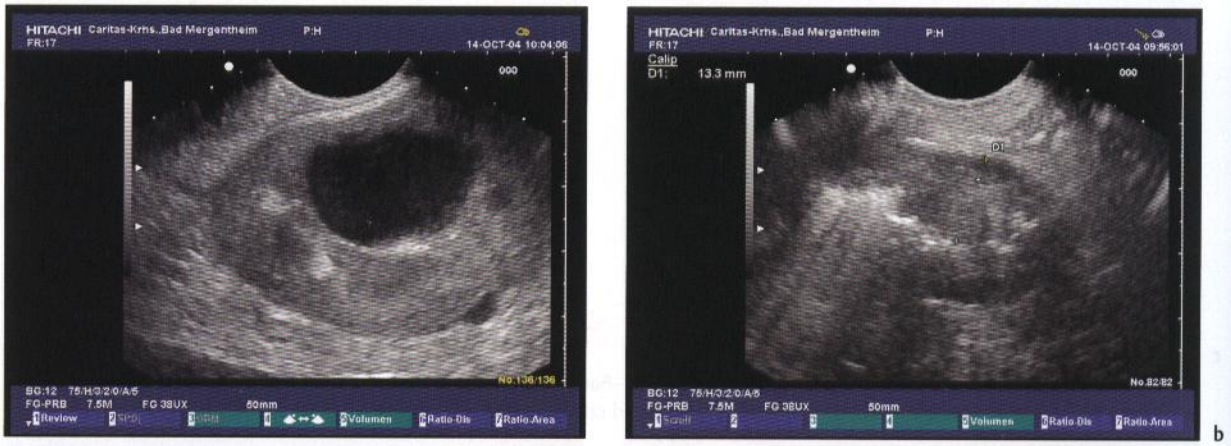


Fig. 23.**12** The most common findings in the kidney are parenchymal cysts (**a**) and physiological sinus pyelectasia (**b**). NBKS: renal sinus; DD: small intestine.



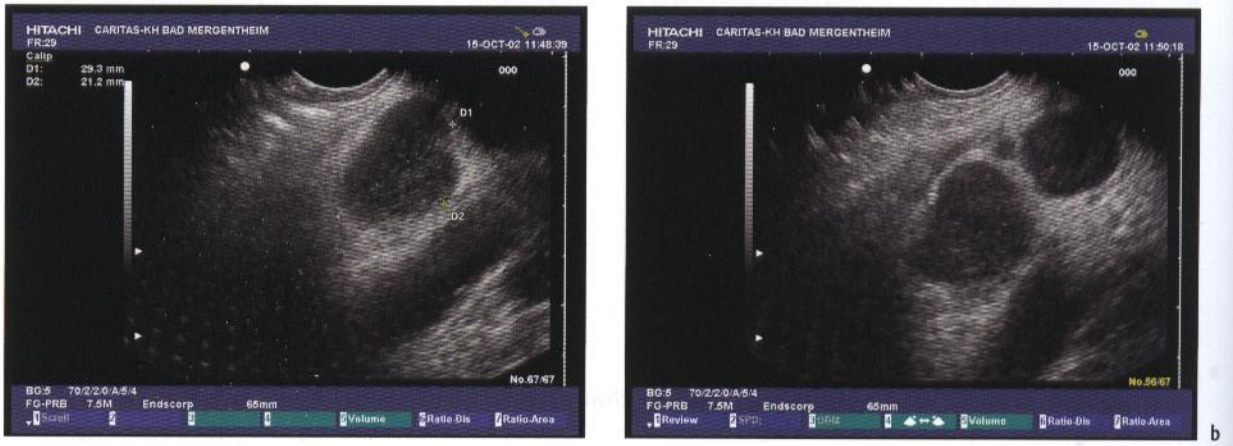
a b

Fig. 23.**13** Ureter. The normal ureter (between the markers), next to the retroperitoneal muscles (iliopsoas, PS), is best imaged from the ascending duodenum. **a** B-mode imaging. **b** Color Doppler imaging. K: kidney; UR: ureter.



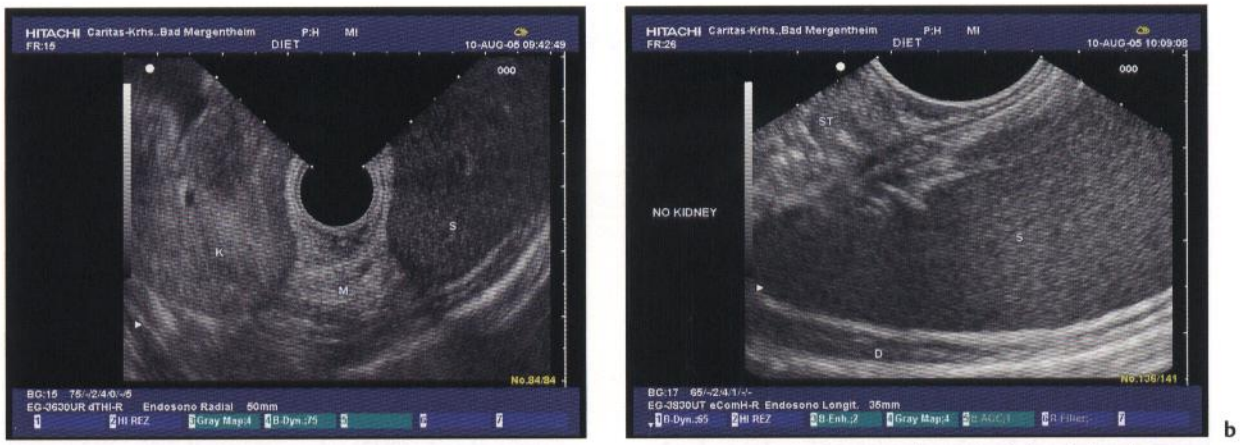
a b

Fig. 23.**14a** An incidental finding of hydronephrosis. **b** This was misinterpreted as a centrally located cyst, due to colorectal carcinoma in the left colon. In a few patients, incidental EUS findings may be diagnostic.



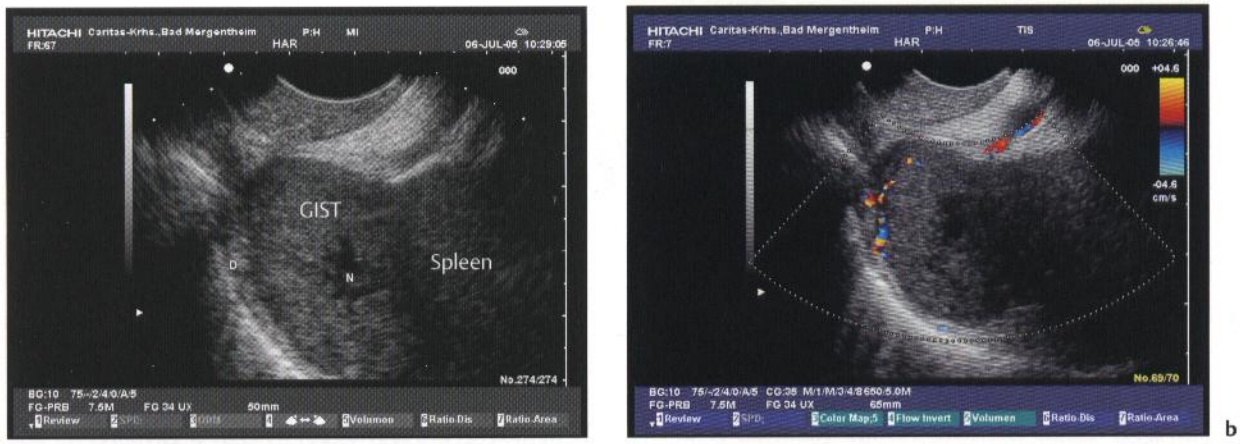
a b

Fig. 23.**15a, b** An incidental finding of non-Hodgkin's lymphoma.



a b

Fig. 23.**16** Normal spleen. **a** Using radial scanning techniques, the spleen (S) can be demonstrated with the kidney (K) in the same image, separated by the stomach (M). **b** The image obtained with the longitudinal technique differs. D: diaphragm; ST: stomach; S: spleen.



a b

Fig. 23.**17a** A gastrointestinal stromal tumor (GIST) infiltrating the spleen is seen in B-mode. D: diaphragm; N: central necrosis. **b** Infiltration of the diaphragm is visible with color Doppler imaging.

Peritoneum. Peritoneal carcinosis can be visualized using EUS, but the clinical value of this has not been determined. EUS-guided fine-needle aspiration is helpful in the final diagnosis (Fig. 23.**18**).

Small intestine. The same principles as in EUS of the esophagus and stomach are applied in the small bowel. Due to the difficult diagnosis of diseases of the small intestine, the value of EUS is variable. Examples (e. g., Osler's disease of the small intestine) are discussed in Chapter 20 (Fig. 23.**19**) [12–14].



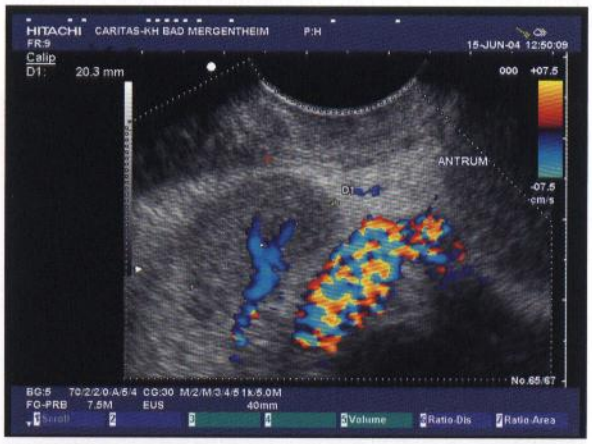
Fig. 23.**18** Peritoneal carcinosis (P CA) can be visualized using EUS.



a



b



c

Fig. 23.**19a** Vasculitis of the small intestine is typically diagnosed due to edema of the circular folds of the small intestine (Kerckring folds) [12–14]. **b** It may also be evident from enlarged peri-intestinal lymph nodes, with a normal architecture. **c** However, it can also present in the form of tumor-like lesions due to necrosis.

References

1. Dietrich CF, Hirche TO, Schreiber D, Wagner TO. [Sonographie von Pleura und Lunge; in German.] Ultraschall Med 2003;24:303–11.
2. Hirche TO, Wagner TO, Dietrich CF. [Mediastinal ultrasound: technique and possible applications; in German.] Med Klin (Munich) 2002;97:472–9.
3. Dietrich CF, Ignee A, Trojan J, Fellbaum C, Schuessler G. Improved characterisation of histologically proven liver tumors by contrast enhanced ultrasonography during the portal venous and specific late phase of SHU 508A. Gut 2004;53:401–5.
4. Dietrich CF. Characterisation of focal liver lesions with contrast enhanced ultrasonography. Eur J Radiol 2004;(51 Suppl):S9–17.
5. Dietrich CF, Wehrmann T, Zeuzem S, Braden B, Caspary WF, Lembcke B. [Analysis of hepatic echo patterns in chronic hepatitis C; in German.] Ultraschall Med 1999;20:9–14.
6. Dietrich CF, Schall H, Kirchner J, Seifert H, Herrmann G, Caspary WF, et al. Sonographic detection of focal changes in the liver hilus in patients receiving corticosteroid therapy. Z Gastroenterol 1997;35:1051–7.
7. Dietrich CF, Stryjek-Kaminska D, Teuber G, Lee JH, Caspary WF, Zeuzem S. Perihepatic lymph nodes as a marker of antiviral response in patients with chronic hepatitis C infection. AJR Am J Roentgenol 2000;174:699–704.
8. Dietrich CF, Zeuzem S. [Sonographic detection of perihepatic lymph nodes: technique and clinical value; in German.] Z Gastroenterol 1999;37:141–51.
9. Dietrich CF, Lee JH, Herrmann G, Teuber G, Roth WK, Caspary WF, et al. Enlargement of perihepatic lymph nodes in relation to liver histology and viremia in patients with chronic hepatitis C. Hepatology 1997;26:467–72.
10. Hirche TO, Russler J, Braden B, Schuessler G, Zeuzem S, Wehrmann T, et al. Sonographic detection of perihepatic lymphadenopathy is an indicator for primary sclerosing cholangitis in patients with inflammatory bowel disease. Int J Colorectal Dis 2004;19:586–94.
11. Dietrich CF, Chichakli M, Hirche TO, Bargon J, Leitzmann P, Wagner TO, et al. Sonographic findings of the hepatobiliary-pancreatic system in adult patients with cystic fibrosis. J Ultrasound Med 2002;21:409–16.
12. Dietrich CF, Lembcke B, Seifert H, Caspary WF, Wehrmann T. [Ultrasound diagnosis of penicillin-induced segmental hemorrhagic colitis; in German.] Dtsch Med Wochenschr 2000;125:755–60.
13. Dietrich CF, Brunner V, Seifert H, Schreiber-Dietrich D, Caspary WF, Lembcke B. [Intestinal B-mode sonography in patients with endemic sprue: intestinal sonography in endemic sprue; in German.] Ultraschall Med 1999;20:242–7.
14. Dietrich CF, Brunner V, Lembcke B. [Intestinal ultrasound in rare small and large intestinal diseases; in German.] Z Gastroenterol 1998;36:955–70.

24 Endoanal and Endorectal Sonography

M. Sailer, H. Allgayer, C.F. Dietrich

Introduction

Sonographic examination of the perineum, anus and rectum, including the surrounding structures, using intraluminal transducers with transanal/rectal imaging—i.e., endoscopic ultrasonography (EUS)—has become increasingly important in clinical practice during the last 10 years [1,2]. Anal and rectal EUS have been shown to be useful tools in evaluating colorectal, anal, and pelvic disorders, due to the high resolution provided, with clearly distinguishable tissue-dependent echo signals [3,4]. The use of anal and endorectal ultrasonography is now recommended for a wide variety of indications, on the basis of the diagnostic and therapeutic guidelines published by technical review groups in various societies representing specialties and/or subspecialties [5].

Normal Anatomy

EUS is able to image the rectal wall layers and adjacent structures, including the pelvic organs, with a high degree of precision. Detailed knowledge of the anatomy and morphology is needed for correct interpretation of the images provided. Modern intraluminal ultrasound probes make it possible to image the anal and pelvic structures in multiple planes relative to the body axis, providing sagittal, frontal, transverse, and longitudinal sections.

Anatomy of the Perineum and Anus

The anal mucosa and internal anal sphincter (IAS) muscle are considered to represent the continuation of the inner rectal ring muscle. They form the innermost structures and can be visualized from the anal lumen. The hyperechoic longitudinal fibers of the corrugator ani muscle are regarded as an extension of the exterior rectal longitudinal muscle. The levator ani muscle is located at the cranial edge of the external anal sphincter (EAS) muscle, which has a funnel-like shape and forms the muscular floor of the pelvis. The funnel-like structure of the levator ani separates the extraperitoneal pelvis from the infraperitoneal and the pelvirectal space. The lateral region corresponds to the obturator internus muscle. The deep transverse perineal muscle and superficial transverse perineal muscle, as well as the ischiocavernous muscle, can also be imaged with EUS. The transverse orientation is the one most commonly used, and it can be varied depending on the height and angle of the corresponding sections (Figs. 24.**1**–24.**11**).

Anal canal. The echogenicity of the various mural layers in the anal canal is very similar to that in the rest of the gastrointestinal tract and is characterized by various well-distinguishable bands when imaged from the lumen. The anal canal is covered with columnar epithelium below the anal crypts. The mucosa is a transitional-cell epithelium and starts at the level of the anal crypts; however, it can only be visualized irregularly as a faintly dark layer with scattered echoes of medium density. The transitional epithelium disappears in the first echodense border area, depending on the type of ultrasound probe used and the frequency being used.

The pectinate line and the crypts are often not visible, mainly due to compression of the anal canal by the endorectal probe. The submucosa and subcutaneous connective tissue appear as a homogeneous echogenic layer, increasing in thickness from the superior to the inferior margin of the anal canal. The rectal venous plexus is normally almost invisible unless very thin probes are used. The IAS can regularly be seen as a



a

Fig. 24.**1a–f** Views of the internal anal sphincter (IAS) as the principal structure at the first level from anal to oral, with six horizontal sections a few millimeters long, which should be seen as a continuum. **a** The subcutaneous part of the external anal sphincter muscle is seen as a strong hyperechoic ring. At this level, the IAS is not visible.

Fig. 24.**2b–f** ▷



b



c



d



e



f

Fig. 24.**1b–d** A hypoechoic inner ring (the IAS) is seen, accompanied by an outer hyperechoic ring representing the external anal sphincter (EAS), with the superficial part initially and the deep part following. LM: longitudinal muscle (the corrugator cutis muscle of the anus); RVP: rectal venous plexus; SM: submucosa.



Fig. 24.**2** The subcutaneous part of the external anal sphincter muscle, seen as a strong hyperechoic ring. At this level, the IAS is not visible.



Fig. 24.**3** A hypoechoic inner ring (the IAS), accompanied by the superficial part of the external anal sphincter (the outer hyperechoic ring).



Fig. 24.**4** A strong puborectal sling is seen here, which is hyperechoic like all the striated muscles in the external anal sphincter, in contrast to the internal anal sphincter, which is seen as a hypoechoic ring internal to the puborectal sling.



Fig. 24.**5** The inner hypoechoic ring is formed by the smooth muscle of the internal anal sphincter. There is also an outer hyperechoic ring, representing the strong and circumferentially intact external anal sphincter (striated muscle).

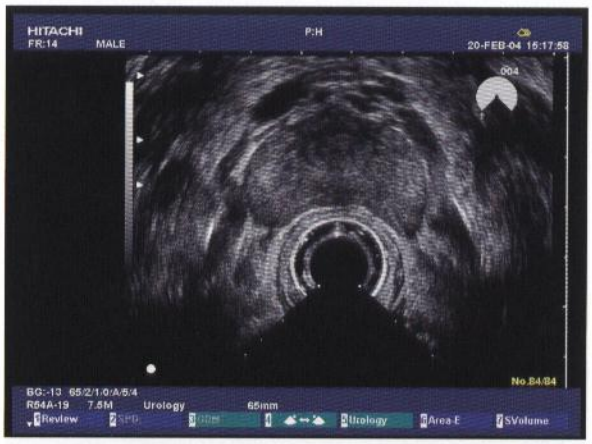


Fig. 24.**6** The normal prostate gland, situated ventrally. This is a useful landmark during routine endorectal ultrasound examinations.



Fig. 24.**7** Normal seminal vesicles, situated cranial to the prostate gland. The moustache shape and symmetry of the structure should be noted.



Fig. 24.**8** A normal pear-shaped uterus, with slight deviation to the left. This is a useful landmark during routine endorectal ultrasound examinations in female patients.



Fig. 24.**9** The normal vagina, situated ventrally between the bladder (the echo-free urine-filled structure above the vagina) and the rectum. Typically, a three-layer morphology is seen, with a fine hyperechoic inner layer.



a



b

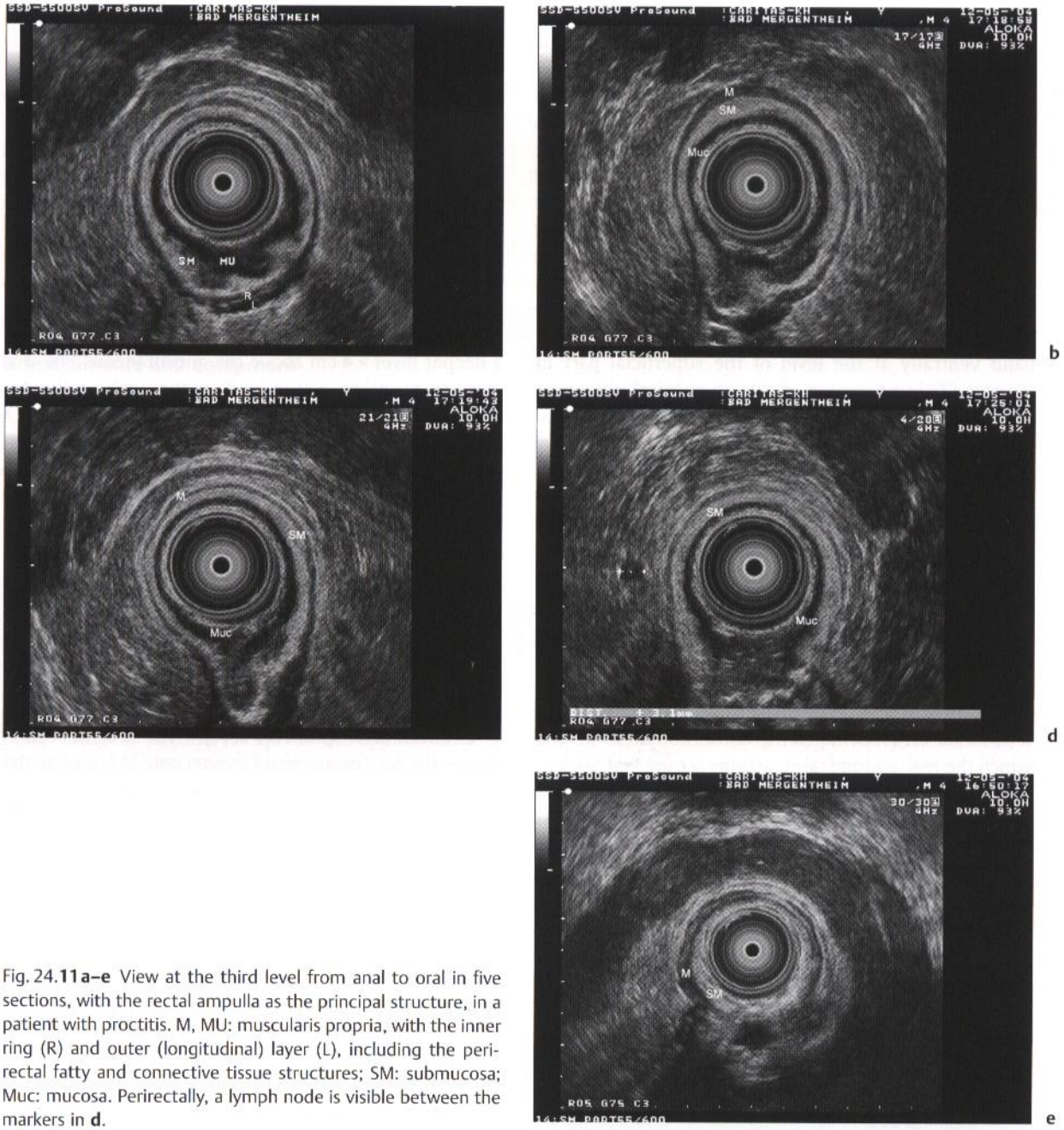


c

Fig. 24.**10a–c** Views of the external anal sphincter (EAS) at the second level from anal to oral, in three sections at very short distances from each other. IAS: internal anal sphincter (seen less prominently); Muc: mucosa; PRM: puborectal muscle and perirectal fatty and connective tissue (i. e., mesorectum); SM: submucosa.

homogeneous hypoechoic layer with a thickness of 2–4 mm, with no significant sex-dependent differences. However, the thickness measured depends on the probes used, as larger probe diameters lead to thinning of the surrounding structures [6]. The echodensity and thickness of the IAS tend to increase with age. However, the normal thickness does not exceed 4 mm even in the elderly. The intersphincteral space, with fibers of the corrugator muscle as a continuation of the rectal longitudinal muscle, is seen endosonographically as a thin hypoechoic layer containing hyperechoic connective-tissue septa, representing the border areas of the hypoechoic IAS and the first less echogenic layer in the EAS. It can be identified at about 2 cm from the anocutaneous line. At this level, the ischioanal fossa, anococcygeal ligament, and coccyx can be visualized, provided that appropriate acoustic penetration is produced.

Adequate differentiation is possible in the hyperechoic border area between the ultrasound probe and the mucosa (or the anal cutis): the hypoechoic, ex-



a b c d e

Fig. 24.**11a–e** View at the third level from anal to oral in five sections, with the rectal ampulla as the principal structure, in a patient with proctitis. M, MU: muscularis propria, with the inner ring (R) and outer (longitudinal) layer (L), including the perirectal fatty and connective tissue structures; SM: submucosa; Muc: mucosa. Perirectally, a lymph node is visible between the markers in **d**.

tremely thin mucosa, which often cannot be recognized as a defined layer, due to a lack of the muscularis and its very thin diameter; the hyperechoic submucosa (and subcutis); and the hypoechoic IAS, with the adjacent partly hypoechoic and partly hyperechoic intersphincteral space corresponding to the corrugator ani muscle.

The EAS contains connective-tissue fibers in increasing amounts toward its distal section and appears as a layer 5–10 mm wide with irregular echo patterns and a series of concentrically bright and gray echo lines, depending on the ultrasound resolution power and, in relation to the thickness, the probe diameter. The EAS continues into the puborectalis muscle at the cranial margin of the anal canal. This part of the puborectalis muscle, with its more echogenic patterns, is only identifiable by its course. More orally, the muscular structures are no longer imaged vertically, so that this part of the muscle produces a weaker and less defined image. Ventrally, this broad muscle layer reaches the inferior part of the pubic bone, with inclusion of the urethra and the inferior part of the prostate or vagina. This typical configuration can be seen in the transverse section at 3 cm from the anocutaneous line between the 10-o'clock and 2-o'clock positions, with visualization of the ure-

thra, prostate, inferior pubic ramus, levator ani muscle (puborectalis muscle), EAS, and ischioanal fossa and pelvirectal fossa.

The EAS consists of three more or less separate parts: the subcutaneous part, the superficial part, and the deep part. It is of great importance to understand that the shape and configuration of the EAS differs significantly between males and females. The anal canal is generally 0.5–1.0 cm longer in males, and the three different parts of the EAS are configured cylindrically around the anus, which means that the muscle shape and length are roughly the same ventrally and dorsally. In contrast, the three sections of the EAS are fused into a narrow band ventrally at the level of the superficial part in females [7,8]. Awareness of this anatomical difference is very important in order not to misinterpret normal anatomical findings.

The subperitoneal/pelvirectal layer and the subcutaneous and ischiorectal space are confluent relative to each other. The remaining muscles forming the levator ani muscle (the coccygeus muscle, iliococcygeus muscle, and pubococcygeus muscle) are identifiable with EUS only to a limited extent, but can be seen as an inhomogeneous, mostly hyperechoic layer with increasing cranial distance to the rectal wall.

It is important to appreciate that the hyperechoic structures are not directly imaged, but instead represent ultrasound artifacts indicating borderline areas behind which the real anatomical structures are imaged, such as the mucosa and muscularis propria—especially when older ultrasound equipment is used. In addition, it is also clinically relevant to note that these two hypoechoic structures are important in the staging of rectal cancers in accordance with the TNM classification.

Table 24.1 Endoscopic ultrasound delineation of anorectal muscles

- Internal anal sphincter muscle
- External anal sphincter muscle
  - Subcutaneous part
  - Superficial part
  - Deep part
- Levator ani muscle
- Obturator internus muscle
- Deep and superficial transverse perineal muscle
- Ischiocavernous muscle

Table 24.2 Normal sphincter values (highly dependent on age, sex, and probe diameter)

Muscle	Depth
Internal anal sphincter	1.5–4.0 mm
External anal sphincter	5–10 mm

Endosonographic Imaging at Different Anatomical Levels

The anatomical relationship between the IAS, levator ani, and ischioanal/iliorectal fossa can only be reconstructed if the operator is sufficiently familiar with the anatomy and has a good spatial imagination. Reproducible documentation and visualization in a single image are only possible with the aid of longitudinal sonographic sections through the anal canal. Systematic and comprehensive categorization can be achieved formally by producing corresponding sections at a superficial level at 0–2 cm, at a second level at 2–4 cm, and at a deeper level > 4 cm above the anocutaneous line. For learning purposes, a step-by-step approach centimeter by centimeter appears helpful.

Internal anal sphincter level. The first section shows the cutis, the transitional epithelium, and the subcutis with the transition to the submucosa, and more orally the IAS surrounded by the transverse perineal muscle and the ischioanal fossa. At this level, the corrugator ani (or longitudinal) muscle, containing hyperechoic connective-tissue fibers, can be distinguished from the IAS, which has weaker echogenicity (i.e., a hypoechoic pattern). Additional points of orientation at this level are the root of the penis with the ischiocavernous muscle and the ramus of the ischium.

External anal sphincter level. The second section shows the less pronounced hypoechoic IAS, and as the principal structure the more prominent EAS with inhomogeneous echo patterns (with a series of concentrically bright and gray areas or lines); more in the distance and posteriorly, the coccyx and coccygeal ligament (the dural part of the filum terminale) are seen. The anorectal muscles delineated with ultrasound are listed in Table 24.1, and normal sphincter values are listed in Table 24.2.

Rectal wall. The third section is at the level of the prostate gland with the urethra; the inferior pubic ramus yields images of the lumen and the variably hyperechoic EAS at an increasing distance, and the transition into the levator ani muscle forming the pelvic floor. The funnel of the levator ani separates the extraperitoneal pelvis into an infraperitoneal or pelvirectal space and a subcutaneous or ischiorectal space. The lateral border corresponds to the obturator internus muscle, with the obturator foramen. At this point, which is distinctly marked by the U-shaped puborectalis, the anal canal terminates and the rectum begins.

The typical ultrasound features of the rectal wall are found above this transition zone. These structures, which appear to have five layers with less sophisticated equipment, consist of the hyperechoic borderline between the probe and the mucosa, the hypoechoic mucosa, the hyperechoic submucosa, the hypoechoic muscularis propria, the hyperechoic serosa, and the border

area to the perirectal fat tissue. More differentiated views are possible with the higher resolution power provided by more advanced equipment. With high-resolution probes, the two parts of the muscularis propria can be differentiated, with a circular layer (inner ring layer) and a longitudinal layer (outer ring layer) separated by a connective tissue-like septum. Further differentiation yields additional layers, such as a superficial layer of the muscularis propria and a deeper one, with a total of up to nine separate ultrasonographically discernible structures.

■ Instruments and Equipment

A transverse section with a 360° transducer is helpful for examining the anal canal, whereas for examining more orally located structures, radial as well as sector scanners can be used. Most modern probes, however, provide 360° transducers, which makes orientation much easier.

Patient preparation. Before rectal/anal EUS is carried out, the patient's history should be carefully noted, with subsequent digital examination, and sigmoidoscopy (rectoscopy, colonoscopy) should be carried out to evaluate potential obstacles (contraindications) and obtain important additional information. No special bowel lavage is needed, except for the application of a cleansing enema 10–20 min before a rectal examination. An enema is not required if only the anal canal is examined (e.g., sphincter evaluation in incontinent patients or patients with anal fistulas). The patient is examined either in the left lateral or the lithotomy position, depending on the examiner's preference. However, reporting of the findings should always use clock points for reference (the pubic symphysis is always at the 12-o'clock position).

Introducing the transducer. Before the ultrasound probe is introduced, a thin layer of jelly is applied to the transducer's outer protective latex cover. The probe itself can either be introduced "blindly," or with the palpating finger, or using a rectoscope (rarely performed). Optimal viewing of the perianal and perirectal processes is achieved when the transducer is directed toward the umbilical region. When lower frequencies are used, a filling balloon may be helpful, but in this case it has to be taken into account that the degree of filling of the water balloon may affect the imaging of the rectal wall and/or pathological processes. Water filling is not required if only the anal region is examined. The rectal wall may be stretched, depending on the extent of the filling, resulting in compression of the single wall layers. Even a tumor can then be overlooked if inappropriate pressure is applied. As in rigid rectoscopy, problems may arise starting at 15 cm above the anocutaneous line. However, there are cases in which viewing with the rigid instrument is already hampered at a level at or just above 10 cm, particularly when the examination is being conducted to search for a tumor. In normal circumstances, the rigid probe can be advanced up to 20 cm above the anocutaneous line.

Examination. The ultrasound examination is carried out during slow, step-by-step withdrawal of the transducer into the anal canal. Orientation is achieved by identifying the principal surrounding structures (bladder, prostate, vagina, puborectal muscle, etc.); details are best seen with appropriate focusing and adjustment of the instrument.

■ Clinical Indications for Endorectal Ultrasound Techniques

Whereas rectal EUS primarily visualizes the rectal wall layers and their surroundings, anal EUS is carried out to examine the sphincter muscles and the pelvic floor. Due to the variability of the organ structures and the complex conditions affecting the precise location of the organs, detailed anatomical knowledge and precise orientation are mandatory for correct interpretation of EUS images. Starting from the lumen, a thin hypoechoic circular structure and a thicker hyperechoic circular structure are seen, which are interpreted as border echoes and subepithelial tissue, respectively, followed by a hypoechoic homogeneous ring pattern, which corresponds to the IAS. This muscle is usually thickest at the level of the pectinate line, with the diameter decreasing in the oral direction. The superposed longitudinal muscle is not always clearly visible with relatively hypoechoic fibers. The EAS consists of horizontally oriented (striated) fibers with complex, mainly hyperechoic structures (Fig. 24.**3**). At the outermost level—i.e., immediately at the anocutaneous junction—the IAS is not visible. Only the subcutaneous portion of the EAS forms the sphincter apparatus at this level, which is recognized by a strong circular band with the typical hyperechoic pattern of striated muscle. More orally, the structures of the levator ani and puborectalis muscle can be seen, the latter passing the rectum dorsally in a U-shaped loop and continuing ventrally as two lateral crura to the pubic bone. Sonomorphologically, these structures are represented by inhomogeneous longitudinal echo patterns lateral to the sphincter organ (Fig. 24.**4**). At this level, the adjacent organs (prostate, seminal glands, urethra, vagina, uterus, and bladder) are also visualized. The indications for anorectal ultrasonography (ARUS) and endorectal ultrasonography (ERUS) are listed in Table 24.**3**.

Table 24.3 Indications for anorectal ultrasonography (ARUS) and endorectal ultrasonography (ERUS)

Anal carcinoma	T and N staging
Rectal carcinoma	T and N staging
Tumor follow-up	Submucosal and extrarectal tumor recurrence
Incontinence	Assessment of sphincter morphology
Extrarectal pathology	Abscess, fistula

Rectal Cancer

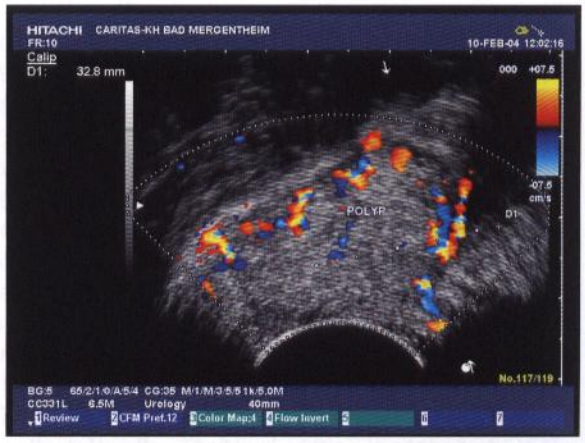
Clinically, rectal cancer is regarded a separate entity, which can be distinguished from colon cancer on the basis of the surrounding anatomy, despite a similar pathogenesis. The treatment options also vary distinctly between rectal and colon cancers—including local excision and neoadjuvant chemoradiotherapy, for example. Accurate preoperative staging using EUS is therefore mandatory in order to allow an individualized approach to treatment in rectal cancer patients.

Tumor Staging

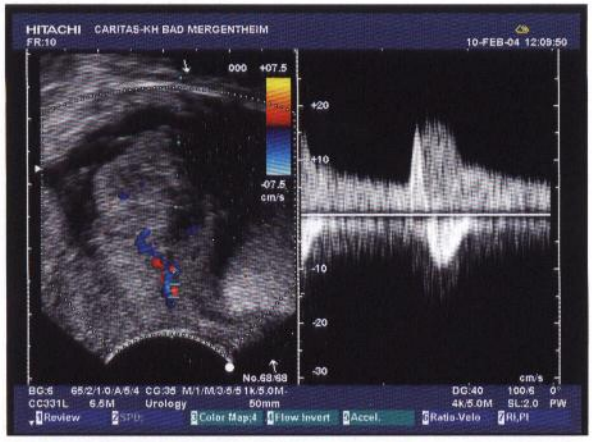
T and N staging. Preoperative assessment of the tumor's penetration depth (T staging) can be carried out precisely with EUS; the endosonographically assessed tumor stage is labeled with the prefix "u" for ultrasound (Figs. 24.**12**–24.**23**). uT1 carcinomas are present when the mucosa/submucosa is involved, the second layer (hypoechoic) is often thickened, and the subsequent hyperechoic layer (layer III) is still intact. In uT2 tumors, the fourth (hypoechoic) layer, corresponding to the muscularis propria, is enlarged, with interruption of the layer located immediately below (III) and hypoechoic thickening of the mucosa (layer II); the outermost layer (V) remains intact. In uT3 tumors, each of the wall layers is involved, including layer V, with extension into the hyperechoic perirectal fat tissue. The continuity of layer V is disrupted. In stage T4, the tumor infiltrates either neighboring organs (such as the prostate, vagina, or bladder), which can be visualized easily with EUS, or the visceral peritoneum, although the latter is not dis-



a



b



c



d

Fig. 24.**12** uT1 carcinoma of the rectum in two patients (patient A in **a–c**, patient B in **d**). **a** Infiltration of the tumor does not reach the muscularis propria (seen between the markers). **b** At the transition to the muscularis, vessels can be misinterpreted as infiltration. **b, c** Color Doppler and spectral analysis can be helpful for identifying blood vessels (arterial flow spectrum). **d** The muscularis should be visualized in all sections, but this is not always possible at one level.

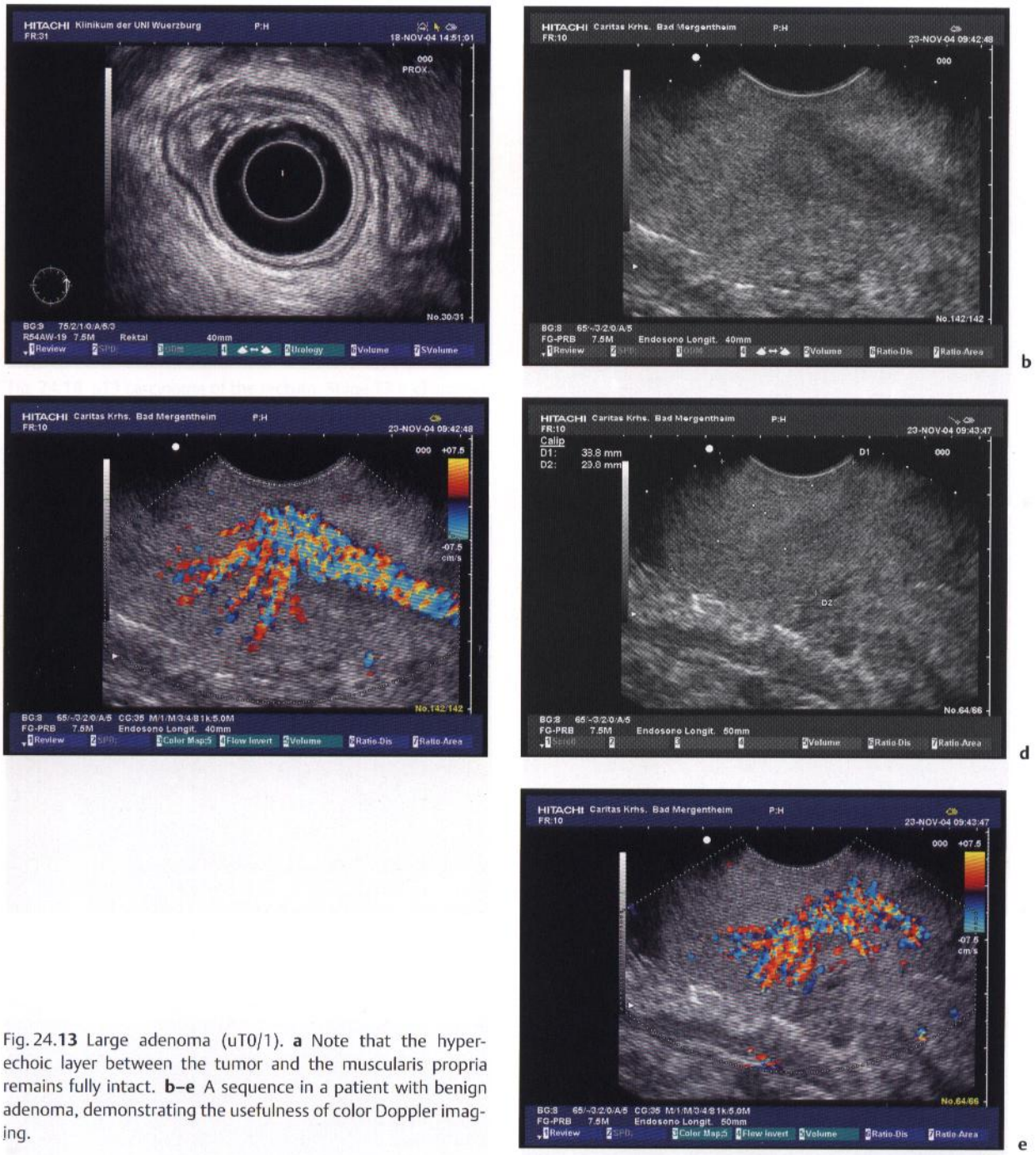
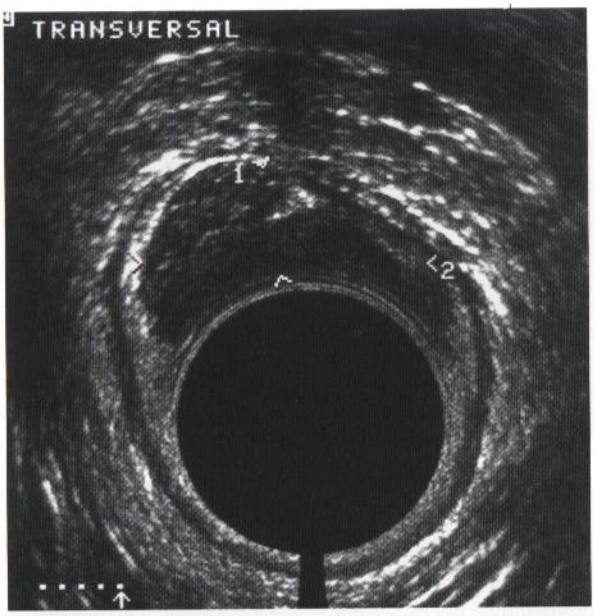
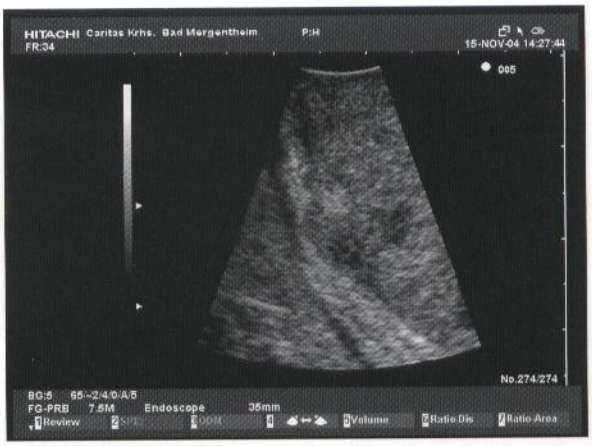


Fig. 24.**13** Large adenoma (uT0/1). **a** Note that the hyperechoic layer between the tumor and the muscularis propria remains fully intact. **b–e** A sequence in a patient with benign adenoma, demonstrating the usefulness of color Doppler imaging.



a

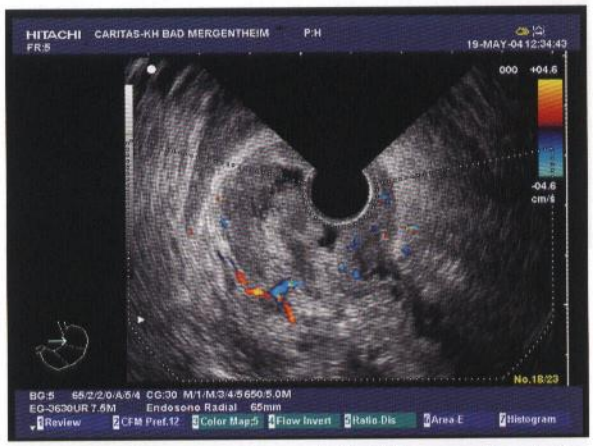


b

Fig. 24.**14a** uT1 and pT1 carcinoma between the 11-o'clock and 1-o'clock positions. **b** Note the intact muscularis propria layer.



a



b

Fig. 24.**15** uT2 Carcinoma of the rectum. **a** Stage T2 is characterized by infiltration of the muscularis, which can be seen on the left lower side of the image. **b** Color duplex imaging, here showing an afferent vessel, may be helpful to provide a better grasp of the architecture.

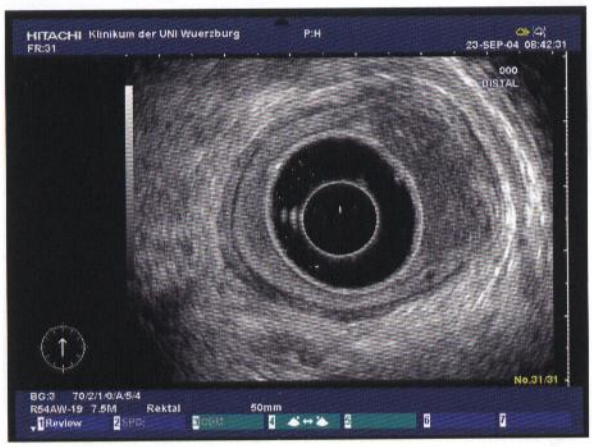
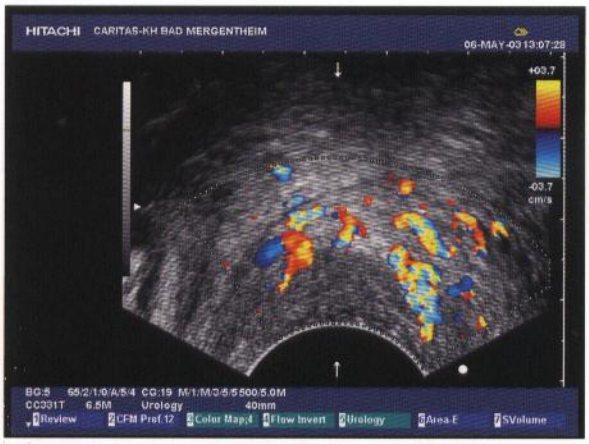


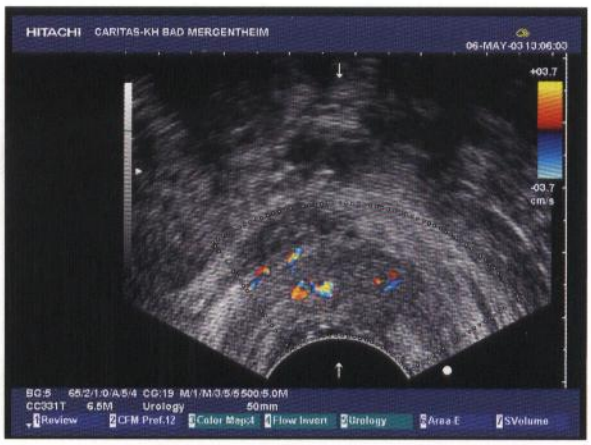
Fig. 24.**16** uT2 carcinoma.



Fig. 24.**17** uT3 carcinoma of the rectum. Stage T3 is characterized by infiltration into the perirectal connective tissue, seen at the lower left side of the image.



a



b

Fig. 24.**18** uT3 carcinoma of the rectum. Stage T3 is characterized by infiltration into the perirectal connective tissue. **a, b** An inflammatory peritumorous tissue reaction can lead to misinterpretation (overstaging). After radiotherapy, no tumor tissue can be visualized in many cases either endoscopically or endosonographically.



Fig. 24.**19** uT3 carcinoma of the rectum. Stage T3 is characterized by infiltration into the perirectal connective tissue, as seen at the left margin here.



Fig. 24.**21** A large uT3 uN+ carcinoma, with a small lymph node at the 8-o'clock position.



a

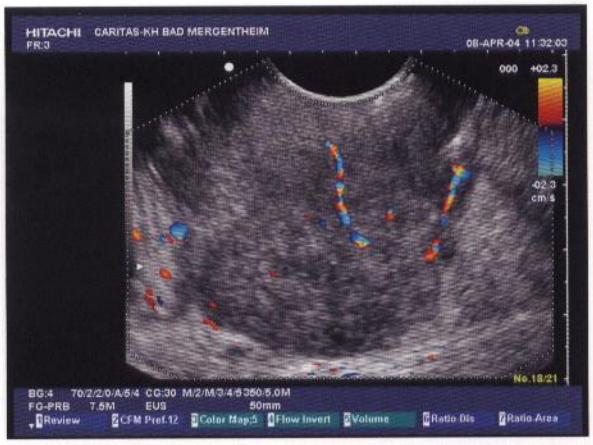


b

Fig. 24.**20** uT3, uN+ carcinoma of the rectum. **a** As a rule, lymph nodes with malignant infiltration (between the markers) are less echogenic. **b** However, when there are also mixed inflammatory signs, it is not possible to assess the benign or malignant status of the lymph node (between the markers) clearly. The echogenicity of this lymph node corresponds to that of the underlying tumor.

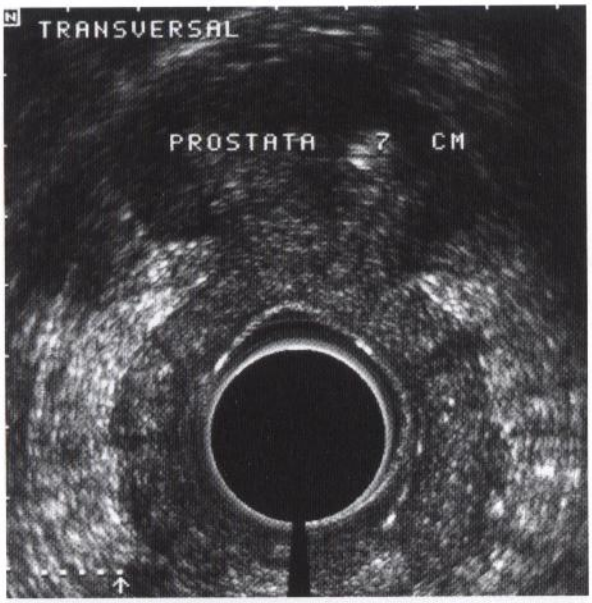


a



b

Fig. 24.**22** uT4 carcinoma of the rectum. **a** Stage T4 stage is characterized by infiltration into adjacent organs, as seen here in a patient with infiltration into the uterus. The infiltration extends beyond the borders of the organ (marked with 1–3). **b** Color duplex imaging is helpful to provide a better grasp of the architecture.

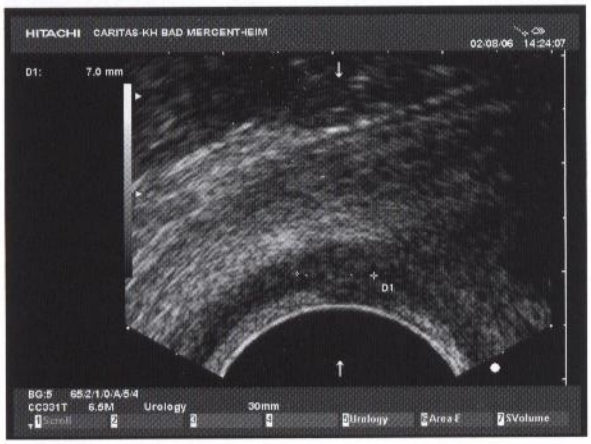


a



b

Fig. 24.**23a, b** A circular uT4 carcinoma with broad infiltration into the prostate (pT4).

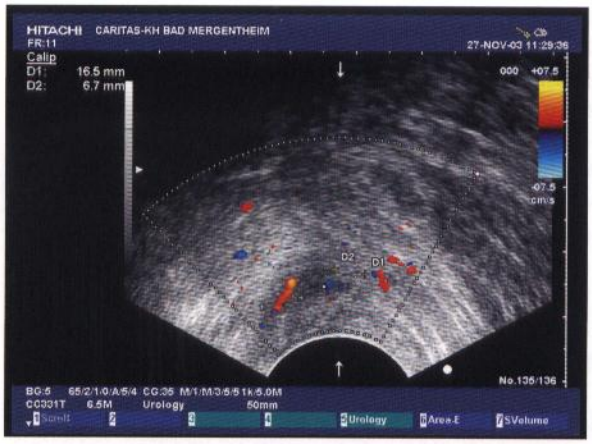


tinguishable as a separate layer. Other malignant and nonmalignant processes can be examined with EUS and provide important additional information. Tumor recurrences (at the anastomosis or perirectal), recurrences in the pelvic floor, tumors in the lower pelvis (e. g., uterus, vagina, or bladder), transmural inflammatory processes (Crohns disease of the colon) and/or fistulas also are accessible to EUS, as well as other forms of disease (Figs. 24.**24**–24.**27**) [9].

Fig. 24.**24** Carcinoid of the rectum. Between the markers, a small carcinoid is seen infiltrating the muscularis propria. Local excision is therefore not an option.



a



b



c

Fig. 24.**25a** Rectal venous plexus. **b** A thrombosed node. **c** A hemangioma. With arterially perfused hemangiomas, hemangiosarcoma has to be considered in the differential diagnosis.

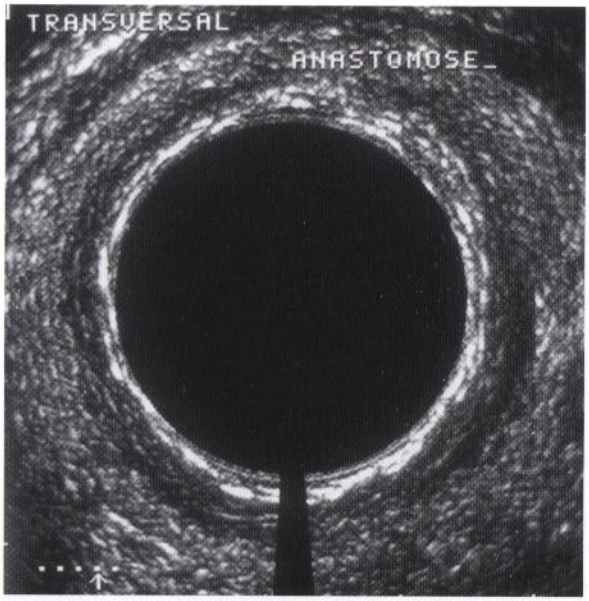


Fig. 24.**26** A normal anastomosis, showing the metal clips from the circular stapler.



Fig. 24.**27** An extramucosal recurrence at the 1-o'clock position. The rectal wall is intact, and the growth is therefore not detectable endoscopically.

Preoperative Diagnosis of Rectal Carcinomas

In the preoperative diagnostic work-up of rectal carcinoma, rectoscopy and/or colonoscopy with biopsies and an abdominal ultrasound examination are mandatory. Computed tomography (CT) is also necessary if abdominal ultrasonography does not provide satisfactory information. EUS imaging is a useful tool for the further evaluation of these tumors, due to its high sensitivity for T staging in particular, which lies in the range of 80–90%—so that this technique can define the tumor location precisely within the rectal wall (Tables 24.**4**, 24.**5**) [1,10–28].

In addition, pathological conditions in the pararectal area also can be visualized, particularly lymph nodes. However, the sensitivity and specificity of ultrasound for lymph-node staging is somewhat lower, in the range of 70–80% (Table 24.**5**) [1,29]. The T stage may be overestimated in individual cases, particularly if a hypoechoic peritumoral inflammatory reaction is present. It should be noted that biopsies taken before the EUS examination can lead to significant mis-staging (usually involving overstaging) of cancers. Again, the explanation for this phenomenon is the inflammatory reaction caused by the biopsy trauma, which in turn leads to blurring and/or pseudoinfiltration of layers that are not primarily involved.

Table 24.**4** T staging (primary tumor) of rectal tumors with endorectal ultrasonography

First author (ref.)	Year	Patients (n)	Accuracy (%)	Sensitivity (%)	Specificity (%)	PPV (%)	NPV (%)
Akahoshi [13]	2000	39	82	83	65	59	87
Akasu [14]	1997	150	89	96	78	88	91
Beynon [15]	1989	99	93	99	91	97	95
Fedyaev [16]	1995	109	95	97	91	96	94
Garcia-Aguilar [17]	2002	545	69	–	–	72	93
Glaser [10]	1990	110	94	96	91	92	96
Herzog [18]	1993	118	93	98	75	90	95
Katsura [19]	1992	112	97	96	100	100	94
Nielsen [12]	1996	100	94	96	87	96	87
Rafaelsen [20]	1994	107	89	96	77	88	91
Rifkin [21]	1989	101	72	67	77	73	72
Sailer [22]	1997	162	89	97	81	83	97
Santoro [23]	2001	–	89	82	93	89	94
Yamashita [24]	1988	122	86	96	52	88	78

NPV: negative predictive value; PPV: positive predictive value.

Table 24.**5** N staging (lymph nodes) of rectal tumors with endorectal ultrasonography

First author (ref.)	Year	Patients (n)	Accuracy (%)	Sensitivity (%)	Specificity (%)	PPV (%)	NPV (%)
Akasu [14]	1997	164	76	77	74	79	72
Beynon [15]	1989	95	83	88	79	78	89
Fedyaev [16]	1995	109	72	94	55	61	92
Frascio [25]	2001	–	75	74	73	–	–
Garcia-Aguilar [17]	2002	238	64	33	64	52	68
Glaser [10]	1990	97	80	80	81	78	82
Herzog [18]	1993	111	80	89	73	71	90
Hildebrandt [26]	1990	113	79	72	83	72	83
Katsura [19]	1992	98	68	80	62	54	85
Kim [27]	2000	–	64	53	75	71	59
Nielsen [12]	1996	81	67	79	56	61	75
Rafaelsen [20]	1994	53	70	58	76	58	76
Rifkin [21]	1989	102	81	50	92	68	84
Saitoh [28]	1986	88	75	73	82	95	42
Santoro [23]	2001	–	74	70	79	72	84

NPV: negative predictive value; PPV: positive predictive value.

In comparison with T staging, evaluation of the lymph nodes is fraught with a greater possibility of errors involving overstaging and understaging, as hypoechoic lymph-node structures can be found in inflammatory as well as in malignant processes. The probability of malignancy increases with increasing diameter of the lymph nodes. In unclear cases, EUS-guided fine-needle biopsy can be carried out using a linear transducer [29,30]. However, if the histology is negative, a metastasis can still not be ruled out, as the biopsy needle may have missed the lymph node or malignant tissue within it. It is therefore the authors' practice to classify all visible lymph nodes as N+, while being fully aware that some tumors may be overstaged in this way.

When T1 tumors are suspected, with histomorphological signs of low-grade carcinoma, and local excision is planned, EUS is considered to be mandatory [31]. With the growing acceptance of neoadjuvant approaches, reliable preoperative staging of rectal cancers is mandatory. Studies have shown that tumors that penetrate through the rectal wall—i.e., T3 cancers and all node-positive tumors—have a better outcome when preoperative radiotherapy or chemotherapy is administered [32,33]. The German Rectal Cancer Trial in particular demonstrated a clear advantage for preoperative treatment in contrast to a postoperative setting [34]. Of course, as has already been common practice for many years, all T4 carcinomas require neoadjuvant chemoradiotherapy. The modern differentiated approach to rectal tumor treatment, ranging from transanal excision to neoadjuvant chemoradiotherapy with subsequent surgery, requires an equally differentiated and precise staging instrument. At present, EUS appears to be the most accurate imaging method in comparison with other techniques such as CT and magnetic resonance imaging (MRI) [35,36].

■ Tumor Follow-Up

EUS is of clinical importance in the follow-up of colorectal carcinoma and is recommended by interdisciplinary guidelines published in 2000, particularly for rectal tumors staged as UICC II or III [5]. The advantage is that pathological submucosal and pararectal (extrarectal) conditions can be detected that normally escape rectal digital and endoscopic examination due to their extraluminal location. In a comparative study, Giovannini et al. found that the additional diagnostic value of this method is due to its ability to detect locoregional recurrences in patients who have undergone surgery and/or radiotherapy in 10–25% of cases, in comparison with more conventional methods such as digital examination, rectoscopy, and/or CT [37].

Recurrences characteristically have a hypoechoic appearance, similar to primary tumors. As with other imaging techniques, it is not possible to distinguish between scarring and malignant tissue solely on the basis of imaging criteria. Increasing growth over time and/or an irregular appearance constitute typical signs of malignancy. However, if there is any doubt, EUS-guided biopsies can be taken, and this is certainly an additional advantage of this technique [9,38,39]. A detailed description of three-dimensional endorectal ultrasonography is provided in Chapter 25.

■ Anorectal Endosonography in Fecal Incontinence

An essential precondition for rational treatment of fecal incontinence is detailed knowledge of individual anatomical and functional defects in the sphincter system and the adjacent structures. Anorectal EUS plays an important role in the evaluation of fecal incontinence and is used as a valuable and noninvasive imaging tool [4,40,41]. On the basis of the combined methods of EUS and rectal perfusion manometry, four major types of fecal incontinence can be distinguished:

- A predominantly sensory form
- A mainly muscular form
- A form with both sensory and muscular components
- A form with predominantly decreased rectal compliance and impaired reservoir function

Each of these requires different therapeutic approaches [42]. Interestingly, when EUS was introduced into the diagnostic work-up for incontinent patients, it was noticed that the vast majority of patients who had previously had conditions described as "idiopathic" did in fact have morphological changes in the sphincter [43,44]. The principal cause of incontinence is obstetric trauma [45], and sphincter disruption is therefore mainly seen at the level of the EAS, somewhere between the 10-o'clock and 2-o'clock positions (i.e., ventrally, between the vagina and anus). With more excessive forces, such as a complete perineal tear in situations with an uncontrolled third stage at birth or instrumental (forceps) delivery, injury even to the IAS can be encountered [46]. Scars in the hyperechoic EAS are usually hypoechoic on EUS imaging, whereas injuries to the hypoechoic IAS result in hyperechoic scar tissue.

The predominantly sensory form is characterized by normal EUS morphology and manometry; the second is characterized by normal endosonographic structures, including the IAS and EAS, the levator ani, and the puborectalis muscle, but shows pathological sphincter pressure (resting and/or squeeze pressure); in the third form, both pathological morphology and manometry are usually present; and in the last form, EUS and manometry may or may not be pathological. Endosonographically, the IAS may be found to be thickened, or its contour may be disrupted, as may also be the case in pa-



a



b

Fig. 24.**28a, b** Crohn's disease with intramural abscess formation, seen between the markers.



Fig. 24.**29** A large abscess in a 31-year-old patient with Crohn's disease.

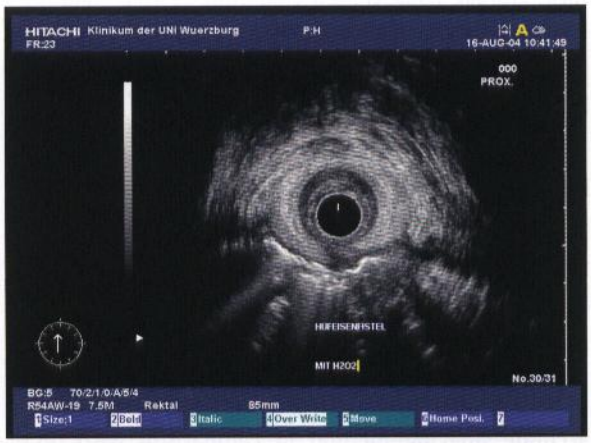


Fig. 24.**30** A dorsal horseshoe fistula, enhanced with hydrogen peroxide through the external opening.

tients with solitary rectal ulcer and/or after hemorrhoidal surgery [47,48].

Various degrees of interruption of the continuity of the EAS mainly are observed in elderly patients with anal incontinence and a history of gynecological/obstetric trauma [49]. Endosonographic features such as structural gaps appear to be clinically relevant when corresponding correlations with clinical and/or functional parameters are present—e. g., decreased sphincter pressure.

It should be mentioned that such disturbances may not always be observed in these patients. In a study including more than 100 patients with different degrees of fecal incontinence, a weak but significant correlation was observed between the diameter of the EAS and the maximal squeeze pressure [50,51]. However, these data need further confirmation, as others have not found such a correlation.

Anal Fistula

EUS can be a valuable tool in the evaluation of anal fistulas, particularly in patients with complex and/or recurrent fistulas, as in Crohn's disease [52]. Precise imaging of the puborectalis loop with the levator ani muscle is mandatory to help in surgical decision-making regarding this region (Figs. 24.**28**–24.**33**). The levator ani extends continuously into the EAS, with a laterocranial continuation to the obturator muscle. Above this strong musculature lies the pelvirectal fossa, below the ischioanal fossa. Familiarity with the anatomy enables the examiner to distinguish between pelvirectal (suprasphincteral) and ischiorectal (infrasphincteral) abscesses and fistulas [4]. Instillation of hydrogen peroxide or even simple mineral water through the external orifice of the fistula allows even better examination of the structures involved. The contrast medium helps delineate

side tracks and fistula extensions that may escape notice in the unenhanced state [53]. EUS examination of complex fistulas is mainly helpful if it is carried out by the operating surgeon himself, as it can help decisively in the planning of the surgical procedure [54]. In acute situations with pain and discomfort, EUS, like any other clinical or instrumental examination, should be carried out with the patient under general anesthesia.

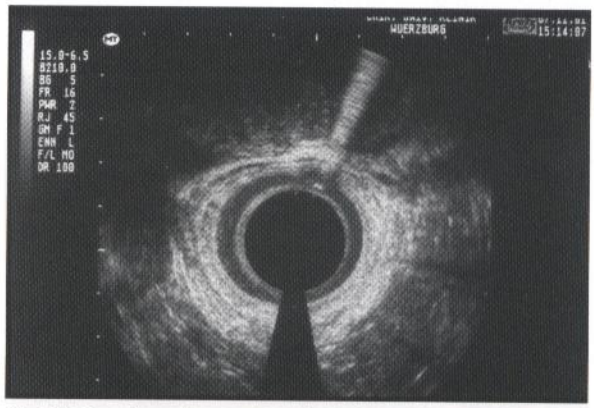


Fig. 24.**31** Echoes from a metal probe in a trans-sphincteral fistula, indicating the internal opening at the 1-o'clock position.

■ Interventional Procedures with Endoscopic Anorectal Ultrasound

EUS-Guided Transrectal Biopsies of Pelvic Tumors

The diagnostic work-up of pelvic tumors can occasionally be laborious. Using imaging techniques such as CT or MRI, or both, in patients with a history of a pelvic malignancy—e.g., rectal, prostate, or cervical cancer—it is often difficult to differentiate between scar tissue and recurrent tumor, particularly if the space-occupying lesion is small and tumor markers are not raised, or raised only slightly. Positron-emission tomography (PET) allows further classification of these lesions into those that do or do not show uptake of the marker, which is usually fluorodeoxyglucose [55]. However, a definitive histological diagnosis needs to be established in order to decide conclusively on further therapeutic strategies, which may range from palliative conservative measures to major surgery such as multivisceral resection. The same applies to patients with no previous history who either present with a symptomatic or incidental pelvic tumor that cannot be clearly classified using either imaging, laboratory investigations, or follow-up examinations by the respective specialists—i.e., the urologist, gynecologist, or colorectal surgeon.

Percutaneous biopsies assisted either by CT or by abdominal ultrasonography have several limitations. The distance from the surface to the lesion can be considerable, making it difficult if not impossible to achieve precise aspiration. Tumors can be obscured by anatomical structures such as the uterus, adnexa, or bowel. In addition, patient discomfort and the risk of intraperitoneal infection should also be borne in mind when this type of approach is used. Transrectal EUS overcomes most of these limitations, and most importantly, its spatial resolution is considerably better than that of any of the other imaging techniques, including PET. EUS is therefore potentially capable of detecting lesions at a stage at which conventional diagnostic tools would fail to do so [56].

We have reported our results with EUS-guided biopsies in a total of 48 patients [9]. Apart from one post-biopsy hemorrhage, which was managed conservatively, no other complications were encountered. Sufficient tissue was removed to allow histological examination



Fig. 24.**32** A large presacral abscess.



Fig. 24.**33** A pararectal abscess in a patient with Crohn's disease.

in all cases. A wide range of diagnoses, including primary and secondary malignancies (n = 25) and benign lesions (n = 23) were established. There were no false-positive cases, but three false-negative histological diagnoses in patients in whom local recurrence of a malignant tumor

was confirmed during the follow-up period. This represents a sensitivity of 88%, a specificity of 100%, a positive predictive value of 100%, and a negative predictive value of 89%. Only 13 tumors (27%) in the series were easily palpable by rectal examination. Theoretically, these tumors could have been approached using simple digitally guided transrectal needle biopsy. However, EUS provides biplanar imaging with very precise target localization and needle monitoring. Lesions can be biopsied under visual guidance, rendering the procedure more controlled and consequently safer.

EUS-guided biopsy of the prostate gland is a well-established method in the field of urology and has gained widespread acceptance in routine practice. Well-documented studies including several thousand patients have shown that the procedure is safe and effective, with little patient discomfort and very low morbidity rates [57]. Infection, although a rare event, is probably the most serious complication, and administration of a prophylactic antibiotic is generally recommended. As the perirectal tissue is not as well vascularized and contained as the prostate, we consider that more thorough preparation, including complete bowel lavage and single-shot antibiotics, is warranted. As with any other invasive procedure, it appears prudent not to carry out EUS-guided transrectal biopsy in patients receiving anticoagulant or thrombolytic medication. If a biopsy is nevertheless needed, medication should either be discontinued if possible, or else the patient should be monitored on an in-patient basis.

Only a few studies have been published in the non-urological and nongynecological literature on transrectal biopsy of pelvic masses. Apart from anecdotal reports including small numbers of patients, two articles described transrectal ultrasound guided biopsies in larger series of patients with suspected recurrences of rectal carcinoma. Hünerbein et al. [38] report 30 patients who underwent transrectal ERUS-guided biopsies during tumor follow-up. They found 10 patients with malignant histological findings, while the remaining patients had no evidence of recurrent disease during a follow-up period of 7 months. No complications were encountered. Löhnert and colleagues [39] used a transperineal approach under local anesthesia in 111 patients with suspicious masses following low anterior resection for rectal cancer. Local recurrences were demonstrated histologically in 52 patients. Potentially curative salvage surgery was possible in 31 patients, 25 of whom had been diagnosed by EUS alone (81% of all curatively resected patients with local recurrences). There were no false-positive or false-negative results. The total numbers of biopsy samples retrieved in each patient are not mentioned in either of these papers. However, taking into consideration our own three cases of false-negative histology, all of which occurred in the early period of the study in which only one or two aspirations were carried out, we would now recommend obtaining at least five tissue samples per patient. Using this policy, we increased the sensitivity of the method to 100%.

According to the urology literature, transrectal ultrasound-guided needle biopsy is generally considered to cause no discomfort or only minimal discomfort and it has therefore been common practice to carry out this procedure without anesthesia or analgesia. We can confirm that the vast majority of patients have no pain, or only insignificant pain. We used a sedative drug in only three patients who expressed anxiety before the biopsy. It appears from the literature that younger patients—i. e., those under 60 years of age—experience more discomfort, so that this subgroup may benefit from analgesia and/or sedation [57].

EUS-Guided Transrectal Aspiration of Pelvic Fluid Collections

As the resolution of EUS is less than 1 mm, even very small lesions that might otherwise evade detection on clinical examination or conventional imaging such as CT can be visualized with great accuracy. In addition, their location and relationship with neighboring structures can be precisely outlined, which greatly increases the safety of any interventional procedures such as endorectal ultrasound-guided biopsies or aspiration of abscesses. We have recently reported our experience in 29 patients who underwent a total of 33 EUS-guided aspiration procedures [58]. No procedure-related complications were encountered. In 22 cases (76%), the lesions were identified following a surgical procedure. Amounts of fluid varied between 5 and 750 mL. The fluids were sterile in 14 cases (42%). The fluid collections consisted of hematomas, seromas, peritoneal cysts, and a mucocele. Microorganisms were found in the remaining 19 aspirations (58%), with lesions consisting of abscesses (n = 16) and infected hematomas (n = 3). A transrectal (n = 14) or transvaginal (n = 2) drainage catheter was placed in 16 patients under endosonographic guidance using the Seldinger technique. Only two patients required a subsequent laparotomy for definitive treatment of the septic focus, while the remaining patients were all treated successfully using this conservative approach. It was demonstrated that transrectal drainage of pelvic fluid collections can be carried out with no morbidity, or only insignificant morbidity, in carefully selected patients. Most cases involve patients with postoperative complications, particularly pelvic abscesses or hematomas with or without anastomotic dehiscence. Transrectal EUS-guided drainage in these circumstances is a comparatively minor intervention, causing only little discomfort to the patient. This report shows that the procedure can be carried out safely and that it avoids the need for further surgery in the great majority of patients. This is not surprising, as interventional drain-

age of infectious foci is a well-known and widely applied principle.

Since no radiation exposure is involved, EUS is also useful in the follow-up of these patients. In cases of abscesses, the cavities can be easily visualized by instilling a few milliliters of hydrogen peroxide through the draining catheter. This allows evaluation of the cavity size and its configuration. Cystic structures need to be reviewed thoroughly to rule out infection or malignancy. However, benign peritoneal cysts are occasionally encountered after pelvic operations, typically following hysterectomies. In suitable patients who present with cyst-related symptoms, obliteration therapy can be attempted. Following the principles of pleurodesis, a sealant such as doxycycline or fibrin glue can be injected into the cyst.

In conclusion, endorectal ultrasound is a useful and complementary imaging technique in the assessment of pelvic pathology. The major advantage of EUS, however, is that it makes it possible to carry out ultrasound-guided punctures and aspirations of extrarectal fluid collections and biopsies of solid lesions. Microbiological, cytological, and/or histological examination of the specimens allows accurate diagnosis. In cases of abscess formation or infected hematoma, a drain can be placed at the same time, avoiding the need for surgery in the majority of patients. EUS-guided interventions are safe and cost-effective and cause minimal discomfort to the patient (Fig. 24.**34**).



Fig. 24.**34** Ultrasound-guided biopsy or aspiration. The needle tip can be seen precisely along the dotted line (the distance between two dots equals 1 cm).

Anal Cancer

Whereas surgical excision used to be the standard method in the treatment of anal malignancies, most tumors are nowadays treated using combined chemoradiotherapy. Only very small cancers of the anal margin can safely be excised without compromising the anal sphincter. Very advanced tumors causing obstruction and/or bleeding or cancers that have failed to respond to chemoradiotherapy also need to be treated surgically, usually with an abdominoperineal resection.

Anal cancers are classified according to their size (T stage). However, with regard to lymph-node metastases, two distinctly different classifications are applied, depending on the precise location of the malignancy (Table 24.**6**). While tumors located at the anal margin tend to involve inguinal lymph nodes as the principal metastatic route, cancers in the anal canal primarily metastasize to the perirectal nodes. The ultrasound appearance of squamous-cell cancers of the anus is typically that of a hypoechoic lesion.

Anal ultrasound is useful for determining not only the precise depth of infiltration, but also for delineating sphincter involvement [59]. Bartram and Burnett proposed a new classification for the endoanal ultrasound staging of anal cancers [60]. They suggest that the T level should not be determined according to the size of the lesion, but according to the anatomical structures involved (Table 24.**7**). In addition, anal ultrasound can be used to monitor the treatment response and for follow-up examinations in these patients [61]. If complete regression is achieved, the ultrasound morphology of the anatomic area involved may revert to normal. However, in most cases some echo patterns differing from the

Table 24.**6** TNM classification of cancers in the anal margin and anal canal. The differences in the N staging should be noted

Stage	Anal canal	Anal margin
Tis	Carcinoma in situ	Carcinoma in situ
T1	Tumor < 2 cm	Tumor < 2 cm
T2	Tumor > 2 and < 5 cm	Tumor > 2 and < 5 cm
T3	Tumor > 5 cm	Tumor > 5 cm
T4	Tumor infiltrates neighboring organs*	Tumor infiltrates extradermal structures (e.g., cartilage, muscle)
N0	No regional lymph nodes involved	No regional lymph nodes involved
N1	Perirectal lymph nodes	Ipsilateral inguinal lymph nodes
N2	Inguinal and/or iliac lymph nodes on one side	
N3	Bilateral and/or perirectal and inguinal lymph nodes on one side	
M0	No distant metastases	No distant metastases
M1	Distant metastases	Distant metastases

The anal sphincter is not a neighboring organ.

Table 24.7 Endosonographic staging of anal cancers proposed by Bartram and Burnett (1991) [60]

Stage	Depth of infiltration
T1	Infiltration into the internal anal sphincter
T2	Infiltration into the external anal sphincter (EAS)
T3	Tumor penetrates through the EAS
T4	Infiltration into neighboring organs

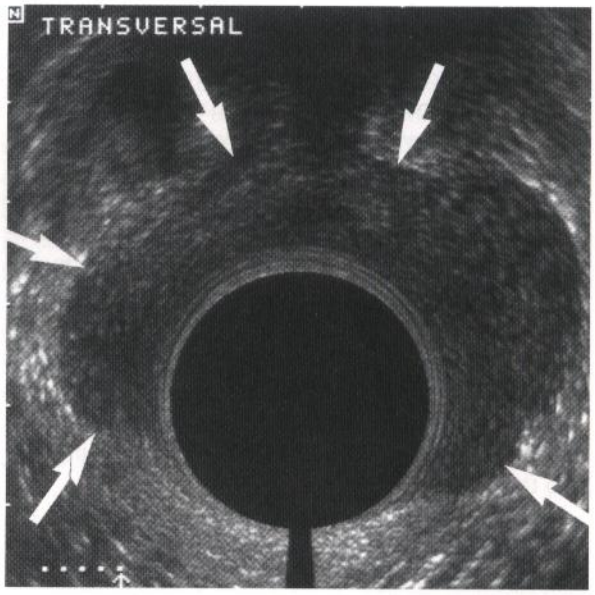


Fig. 24.**35** A large carcinoma at the anal margin (arrows), infiltrating the subcutaneous part of the external anal sphincter.



a



b

Fig. 24.**36a, b** Perineal transcutaneous ultrasound is especially effective in demonstrating trans-sphincteral and extrasphincteral locations that are often difficult to demonstrate with endorectal ultrasound. FI: fistula.

neighboring healthy tissue are seen representing the residual scar.

There have been reports that three-dimensional (3D) anal ultrasonography may be able to improve the accuracy of staging further [62]. Löhnert and co-workers describe an interesting new application of 3D ultrasound in the treatment of anal tumors [63]. They used 3D reconstructions for radiotherapy simulation in order to improve the radiation dose to the target field. They also implanted afterloading needles using endosonographic transperineal guidance. They concluded that this new technique is capable of minimizing radiation-induced damage to adjacent organs and/or healthy tissue (Fig. 24.**35**).

Perineal Transcutaneous Ultrasound

Perineal transcutaneous ultrasound (PTUS) is very effective but is rarely considered in the imaging work-up for perianal inflammatory lesions, e. g. in Crohn's disease. In contrast to the established methods, perineal ultrasound is an easy and cost-effective method of imaging for perianal abscesses and fistulas (Fig. 24.**36**).

References

1. Brugge WR. Endoscopic ultrasonography: the current status. Gastroenterology 1998;115:1577–83.
2. Sailer M, Leppert R, Fuchs KH, Thiede A. Die endorektale Sonographie. Coloproctology 1995;17:149–57.
3. Löhnert M, Dohrmann P, Stoffregen C. Endorektale Sonographie in der Proktologie. In: Braun B, editor. Ultraschall-

diagnostik. Lehrbuch und Atlas. Munich: Ecomed, 1990; 76–89.
4. Poen AC, Felt-Bersma RJ. Endosonography in benign anorectal disease: an overview. Scand J Gastroenterol Suppl 1999;230:40–8.
5. Hermanek P. Qualitätssicherung in der Onkologie, Diagnose und Therapie maligner Erkrankungen. Kurzgefasste Interdisziplinäre Leitlinie 2000. Munich: Zuckerschwert, 2000.
6. Sailer M, Leppert R, Fuchs KH, Thiede A. [Endo-anal sonography in diagnosis of fecal incontinence; in German.] Zentralbl Chir 1996;121:639–44.
7. Stelzner F. Die anorectalen Fisteln, 3rd ed. Berlin: Springer, 1981.
8. Fritsch H, Brenner E, Lienemann A, Ludwikowski B. Anal sphincter complex: reinterpreted morphology and its clinical relevance. Dis Colon Rectum 2002;45:188–94.
9. Sailer M, Bussen D, Fein M, Freys S, Debus SE, Thiede A, et al. Endoscopic ultrasound-guided transrectal biopsies of pelvic tumors. J Gastrointest Surg 2002;6:342–6.
10. Glaser F, Schlag P, Herfarth C. Endorectal ultrasonography for the assessment of invasion of rectal tumours and lymph node involvement. Br J Surg 1990;77:883–7.
11. Kuntz C, Glaser F, Buhr HJ, Herfarth C. [Endo-anal ultrasound: indications and results; in German.] Chirurg 1994;65:352–7.
12. Nielsen MB, Qvitzau S, Pedersen JF, Christiansen J. Endosonography for preoperative staging of rectal tumours. Acta Radiol 1996;37:799–803.
13. Akahoshi K, Kondoh A, Nagaie T, Koyanagi N, Nakanishi K, Harada N, et al. Preoperative staging of rectal cancer using a 7.5 MHz front-loading US probe. Gastrointest Endosc 2000;52:529–34.
14. Akasu T, Sugihara K, Moriya Y, Fujita S. Limitations and pitfalls of transrectal ultrasonography for staging of rectal cancer. Dis Colon Rectum 1997;40(10 Suppl):S10–5.
15. Beynon J, Mortensen NJ, Foy DM, Channer JL, Rigby H, Virjee J. Preoperative assessment of mesorectal lymph node involvement in rectal cancer. Br J Surg 1989;76:276–9.
16. Fedyaev EB, Volkova EA, Kuznetsova EE. Transrectal and transvaginal ultrasonography in the preoperative staging of rectal carcinoma. Eur J Radiol 1995;20:35–8.
17. Garcia-Aguilar J, Pollack J, Lee SH, Hernandez DA, Mellgren A, Wong WD, et al. Accuracy of endorectal ultrasonography in preoperative staging of rectal tumors. Dis Colon Rectum 2002;45:10–5.
18. Herzog U, von Flue M, Tondelli P, Schuppisser JP. How accurate is endorectal ultrasound in the preoperative staging of rectal cancer? Dis Colon Rectum 1993;36:127–34.
19. Katsura Y, Yamada K, Ishizawa T, Yoshinaka H, Shimazu H. Endorectal ultrasonography for the assessment of wall invasion and lymph node metastasis in rectal cancer. Dis Colon Rectum 1992;35:362–8.
20. Rafaelsen SR, Kronborg O, Fenger C. Digital rectal examination and transrectal ultrasonography in staging of rectal cancer: a prospective, blind study. Acta Radiol 1994; 35:300–4.
21. Rifkin MD, Ehrlich SM, Marks G. Staging of rectal carcinoma: prospective comparison of endorectal US and CT. Radiology 1989;170:319–22.
22. Sailer M, Leppert R, Bussen D, Fuchs KH, Thiede A. Influence of tumor position on accuracy of endorectal ultrasound staging. Dis Colon Rectum 1997;40:1180–6.
23. Santoro GA, Pastore C, Barban M, DiFalco G. Role of endorectal ultrasound in the management of rectal cancers. Hepatogastroenterology 2001;48:133–39.
24. Yamashita Y, Machi J, Shirouzu K, Morotomi T, Isomoto H, Kakegawa T. Evaluation of endorectal ultrasound for the assessment of wall invasion of rectal cancer: report of a case. Dis Colon Rectum 1988;31:617–23.
25. Frascio F, Giacosa A. Role of endoscopy in staging colorectal cancer. Semin Surg Oncol 2001;20:82–5.
26. Hildebrandt U, Klein T, Feifel G, Schwarz HP, Koch B, Schmitt RM. Endosonography of pararectal lymph nodes: in vitro and in vivo evaluation. Dis Colon Rectum 1990;33:863–8.
27. Kim HJ, Wong WD. Role of endorectal ultrasound in the conservative management of rectal cancers. Semin Surg Oncol 2000;19:358–66.
28. Saitoh N, Okui K, Sarashina H, Suzuki M, Arai T, Nunomura M. Evaluation of echographic diagnosis of rectal cancer using intrarectal ultrasonic examination. Dis Colon Rectum 1986;29:234–42.
29. Giovannoni M, Bernardini D. Biopsie guidée sous echoendoscopie des lésions péri-rectales et peri-coliques. Acta Endosc 1998;28:45–51.
30. Giovannini M. Endoscopic ultrasonography with a curved array transducer: normal echoanatomy of retroperitoneum. Gastrointest Endosc Clin N Am 1995;5:523–8.
31. Sailer M, Leppert R, Kraemer M, Fuchs KH, Thiede A. The value of endorectal ultrasound in the assessment of adenomas, T1- and T2-carcinomas. Int J Colorectal Dis 1997;12: 214–9.
32. Improved survival with preoperative radiotherapy in resectable rectal cancer. Swedish Rectal Cancer Trial. N Engl J Med 1997;336(14):980–7.
33. Kapiteijn E, Marijnen CA, Nagtegaal ID, Putter H, Steup WH, Wiggers T, et al. Preoperative radiotherapy combined with total mesorectal excision for resectable rectal cancer. N Engl J Med 2001;345:638–46.
34. Sauer R, Becker H, Hohenberger W, Rodel C, Wittekind C, Fietkau R, et al. Preoperative versus postoperative chemoradiotherapy for rectal cancer. N Engl J Med 2004;351: 1731–40.
35. Kwok H, Bissett IP, Hill GL. Preoperative staging of rectal cancer. Int J Colorectal Dis 2000;15:9–20.
36. Maier A, Fuchsjager M. Preoperative staging of rectal cancer. Eur J Radiol 2003;47:89–97.
37. Giovannini M. [What is the role of endo-rectal echography in monitoring of patients operated on for rectal cancer? In French.] Gastroenterol Clin Biol 1998;22(3):266–268.
38. Hünerbein M, Schlag PM. Three-dimensional endosonography for staging of rectal cancer. Ann Surg 1997;225:432–8.
39. Löhnert MS, Doniec JM, Henne-Bruns D. Effectiveness of endoluminal sonography in the identification of occult local rectal cancer recurrences. Dis Colon Rectum 2000;43: 483–91.
40. Barnett JL, Hasler WL, Camilleri M. American Gastroenterological Association medical position statement on anorectal testing techniques. American Gastroenterological Association. Gastroenterology 1999;116:732–60.
41. Kumar A, Rao SS. Diagnostic testing in fecal incontinence. Curr Gastroenterol Rep 2003;5:406–13.
42. Nielsen MB, Hauge C, Pedersen JF, Christiansen J. Endosonographic evaluation of patients with anal incontinence: findings and influence on surgical management. AJR Am J Roentgenol 1993;160:771–5.

43. Law PJ, Kamm MA, Bartram CI. Anal endosonography in the investigation of faecal incontinence. Br J Surg 1991;78: 312–4.
44. Eckardt VF, Jung B, Fischer B, Lierse W. Anal endosonography in healthy subjects and patients with idiopathic fecal incontinence. Dis Colon Rectum 1994;37:235–42.
45. Sultan AH, Kamm MA, Hudson CN, Thomas JM, Bartram CI. Anal-sphincter disruption during vaginal delivery. N Engl J Med 1993;329:1905–11.
46. Oberwalder M, Connor J, Wexner SD. Meta-analysis to determine the incidence of obstetric anal sphincter damage. Br J Surg 2003;90:1333–7.
47. Christiansen J, Roed-Petersen K. Clinical assessment of the anal continence plug. Dis Colon Rectum 1993;36:740–2.
48. Abbasakoor F, Nelson M, Beynon J, Patel B, Carr ND. Anal endosonography in patients with anorectal symptoms after haemorrhoidectomy. Br J Surg 1998;85:1522–4.
49. Marshall M, Halligan S, Fotheringham T, Bartram C, Nicholls RJ. Predictive value of internal anal sphincter thickness for diagnosis of rectal intussusception in patients with solitary rectal ulcer syndrome. Br J Surg 2002;89:1281–5.
50. Kamm MA. Obstetric damage and faecal incontinence. Lancet 1994;344:730–3.
51. Schafer R, Heyer T, Gantke B, Schafer A, Frieling T, Haussinger D, et al. Anal endosonography and manometry: comparison in patients with defecation problems. Dis Colon Rectum 1997;40:293–7.
52. Leppert R, Sailer M, Fuchs KH, Thiede A. Endosonography of anal fistulas and abscesses and their relation with the sphincter complex. Coloproctology 1994;16:327–29.
53. Poen AC, Felt-Bersma RJ, Eijsbouts QA, Cuesta MA, Meuwissen SG. Hydrogen peroxide-enhanced transanal ultrasound in the assessment of fistula-in-ano. Dis Colon Rectum 1998;41:1147–52.
54. Sailer M, Fuchs KH, Kraemer M, Thiede A. [Stepwise concept for treatment of complex anal fistulas; in German.] Zentralbl Chir 1998;123:840–5.
55. Arulampalam TH, Costa DC, Loizidou M, Visvikis D, Ell PJ, Taylor I. Positron emission tomography and colorectal cancer. Br J Surg 2001;88:176–89.
56. Sailer M, Leppert R, Fuchs KH, Thiede A. [Endorectal ultrasound for evaluating perirectal processes]. Chirurg 1995; 66:34–9.
57. Rodriguez LV, Terris MK. Risks and complications of transrectal ultrasound guided prostate needle biopsy: a prospective study and review of the literature. J Urol 1998;160: 2115–20.
58. Sailer M, Bussen D, Fuchs KH, Thiede A. Endoscopic ultrasound-guided transrectal aspiration of pelvic fluid collections. Surg Endosc 2004;18:736–40.
59. Sailer M, Bussen D, Leppert R, Fuchs KH, Thiede A. Endosonography of anal carcinomas. Coloproctology 1997;19: 84–8.
60. Bartram CI, Burnett JD. Atlas of anal endosonography. Oxford: Butterworth-Heinemann, 1991.
61. Magdeburg B, Fried M, Meyenberger C. Endoscopic ultrasonography in the diagnosis, staging, and follow-up of anal carcinomas. Endoscopy 1999;31:359–64.
62. Christensen AF, Nielsen MB, Engelholm SA, Roed H, Svendsen LB, Christensen H. Three-dimensional anal endosonography may improve staging of anal cancer compared with two-dimensional endosonography. Dis Colon Rectum 2004; 47:341–5.
63. Löhnert M, Doniec JM, Kovacs G, Schroder J, Dohrmann P. New method of radiotherapy for anal cancer with three-dimensional tumor reconstruction based on endoanal ultrasound and ultrasound-guided afterloading therapy. Dis Colon Rectum 1998;41:169–76.

25 Three-Dimensional Endorectal Ultrasound (ERUS) and Rectal Cancer

M. Giovannini

Introduction

Several studies in the field of endoscopic ultrasound (EUS) technology have reported advantages with three-dimensional (3D) EUS [1–13]. However, most 3D EUS studies have been conducted using catheter-type miniature probe systems [3,6–9]. Some studies have previously reported benefits of a prototype 3D EUS system using a linear-array echoendoscope for 3D guidance of interventional procedures, but the scanning method used in this system has limitations and, as the ultrasound probe was not positioned at the tip of the endoscope, it was difficult to obtain clinically adequate images in the stomach without geometrical distortion [14–16]. A recent study attempted to resolve this problem and maximize the performance of 3D EUS using a linear echoendoscope with a miniature electromagnetic position sensor attached to the tip of the scope, which can be used for freehand scanning in any position [17]. However, the problem with this technique is that the electromagnetic sensor increases the size of the probe. This chapter reports on experience with a totally new 3D EUS software program that works without the need for an electromagnetic sensor and can be used even with electronic radial or linear rectal probes.

Basic Principles of 3D Ultrasound

Two types of system have been developed, making use of either a series of two-dimensional (2D) images produced by one-dimensional arrays, or using 2D arrays to produce 3D images directly. Two criteria have to be met to avoid inaccuracies: the relative position and angulation of the acquired 2D images need to be known accurately; and the images have to be acquired rapidly and/or gated to avoid artifacts caused by respiratory, cardiac, and involuntary motion.

Tracked free-hand systems. The operator holds an assembly consisting of the transducer and an attachment, and manipulates it over the anatomy. Two-dimensional images are digitized as the transducer is moved, while meeting two criteria: the precise relative angulation and position of the ultrasound transducer have to be known for each digitized image; and the operator has to ensure that no significant gaps are left when scanning the anatomy.

3D reconstruction. The three-dimensional reconstruction process involves generating a 3D image from a digitized set of 2D images. The approach used was the voxel-based volume. The 2D images are built into a 3D voxel-based volume (3D grid) by placing each digitized 2D image into its correct location in the volume. The main advantages of this is that no information is lost during the 3D reconstruction and that a variety of rendering techniques are possible; however, large data files are generated.

Visualization of 3D ultrasound images. The ability to visualize information in the 3D image depends critically on the rendering technique. Three basic methods are used:

- *Surface-based viewing technique.* An operator or algorithm identifies the boundaries of structures in order to create a wire-frame representation. These boundaries are shaded and illuminated, so that surfaces, structures, and organs are visualized.
- *Multiplane viewing techniques* (Fig. 25.**1**).
  - Orthogonal views: three perpendicular planes are displayed simultaneously and can be moved or rotated.
  - Polyhedron: the 3D images are presented as a multiple-sided volume (polyhedron). The appropriate ultrasound image is "painted" onto each face of the polyhedron, which can be manipulated.
- *Volume-based rendering techniques.* The 3D image is projected onto a 2D plane by casting rays through the 3D image. The voxel values intersected by each ray can be multiplied by factors and summed to produce different effects: multiplied by one and then added, to form a radiography-like image; multiplied by factors to produce translucency; or displaying only the voxel with the maximum intensity along each ray.

Results of 3D ERUS in the Literature

Our experience. From May 2003 to March 2004, we carried out 35 3D ERUS examinations using this new software program. The indication for EUS was local staging of rectal cancer in all 35 cases. Before 3D ERUS scanning, a standard ERUS examination was carried out. Three-dimensional rectal examinations were conducted using a radial electronic rigid probe (Hitachi R 54). The 3D software is included in the new ultrasound

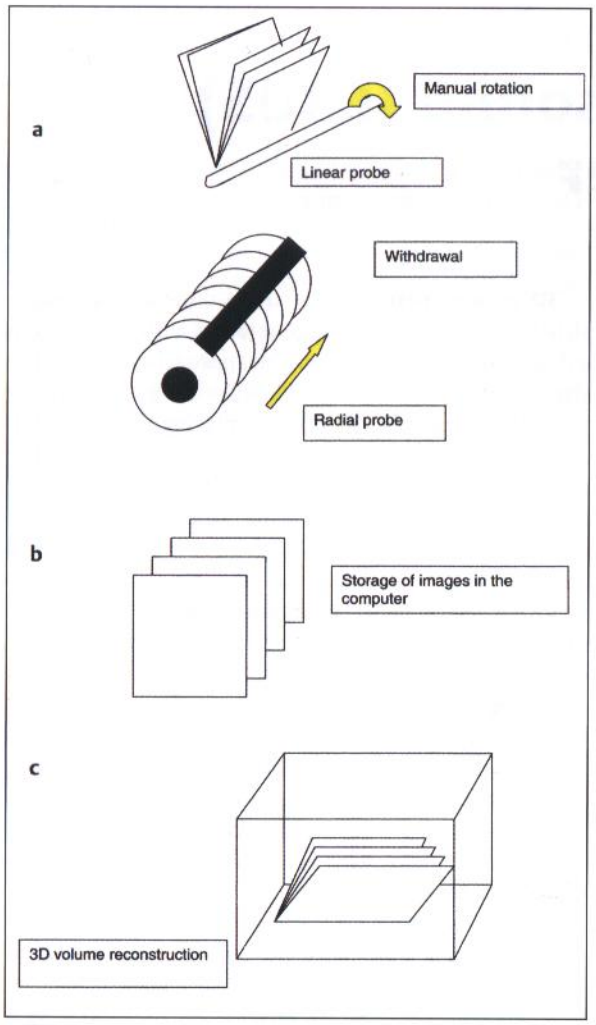


Fig. 25.**1a–c** The various steps involved in three-dimensional endoscopic ultrasound (3D EUS) scanning using radial or linear echoendoscopes.

Table 25.**1** Accuracy of three-dimensional endorectal ultrasonography (3D EUS) staging of rectal cancer

	T1/T2N0	T3N0	T3N1	T4N1
2D EUS	5	15	12	3
3D EUS	5	9	18	3
Surgical findings	4	6	22	3

scanning machine (Hitachi 6500 or 8000) and allows reconstruction of the 2D EUS pictures in six different scans. The acquisition time is very fast, at around 10–25 s. The acquisition time was function of the number of images recorded.

Thirty-five rectal cancers were assessed using 2D and 3D EUS. All of the tumors were located in the middle and lower part of the rectum, and stenotic tumors were excluded from the study. Three-dimensional EUS was possible in all cases. Two-dimensional EUS data classified the tumor into stages T1N0 (two patients), T2N0 (three patients), T3N0 (15 patients), T3N1 (12 patients) and T4N1 (three patients). Using 2D imaging, it was not possible to establish the degree of involvement of the mesorectum (more or less than 50%) precisely. No differences were found using 3D ERUS for superficial tumors (T1 and T2N0), but in six of the 15 patients staged with T3N0, 3D ERUS identified malignant lymph nodes, which were confirmed surgically in five of the six cases (Table 25.**1**).

By contrast, 3D EUS allowed precise assessment of the extent of infiltration into the mesorectum (Fig. 25.**2**) in all cases and showed quite complete invasion of it in eight cases. These findings were confirmed in all cases by the surgical data. To summarize the findings for rectal cancer: 2D EUS assessed 25 of 35 rectal tumors (71.4%) correctly with regard to the T and N staging, and 3D EUS increased this result to 31 correct evaluations out of 35 (88.6%).

With regard to the accuracy of 2D and 3D imaging in relation to the T staging (T1–2 vs. T3–T4), there were no differences (34 of 35 accurate staging findings using both techniques). However, patients staged with 3D imaging as T3N0 developed fewer liver metastases than those classified as T3N0 with 2D imaging (one of nine versus six of 15; 11% vs. 40%; $P = 0.002$). This difference was due to the fact that seven of the 15 rectal cancers staged as T3N0 with 2D imaging proved to be pT3N1 in the resected specimens. On the other hand, eight of the 35 patients in whom 3D ERUS showed extensive mesorectal infiltration (more than two-thirds of the thickness of the mesorectum) also developed more metastases (liver or peritoneal carcinomatosis) (four of eight versus seven of 27; 50% vs. 26%; $P < 0.001$).

Literature data. Three-dimensional ERUS is a new technique that is still undergoing development. Sumiyama et al. [15,17] recently reported their experience using 3D EUS and an electronic linear probe. They concluded that 3D EUS with a linear-array echoendoscope is accurate and represents a consistent method. They report that 3D EUS facilitates the anatomical interpretation of sonographic images and reduces the procedural difficulty of scanning.

Previous experience with 3D EUS using mechanical miniprobes has been reported for cardiovascular procedures [18], and using rigid electronic probes for gynecological tumor assessment [19,20]. More recently, results with 3D EUS using mechanical miniprobes have also been published for pancreaticobiliary diseases [3,6,9] and anal diseases [7].

Our own experience is slightly different, as we are using 3D ERUS with a new software program that allows linear-curved or radial electronic probes to be used, as the software is integrated into the ultrasound system's computer and an external sensor attached to the tip of the EUS scope is not needed. However, the most important question is whether 3D EUS is useful [21,22].

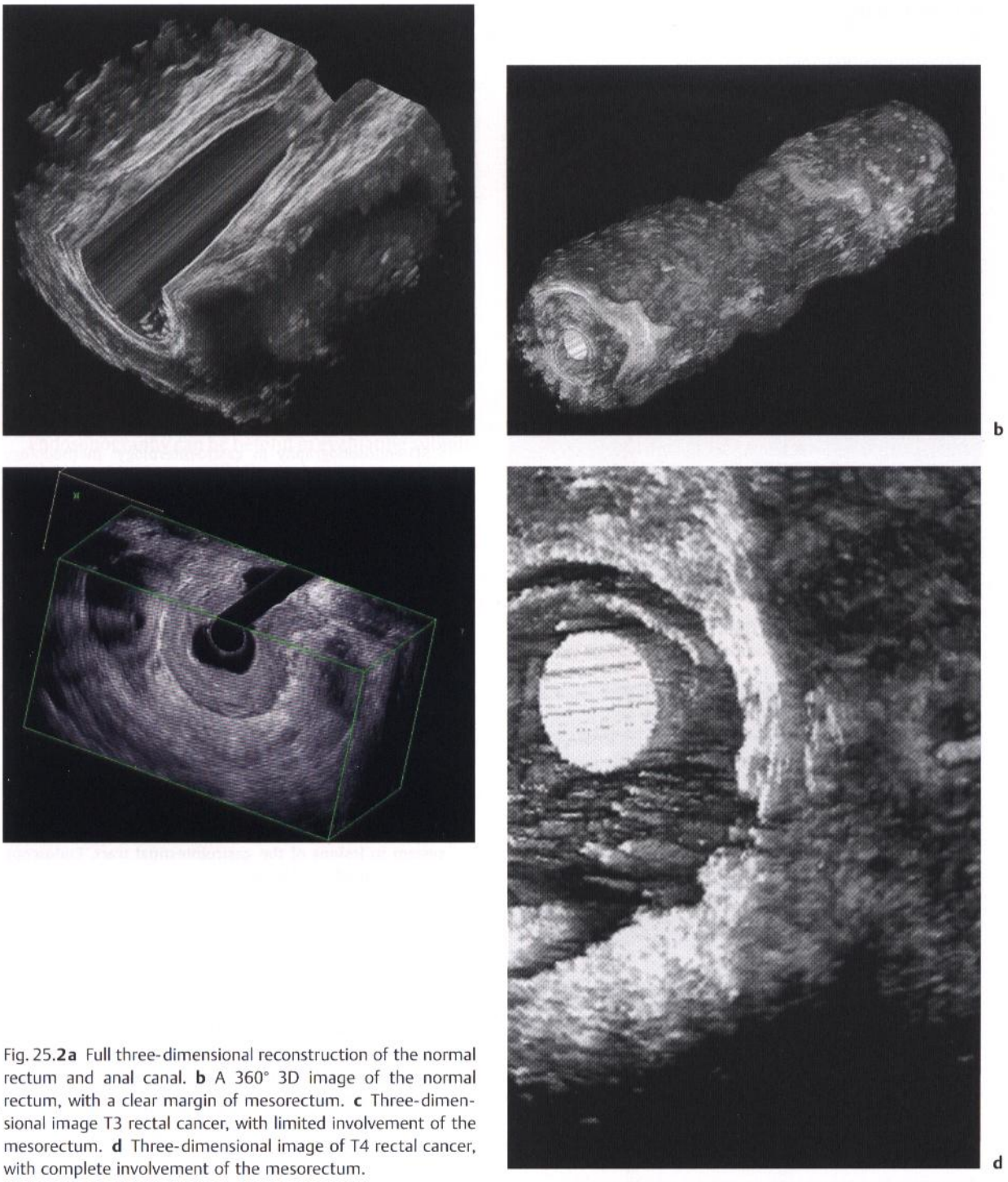


Fig. 25.**2a** Full three-dimensional reconstruction of the normal rectum and anal canal. **b** A 360° 3D image of the normal rectum, with a clear margin of mesorectum. **c** Three-dimensional image T3 rectal cancer, with limited involvement of the mesorectum. **d** Three-dimensional image of T4 rectal cancer, with complete involvement of the mesorectum.

With regard to the locoregional staging of rectal cancer, several studies have reported interesting results, with better parietal staging [4,5], accurate staging even in cases of stenotic lesions, and more precise EUS guidance for biopsies [23]. Our own results show that the mesorectal margins are better defined with 3D EUS than with 2D EUS, allowing more accurate parietal staging. This precise definition of mesorectal involvement has a direct impact on therapeutic decision-making, since cancer reaching the margins of the mesorectum is regarded as a T4 lesion, even without the involvement of a pelvic organ [24]. Such lesions have to be treated with preoperative chemoradiotherapy.

Conclusions

Three-dimensional ERUS with new software program described here is currently available and is easy to perform. As there is no need for an external sensor mounted at the tip of the probe, manipulation of the rectal probe is facilitated. Three-dimensional ERUS has a direct therapeutic impact on the pretherapeutic staging of rectal cancer, and allows more precise definition of the mesorectal margins, with a direct impact on therapeutic decision-making.

References

1. Kallimanis G, Garra BS, Tio TL, Krasner B, al-Kawas FH, Fleischer DE, et al. The feasibility of three-dimensional endoscopic ultrasonography: a preliminary report. Gastrointest Endosc 1995;41:235–9.
2. Odegaard S, Nesje LB, Molin SO, Gilja OH, Hausken T. Three-dimensional intraluminal sonography in the evaluation of gastrointestinal diseases. Abdom Imaging 1999;24:449–51.
3. Kanemaki N, Nakazawa S, Inui K, Yoshino J, Yamao J, Okushima K. Three-dimensional intraductal ultrasonography: preliminary results of a new technique for the diagnosis of diseases of the pancreatobiliary system. Endoscopy 1997;29:726–31.
4. Hunerbein M, Schlag PM. Three-dimensional endosonography for staging of rectal cancer. Ann Surg 1997;225:432–8.
5. Ivanov KD, Diavoc CD. Three-dimensional endoluminal ultrasound: new staging technique in patients with rectal cancer. Dis Colon Rectum 1997;40:47–50.
6. Tokiyama H, Yanai H, Nakamura H, Takeo Y, Yoshida T, Okita K. Three-dimensional endoscopic ultrasonography of lesions of the upper gastrointestinal tract using a radial-linear switchable thin ultrasound probe. J Gastroenterol Hepatol 1999;14:1212–8.
7. Gold DM, Bartram CI, Halligan S, Humphries KN, Kamm MA, Kmiot WA. Three-dimensional endoanal sonography in assessing anal canal injury. Br J Surg 1999;86:365–70.
8. Calleja JL, Albillos A. Three-dimensional endosonography for staging of rectal cancer. Gastrointest Endosc 1998; 47:317–8.
9. Marusch F, Koch A, Schmidt U, Zippel R, Kuhn R, Wolff S, et al. Routine use of transrectal ultrasound in rectal carcinoma: results of a prospective multicenter study. Endoscopy 2002;34:385–90.
10. Liu J, Miller LS, Chung CY, Overton DA, Sheera M, Forsberg F, et al. Validation of volume measurements in esophageal pseudotumors using 3D endoluminal ultrasound. Ultrasound Med Biol 2000;26:735–41.
11. Chung CY, McCray WH, Dhaliwal S, Haywood T, Black M, Liu JB, et al. Three-dimensional esophageal varix model quantification of variceal volume by high-resolution endoluminal US. Gastrointest Endosc 2000;52:87–90.
12. Hunerbein M, Ghadimi BM, Gretschel S, Schlag PM. Three-dimensional endoluminal ultrasound: a new method for the evaluation of gastrointestinal tumors. Abdom Imaging 1999;24:445–8.
13. Hunerbein M, Gretschel S, Ghadimi BM, Schlag PM. Three-dimensional endoscopic ultrasound of the esophagus: preliminary experience. Surg Endosc 1997;11:991–4.
14. Tamura S, Hirano M, Chen X, Sato Y, Narumi Y, Hori M, et al. Intrabody three-dimensional position sensor for an ultrasound endoscope. IEEE Trans Biomed Eng 2002;49: 1187–94.
15. Sumiyama K, Suzuki N, Kakutani H, Hino S, Tajiri H, Suzuki H, et al. A novel 3-dimensional EUS technique for real-time visualization of the volume data reconstruction process. Gastrointest Endosc 2002;55:723–8.
16. Molin S, Nesje LB, Gilja OH, Hausken T, Martens D, Odegaard S. 3D-endosonography in gastroenterology: methodology and clinical applications. Eur J Ultrasound 1999;10:171–7.
17. Sumiyama K, Suzuki N, Tajiri H. A linear-array freehand 3-D endoscopic ultrasound. Ultrasound Med Biol 2003;29: 1001–6.
18. Klingensmith JD, Schoenhagen P, Tajaddini A, Halliburton SS, Tuzcu EM, Nissen SE, et al. Automated three-dimensional assessment of coronary artery anatomy with intravascular ultrasound scanning. Am Heart J 2003;145: 795–805.
19. Ayoubi JM, Fanchin R, Ferretti G, Pons JC, Bricault I. Three-dimensional ultrasonographic reconstruction of the uterine cavity: toward virtual hysteroscopy? Eur Radiol 2002;12: 2030–3.
20. Liu JB, Miller LS, Bagley DH, Goldberg BB. Endoluminal sonography of the genitourinary and gastrointestinal tracts. J Ultrasound Med 2002;21:323–7.
21. Yoshimoto K. Clinical application of ultrasound 3 D imaging system in lesions of the gastrointestinal tract. Endoscopy 1998;30(Suppl 1):A145–8.
22. Yoshino J, Nakazawa S, Inui K, Katoh Y, Wakabayshi T, Okushima T, et al. Surface-rendering imaging of gastrointestinal lesions by three-dimensional endoscopic ultrasonography. Endoscopy 1999;31:541–5.
23. Hunerbein M, Dohmoto M, Haensch W, Schlag PM. Evaluation and biopsy of recurrent rectal cancer using three-dimensional endosonography. Dis Colon Rectum 1996;39: 1373–8.
24. Heald RJ, Ryall RD. Recurrence and survival after total mesorectal excision for rectal cancer. Lancet 1986;i:1479–82.

26 Endoscopic Ultrasound of the Colon

C.F. Dietrich, J. Mertens

Introduction

Endoscopic ultrasound (EUS) examination of the colon is possible, particularly using radial scanning techniques with an orthograde endoscopic view. Longitudinal probes in which the endoscopic view is not orthograde are more difficult to use, and this may complicate examinations in certain cases.

Endosonography can be helpful in evaluating submucosal colonic tumors in which the benign or malignant status is unknown. In these cases, the ideal combination of diagnostic methods—such as colonoscopy for precise localization and visualization of the findings and subsequent endosonography (e.g., using instilled water for optimal imaging conditions)—remains a challenge.

Miniprobe technology has proved to be superior to conventional endosonography in the colon (with the exception of the rectum), since tumors or polyps can be visualized, examined, and classified in the same way as in the approach used for esophageal, gastric, and duodenal wall endosonography. Although the place of miniprobe technology has not yet been sufficiently evaluated, it will probably offer a wide range of further indications.

Clinical Relevance

The relevance of flexible endosonography techniques in the lower intestinal tract is a matter of controversy [1–14]. There are as yet no universally accepted indications for endosonography of the colon. In contrast, rectal endosonography using rigid probes is widely used and, in the hands of an experienced examiner, can play an important role in the diagnosis of complicated fistulas and in the staging of rectal carcinomas. In some cases, endosonography may also be helpful for EUS-guided puncture. With further technical improvements and more widespread use of high-frequency miniprobe technology, an extended range of indications for endosonography in the lower gastrointestinal tract can be expected, particularly since lesions can be visualized endoscopically and their intramural and transmural extension can be assessed during the same examination.



Fig. 26.1 The prostate, with the urethra.

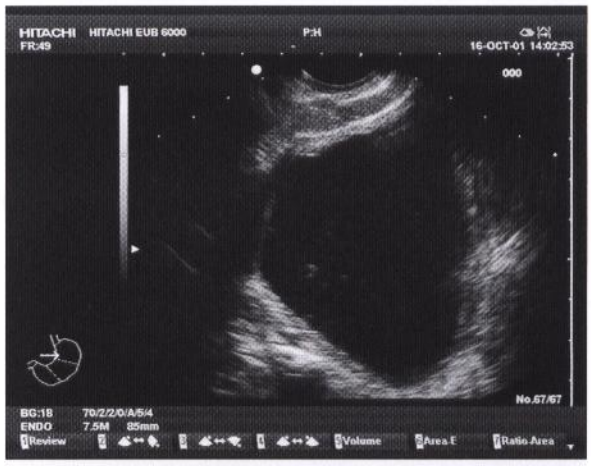
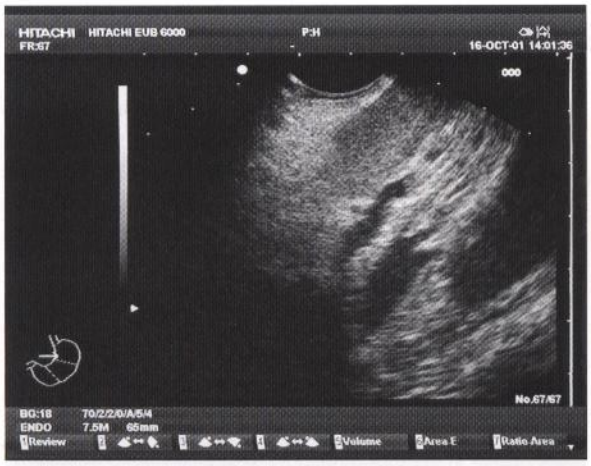


Fig. 26.2 The urinary bladder, with sporadic echoes caused by sediment.

The cecal pole and ileocecal valve can be reached with guidance from landmark structures and surrounding organs such as the prostate, seminal vesicle, urinary bladder, psoas muscle, left kidney with hilum, spleen, pancreas, gallbladder, liver, right kidney, and head of the pancreas (Figs. 26.**1**–26.**15**). Fistulas, abscesses, and other pathological transmural findings can be visualized with a high level of sensitivity (Figs. 26.**16**, 26.**17**).

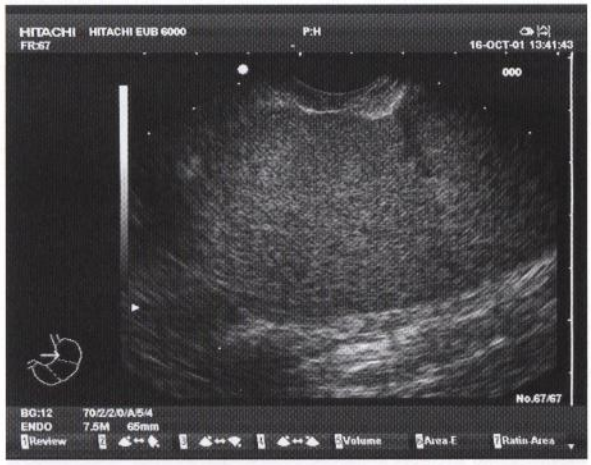


a

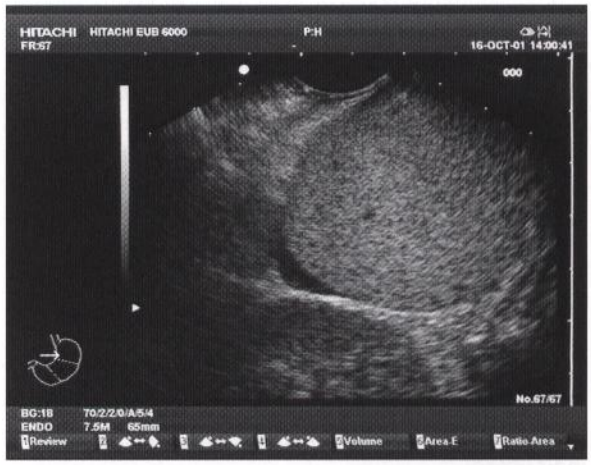


b

Fig. 26.3 **a** The left kidney, with the vascular hilum. **b** The renal parenchyma, as seen from the descending colon.



a



b

Fig. 26.4 The spleen. **a** With a small amount of physiological perisplenic free fluid toward the kidney. **b** With diaphragmatic borders, as seen from the splenic flexure of the colon.



Fig. 26.5 The pancreatic body, with the pancreatic duct, visualized from the transverse colon.

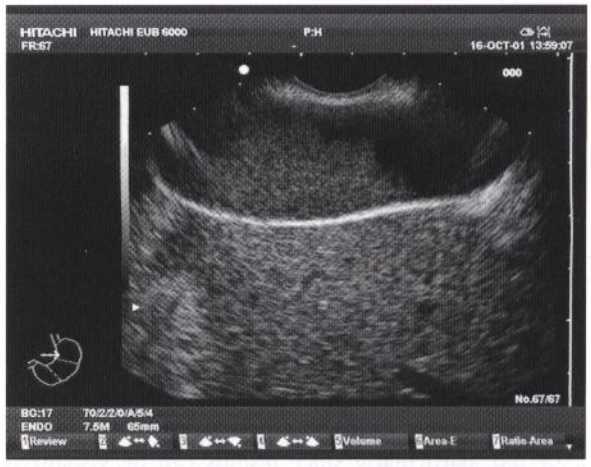


Fig. 26.6 The gallbladder with sludge, visualized from the hepatic (right) flexure of the colon.

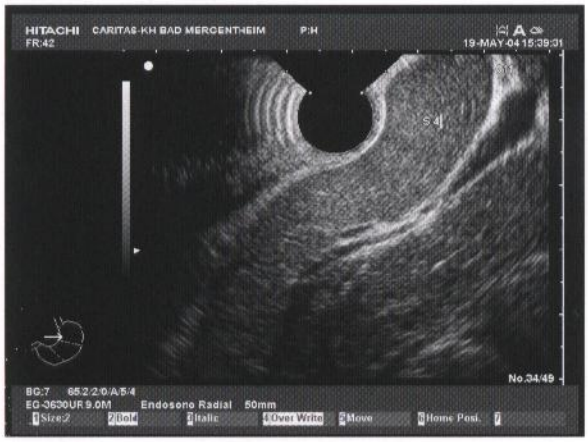


Fig. 26.**7** Imaging of the liver from the colon, demonstrating the echogenic borders of the portal vein branches. S4: quadrate lobe.

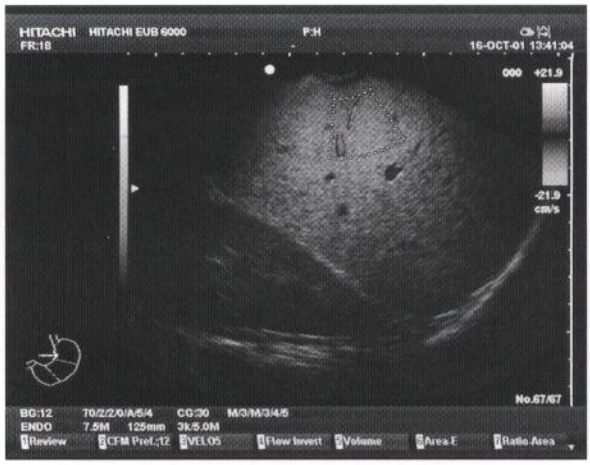


Fig. 26.**8** Imaging of a fatty liver echo texture, including comparison of the parenchymal imaging characteristics of the liver and kidney. It is also possible to assess the vessels using color Doppler imaging.



Fig. 26.**9** The head of the pancreas, as seen from the ascending colon.

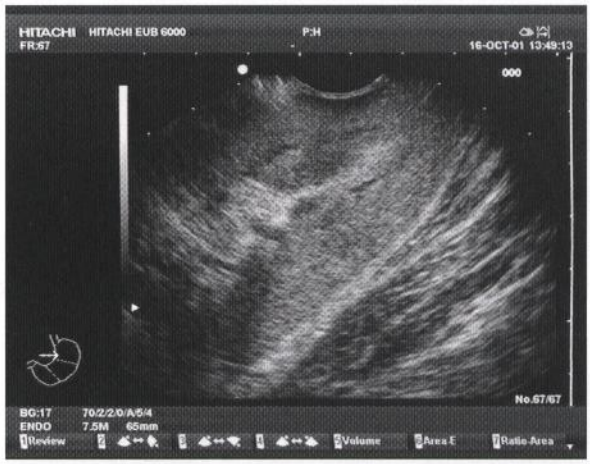
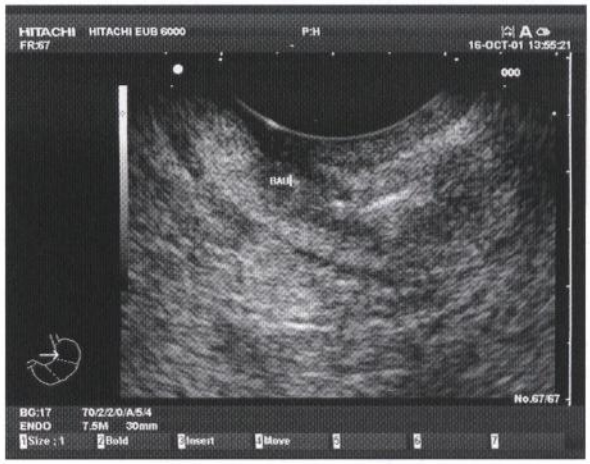


Fig. 26.**10** The right kidney, as seen from the ascending colon.



a

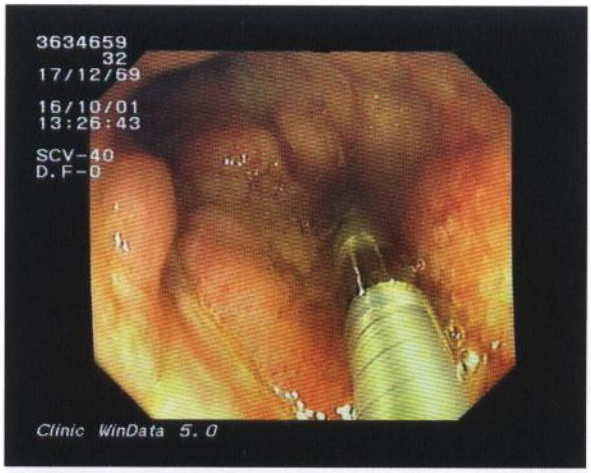


b

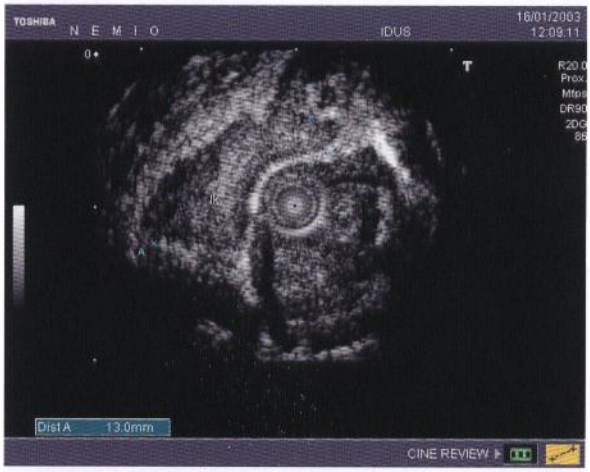
Fig. 26.**11a** The ileocecal valve. **b** With the orifice of the terminal ileum. BAU: Bauhin's valve.



a



b



c

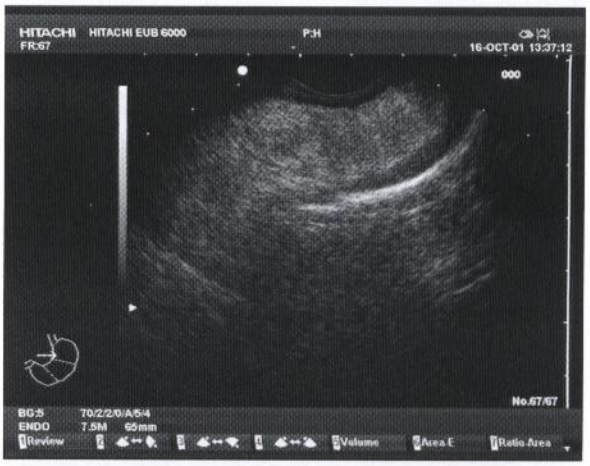
Fig. 26.**12a** The terminal ileum (ti), examined with miniprobe ultrasound, with visualization of small (physiological) lymph nodes (lk) in the immediate vicinity. **b, c** Pathological lymph nodes due to Crohn's disease (**b**, endoscopic image; **c**, miniprobe image).



Fig. 26.**13** A fistula in Crohn's disease. There is a transmural inflammatory reaction, with a blind-ending fistula (F). Fissural ulcerations corresponding to the endoscopic image were visible, the transmural size of which was only capable of being evaluated with miniprobe endosonography.



a



b

Fig. 26.**14** Imaging of a fistula with a surrounding transmural inflammatory mesenteric reaction, with echogenic air outside the intestinal wall. **a** Miniprobe imaging. **b** Conventional endosonography.

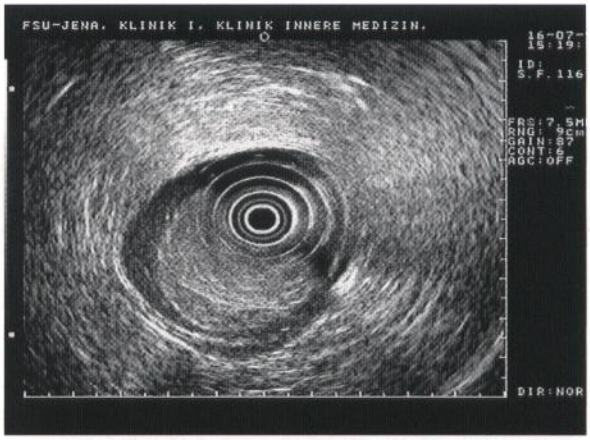
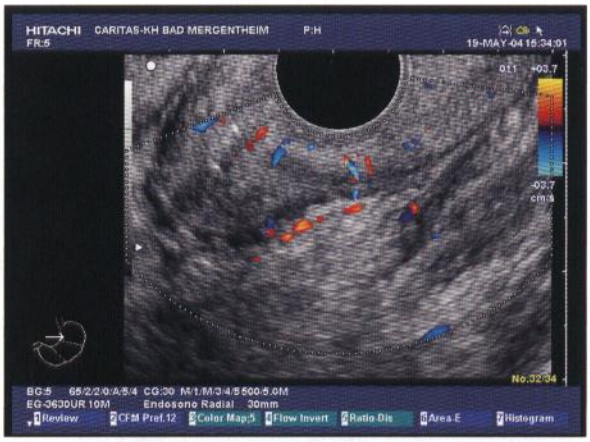


Fig. 26.**15** A lipoma in the transverse colon. As in the upper gastrointestinal tract, submucous tumors can be assigned to a specific layer of the intestinal wall—e. g., the submucosa with lipomas.

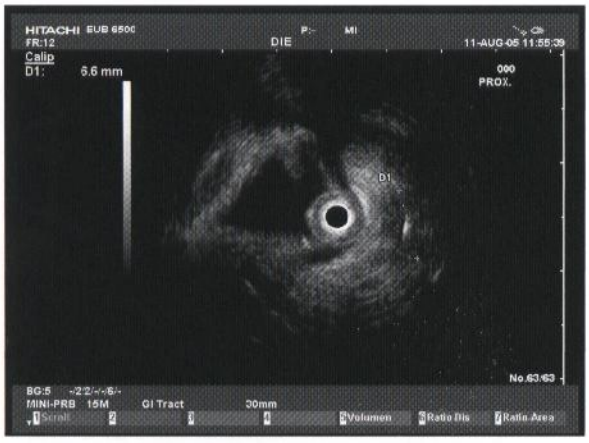


a



b

Fig. 26.**16a, b** Hemorrhagic segmental colitis, with circumscribed ischemic thickening in the right colon.



a



b

Fig. 26.**17a, b** Diverticula (between the markers) visualized using miniprobe endosonography.

References

1. Ahmad NA, Kochman ML, Long WB, Furth EE, Ginsberg GG. Efficacy, safety, and clinical outcomes of endoscopic mucosal resection: a study of 101 cases. Gastrointest Endosc 2002;55:390–6.
2. Bhutani MS, Nadella P. Utility of an upper echoendoscope for endoscopic ultrasonography of malignant and benign conditions of the sigmoid/left colon and the rectum. Am J Gastroenterol 2001;96:3318–22.
3. Dietrich CF, Lembcke B, Seifert H, Caspary WF, Wehrmann T. Sonographische Diagnostik der Penicillin-induzierten seg-

mentär-hämorrhagischen Colitis. Dtsch Med Wochenschr 2000;125:755–60.
4. Giovannini M, Bernardini D, Seitz JF, Moutardier V, Hoevenaeghel G, Monges G, et al. Value of endoscopic ultrasonography for assessment of patients presenting elevated tumor marker levels after surgery for colorectal cancers. Endoscopy 1998;30:469–76.
5. Hirata N, Kawamoto K, Ueyama T, Iwashita I, Masuda K. Endoscopic ultrasonography in the assessment of colonic wall invasion by adjacent diseases. Abdom Imaging 1994; 19:21–6.
6. Hizawa K, Suekane H, Aoyagi K, Matsumoto T, Nakamura S, Fujishima M. Use of endosonographic evaluation of colorectal tumor depth in determining the appropriateness of endoscopic mucosal resection. Am J Gastroenterol 1996; 91:768–71.
7. Hunerbein M, Handke T, Ulmer C, Schlag PM. Impact of miniprobe ultrasonography on planning of minimally invasive surgery for gastric and colonic tumors. Surg Endosc 2004;18:601–5.
8. Lew RJ, Ginsberg GG. The role of endoscopic ultrasound in inflammatory bowel disease. Gastrointest Endosc Clin N Am 2002;12:561–71.
9. Okada N, Hirooka Y, Itoh A, Hashimoto S, Ishikawa H, Itoh T, et al. Cholecystocolonic fistula preoperatively diagnosed by endoscopic ultrasound of the colon. J Gastroenterol Hepatol 2005;20:1621–4.
10. Sasaki Y, Niwa Y, Hirooka Y, Ohmiya N, Itoh A, Ando N, et al. The use of endoscopic ultrasound-guided fine-needle aspiration for investigation of submucosal and extrinsic masses of the colon and rectum. Endoscopy 2005;37:154–60.
11. Stergiou N, Haji-Kermani N, Schneider C, Menke D, Kockerling F, Wehrmann T. Staging of colonic neoplasms by colonoscopic miniprobe ultrasonography. Int J Colorectal Dis 2003;18:445–9.
12. Tsuga K, Haruma K, Fujimura J, Hata J, Tani H, Tanaka S, et al. Evaluation of the colorectal wall in normal subjects and patients with ulcerative colitis using an ultrasonic catheter probe. Gastrointest Endosc 1998;48:477–84.
13. Watanabe F, Honda S, Kubota H, Higuchi R, Sugimoto K, Iwasaki H, et al. Preoperative diagnosis of ileal lipoma by endoscopic ultrasonography probe. J Clin Gastroenterol 2000;31:245–7.
14. Waxman I, Saitoh Y, Raju GS, Watari J, Yokota K, Reeves AL, et al. High-frequency probe EUS-assisted endoscopic mucosal resection: a therapeutic strategy for submucosal tumors of the GI tract. Gastrointest Endosc 2002;55:44–9.

27 Mediastinum

C.F. Dietrich, M. Hocke

Introduction

Endoscopic ultrasound (EUS) diagnostic techniques are extremely valuable in the mediastinum, but this has not yet been fully exploited in everyday clinical practice. It is not possible to evaluate the mediastinum adequately using only one method of examination; instead, a combination of endoscopic methods (e.g., bronchoscopy), radiographic methods (e.g., conventional techniques, computed tomography, magnetic resonance imaging), surgical methods (e.g., mediastinoscopy, thoracoscopy, thoracotomy) and ultrasound methods is necessary.

Conventional radiography is undoubtedly important at the start of diagnostic work-up in the mediastinal region. The upper and anterior mediastinum can be seen adequately with *transthoracic mediastinal ultrasonography,* which is easily carried out and also allows targeted aspiration of tumors in order to obtain histological confirmation of the suspected diagnosis [1–5]. However, examination of the aortic lymph nodes and lymph-node groups in the lower and posterior mediastinum is not adequate with this method. *Computed tomography* (CT) allows the mediastinum to be examined accurately, but aspiration and collection of histological specimens from structures deep in the mediastinum require a separate procedure. *Transesophageal endoscopic ultrasonography* allows examination of the posterior mediastinum, as well as visualization and targeted aspiration of even the smallest structures in this area. On the other hand, the examination of pretracheal and paratracheal structures using endoscopic ultrasonography is not adequate (with the exception of the 2L and 4L nodes). *Transbronchial endoscopic ultrasonography* shows signs of being a promising method, but so far has only been used in a few centers and has not yet been fully evaluated.

The diagnostic confirmation of mediastinal tumors and staging of bronchial carcinoma are therefore still dependent on mediastinoscopy, video-assisted thoracoscopy, and thoracotomy and mediastinotomy if necessary. Each of these methods only has a limited range of indications. Coordinating the application of the methods is even more difficult, since ultrasound techniques are not yet fully developed in the field of pneumology. Transesophageal endoscopic ultrasound is often carried out by gastroenterologists, and interdisciplinary collaboration may be inadequate. A further disadvantage is that there is a relatively small number of pneumology centers in Europe in comparison with the USA, for example.

Anatomy

The mediastinum is a complex space in which the lymph nodes of the upper mediastinum, the aortic lymph nodes, the lymph nodes of the lower mediastinum, and the pulmonary lymph nodes have to be distinguished. The pulmonary lymph nodes (hilar, interlobar, lobar, segmental, and subsegmental) are known as the N1 lymph nodes; the mediastinal and subcarinal lymph nodes as the N2 lymph nodes; and the supraclavicular and scalene lymph nodes as the N3 lymph nodes. The mediastinal lymph nodes are classified in accordance with the Mountain and Dresler system [6], which is adapted from an earlier classification by Tsuguo Naruke.

The paratracheal lymph-node groups (level 2L and 4L; L = left), the lymph-node groups in the aortopulmonary window (level 5), the subcarinal (level 7), and in particular the paraesophageal lymph nodes (level 8) can be viewed and punctured with real-time visualization. This is also possible in part for the lymph nodes in the region of the inferior pulmonary ligament (level 9). The same is true of metastases in the left adrenal gland, determining the prognosis in up to 5% of cases [7].

Lymph-node levels 1, 2R, 3, and 4R (R = right), as well as 6, are not capable of being assessed in most patients with normal-sized lymph nodes, due to interference from the larger airways (Fig. 27.**1**). EUS imaging may be possible in patients with larger lymphomas.

It has been shown that CT, which simply determines the size of mediastinal lymph nodes, is inadequate, with an accuracy level of 50–80%. The longitudinal position of the lymph nodes in the mediastinum is the critical factor, as this means that the lymph nodes can only be imaged from the side or at an angle. This is the reason for the notable inaccuracy of CT for determining the size of the lymph nodes. Endoscopic ultrasonography is able not only to assess the criteria relative to size, but also changes pertaining to the echo pattern, architecture, and localized infiltration.

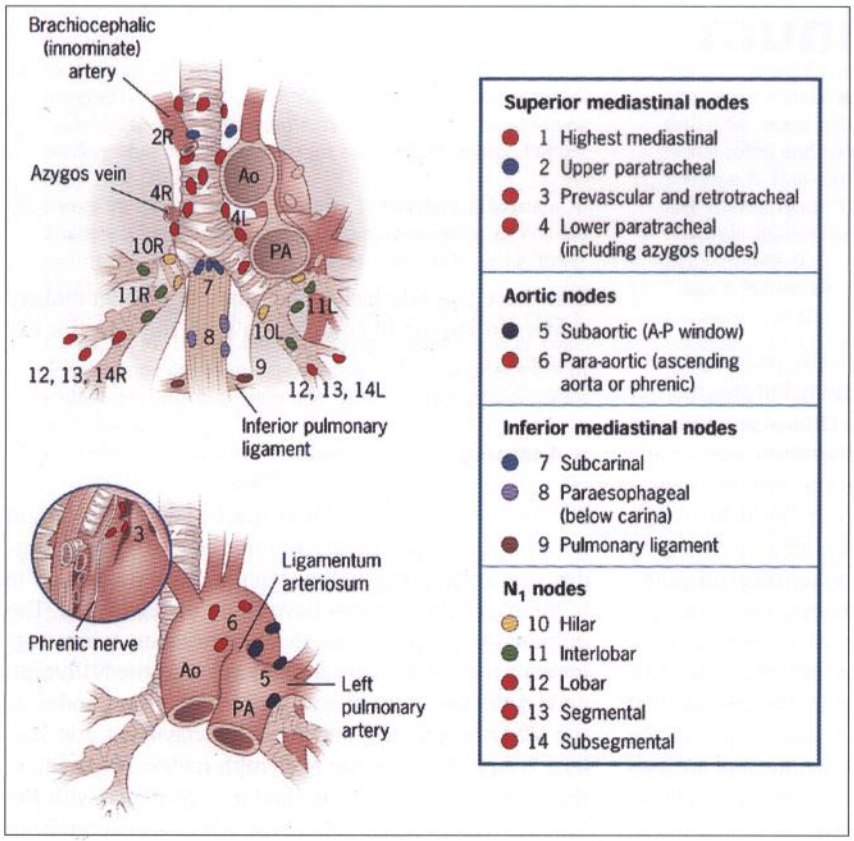


Fig. 27.1 Classification of the mediastinal lymph nodes according to Mountain and Dresler [6] (reproduced with permission from Chest, Vol. 111, 1997).

■ Examination Techniques

General

Radial and linear instruments are available for transesophageal endoscopic ultrasonography in the mediastinum, but the radial technique does not allow aspiration, and the longitudinal scanner is therefore preferable from the pneumological point of view. Aspiration specimens obtained with EUS can be assessed using either cytology or molecular biology.

When enlarged lymph nodes are present, detection is also easier. When lymph nodes are detected, biopsy of the lymph node (or an adrenal lesion) that is considered to be the most distant should be carried out first, to avoid spreading malignant cells from local lymph nodes to more distant ones.

Prerequisites. Esophagogastroduodenoscopy (EGD) should be carried out before EUS in order to exclude stenosis and minimize the risk of perforation by the relatively inflexible endoscopic ultrasound instrument. Extra care should be taken in inserting the instrument into the middle esophagus if a traction diverticulum is suspected and during passage through the gastroesophageal junction, where there is an increased risk of perforation due to aggressive forward movement. The explanation of the procedure given to the patient should be the same as for any endoscopic procedure in the upper gastrointestinal tract, with extra emphasis being given to the increased risk of perforation in comparison with conventional EGD. The patient should be informed about the risk of bleeding and infection (including potentially fatal progressive mediastinitis). The risk of bleeding is small when coagulation is adequate (Quick test > 50%, thrombocytes > 50/nL).

Endoscopic ultrasound examination of the mediastinum can be carried out as an outpatient procedure. After it has been explained to the patient, the examination requires 5–20 min, depending on the practitioner's level of experience. It has proved helpful to work with a cytologist present during the examination, although this topic is a matter of controversy.

Some authors have found that suction during fine-needle aspiration of lymph nodes increases the bloodiness of the specimen and does not necessarily increase the yield. The aspiration procedure is described elsewhere (see Chapter 10).

Sedation. Sufficient sedation is extremely important. EUS-guided aspiration should only be carried out with adequate sedation, without cough stimulation or patient movement, as accidental puncture of the heart or large mediastinal vessels has to be avoided. Anesthesia that can be easily controlled is therefore necessary. In our experience, propofol (Disoprivan) is more suitable than midazolam for this purpose, but comparative studies on this topic are lacking.

Procedure

The instrument is guided into the esophagus with endoscopic visualization. From the upper esophagus (18–20 cm past the incisor line), insertion can then continue using either endoscopic or endoscopic ultrasound viewing.

Although orientation may be possible using the surrounding structures while the scope is being inserted, systematic examination starts distally, as control is much better when the scope is withdrawn. When the scope is rotated, the tracheal and bronchial airways ventrally, the echo-free vessels mainly laterally, and the hyperechoic bone structures dorsally can all be used as simple landmarks for orientation.

The systematic examination of the mediastinum starts distally, with the instrument in the cardiac region at the level of the thoracoabdominal junction. In this position, one can identify the liver, hepatic veins, inferior vena cava, heart chambers and heart valves, the left and right ventricular outflow ducts, the ascending aorta, the pulmonary trunk with the pulmonary arteries, and the aortic arch with the aorticopulmonary window. When the endoscope is turned and one orients oneself along the reflexogenic spine, it becomes possible to identify the descending aorta paravertebrally on the left and the azygos vein on the right. Further up, the vessels emerging from the aorta, particularly the cervical vessels (the common carotid artery and jugular vein), the thyroid, and the paratracheal lymph-node groups can be observed from the tracheal bifurcation up to the mouth of the esophagus. The pretracheal lymph nodes are beyond the range of endoscopic ultrasound, as they are concealed behind the air-filled trachea. The pneumological examination using endoscopic ultrasound is completed by imaging the left adrenal gland and if possible the right adrenal gland (see Chapter 21) and by examining the lymph nodes of the celiac trunk. One can also start assessing the more distally located structures here, with the transduodenal and transgastric part of the examination taking place to begin with. The mediastinal lymph-node groups are examined using the following markers: the echo-free heart chambers and vascular paths; the ventral hyperechoic (air-filled) tracheobronchial system; and the dorsal echogenic bone structures of the spine. Directly next to the esophagus are the periesophageal and paravertebral lymph-node groups. The paracardiac lymph nodes can be found in the immediate neighborhood of the heart. Along the contour of the heart on the upper side of the atrium, the subcarinal lymph nodes can be detected in the tracheobronchial region, and the lymph nodes of the pulmonary ligament are located somewhat further distally.

The course of a typical examination is described in Chapter 2. Figures 27.**2**–27.**12** focus on the anatomy of the mediastinal vessels using color Doppler imaging and



Fig. 27.**2** The diaphragm, with the confluence of the hepatic veins (CLV) at the inferior vena cava (VCI).

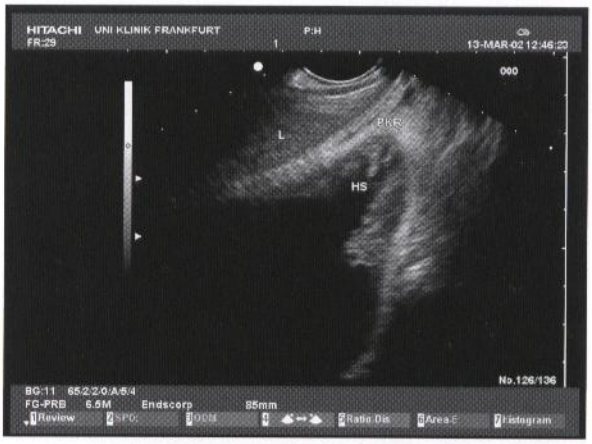


Fig. 27.**3** The pericardial cavity (PKR) with the left lobe of the liver (L) and tip of the heart (HS).

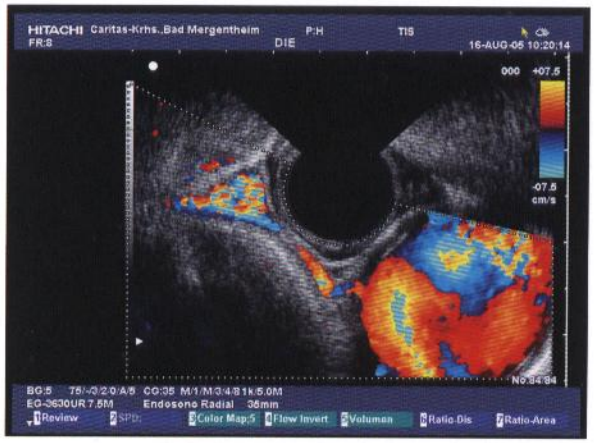
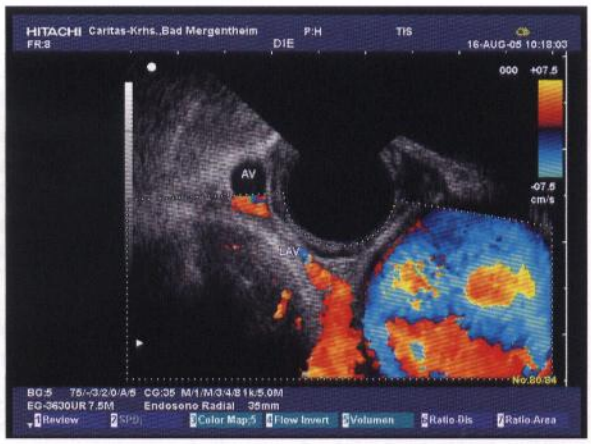


Fig. 27.**4** The arterial branches of the aorta can be visualized using color Doppler imaging. The azygos vein can be viewed in its contralateral position on the right in front of the spine. Visualizing the vertebrae (left lower corner of the image) has proved helpful.



a

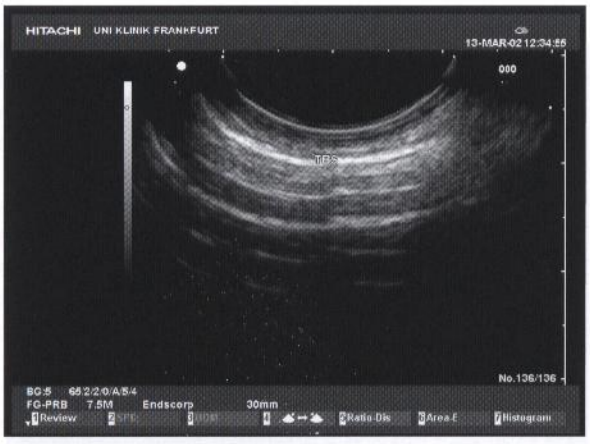


b

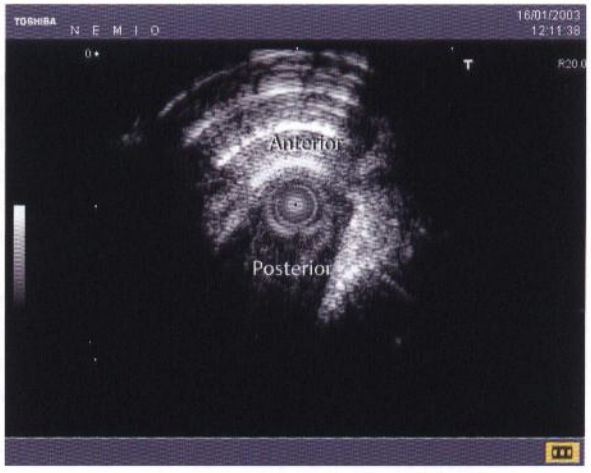


c

Fig. 27.5 The azygos vein (AV) can be accurately viewed in its lateral position on the right in front of the spine. Visualizing the aorta (AO) on the left of the cervical vertebrae (CV) has proved helpful. **a** The left azygos vein (LAV) is also visible here (B-mode). **b** Color Doppler imaging. **c** Miniprobe ultrasonography.



a



b

Fig. 27.6 The trachea (TBS) can be imaged with both conventional EUS (a) and miniprobe EUS (**b**) by identifying the air echoes ventrally. The lumen is therefore posterior in **b**.

miniprobe ultrasonography of the mediastinum, and showing potential artifacts.

■ Literature Review

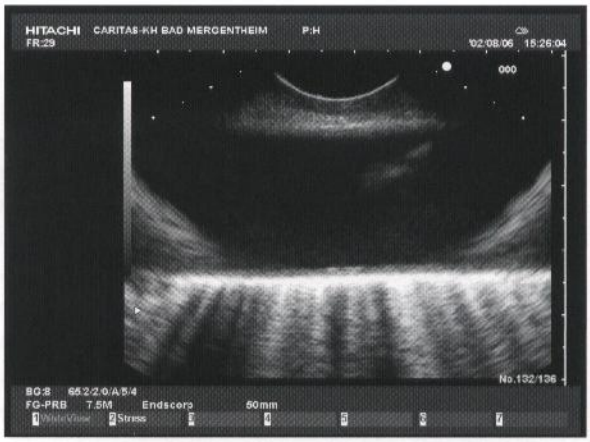
Information about the importance of the lymph-node structure in distinguishing between malignant and benign changes in lymph nodes is mainly derived from high-resolution ultrasonography (7.5–12 MHz). Most research has concentrated on the results of cervical lymph-node ultrasonography. Attempts to assess malignancy on the basis of size (malignant > 1 cm), appearance (malignant: round, benign: oval), and internal structure (malignant with no signs of a hilum, benign with identification of a hilum) have shown success rates of 57–94% in various studies [8–13].

Combining these findings with the use of power Doppler to examine the vascular distribution can improve the accuracy of the diagnosis. In this way, it is possible to observe that benign lymph nodes show hilar vascularization and that malignant lymph nodes usually show vascularization coming from the edge. However, these results, from a study that reported a sensitivity of 92% and a specificity of 100%, need to be tested in further investigations [14]. The criteria may also be easier to image and evaluate with the use of ultrasound contrast enhancement [15]. It would be logical to extend the results to the lymph nodes in the mediastinum and abdominal cavity using high-resolution endoscopic ultrasonography. Initial results from an as yet unpublished study currently being conducted to differentiate between malignant and benign lymph nodes using endoscopic ultrasonography show promising results.

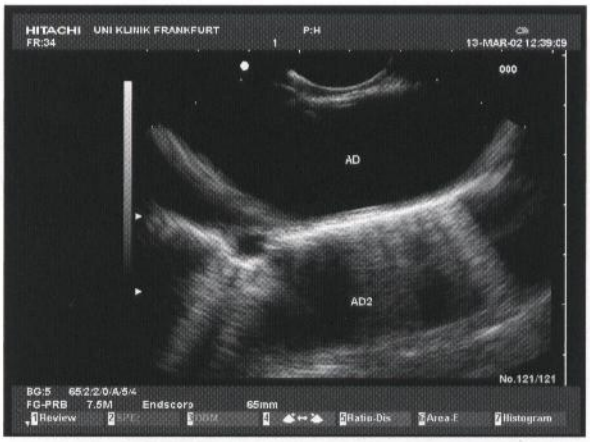
EUS-Guided Fine-Needle Aspiration in the Mediastinum

The aim of endoscopic ultrasound-guided fine-needle aspiration (EUS-FNA) in the mediastinum is either to stage mediastinal lymph nodes in lung cancer or to diagnose other diseases involving the lymph nodes or lesions of unknown origin in the mediastinum. More than 20 studies focusing on mediastinal staging of lung cancer and EUS-FNA have been published, including a total of more than 1200 patients. The reported sensitivity of EUS-FNA for detecting mediastinal malignancy ranges from 0.61 to 1.00 (median 0.90), with specificities of 0.71–1.00 (median 0.99) (Table 27.**1**) [16–31].

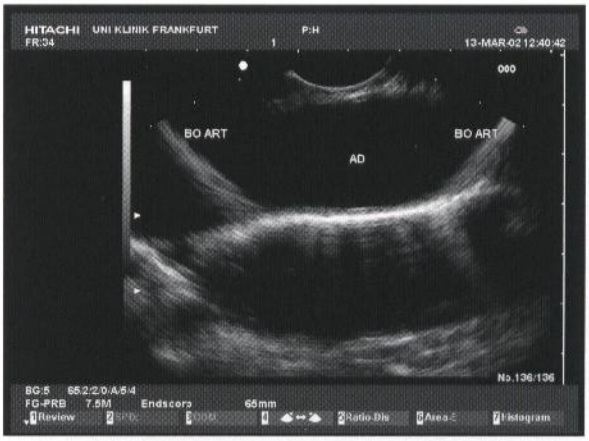
No fatal complications of EUS-FNA have been reported in the literature so far. FNA of a cystic mediastinal lesion should be avoided, or when necessary it can be preceded by prophylactic antibiotic administration. The use of ultrasound contrast enhancement specifically for lymph nodes may make it easier to detect localized infiltration of lymphatic tissue in the future.



a



b



c

Fig. 27.**7** The descending aorta (AD). Due to the extreme differences in acoustic impedance between the blood in the aorta and the surface of the lung, the descending aorta can be imaged in various cross-sections with different artefacts. **a** Typical morphology. **b** Mirror artefact. **c** Arch artefacts.

Table 27.1 Endoscopic ultrasound–guided fine-needle aspiration (EUS-FNA) cytology for mediastinal malignancy in the mediastinum, mainly in patients with non–small-cell lung cancer: literature review

First author (ref).	Year	Patients (n)	Sensitivity (%)	Specificity (%)	Accuracy (%)	PPV	NPV
Giovannini [16]	1995	42	0.81–0.89	1.00	0.83–0.89	–	–
Pedersen [17]	1996	9	0.91	1.00	0.92	1.00	0.67
Silvestri [18]	1996	27	0.89	1.00	0.93	1.00	0.82
Gress [19]	1997	24	0.93	1.00	0.96	–	–
Wiersema [20]	1997	171	0.92	0.93	0.92	1.00	0.86
Hünerbein [21]	1998	25	0.89	0.83	–	1.00	0.75
Williams [22]	1999	82	0.87	1.00	0.90	–	–
Roberts [23]	2000	20	0.86	1.00	–	–	–
Fritscher-Ravens [24]	2000	153	0.88–0.97	1.00	0.94–0.98	1.00	0.88–0.95
Laudanski [25]	2001	92	0.70	0.81	0.77	0.64	0.85
Wiersema [26]	2001	86	0.96	1.00	0.98	–	–
Wallace [27]	2001	121	0.87	1.00	0.89	1.00	0.64
Larsen [28]	2002	79	0.92	1.00	0.94	1.00	0.80
Wallace [29]	2004	69	0.61	0.98	0.83	0.94	0.78
Annema [30]	2004	36	0.93	1.00	0.94	1.00	0.80
Kramer [31]	2004	81	0.78	0.71	0.77	1.00	0.45

NPV: negative predictive value; PPV: positive predictive value.

Indications for EUS-FNA. Aspiration is specifically indicated:

- In cases of submucosal tumors of the esophagus in which the patient's operability is doubtful or impossible to confirm.
- In cases of confirmed bronchial carcinoma in patients in whom it is an open question whether the contralateral lymph nodes may be affected, so that surgical treatment is inappropriate (we recommend carrying out EUS before mediastinoscopy, since the latter is much more stressful procedure and can be avoided if the FNA results are positive for malignancy).
- In cases of unexplained enlargement of mediastinal lymph nodes.
- In cases of suspected paraesophageal bronchial carcinoma in which bronchoscopic confirmation is not possible.
- In cases of unknown mediastinal masses (there is a higher risk of infection in cystic masses, and the indication therefore has to be strong).
- In cases of re-staging after induction chemotherapy (Figs. 27.**8**–27.**11**).

Drainage of mediastinal abscesses using endoscopic ultrasound has been reported, but caution should be exercised when resorting to this procedure, as there is a danger of permanent fistula formation in the esophagus (Fig. 27.**12**).

Clinical value in pneumology. The available options for diagnosing disease in the mediastinum and surrounding organs using transesophageal EUS-FNA are not currently being fully exploited. However, if the aspiration is carried out correctly, cytological and possibly histological assessment of unclear changes can significantly shorten the diagnostic procedure in everyday routine work for many patients, allowing malignant infiltration to be confirmed and tumors to be classified.

Non–Small-Cell Lung Cancer

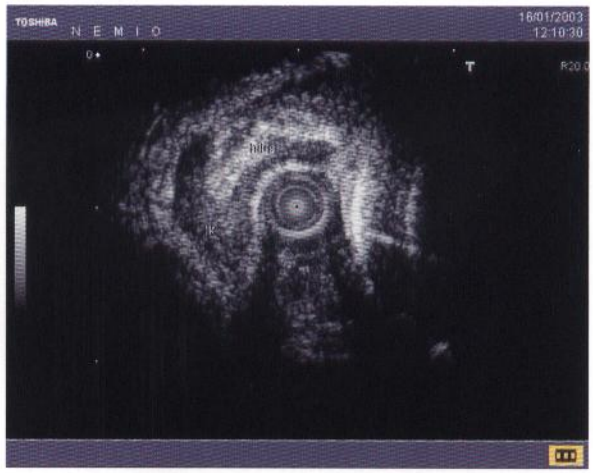
The problem. In patients with non–small-cell lung cancer (NSCLC) who undergo surgery, the procedure may be futile due to advanced mediastinal disease in up to 50% of cases. This is particularly important in up to 25% of patients who are found to have normal-sized lymph nodes (< 1 cm) on chest CT. Up to 15% of operations for NSCLC result in exploratory thoracotomies without tumor resection; in addition, up to 35% of the operations are unsuccessful due to postoperative tumor recurrence.

The treatment of NSCLC is stage-dependent. Surgical resection is considered if no spread outside the lung is found (stages I and II). Induction chemotherapy followed by resection is considered in patients with ipsilateral mediastinal lymph-node disease (stage IIIA). Chemotherapy or chemoradiotherapy are considered if contralateral mediastinal lymphadenopathy or distant metastases are present (stages IIIB and IV).

Lymph-node staging. When a tumor has been histologically confirmed and is thought to be potentially operable, lymph-node staging is required in order to examine the contralateral mediastinal lymph-node



a



b



c

Fig. 27.**8** The subcarinal lymph-node groups on the roof of the left atrium: imaging of the normal lymph-node architecture with a lymph-node sinus (LKS). **a** Conventional EUS. **b** Mini-probe EUS. **c** Pathological lymph nodes often show changes in the architecture, seen here in a patient with bronchial carcinoma (BC).

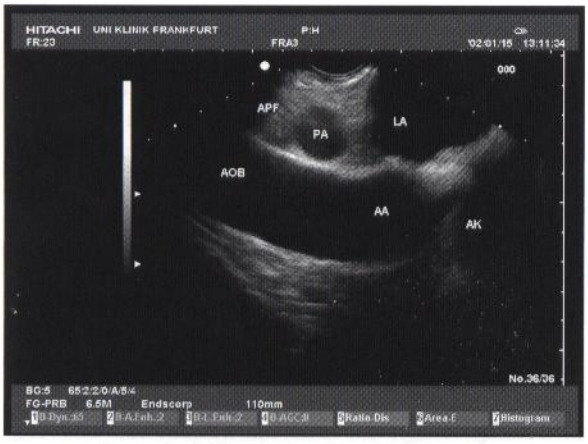


Fig. 27.**9** The aortopulmonary window (APF). The left atrium (LA), pulmonary artery (PA), aortic arch (AOB), ascending aorta (AA), and aortic valve (AK) are also shown. The pulmonary artery separates the aortopulmonary window from the subcarinal lymph-node groups on the roof of the left atrium.



Fig. 27.**10** A normal periesophageal lymph node. A very narrow, longitudinally positioned lymph node with normal architecture is shown between the markers. PA: pulmonary artery.

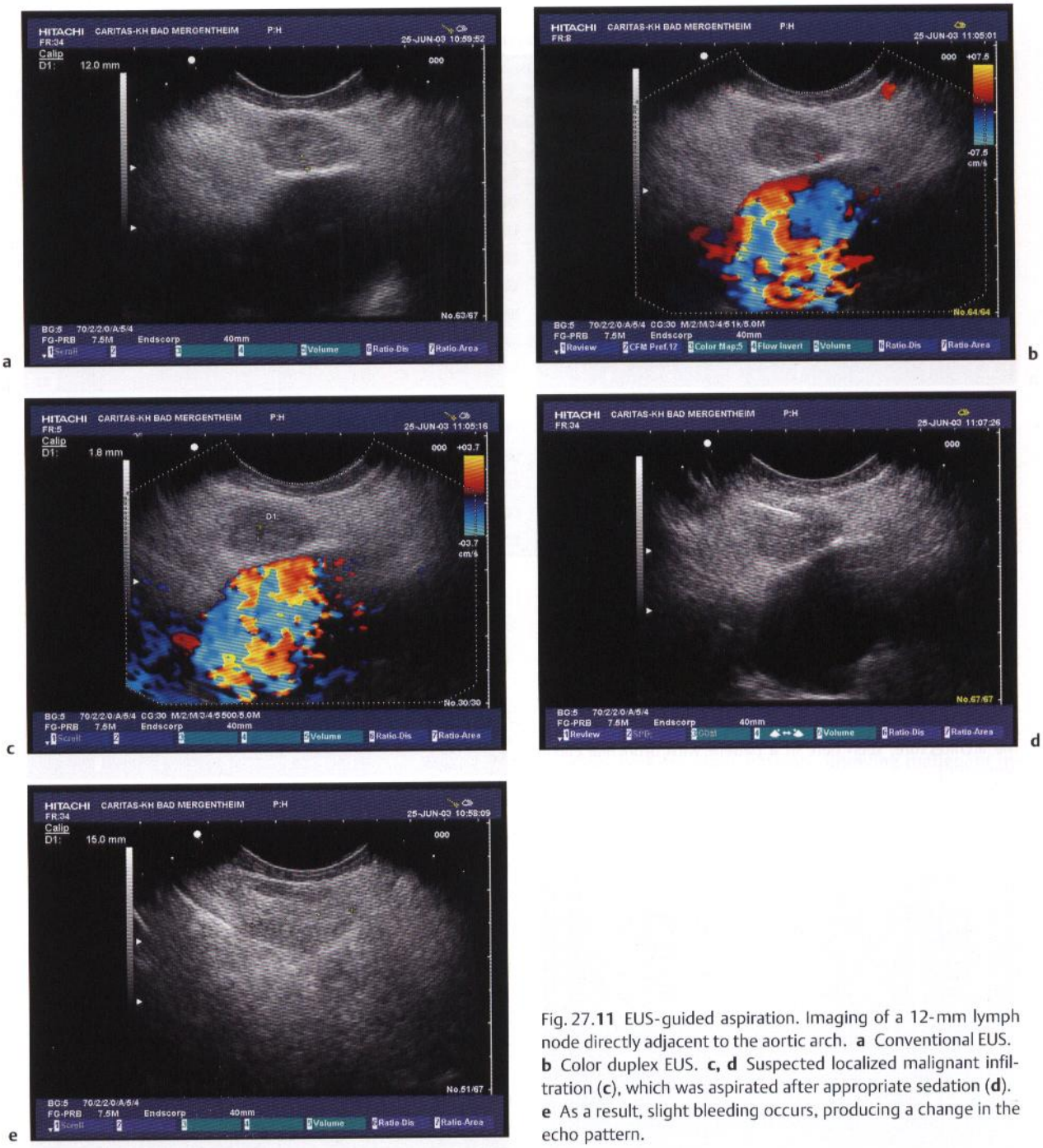


Fig. 27.**11** EUS-guided aspiration. Imaging of a 12-mm lymph node directly adjacent to the aortic arch. **a** Conventional EUS. **b** Color duplex EUS. **c, d** Suspected localized malignant infiltration (**c**), which was aspirated after appropriate sedation (**d**). **e** As a result, slight bleeding occurs, producing a change in the echo pattern.

groups (the patient is considered to be inoperable if these are positive).

Imaging methods. Chest radiography, thoracic CT, and bronchoscopy are the main imaging methods and are a prerequisite for further investigations (such as EUS, mediastinoscopy, and video-assisted thoracoscopy).

EUS. The advantage of endoscopic ultrasound over CT is that it provides an opportunity to assess the fine lymph-node structure through the echo patterns. Localized malignant lymph-node infiltrations can be recognized more easily using endoscopic ultrasound, even when computed tomography produces negative results.

EUS-FNA in CT-negative patients. EUS-FNA is able to demonstrate mediastinal lymph-node metastases in a significant number of patients who are not found to have enlarged mediastinal lymph nodes on CT. This is suggested by limited experience in two studies in which EUS-FNA demonstrated mediastinal malignancy in 10 of

24 CT-negative patients (42%) and four of 18 CT-negative patients (22%), respectively [32,33]. In addition, Wallace et al. [29] evaluated EUS-FNA in a study including 69 patients with NSCLC and lymph nodes less than 1 cm in size on CT. A sensitivity of 61% and a specificity of 98% for advanced lung cancer was found with EUS-FNA. EUS detected advanced disease in 25% of the CT-negative patients (17 of 69; nine with N2–3, one with M1, and one with T4).

EUS-FNA after induction chemotherapy. EUS-FNA appears to be indicated for down-staging evaluation after induction chemotherapy. In one study, 19 consecutive patients with NSCLC and confirmed ipsilateral or subcarinal lymph-node metastases who had been treated with induction chemotherapy underwent mediastinal re-staging using EUS-FNA. Patients were assessed as having either a partial response or stable disease on the basis of sequential CT scans of the thorax. When EUS-FNA re-staged the mediastinum as showing no regional lymph-node metastases (N0), surgical resection of the tumor with lymph-node sampling or dissection was carried out. The positive predictive value, negative predictive value, sensitivity, specificity, and accuracy were 100%, 67%, 75%, 100%, and 83%, respectively, showing that EUS-FNA is an accurate method for re-staging of mediastinal lymph nodes after induction chemotherapy in patients with NSCLC. EUS-FNA appears to be able to identify a subgroup of down-staged patients who may benefit from further surgical treatment.

Limitations and prospects. Most of the studies discussed above were retrospective rather than consecutive and included only selected patients. No blinding was carried out in comparisons between EUS-FNA, mediastinoscopy, and transbronchial aspiration. Most of the published results are from expert centers.

Mediastinoscopy. Mediastinoscopy is regarded as the gold standard for mediastinal staging, and recently published guidelines recommend invasive mediastinoscopy (with a complication rate of 2–3%) before resection with curative intent is carried out. However, mediastinoscopy is limited to the anterior mediastinum (with examination of the pretracheal and paratracheal lymph-node groups) and N2–3 disease is found in up to 15% of patients who undergo thoracotomy after negative mediastinoscopy findings.

Diagnostic work-up:

- Chest radiography, thoracic CT, and bronchoscopy should be carried out in all patients using the best available equipment.
- EUS of the mediastinum, including potential fine-needle aspiration of lymph nodes, should be used as a secondary diagnostic method if it is not possible to classify peripheral tumors using bronchoscopy (with transbronchial biopsy).



Fig. 27.**12** Aspiration of a mediastinal empyema, followed by insertion of a drain via the puncture canal.

- Mediastinoscopy, covering the anterior mediastinum, and EUS-FNA, covering the posterior mediastinum, have been regarded as complementary. However, there have been no studies actually comparing the two methods with a controlled and blinded design. Mediastinoscopy is indicated for enlarged lymph nodes in groups 2 and 4. The prevascular and retrotracheal lymph-node group 3 and the N1 groups require supplementary examination procedures.
- Transthoracic puncture can be done using CT or transthoracic ultrasonography.
- It has been postulated that transbronchial miniprobe EUS might be helpful for lymph-node staging in patients in whom N1 groups are affected.

■ Prospects and Limitations

The limitations of EUS examination of the mediastinum and fine-needle aspiration are especially clear in the case of the pretracheal and right-sided paratracheal lymph-node groups (2R, 4R), which are often affected, since air in the tracheobronchial tree makes the ultrasound examination impossible. Transesophageal mediastinal EUS and mediastinoscopy are complementary in the area of the pretracheal lymph-node groups, since mediastinoscopy offers in particular a good approach to the pretracheal and paratracheal lymph-node groups, which cannot be assessed adequately with EUS. EUS examination of the mediastinum has advantages for evaluating periesophageal, subcarinal, and aortopulmonary lymph-node groups, in addition to the region around the pulmonary ligament.

Conclusions

Radial and linear instruments are available for transesophageal EUS of the mediastinum, but the radial technique does not allow puncture to be carried out. Longitudinal scanners are therefore preferable for pneumological purposes. The lymph nodes in the aortopulmonary window, subcarinal nodes, and nodes in the paraesophageal region can be examined with EUS-FNA. This is also possible with some of the lymph nodes in the region of the inferior pulmonary ligament and left paratracheal region. Lymph-node levels 1, 2R, 3, 4R, and 6 are not always capable of being assessed, due to the interference from the larger airways. The left adrenal gland should always be examined as well, as it determines the prognosis in up to 5% of cases.

References

1. Dietrich CF, Braden B, Wagner TOF. Thorax- und Lungensonographie. Dt Aerzteblatt 2000;97:A103–110.
2. Dietrich CF, Hirche TO, Schreiber D, Wagner TO. [Sonographie von Pleura und Lunge; in German.] Ultraschall Med 2003;24:303–11.
3. Dietrich CF, Chichakli M, Bargon J, Wehrmann T, Wiewrodt R, Buhl R, et al. Mediastinal lymph nodes demonstrated by mediastinal sonography: activity marker in patients with cystic fibrosis. J Clin Ultrasound 1999;27:9–14.
4. Dietrich CF, Viel K, Braden B, Caspary WF, Zeuzem S. [Mediastinal lymphadenopathy: an extrahepatic manifestation of chronic hepatitis C? In German.] Z Gastroenterol 2000; 38:143–52.
5. Dietrich CF, Liesen M, Buhl R, Herrmann G, Kirchner J, Caspary WF, et al. Detection of normal mediastinal lymph nodes by ultrasonography. Acta Radiol 1997;38:965–9.
6. Mountain CF, Dresler CM. Regional lymph node classification for lung cancer staging. Chest 1997;111:1718–23.
7. Dietrich CF, Wehrmann T, Hoffmann C, Herrmann G, Caspary WF, Seifert H. Detection of the adrenal glands by endoscopic or transabdominal ultrasound. Endoscopy 1997;29: 859–64.
8. Ahuja A, Ying M. An overview of neck node sonography. Invest Radiol 2002;37:333–42.
9. Vassallo P, Wernecke K, Roos N, Peters PE. Differentiation of benign from malignant superficial lymphadenopathy: the role of high-resolution US. Radiology 1992;183:215–20.
10. Vassallo P, Edel G, Roos N, Naguib A, Peters PE. In-vitro high-resolution ultrasonography of benign and malignant lymph nodes: a sonographic–pathologic correlation. Invest Radiol 1993;28:698–705.
11. Hajek PC, Salomonowitz E, Turk R, Tscholakoff D, Kumpan W, Czembirek H. Lymph nodes of the neck: evaluation with US. Radiology 1986;158:739–42.
12. Van den Brekel MW, Castelijns JA. Imaging of lymph nodes in the neck. Semin Roentgenol 2000;35:42–53.
13. Van den Brekel MW, Castelijns JA, Stel HV, Golding RP, Meyer CJ, Snow GB. Modern imaging techniques and ultrasound-guided aspiration cytology for the assessment of neck node metastases: a prospective comparative study. Eur Arch Otorhinolaryngol 1993;250:11–17.
14. Ariji Y, Kimura Y, Hayashi N, Onitsuka T, Yonetsu K, Hayashi K, et al. Power Doppler sonography of cervical lymph nodes in patients with head and neck cancer. AJNR Am J Neuroradiol 1998;19:303–7.
15. Schade G. [Experiences with using the ultrasound contrast medium Levovist in differentiation of cervical lymphomas with color-coded duplex ultrasound; in German.] Laryngorhinootologie 2001;80:209–13.
16. Giovannini M, Seitz JF, Monges G, Perrier H, Rabbia I. Fine-needle aspiration cytology guided by endoscopic ultrasonography: results in 141 patients. Endoscopy 1995;27: 171–7.
17. Pedersen BH, Vilmann P, Folke K, Jacobsen GK, Krasnik M, Milman N, et al. Endoscopic ultrasonography and real-time guided fine-needle aspiration biopsy of solid lesions of the mediastinum suspected of malignancy. Chest 1996;110: 539–44.
18. Silvestri GA, Hoffman BJ, Bhutani MS, Hawes RH, Coppage L, Sanders-Cliette A, et al. Endoscopic ultrasound with fine-needle aspiration in the diagnosis and staging of lung cancer. Ann Thorac Surg 1996;61:1441–5.
19. Gress FG, Savides TJ, Sandler A, Kesler K, Conces D, Cummings O, et al. Endoscopic ultrasonography, fine-needle aspiration biopsy guided by endoscopic ultrasonography, and computed tomography in the preoperative staging of non–small-cell lung cancer: a comparison study. Ann Intern Med 1997;127(8 Pt 1):604–12.
20. Wiersema MJ, Vilmann P, Giovannini M, Chang KJ, Wiersema LM. Endosonography-guided fine-needle aspiration biopsy: diagnostic accuracy and complication assessment. Gastroenterology 1997;112:1087–95.
21. Hunerbein M, Dohmoto M, Haensch W, Schlag PM. Endosonography-guided biopsy of mediastinal and pancreatic tumors. Endoscopy 1998;30:32–6.
22. Williams DB, Sahai AV, Aabakken L, Penman ID, van Velse A, Webb J, et al. Endoscopic ultrasound guided fine needle aspiration biopsy: a large single centre experience. Gut 1999;44:720–6.
23. Roberts JR, Shyr Y, Christian KR, Drinkwater D, Merrill W. Preemptive gastrointestinal tract management reduces aspiration and respiratory failure after thoracic operations. J Thorac Cardiovasc Surg 2000;119:449–52.
24. Fritscher-Ravens A, Sriram PV, Bobrowski C, Pforte A, Topalidis T, Krause C, et al. Mediastinal lymphadenopathy in patients with or without previous malignancy: EUS-FNA-based differential cytodiagnosis in 153 patients. Am J Gastroenterol 2000;95:2278–84.
25. Laudanski J, Kozlowski M, Niklinski J, Chyczewski L. The preoperative study of mediastinal lymph nodes metastasis in lung cancer by endoscopic ultrasonography (EUS) and helical computed tomography (CT). Lung Cancer 2001;34 (Suppl 2):S123–6.
26. Wiersema MJ, Vazquez-Sequeiros E, Wiersema LM. Evaluation of mediastinal lymphadenopathy with endoscopic US-guided fine-needle aspiration biopsy. Radiology 2001;219: 252–7.
27. Wallace MB, Kennedy T, Durkalski V, Eloubeidi MA, Etamad R, Matsuda K, et al. Randomized controlled trial of EUS-guided fine needle aspiration techniques for the detection of malignant lymphadenopathy. Gastrointest Endosc 2001; 54:441–7.
28. Larsen SS, Krasnik M, Vilmann P, Jacobsen GK, Pedersen JH, Faurschou P, et al. Endoscopic ultrasound guided biopsy of

mediastinal lesions has a major impact on patient management. Thorax 2002;57:98–103.
29. Wallace MB, Ravenel J, Block MI, Fraig M, Silvestri G, Wildi S, et al. Endoscopic ultrasound in lung cancer patients with a normal mediastinum on computed tomography. Ann Thorac Surg 2004;77:1763–8.
30. Annema JT, Hoekstra OS, Smit EF, Veselic M, Versteegh MI, Rabe KF. Towards a minimally invasive staging strategy in NSCLC: analysis of PET positive mediastinal lesions by EUS-FNA. Lung Cancer 2004;44:53–60.
31. Kramer H, Nieuwenhuis JA, Groen HJ, Wempe JB. Pulmonary tuberculosis diagnosed by esophageal endoscopic ultrasound with fine-needle aspiration. Int J Tuberc Lung Dis 2004;8:272–3.
32. Fritscher-Ravens A, Davidson BL, Hauber HP, Bohuslavizki KH, Bobrowski C, Lund C, et al. Endoscopic ultrasound, positron emission tomography, and computerized tomography for lung cancer. Am J Respir Crit Care Med 2003; 168:1293–7.
33. Fritscher-Ravens A, Bohuslavizki KH, Brandt L, Bobrowski C, Lund C, Knofel WT, et al. Mediastinal lymph node involvement in potentially resectable lung cancer: comparison of CT, positron emission tomography, and endoscopic ultrasonography with and without fine-needle aspiration. Chest 2003;123:442–51.

28 Endobronchial Ultrasound with Miniprobe Radial Scanning

H.D. Becker

Introduction

In the bronchi, the endoscopist's view is restricted to the lumen and internal surface of the airways. Intramural processes and those adjacent to the airways can only be assessed using indirect signs. The clinical staging of lung cancer corresponds to pTNM in only 60% of cases. For these reasons, there was a need to improve the tools available for endoscopic diagnosis. As external mediastinal ultrasonography and transesophageal endosonography were insufficient for the imaging of mediastinal structures, there was a need for a different solution involving the use of miniaturized probes of the type used for endoscopic ultrasonography (EUS) [1] and cardiovascular endosonography, preliminary experience with which had been reported in endovascular sonography of the pulmonary artery to exclude tumor invasion [2].

Miniprobes: General Considerations

During the 1990s, miniaturized probes with a frequency of 7.5 MHz began to be used. Probes with 12 and 20 MHz also became available later. The first probes had a diameter of 3 mm, with a mechanical single-element transducer at the tip rotating at approximately 400 rpm and producing a 360° image perpendicular to the axis. Due to the large diameter of the probe, it was mainly used during rigid bronchoscopy, with a metallic tube serving as a guide. To achieve better contact with the tracheobronchial wall, a latex balloon was attached at the tip of the probe, which was filled with sterile water via a side port. Later, models with a diameter of 2.5 mm became available that were capable of being introduced via biopsy channels at least 2.8 mm in diameter in regular flexible fiberscopes. These have been available commercially since 1999 (Olympus UM-2R/3R, with an MH-240 driving unit and EU-M20 and 30 processors). In addition, dedicated balloon catheters are available that can be attached to the probe at the connector for the driving unit (Olympus UM-BS20-26R) (Fig. 28.1).

A special feature is the O-ring at the tip, which fits to a notch at the tip of the probe (Olympus UM-BS20-26R). When the balloon is overinflated or pressure is exerted due to coughing, the tip slips off the probe, preventing rupture with fragments dislodging into the lung. This comparatively simple device meets three requirements for optimal imaging: firstly, 20-MHz probes, with their high resolution, can be used; secondly, as the water in the balloon in front of the transducer shifts the focus to the periphery, the depth of penetration is sufficient for imaging the surrounding mediastinal structures; and thirdly, the balloon provides complete circular contact with the airway wall, which is essential for orientation.

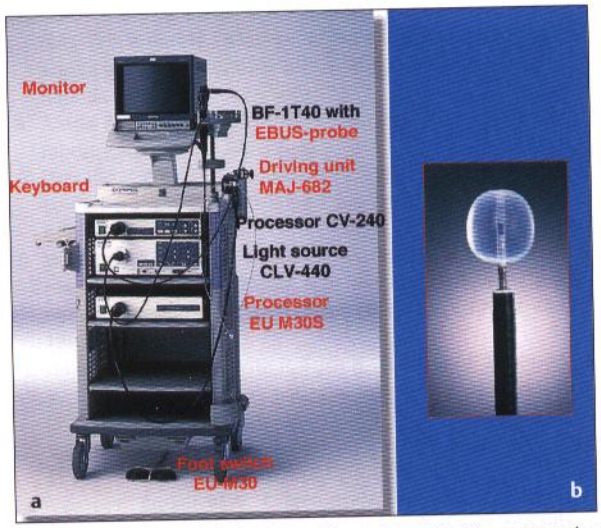


Fig. 28.1 **a** The complete miniprobe system. **b** The miniprobe is introduced via the biopsy channel of a video bronchoscope. The probe is armed with a balloon catheter. The grayish mechanical rotating transducer can be seen inside the balloon (arrow).

Handling of Miniprobes

Storage and Preparation

Miniprobes are fragile and have to be handled very delicately. The transducer and connecting driving wire are protected from friction inside the plastic sheath by applying a gel solution. As this is not completely air-sealed, small air bubbles may collect in front of the transducer and interfere with the image. The devices should therefore be stored in a hanging position, with the connector upward and the tip of the probe downward. If a bubble has collected in front of the transducer,

the catheter should be held approximately 40 cm proximal from its tip and the end should be gently rotated like a lasso, so that the centrifugal force drives the gel toward the tip and the bubble travels proximally. After the probe has been inserted into the balloon catheter and fixed at the connector, the balloon catheter should be completely filled with sterile water until drips appear at the distal end. Saline solution should not be used, as the salt may crystallize on the tip of the probe and interfere with the ultrasonic signal. After filling of the catheter, the O-ring of the balloon is slipped onto the groove on the tip of the catheter. This can be achieved with the fingertip or with the help of a dedicated rubber device. Exerting too much force on the tip, which results in bending or even kinking of the tip, should be avoided. The balloon is then refilled. If a few air bubbles are still observed, the balloon is kept with its tip downward, so that the air collects at the end of the catheter. The air is evacuated by suctioning the water from the balloon with the syringe. This should always be held in such a way that the air is above the fluid and is not flushed back into the catheter.

Application

The miniprobes should always be used with bronchoscopes that have an appropriate biopsy channel at least 2.8 mm in diameter when applied with the balloon sheath. We prefer to use a little medical silicone on the tip before insertion. During introduction, the assistant should apply suction in order to completely evacuate the balloon, preventing dislocation from the tip or damage due to friction within the biopsy channel. The probe should never be advanced when the tip of the endoscope is in a sharply bent position. It should also not be activated then, as the transducer may be fixed while the wire is still rotating and could therefore shear off. Force should never be used while advancing the probe, neither when there is resistance against the tip nor by pushing the probe forcefully sideways against the wall. Inside stenoses and in the periphery as well, the probe should never be advanced using force, as the tip easily becomes kinked in this way. The balloon should be never overinflated. Particularly when the probe is being advanced inside narrowing airways or if the patient coughs, the balloon's safety feature will not work with overinflation, as the O-ring is not able to slip off; in this case, the balloon may fracture and latex fragments may be lost inside the lung.

■ Technique of EBUS

The miniprobes are inserted through the biopsy channel of flexible scopes with a diameter of at least 2.8 mm. Precise placement is carried out with endoscopic visualization, and once the balloon is in place, it is filled with sterile water until firm contact with the wall is established. Adequate contact is confirmed by a complete circular image of the bronchial wall and the surrounding structures. The development of the image can be compared to a sunrise, in which all of the structures gradually become visible. With the patient under local anesthesia, complete inflation of the balloon is possible in bilaterally ventilated lungs after sufficient preoxygenation, up to the main bronchi and even the trachea. Complete obstruction of a remaining main bronchus after contralateral resection, or resection of the trachea, can therefore be tolerated for up to 2 min with sufficient sedation. If necessary, the bronchoscope can be introduced via a larynx mask. In these cases, general anesthesia may be preferable, as it can provide additional time for imaging of the mediastinal structures. In our view, this procedure is well justified due to the useful additional information that can be obtained. We have never observed barotrauma during complete obstruction, since according to our measurements even with high-frequency jet ventilation, the pressure distal to the balloon during filling rapidly drops to zero after complete inflation. If the patient is not able to tolerate complete obstruction at all, the balloon can be partially filled and applied with semicircular contact.

Imaging Artifacts

Motion artifacts with irregular rotation were observed when early probes were used inside calibration phantoms, causing considerable distortion of the circumferential sector images—whereas the radial distances were measured correctly, as reported with other systems. However, the image construction is still slow enough for respiratory motion to create artifacts. As these are not synchronous, they can be readily differentiated from pulsations. Most frequently, a multiple ring reflection is caused by the strong echo of the balloon. As the airways are surrounded by strongly reflecting structures, multiple reflex echoes and mirror and comet artifacts are observed in endoscopic bronchial ultrasonography (EBUS), as in other applications. This applies in particular to the adjacent lung surface, vertebral column, calcified cartilage, and lymph nodes. Triangular distortion of lymph nodes and attenuation of the outer contours in echogenic structures is also very common with 20-MHz probes. Air bubbles in the balloon can cause shadows or images distortions resembling a "rabbit's ear" (Fig. 28.**2**).

Sonographic Anatomy

In animals and in resected human specimens, we have observed a seven-layered structure in the central airways in vitro. This is in contrast to the findings of other groups, who have described three layers, or more re-

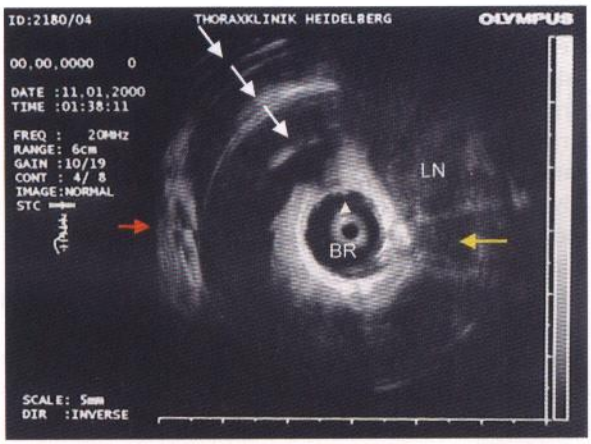


Fig. 28.**2** Artifacts in bronchial imaging. *Rotation artifact:* on the left, in the 9-o'clock position, there is an interruption in the contour of the wall and the adjacent pulmonary artery (red arrow). In this position, the image is refreshed after one circulation of the transducer. If the structures have in the meantime been displaced by breathing, pulsation, or movement of the bronchoscope, the interruption can be observed. *Repeat echoes:* in the 11-o'clock position, there is insufficient contact between the balloon and the bronchial wall. The strong echo from the balloon is repeatedly reflected in quarter-circles (three arrows). *Shadows due to air:* also in the 11-o'clock position, small bubbles have collected inside the balloon (arrowhead). These are causing the triangular shadow, in which the structures are lost. However, the strong echoes from the balloon are still visible. Another shadow is seen in the 3-o'clock position (yellow arrow), where a bronchial branch is emerging and the air inside is reflecting the ultrasound and causing the shadow. *Fading:* as the lower energy from the 20 MHz is dissipating inside the tissue by dispersion and absorption, the external boundary of the lymph node (LN) is not visible.

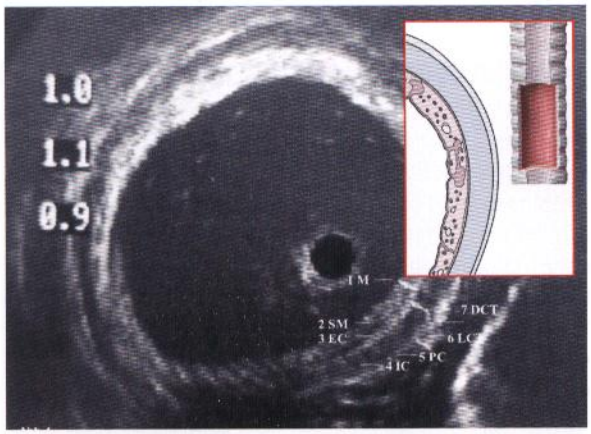


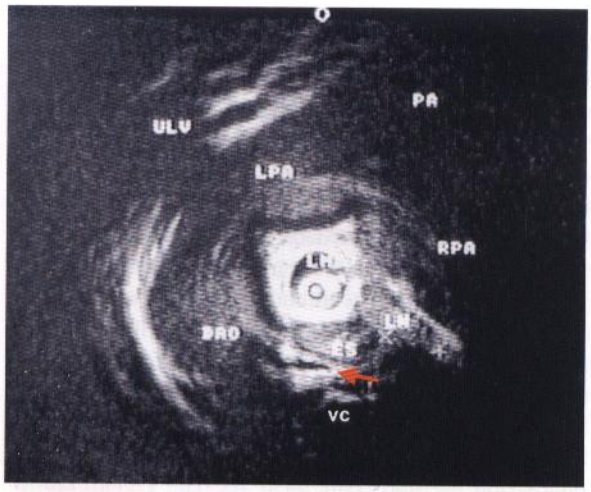
Fig. 28.**3** The structure of the wall of the central airways. At high magnification, the seven-layered structure is clearly visible with the 20-MHz probe. The three layers of cartilage, consisting of endochondrium (EC), an internal spongiform structure (IC), and perichondrium (PC), are accompanied by mucosa (M) and submucosa (SM) on the inside and loose connective tissue (LCT) and dense connective tissue (DCT) on the outside. The anatomical illustration shows the high resolution provided by the ultrasound image, at less than 1 mm.

cently five [3,4], in some cases due to the use of probes with a lower resolution. The first innermost layer, the mucosa, has a highly echogenic structure that is mostly confluent with the echo of the balloon and only becomes visible with high magnification. The second layer has low echogenicity and represents the submucosa. In normal conditions, it can be easily differentiated from the mucosa and from the third layer, the strongly reflecting internal surface of the cartilage, which I call "endochondrium." The spongiform internal structure of the cartilage, the fourth layer, is hypoechoic again, whereas a fifth hyperechoic layer represents the external surface of the cartilage (perichondrium). It is a little-known fact that the central airways are surrounded by a double layer of loose and dense connective tissue, representing the sixth (hypodense) and seventh (hyperdense) ultrasonic layers (Fig. 28.**3**). This seven-layered structure has been confirmed in another prospective experimental study [5].

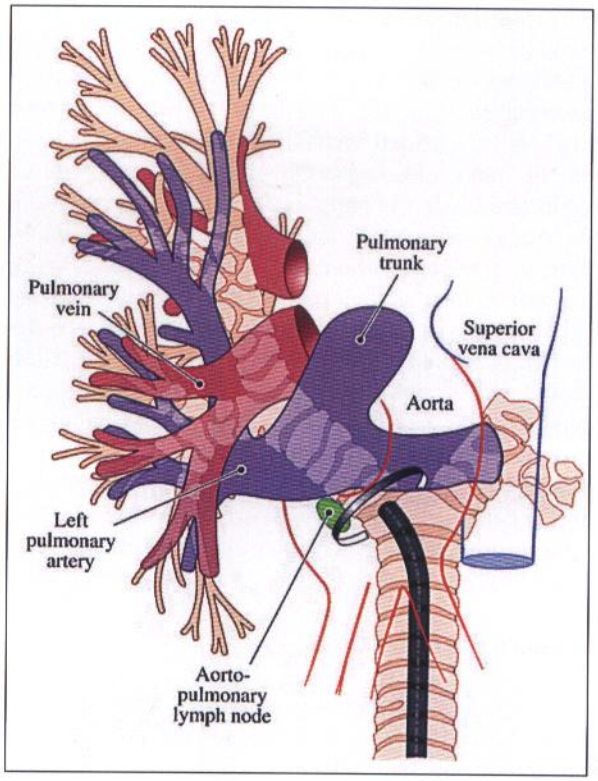
In vivo, the complex structure can be only seen with high magnification, whereas at medium and low-powered magnification, the delicate layers are confluent with the strong echo from the supporting cartilages. At the dorsal membranous wall and in the periphery distal to the lobar bronchi, the structure only consists of three layers. The layered structure is not visible with the 7.5-MHz ultrasound bronchoscope.

Orientation within the mediastinum is difficult. This is mainly due to the complex anatomy, as well as to motion artifacts and pulsation, but it is also due to the very unusual planes that are present. The plane of the circumferential image of the miniprobe is perpendicular to the axis of the probe. While the planes inside the trachea are comparable to those in horizontal computed tomography (CT) images, following the oblique course of the airways, the images tilt more and more as one follows the main bronchi until a coronary plane is reached in the distal left main bronchus, or even an inverse horizontal plane on entering the apical segments of the upper lobes.

For orientation, it is useful to recognize key anatomical structures and their relationship to the airways and to each other, rather than to observe the position of the probe. Familiarity with the anatomy is essential for orientation. The image has to be set accordingly, so that landmark structures that are found only ventral or dorsal to the bronchus, such as the esophagus or pulmonary artery, are in the correct position. It is helpful to place the tip of the bronchoscope close to the balloon, or even better to look inside the balloon and follow the motion of the probe on the ultrasound image, while the tip of the bronchoscope is flexed up and down. Once the sagittal orientation is set and the EBUS image is adjusted with the scroll ball on the keyboard, right and left orientation can be set accordingly, with lateral motion



a



b

Fig. 28.4 Mediastinal anatomy. **a** The typical ultrasound anatomy of the proximal left main bronchus and surrounding structures. Dorsally lies the esophagus (ES, above the red arrow); to the right of the esophagus, there is a borderline lymph node (LN); on the left lie the descending aorta (DAO) and the beginning of the aortic arch. Behind the esophagus and in front of the vertebral column (VC), an intercostal artery is crossing to the right (red arrow). Ventrally, the main pulmonary artery (PA) and its left (LPA) and right (RPA) branches are visible. On the left, the pulmonary upper lobe vein (ULV) crosses towards the left atrium. **b** The diagram illustrates the anatomy and the ultrasound plane (reproduced with permission of the author from Wang et al. [6]).

being observed on the ultrasound image and the reverse key being used if necessary.

Vessels are easily recognized by their low echogenicity and by pulsations; arteries and veins differ in characteristic ways. However, in the periphery the variations are so complex that this may become impossible. Observation of the pulse oximeter is often helpful. Lymph nodes are easily differentiated by their comparatively higher echogenicity.

As filling of the balloon catheter with water shifts the focus more distally, even with the 20-MHz probes the depth of penetration can be up to 5 cm. Thus, the left atrium and mitral valve can frequently be seen from the left main bronchus. Near the bifurcation, the main pulmonary artery and its branching into the left and right main arteries can be seen ventrally. Dorsally, the descending aorta, the multilayered structure of the esophagus, and the vertebral column are clear landmarks for orientation. The aortopulmonary window can be inspected and approached from the left main bronchus (Fig. 28.**4**) [6].

Ventral to the right main bronchus, the right pulmonary artery is always found, crossed by the azygos vein, which can often be followed as far as its confluence with the vena cava, which is situated beside the root of the aorta. Slightly more proximally, at the level of the tracheobronchial angle, the esophagus is seen crossing to the left, accompanied by the azygos vein, which crosses forward at the right toward the vena cava. Pathological soft-tissue structures are easily differentiated from these structures. Further distally, in the intermediate bronchus, the pulmonary artery and pulmonary vein are found ventrally. At the level of the middle lobe bronchus, the segmental artery for the apical segment of the lower lobe (S6) can be seen crossing laterally beside the intermediate bronchus, whereas the bright reflection of the adjacent pleura of S6 is a significant dorsal landmark.

In the periphery, conditions are less favorable, as the surrounding air is strongly reflective and thus frequently prevents detailed analysis of the bronchial wall and adjacent vessels. Despite this, some Japanese authors have even succeeded in analyzing the alveolar structures with EBUS [7]. However, solid and cystic structures are clearly demarcated against the hyperechoic lung structure by their lower echogenicity. EBUS is thus useful for guiding biopsy procedures in these lesions.

■ Clinical Results

In a prospective study including 648 patients, we demonstrated that EBUS has a very low complication rate and only adds an average of 6.3 min per bronchoscopy,

with 18.9 min for the whole procedure [8]. Complications were rare and minor; 5% of the patients required additional oxygen. Transient minor arrhythmias were observed in 18 of 103 patients (17%) who underwent blockage of the left main bronchus by the balloon. Rarely, minor bleeding occurred during placement of the probe inside the periphery of the lung. In addition, the study confirmed the cost-effectiveness of the procedure, with re-sterilization and reuse of the probes being possible as long as they resisted the mechanical stress [9]. EBUS is now reimbursed in the USA. However, the system is also cost-effective in Europe, in view of the more invasive and expensive procedures that the procedure makes it possible to avoid. We have carried out prospective studies to validate EBUS for various indications [10–13]. The results have been confirmed by other authors and demonstrate that EBUS is comparable with other procedures and in many instances even superior.

■ Staging of Lung Cancer

The purpose of staging is to provide precise classification in accordance with the TNM system as a rational basis for treatment. The bronchoscopic criteria for tumor spread are documented in the recent UICC classification [14]. Small, radiographically invisible tumors have to be located in individuals who are at risk or have positive sputum cytology. The decision on whether to carry out treatment is taken on the basis of tumor spread and the depth of infiltration into the layers of the bronchial wall. The decision also depends on the histological assessment of biopsy specimens. Lymph-node involvement in hilar and mediastinal nodes can be assessed using transbronchial needle aspiration (TBNA). In addition to the size and extent of the lesion, its internal structure and relationship to mediastinal structures are of interest. Metastasis can also involve the parabronchial mediastinal structures, central airways, lung, and pleura. EBUS provides useful information, particularly in regions that are not directly visible through the bronchoscope.

Primary lung cancer: endobronchial extent. *Early cancer.* Early cancer was until recently considered to be radiographically invisible. This has changed since the introduction of endobronchial ultrasonography. It is known from earlier radiographic studies that only 75% of bronchologically visible tumors are radiographically detectable [15]. Radiographically invisible tumors included lesions that had already penetrated into the deeper layers of the wall. In several patients referred to our institution for endobronchial treatment of supposedly early cancer, transmural invasion and even local lymph-node involvement were detected that had escaped all previous diagnostic procedures.

By pathological definition, early cancer is limited to the bronchial wall, whereas in-situ carcinoma does not cross the lamina propria. In all cases of macroscopic alteration of the mucosa, alterations in the texture were identified on endosonography. Depending on the extent of infiltration, the wall is thickened and the architecture is altered. As has been reported for other tumors, hyperechoic structures were found, although hypoechoic structures were more frequent. Extensive submucosal tumor spread and even infiltration beyond the cartilage is sometimes detected with EBUS even in macroscopically intact mucosa. When there are no signs of infiltration of the deeper layers or lymph-node involvement, tumors of this type that are limited to the bronchial wall can be treated with curative intent using endoscopic methods [16].

With the development of autofluorescence bronchoscopy for detection of tumors that are invisible with white-light bronchoscopy, there has been renewed interest in early detection. Extinction of autofluorescence can be also caused by benign lesions such as inflammation, granuloma, scars, and dysplasia. We have shown that analyzing the structure of the wall with EBUS improves the specificity significantly and can clarify the nature of a lesion with a high degree of reliability [17]. In our experience, correlation with the histology was improved from 58% to 92% (Fig. 28.**5**).

Despite the curative potential of endoscopic treatment modalities using electrocautery or photodynamic therapy (PDT), the relapse rate reported in the literature is as high as 50% [15,18]. This has been attributed to failure of treatment. Since the introduction of EBUS, we have shown that cancers detected using autofluorescence have often penetrated the deeper layers of the wall and are not really early lesions. This has been confirmed by Miyazu et al. [19], who showed that all tumors that were found to be limited to the internal layers of the bronchial wall using both autofluorescence and EBUS were associated with long-term complete remission after PDT. This proves that EBUS is currently the only reliable method for precise staging of localized early cancer. In the future, therefore, screening using molecular cytodiagnosis in the sputum, blood, or swabs from the buccal mucosa, along with localization using autofluorescence and local staging with EBUS, will be the three pillars of early detection and local minimally invasive treatment for central early lung cancer [20].

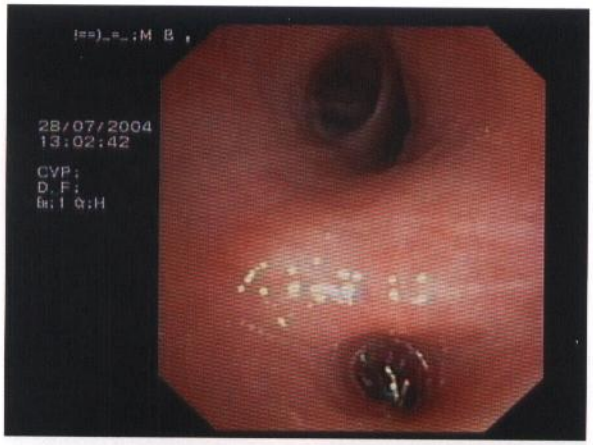
Local T staging of advanced lung cancer. Computed tomography is still the gold standard for the diagnosis of local tumor spread. However, clinical staging is confirmed by surgery in only 60–70% of cases [21]. In locally advanced cancer, EBUS also provides important information to support treatment decisions. In patients with complete obstruction of the airway, we have been able to localize the base and surface of the occluding tumor, diagnose the extent to which the tumor has penetrated

into the wall and into the mediastinum, and assess whether the distal airways were patent. Particularly for the surgical strategy, it is essential to know the precise intended resection lines. Involvement of the main bronchi, main carina, or trachea requires more extensive resection and frequently precludes operability. A combination of autofluorescence and EBUS also proved useful here for detecting submucosal tumor spread. In particular, the potential to diagnose involvement of the pulmonary vessels influences decisions regarding intervention [22]. Perfusion of the lung can be shut down by the Euler–Liljestrand reflex even when the pulmonary artery is patent. Usually, one then has to exclude organic obstruction using conventional or CT angiography, as endoscopic obliteration in this case would merely increase dead-space ventilation. Passing through the stenosis with the miniprobe enabled us to diagnose infiltration of the pulmonary artery (Fig. 28.**6**) and also made it possible to see whether the bronchi distal to the stenosis were patent. In some patients, application of the ultrasound bronchoscope can provide additional quantitative information on blood flow, using the Doppler function.

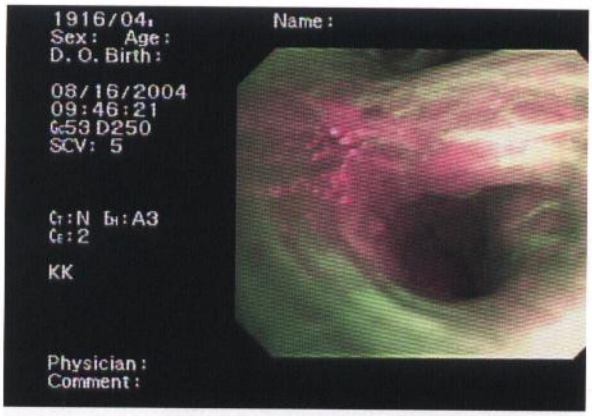
Mediastinal infiltration: trachea, pulmonary artery, esophagus, large vessels. Diagnosis of infiltration of the large mediastinal vessels—the aorta, vena cava, and main pulmonary artery—is crucial and can be difficult using radiographic methods. Tumors located in the trachea, left main bronchus, and left hilum are located in the close vicinity of the esophagus, and we have been able to detect direct infiltration using EBUS in several cases (Fig. 28.**7**).

In addition, tumor invasion of the aortic arch, descending aorta, and main pulmonary artery can be diagnosed from the main bronchi and the trachea. Infiltration of these structures usually excludes surgical procedures. However, if there is a distinct sonographic interface between the tumor and these structures, operability is possible, as has been confirmed in many of our patients. Particularly with miniprobes, infiltration of the external layers of the trachea and main bronchi can be reliably diagnosed and distinguished from impression without infiltration. In a prospective study, CT was only found to have a sensitivity of 25% and a specificity of 80% (accuracy 51%) in comparison with EBUS, which had an accuracy of 94%, a sensitivity of 89%, and specificity of 100% [10]. The 7.5-MHz resolution provided by the ultrasound bronchoscope is insufficient for this purpose.

Lymph nodes: location, size, structure, infiltration, and biopsy. Infiltration of local lymph nodes has an even greater influence on the prognosis than the local tumor extent. This is why preoperative staging of the lymph nodes is essential. Using miniprobes, lymph nodes as small as 2–3 mm can be detected, and their internal structures (folliculi and sinuses), as well as the connect-



a

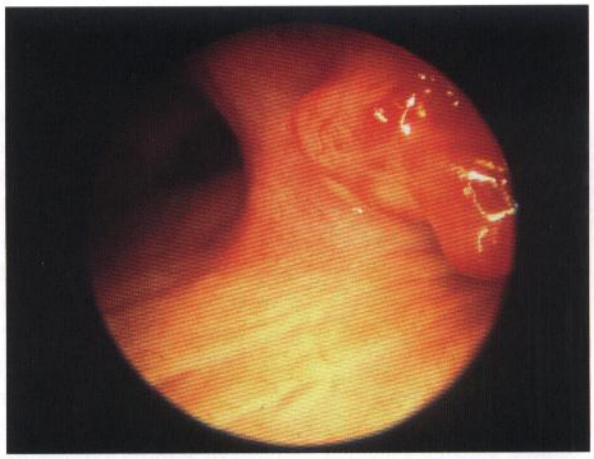


b

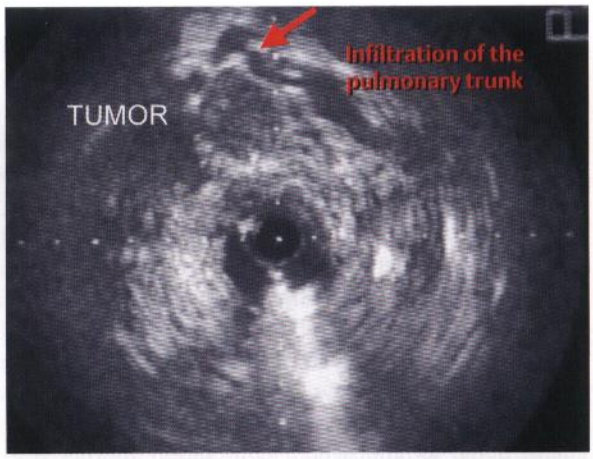


c

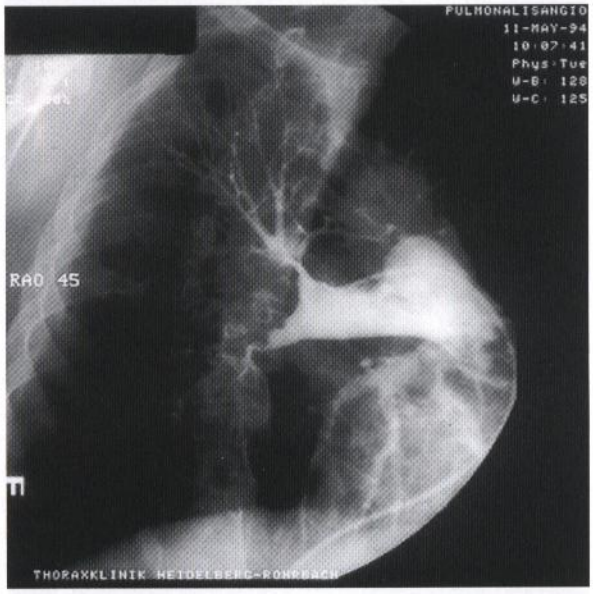
Fig. 28.**5** Early cancer. **a** The carina of the left apical lower lobe segment is widened in comparison with the distal segments, and the light reflex is irregular (white-light imaging). **b** With blue-light autofluorescence (AFI System, Olympus, Tokyo, Japan), the true submucosal extent of the lesion is visible from the magenta discoloration in comparison with the normal greenish color. **c** It is only with endobronchial ultrasound that the true intramural extent of the tumor (TU) becomes visible—4.2 mm in comparison with the normal wall (N) of 1.5 mm—as well as a 1-cm lymph node (LN). Histological assessment of a deep biopsy identified a squamous-cell cancer that was beginning to penetrate but was still limited to the bronchial wall. In accordance with the ultrasound findings, the tumor was treated with curative intent by bronchoscopic brachytherapy, as the patient was not able to undergo surgery following right-sided pneumonectomy.



a



b



c

Fig. 28.6 Infiltration of the pulmonary artery. **a** On bronchoscopy, the left upper lobe bronchus is seen to be obstructed by a tumor. **b** On ultrasonography, the upper lobe artery is seen to be invaded by the tumor and almost completely obstructed. **c** This finding was confirmed on angiography. We now rely on endobronchial ultrasound and no longer carry out conventional or computed-tomographic angiography for confirmation.

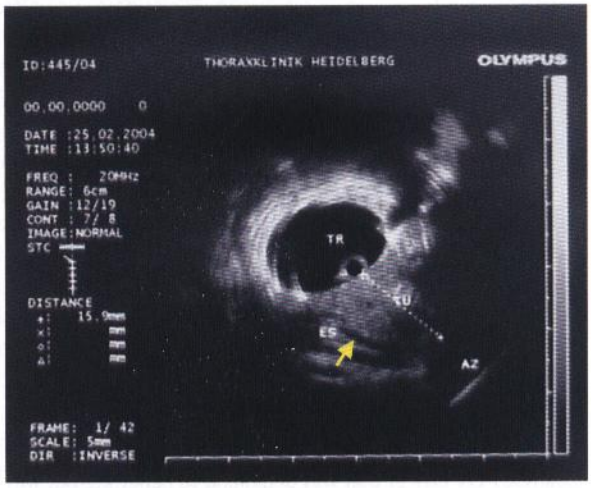


Fig. 28.7 Infiltration of the esophagus. The dorsal wall of the trachea (TR) has been infiltrated by an extensive tumor (TU), and the layer structure has been disrupted. The tumor is penetrating the esophagus (ES) and has disrupted its structure as well. Whether or not the azygos vein is also involved is not clear from the 20-MHz ultrasound image, as the depth of penetration is not sufficient.

ing lymph vessels, can be visualized. However, in contrast to tumors in other locations, we have not found any reliable criteria for malignant infiltration.

In a prospective study of 84 resected lymph nodes from 14 patients who underwent surgery for lung cancer, we examined the specimens in vitro in favorable conditions. However, neither the size, echogenicity, or homogeneity of the internal structures, nor their demarcation from the surrounding tissue, made it possible to identify reliable criteria for infiltration, although the resolution was well under 1 mm. These findings were recently confirmed with computer-assisted analysis of the internal structures. In our opinion, this is due to the high rate of alterations of the internal structure by nonspecific infiltrates in postobstructive pneumonia, silicotic and tuberculotic scars, and other forms of pathology. The importance of transbronchial and transtracheal needle aspiration has been described elsewhere.

Mediastinal lesions can be explored using the miniprobe and approached with TBNA if they are in contact with the tracheobronchial tree or if a vessel provides an acoustic window. For exploration of the retrosternal and paravertebral mediastinum, the depth of penetration provided by the 20-MHz probe is insufficient; use of the ultrasound bronchoscope is superior here. Using the latter instrument, we have been able to diagnose tumor infiltration into the lateral wall of the aorta and the dorsal wall of the esophagus. Lesions in the anterior and dorsal mediastinum can also be located and approached with a long needle, provided there are no intervening vessels. Mediastinal, pericardiac, and bronchogenic cysts can be easily diagnosed on the basis of their low echogenicity, and septations are often seen inside them. In the case of infection or internal hemorrhage, the echoes are brighter and the structure is more irregular. Using evacuation with a needle, bland cysts can be collapsed. In contrast to reports of infections and septicemia after transesophageal needle aspiration of cysts, we have never observed such complications after transbronchial puncture. We attribute this to the less contaminated environment in the airways.

In lymphomas, goiter, thyroid cancer, and metastatic disease, differentiation between compression and infiltration with EBUS is as important as in primary lung cancer. In tumors of the thymus and other organs located in the left anterior mediastinum, access with the miniprobe inserted into the apical segment of the left upper lobe can sometimes be useful. In several instances, compression of the left main bronchus by esophageal tumors has been clearly attributable to intramural leiomyomas of the esophagus, which are characteristic in their connection with the spiral muscular layers.

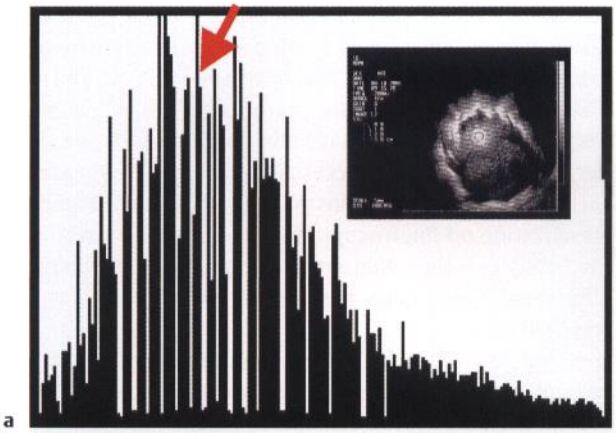
Intrapulmonary lesions. Ultrasound is strongly reflected by air, and we were therefore initially skeptical about its application. However, Hürter and Hanrath [3,4] have reported that ultrasound is useful for detecting peripheral lesions, and it even appears to be possible to analyze the structure of pulmonary tissue using high-frequency ultrasound [7]. We have been able to locate solid and cystic lesions in the periphery of the lung using the miniprobe [3,4]. We have also confirmed that localization for biopsy was successful in up to 80% of cases [12]. Particularly in lesions < 3 cm in size with poor visualization on fluoroscopy, and lesions hidden behind the heart or other anatomical structures and behind pleural effusions, EBUS has proved to be significantly superior.

If the probe can be placed inside the lesion and a catheter is used as an extended working channel for biopsy procedures with forceps, curette, brush, or catheter, the results approximate 100%. The high resolution provided by 20-MHz ultrasound allows detailed imaging of the internal structure of these lesions, correlating significantly with the histological diagnosis [23]. Using computer-assisted image analysis, we have been able to predict the nature of such lesions in 92% of cases [24] (Fig. 28.**8**).

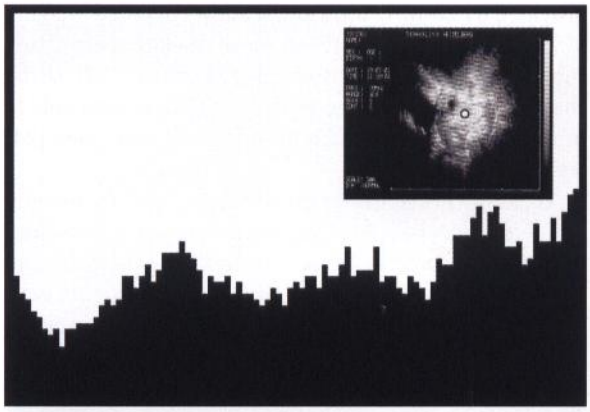
This may prove useful in the future, when screening for peripheral lesions using high-resolution low-dose helical CT becomes routine and further diagnostic and therapeutic decisions need to be made. In patients with atelectasis, EBUS is useful in providing information on the cause—for example, bronchial compression by lymph nodes or external compression of the lung by pleural effusions or solid structures. In several instances, we have diagnosed intrapulmonary cavities due to tuberculosis, necrotizing tumors, or mycetomas, and EBUS has been helpful in guiding the placement of pigtail catheters for drainage and local instillation of drugs.

Pleura and neighboring organs. If there is an acoustic window due to atelectasis, or a fluid collection close to the bronchi, the pleura and neighboring structures—such as solid structures in the visceral, mediastinal, and parietal pleura, or on the pericardium—can be visualized (Fig. 28.**9**).

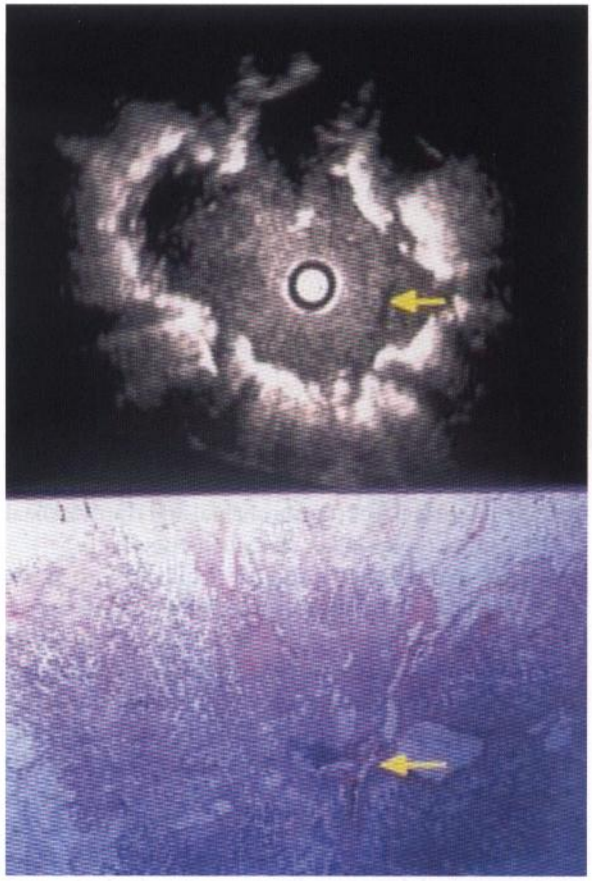
Imaging of the heart and thyroid has been already mentioned. EBUS is particularly useful for diagnosing infiltration of the esophagus by tumors of the central airways. In these cases, surgery is no longer feasible in most instances, and bronchoscopic interventions also have to be carried out very cautiously, since there is a very high risk of esophagobronchial fistulas after extensive laser resection and additional radiotherapy, for example. In these cases, simultaneous exploration of the esophagus with the miniprobe is very useful.



a

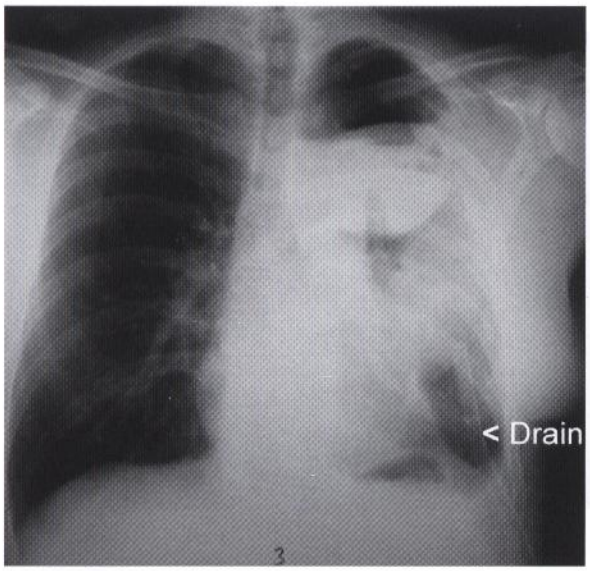


c

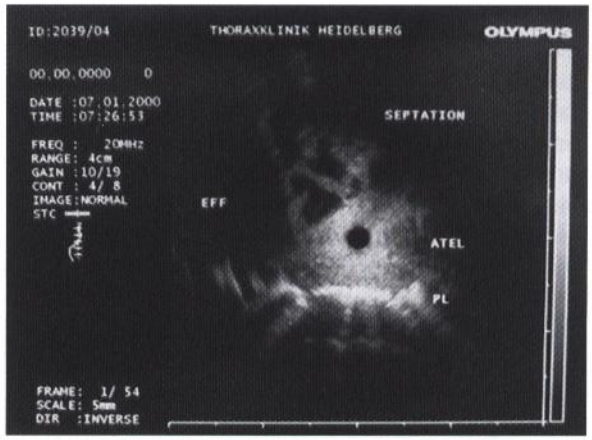


b

Fig. 28.8 Structural analysis of pulmonary nodules. **a** Endobronchial ultrasound imaging of a coin lesion (nodular opacity) shows a detailed image of vessels, small airways, and irregular boundaries to the surrounding lung tissue (image courtesy of Dr. Kurimoto). **b, c** The ultrasound images of a malignant lesion (**b**) and a benign lesion (**c**) show a similarly detailed internal structure. Using commercial computer programs (e.g., Picture Publisher), the distribution of signals can be quantified. Almost all malignant lesions have a characteristic peak in the dark spectrum, probably correlating with the vascularization.



a



b

■ EBUS in Therapeutic Bronchoscopy

The value of EBUS in decision-making and in guiding treatment applications was mentioned above. In our institution, 20% of all bronchoscopies conducted include therapeutic procedures. In 48% of these interventions, ultrasound provides useful additional information, which has strategic importance for the planning of the procedure in 43% of cases [13]. Exploration of central airway stenoses with EBUS to assess the extent and cause of the lesion and its relation to surrounding structures is helpful in decision-making regarding the appropriate technique—e.g., mechanical dilation, laser resection, argon plasma coagulation, or stenting—and for checking the effectiveness of the treatment during the follow-up period. Before the resection of granulomas and scars, precise evaluation of their thickness and vascularization is important in order to avoid perforation or hemorrhage.

Particularly in potentially curative bronchoscopic treatment of localized malignancies using photodynamic therapy or brachytherapy, precise diagnosis of the extension of the lesions into the bronchial wall is essential for success. EBUS is superior to all other imaging modalities in this context for analyzing the delicate layers of the tracheobronchial wall. Complications in the healing of anastomoses after bronchoplastic procedures can be difficult to recognize using bronchoscopy alone, and it can be difficult to differentiate between edema with superficial necrosis of the mucosa and incipient dehiscence. EBUS is useful here for checking the integrity of the bronchial layers and particularly for assessing the adjacent pulmonary artery. Thus, in cases of local abscess formation with peribronchial fluid collections, the decision on whether or not to carry out a surgical intervention can be taken before hemoptysis signals fatal hemorrhage.

■ EBUS in Pediatric Bronchoscopy

EBUS has also proved to be useful in many instances in pediatric bronchoscopy, as conventional imaging in small patients can be even less reliable due to motion artifacts and restrictions on radiation exposure [25]. In 412 children (3% of all patients), with a median age of 4.2 years, whom we examined between January 1998 and December 2001, EBUS was used in 140 cases (34%)—almost equivalent to the frequency in adults. The indications included analysis of structures in stridor and intermittent dyspnea, which especially in these patients can be caused by vascular malformations such as pulmonary slings. We detected 11 of these, in some cases even after cardiovascular exploration had been negative [26]. Solid lesions, perforating lymph nodes, atelectasis, and pneumonia were among the other indications. Children tolerated EBUS as well as adults did, and the time required for the examination was not longer.

■ Training and Learning Curve in EBUS

By comparison, EBUS is more difficult to learn and apply than many other bronchoscopic techniques. This is due in the first place to a general lack of training in ultrasound among most bronchoscopists, who have only very recently started to learn the handling of the devices and the interpretation of ultrasound images. Secondly, the application is more demanding, as the airways cannot be occluded for a longer period, and especially in patients receiving local anesthesia, the time available for the examination is short and the procedure has to be repeatedly interrupted. Finally, the anatomy of the airways and mediastinum is very complex, and orientation is difficult. This is the why the use of EBUS is only becoming more widespread very slowly. In our experience, following training in the theory of the procedure through reading, lectures, and the use of digital media, attendance at a 1-week course in a training center is useful for obtaining anatomical orientation and taking the initial steps in interpreting the images. Posters illustrating the anatomy and the corresponding ultrasound images, including the location of lymph nodes, are available for this purpose, and digital media (CDs and DVDs) are available for interactive learning. This has to be intensified by personal practical experience in patients, for which approximately 50 procedures are necessary. According to Falcone et al. [27], 20 procedures are necessary for image interpretation, and sufficient expertise was gained after 6–24 months, depending on the frequency of examinations—illustrating the difficulty of this method in comparison with other techniques. The development of interactive virtual training models could be very effective in shortening the learning curve, since at present neither training in phantom models nor in animal models is capable of replacing experience in real patients.

◁ Fig. 28.**9** Septated pleural effusion after surgery. **a** Pulmonary radiograph after resection of the upper lobe due to squamous-cell cancer. Despite suction with drainage, the lung is still partially collapsed, and the apical segment of the lower lobe is infiltrated. **b** Endobronchial ultrasound shows an extensive septated effusion (EFF), which has not been drained, and the lung is atelectatic (ATEL). The visceral pleura (PL) shows strong echoes. This situation usually has to be treated using video-assisted thoracoscopy.

Cost-Effectiveness

As with all new procedures, cost-effectiveness is an important issue in EBUS as well. In the United States, EBUS is reimbursed as separate procedure. For Europe, we carried out a cost assessment using the example of lymph-node staging. The costs involved in the acquisition and write-off of the equipment, costs for the physician and staff, and the costs of the disposable materials amount to approximately € 138 per procedure (excluding costs for bronchoscopy, which are the same for all calculation models). If 100 patients with enlarged lymph nodes undergo mediastinoscopy for preoperative staging, the total costs amount to € 162 000, calculated on the basis of € 1620 per procedure. If staging is carried out, including conventional CT-guided TBNA, the costs can be calculated as follows: the costs for disposables, needles, staff, and pathologist amount to € 57. Calculating an accuracy rate of 60% (an optimistic figure), 40 patients will need additional mediastinoscopy. Thus, the total costs will amount to € 70 000 (100 × € 57 for TBNA and 40 × € 1620 for mediastinoscopy). Improving the results of TBNA to 80% using EBUS, 100 × € 57 for TBNA have to be added to 100 × € 138 for EBUS. Since with this strategy only 20 patients would need additional mediastinoscopy (20 × € 1620), the total is € 51 000. This demonstrates that EBUS-guided TBNA is the most cost-effective strategy for lymph-node staging. Since reimbursement in Germany, for example, is currently in accordance with a system aimed at further rationalization of resources, it can be expected that EBUS-guided TBNA will continue to be applied more extensively.

Conclusions and Future Prospects

EBUS with miniprobes is currently being carried out in approximately 100 institutions throughout the world, and the results have been largely consistent. EBUS is beginning to replace other methods for several indications, as it has proved to be superior. These include the staging of early lung cancer and TBNA. Currently, the new ultrasonic endoscope is attracting wide attention, and this will increase the use of EBUS, as the technology is more similar to what bronchoscopists are used to handling. However, it should be borne in mind that the two methods are complementary rather than competing (Table 28.**1**).

EBUS using the miniprobe is superior for analyzing the delicate structures of the bronchial wall to detect early cancer and invasion by mediastinal lesions. This can make it possible to avoid inappropriate bronchoscopic treatment and futile surgery. Stenoses can be passed to allow precise staging. Peripheral lesions can be located and biopsied to allow histological assessment without the need for fluoroscopy. Unnecessary surgical resections of benign lesions might be avoided in this way in many cases. At our institution, approximately two-thirds of EBUS procedures are currently carried out using the miniprobe and one-third with the echo bronchoscope.

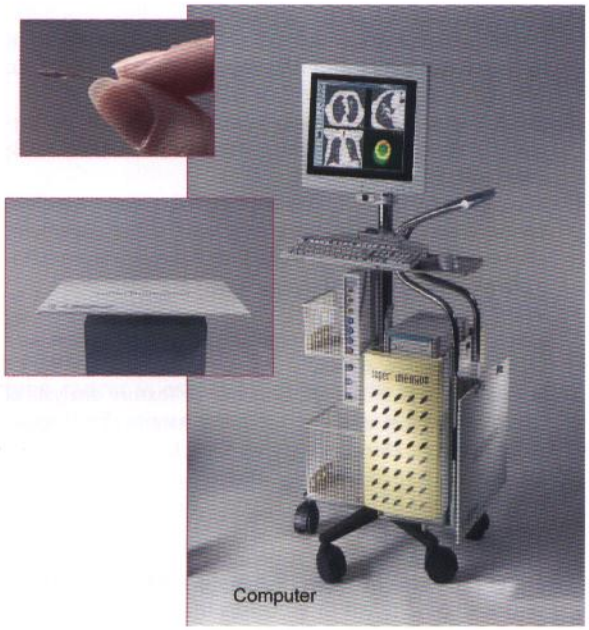
Table 28.**1** Various applications of endobronchial ultrasound probes

	Miniprobe	Puncture scope
Range	+++ (Central/lung)	++ (Central)
Maneuverability	+++	++
Orientation	+++	+
Layers	+++	Negative
Lymph nodes	++ (80–90%)	+++ (95–100%)
Mediastinum	+	+++
Vessels	++ (small)	+++ (Doppler)
Lung	+++ (75%)	Negative
Stenosis	+++	Negative
Intervention	Peripheral navigation	Central control

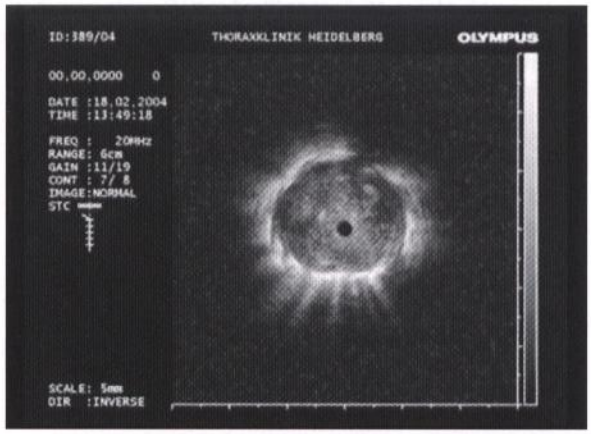
Further developments might include higher resolution, with 30-MHz ultrasonography to analyze vascularization (e.g., after bronchoplastic procedures or in patients with inflammation and neoplastic neovascularization). With regard to the use tissue analysis and computerized image analysis, color-coded tissue characterization using algorithms quantified with a learning vector might become useful and could increase the sensitivity and specificity in detecting early central and peripheral cancer and lymph-node metastasis [21, 28].

An additional channel in the miniprobe might be useful to increase the yield of biopsies in peripheral lesions [4]. We are currently exploring the application of EBUS miniprobes in connection with electromagnetic navigation in the diagnosis of peripheral lesions. For this purpose, EBUS probes, ultrathin bronchoscopes, biopsy instruments, and therapeutic instruments can be introduced using a catheter as an extended working channel, positioned inside the lesion with navigational assistance using a steerable electromagnetic sensor [29] (Fig. 28.**10**). In our experience, this technology is very promising for diagnosis, and in a pilot study we have already used it to carry out bronchoscopic treatment of inoperable peripheral lesions by intralesional placement of brachytherapy catheters. In this context, EBUS not only helped by confirming the precise location of the catheters, but also provided information regarding the tumor response through computerized image analysis that corresponded with the histological findings.

As the results in the treatment of advanced lung cancer are disappointing, early detection has recently been attracting increased attention. Screening of populations that are at risk for developing lung cancer, using molecular-biological methods and localization of lesions with autofluorescence methods, will play an increasing



a



b

Fig. 28.**10** Endobronchial ultrasonography in combination with electromagnetic navigation. The patient is placed on an electromagnetic table. A sensor is introduced via the bronchoscope, along with a catheter that serves as an extended working channel in the periphery of the lung. **a** The sensor, electromagnetic table, and computer allow navigation to be displayed in three planes, with the target shown in a frontal view on the monitor. Navigation of the steerable sensor is carried out using virtual bronchoscopy with three-dimensional computed tomography and the target coordinates. Fluoroscopy is not needed. **b** The precise position of the catheter inside the lesion is confirmed using endobronchial ultrasound. Afterwards, a brachytherapy catheter with a dummy probe is inserted for high-dose radiotherapy.

role. In this context, EBUS is the ideal tool for local staging of these lesions and detection of lymph-node metastases before local endobronchial therapy is considered [9,16].

It can be expected that increasing numbers of small pulmonary lesions will be detected with CT screening for peripheral lesions. A large number of these will be benign and will not require intervention. In this context, EBUS could play an important role in guiding diagnostic procedures and helping in decision-making through image analysis.

It is also possible that endobronchial ultrasonography could be applied using higher focused energies for thermal ablation and noncontact destruction of lesions. This could include early central lesions, as well as peripheral nodular lesions in the lung. As the EBUS image changes depending on the water content, computerized analysis of impedance changes in EBUS images could then serve to check the effectiveness of treatment.

Precise control of the needle using the ultrasonic bronchoscope might become useful for inserting radiofrequency ablation needles in order to treat extramural lesions adjacent to the central airways. In particular, changes in impedance after heat application might be useful as tools for checking these procedures; local transmural intratumoral deposition of cytotoxic agents could also be much more easily assessed with the additional use of EBUS.

In conclusion, EBUS has now become potentially just as important as endoscopic ultrasonography is in the esophagus, but is not yet as widely used. Currently, however, it is complementing the existing armamentarium of diagnostic and therapeutic tools in bronchoscopy, and in many respects it is already replacing less effective technologies. Diagnostic and therapeutic decisions can be assisted with EBUS directly during bronchoscopy, without the need for further time-consuming and costly procedures. As has been shown by the recent introduction of the ultrasound bronchoscope, interest in this new technology has been increasing significantly, and we are currently observing the beginnings rather than the end of a new development that is likely to provide an ever-increasing range of instruments and applications.

References

1. Koga T, Ogata K, Hayashida R, Hattori R. Usefulness of transluminal ultrasonography in the evaluation of bronchial stenosis secondary to tuberculosis. J Jpn Soc Bronch 1994; 16:477–82.
2. Frank N, Holzapfel P, Wenk A. Neue Endoschall Minisonde in der täglichen Praxis. Endosk Heute 1994;3:238–44.

3. Hürter T, Hanrath P. [Endobronchial sonography in the diagnosis of pulmonary and mediastinal tumors; in German.] Dtsch Med Wochenschr 1990;115:1899–905.
4. Hürter T, Hanrath P. Endobronchial sonography: feasibility and preliminary results. Thorax 1992;47:565–7.
5. Netter FH. Atlas of human anatomy, 2nd ed. Summit, NJ : Novartis Pharmaceuticals, 1998.
6. Wang KP, Mehta AC, Turner JF, editors. Flexible bronchoscopy, 2nd ed. Malden, MA: Blackwell, 2004.
7. Omori S, Takiguchi Y, Hiroshima K, Tanabe N, Tatsumi K, Kimura H, et al. Peripheral pulmonary diseases: evaluation with endobronchial US initial experience. Radiology 2002; 224:603–8.
8. Herth F, Becker HD, Manegold C, Drings P. Endobronchial ultrasound (EBUS): assessment of a new diagnostic tool in bronchoscopy for staging of lung cancer. Onkologie 2001; 24:151–4.
9. Becker HD. Options and results in endobronchial treatment of lung cancer. Minim Invasive Ther Allied Technol 1996; 5:165–78.
10. Herth F, Ernst A, Schulz M, Becker H. Endobronchial ultrasound reliably differentiates between airway infiltration and compression by tumor. Chest 2003;123:458–62.
11. Herth FJ, Becker HD, Ernst A. Ultrasound-guided transbronchial needle aspiration: an experience in 242 patients. Chest 2003;123:604–7.
12. Herth FJ, Ernst A, Becker HD. Endobronchial ultrasound-guided transbronchial lung biopsy in solitary pulmonary nodules and peripheral lesions. Eur Respir J 2002;20:972–4.
13. Herth F, Becker HD, LoCicero J III, Ernst A. Endobronchial ultrasound in therapeutic bronchoscopy. Eur Respir J 2002; 20:118–21.
14. Mountain CF. Revisions in the international system for staging lung cancer. Chest 1997;111:1710–7.
15. Naidlich DP. Staging of lung cancer. Controversy: computed tomography versus bronchoscopic needle aspiration: pro computed tomography. J Bronchol 1996;3:73.
16. Becker HD. [Endobronchial ultrasound: a new perspective in bronchology; in German.] Ultraschall Med 1996;17: 106–12.
17. Herth F, Becker HD, LoCicero J, Ernst A. Endobronchial ultrasound improves classification of suspicious lesions detected by autofluorescence bronchoscopy. J Bronchol 2003;10: 249–52.
18. Ono R, Suemasu K, Matsunaka T. Bronchoscopic ultrasonography in the diagnosis of lung cancer. Jpn J Clin Oncol 1993; 23:34–40.
19. Miyazu Y, Miyazawa T, Kurimoto N, Iwamoto Y, Kanoh K, Kohno N. Endobronchial ultrasonography in the assessment of centrally located early-stage lung cancer before photodynamic therapy. Am J Respir Crit Care Med 2002;165: 832–7.
20. Lam S, Becker HD. Future diagnostic procedures. Chest Surg Clin N Am 1996;6:363–80.
21. Basset O, Sun Z, Mestas JL, Gimenez G. Texture analysis of ultrasonic images of the prostate by means of co-occurrence matrices. Ultrason Imaging 1993;15:218–37.
22. Becker HD. Endobronchialer Ultraschall—eine neue Perspektive in der Bronchologie. Endosk Heute 1995;1:55–6.
23. Kurimoto N, Murayama M, Yoshioka S, Nishisaka T. Analysis of the internal structure of peripheral pulmonary lesions using endobronchial ultrasonography. Chest 2002;122: 1887–94.
24. Becker HD, Herth F, Shirakawa T. Computer-assisted analysis of endosonographic images of solitary pulmonary nodules (SPN). Eur Respir J 2001;20:462.
25. Herth F, Becker H. Endoluminaler Ultraschall. Atemweg Lungenkrankh 2003;29:460–75.
26. Link B, Liman ST, Becker HD, Dienemann H. [Endobronchial juvenile hemangioma in infancy: removal by main bronchus cuff resection. Case report; in German.] Chirurg 2001;72:584–7.
27. Falcone F, Fois F, Grosso D. Endobronchial ultrasound. Respiration 2003;70:179–94.
28. Wagner RF, Insana MF, Brown DG. Unified approach to the detection and classification of speckle texture in diagnostic ultrasound. Opt Eng 1986;25:738–42.
29. Becker HD, Mehta A, Ernst A, Herth F, Shirakawa T. Bronchoscopic biopsy of isolated, peripheral lung lesions under electromagnetic guidance: a pilot study. J Bronchol 2005;12.

29 Endobronchial Ultrasound

F.J.F. Herth, R. Eberhardt, M. Krasnik, P. Vilmann

Introduction

Pathological evaluation of mediastinal lymph nodes in lung cancer is essential for accurate staging and planning of effective treatment [1]. Locoregional spread involves mediastinal lymph-node involvement, and this is a major determinant of surgical resectability. Despite the advances in surgical treatment and multimodality treatment, lung cancer is still the leading cause of death from malignant diseases worldwide. Accurate staging of the disease is important not only in order to determine the prognosis, but also to decide the most suitable treatment plan for both operable and inoperable patients with non–small-cell lung cancer (NSCLC). During the staging process, accurate mediastinal lymph-node staging is one of the important factors that affect the management of patients. Conventional imaging methods available for evaluating the mediastinum, such as computed tomography (CT), are inaccurate in the diagnosis of mediastinal lymph-node metastasis [2]. Positron-emission tomography (PET) has been reported to increase the diagnostic yield [3].

The increasing use of minimally invasive techniques and day-case procedures has renewed interest in the use of transbronchial needle aspiration (TBNA) for mediastinal lymph-node staging. Conventional TBNA relies on "blind" needle puncture, guided by static CT scans. The technique is highly operator-dependent, and reported sensitivities vary widely, between 15% and 78% [4]. Higher yields are noted from the subcarinal station and when lymphadenopathy is present. However, due to the discouraging results that many operators obtain during their initial experience with the technique, recent surveys have shown that only 25% of pulmonologists use TBNA [5,6].

Endobronchial ultrasound (EBUS) using a radial probe is an imaging technique capable of detecting even small mediastinal lymph nodes [7]. However, imaging alone is inaccurate. Tissue confirmation of suspected malignant lymphadenopathy is therefore required, especially before surgical resection. Various invasive and noninvasive methods have been used to obtain tissue confirmation. In particular, endoscopic ultrasound–guided fine-needle aspiration (EUS-FNA) is a well-known modality with a high yield for tissue sampling of the mediastinum.

Lymph-Node Staging

In favorable conditions, lymph nodes can be detected with EBUS down to a size of 2–3 mm, and the internal structure (sinuses and folliculi) as well as small lymph vessels can be analyzed. The results of transbronchial needle aspiration (TBNA) can be significantly improved using endosonographic localization of lymph nodes, with a sensitivity of up to 85% [8]. This is especially true for positions in which reliable landmarks on the CT are missing—e.g., in high and low paratracheal locations. Herth et al. [9] investigated the results of EBUS-guided TBNA in comparison with conventional TBNA. In this randomized study, the authors confirmed that the yield of EBUS-guided TBNA is higher than that of conventional TBNA (85% vs. 66%). In an additional analysis of the lymph-node stations, they showed that particularly in locations that lack endoscopic landmarks (lymph-node stations 2, 3, and 4 in the Mountain and Dresler scheme [10]), the detection technique is helpful for increasing the yield. On the other hand, it was also demonstrated that when there are enlarged subcarinal nodes, conventional TBNA has the same yield as TBNA after EBUS detection [7].

Since the development of the EBUS-TBNA scope, the use of miniprobes for TBNA guidance has dramatically declined.

Description of the EBUS-TBNA Endoscope and Needle

The flexible ultrasonic bronchoscope (Olympus XBF-UC40P; Olympus, Tokyo, Japan) (Fig. 29.**1**) has an outer diameter of the insertion tube of 6.7 mm, with a working length of 550 mm (total length 870 mm). The instrument has a small, curved linear-array electronic transducer 10 mm long located at the distal end of the endoscope in front of a 30° degree oblique forward viewing fiberoptic lens (with an angle of view of 80°) (Fig. 29.**2**). The diameter of the distal end of the endoscope with the transducer is 6.9 mm. The angulation range of the distal end of the endoscope is 160° upward and 90° downward. The endoscope has a biopsy channel of 2 mm. The ultrasonic frequency is 7.5 MHz, with a penetration depth of 4–5 cm. The depth of imaging can be adjusted from 2 to 9 cm at 1-cm intervals. The scanning direction



Fig. 29.**1** The linear-array ultrasound bronchoscope (Olympus BF-UC40F-OL5; Olympus Ltd., Tokyo, Japan).

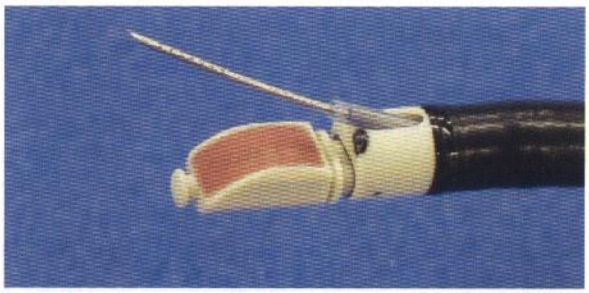


Fig. 29.**2** The needle is extended through the working channel and exits obliquely.



Fig. 29.**3** The 22-gauge needle.

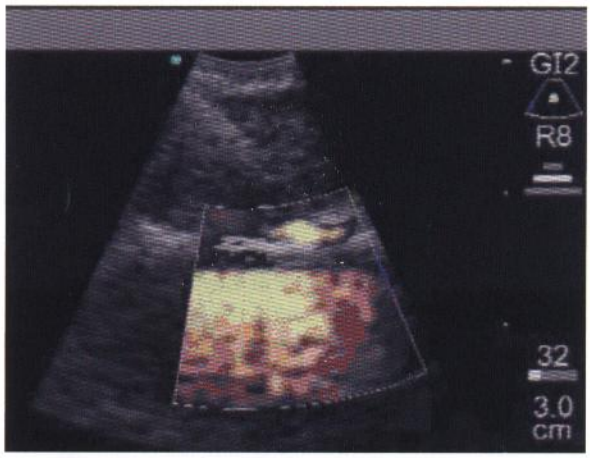


Fig. 29.**4** Checking the vessels during a puncture procedure. The needle is visible within the lymph node.

is parallel to the longitudinal axis of the endoscope, with a scanning angle of 50°. This allows full ultrasonic monitoring of a needle when inserted via the biopsy channel during scanning. The endoscope can either be connected to an Olympus ultrasound processor (Olympus EU-121 C2000) or to an Aloka ultrasound scanner. A balloon, which can be filled with water, can be mounted around the transducer for better ultrasonic coupling with the bronchial wall. The ultrasound images can be frozen, and the size of lesions can be measured in two dimensions by placing cursors. The system also has a Doppler mode.

A dedicated 22-gauge needle (Olympus NA-201SX-4022) was developed for carrying out transbronchial aspiration (Fig. 29.**3**). The inner diameter of the needle is nearly equal to that of a conventional 21-gauge needle, which allows sampling of histological cores in some cases. The needle is also equipped with an internal sheath, which is withdrawn after the bronchial wall has been passed, avoiding contamination during EBUS-TBNA. The needle can be visualized through the lenses and on the ultrasound image.

■ Procedure

The ultrasonic bronchoscope is introduced to the area of interest via an endotracheal tube under visual guidance and with the patient under local anesthesia, usually as an outpatient procedure. The bronchoscope is inserted orally, with additional sedation usually with 2 mg midazolam. Patients have to be monitored for electrocardiography, pulse oximetry, and blood pressure if an anesthesiologist is not present. Images can be obtained by directly contacting the probe or by attaching a balloon to the tip and inflating it with saline. Since the balloon is designed not to overinflate, it will not occlude the central airway. No experiences of technical difficulties using the balloon have been reported.

When a lesion is outlined, the needle is introduced via the endoscope's biopsy channel. Power Doppler imaging is used immediately before the biopsy in order to avoid unintended puncture of vessels between the wall of the bronchi and the lesion (Fig. 29.**4**). With real-time ultrasonic guidance, the needle is inserted into the lesion. Suction is applied with a syringe, and the needle is moved back and forth inside the lesion, as in the EUS-FNA procedure (Figs. 29.**5**, 29.**6**).

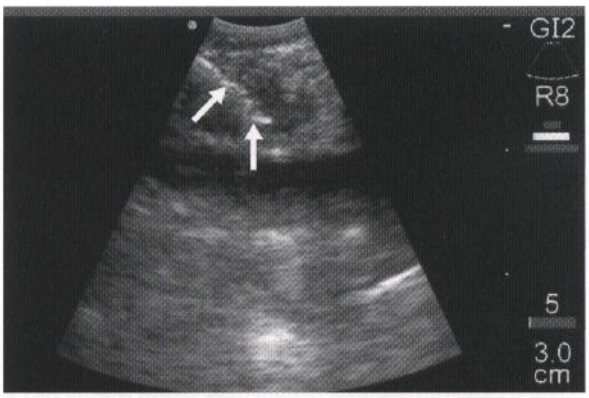


Fig. 29.**5** Puncture of an 8-mm lymph node in position 4r. The needle (arrows) is visible within the node.

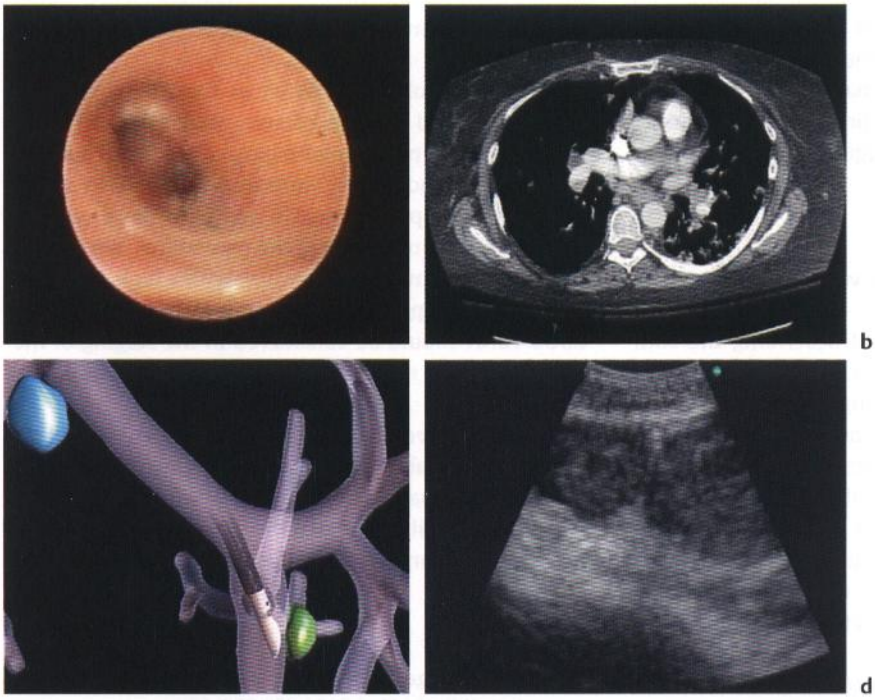


Fig. 29.**6a** Endoscopic view of enlarged nodes in 11l. **b** Computed tomography. **c** Schematic view. **d** Endoscopic bronchial ultrasound image. Cytological proof of N3 positive squamous-cell cancer was obtained.

■ Results

Several papers have been published on this procedure. Krasnik et al. [11] reported on 11 patients in whom 15 lesions were punctured, without complications. The lesions were located as follows: four in region 10L, four in region 10R, one in region 4L, three in region 4R, one in region 1, one in region 7, and one in region 2R. The lesions ranged from 7 mm to 80 mm in size. Biopsies obtained with EBUS-FNA showed malignant cells in 13 lesions and benign cells in two.

Yasufuku et al. [12] published their first experience in a few patients in 2004. In a second trial [13], they examined 70 patients with mediastinal lymph nodes (n = 58) and hilar lymph nodes (n = 12). The sensitivity, specificity, and accuracy of EBUS-TBNA for distinguishing between benign and malignant lymph nodes were 95.7%, 100%, and 97.1%, respectively. There were no complications.

In a recent paper by Rintoul et al. [14], EBUS-TBNA was used in 18 patients. Cytology revealed N2/N3 nodal disease in 11 patients and provided a primary diagnosis in eight patients. The cytology results for EBUS-TBNA samples were negative in six patients, and mediastinoscopy or clinical follow-up confirmed this result in four. The sensitivity, specificity, and accuracy of EBUS-TBNA were 85%, 100%, and 89%, respectively.

The largest trial published to date reported the results of the method in 502 patients [15]. A total of 572 lymph nodes were punctured, and 535 (94%) of the procedures resulted in a diagnosis. Biopsies were taken from all of the accessible lymph-node stations (2l, 2r, 3, 4r, 4l, 7, 10r, 10l, 11r, and 11l). The mean (SD) diameter of the nodes was 1.6 ± 0.36 cm (range 0.8–3.2 cm). The

sensitivity was 92%, the specificity was 100%, and the positive predictive value was 93%. As in all of the other trials, no complications occurred.

The Danish–German group [16] also examined the accuracy of EBUS-TBNA for sampling nodes less than 1 cm in diameter. Among 100 patients, 119 lymph nodes 4–10 mm in size were detected and sampled. Malignancy was detected in 19 patients, but missed in two others; all of the diagnoses were confirmed by surgical findings. The mean diameter of the punctured lymph nodes was 8.1 mm. The sensitivity of EBUS-TBNA for detecting malignancy was 92.3%, the specificity was 100%, and the negative predictive value was 96.3%. Again, no complications occurred. The authors concluded that EBUS-TBNA is capable of sampling even small mediastinal nodes, so that unnecessary surgical exploration can be avoided in the one in five patients who have no CT evidence of mediastinal disease. Potentially operable patients with clinically nonmetastatic NSCLC may benefit from presurgical EBUS-TBNA biopsies and staging.

■ EBUS-TBNA in Combination with EUS-FNA

Two papers have been published describing the combined approach. Again, Herth et al. [17] showed that the sensitivity and the specificity using both techniques led to the same results as a routine mediastinoscopy.

A recent study [18] has reported promising results with regard to the combination of EUS-FNA and EBUS-TBNA. A comparison of EUS-FNA and EBUS-TBNA was carried out in 33 patients, for lung cancer staging in patients with an established diagnosis of NSCLC (n = 20) or for diagnosis of suspected malignant lesions in the mediastinum in patients with suspected lung cancer (n = 13). The diagnoses were verified in 28 of 31 patients either by thoracotomy (n = 9) or through clinical follow-up (n = 18). A total of 119 lesions were sampled by EUS-FNA (n = 59) and EBUS-TBNA (n = 60). EUS-FNA and EBUS-TBNA identified cancer in 26 and 28 lesions, respectively, and benign cytology in 30 and 28 lesions, respectively. Suspicious cells were found in three lesions with EUS-FNA and four lesions with EBUS-TBNA. When the 60 EBUS-TBNA samples were compared with the 59 EUS-FNA samples, 11 additional cancer diagnoses and three samples with suspicious cells were obtained with EBUS-TBNA that had not been obtained with EUS-FNA. In contrast to this, EUS-FNA diagnosed 12 additional cancer diagnoses, one suspicious and one specific benign diagnosis (sarcoidosis) in addition to EBUS-TBNA. With regard to the results with the combined approach (EUS-FNA + EBUS-TBNA) in 28 of 31 patients in whom a final diagnosis was obtained in relation to the evaluation of cancer involving the mediastinum, 20 patients were found to have mediastinal involvement, whereas no mediastinal metastases were found in eight patients. The accuracy of EUS-FNA and EBUS-TBNA, in combination, for the diagnosis of mediastinal cancer was 100% (95% CI, 83–100%). The authors concluded that EUS-FNA and EBUS-TBNA appear to be complementary methods.

■ Conclusion

Endobronchial ultrasonography has been widely available for more than 5 years. A growing body of good-quality research studies support the view that it has a significant role to play in airway assessment and procedural guidance. A further step in technological development has been made with the introduction of the EBUS-TBNA scope.

The results of the trials show that there is a high diagnostic yield for the correct prediction of lymph-node staging in patients with lung cancer in comparison with other modalities. Moreover, EBUS-TBNA avoids many invasive procedures. In addition, there were no complications during any of the procedures. EBUS-TBNA is a minimally invasive procedure with a high diagnostic rate, and many patients can benefit from the procedure. EBUS-TBNA should be considered in the staging of mediastinal lymph nodes as well as in the diagnosis of lung cancer.

The combined approach with EUS-FNA and EBUS-TBNA may be able to replace more invasive methods for evaluating patients with lung cancer in whom there are suspected hilar or mediastinal metastases, as well as for evaluating unknown mediastinal or hilar lesions.

References

1. Spira A, Ettinger DS. Multidisciplinary management of lung cancer. N Engl J Med 2004;350:379–92.
2. Sihoe AD, Yim AP. Lung cancer staging. J Surg Res 2004;117: 92–106.
3. Toloza EM, Harpole L, Detterbeck F, McCrory DC. Invasive staging of non-small cell lung cancer: a review of the current evidence. Chest 2003;123:157–66.
4. Mehta AC, Kavuru MS, Meeker DP, Gephardt GN, Nunez C. Transbronchial needle aspiration for histology specimens. Chest 1989;96:1268–72.
5. Prakash VB, Offord K, Stubbs SE. Bronchoscopy in North America: the ACCP survey. Chest 1991;100:1668–75.
6. Haponik EF, Sture D. Underutilization of transbronchial needle aspiration: experience of current pulmonary fellows. Chest 1997;112:251–3.
7. Herth F, Becker HD, Ernst A. Conventional vs Endobronchial ultrasound-guided transbronchial needle aspiration: a randomized trial. Chest 2004;125: 322–5.
8. Herth F, Becker HD. Endobronchial ultrasound of the airways and the mediastinum. Monaldi Arch Chest Dis 2000; 55:36–45.
9. Herth F, Hecker E, Hoffmann H, Becker HD. Endobronchial ultrasound for local tumour and lymph node staging in

patients with centrally growing lung cancer. Ultraschall Med 2002;23:251–5.
10. Mountain CF, Dresler CM. Regional lymph node classification for lung cancer staging. Chest 1997;111:1718–23.
11. Krasnik M, Vilmann P, Larsen SS, Jacobsen GK. Preliminary experience with a new method of endoscopic transbronchial real time ultrasound guided biopsy for diagnosis of mediastinal and hilar lesions. Thorax 2003;58:1083–6.
12. Yasufuku K, Chhajed PN, Sekine Y, Nakajima T, Chiyo M, Iyoda A, et al. Endobronchial ultrasound using a new convex probe: a preliminary study on surgically resected specimens. Oncol Rep 2004;11:293–6.
13. Yasufuku K, Chiyo M, Sekine Y, Chhajed PN, Shibuya K, Iizasa T, et al. Real-time endobronchial ultrasound-guided transbronchial needle aspiration of mediastinal and hilar lymph nodes. Chest 2004;126:122–8.
14. Rintoul RC, Skwarski KM, Murchison JT, Wallace WA, Walker WS, Penman ID. Endobronchial and endoscopic ultrasound-guided real-time fine-needle aspiration for mediastinal staging. Eur Respir J 2005;25:416–21.
15. Herth FJF, Eberhardt R, Vilmann P, Krasnik M. EBUS-TBNA: a new device for endoscopic transbronchial real time ultrasound guided biopsy for diagnosis and staging of mediastinal lymph nodes. Thorax [in press].
16. Herth FJF, Krasnik M, Eberhardt R, Ernst A, Vilmann P, Dienemann H. EBUS guided biopsy for the staging of mediastinal lymph nodes in a radiologically normal mediastinum. Lung Cancer 2005;49:26.
17. Herth FJ, Lunn W, Eberhardt R, Becker HD, Ernst A. Transbronchial vs. transesophageal ultrasound-guided aspiration of enlarged mediastinal lymph nodes. Am J Respir Crit Care Med 2005;171:1164–7.
18. Vilmann P, Krasnik M, Larsen SS, Jacobsen GK, Clementsen P. Endoscopic trans-esophageal and endoscopic-ultrasound guided biopsy: a combined approach in the evaluation of mediastinal lesions. Endoscopy 2005;37:833–9.

30 EUS-Guided Neurolysis of the Celiac Plexus

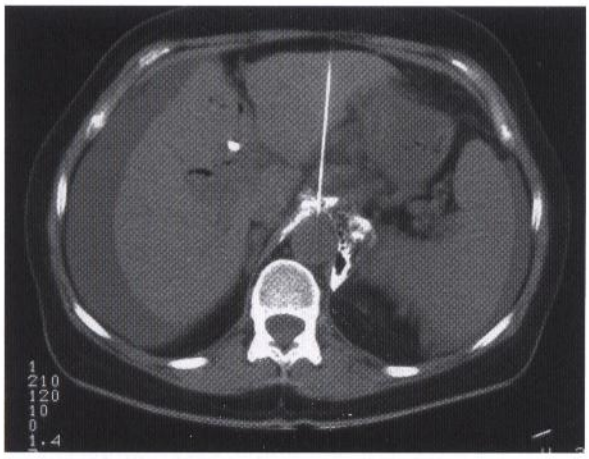
S. Hollerbach

Introduction

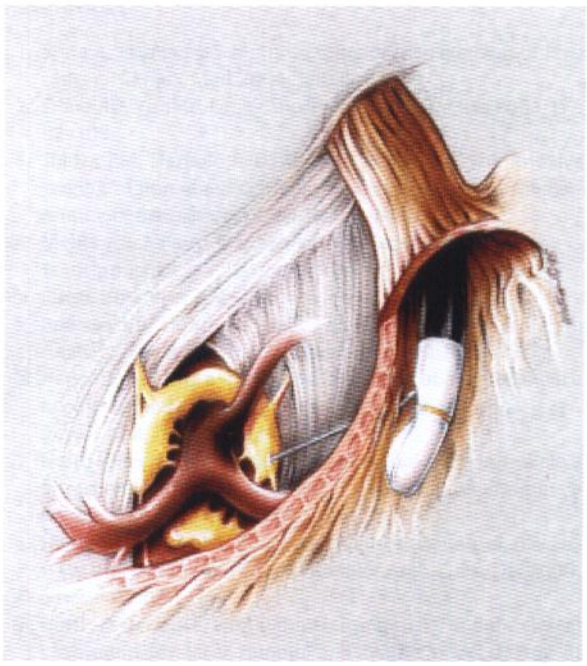
Celiac plexus neurolysis has been used since 1950 to treat severe visceral pain syndromes. The initial clinical studies were carried out using dorsal and paraspinal routes or transabdominal techniques with fluoroscopic guidance in order to access the region of the celiac trunk. These techniques were mainly used in large treatment centers to treat intractable pain caused by pancreatic carcinoma, and sometimes in chronic pancreatitis. However, because of the high level of expertise and specialization required to carry out such invasive procedures safely in patients, the techniques did not come into widespread use outside a few tertiary care centers. Alternative surgical methods also never became treatment options, as they were even more invasive and were not an attractive option for use in terminally ill groups of patients. With the advent of various highly effective and potent analgesic drugs and anesthetics, interest in developing additional invasive methods of treating cancer pain declined even further. However, when computed tomography (CT) techniques were further refined during the 1980s, interest among clinicians gradually returned to the issue of celiac plexus neurolysis (Fig. 30.**1a**).

Since then, a few specialized pain centers have reported clinical "success rates" in the range of 60–85% with CT-guided interventions in uncontrolled open studies, although evidence from controlled studies is still largely lacking. A relatively high rate of complications was encountered with CT-guided techniques, which is one of the major reasons for continuing efforts since the mid-1990s to develop novel techniques such as endoscopic ultrasound (EUS)-guided plexus neurolysis. This approach always appeared attractive, as it offers the advantages that it is carried out with the patient in intravenous sedation and is considerably less invasive, since very fine needles are used (22–25 G) with direct ultrasound visualization, very close to the anatomical structures that indicate the location of the celiac plexus—the neural ganglionic structures of which are not visible themselves with any imaging methods (Fig. 30.**1b**).

Initial uncontrolled clinical studies [1,2] provided encouraging results with regard to the feasibility and safety of EUS-guided fine-needle injection (FNI) in this setting. Success was reported in 80–90% of cases, with reduced analgesic requirements and stabilization of the pain. Relevant side effects of EUS-FNI included transient diarrhea, hypotension, and rare cases of infection. No



a



b

Fig. 30.**1a** Computed tomography–guided celiac plexus neurolysis. **b** Endoscopic ultrasound–guided celiac plexus blockade, showing some of the anatomical landmarks.

randomized controlled clinical studies have yet been published on the topic, although several clinical trials are currently being conducted in different countries.

Minimally invasive interventional therapeutic endosonography is a novel technique. With the advent of improved endoscopic technology and the development of longitudinal scanners, it became possible some 12 years ago to combine ultrasonography and endoscopy in such a way that ultrasound-guided transmural needle interventions (biopsies) became possible during the same endoscopy session. This method has the unique advantage that even small and previously inaccessible pathological lesions (≥ 5 mm) can be reached with EUS guidance even if they are located in the posterior mediastinum, around the cardia, the cranial retroperitoneum, the adrenal glands, the hilum of the liver, the pancreatic region, and the rectum [3–8]. These techniques were initially used only to obtain EUS-guided fine-needle aspiration (FNA) biopsies for diagnostic purposes, but today they are increasingly being used for transvisceral therapeutic procedures [1,2,9,10]. The variety of options available and the fact that the complication rate is relatively low makes EUS-guided interventions particularly attractive. However, EUS-guided interventions are technically highly demanding, and considerable endoscopic and ultrasound training is needed in order to carry out procedures of this type safely. Skill and expertise in EUS-guided interventions are necessary before these rather delicate methods can be safely conducted in patients. Table 30.1 provides an overview of the current routine and experimental indications for diagnostic and therapeutic uses of EUS-FNA.

This chapter provides an overview of one of the most useful clinical applications of EUS-guided therapy: celiac plexus neurolysis in the treatment of severe visceral pain in malignant disease, using injection therapy. It should be borne in mind that this form of treatment is largely supportive, although it can make a significant contribution to a comprehensive and interdisciplinary approach to pain management in malignant disease. It helps the clinician control pain in patients with end-stage disease and adds valuable nonpharmacological options. However, there is still a lack of prospective and controlled clinical studies.

Table 30.1 Indications for diagnostic and therapeutic endoscopic ultrasound-guided fine-needle aspiration (EUS-FNA)

Diagnosis and/or local staging
• Mediastinal lymphomas (bronchial carcinoma, Hodgkin's lymphoma, non-Hodgkin's lymphoma, tuberculosis, sarcoidosis)
• Mediastinal tumors (bronchial carcinoma, germ-cell tumor, thymoma, metastases, inflammatory pseudotumors, etc.)
• Mediastinal abscess (perforating abscess, tuberculosis), fluid collections in the posterior mediastinum
• Pathological lesions in the thyroid and parathyroid *
• N/M1A staging of esophageal carcinoma
• Intramural esophageal tumors
• Submucous tumors in the esophagus, stomach, and duodenum
• Diagnosis of the type and N/M staging of tumors, metastases, lymph nodes, abscesses, and fluid collections in the peritoneum and retroperitoneum
• Diagnosis of periampullary tumors and malignant pancreatic tumors (including N and local M staging)
• Diagnosis of pathological lesions in the left lobe of the liver and central segments of the liver and hilar region (metastases, hepatocellular carcinoma, cholangiocarcinoma, adenoma, hilar lymph nodes, abscesses)
• Diagnosis of lesions in the left adrenal gland (metastases, adenomas, multiple endocrine neoplasia, tuberculosis)
• Circumscribed lesions of the spleen (non-Hodgkin's lymphoma, Hodgkin's disease, metastases)
Therapy
Celiac plexus block (neurolysis) for pain treatment in pancreatic and papillary carcinoma, as well as chronic pancreatitis
EUS-targeted drainage treatment for pancreatic pseudocysts (with stent placement)
EUS-targeted drainage treatment in cholestasis* and accessible dilated bile ducts (with stent placement)
EUS-guided endoscopic mucosal resection
EUS-guided intratumoral fine-needle injection therapy

If these procedures are not easier with EUS-FNA, percutaneous access is also possible.

■ Prerequxisites for EUS-Guided Celiac Plexus Neurolysis and Other Treatments

The effectiveness of therapeutic EUS depends on a variety of different factors:

- *General experience and skill.* One of the most important prerequisites for carrying out EUS-guided treatments successfully is excellent endoscopic skills, with full mastery of all of the conventional endoscopic techniques using straight-viewing and side-viewing endoscopes, including esophagogastroduodenoscopy and endoscopic retrograde cholangiopancreatography. In addition, comprehensive training in interventional transcutaneous sonography, including fine-needle puncture and drainage techniques, is needed in order to meet the high requirements for interventional therapeutic EUS.
- *Specialized endosonography skills.* Endoscopic ultrasonography with fine-needle aspiration (EUS-FNA) is probably one of the most technically demanding and training-intensive endoscopic examination procedures. Experience with at least 250–300 previous endosonographic examinations, including fine-needle biopsies, is needed to ensure that treatments in this field are carried out safely and successfully in routine clinical conditions in patients.
- *Cost-effectiveness.* Interventional EUS for routine use in an endoscopy department generally involves sub-

stantial costs, including the high initial investment and installation costs and expenses for repair procedures, as well as additional costs for accessory materials such as puncture needles and other appliances. These additional materials are usually much more expensive than any of the catheters and needles used for percutaneous procedures. Depending on the type of needle used and local price negotiations, the cost of a biopsy needle as a single-use device can amount to € 150–300. On top of this, costs for sedatives and anesthetics, cytology and/or histology, and microbiology have to be taken into account, representing an additional € 50–150, depending on the severity and type of disease and procedure. With therapeutic interventions, even higher total costs have to be calculated (between approximately € 850 and € 1500 per drainage procedure) if metal stents are not inserted; metal stents can increase the cost up to a total of € 1500–2500. Finally, the amount of time and the numbers of staff needed for demanding procedures such as these mean that the use of the techniques outside specialized care centers, with reasonable numbers of patients with special needs, is questionable and unattractive. In general, only specialized clinical care centers dealing with a significant number of complex gastroenterology and oncology cases, which also offer a wide range of minimally invasive visceral surgical procedures per year, should consider installing therapeutic EUS facilities in order to serve as a center of expertise. Any other institutions would need to weigh up the benefits of such niche techniques carefully against the medical and financial risks, since basic endosonographic problems can be reasonably assessed with radial-scanning echoendoscopes, allowing appropriate selection of patients with special medical needs who can still be referred to secondary or tertiary care centers for therapeutic EUS.

■ Indications for Therapeutic EUS

Several new applications for interventional EUS techniques are in principle feasible and are currently being investigated. Only a few therapeutic EUS techniques have yet made their way into prospective clinical studies that allow preliminary evidence-based conclusions to be drawn (Table 30.**1**). Clinically approved therapeutic EUS techniques currently include:

- Celiac plexus neurolysis (with EUS-FNI) to achieve better control of chronic visceral pain in patients with pancreatic and periampullary carcinoma and other types of retroperitoneal tumor (clinical efficacy approximately 50–80%, depending on the definition of the outcome; however, further research is still required).
- EUS-guided drainage of pancreatic pseudocysts and necroses, including one-step placement of stents and drainage catheters.
- EUS-guided drainage of obstructed bile ducts in the left liver lobe, as an alternative technique to percutaneous transhepatic cholangiographic drainage (PTCD).
- EUS-guided drainage of obstructed pancreatic ducts and placement of transpapillary pancreatic guide wires (experimental).

Other experimental therapeutic EUS options and techniques include:

- EUS-guided intratumoral injection therapy with cytotoxic agents (local chemotherapy), immunomodulators (e.g., mixed allogenic lymphocyte populations or lectins), and other agents.
- EUS-guided radiofrequency ablation of tumors (pancreas, liver metastasis, retroperitoneal tumors).
- EUS-guided local laser ablation therapy or photodynamic therapy.

■ Contraindications to Therapeutic EUS

In general, EUS-FNA applications are considered to be very safe. Most of the contraindications are therefore only relative, but the benefits need to be carefully weighed up against the potential risks in each individual patient affected by the relative contraindications. The most frequent complications are listed in Table 30.**2**. Diagnostic puncture biopsies with fine needles (19–25 gauge) are generally safe, while therapeutic procedures involve a small but considerable risk of side effects, particularly in severely ill patients with multiple risk factors such as severe coagulopathy. The contraindications to diagnostic fine-needle injection therapy—e.g., for celiac plexus neurolysis and other therapeutic procedures—are:

- Lack of informed consent from the patient
- Poor clinical status of the patient (Karnofsky index < 70%)
- Large vessels blocking the needle path
- Lack of visualization of the needle tip
- Severe coagulopathy (Quick test < 30%, thrombocyte count < 40 000)

■ Materials

Echoendoscopes

There are at present three manufacturers producing echoendoscopes that allow diagnostic and therapeutic EUS procedures. These consist exclusively of longitudi-

nal-scanning endoscopes with a biopsy channel (longitudinal convex-array scanners).

Hitachi (Hitachi Medical Corporation Tokyo, Japan), in collaboration with Pentax (Pentax Europe Ltd., Hamburg, Germany), has the longest record with longitudinal EUS and currently produces several ranges of fiberoptic echoendoscopes (Pentax FG-34UX, FG-48UX) and digital video endoscopes (Pentax FG-3830) for diagnostic and therapeutic interventions. Fiberoptic ultrasound endoscopes have an oblique-viewing 60° lens with a longitudinal echo transducer at the tip of the scope. The working channels for biopsies have two different sizes (2.0 or 3.2 mm). The electronic curved-array transducer produces a sector-like 120° image along the longitudinal scope axis that allows fully EUS-guided interventional maneuvers under full vision. The transducer frequency can be switched between 5 and 10 MHz. A water-filled balloon around the tip of the instrument enhances contact between the ultrasound beam and the mucosal surfaces and minimizes disturbing air reflexes within the gastrointestinal tract. All of the endoscopes are equipped with a color Doppler device and continuous-wave Doppler to facilitate the analysis of vascular structures.

Toshiba. Another manufacturer of longitudinal echoendoscopes with working channels for biopsies is Toshiba (Toshiba Medical Systems Europe, Zoetermeer, Netherlands), which produces the ultrasound unit for a dedicated Fujinon scope (Fujinon Europe Ltd., Willich, Germany). The local resolution provided by this device is quite good, although the biopsy channel requires considerable experience and does not contain an elevator. Due to the limited distribution of these endoscopes, clinical experience with them is very limited and it is not very likely that this collaboration will lead to the development of any novel EUS equipment.

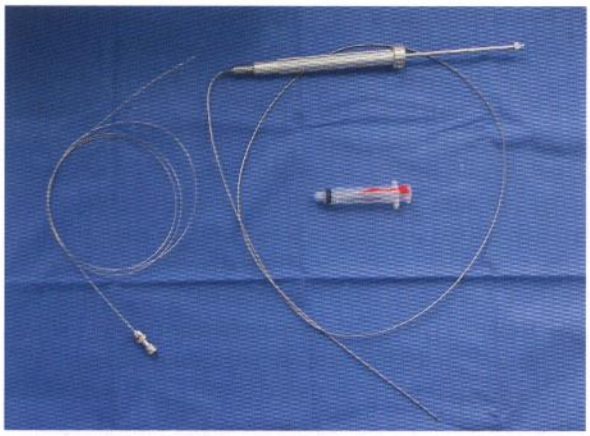
Olympus (Olympus Europe Ltd., Hamburg, Germany) has now developed a relatively wide range of different radial and longitudinal echoendoscopes, including digital radial scanners and longitudinal scopes that contain large working channels for therapeutic maneuvers. These endoscopes maintain the same high solid-state standards as those of the conventional endoscopes the company produces. The latest addition involves exclusively ultrasound scanners and machines, which are produced by Aloka (Aloka Europe Ltd., Zug, Switzerland). The Aloka GF-UCT140-AL5 and GF-UC 140P-AL5 for standard processors and the GF-UCT160-OL5 and GF-UC160P-OL5 series for Exera II processors should be mentioned in particular. These scopes have working channels ranging from 2.8 up to 3.8 mm for therapeutic applications, and they all incorporate color Doppler units. However, there is one series that can be combined with equipment from ATL Ultrasound, Inc. The longitudinal puncture endoscopes manufactured by Olympus are all equipped with an elevator that facilitates introduction of the biopsy needle under ultrasound guidance, within certain limits.

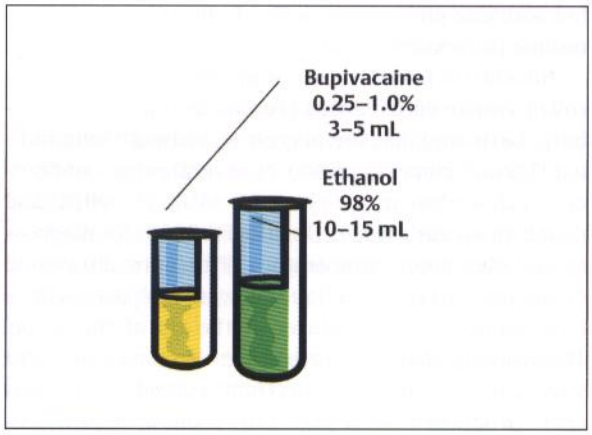
The specific choice of interventional EUS equipment to be used certainly depends on many different factors, including individual preferences, previous experience, the local ultrasound and endoscope equipment available, and the financial options at one's disposal. For instance, there are differences between the manufacturers' products with regard to ultrasound resolution, flexibility, and appliances, but also in terms of mechanical properties and electronic endoscope quality. These factors need to be individually weighed up against each other to reach a final decision relative to the available budget. Successful EUS procedures are certainly also highly dependent on the operator's skills and experience, while the endoscope facilities and ultrasound applications are clearly of secondary importance.

Materials for Therapeutic EUS Procedures

Various commercially available needle systems can be used to carry out EUS-guided fine-needle injections for celiac plexus neurolysis. At present, a wide range of different needle systems are available on the medical product market. The main players in this field are the companies GIP/Medi-Globe Ltd. (Achenmühle, Germany), Wilson-Cook (Cook Endoscopy, Winston-Salem, North Carolina, USA), and Olympus. However, successful treatment is possible with almost any of the products available, and in many cases it is the price of the needle that determines preferences in an individual EUS department. The least expensive needle currently available is the Hancke–Vilmann metal needle (Medi-Globe), which consists of a metal needle made of stainless steel (170 cm/0.8 mm, 22 gauge). It has a metal stylet, a reusable metal spiral sheath, and a grip with a piston (Fig. 30.**2**) to guide the needle tip properly. Numerous pioneering clinical studies have been conducted using this needle, which has been the standard in EUS-FNA for many years now. For therapeutic applications, however, a similar 19-G needle is available—e.g., for pancreatic pseudocyst drainage procedures. This needle has a larger lumen and is also practical for injection therapy, while the price is still the lowest on the market due to the reusable outer parts. However, there are problems in that the visibility of these needles is in some cases very limited, while the outer sheath is rather rigid.

Other diagnostic and therapeutic needle systems at higher prices are available in different sizes and styles (19–25 G) from Wilson-Cook and Olympus. The Olympus needles are solid-state metal ones (22 G) that can be used primarily for diagnostic EUS-FNA and injection treatments such as plexus neurolysis. They have fair to good visibility in tissue and are rather flexible, whilst the price is considerable. Cook supply the widest range of specialized and dedicated diagnostic and therapeutic





a b

Fig. 30.2 Materials required for EUS-guided celiac plexus neurolysis (EUS-CPN). **a** Standard Hancke–Vilmann biopsy needle, including the piston, protective sheath, stylet and needle, and Luer aspiration syringe. **b** Injection solutions.

needles (e.g., the 22-gauge EchoTip EUSN-1, EUSN-1-T, EUSN-1-CS, and EUSN-3 needles; the 19-gauge EchoTip EUSN-19-T; and the 25-gauge EchoTip EUSN-25), and have also developed a novel dedicated cutting needle for histological purposes (the 19-gauge Quick-Core EUSN-19-QC). They have also developed the only specially designed spray needle for celiac plexus neurolysis, with multiple side holes and a diameter of 20 gauge (EchoTip EUSN-20-CPN). However, good though these needles may be, there is no scientific evidence as yet that the high cost of these appliances is justified by their individual performance status, which remains to be demonstrated in ongoing clinical studies in several EUS centers around the world.

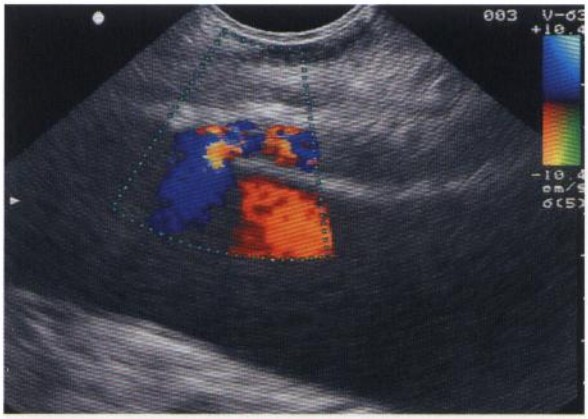
Injectant solutions are required for celiac plexus neurolysis. These consist of a local anesthetic and absolute alcohol solution for final and permanent neurolysis, with an amount 5–15 mL of a commercially available local anesthetic—procaine benzylpenicillin (novocaine), lidocaine, or mepivacaine and lauromacrogol 400 (Scandicain)—which is followed by 20–30 mL of absolute alcohol (98% ethanol). Figure 30.**2** shows the equipment and solutions required for EUS-guided celiac plexus neurolysis (CPN).

■ Celiac Plexus Neurolysis

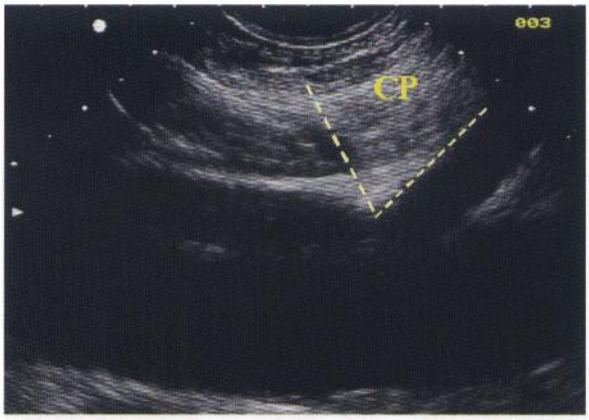
Preparation for the Procedure

The patient should be placed in the left lateral decubitus position, as recommended for conventional esophagogastroduodenoscopy (EGD) procedures. However, in some cases it can be helpful to rotate the patient's body toward the abdomen during the EUS intervention, to provide a better overview of the celiac plexus region. Topical anesthetic sprays are strongly recommended (e.g., with lignocaine/Xylocaine) to ensure event-free endoscope insertion. Intervenous sedative medication should always be administered to facilitate the EUS procedure. The recommended agents are the same as those used for standard EGD and colonoscopy procedures, including midazolam (Dormicum, 5–10 mg), propofol (Disoprivan, 50–200 mg) and/or pethidine (Dolantin, 25–75 mg). Additional use of hyoscine butylbromide (Buscopan) or atropine can only be recommended in exceptional cases—for instance, when the duodenal bulb cannot be reached easily or if cramps and spasms inhibit the insertion of the scope into the second part of the duodenum. Monitoring devices for continuous measurement of blood pressure and pulse oximetry are mandatory to ensure safe surveillance of vital signs during echoendoscopy in all cases. If high-risk patients are being examined—e.g., patients with concomitant severe respiratory and cardiovascular problems—portable or stationary electrocardiography (ECG) monitors should be used as well. Facilities for continuous oxygen administration via nasal or oral probes or masks during endoscopic procedures are essential, and oxygen should be administered even during episodes of slight hypoxemia.

The side-viewing echoendoscope is then introduced under proper sedation, with minimal pressure during pharyngeal and laryngeal passage into the esophagus. In routine conditions, 2.5–5.0 mg midazolam is recommended, and this should be combined with bolus administration of propofol in boluses of 30–50 mg with continuous monitoring of oxygenation and blood pressure. Alternatively, 25–50 mg pethidine can be used, particularly in countries that do not permit the use of propofol for this indication. Several countries restrict the use of propofol to endoscopy units with physicians present who have formal training in intensive-care treatment, since the agent is an intravenous anesthetic that can potentially cause severe respiratory depression and hypoventilation, including life-threatening hypoxia,



a



b

Fig. 30.**3** Endosonographic appearance of the target region for EUS-guided celiac plexus neurolysis (EUS-CPN). **a** Identification of the celiac trunk with color duplex ultrasound scanning, and positioning of the longitudinal transducer above the abdominal aorta. **b** The presumed anatomical position of the major celiac plexus (CP) ganglion network, indicated by the triangular line. The tip of the injection needle is also visible.

if not administered correctly. However, with the necessary experience, careful bolus administration, and continuous patient monitoring, we have found that propofol is very helpful and safe in our experience. We therefore strongly recommend the combination of low-dose midazolam and propofol as the sedation method of choice in most cases, particularly if EUS-guided therapy is planned or scheduled.

Antibiotic prophylaxis. In accordance with standard endocarditis prevention guidelines, prophylactic antibiotics should be administered before the EUS intervention in all patients who have an increased risk of endocarditis or other systemic infections (artificial valve, valvular stenoses or insufficiencies, shunts). In addition, if cystic lesions are being punctured during EUS-FNA or EUS-FNI, antibiotic prophylaxis should also be administered intravenously. Recommended single antibiotic substances include amoxicillin, ampicillin, piperacillin, ceftriaxone, and cefuroxime. Before administration, however, the individual risk situation should be assessed and the choice of antibiotics should be tailored to the specific situation, as recommended in the current endocarditis prevention guidelines.

Prophylaxis in EUS-FNI. Intravenous antibiotics should be administered prophylactically before EUS-FNI if there is an increased risk of endocarditis and/or if spontaneous bacterial peritonitis has to be avoided. Suitable antibiotics include ampicillin, amoxicillin, or ceftriaxone. It is not known whether administration of proton-pump inhibitors (PPIs) is helpful in preventing ulcer complications after therapeutic EUS procedures. However, in the absence of solid data, we would currently recommend avoiding PPI administration in severely ill patients, if clinically feasible, as the agents could theoretically increase bacterial overgrowth.

Procedure

Using an echoendoscope with a linear transducer, the region at the root of the celiac ganglion, arising just cephalad and anterior to the celiac artery, can be reached in most patients (Fig. 30.**3**). The echoendoscope is pulled back just below the cardia, approximately 40–45 cm from incisors, and placed a few centimeters below the phrenic hiatus, with the transducer curved posteriorly against the stomach wall. After this position has been achieved, either a 22-gauge diagnostic FNA needle or a specially designed 20-gauge needle with side holes is introduced through the endoscope's working channel and carefully inserted through the stomach wall. With close observation of the tip of the needle, the operator advances the needle under direct vision until the wall of the common celiac trunk is just touched, and the scope is then withdrawn 3–5 mm on reaching the arterial wall. In cases of doubt or uncertainty, the needle position can also be visualized by injecting contrast agents for fluoroscopy (Fig. 30.**4**). Before anything is injected, aspiration should be applied to exclude intravascular positioning of the needle tip—e. g., in the celiac artery. The best results are achieved when the injection starts approximately 2 mm cephalad to the celiac trunk, to spread the injection agent widely in the soft tissue surrounding the retroperitoneal region. This procedure requires considerable skill and should only be carried out by experienced EUS interventionists. Subsequently, 10–15 mL bupivacaine (0.25%) is instilled for local anesthesia on both sides of the celiac axis, whenever anatomically possible, by repositioning the endoscope and needle. This injection is extremely important in order to avoid severe local pain after administration of the neurolytic agent (absolute alcohol).

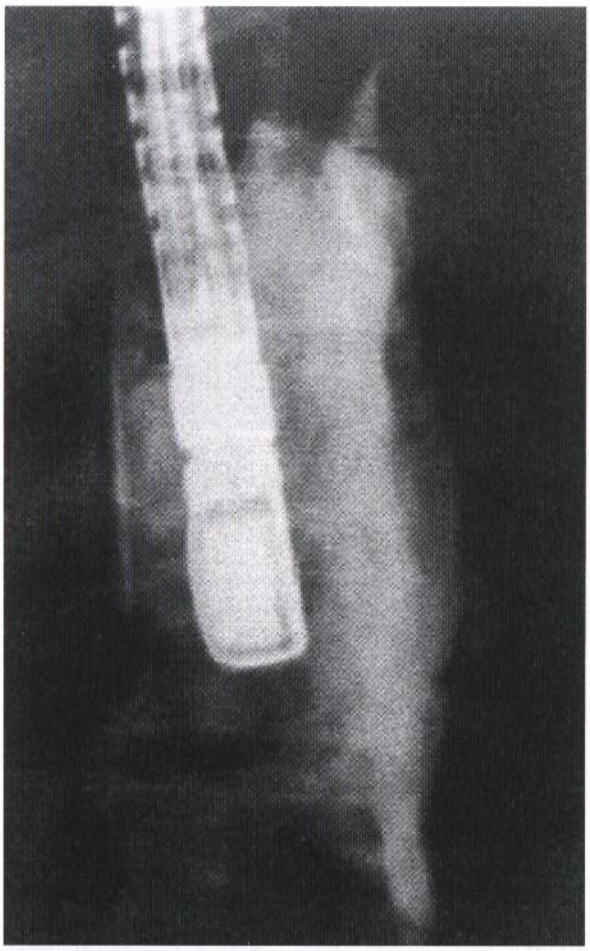
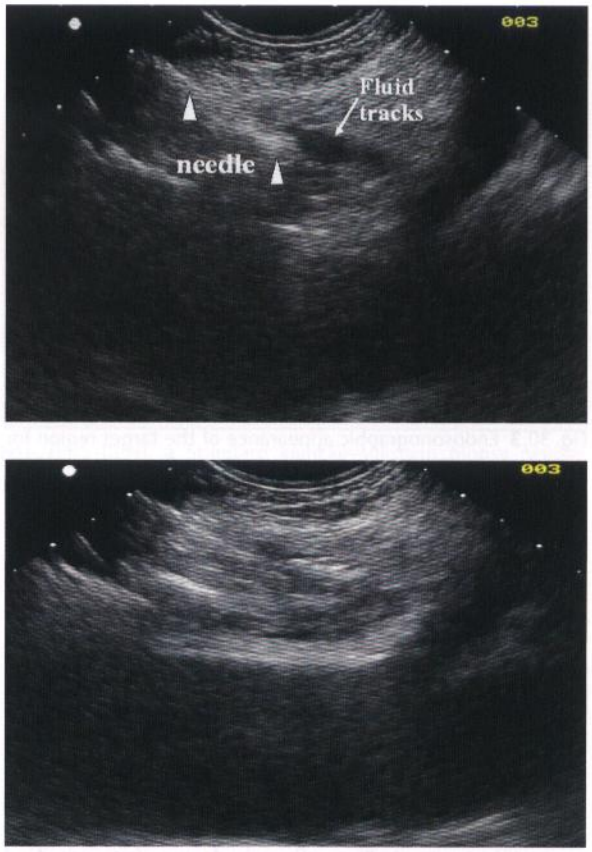


Fig. 30.4 Fluoroscopic image of the celiac trunk and its surroundings after EUS-guided fine-needle injection of contrast material before celiac plexus neurolysis. The wide distribution of the injection fluid is well demonstrated.



a

b

Fig. 30.5 EUS-guided celiac plexus neurolysis. **a** The celiac plexus is located directly cephalad and anterior to the celiac trunk arteries as they emerge from the aorta. The EUS-guided fine needle is carefully introduced and advanced close to the wall of the celiac trunk. **b** The local anesthetic agent is then sprayed or injected, followed by injection of the absolute alcohol, which is sprayed or injected in equal aliquots on both sides of the celiac trunk.

The utmost care should be taken to keep the tip of the needle away from the arterial wall, to prevent significant complications such as arterial bleeding and embolization during the injection. Subsequently, 10–15 mL 98% ethanol (absolute alcohol) is injected first and the injection is then repeated after repositioning of the EUS instrument by angling the tip by approximately 90°. When the alcohol is injected under ultrasound vision, the image of the needle becomes increasingly blurred, as the injectant solution produces highly echogenic cloud-like ultrasound artifacts (Fig. 30.5). The treatment should therefore be carried out rapidly as a bolus injection to both application sides of the celiac trunk, and the procedure should be terminated immediately after the end of the injection.

This procedure can be carried out on an outpatient basis, as it rarely causes any lasting side effects. Celiac plexus neurolysis can also be carried out at the end of a diagnostic tumor-staging procedure for pancreatic carcinomas. In this case, morphological EUS staging of the tumor and locoregional lymph-node staging is carried out first, in combination with diagnostic EUS-FNA to allow histological assessment of the tumor, followed by the EUS-CPN procedure as described above.

Problems and Complications

Most EUS-guided therapeutic interventions are still regarded as experimental. In addition to the general risks and side effects of standard endoscopy, therefore, the specific procedure-related risks associated with EUS-guided treatments have to be assessed before the treatment. If it is carried out correctly, EUS-guided celiac plexus neurolysis usually only causes mild complications such as transient diarrhea or mild local tenderness. However, a few individual cases of major complications have been reported, including pancreatic abscess, arteriovenous malformations, and bleeding, which suggests that careful clinical observation is absolutely mandatory after all interventional measures. EUS-guided treat-

ments are extremely safe when carried out by experienced interventional endoscopists, with careful technique and the use of safe injection materials, although there are as yet only limited data for safety assessments. Our experience in more than 50 patients treated with EUS-FNI is positive; only three of the patients (1.5%) developed mild, transient, and self-limiting complications, and no severe complications requiring interventional treatment developed. Table 30.**2** lists the published types and frequency of potential complications related to EUS-FNI.

Postinterventional Measures

In principle, all EUS-guided interventions can be carried out in an outpatient setting. However, postinterventional in-hospital surveillance should be considered in patients with a high risk of complications—e. g., patients with coagulation disorders or severe respiratory and cardiac problems. In view of the favorable safety profile of EUS-guided interventions such as EUS-FNA and EUS-FNI, severe complications occur extraordinarily rarely if the techniques are applied correctly. In all routine cases of EUS-FNI, surveillance after the intervention follows the general principles for diagnostic and therapeutic outpatient endoscopy with the use of sedatives and anesthetics. The patients should fast for at least 1 h after the intervention due to the use of local anesthetics and potential nausea or vomiting. Depending on the duration, dosage, and depth of the sedation used, adequate clinical monitoring of patients after endoscopic interventions must include careful clinical monitoring (observation, repeated measurements of blood pressure and pulse rate, oximetry). When sedatives or anesthetics are administered, the patient must be instructed not to drive a vehicle for 24 h. In addition, the patient must be absent from work and should have no responsibility for major business activities on the day of the operation, and prior consent should be obtained to ensure this. High-risk patients and those in whom difficult EUS-guided interventions are planned should be offered an in-hospital procedure with overnight observation.

Table 30.**2** General complications of endoscopic ultrasound-guided fine-needle aspiration (EUS-FNA)

Complications	Frequency (approx.)
Cervical perforation	0.03%
Other types of perforation	Only in high-grade stenosis (caution required)
Significant bacteremia (solid processes)	< 0.05%
Infections (cystic processes)	Up to 10% (antibiotic prophylaxis required)
Significant extraluminal hemorrhage	1.3%
Mild transient pancreatitis (only in pancreatic fine-needle aspiration)	0.5%
Aspiration	0.2%

* Literature reports all describe bleeding as resolving spontaneously, without the need for therapeutic interventions.

References

1. Wiersema M, Wiersema L. Endosonography-guided celiac plexus neurolysis (EUS-CPN) in patients with pain due to intra-abdominal malignancy (IAM) [abstract]. Gastrointest Endosc 1996;43:A565.
2. Will U, Burmester E, Erk J. Normal anatomy and landmarks. In: Rösch T, Will U, Chang KJ, editors. Longitudinal endosonography: atlas and manual for use in the upper gastrointestinal tract. Berlin: Springer, 2001: 2:22–55.
3. Rösch T, Lightdale CJ, Botet JF, Boyce GA, Sivak MV Jr, Yasuda K, et al. Localization of pancreatic endocrine tumors by endoscopic ultrasonography. N Engl J Med 1992;326: 1721–6.
4. Vilmann P, Hancke S, Henricksen FW, Jacobsen GK. Endoscopic ultrasonography-guided fine-needle aspiration biopsy of lesions in the upper gastrointestinal tract. Gastrointest Endosc 1995;41:230–5.
5. Caletti G, Fusaroli P, Bocus P. Endoscopic ultrasonography. Digestion 1998;59:509–29.
6. Wiersema MJ, Vilmann P, Giovannini M, Chang KJ, Wiersema LM. Endosonography-guided fine-needle aspiration biopsy: diagnostic accuracy and complication assessment. Gastroenterology 1997;112:1087-1095.
7. Giovannini M, Seitz JF, Monges G, Terrier H, Rabbia I. Fine-needle aspiration cytology guided by endoscopic ultrasonography: results in 141 patients. Endoscopy 1995;27: 171–7.
8. Hollerbach S, Klamann A, Topalidis T, Schmiegel W. Endoscopic ultrasonography–guided biopsy (EUS-FNA) aids in the diagnosis of chronic pancreatitis. Endoscopy 2001;33: 824–31.
9. Chang KJ, Nguyen PT, Thompson JA, Kurosaki TT, Casey LR, Leung EC, et al. Phase I clinical trial of allogeneic mixed lymphocyte culture (cytoimplant) delivered by endoscopic ultrasound-guided fine-needle injection in patients with advanced pancreatic carcinoma. Cancer 2000;15:1325–35.
10. Pfau PR, Chak A. Endoscopic ultrasonography. Endoscopy 2002;34:21–8.

31 EUS-Guided Bile Duct Drainage

J. Niehaus, E. Burmester

Introduction

Endoscopic retrograde cholangiography with stenting of the bile duct is an established procedure for palliative treatment of malignant pancreaticobiliary strictures [1,2]. In 5–10% of cases, it is not possible to place a stent with the duodenoscope. This may be due to previous surgical procedures such as gastrectomy with Roux-en-Y loop, Billroth II resection, or Whipple procedures. Other reasons may include complete stenosis of the common bile duct, obstruction of the pylorus or duodenum due to tumor infiltration, and anatomic variants such as upside-down stomach. Percutaneous transhepatic cholangiographic drainage (PTCD) has so far been the alternative method, with a complication rate of up to 15% [3–6] (Table 31.**1**).

Table 31.1 Complications of percutaneous transhepatic cholangiographic drainage

- Biliary peritonitis
- Occlusion
- Cholangitis
- Hemorrhage
- Dislocation
- Hemobilia
- Liver abscess
- Perforation
- Pain
- Pneumoperitoneum

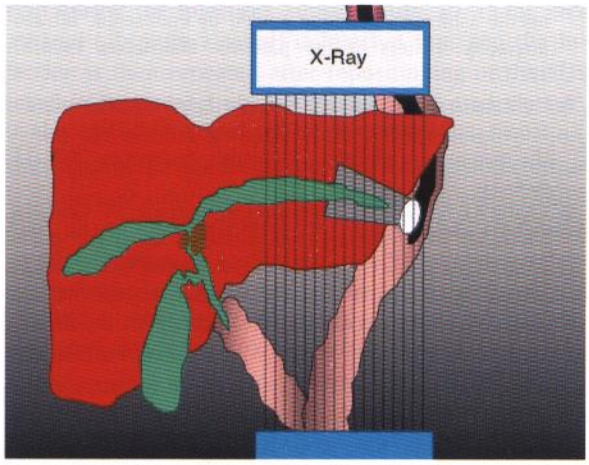


Fig. 31.1 Good visualization of the dilated left hepatic bile duct after gastrectomy with a Roux-en-Y anastomosis.

Since the introduction of metallic stents, the insertion of a PTCD with internal drainage has been possible in up to 90% of the patients [5]. These procedures are not only time-consuming, but may be very painful for the patient in cases in which an internal drain fails and only external drainage is possible. This represents a significant reduction in the quality of life for these patients with malignant diseases.

To date, the most important EUS-guided procedures have been transgastric or transduodenal drainage of pancreatic pseudocysts and celiac plexus neurolysis [7–12]. There have been reports of EUS-guided injection of botulinum toxin or antitumor agents. Wiersema et al. were the first to report on EUS-guided cholangiography [11], and a two-step drainage procedure for the bile duct has also been described.

The dilated intrahepatic bile ducts are well visualized with EUS, even in patients who have undergone partial or complete gastrectomy, particularly if the device is positioned near the left liver lobe. This anatomical correlation makes it possible to carry out EUS-guided drainage of the bile duct for palliative purposes in patients with symptoms of cholestasis who decline PTCD or in those in whom all of the alternative methods have failed due to anatomic variations (Figs. 31.**1**, 31.**2**).

Technique

A modification of the one-step technique described by Seifert [7] for the drainage of pancreatic pseudocysts is used for puncture of the intrahepatic or common bile duct. The puncture can be carried out with a specially prepared device consisting of a 19-gauge fistulotome with a 0.25-inch guide wire, a pusher tube (Mandel Rupp, Erkrath, Germany), and an 8.5-Fr, 5–7 cm plastic stent attached with a 3–0 nylon suture (Fig. 31.**3**).

The dilated intrahepatic bile ducts are visualized with the EUS transducer positioned at the level of the left liver lobe. Color Doppler imaging is used to detect and avoid any interposed vessels. After puncture, contrast medium is injected, and the stent is inserted over the guide wire with fluoroscopic guidance via a transgastric,



Fig. 31.**2** Dilation of the left intrahepatic bile duct.



Fig. 31.**4** A dilated intrahepatic bile duct, with color Doppler mode being used to visualize possible vessels.

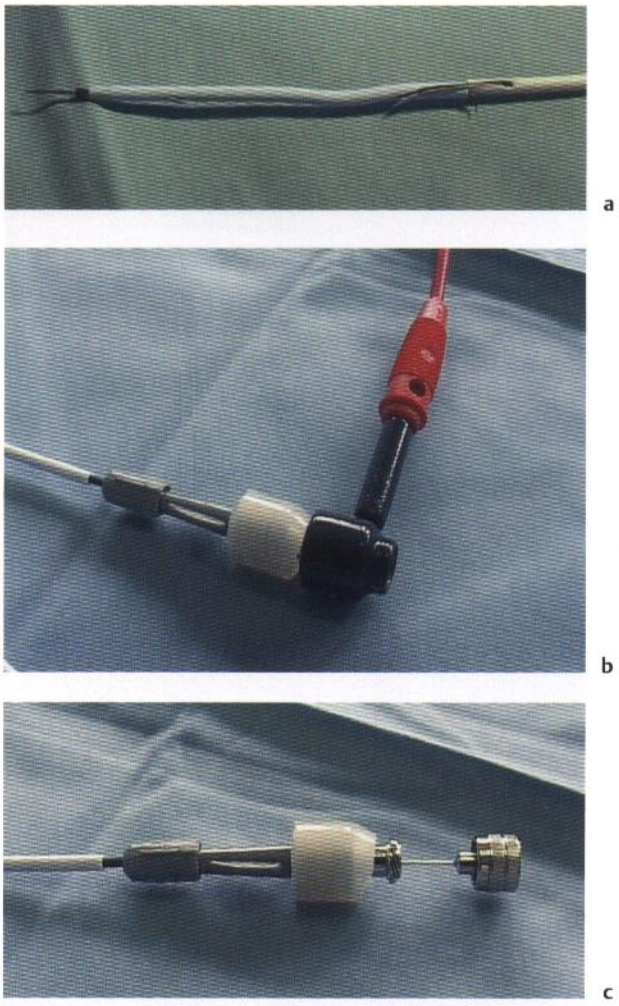


Fig. 31.**3a–c** Device for the puncture of the intrahepatic or common bile ducts.

transduodenal, or transjejunal route into the dilated bile duct (Figs. 31.**4**–31.**11**).

■ Results

Since the first report of this one-step technique, which was carried out successfully on three of four patients with extrahepatic cholestasis due to advanced malignant diseases, no serious complications have been reported with the procedure [13]. In all patients in whom stent insertion was possible, cholestasis resolved and the stents remained patent for relatively long periods of time—up to 9 months. Since 2002, a further four patients have been successfully treated with this technique in our own institution. In two cases, revision of the stent was possible after occlusion.

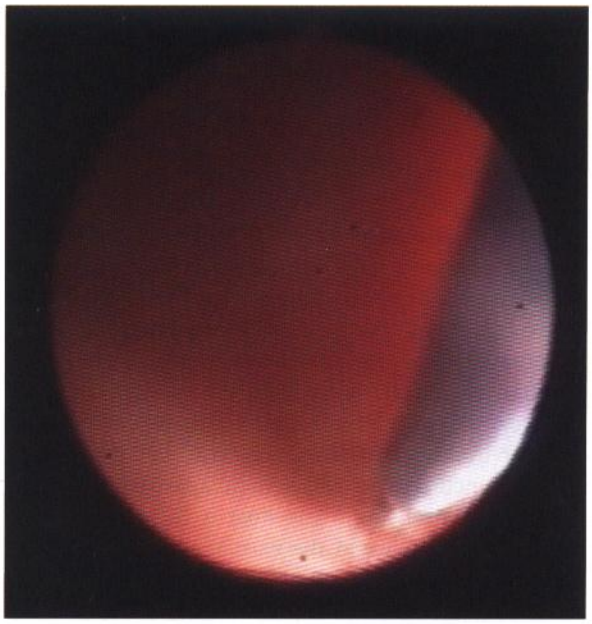


Fig. 31.**5** Endoscopic view of the fistulotome with the loaded stent.

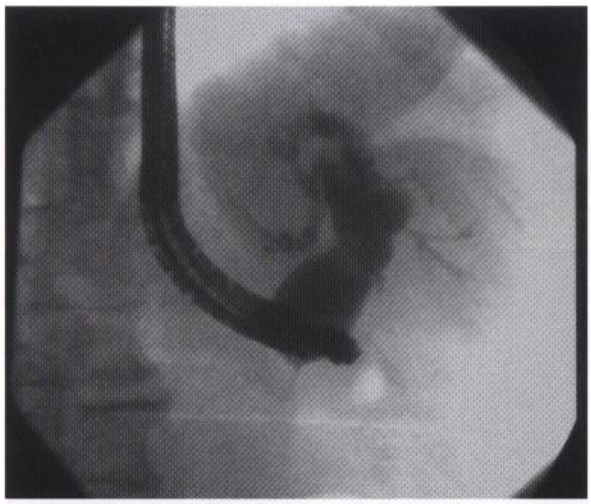


Fig. 31.6 Fluoroscopy, with visualization of the dilated intrahepatic ducts.



Fig. 31.7 EUS-guided insertion of the guide wire into a dilated intrahepatic bile duct.

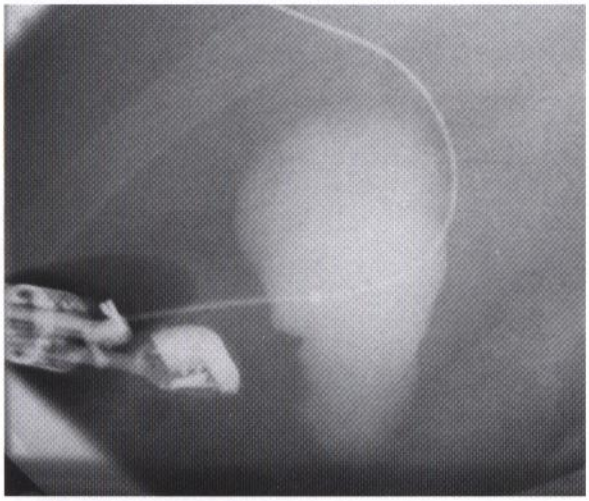


Fig. 31.8 Fluoroscopy with documentation of the correct position of the guide wire.



Fig. 31.9 EUS-guided insertion of the stent into the dilated bile duct by current application on the fistulotome.

Conclusions

Endoscopic ultrasound-guided biliary drainage appears to be a good and safe alternative to PTCD and endoscopic retrograde cholangiopancreatography in the palliative treatment of patients with malignant biliary obstruction, particularly those who have undergone gastrectomy or Billroth II resection. The main advantage is the proximity of the transducer to the dilated extrahepatic or intrahepatic ducts, which allows direct EUS-guided puncture. The transhepatic approach for drainage of the intrahepatic bile duct is technically easier than direct puncture of the extrahepatic duct through the duodenal wall. The one-step technique reduces the risk of guide-wire dislocation, in contrast to the two-step method.

The two main risks of EUS-guided biliary drainage may be hemorrhage and bile leakage into the abdomen, with subsequent biliary peritonitis, especially if stent placement fails. To reduce the risk of bleeding, it is very helpful to use color Doppler imaging to detect vessels. Although EUS-guided biliary drainage is still an experimental technique, it may be very useful in special cases for drainage of a dilated biliary tree caused by malignant stenosis, especially when other methods have failed. A prospective trial including larger numbers of patients is needed to assess the value of EUS-guided biliary drainage in comparison with PTCD.



Fig. 31.**10** Endoscopic view of the correct position of the stent just before the fistulotome is retrieved.

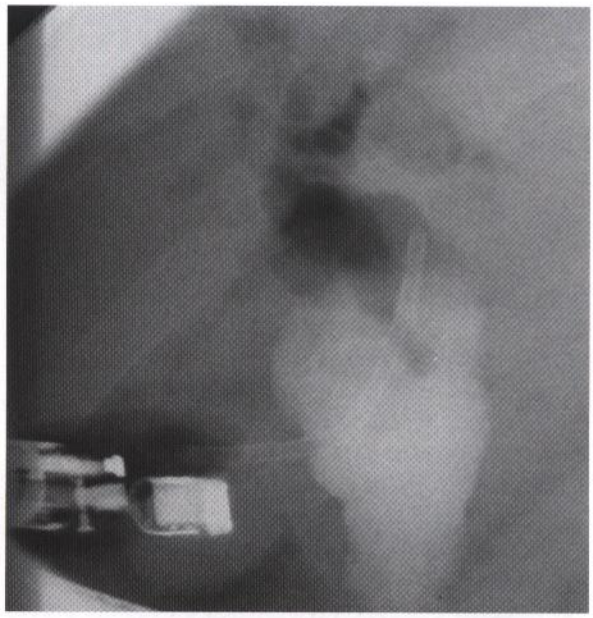


Fig. 31.**11** Radiograph showing aerobilia and correct positioning of the stent.

References

1. Schöfl R. Diagnostic retrograde cholangiopancreatography. Endoscopy 2001;33:147–57.
2. Fogel EL, Sherman S, Devereaux BM, Lehmann GA. Therapeutic biliary endoscopy. Endoscopy 2001;33:31–8.
3. McPherson SJ, Gibson RN, Collier NA, Speer TG, Sherson ND. Percutaneous transjejunal biliary intervention: 10-year experience with access via Roux-en-Y loops. Radiology 1998;209:883–4.
4. Perry LJ, Stokes KR, Lewis WD, Jenkins RL, Clouse ME. Biliary intervention by means of percutaneous puncture of the antecolic jejunal loop. Radiology 1995;195:163–7.
5. Beissert M, Wittenberg G, Sandstede J, Beer M, Tschammler A, Burghardt W, et al. Metallic stents and plastic endoprosthesis in percutaneous treatment of biliary obstruction. Z Gastroenterol 2002;40:503–10.
6. Born P. Arterial bleeding as an unusual late complication of percutaneous transhepatic biliary drainage. Endoscopy 2003;35:978–79.
7. Seifert H. Interventional therapeutic endosonography: current status. In: Rösch T, Will U, Chang KJ, editors. Longitudinal endosonography. Heidelberg: Springer, 2001: 157–63.
8. Wiersema M, Wiersema L. Endosonography guided celiac plexus neurolysis in patients with pain due to intra-abdominal malignancy [abstract]. Gastrointest Endosc 1996;43:424.
9. Hoffmann BJ, Knapple W, Bhutani MS. EUS-guided injection of botulinum toxin for achalasia [abstract].Gastrointest Endosc 1996;43:432.
10. Chang K, Nguyen P, Thompson J. Phase I clinical trial of allogenic mixed lymphocyte culture (cytoimplant) delivered by endoscopic ultrasound guided (EUS)-guided fine needle injection in patients with advanced pancreatic carcinoma [abstract]. Gastrointest Endosc 1998;47:AB 144.
11. Wiersema MJ, Sandusky D, Carr R, Wiersema LM, Erdel WC, Frederick PK. Endosonography-guided cholangiopancreatography. Gastrointest Endosc 1996;43(2 Pt 1):102–6.
12. Giovannini M, Moutardier V, Persenti C, Bories E, Lelong B, Delpero JR. Endoscopic ultrasound-guided bilioduodenal anastomosis: a new technique of for biliary drainage. Endoscopy 2001;33:898–900.
13. Burmester E, Niehaus J, Leineweber T, Huetteroth T. EUS-cholangio-drainage of the bile duct: report of 4 cases. Gastrointest Endosc 2002;57:246–51.

32 Laparoscopic Ultrasound Scanning

P. Vilmann, C. Ortiz-Moyano

Introduction

Intraoperative ultrasound scanning has been in use for more than 40 years, and its value for detecting lesions in the pancreas, liver, and retroperitoneum is well documented. During the past 10–15 years, diagnostic laparoscopy and laparoscopic surgery have replaced many of the open procedures. This has led to an increasing need to find a substitute for the tactile feedback that manual palpation provides during open surgery. Recent technology has provided specially designed ultrasound probes that can pass through standard laparoscopic trocars in order to perform intra-abdominal as well as intrathoracic examinations and ultrasound-guided interventions (Table 32.**1**). Laparoscopic ultrasound scanning (LUS) represents a significant technical improvement in diagnostic laparoscopy and therapeutic laparoscopic interventions. This chapter provides a description of the procedure and the instruments used for LUS, with special focus on a new-generation LUS probe designed for LUS-guided interventions, as well as a review of the literature.

Equipment

The dedicated LUS probes currently available use electronic transducers with a linear or convex array mounted on a rigid or a flexible tip on the instrument. Movement of the flexible tip is controlled by a steering wheel located on the instrument's shaft. Depending on the manufacturer, the tip can be moved in either two or four directions (Table 32.**1**). The frequency is either fixed at 5.0–7.5 MHz or variable, ranging from 4 or 5 MHz to 10 MHz. The new laparoscopic probes have additional features such as power Doppler and color Doppler. This is especially valuable for differentiating between vascular structures and tubular structures in which there is no flow, such as the common bile duct.

Only one manufacturer (B-K Medical, Herlev, Denmark) offers an ultrasound unit that can be fully integrated into the laparoscopic rack. A remote control that operates the different ultrasonic functions is also available from the company. It is of course important for the operator to be able control the ultrasound features personally instead of having a second person manipulating the ultrasound console. The laparoscopic image and the

Table 32.**1** Laparoscopic ultrasound probes

Manufacturer	Frequency range (MHz)	Shaft diameter (mm)	Color Doppler	Flexible tip	Biopsy facility
ATL	5.0–9.0		Yes	Yes (4-way)	No
Aloka (SSD 1700)	4.0–10.0		Yes	Yes (2-way)	No
Aloka (UST 5222L-7.5)	7.5	10	No	No	No
B-K Medical (8666)	5.0–10	Fits into a 12-mm port	Yes	Yes (4-way)	Yes
Esaote Biomedica (LP13, AU4)	7.5–10.0	Fits into a 10-mm port	Yes	Yes (4-way)	No
Hitachi	5.0–7.5		Yes	Yes (4-way)	No
Hitachi (EUP-OL531)	5–10	11.8	Yes	Yes (4-way)	Yes
Siemens (LAP8-4)	4.0–8.0	10	Yes	Yes (4-way)	No
Toshiba	7.0		Yes	Yes (4-way)	No
Toshiba (PVM-787LA)	5–9	14.8	Yes	No	Yes
Olympus (MH-300)	7.5	?	?	Yes	No

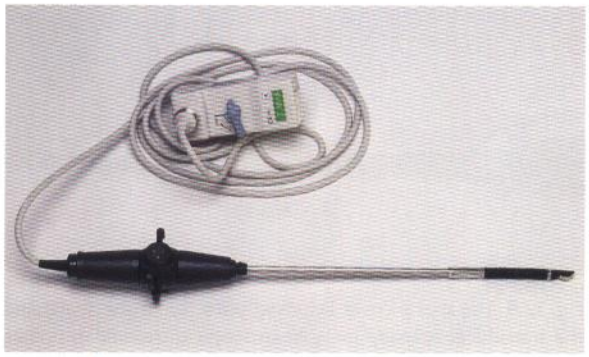


Fig. 32.**1** The laparoscopic ultrasound probe without its biopsy covering (Hitachi OL-531).



Fig. 32.**2** The transducer is electronic, with a scanning angle of 60° and a lateral and slightly oblique forward view.



a



b

Fig. 32.**3a, b** Mounted at the flexible tip of the instrument, the transducer can be moved 90° degrees up or down and left or right.

ultrasound image should preferably be superimposed (picture-in-picture). This option is important, because the movement of the transducer has to be coordinated with the real-time ultrasound image.

Adequate sterilization has been one of the limitations of laparoscopic LUS. The transducers do not tolerate heating to more than 50–55 °C. Until recently, cleaning has therefore either been carried out using disinfection with glutaraldehyde or similar detergents, or alternatively, gas sterilization. Others have used sterile plastic coverings. However, none of these methods has been perfect. Recently, materials have been developed for the probes that allow Sterrad or Sterris sterilization (Advanced Sterilization Products, Irvine, California, USA) without damaging the transducers.

The diameter of the probes is up to 1 cm, so that they can be introduced into the abdominal cavity through a standard trocar with a diameter of either 10 mm or 12 mm. There are at present only three manufacturers that provide biopsy facilities with the laparoscopic probe. The B-K probe was the first on the market. The biopsy channel is not fully integrated into the shaft of the probe. A flexible channel passes outside parallel to the probe, ending in a hole near the transducer [1,2]. This means that a needle has to pass a flexible sheath that is not supported by the probe and that the tip of the needle has to be directed into an inlet near the transducer when a biopsy is needed. This maneuver is somewhat cumbersome, and this may be the reason why this procedure has not come into widespread use. The second company offering biopsy facilities with their probe is Toshiba (PVM-787LA). However, this probe is stiff, with a forward-viewing transducer and a diameter of 24 mm [3]. The probe is primarily produced for radiofrequency ablation (RF) of liver lesions. Only one company has the biopsy channel fully integrated into a probe (Hitachi OL-531), with the probe being introduced via a standard trocar (Fig. 32.**1**).

This probe was recently developed by the present author (P.V.) and the Hitachi company in collaboration. It has a diameter of 11.8 mm and fits into a 12-mm port. The total length of the instrument is 67 cm and the length of the insertion tube is 42 cm. The transducer is electronic, with a scanning angle of 60° and a lateral and slightly oblique forward view (Fig. 32.**2**).

The curve radius is 10 mm. The central frequency is 7.5 MHz, with a bandwidth of 5–10 MHz. The transducer mounted at the flexible tip of the instrument can be moved 90° up or down and left or right (Fig. 32.**3**). A removable metal needle cover case around the body of the probe shaft forms a biopsy channel with a diameter of 3.2 mm (Figs. 32.**4**, 32.**5**). The biopsy channel can be reduced to 2.4 mm with a mountable inner plastic tube (Figs. 32.**6**, 32.**7**), allowing use of a modified 22-guage or 19-gauge aspiration biopsy needle (SonoTip II, MediGlobe Ltd., Achenmühle, Germany) (Fig. 32.**8**). When it



Fig. 32.**4** A removable metal needle cover case around the body of the probe shaft forms a biopsy channel with a diameter of 3.2 mm. The image shows a proximal and oblique image of the metal cover, with a view into the biopsy channel inlet.

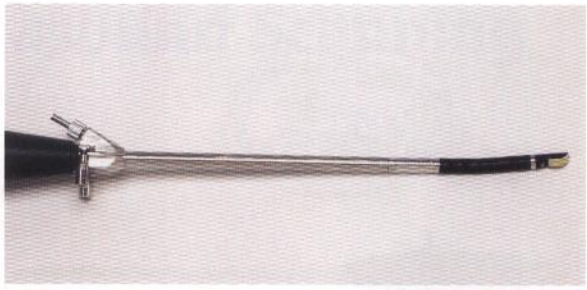


Fig. 32.**5** The metal cover is locked onto the probe shaft, and the transducer is ready for a laparoscopic ultrasonic examination with biopsy of a lesion.

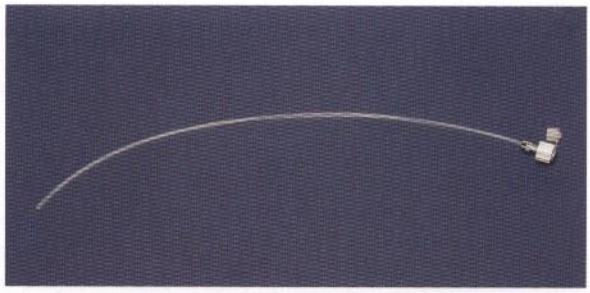


Fig. 32.**6** The biopsy channel can be reduced to 2.4 mm with an inner plastic tube.

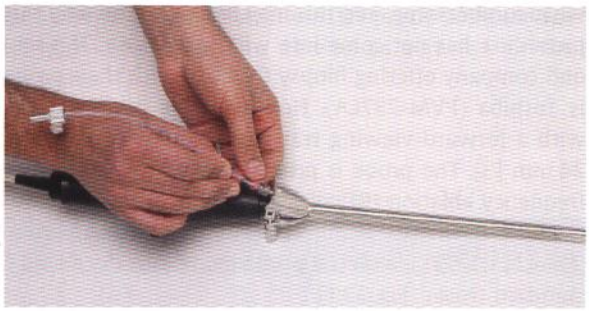


Fig. 32.**7** The inner plastic tube being introduced via the inlet on the metal cover.

is not reduced, the biopsy channel allows the introduction of a standard-sized radiofrequency needle. The probe can be connected to a Hitachi ultrasound scanner (EUB-6500 or EUB-8500) with power and color Doppler facilities. The probe can be fully sterilized with Sterrad (H2O2 plasma) and ETO gas sterilization.

Laparoscopic ultrasound–guided biopsy has hitherto been a difficult and cumbersome procedure using the probes available on the market. The biopsy procedure with the new probe can be carried out without difficulty during routine laparoscopic scanning. The probe also allows radiofrequency ablation of hepatic lesions during laparoscopic ultrasound scanning. A needle is at present under construction (the HiTT-Flex monopolar radiofrequency needle, compatible with the Elektrotom HiTT 106 ablation system; Berchtold Ltd., Tuttlingen, Germany) (Fig. 32.**9**). The construction of the new laparoscopic probe for guided interventions is a fresh advance toward minimally invasive procedures for primary diagnosis, staging, and treatment guided by laparoscopic ultrasound scanning.

■ Examination Procedure

The procedure is carried out with the patient under general anesthesia. Several examination procedures have been described. The presetting of the image direction is, as usual, with distal to the right and proximal to the left in the ultrasound image. This provides images very similar to the endoscopic ultrasound (EUS) images obtained with linear transducers. The access site for the laparoscope and probe is selected depending on the indications for the examination. Most frequently, a supraumbilical or infraumbilical access site is chosen for the laparoscope itself. Some authors favor access via the right upper abdominal quadrant for the second port when the liver and hepatobiliary region have to be examined. Others use a port in the left upper quadrant. The aim is to obtain good access and to examine the region or organ in question in two directions. This can be accomplished by switching ports between the laparo-

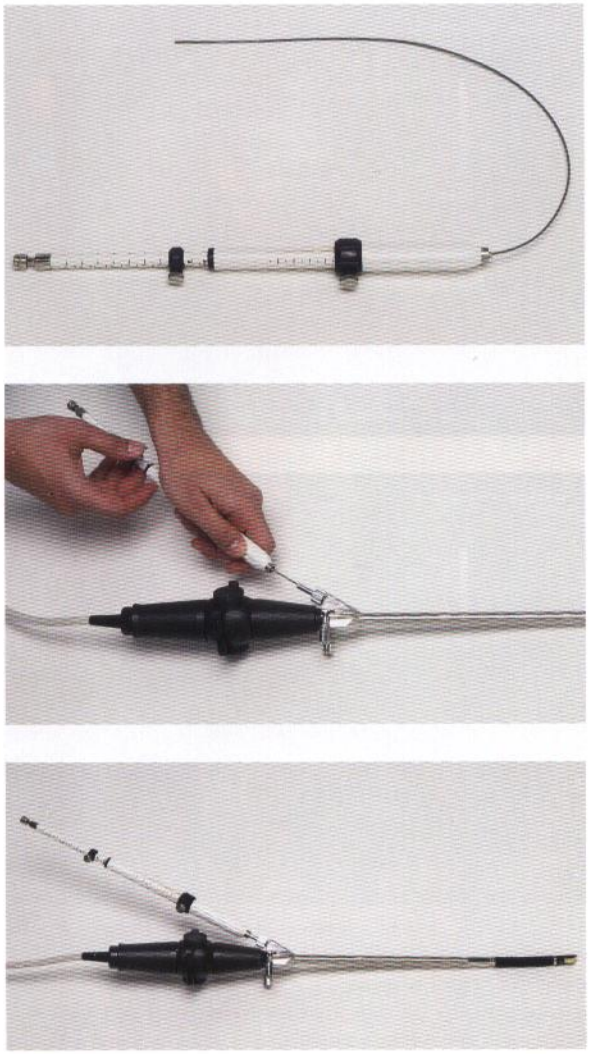


Fig. 32.**8a** A prototype modified 22-gauge aspiration biopsy needle (SonoTip II, Medi-Globe Ltd., Achenmühle, Germany). **b** The needle is introduced via the biopsy inlet of the laparoscopic probe. **c** The needle is now mounted on the laparoscopic probe, ready for a biopsy to be taken.

scope and the probe. For the staging of upper gastrointestinal cancer, the present authors prefer the left upper quadrant and the supraumbilical port (Fig. 32.**10**).

This provides good access to the left liver lobe, the region of the cardia, the hepatoduodenal ligament in a longitudinal scanning direction, and the pancreas in horizontal section. The aorta and the celiac vessels can be seen from the umbilical port, and the right liver lobe can be examined as well. LUS has to be carried out in a systematic way, including all segments of the liver, the hepatoduodenal ligament, and the celiac trunk and superior mesenteric artery. The intra-abdominal examination follows the same principles as transcutaneous ultrasonography.

The images obtained during LUS are frequently excellent, with optimum scanning conditions, due to

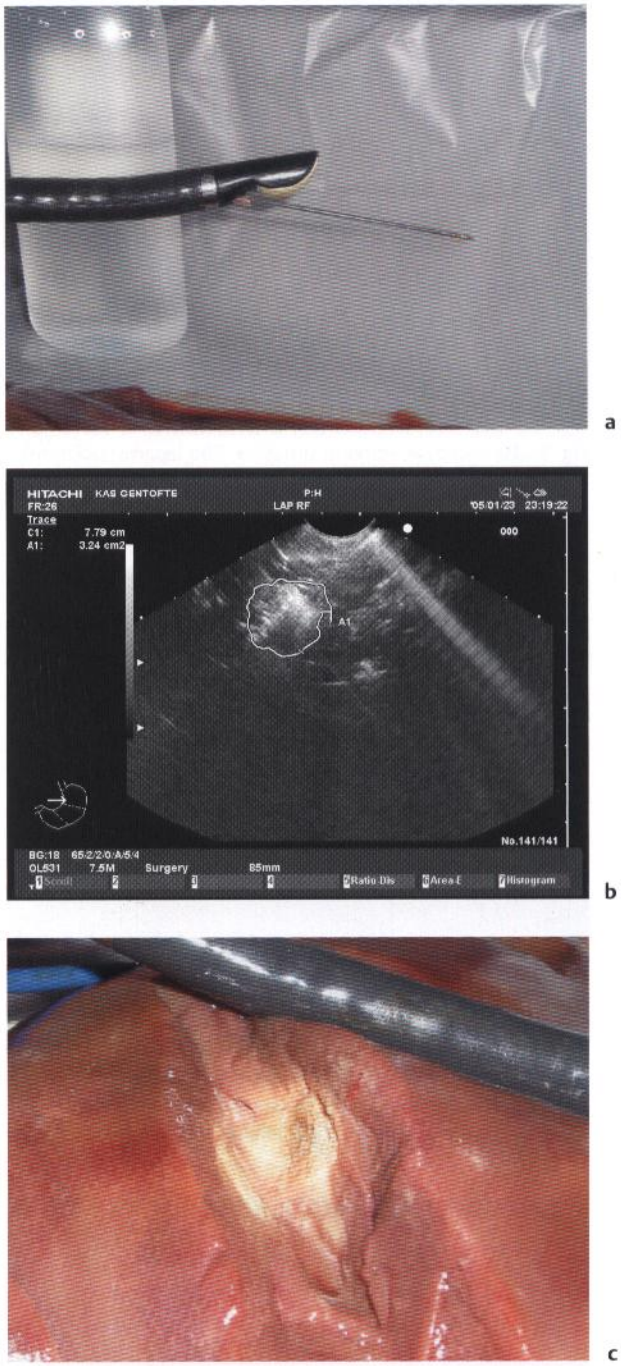


Fig. 32.**9** The probe also allows radiofrequency ablation of hepatic lesions during laparoscopic ultrasound scanning. **a** The radiofrequency needle (HiTT-Flex) has been introduced. **b** The image shows the burning effect visible during radiofrequency ablation of the liver in a swine model. **c** The necrosis seen after laparoscopic ultrasound-guided radiofrequency ablation in the liver.



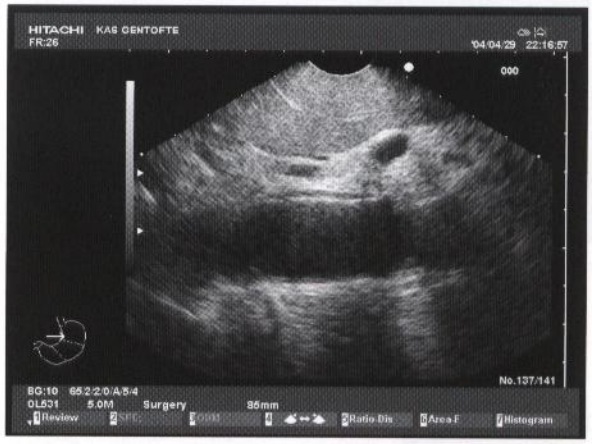
Fig. 32.**10** A typical working situation. The laparoscopic probe and the laparoscope have been introduced via two ports. The ultrasound scanner and the laparoscopic rack are seen, and the images are visible simultaneously.



Fig. 32.**12** A hepatic metastasis approximately 10 mm in size in the right liver lobe.



a



b

Fig. 32.**11** The images obtained during laparoscopic ultrasonography are frequently excellent, with optimum scanning conditions due to close proximity to the intra-abdominal organs. **a** A laparoscopic ultrasound image of the aorta with the celiac trunk, seen with color Doppler. **b** A view of the aorta with the celiac trunk and the left gastric artery just below part of the left liver lobe.

the close proximity to the intra-abdominal organs (Fig. 32.**11**).

Generally, the contact technique is used to scan solid organs such as the liver. In the upper abdomen, the liver is usually also used as an acoustic window for more deeply located structures. Better image quality is sometimes obtained with indirect scanning through a saline solution. This method improves discrimination of individual wall layers and offers higher resolution in the transducer's focal zone. When the liver is scanned, the transducer is placed directly on the left or right liver lobe. The liver is scanned systematically by moving the probe over all segments while simultaneously following it optically with the laparoscope, manipulated by an assistant (Fig. 32.**12**).

The caudal parts of the liver should be examined from both the anterior and posterior surface. This is important, as small lesions just under the liver capsule can easily be missed due to their close proximity to the transducer. The location, number, and size of hepatic lesions must be documented. Relevant anatomic structures such as the portal and hepatic veins and bile ducts can be visualized. The segmental anatomy of the liver can be delineated and the relation of the tumor to these structures allows assessment of the extent of resection and the amount and function of the remaining liver tissue. The structures of the porta hepatis can be best assessed (in longitudinal section) when the probe is introduced through the left subcostal trocar and placed on segment IV of the liver. The distal part of the common bile duct is identified by positioning the transducer directly on the hepatoduodenal ligament. The stomach can be visualized by direct-contact scanning, or using the liver as an acoustic window. Acoustic shadowing of the posterior wall of the stomach and the pancreas can be avoided by aspi-

ration of air and if necessary instillation of 300–500 mL saline solution through a nasogastric tube into the stomach. The branches of the celiac axis, portal vein, superior mesenteric artery, and aorta are displayed in transverse sections from the left subcostal trocar. Lymph nodes along these vessels are classified in accordance with the TNM classification (Fig. 32.**13**).

Metastatic lymph-node involvement is characterized by a hypoechoic pattern, round shape, and well-delineated boundaries. Color Doppler examinations can be helpful in delineating the vascular anatomy and distinguishing vessels from lymph nodes (Fig. 32.**14**).

Biopsy of lymph nodes is always relevant if a biopsy confirming malignancy will alter the management of the patient.

■ Biopsy Procedure

Until recently, LUS-guided biopsy was if not impossible, then at least cumbersome. The needle had to be introduced through the anterior abdominal wall, and free-hand guidance by the transducer had to be used [4–6]. Alternatively, as with the B-K probe, the needle has to pass through an exterior floppy biopsy sheath before the biopsy maneuver is started [2,7]. With the new LUS probe from Hitachi, the procedure has become simple and easy. After a lesion is outlined, the needle is simply introduced via the biopsy inlet of the probe and firmly connected to the Luer-lock biopsy inlet (Fig. 32.**8b**, **c**). The stylet is withdrawn a few millimeters. The needle can then be advanced under ultrasound guidance directly into the lesion (Fig. 32.**15a**). The stylet is removed completely, and a vacuum is applied to the needle. To-

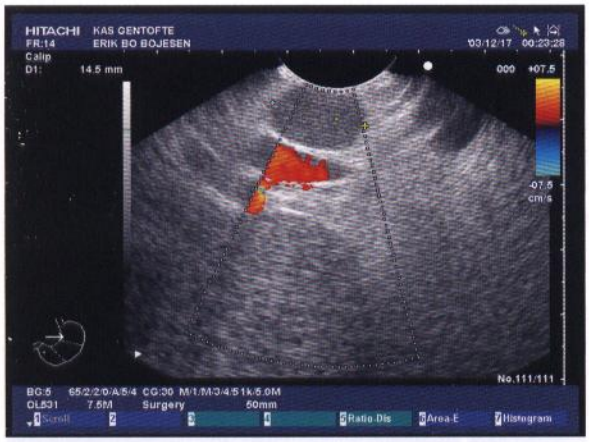


Fig. 32.**13** A 14.5-mm hypoechoic lymph node in the retroperitoneum in a patient with gastric cancer.

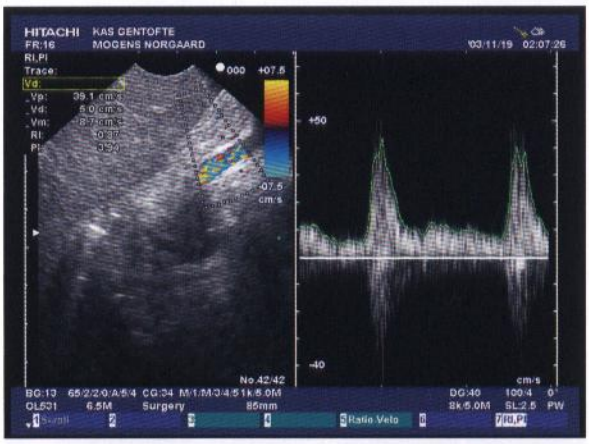
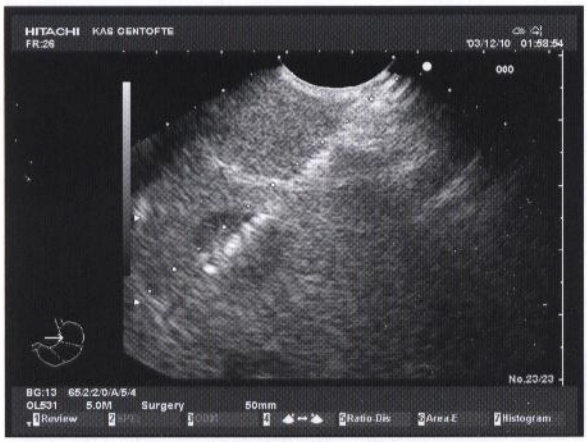
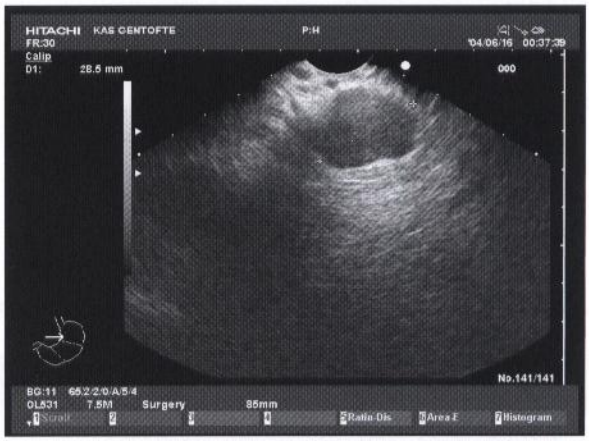


Fig. 32.**14** Color Doppler examination is extremely valuable. The image shows a duplex scan of an abdominal vessel with color Doppler, pulsed Doppler, and B-mode scanning.



a



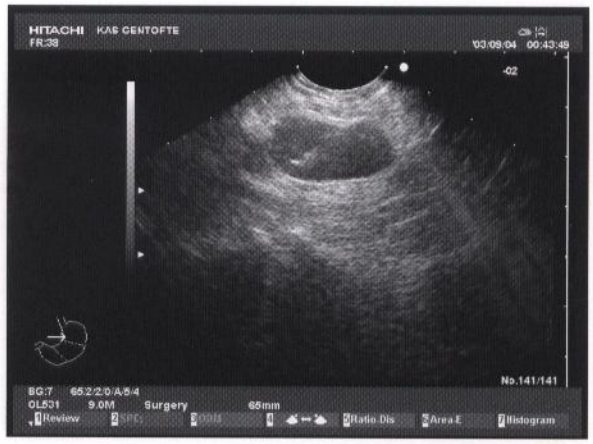
b

Fig. 32.**15** The biopsy needle is introduced and a guided biopsy of a hepatic metastasis is taken. **a** Note the deflections from the needle just below the needle guide line. **b** A suspicious hypoechoic lesion in the left adrenal gland in a patient with gastric cancer. The laparoscopic ultrasound (LUS)-guided biopsy revealed malignant cells, and the patient was ultimately staged as having incurable disease (M1).

Fig. 32.**15c–e** ▷



c



d

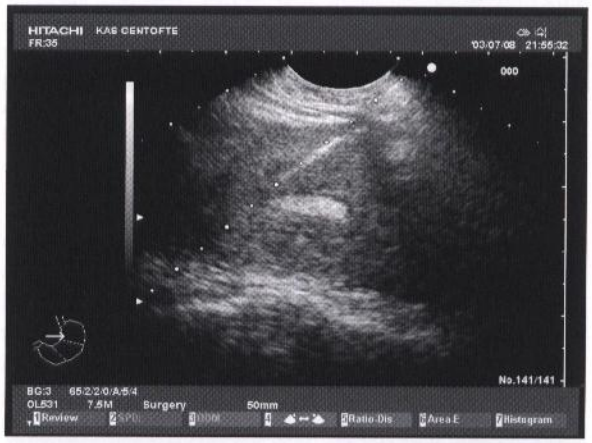


e

Fig. 32.**15c** LUS-guided biopsy of a hypoechoic hepatic metastasis 7 mm in size. **d** LUS-guided biopsy of an enlarged suspicious lymph node in the retroperitoneum in a patient with cancer of the gastric cardia. **e** A cystic neoplasm in the tail of the pancreas. The biopsy confirmed malignancy. The multiple cysts inside the solid tumor are notable.



a



b

Fig. 32.**16** A laparoscopic ultrasound (LUS) image in a patient with retroperitoneal fibrosis. **a** There is a hypoechoic, thickened rim of fibrosis compressing the aorta, seen in color Doppler mode. **b** An LUS-guided histological needle biopsy was carried out, demonstrating fibrosis.

and-fro movements are carried out, still with ultrasound guidance (Fig. 32.**15b–e**).

The entire biopsy instrument is then removed, and the material is expelled onto glass slides and smeared for cytological evaluation. At present, only needles for fine-needle biopsy have been developed for this probe, but a Tru-Cut histological needle is commercially available for the B-K probe. It is only a matter of time before a histological needle becomes available for the Hitachi probe as well. In a single case in which fine-needle biopsy was not sufficient, the authors have used the Tru-Cut needle designed for the B-K probe together with the OL-531 probe (Fig. 32.**16**). However, it should be emphasized that for safety reasons this is not at

present recommended before a dedicated histological needle has been manufactured (the main risk being transducer damage).

Review of the Literature

Staging of Gastrointestinal Cancers

Patients with upper gastrointestinal cancer frequently present at an advanced stage of the disease in which curative treatment is not possible. The prognosis in gastrointestinal cancer is poor, but it is closely related to the TNM stage of the tumor. It is therefore mandatory to evaluate the preoperative stage carefully to avoid unnecessary and futile surgery in patients with disseminated disease, and to select patients with locally advanced disease who may benefit from neoadjuvant chemoradiotherapy before surgical resection.

Endoscopic ultrasound scanning has proved to be significantly more accurate for assessing the TN staging preoperatively in comparison with transabdominal ultrasonography, computed tomography (CT) and magnetic resonance imaging (MRI). However, the method has some limitations. EUS is not capable of detecting metastases in the right liver lobe, superficial liver metastases, or peritoneal carcinosis. In addition, if impassable stenotic tumors are present in the esophagus or stomach, the staging evaluation is insufficient.

Laparoscopy in combination with LUS has been shown to allow excellent staging and resectability evaluation of gastrointestinal cancers in comparison with other imaging modalities such as CT, transabdominal ultrasound, and MRI. This superiority has been thoroughly documented, and if LUS is combined with EUS, the rate of futile operations such as unnecessary exploratory laparotomy can be reduced from 30–40% down to less than 5% [8–11].

There appears to be some variance in the clinical impact of LUS staging depending on the cancer evaluated [12]. According to van Dijkum et al. [12], in a study including more than 400 patients, laparoscopic staging avoided laparotomy in 20% of the patients: 5% of those with an esophageal tumor, 20% of those with a gastroesophageal junction tumor, 15% of those with a periampullary tumor, 40% of those with a proximal bile duct tumor, 35% of those with a liver tumor, and 40% of those with a pancreatic body or tail tumor.

LUS in Esophagogastric Cancer

The presence of liver metastases, malignant ascites, or peritoneal carcinosis and specific cases of invasion of adjacent organs (stage T4) in patients with esophageal and gastric cancer are in most centers regarded as a contraindication for major surgical resections. Laparoscopy with laparoscopic ultrasound scanning has been shown to add significant staging information to the preoperative evaluation of patients with cancer of the stomach and gastric cardia, whereas the added value in patients with cancer of the middle and upper esophagus is more limited [13–16]. The reported accuracy of LUS in the evaluation of resectability is in the range of 50–100% [9–11]. The impact on therapy is such that laparotomies can be avoided in 25–63% of patients examined with LUS [9,12–17]. In many of the publications, LUS-guided biopsy was not possible [15].

In a large study by Stein et al. [13], laparoscopy and LUS yielded a 24% rate of relevant new findings not seen with standard preoperative staging modalities in patients with cancer of the esophagus or cardia. Laparoscopy including LUS is at present considered mandatory in the preoperative staging evaluation of patients with locally advanced carcinoma of the distal esophagus or gastroesophageal junction who are being considered for neoadjuvant therapy or primary resection (Table 32.**2**) [13–15,18].

LUS in Pancreatic Cancer

Carcinoma of the pancreas is associated with a dismal prognosis, with an overall 5-year survival rate of about 5%. At the time of diagnosis, pancreatic cancer is a disseminated disease in the majority of cases. Pancreatic cancer either spreads by invading adjacent structures and organs, or sends metastases to the lymph nodes, peritoneum, liver, or lungs. The only chance of cure is surgery. Exact staging prior to treatment decisions is therefore paramount in order to avoid futile laparotomies in incurable patients. A variety of image modalities are at present available in the evaluation of pancreatic cancer. However, none of these are sufficiently accurate

Table 32.**2** Laparoscopy and laparoscopic ultrasonography in the staging of regional and distant metastases in esophageal, gastric, and cardia carcinoma

First author (ref.)	Lesion	Location	Patients (n)	Sensitivity (%)	Specificity (%)	Accuracy (%)
Stein 1997 [13]	Esophagus and cardia	Celiac axis	127	67	92	
Romijn 1998 [15]	Esophagus and cardia	Distant metastases	60	81	100	
Hulscher 2000 [14]	Gastric cardia	Distant metastases	48	79		
Lavonius 2002 [18]	Gastric tumors	Distant metastases	37	63	100	83

Table 32.3 Studies combining laparoscopy and laparoscopic ultrasonography to assess unresectability in pancreatic and ampullary tumors

First author (ref.)	Patients (n)	Sensitivity (%)	Specificity (%)	PPV (%)	NPV (%)	Accuracy (%)
Durup Scheel-Hincke 1999 [9]	35	86	100	100	80	
Minnard 1998 [25]	90	98	100	100	98	
Merchant and Conlon 1998 [29]	90	91		100	98	
Catheline 1999 [24]	26	94				80.7
Pietrabissa 1999 [27] *	50	94	80			87
Jimenez 2000 [30]	125	97				
Schachter 2000 [20]	67	100	88	89	100	
Menack 2001 [22]	27	77	100	100	90	
Taylor 2001 [26]	51	67	100	100	91	92

* Vascular invasion. NPV: negative predictive value; PPV: positive predictive value.

as single methods. To date, dynamic contrast-enhanced CT has been the preoperative imaging modality of choice. However, when CT is used in the evaluation of resectability, about half of the patients undergo exploratory surgery because disseminated disease is detected, preventing radical resection. The sensitivity and positive predictive value of CT in defining resectability are only 75% and 38%, respectively [19]. Improvements in assessing resectability are seen when laparoscopy is used, and 24–40% of patients deemed to have resectable disease at CT have been demonstrated to have incurable disease at laparoscopy. Endoscopic ultrasound scanning appears to be comparable to multiple-slice CT in the evaluation of vascular infiltration, but may be preferable due to the biopsy facilities available if disseminated disease is outlined, either in the form of suspicious lymph nodes or small liver metastases. LUS has been shown to improve pancreatic carcinoma staging over laparoscopy alone, providing additional surgical information in 14–25% of cases [20–28]. In a study by Taylor et al. [26] including 51 patients, LUS prevented unnecessary extensive surgery in 53% of patients deemed resectable by CT. Another study in 214 patients [12] showed that LUS resulted in a change in the decision regarding surgical intervention in 40% of the patients.

LUS has also been shown to be valuable for the detection of insulinomas, with subsequent laparoscopic resection or enucleation [28].

There is no doubt that LUS represents an advance in the evaluation of pancreatic lesions (Table 32.3) [9, 20, 22, 24–30].

LUS in Colonic Cancer

Laparoscopic colectomy has developed rapidly as a minimally invasive method in colonic surgery, reducing the stress response usually seen after an open surgical procedure. However, one of the limitations of laparoscopy is the inability to palpate organs and tissue with this modality. LUS has been described as the only real alternative to manual exploration [31–34]. Despite full preoperative staging with transabdominal ultrasound and CT, intraoperative ultrasonography has been shown to find additional liver metastases in 10–30% of patients with cancer of the colon. Theoretically, LUS should therefore be able to add valuable staging information in patients scheduled for laparoscopic colonic resection. Several studies have focused on LUS in the detection of liver metastases in patients with colonic cancer, but only one study has evaluated the role of LUS in the complete TNM staging of colorectal cancer [31]. In the study by Goletti et al. [31], the therapeutic program was changed thanks to laparoscopy and LUS in 33% of cases. The added value of LUS was 12%. The accuracy of T staging was 97%. LUS had a sensitivity in the detection of hepatic metastases of 100%, compared with 63% and 75% with preoperative radiographic methods and laparoscopy, respectively. Nodal metastases were diagnosed with a sensitivity of 94%, compared with 18% in preoperative staging and 6% with laparoscopy, but the method had a low specificity of 53% and an overall accuracy of 72%—comparable with the evaluation of lymph-node metastases with EUS imaging in most other gastrointestinal cancers. However, no LUS-guided biopsies were taken, and this might potentially change the low specificity obtained with imaging alone, as when EUS-guided fine-needle aspiration is used in upper gastrointestinal cancers.

LUS in Gallstone Disease

Intraoperative cholangiography (IOC) has traditionally been used for the detection of choledocholithiasis during open and laparoscopic cholecystectomy. An additional benefit of IOC is the definition of the biliary anatomy, allowing the detection of anomalies and possible protection against bile duct injury during surgery. However, there are some limitations with the method, and in a number of cases IOC cannot be carried out either due

to contraindications (e. g., pregnancy) or difficult cannulations [24]. A number of studies have been published describing the value of LUS in the detection of stones in the common bile duct (Table 32.**4**) [35–45]. The sensitivity of the method for detecting common bile duct (CBD) stones lies in the range of 80–96% (Table 32.**4**). According to the studies, LUS is comparable with IOC and as such may replace or at least be able to serve as an adjunct to IOC in the evaluation of the biliary tree during laparoscopic cholecystectomy.

In a large prospective study including 900 patients [42], the combination of IOC and LUS was found to have a sensitivity of 95% and a specificity of 98%. In another prospective, single-blinded study [41] including 135 patients, the bile ducts were satisfactorily identified using LUS and IOC in 131 and 121 cases, respectively. The sensitivity of LUS for detecting CBD stones was 96%, in comparison with 86% with IOC, while the specificity values were 100% and 99%, respectively. In a randomized comparative study in 518 patients, the overall accuracy of LUS for identifying unsuspected CBD stones was 99.2%, in comparison with 98.9% with IOC [35]. The conclusion of these studies is that LUS is equal to or superior to IOC for detecting CBD stones during laparoscopic cholecystectomy. An additional benefit of LUS is that the time required for the procedure is approximately half of that needed for IOC [35,37].

LUS in Liver Disease

The use of LUS to examine the liver has become an important part of surgical oncology, especially for the screening of metastatic lesions (Fig. 32.**17**). In patients in whom there is already a known liver malignancy, whether primary or metastatic, however, LUS has also been effective in detecting previously unrecognized additional malignant foci within the hepatic parenchyma (Fig. 32.**18**). In patients scheduled for liver resection, LUS can detect possible unresectability or incurability and thereby avoid futile laparotomies (Table 32.**5**) [32, 33, 46–57]. In addition to this, LUS is used to guide the surgical procedure. Limited hepatic resections can be carried out laparoscopically, and LUS can be helpful in locating the lesion and confirming resectability, as well as during the resection. In recent years, the indications for the resection of hepatic metastases have changed toward a more aggressive approach, with local or segmental resection for multiple lesions even in patients with bilobar disease. A better understanding of liver anatomy and familiarity with intraoperative ultrasonography has led to a practical, segment-oriented approach to hepatic resections [52]. The use of local ablation techniques such as radiofrequency ablation and microwave ablation may further extend the options for curative surgical treatment.

Table 32.**4** Diagnostic values for laparoscopic ultrasonography in the detection of bile duct calculi during laparoscopic cholecystectomy

First author (ref.)	Patients (n)	Sensitivity (%)	Specificity (%)	PPV (%)	NPV (%)
Birth 1998 [35]	518	83.3	100	100	99.2
Thompson 1998 [36]	360	90	100	100	98.4
Machi 1999 [37]	100	88.9	100	100	98.9
Kimura 1999 [38]	184	82.4	100		
Siperstein 1999 [39]	300	96.2	100	100	99.6
Tranter 2001 [40]	367	92	100	100	98
Tranter 2002 [41]	135	96	100	100	98
Catheline 2002 [42]	900	80	99	89	99

NPV: negative predictive value; PPV: positive predictive value.

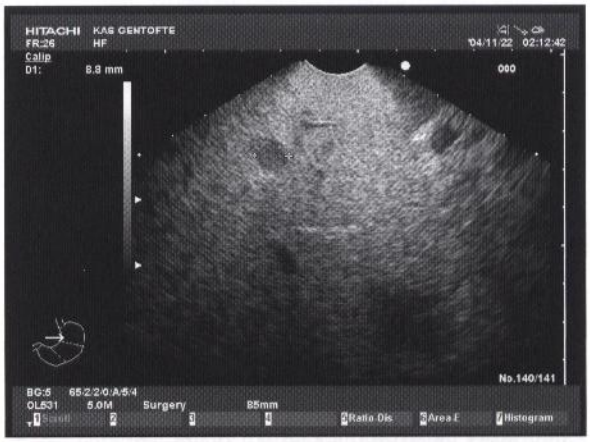


Fig. 32.**17** A small hepatic metastasis detected during a staging procedure. The lesion had not been seen with conventional image modalities before the LUS examination. The LUS-guided biopsy revealed malignant cells.



Fig. 32.**18** Color Doppler examination of a 6 cm malignant tumor in the right lobe of the liver.

Table 32.5 Diagnostic values for laparoscopic ultrasonography in assessing the resectability of primary liver tumors and metastases

First author (ref.)	Lesions	Patients (n)	Sensitivity (%)	Specificity (%)	Accuracy (%)
Callery 1997 [46]	HBP malignancies	50	96	92	
Barbot 1997 [47]	Liver tumors	23	100	40	
Rahusen 1999 [33]	Colorectal cancer and lesions in the liver	50	89		
Jarnagin 2000 [48]	HBP malignancies	186	97		
Lo 2000 [49]	HCC	184	59.6	100	89.4
Milsom 2000 [32]	Colorectal cancer and lesions in the liver	77	95		

HBP: hepatobiliary and pancreatic; HCC: hepatocellular carcinoma.

In a study by de Castro et al. [52] including 84 patients with 33 primary liver tumors and 51 secondary liver tumors, resectability was correctly predicted with LUS in 72% of the patients. LUS found additional lesions not seen on preoperative CT in 36% of the patients with primary liver malignancies. Additional lesions were found with LUS in 25% of patients with secondary liver malignancies.

In a study by Montorsi et al. [58] including 68 patients with primary liver cancer, additional information was found in 57%, including new hepatocellular cancer nodules in different hepatic segments and an adrenal metastasis in 22% of the cases. In another study by Foroutani et al. [51], LUS detected all 201 tumors seen on preoperative CT and detected 21 additional lesions in 11 patients. It appears from this study that small lesions in particular are liable to be overlooked with CT. In a study by Lo et al. [49], the addition of LUS avoided exploratory laparotomies in 31 of 52 patients (62%) with unresectable disease that had not been detected in preoperative studies.

LUS has also been reported to be helpful in the detection and subsequent management of hepatic cysts with laparoscopic deroofing [57].

Miscellaneous Applications of LUS

LUS has also been used in gynecological, urological, laparoscopic, and thoracoscopic procedures [59–61]. Laparoscopic surgery is increasingly being used in the management of patients with gynecologic malignancies [59,60]. LUS can be used either to detect ovarian tumors during laparoscopy, to assist with the surgical resection, or to localize pelvic and para-aortic lymph nodes in patients with cervical carcinomas. In a study by Cheung et al. [60], the sensitivity and specificity of LUS in detecting pelvic lymph-node metastases were 91% and 100%, respectively. The authors concluded that the LUS procedure was simple, easy to learn, and highly sensitive.

In urology, LUS appears to be a promising adjunct to four current procedures: difficult pelvic lymphocele marsupialization, renal cyst decortications, nephrolithotomy and other forms of renal stone surgery, and cryotherapy or radiofrequency therapy of renal masses [61].

The role of ultrasound scanning during video-assisted thoracic surgery has been evaluated in a study by Coppola et al. [62]. Thoracoscopic ultrasonography was carried out with an LUS probe in 35 patients in order to localize pulmonary nodules suspected of malignancy. In 37 of 40 lesions (sensitivity 93%), ultrasonography was able to locate lesions preoperatively detected by CT. In addition, ultrasonography also located two nodules not visualized with helical CT. Eighteen nodules were not visible or palpable at the thoracoscopic examination and were only identified with thoracoscopic ultrasonography. Further studies are needed before final conclusions can be drawn.

LUS-Guided Therapy

LUS-guided therapy has been primarily reported in the treatment of hepatic lesions such as primary hepatocellular carcinomas (HCC) and hepatic metastases. The treatment options have been either ethanol injection, microwave coagulation, cryoablation, or radiofrequency ablation [63–68]. Most authors prefer radiofrequency ablation, due to the potentially larger coagulation size. Patients treated with radiofrequency ablation have long-term survival rates that are comparable to those in patients treated with hepatectomy. Although most of the patients can be treated percutaneously, there are some cases in which percutaneous ultrasound guidance is not appropriate. Laparoscopic access allows easier detection and more accurate targeting of the tumor in comparison with percutaneous access and can minimize complications. It is therefore an attractive treatment modality for localized hepatocellular carcinoma and hepatic metastases. In addition, the method is favorable in terms of the length of hospital stay and with regard to cost-effectiveness, as it is completed in a single session [65]. Lesions located in the subphrenic area of hepatic segment VIII (right posterior medial segment) or segment III (left anterior lateral segment) may often be difficult to demonstrate using percutaneous ultrasonography. Tumors located adjacent to the gallbladder may cause serious complications when treated percutaneously. Caution may be required with other tumors located on the surface of the liver or protruding from the

liver surface in order to avoid injuring the peritoneum or adjacent organs. Although a laparoscopic approach for local ablation plays an important role in treating hepatic lesions near the liver surface, precise targeting of ablation has been difficult using conventional linear ultrasound probes. One problem has been the lack of LUS probes with proper needle-guiding facilities. Most studies of LUS-guided radiofrequency ablation have therefore used an indirect method of guidance, with needle insertion via a route different from that of the LUS probe.

In a study by Noguchi et al. [67] including 51 patients with HCC, the survival after treatment with laparoscopic ablation was 95.2% after 1 year and 82.4% after 3 years. The tumor stage was a significant prognostic factor ($P < 0.0001$). There were no local recurrences within 6 months of the treatment in the successfully treated patients.

In another study by Machi et al. [66] including 46 patients, both hepatic metastases and HCCs were treated using percutaneous (81 lesions), laparoscopic (14 lesions), and open surgical approaches (109 lesions). Local tumor recurrence at the radiofrequency ablation site was diagnosed in 18 of 204 tumors (8.8%) during a mean follow-up period of 20.5 months. The risk factors for local recurrence included large tumor size and major vessel invasion. The recurrence rates for tumors less than 4 cm, 4–10 cm, and over 10 cm, and for those with vascular invasion, were 3.3%, 14.7%, 50%, and 47.8%, respectively. Ten of 18 tumors recurring locally were re-treated with radiofrequency ablation, and eight of them showed no further recurrence. The authors concluded that ultrasound-guided radiofrequency ablation is a relatively safe, well-tolerated, and versatile treatment option that offers excellent local control of primary and metastatic liver tumors. The appropriate use of percutaneous, laparoscopic, and open surgical radiofrequency ablation is beneficial in the management of patients with liver tumors in a variety of situations.

There appears to be a clear need for safe and accurate needle guidance during LUS in patients with liver lesions. We have tested the Hitachi LUS probe (OL-531) with a semiflexible radiofrequency needle in a porcine model and were able to insert the needle via the channel without any problems and to create a coagulation necrosis (Fig. 32.**9**). Other needle systems are currently being developed, and it is expected that LUS-guided radiofrequency ablation of liver lesions will become a standard option as a minimally invasive approach in a selected group of patients with malignant liver lesions in the near future.

References

1. Mortensen MB, Durup J, Pless T, Plagborg GJ, Ainsworth AP, Nielsen HO, et al. Initial experience with new dedicated needles for laparoscopic ultrasound-guided fine-needle aspiration and histological biopsies. Endoscopy 2001;33: 585–9.
2. Durup Scheel-Hincke J, Mortensen MB, Pless T, Hovendal CP. Laparoscopic four-way ultrasound probe with histologic biopsy facility using a flexible Tru-Cut needle. Surg Endosc 2000;14:867–9.
3. Hozumi M, Ido K, Hiki S, Isoda N, Nagamine N, Ono K, et al. Easy and accurate targeting of deep-seated hepatic tumors under laparoscopy with a forward-viewing convex-array transducer. Surg Endosc 2003;17:1256–60.
4. Santambrogio R, Podda M, Zuin M, Bertolini E, Bruno S, Cornalba GP, et al. Safety and efficacy of laparoscopic radiofrequency ablation of hepatocellular carcinoma in patients with liver cirrhosis. Surg Endosc 2003;17:1826–32.
5. Berber E, Garland AM, Engle KL, Rogers DSJ, Siperstein AE. Laparoscopic ultrasonography and biopsy of hepatic tumors in 310 patients. Am J Surg 2004;187:213–8.
6. Ido K, Nakazawa Y, Isoda N, Kawamoto C, Nagamine N, Ono K, et al. The role of laparoscopic US and laparoscopic US-guided aspiration biopsy in the diagnosis of multicentric hepatocellular carcinoma. Gastrointest Endosc 1999;50: 523–6.
7. Mortensen MB, Durup J, Pless T, Plagborg GJ, Ainsworth AP, Nielsen HO, et al. Initial experience with new dedicated needles for laparoscopic ultrasound-guided fine-needle aspiration and histological biopsies. Endoscopy 2001;33: 585–9.
8. Rau B, Hunerbein M, Schlag PM. Is there additional information from laparoscopic ultrasound in tumor staging? Dig Surg 2002;19:479–83.
9. Durup Scheel-Hincke J, Mortensen MB, Pless T, Hovendal CP. Laparoscopic ultrasonography: a method for staging of upper gastrointestinal cancer. Eur J Ultrasound 1999;9: 177–84.
10. Olsen AK, Bjerkeset OA. Laparoscopic ultrasound (LUS) in gastrointestinal surgery. Eur J Ultrasound 1999;10:159–70.
11. Tang CN, Siu WT, Ka-Wah-Li M. Use of diagnostic laparoscopy and laparoscopic ultrasound in the management of upper gastrointestinal malignancy. Ann Coll Surg HK 2001; 5:19–24.
12. Van Dijkum EJN, de Wit LT, van Delden OM, Kruyt PM, van Lanschot JJ, Rauws EAJ, et al. Staging laparoscopy and laparoscopic ultrasonography in more than 400 patients with upper gastrointestinal carcinoma. J Am Coll Surg 1999;189: 459–65.
13. Stein HJ, Kraemer SJ, Feussner H, Fink U, Siewert JR. Clinical value of diagnostic laparoscopy with laparoscopic ultrasound in patients with cancer of the esophagus or cardia. J Gastrointest Surg 1997;1:167–73.
14. Hulscher JB, Nieveen van Dijkum EJ, de Wit LT, van Delden OM, van Lanschot JJ, Obertop H, et al. Laparoscopy and laparoscopic ultrasonography in staging carcinoma of the gastric cardia. Eur J Surg 2000;166:862–5.
15. Romijn MG, van Overhagen H, Spillenaar Bilgen EJ, Ijzermans JN, Tilanus HW, Lameris JS. Laparoscopy and laparoscopic ultrasonography in staging of oesophageal and cardial carcinoma. Br J Surg 1998;85:1010–2.

16. Flett ME, Lim MN, Bruce D, Campbell SH, Park KG. Prognostic value of laparoscopic ultrasound in patients with gastro-esophageal cancer. Dis Esophagus 2001;14:223–6.
17. Tsioulias GJ, Wood TF, Chung MH, Morton DL, Bilchik A. Diagnostic laparoscopy and laparoscopic ultrasonography optimize the staging and respectability of intraabdominal neoplasms. Surg Endosc 2001;15:1016–9.
18. Lavonius MI, Gullichsen R, Salo S, Sonninen P, Ovaska J. Staging of gastric cancer: a study with spiral computed tomography, ultrasonography, laparoscopy, and laparoscopic ultrasonography. Surg Laparosc Endosc Percutan Tech 2002;12:77–81.
19. Giger U, Schafer M, Krahenbuhl L. Technique and value of staging laparoscopy. Dig Surg 2002;19:473–8.
20. Schachter PP, Avni Y, Shimonov M, Gvirtz G, Rosen A, Czerniak A. The impact of laparoscopy and laparoscopic ultrasonography on the management of pancreatic cancer. Arch Surg 2000;135:1303–7.
21. Kwon AH, Inui H, Kamiyama Y. Preoperative laparoscopic examination using surgical manipulation and ultrasonography for pancreatic lesions. Endoscopy 2002;34:464–8.
22. Menack MJ, Spitz JD, Arregui ME. Staging of pancreatic and ampullary cancers for resectability using laparoscopy with laparoscopic ultrasound. Surg Endosc 2001;15:1129–34.
23. Koler AJ, Lilly MC, Arregui ME. Suprapancreatic and periportal lymph nodes are normally larger than 1 cm by laparoscopic ultrasound evaluation. Surg Endosc 2004;18:646–9.
24. Catheline JM, Turner R, Rizk N, Barrat C, Champault G. The use of diagnostic laparoscopy supported by laparoscopic ultrasonography in the assessment of pancreatic cancer. Surg Endosc 1999;13:239–45.
25. Minnard EA, Conlon KC, Hoos A, Dougherty EC, Hann LE, Brennan MF. Laparoscopic ultrasound enhances standard laparoscopy in the staging of pancreatic cancer. Ann Surg 1998;228:182–7.
26. Taylor AM, Roberts SA, Manson JM. Experience with laparoscopic ultrasonography for defining tumour resectability in carcinoma of the pancreatic head and periampullary region. Br J Surg 2001;88:1077–83.
27. Pietrabissa A, Caramella D, Di Candio G, Carobbi A, Boggi U, Rossi G, et al. Laparoscopy and laparoscopic ultrasonography for staging pancreatic cancer: critical appraisal. World J Surg 1999;23:998–1002.
28. Jaroszewski DE, Schlinkert RT, Thompson GB, Schlinkert DK. Laparoscopic localization and resection of insulinomas. Arch Surg 2004;139:270–4.
29. Merchant NB, Conlon KC. Laparoscopic evaluation in pancreatic cancer. Semin Surg Oncol 1998;15:155–65.
30. Jimenez RE, Warshaw AL, Fernandez-Del Castillo C. Laparoscopy and peritoneal cytology in the staging of pancreatic cancer. J Hepatobiliary Pancreat Surg 2000;7:15–20.
31. Goletti O, Celona G, Galatioto C, Viaggi B, Lippolis PV, Pieri L, et al. Is laparoscopic sonography a reliable and sensitive procedure for staging colorectal cancer? A comparative study. Surg Endosc 1998;12:1236–41.
32. Milsom JW, Jerby BL, Kessler H, Hale JC, Herts BR, O'Malley CM. Prospective, blinded comparison of laparoscopic ultrasonography vs. contrast-enhanced computerized tomography for liver assessment in patients undergoing colorectal carcinoma surgery. Dis Colon Rectum 2000;43:44–9.
33. Rahusen FD, Cuesta MA, Borgstein PJ, Bleichrodt RP, Barkhof F, Doesburg T, et al. Selection of patients for resection of colorectal metastases to the liver using diagnostic laparoscopy and laparoscopic ultrasonography. Ann Surg 1999;230:31–7.
34. Hartley JE, Kumar H, Drew PJ, Heer K, Avery GR, Duthie GS, et al. Laparoscopic ultrasound for the detection of hepatic metastases during laparoscopic colorectal cancer surgery. Dis Colon Rectum 2000;43:320–4.
35. Birth M, Ehlers KU, Delinikolas K, Weiser HF. Prospective randomized comparison of laparoscopic ultrasonography using a flexible-tip ultrasound probe and intraoperative dynamic cholangiography during laparoscopic cholecystectomy. Surg Endosc 1998;12:30–6.
36. Thompson DM, Arregui ME, Tetik C, Madden MT, Wegener M. A comparison of laparoscopic ultrasound with digital fluorocholangiography for detecting choledocholithiasis during laparoscopic cholecystectomy. Surg Endosc 1998;12:929–32.
37. Machi J, Tateishi T, Oishi AJ, Furumoto NL, Oishi RH, Uchida S, et al. Laparoscopic ultrasonography versus operative cholangiography during laparoscopic cholecystectomy: review of the literature and a comparison with open intraoperative ultrasonography. J Am Coll Surg 1999;188:360–7.
38. Kimura T, Umehara Y, Yoshida M, Sakuramachi S, Kawabe A, Suzuki K. Laparoscopic ultrasonography and operative cholangiography prevent residual common bile duct stones in laparoscopic cholecystectomy. Surg Laparosc Endosc Percutan Tech 1999;9:124–8.
39. Siperstein A, Pearl J, Macho J, Hansen P, Gitomirsky A, Rogers S. Comparison of laparoscopic ultrasonography and fluorocholangiography in 300 patients undergoing laparoscopic cholecystectomy. Surg Endosc 1999;13:113–7.
40. Tranter SE, Thompson MH. Potential of laparoscopic ultrasonography as an alternative to operative cholangiography in the detection of bile duct stones. Br J Surg 2001;88:65–9.
41. Tranter SE, Thompson MH. A prospective single-blinded controlled study comparing laparoscopic ultrasound of the common bile duct with operative cholangiography. Surg Endosc. 2003;17:216–9.
42. Catheline JM, Turner R, Paries J. Laparoscopic ultrasonography is a complement to cholangiography for the detection of choledocholithiasis at laparoscopic cholecystectomy. Br J Surg 2002;89:1235–9.
43. Kelly SB, Remedios D, Lau WY, Li AK. Laparoscopic ultrasonography during laparoscopic cholecystectomy. Surg Endosc 1997;11:67–70.
44. Santambrogio R, Bianchi P, Opocher E, Verga M, Montorsi M. Prevalence and laparoscopic ultrasound patterns of choledocholithiasis and biliary sludge during cholecystectomy. Surg Laparosc Endosc Percutan Tech 1999;9:129–34.
45. Catheline JM, Turner R, Rizk N, Barrat C, Buenos P, Champault G. Evaluation of the biliary tree during laparoscopic cholecystectomy: laparoscopic ultrasound versus intraoperative cholangiography: a prospective study of 150 cases. Surg Laparosc Endosc 1998;8:85–91.
46. Callery MP, Strasberg SM, Doherty GM, Soper NJ, Norton JA. Staging laparoscopy with laparoscopic ultrasonography: optimizing resectability in hepatobiliary and pancreatic malignancy. J Am Coll Surg 1997;185:33–9.
47. Barbot DJ, Marks JH, Feld RI, Liu JB, Rosato FE. Improved staging of liver tumors using laparoscopic intraoperative ultrasound. J Surg Oncol 1997;64:63–7.
48. Jarnagin WR, Bach AM, Winston CB, Hann LE, Heffernan N, Loumeau T, et al. What is the yield of intraoperative ultrasonography during partial hepatectomy for malignant disease? J Am Coll Surg. 2001;192:577–83.

49. Lo CM, Fan ST, Liu CL, Poon RT, Lam CM, Yuen WK, et al. Determining resectability for hepatocellular carcinoma: the role of laparoscopy and laparoscopic ultrasonography. J Hepatobiliary Pancreat Surg 2000;7:260–4.
50. Potter MW, Shah SA, McEnaney P, Chari RS, Callery MP. A critical appraisal of laparoscopic staging in hepatobiliary and pancreatic malignancy. Surg Oncol 2000;9:103–10.
51. Foroutani A, Garland AM, Berber E, String A, Engle K, Ryan TL, et al. Laparoscopic ultrasound vs. triphasic computed tomography for detecting liver tumors. Arch Surg 2000; 135:933–8.
52. De Castro SM, Tilleman EH, Busch OR, van Delden OM, Lameris JS, van Gulik TM, et al. Diagnostic laparoscopy for primary and secondary liver malignancies: impact of improved imaging and changed criteria for resection. Ann Surg Oncol 2004;11:522–9.
53. Grobmyer SR, Fong Y, D'Angelica M, Dematteo RP, Blumgart LH, Jarnagin WR. Diagnostic laparoscopy prior to planned hepatic resection for colorectal metastases. Arch Surg 2004;139:1326–30.
54. D'Angelica M, Fong Y, Weber S, Gonen M, DeMatteo RP, Conlon K, et al. The role of staging laparoscopy in hepatobiliary malignancy: prospective analysis of 401 cases. Ann Surg Oncol 2003;10:183–9.
55. Lo CM, Lai EC, Liu CL, Fan ST, Wong J. Laparoscopy and laparoscopic ultrasonography avoid exploratory laparotomy in patients with hepatocellular carcinoma. Ann Surg 1998;227:527–32.
56. Catheline JM, Champault G. Ultrasonographic laparoscopy of the liver. Chirurgie 1999;124:568–76.
57. Schachter P, Sorin V, Avni Y, Shimonov M, Friedman V, Rosen A, et al. The role of laparoscopic ultrasound in the minimally invasive management of symptomatic hepatic cysts. Surg Endosc 2001;15:364–7.
58. Montorsi M, Santambrogio R, Bianchi P, Opocher E, Cornalba GP, Dapri G, et al. Laparoscopy with laparoscopic ultrasound for pretreatment staging of hepatocellular carcinoma: a prospective study. J Gastrointest Surg 2001;5:312–5.
59. Helin HL, Kirkinen P. Laparoscopic ultrasonography during conservative ovarian surgery. Surg Endosc 2000;14:161–3.
60. Cheung TH, Yang WT, Yu MY, Lo WK, Ho S. New development of laparoscopic ultrasound and laparoscopic pelvic lymphadenectomy in the management of patients with cervical carcinoma. Gynecol Oncol 1998;71:87–93.
61. Matin SF, Gill IS. Laparoscopic ultrasonography. J Endourol 2001;15:87–92.
62. Coppola F, Papa S, Pilotti V, Mattioli S, Gavelli G. Ultrasonographic localization of occult pulmonary nodules during video-assisted thoracic surgery. Eur Radiol 2003;13: 2358–64.
63. Santambrogio R, Podda M, Zuin M, Bertolini E, Bruno S, Cornalba GP, et al. Safety and efficacy of laparoscopic radiofrequency ablation of hepatocellular carcinoma in patients with liver cirrhosis. Surg Endosc 2003;17:1826–32.
64. Kim RD, Nazarey P, Katz E, Chari RS. Laparoscopic staging and tumor ablation for hepatocellular carcinoma in Child C cirrhotics evaluated for orthotopic liver transplantation. Surg Endosc 2004;18:39–44.
65. Nagae G, Ido K, Isoda N, Sato S, Kita H, Sugano K. Laparoscopic ablation therapy for hepatocellular carcinoma. Dig Endosc 2005;17:1–8.
66. Machi J, Uchida S, Sumida K, Limm WM, Hundahl SA, Oishi AJ, et al. Ultrasound-guided radiofrequency thermal ablation of liver tumors: percutaneous, laparoscopic, and open surgical approaches. J Gastrointest Surg 2001;5:477–89.
67. Noguchi O, Izumi N, Nishimura Y, Ueda K, Tsuchiya K, Hamano K, et al. Laparoscopic ablation therapy for hepatocellular carcinoma: clinical significance of a newly developed laparoscopic sector ultrasonic probe. Dig Endosc 2003; 15:179–84.
68. Ido K, Isoda N, Sugano K. Microwave coagulation therapy for liver cancer: laparoscopic microwave coagulation. J Gastroenterol 2001;36:145–52.

33 EUS-Guided Endosurgery

A. Fritscher-Ravens

Introduction

Interventional endoscopic ultrasound (EUS)-guided procedures such as cyst drainage and celiac block have now proved to be feasible, opening a window of opportunity for further and more invasive procedures. Such procedures might include needles or larger instruments to penetrate into the peritoneal cavity, or more invasive manipulations, including cutting through the gastric wall.

Most recently, the new and experimental field of transluminal endoscopic interventions has been developing, allowing minimally invasive endoscopic surgery [1–5]. Parallel to the endoscopic expansion, new indications for therapeutic EUS-guided interventions have been developed in areas that were previously purely surgical. Since EUS allows visualization of organs adjacent to the gastrointestinal tract, such as mediastinal and gastric lymph nodes, the gallbladder, small bowel, or parts of the diaphragm, it seems feasible to attempt to develop endoscopic surgical procedures that otherwise require open or laparoscopic surgery. Examples of such possibilities include gastropexy to the diaphragm or pacing of the diaphragm [6,7], gastrojejunostomy, or cholecystoduodenostomy [8,9]. EUS guidance allows the deployment of devices under direct ultrasound vision into structures beyond the gastrointestinal wall and thus the involvement of other organs. New suturing and anchoring devices allow a transgastric approach to be performed in such a way that the peritoneal or mediastinal cavity is not penetrated with a nonsterile endoscope [10]. The present chapter presents these new methods, which to date have only been carried out in animals, but have considerable future potential for patients.

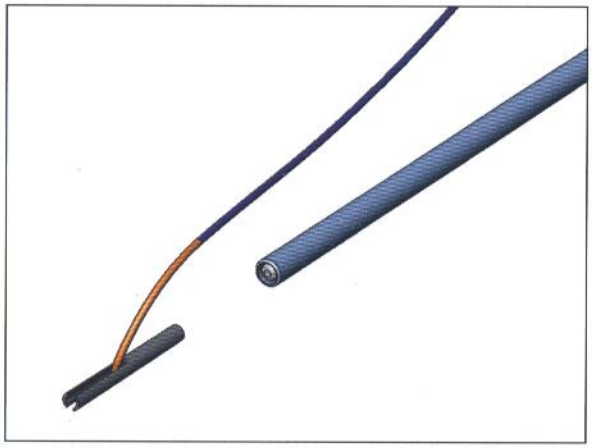


Fig. 33.1 A metal anchor with a spring-forked tail, constructed like a T-bar, is attached to a thread and then loaded into a 19-g EUS needle.

New Devices

Suturing System

An endoscopic suturing device has been developed, capable of being used in combination with any endoscope with a 2.8-mm accessory channel. The device allows stitches to be placed under EUS guidance at any desired depth in the gastric, esophageal, or duodenal wall [10]. It can also be used to place stitches beyond the wall of the gastrointestinal tract, to fix organs or structures to the stomach. The device had to be sufficiently small to fit into the inner hollow part of a 19-gauge EUS needle. A metal anchor, constructed like a T-bar, was made with a sprung forked tail, which allowed some friction to be exerted to prevent premature ejection of the system out of the 19-gauge needle (Fig. 33.**1**). The anchor is attached to a polypropylene thread, which is held alongside the needle. The thread is guided outside the endoscope through a perforated custom-made plastic interface, which is screwed onto the accessory channel (Fig. 33.**2**). The original needle stylet was modified to pass 3 mm beyond the tip, thus ejecting the tag and thread from the hollow needle into the desired target [10]. It has always been possible to identify the exact location of the tag on the ultrasound screen. The metal anchor appears as a hyperechoic reflection without shadowing and is easily moved by gentle traction on the thread (Fig. 33.**3**).

Once an anchor or several anchors have been placed, the threads emerging out of the esophageal or gastric wall need to be fixed to the wall or knotted (locked) together (Figs. 33.**4**, 33.**5**). If tight knotting or fixation to the gastric wall is desired, a pledget may be necessary to spread the force over a larger surface area of the gastric wall. A pledget is a flat piece of nonabsorbable material, which is pushed down over the thread to reduce the chance of the stitch cutting out.

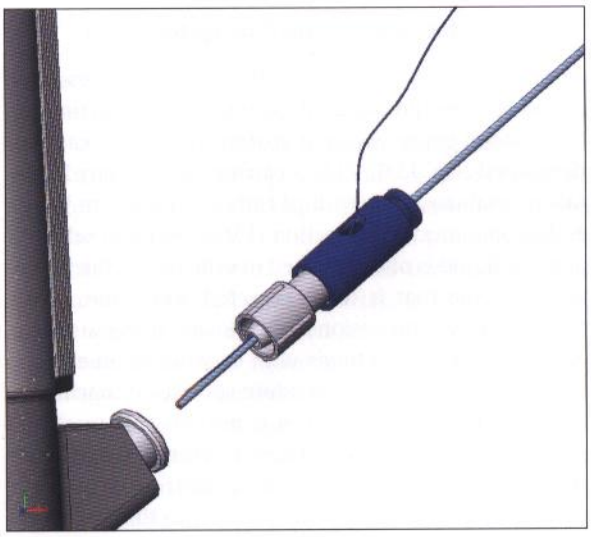


Fig. 33.2 When the anchor is loaded, the thread runs alongside the EUS needle in the echoendoscope's accessory channel. It is guided to the outside part of the scope through an additional custom-made perforated plastic piece, which is screwed on top of the endoscope channel.



Fig. 33.3 Ultrasound image of the anchor, which has been ejected just beyond the gut wall. There is a distinct white echo reflex, representing the piece of metal.

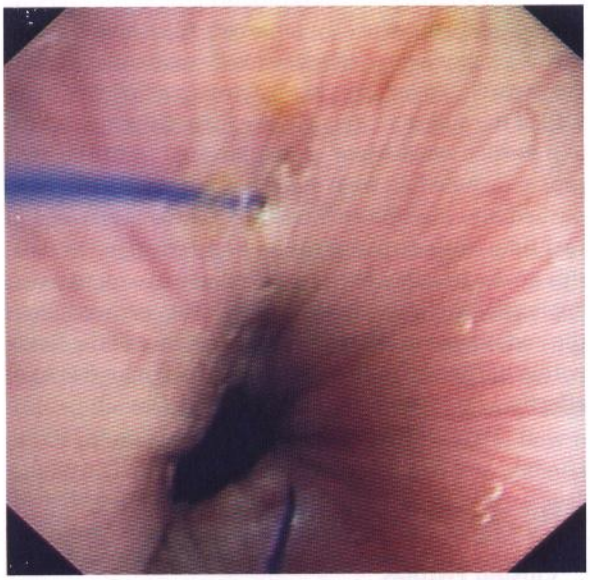


Fig. 33.4 Endoscopic image showing two threads appearing in the esophageal lumen. They are attached to anchors ejected beyond the gut wall.



Fig. 33.5 Endoscopic image of a custom-made locking device. Two threads with anchors beyond the gut wall have been tied together and have been captured within this locking device in the stomach.

One or several threads can be locked into a small metal or plastic locking device, which will pass through a 2.8-mm endoscope channel (Fig. 33.5). The threads are guided through holes in a small metal cylinder. Another cylinder can be moved into position over the threads and inner cylinder, exerting friction on the thread. The lock is then released from its applicator. The thread is cut using endoscopic scissors.

Recently, another type of suturing device, the "Eagle Claw," (Olympus Opt., Tokyo, Japan) has been described and comparisons with tying knots were carried out in bench experiments, none of which used endoscopic ultrasound for guidance [11,12].

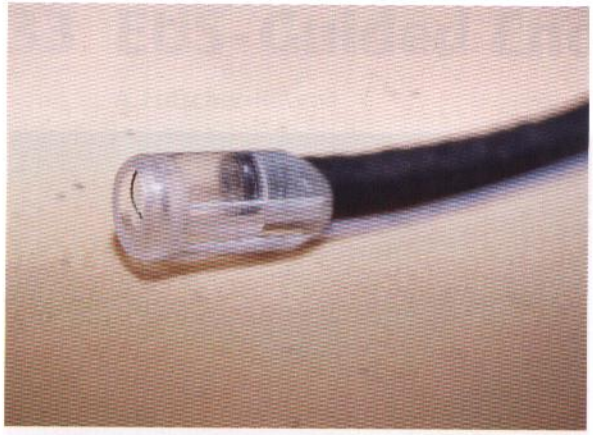


Fig. 33.**6** Gastroscope with an end cap, specially designed for EUS miniprobe examination. There is a snare mounted onto a rim at the distal end of the end cap, and a hollow part for the miniprobe.

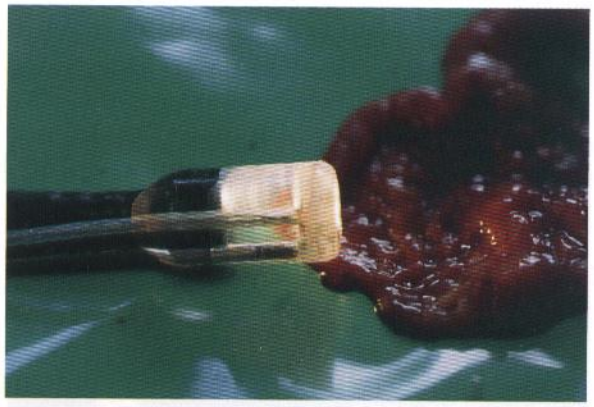


Fig. 33.**7** Alongside the end cap, a channel is aligned, into which an EUS miniprobe can be inserted, so that it forms part of the inner wall of the end cap.



Fig. 33.**8** EUS image showing the result of saline injection, represented by a hypoechoic area, with a snare across the tissue and the injection.

EUS-Guided Snare Resection System

To be able to visualize any difficult mucosal resection and to observe the extent of the resection in real time, an EUS-guided snare within a custom-made end cap was developed (Fig. 33.**6**). EUS is carried out in many hospitals to evaluate the depth of tumor penetration before endoscopic mucosal resection (EMR). At EMR, saline or another liquid is often injected in order to lift the pathological tissue that is to be resected above the serosa. Subsequently, the lesion is removed using a snare. Although various methods with or without an end cap are available, the main procedure consists of snaring the lesion. However, with EMR it is not possible to ensure reliably that the serosal surface has not been included in the tissue grasped—resulting in perforation or bleeding in rare cases. Nor is it possible to ensure that the entire area aimed for has been resected with this method.

In the context of EMR, real-time EUS vision before and during the cutting process might help reduce risk of perforation (Fig. 33.**8**) [13]. For this purpose, the modified end cap was developed and attached to the tip of a conventional endoscope (Figs. 33.**6**, 33.**7**). The targeted tissue can be sucked into the hollow part of the end cap, snared, and subsequently removed. Alongside the end cap, a channel into which an EUS miniprobe can be inserted is aligned so that it forms part of the inner wall of the end cap (Fig. 33.**7**). A channel, through which a preloaded open snare can be inserted to fit the end-cap, is included as well. Once the miniprobe has been pushed into the side channel, EUS can be performed in real time during snare capture and resection. To date, this device has only been tested in animal experiments; applications in humans are awaited. The method allows the endoscopist to view the serosal surface of the tissue within the end cap and to check that the tumor has been effectively trapped before snare closure.

■ EUS-Guided Therapy

Closing Fistulas

Esophageal fistulas can occur after radiotherapy for cancer or after esophageal surgery, and represent a major treatment challenge. Hanging plastic tubes have been inserted, and covered metal stents have recently been deployed to bridge the defect in order to allow the patient to swallow without complications [14].

After the development of the EUS-guided suturing system, it was tested to investigate whether it might be possible to sew patches across the esophageal lesion in order to close the fistula [15]. Attaching patches to the esophageal wall might allow better management of these patients. The choice of material, as well as its weight, elasticity, and the development of rapid and

reliable attachment mechanisms, may influence the success of this type of EUS-guided intervention. In an experimental porcine model, patches 0.4–2.0 cm in size of various materials were attached to the esophageal wall or gastroesophageal junction, using the suturing device described above [15]. Patches used to close fistulas were compared with flaps that prevented food entering the mediastinum but allowed pus to drain into the esophagus. The number of stitches used ranged from one to six, and different materials used to cover the lesion were tested for their capacity to deform in accordance with the movements of the esophagus. Although most of the flexible plastic materials failed to conform to the esophageal wall during peristalsis and respiration, modified small-intestinal submucosa with growth factor (SIS, Wilson-Cook, Winston-Salem, North Carolina, USA) performed well and remained attached to the wall even when the esophagus was inflated with air and deflated (Fig. 33.**9**) [15]. Although these were preliminary studies, there may be a potential for further developments using this type of material. It might even be worth considering using only the suturing device, as described above, to simply close the defects. However, as it may not be possible for pus to drain once the defect is closed, there might be situations in which a cover without defect closure for further drainage could be indicated. These studies have only been conducted in animals, and experience in patients is awaited.

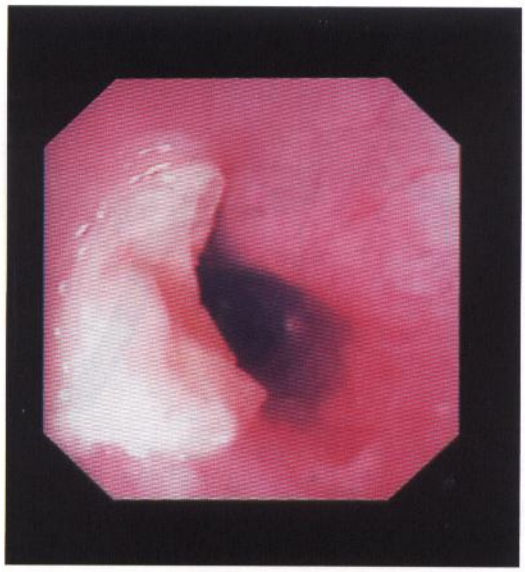


Fig. 33.**9** Endoscopic image of the esophagus. To close the fistula, small-bowel mucosa (SIS, Wilson-Cook, Winston-Salem, North Carolina, USA) has been attached to the esophageal wall using the suturing device. The shape of the patch adapts to the varying shapes of the esophageal wall.

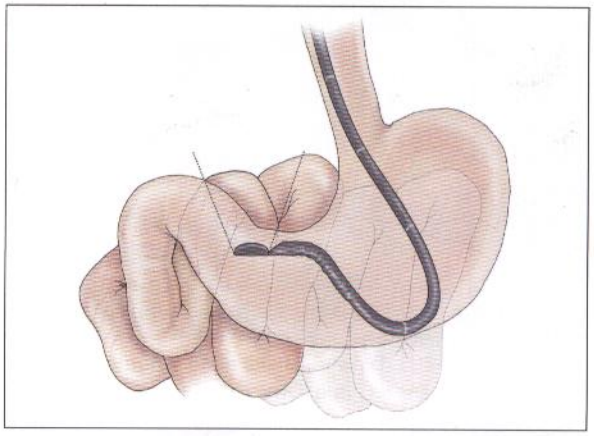


Fig. 33.**10** Schematic drawing of the angle of the linear endoscopic ultrasound view and the small bowel relative to the gastric wall.

Transgastric Anastomosis

One of the first uses of EUS-guided transgastric surgery, as well as endoscopic transgastric surgery without EUS, was in creating an endoscopic gastrojejunostomy [2,16]. Some problems appeared to be difficult to solve with an endoscopic transgastric procedure alone. These included the task of sterilizing the gastric lumen to allow a "clean" endoscope into the peritoneal cavity; how to capture a loop of small bowel; and how to stop potential bleeding whilst making an incision into the gastric wall, with the potential risk of hitting an intervening vessel. The combination with endoscopic ultrasound has a number of advantages: it is not necessary to penetrate the peritoneal cavity with a nonsterile endoscope, and the bowel loop can be easily captured with the anchor described. As in endoscopic ultrasonography, color Doppler or even power Doppler imaging is available. Therefore, most potentially intervening vessels can be seen on the ultrasound screen and can be avoided by repositioning the echoendoscope [8,9].

Once a malignant tumor has occluded the lumen of the bowel and the patient appears to be inoperable, there is a need to create a bypass—e. g., with a gastrojejunal anastomosis. This is usually achieved with open or laparoscopic surgery, which may create an additional burden for the severely ill patient. The invention and development of an endoscopic transgastric approach to create an anastomosis (with or without EUS guidance), requiring only single-lumen access (via the gastric lumen) for the entire procedure, might be of benefit for these patients.

The technical process using the EUS-guided approach starts by identifying an appropriate small-bowel loop on the EUS screen (Fig. 33.**10**). With real-time EUS visualization, a 19-gauge EUS needle loaded with the anchor system described above can be advanced through the gastric wall into the loop (Fig. 33.**11**). The anchor is then released by pushing the stylet down the inner part of the needle. Once ejected, it can help appose the small-bowel loop against the gastric wall. When the examiner pulls

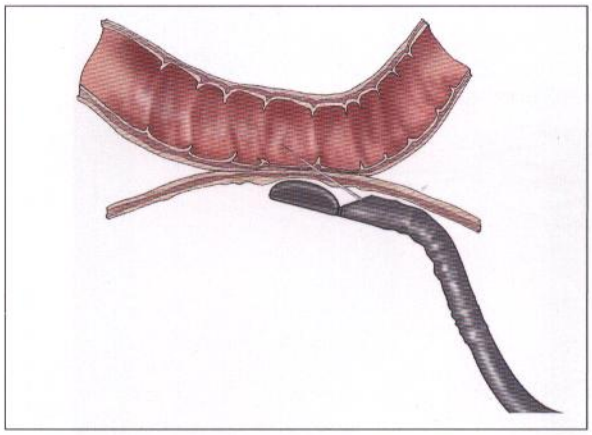


Fig. 33.**11** A 19-gauge EUS needle loaded with the anchor system can be pushed forward through the gastric wall into a small bowel loop with real-time EUS visualization.

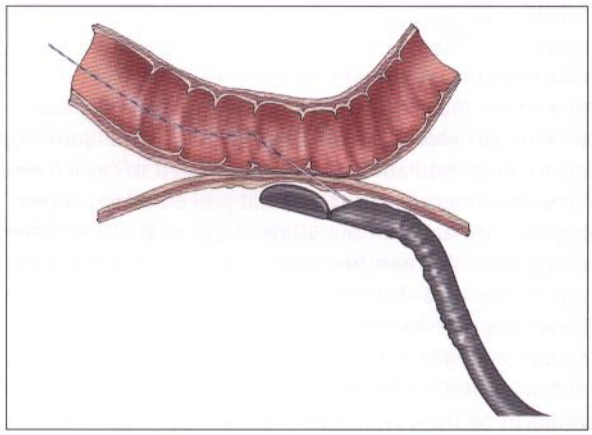


Fig. 33.**12** Subsequently, the guide wire can be pushed into the otherwise inaccessible small-bowel lumen.



Fig. 33.**13** A balloon is pushed over the guide wire into the small bowel lumen.

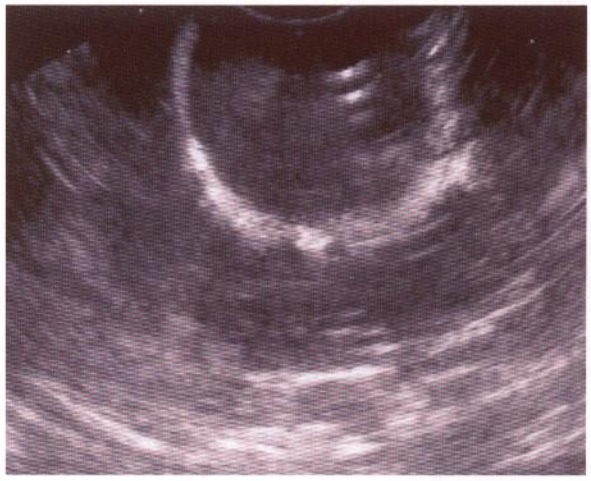


Fig. 33.**14** EUS image of the inflated and water-filled balloon that has been guided over a wire into the small-bowel lumen.

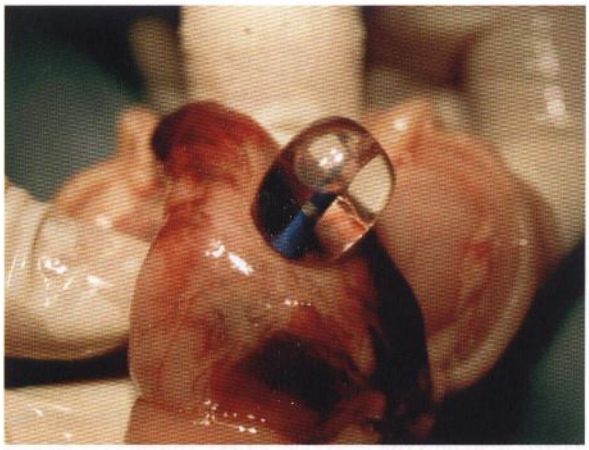


Fig. 33.**15** Autopsy photograph showing the inflated balloon filled with water in the small bowel.

on the anchor thread from the outside of the endoscope, the attached anchor captured within the small bowel will pull the organ with it to the gastric wall. The stylet can be removed leaving the inner hollow part of the needle available to host a guide wire, which can be pushed into the otherwise inaccessible small-bowel lumen (Fig. 33.**12**). Subsequently, a balloon can be pushed over the guide wire and inflated and filled with water once it is inside the small-bowel lumen (Figs. 33.**13**–33.**15**) [8].

This serves to provide counter-pressure from the inaccessible side for an anastomosis device, which is deployed endoscopically from the gastric side. The anastomosis device can either consist of a plate to spread the force, spring, and lock, or of a second balloon to be pressed against the one in the small bowel, guided by the access catheter. If a plate-like anastomosis device is used and guided over the catheter to the point where it

emerges from the gastric wall, a spring has to be deployed and then compressed against the plate and the counter-pressure balloon in the small bowel (Fig. 33.**16**). To perform this part of the procedure, it is advisable to exchange the echoendoscope for a gastroscope, onto which the device is back-loaded. A double balloon (that can be inflated from either side of the two walls) can be used as an alternative device. Both of these systems force the two walls (the small bowel and stomach) together with a pressure greater than 200 mmHg, which is generally high enough to cause ischemia in the tissue in between. Locks have to be deployed at this stage to keep the system in place [8]. Within about 2 days, an opening is formed between the small bowel and the gastric wall (Fig. 33.**17**). The anastomosis can be very small but, once a balloon is used, may be up to 17 mm in diameter. However, even this may be too small for a long-lasting anastomosis suitable for appropriate food intake. As anastomoses tend to heal very quickly, implying self-fulfilling closure of the opening, care needs to be taken to achieve a large enough hole. As this may vary considerably between individuals, it may be necessary to deploy a short stent such as the Joyo stent from Wilson-Cook to bridge the two organs and keep them open. The hole created can also be cut larger with a needle-knife. Survival studies in animals have been conducted successfully [8,9] and studies in humans are awaited.

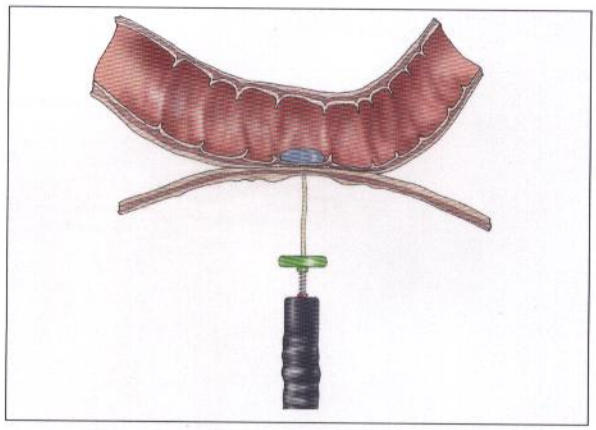


Fig. 33.**16** A plate-like anastomosis device with a spring is used and guided over the catheter to the point at which it emerges from the gastric wall. When the endoscope is pushed against the gastric wall, the spring is compressed against the plate and the counter-pressure balloon in the small bowel, causing pressure on the gut walls.

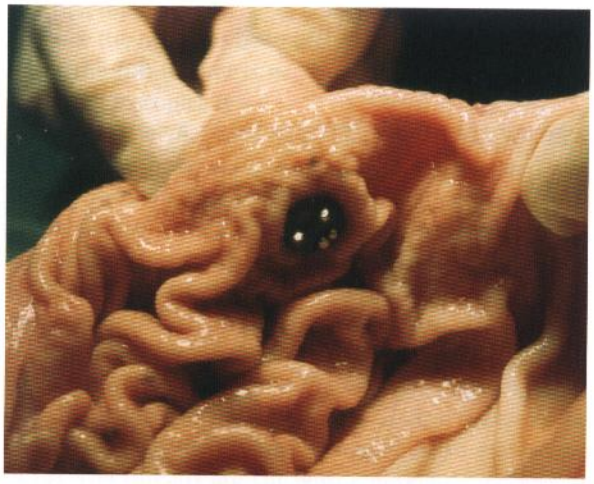


Fig. 33.**17** Autopsy of an animal in which EUS-guided anastomosis formation has been carried out. The anastomosis created is the size of a therapeutic gastroscope.

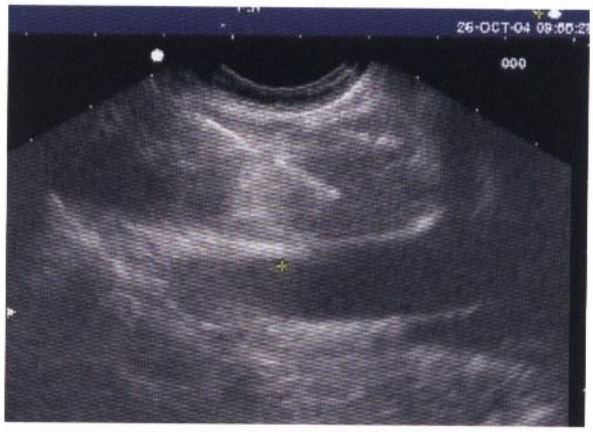


Fig. 33.**18** EUS image of the median arcuate ligament, situated between the aorta and the celiac axis. An EUS needle, used to deploy an anchor, can be seen within the ligament.

EUS-Guided Posterior Gastropexy for Reflux Disease

Traditionally, any approach to repair a hiatus hernia causing reflux disease has been surgical, either with laparoscopy or laparotomy. Currently, the most frequently used procedure is Nissen fundoplication, although the best results are reported using Hill's operation [17,18].

Endoscopic procedures for reflux disease are constrained by the internal gut wall. This limitation makes it difficult to alter the angle of His, which is necessary to achieve long-term success by repositioning the lower esophageal sphincter.

EUS enables the examiner to view beyond the gut wall, so that some structures relevant to reflux surgery, such as parts of the diaphragm—e. g., the right crus and median arcuate ligament (MAL)—can be identified (Fig. 33.**18**). Stitches can be placed into these muscular components to attach the lower esophageal sphincter to the MAL or right crus with real-time time vision (Figs. 33.**18**, 33.**19**). Real-time images allow precise placement of the stitches or anchors into the desired muscle, while EUS serves just as the imaging technique to guide the correct placement of tools or devices for fixation of the lower esophageal sphincter (LES) [6]. The combination of the abilities to "see" and "fix" parts of the

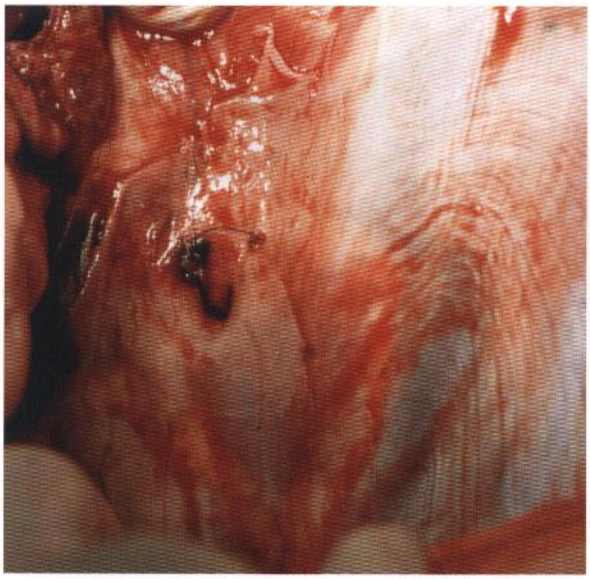


Fig. 33.**19** Autopsy photograph showing the anchor placed in the median arcuate ligament.

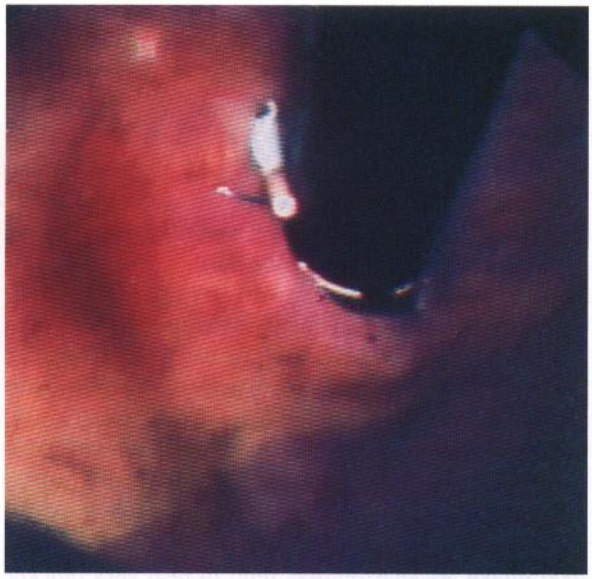


Fig. 33.**20** Endoscopic image of a lock, which captures both the threads out of the median arcuate ligament and the one ejected beyond the cardia wall. The view is with the endoscope in retroflexed position.

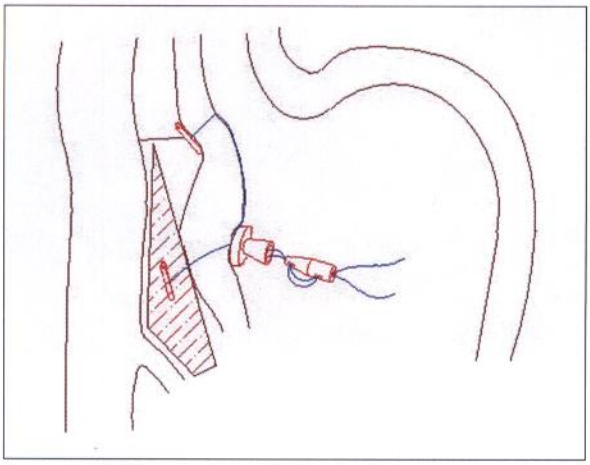


Fig. 33.**21** Schematic drawing, showing the principle of the two anchors with threads and the way in which they lock in the gastric lumen.

diaphragm without a transabdominal approach has been used to develop an experimental approach to conducting an endoscopic posterior gastropexy for reflux disease. The approach we used was similar to, and inspired by, the surgical procedure developed by Prof. Lucius Hill [17,18].

Under constant real-time EUS control, an anchor and a thread are fired through the wall of the stomach into the MAL. Subsequently, a second anchor is placed through the full thickness of the gastrointestinal wall posteriorly, immediately below the lower esophageal sphincter. Both threads, which are fixed to the anchors, will appear in the lumen of the stomach and can be locked together endoscopically (Figs. 33.**20**, 33.**21**) [10].

Manometry before the procedure can be used to establish a baseline sphincter pressure. Intraoperative and postoperative manometry are used to measure the alterations in the pressure in the LES during and after the examination. In experimental procedures conducted in more than 20 survival studies in pigs, the median sphincter pressure increased significantly from 11.2 mmHg to 21 mmHg ($P < 0.05$) [6]. The median length of the LES increased from 2.8 to 3.5 cm. Even 4 weeks after the procedure, these data were reproducible [6,10]. Although studies in humans have yet to be performed, this procedure appears to have a high potential to achieve an interventional endoscopic treatment for reflux disease without surgery. One of the positive aspects of the new approach may be that it is reversible if the results do not appear to be having the desired effect, if the effect is too strong, or if the patient feels uncomfortable with it. It also has the additional benefit of not precluding possible later surgery.

EUS-Guided Lymph Node Removal

As discussed above, EUS can be used to help carry out examinations that would otherwise be more interventional or purely surgical. It can also be used as a guide for purely endoscopic surgery.

Enlarged mediastinal or perigastric lymph nodes may need to be removed for histological assessment, to obtain insights into the underlying disease. Nodes located in the mediastinum or intra-abdominally cannot always

be removed easily, as nonsurgical access is difficult. Especially in these areas, there may be strong reasons for retrieving such nodes, especially if difficult diseases such as non-Hodgkin's lymphomas are suspected, or other attempts to reach a diagnosis have been fruitless.

Sentinel lymph nodes in direct proximity to a T1 or T2 gastrointestinal carcinoma are also of interest. As T1 or T2 carcinomas in defined areas of the upper gastrointestinal tract may be removable by endoscopic mucosal resection, these nodes may limit this endoscopic approach. They would need to be removed in order to offer the patient an attempt at curative treatment. Surgery is currently carried out in these cases.

Although EUS has been shown to be very effective for obtaining biopsies from nodes in close proximity to the gut wall, these indications may make the entire removal of such nodes necessary.

Using EUS, it is possible to detect even small (< 1 cm) periesophageal or/and perigastric nodes, as well as to select "suspicious" nodes on the basis of their ultrasound morphology. It also makes it possible to identify potential intervening blood vessels between the gut wall and the node, allowing safe access.

EUS-guided endoscopic lymphadenectomy starts with the EUS-guided selection of a lymph node [19]. A 19-gauge EUS needle (Wilson-Cook) with the custom-made anchor and thread (as described above) inside its inner hollow part can then be passed through the esophageal/gastric wall into and then through the full length of the node (Fig. 33.**22**). Once the needle tip is visualized on the opposite side of the entrance of the needle into the node, the anchor and thread can be released from the needle. This is achieved by pushing the inner stylet of the needle forward. Once the needle is removed and the examiner starts pulling on the thread from the outer side of the biopsy channel of the echoendoscope, the T-bar anchor should tilt into a horizontal position to catch the node. Capture of the lymph node can be seen on the ultrasound screen. The thread pulls the node against the gastric wall, and when released, the node bounces back into its original position. When pulled on the thread, the node may indent into the gastric lumen (Fig. 33.**22**) [19].

Subsequently, the echoendoscope has to be replaced by a gastroscope, and the thread is reloaded into its biopsy channel. Endoscopic incision into the gastric wall using a needle-knife is the next step to be performed. This can also be done with the echoendoscope in place. However, straightforward viewing with a gastroscope ensures that the cutting process can be adequately visualized. Gastric wall dissection has to be carried out in close proximity to the point of exit of the thread from the stomach. Care has to be taken, as electrocautery may damage or cut the thread. The gastric incision can be very small. The lymph node is removed by pulling on the thread, which forces the anchor

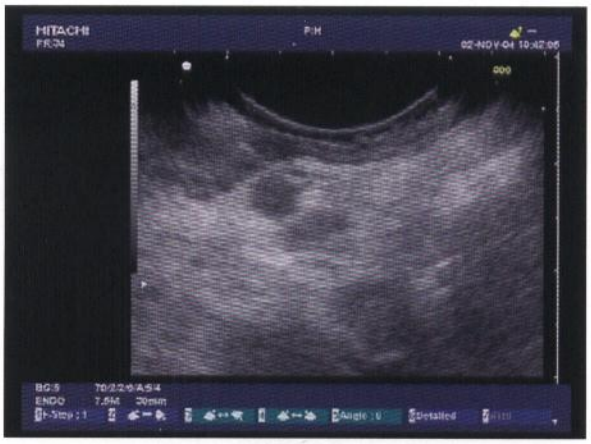


Fig. 33.**22** EUS image showing a hypoechoic lymph node. An anchor has been ejected into it, and it is pulled against the gastric wall.

to take the node with it through the incision into the gastric lumen [19].

Once the node has been secured outside the patient's body, the full-thickness gastric wall incision has to be closed endoscopically.

The EUS needle, with an anchor and thread identical to those the node was captured with, is reloaded and passed through the accessory channel of the gastroscope. When in close proximity to the incision, the needle has to puncture the gastric wall, and the anchor is released beyond the gastric wall. The process has to be repeated with further deployment of a second anchor on the opposite side of the incision. Once two stitches or more have been placed, the threads are locked together with a newly developed locking device that can be passed through the accessory channel of an endoscope [4,10]. The threads are cut with endoscopic scissors or with a cutter incorporated into the locking device.

This approach has proved to be feasible in a few animal survival studies. Further animal studies are needed before studies in humans are embarked on.

Conclusion

Although the EUS-guided techniques described in this chapter are purely experimental, they are exciting in themselves. They also allow EUS-guided endosurgery using methods that will make a wide variety of interventions possible in the future. At present, all of the interventional techniques described have only been carried out in animal studies. The need to develop tools and devices that have been approved for human use may delay patient-orientated studies for a few more years, but such studies will undoubtedly follow. A great deal of enthusiasm has been raised, which may lead not only to overestimation of the prospects for techniques such as

these but also to underestimation of the problems that might arise when the methods are introduced for patients. However, even when they are viewed with the appropriate skepticism, these new concepts have already at this early stage opened up new prospects that can be neither ignored nor disregarded.

References

1. Seifert H, Faust D, Schmitt T, Dietrich C, Caspary W, Wehrmann T. Transmural drainage of cystic peripancreatic lesions with a new large-channel echo endoscope. Endoscopy 2001;33:1022–6.
2. Kalloo A, Kantsevoy S, Jagannath S, Niiyama H, Magee CA, Vaugh C, et al. Endoscopic gastrojejunostomy with long-term survival in a porcine model [abstract]. Gastrointest Endosc 2002;55:AB 96.
3. Kalloo AN, Singh VK, Sanjay B, Jagannath SB, Niiyama H, Hill SL. Flexible transgastric peritoneoscopy: a novel approach to diagnosis and therapeutic intervention in the peritoneal cavity. Gastrointest Endosc 2004;60:114–7.
4. Ikeda K, Fritscher-Ravens A, Mosse CA, Mills T, Tajiri H, Swain CP. Endoscopic full-thickness resection with sutured closure in a porcine model. Gastrointest Endosc 2005;62: 122–9.
5. Hu B, Chung SCS, Sun LCL, Kawashima K, Yamamoto T, Cotton PB, et al. Transoral obesity surgery: endoluminal gastroplasty with an endoscopic suture device. Endoscopy 2005;37:411–4.
6. Fritscher-Ravens A, Mosse CA, Mukherjee D, Yazaki E, Park PO, Mills T, et al. Transgastric gastropexy and hiatal hernia repair for GERD under EUS control: an experimental study in a porcine model. Gastrointest Endosc 2004;59:89–95.
7. Fritscher-Ravens A, Mosse AC, Ikeda K, Swain P. Interventional endoscopic ultrasound for hiatus hernia and the diaphragm [abstract]. Gastrointest Endosc 2005;61:AB 278.
8. Fritscher-Ravens A, Mosse CA, Mukherjee D, Mills T, Park PO, Swain CP. Transluminal endosurgery: single lumen access anastomotic device for flexible endoscopy. Gastrointest Endosc 2003;58:585–91.
9. Fritscher-Ravens A, Mosse CA, Mukherjee D, Swain CP. Balloon compression anastomosis at flexible endoscopy [abstract]. Gastrointest Endosc 2003;57:AB 6.
10. Fritscher-Ravens A, Mosse CA, Mills TN, Mukherjee D, Park PO, Swain CP. A through-the-scope device for suturing and tissue approximation under EUS control. Gastrointest Endosc 2002;56:737–42.
11. Hu B, Sun LC, Karmakar M, Cotton PB, Gostout CJ, Hawes RH, et al. Assessing the adequacy of endoscopically tied knots: a functional approach. Endoscopy 2005;37:415–7.
12. Hu B, Chung SCS, Sun LCL, Kawashima K, Yamamoto T, Cotton PB, et al. Transoral obesity surgery: endoluminal gastroplasty with an endoscopic suture device. Endoscopy 2005; 37:411–4.
13. Fritscher-Ravens A, Appleyard M, Swain P. Real time echoendoscopic control of submucosal resection and polypectomy [abstract]. Gastrointest Endosc 2001;53:AB 128.
14. Siersema PD, Homs MY, Haringsma J,Tilanus HW, Kuipers EJ. Use of large-diameter metallic stents to seal traumatic nonmalignant perforations of the esophagus. Gastrointest Endosc 2003;58:356–61.
15. Fritscher-Ravens A, Park PO, Swain CP. Esophageal patches and valves: material, design and endoscopic attachment methods [abstract]. Gastrointest Endosc 2003;57:AB 83.
16. Fritscher-Ravens A, Appleyard M, Swain P. Experimental studies on anastomosis using endoscopic ultrasound [abstract]. Gastrointest Endosc 2001;53:AB 57.
17. Hill LD, Tobias J, Morgan EH. New concepts of pathophysiology of hiatal hernia and esophagitis. Am J Surg 1966; 111:70–9.
18. Low D, Anderson RP, Ilves R, Ricciardelli E, Hill LD. Fifteen- to twenty-year results after the Hill antireflux operation. J Thorac Cardiovasc Surg 1989;98:444–450.
19. Fritscher-Ravens A, Mosse AC, Ikeda K, Swain P. Transgastric endosurgical approaches to lymph nodes using EUS guidance [abstract]. Gastrointest Endosc 2005;61:AB 226.

Index

Bold type indicates illustrations.

A

abdominal ultrasonography, and chronic pancreatitis, 161, 162
abdominal vessels, 198, **198**
abscess
  after EUS-FNA, 89
  and chronic pancreatitis, 171
  colon, 317
  Crohn's disease, **306**
  liver, **125**
  pancreatic, transmural drainage, **241**
  pararectal, **307**
  presacral, **307**
  submucosal, **134**
accessory pancreatic duct, 199, **200**
accuracy
  diagnostic tests, defined, 251
  of EUS, esophageal tumors, 103
acinar-cell carcinoma, 216, **219**
acquired immune deficiency syndrome (AIDS), and pancreatic lymphoma, **222**
acute pancreatitis, Atlanta classification, 231, 232, 233
Addison's disease, and adrenal atrophy, **269,** 271
adenocarcinoma
  mucinous, pancreas, 183, 185
  pancreas, 196–207
  pancreatic duct, 276
  retropapillary, pancreas, **220–221**
  small bowel, 118, 119
adenoma
  adrenal glands, **268, 269**
  microcystic, sonoelastography, **68**
  pancreas, aspiration, **185**
  papilla, 29, **30**
  papilla of Vater, **256,** 256–257, **257**
  polycystic serous, pancreas, **231**
  rectum, **299**
  serous, *vs.* duodenal diverticulum, **222**
  small bowel, 118, 119
adenomatosis, papillary, 30, **32**
adenomyomatosis, papilla of Vater, 257–258, **258**
adrenal glands
  adenoma, **268, 269**
  adenomas, *vs.* subepithelial tumors, 123
  atrophy, **269,** 271
  calcification, **269**
  carcinoma, pancreatic metastasis, **40**
  contrast-enhanced imaging, **268**
  cross-section, 5, **5**
  diffuse enlargement, **267**
  ectopic tumors, 270
  EUS-FNA, 271
  EUS imaging, 264–272
  examination technique, 264–266
  hyperplasia, 268, **269**
  incidentalomas, 267, **267, 268**
  indications for EUS, 266
  insufficiency, **269,** 271
  left, 11, **12,** 264, 265, **265**
  in mediastinal examination, 325
  miniprobe imaging, **266**
  morphology, 266
  nodular transformation, **268**
  pathological findings, 266–271
  pheochromocytoma, **271**
  radial *vs.* longitudinal scanning, **39, 40**
  right, 14, **16,** 265–266, **267**
  small tumor, **268**
  tumors, 266–267, 268, 270, **270, 270–271**
adrenal hilum, **266, 267**
adrenal vessels, **266**
aerobilia, **257, 363**
afterloading needles, 310
AIDS, *see* acquired immune deficiency
air, in EUS examinations, 1
air-drying fixation, 84, 85
air embolism, in pancreatic interventions, 245
airways
  in mediastinal examination, 325
  wall structure, 335–336, **336**
Albarran lever, 72, 79, 80
Albunex, 276
alcohol abuse, and chronic pancreatitis, 169
aldosteronism, primary, **268**
allergic reactions, contrast imaging, 57
Aloka echoendoscopes, 355
alveolar structures, in EBUS, 337
amplitude mode (A-mode), 60
ampulla of Vater, 199, **200**
ampullary tumors, 372
amyloidosis, colon and rectum, 140
anal canal, 291, 294–296
  cancer, TNM classification, 309
  3D EUS, **315**
anal cancer, 309–310
anal crypts, 291
anal fistula, **306,** 306–307, **307**
anal margin
  cancer, TNM classification, 309
  carcinoma, **310**
anal sphincter, *see* external anal sphincter; internal anal sphincter
anal ultrasonography, three-dimensional, 310
anaphylactic risk, contrast ultrasound, 57
anastomosis
  rectum, **303**
  transgastric, **381,** 381–383, **382, 383**
anatomy
  anus, 291
  celiac plexus, 352, **352**
  from duodenum, 13–14, **15–17**
  from esophagus, 8–9, **8–10**
  EUS, longitudinal, 8–17
  heart, 9, **10**
  landmarks, EUS, 8
  levels, endoanal sonography, **295,** 296–297
  longitudinal EUS, 8–17
  mediastinum, 323
  pancreatic drainage, 238–239
  perineum, 291
  sonographic, EBUS, 335–337
  from stomach, 11, **11, 12–14,** 13
  Voxel-Man, 19, **19, 20–21**
anchor
  for endoscopic suturing, 378, **378, 379**
  in EUS-guided gastropexy, 383, 384
  in transgastric anastomosis, **382**
anesthesia, celiac plexus neurolysis, 357, **358**
aneurysms, *vs.* subepithelial tumors, 123
angiomyosarcoma, left atrium, **282**
Ann Arbor classification, lymphomas, 156
anorectal EUS
  fecal incontinence, 305–306
  interventional procedures, 307–308
anorectal muscles, EUS delineation, 296
anorectal ultrasonography (ARUS), 297, 298
antibiotic prophylaxis
  celiac plexus neurolysis, 358
  pancreatic interventions, 239, 243
anus, anatomy, 291
aorta
  arterial branches, **325**
  ascending, in mediastinal examination, 325
  descending, **20, 327**
  fibrosis, laparoscopic ultrasound, **370**
  as landmark in linear EUS, 8
  in laparoscopic ultrasonography, **368**
  thoracic, 11, **11**
  Voxel-Man and EUS, **22**
aortic arch, 8, **9,** 325
aortic lymph nodes, 323
aortopulmonary lymph nodes, 331
aortopulmonary window, 9, **9,** 323, 325, **329**
arterial aneurysms, *vs.* subepithelial tumors, 123
arteriovenous malformations, 123
artifacts, 48–49, 335, **336**
ascites, 240
aspiration, and diagnostic EUS, 88–89
aspiration biopsy needle, **367**
aspiration cyst, 89
aspirin, and hemorrhage after EUS-FNA, 92
Atlanta classification, 231, 232, 233
atrium, left, **20, 329**
attenuation threshold, microbubbles, 47
autocorrelation method, 65
autofluorescence bronchoscopy, 338, **339**
autoimmune pancreatitis, 179
axes, in 3D cube, 61, **61**
azygos vein, **325, 326**
  in EBUS, 337
  in mediastinal examination, 325

B

backscattering, in ultrasound contrast, 46
bacteremia, 89–90
bacterial infection, 240, 243
balloon catheters, 334
balloon dilation
  bile duct strictures, 29
  in pancreatic interventions, 243
balloons, and miniprobe imaging, 24
Bauhin's valve, **319**
bedside cytology, 85, **85**
benign diseases/tumors/lesions
  esophagus, 102
  small bowel, 118
  stomach, 110–111, **112**
bile duct
  anatomy, **28**
  calculi, and laparoscopic ultrasound, 373
  carcinoma, contrast imaging, 276
  drainage, EUS-guided, 360–363
  as examination landmark, 3
  IDUS, 27, **28**
  injury, in pancreatic interventions, 247
  intrahepatic, dilated, **361, 362**
  obstruction, 94
  stones, *see* choledocholithiasis
  strictures, 29–30, **31,** 33
  tumor evaluation, 256
  wall layers, 27
  see also cholangitis; hepatobiliary system
bile leakage, after biliary drainage, 362
biliary peritonitis, 90, 362

biliary tract, papillomatosis, 30, **32**
Billroth II resection, 360
biopsy
  buttonhole, 121, **123**
  channel, in LUS, 365, **366**
  equipment and technique, 71–81
  EUS-guided, *see* EUS-guided biopsy
  with linear EUS, 38–39
  in LUS, 366, 369–371
  procedure, 77–80
  transrectal, pelvic tumors, 307–308
biopsy needles, 72–76
  aspiration, **367**
  Hancke–Vilmann system, **73**
  in laparoscopic ultrasound, **369**
  nitinol, 75, **76**
  and piston locking, 73, **73**
  sheaths, 75, **75**
  stylets, **73,** 74, **74**
  tips, **76**
B-K laparoscopic ultrasound equipment, 364, 365
bleeding, *see* hemorrhage
blood pool contrast agents, 45
blood vessels, injury, in pancreatic interventions, 243, **244, 245**
bolus injection, ultrasound contrast, 47
bolus kinetics, 53–54, **54**
breast, tissue elasticity, **65**
bronchi
  anatomy, in EBUS, 335–337
  carcinoma, 328
  in mediastinal examination, 325
bronchial carcinoma, 323
bronchogenic cysts, 341
bronchoscopes, 335, 347–348, **348**
bronchoscopy, 330
  autofluorescence, 338, **339**
  mediastinum, 323
  pediatric, 343
  therapeutic, 343
Brunner's gland hyperplasia, 130, 131
buttonhole biopsy, 121, **123**

C

calcification/calculi
  adrenal glands, **269**
  and chronic pancreatitis, 166, 177, **178**
  pancreas, 169, **170**
Cambridge classification, chronic pancreatitis, 161, 162, 165, 171, 190
cancer, gastric, 112–114, **114–117**
capsule endoscopy, 156, **156**
carcinoembryonic antigen (CEA), 184, 243
carcinoid, 118, 119, 138
carcinoma
  bronchial, 323, 328
  cardia, 371
  esophagus, 102
  lungs, in situ, 338
  pancreatic head, 90
  papilla of Vater, **259**
  rectal, radial *vs.* miniprobe scanning, **42**
  small bowel, 118
  uT1, rectum, **299**
  see also cancer; staging; tumor; *specific lesions and organs*
carcinosis, peritoneal, **117, 289**
cardia
  carcinoma, staging, 371
  varices, **129**
cardiac region, in mediastinal examination, 325
Caroli's disease, **285**
cavernoma, portal vein, **130**
cavernous hemangioma, 128, **130**
cavitation, ultrasound-induced, 57
celiac plexus block/neurolysis, 360
  anesthesia, 357
  complications, 358–359
  CT-guided, 352
  EUS-guided, 90, 352–359, **357, 358**
  materials, 355–356, **356**
  postinterventional measures, 359
  preparation, 356–357
  procedure, **357,** 357–358, **358**
  sedation, 357
celiac trunk, 197, **197**
  in laparoscopic ultrasonography, **368**
  wide-band harmonic imaging, 277
chemical fixation, 84, 85
chemoradiotherapy, re-staging after, 108
chemotherapy
  gastrointestinal lymphomas, 159
  induction, EUS-FNA after, 331
chest radiography, and EUS, 330, 331
cholangiocellular carcinoma, 258
  IDUS, 30, **32,** 33
  and miniprobe EUS, 24
cholangiofibromas, **283**
cholangiography, EUS-guided, 360
cholangitis
  after EUS-FNA, 90
  chronic, and periductal fibrosis, **261**
  primary sclerosing, 30, **31**
  sclerosing, contrast-enhanced EUS, 276
cholecystectomy, 255
  laparoscopic, and LUS, 373
cholecystolithiasis, 251, **286**
  detection rates with TUS, 251
  EUS imaging, 255
choledocholithiasis, 251, 259, **260–261**
  detection rates, 252, 253
  differential diagnosis, 254
  EDUS imaging, **255**
  elastography, 259, **261**
  IDUS imaging, 28–29, **29, 30**
  miniprobe imaging, **260–261**
  transabdominal ultrasound, **251**
cholelithiasis, 251
chronic pancreatitis, 161–194, 230
  accuracy of EUS, 168
  calcification, 177, **178**
  Cambridge classification, 161, 162, 165, 171, 190
  and common bile duct stenosis, **177**
  complications, 171, **172–175**
  contrast imaging, **273**
  diagnosis, 161, 179–187
  ductal criteria, 165–166, **166**
  and enlarged lymph node, **181**
  ERCP criteria, 168
  etiology, 171, 177, 179
  EUS criteria, 165–167, **165–167,** 169, **170**
  and EUS-FNA, 168
  EUS-guided treatment, 187–189
  and EUS-TCB, 169
  and false aneurysm, **175**
  and focal lesions, 183
  hypoechoic mass lesions, **180**
  intrapancreatic collateralization, **174**
  and malignant neoplasia, 274, 276
  Milwaukee classification, 165, 166
  vs. pancreatic carcinoma, **228**
  and pancreatic head cancer, **179**
  parenchymal criteria, 165, **166**
  pitfalls, 169
  portal vessels, thrombosis, **172**
  practical hints, 179
  and pseudocysts, **167,** 233
  staging, 171, 190
  treatment, 189
ciprofloxacin, 243
classifications
  Ann Arbor, 156
  Atlanta, 231–233
  Cambridge, 161, 162, 165, 171
  contrast agents, 45
  gastric cancer, histological, 112, 113
  lymph nodes, mediastinal, **324**
  Milwaukee, chronic pancreatitis, 165, 166
  Milwaukee, sphincter of Oddi dysfunction, 258
  non-Hodgkin's lymphoma (NHL), 155
  pancreas, 208, 230–233
  small bowel tumors, 119
  stomach cancer, 112, 113
  subepithelial tumors/lesions, 126–132, 128
  TNM, 112, 113, 156, 309
  UICC, gastric cancer, 113
  WHO, 155, 208
clinical cytology, 85, **85**
clinical indications, contrast ultrasound, 55–57
coin lesion, lungs, **342**
colitis, hemorrhagic segmental, **321**
colitis cystica profunda, 130
collateralization, intrapancreatic, **174**
collateral vessels, pancreas, **188**
colon, 317–322
  cancer, and laparoscopic ultrasound, 372
  hemorrhagic segmental colitis, **321**
  transverse, lipoma, **321**
color-coded duplex sonography (CCDS)
  and chronic pancreatitis, 161, 181, **182,** 183
  and complications, 95
  and false aneurysm, pancreas, **175**
  and hemorrhage risk, 93
  peripancreatic collateral vessels, **175**
  and subepithelial lesions, 126, **127**
  subepithelial tumors/lesions, 126, **127**
color Doppler imaging
  abdominal vessels, in LUS, **369**
  EUS-guided bile duct drainage, 360, **361**
  and subepithelial lesions, 127
colorectal carcinoma/neoplasm
  and miniprobe EUS, 24, 25
  sonoelastography, **68**
color power angio (CPA) mode
  chronic pancreatitis, **167**
  and complications, 95
  intrapancreatic collateralization, **174**
  and subepithelial lesions, 127
comet artifact, 335
common bile duct, 14, **15, 16,** 162, 199, **200**
  collateral vessels, in chronic pancreatitis, **173**
  contrast-enhanced EUS, 276
  dilation, 257
  EDUS, 255–256
  IDUS, 256
  orifice, imaging, **255**
  stenosis, 171, **177,** 360
  stone, EDUS, 177, **178**
  Voxel-Man and EUS, **21**
  wall thickening, concentric, 180
  see also bile duct; choledocho-
common carotid artery, 325
common hepatic artery, 277, **278**
complication rates
  endoscopic sphincterotomy (EST), 254
  ERCP, 254
  prospective *vs.* retrospective studies, 96
complications
  celiac plexus neurolysis, 358–359
  chronic pancreatitis, 161
  EUS-guided biopsy, 80–81
  EUS-related, 2, 93–96
  EUS-specific factors, 87, 88
  fine-needle interventions, 88, 89–96
  infectious, after EUS-FNA, 89–90, 95
  prevention, 87–99

septic, pancreatic interventions, 239
subepithelial lesions, 147
compression, and tissue elasticity, **66**
computed tomography (CT), 2
celiac plexus neurolysis, 352, **352**
choledocholithiasis detection rates, 252
and chronic pancreatitis, 161, 162
cystic pancreatic lesions, 230
vs. EUS-FNA, 94
vs. EUS-guided biopsy, 307
helical, *vs.* 3D EUS, 60
mediastinum, 323, 330–331
pancreatic adenocarcinoma, 200
and pancreatic adenocarcinoma, 196
and pancreatic interventions, 240
retroperitoneal necrosis, **242**
subepithelial tumors, 122
confidence levels, in EUS practice, 6–7
Conn's syndrome, adrenal gland adenoma, **268**
contraindications, therapeutic EUS, 354
contrast agents, 44–59
artifacts, 48–49
classification, 45
dosage and administration, 46–48
doses, recommended, 48
drug-delivery systems, 45
dynamics, 53
echogenic properties, 46
intracavitary, 45
microbubbles, 45, **47**
microscopic structure, **46**
mode of action, 45–46
optimal dose, 48
oral, 45
phases in liver, **53**
specific imaging procedures, 50
see also Albunex; Levovist; Optison; SonoVue
contrast-enhanced EUS, 44–59
adrenal glands, **268**
allergic reactions, 57
bile duct drainage, 360
in chronic pancreatitis, **180, 182**
findings, 276–277
history, 44
indications, clinical, 55–57
intraductal interruption, on ERCP, 189
lymph nodes, 277, 280–281
and malignancy, 273–274
neuroendocrine tumors, **228, 275**
pancreatic EUS, 162
pancreatic masses, 202
qualitative evaluation, 52–53
quantitative evaluation, 53–55
risk, 57–58
safety, 57–58
sarcoidosis, **279–280**
contrast-specific imaging, 49–52
contrast–tissue ratio, **51**
conventional EUS, *vs.* miniprobe EUS, 37
cost-effectiveness, 37, 344, 353–354
C-reactive protein (CRP), 244, 247
Crohn's disease, 111, 302, **306, 320**
cross-section, anatomical
EUS, 2–6
and Voxel-Man, 19
Cruveilhier–Baumgarten syndrome, **287**
Cushing's syndrome, and adrenal tumors, 268
cystadenocarcinoma, 183, 210, **211–212**
cystadenoma
and complications of EUS-FNA, 95
mucinous, 210, **211**
serous, 181, 212, 215, **215**
cystic duct, lymph node, **261**
cystic hamartoma, EUS follow-up, 148
cystic lesions/neoplasms, 145, **285**
pancreas, *see* pancreas
papillary, 215, **216**
cyst infection, after EUS-FNA, 89
cystointestostomy, 236
Cystotome, 243
cysts
bronchogenic, 341
esophagus, 102
kidney, **287**
lymphatic, 130
pancreas, differential diagnosis, 183–185
cytological aspiration biopsy, 82
cytology, 82–83
capabilities and limitations, 86
cystic neoplasms, pancreas, 209
documentation, 86
mediastinal specimens, 324

D

debridement, pancreatic necroses, 237, 248
Delaunay solution, 85
delineation, contours, 55
depletion kinetics, 54–55
destruction artifacts, 48
detection rates, cholecystolithiasis, 251, **251**
detection threshold, microbubbles, 47
diagnosis
choledocholithiasis, 254
chronic pancreatitis, 179–187, 190
cystic lesions, pancreas, **184,** 209–210, **220**
definitions of terms, 251
EUS, complications, 87–89
intraductal papillary mucinous neoplasm, 212
neuroendocrine tumors, pancreas, 223
pancreas, **247,** 247–248
preoperative, rectal carcinoma, 304
serous adenoma *vs.* diverticulum, **222**
diameter, miniprobes, 23
diaphragm, **325**
diathermy, 241, 242, 243
dilation
EUS staging after, **108**
perforation risk, 88
diverticulum, **222, 321,** 324
documentation, cytology, 86
Doppler imaging, 48–49, 49, 55, 240
dosage, contrast agents, 46–48
drainage, pseudocysts, 187–188, **188,** 238–240
drug-delivery systems, ultrasound contrast, 45
duodenal bulb, cross-section, 3, **4**
duodenal diverticulum, *vs.* serous adenoma, **222**
duodenal papilla, EDUS, 256
duodenum
descending, cross-section, 2–3, **3**
EUS anatomy imaged from, 13–14, **15–17**
subepithelial tumors, **139, 143**
wall layers, 100
duplex sonography, color-coded, *see* color-coded duplex sonography
duplication cyst, foregut, infection, 89
dynamics, contrast agents, 53
dysphagia, 121

E

Eagle Claw suturing device, 379
echoendoscopes, 354–355
diameter, 37
flexible longitudinal, **36**
rigid rectal probe, **36**
echo signal, nonlinear, in ultrasound contrast, 46
EchoTip needles, **74,** 357
edema, mucosa, 100
education and training, EUS, 8
elasticity, tissue, **65,** 65–70
elastography
cholangiofibromas, **283**
and choledocholithiasis, 259, **261**
gastric cancer, **116**
liver metastases, **284**
and pancreatic metastasis, **40**
see also sonoelastography
electromagnetic navigation, and EBUS, 344, **345**
electromagnetic sensor, in 3D EUS, 62
elevators, 72, 79, 80
embolic risk, contrast ultrasound, 57
embolism, air, in pancreatic interventions, 245
empyema, 130
endoanal sonography, 291–312
anatomical levels, **295,** 296–297
examination, 297
endobronchial ultrasound (EBUS), 24, 347–351
applications, 344
artifacts, 335, **336**
clinical results, 337–338
learning curve, 343
procedure, 348, **348, 349**
technique, 335–337
endometriosis, rectum, 139, **139**
endorectal ultrasonography (ERUS), 291–312
three-dimensional, 313–316
endoscopes
EBUS-TBNA, 347–348
for EUS-guided biopsy, **71,** 71–72, **72**
flexible longitudinal, **36**
rigid rectal, **36**
rotation, in linear EUS, 9, **10,** 11, **13,** 14, **17**
sideways movement, 2
endoscopic mucosal resection (EMR), 24–25, 102
endoscopic retrograde cholangiography (ERC), 27, 360
endoscopic retrograde cholangiopancreatography (ERCP)
aerobilia after, **257**
and choledocholithiasis, 251, 253
and chronic pancreatitis, 161, 162, 167–169
complication rates, 254
and cystic pancreatic lesions, 230, 233
vs. EUS-guided biliary drainage, 362
and IDUS, 28
intraductal contrast interruption, 189
and linear EUS, 8
and pancreatic adenocarcinoma, 196
and pancreatic interventions, 240
endoscopic sphincterotomy (EST), 251, 254
endoscopic ultrasonography (EUS), 37
accuracy, 103, 114, 158, 200
adenomyomatosis of papilla of Vater, 258
adrenal glands, 264–272
bile duct drainage, 360–363
biopsy, *see* EUS-guided biopsy
and choledocholithiasis, 251, 252, 253, 254
and chronic pancreatitis, 161–194, 190
colon, 317–322
complications, 87–99
conventional *vs.* IDUS, in choledocholithiasis, 28
criteria, subepithelial tumors/lesions, 129
vs. CT, 113, 114, 122, 200
vs. CT and ERCP, pancreatic adenocarcinoma, 196
diagnostic, complications, 87–88
and endosurgery, 378–386
vs. ERCP, in chronic pancreatitis, 167–169
esophageal squamous-cell carcinoma, **38**
esophagus, 97–109, 101
experimental techniques, 378–385
fine-needle-aspiration, *see* EUS-FNA
freehand, 61–62
future techniques, 42–43
history, 36–37
indications, 18, 36, 37

endoscopic ultrasonography (EUS)
linear/longitudinal, *see* linear/longitudinal EUS
lymph-node removal, 384–385
and neuroendocrine tumors, 223
radial, *see* radial EUS
rigid rectal probe, **36**
rigid *vs.* flexible radial, rectal polyp, **39**
skills rating, 6–7
small bowel, 118
snare resection system, 380, **380**
staging, and stricture dilation, 94
stomach, 109–117
subepithelial tumors, 141, 142
therapeutic, 354
three-dimensional linear, 60–64
transbronchial, 323
transesophageal, 323, 331
Tru-Cut biopsy, and chronic pancreatitis, 169
endoscopy, before transmural pancreatic drainage, 240
endosonography, *see* endoscopic ultrasonography; EUS-
endosurgery, EUS-guided, 378–386
epidemiology
cystic pancreatic lesions/neoplasms, 209, 233–234
intraductal papillary mucinous neoplasm, 212
neuroendocrine tumors, pancreas, 223
esophageal cancer/carcinoma
fine-needle aspiration, 105, 108–109
mesenchymal, 121
miniprobe EUS staging, 24
staging, 38, 102, 103–105, **105–108**
and tracheal bifurcation, 109
esophagogastric cancer, 371
esophagogastroduodenoscopy, 155, 324
esophagus
anatomy imaged from, 8–9, **8–10**
benign diseases, 102
cancer, *see* esophageal cancer/carcinoma
EUS, 97–109
examination, optimizing, 110
fistulas, 380–381, **381**
granular-cell tumor, EUS-guided resection, **146**
leiomyoma, **136,** 341
leiomyosarcoma, **138**
and lung cancer, 339, **340,** 341
malignant tumors, 102–104
orientation, 101
squamous-cell carcinoma, **38**
subepithelial tumors, **121**
submucosal tumors, 328
tumors, *see* esophageal cancer/carcinoma
varices, 102, **103,** 276
wall layers, 100, **100, 101**
EUS, *see* endoscopic ultrasonography
EUS-FNA, 18–19, 71, 72, 82
acute recurrent pancreatitis, **181**
adrenal glands, 271
biopsy, 37, 39, 42, 82, 86, **86,** 87
and chronic pancreatitis, 168
complications, 87, 88, 89–93
contraindications, 94–95
esophageal carcinoma, 105, 108–109
indications, 189, 353
levels of difficulty, 77
limitations, 189
mediastinum, 327–328, **330,** 330–331
and neuroendocrine tumors, 223, **227**
and pancreatic cysts/lesions/neoplasms, 89, 185, **185,** 203, **204,** 204–206, **205,** 209, 274
rectal carcinoma, 305
sepsis after, 89
and subepithelial lesions, 126, **127,** 144–145
with TBNA, 350
tips and tricks, 82–86
and tumor staging, 100
EUS-guided biopsy, 71–81
and clinical data, 85
complications, 80–81
fixation and staining, 83–85, **85**
insulinoma, **79**
needle movement in lesion, 80, 83, **83**
needle system attachment, **78**
needle tip markings, 76, **76**
specimen handling, 83, **83**
tips and tricks, 78
EUS Meets Voxel-Man, 18–22
examination
3D EUS, in patients, 63–64
endoanal sonography, 297
esophagus, 101
mediastinum, 324–325
procedures, 2
sequence, longitudinal EUS, 8
stomach, 109–110
systematic, 20
technique, adrenal glands, 264–266
time, IDUS, 27
Exera II processors, 355
extended combined autocorrelation method, 65
external anal sphincter, 291, **292, 293,** 294, **294,** 295
as anatomical level in EUS, 296
normal values, 296
parts, 296
sonoelastography, **68**
extraductal ultrasonography (EDUS), 24, 26
choledocholithiasis, 177, **178, 255**
common bile duct, 255–256
duodenal papilla, 256
and pancreatic duct obstruction, 177
extraluminal lesions, gastrointestinal tract, 121
extramural impressions, 122–123, **124**
EZ Shot, biopsy needles, **75**

F

fecal incontinence, 305–306
fibrolipomas, 132
fibroma, 102, 119
fibrosarcoma, small bowel, 119
fibrosis, retroperitoneal, laparoscopic ultrasound, **370**
fibrovascular polyps, 132
filter procedures, frequency, 49
fine-needle aspiration/puncture, *see* EUS-FNA
fine-needle intervention (FNI), 88, 358
finite element method, 3D, 67
fistulas
closing, 380–381, **381**
colon, 317
Crohn's disease, **320**
horseshoe, **306**
miniprobe imaging, **320**
pancreas, 240
and pancreatic pseudocysts, 235
trans-sphincteral, **307**
fistulotome, biliary drainage, **361, 363**
fixation, EUS-guided biopsy, 83–85, **84**
flash echo imaging, 52
flow rates, spectral Doppler, 48–49
fluid collections
pancreas, 234, 238–240
pelvic, 308–309, **309**
peripancreatic, 231–232
postacute, 231
fluoroscopy, 341, 360
focal lesions, 55, 56, **56**
vs. pancreatic cancer, 179–183
foregut duplication cyst, infection after EUS-FNA, 89
foveolar hyperplasia, stomach, 111
freedom of movement, in 3D EUS, 62
freehand ultrasound
in 3D imaging, 61–62
tracked, 313
free radicals, and contrast ultrasound, 57
frequency filter procedures, 49
Fujinon echoendoscopes, 355
fundic varices, **174**

G

gallbladder, 14, **17, 21,** 282, 286
carcinoma, 259
collateral vessels, in chronic pancreatitis, **173**
and contrast-enhanced EUS, 277
imaging from colon, **318**
impression on gastric fundus, **124**
malignancy, contrast imaging, 276
microcalculi, 177, **178**
gallstones, 251, 254–255, 372–373
ganglioneuromas, 183
gas, contrast microbubbles, 46
gastrectomy, and bile duct drainage, 360, **360**
gastric artery, left, **20,** 197, **197, 368**
gastric cancer, 147
elastography, **116**
in laparoscopic ultrasound, **369**
staging, **114, 115, 116**
gastric mapping, 155
gastric mucosa, heterotopia, 130, 131, **132**
gastric varices, and pancreatic pseudocysts, 235
gastric vein, left, Voxel-Man and EUS, **20**
gastric wall, 14, 16, **17, 110,** 385
see also stomach
gastrinoma, 33, 119, 223
gastritis, large-fold, **41,** 111, **112**
gastritis cystica profunda, 130, **132**
gastrointestinal cancer, laparoscopic ultrasound staging, 371
gastrointestinal lymphoma, **157,** 159, **159**
Ann Arbor classification, 156
capsule endoscopy, 156, **156**
chemotherapy, 159
clinical presentation, 155
diagnosis, 155–156, 155–160
diagnosis and treatment planning, 155–160
EUS appearance, 159
EUS relevance, 156–158
and *H. pylori* eradication, 159
prognosis, 156
radiotherapy, 159
staging, 155–156
treatment planning, 159
gastrointestinal perforation, risk in EUS, 87
gastrointestinal stromal tumor (GIST), 128, 134–135, 143, **143,** 148, 149, **289**
colon and rectum, 139
prognostic criteria, 135
rectum, **141**
stomach, **121, 123,** 125, 126, **127,** 137–138, **138**
gastrointestinal tract
mass lesions, 121
subepithelial tumors, 121–154
tumor staging, 38
varices, 121
wall, examination, 14, 16, **17**
gastrojejunal anastomosis, 381
gastrojejunostomy, endoscopic, 381
gastropexy, **383,** 383–384, **384**
gastroscope
in endoscopic lymphadenectomy, 385
snare resection system, 380, **380**
geometrical relationship, 2D images in 3D cube, 61, **61**

Giovannini Needle Wire, 243
GIP/Medi-Globe needle systems, 355
golden rules, EUS, 1
granular-cell tumors, 136–137, 138, 140, **146**
guide wires, 242, 360, **362**
gynecology, and laparoscopic ultrasound, 374

H

hamartoma, 118, 119, 130, 131, 148
Hancke–Vilmann needles, **73, 83,** 355, **356**
hardening of tissue, 65
harmonic imaging, 49, **49, 51**
harmonic oscillations, in ultrasound contrast, 46
harmonic power Doppler, 49
heart, 9, **10, 20,** 282, **282,** 325, **325, 329**
heavy cube transmitter, in 3D EUS, 62, **62**
Helicobacter pylori, 155, 159
Hemacolor staining kit, **85**
hemangioma, **283**
  cavernous, 128, **130,** 136
  esophagus, 102
  EUS follow-up, 148
  rectal venous plexus, **303**
  small bowel, 119
hemangiosarcoma, small bowel, 119
hematoma, after EUS-FNA, 90, **91**
hematothorax, 90
Hemoclips, 243
hemolysis, and contrast ultrasound, 57
hemorrhage/bleeding
  after EUS-FNA, 89, 90–93, **91, 92**
  after EUS-guided biliary drainage, 362
  gastrointestinal, 121
  and GISTs in stomach, 138
  intraluminal, after EUS-guided intervention, 93, **93**
  pancreatic pseudocysts, 235
  risk, 93, 324
  subepithelial lesions, **122,** 147
  and transmural puncture, pancreatic fluid collections, 239
hemosuccus pancreaticus, 235
heparin, low-molecular-weight, 90
hepatic vessels, 13, 14, **14, 17,** 197, **197,** 325
hepatobiliary system, 27, 251–263
hepatocellular carcinoma, and laparoscopic ultrasound, 374
heterotopia, pancreatic, 130, 131–132, **132, 133,** 145, 148
hiatus hernia, and EUS-guided gastropexy, 383
hilar vascularization, 327
histological classification, gastric cancer, 113
histology, cystic neoplasms, pancreas, 209
history of ultrasound, 36–37, 44
Hitachi instruments, 355, 365, **365**
honeycomb pattern, pancreas, 165, **166, 222**
horizontal rotation, in 3D EUS, 61
horseshoe fistula, **306**
hydrogen peroxide instillation, anal fistula, 306
hydronephrosis, **288**
hyperaldosteronism, 268, **269**
hyperparathyroidism, 240
hyperperfusion, 53
hypervascularization, 273–274
hypoechoic subepithelial tumors, 137, 141–143
  benign, **142**
  colon and rectum, 139–140
  duodenum, 138–139
  esophagus, 136–137
  malignant, **143**
  stomach, 134, 137–138
hypoperfusion, 53, 276

I

ileocecal valve, **319**
ileum, terminal, **319, 320**
implantation metastasis, 93
incidental findings, 282–290
incidentalomas, 267, **267, 268**
indications
  anorectal ultrasonography (ARUS), 298
  contrast ultrasound, 55–57
  endorectal ultrasonography (ERUS), 297, 298
  esophageal EUS, 101
  EUS-FNA, 353
  EUS in stomach, 110
  therapeutic EUS, 354
infection, spontaneous, pseudocysts, 235
infectious complications, EUS-FNA, 95
inferior pulmonary ligament, 323
inferior vena cava (IVC), 14, **16, 22,** 325
  involvement by adrenal tumor, **270–271**
  as landmark in linear EUS, 8
inflammatory fibroid polyps, 134, 136, 137, 138
inflammatory vascular polyp, 138
insonation power, low, 51–52
instruments
  EBUS-TBNA, 347–348
  endoanal sonography, 297
  mediastinal EUS, 332
  mediastinal examination, 324
  positioning in stomach, 1
  see also echoendoscopes; endoscopes; miniprobes; probes
insulinoma, 33, **79,** 119, 223, **224–225,** 276
internal anal sphincter, 291, **291–292, 293,** 294, 295
  as anatomical level in EUS, 296
  normal values, 296
  sonoelastography, **68**
interobserver variation, EUS in pancreas, 219
interventional procedures
  anorectal EUS, 307–308
  fine-needle, complications, 88, 89–96
  with linear EUS, 38–39
  pancreas, 230–250
  transluminal EUS, 378
intestinal lymphoma, 155, 156
intestinal obstruction, 121
intra-abdominal examinations, 364
intraductal papillary mucinous neoplasms/tumors, 177, 183, 185, **186,** 210, 212, **213–215**
  branch duct type, 210
  main duct type, 210, 212
  peritoneal dissemination, 93
intraductal ultrasonography (IDUS), 23, 24, 27–35
  choledocholithiasis detection rates, 253
  common bile duct, 256
  indications, 34
intrahepatic bile duct, dilated, **361, 362**
intraoperative ultrasonography (IOUS), 227
intrapulmonary lesions, 341
intrathoracic examinations, 364
ischemia, contrast diagnosis, 55
ischiorectal space, 296
islet-cell tumors, cystic, 183
islet transplantation, autologous, 237

J

jugular vein, 325
jumbo biopsies, risk, 121

K

Kaposi's sarcoma, small bowel, 118, 119
Kerckring folds, **290**
kidney, 11, **12,** 286, **289**
  imaging from colon, **318, 319**
  parenchymal cysts, **287**
  right, 14, **16**
kinetics
  depletion, 54–55
  replenishment, 54, **54**
Klatskin tumor, 256

L

landmarks, anatomical, Voxel-Man, 20–21, **20–21**
laparoscopic ultrasound (LUS), 364–377
  and ampullary tumors, 372
  and bile duct calculi, 373
  biopsy procedure, 369–371
  and cardia carcinoma, 371
  colon cancer, 372
  equipment, 364–366, **365, 366, 367**
  and esophagogastric cancer, 371
  and gallstone disease, 372–373
  and laparoscopic cholecystectomy, 373
  and liver disease, **373,** 373–374
  and pancreatic cancer, 371–372
  procedure, 366–369
  and treatment, 374–375
  working situation, **368**
Lauren histological classification, 113
learning curve, EBUS, 343
leiomyoblastoma, 125, 134, 138
leiomyoma, 121, 134, 135
  colon and rectum, 139
  duodenum, 138
  esophagus, 102, **102, 136,** 341
  small bowel, 118, 119
leiomyomatosis, esophageal, 136
leiomyosarcoma, 134
  colon and rectum, 139
  esophagus, **138**
  small bowel, 119
levator ani muscle, 291, 296
Levovist, detection of malignancies, pancreas, 274
lightweight sensor, in 3D EUS, 62, **62**
linear/longitudinal EUS, 8–17, 18, 36, 37–39
  adrenal gland, **39, 40**
  mediastinum, 324
  vs. miniprobe, large-fold gastritis, **40**
  pancreatic metastasis, **40**
  subcarinal lymph nodes, **40**
  three-dimensional, *see* three-dimensional linear EUS
lipoma
  colon and rectum, 139
  esophagus, 102, **102**
  resected, **146**
  small bowel, 118, 119
  submucosal, 132, **133, 134**
  transverse colon, **321**
liposarcoma, small bowel, 119
liver, **325**
  abscess, **125**
  contrast phases, **53**
  as examination landmark, 4
  fatty, **285, 319**
  hilum, **17,** 197, **197**
  imaging from colon, **319**
  left lobe, 4, 13, **14,** 282
  lesions, contrast diagnosis, 56, **56**
  and LUS, 368, **373,** 373–375, 374
  metastases, **283–284, 368, 369, 370, 373**
  vessels, 14, **17**
  Voxel-Man and EUS, **21**
  see also hepatic; hepatobiliary system; hepatocellular; perihepatic
longitudinal EUS, *see* linear/longitudinal EUS
longitudinal muscle, in endorectal ultrasound, 297

longitudinal scanners, 8
low mechanical index imaging, 51–52
low-molecular-weight heparin (LMWH), 90
Lugano lymphoma classification, 156
luminal narrowing, and complications, 94
lung cancer
  esophageal infiltration, 339, **340**
  mediastinal infiltration, 339
  non–small-cell, 328–331
  primary, 338–339, 341
  pulmonary artery infiltration, 339, **340**
  staging, 338–341
lungs
  embolism, **282**
  intrapulmonary lesions, 341
  lymph nodes, 323
  parenchyma, 282
  see also pulmonary
LUS, *see* laparoscopic ultrasound
lymphadenectomy, endoscopic, 385
lymphangioma
  cavernous, 131
  colon and rectum, 139
  cystic, 130, 131, 183
  esophagus, **131**
  EUS follow-up, 148
  small bowel, 119
lymphangiosarcoma, small bowel, 119
lymphatic cysts, 130
lymph nodes
  aortic, 323
  aortopulmonary, 331
  contrast-enhanced EUS, 277, 280–281
  enlarged, and chronic pancreatitis, 189
  EUS-guided biopsy, 281
  infiltration, gastric cancer, **116**
  involvement, LUS scanning, 369
  levels, mediastinum, 332
  in lung cancer, 339, 341
  malignancy criteria, pancreas, 203, **204**
  malignant, *vs.* GIST, 125
  mediastinal, 323, **324,** 327, 328
  metastases, esophagus, 102
  N1–N3, 323
  paraesophageal, 323
  paratracheal, 323, 325
  periesophageal, **329,** 331
  perihepatic, **278, 286**
  pulmonary, 323
  puncture, EBUS, **348, 349**
  radial *vs.* longitudinal scanning, **40, 41**
  removal, EUS-guided, 384–385
  scalene, 323
  sentinel, 385
  staging, 328–329, 347
  subcarinal, 323, 325, **329,** 331
  supraclavicular, 323
lymphoma
  and complications of EUS-FNA, 95
  and extramural impression, 123
  gastrointestinal, *see* gastrointestinal lymphoma
  intestinal, 155, 156
  and miniprobe EUS, 24
  non-Hodgkin's, **288**
  pancreas, 219, **222**
  small bowel, 118, 119
  T-cell, stomach, **139**

M

magnetic resonance cholangiopancreatography (MRCP)
  choledocholithiasis detection rates, 253
  and chronic pancreatitis, 161
  and cystic pancreatic lesions, 233
magnetic resonance imaging (MRI)
  bile duct, 28
  vs. 3D EUS, 60
  vs. EUS, cystic pancreatic lesions, 230
  vs. EUS-guided biopsy, 307
  mediastinum, 323
  and pancreatic interventions, 240
main pancreatic duct, dilation, 185, **185,** 187
malignancy, and lymph node size, 327
malignancy criteria
  bile duct strictures, 29, 33
  pancreatic duct strictures, 33
malignant lesions/tumors
  and chronic pancreatitis, 276
  and contrast enhancement, 273–274, **274**
  small bowel, 118
manometry, in EUS-guided gastropexy, 384
mapping, gastric, 155
marginal-zone B-cell lymphoma, stomach, **157**
mass lesions
  fluid, impression on gastric wall, **125**
  gastrointestinal tract, 121
  pancreatic, 90
May–Grünwald–Giemsa staining, **84,** 85
mechanical index (MI), 51
mechanical transducer, 334
mediastinitis, risk, 324
mediastinoscopy, 323, 331, 344
mediastinum, 323–333
  anatomy, 323, 336, **337**
  central, cross-section, 5, **6**
  cysts, *vs.* subepithelial tumors, 123
  diagnostic work-up, 331
  EUS-FNA, 327–328, 328, **330**
  examination procedure, 325
  examination techniques, 324–325
  hematoma, after EUS-FNA, 90, **91**
  imaging methods, 330–331
  infiltration, lung cancer, 339
  lesions, lung cancer, 341
  limitations of EUS, 331
  lower, cross-section, 5, **5**
  lymph nodes, 323, **324,** 328, 347, 384–385
  masses, unknown, 328
  mass lesions, and complications of EUS-FNA, 95
  orientation in EBUS, 336
  posterior, 323
  transesophageal EUS, 331
  ultrasonography, transthoracic, 323
  upper, cross-section, 5–6, **6**
Medi-Globe biopsy needles, 73, 74, **74,** 75, **76,** 355
melanoma metastasis, EUS-FNA, 93
Ménétrier's disease, 111, **112**
mesenchymal tumors, 121, 130, 134, 149
  colon and rectum, 140
  phenotypic characterization, 135
mesenteric vessels, 199, **199**
mesorectal tumor involvement, 3D EUS imaging, 315
metal spiral, in EUS-guided biopsy, 77, 78
metastases
  adrenal glands, 271
  hemorrhage risk, 90
  liver, **283–284**
  stomach, 138
MI, *see* mechanical index
microbubbles, 46
  attenuation threshold, 47
  concentration after bolus administration, **47**
  detection threshold, 47
  insonation behavior, **47**
  oscillation in sound field, **47**
  shell, 45
microlithiasis, **286**
Milwaukee classification
  chronic pancreatitis, 165, 166
  sphincter of Oddi dysfunction, 258
miniprobe endobronchial ultrasound, 334–346
miniprobe EUS, 23–26
  adrenal glands, **270**
  application, 24–26, 335
  choledocholithiasis, **260–261**
  colon examination, 317
  vs. conventional EUS, 37
  and 3D EUS, 314
  diseases evaluated, 25
  durability and price, 24
  endobronchial ultrasound, 334–346
  esophageal cancer, **105, 107**
  fistulas, **320**
  frequencies, 23, 27
  future developments, 26
  and gastrointestinal lymphomas, 158
  handling, 334–335
  hepatobiliary lesions, 255
  history, 36–37
  in IDUS, 23, 24, 27
  penetration depth, 37
  preparation, 334–335
  vs. radial, rectal carcinoma, **42**
  vs. radial *vs.* linear, 36–43, **41**
  selection, to prevent complications, 94
  storage, 334–335
  subcarinal lymph nodes, **329**
  technical considerations, 23–24
  transbronchial, 331
  for vessel identification, 245
  wear and lifespan, 27
Mirizzi syndrome, and IDUS, 29
mirror artifact, 335
molecular biology, mediastinal specimens, 324
morbidity rates, EUS and EUS-FNA, 96
mortality, EUS, 88, 96
mucinous cystadenoma, 210, **211**
mucinous duct ectasia, 210, 212
mucinous tumors, 181
mucoceles, 130
mucosa-associated lymphoid tissue (MALT) lesions, 25, **157,** 159
mucosal edema, 100
mucus-producing tumor, pancreas, **231**
multiplane viewing technique, 3D ultrasound, 313
mural abscess, 130
muscularis propria, endoanal sonography, 296
myogenic tumors, 135
myxoma, esophagus, 102

N

narrowing, luminal, and complications, 94
nasocystic catheter, 243
nasocystic drains, pancreatic interventions, 240
nasocystic irrigation, after pancreatic intervention, 243
nasogastric irrigation, after pancreatic intervention, 245
navigation, electromagnetic, and EBUS, 344, **345**
necrosis
  gastric wall, **242**
  infected, pancreas, 233, 240
  pancreatic, debridement, 241, 244
  retroperitoneal, **242**
necrotic cavity, retroperitoneal, 244, **246**
needle guidance, in LUS, 375
needle-knife papillotome, 242
needles
  cover case, laparoscopic ultrasound, **366**
  EBUS-TBNA, 347–348, **348**
  in endoscopic lymphadenectomy, 385
  for EUS-guided pancreatic drainage, 241
  movement in lesion, 80, 83, **83**

movement in ultrasound field, **18,** 19
systems, 355–356
tip, markings, 76, **76**
needle-tract seeding, in EUS-FNA, 93
negative predictive value, defined, 251
neoplasms, cystic, *see* cystic lesions/neoplasms
neurilemmoma, small bowel, 119
neuroendocrine tumors, 181
colon and rectum, 139–140, **140**
and complications of EUS-FNA, 95
hemorrhage risk, 90, **91**
mimicking gastric carcinoma, **117**
pancreas, 33, 223–228, **225, 275**
papilla of Vater, **259**
somatostatin-receptor scintigraphy, 227
stomach, 138
neurofibroma, 119, 134
neurofibrosarcoma, small bowel, 119
neurogenic tumors, 134, 135
neurolysis, celiac plexus, 352–359
nitinol biopsy needles, 75, **76**
N1–N3 lymph nodes, 323
non-Hodgkin's lymphoma (NHL), 155, **222, 288**
nonlinear echo signal, in ultrasound contrast, 46
non–small-cell lung cancer (NSCLC), 328–331
nonsteroidal anti-inflammatory drugs (NSAIDs), and hemorrhage, 92
N staging
esophageal tumors, 104, 105
gastric cancer, 114
rectal cancer, 304, 314

O

obstruction, intestinal, 121
Olympus biopsy needles, 73, 74, **75**
Olympus echoendoscopes, 355
operating costs, EUS, 37
Optison, and pancreatic adenocarcinoma, 276
oral contrast agents, 45
orientation
esophagus, 101
radial EUS, **2**
stomach, 109
Osler's disease, **284**
vs. submucosal tumor, stomach, **117**
ovarian carcinoma, subepithelial metastasis, **139**
overstaging, rectal carcinoma, 305

P

pancreas, 11, **12,** 13
abscess, transmural drainage, **241**
adenocarcinoma, *see* pancreatic adenocarcinoma
adenoma, aspiration, **185**
AIDS and lymphoma, **222**
anatomic variants, 169
anatomy, and transmural drainage, 238–239
and biliary IDUS, 27
biopsy, **79,** 79–80
cancer/carcinoma, *see* pancreatic cancer/carcinoma
collateralization, **174**
contrast-enhanced EUS, 273–281
cystic lesions/neoplasms, *see* pancreatic cystic lesions/neoplasms
differential diagnosis, **247,** 247–248
ductal adenocarcinoma, 276
ductal carcinoma, *vs.* pseudocyst, 219, **220**
EUS, 162–165, **163–165,** 197–199, **197–199**
fluid collections, etiopathogenesis, 234
function tests, 161
golden V view, 3
head, imaging from colon, **319**
infected necrosis, 233
interventions, 230–250, 239, 243, **244, 245,** 246
intraductal papillary mucinous neoplasm/tumor, 185, **186,** 210, 212, **213–215**
as landmark in linear EUS, 8
lesion, cystic, after EUS-FNA, 89
lymphoma, 219, **222**
malignancy, 180, 271
masses, and complications of EUS-FNA, 95
mass lesions, 90
metastasis, radial *vs.* longitudinal scanning, **40**
mucus-producing tumor, **231**
necroses, 237, 248
neuroendocrine tumors, 33, 223–228, **275**
normal findings, 163
operability, and contrast-enhanced EUS, 277
parenchymal calcification, **170**
peripancreatic collaterals, **175**
polycystic serous adenoma, **231**
pseudocysts, *see* pancreatic pseudocysts
puncture position, 243
puncture sets, 243
rare neoplasms, 216, 219, **219, 220–222**
resection, left, 237
solid lesions/neoplasms, 177, 190
stenosis, papilla, 185, **186**
stones, **170**
surgery, 247
teratoma, 216, **217–218**
therapeutic approaches, 234–247
transmural drainage, and retroperitoneal necrosis, **242**
transmural operation, 240–247
tumors, *see* pancreatic cancer/carcinoma
vascular structures, 202
Voxel-Man and EUS, **21**
see also pancreatic body; pancreatic duct; pancreatic head; pancreatic tail
pancreas divisum, 162
pancreatic adenocarcinoma, 196–207
CT *vs.* EUS, 200
differential diagnosis, 201
EUS-FNA, **204,** 204–206, **205**
lymph-node assessment, 203
M stage, 203–204
N stage, 203, **204**
retropapillary, **220–221**
staging, 200–203
T stage, 200–203, **201**
pancreatic body, 11, **12, 197**
imaging from colon, **318**
Voxel-Man and EUS, **21**
pancreatic cancer/carcinoma, **125,** 200, **203**
vs. chronic pancreatitis, **228**
classification, 208
contrast imaging, **274**
cystic, 33, 208–229
differential diagnosis, 201
epidemiology, 196
EUS-FNA, 274
vs. focal inflammatory masses, 179–183
and laparoscopic ultrasound, 371–372, 372
pancreatic cystic lesions/neoplasms, 177, 190, 208–229, 243
aspiration, 243
classification, 230–233
definition, 230
differential diagnosis, 183–185, **184,** 209–210
epidemiology, 209, 233–234
EUS-FNA, 185, **185**
hemorrhage after EUS-FNA, **92**
MRCP, 233
papillary, 215, **216**
pitfall, **222**
therapy, 210
pancreatic duct, 13, **13,** 14, **15, 16,** 161, 199, **200**
accessory, 199, **200**
adenocarcinoma, contrast-enhanced EUS, 276
dilation, **167,** 189
EUS-guided drainage, 90
as examination landmark, 3
IDUS, 27, **28,** 33
main, dilation, 185, **185,** 187, 201, **202**
orifice, imaging, **255**
stones, 3D imaging, **63**
strictures, malignancy criteria, 33
system, 161
Voxel-Man and EUS, **21**
pancreatic flow, 246
pancreatic head, 13, **13, 15,** 198, **199**
cancer, and chronic pancreatitis, **179**
carcinoma, 90
honeycomb pattern, **222**
tumor, 201, **201, 202**
tumors, EUS-FNA, **205**
Voxel-Man and EUS, **21**
pancreatic heterotopia, 130, 131–132, **133**
EUS follow-up, 148
stomach, 145
pancreaticobiliary strictures, 360
pancreaticoduodenal artery, **20**
pancreaticoduodenectomy, 236
pancreaticojejunostomy, 236
pancreatic pseudocysts, **125, 176,** 187, **188,** 208, 237, 360
and chronic pancreatitis, **167,** 171, 233
conservative treatment, 236
and contrast-enhanced EUS, 277
diagnostic issues before EUS, 187
differential diagnosis, 183–185
drainage, **19,** 187–188, **188,** 237, 238–240, **244, 246,** 248
interventional treatment, 236–237, 239
pancreatic tail, **174**
spontaneous course, 234, 235–236
spontaneous infection, 235
spontaneous rupture, 235
pancreatic tail
mass *vs.* chronic pancreatitis, **182**
pseudocyst, **174**
pancreatitis, 237
acute, 89, 90–93, 161, 231, 232
acute recurrent, 171, **181,** 185
autoimmune, 179
chronic, *see* chronic pancreatitis
complications, morphological, **247,** 247–248
and hyperparathyroidism, 240
idiopathic, after EUS-FNA, 90
idiopathic recurrent, 171
and IDUS, 33
lymphoplasmacytic sclerosing, 179, 180
pancreatoduodenectomy, pylorus-preserving, 34
pancreatogastrostomy, EUS-guided, 90
pancreatography, EUS-assisted, 189
Papanicolaou solution, 85
papilla, adenoma, 29, **30**
papilla of Vater, 14, **15, 16,** 199, **200**
adenoma, 34, **256,** 256–257, **257**
carcinoma, **259**
criteria for noninvasive neoplasm, 258
criteria for tumor, 258
cross-section, 3, **3**
inflammation, **257**
neuroendocrine tumor, **259**
papillary cystic neoplasm, 215, **216**
papillitis, papilla of Vater, **257**
papillomatosis, biliary tract, 30, **32**
para-aortic region, cross-section, 4, **4**
paragangliomas, 183
parametric imaging, 54–55
paratracheal lymph nodes, 323, 325
paratracheal structures, 323
parenteral nutrition, and pancreatic pseudocysts, 236

Paris staging system, gastrointestinal lymphomas, 156
Partington–Rochelle pancreaticojejunostomy, 236
patches, for esophageal fistula closure, 380–381, **381**
patients
  cooperation, in EUS-guided biopsy, 77
  information, 240, 324
  position, and imaging from duodenum, 14
  preparation, 2, 77, 297
pectinate line, 291
pediatric bronchoscopy, 343
pelvic fluid collections, 308–309, **309**
pelvic tumors, transrectal biopsy, 307–308
penetration depth
  IDUS, 27
  miniprobe EUS, 37
Pentax echoendoscopes, 355
percutaneous drainage, pancreatic pseudocysts, 237
percutaneous endoscopic gastrostomy (PEG), 243, 245
percutaneous transhepatic cholangiographic drainage (PTCD), 360
perforating veins, contrast imaging, 276
perforation
  EUS-guided treatment, 145, 147
  risk, 2, 87, 88
  and stricture dilation, 94
perfusion
  abnormalities, 53, **53**
  in contrast imaging, 53, 55
  real-time imaging, 51
pericardial cavity, **325**
pericholangitis, **261**
periesophageal lymph nodes, **329,** 331
periesophageal structures, assessment, 108–109
perigastric lymph nodes, 384–385
perihepatic varices, **287**
perineum, 291, 310, **310**
peristaltic movements, and instrument position, 1
peritoneal carcinosis, **117, 289**
peritoneal dissemination, IPMT, 93
peritoneum, 289
peritonitis, biliary, 90, 362
phase inversion imaging, 49
pheochromocytoma, adrenal glands, 270, **271**
photodynamic therapy, lung cancer, 338
piston locking, biopsy needles, 73, **73**
pitfalls
  chronic pancreatitis diagnosis, 169
  subepithelial tumors/lesions, 125–126, 128, 143–144, **144,** 145, **146,** 147
pleura, and lung cancer, 341
pneumology, and mediastinal EUS-FNA, 328
polypoid lesions, bile ducts, 30
polyps
  fibrovascular, 132
  gastric, 110, **111**
  inflammatory fibroid, 134, 136, 137, 138
  rectal, rigid *vs.* flexible radial EUS, **39**
portal hilum, Voxel-Man and EUS, **21**
portal hypertension, 111, **112**
  hemorrhage risk, 90
portal vein, **172**
  cavernoma, **130**
  contrast-enhanced EUS, **278**
  obstruction, 198
  thrombosis, **172**
  wide-band harmonic imaging, 277
portal venous confluence, 11, **13**
portal vessels, thrombosis, **173**
portosplenic vessels, **172**
portosystemic shunts, and chronic pancreatitis, 171
positioning/tracking system, in 3D EUS, 62
positive predictive value, defined, 251
postacute fluid collections, 231
power Doppler imaging, 327
PowerShot, biopsy needles, **75**
pretracheal structures, 323
primary sclerosing cholangitis, IDUS, 30, **31**
probes, miniaturized, *see* miniprobes
procalcitonin, 240
procedure, results, 349–350
proctitis, **295**
propofol sedation, 240
prostate gland, **293,** 295, 308, **317**
pseudoallergic reactions, contrast, 57
pseudoaneurysm, pancreas, 183–185
pseudocystoduodenostomy, 236
pseudocystogastrostomy, **93,** 236
pseudocystojejunostomy, 236
pseudocysts, *see* pancreatic pseudocysts
pseudolymphoma, small bowel, 119
pseudopapillary tumors/neoplasms, 183, 215, **216**
puborectalis muscle, 295
pulmonary artery, 325, 336, 337, 339, **340**
pulmonary complications, pancreatic interventions, 246
pulmonary ligament, 331
pulmonary lymph nodes, 323
pulmonary nodules, structural analysis, **342**
pulmonary trunk, 325
pulse inversion imaging, 49
pulse summation procedures, 49–51, **50, 51**
puncture, transmural, 238
puncture sets, 243
pusher tube, bile duct drainage, 360
pyelectasia, **287**
pyloric sphincter, hypertrophy, 125, **125, 126**

Q

qualitative evaluation, contrast, 52–53
quantification, in sonoelastography, 67, 69
quantitative evaluation, contrast, 53–55
Quick-Core needle, 76

R

rabbit's ear artifact, 335
radial EUS, 1–7, 8, 18, **18,** 36–43
  adrenal gland, **39, 40**
  history, 36
  large-fold gastritis, **41**
  vs. linear/longitudinal, 37–39
  lymph nodes, **40, 41**
  orientation, **2**
  and orientation in esophagus, 101
  pancreatic metastasis, **40**
  rectal carcinoma, **42**
  rigid *vs.* flexible, rectal polyp, **39**
  three-dimensional, 60
radiofrequency ablation, **367**
radiography, conventional, 323
radiotherapy, 159, 380
real-time perfusion imaging, 51
reconstruction, three-dimensional, 313
rectal cancer/carcinoma, **140,** 298
  EUS-guided biopsy, 308
  follow-up, 305
  N staging, 304
  preoperative diagnosis, 304
  radial *vs.* miniprobe scanning, **42**
  recurrences, 139, 305, 308
  staging, 3D EUS, 314, 315
  T staging, **298, 300, 301,** 304
rectum
  adenoma, **299**
  anastomosis, **303**
  cancer, *see* rectal cancer/carcinoma
  carcinoid, **302**
  cavernous hemangioma, **130**
  3D EUS, **315**
  extramucosal recurrence, **303**
  gastrointestinal stromal tumors (GISTs), **141**
  polyp, rigid *vs.* flexible radial EUS, **39**
  subepithelial tumors, **141**
  venous plexus, 291, **303**
  wall, as anatomical level, 296
reference positions for EUS, 20–21, **20–21**
reflex echoes, 335, **336**
reflux disease, and EUS-guided gastropexy, 383
renal-cell carcinoma, 181
rendering techniques, 3D ultrasound, 313
replenishment kinetics, 54, **54**
resolution, 27, 37
re-staging after chemoradiotherapy, 108
retention cysts, pancreas, 208
retroperitoneum, 244, **246,** 286, **369**
rigidity, miniprobes, 23
risk
  buttonhole biopsies, 121
  of EUS, 2, 87–99, 96
rotation
  artifact, **336**
  of endoscope, in linear EUS, 9, **10,** 11, **13,** 14, **17**
  transducer, in 3D imaging, 61
Roux-en-Y loop, and EUS-guided bile duct drainage, 360, **360**
rupture, spontaneous, pancreatic pseudocysts, 235

S

safety of EUS, 57–58, 87, 95, 96
salt-and-pepper texture, pancreas, 199
sampling errors, FNAB, 86, **86**
Santorini's duct, 199, **200**
sarcoidosis, **279–280**
sarcoma, small bowel, 118
saturation artifacts, 48
scalene lymph nodes, 323
schwannoma, 134, 135
  colon and rectum, 140
  duodenum, 138
  stomach, 138, **138**
sclerosing cholangitis, 276
scope, *see* endoscope
secretin–pancreozymin test, 161
secretin test, 165
sedation, 2
  for adrenal gland examination, 265
  for celiac plexus neurolysis, 357
  in mediastinal examination, 324
  pancreatic interventions, 240
seminal glands, 297
seminal vesicles, **293**
sensitivity
  diagnostic tests, 251
  T staging, 104
sensor, in 3D EUS, 62, **62,** 64
sentinel lymph nodes, 385
sepsis, 89, 239
serous cystadenoma, 212, 215, **215**
shadow artifacts, 48, **336**
sheaths, for biopsy needles, 75, **75**
sideways movement, endoscope, 2
signal–clutter ratio, 49
signal enhancers, 55
simple cysts, pancreas, 208
sinus pyelectasia, **287**
skill in EUS, 6–7, 353
small bowel, 118, 289
  and transgastric anastomosis, 381, **381**
  tumor classification, 119
  vasculitis, **290**

small-cell lung cancer, **117**
small intestine, *see* small bowel
smear preparation/technique, 80, 83, **84, 85,** 86
smoking, and chronic pancreatitis, 169, 179
snare resection system, EUS-guided, 380, **380**
solid pseudopapillary neoplasm, 215, **216**
somatostatin analogue treatment, 236
somatostatin-receptor scintigraphy, 227
sonoelastography, 65–69
  anal sphincter, **68**
  colorectal carcinoma, **68**
  gastric cancer, **116**
  microcystic adenoma, **68**
  teratoma of testis, **69**
  see also elastography
sonoporation, 45, 57
SonoTip biopsy needles, **74, 367**
SonoVue
  administration, **228**
  adrenal gland imaging, **268**
  chronic pancreatitis, **180, 182**
  lymph node assessment, **279–280**
  pancreatic malignancy, 274
specificity, diagnostic tests, 251
specimen handling, FNAB, 83, **83, 84,** 86
spectral Doppler imaging, 48–49
sphincter, anal, *see* external anal sphincter; internal anal sphincter
sphincter of Oddi, 251, 254
  dysfunction, 34, 258
  manometry, and idiopathic recurrent pancreatitis, 171
sphincterotomy, and IDUS, 33
spine, 325, **325, 326**
spiral, metal, in EUS-guided biopsy, 77, 78
spleen, **125,** 286, **289, 318**
splenectomy, 237
splenic artery, **21,** 197, **197,** 198
  impressions on gastric fundus, **124**
  wide-band harmonic imaging, 277
splenic vein, 197, **197**
  thrombosis, **130,** 171, **174, 175,** 235, **245**
splenomesenteric confluence, 197, **197**
splenoportal confluence, Voxel-Man and EUS, **21**
spontaneous rupture, pancreatic pseudocysts, 235
staging
  anal cancer, 310
  esophageal tumors, 103–105, **105–108**
  gastrointestinal cancer, 371
  gastrointestinal lymphoma, 155–156
  lung cancer, 338–341
  lymph nodes, NSCLC, 328–329
  pancreatic adenocarcinoma, 200–203
  rectal cancer, 298, **299–302,** 302, 314, 315
staining, EUS-guided biopsy, 85
staining kit, 85, **85**
stenosis
  common bile duct, 360
  and endoscope diameter, 37
  esophagus, EUS staging after, **108**
  see also stricture
stent, bile duct drainage, **263,** 360, 361, **361, 362**
sterilization, and LUS, 365
stimulated acoustic emission (SAE) imaging, 46, 52, **52**
stomach
  anatomy imaged from, 11, **11, 12–14,** 13
  benign lesions, 110–111, **112**
  cancer, 112–114, **114–117,** 131
  cross-section, 4, **4**
  EUS, 109–117
  examination, 109–110
  extramural impressions, **124–125**
  fistula, 235
  foveolar hyperplasia, 111
  fundic varices, **174**
  gallbladder impression, **124**
  heterotopic pancreatic tissue, **133**
  indications for EUS, 101
  intramucosal metastasis, **117**
  leiomyoma, **136**
  marginal-zone B-cell lymphoma, **157**
  mesenchymal tumors, 121
  metastases, 138
  neuroendocrine tumor, *vs.* carcinoma, **117**
  orientation, 109
  Osler's disease, *vs.* submucosal tumor, **117**
  pancreatic heterotopia, 145
  polyps, 110, **111**
  pseudocyst impression, **125**
  schwannoma, 138, **138**
  subepithelial tumor, **121, 122, 142, 143**
  T-cell lymphoma, **139**
  transmural window, 246, **246**
  ulcers, 110
  varices, and pancreatic pseudocysts, 235
  wall dissection, in endoscopic lymphadenectomy, 385
  wall layers, 100
  see also gastric
stones
  bile duct, *see* choledocholithiasis
  pancreatic duct, 3D imaging, **63**
strain field, and tissue elasticity, 66–67
strictures
  bile duct, IDUS, 29–30, **31,** 33
  and complications, 94
  pancreaticobiliary, 360
  see also stenosis
stromal tumors, esophagus, 102
stylets, biopsy needles, **73,** 74, **74**
  retraction, 79, 83
subcarinal lymph nodes, 323, **329,** 331
  radial *vs.* longitudinal scanning, **40**
subclavian artery, left, 8, **9**
subepithelial lesions/tumors, 95
  classification, 128
  complications, 147
  cystic, 130–132
  description and classification, 126–132
  diagnostic strategy, 147–149
  differentiation, **128**
  duodenum, **139**
  esophagus, **121**
  EUS criteria, 129
  and EUS-FNA, 95, 148
  EUS follow-up criteria, 148
  EUS-guided resection/treatment, 145, **146,** 147
  vs. extramural impressions, 122–123, 125–126
  gastric body, **121**
  hypoechoic, 134, 136–143, **143**
  malignant, **139**
  pitfalls, 128, 135–136, 143–144, **144**
  practical hints, 126, 136
  vs. pyloric sphincter hypertrophy, 125, **125, 126**
  rectum, **141**
  resection criteria, 148
  solid, 132–135
  solid cystic, 130–132
  therapeutic strategy, 147–149
  Tru-Cut biopsy, 148
  vascular, 128, **129, 130**
subjectiveness of imaging, 1
submucosal lesions, esophagus, 102
superior mesenteric artery (SMA), as landmark, 11, **11, 13**
superior mesenteric vessels, 14, **15**
supraclavicular lymph nodes, 323
surface-based viewing technique, 313
surgery, pancreas, 247
suturing system, endoscopic, **378,** 378–379, **379**
system saturation, contrast agents, 47

T

teratoma
  cystic, 183
  pancreas, 216, **217–218**
  testis, sonoelastography, **69**
therapeutic bronchoscopy, 343
therapeutic EUS
  contraindications, 354
  indications, 354
  intraductal papillary mucinous neoplasm, 212
  materials, 355–356
  pancreas, 210, 234–247
thoracic aorta, *see* aorta
thoracoscopy, 323, 374
three-dimensional EUS
  anal, 310
  endorectal, 313–316
  linear, 60–64, **62, 63**
  principles, 313
  radial, 60
  reconstruction, 27, 313
  rectal cancer staging, 314
  results, 313–315
  scanning steps, **314**
  vascular imaging, 52–53, **53**
  viewing techniques, 313
  volume image, **63**
thrombosis, portosplenic, 128
thyroid, 282
  in mediastinal examination, 325
tissue diagnosis, pancreatic adenocarcinoma, 204
tissue elasticity, **65,** 65–70, **66**
tissue glue, in pancreatic interventions, 240
tissue-specific contrast agents, 45
TNM classification
  anal margin and canal cancer, 309
  cholangiocellular carcinoma, 258
  gallbladder carcinoma, 258
  gastric cancer, 112, 113
  gastrointestinal lymphomas, 156
  pancreatic adenocarcinoma, 200, 201
Toshiba echoendoscopes, 355
toxicological risk, contrast ultrasound, 57
trachea, 9, **10, 20, 326**
  adjacent structures, 323
  bifurcation, and esophageal cancer, 109
  lung cancer infiltration, 339
  in mediastinal examination, 325
tracheobronchial region, 325
tracked free-hand systems, 3D ultrasound, 313
tracking system, in 3D EUS, 62
traction diverticulum, 324
training, 8, 18–22, 93–94, 343
transabdominal ultrasound (TUS), 23
  choledocholithiasis, 251, **251,** 252
  and 3D EUS, 60
transbronchial EUS, 323
transbronchial needle aspiration (TBNA), 338, 341, 347
  cost-effectiveness, 344
  with EUS-FNA, 350
transcutaneous ultrasound, perineal, 310, **310**
transducer
  mechanical, 334
  parallel guidance, in 3D imaging, 61
  positioning for EUS-guided biopsy, 77, **77,** 79, **79**
  rotation, in 3D imaging, 61
transesophageal EUS, 323
transgastric anastomosis, **381,** 381–383, **382, 383**

transit time analysis, 54
transluminal endoscopic interventions, 378
transmural drainage, pancreas, 238–240, **241,** 243, **244, 245,** 248
transmural operation, pancreas, 240–247
transmural window, stomach, 246, **246**
transpapillary therapy, 240, 246, 247
transrectal aspiration, EUS-guided, 308–309, **309**
transthoracic mediastinal ultrasound, 323
traumatic injuries, 55
treatment, *see* therapeutic EUS
Tru-Cut biopsy (TCB), 87, 126, 148
Tru-Cut needles, 76, **76**
  and complications of EUS-FNA, 95
  in laparoscopic ultrasound, 370
true cysts, pancreas, 208
T staging
  accuracy of EUS, 37–38
  esophagus, 103–105, **105–108**
  EUS-FNA, 100
  gastric cancer, 114
  rectal cancer/carcinoma, 298, 304, 314
tuberculomas, 130
tuberculosis, adrenal, **269**
tumor cell seeding, after fine-needle biopsy, 93
tumors
  bile ducts, 30
  biopsy, 79, 307–308
  liver, and LUS, 374–375
  neurogenic, 134
  staging, *see* T staging
  subepithelial, *see* subepithelial lesions/tumors
  and tissue elasticity, 67, **67**
TUS, *see* transabdominal ultrasound
two-dimensional EUS, *vs.* 3D, 314
two-step drainage, 360

U

UICC classification, gastric cancer, 113
ulcer, gastric, 110
ultrasonography, *see* contrast-enhanced EUS; endoscopic ultrasonography; laparoscopic ultrasound
ultrasound contrast agents, *see* contrast agents
ultrathin sensor, in 3D EUS, 64
uncinate process, 198, **199,** 204
understaging, rectal carcinoma, 304
ureter, **288**
urethra, imaging from colon, **317**
urinary bladder, imaging from colon, **317**
urogenital system, 286
urology, and LUS, 374
uterus, **293,** 297

V

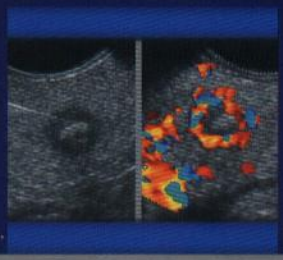
vagina, **294,** 295
varices, 102, **103,** 121, **129,** 147, **245,** 276, **287**
vascular flow, Doppler signal enhancement, 55
vascular geometry, 52–53, **53**
vascular imaging, 3D reconstruction, 52–53, **53**
vascular injury, pancreatic interventions, 243, **244, 245**
vascular malformations, subepithelial, 126
vascular pattern, in malignancy, **273, 274**
vascular polyp, inflammatory, 138
vascular structures, pancreas, 202–203
vasculitis, small intestine, **290**
venous plexus, rectal, 291
ventricular outflow ducts, 325
vertebrae, **326**
vertical rotation, in 3D EUS, 61
volume-based rendering techniques, 3D ultrasound, 313
volume image, 3D, **63**
Voxel-Man, 18–22, **19, 20–21**
voxel values, 3D ultrasound, 313

W

wall layers
  bile duct, 27
  central airways, 335–336, **336**
  gastrointestinal tract, 100, **110**
  tracheobronchial, 343
wash-in kinetics, 53, **53**
wash-out kinetics, 53
water filling, 1, 94
Whipple procedure, 34, 236, 360
wide-band harmonic imaging, 49, **51,** 277, **278**
Will, Uwe, ten golden rules of EUS, 1
Wilson-Cook biopsy needles, 73, 74, **74,** 75, **75**
Wirsung's duct, **200, 202**
  see also pancreatic duct
working channel, damage, 74, 78–79
World Health Organization (WHO) classifications
  non-Hodgkin's lymphoma (NHL), 155
  pancreatic tumors, 208

Y

Youden index, defined, 251
Young's modulus, 67



Endoscopic Ultrasound

Endoscopic ultrasound (EUS) is now considered one of the most essential and cost-effective techniques in the assessment of a wide range of gastrointestinal diseases. A remarkably versatile, minimally invasive procedure, it also calls for a high level of anatomic knowledge and manual dexterity. This lavishly illustrated volume—a textbook and atlas in one—offers medical professionals the most comprehensive overview of EUS available, as well as a wealth of valuable insights from diverse leaders in the field.

Features:

- More than 900 up-to-date, superior-quality images
- Clear, step-by-step instructions for all current procedures and techniques
- Logical, easy-to-use structure throughout, including the requisite anatomy and pathology
- Strategies for selecting patients and procedures, including hygiene requirements, informed consent, patient positioning and monitoring, and more
- Precise clinical descriptions and valuable tips and techniques for diagnosis and treatment
- Guidance on the secure handling of needling and catheters
- Insightful discussions of the uses and limitations of evolving techniques
- Chapters on contrast-enhanced EUS techniques and ultrasound elastography

Tailored to the needs of specialists and trainees in gastroenterology, pneumology, and surgery, *Endoscopic Ultrasound*—with its broad scope and up-to-date information—is also essential reading for anyone wishing to explore and exploit the potential of state-of-the-art EUS.

The Americas
ISBN 1-58890-490-3
ISBN 978-1-58890-490-4
9 781588 904904

www.thieme.com

Rest of World
ISBN 3-13-143151-2
ISBN 978-3-13-143151-6
9 783131 431516